Morphological variability in dogs and red foxes from the first European agricultural societies : a morpho-functional approach based on the mandible

Colline Brassard

MUSÉUM NATIONAL D'HISTOIRE NATURELLE

École Doctorale 227
Sciences de la nature et de l'Homme : évolution et écologie

Année 2020 **N°attribué par la bibliothèque**
|_|_|_|_|_|_|_|_|_|_|_|_|

THÈSE

Pour obtenir le grade de

DOCTEUR DU MUSÉUM NATIONAL D'HISTOIRE NATURELLE

Spécialité : Anatomie fonctionnelle

Présentée et soutenue publiquement par

Colline Brassard

Le 3 décembre 2020

VARIABILITE MORPHOLOGIQUE DES CHIENS ET RENARDS ROUX DANS LES PREMIERES SOCIETES AGRICOLES D'EUROPE : APPROCHE MORPHO-FONCTIONNELLE BASEE SUR LA MANDIBULE

Sous la direction de :

Dr **Anthony HERREL** – Directeur de recherche - CNRS, Muséum national d'Histoire Naturelle, Paris – Directeur
Dr **Stéphanie BREHARD** – Maître de conférences, Muséum national d'Histoire Naturelle, Paris – Co-directrice
Dr **Raphaël CORNETTE** – Ingénieur de recherche, Muséum national d'Histoire Naturelle, Paris – Encadrant
Dr **Cécile CALLOU** – Maître de conférences, Muséum national d'Histoire Naturelle, Paris – Encadrante

Devant le jury :

Pr **Laszlo BARTOSIEWICZ** – Department of Archaeology and Classical Studies, Stockholm University, Sweden – Rapporteur
Dr **Adam HARTSTONE-ROSE** – Department of Biological Sciences, NC State University, United States of America – Rapporteur
Dr **Rose-Marie ARBOGAST** – Directrice de recherche - CNRS, Université de Strasbourg – Examinatrice
Dr **Allowen EVIN** – Chargée de recherche, CNRS, Université Montpellier 2 – Examinatrice
Dr **Anthony HERREL** – Directeur de recherche - CNRS, Muséum national d'Histoire Naturelle, Paris – Directeur
Dr **Stéphanie BREHARD** – Maître de conférences, Muséum national d'Histoire Naturelle, Paris – Co-directrice
Dr **Claude GUINTARD** – Maître de Conférences ONIRIS Nantes – Invité

Morphological variability in dogs and red foxes from the first European agricultural societies: a morpho-functional approach based on the mandible

Abstract

The major cultural and techno-economic changes that occurred in Europe between 7,000 and 4,000 BC, including the development of agriculture, had major repercussions on the animals that lived close to humans. The dog, the only animal that has been domesticated for thousands of years is probably a good marker of the evolution of human societies at that time. Although many data inform us about its status and genetic diversity, very few studies have documented its morphological variability and the resulting possible functional adaptations in relation to anthropogenic constraints. Furthermore, to date no studies have explored the variability in ancient red foxes although they are likely to develop the same adaptations as dogs (but to a lesser extent due to their commensal nature). In this thesis, an innovative morpho-functional approach is used to describe the evolution of mandible (the best preserved bone in archaeological series and an important functional element of the masticatory apparatus) from the Mesolithic to the very early Bronze Age in Western Europe and Southern Romania. Photogrammetry and geometric morphometrics are used to quantify the shape of the bones in 3D. In a first step, shape drivers and form-function relationships within the masticatory apparatus are explored in a sample of modern dogs and foxes. The masticatory muscles of approximately 120 dogs of various breeds and foxes were dissected. A biomechanical model for estimating bite force using muscle data is established and validated by *in vivo* measurements. Strong interrelationships between the cranium, mandible, masticatory muscles and bite force are demonstrated for both species, highlighting the strong integration despite the extreme artificial selections in modern dogs. A predictive model of bite force using the shape of mandibular fragments is therefore developed to interpret the variations in shape in the archaeological sample. The impacts of developmental and environmental factors (climate, urbanism, diet) on the form or function are quantified by studying 433 Australian foxes. Secondly, the variability of ancient dogs and foxes (528 dogs and 50 foxes) is compared with that of modern canids (70 dogs, 8 dingoes, 8 wolves, 68 foxes). Strong morphological differences are demonstrated for both species, suggesting functional differences. Ancient dogs appear highly variable in terms of size and shape, although less variable than modern dogs. Modern hypertypes have no equivalent in our archaeological sample. More surprisingly, some ancient shapes are not found in the extant sample. Finally, the variability existing in dogs prior to the Bronze Age is explored and linked to the information already available. Strong differences between eastern and western Europe are highlighted, reflecting the very different histories of dog populations in these two areas. In each geographical area, temporal but also cultural differences in the size and shape of the dogs are demonstrated. The study of foxes, although limited due to the scarcity of remains, reveals the existence of a relatively large diversity. Variation in size and shape are then probably more related to geographical and climatic variation than to anthropogenic constraints. Differences in bite force over time are suggested for both dogs and foxes, suggesting changes in dog function, and possibly functional adaptations to a diet that has become increasingly influenced by human practices.

Key words: canid, *Canis familiaris*, *Vulpes vulpes*, Neolithic-Chalcolithic, geometric morphometrics, masticatory apparatus

Résumé

Les changements culturels et techno-économiques majeurs survenus en Europe entre 7000 et 4000 ans avant J.-C., notamment le développement de l'agriculture, ont eu d'importantes répercussions sur les animaux qui vivaient près des hommes. Le chien, seul animal domestiqué depuis déjà plusieurs millénaires, est probablement un bon marqueur de l'évolution des sociétés humaines à cette époque. Bien que de nombreuses données nous informent sur son statut et sa diversité génétique, très peu d'études ont documenté sa variabilité morphologique et les éventuelles adaptations fonctionnelles en découlant, en lien avec les contraintes anthropiques. En outre, à ce jour, aucune étude n'a exploré la variabilité des renards roux anciens, bien qu'ils soient susceptibles de développer les mêmes adaptations que les chiens (mais dans une moindre mesure en raison de leur nature commensale). Dans cette thèse, une approche morpho-fonctionnelle innovante est utilisée pour décrire l'évolution de la mandibule (l'os le mieux préservé dans les séries archéologiques et un élément fonctionnel important de l'appareil masticateur) du Mésolithique au tout début de l'âge du Bronze en Europe occidentale et au sud de la Roumanie. La photogrammétrie et la morphométrie géométrique sont utilisées pour quantifier la forme des os en 3D. Dans un premier temps, les facteurs de forme et les relations forme-fonction au sein de l'appareil masticateur sont explorés dans un échantillon de chiens et de renards modernes. Les muscles masticateurs d'environ 120 chiens de différentes races et de renards ont été disséqués. Un modèle biomécanique d'estimation de la force de morsure à partir des données musculaires est établi et validé par des mesures *in vivo*. De fortes interrelations entre le crâne, la mandibule, les muscles masticateurs et la force de morsure sont démontrées pour les deux espèces, soulignant la forte intégration malgré les sélections artificielles extrêmes chez les chiens modernes. Un modèle prédictif de la force de morsure utilisant la forme des fragments mandibulaires est donc développé pour interpréter les variations de forme dans l'échantillon archéologique. Les impacts des facteurs de développement et environnementaux (climat, urbanisme, alimentation) sur la forme ou la fonction sont quantifiés par l'étude de 433 renards australiens. Ensuite, la variabilité des chiens et des renards anciens (528 chiens et 50 renards) est comparée à celle des canidés modernes (70 chiens, 8 dingos, 8 loups, 68 renards). De fortes différences morphologiques sont démontrées pour les deux espèces, ce qui suggère des différences fonctionnelles. Les chiens anciens semblent très variables en termes de taille et de forme, bien que moins variables que les chiens modernes. Les hypertypes récents n'ont pas d'équivalent dans notre échantillon archéologique. Plus surprenant, certaines formes anciennes ne sont pas trouvées dans l'échantillon moderne. Enfin, la variabilité existant chez les chiens avant l'âge du Bronze est explorée et mise en relation avec les informations déjà disponibles. De fortes différences entre l'Europe de l'Est et de l'Ouest sont mises en évidence, reflétant les histoires très différentes des populations canines dans ces deux régions. Dans chaque zone géographique, des différences temporelles mais aussi culturelles dans la taille et la forme des chiens sont démontrées. L'étude des renards, bien que limitée en raison de la rareté des restes, révèle l'existence d'une diversité relativement importante. Les variations de taille et de forme sont alors probablement plus liées à des variations géographiques et climatiques qu'à des contraintes anthropiques. Des différences dans la force de morsure au fil du temps sont suggérées pour les deux espèces, ce qui laisse supposer des changements dans la fonction du chien, et peut-être des adaptations fonctionnelles à un régime alimentaire de plus en plus influencé par les pratiques humaines.

Mots clefs : canidé, *Canis familiaris*, *Vulpes vulpes*, Neolithique-Chalcolithique, morphométrie géométrique, appareil masticateur

I dedicate this thesis to the memory of Anne Tresset, who strongly contributed to the elaboration of this PhD subject and its supervision during the first year. This exceptional woman and researcher will remain engraved in my memory as a model of strength, will and courage, and her insatiable curiosity and passion for transdisciplinary subjects will continue to inspire me. I am grateful to her for allowing me to work in two dynamic laboratories with wonderful, caring and passionate people and – though my original skills and training were still far from this research's contextual foundations – for trusting me to carry out this project.

From the bottom of my heart, thank you.

Je dédie cette thèse à la mémoire d'Anne Tresset, qui a fortement contribué à l'élaboration de ce sujet de thèse et à son encadrement, la première année de sa réalisation. Cette femme et chercheure exceptionnelle restera gravée dans ma mémoire comme un modèle de force, de volonté et de courage, et sa curiosité et sa passion insatiables pour des sujets transdisciplinaires continueront de m'inspirer. Je lui suis extrêmement reconnaissante de m'avoir permis de travailler dans deux laboratoires dynamiques, avec des personnes formidables, bienveillantes et passionnées, et pour m'avoir fait confiance pour mener à bien ce projet, dont les fondements contextuels étaient pourtant bien éloignés de mes compétences et de ma formation originelle.

Du fond du cœur, merci.

Anne Tresset

Chercheuse en archéozoologie

Médaille d'argent du CNRS 2016

Anne Tresset s'efforce de décrypter les relations que notre espèce a su nouer avec les animaux, notamment à travers les processus de domestication. Ses travaux ont permis de réévaluer les modalités de diffusion et d'adaptation d'espèces clés dans l'économie des sociétés néolithiques depuis le Proche-Orient jusqu'aux confins de l'Europe. Anne Tresset a produit ces dernières années plusieurs synthèses internationalement reconnues sur ce sujet. Au sein d'une équipe de quinze personnes qu'elle dirige depuis 2006, la scientifique a ouvert son domaine de recherche à de nouvelles méthodes d'investigations telles que la biogéochimie isotopique, la paléogénétique, la morphométrie géométrique ou la modélisation

Acknowledgements / Remerciements

Ce manuscrit marque l'aboutissement de trois années de travail (2017-2021) d'un contrat doctoral réalisé au Muséum national d'Histoire naturelle, au sein principalement des UMR 7179 (Mécanismes adaptatifs et évolution) et des UMR 7209 (archéozoologie, archéobotanique : sociétés, pratiques et environnement), que je remercie pour leur accueil et pour m'avoir donné les moyens et financiers de parvenir à l'aboutissement de mes recherches dans le temps imparti. Ce manuscrit marque aussi l'aboutissement d'une formation nécessaire à la réalisation de mon rêve d'enfant, celui de devenir, un jour, chercheur en sciences du vivant, et pour cela de faire une thèse, « comme papa ».

Cette période courte mais intense a été marquée par de nombreuses rencontres et collaborations avec des personnes formidables. Ces remerciements seront donc longs… Ils se devaient bien de l'être après tout, pour tenter de rendre compte de l'ampleur de l'investissement des personnes qui m'ont permis de mener à bien, de près ou de loin, ce projet fantastique.

D'abord, merci à mes directeurs et encadrants de thèse, sans contexte les meilleurs du monde. Je n'aurais pas pu espérer meilleure équipe encadrante. D'abord et toujours bienveillante, toujours disponible pour m'aider lors de mes interrogations méthodo existentielles, pour m'aider à trancher, et pour me faire progresser. Merci de m'avoir fait sortir un peu de ma zone de confort pendant ces trois années. Merci de m'avoir permis de participer à des enseignements, en parallèle de mes recherches, me permettant de prendre conscience de mon goût pour l'enseignement, la diffusion et la vulgarisation. Merci d'avoir été flexibles, compréhensifs, et de m'avoir donné des modèles à aduler 😊. Vous êtes les encadrants dont tous les doctorants rêvent ! Merci pour vos apports individuels foncièrement complémentaires, qui ont fait de cette équipe encadrante un modèle de soutien absolument sans faille pendant cette période. Du fond du cœur, un grand merci à tous les quatre. J'espère que nous aurons l'occasion de travailler encore longtemps ensemble.

Plus individuellement, maintenant.

Merci d'abord à Anthony Herrel, pour… La liste est longue ! 😊 D'abord pour ta grande gentillesse, ton empathie et ta bienveillance. Ensuite pour avoir vu ton rôle de directeur de thèse comme un rapport maître/apprenti, ou une mission d'intégration dans la recherche sur le long terme. Tu ne comptes pas tes heures pour tes étudiants, et tu es toujours là pour eux ! Pour ta curiosité permanente, pour être toujours partant pour un nouveau projet, même s'il s'éloigne un peu de tes recherches habituelles… Merci d'avoir toujours tenu compte de mes aspirations et avoir écouté avec intérêt mes projets de travail sur l'Egypte ancienne, pour

m'avoir permis de discuter de mon projet de post-doc et avoir donné un œil « critique », mais bienveillant. Pour m'avoir permis d'encadrer des étudiants supers pendant leur master. Pour ne pas qualifier ce que tu fais de « travail » mais plus comme un amusement, et montrer qu'il est possible de vivre de sa passion (ma vision du métier de rêve n'est donc pas un fantasme !). Pour voir aussi clair dans les futurs projets et publications et redonner de l'ordre dans les idées d'un doctorant paumé en moins de temps qu'il n'en faut pour dire « zygomaticomandibularis », pour la mission surprise en Australie, pour les congélateurs en Tunisie, pour m'avoir formée et aidée dans les dissections, pour les nombreuses relectures et corrections toujours super rapides et intéressantes… pour des articles dont tu n'étais parfois même pas auteur ! J'espère arriver un jour à être un chercheur aussi formidable que toi.

Ensuite, merci à Stéphanie Bréhard. Là aussi, la liste est très longue ! Pour avoir pris la relève d'Anne au pied levé, et surtout pour avoir toujours mis au centre de ton encadrement l'aspect humain. Pour avoir su concilier avec brio la bienveillance et l'empathie d'un côté, avec la neutralité et l'objectivité de la recherche de l'autre. Pour ne pas avoir compté tes heures pour me former sur un sujet que j'ai eu du mal à apprivoiser, pour avoir toujours été extrêmement patiente et avoir accepté de répéter 1000 fois sans broncher. Pour ton organisation, m'enlevant beaucoup de charge mentale, pour ton approche humaine et éthique de la recherche et du terrain, pour ta méthodologie hyper carrée, et pour m'avoir donné les « codes » de ce monde pas toujours facile, m'épargnant j'en suis sûre de nombreuses situations épineuses. Pour m'avoir protégée et portée pendant ces 3 années dans un univers bien éloigné de ma formation de départ !

Merci à Raphaël Cornette, pour ta gentillesse, pour être toujours partant et de bonne humeur quand il s'agit de venir mesurer des forces de morsure, pour t'être toujours rendu disponible pour répondre à mes questions existentielles en morphométrie et pour avoir apporté des solutions à des « beugs » insolites…

Merci à Cécile Callou, pour m'avoir dans un premier temps aiguillé vers cette thèse sur le chien, pour m'avoir suivie depuis le master (supportant même la fabuleuse toge pourpre de véto), pour m'avoir toujours donné les bons conseils pour avancer dans ce monde pas toujours évident, pour les TDs d'osétologie, pour avoir replacé Poulopot qui a su prendre la première place dans sa nouvelle maison, pour ton soutient quand ça n'allait pas…

I am also deeply thankful to the two external examiners (Adam Hartstone-Rose and Laszlo Bartosiewicz) for their thoughtful review of this manuscript and their valuable suggestions during the defence, which will be of great interest to make the most of this work. Je remercie aussi les autres membres externes du jury (Allowen Evin, Rose-Marie Arbogast, Claude Guintard), qui m'ont aussi apporté des pistes de réflexions très intéressantes pour la suite de cette étude.

Ces 3 années de thèses ont été l'occasion de poursuivre voire créer de nombreuses collaborations. Un immense merci à tous ceux, dans tous les champs disciplinaires, qui ont contribué à mes recherches, en donnant accès à du matériel moderne ou archéologique, en participant aux manips, en me formant, en discutant des résultats, en me donnant accès à des données inédites pour réfléchir à plus grande échelle, ou pour discuter de perspectives futures. C'est grâce à vous tous que j'ai pu mener à bien cette thèse. La liste est longue et j'espère n'oublier personne…

Au Muséum, merci à Arnaud Delapré (pour son aide précieuse pour la photogrammétrie et Avizo, pour avoir toujours cherché des solutions à mes problèmes et avoir toujours été disponible), à Céline Houssin (pour sa bonne humeur, sa venue lors des séances de mesures in vivo).

A l'école vétérinaire de Nantes (Oniris), merci à Claude Guintard (pour son aide immense dans la collecte des renards et des chiens et son accueil à Nantes bien sûr, mais aussi et surtout pour sa curiosité insatiable dans la recherche, pour mettre l'humain avant tout, sa grande gentillesse, ses conseils toujours avisés et bienveillants, pour cette collaboration formidable qui j'espère durera longtemps, et pour rendre les trajets de tram si passionnants qu'on en oublie 3 fois de suite le bon arrêt), à Eric Betti (pour sa gentillesse et sa patience lors des TDs de dissection à Oniris), à Manuel Comte et Fred (pour m'avoir beaucoup aidée et tenu compagnie lors de mes séances de dissection).

A l'ANSES de Nancy et la station expérimentale d'Atton, merci à Elodie Monchâtre-Leroy, Jacques Barrat et Sandrine Lesellier, pour leur aide substantielle dans la collecte des chiens et des renards argentés, pour leur accueil toujours chaleureux pour venir mesurer des forces de morsure à la station d'Atton.

De la grande famille de la SCC, merci à Nathalie, Stéphane et Adrien Bausmayer et Michel Beyer (pour nous avoir permis de mesurer des forces de morsures et pour nous avoir montré toute la beauté du jeu du dressage au mordant) et à André Varlet (pour la mise en contact avec des chasseurs et la famille Bausmayer).

Merci à Raymond Triquet pour m'avoir fourni la grande majorité des renards de ma thèse, pour ses relectures et son investissement dans le papier sur les renards, pour sa gentillesse et le temps qu'il m'a consacré au téléphone, partageant sa curiosité pour le monde naturel et son amour de la langue anglaise, achevant de me convaincre qu'il s'agissait là d'une langue formidable qu'il était « facile de mal parler ». Merci aussi à Arnaud Larralle et Hélène Garès pour la collecte des renards.

To the veterinary school of Life Science (Murdoch University), thanks to Trish Fleming for taking care of me for the three wonderful weeks I spent in Australia, for her great kindness, for helping me so much in my research, even during the weekend, for the dissections that were not planned, for the improvised barbecue of fox heads and dingoes in her garden, for the jacuzzi on Saturday evening with red wine, for putting stars in my eyes. I hope to have the opportunity to come back soon, why not for a longer period! Thanks also to John Mullen, Jesse L. Forbes-Harper, Heather M. Crawford, John-Michael Stuart, Natasha Elisabeth, Nathalie M. Warburton, Michael C. Calver, Peter Adams, for having all been so kind to me during my stay!

Merci à tous les archéozoologues qui m'ont répondu, lorsque je les ai sollicités pour accéder à du matériel, voire même qui ont pu me recevoir pour que j'étudie ce matériel. Merci pour votre disponibilité, votre temps, votre accueil toujours chaleureux.

En Allemagne, merci à Andrea Zeeb-Lanz pour m'avoir merveilleusement accueillie lors de ma mission à Speyer pour étudier le matériel de Herxheim.

En France, merci à Rose-Marie Arbogast (pour m'avoir aidée lors de ma mission à Lons le Saunier pour l'étude du matériel de Chalain-Clairvaux, pour avoir répondu à mes questions concernant le matériel de Twann, pour avoir fourni les numéros d'inventaires de Herxheim, et enfin pour avoir présidé mon jury de thèse), Vianney Forest (pour m'avoir lancé dans le monde merveilleux de la recherche et de l'archéozoologie, pour sa pédagogie, pour son accueil dans le sud, pour son temps, sa gentillesse, ses discussions), Morgane Ollivier (pour avoir fait partie de mon comité de thèse, pour son investissement sans faille, sa grande gentillesse et ses travaux passionnants), Aurélie Manin (pour avoir partagé des résultats inédits, me permettant de prendre cela en considération dans les interprétations), Marie Balasse (pour sa gentillesse, sa super gestion de l'équipe PRESAGE), Myriam Boudadi-Maligne (pour l'organisation du colloque Hommes-Canidés et les échanges, en espérant que nous aurons l'occasion de travailler ensemble dans le futur), Aline Averbouth (pour m'avoir mise en contact avec des personnes susceptibles de m'aider et m'avoir permis de faire pension pour hérisson une soirée, pour son partage de l'amour des animaux et de la nature). Merci aussi à Isabelle Carrère, Véronique Fabre, Muriel Gandelin, Fabien Convertini, Alain Beeching, Jacques-Léopold Brochier, Charlotte Leduc, Lamys Hachem, Evelyne Crégut, Céline Bémilli, l'Institut de Paléontologie Humaine, Axelle Davadie.

En Suisse, pour l'étude du matériel de Twann, merci à Adriano Boschetti, Rebecca Vogt (chargée de l'inventaire des collections, que j'ai torturé à sortir presque toutes les caisses de l'entrepôt pour tenter de mettre la main sur ces maudits renards introuvables), Carole, Barbara Chevallier, Winkelmann Ulrich pour m'avoir donné accès au service le weekend !

En Roumanie, un grand merci à Adrian Balasescu (pour son accueil hyper chaleureux à Bucarest, pour l'organisation du colloque auquel il m'a permis de participer, pour son aide précieuse pour les contextes archéologiques, et pour avoir mis à disposition une grande quantité de matériel), Adina Boroneant (pour l'accès au matériel et les contextes archéologiques), et Valentin Radu.

Enfin, merci à tous les autres, qui ont contribué, de près ou de loin, à enrichir ces trois années de construction dans l'univers de la recherche.

Thanks to to Ardern Hulme-Beaman for his enthousiasm and for, I hope, the future projects that will bring a new life to these canid mandibles and maybe extend the perspectives of application to much more archaeological material.

Merci à Fabien Belhaoues pour les discussions enflammées sur le monde de la recherche et les bières à Montpellier (on les écrit quand ces articles ? 😊).

Merci à Margot Michaud et Lysianna Ledoux pour leur expérience du post-doc Fyssen.

Merci aux merveilleuses étudiantes que j'ai contribué à former (quel plaisir de pouvoir allier enseignement et recherche, pile dans son domaine de compétences !). Merci à Marilaine Merlin, une fabuleuse étudiante du Muséum, hyper investie et à l'écoute, qui a aidé de façon

substantielle dans l'acquisition des données (dissections et morphométrie sur les crânes) et dont les qualités artistiques (et culinaires) étaient plus que bienvenues ! 😊 Merci aussi à Lauriane Quiblier, là encore une étudiante très investie, malgré des conditions sanitaires qui ont bouleversé son calendrier de travail. Merci à vous deux de m'avoir permis de sortir un peu du « tout recherche » de la thèse en me permettant d'y ajouter un peu de formation.

Merci aux responsables des missions de statistiques (Loïc Ponger et Sandrine Pavoine) pour m'avoir permis de faire partie, pendant ces 3 années, de l'équipe enseignante, ce qui a été une vraie révélation.

Merci à Jérôme Sueur et Véronique Barriel pour leur aide dans les moments difficiles et leur grand soutient.

Je remercie également chaleureusement les personnes qui m'ont accompagné pour les aspects administratifs / techniques au Muséum : Samia Chentout, Anne-Cécile Haussonne, Yamso Sepkon, Nadine Comte, Karyne Debue et Isabelle Baly.

Merci aussi à Farid Hadj Rabah pour l'impression des exemplaires papier de la thèse.

Enfin, un énorme merci à tous mes co-bureaux, co-promo de choc et collègues de labo, qu'ils soient de MECADEV ou d'AASPE, pour tous les bons moments passés au bureau. C'est dans les moments de confinement qu'on apprécie d'autant plus le souvenir de ces moments et qu'on se rend compte à quel point ils comptent vraiment ! Merci donc à Maxime Taverne, Rohan Mansuit, Christophe Mallet, Rémi Lefèbvre, Ana Phelippeau, Julie Solpesa, Priscila Rothier, Cyril Etienne, Marjorie Roscian, Louise Le Meillour, Marine Durocher, Hugo Harbers, Manon Leneün, Nicolas Morrand, Nicolas Lazzerinni, Anaïs Marrast, Olivier Trombet… et tous les autres !

Merci à mes amis de toujours, vétos ou non, toujours avec ce qu'il faut de folie pour se vider la tête et mieux repartir, mais qui savent garder la tête sur les épaules et qui ont compté pendant ces trois années. En particulier un grand merci à Rachel Colombe, pour tout ce qu'elle est : juste, brillante, bienveillante. Merci aussi à Philippe Théophile, Thomas Brinjean, Agathe Champetier, Tanguy Combe, Aliénor Lepetit, Raphaël Hanon, Camille Marsan, Xavier Ballet, Anne-Cécile et Thomas Sibarita, Marion Strauss, Arthur Humbert, Elodie Jacob et Lionel Communal, la tribu Sperber, Laura Vallance, Dominique Mias-Lucquin… Et bien sûr un grand merci à Florian Le Gall, pour avoir rendu la fin de thèse aussi agréable et facile, si improbable que cela puisse paraître.

A Canelle, une alliée de choix pendant les mois de confinement et de rédaction, non moins contente de voir disséqués tous ces fichus clébards !

Enfin, un grand merci (le mot paraît bien court pour qualifier tout ce qu'il représente) à mes parents, pour leur soutien sans faille pendant ces 29 années et pour m'avoir porté jusqu'au bout de mes études… (Maintenant c'est fini, promis !)

Et bien sûr merci à Alexandra Elbakyan, sans qui ma biblio aurait été bien moins fournie !

Abbreviations

BC / BP: Before Christ / Before present

[xxx] cal BC / BP: calibrated years before Christ / before present

BF: Bite Force

CVA: Canonical Variate Analysis

DNA: Desoxyribonucleic acid

DNAmt: Mitochondrial DNA

Hg: Haplogroup

MP: Mechanical potential

NISP: Number of individuals by skeletal part

PCA: Principal Component Analysis

PCSA: Physiological Cross-Sectional Area

2B-PLS: Two-blocks partial least-square analysis

Table of contents

Introduction

Among all animals, dogs have revealed one of the most fascinating evolutionary stories, owing to their close interconnection with humans and their proper evolutionary history. Accordingly, they have long been the object of scientific curiosity.

Although widely documented, the sequence of events leading to the domestication of the wolf and the origin of the dog is not fixed and continually evolves with new archaeological and (paleo)genetic discoveries. The dog is considered to be the first animal ever domesticated, and its domestication dates back to at least 13,000 years BC. Hunter-gatherers in many parts of the world, including some in Western Eurasia, are said to have gradually selected the most docile wolves and encouraged their reproduction, taking advantage of their companionship, especially for hunting. The result was the rapid modification of their phenotype and a morphological difference that became clearer and clearer over the generations compared to their wild ancestors.

Long after their domestication, when dogs were already well differentiated from wolves, major cultural and techno-economic changes occurred in the Near-East and gradually spread to South-Eastern Europe and then to Western Europe between 7,000 and 4,000 years BC. This Neolithic revolution was marked by profound changes in the ways of life and subsistence of humans, which had strong repercussions on animals, especially those living closest to humans such as dogs. From hunter-gatherers, humans became farmers. Regionally and chronologically, human groups have developed different cultural identities succeeding or overlapping in a complex mosaic, and consequently considerations towards dogs vary between cultures and geographic localities. Indeed, depending on the period and culture, dogs may have had many different statuses and functions, with clues to these roles provided by archaeological data.

In this PhD thesis, we focus on two geographical areas: Western Europe and South-Eastern Europe, since they are characterized by different neolithisation processes and the dog populations at these sites thus have undergone different evolutionary histories. We concentrate on the period from the Mesolithic (period of the last European hunter-gatherers), to the very early Bronze Age. Throughout the manuscript, this period will be referred to as the "pre-Bronze Age period".

Humans and dogs co-evolved during this period, both adapting in parallel to the new anthropic constraints and modifications of the environment. For example, both developed the ability to digest the starch contained in cereals and pulses and more and more present in the diet and food waste of the first farmers. Dogs also followed Neolithic human groups in their movements from east to west, leading to changes in the genetic make-up of populations over time.

While many studies have explored the diversity and adaptations of dogs at the genetic level during this period, work on their morphology is much rarer and data are often scattered. The objective of this PhD thesis was therefore to document the variability and evolution of the

morphology of dogs that existed during this period (hence well after domestication and before the Bronze Age), and to interpret the results in the light of available data concerning archaeology and genetics.

To explore and better understand the impact of the proximity between humans and animals, we also studied the variability and morphological evolution of a canid species that has remained commensal and has been little studied to date in archaeozoology: the red fox.

We based our work on a bone that is generally well preserved in archaeological series and is likely informative of the skull and thus of the overall morphotype: the mandible. We here propose an innovative morpho-functional approach. Form is approached by means of the 3D reconstruction of the bones by photogrammetry and the use of 3D geometric morphometrics. Variation in form is interpreted in functional terms, by estimating the bite force and the relative contribution of the masticatory muscles to this force.

To do so, we first explored the relations between form and function in the masticatory apparatus of modern canids (mostly red foxes and dogs). In particular, we investigated whether the form of the mandible is a good proxy for inferring the overall morphotype, muscle data, or bite force. To do so, we dissected the jaw muscles of dogs, foxes, and dingoes and obtained *in vivo* measures of bite force allowing to validate our models.

This thesis consists of 3 parts.

In the first (bibliographical) part, we establish the global framework in which this work was carried out, by returning to notions of evolutionary biology and archaeozoology necessary for the study of canids. We retrace the evolutionary history of canids from their appearance to the present day, evoking domestication, the Neolithic period and also the very recent selection at the origin of modern dog breeds. Next, we establish a non-exhaustive inventory of the occurrences of canids in the archaeological record and the types of status granted by prehistoric humans to these canids before the Bronze Age in Europe. This introductory part allows us to detail the chrono-cultural context as the basis for the research questions explored in this thesis.

The second part is presented in the form of a compilation of published articles or manuscripts. Its objective is to explore the architectural and functional relationships between the mandible, the cranium, the masticatory muscles and bite force in relation to other parameters (environment, urbanisation, diet) in modern dogs and foxes. In this part, the general methodology and the notions necessary for the study of form and function are detailed.

In the third part, the methods are adapted and then applied to our archaeological corpus of dogs and foxes. In this part, modern and ancient (pre-Bronze Age) canids are compared to ensure the transposability of the methods, on the one hand, and also to document the evolution of forms over time.

Given the interdisciplinary nature of this thesis and in order to facilitate the reading of the manuscript and its understanding by non-specialists, we regularly summarize the key points of the different sections and/or chapters. At the end of the second part, we discuss more specifically the aspects of functional anatomy resulting from the study of modern canids. In the general discussion, we focus on the results obtained when applying the methods to pre-Bronze Age canids. We try to answer the questions formulated at the end of part 1 and discuss the prospects for future study.

Part 1

Chapter 1.
The natural and cultural history of canids in Europe from origin to the very early Bronze Age, state of the art

This chapter aims to provide a general framework for our research and to formulate the questions we explored in this PhD thesis. First, we retrace the evolutionary history of canids from their origin to modern times, in order to recall some key concepts in evolutionary biology and archaeozoology. Then, through a synthetic bibliographical review, we focus on the representation of canids in proto-historic societies from Europe/Western Eurasia, before retracing the different typologies of relationships they have entertained with humans. Finally, existing data on the morphological variability of these protohistoric canids will be reviewed. The main questions that will be addressed in this thesis will be presented in the conclusion of this chapter.

1. The origins of extant canids in Europe: an history between commensalism and domestication

Before addressing the core research questions of this thesis, it is essential to bear in mind a certain number of concepts with regards to the evolutionary history of canids, from their origin to their current presence by our side. Accordingly, in this section, we will briefly discuss the phylogeny of canids, as well as the evolution of their distribution in Eurasia (in other words, phylogeography[a]). More precisely, we will summarize the evolutionary history of the wolf and its relatives (dog, dingo) and the red fox and its relatives (silver fox) since their emergence, focussing on Europe.

The aim is not to be exhaustive, but to provide the necessary basis for understanding the genetic and morphological diversity existing within these species through time and to link them to natural phenomena first, and then to anthropogenic changes. We will deliberately be synthetic and invite the reader to refer to the articles of Edwards *et al.* (2012) and Statham *et al.* (2012) for more details on the phylogeography of foxes, and to those of Loog *et al.* (2018) and Pilot *et al.* (2010, 2019) for the phylogeography of wolves.

1.1. Phylogeny

The Canidae family (Fischer, 1817), which has been estimated to diverge about 50 million years ago (Wayne, Benveniste and O'Brien, 1989), is part of the order Carnivora, and currently comprises 13 genera and 36 species (updated from ITIS1 on 22 July 2020, https://www.itis.gov/). Among them, we will focus in this PhD thesis on the grey wolf *Canis lupus* (Linnaeus, 1758), its domesticated subspecies *Canis lupus familiaris* (Linnaeus, 1758), its feral subspecies *Canis lupus dingo* (Meyer, 1793) and the red fox *Vulpes vulpes* (Linnaeus, 1758).

Numerous studies, mainly relying on morphology and cytogenetics, have been conducted to elucidate the phylogenetic relationships of canids, but the results of these studies are quite unstable (see Zrzavý *et al.*, 2018). However, studies based on molecular data (especially on nuclear markers; e.g. Lindblad-Toh *et al.*, 2005; Zrzavý *et al.*, 2018), converge towards a single tree typology supported by combined molecular and morphological data. Accordingly, two groups of recent Canidae can be distinguished, the "fox-like" monophyletic Vulpini (genera *Nyctereutes*, *Otocyon*, *Urocyon*, *Vulpes*) and the "dog-like" monophyletic Canini, the latter group being divided into two other groups: the South American Cerdocyonina (genera *Atelocynus*, *Cerdocyon*, *Chrysocyon*, *Dusicyon*, *Lycalopex*, *Speothos*) and the Afro-Holarctic "wolf-like" Canina (genera Canis s. str, Cuon, Lupulella, Lycaon). Canini and Vulpini separated

[a] Phylogeography is the study of the historical processes that are responsible for the contemporary geographic distributions of individuals. This is accomplished by considering the geographic distribution of individuals in light of genetics, particularly population genetics.

more than 8 million years ago, so the phylogenetic distance between wolves and foxes is rather great (Lindblad-Toh *et al.*, 2005; Zrzavý *et al.*, 2018). The species descending from these clades (wolves and dogs on the one hand and foxes on the other hand) are therefore very distant cousins.

The tree proposed by Zrzavý *et al.* (2018, Figure 1) summarizes the phylogenetic relationships of 36 extant and 42 extinct species of Canidae, based on 360 morphological, developmental, ecological, behavioural and cytogenetic characters and on 24 mitochondrial and nuclear markers. However, the position of fossil canids in the tree is likely to be heavily influenced by the almost exclusive use of morphological traits related to the skull, as these are often the only traits available. Additionally, comparisons of morphological and genetic phylogenies suggest that there are strong morphological convergences between species that are very distant from each other, which can be linked to the phenomenon of hypercarnivory (diet consisting of at least 75% meat). Indeed, in morphologically based phylogenetic trees, all canid species assumed to be hypercarnivorous and/or large-tailed tended to form a deeply nested clade, often next to *Canis lupus* (Zrzavý *et al.*, 2018). Relatively hypercarnivorous species share several cranial and dental features that could also be found in fossils: relatively short and deep jaws and a very robust skull (Slater, Dumont and Van Valkenburgh, 2009). Shortened jaws are associated with an enlarged palate, enlarged incisors and canines, the compression of the premolars, adaptations of anterior upper molars for grinding, and reduction or loss of postcarnassian molars (Van Valkenburgh, 1989; Van Valkenburgh and Koepfli, 1993; Wang *et al.*, 2004). On the contrary, in molecular trees, no unified 'hypercarnivorous clade' exists and no recent hypercarnivore is closely related to the grey wolf. Thus, morphology alone groups species that are distant phylogenetically, yet that show convergences in response to similar ecological and functional constraints.

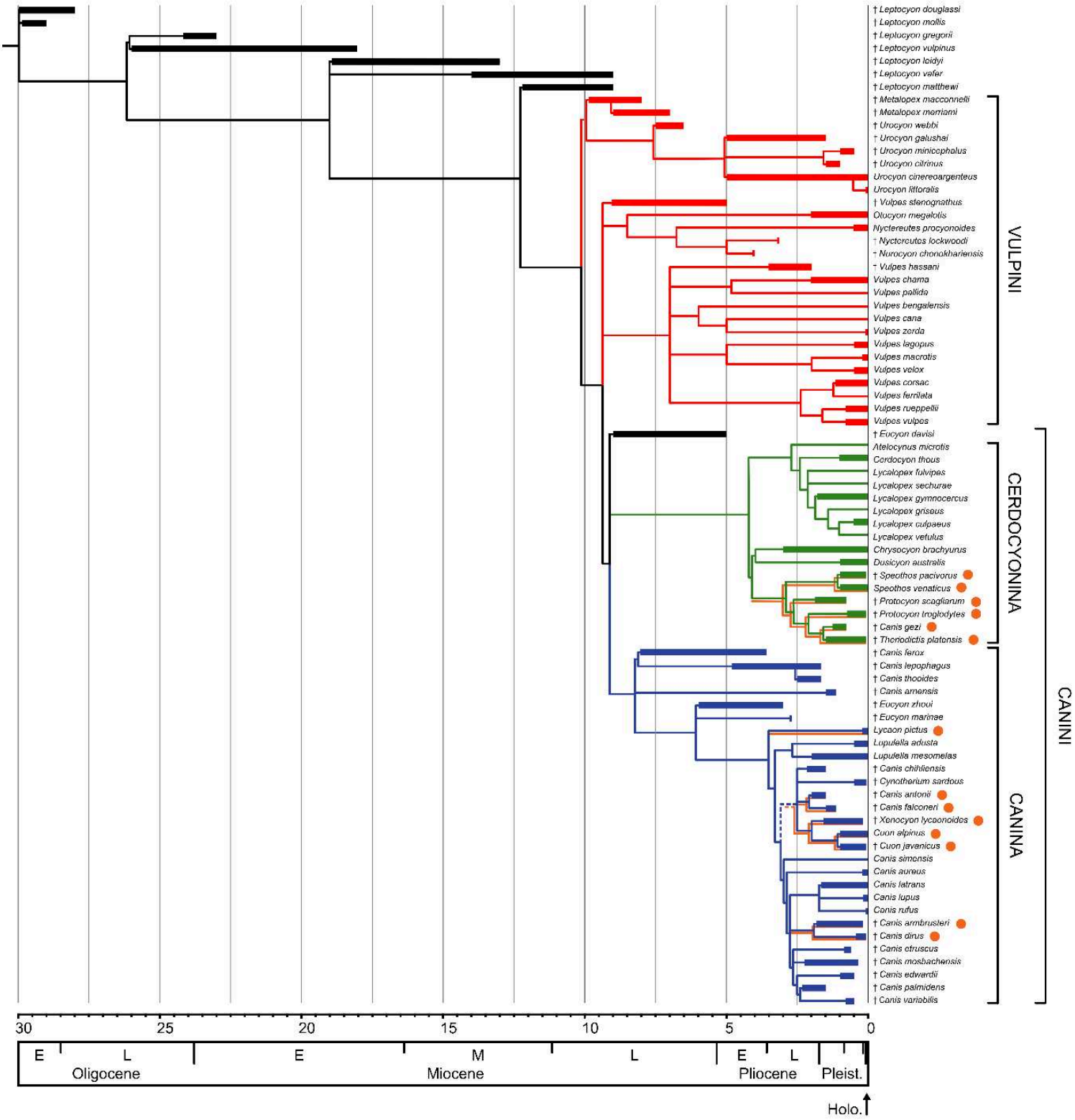

Figure 1. The phylogeny of extant and extinct canids proposed by Zrzavý *et al.* (2018).

Dotted lines represent uncertain phylogenetic relationships, thick lines the known stratigraphic extent. Divergence times are derived from Wang *et al.* (2008) and molecular clock analyses (Lindblad-Toh *et al.*, 2005; Perini *et al.*, 2010; Nyakatura & Bininda-Emonds, 2012; vonHoldt *et al.*, 2016; cited in Zrzavý *et al.*, 2018). Vulpini are in red; Canina are in blue; Cerdocyonina are in green; HCs are in orange; extinct taxa (†) are in black.

1.2. Wolves and red foxes from their appearance to the early Holocene

1.2.1. First red foxes and wolves in Europe

1.2.1.1. *Red foxes*

The first Vulpini first appeared in North America at the end of the Miocene (~9 Ma; Wang and Tedford, 2008). They only appeared and diversified in Eurasia at the beginning of the Pliocene (~4 Ma). During the Plio-pleistocene, many species of foxes appeared, including the Arctic fox (Wang, Tedford and Antón, 2010).

Fossil remains suggest that red foxes *Vulpes vulpes* have been present in continental Europe for at least 71 kyrs (Sommer and Benecke, 2005; Edwards *et al.*, 2012). Mitochondrial DNA analysis suggest that all current foxes are from the Middle East (Statham *et al.*, 2012) and that the primary North American clade is 400 +/- 139 kyrs of age.

1.2.1.2. *Wolves*

Paleontological records attest to the appearance of the wolf *Canis lupus* in Europe about 800 kyrs ago, in the middle Pleistocene (Wang, Tedford and Antón, 2010, p. 148). Older evidence of wolf occurrence is only known from Siberia and Alaska (Beringia). Wolves are thus thought to have originated in the Palearctic (Kahlke, 1999 in Sommer and Benecke, 2005) and more specifically in Beringia, before spreading throughout the Holarctic (Wang, Tedford and Antón, 2010).

The wolf appears to have been well established in Europe for about 400 kyrs (Meloro *et al.*, 2011) and its presence has even become continuous in the Northern hemisphere for at least 300 kyrs (see additional information 1 in Loog *et al.* (2018). Remains of grey wolves found in Saalian glacier assemblages (230 to 130 kyrs) attest to a very robust form (Sommer and Benecke, 2005).

1.2.2. Evolution through the Pleistocene and early Holocene

Both wolves and foxes maintained a wide geographical distribution in the Northern hemisphere throughout the Pleistocene and Holocene[b] (Loog *et al.*, 2018; Pilot *et al.*, 2019). This is likely related to the frequent introgression of ecologically diverse conspecific and congeneric populations that could have facilitated adaptation to novel environmentals (Pilot *et al.*, 2019), resulting in a great ecological flexibility. However, their demography has undergone some major variations. In particular, during the late Pleistocene, profound climatic and anthropogenic changes occurred and caused the extinction of many large mammals (Lorenzen *et al.*, 2011). Those species that survived – including grey wolves and red foxes – experienced major demographic bottlenecks, local extinctions and phylogeographic changes (Edwards *et al.*, 2012; Statham *et al.*, 2012; Loog *et al.*, 2018; Pilot *et al.*, 2019). In addition, the Pleistocene glaciations had a profound effect on intraspecific genetic differentiation, and the divergence of

[b] The Holocene is a geoclimatic period of gradual warming that succeeded to the Pleistocene around 10,000 years ago at the end of the last ice age (Würm-Wisconsin).

the corresponding subpopulations is at the origin of many extant species. Ancestral lineages may have been isolated in different glacial refugia during the last glaciation (~50 kyrs) up to the Last Glacial Maximum (LGM, 21-17 kyrs BP), which may have induced their long-term geographic separation (Pilot *et al.*, 2010).

1.2.2.1. *Geographical distribution*

Red fox

During the last glaciation and up to the LGM the Iberian Peninsula, the Italian Peninsula and the Balkans, and the Carpathians and Crimean Peninsula acted as glacial refuges for red foxes (Sommer and Benecke, 2005). After a demographic bottleneck, they underwent a major expansion in Eurasia (as suggested by mitochondrial DNA analyses of around 1000 red foxes, Statham *et al.*, 2012). This expansion was accompanied by a secondary transfer of a single matrilineage (Holarctic) to North America.

During the last warmest interstage of the pleniglacial period (38-25 kyrs BC), the red fox was present in Central Europe and its distribution extended at least partly to Southern England (Sommer and Benecke, 2005). At that time, the Arctic fox (*Alopex lagopus*) and red fox were probably sympatric in parts of their range.

During the LGM (22-18 kyrs BC), the arctic fox was distributed exclusively in Central Europe, in addition to being present in glacial refuges. The combined distribution of the artic fox and red fox persisted after the LGM and during the Late Glacial (15-9,5 kyrs BC) in Central Europe, with the probable exception of the Allerød interstadial (Sommer and Benecke, 2005). The range of the arctic fox regresses towards the Northernmost regions of Europe during the Holocene.

After the LGM, the earliest well-documented records of *Vulpes vulpes* in Central Europe are between 14 and 13,5 kyrs BC (Sommer and Benecke, 2005).

Wolf

During the last pleniglacial period (75 to 15 kyrs BC), the wolf was already present in geographical regions that served as glacial refuges for species more adapted to warm climates as evidenced by bone remains: France, Spain, Ireland, Great Britain, Germany, Italy, Greece, Moldavia and Ukraine(Sommer and Benecke, 2005). No drastic decrease in the distribution of grey wolves is assumed (Sommer and Benecke, 2005). The omnipresence of the wolf during the Holocene is likely not due to a recolonisation.

1.2.2.2. *Genetic diversity (haplogroups history)*

Red foxes

Analyses of the mitochondrial DNA of modern and ancient red foxes have suggested that they show a high degree of phylogenetic structure throughout Europe (Edwards *et al.*, 2012). Only a few of the existing haplotypes were found in several locations. Among them, haplotype A1 is one of the most common and it has the widest geographical distribution (it is present worldwide), haplotype A2 is mainly present in Scandinavia and Central Europe, haplotypes B

and D are mainly found in the British Isles. Southern regions are less well connected than Northern regions and Iberian foxes are relatively isolated from other European regions (Frati *et al.*, 1998; Edwards *et al.*, 2012).

Wolves

Analyses of the mitochondrial DNA of modern and ancient wolves have revealed that there are two European haplogroups (Pilot *et al.*, 2010). Haplogroup 1 is also present in North America, unlike haplogroup 2. These two hapologroups include European and Asian haplotypes and overlap geographically, but differ significantly in frequency between populations in South-Eastern and Western Europe. Haplogroup 1 predominates in Eastern Europe and the Iberian Peninsula, while haplogroup 2 predominates in the Apennine Peninsula (a mountain range in the Alpine belt that runs through Italy). Italian wolves are thought to have been genetically isolated for thousands of generations south of the Alps, but the presence of a shared haplotype between the Iberian Peninsula and Eastern Europe strongly suggests the existence of a past gene flow between these two populations, thus implying the presence of haplogroup 1 in the extinct intermediate populations of Central and Western Europe. Surprisingly, all ancient wolves in Central and Western Europe (42 kyrs BC to 750 AC) have haplotypes belonging to haplogroup 2. The dominant haplogroup would therefore have changed from haplogroup 2 to haplogroup 1 over the last 40,000 years, before and after the LGM, which may be related to ecological changes that occurred after the LGM (Pilot *et al.*, 2010, Figure 2). The turnover was incomplete in Central and Western Europe (haplogroup 2 persisted) while it was complete in Northern America. Haplotypes of haplogroup 1 appeared in samples of wolves from Western Germany date to 250 to 550 AC (Pilot *et al.*, 2010).

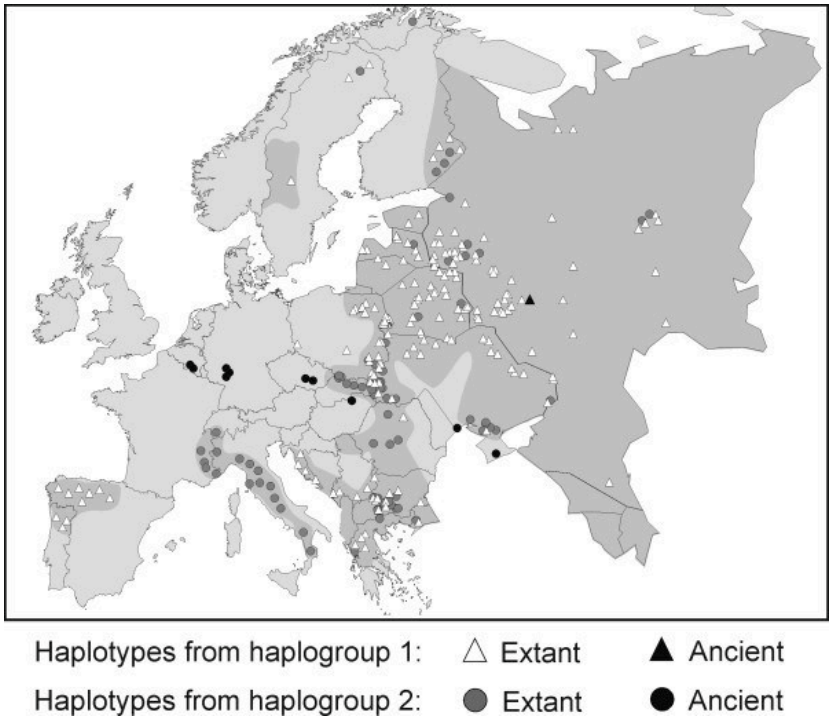

Figure 2. Distribution of haplogroups 1 and 2 in extant and ancient European wolves. From Pilot et al (2010).

Other DNA analyses revealed that at the end of the Pleistocene, wolf populations in North America would have experienced a bottleneck, following the diffusion of a maternal lineage of Greenland wolves (contrary to previous studies that suggested an extinction replacement event) but the authors found no argument for a similar bottleneck in Eurasia (Ersmark *et al.*, 2016). Loog and colleagues (2018) hypothesized the existence of this bottleneck in Eurasia based on

the analysis of 90 whole mitochondrial genomes of modern wolves and 45 mitochondrial genomes of ancient wolves from the Northern Hemisphere, the latter covering a period of 50 kyrs. Their results suggest that the wolves that exist today all originate from a single Late Pleistocene ancestral population from Beringia (or a Northeast Asian region in close geographical proximity). A bottleneck occurred (between 38 and 13 kyrs BC) with limited gene flow between neighbouring demes, and the population rapidly expanded at the end of the LGM (around 23,5 kyrs BC, between 31-12 kyrs BC), replacing indigenous Pleistocene wolf populations across Eurasia (Loog *et al.*, 2018). Despite this bottleneck, genetic variation remained high throughout Europe until the last few centuries (Dufresnes *et al.*, 2018).

1.3. The domestication of the wolf as a dog during the late Pleistocene

Contrary to the evolutionary origins of the wolf and the fox, the origins of dogs are more anthropic than natural, as they are intrinsically linked to humans. In return, dogs are suspected of having profoundly influenced the course of human history and the development of the first civilisations (Shipman, 2015b).

In this PhD thesis, we will not examine the first domestic dogs, but rather their evolution in later times, when the domestication was certain and no confusion between them and their wild ancestor was possible. However, in order to understand some of the questions that will be addressed in this work, some background information on the process of domestication, and in particular on the biological and anthropic phenomena that led to a divergence in the history of dogs compared to their wild relatives, seemed useful.

1.3.1. The ancestral lineage of wolf at the origin of dogs

Grey wolves *Canis lupus* are the ancestors of the subspecies *Canis lupus familiaris*, in other words, dogs. However, extant wolves are not believed to be the direct ancestors of modern dogs (Freedman *et al.*, 2014). In fact, during the late Pleistocene, one ancestral lineage of European grey wolves – that occupied the tundra steppes more than 20 kyrs ago (~60-20 kyrs according to Frantz *et al.*, 2016)– would have diverged in a very short time to give rise to dogs through a process of **domestication** (Thalmann *et al.*, 2013; Freedman *et al.*, 2014; Fan *et al.*, 2016; Freedman and Wayne, 2017), ensuring the evolutionary success of this lineage. Domestication is associated with a first severe bottleneck, causing the divergence between dogs and wolves (Freedman *et al.*, 2014). Dogs occupied a new ecological niche, and found themselves favoured in competition for resources, disease transfer or mixing with non domesticated lines (Lescureux and Linnell, 2014; Pilot *et al.*, 2019). Soon after their divergence from dogs, another major bottleneck occurred in wolves. This means that dogs come from a population of wolves that was much more genetically variable than the modern population of wolves (Freedman *et al.*, 2014). The ancestral lineage of wolf responsible for domestication is now extinct. Morphological and isotopic data suggest that their extinction was linked to that of their megafauna prey (Leonard *et al.*, 2007). These populations were subsequently replaced by modern lines of wolves (Larson *et al.*, 2012).

1.3.2. Domestication was initiated by a phase of commensalism

Somewhere in the last 11 to 35 kya BP, Late Pleistocene wolves were likely attracted to hunter-gatherer encampments to feed on human food waste (Coppinger and Coppinger 2001; Morey 1994 in Zeder, 2012; Freedman and Wayne, 2017). They would have followed humans to take advantage of the carcasses they left behind in the landscape (Shipman, 2015b, 2015a). This forced some wolves to migrate towards a human niche, reflecting their demographic divergence from established territorial wolves (Freedman and Wayne, 2017). This would therefore have been the beginning of a commensal relationship. This is the hypothesis put forward by Zeder (2012). At this stage, the "proto-dog" benefited from the relationship with man, while man does not really benefit from this relationship. The animals most likely to have been attracted to human groups were probably not the alpha males (the most aggressive), but rather members of the subdominant pack, wolves that were less aggressive but still distrustful of males. These individuals, with higher stress thresholds, were probably better candidates for domestication. Next, humans likely started to select these less aggressive wolves/dogs, which would have paved the way for a domestic relationship for the first time in the animal world[c]. This hypothesis was confirmed by the farm-fox experiment, as we will see in the next paragraph.

The association then became more and more mutualistic, involving common activities from which men now derived tangible benefits from this collective intelligence (hunting or protection of the group against other humans or carnivores; Zeuner, 1963; Clutton-Brock, 1999; Vigne, 2012; Freedman and Wayne, 2017), which, however, remains difficult to deduce from the archaeological remains (Boudadi-Maligne *et al.*, 2020). Hunter-gatherers and proto-dogs thus progressively developed closer social bonds.

Later on, the transition to a more sedentary lifestyle and the development of agriculture, starting at around 11.5 kyrs BP in Western Eurasia, would probably have involved the selection of modified phenotypes and the appearance of dogs of very different sizes, resulting in a marked phenotypic divergence from their ancestors. This point will be discussed in further details in section 2.3 and in Conclusion and discussion of Part 2 and perspectives for Part 3.

1.3.3. A unique but reproducible situation in other canids

The **farm-fox experiment** was a key stage in the comprehension of the domestication process. It was carried out over several decades by a group of Russian researchers in Siberia starting in the 1960s (Trut, 1999; Trut, Oskina and Kharlamova, 2009, 2012). They monitored the evolution of a population of silver foxes originating from fur farms in Eastern Canada, reproducing the first supposed stages of domestication. Silver foxes are eumelanic variants of the red fox, thus belonging to the same species (*Vulpes vulpes*), although they may differ slightly in osteological dimensions. These original silver foxes were already selected for their fur but not domesticated.

[c] The dog is the first domesticated animal, since the other domestications coincide with or are posterior to the development of agriculture, around 11.5 kyrs BP (Vigne, 2011; Zeder, 2012).

At the beginning of the experiment, Dr. Dimitry Belyaev and his colleagues selected the least shy individuals and eliminated the most aggressive ones from reproduction. In only a few generations (6-15), they observed the same morphological, behavioural and beahvioral variations as those observed between wolves and dogs (and consistently found in the domestication of other species, which is called the “domestication syndrome”). These results supported Belyaev's original idea that intentional selection on tameness and strictly behavioural traits determined the establishment of the domestication syndrome.

Subsequent authors have contested these results, arguing that this study was biased because most of the traits attributed to behavioural selection for tameness were prior to the experiment (Lord *et al.*, 2020). However, the quantitative evolution of these traits over the course of the experiment does not affect, to our mind, the fact that behavioural selection influenced morphological or physiological traits. These traits, although already existing in a small proportion in the population prior to the experiment, have become increasingly frequent over the generations, under the effect of the drastic selection.

These results reinforce the hypothesis that dogs rapidly emerged from a commensal relationship and from the preferential breeding of docile and tame animals. However, strong selection pressures were imposed during the experiment (only 3% of males and 8–10% of females were allowed to breed in each generation, Trut, Plyusnina and Oskina, 2004) and these are not directly transposable to prehistoric hunther-gatherers. The domestication process may therefore have taken longer, and hybridisation with wild wolves may have complicated the process as compared to the farm-fox experiment.

This selection for behaviroural traits had many biological effects, such as a modification in the secretion of cortisol (hormone of stress) and serotonine, thus encouraging the development of tame individuals through generations (Trut, 1999, Figure 3G) and the appearance of new morphological traits (Trut, 1999, Figure 3G) and the appearance of new morphological traits (cf section 1.3.4, Figure 3). A specific selection for morphological traits may have occurred only later on, reinforcing the domestication syndrome characterictics (Trut, 1999; Saetre *et al.*, 2004).

Interestingly, this experiment proved that foxes can respond in the same way as proto-dogs to anthropogenic constraints. However, in their evolutionary history, it has been otherwise. The fox has never been domesticated and has remained commensal, although some evidence of a special relationship between foxes and dogs in the past are attested to (see section 2). Never very far from human settlements from which it benefits, it has always kept a certain distance and remains more subject to natural selection pressures. The dog is the only large carnivore and only canid that has ever been domesticated.

1.3.4. Changes related to domestication

Examination of wolf and dog remains in the early phases of domestication and experimental studies on the domestication process have shown that the domestication has been accompanied by a large number of genetic, morphological, physiological or even behavioural modifications (e.g. Wayne, 1986; Trut, 1999; Horard-Herbin and Vigne, 2005; Trut, Oskina and Kharlamova, 2009, 2012; Pionnier-Capitan, 2010; Horard-Herbin, Tresset and Vigne, 2014; Miklósi, 2014; Lord *et al.*, 2020).

Among the morphological manifestations of domestication in dogs, we notice:

- fur depigmentation, revealing a "star pattern" (Figure 3A) or specifically localized depigmentation spots (mottling or piebaldness, Figure 3B,C), apparition of droopy ears (Figure 3D) and an upward curled tail (or shortening of the tail, Figure 3E);
- reduction in length and torsion of the limbs;
- preservation of paedomorphic characteristics: juvenile traits are maintained, which is especially observable in cranial morphology. This resulted in changes in cranial dimensions, including a decrease in skull height and width, widening of the palate and shortening of face and muzzle (Figure 3F), thus leading to the apparition of a marked "stop" (a depression located between the frontal and the nasal regions). Brain capacity also decreases (Kruska, 1988);
- these cranial modifications lead to a reduction in the space available for the teeth, causing frequent tooth rotation, a reduction in size and number, overlap or occlusal problems with an offset between the upper and lower rows of teeth, or reduction in the length of premolar or molar rows;
- a decrease in sexual dimorphism, including within the skull, with the acquisition in some males of morphological traits reminiscent of females;
- decrease in size and bone dimensions.

All domesticated species share the majority of these changes, which characterize the "domestication syndrome" (Lord *et al.*, 2020). The existence of such a syndrome is appealing because it makes it possible to identify domestic animals dichotomously from their wild counterparts. Consequently, many studies have used these morphological characteristics or have compared the skeleton of wolves and dogs to identify specific osteologic criteria (Belhaoues, 2018) to distinguish wolves and dogs in the archaeological record (Horard-Herbin, 2014), particularly to identify the first domestic dogs (e.g. Pionnier-Capitan, 2010; Pionnier-Capitan *et al.*, 2011; Horard-Herbin, Tresset and Vigne, 2014). However, these modifications were not yet very marked at the beginning of the domestication process and are likely blurred by hybridisation (Ardalan *et al.*, 2011; Freedman *et al.*, 2014). Additionally, the morphological variability of ancient wolves (especially in the Pleistocene) is not well known because there are few remains (Janssens *et al.*, 2019). As in extant wolves, it seems to have been relatively important as early as the Pleistocene (Boudadi-Maligne and Escarguel, 2014), making strict identification of the subspecies difficult, especially in the early stages of domestication. The length, height, and size of the skull, the width of the muzzle, the orbital angle and the mesio-distal diameter P4 - M1 can however help, to a limited extent, to distinguish the frst dogs from wolves (Janssens *et al.*, 2019)

Figure 3. morphological and behavioural transformations observed in foxes during the domestication experiment conducted by Belyaev. From Trut, Plyusnina and Oskina (2004)

A: Star pattern; B: Localized depigmented spots (piebaldness); C: Localized yellow-brown spots (mottling); D: Floppy-ears; E: Curly tail; F: crania of female foxes from the domesticated population: norm (left) and shortened and widened face (right); G: The behavior of an animal from the domesticated population.

1.3.5. Geographical origins and timing of domestication

1.3.5.1. *Methodological difficulties, a subject under debate*

The precise timing, geographical origin and ecological context of early domestication are still debated in the scientific community. This is due to many methodological difficulties. Firstly, archives are fragmented in time and space, as ancient remains are rare (Larson *et al.*, 2012).

It is also necessary to underline the difficulty of the osteological distinction between the dog and the wolf, partly due to the possibility of hybridisation. Mixtures between dogs and other wild canine lines (a large gene flow between the wolf-dog ancestor and golden jackals has been demonstrated, Freedman *et al.*, 2014 , or between resident native dogs and dogs from elsewhere, may complicate the exploration of the evolutionary history of dogs based on genomic data (Freedman and Wayne, 2017). Furthermore, early dogs were probably morphologically very similar to wolves (Larson *et al.*, 2012), perhaps even indistinguishable. It is thus very difficult to know whether the remains of supposed dogs did not in fact belong to the ancestral lineage of wolves at the origin of modern dogs, which could be morphologically distinct from modern wolves (smaller for example), or whether they could not belong to a lineage other than the ancestral lineage at the origin of modern dogs, as part of a failed domestication process (Larson *et al.*, 2012; Freedman *et al.*, 2014).

1.3.5.2. *Earliest remains*

The location of the oldest remains of dogs is of interest to clarify the geographical and temporal origin of domestication (see section 1.3.5.3) and to document the morphological variability existing at such early periods (we will come back to this in section 2.4.2.1). This is why we linger in this section to list the discoveries of the oldest dogs.

Fossil wolf remains have been found in association with hominids as early as 400 kyrs (Clutton-Brock, 1995), but the first evidence of dog remains is much more recent.

In Europe, the first remains classified as dogs were found at Predmosti in Czech Republic (estimated to ~27 kyrs; Germonpré *et al.*, 2012), and at the Goyet cave in Belgium (~36 kyrs; Germonpré *et al.*, 2019). However, subsequent studies have challenged these attributions, and suggested the canids were more likely to be wolves (Boudadi-Maligne and Escarguel, 2014; Drake, Coquerelle and Colombeau, 2015; Frantz *et al.*, 2016; Freedman and Wayne, 2017), perhaps descended from an extinct wolf lineage (Crockford and Kuzmin, 2012; Morey, 2014; see response to these criticisms in Germonpré *et al.*, 2013, 2015).

Analysis of the entire mitochondrial genome of the Goyet dog revealed that it belonged to a sister group (i.e. reciprocally monophyletic group) to all extant dogs and wolves (Thalmann *et al.*, 2013), suggesting that it was the result of an abortive domestication event or that it was a morphologically distinct and now extinct wolf population adapted to megafauna hunting in Beringia in the late Pleistocene (Leonard *et al.*, 2007; Thalmann *et al.*, 2013). Sequencing of the mitochondrial genome of the Taimyr wolf, a 35 kyrs fossil specimen found in Northern

Siberia, supports the existence of such a lineage (Skoglund *et al.*, 2015). The results showed that this wolf was reciprocally monophyletic with a clade consisting of an interbreeding of ancient and extant wolf and dog lines, again suggesting an early divergence between wolves and modern dogs from an ancient wolf population now extinct.

Remains clearly attributable to the dog during the Upper Paleolithic in Western Europe have been listed by Pionnier-Capitan *et al.* (2011 , Figure 5, Table 1). Accordingly, dogs are present in Western Europe from at least the Middle Magdalenian (i.e. from 13,000 cal. BC).

In Romania, there is to our knowledge no mention of Upper Paleolithic dogs (Bălăşescu, Radu and Moise, 2005).

In the Middle East, the most ancient dogs originate from Iraq (~13 kyrs; Zeder, 2012).

In Asia, the oldest dog-like canid remains are found in the Razboinichya cave in the Altai Mountains of Siberia (~33 kyrs; Ovodov *et al.*, 2011). According to the authors, this could be an attempt at domestication that failed due to climate and cultural changes associated with the LGM and that did not lead to late Holocene lineages. The attribution to the dog was nevertheless confirmed by genetic analysis of mtDNA (Druzhkova *et al.*, 2013).

In East Asia, very few ancient remains have been found, the oldest (~ 12-13 kyrs in Kamchatka, Russia and Northern China; Freedman and Wayne, 2017) being younger than the oldest undisputed fossils in Europe (15 kyrs) and as old as the oldest remains found elsewhere in Central Asia or in the Near and Middle East (5-13 kyrs).

The earliest American dogs very likely come from dog lines from the Old World (Leonard *et al.*, 2007), with the oldest confirmed remains from Koster, IL dated to ~9.9 cal. kyrs BP (Leathlobhair *et al.*, 2018).

Figure 4. Location of sites in Western Europe containing upper Palaeolithic dogs. Sites are listed in Table 1.
1: Erralla;
2: pont d'Ambon (France);
3: le Closeau (France);
4: Montespan (France);
5: grotte Jean-Pierre 1 (France);
6: le Morin (France);
7: grotte-abri du Moulin(France);
8: Hauterives-Champréveyres (Switzerland);
9: Kesslerloch (Switzerland);
10: Bonn-Oberkassel (Germany);
11: Kniegrotte (Germany);
12: Teufelsbrücke (Germany);
13: Ölknitz (Germany);
14: Mezin (Ukraine);
15: Eliseevichi I (Russia).

Table 1. Sites with dog remains from the Upper Paleolithic in Western Europe and illustrated in Figure 4. Completed from Horard-Herbin, Tresset and Vigne, 2014.

Location	Site and code in the map	Timing	Reference
Iberian Peninsula	Erralla, Spain (1)	Early Magdalenian ~ 19,000 BP or Allerod ~12,500 BP	Altuna, Baldeón and Mariezkurrena, 1985 García-Moncó, 2005 Vigne, 2005
France	Pont d'Ambon, Bourdelles (2)	upper Azilian layer, preboreal 12,952-12,451 cal. BP dating on canid bone	Célérier and Delpech, 1978 Célérier *et al.*, 1999
	Le Closeau (3)	14,999-14,319 cal. BP 14,596-14,055 cal. BP	Pionnier-Capitan *et al.*, 2011
	Montespan (4)	Middle Magdalenian 15,500-13,500 cal. BP	García-Moncó, 2005 Pionnier-Capitan *et al.*, 2011
	Grotte Jean-Pierre 1, Saint-Thibault-de-Couz (5)	10,050 ± 100 BP from pollens 12,027-11,311 cal. BP from the canid skull	Lequatre, 1994 Chaix, 2000
	Grotte de le Morin, Pessac-sur-Dordogne (6)	15,005-14,155 cal. BP (OxA-23628) 15,114-14,237 cal. BP (OxA-23627)	Boudadi-Maligne *et al.*, 2012
	Grotte-abri du Moulin, Troubat (7)	Middle Magdalenian, Azilian 12,475-12,429 cal. BP (OxA-36550) from a dog tibia	Boudadi-Maligne *et al.*, 2020
Swizerland	Hauterives-Champréveyres, Neuchâtel (8)	13,000 BP (15,000-14,000 cal. BP)	Morel *et al.*, 1997 Morel et Müller, 1997
	Kesslerloch (9)		Napierala and Uerpmann 2012
Germany	Bonn-Oberkassel (10)	14,708-13,874 cal. BP	Nobis, 1981 Street, 2002 Bales 2006
	Kniegrotte (11)	Late Magdalenian 16,700-13,800 BP	Musil, 1974, 2000
	Teufelsbrücke (12) and Ölknitz (13)	Early Dryas 15,770-13,957 cal. BP	Musil, 2000
Ukraine	Mezin (14)	Epigravettian 14,700-14,300 BP	Pidoplichko, 1969, cited by Benecke, 1987
Russia	Eliseevichi I (15)	16,945-16,190 cal. BP	Sablin et Khlopachev, 2002, 2003

All these studies therefore tend to suggest that Eurasian dogs appeared at least 15 kyrs cal. BP (Pionnier-Capitan *et al.*, 2011, Figure 5), maybe even as early as 33 kyrs.

Figure 5. Geographic origins and age of the oldest validated dog remains in Eurasia
From Freedman et Wayne (2017), which is modified from Frantz *et al.* (2016).
Dots represent sites containing dog remains and coloring is indicative of the timing.

1.3.5.3. *Scenario and timing*

The study of genetic diversity and phylogenetic relationships observed between ancient and modern dogs and wolves, and even other canine species such as the dingo, through mitochondrial DNA and Y chromosomes analyses, lead scientists to propose two kinds of scenarios: either domestication took place independently in several places around the globe, or an initial domestication event resulted in a first monophyletic clade (clade I) that subsequently underwent repeated cycles of hybridisation and selection for phenotypic variation (Vilà *et al.*, 1997).

Three locations have been suggested as possible centres of domestication: Europe, Southeast Asia, and the Middle East (Savolainen *et al.*, 2002; Pang *et al.*, 2009; Vonholdt *et al.*, 2010; Brown *et al.*, 2011; Larson *et al.*, 2012; Thalmann *et al.*, 2013; Freedman *et al.*, 2014; Wang *et al.*, 2016; Freedman and Wayne, 2017).

The dates of domestication are variable and depend on the methodologies (Vilà *et al.*, 1997; Savolainen *et al.*, 2002; Wang *et al.*, 2013, 2016; Skoglund *et al.*, 2015; Frantz *et al.*, 2016; Freedman and Wayne, 2017). For example, the oldest archaeological remains in Eurasia are dated to about 15 kyrs BP (see previous section), but dogs could have been domesticated as early as 135 kyrs according to Vilà *et al.* (1997) who use mutation rates to estimate the divergence between wolves and coyotes. This order of magnitude proved to be too large. Savolainen *et al.* (2002) estimated the origins of dogs at 14±4 kyrs for clade A (1 founder), 11 ± 4 kyrs for clade A1, 16 ± 3 kyrs for clade A2, 26 ± 8 kyrs for clade A3, 13 ± 3 kyrs for clade B and 17 ± 3 kyrs for clade C. Their conclusion was that dogs either came from clade A (around 40 kyrs BP) or that they came from a group of founders from all three clades (around15 kyrs BP). Based on by the mutation rate, Wang *et al.* (2013) estimated that domestication occurred around 32 kyrs BP and then corrected the date to around 33 kyrs BP (Wang *et al.*, 2016), assuming an outbreak in Southeast Asia. Freedman and Wayne (2017) deduced a dog-wolf divergence moment of 11-16 kyrs BP, and expanded to 11-34 kyrs BP. Using the Taimyr wolf sample (dated to 35 kyrs BP), Skoglund *et al.* (2015) moved the previously reported wolf-dog divergence from around11-16 kyrs BP (Freedman *et al.*, 2014) to around 27-40 kyrs BP. Frantz *et al.* (2016) used archaeological samples to infer a mutation rate and suggested that dogs originate to around 14-6.4 kyrs BP.

Today, the scientific community considers that dogs have been living with humans for at least 15,000 years (Pionnier-Capitan *et al.*, 2011; Boudadi-Maligne and Escarguel, 2014; Perri, 2016; Janssens *et al.*, 2019; Boudadi-Maligne *et al.*, 2020).

The current consensus is the scenario proposed by Frantz *et al.* (2016). The authors proposed that dogs may have been domesticated independently from geographically and genetically differentiated wolf populations in East Asia first, and in Western Eurasia, and that East Asian dogs then partially replaced those originating from Western Eurasia. The discrepancy between East Asian and Western Eurasian dogs would date from ~14-6.4 kyrs, which is later than the known presence of dog remains in these two regions. This suggests that dogs must have been present in both regions before. Indeed, they showed that there was a significant turnover of

mitochondrial DNA haplotypes between ancient and modern dogs, during which clade A increased in terms of frequency, while haplotypes B, C and D decreased in frequency, which could not be explained by genetic drift (Frantz *et al.*, 2016).

1.4. Return to the wild: the case of the dingo

The **dingo**, *Canis lupus dingo* (Meyer, 1793), is another subspecies of the grey wolf. It probably originates from a very small population of domestic dogs from Southeast Asia (Savolainen *et al.*, 2004) that returned to the wild (this is what we call a feral dog) during prehistoric times.

The earliest remains (around 5,500 years BP) have been found in Ban Chiang (Thailand), one of the oldest sites in Asia that testifies to the transition from hunter-gatherers to sedentary farmers (Corbett, 1995). In Australia, the oldest remains are dated to 3,450 ± 95 BP (Corbett, 1995) and its arrival has been dated by the molecular clock to around 4,600-5,400 years BP (Savolainen *et al.*, 2004).

Today, the dingo and its counterparts (e.g. the yellow dog of New Guinea) are widely distributed in Southeast Asia. Isolated for more than 3,500 years, they represent a unique isolate of early undifferentiated dogs. Accordingly, dingoes likely provide a good and unique picture of what the first dogs looked like when they were still subject to natural constraints rather than to strong anthropic selections for strictly aesthetic reasons. Nowadays, dingoes live in a commensal relationship with the indigenous populations of humans. Indeed, they live in close association with human groups, serving as guardians, hunting companions, or for companionship (Clutton-Brock, 1989; Corbett, 1995; Koungoulos and Fillios, 2020, Figure 6). However, these dogs remain relatively independent.

Figure 6. Australian Aborigines and their dingoes (Clutton-Brock, 1989)

1.5. Extant worldwide distribution and diversification of red foxes, wolves and dogs

Foxes, wolves and dogs are still interacting in a large part of the Northern hemisphere. (Lescureux and Linnell, 2014) since they do not have exactly the same ecological niches and can therefore coexist (in particular, diets are somewhat different, Macdonald and Sillero-Zubiri, 2004).

Today, *Vulpes vulpes* and *Canis lupus* are the two species of wild carnivores with the widest geographic distribution. They are found on all continents except Antarctica. These species are thus able to colonize biotopes with very different and sometimes extreme environmental conditions, thanks to their great adaptability and even morphological, physiological and behavioral plasticity (Macdonald and Sillero-Zubiri, 2004).

The red fox, which has remained commensal, has furthermore accommodated well to growing urbanism, taking advantage of the resources available in the cities (Hulme-Beaman *et al.*, 2016).

On the contrary, grey wolf populations have drastically decreased over the last two centuries as a result of persecution, although they have recovered well in recent decades (Lescureux and Linnell, 2014; Ersmark *et al.*, 2016). Wolves have even come close to being totally exterminated in Western Europe. As a result, diversity collapsed dramatically at the beginning of the 20th century and recolonisation from a few homogeneous relict populations induced drastic changes in the genetic composition (Dufresnes *et al.*, 2018). Modern wolves are thus significantly different from the prehistoric wolves that lived in this region. On the other hand, in Eastern Europe, human persecution has had less effect on wolf demography. Diversity has thus been less impacted (Dufresnes *et al.*, 2018).

Another reason for the decrease in wolf populations is the tremendous increase in those of dogs, directly threatening wolves through hybridisation, disease transfer, and competition. The story of dogs has been a real success, thanks to their importance to humans and their great plasticity. They rapidly expanded to Africa, America, and even Australia by following humans. They have become widely used for a variety of purposes (e.g. as a source of food and fur, for hunting, guarding, fighting, or for companionship). Thus, dogs have become the most common carnivore, and are estimated to be close to 900 million individuals, worldwide (Gompper, 2014), and their population is still increasing (Lescureux and Linnell, 2014).

This population explosion has been accompanied by an explosion of genetic and phenotypic variability. Hence, from the Chihuahua to the Rottweiller, the dog is currently the most variable carnivore in terms of overall morphology, size and proportions (Drake and Klingenberg, 2010).

Numerous studies have explored the genetic basis of this morphological variability (Lindblad-Toh *et al.*, 2005; Freedman *et al.*, 2014). It turns out that the evolutionary history of dogs up to the time of breed formation is extremely complex. Indeed, it encompasses many bottlenecks (after the first severe bottleneck related to domestication), local population expansions, contractions, extinctions and replacements, as well as and gene flows with wolves (Freedman and Wayne, 2017). Long after the initial process of domestication, and especially during the last 200 years, dogs have undergone rapid phenotypic changes, with the creation of

breeds through strong artificial selection and closed breeding systems imposed by humans (Freedman and Wayne, 2017).

The term "**breed**" refers to a single population within a single species with distinct hereditary, morphological and physiological traits as defined by standards in books that have been established only since the nineteenth century (Pionnier-Capitan, 2010; Horard-Herbin, Tresset and Vigne, 2014). The 353 breeds of dogs currently recognized by the FCI (Fédération Cynologique Internationale, International Canine Federation, http://www.fci.be), are the result of a very recent selection on specific physical or behavioral traits, in order to satisfy functional needs (e.g. for work, hunting, or running) or for strictly aesthetic reasons. Moreover, some authors have even drawn a parallel between cranial morphology and certain car models, associating an emotional value to certain morphological traits. Hence, Bartosiewicz (2018) stated that models of economy cars with a rather "cute" face (Käfer model, i.e. beetle in German, such as the Volkswagen Typ 1 or the two-horsepower Citroën 2 CV) recall the neotenic traits of the highly modified small dog breeds such as the pug, while sports car models are more reminiscent of a wolf's skull, with oversized engines and a small cabin size recalling the cranial proportions (large splanchnocranium, small neurocranium) of adult wolves (Figure 7).

Figure 7. Neotenic features of a Fiat 500 (1967, left) and a Porsche 356B Coupe (1962, right), in comparison with the cranial proportions of a pug (left) and wolf (right). Figure 6 from Bartosiewicz (2018).

Although the notion of breed is very recent and therefore cannot be applied to ancient dogs, morphological groups (**morphotypes**, characterized by different cranial proportions) are already identifiable as early as the Bronze Age and Antiquity (Belhaoues, 2018), and the phenomenon intensifies in the Middle Ages and during modern times (Horard-Herbin, Tresset and Vigne, 2014). We will explore the variability in early periods (before the Bronze Age) in section 2.3.6.4 and in the course of this thesis. In order to describe shape variation, a division into **dolichocephalic** (elongated and narrow skull, akin to greyhounds), **brachycephalic** (broad and short skull, akin to mastiffs or bulldogs) and intermediate **mesocephalic** types can be used.

The intensive selection of dog breeds has not been without consequences regarding their genetic integrity and the population health. Strict selection based on a set of strict standards has helped to homogenize breeds, reducing genetic diversity and led to the fixation of certain pathological traits. Moreover, mitochondrial DNA analysis has demonstrated that indigenous African village dogs have greater genetic diversity than purebred dogs (Boyko *et al.*, 2009).

Thus, skeletal anomalies are frequent in some breeds and are even ancient. For example, chondrodysplasia (dwarfism resulting in a reduction in the size of the limbs and their torsion, as for example in the dachshund) is already known in ancient Egypt (Brassard, 2018) and is found in sites dating to the Roman period (Teichert, 1987). In addition, most brachycephalic breeds are affected by a brachycephalic syndrome resulting, among other things, in severe

respiratory disorders. It should be remembered that some breeds would not be naturally viable after this strict selection (many births are artificially supported in some breeds). Today, the standards tend to integrate clauses ensuring the well-being and integrity of animal health, by allowing more genetic variability.

Conclusion

By retracing the evolutionary history of canids likely to be found in archaeological sites in Europe after the domestication of the dog (wolves, dogs, and red foxes), the following key points emerge:

KEY POINTS

Red foxes, wolves and dogs have had very different evolutionary histories.
Red foxes have remained commensal and are today among the most widespread carnivores on the planet, wolves have rarified and have remained wild, and dogs emerged from an ancestral lineage of wolves at least 15,000 years BP through a process of domestication likely because of drastic selection upon behavioural traits. They have extraordinarily diversified these two last centuries.

- ⇨ The **different trajectories of dogs** (anthropogenic or even artificial evolutionary history) **and red foxes** (more natural evolutionary history, although it has been likely also impacted by anthropogenic activities, due to its commensal nature) **may be interesting to compare.**

Extant wolves are not the direct descendants of the ancestral lineage of wolfs that were domesticated into dogs, which should be considered when comparing ancient and modern wolves.

Although Canini (wolves and dogs) and Vulpini (red foxes) have been separated for millions of years, experimental studies showed that the red fox is likely to respond similarly to wolves/dogs to anthropogenic constraints.

- ⇨ **Red foxes are thus a good model to compare with dogs in order to evaluate the effect of the proximity to humans.**

The genetic and morphological variability in dogs has exploded very recently with the creation of breeds, leading to extreme morphologies in modern dogs. However, a certain variability, recalling some modern breeds, already existed in the Bronze Age and Antiquity, as testified by bone remains. Considering that dogs were domesticated at least in two places (East Asia and Western Eurasia), a somewhat important variability probably existed from the very beginning.

In the following section, we discuss what happened after the domestication and before the Bronze Age, during the emergence of the first agricultural societies.

2. The evolution of canids from the Mesolithic to the Bronze Age: state of the art

Previously, we recalled the general evolution of dogs and red foxes, by insisting on their origin and evolution during the last centuries. If the most radical upheavals concerning dog history dates back to the time of wolf domestication or are very recent (with the creation of breeds in the last two centuries and the increasing impact of urbanism on commensal species), the history of these two species has not been without upheaval in more distant times. In his thesis, Belhaoues (2018) argues that during the Bronze Age, dogs appeared rather commensal and that they escaped from human control, while canine morphotypes greatly diversify in Roman Antiquity, attesting to voluntary human selection to satisfy specific demands.

Even before that, tremendous transformations in human societies, in particular the emergence of agriculture during the Neolithic period, are known to have had repercussions on animals living close to humans. Given that dogs were already domesticated at this time, the question is how they were impacted by these profound socio-economic changes. However, as we shall see in the following sections, although genetic or contextual archaeological data are abundant, data on the morphology of dogs have been much less exploited and are relatively scattered throughout the litterature.

For these reasons, we focus on the Neolithic period in this thesis, rather than on the early stages of dog domestication or on later periods after the Bronze Age, that have already been studied in detail.

2.1. The Neolithic transition: a period of major interest for studying dog populations?

During the late Pleistocene (23-10 kyrs BC), due to the glacial climate, living conditions were extremely difficult and not conducive to the exploitation of natural resources. After the end of the last glaciation, about 12 kyrs ago, the climate warmed and stabilized, and natural upheavals greatly diminished in magnitude. However, another upheaval took place, this time of anthropogenic origin. The growing of the modern human population was accompanied by major changes in their lifestyle, which strongly impacted the environment. Changing from a nomadic to a sedentary lifestyle, human groups settled, first in hammlets and then in villages, and gradually moved from a way of life based on hunting, fishing and gathering (during the Epipaleolithic and Mesolithic periods) to a subsistence economy based on animal husbandry and agriculture, resulting in the domestication of many animal and plant species (during the Neolithic and later periods, Cauwe *et al.*, 2007; Zeder, 2008; Vigne, 2011; Willcox, 2013). Other innovations of this period include, in Western Eurasia, included architectural changes, long-distance trade, the making of ceramic pottery, the establishment of a social hierarchy and the use of symbolic expressions (Fowler, Harding and Hofmann, 2015). These major technological, economic and cultural changes correspond to the so-called **Neolithic Revolution** (the term was proposed for the first time by Vere Gordon Childe in 1936).

This decisive transition in the History of Humanity took place between around 9,5 and 4 kyrs BC (Cauwe *et al.*, 2007) in Western Eurasia. It began in the Near East and the Neolithic way of life gradually spread into Europe between 7 and 4 kyrs cal. BC (Tresset and Vigne, 2011). The Neolithic transition first impacted the south-eastern part of Europe, the Balkan Peninsula and its margins, during the 7th millennium cal. BC. These areas retained a strong influence from the Near-Eastern Neolithic. The Neolithic spread in Central and Western Europe from the 6th millennium cal. BC and throughout the 5th millennium. It happened through two main diffusion streams: the Impressa-Cardial cultures along the Northern coastline of the Mediterranean (Mediterranean stream) and the Linienbandkeramik culture (**LBK**, "culture Rubanée" or Danubian culture) through the Danubian corridor (danubian or continental stream, Figure 8). The LBK culture is thus the earliest Neolithic culture in Central Europe, and dates to 5,5-4,7 kya BC. It is present from Slovakia to the Netherlands, through Moldavia, Ukraine, Romania, Hungary, the Czech Republic, Western Germany, Northern France and Belgium. This population replaced or co-existed with hunter-gatherer populations.

Eastern and Western Europe thus have somewhat different histories, in terms of cultures and chronologies. The Danubian area retained some characteristics from the Balkan Neolithic but also incorporated late indigenous hunter-gatherer features, resulting in both cultural and genetic mixing (Cauwe *et al.*, 2007; Ollivier *et al.*, 2018). On the Northern and Western plain margins of Europe, the transition occurred much later. In the Northern plains of Central Europe, hunting, fishing and gathering remained the dominant economy until 4-3,8 kyrs BC. In North-Western Russia, the first signs of agricultural development were observed between 2,7 and 2 kyrs BC (Fowler, Harding and Hofmann, 2015).

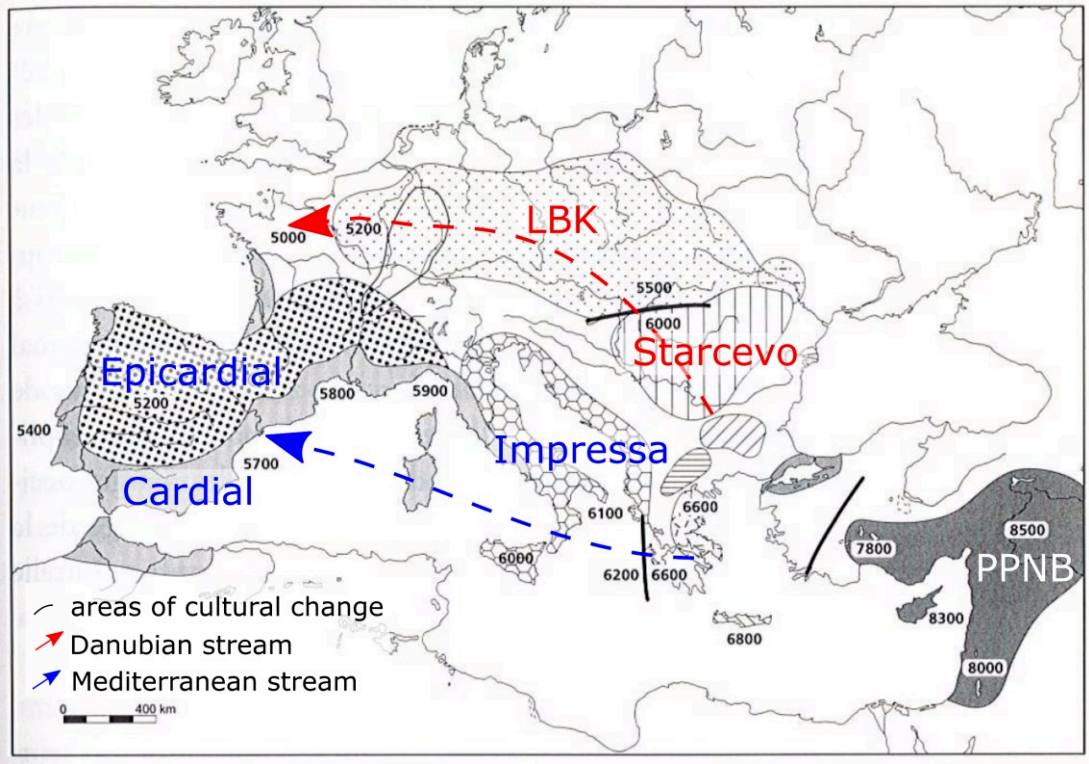

Figure 8. Chronological spread of the Neolithic across Europe. The two main diffusion streams are drawn and some of the oldest cultures (and further cited in the manuscript) are reported on the map. Modified from Guilaine (2003).

Some studies have suggested that farmers from the Near East would have immigrate to Europe (Fowler, Harding and Hofmann, 2015) and substantially replaced the local hunter–gatherer population, except on the Western and Northern margin of the continent, where Mesolithic societies persisted longer (Haak *et al.*, 2015). DNA analysis have revealed an unbroken chain of ancestry from Central and SouthWestern Europe to Greece and NorthWestern Anatolia, suggesting that these migrations would have been rather limited (Hofmanová *et al.*, 2016). The progression of the Neolithic from east to west would thus have occured mainly through the diffusion of ideas. However, the scenario is very complex and involves a combination of processes of the diffusion of ideas, physical migration (e.g. from Anatolia to Greece and Bulgaria), acculturation and the contribution of local hunter-gatherer populations.

These farmers were accompanied by several domesticated species (Zeder, 2008; Tresset and Vigne, 2011), including dogs (Ollivier *et al.*, 2018). Indeed, although dogs were already domesticated prior to the Neolithic, they were an integral component of the Neolithic farming package. Through the analyses of mitochondrial DNA of 99 ancient European and Near Eastern dogs spanning the Upper Palaeolithic to the Bronze Age, Ollivier *et al.* (2018) have suggested that during the Neolithic transition, dogs spread from the Near East into Europe, alongside other domestic animals such as pigs, cows, sheep and goats. In Eastern Europe, incoming farmers would have brought Near Eastern dogs with them rather than having primarily adopted indigenous European dogs after they arrived, changing deeply the population. In Western and Northern Europe, these migrating dogs got diluted into the native population.

During the Neolithic transition, the domestication of animals and plants greatly facilitated food access, for both humans and the dogs that surrounded them (Freedman and Wayne, 2017). This has been demonstrated by the coincidental between the regional advent of agriculture and the increasing in the number of **AM2YB gene** copy in dogs through the Neolithic transition around 7 kyrs BC (Arendt *et al.*, 2016; Ollivier *et al.*, 2016, Figure 9). Thus, the growing input of cereals and pulses in the diet of dogs has resulted in an increasing in the efficiency of starch digestion, as it was previously reported in humans (Perry *et al.*, 2007). In modern wild canids (wolves and dingoes) and Huskies, the number of copies remains low (Freedman *et al.*, 2014). Within a single archaeological site (Borduşani and Hârşova, Romania) individuals with low or high copy numbers coexisted, suggesting that the expansion of the gene was not yet fixed in dogs populations associated with agricultural Neolithic societies. However, it must be considered that dogs posessing the genetic background to digest starch may still have had a predominantly carnivorous diet. This was supported by isotope analyses which demonstrated that dogs from Eastern European Chalcolithic sites (Borduşani, Hârşova and Vităneşti) had a diet rich in meat, even though they had a sufficient number of AMY2B copies to be able to digest starch (Balasse *et al.*, 2016).

The Neolithic transition therefore seems to be a period of significant co-evolution between humans and dogs. Indeed, the major changes in human lifestyles could not have been without consequences on the dogs that lived with them. So far, there is no comparative data for commensal species such as red foxes, but it is likely that they could have benefited from this

increased access to food resources as well (by feeding on the garbage or on the small rodents attracted by cereal storages).

Afterwards, the European Neolithic became a very complex mosaic of cultures (mostly defined by ceramics) that vary greatly and succeeded or superimposed each other in time and space, testifying to very different ways of life and social organisation. The Neolithic ends with the invention and spread of copper metallurgy (which corresponds to the Chalcolithic) and then the bronze metallurgy (which defines the Bronze Age, around the beginning of the third millennium BC to the second millennium BC).

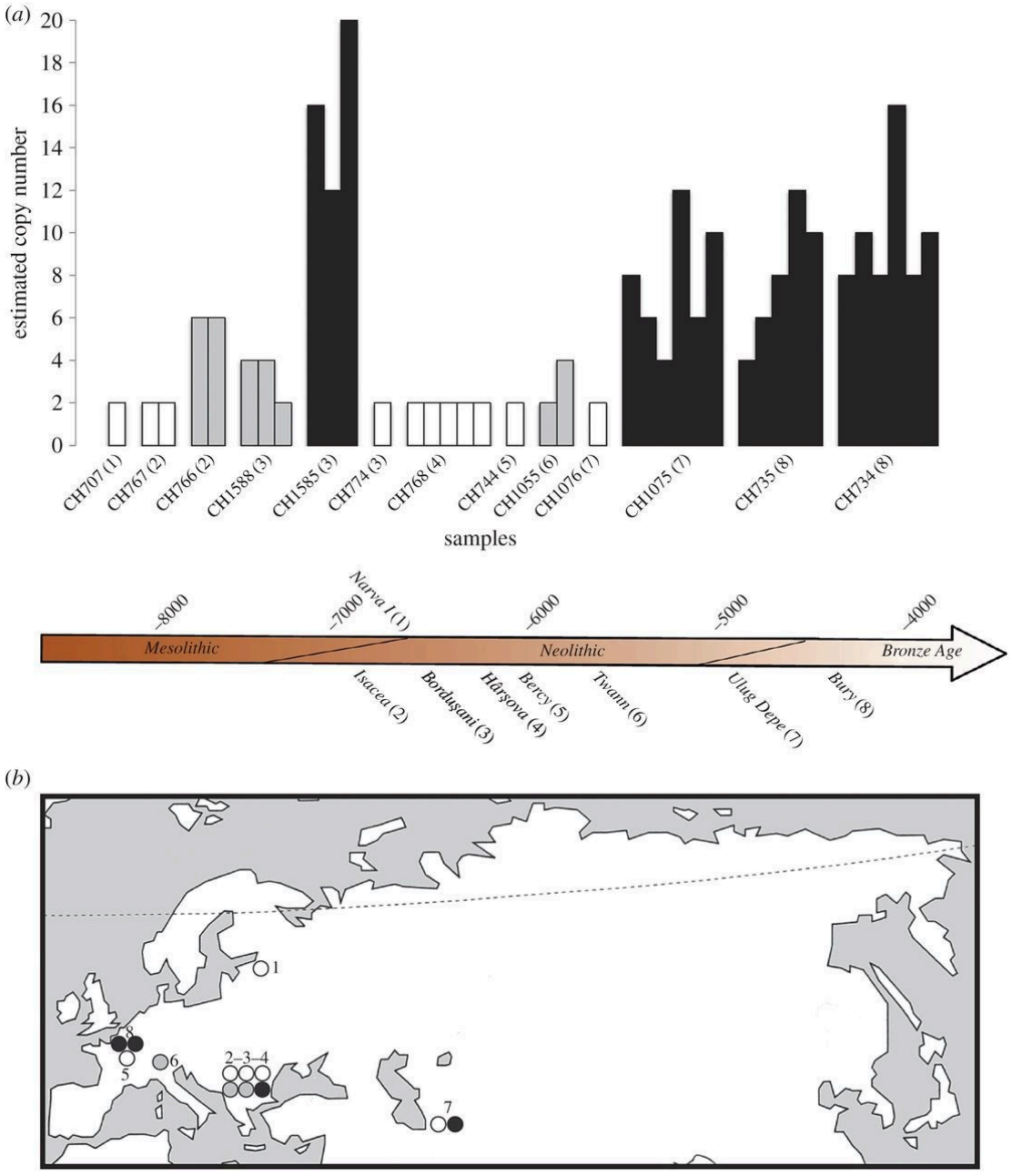

Figure 9. Distribution of estimated Amy2B gene copy numbers between the Upper Palaeolithic and the Bronze Age (a) through Eurasia (b). Figure 1 from Ollivier *et al.* (2016)
white: 2 copies, grey: 2-8 copies, black: more than 8 copies.

2.2. Non-exhaustive occurrence of canid remains in the archaeological record from the Mesolithic to the early Bronze Age

The first step of our study was to collect information on the **occurrences** of canids around the Neolithic period (dogs, wolves and red foxes, the only species attested in Europe at this time, as seen in section 1[d]), in order to conceive our archaeological corpus. This long and fastidious research has allowed us to describe (in a very general way) the evolution of the frequency of canid remains in the chrono-geographic range relevant for our study. Subsequently, this bibliographical research also allowed us to document the variability in relationships between humans and dogs (see section 2.3).

The summary presented in this section is not meant to be exhaustive, given the abundance of and frequent non-publication of faunal lists and the difficulty to access to some of the bibliographical resources. However, this step enabled us to highlight some methodological limitations related to the availability or even to the existence of archaeological material. Indeed, our research has shown that the remains could be very rare for some species, or for some chronological periods or geographical areas.

We will discuss some specificities on dog findings in the sites listed in this section in more detail in the next section (section 2.3).

[d] For the periods from the Mesolithic to the Bronze Age, no remains of *Vulpes corsac* or *Cuon alpinus* were found in Europe (Sommer and Benecke, 2005). The documented Neolithic remains of *Canis aureus* originate from Greece (Sommer and Benecke, 2005) and are therefore out of our area of interest.

2.2.1. Methodology

Given that the aim was to study the evolution of the dog around the Neolithic transition, we limited our research to the period from the Mesolithic to the Chalcolithic in South-Eastern Romania and to the very early Bronze Age in Western Europe.

In South-Eastern Romania, the Neo-Chalcolithic era is divided into Early Neolithic, Late (or developed) Neolithic and the Chalcolithic, which is devided into Early and Late (or developed) Chalcolithic (Bălăşescu, Radu and Moise, 2005, Table 2).

Table 2. Chronological periods and related cultures considered in this thesis for South-Eastern Romania, from Bălăşescu, Radu and Moise, 2005. Dates are in BC.

Dates	Period		Culture
~4,600/4,500-3,800/3,700	Chalcolithic	Late/Developped Chalcolithic	Gumelniţa – Sălcuţa – Cernavodă I
~5,000-4,500		Early Chalcolithic	Vădastra – Hamangia III – Bolintineanu – Boian – Stoicani-Aldeni
~5,500-5,000	Late/Developed Neolithic		Vinča – Dudeşti – Hamangia I et II
~6,600-5,500	Early Neolithic		preCris – Starčevo-Criş

In Western Europe, to provide an effective framework, we split the Neolithic period into three stages: Early, Middle and Late[e] Neolithic (Table 3).

Table 3. Chronological periods and related cultures considered in this thesis for France and Western Europe (modified from Demoule, 2007; Ghesquière and Marchand, 2010). Dates are in cal. BC.

Dates	Period		Culture
2,200/2,100	Early Bronze Age		
2,200/2,100-2,500	Neolithic	Late Neolithic	Campaniforme
2,500-3,500			Ferrières – Couronnien – Vienne – Charente – Seine-Oise-Marne – Clairvaux – Horgen, …
3,500-4,800		Middle Neolithic	Cerny – Chambon – Chasséen – Noyen – Michelsberg – Cortaillod, …
4,800-5,800		Early Neolithic	LBK (Rubané) – Villeneuve Saint Germain Impressa – Cardial-Epicardial, …
5,500-9,500	Mesolithic		Castelnovien – Cuzoul – Gazel Sauveterrien – Beuronien – Montclusien
8,000-9,500	Paleolithic	Epipaleolithic Upper Paleolithic	Azilien Magdalénien – Solutréen – Gravettien – Aurignacien – Châtelperronien
33,000 BC			

[e] That gathers both the French “récent” and “final” Neolithic, as well as the French Chalcolithic.

We have focused our research mainly on France and Romania because the Neolithisation processes are different (see section 0) and dogs have been well studied in both areas (e.g. (Arbogast *et al.*, 2005; Pionnier-Capitan, 2010; Pionnier-Capitan *et al.*, 2011; Ollivier *et al.*, 2013, 2016, 2018; Frantz *et al.*, 2016). Our research led us to include Romania, France and some countries bordering France (Switzerland, Germany, Belgium).

In this section, we focus on the dog and the red fox, since the study of the wolf is beyond the scope of this thesis.

To list the occurrences of dog and red fox, we used several tools. The aim was not to be exhaustive but to provide an overall picture for the two geographical areas studied.

For the red fox, we started from the synthesis provided by Fosse (1988).

For the dog, we used the unpublished synthesis of Bréhard *et al*. (2014) for French Early and Middle Neolithic. This synthesis is broad but not exhaustive for the Early Neolithic, since it does not include the Early Neolithic of Eastern France for example.

To list the presence of the two species in Southern Romania, we used mainly the synthesis published by Bălăşescu *et al.* (2005a).

We also refer to Sommer and Benecke (2005) which lists a large pannel of canid remains throughout Europe. Our database is complementary but cannot replace it, since our objective was not the same as that of the authors: their approach was more naturalistic, and thus more chronological than cultural.

We supplemented these data with archaeological databases.

An extraction from the **I2AF database** [f] was carried out by C. Callou on August 2018. This database contains only very fragmentary data. We are limited by the state of encoding in the database (all publications or reports are far from being recorded).

An extraction from the **OBRESOC database**[g] was carried out by S. Bréhard on March 2018. This research database focused on an essential cultural group for the continental Early Neolithic: the LBK culture. We will therefore be able to focus on this cultural group for which the work was exhaustive at the time of the construction of the database (10 years ago).

Considering that the Neolithic history is different in Eastern and Western Europe, we focused on several spatio-temporal entities:

- Mesolithic in Romania and France;
- Neo-Chalcolithic in Romania;
- LBK culture (OBRESOC data especially) in Europe;
- Early Neolithic in France;
- Middle Neolithic in France/Switzerland;
- Late Neolithic in France/Switzerland

[f] I2AF : Inventaires archéozoologiques et archéobotaniques de France, inpn.mnhn.fr

[g] OBRESOC : Un observatoire rétrospectif d'une société archéologique : La trajectoire du néolithique Rubané, https://trajectoires.cnrs.fr/actualite/anr-obresoc/

2.2.2. Mesolithic dogs and red foxes in France and Romania

2.2.2.1. *Romania*

In the Romanian Mesolithic, the presence of dogs is well attested in some sites of the Iron Gates (Table 4, Figure 10), such as Ostrovul Corbului (Haimovici, 1987) and Ostrovul Banului (Bălăşescu, Radu and Moise, 2005). In Icoana, the identification is limited to "*Canis sp*." but the presence of dogs is very likely likely (Bălăşescu, *pers. comm*.). In Cuina Turcului II, among the 78 wolf remains it is very probable that there are also some dogs. Cranial remains are fairly well represented, especially the remains of the mandible. Dog remains are attested at Alibeg, but their attribution to the Mesolithic or early Neolithic levels has to be confirmed. Dogs are attested in the Serbian Iron Gates: at the sites of Padina (including 42 mandibles), Vlasac (26 mandibles), Lepenski Vir (18 mandibles) and at Hajdučka Vodenica (Dimitrijević and Vuković, 2015). For the sites I could obtain the faunal list of, three contain fox remains: Cuina Turcului, Ostrovul Banului and Ostrovul Corbului (Table 4).

2.2.2.2. *France*

In France, our research (mainly using the I2AF database) reveals that, during the Mesolithic, sites yielding dog remains are rare and few have been excavated (Figure 10). However, published data are scarce. In addition, there is no review article listing French Mesolithic sites containing dogs.

We have not mentioned the site of Noyen-sur-Seine where 11 canid remains were excavated from the Mesolithic layer, because it is not clear whether the remains belong to dogs or wolves (the cranial measurements are compatible with wolves, Vigne and Marinval-Vigne, 1988).

French Mesolithic sites that have yielded red foxes are also rare, although slightly more numerous. Fosse (1988) counted 5 Mesolithic sites, we counted about 23 based on the records in the I2AF data base. Most often, the dog is not present on the sites that delivered foxes. Badger and fox are often associated, which possibly indicates modern intrusions. In these conditions, it is difficult to conclude that the fox could have been a prey to humans. As Fosse (1988) already pointed out, the presence of red foxes is not systematic in all the sites nor in all the mesolithic layers of the same site (for example at Gazel porche and ‘Abri III de Chinchon’, only one of the five Mesolithic layers contained red foxes; and at Rouffignac the fox was absent whereas the wolf, wildcat and marten were present; Fosse, 1988; Rozoy, 1978). Fox remains are therefore rather occasional during Mesolithic.

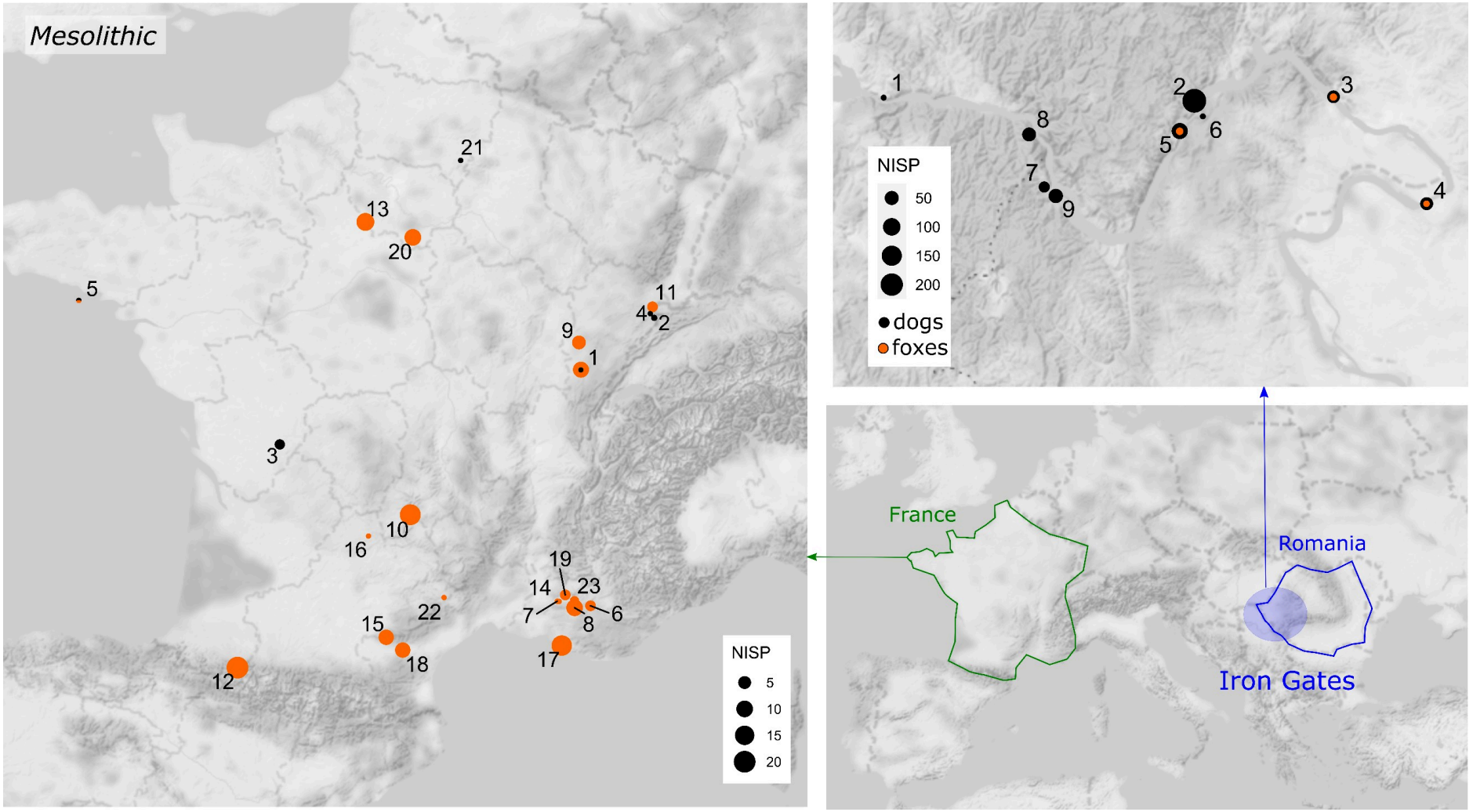

Figure 10. Romanian and French sites that have delivered remains of Mesolithic dogs or red foxes according to the literature. The sites are inventoried in Table 4 and Table 5. Dot size is proportional to the number of remains (NISP[h]) of the species of interest on the site. Where data were not available, the size is the smallest (1).

[h] NISP: number of identified specimens.

Table 4. Remains of Mesolithic dogs found in Romania.

Map code	site	species	Total NISP	NISP	Ref
1	Alibeg	dog	1+		Bălăşescu unpublished
2	Icoana	Canis sp.	8006	236	Bolomey, 1973
3	Ostrovul Banului	dog	269	35	Bălăşescu and Radu, 2012
3	Ostrovul Banului	fox	269	11	Bălăşescu and Radu, 2012
4	Ostrovul Corbului	dog	3314	38	Haimovici, 1987
4	Ostrovul Corbului	fox	3314	8	Haimovici, 1987
5	Cuina Turcului II	wolf - probably dog	684	78	Bolomey, 1973
5	Cuina Turcului II	fox	684	15	Bolomey, 1973
6	Hajdučka Vodenica	dog	1+		Dimitrijević and Vuković, 2015
7	Lepenski Vir	dog	1+	21	Dimitrijević and Vuković, 2015
8	Padina	dog	1+	48	Dimitrijević and Vuković, 2015
9	Vlasac	dog	1+	53	Bökönyi, 1978 Bökönyi 1978 Dimitrijević and Vuković, 2015

Table 5. Remains of Mesolithic dogs and red foxes recorded in France (mainly from I2AF and Fosse, 1988).

species	Map code	site	Total NISP[i]	NISP	Ref
dog	1	A Daupharde, Ruffey-sur-Seille, France	226	1	Séara, Rotillon and Cupillard, 2002
dog	2	Grotte de la Baume de Montandon, Saint-Hippolyte, France	173	2	Cupillard *et al.*, 2000
dog	3	grotte des Perrats, Agris, France	170	3	Arbogast, inédit
dog	4	Rochedane, Villars-sous-Dampjoux, France	362	1	Bridault, 1993
dog	5	Téviec, France	566	1+	Péquart *et al.*, 1937; Jeunesse, 2001; Schulting and Richards, 2001; Pionnier-Capitan et Tresset, unpublished; Tresset, unpublished
fox	1	A Daupharde, Ruffey-sur-Seille, France	804	9	Lena in Séara, Rotillon and Cupillard, 2002
fox	5	Téviec, France		1+	Rozoy, 1978
fox	6	Abri de Saint-Mitre, Reillanne, France	176	3	Helmer, 1979
fox	7	Abri III de Chinchon, saumanes, France	38	1	Helmer, 1979
fox	8	les Agnels, Apt, France	1478	10	Rillardon, 2010
fox	9	Aux Champins, Choisey, France	411	6	Léna in Séara, Rotillon and Cupillard, 2002
fox	10	les Baraquettes, Velzic, France	241	18	Fontana, 2000
fox	11	Bavans, France	254	3	Arbogast, Jeunesse and Schibler, 2001
fox	12	grotte du Bignalats, Arudy, France	622	20	Altuna and Marsan, 1986
fox	13	parc du Château, Auneau, France		12	Dubois *et al.*, 1998
fox	14	Chinchon 2, Saumane-de-Vaucluse, France	40	1	Crégut-Bonnoure, 1988; Rillardon, 2010
fox	15	Dourgne, France	801	8	Geddès, 1993
fox	16	grotte des Escabasses, Thémines, France		1	Rivière, 2006
fox	17	Font-aux-Pigeons, Châteauneuf-les-Martigues, France	3601	17	Ducos, 1958; Geddès, 1980; Poulain, 1984
fox	18	Gazel, Sallèles-Cabardès, France	664	8	Geddès, 1980
fox	19	Gramari, méthamis, France	462	3	Guilbert *et al.*, 2003; Rillardon, 2010
fox	20	Grotte à la peinture, Larchant, France	402	10	Bridault and Bautista, 1993
fox	21	l'abri Tardenoisien de la chambre des Fées, Coincy, France	12	1	Poulain, 1964
fox	22	abri du Roc Troué, Sainte-Eulalie-de-Cernon, France	83	1	Poulain, 1992
fox	23	grotte du Vauloubeau, Saint-Pierre-Quiberon, France	26	2	Crégut-Bonnoure, 2008; Rillardon, 2010

[i] NISP: number of identified specimens.

2.2.3. Neo-Chalcolithic in Romania

During the Romanian Neolithic, identified sites yielding dogs and foxes are locaed in South-Western Romania, whereas those containing remains dated to the Chalcolithic are located in the South-Eastern part of the country. This is mainly related to the state of the archaelogical excavations.

With regard to dog remains, there is a strong disproportion between the number of sites and the number of remains according to the period (Figure 11). The number of dog remains (as well as the number of sites containing dogs) is very low in the Early Neolithic and increases in later periods. Dogs are frequent in the Vinča and Boian cultures (in Isaccea-Suhat dogs are in second place after cattle but they surpass both ovicaprines and pigs, in terms of NISP; dogs also surpass pigs at Hârşova-tell during the Boian culture) and a peak is even reached during the Gumelniţa (Late Chalcolithic; Bălăşescu, Radu and Moise, 2005). Still, it should be noted that in the majority of Gumelniţa sites, the frequencies (% NISP) of dogs do not exceed 5% of mammalian remains. However, it occupies the first place ahead of other domestic animals at Căscioarele during the Gumelniţa culture (in terms of NISP), which is closely correlated with the good representation of game species that reaches more than 70% (Bălăşescu, Radu and Moise, 2005). During the same culture (Gumelniţa) at Borduşani-Popină it comes in second place, ahead of ovicaprines and cattle species.

During the Neo-Chalcolithic, the red fox is present in most of South-Eastern Romanian sites but the number of remains is often very low (Figure 11, Table 6). Like other wild carnivores, it seems to have been hunted only sporadically. The number of foxes, as well as the number of wolves is relatively more important during the cultures Vinča, Boian (where it represents almost half of the carnivore sample) and Gumelniţa (especially at Vităneşti, Borduşani and Hârşova-tell). This is likely related to the anthropophilia of the species (it was attracted by human settlements to find its food).

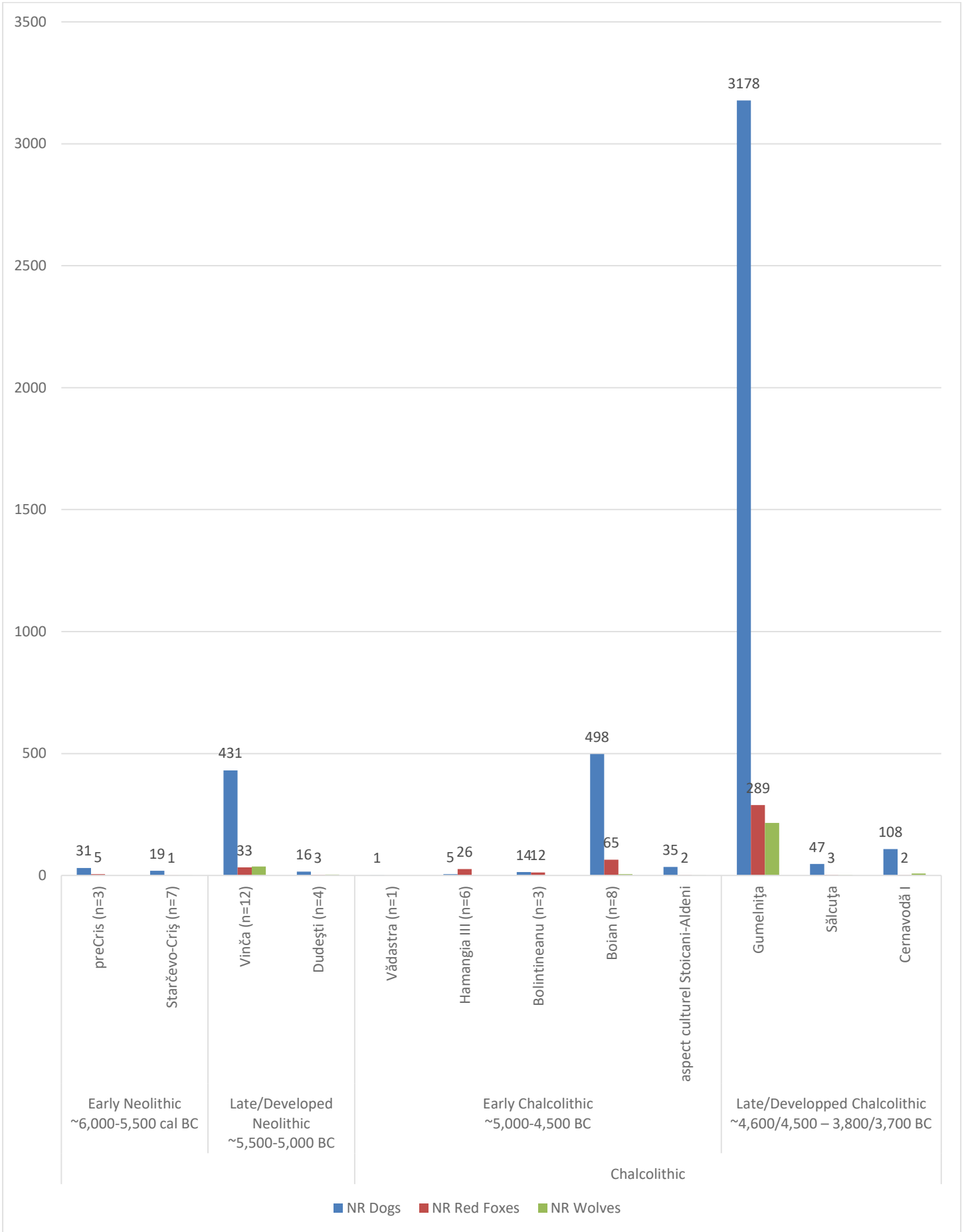

Figure 11. Occurrences of canid remains from the Early Neolithic to the Chalcolithic in South-Eastern Romania – synthesis by culture, from Bălășescu, Radu and Moise (2005)

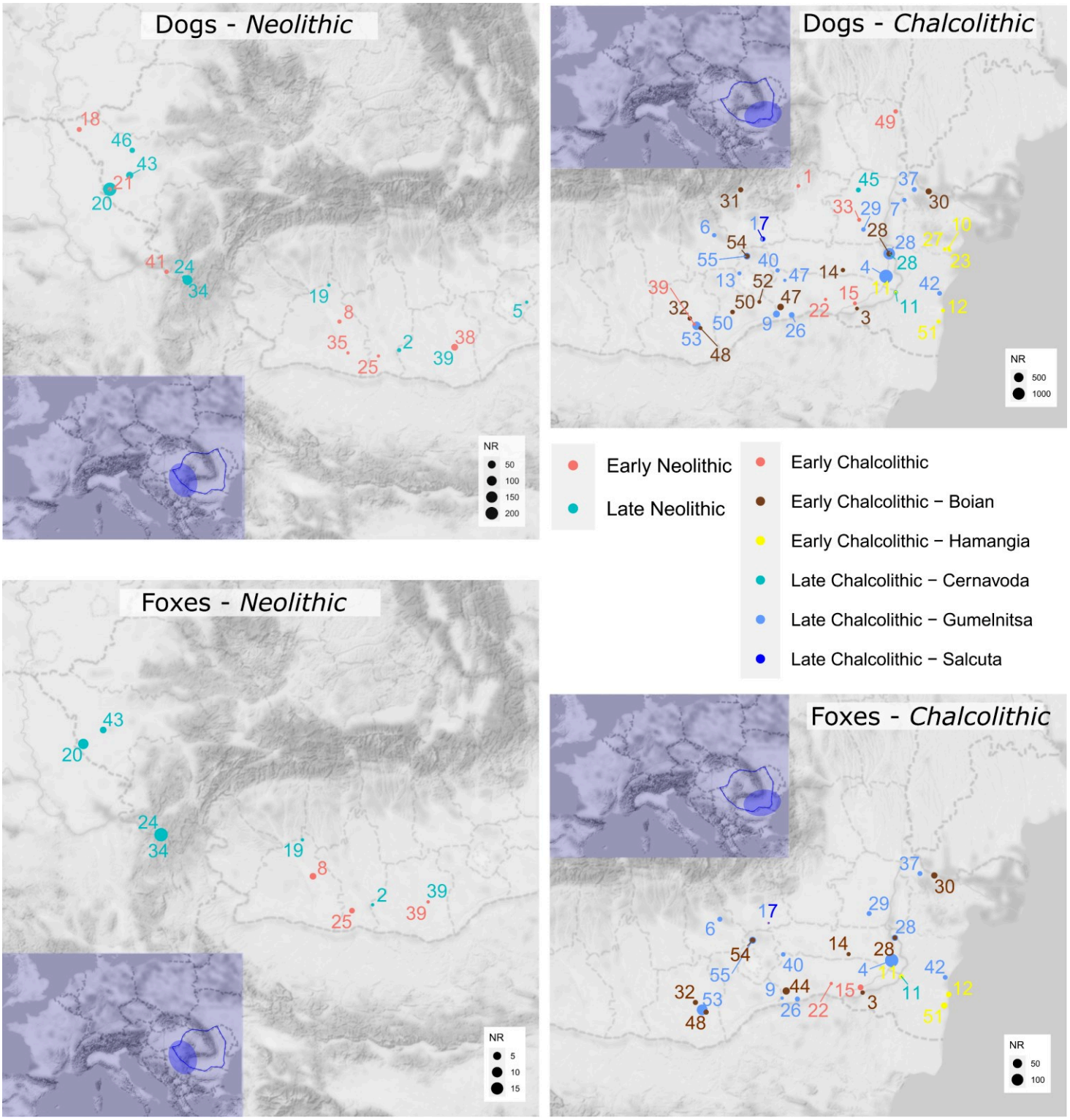

Figure 12. Sites that have delivered remains of Neolithic or Chalcolithic dog or red foxes in Romania/Serbia according to the literature. The sites are inventoried in Table 6. Dot size is proportional to the number of remains (NISP) of the species of interest on the site. Where data were not available, the size is the smallest (1).

Table 6. Occurrences of canid remains from the Early Neolithic to the Chalcolithic in South-Eastern Romania – details by site, from Bălăşescu, Radu and Moise (2005).

Period	Cultural group	Map code	Site	Dogs	Foxes	Wolves	NISP
Early Neolithic ~6,000-5.500 cal BC	Gura Baciului-Cârcea preCris	8	Cârcea-La Hanuri		3		235
		25	Grădinile	1	2		852
		38	Magura-Boldul	30			4416
	Starčevo-Criş	8	Cârcea-La Viaduct	3		1	349
		18	Dudeştii-Vechi	8			564
		21	Foeni-Gaz	1			502
		21	Foeni-Sălaş	2			261
		39	Măgura-Buduiasca		1		66
		35	Locusteni	1			331
		41	Moldova Veche-Rât	4			424
Late/Developed Neolithic ~5,500-5.000 BC	Vinča	24	Gornea-Căuniţa de Sus	7	1	3	1612
		20	Foeni-Cimitirul Ortodox 1998	37			3765
		20	Foeni-Cimitirul Ortodox 2003	234	10	3	16037
		34	Liubcova-Orniţa 1977	83	18	26	4774
		34	Liubcova-Orniţa IV-III	16		1	1668
		34	Liubcova-Orniţa II-I	6	1		1107
		43	Parţa I 1998	8	2		1267
		43	Parţa I 1995	10		3	4296
		43	Parţa II	18	1		2012
		46	Sânandrei cultura Banatului	2		1	150
		46	Sânandrei Vinča C				151
		46	Sânandrei post Vinča C	10			1703
	Dudeşti	2	Beciu	3	1		129
		5	Brăneşti-Vadu Ana	1			20
		19	Fărcaşu de Sus	+	1		345
		39	Măgura-Buduiasca	12	1	4	594
	Hamangia II	12	Goloviţa (Hamangia II)	+			92
Early Chalcolithic ~5.000-4.500 BC	Vădastra	39	Măgura-Buduiasca	1			60
	Hamangia	11	Cernavodă (Hamangia II-III)		4		354
		12	Cheia (Hamangia III)	6	8		1444
		27	Hamangia (Hamangia III)	3			70
		51	Techirghiol (Hamangia III)	7	14		1094
		10	Ceamurlia de Jos (Hamangia III)	+			147
	Bolintineanu	15	Coslogeni	6	10		433
		22	Gălăţui	1	1		363
		36	Lunca	7	1		394
	Boian, Giuleşti	3	Bogata	4	3		170
		14	Ciulniţa	14	2		2489
		30	Isaccea-Suhat	106	14		795
		32	Lăceni-Măgura	9	6		226
		48	Siliştea-Conac	8	6		141
	Boian-Vidra	52	Vărăşti	7			260
		54	Vlădiceasca	46	7	2	2655
	Boian-Spanţov	28	Hârşova-tell	77	4		1527
		31	Izvoarele	50		2	1136
		32	Lăceni-Măgura	10			252
		44	Radovanu	142	23	1	4703
		50	Tangâru	25			421
	Stoicani-Aldeni	1	Aldeni	3			28
		17	Drăgăneşti	7	2	1	674
		33	Lişcoteanca	7			515
		49	Suceveni	18			806

Period	Cultural group	Map code	Site	Dogs	Foxes	Wolves	NISP
Late/Developped Chalcolithic ~4.600/4.500 - 3.800/3.700 BC	Gumelniţa	4	Borduşani	1343	143	64	9317
		7	Carcaliu	13			481
		13	Chitila	8			481
		28	Hârşova-tell	896	14	26	5310
		29	Însurăţei	20	5	5	581
		37	Luncaviţa	21	4	6	924
		37	Luncaviţa G	16	1	2	548
		42	Năvodari	27	4	12	425
		47	Şeinoiu	1			97
		50	Tangâru	4			256
		6	Bucşani	15	5		808
		9	Căscioarele	166	1	3	2829
		40	Măriuţa	13	3		526
		17	Drăgăneşti-Olt A	14	1		719
		17	Drăgăneşti-Olt B	35	2		1515
		26	Gumelniţa A	62	3	2	1886
		26	Gumelniţa B	14	2	2	476
		53	Vităneşti A2	252	61	72	9089
		53	Vităneşti B1	90	19	18	3662
		55	Vlădiceasca GA1	18	4		475
		55	Vlădiceasca GA2	127	15	3	3518
		55	Vlădiceasca GB1	23	2		1013
	Sălcuţa	16	Cuptoare-Sfogea	27	1		994
		17	Drăgăneşti-Olt	20	2	2	887
	Cernavodă I	11	Cernavodă	11	2		285
		28	Hârşova-tell	63		3	358
		45	Râmnicelu	34		5	2838

2.2.4. Neolithic in France – general trends

The synthesis of Bréhard *et al.* (2014) revealed a large imbalance in the number of sites and the number of dog remains for each period/culture, as it has been observed in the previous section for Eastern Europe. There is almost the same (consistent) number of sites dated to the VSG culture, Cardial-Epicardial cutures (Early Neolithic) and Chasséen or Cortaillod cultures (Middle Neolithic). However, the number of dog remains is much lower during the Early Neolithic compared to the Middle Neolithic. Dog remains are especially numerous during the Chasséen culture and even more during the Cortaillod culture, despite the fact that the number of sites is not that different than during the Early Neolithic (Figure 13).

A.

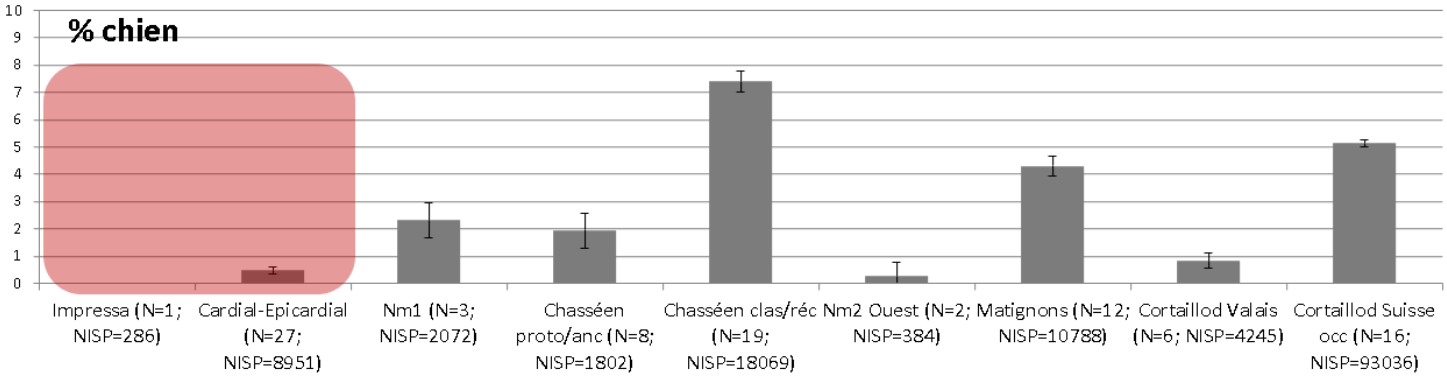

B.

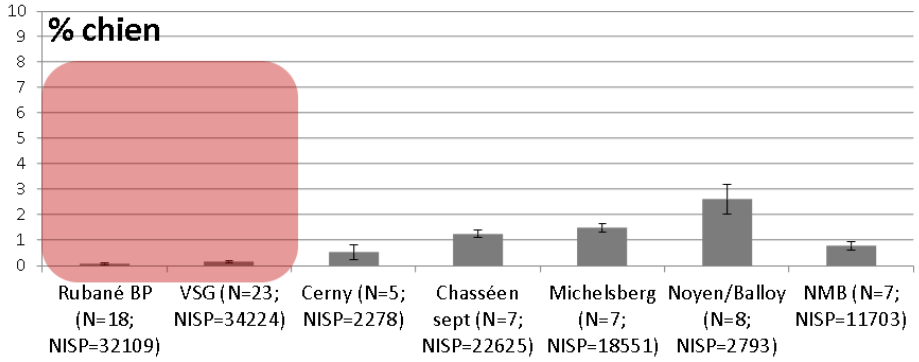

Figure 13. Evolution of the frequency of dog remains in the Early and Middle Neolithic sites of France according to chrono-cultural groups. A: South of France (Middle Neolithic sites from Swizterland are included); B: North of France. Matignons culture is from the very beginning of the Late Neolithic. From Bréhard *et al.* (2014).

In the following sections, we augmented the database of Bréhard *et al.* (2014) with Early Neolithic sites from the Eastern part of France and with sites studied after the completion of the synthesis.

2.2.5. Early Neolithic in France and LBK culture in Europe

During the Early Neolithic in France, dog remains are rare (both in terms of number of sites and number of remains per site, Table 7, Figure 13, Figure 14). However, it is likely that the canine population at that time was much larger than suggested by the excavated dog remains (Arbogast, 1995). Indeed, frequent dog bite or chewing marks are observed on the bones of other species (for example in Armeau, Poplin, 1975). The geographical distribution of the sites which yielded dog remains is linked to both the state of archaeological excavations and to the fact that our synthesis is not exhaustive.

The scarcity of dog remains may relate to their status during this period. Some authors have suggested that dogs were not found in household refuses because the dogs would have been rarely eaten and would hence have benefited from a special position relative to humans (Poplin, 1975; Arbogast, 1989).

The number of red fox remains is also pretty low during the Early Neolithic (Table 7, Figure 14), as already reported by Bedault (2012). They are sometimes associated with other digging animals, notably the badger, as at Fontbrégoua, Saint Mitre, Gazel I, Jean-Cros or “Les Obeaux”, where the red fox may be intrusive (Helmer, 1979; Poulain, 1979; Fosse, 1988). However, they are often associated with other fur-bearing carnivores. This is consistent with the fact that among wild species, aurochs, deer, wild boar and roe deer were the most frequent game species at this period, even though the hunting of numerous fur-bearing carnivores, rodents and lagomorphs (badger, marten, weasel, beaver, hare) likely had a significant secondary role (Arbogast, 1994).

Foxes and dogs are found together at a few sites.

Northern Fance was neolithicized by the LBK culture (or “culture Rubanée”), a major pan-European culture (see section 2.1). The OBRESOC database allowed us to extend the referencing of sites dated to the LBK containing dog and/or red fox remains in Europe (Figure 14, Table 7). These data confirm what we already observed in France. Although sites are more numerous, the number of dog remains is generally very low with the exception of some sites such as Herxheim, which reveals singular cultural practices for that period (see section 2.3.4.2).

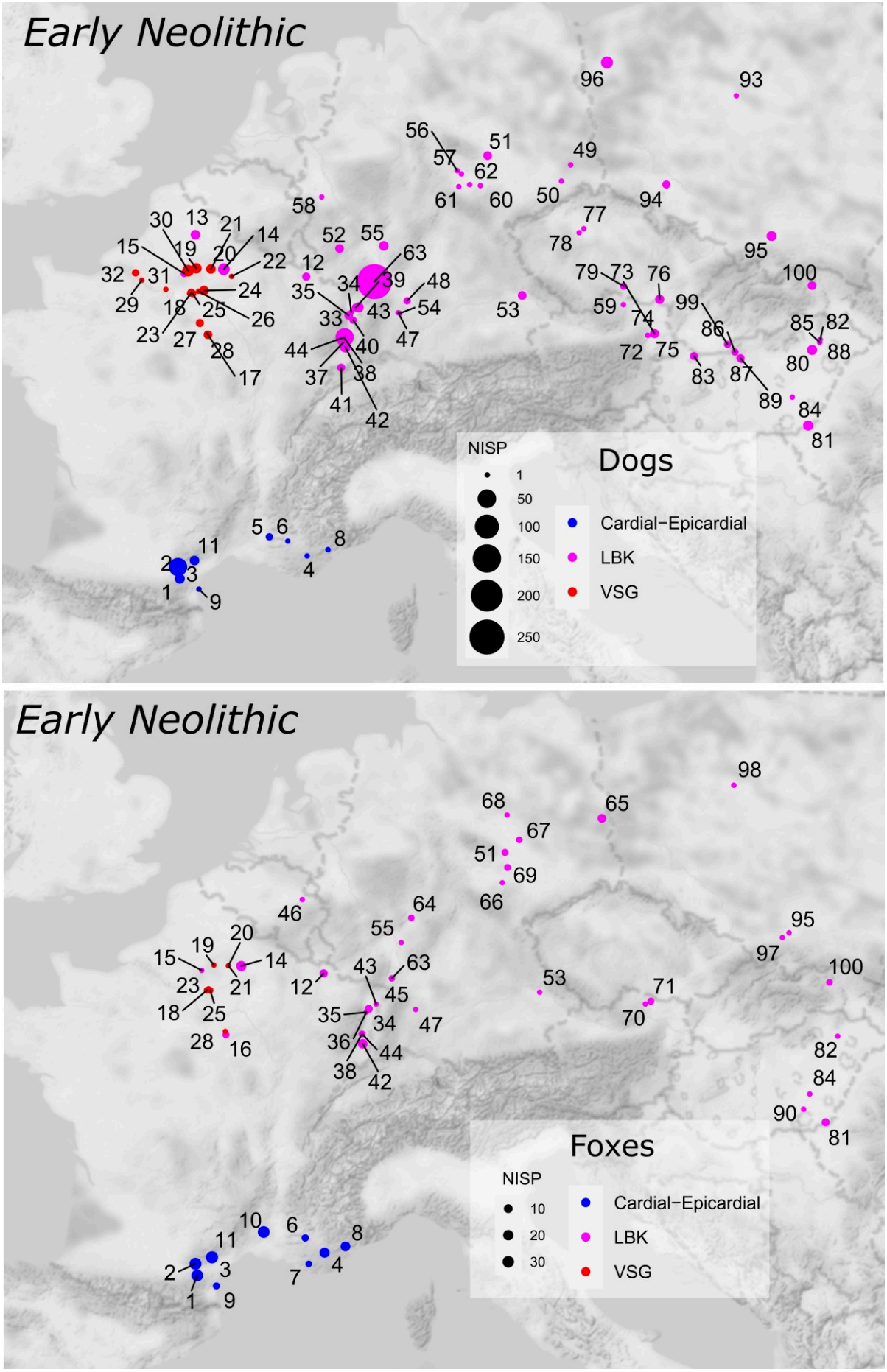

Figure 14. Remains of dogs and red foxes from the Early Neolithic in France and from the LBK culture in Europe. Sites are listed in Table 7. Dot size is proportional to the number of remains (NISP) of the species of interest on the site. Where data were not available, the size is the smallest (1).

Table 7. Occurrences of dog and fox remains from the Early Neolithic in France and LBK culture in Europe. From Bréhard and Vigne (*in press*); Bedault (2012); Bréhard *et al.* (2014) for Southern and Northern France, from I2AF database for Eastern France, and from OBRESOC database for the LBK in Europe.

Country	Map code	Culture	Sites	Reference	NISP dogs	NISP foxes
Southern France	**1**	Péricardial	Jean-Cros (2a-b)	Poulain, 1979	7	32
	2	Cardial ancien	Gazel I (sensu Manen)	Geddès, 1980 modified by Vigne, 2007	5	20
	3	Cardial ancien	grotte de l'Aigle (c5)	Khawam, 2016	5	35
	4	Cardial ancien	grotte de Fontbrégoua (C48-45)	Helmer, 1979	1	9
	4	Cardial récent	grotte de Fontbrégoua (C44-41)	Helmer, 1979		9
	5	Cardial	Abri de Fraischamp 2 (C4-C3)	Helmer, 1979	2	
	6	Cardial	Saint Mitre (C3)	Helmer, 1979	1	4
	7	Cardial	Baume Saint-Michel (C5b)	Helmer in Hameau *et al.*, 1994		2
	8	Cardial récent	grotte Lombard	Helmer, 1991	1	16
	9	Cardial/Epicardial	Leucate-Corrège	Geddes, 1984	1	3
	10	Epicardial ancien	**"Le Taï"**	Bréhard and Vigne, in press		33
	2	Epicardial ancien	Gazel II	Geddès, 1980 modified by Vigne, 2007	20	11
	11	Epicardial ancien	**grotte de Camprafaud (C18-C19)**	Doumerc, 2016	3	8
	11	Epicardial récent	grotte de Camprafaud (C17)	Doumerc, 2016	3	
	2	Epicardial récent	Gazel III	Geddès, 1980 modified by Vigne, 2007	23	4
Northern France	**12**	RBP Ancien et Moyen	Ay-sur-Moselle	Arbogast, 2001 unpublished	3	7
	13	RBP Ancien et Moyen	Menneville "Derrière le Village"	Hachem, 1996a	3	
	14	RBP Ancien et Moyen	Cuiry les Chaudardes "Les Fontinettes" (Phases 1-4)	Hachem, 1996b	12	19
	15	RBP Ancien et Moyen	Pont-Saint-Maxence "Le Joncoire"	Arbogast, Jeunesse and Schibler, 2001	2	1
	16	RBP Ancien et Moyen	Armeau	Poplin, 1975		3
	17	RRBP/Rubané final	Etigny	Carré, 2004	1	
	13	RRBP/Rubané final	Menneville "Derrière le Village"	Hachem, 1996a	3	
	18	VSG	Jablines "La Pente de Croupetons"	Bostyn, Hachem and Lanchon, 1991; Hachem in process	1	2
	19	VSG	Trosly-Breuil "Les Obeaux"	Arbogast, 1993 and unpublished	8	1
	20	VSG	Bucy le Long "La Fosse Tounise"	Bedault, 2012	6	1
	21	VSG	Bucy le Long "Le Fond du Petit Marais/le Grand Marais"	Bedault, 2012	3	1
	22	VSG	Tinqueux "La Haubette"	Bedault, 2012	1	
	23	VSG	Vignely "La Porte aux Bergers"	Bedault, 2012	3	2
	24	VSG	Luzancy "Le Pré aux Bateaux"	Bedault, 2012	6	
	25	VSG	Mareuil-lès-Meaux "Les Vignolles"	Arbogast, Schaefer, inédit	2	2
	26	VSG	Changis-sur-Marne "Les Pétreaux"	Hachem in Lanchon *et al.*, 2008	1	
	27	VSG	Villeneuve-la-Guyard "Les falaises de Péproux"	Bedault, 2012	3	
	28	VSG	Passy "La Sablonnière"	Bedault, 2012	4	1
	29	VSG	Aubevoye "La Chartreuse"	Bedault, 2012	1	
	30	VSG	Longeuil-Sainte-Maris "La butte de Rhuis III"	Arbogast, 1995	12	
	31	VSG	Maurecourt "La Croix de Choisy"	Bémilli, 2006	1	
	32	VSG	**Alizay-la-Chaussée str 506**	Bemilli unpublished	2	
Eastern France	**33**	Rubané ancien	Bischoffsheim Le village	Arbogast, 1991	1	
	34	Rubané ancien	Dachstein "Am Geist"	Arbogast, 1994	1	6
	35	Rubané récent	Rosheim "Sainte-Odile"	Arbogast unpublished	4	1
	36	Rubané récent	Rosheim "Sablière Helmbacher"	Poulain in Thévenin and Sainty, 1979	7	
	37	Rubané récent	Rouffach "Gallbühl"	Poulain, 1984	2	1
	38	Rubané final	Wettolsheim "Ricoh"	Arbogast, 1994	3	
	39	Rubané final	Pfulgriesheim "Langgarten" and "Buetze"	Meunier, Sidéra and Arbogast, 2003	2	
	40	Rubané final	Westhouse "Ziegelhof"	Lefranc *et al.*, 1998		1
	41	Rubané	Oberlarg "Mannlefelsen 1"	Poulain, 1984	3	
	42	Rubané	Ensisheim "Ratfeld"	Arbogast, 1994	9	15
	43	Rubané	Reichstett	Poulain-Josien, 1978	7	1
	44	Rubané	Colmar "route de Rouffach"	Poulain, 1989	47	3
	45	Rubané ancien à récent	Reichstett "Schamli"	Poulain-Josien, 1978		1
Belgium	**46**	Culture omalienne	Liège "Place Saint-Lambert"	Otte, 1984		1
Germany	**47**	LBK	Ammerbuch-Reusten	Uerpmann, 2001	1	1
	48	LBK	Stuttgart "Cannstatt 1"	Brunnacker *et al.*, 1967	2	
	49	LBK	Großgrabe "Gebinde"	Müller, 1964	1	
	50	LBK	Dresden "Cotta (Fpl. 4)"	Benecke, 1999	1	
	51	LBK	Eisleben "Voswelle"	Döhle, 1994	4	3
	52	LBK	Langweiler 8	Uerpmann in Boelicke and Aniol, 1988	4	
	53	LBK	Straubing "Lerchenhaid Fundplatz A"	Ziegler, 1985	4	1
	54	LBK	Ammerbuch-Pfäffingen "Lüsse"	Stork, 1993	1	
	55	LBK	Riedstadt/Godelau "Nachtweide"	Uerpmann, 2001	6	1
	56	LBK	Schlotheim	Müller, 1964	1	
	57	LBK	Bruchstedt "Strasse der Einheit"	Müller, 1964	1	
	58	LBK	Müddersheim "Strasse Düren-Zülpich, Ziegelei St. Antonius"	Schietzel and Stampfli, 1965	1	
	59	LBK	Zauschwitz/Weideroda	Müller, 1964	1	
	60	LBK	Ehringsdorf/Weimar	Müller, 1964	1	
	61	LBK	Gotha "Körner (Lehmgrube der Ziegelei)"	Müller, 1964	1	
	62	LBK	Erfurt "Rankestraße"	Müller, 1964	1	
	63	LBK	**Herxheim**	Jeunesse, Boulestin and Zeeb-Lanz, 2009	250	2

Country	Map code	Culture	Sites	Reference	NISP dogs	NISP foxes
	64	LBK	Bruchenbrücken	Uerpmann, 2001		2
	65	LBK	Dammendorf (Windmühlenberg)	Müller, 1964		10
	66	LBK	Hohlstedt	Müller, 1964		1
	67	LBK	Köthen"Scherbelberg"	Müller, 1964		2
	68	LBK	Barleben "Schweinemästerei"	Müller, 1964		1
	69	LBK	Tröbsdorf/Burgscheidungen	Müller, 1964		3
Austria	**70**	LBK	Mold "Im Doppel"	Schmitzberger, 2010		1
	71	LBK	Pulkau	Wolff, 1980		3
	72	LBK	Poigen "Bachrain"	Wolff in Lenneis, 1977	1	
	73	LBK	Schwechat "Unteres Feld"	Ruttkay, 1971	1	
	74	LBK	Unteres Feld grupe 1-14-6	Ruttkay, 1971	5	
	75	LBK	Brunn am Gebirge "Fundstelle 1, Wolfsholz"	Pucher, 1998	2	
Czech Republic	**76**	LBK	Mikulov "Jelení-Louka"	(Kratochvíl, 1973)	5	
	77	LBK	Roztoky	(Peške, 1991)	1	
	78	LBK	Hostivice "Sadová"	Kovačiková, 2011	1	
	79	LBK	Chotěbudice	Kovačiková, 2011	2	
Hungary	**80**	LBK	Folyás "Fundstelle Szilmeg"	Bökönyi, 1959	7	
	81	LBK	Battonya "Gödrösök"	Bökönyi, 1984	7	6
	82	LBK	Tiszalök "Hajnalos"	Vörös, 1989 in Arbogast, Jeunesse and Schibler, 2001	1	1
	83	LBK	Győr "Pápai Vám"	Bökönyi, 1974	3	
	84	LBK	Szarvas	Bökönyi, 1987 in Arbogast, Jeunesse and Schibler, 2001	1	1
	85	LBK	Tiszavasvári "Keresztfal"	Bökönyi, 1974	1	
	86	LBK	Pilismarót "Szobi Rév"	Bökönyi, 1974	2	
	87	LBK	Vörös Csillag Tsz	Bökönyi, 1974	1	
	88	LBK	Tiszavasvári "Deakhalmi dülö"	Bökönyi, 1974	1	
	89	LBK	Pomaz "Zdravlyák"	Bökönyi, 1959	3	
	90	LBK	Borsod "Derekegyházi Dülö"	Bökönyi, 1959		1
Moldova	**91**	LBK	Floreşti 1	Calkin 1970 in Arbogast, Jeunesse and Schibler, 2001	1	
	92	LBK	Novye-Rusesty 1	David and Markevic, 1967 in Arbogast, Jeunesse and Schibler, 2001	18	25
Poland	**93**	LBK	Brzesc Kujawski	Bogucki, 1982 in Arbogast, Jeunesse and Schibler, 2001	1	
	94	LBK	Gniechowice	Kulczycka-Leciejewiczowa and Romanow, 1985	3	
	95	LBK	Lagiewniki 5	Sobociński, 1981	7	1
	96	LBK	Zalecino 4	Sobocinski, 1984	13	
	97	LBK	Grabie 4	Sobocinski, 1985		1
	98	LBK	Lojewo 1/22	Sobocinski, 1985		1
Slovakia	**99**	LBK	Berek, Bíňa	Ambros unpublished in Arbogast, Jeunesse and Schibler, 2001	2	
	100	LBK	Fedelemka, Sarisské Michalany	Šiška, 1989	4	2
Ukraine	**101**	LBK	Girka Polonka	Kotova, 2003	1	
	102	LBK	Rovno	Kotova, 2003	5	2
	103	LBK	Gnidava	Kotova, 2003	1	
	104	LBK	Golysev 2	Kotova, 2003	3	

2.2.6. Middle Neolithic in France and Switzerland

In France, the Middle Neolithic is a complex mozaic of cultures. Indeed, it is characterised by the co-existence and succession of several cultures in the north (Cerny, Michelsberg, Northern Chasséen, Noyen group) and the existence of a cultural complex that dominated in the south (Southern Chasséen). Many exchanges and influences occurred between these regional cultures, as well as with those in Eastern France and Switzerland (Cortaillod, Middle Burgundian Neolithic NMB, Bostyn *et al.*, 2011).

Our synthesis shows that there are many more sites and more information on canid bones in the Middle Neolithic than in the Early Neolithic (Figure 14, Figure 15). However, there are still some lacuna in data from Central France or Brittany, likely linked to the state of archaeological excavations or research.

The number of dog remains increases considerably while the number of fox remains remains relatively low (Figure 14, Figure 15). This is particularly evident during the Chasséen and the Cortaillod. Dog remains belong to complete individuals or to scattered remains of many different animals. This thus suggests two different types of human-dog relationships. We will detail this further in section 2.3.

The possibility that the fox was intrusive still exists at this period, in particular at Collombey-Barnaz II where it was associated with the bear, and perhaps at Dourgne C4 (Fosse, 1988).

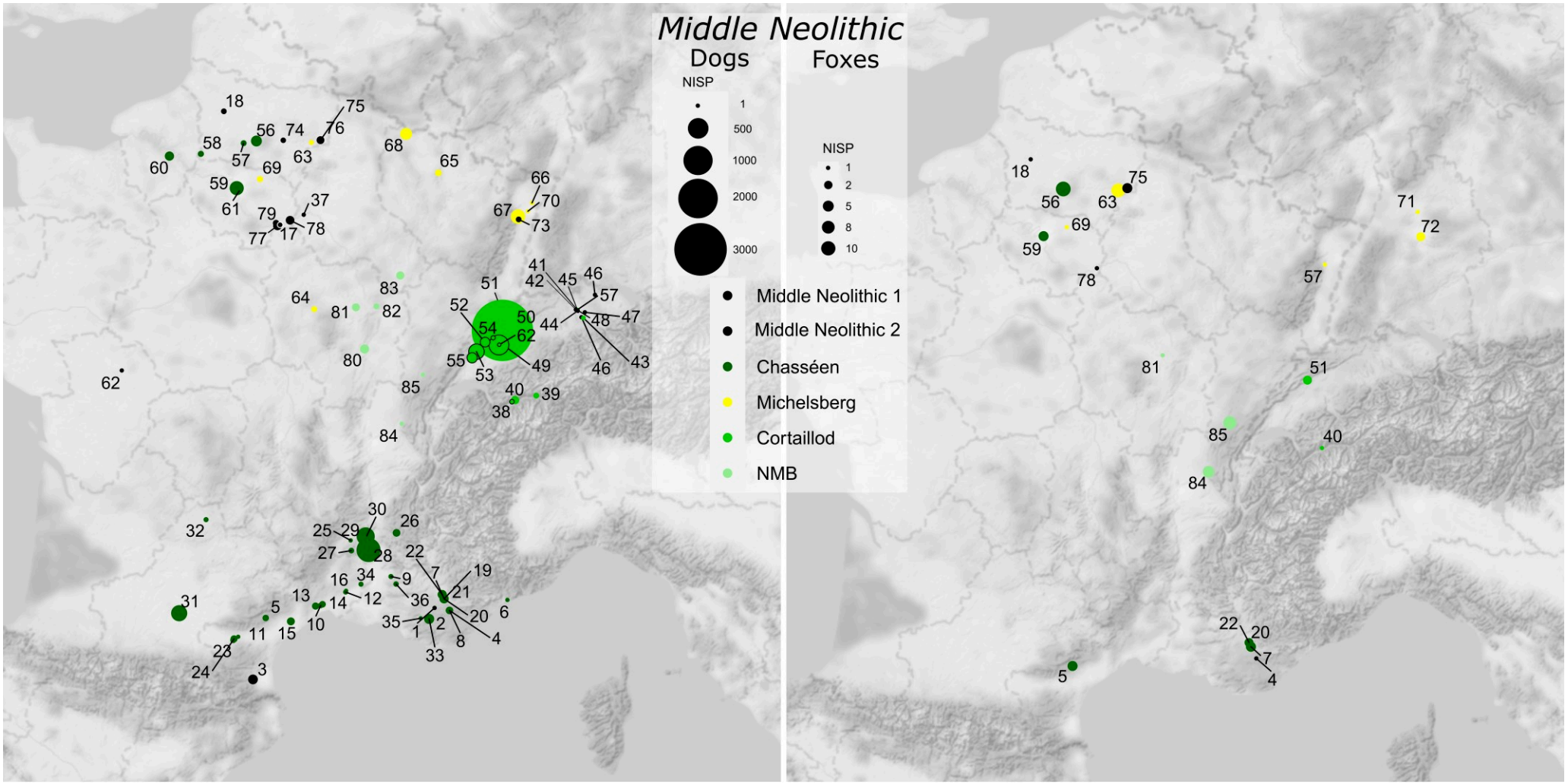

Figure 15. Remains of dogs and red foxes from the Middle Neolithic in France. Sites are listed in Table 8. Dot size is proportional to the number of remains (NISP) of the species of interest on the site. Where data were not available, the size is the smallest (1).

Table 8. Occurrences of dog and fox remains from the Middle Neolithic in France, from Bréhard (2011), Hachem (2011), Bréhard *et al.* (2014) and the I2AF database.

Cultural phase	Map code	Sites	Reference	NISP dogs	NISP foxes
Middle Neolithic 1					
Southern France					
– transition between Early and Middle Neolithic	1	Chemin de Barjols FS 1069	Cockin and Furestier, 2009 cited in Remicourt *et al.*, 2012	1+	
– Middle Neolithic 1	2	Saint-Maximin-la-Sainte-Baume "Le clos de Roque"	Blaise in Remicourt *et al.*, 2012	1	
– Montbolo	3	Grotte de Montou	Loirat, 2000	48	
– Pré-Chasséen	4	Grotte de Fontbrégoua (C30-36)	Helmer, 1979	3	1
– Chasséen	5	Grotte de Camprafaud (C14-15)	Poulain, 1985	2	
– Early Chasséen	6	Giribaldi à Nice	Helmer, 2004	1	
	7	Grotte de l'Eglise supérieure (C7-8)	Helmer, 1979	16	1
	8	Grotte de Fontbrégoua (C20-29 and C19-8)	Helmer, 1979	11	
	9	Grotte d'Unang (ensemble 3)	Poulain-Josien, 1993	2	
	10	Castelnau-le-Lez "jardins de vert-Parc"	Vignaud, 2003	4+	
	11	Berriac "Les Plots"	Vaquer, 1998	1+	
	12	**Nîmes "Cadereau d'Alès"**	Hasler and Noret, 2004 ; Chevrier, 2014	2+	
	13	**Juvignac "ZAC de Caunelle"**	Convertini *et al.*, 2014 ; Chevrier 2014; Bréhard unpublished	14+	
	14	**Béziers "le Crès"**	Loison and Schmitt, 2009	9+	
	15	**Valros "le Pirou"**	Caillat in Gandelin, 2015	22+	
	16	**Mas de Vignolles IV**	Forest in Jallot, 2004	1+	
Northern France – Cerny	17	Balloy les Réaudins LRE	Tresset, 1996b	8	
	18	Zac Dunant à Conty	Hachem, 2011; Bostyn *et al.*, 2016	4	1
Middle Neolithic 2					
Late Chasséen	19	Grotte de l'Eglise (C5-6 ; C8-9)	Helmer, 1979 Helmer, 1979	1	
	20	Grotte de l'Eglise supérieure (C6-3)	Helmer, 1979	41	4
	8	Grotte de Fontbrégoua (C19-8)	Helmer, 1979	7	
	21	Grotte C	Poulain, 1971	18	
	22	Grotte Murée (C11-7b)	Helmer, 1979	39	3
	5	Grotte de Camprafaud (C12-13)	Poulain, 1985	6	4
	23	Cavanac "La Toronde"	Carrère, 1986	6	
	24	**Auriac, sol P IV**	Bréhard, 2011	13	
	25	Combe Obscure (C5)	Helmer, 1991b	1	
	26	Trou Arnaud (c. A, B, E)	Helmer in Blaise, 2009	19	
	27	Baume d'Oullen (C4)	Helmer and Vigne in Blaise *et al.*, 2009	4	
	28	**Saint Paul-Trois-Châteaux "les Moulins"**	Bréhard, 2011	624	
	29	**Châteauneuf-du-Rhône "la Roberte"**	Bréhard, 2011	307	
	30	Montélimar "le Gournier", zone E-F	Bréhard, 2011	25	
	31	Villeneuve-Tolosane "la Terrasse", puits R21-1	Fontaine, 2002	226	
	32	Montesquieu-de-Lauragais "Narbons" (fosse 1020)	Martin in Tchérémissinoff *et al.*, 2005	2	
	33	Saint-Maximin-la-Sainte-Baume "chemin d'Aix"	Martin *et al.*, 2008	55	
Chassén	34	**"le Taï"**	Bréhard et Vigne in press	2	
	35	Trets "Bastidonne"	D'Anna, 1993	1+	
	36	Rousillon "Les Martins"	Vaquer, 1998	3+	
Middle Neolithic 2	37	Pont-sur-Seine "la Ferme de l'Ile"	Hachem, 2009	1	
Cortaillod Valais	38	Sion "Petit-Chasseur I"	Chaix, 1988	3	
	39	Rarogne-Heidnisch-Bühl II	Chaix, 1976	5	
	40	Saint Léonard "sur le Grand Pré"	Chaix 1976	27	1
Eastern Switzerland					
– Egolzwil	41	Kleiner Hafner 5A+B	Arbogast *et al.*, 2005	1+	
– Cortaillod	41	Kleiner Hafner 4A-4C-A-3-4D-4E-4F-4G	Arbogast *et al.*, 2005		
	42	Mozart Str. 6u, Str 60, str. 5u, str. 5o	Arbogast *et al.*, 2005	1+	
	43	Meilen Rohrenhaab 5	Arbogast *et al.*, 2005	1+	
– Pfyn	44	Seefeld 9	Arbogast *et al.*, 2005	1+	
	45	Pressehaus L	Arbogast *et al.*, 2005	1+	
	46	Feldmeilen Vor. 9-8-6	Arbogast *et al.*, 2005	1+	
	44	Seefeld 8-7-5	Arbogast *et al.*, 2005	1+	
	45	Pressehaus J	Arbogast *et al.*, 2005	1+	
	46	Gachnang Niderwil	Arbogast *et al.*, 2005	1+	
	47	Horgen Dampfschif.	Arbogast *et al.*, 2005	1+	
	43	Meilen Rohrenhaab 3	Arbogast *et al.*, 2005	1+	
	42	Mozart Str. 4u - Str. 4m - Str. 4o	Arbogast *et al.*, 2005	1+	
Western Switzerland			Arbogast *et al.*, 2005		
– Egolzwil	48	Egolzwil 3	Arbogast *et al.*, 2005	1+	
– Cortaillod	49	Muntelier/Fischergässli	Arbogast *et al.*, 2005	1+	
	50	Burgäschisee SW- Süd	Arbogast *et al.*, 2005	1+	
– Cortaillod classique	51	**Twann US(B)**	Becker 1981 in Chiquet, 2012	185	1+
	51	**Twann US(G)**	Grundbacher and Stampfli in Chiquet, 2012	147	
	49	Montilier Strandwerg	Reynaud Savioz, 2005 in Chiquet, 2012	231	
	49	Montilier Fischergassli	Morel, 2000 in Chiquet, 2012	168	
	49	Montilier dorf	Lopez, 2003 in Chiquet, 2012	37	
	52	Auvernier-Port Vb-c	Chaix in Chiquet, 2012	11	

	52	Auvernier-Port Va-a'	Chaix in Chiquet, 2012	7	
– Cortaillod moyen	53	Concise-sous-Colachoz (E2B, E3B)	Chiquet, 2012	209	
Cultural phase	**Map code**	**Sites**	**Reference**	**NISP dogs**	**NISP foxes**
	54	Thielle-Mottaz	Chaix, 1979 in Chiquet, 2012	2	
	55	Yverdon Garage-Martin, c18-19	Chaix, 1976 in Chiquet, 2012	58	
– Cortaillod tardif	53	Concise-sous-Colachoz (E4A; E6)	Chiquet, 2012	28	
	51	**Twann OS**	Becker and Johansson 1981 in Chiquet, 2012	1994	
	55	Yverdon Garage-Martin, c14-16b	Chaix 1976 in Chiquet, 2012	18	
	52	Auvernier-Port III	Chaix in Chiquet, 2012	46	
– Cortaillod moyen et tardif	51	**Twann MS**	Becker and Johansson 1981 in Chiquet, 2012	1629	2+
Northern Chasséen	56	Jonquières "le Mont d'Huette"	Poulain, 1984b	71	11
	57	Catenoy "le camp de César"	Méniel, 1984	5	
	58	Boury-en-Vexin "le Cul Froid", dépotoirs	Méniel, 1984	6	
	59	**Paris "Bercy", Quartier Sud (couches et chenal)**	Tresset, 1996	155	4
	60	Louviers "La Villette"	Tresset, 2005	40	
	61	Maisons-Alfort "Zac d'Alfort"	Hachem *et al.*, 2002	3	
Western Middle Neolithic	62	Migné-Auxances "Temps-Perdu"	Braguier, 1999	1	
Michelsberg	63	Maizy "Les Grands Aisements"	Hachem, 1989	2	9
	64	Bazoches "le Bois de Muisemont"	Hachem, 1987, 2011	5	
	65	Arnaville "Le Rudemont"	Thévenin, 1981; Blouet *et al.*, 1984; Arbogast, 1989	10+	
	66	Vendenheim "the Gates of the Kochersberg"	Lefranc *et al.*, 2015	1+	
	67	Rosheim	Poulain in Thévenin, Sainty and Poulain, 1977	166	
	67	Rosheim "Sainte-Odile"	Poulain in Thévenin, Sainty and Poulain, 1977	4	1
	67	Rosheim "Leimen"	Lefranc, Arbogast and Boës, 2007; Arbogast *et al.*, 2013	1+	
	68	Mairy "Les Hautes Chanvières"	Arbogast, 1994	94	
	69	Vignely "la Noue Fenard"	Claudet, 2003	7	1
	70	Holtzheim	Kuhnle *et al.*, 1999	1	
	71	Heilbronn-Klingenberg "Schlossberg", structure 619	Seidel *et al.*, 2008		1+
	72	Münster "Schnarrenberg"	Joachim, 1984		3+
Grossgartach/Roessen	73	Obernai	Guthmann, Lefranc and Arbogast, 2016	4	
Rössen final/tardif	74	La Terre saint Mard, Osly-Courtil	Hachem, 2011	3	
Epi-Roessen	75	Berry au Bac "La Croix Maigret"	Méniel, 1984a	21	4
Epi-Roessen	76	Saint-Julien-lès-Metz "Ferme Grimont"	Brunet *et al.*, 2006	1	
Groupe de Noyen	77	Gravon, enceinte FA	Tresset, 1996b	32	
	78	Noyen-sur-Seine "le Haut des Nachères" Fd (fossé+enceinte)	Tresset, 1988	31	1
Grpe de Balloy	79	Châtenay "le Maran", enceintes F, FA	Tresset, 1996b	2	
	79	Châtenay "la Bachère"	Tresset, 1996b	8	
Middle Neolithic in Burgundy	80	La Redoute "Camp de Chassey" (niv 6)	Poulain, 2005	38	
	81	Vitteaux "Camp de Myard" (secteurs 3, 7, 10 & 11)	Poulain, 2003b	22	1
	82	Châtelet d'Etaules (secteur 3 c. IIIb)	Poulain, 2003a	5	
	83	Cohons "La Vergentière" (sondages 1, 2 et 6)	Poulain, 1992	25	
	84	Grotte du Gardon (c46-43)	Chiquet, 2013	1	6
	85	**Clairvaux XIV**	Arbogast *et al.*, 2005	1+	8+

2.2.7. Late Neolithic in France

Contrary to the Early and Middle Neolithic, no synthetic and critical work has been done on sites providing dog remains for the end of the Neolithic in France. Our work is only based on I2AF database, without a critical approach of the chrono-cultural attribution of the sites or on the taxonomic identification of the remains.

We did not include the sites recorded as from the transition between the Late Neolithic and the Bronze Age.

Sites containing dogs are always very numerous through the Late Neolithic and the number of dog remains is much higher than that of foxes (Table 9, Figure 16). Data is still incomplete in central France and Brittany.

The presence of foxes is certainly intrusive at “Pierre levee” in Nieul-sur-l'Autise (Campaniforme) and at Gimel and at “l’Homme mort” (Fosse, 1988).

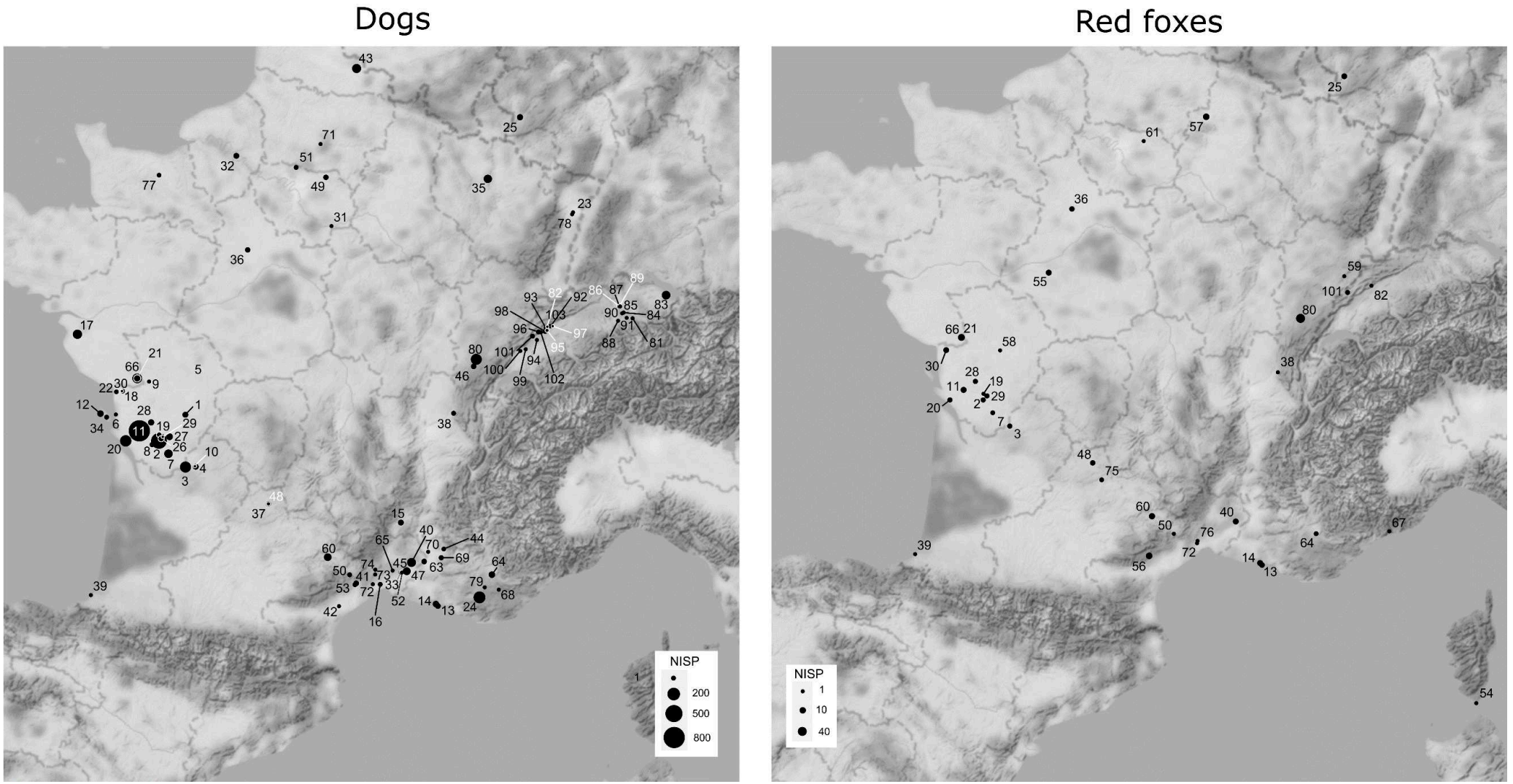

Figure 16. Remains of dogs and red foxes from the Late Neolithic in France, mainly from the I2AF database. Sites are listed in Table 9. Dot size is proportional to the number of remains (NISP) of the species of interest on the site. Where data were not available, the size is the smallest (1).

Table 9. Occurrences of dog and fox remains from the Late Neolithic in France, mainly from the I2AF database.

Country	Map code	Culture	Sites	Reference	NISP dogs	NISP foxes
France	1	Matignons	Chenommet FIII "Bellevue"	Bréhard, Beeching and Vigne, 2010	**11**	
	2	Matignons	Juillac-le-Coq "Matignons" - camps 1 et 2	Poulain-Josien, 1966	**369**	**3**
	3	Matignons	Festalemps "Bois de Fau"	Braguier, 2000	**134**	**3**
	4	Artenac	Douchapt "Beauclair"	Braguier, 1997	**10**	
	5	Artenac	Aslonnes "Camp Allaric"	Thévenin, Sainty and Poulain, 1977	**?**	
	6	Artenac	Port-des-Barques "Piedmont"	Braguier, 1997	**1**	
	7	Artenac/Peu-Richard	Challignac "le Camp"	Braguier, 1997	**55**	**2**
	8	Artenac/ Peu-Richard	Jarnac-Champagne "Mercière"	Braguier, 2000	**4**	
	9	Artenac/Matignons/Peu-Richard	Échiré "Les Loups"	Burnez, 1986	**1+**	
	10	Artenacien	Saint-Méard-de-Drône "Gros Bost"	Braguier, 2000	**1**	
	11	Artenacien/Peu-Richard	Saintes "Diconche"	Bökönyi and Bartosiewicz, 1999	**803**	**7**
	12	Artenacien/Peu-Richard	Saint-Georges-d'Oléron "Ponthezière"	Tresset, in press, Laporte, 1990, Laporte 1994 in Braguier, 1997	**18**	
	13	Couronnien	Martigues "Collet-Redon"	Durrenmath *et al.*, 2003	**6**	**1**
	13	Campaniforme	Martigues "Collet-Redon"	Durrenmath *et al.*, 2003	**2**	**3**
	14	Couronnien	Martigues "Ponteau-Gare"	Margarit, Durrenmath and Gilabert, 2002	**16**	**7**
	15	Ferrières	Chauzon "Beaussement"	Poulain-Josien, 1965	**10**	
	16	Ferrières	Saint-Aunès "Saint-Antoine" (ZAC), tranche 3	Ott *et al.*, 2008	**3**	
	17	Groupe de Kerugou	Machecoul "les Prises"	Boujot and l'Helgouach 1987 in Braguier, 1997	**75**	
	18	Matignons ; Peu-Richard	Nuaillé-d'Aunis "la Mastine"	Cassen and Scare 1987 in Braguier, 1997	**2**	
	19	Matignons et Peu Richard	Gensac-la-Pallue "Soubérac"	Poulain-Josien, 1965	**15**	**1**
	20	Matignons/Peu Richard	Semussac "Chez Reine"	Poulain-Josien 1965,1967b, 1984, Cassen 1986 in Braguier, 1997	**147**	**3**
	21	Matignons/Peu Richard/Artenac	Nieul-sur-l'Autise "Champ Durand"	Braguier, 1999b	**89**	**1**
	22	Matignons/Peu-Richard	Villedoux "le Rocher"	Braguier, 1999b et Braguier, 1997	**2**	
	23	Munzingen	Holtzheim	Kuhnle *et al.*, 1999	**1**	
	24	Néo final	Saint-Maximin-la-Sainte-Baume "Le clos de Roque"	Blaise in Remicourt *et al.*, 2014	**167**	
	25	Néolithique final+ récent	Baume de Layrou	Collonge, 2000	**13**	**6**
	26	Peu-Richard	Segonzac "Fontbelle"	Braguier, 2000	**23**	
	27	Peu-Richard	Vibrac "la Grande Plaine"	Burnez, in press, in Braguier, 1997	**23**	
	28	Peu-Richard	Authon-Ébéon "le chemin Saint-Jean"	Louboutin, Burnez and Braguier, 2003	**14**	**3**
	29	Peu-Richard	Mainxe "Montagan"	Braguier, 1997	**1**	**3**
	30	Peu-Richard/Bronze final	Longèves "Pied-Lizet"	Cassen, Scare 1987 in Braguier, 1997	**1**	**6**
	31	SOM	Marolles-sur-Seine "Gours aux Lions"	Poulain, 1984c	**1**	
	32		Val-de-Reuil "Butte Saint-Cyr"	Billard, Guillon and Verron, 2010	**10**	
	33		**Nîmes "Cadereau d'Alès"**	Hasler and Noret, 2004	**1+**	
	34		Dolus-d'Oléron "Ecuissière"	Braguier, 2009	**3**	
	35		Pagny-sur-Moselle "En Navut"	Arbogast, 1994	**51**	
	36		Lutz-en-Dunois "Eteauville"	Poulain-Josien, 1965b	**6**	**4**
	37		Thémines "grotte des Escabasses"	Braguier in Valdeyron, 1998	**5**	
	38		Grotte du Gardon (c37)	Ansermet, 1999	**3**	**1**
	39		Biarritz "grotte du Phare"	Lehnebach, 2003	**1**	**1**
	40		Le Taï	Manen, 2005	**65**	**7**
	41		Saint-André-de-Sangonis "Lagarel, A750"	Georjon *et al.*, 2007	**8**	
	42		Béziers "le Gasquinoy"	Forest in Buffat *et al.*, 2008	**1**	
	43		Valenciennes "les Lauréades"	Deckers *et al.*, 2009	**69**	
	44		Bédoin "Limon-Raspail"	Cauliez *et al.*, 2005	**2**	
	45		Mas de Vignoles IV	Hasler and Noret, 2004	**1+**	
	46		**Clairvaux-les-Lacs "Motte-aux-Magnins"**	Chenevoy and Chaix, 1985	**7**	
	47		Manduel "Fumérian"	Hasler *et al.*, 2011	**40**	
	48		Thémines "Roucadour"	Mougne, 2006	**3**	**4**
	49		Meaux "route de Varreddes"	Bémilli, 2005	**6**	
	50		Saint-Etienne-de-Gourgas	Poulain-Josien, 1972	**3**	**1**
	51		**Bury**	Salanova, 2007	**3+**	
	52	Fontbouisse	Caissargues "Moulin Villard"	Carrère and Forest, 2003	**1+**	
	53	Fontbouisse	Cambous	Poulain 1978b in Carrère and Forest, 2003	**3**	
	54		Bonifacio "Araguina-Sennola"	Vigne, 1988		**1**
	55	SOM	Sublaines "Dolmen de Villaine"	Poulain, 1972		**7**
	56		Grotte de Camprafaud (C7-C8)	Poulain, 1985		**7**
	56		Grotte de Camprafaud (C3)	Poulain, 1985		**4**
	57	SOM	Tinqueux "l'Homme mort"	Thérèse Poulain, 1984c		**11**
	58	Peu-Richard/Artenac	Sainte-Soline "Montiou"	Guinot in Germond, Bizard and Guinot, 1987		**1**
	59		Bretonvillers "Roche-Chêvre"	Baudais *et al.*, 1993		**1**
	60	Treilles (groupe des) / Chalcolithique	Saint-Rome-de-Cernon "grotte 1 de Sargel"	Erroux and Poulain, 1984	**37**	**9**
	61		Vignely "la Noue Fenard" str 264	Brunet *et al.*, 2020		**1**
	63	Campaniforme	Avignon "La Balance - Rue ferruce", C9-10-11-12	Helmer, 1979	**7**	

	64	Campaniforme	Montagnac-Montpezat "La grotte murée" C6-C7	Helmer, 1979	**18**	**2**
Country	**Map code**	**Culture**	**Sites**	**Reference**	**NISP dogs**	**NISP foxes**
	65	Campaniforme	Saint-Côme-et-Maruéjols "Bois Sacré"	Poulain, 1974	**1**	
	66	Campaniforme	Nieul-sur-l'Autise "Pierre levée"	Thérèse Poulain, 1979	**42**	**14**
	67	Campaniforme	Castellar "Abri Pendimoun"	Binder, 2002		**1**
	68		Fontbregoua "Baume"	Helmer, 1979	**1**	
	69		Venasque "Capty"	Helmer, 1979	**4**	
	70		Courthézon "Plaine des blancs"	Helmer in Muller *et al.*, 1986	**1**	
	71		Compiègne "Gord"	Méniel, 1984a	**1**	
	72		Grabels "Gimel"	Poulain-Josien, 1957	**1**	**1**
	73		Saint-Mathieu-de-Tréviet "le Lébous"	Carrère and Forest, 2003	**1+**	
	74		Claret "Rocher du Causse"	Carrère and Forest, 2003	**1+**	
	75		Saint-André-de-Cruzières "grotte Chazelles"	Favrie, 2003		**2**
	76		Saint-Gély du Fesc "Les Vautes"	Carrère and Forest, 2003		**1+**
	77		Bretteville-le Rabet	Arbogast, 1989	**2+**	
	78		Entzheim "Aeropark"	Croutsch *et al.*, 2007	**1+**	
	79		Chemin de Barjols	Gourichon in Cockin and Furestier, 2009	**1+**	
	80	Clairvaux	**Chalain station 19**	Pétrequin *et al.*, 2002	**3+**	
	80	Clairvaux	**Chalain station 3**	Arbogast, 1997	**16**	**29**
	80	Horgen	**Chalain station 3**	Arbogast, 1997	**113**	**11**
Switzerland	81		PfäffikonBurg	Deschler-Erb and Marti-Grädel, 2004	**1+**	
	82	Horgen	**Twann UH MH OH**	Arbogast, Jeunesse and Schibler, 2001	**1+**	**1+**
	83	Horgen	Arbon-Bleiche 3	Deschler-Erb and Marti-Grädel, 2004	**58**	
	84	Horgen/Cordé	Feldmeilen vor. 4-3-1-1y-1x	Deschler-Erb and Marti-Grädel, 2004	**1+**	
	85	Horgen/Cordé	Seefeld 4-3-2-F-E-D-C/B-A	Arbogast *et al.*, 2005	**1+**	
	86	Horgen/Cordé	Pressehaus G-E-C2	Arbogast *et al.*, 2005	**1+**	
	87	Horgen/Cordé	Mythenschloss 3 -2.4- 2.2-3 -	Arbogast *et al.*, 2005	**1+**	
	88	Horgen/Cordé	Zug-Schützenmatt	Arbogast *et al.*, 2005	**1+**	
	89	Horgen/Cordé	Mozart Str. 3u-3a-3o-2u-2o	Arbogast *et al.*, 2005	**1+**	
	90	Horgen/Cordé	Scheller S4-S3	Arbogast *et al.*, 2005	**1+**	
	91	Horgen/Cordé	Sennweid S5-S4	Arbogast *et al.*, 2005	**1+**	
	92	Horgen Port Conty	Lattrigen VI	Arbogast *et al.*, 2005	**1+**	
	93	Horgen occidental	Neuveville-Schaffis	Arbogast *et al.*, 2005	**1+**	
	94	Horgen occidental	Portalban les Grèves	Arbogast *et al.*, 2005	**1+**	
	95	Horgen occidental	Lüscherz-Binggeli	Arbogast *et al.*, 2005	**1+**	
	96	Horgen occidental	Saint-Blaise Dames 9	Deschler-Erb and Marti-Grädel, 2004; Arbogast *et al.*, 2005	**1+**	
	97	Horgen occidental	Nidau 3	Arbogast *et al.*, 2005	**1+**	
	98	Lüscherz Suisse occ	Vinelz 1960	Arbogast *et al.*, 2005	**1+**	
	99	Lüscherz Suisse occ	Yvonand IV	Arbogast *et al.*, 2005	**1+**	
	100	Lüscherz Suisse occ	Yverdon Garage-Martin, c11-12	Arbogast *et al.*, 2005	**1+**	
	96	Lüscherz Suisse occ	Saint-Blaise Dames 7	Arbogast *et al.*, 2005	**1+**	
	101	Lüscherz Suisse occ	Auvernier "Brise Lames"	Deschler-Erb and Marti-Grädel, 2004; Arbogast *et al.*, 2005	**1+**	
	102	Lüscherz Suisse occ	Pont-de-Thielle	Arbogast *et al.*, 2005	**1+**	
	95	Lüscherz Suisse occ	Lüscherz-Dorf, äus. Stat	Arbogast *et al.*, 2005	**1+**	
	101	Auvernier/Cordé Suisse occ	Auvernier	Stampfli 1976b in Marti-Grädel and Stopp, 1997		**1+**
	101	Auvernier/Cordé Suisse occ	Auvernier-La Saunerie	Arbogast *et al.*, 2005	**1+**	
	98	Auvernier/Cordé Suisse occ	Vinelz-Hafen	Arbogast *et al.*, 2005	**1+**	
	103	Auvernier/Cordé Suisse occ	Sutz-Rütte	Arbogast *et al.*, 2005	**1+**	
	98	Auvernier/Cordé Suisse occ	Vinelz-Alte Stat, NW	Arbogast *et al.*, 2005	**1+**	
	96	Auvernier/Cordé Suisse occ	St-Blaise Bain Dames Auvernier-E-F-G-H	Arbogast *et al.*, 2005	**1+**	

Conclusion

Concerning the evolution of the occurrence of dog remains from the Mesolithic to the pre-Bronze Age in Western Europe and in Romania, the following key points emerge:

KEY POINTS – dogs

In South-Eastern Romania, dog remains are more abundant in the later periods, especially in the Gumelnița culture.

In Western Europe, the trend is the same. The importance of dogs in archaeological sites from the Mesolithic to the pre-Bronze Age increases over time, which has already been suggested by some authors (Arbogast, 1995). They are little represented in the Mesolithic and Early Neolithic, but the number of remains explodes in the Middle Neolithic, with the presence of many complete skeletons in connection or, on the contrary, isolated bones in food refuses (see section 2.3).

About the evolution of the occurrence of red foxes remains from the Mesolithic to the pre-Bronze Age in Western Europe and in Romania, the following key points emerge:

KEY POINTS – red foxes

Red foxes are poorly represented in sites from the Mesolithic to the pre-Bronze Age, in both Western Europe and Romania. This is due to several reasons. First, fox remains may have not always been correctly identified (some were only identified as Canidae without further precision). Moreover, it also illustrates a reality of the material: foxes are not very frequent in excavated sites. This is explained by the natural behavior of the fox: it tends to keep a distance from human settlements and is therefore unlikely to be found in food waste. Accordingly, studying fox remains for comparative purposes with dogs needs a lot of time and energy, which may have discouraged zooarchaeologists.

Interestingly, the percentage of fox remains tends to decrease over time, which is particularly evident in some Neolithic stratified sites. For example, at Gazel and Camprafaud, the percentage of red fox remains is maximal at the Early Cardial Neolithic, to become zero during the Epicardial and remains either very low (Camprafaud) or null (Gazel) in later periods (Vigne, 1988). The same can be observed in the stratified site of Fontbrégoua or the 'grotte de l'Eglise' (Helmer, 1979). This trend is confirmed when looking at other Early Neolithic sites such as 'Eglise supérieure", or even Late Neolithic sites such as 'la grotte Murée' (Helmer, 1979; Vigne, 1988).

2.3. The place of canids in European societies of the pre-Bronze Age

In this section, we use the information collected in the previous section (2.2) to document the variability of status conferred by protohistoric humans to canids in the chrono-geographic range relevant for our study. We do so by assessing the impact of the transition from a predation economy (Mesolithic) to a production economy based on agriculture (Neolithic) in Western Europe and Romania. In this section we do not aim to be exhaustive. We only provide a few examples, by recalling some of the sites listed in section 2.2. This will give a global framework to the corpus we studied in the Conclusion and discussion of Part 2 and perspectives for Part 3, and will bring to light some major questions we will raise in conclusion of this Part 1, and that we will try to answer in Part 3.

One of the major problems when looking at foxes in archaeological contexts is the lack of data. Not only are the remains scarce, but information on the skeletal parts is far from being systematically provided. Anthropogenic marks are only exceptionally mentioned in publications of archaeozoologists. The interpretation of red fox remains is also particularly tricky because it is a digging animal (like a badger) that can simply and relatively frequently be intrusive, especially in cave sites, as highlighted it in the previous section. It is then essential to look more closely at the skeletal parts that have been excavated and at possible anthropogenic marks, and to look at the species which are associated with the fox (hunted species, furbearing species, humans). In the case of the simultaneous presence of several diggers, either the site was used for a long time as a burrow/hole, or the site testifies to a specialized hunting of animals for fur (Mallye, 2007). It is not uncommon to find several associated commensal animals (notably foxes and badgers), as badger dens may serve as a den for foxes (San, 2002; Mallye, 2007). This is a real issue because the remains can be either contemporary to humans, or the deposit could have been made more recently, after humans abandoned the site. It then is difficult to replace the remains in a reliable chrono-cultural context and to interpret their status with certainty. For example, in the case of a complete skeleton, the fox can either be considered as intrusive (it can be either sub contemporaneous to the other structures or much posterior in time) or as being intentionaly buried by humans (Fosse, 1988).

2.3.1. The omnipresence of dogs in the life and mental representations: evidence from art

The cultural importance of the dog is underlined by the representations of this animal in the art. Dogs are depicted on the walls of tombs since the earliest Neolithic periods. For example, the famous sculptures/engravings at Göbekli Tepe from the early PPNA/PPNB depict cats, cattle, snakes and pigs, as well as dogs (Klaus Schmidt, 2010; Zalai-Gaál *et al.*, 2011). Dogs and foxes are also represented on ceramics or dishes, with engravings (e.g. at Hallan Çemi Tepesi), sculturing (e.g. at Codžadermen VI in Gorni Pasarel during the Karanovo-Gumelniţa culture, or at Vinča where a four-legged container probably representing a dog was found) or even paintings (e.g. Gimbutas, Zalai-Gaál *et al.*, 2011). Another example consists of tiny argile sculptures representing dogs in the Lengyel culture, or in the Chalcolithic levels of Großwardein-Salca ("Herpály-Salca", Zalai-Gaál *et al.*, 2011). These representations reinforce the idea that canids were omnipresent in protohistoric human life and they attest to the overall perception of the dog's spiritual qualities in human communities (Zalai-Gaál *et al.*, 2011).

2.3.2. Commensal animals living close to humans, or even daily allies

Dogs were probably wandering around settlements and likely took advantage of the garbage left by humans. Canine coprolites and traces of chewing on human food wastes are often found in sites from the Epipaleolithic (Natoufian sites in the Northern and Southern Levant, Vigne and Guilaine, 2004) or Early Neolithic in Europe (Poplin, 1975; Arbogast, 1989; Horard-Herbin, Tresset and Vigne, 2014). This attests to the presence of live dogs, even when their bone remains are rare, Neolithic dogs may have acted like 'garbage collectors' around the villages.

In addition, mixed diets in dogs and humans are attested to since the Mesolithic as evidenced by isotope analysis of Mesolithic dogs in the Iberian Peninsula (7,903-7,570 years cal. BP). This revealed that dogs included a high percentage of aquatic food in their diet, similar to humans (Grandal-d'Anglade *et al.*, 2019). Similar evidence exists for many Neolithic sites in France, China, Anatolia and in the Iberian Peninsula (e.g. Pechenkina *et al.*, 2005; Guiry, 2012; Le Bras-Goude, Herrscher and Vaquer, 2013; Pearson *et al.*, 2015). Later, the introduction of cereals and pulses in the human diet likely encouraged dogs (and probably red foxes) to stay close to human groups, as they could fed on it and gained time and energy to obtain food. This is supported by genetic analyses of Neolithic and Chalcolithic dogs, revealing the acquisition of the ability to digest starch (Ollivier *et al.*, 2016) and isotope analyses on late Neolithic dogs and foxes from the Iberian Peninsula, revealing that both canids had anthropogenic diets (Grandal-d'Anglade *et al.*, 2019).

This type of commensal relationship is higly plausible, considering that it is commonly observed in indigenous societies traditionally living with dogs (Digard, 2006), such as among the Sentinels (Figure 17). The Sentinels are a hunter-gatherer tribe that has been living in autarky on the North Sentinel Island in the Andaman Islands, an archipelago in the Indian Ocean, for around 50,000 years. Their African ancestors are believed to have colonized the island about 50,000 years ago. Some geneticists consider them to be the direct descendants of the first humans to colonize Asia in the Paleolithic, before the invention of agriculture (Endicott *et al.*, 2003).

Figure 17. Jarawa hunter-gatherers and their dogs (from https://www.ouest-france.fr/)

Moreover, dogs may have been allies in hunting, for guarding the settlements against wolf attacks and for herd control, especially in agricultural societies where hunting was not a crucial activity anymore, as deduced from ethnographic information (Coppinger and Schneider, 1995; Albizuri *et al.*, 2019). They may even have been appreciated for companionship. However, these roles are difficult to demonstrate based on archaeological data (Digard, 2006; Horard-Herbin, Tresset and Vigne, 2014). However, some archaeological fndings provide clues. We indeed observed in section 2.2 that during the Early Neolithic, dog remains were rare in habitat structures. Additionally, sometimes no cut marks or evidence for cynophagy is obvious. It is thus likely that the dog had a function other than food (Bedault, 2012) or other economic roles (Arbogast, 1995). It may have had a privileged status, perhaps "already playing its role as a herdsman and companion", as suggested by Poplin (1975). In the Late Neolithic at Diconche (Artenac, Peu-Richard), dogs were mostly old animals, suggesting that they were not bred primarily for their meat, but maybe rather as associates for hunting and/or herding and housekeeping (Braguier, 1997; Bökönyi and Bartosiewicz, 1999).

Archaeological remains rarely allow us to conclude on the function occupied by the canids during their lifetime and the hypotheses advanced can hardly be definitively proven. We know much more about their use after their death, thanks to osteoarchaeozoology.

2.3.3. Use as raw material

Canids (both domestic and wild) have been intensively used as raw material in all periods since the Paleolithic, for their fur or for the manufacture of ornaments or symbolic objects.

2.3.3.1. *Fur*

There are several archaeozoological indications of pelting activity (Helmer, 1992; Arbogast *et al.*, 2005). Among them are: the selective presence of certain parts of the skeleton which are likely to remain attached to the skin after skinning (skull, caudal vertebrae and extremities of the limbs, i.e. phalanges, metapodes), the presence of specific cut marks (the most explicit marks being located on the less fleshy parts, where the skin is in direct contact to the bone, e.g. on the metapodes, just above and around the muzzle, or on the rostro ventral border of the mandible), and the presence of other fur species. However, these indicators are often confusing and fur exploitation can rarely be definitively proven. Indeed, skinning marks are often slight and difficult to discern, and not highly specific to skinning. In many cases, cut marks suggest that both fur and meat were collected jointly likely not to spoil ressources.

Skinning marks are frequently attested in wild species (foxes and wolves) in all periods, but it is not clear wether skinning preceeded the recuperation of the fur only, or if the flesh was also eaten.

A few cases suggest fur use in dogs as soon as the Upper Paleolithic. For example, skinning marks are visible on the dog remains of Pont d'Ambon (Pionnier-Capitan *et al.*, 2011) and Hauterive-Champréveyres (Studer, 1989 cited in Arbogast *et al.*, 2005). Evidence has also been found on dogs of other sites from Western Europe (see Pionnier-Capitan *et al.*, 2011) and in Romania (see Bălăşescu, Radu and Moise, 2005; Pionnier-Capitan *et al.*, 2011). For example, skinning marks have been observed in sites dated to the Vinča, Dudeşti, Boian and Gumelniţa cultures.

2.3.3.2. *Ornaments*

Some elements of the skeleton could be used as ornamental objects, such as canines (e.g. in **Twann** and in Pfulgriesheim, Arbogast in Meunier, Sidéra and Arbogast, 2003; Mallye, 2007; Figure 18A), metapodial elements (e.g. in **Chalain 4,** Maréchal *et al.*, 1998, Figure 18B; and in **Twann**, Schibler, 1981), or even mandibles (e.g. in Sultana, Romania, Lazăr, Mărgărit and Bălăşescu, 2016, Figure 18C).

This use of canid teeth/bones to make pendelocks was very widespread since the Upper Paleolithic, and does not seem to be representative of a given cultural context (Braguier, 1997; Arbogast in Meunier *et al.*, 2003).

The distinction between bones or teeth of foxes and dogs can be difficult when fragmented, but the literature suggests that wild animals would have been used preferentially. However, sometimes, although rather rare, the dog was privileged. This was notably the case at the end of the Neolithic period in the French and Swiss lakeside settlements (Arbogast *et al.*, 2005). Indeed, perforated canines of canids (foxes, dogs or wolves, sometimes associated) gained importance among the pierced teeth, dogs being given a prominent position (dog and bear predominated, followed by fox, wolf, badger and wildcat, Maréchal *et al.*, 1998). The same

goes for the use of metapods during the late Cortaillod in Western Switzerland sites (Maréchal *et al.*, 1998). At **Chalain 4**, for example, a group of pierced metatarsals and metacarpals were assigned to both domestic (dog) and wild (fox) canids (Maréchal *et al.*, 1998, Figure 18B). Additionally, the use of dogs for ornaments or manufactured objects was rare but well documented throughout the Neolithic to the Bronze Age, for example in Hungary (Vretemark and Sten, 2010; Horard-Herbin, Tresset and Vigne, 2014) and Romania (Lazăr, Mărgărit and Bălăşescu, 2016, Figure 18C).

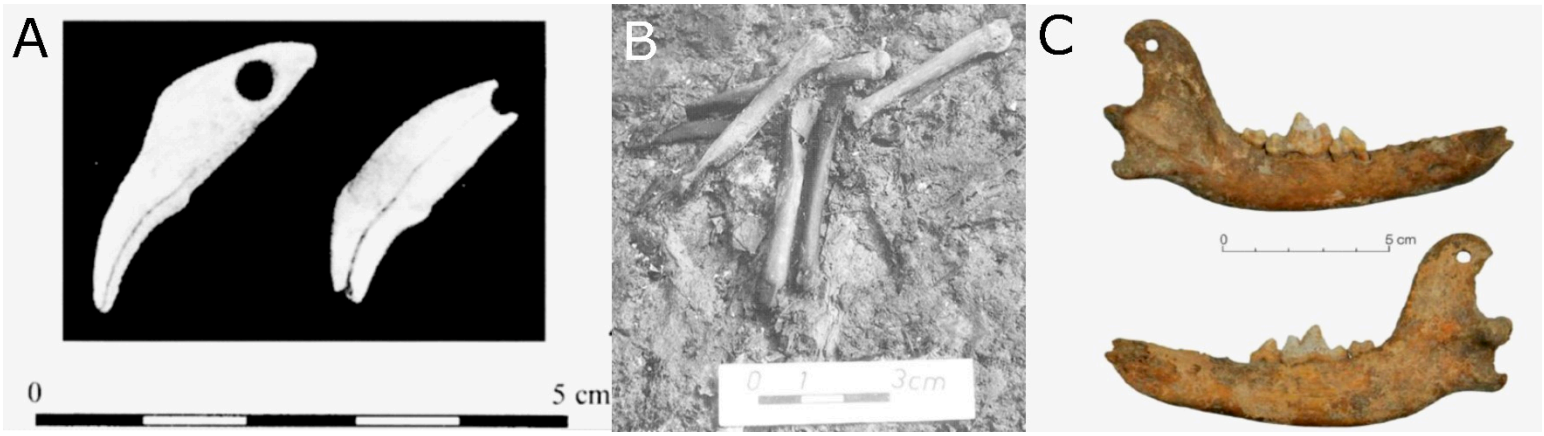

Figure 18. Use of canid teeth and bones as ornaments.
A: Pierced canines of canids, used as pendelocks, Pfulgriesheim, France, Entzheim group (limit between Middle and Late Neolithic), from Meunier *et al.* (2003).
B: Grouping of dog and fox pierced metapodes, Chalain 4, Switzerland, Late Neolithic, 3,000 BC, from Maréchal *et al.*, 1998.
C: Pierced dog mandible used as a pendelock, Sultana, South-Eastern Romania, Chalcolithic, Gumelnița culture, from Lazăr, Mărgărit and Bălăşescu (2016).

Decoratively modified dog bones or teeth were sometimes placed with human burials (Morey, 2006). This was a widespread custom in the LBK, and was already attested in the Mesolithic Vedbaek in Denmark (Zalai-Gaál *et al.*, 2011). These ornamental objects are indeed often excavated in sites of high symbolic power or in sepultures. The authors have given these objects a cultural or religious significance, particularly when they are found in a funerary context (Braguier, 1997). A symbolic significance is provided to these objects when they are distinguished from the "statistical inventory of the fauna consumed" (Leroi-Gourhan and Bernot, 1988) and when the choice does not appear to be related to the abundance of the species hunted, and therefore not directly related to survival (Taborin, 2004), or a trophy or magic value related to hunting (amulet), especially when wild animals are favoured (Arbogast *et al.*, 2005). They could also be objects of exchange, identity markers, etc. (Arbogast *et al.*, 2005). The increased use of the dog is likely more closely linked to its symbolic role, since hunting activities (and accordingly the involvement of dogs in these activities) were limited in late periods (Arbogast *et al.*, 2005).

2.3.4. Dog burials or dogs directly associated with human burials

Complete or almost complete dog skeletons can sometimes be found in connexion which may suggest special care towards the animal body. In many locations distributed worldwide, since the Mesolithic and throughout the Holocene, canids, and especially dogs, have been buried more or less closely to deceased people. This warrants some particular consideration and perhaps even provides evidence for an affectionate rather than a gastronomic relationship between humans and dogs (Davis and Valla, 1978a).

Humans sometimes treat other animals in such a fashion (wild animals of economic use such as the reindeer have figured into the sacrificial practices of ancient humans as well), but not as often as dogs (Morey, 2006). Unique care was devoted to this species for the past 12-14 kyrs (see Table 1 in Morey, 2006). Before the Epipaleolithic, dog burials are unknown.

These descoveries raise the question of the status of these animals and their possible symbolic association with the dead: were they considered as offerings or did they correspond to authentic dog burials? The conclusion often remains difficult to establish. These findings do not inherently reflect the status of these animals as friends, especially taking into account the frequency with which dogs were sacrificied before being placed with (sometimes sacrificied) humans (Morey, 2006).

According to Larsson (1990), there are three different contexts for dog burials, that have different symbolic significance:

- the skeleton is complete and associated with a human skeleton[j], such a bond reflecting how people perceived dogs and gave them spiritual qualities, maybe even wanting to continue the association in the spirit world (Morey, 2006);
- only a part of the skeleton is buried associated with a human skeleton;
- the skeleton is complete and isolated (this is the most frequent situation according to Morey, 2006). Skeletons of complete canids are sometimes accompanied by objects and can therefore be interpreted as ritual deposits, offerings addressed to higher entities (Larsson, 1990).

The literature reveals that singular and different practices took place from the Epipaleolithic to the Bronze Age. We will therefore come back to some of the major discoveries in the following pages.

[j] The presence of lithics and/or worked bone can replace that of a human skeleton (Larsson, 1990).

2.3.4.1. *Epipaleolithic and Mesolithic*

The dog had already considerable symbolic significance for hunter-gatherers. Indeed, dog burials are known from the Near-Eastern Natufian (10–8 kyrs BC, Davis and Valla, 1978b; Tchernov and Valla, 1997) or in the European Mesolithic (Larsson, 1990).

In the Near-East, associations between dogs and humans indicate a close relationship between them at very early stages, likely more akin to an affective relationship than to a gastronomic one. For example, in the Natufian site (around 12-10 kya BP) of Ain Mallaha in the Near East, a puppy of 4-5 months was found clearly associated with a human burial with the person's hand lying on the body of the animal (Davis and Valla, 1978b; Tchernov and Valla, 1997, Figure 19). One grave from Hayonim Terrace (Late Natufian, 11th millennium BC) contained the skeletal remains of three humans and two complete dogs.

Figure 19. Tomb H.104 at Mallaha, showing the human skeleton and puppy.

In Northern Europe, the Mesolithic site of Skateholm in Sweden, dated to around 5 kya BC, is particularly remarkable (Larsson, 1990, 1994). Dogs were sometimes placed in human graves next to human bodies (in one case, the dog was even likely sacrificed before being buried with the person, as its neck was broken), or sometimes dismembered. Finally, in other cases, dogs were placed in authentic sepultures, all grouped together in a well-defined area. Their bodies were accompanied by occasional deposits, some of these burials being even more richly furnished than most human graves. Post-inhumation manipulations similar to humans are attested on some dog bodies, suggesting that the same symbolism may have applied to both humans and dogs. Other cases are attested in Mesolithic Denmark and the Netherlands (e.g. Larsson, 1990; Kannegaard Nielsen *et al.*, 1993; Verjux, 2004; Louwe Kooijmans, 2011).

Similar practices have been documented in hunter-gatherer populations in Asia, North America and Australia (Hasler and Noret, 2004).

Interesting cases are also known during the Mesolithic in the Iberian Peninsula. For example, in the Muge shell-middens (Cabeço da Arruda, Portugal), some 200 human skeletons have been excavated, as well as canid remains (including an almost complete dog) without evidence of cut or burn marks or fractures, suggesting that dogs were probably not consumed but buried intentionally, although there is no direct association with a human burial (Detry and Cardoso,

2010; Pires *et al.*, 2019). In Poças de São Bento (Sado Valley), human graves have been found as well as a dog burial, and the authors suggested the dog may have been deliberately buried, perhaps as part of a ritual (Arias *et al.*, 2015; Pires *et al.*, 2019).

At the Iron Gates, in Serbia, associations between human skeletons and fragments of dog skeletons are also found during the Mesolithic. In Lepenski Vir, skeletons of men were associated with dog skulls, while a dog without skull was associated with a woman (Zalai-Gaál *et al.*, 2011). On the same site, whole parts of dog skeletons were found correctely connected, suggesting that the dog may have served as a sacrificial animal (according to Bökönyi in Bălăşescu, Radu and Moise, 2005; Zalai-Gaál *et al.*, 2011).

2.3.4.2. *Early Neolithic in Western Europe*

Interestingly, during the the Early Neolithic in Eastern and Western Europe, dog burials are almost inexistant. A very special site at this period is **Herxheim** (LBK, Germany). Human remains testify of a very singular treatment of the human body, and cannibalism has been demonstrated. More than 200 dog remains, associated with these human remains, have been excavated. They correspond mostly to skeletal segments, belonging to at least thirteen animals. They showed burn or cut marks (Figure 72), but no fracture (to collect bone marrow), contrary to the other taxa. These dogs were eaten and the anthropogenic marks testify to a special treatment of the carcasses (roasting, skull removal) whose aim remains unknown (Arbogast, 1989; Zeeb-Lanz *et al.*, 2009). This confirms the very special relationship between humans and dogs at these early periods.

2.3.4.3. *Middle Neolithic in Western Europe*

In later periods of the Neolithic in Western Europe, complete skeletons in connection are relatively frequent, particularly during the Chasséen in Southern France. Dog deposits in funeral and habitat contexts are indeed a cultural component of the Southern Chasséen (Loison and Schmitt, 2009). These descoveries raise several questions: were these burials authentic dog burial, or were they offerings (Hasler and Noret, 2004)?

Sites where dogs and humans are directly associated

Sometimes, dogs are closely associated with humans, maybe illustrating a greater closeness between them (Arbogast *et al.*, 2005).

For example, in the necropolis dated to the early Chasséen of **"Le Crès"** in Béziers**,** one grave associate a complete dog in connection with a human (SP13, Amt 107). They are deposited top to tail, opposite each other in the pit (Loison, Fabre and Villemeur, 2003; Loison and Schmitt, 2009). In parallel, seven complete dogs in connection but isolated have been found buried in three pits (Loison and Schmitt, 2009). These dogs were given funeral treatment identical to humans.

In Obernai, the skeletons of four complete dogs were found on the same level and in strict contact with the remains of two children (Guthmann, Lefranc and Arbogast, 2016). They probably belong to the Grossgartach or Roessen occupation (Middle Neolithic) of the site.

More or less complete and connected canids were also found associated with human deposits at the Chasséen sites of "la Bastidonne" at Trets and "les Martins" at Roussillon (D'Anna, 1993; Vaquer, 1998).

Sometimes, the contemporaneity of the human and dog deposits is not assured. For example, more than 10 dog skelettons were found associated with human deposits at Arnaville "Le Rudemont" during the Michelsberg culture (Thévenin, 1981; Blouet *et al.*, 1984; Arbogast *et al.*, 1989). However, the direct association could not be verified and many cut marks were observed on the bones, rendering the hypothesis of a burial of the complete bodies unlikely. Another hypothesis is the deposit of dogs or part of dogs as inventory offerings. Another example is at **"Les Moulins"** in Saint-Paul-Trois-Châteaux (Late Chasséen), where a pit containing the grave of an adolescent girl also yielded some scattered remains of a dog with cut marks, but the dog remains are unlikely to come from the same stratigraphic unit than the human (Crubézy, 1991; Beeching and Crubézy, 1998; Bréhard, 2007).

Complete dogs in connexion but isolated, in sites that yielded human burials

Sometimes, complete dog skeletons are excavated in contemporaneous but distinct structures than those that yielded human burials.

For example, at **"Le Pirou"** in Valros (early Chasséen, dated to the second half of the 5th millennium cal. BC), 10 funerary pits with complete (or almost complete) dog skeletons have been excavated in a habitat context, besides pits with human remains (Gandelin, unp. report 2015, Figure 20).

Figure 20. Complete dog skeleton in a pit in Le Pirou at Valros, early Chasséen, second half of the 5th millennium cal. BC (from https://multimedia.inrap.fr/)

In a pit in **"Cadereau d'Alès"**, two complete canid skeletons from the early Chasséen were discovered, laying on a pile of stones (Hasler and Noret, 2004, Figure 21). The position of the two bodies may suggest that they were intentionally deposited rather than simply dumped in the pit. However, no internal elements in the pit neither physical links between this structure and the individual human burial one metre away allow to prefer either of these hypotheses (Hasler and Noret, 2004).

Figure 21. Dog skeletons from pit 1094 of Cadereau d'Alès, early Chasséen (Photo by Vianney Forest in Hasler and Noret, 2004)

At **"Mas de Vignoles IV"**, several dog skeletons were exhumed (Jallot, 2004). One is attributed to the Chasséen, another to the Late Neolithic Fontbouisse, but most of them can not be attributed to a precise chrono-cultural period (Hasler and Noret, 2004).

In the site "jardins de Vert-Parc" at Castelnau-le-Lez, a pit provided the remains of four dogs (early Chasséen, Vignaud, 2003). Similar deposits were recorded on the site of "les Plots" at Berriac (early Chasséen, Vaquer, 1998). At these sites pits with human skeletons have also been excavated.

At Boury-en-Vexin "Le Cul froid" (Northern Chasséen), three young adult dogs, including one complete, were excavated among the exceptional animal deposit layer of the ditch; these deposits have been interpreted as having a religious function (Méniel, 1987).

Other dog burials in sites where human burials have been excavated are reported in the Middle Neolithic 1, notably at "Chemin de Barjols" (pit FS1069, 4,800-4,400 BC, Cockin and Furestier, 2009; Remicourt *et al.*, 2012) and likely in Clos-de-Roque at Saint-Maximin-la-Sainte-Baume (Cockin and Furestier, 2009; Remicourt *et al.*, 2012, p. 267).

There are also finds from the Michelsberg culture. For example:

- at Rosheim "Sablière Maetz": two complete dog skeletons in connection – an adult male and a puppy –, were found in a pit (Poulain in Thévenin, Sainty and Poulain, 1977, p. 619);
- at Rosheim "Leimen" (ST87, Michelsberg/Munzingen): the complete skeleton of an old female dog was placed in a position that seemed to indicate "careless handling, as if the animal had been lifted by its legs to be placed in the pit on its back, head first" (Arbogast *et al.*, 2013). No anthropogenic marks were noticed. Three human adults and a child were found in separate structures;
- in Vendenheim "The Gates of the Kochersberg", where a dog was placed in a pit and a child was placed on top after filling, the deposits being clearly separated in time (Lefranc *et al.*, 2015).

Interestingly, no complete dog skeleton was found during the Middle Neolithic (mainly Cortaillod culture) in French or Swiss lakeside settlements (Arbogast *et al.*, 2005).

At the end of the Middle Neolithic, cases are known in Germany, for example in Regensburg "Kumpfmühle" (Münchshöfen culture, 4,6-4,2 kyrs BC). A complete dog in connection was found mixed with the remains of four anatomically disordered humans and a pig (Lichardus and Lichardus-Itten, 1985; Meixner, 2009; Bánffy, 2017).

There are also cases in the Iberian Peninsula (Villalba, 1999; Martín Cólliga *et al.*, 2005; Albizuri *et al.*, 2019) and Northern Italy (Beyneix, 2003; Hasler and Noret, 2004; Bernabò Brea *et al.*, 2010) in the Middle Neolithic (from the end of the 5th millennium BC). The presence of dogs was interpreted as a stereotyped ritual activity and an evidence of accompanying offerings. The significant number of cases would be related to the development of ceremonial activities based on dog sacrifice. These persisted for hundreds of years in different cultural environments, even during the Chalcolithic and the Bronze Age. Interestingly, the isotopic analyses conducted by Albizuri *et al.* (2019) suggested that most of these dogs shared their diet with human communities.

2.3.4.4. *Late Neolithic in Western Europe*

At the end of the Neolithic period dog burials were still evidenced in Southern France although they seem less frequent than during the Middle Neolithic.

Among cases of complete dogs clearly associated with humans in a funerary context, one can mention the Late Neolithic occupation of **"Cadereau d'Alès"**. In the tomb 1213 of the funerary complex 1070, the skeleton of a dog was found located about 40 centimetres from the skeleton of a child, arranged on the same plane and in the same orientation (Hasler and Noret, 2004). In **"Mas de Vignoles IV"** as well, a dog skeleton was found under a human body from which it was isolated only by a few slabs (Hasler and Noret, 2004). In the site "Aeropark" in Entzheim, a dog was buried about 15 centimeters above the skull of an adult man in a pit dated to the Late Neolithic (3,800-3,640 cal. BC, Croutsch *et al.*, 2007, p. 233).

In “Chemin de Barjols”, complete dog skeletons were also found during the Late Neolithic, additionally to the dog burial dated to the Middle Neolithic (pit 1057, Gourichon in Cockin and Furestier, 2009). In Bretteville-le Rabet, a pit yielded dog skeletons (from an adult and a juvenile, Arbogast *et al.*, 1989) but we could not verify the presence of human remains at the site.

We also find complete or partial dog skeletons in the habitat zone, outside the sepulture settings, in Diconche, Champ Durand (Braguier, 1997), Feldmeilen, PfäffikonBurg, Auvernier Brise Lames, Saint-Blaise and Arbon-Bleiche 3 (Figure 22, Deschler-Erb and Marti-Grädel, 2004). At **Chalain 19** (Switzerland), the skeletons are on the contrary located at the periphery of the habitat zone, suggesting that they correspond to an evacuation of naturally dead animals (Arbogast *et al.*, 2005).

Figure 22. Dog skeleton elements in anatomical proximity in Arbon-Bleiche 3. From Arbogast *et al.*, 2005.

2.3.4.5. *Neo-Chalcolithic in Eastern Europe*

Interestingly, in South-Eastern Romania, no complete dog skeleton has been excavated, neither for the Neolithic nor for the Chalcolithic period (Bălăşescu and Radu, 2004; Bălăşescu, Moise and Radu, 2005; Bălăşescu, Radu and Moise, 2005; Lazăr, Mărgărit and Bălăşescu, 2016; Bălăşescu *pers. comm.*). However, complete dog skeletons closely associated with humans or isolated in stuctures in sites that yielded human burials are known in geographically close areas, as for example in Hungary, since the Vinča culture. Dogs where also sometimes used as offering deposits in these neighboring areas (Lazăr, Mărgărit and Bălăşescu, 2016).

Remains of more or less complete dogs (sometimes only the skull) associated with humans or objects can also be found in sites of the Late Neolithic Lengyel culture or from the contemporary neighbouring cultures in Hungary and Central Europe (cf Zalai-Gaál *et al.*, 2011). For example, at the site of Alsónyék-Bátaszék in Hungary**,** during the Lengyel occupation (first half of the 5th millenium cal. BC), complete dog skeletons or skulls were discovered beside the deceased (Zalai-Gaál *et al.*, 2011, Figure 23; Osztás *et al.*, 2016). We observe deposits very similar to those from the Chasséen.

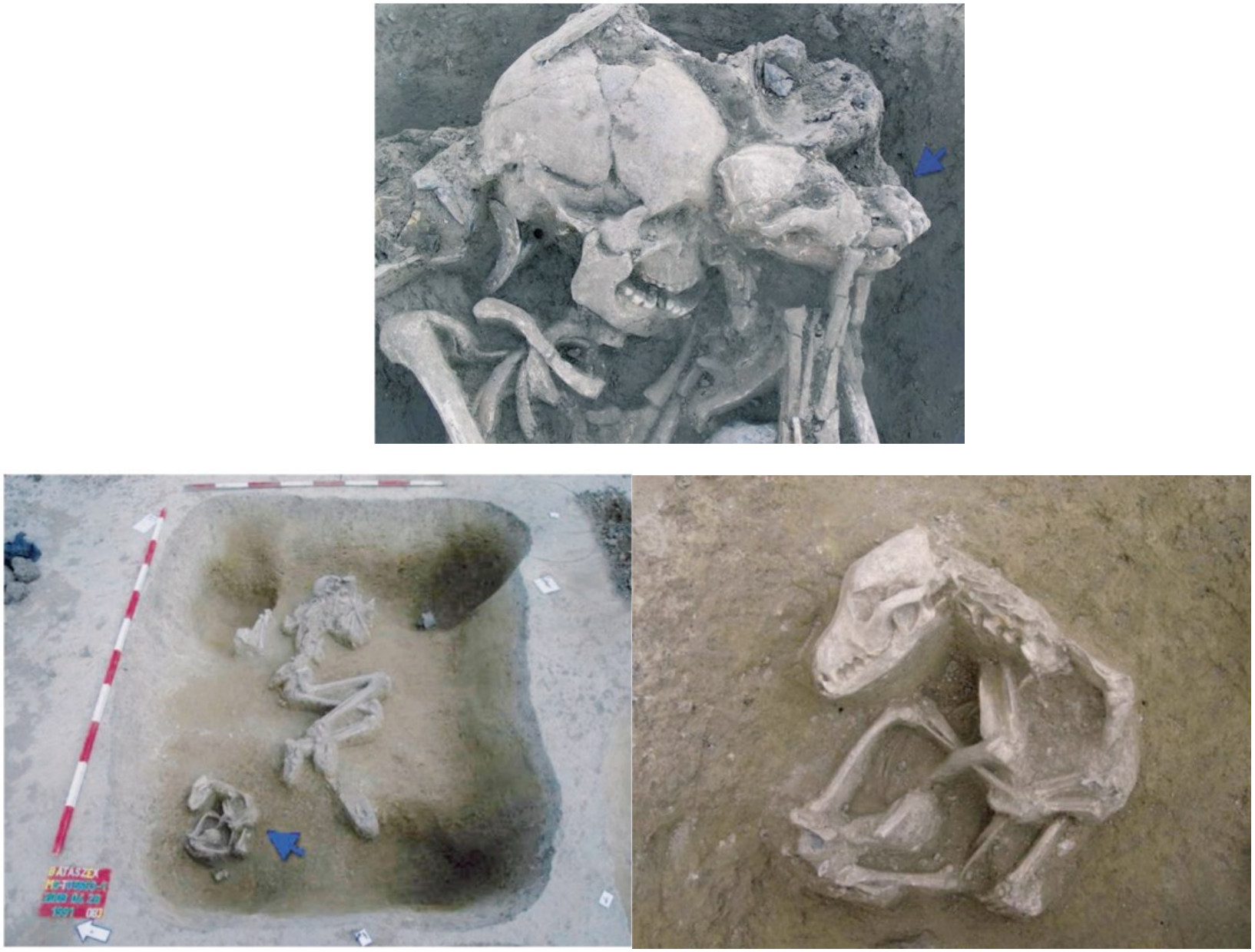

Figure 23. Dog and human burials in Alsónyék-Bátaszék. Top: M6-To-5603/1, tomb 964; Bottom: M6-To-5603/1, tomb 1991. From Zalai-Gaál *et al.*, 2011.

2.3.5. Fox burials

There are a few cases of complete fox skeletons associated with funerary objects or human remains evoking the existence of wild canid burials.

The oldest attestation dates back to the Epipaleolithic in the Near East. In parallel with dog remains found associated with human burials (see previous section), a case of fox-man burial is attested in the pre-Natoufian period at the site of "Uyun al-Hammam" (Maher *et al.*, 2011). The remains of a fox were spread between two tombs. According to the authors, a human (Tomb 1) and a fox (Tomb 8) were buried side by side in two adjacent graves. Then tomb 1 was reopened to remove the human skull, and the fox's grave was also reopened. The bones of the two individuals were mixed together. The treatment of the bodies is reminiscent of the treatment of human remains. The authors therefore suspected that the fox was not a grave good but rather a familiar animal appreciated for its companionship. The special relationship with this animal would have been honoured. The authors even argued that the fox may have been killed to be buried next to the human when the human died. Then, when the grave was reopened, the bones would have been moved to maintain this link in the afterlife. This hypothesis is likely when considering some similar contemporary burials involving wild animals, such as the 8-month-old cat in Shillourokambos (Cyprus) that was buried about 20 centimeters from an adult human (Vigne *et al.*, 2004).

The other published cases are much more recent.

Two Middle Neolithic sites in Germany (dated to the Michelsberg culture) have delivered connected fox remains (skull and mandibles at Heilbronn-Klingenberg "Schlossberg" and complete skeletons of three individuals resting on a charred stone at Münster "Schnarrenberg").

In France, only one case of fox burial is attested in the Late Neolithic (Munzingen B culture, 3,783-3,695 cal. BC), at "Terres de la Chapelle" in Enthzeihm (Guthmann, Lefranc and Arbogast, 2016, Figure 24). The complete skeleton of an adult male red fox, in perfect anatomical connexion, was found in a pit. No anthropogenic marks were observed. It was oriented east-west in the cranio-caudal direction, resting on his right flank, with his head on his left side, which resulted in a very acute angle, with his limbs strongly bent and his extremities leaning against the north wall of the pit, as if, according to the authors, he had been intentionaly placed into a resting position. The animal was closely associated with the fragments of a goblet, a femur and a tibia of a young bovine. Pit filling appears to have been rapid after the animal was placed in the structure. As in "Uyun al-Hammam", the authors have suggested that this would be a burial of a tamed animal rather than a grave offering. However, this case remains controversial, and the unnatural position of the skull raises questions (Claude Guintard, *pers. comm.*). The burial of a wild animal that died naturally can not be excluded.

On the necropolis of Van-Yoncatepe, in Eastern Anatolia (first millennium BC), the remains of five foxes were discovered associated with human skeletal remains (Onar, Belli and Owen, 2005).

Four foxes (as well as a large number of dogs) have been found in Can Roqueta (Barcelona) and Minferri (Lleida), in graves from the Early-Middle Bronze Age. As stated above (see section 2.3.1), isotopes analyses have revealed shared diets between humans, dogs and foxes, suggesting a controlled feeding by humans (Grandal-d'Anglade *et al.*, 2019).

Figure 24. The fox from Entzheim in its pit. Late Neolithic (Munzingen B, 3,783-3,695 cal. BC). From Guthmann, Lefranc and Arbogast, 2016.

2.3.6. Meat consumption

2.3.6.1. *General trends*

The presence of scattered remains of canids in garbage structures, as well as cut marks (filleting, dismembering) or localized burn marks on the bones, attest to a significant implication of canids in the butchering activities from the Upper Paleolithic to the Bronze Age all over Europe.

The consumption of red fox (or wolf) flesh is attested since the Palaeolithic (Helmer, 1979). Helmer (1979) estimates that a fox can provide with 4 kg of meat in average. However, this consumption seems rather opportunistic, and wild canids seem to have been exploited primarily for their fur rather than for their meat. During the Paleolithic and Mesolithic periods, while food resources consisted mainly of large herbivores, wild carnivores roaming near settlements were certainly an important supplementary meat resource for hunter-gatherers (Hainard and Perrot, 1961). Fox hunting was thus more likely related to its abundance near prehistoric sites rather than to a selective hunting (Fosse, 1988).All the parts of the body were thus probably exploited to avoid spoiling anything (Fosse, 1988; Arbogast and Pétrequin, 1993). Thereafter, their consumption seems to decrease through time, and was rather neglected in the Neolithic period.

As for dogs, they were consumed frequently in Europe during the Neolithic (e.g. (Helmer, 1979; Arbogast *et al.*, 2005; Bălăşescu, Moise and Radu, 2005; Bălăşescu, Radu and Moise, 2005; Bréhard, 2007; Pionnier-Capitan, 2010; Horard-Herbin, Tresset and Vigne, 2014) although they were not a primary food resource in most protohistoric European cultures (Zalai-Gaál *et al.*, 2011). Although secondary and relatively marginal in terms of quantity, the consumption of dog meat is attested continuously from the upper Paleolithic (nine remains show marks of disarticulation and filleting in Pont d'Ambon, Pionnier-Capitan *et al.*, 2011) to the Iron Age (Horard-Herbin, 2014). It declined in the Roman era and gradually stopped, for example, in Gaul in the second century AD (Lepetz, 1996). However, it should be noted that there were canine butcheries until the beginning of the 20th century in Europe. Today, no French law prohibits dog meat consumption, as long as their slaughtering respects the hygiene and slaughter rules that are stipulated in the rural code. Nowadays, dog meat is mostly consumed in South Korea and China.

In the following pages, we will go into a little more detail about the different periods from the Mesolithic to the end of the Neolithic period in Western Europe and we will summarize occurences in the Neo-Chalcolithic in Romania and Serbia.

2.3.6.2. *Mesolithic*

During the Mesolithic period, meat was entirely obtained by hunting activities. It is likely that Mesolithic humans were not reluctant to use and exploit all available resources to the fullest. The red fox and the wolf were therefore probably part of the kill count. Besides, dismembering marks were visible on the neck of the femur of a Mesolithic wolf at Noyen-sur-Seine (Vigne and Marinval-Vigne, 1988).

In France, in the late Mesolithic site of **Téviec** (Péquart *et al.*, 1937; Schulting and Richards, 2001), animals and deceased persons were intimately connected, animals having been assigned different statuses (food waste, decorative element of the tomb, offering, and ornament; Fontan, 2019). However, dog remains, scattered and fragmented, were found among the food refuse and not directly associated with human sepultures. It is thus likely that they were eaten (Ollivier *et al.*, 2018, supplementary data). We did not find any indication regarding the presence of anthropogenic marks on dog or fox remains from other Mesolithic sites in France. Evidence of meat use therefore remains difficult to attest for dogs at this period.

Cynophagy is however attested in Eastern Europe, in the Late Mesolithic site of Zamostje 2 (Russia, Chaix, 2013, p. 20) where different types of cut marks have been observed on dog remains, demonstrating a full range of technical operations linked with skinning, defleshing and disarticulation.

In South-Eastern Europe, in Serbia, the dog would have been sacrificied and consumed in Lepenski-Vir III (Schela Cladovei culture). Indeed, cut and burn marks have been found on the dog remains (Bălăşescu *et al*., 2005, see section 2.3.4.1).

2.3.6.3. *Neo-Chalcolithic in Romania*

In Romania, the dog was widely consumed and its fur was often taken jointly, as evidenced by cutmarks (skinning, dismembering and filleting marks) and localized burn marks observed at many sites from the Neolithic and Chalcolithic. Evidence has been found in the cultures of Dudeşti (Beciu and Măgura-Buduiasca, Figure 25), Vinča (Liubcova-Orniţa, as well as in Divostin in Serbia), Boian (**Isaccez-Suhat**, Siliştea-Conac, **Hârşova-tell**, Izvoarele) and Gumelniţa (**Hârşova-tell**, **Borduşani-Popină**, Măriuţa, **Vităneşti**).

To date, no evidence of meat consumption nor fur sampling has been identified on the dog bones during the Starčevo-Criş or the Hamangia cultures in Romania (Bălăşescu, Radu and Moise, 2005). However, evidence for these cultures has been found in other neighbouring countries in Eastern Europe (Lazăr, Mărgărit and Bălăşescu, 2016).

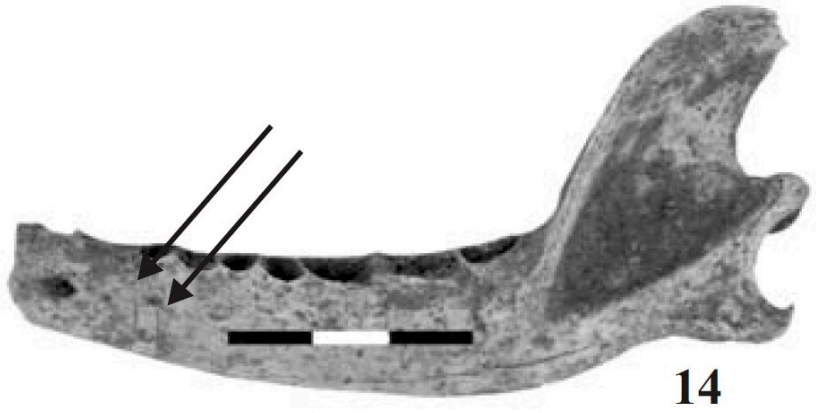

Figure 25. Dog mandible with skinning marks, Magura-Buduiasca, Dudesti culture, Neolithic. From Bălăşescu, Radu and Moise, 2005.

Borduşani and Hârşova show similar slaughter profiles: dogs were mostly slaughtered when still young, i.e. before three years according to Horard-Herbin (2000; Pionnier-Capitan, 2010; Figure 26). This is likely because animals had reached weight maturity and had became ideal targets for meat consumption.

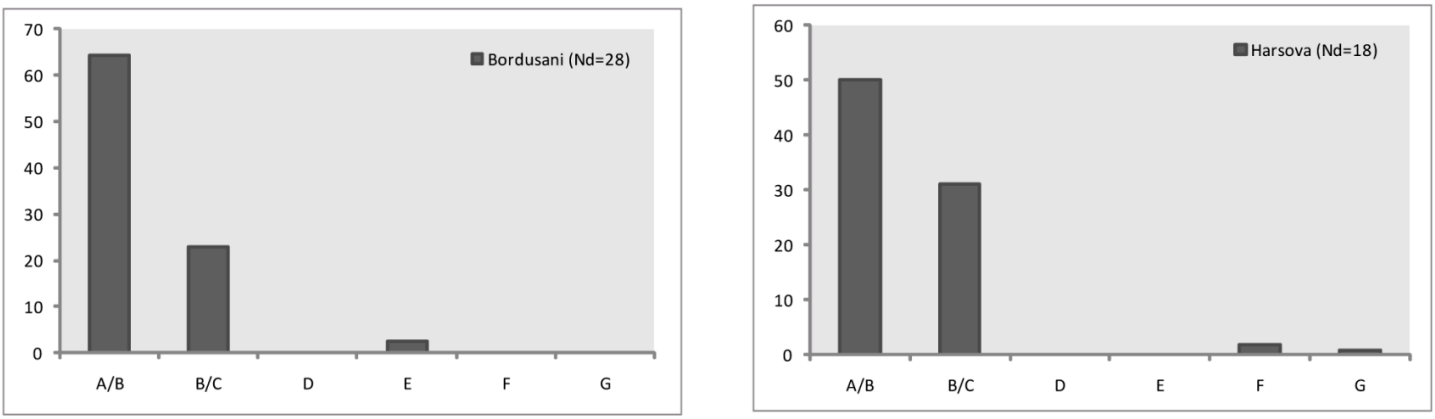

Figure 26. Slaughter profiles of dogs from Borduşani and Hârşova with the age classes proposed by Horard-Herbin, 2000 (see Figure 55). Nd: number of teeth. From Pionnier-Capitan, 2010, p. 108

2.3.6.4. *Early Neolithic in France*

During the Early Neolithic, cut or burn marks are attested on the remains of red foxes and even on those of burrowing animals that one might think intrusive. Carnivores were however never hunted in large quantities during the Early Neolithic. They rather constituted an additional opportunity more than a selective prey, but they were probably prized more for their fur.

For example, on the fox remains dated to the Early Neolithic in **"Le Taï"** at Remoulins (Epicardial culture), dismembering and filleting marks were observed on the acetabulum of a coxa and on the inside of a rib, and under the head. Localized burn marks were also identified on a lumbar vertebra and a metatarsal, indicating that these animals were not exploited solely for their fur, but that the carcasses were also prepared for meat consumption (Bréhard and Vigne, *in press*). The same is true for the badger.

At **Camprafaud C19** (Epicardial culture), a femoral head as well as other fox bones (ulna, distal extremities) show burn marks (Doumerc, 2016). Furthermore, different skeletal parts are present, suggesting that foxes were used for all the resources they could offer (meat and possibly the fur). In addition, other fur animals show anthropogenic marks on this site during the Early Neolithic: the cranial fragment of a badger revealed cut marks (in C18), and lagomorph remains (coxal, ribs, scapula) showed cut and/or localized burn marks (in C18-C19, Doumerc, 2016). This confirms the meat consumption of small fur animals at this period in this site.

Similarly, in Leucate-Corrège, the burned tibia of a fox was found in association with a rib, as well as leg tips and skull remains, suggesting a use of the meat and/or skin (Fosse, 1988).

For dogs, evidence is almost inexistent. We only recall here the case of **Herxheim** (cf p. 88), where Early Neolithic dogs show localized typical marks of cooking (burn marks on the upper teeth, Arbogast, 2018).

2.3.6.5. *Middle and Late Neolithic in France-Switzerland*

Fox remains are never very numerous in the Middle and Late Neolithic, but when present, they are often the only representative carnivores (Fosse, 1988). During these periods, clear evidence of fox meat consumption is rarer than in earlier periods. It seems that foxes occupied only a marginal role in meat resources, when the consumption of wild species was already very limited.

On the contrary, dog meat consumption is very well documented in the second half of the Neolithic period, especially in the Chasséen and Michelsberg cultures from the Middle Neolithic and during the Late Neolithic (Arbogast, 1995; Arbogast *et al.*, 2005; Bréhard, 2007; Pionnier-Capitan, 2010). Here are a few examples.

In **"Les Moulins"** at Saint Paul-Trois-Châteaux, and **"La Roberte"** at Châteauneuf-du-Rhône (late Chasséen), skinning, dismembering and filleting marks, as well as localized burn marks observed on dog bones demonstrate meat consumption. Moreover, dog remains represent as much as 25% of the mammal remains on these sites (compared to a mean of 7% for Southern Chasséen: Figure 13) and most of their remains are concentrated in a few pits. Given these results, Bréhard (2007, 2011) proposed that dogs were consumed during collective meals, when different groups of people gathered at these two sites.

In "Hautes Chanvières" at Mairy (Michelsberg culture), a cut mark characteristic of filleting was evidenced on a femur, and localized incisions were observable on a metatarsal, probably resulting from skinning. This does not seem to be the most common treatment for this animal in Michelsberg settlements (Arbogast, 1995), but cut marks have been observed on the dogs from Rudemont (see page 88).

The use of dog meat as a complemental resource would have been all the more opportune as the development of herding played a secondary role (Hüster-Plogmann and Schibler, 1997; Arbogast *et al.*, 2005). Accordingly, in some French or Swiss lakeside settlements, dog remains reach or even exceed 10% of the total NISP, and the consumption of dog meat may have been as important as that of small domestic ruminants (Arbogast *et al.*, 2005). In **Twann**, many butchering marks (skinning, dismembering and filleting) have been observed on the skull or long bones of dogs dated to the Cortaillod culture (Pionnier-Capitan, 2010; cf Part 3 section 3.1.2.2, Figure 87). Additionnaly, the distribution of ages at death (slaughter profile) suggests that some dogs were preferably selected to be eaten (Arbogast *et al.*, 2005; Pionnier-Capitan, 2010, pp. 107–109). In Twann, dogs were mostly 6 to 12 months old when they died (Figure 27, Becker and Johansson, 1981). These animals therefore had reached weight maturity and had became ideal targets for meat. The same applies during the Horgen culture (Late Neolithic) in Zurich lakes (Hüster-Plogmann and Schibler, 1997) and Arbon-Bleiche 3 (Deschler-Erb and Marti-Grädel, 2004), where frequent cut marks were reported, confirming the intention to dismember the carcasses and remove the flesh. In the latter site, there were many puppies under six months of age which could be related to population regulation practicies, although animals could also have been eaten. Dog meat consumption is also well attested in the likeside villages

of Neuchâtel and Bienne at the end of the Neolithic and early Bronze Age (Arbogast *et al.*, 2005).

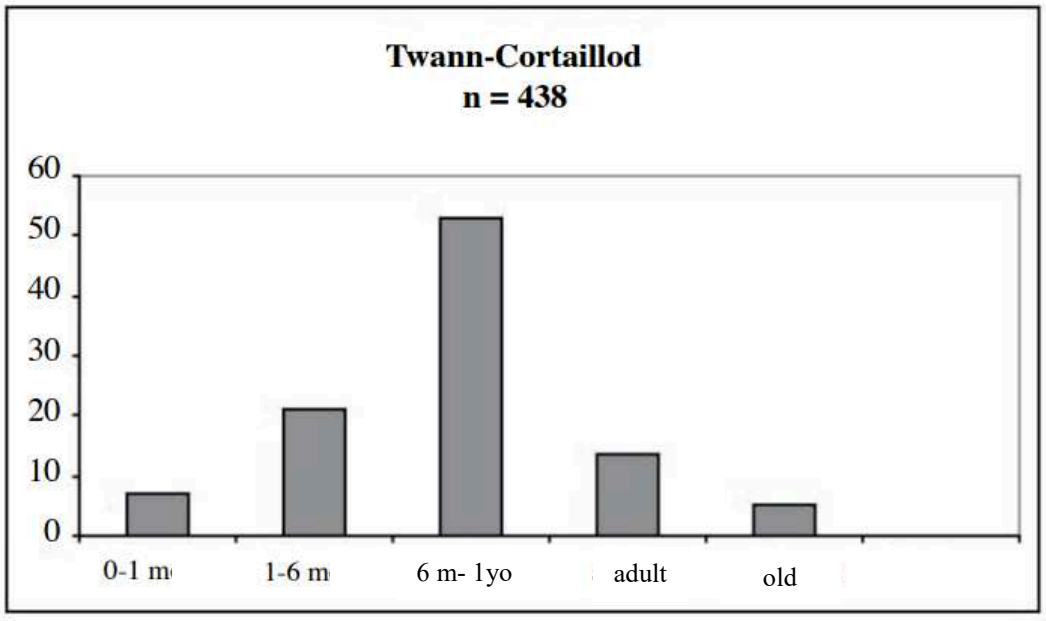

Figure 27. Slaughter profile of the dogs from Twann during the Cortaillod culture, based on the state of tooth eruption and tooth wear. Translated from Arbogast *et al.*, 2005. m: month, yo: years old.

Dog were probably also eaten during the Late Neolithic at "Soubérac" in Gensac-la-Pallue (where a partially burned mandible was found) and in "Clos-de-Roque" at Saint-Maximin-la-Sainte-Baume (some bones show cut marks and dog remains were found associated with other domestic animals, especially in St2096, Remicourt *et al.*, 2012).

Conclusion

KEY POINTS

All these data illustrate the **variety of relationships that existed between hunther-gatherers or farmers and canids**, from the Mesolithic to the Bronze Age. Dogs and red foxes may have been considered as individuals on their own, the companion of a deceased person, a sacrificial object, or the source of raw material necessary for survival, or for ornements. These **uses varied over time, but they often combined**, and some periods were very complex because **uses may have been diverse, even within the same site and occupation.**

The status depends in part on the **domestic/wild status** of the animal, as **dogs seemed to be buried more than other canids**, showing a special bond with humans, in both life and the afterlife, and from the earliest periods. Indeed, during the European Mesolithic, the burial of complete dogs is attested in several areas and seemed to reflect a symbolic function of accompanying the deceased to the afterlife (especially in Western and Northern Europe) or ritual practices (associated with consumption at the Iron Gates sites in Romania or Serbia). This status could also have been granted to some wild, perhaps tamed, foxes, but generally this happened at later periods.

During the Early Neolithic, dogs were little represented in faunal remains in most part of Europe. Dogs may have played the privileged role of **companion** – as allies for hunting, herding or protecting villages – especially in Western Europe, where the site of **Herxheim** stands out. Indeed, it yielded a significant number of dog remains belonging to a small number of individuals, but the site was very unusual, due to the practice of **cannibalism associated with ritual animal meat consumption**. But otherwise, dogs were not much consumed and they were rather evacuated outside the settlements after their death without further consideration.

KEY POINTS

The **presence of dogs then increased and reached a peak** in Western and South-Eastern Europe during the **Middle and Late Neolithic** in the first case, and in the **Chalcolithic Boian and Gumenlitsa** cultures in Romania.

Interestingly**, a much greater diversity of statuses seems to have been attributed to dogs in Western Europe than in Romania** during these periods. **In Romania, dogs were widely eaten and their fur was collected**, although they certainly also played other roles, such as guarding (of herds and settlements), hunting, or simply providing companionship.

In Western Europe, the diversity of dog statuses, sometimes even simultaneously, is more obvious. They may even seem sometimes ambiguous since dogs were considered as an animal for slaughter, the object of an offering or sacrificial deposit (associated with meat consumption or not) and probably also as a companion and an auxiliary in life. They lived close to humans in the settlements, and some authors have hypothetised that populations could have been regulated to prevent dogs from swarming. They were sometimes thrown unceremoniously outside settlements, or carefully placed in pits close to dwellings, or even placed with humans. They were in other cases dismembered, eaten and mixed with other food remains; this dog meat consumption is likely to have sometimes occurred in the framework of collective events.

Red foxes seem to have been primarily hunted for their fur, especially in the early periods, and hunter-gatherers probably also consumed their meat to optimize resources. Their importance seems to have diminished over time, like that of other wild animals. However, there are some particular deposits attesting to a special link (perhaps taming) between humans and wild animals at the very end of the Neolithic and the beginning of the Bronze Age. We have not been able to explore the presence of the red fox in Europe as widely as that of the dog, however, and our conclusions are drawn mainly from our observations in France.

2.4. Morphological evolution of dogs from the Epipaleolithic to the pre-Bronze Age: state of the art

In this section we synthesise available information on the morphology of dogs. This encompasses genetic data that provides information on the colour of their coat (Ollivier *et al.*, 2013, see section 2.4.1), and osteometric data that provides indications on the stature, wither height, gracility or, more rarely, on variability in skull shape (see section 2.4.2). This synthesis should allow to identify limitations of previous studies and missing knowledge about the morphological variability that existed within canids prior to the Bronze Age. This should enable to raise questions that we will address in the conclusion of Part 1 and that we will try to answer in the course of this thesis.

2.4.1. Variations in coat colour

Ollivier *et al.* (2013) analyzed the genome of 15 ancient dogs and 19 ancient wolves from 14 different archeological sites, throughout Eurasia, spanning from the end of Upper Palaeolithic (12 kyrs cal. B.P.) to the Bronze Age (4 kyrs cal. BP). They have demonstrated that the alleles and genes responsible for a light coat (allele R301C of the gene *Mc1r*[k]), or for a dark coat (allele K^B of the gene *CBD103*[l]) were both present on wolf or dog-like canids as early as the Mesolithic (around 11-8 kyrs cal. BP, in Icoana, Romania, Figure 28). These mutations then persisted in different areas in Eurasia, through the Neolithic and the Bronze Age.

In modern canids, the allele R301C of the gene *Mc1r* is only retrieved in Siberian Husky and Alaskan Malamute, but not in any other modern dog breed nor the modern wolves in their sample. In contrast, the K^B allele is widely distributed among modern domestic dogs (including ancient breeds originating in Asia and Africa). However, the allele K^B is very rare in the wild (it has been reported in wolves from North America and Italy only), suggesting that a strong natural selection against this mutation seems to exist in wild contexts. Its presence in wolves is likely derived from past hybridisation with domestic dogs. The authors have hypothethised that the allele K^B could come from the wolves that formed the population where the domestication process occurred, or it could be explained by some mutations related to the relaxation of natural selection, which could explained why it was found such early in the history of dogs (Ollivier *et al.*, 2013).

[k] Melanocortin 1 Receptor.
[l] Canine-β-defensin.

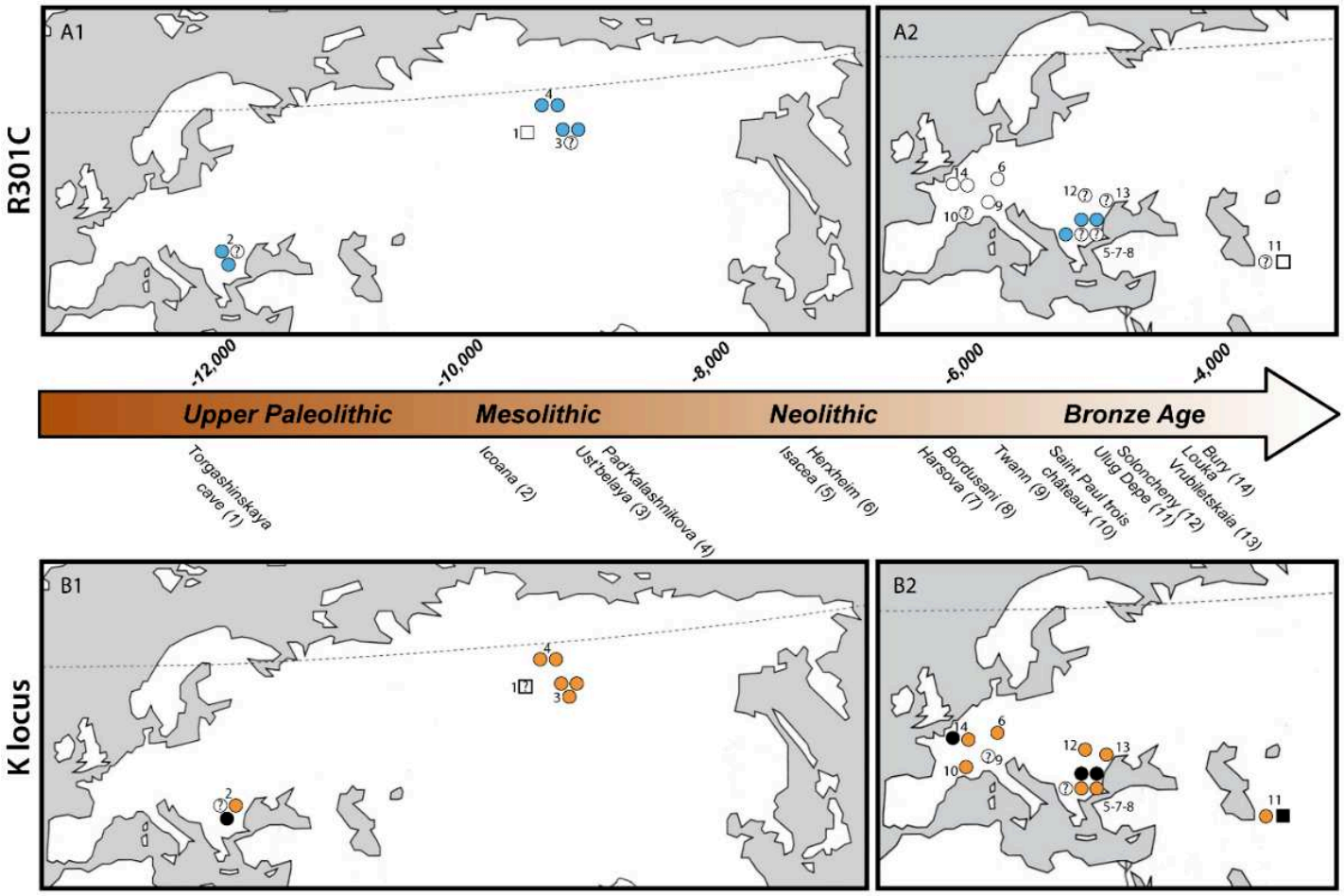

Figure 28. Distribution of the R301C mutation (A1, A2) and of the K^B allele (B1, B2), before (A1, B1) and after (A2, B2) the neolithisation. From Ollivier *et al.* (2013). Blue: presence of R301C mutation, white: absence of R301C mutation, black: presence of K^B allele, orange: absence of K^B allele, question mark: undetermined.

2.4.2. Variation in osteometric measurements

The aim of this last section is to synthesise the available osteometric information of canids from the Upper Paleolithic to the early Bronze Age. The information related to the form of a bone can be split into two components: information about the **size**, and information about the proportions between the different parts of the bone (i.e. **shape**). Throughout the following section, we follow this decomposition, by treating information relating to size and information relating to shape in parallel. Moreover, observed trends are confronted to the paleogenetic data on canid haplogroups, in order to cross information on morphological and genetic variability (Ollivier *et al.*, 2018).

Our survey revealed that osteometric data on canids are often scattered in the literature. To date, there is no complete synthesis in a global diachronic framework Only some unpublished archaeozoological studies have attempted to explore the diachronic evolution of dogs at the European scale. One must also mention the PhD thesis of Maud Pionnier-Capitan (2010) about the domestication of the dog in Eurasia, and the master thesis of Andréa Filippo (2017) about the exploration of the morphological diversity in dog mandibles in Europe and the Middle East, from the Epipaleolithic to the early Bronze Age. There are also a few rare synthetic publications, which compile available osteometric data for some particular chrono-cultural groups or areas where dogs were well represented. This is for example the case of the publication by Arbogast *et al.* (2005), which reports findings on the dog remains from the Middle and Late Neolithic in Swiss and French lakeside settlements, or in Bălăşescu, Radu and Moise (2005) for the whole Neolithic-Chalcolithic period in the South-Eastern part of Romania. We therefore started from these studies and supplemented it with osteometric information collected from publications listed in section 2.2.

Additionnaly, our survey revealed that the exploitation of osteometric data is, so far, very limited and uncomplete. It is often limited to the use of simple linear measurements, which mainly provide an indication of bone size, or of that the stature by means of equations to estimate wither heights. However, these equations only give a very approximate indication of the size of the individual. Sometimes, two measurements are used jointly (e.g. gracility index) and provide information on robustness. Analyses taking into account more than two dimensions (using PCAs, see section 2.2.4) and decomposing form into size and shape using the log-shape ratio method of Mosimann (1970) are very rare (and only limited, to our knowledge to Bréhard, 2007 and Filippo, 2017). However, even these more advanced multivariate methods do not account for the geometry of the bones, as is possible by means of geometric morphometrics (see section 2.2.3). Very few publications have used geometric morphometrics to describe dogs prior to the Bronze Age. Only two studies testify to early attempts. The PhD thesis of Pionnier-Capitan (2010) presents an attempt on the lower carnassial tooth, but few results have emerged, teeth being extremely conservative (see Part 2). Additionnaly, the unpublished master thesis of Filippo (2017) presents an attempt on the mandible, although the overall sample size remains rather low.

For the red fox, there is to our knowledge no synthesis that provides information on their morphological variability from the Upper Paleolithic to Bronze Age in Europe. Data are scattered in the literature and they are very limited. We will therefore only focus on the dog in the following pages. Helmer (1979), however, noted that Neolithic foxes from South-Eastern France were of equal or greater size compared to modern foxes, unlike the Neolithic foxes of Burgäschisee Süd which were smaller than present-day Swiss animals.

2.4.2.1. *Late Upper Paleolithic*

Dogs in Western Eurasia already displayed a wide variety of statures even before the Holocene. Pionnier-Capitan *et al.* (2011) reports the simultaneous existence of several morphological groups, that were confirmed by later discoveries (Boudadi-Maligne *et al.*, 2012, 2020; Horard-Herbin, 2014, see Table 1 for more informations on the cited sites):

- **Dogs of medium size** (wither height estimated to 45-60 cm) with a rather modified morphology (strong allometric differences) in the Near East during the Natufian and in Northern Zagos contemporary cultures (Tell Mureybet, Syria; Hayonim Terrace and Ein Mallaha, Israel; Pelagawra's cave, Zagros), or in South-Western France during the Azilian (Grotte abri du Moulin, Troubat).

- **Dogs of medium to large size** (wither height estimated to more than 60 cm) and fairly robust, with a morphology similar to modern wolves held in captivity, in Eastern Europe (some of these "large dogs" were probably wolves according to Boudadi-Maligne and Escarguel, 2014), and France (Kniegrotte, Germany; Mezin, Ukraine; Eliseevichi I, Russia; Le Closeau, France).

- **Small to very small dogs** (wither height estimated to 30-45 cm or less than 30) in Western Europe (Bonn-Oberkassel, Teufelsbrücke and Ölknitz, Germany; Hauterive-Champréveyres, Switzerland; Grotte Jean-Pierre 1, Pont d'Ambon, Montespan, Grotte de le Morin, France; Erralla, Spain, Iberian Peninsula). The smallest dogs have been found in the Westernmost regions (France, Iberian Peninsula). One example is the small dog of Montespan (France), dating from the Middle Magdalenian (15,5-13,5 kyrs cal. BP; Pionnier-Capitan *et al.*, 2011), more or less contemporary with the first large dogs of Russia (Sablin and Khlopachev, 2002).

At this period, all European dogs, however, belong to the same haplogroup C but very few data are available (Ollivier *et al.*, 2018).

2.4.2.2. *Mesolithic*

Very few osteometric data are available for the European Mesolithic (see section 2.2.2), and they only provide indications on the size of the bones or individuals.

Dogs of the European Mesolithic were already well distinguished from wolves. Indeed, Mesolithic dogs from Northern France would have been smaller than Mesolithic wolves, based on humerus lengths (Pionnier-Capitan *et al.*, 2011, Figure 29), but the number of wolf specimens is too low to be sure. Additionally, we have seen in section 2.4.1 that black coats were already present in dogs of the Romanian Mesolithic at Icoana, or in wolf/dog hybrids, but not in strictly wild wolves (Ollivier *et al.*, 2013).

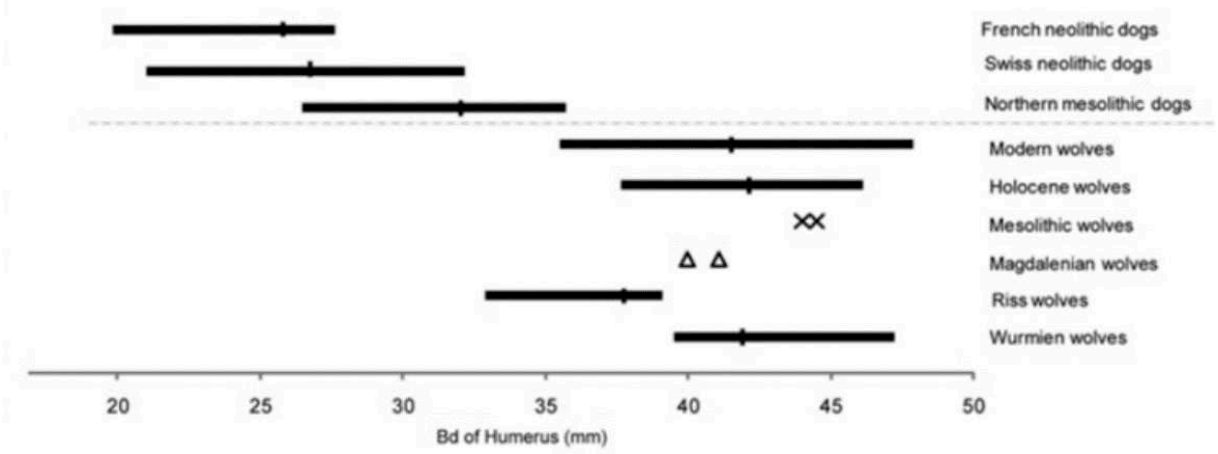

Figure 29. Humeral measurements on canids from the Mesolithic and Neolithic, modified from Pionnier-Capitan *et al.* (2011)

Some dogs are **large and reminiscent of wolves**. Accordingly, Romanian Mesolithic dogs of Ostrovul Banului and Icoana (and perhaps of Ostrovul Corbului) have a jugular dental row whose dimensions are quite similar to those of the wolf, although the molar row is smaller (Pionnier-Capitan, 2010). The two Mesolithic "*Canis* sp." from Noyen-sur-Seine (France, seventh millennium BC; Vigne and Marinval Vigne, 1988) are thought to be wolves with some morphological characteristics reminiscent of modern wolves held in captivity (shortened snout for one, strong depression of the sagital gutter for the other), which leads the authors to suggest the possibility of proto-breeding.

Other dogs are of more **average size**. For example, in Montandon, a wither height of 51.1 to 52 cm is given (Cupillard *et al.*, 2000). At Cabeço da Amoreira in the Muge Valley in Portugal, a wither height of 48.5-51cm was estimated from an almost complete skeleton of Mesolithic *Canis*, and the authors suggest that this medium-sized dog was reminiscent of the Dalmatian, English Springer Spaniel or the Portuguese water-dog (Detry and Cardoso, 2010, Figure 30).

Other Mesolithic dogs are much **smaller**, as for example in Téviec (France, 6th millennium BC; Pionnier-Capitan, 2010).

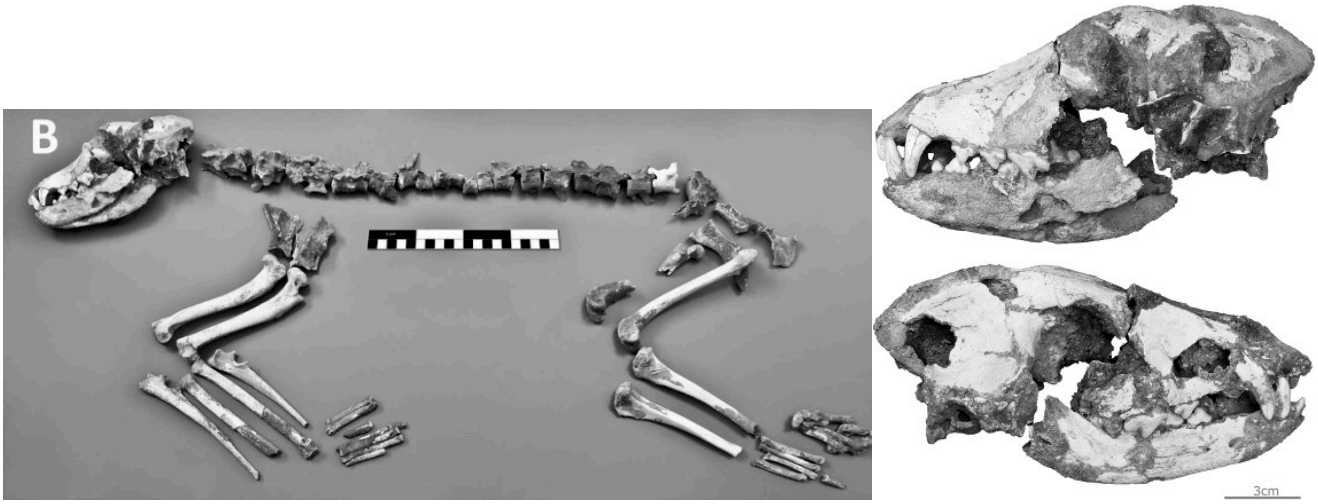

Figure 30. Mesolithic Dog of Cabeço da Amoreira in the Muge Valley in Portugal, from Detry and Cardoso (2010)

Our appreciation of the overall variability in canids at this time is very limited, but morphological variability thus already seemed to exist (presence of black dogs from the Mesolithic period, and small dogs of less than 30 cm since the Epipaleolithic). At this period, European dogs belong to haplogroup C (Ollivier *et al.*, 2018), but a high frequency of haplogroup A was found in Mesolithic dogs from the Iberian Peninsula (7,903-7,570 cal. BP), suggesting that some geographic variation and genetic variability already existed (Pires *et al.*, 2019).

2.4.2.3. *From the Mesolithic to the very early Bronze Age*

2.4.2.3.1. Dogs versus wolves

Size

In Eastern and Western Europe, **Neolithic dogs were much smaller than wolves**, making confusion unlikely. This was demonstrated by many studies, based on the length and width of the lower first molar (Pionnier-Capitan *et al.*, 2011, Figure 29), on measurements taken on the mandible (Filippo, 2017, Figure 32), or on long bones and size estimates (Arbogast *et al.*, 2005; Forest and Rodet-Belarbi, 2018).

Shape

The multivariate statistical analyses of linear mandibular measurements (traditional morphometrics), or landmarks (geometric morphometrics) by Filippo (2017) have shown that the morphological spaces of ancient wolves was included within that of ancient dogs, all periods confounded, suggesting that ancient dogs are close in shape to their wild relatives. However, although this study has shown that the variability of modern dogs overlaps that of ancient dogs much, a proportion of Eastern and Western European dogs are outside this variability (Figure 31) suggesting that some ancient morphologies could have no modern equivalent and that the **variability in shape may have been, surprisingly, greater in the past**.

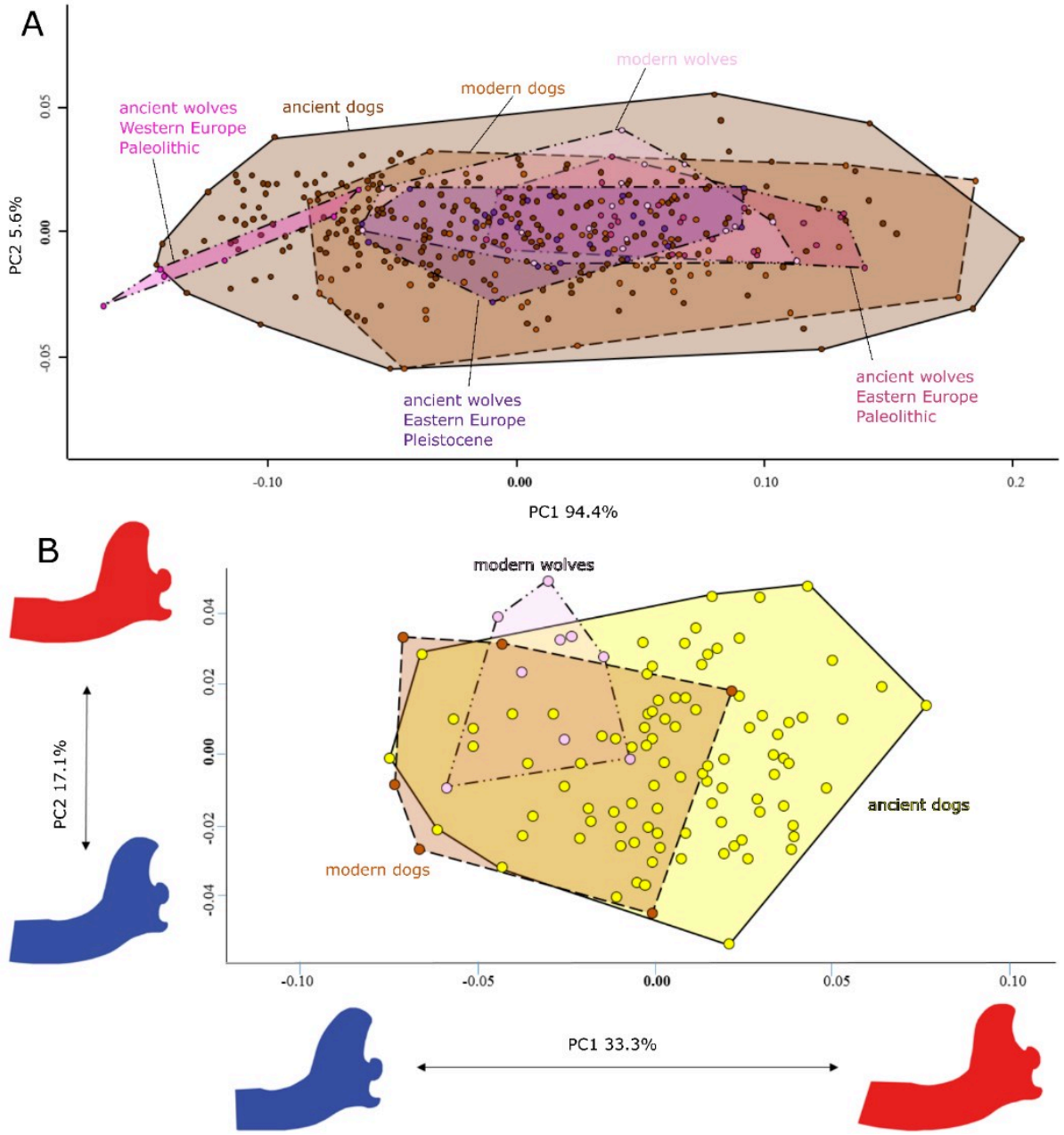

Figure 31. Variability in mandibular shape shown by Principal Component Analyses performed on (A) three mandibular measurements (von den Driesch's dimensions 9, 10 and 11) or (B) 2D coordinates of landmarks on the mandible of ancient dogs and modern dogs and wolves. From Filippo, 2017.

2.4.2.3.2. Variations in size – general trends

Many studies have suggested that, from the Mesolithic to the pre-Bronze Age, in both Eastern and Western Europe, **dogs progessively decreased in mean size and the variability in size tended to increase** (Arbogast *et al.*, 2005; Bălășescu, Radu and Moise, 2005; Clark, 2006; Pionnier-Capitan *et al.*, 2011; Filippo, 2017, Figure 32)**.** This was for example illustrated in the increasing of coefficients of variation for isolated measurements of cranial and post-cranial skeletal elements in the study of Pionnier-Capitan *et al*. (2011).

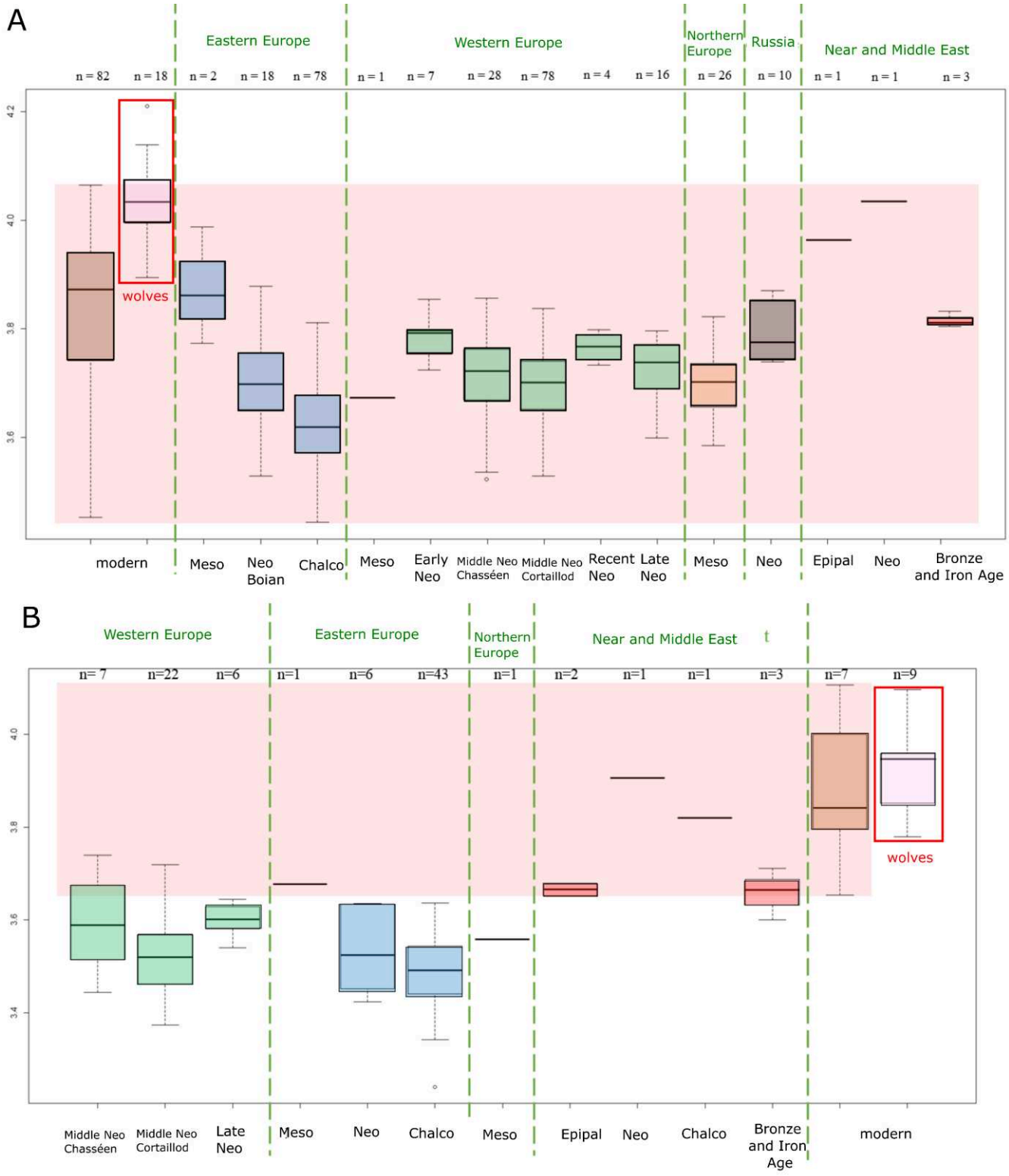

Figure 32. Variation in mandibular size in dogs over time in Europe, Eastern Russia and the Near and Middle East. Translated from(Filippo, 2017).
A: size is approximated from the geometric mean of mandibular dimensions, following the log-shape ratio procedure proposed by Mosimann (1970).
B: size is approximated from the geometric mean of Euclidean distance between two-dimensional landmarks.
Epipal: Epipaleolithic; Meso: Mesolithic; Neo: Neolithic; Chalco: Chalcolithic

Eastern Europe

Cranial remains are well represented in South-Eastern Romania, especially the mandibles, which allowed to estimate the length of the corresponding skulls (Table 10). The post-cranial skeleton is also well represented, but rather fragmented, so only a few complete bones could be used to estimate the wither heights (Table 10).

Osteometric data seem to attest to the existence of a fairly homogeneous and similar population throughout the Neo-Chalcolithic of South-Eastern Romania, with dogs of medium size and medium robustness, and smaller than in the Mesolithic of Ostrovul Corbului (Bălăşescu, Radu and Moise, 2005). The lower first molar (M1) is constantly decreasing in size between the Mesolithic (Icoana), Early Neolithic (Cuina Turcului, Starčevo-Criş) and Chalcolithic Boian and Gumelniţa cultures (Bălăşescu, Radu and Moise, 2005). The same is observed when considering the mean centroid sizes of the mandibles in multivariate analyses (Filippo, 2017, Figure 32). The decrease in mean sizes is related to an increased variability and the presence of **small to very small dogs, notably** at Borduşani and Hârsova during the Gumelnița culture (33 cm, Bălăşescu, Radu and Moise, 2005). Besides, many of the Gumelniţa dogs show a phenomenon of oligodontia with the absence of the lower third molar for at least 15% of the total number of mandibles analysed at Borduşani-Popină and Hârşova-tell (Pionnier-Capitan, 2010). Dogs from the Gumelnița are, on average, smaller than dogs from the Boian culture. The dogs at Borduşani-Popină are smaller, which may reflect the isolation of the community.

Table 10. Cranial lengths and wither heights estimated for Romanian Neolithic dogs. From Bălăşescu, Radu and Moise, 2005.

Culture	Site	Cranial length				Wither height				
		N	mean	min	max	N	mean	min	max	robustness
Gura Baciului-Cârcea		/	/	/	/	/	/	/	/	/
Starčevo-Criş		/	/	/	/	3	44.2	40.5 Moldavie Veche-Rât	50.8 Dudeştii Vechi	7.4
Vinča		17	139.5	118.4 cimetière Foeni-Orthodox	154.7 Part-tell II			40.1 Part-tell II		
Dudeşti		1		139.3 Măgura-Buduiasca				47.9 Măgura-Buduiasca		
Vădastra								45.5 Vădastra		
Hamangia		3		135.5 Loa Cle	142.5 and 153.2 Hamangia			46.8 Cheia		7.3
Boian		14	139.9	127.1	153.2	3	40.5	37.4	44.8	
Gumelniţa	All	92	131.9	98	39		40.2	33.4	46.8	
	Borduşani-Popină	36	124.4	99	13		40.4	33.4	46.8	
	Hârşova-tell	17	132.5	118.4	23		39.9	34.1	43.6	
	Însurăţei	1	148.8							
	Luncaviţa	3		98 and 99.7	179					
	Vlădiceasca	28	139.9	119.8	163.4				42.3	
	Vităneşti	7	137.9	121.3	144.5			40	44.2	
Cernavoda	Hârşova-tell		127.1				45.1			
Bolintineanu, Sălcuţa et Stoicani-Aldeni	/	/	/	/	/		/	/	/	/

Western Europe

Few remains of dogs dated to the Mesolithic or **Early Neolithic** are available (see section 2.2.5), and osteometric data are scarce, rendering our evaluation of the variability in size at that time very uncomplete. Available data suggest that Mesolithic dogs are on average bigger than Neolithic dogs but the scarcity of data for the earliest periods makes it very hypothetical (Figure 32). Measurements taken in Herxheim (Germany, LBK, end of the sixth millennium cal. BP), indicate that these **Early Neolithic dogs were relatively large** (although significantly smaller than wolves). In addition, they had a shortened face and teeth were often missing (Pionnier-Capitan, 2010; Arbogast, 2019).

More information is available for the **Middle Neolithic**, with series of measurements for large populations, particularly in Swiss and French lakeside settlements, providing us with a more comprehensive idea of the variability that existed at that time, and even between regions, periods and cultures. **Dogs of the Middle and Late Neolithic were of medium to small size**, with wither heights ranging from 35 and 55 cm. There is indeed concordant evidence in many regions (Table 11). Dogs seem relatively larger during the Late Neolithic in Switzerland.

Dog size decreases during the Middle Neolithic and up to the end of the Neolithic. This decrease in mean size is accompanied by **an increase in the variability**.Indeed, through the comparison of measurements of long bones from sub-complete dogs from Mairy, Bercy, Boury-en-Vexin, les Magnins with modern dogs (a female small Dane and a male large bullhead), Bréhard (2007) shows that a variability seemed to exist within the animals of the Middle Neolithic. Measurements of the mandibles of "Les Moulins" and "La Roberte" also show clear variations in size (Bréhard, 2007).

The decrease in size is related to **the presence of small to very small dogs i**n many sites of the Chasséen complex during the Middle Neolithic (Bercy, "les Moulins", "la Roberte", "Champ du poste" in Carcassonne) or associated cultures (Pionnier-Capitan, 2010; Horard-Herbin, Tresset and Vigne, 2014; Forest and Rodet-Belarbi, 2018). These small dogs do not appear in the earliest period, but the scarcity of the material does not allow to exclude their presence in dog populations.

To date, no very large dogs are attested in the Middle Neolithic period in France (Bréhard 2007). They **do not reappear until the end of the Neolithic period** (Bréhard, 2007; Pionnier-Capitan, 2010). For example, the dogs of Bury (extreme end of the Neolithic; (Salanova *et al.*, 2017) were large, with a slightly shortened face. DNA analysis revealed that at least one of them was black, while another still retained the colour of the wild coat (Ollivier *et al.*, 2013). In Switzerland as well dogs increased in size significantly from the Late Neolithic to the Late Bronze Age (from 47 cm to 61 cm), to become much more robust (Arbogast *et al.*, 2005). However, the scarcity of measurements for the Bronze Age does not ensure that this increase in size was significant, neither generalisable to other regions, nor constant over time. This increase in size would have been accompanied by an increase in variability (but which remains reasonable), since medium to small dogs similar to those of the Neolithic period

persisted. Larger bodies were likely less adapted in these geographical isolates were living conditions were more difficult, or medium to small dogs would have been preferred to ensure tasks specific to montain environments (Arbogast *et al.*, 2005). It is also possible that this was related to selection and the preferred use of larger dogs that were likely to provide more meat. This remains difficult to prove, but it is supported by the fact that the increase in size was not accompanied by any change in bony proportions, and it is consistent with the methods of dog selection observed at Hauterive-Champréveyres (Arbogast *et al.*, 2005).

Table 11. Wither heights reported in the literature for some sites dated to the Middle or Late Neolithic.

Period – Culture	Region	Site	Wither heights	Ref
Middle and Late Neolithic	Southern France	"La Farigoule 2" "Le Crès" "Vert-Parc" "Mas de Vignoles IV » "Cadereau d'Alès"	37-52 cm	Forest and Rodet-Belarbi, 2018.
	Swiss or French lakeside settlements	Auvernier Twann Chalain-Clairvaux Zurich Arbon Feldmeilen	40-55 cm	Arbogast *et al.*, 2005)
Middle Neolithic – Michelberg	North-Eastern France	"les Grands Aisements"	40-50 cm	
		"Les Hautes Chanvrières" in Mairy	35.5-47.8 cm	Bréhard, 2007
Middle Neolithic – Chasséen	Northern France	"Cul froid" in Boury-en-Vexin	idem	
		Bercy	39.2-47.6 cm	Bréhard, 2007
	Southernof France	"Les Moulins"	35 - 46 cm	Bréhard, 2007
Middle/Late Neolithic	Switzerland	"La Motte aux Magnins"	49-51.3cm	Chaix 1989 in Bréhard, 2007
Late Neolithic	France	Machecoul	42 cm	Braguier, 1997
		"Camp 1 des Matignons"	42-46 cm "size of a French spaniel"	Braguier, 1997
		Diconche	42.3 cm (37.1-44.8 cm)	Bökönyi and Bartosiewicz, 1999
		Mas de Vignolles IV	45 cm	Convertini *et al.*, 2004

2.4.2.3.3. Variations in shape – general trends

General view of dog morphotypes

Previous authors have described some **morphological types in Neolithic dogs**. These types were defined by some morphological characteristics and generally correspond to specific geographical regions and periods. They illustrate the existence of a global variability if we consider the Neolithic as a whole (Studer, 1901; Ducos, 1968; Helmer, 1979; Bökönyi, 1988; Arbogast *et al.*, 2005; Pionnier-Capitan, 2010). These types are, however, "only landmarks among a multitude of forms" (Ducos, 1968).

Among these types are:

- ***Canis familiaris ladogensis*** or ***Canis familiaris inostranzevi*** (Anoutchine 1882). This type corresponds to rather large and wide dogs, dating from the Early Neolithic in the region of Lake Ladoga in Russia.

- ***Canis familairis palustris*** (Rütimeyer 1862) or “dog of the peat bogs” or “dog of the the palaffites". This type, rather homogeneous, corresponds to dogs of rather smaller size (like the modern spitz type), with a broad, rounded cranial cavity and a sharp muzzle. It dates back to the Middle Neolithic and was found in Swiss or French lakeside settlements. However, in their synthesis, Arbogast *et al.* (2005) wrote that it is difficult to recognise this type specifically, since it sometimes correspond to the description of dogs outside the area of the Swiss lakes (for example in Mairy, Michelsberg, Arbogast *et al.* (2005) or even later in the Late Neolithic (as in Diconche, Artenacian/Peu-Richard, Bökönyi and Bartosiewicz, 1999).

- ***Canis poutiatini*** (Studer 1906, cited by Bökönyi, 1988), whose morphology remind that of the Australian dingo.

- dogs of intermediate size: ***Canis familairis intermedius*** et ***Canis familairis matris-optimae*** (Bökönyi, 1988).

Differences between Eastern and Western Europe

Dogs from Western Europe seem to be distinct from those from Eastern Europe, based on the multivariate analyses conducted by Filippo (2017) on three or eight of the Von den Driesch’s standardised dimensions (1976, traditional morphometrics, Figure 33A,B) or on 2D coordinates of landmarks (geometric morphometrics, Figure 33C).

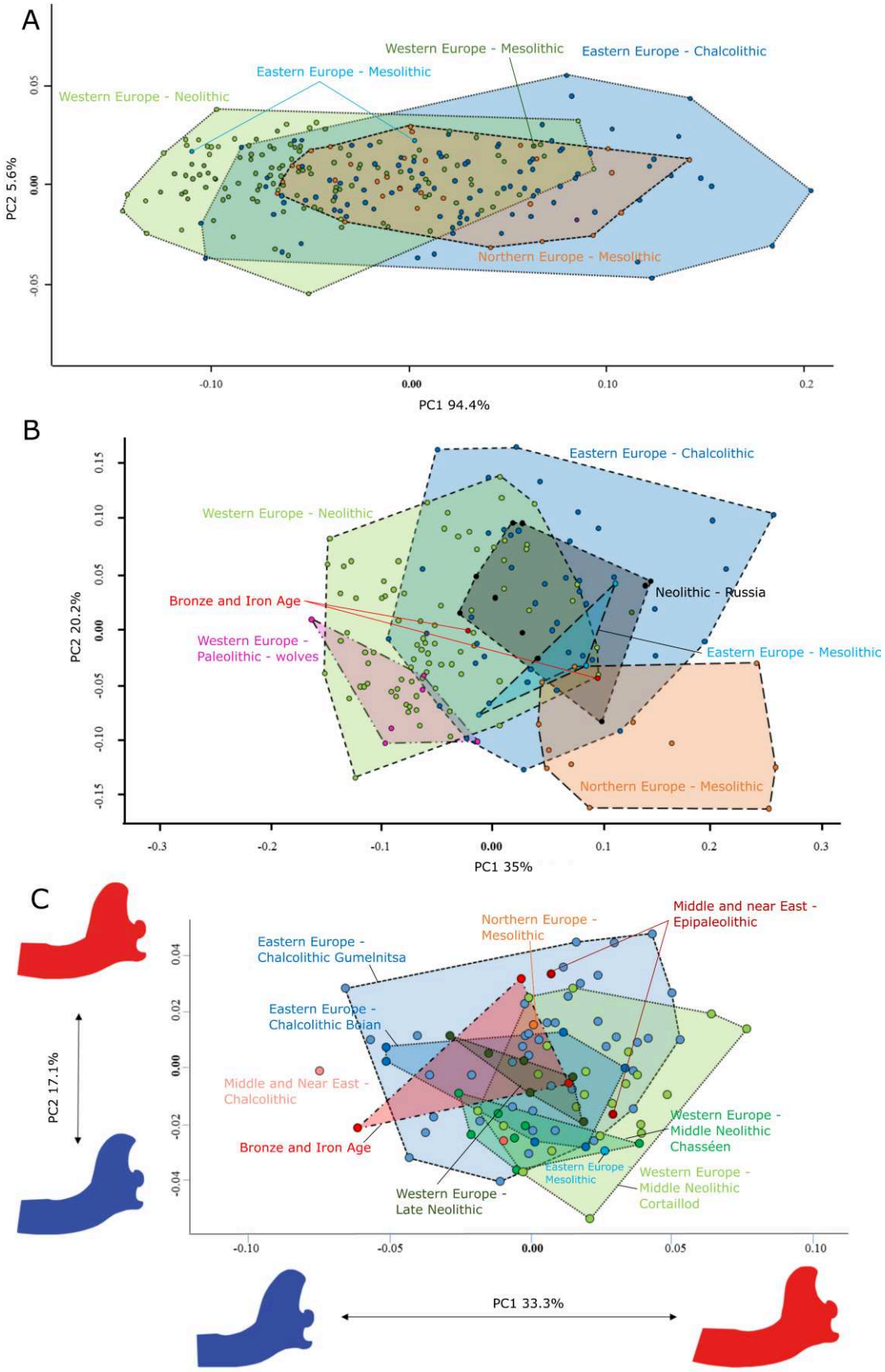

Figure 33. Variation in mandibular shape in dogs from the Epipaleolithic to the Bronze Age, modified from Filippo, 2017. Only the first two axes of the principal component analyses are represented. Analyses were performed on: (A) three dimensions (von den Driesch measurements 9, 10 and 11), (B) eight dimensions (von den Driesch measurements 9, 10, 11, 13L, 13B, 14, 17 and 20) or coordinates of 2D landmarks (C).

Variability of Neolithic dogs in Western Europe between periods and cultures

The multivariate study of Filippo (2017) suggested that **in Western Europe, some shapes would have been maintained over time while new ones would have appeared** (Filippo, 2017, Figure 34).

Variability of Neolithic and Chalcolithic dogs in Eastern Europe between periods, cultures and contemporary sites

In her multivariate study, Filippo (2017) had too few early dogs to clearly distinguish Mesolithic or Early Neolithic dogs from Chalcolithic dogs. No clear distinction between dogs from the Boian and Gumelnița cultures appear but **some differences seem to appear between contemporary and similar Chalcolithic sites (as regards the list of faunal remains) of Hârşova and Borduşani and the Boian sites of Varasti and Isaccea**, suggesting regional differences (Filippo, 2017, Figure 33).

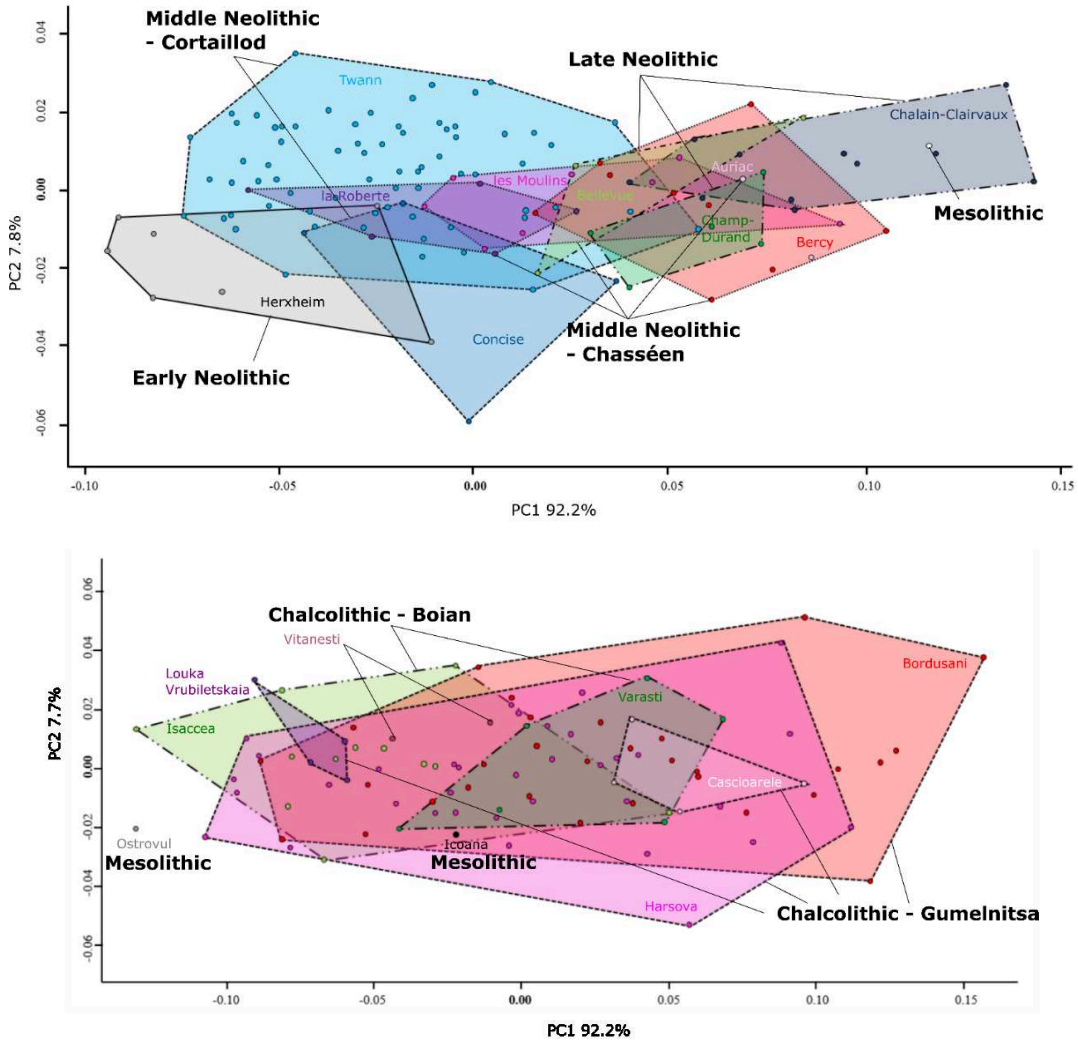

Figure 34. Variation in mandibular shape based on a Principal Component Analysis performed on three mandibular measurements (Von den Driesch's dimensions 9, 10 and 11) of dogs from Western Europe between the Mesolithic and Late Neolithic (up), or from Eastern Europe between the Mesolithic and the Chalcolithic (bottom).Modified from Filippo, 2017.

2.4.2.3.4. Variability in size and shape of dogs from French and Swiss lakeside settlements

Arbogast *et al.* (2005) first underlined the **relative homogeneity of the measurements in the Middle and Late Neolithic in the French and Swiss lakeside settlements**, both regionally and between regions, and even over a short time span, since the median values are fairly close and the variability remains limited. This could be explained in part by repeated interbreeding, leading to convergence towards the same morphological type (rather medium-sized and slender dogs) showing little differentiation (Arbogast, 1994). **The selection of particular morphological types therefore does not seem to have been a major concern in the Neolithic period,** at least in this geographical area (Arbogast *et al.*, 2005).

Regional variation

Middle Neolithic dogs from French lakeside settlements would have been slightly larger than their counterparts at sites in Western Switzerland, suggesting **regional variation within the same cultural group**. These differences persisted over time, as a parallel increase in size is observable in both regions (cf above, Arbogast *et al.*, 2005). Additionally, during the Chasséen, the dogs from Chalain were slightly larger than those – contemporary – of "la Roberte" (Pionnier-Capitan, 2010).

However, these studies mostly reflect variation in size, and do not accurately describe variations in shape. The multivariate study of Filippo (2017), providing a more accurate description of shape, reported morphological variations in sites from this region. For example, dogs from Twann (Middle Neolithic, Cortaillod) were clearly different in shape than dogs from Chalain-Clairvaux (Late Neolithic, Figure 34), from which they are separated by a gap of around 300-500 years. However, it is not clear whether shape differences are related to differences in location and/or differences in period and culture.

Intra-site variability

Additionnaly, the same study as suggested that **an important variability may be observable on the site of Twann** (Middle Neolithic, Cortaillod culture). The very large number of mandibles and long bones excavated allowed to explore the variability within the same geographic context and within the same occupation phase. Even visually, one can assess "the extraordinary range of morphologies that may have existed at that time" (Becker and Johansson, 1981; Pionnier-Capitan, 2010, Figure 35). In her PhD thesis, Maud Pionnier-Capitan (2010) calculated the coefficients of variation for 20 mandibular measurements on 45 complete mandibles, and obtained high values, ranging from 6 to 9%. However, these results, above all, reflect the high variability in mandible sizes. The high variability in shape is suggested by the multivariate study of Filippo (2017, Figure 35).

Figure 35. Dog mandibles from the same stratigraphic layer of Twann (Middle Neolithic, Switzerland). From Pionnier-Capitan (2010).

2.4.2.3.5. Haplogroups

During the Mesolithic, Europe possessed the mitochondrial haplogroups C and A (haplogroup A is only present in the Iberian Peninsula), and during the Neolithic these haplogroups were accompanied in Europe by haplogroup D. This strongly suggests the introduction of non-indigenous domestic dogs, probably coming from the Near-East. In France-Switzerland, the earliest dogs of haplogroup D arrived during the Middle Neolithic, in the Chasséen around 5,900-5,700 cal. BP (S. Bréhard, M. Ollivier and A. Manin, *pers. comm.*), and in the Cortaillod (Ollivier *et al.*, 2018). In Western and Northern Europe, the turnover was incomplete and haplogroup C persisted well into the beginning of the Bronze Age at least. In SouthEastern Europe (including Romania) the haplogroup D became dominant at the early Chalcolithic and then was the only haplogroup represented during the Late Chalcolithic-Gulmenitsa culture (Table 12). In Western Europe, haplogroup C remained dominant during the Neolithic, but haplogroups A, D and B were also present (Table 19). Thus, dogs from Western and South-Eastern Europe did not have the same evolutionary histories, which may have resulted in different morphologies in the two poles. In Western Europe, dogs coming from an Epipaleolithic and Mesolithic matriline still dominated during the Neolithic. Local human populations thus did not seem to have replaced their dogs much with dogs from elsewhere.

Table 12. Representation of the different dog haplogroups following the different chrono-cultural contexts. Up-to-date unpublished results, personal communication from M. Ollivier, A. Manin and S. Bréhard.

Haplogroup	**C**	**D**	**A**	**B**
South-Eastern Europe				
Mesolithic	6			
Chalcolithic – Hamangia and Boian	2	5		
Chalcolithic – Gumelnița	0	14		
Western Europe				
Epipaleolithic – Mesolithic	2			
Early Neolithic – Herxheim	1	1		
Middle Neolithic – Chasséen	18	1	2	1
Middle Neolithic – Cortaillod – Twann	6	2		
Late Neolithic	5	1		

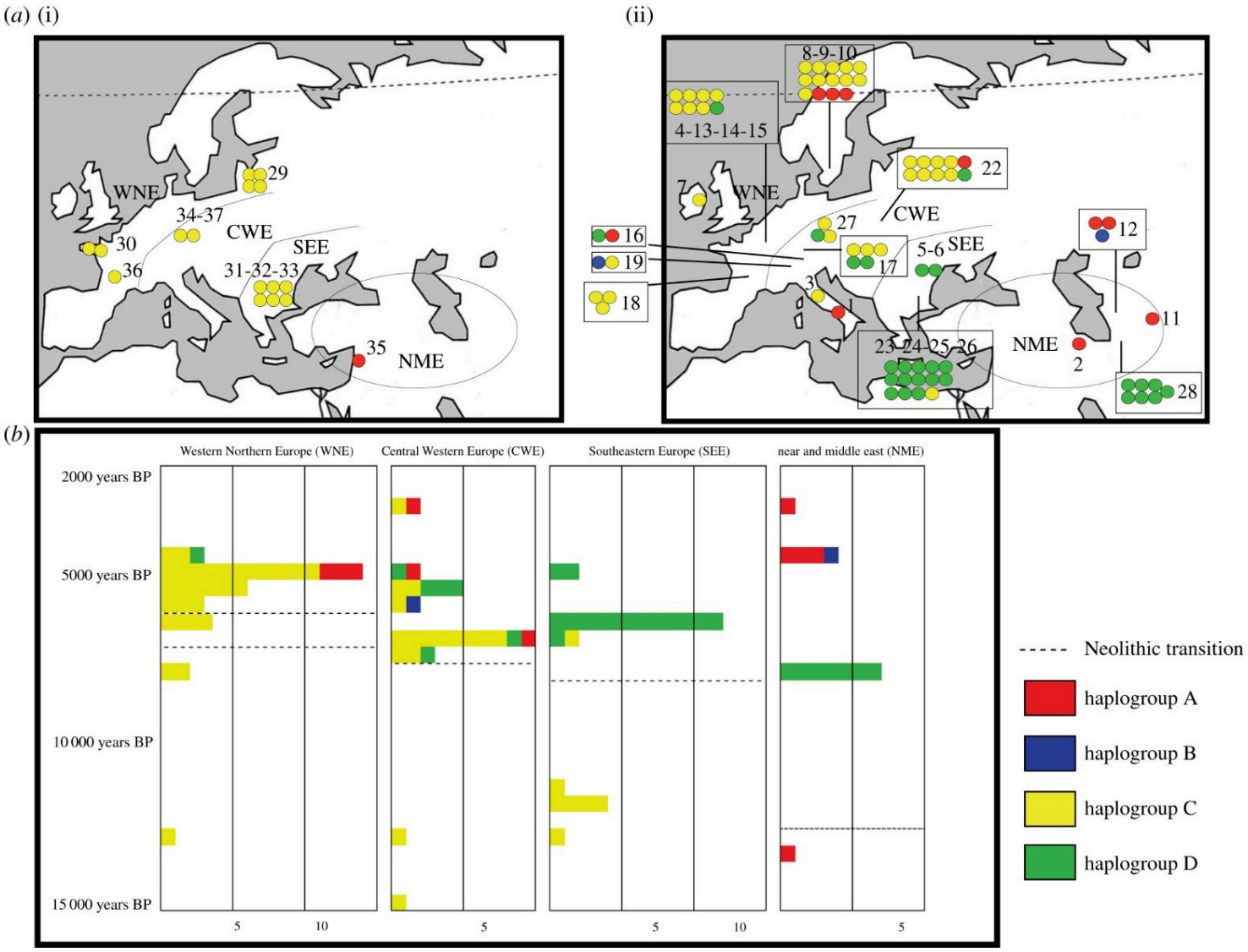

Figure 36. Genetic, geographical and chronological pattern of ancient dogs in the Middle East and Europe from the pre-neolithic (a) (i) to during and after the Neolithic transition (a) (ii), and chronological distribution of dog haplogroup frequencies (b). The dashed line represents the Neolithic transition. From Ollivier *et al.*, 2018.

2.4.1. Evolution in masticatory abilities

To date, the Master thesis written by Andréa Filippo (2017) is the only study that has attempted to interpret the observed variations in form from a functional perspective. The masticatory function is approached by calculating the **mechanical potential**, which provides a rough estimate of the efficacy of the temporalis muscle and the jaw morphology in generating bite force if the mandible is considered as a simple lever. Since it is a measurement ratio, the mechanical potential provides an indication on the bite force relative to the size of the individuals. This simple model is useful to attribute a functional interpretation to linear measurements, but it lacks precision because it does not take into account the architecture of the muscles nor the finer variations in shape.

This previous study has suggested, on a relatively large sample of mandibles, that **the mean mechanical potential tended to decrease between the Boian and Gumelnița cultures**, but the sample size for the Boian culture is very small. The mechanical potential **tends to decrease on average between the Chasséen and Cortaillod cultures** during the Middle Neolithic in Western Europe and **dogs dated to the Late Neolithic have in average similar mechanical potential values as during the Chasséen culture**. However, the sample size of both groups is small and likely does not reflects the true variability in function at that times. Additionnaly, **dogs with the highest mechanical potential during the Boian culture in South-Eastern Romania seem to have no equivalent in Western Europe**. Moreover, although the modern samples of dogs and wolves are small, the variation in the mechanical potential of modern dogs covers almost the entire variation in the mechanical potential of ancient dogs, and the mechanical potential of modern wolves is on average lower than that of ancient dogs.

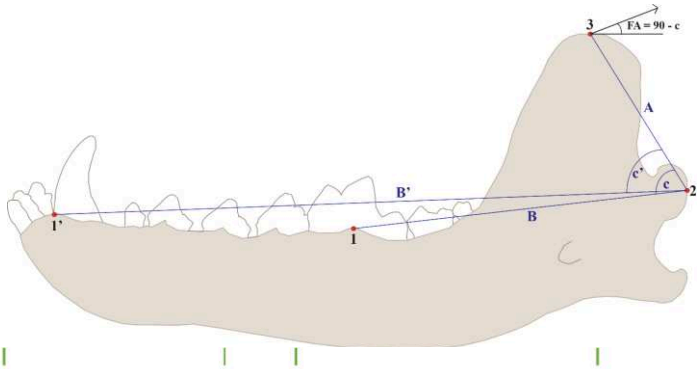

Figure 37. Measurements used for the calculation of the mechanical potential (MP): MP = A/B cos (FA). From Filippo, 2017.

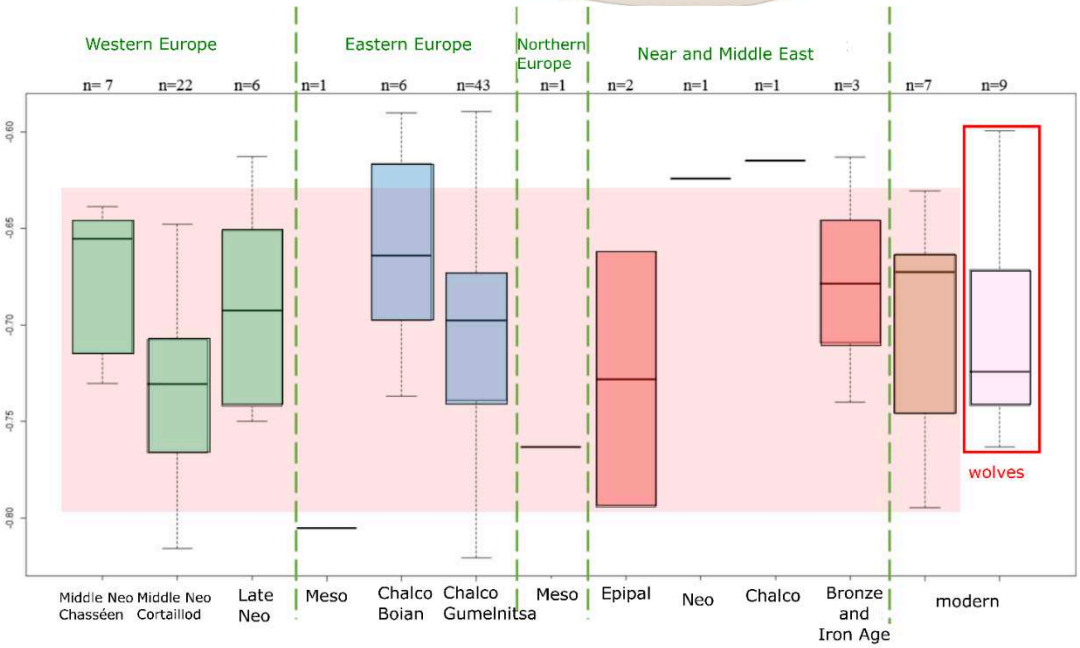

Figure 38. Variation in the mechanical potential of dogs from Europe and Near and Middle East. Translated from Filippo, 2017. Epipal: Epipaleolithic; Meso: Mesolithic; Neo: Neolithic; Chalco: Chalcolithic.

Conclusion of Part 1: Formulation of the research problem

This first bibliographical part enabled us to review current knowledge on the place of canids – in particular the dog – in the archaeological record and in the life of the first farmers, as well as their genetic and morphological variability in the first agricultural societies. This allowed us to define more precisely our research questions, to choose the best methodology to address these questions, and to put some limitations to our work.

The dog is an animal of major interest as it is the witness of the transition from hunther-gatherers to farming societies and of the evolution of the first agricultural societies. Moreover, the Neolithic societies are the first for which a large number of dog remains are available, even if remains are rare in the early phases. Moreover, the distinction between dogs and wolves is problematic in the Epipaleolithic because crossbreeding between wolves and dogs is not excluded in the early phases of domestication, and because the remains are rare and often fragmented. From the Mesolithic onwards, dogs and wolves seem to be clearly distinguishable, particularly in terms of size, the risk of confusion thus being minimal.

Contrary to the dog, the red fox has yielded a much smaller number of remains, is much less documented, and the interpretation of its presence is often problematic. Osteometric data are very rare and are often only used to diagnose differences from dogs. We will therefore focus primarily on the dog in this thesis. The study of the red fox, carried out for exploratory and comparative purposes remains preliminary.

The overview conducted in this part has shown that a great amount of data is already available on the (great) diversity of the status that humans granted to dogs in societies from the Mesolithic to the pre-Bronze Age in Europe, but also on their genetic diversity (haplogroups), their functional adaptations in relation to the major changes in human societies that occurred in this period (acquisition of the ability to digest starch from cereal or pulse), and also on their morphological diversity (coat colour, size, overall robustness).

Previous morphometric studies all provide some concordant information. **In Western Europe, dogs would have decreased in size from the Mesolithic to the end of the Middle Neolithic and then increased in size with the appearance of larger dogs during the Late Neolithic**. **In Eastern Europe, dogs would also have decreased in size from the Mesolithic to the Chalcolithic**. In both areas, a **certain variability already existed in the past, both in terms of size (very small dogs are attested during the Chasséen, Cortaillod and Gumelnița cultures) and shape (**ancient dogs would be relatively similar in shape but much smaller to their wild relatives, yet some studies suggested that some shapes may have no equivalent among modern dogs).

However, these morphometric data are rarely related to other data, such as the affiliation to a given **haplogroup**, the **colour of the fur**, the ability to **digest starch** (data provided by genetics), or to the **relationships** that the canids entertained with humans (data provided by archaeological contexts and osteoarchaeology).

Moreover, **studies that have explored morphological variability in canids are quite unsatisfactory** for several reasons. Almost all these studies rely on a traditional metric approach (traditional morphometrics), i.e. measurements taken directly on the bone remains with a caliper, following standards to ensure a certain repeatability (Von den Driesch, 1976). Statistical analyses are often uni- or bivariate and conclusions are limited to comparisons in size (sometimes by estimating wither heights) or coefficient of variation (only one dimension is used), or comparisons of robustness (two dimensions are used: width and length). Shape is therefore poorly and uncompletely described. To our knowledge, the only attempts that have been done to explore shape variability with finer approaches, such as 2D geometric morphometrics, are based on landmarks put on photographs. Moreover, this is the only study that has attempted to interpret the variation in form from a functional point of view, thus connecting anatomical shape with biological function. To date, there is **no study that uses three-dimensional data**, which would yet allow much more precise descriptions of shapes and more accurate functional inferences. Given the variability suggested by the 2D data alone, **the use of 3D appeared to be a very interesting method for this thesis.** Moreover, **osteometric data are rather scattered in the literature**. Indeed, studies comparing sites are rare and comparisons are often regional and limited to a short chrono-cultural phase. Comparisons at a European scale are so far almost non-existent and refer to very limited sample sizes. They only provide a fragmentary idea of the morphological variability that existed in dogs before the Bronze Age. This will be a main motivation in the further development of this work.

Cranial remains are far too rare to allow a thorough study of shape, but **mandibles are among the most numerous and best preserved remains** as evidenced by some previous work exploring the morphological variability of prehistoric dogs. Additionally, its great **plasticity** and **close relationships with the cranium and masticatory functions** (this will be detailed further in Part 2) make it a subject of major interest and more promising than teeth, that are very conservative, for following rapid evolutionary phenomena.

We could access to large samples coming from different sites of our two geographical areas of interest (**Western Europe: France-Switzerland, and Eastern Europe: Romania**). For these sites, rich contextual data are already available (archaeological context, DNA data). Since in these two areas the neolithisation processes differ, as well as the evolutionary histories of dogs (according to haplogroup data), they will be considered in parallel analyses.

We can therefore formulate the following problem:

How does mandibular shape inform us about the evolution of the morphological variability and chewing abilities in dogs from the first European agricultural societies?

A number of sub-questions can be identified from this major question:

Q1: What was the morphological variability in dogs before the Bronze Age compared to modern canids?

Previous studies suggested that ancient dogs were smaller than both modern and ancient wolves, but were indistinguishable from them in terms of proportions. Most studies seem to suggest that the variability of dogs was lower in the past, but that of Filippo (2017), which included many ancient and modern specimens suggested that some shapes may have disappeared, and that the variability may have been much greater than previously thought. What if the canid sample is enriched and the tools for analysing the shape are finer?

Q2: Are there different morphotypes in Eastern and Western Europe?
Q3: Can we understand the temporal and cultural variations in form or masticatory function for a same region (Eastern or Western Europe)?
Q4: Can the different haplogroups be linked to significant morphological differences?

Previous studies have put forward the possibility that dogs from Eastern Europe were different from those from Western Europe (in terms of both genetic composition and jaw shape) and that jaw shape varied between periods and cultures. This could be consistent with mitochondrial data on haplogroups which show that the two geographical poles were marked by different evolutionary histories.
It would indeed be interesting to morphologically characterise the dogs in Western Europe coming from the influx of dogs from the Near East (haplogroup D). Do they differ in size, proportions and robustness? Has there been a progressive replacement of the existing population in Western Europe (which would result in an irreversible change in morphology) or have the native morphotypes persisted and have the populations mixed (resulting in mixed morphologies)?

Q5: Can particular morphotype be linked to particular status/use?

Dog status seem to have been more variable in Western Europe than in Romania, where the deposit or burial of complete animals is, to date, not attested. In Western Europe, some morphotypes may have been favoured to ensure specific functions (consumption versus non-consumption). So far, the methods employed to describe shape variation were to incomplete to test for this phenomenon. Did the complete buried dogs present

particular morphologies? Are morphological similarities observed for consumed dogs? This is relevant when considering that in some modern societies (e.g. South Korea), specific breeds of dogs are dedicated to meat production (Milliet, 1995).

Q6: Has the appearance of the ability to digest starch been accompanied by changes in mandibular morphology, which could result in changes in masticatory abilities over time, in both Eastern and Western Europe?

One could expect early dogs with a low copy number of the gene AMY2B (and which are therefore not able to digest starch that much) to have jaws that are more adapted to feed on animal prey than on a diet that is rich in cereals from human food refuse. They must produce relatively high bite forces at large gape angles, useful to feed on a mostly carnivorous diet. On the contrary, dogs with a greater number of copies (and that are adapted to digest starch) should privilege bites at low gapes and lateral movments for mastication of a diet that is more varied and richer in cereals. As the mandible is directly involved into mastication, these differences should be traceable based on differences in mandible shape.

Q7: Can we understand the temporal and cultural variations in form or masticatory function within a single site providing material over a long and rich chrono-stratigraphic period (e.g. Twann)?

Q8: For contemporary and similar sites with regard to food acquisition strategy (e.g. Hârşova and Borduşani), are there differences in shape between dog populations?

These would more likely result of anthropic constraints (e.g. selection for aesthethics or functional purposes, strong endogamy) than to natural constraints.

Q9: What can be learned from the comparison of the results obtained for dogs and red foxes?

Comparing the morphological and functional evolution of a domestic canid (the dog), which has obviously maintained a rather commensal relationship with humans, with that of a canid which has remained strictly commensal is interesting to evaluate the impact of the proximity between humans and canids on their morphological and functional adaptations. One might expect to observe either parallel evolutionary trajectories if and when dogs were commensal and humans did not voluntarily select particular morphotypes. Conversely, should humans have selected for certain morphologies then different trajectories for the two canids, one remaining mostly subject to natural constraints, and the other being subject to stronger anthropic constraints should be observed.

These questions raise other questions of a more methodological nature:

- How does the state of the archaeological material (availability, fragmentation) limit the results/interpretations of our study?
- Is mandibular shape a good indicator of the overall morphotype, of the shape of the complete skull?
- How can mandibular shape be used to make functional inferences? In other words, if and how can variations in masticatory ability be inferred from variation in mandibular shape (development of masticatory muscles, bite force)?
- How are natural abiotic (sex, age, size) or biotic (environmental conditions, diet, proximity to humans) factors likely to impact the shape of the mandible or masticatory capacities?

To adress these questions, the use of modern specimens for which muscular and contextual data are available is inevitable. It will indeed be necessary to make the connection between morphology and the other parameters likely to be of interest to us (masticatory muscles, bite force, age, sex, size, diet, proximity to human settlements). However, this raises a crucial question: are modern canids good models for interpreting canids prior to the Bronze age?

To sum up, we aim to gather a corpus of dog and red fox mandibles from the Mesolithic to the pre-Bronze Age in Western Europe and Romania, that is as comprehensive as possible, in order to explore the morphological variability that existed in dogs in the first agricultural societies. Three-dimensional geometric morphometrics will be used to describe variation in shape. This variability will be examined in relation to data on haplogroups, cultural context, temporality, and geography. Dogs and red foxes will be compared to investigate the impact of the proximity between human and canids. In order to interpret the morphological variability in functional terms, we will need to understand the relationships between the shape of the mandible, the shape of the skull, the development of masticatory muscles and the production of bite force. To do this, we will have to make use of modern canids. If strong relationships are attested, then predictive models may be derived and applied to archaeological remains to infer function from mandibular shape. These modern canids will also enable us to explore the effect of other factors such as diet, human-animal proximity, age, sex, or size. We will compare the existing variability with that in the past to better understand what this represents and discuss the relevance of using modern canids to interpret remains prior to the Bronze Age.

Part 2

Developing morpho-functional tools on the mandible of extant canids

The purpose of this second part is to develop methodological tools on modern canids which will be applied to the archaeological mandibles of canids in Part 3. This part is mostly a compilation of manuscripts and published articles, each one addressing a specific biological question.

As we aim to make this relatively technical part accessible to readers who are not specialists in morphometry or functional anatomy, in a first chapter (Chapter 2), we will provide basic knowledge that will be useful to apprehend the following chapters (3, 4 and 5). Anatomical and functional basics will be provided to help understand the organisation of the mandible within the masticatory apparatus. We will briefly describe the overall methodology used in this thesis and also recall some statistical bases useful to explore morphological variation in multivariate datasets. The biological questions, as well as the reference sample constituted to address these questions in the following chapters will be presented.

Before each chapter is presented, key points pertinent to the application to the archaeological canids will be highlighted.

In the conclusion of this part 2, we will summarize the main findings provided by the study of modern canids and discuss future perspectives. Above all we will draw conclusions on the application of these results to interpret the archaeological remains of dogs prior to the Bronze Age in part 3.

Chapter 2.
General methodology

In this chapter the aim is to provide a basis of understanding for the following chapters, where the specialised bibliography will be more specifically addressed.

In addition to being resistant to post-burial processes and thus well preserved in archaeological contexts, the mandible provides interesting insights into the morphological and functional variability within canids, since it is a key architectural and functional part of the head.

To convince the reader thereof, first, the anatomy of the masticatory apparatus and the integration of the mandible into this apparatus to allow mastication will be briefly described. The factors that may affect the morphological variability of the mandible and its function will be highlighted, leading to a number of biological questions that will be addressed in the following chapters.

The mechanical principles needed to approach the functioning of the masticatory apparatus, as well as the geometric tools required to describe the three-dimensional shape of the mandible as faithfully as possible will be presented next. Additionally, basic notions of the statistical tools used in the articles will be provided to clarify their principle and limitations.

In conclusion, we will describe how our reference sample of modern canids is constituted (and outline its limitations), and finally list the research questions that will be addressed in the next chapters (articles) of this part of the thesis.

1. The mandible within the bony head of canids: from integration to plasticity

In this section, the anatomical description of the head is oriented towards morpho-functional purposes allowing to highlight the relations between morphology and function.

1.1. The mandible, a component integrated into the masticatory apparatus

The skeleton of the head is made up of two main bony complexes. The dorsal complex (the **cranium**) is composed of an assemblage of flat mostly dermal bones. It contains the cerebral and nasal cavities, and thus protects the central nervous system and the sense organs, including the initial parts of the respiratory system. Upfront, the premaxillary and maxillary bones constitute the jaws that bear the teeth in two symmetrical arranged arcades. The ventral complex is made up of two hemi-**mandibles** (here called mandible for simplification purposes) that form the lower jaw. The cranium and mandibles are articulated at the temporo-mandibular joint and are joined by the masticatory muscles which originate on the skull and attach to the posterior part of the mandibles (Figure 39).

Among the **masticatory muscles**, some are **adductors** (they raise the mandible: temporal, masseter, and pterygoid muscles) and others are abductors (they lower the mandible: digastric muscle).

By raising and lowering of the mandible, these muscles are responsible for biting, which plays a role in defense against competitors or predators, prey acquisition, and chewing (mastication, i.e. the first stage of digestion). By contracting, the muscles actually bring the jaws that carry the teeth closer together, producing the **bite force**, and allowing the incisor teeth in the front to cut food, the well-developped canine teeth and premolars (that are secodont), to tear food, and the bunodont molars at the back to grind food. The secobunodont carnassials are in close contact (premolar 4 on the upper jaw P^4 and molar 1 on the lower jaw M_1) and act as scissors to tear and grind food.

The masseter, temporal (which is very developed in carnivores), and digastric muscles allow mainly vertical movements, while the pterygoid (which is poorly developed in carnivores), allows horizontal movements necessary for food grinding. The associated contraction of the masseter and pterygoid muscles increases the force produced during the bite, while the temporal muscle is mainly involved in generating bite speed and is optimized for biting at large gapes. The anatomy of the muscles is in fact more complex since each muscle complex is actually divided into several layers distinguishable by their attachment on the cranium and mandible (Figure 39).

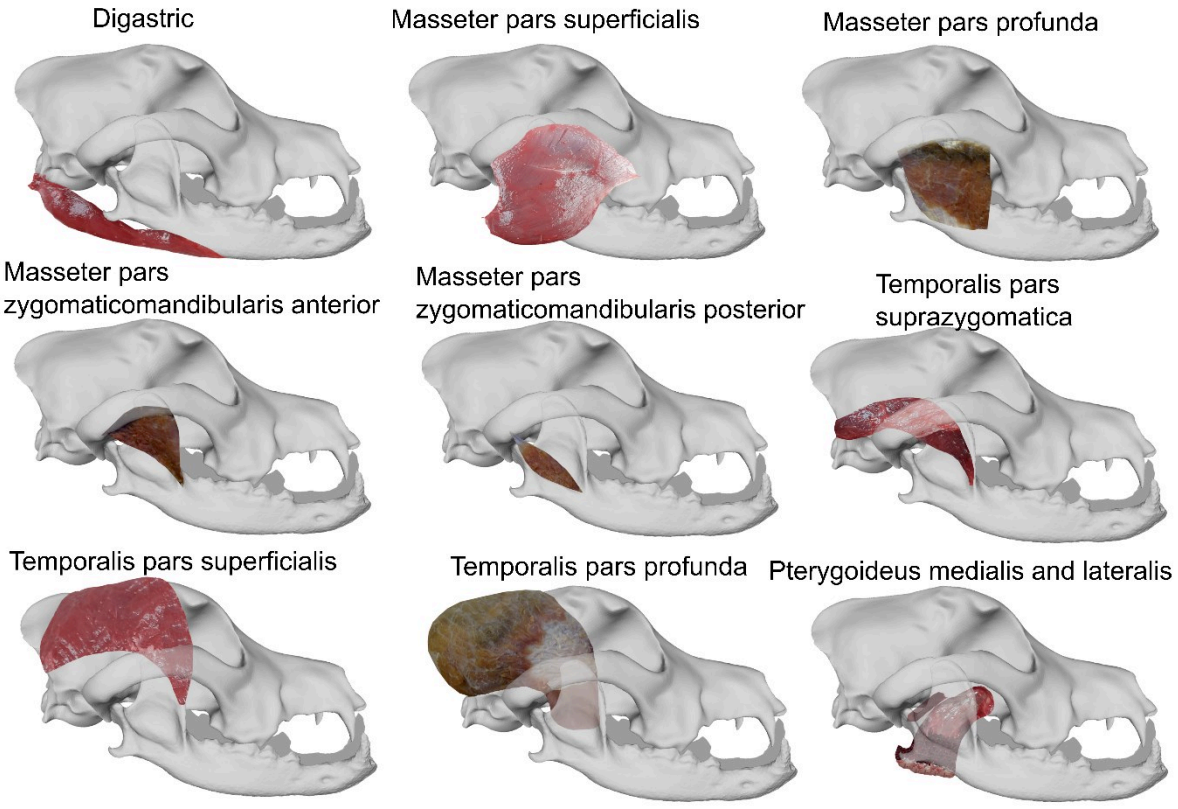

Figure 39. Masticatory muscles in dogs and their different bundles.

The fact that the cranium, mandibles and muscles are in direct contact suggests strong developmental and functional constraints.

Thus, morphological variations in one bone complex are likely to be reflected on the other. To this extent, the shape of the mandible is likely informative of the shape of the skull, and may provide an appreciation of the overall morphotype (which, it should be remembered, refers to cranial proportions, making it possible to define the dolichocephalic, mesocephalic and brachycephalic types, cf Part 1 – 1.5).

Likewise, as the skull serves as a framework for the muscles which are inserted upon it, the development of the muscles is limited by that of the bones, whilst shaping them simultaneously. Thus, the shape of the mandible is likely informative of the volume occupied by the muscles, and the strength they are able to develop (individually or collectively through the production of bite force). Moreover, the mandible is more specifically oriented towards biting than the cranium, which is also involved in other functions, since it houses the brain and the sense organs. Thus, the mandible may have a stronger relationship with the masticatory muscles or bite force.

This relationship between the various elements of the masticatory apparatus is often referred to as its **integration**. Integration is "the tendency of different traits to vary jointly, in a coordinated manner, throughout a morphological structure or even a whole organism" (Klingenberg, 2014). Integration can also occur at a smaller scale, e.g. within each bone complex. For example, the shape of the anterior part of the cranium (one module) is likely to be correlated with that of the posterior part of the cranium (another module), due to developmental and functional constraints. This is called **modularity** (Klingenberg, 2014). The concepts of morphological integration and modularity are thus inherently connected.

In addition to the mechanical constraints, there are also developmental factors that may play an important role in maintaining and shaping the integrity of the system. For example, sexual dimorphism is often observed, particularly in wild canids, generally resulting in larger size and more developed muscles in males than in females. Additionally, variations in the overall shape or in the shape of different parts of the skull are intrinsically linked to variations in size in order to maintain the integrity of the system. This is called **allometry**. Allometry can be age-related (ontogenic or static allometry, if we look at the impact of size during development in the same individual or in different individuals from the same population, respectively), or species-related if we compare different species (evolutionary allometry).

1.2. The mandible, a plastic component of the masticatory system

Skull shape, muscle development and bite strength have a genetic basis but also may respond to environmental constraints due to **phenotypic plasticity**. Phenotypic plasticity is "the ability of an organism to change in response to stimuli or inputs from the environment. The response may or may not be adaptive, and it may involve a change in morphology, physiological state, or behavior, or some combination of these, at any level of organisation, the phenotype being all of the characteristics of an organism other than its genes" (*Encyclopedia of Ecology | ScienceDirect*).

Bones are much more plastic than teeth, which are more **conservative** and evolve very slowly. The mandible is therefore more interesting to capture relatively rapid changes through time.

Morphology can thus provide information on the ecology of the species (ecomorphology), which has been shown for many vertebrates. Similarly, for plastic structures, morphology may reflect the changes of an animal in response to its environment during its lifetime (see bibliography in the following chapters).

It has been demonstrated that skull morphology and bite force are related to **diet** in numerous vertebrate species. For example, strict carnivore clades will not have the same functional adaptations (reduction in the number of teeth, that are also sharper/more secondont; more strongly developed masticatory muscles, resulting in a more developed sagittal crest) compared to herbivores (continuously growing/selenodont teeth, masticatory muscles allowing more important horizontal movements). Christiansen and Wroe (2007) showed that the relationship between bite force and diet even overcomes phylogenetic constraints on cranial morphology in carnivores, for example. Plant consumers and carnivores that capture large prey have higher bite forces than omnivores and carnivores that capture small prey.

It is also possible to link morphology to other environmental parameters, including geographical or climatic data (if populations are isolated, morphological differentiation can occur) or even anthropogenic data.

However, while these effects have been extensively studied at the scale of large clades, studies focusing on the impact of diet or environmental parameters on morphology within the same species are rarer. This is particularly the case in canid species, where the description of variation in shape generally concerns only the cranium and not the mandible, and calls for a more detailed anatomical description.

One consequence of the important functional role is that individuals of different species can share certain morphological traits. This is a phenomenon of **convergence**.

1.3. A system subject to considerable morphological variability in canids

One of the peculiarities of canids is their extreme morphological variability (or **morphological disparity**). The interspecific variability is enhanced by an exceptional intraspecific variability for some species such as the dog. Recent artificial selection for the creation of breeds has resulted in an extraordinary diversity of sizes and shapes, which is well reflected in the head. Consequently, "the amount of shape variation among domestic dogs far exceeds that in wild species, and it is comparable to the disparity throughout the Carnivora" (Drake and Klingenberg, 2010, Figure 40).

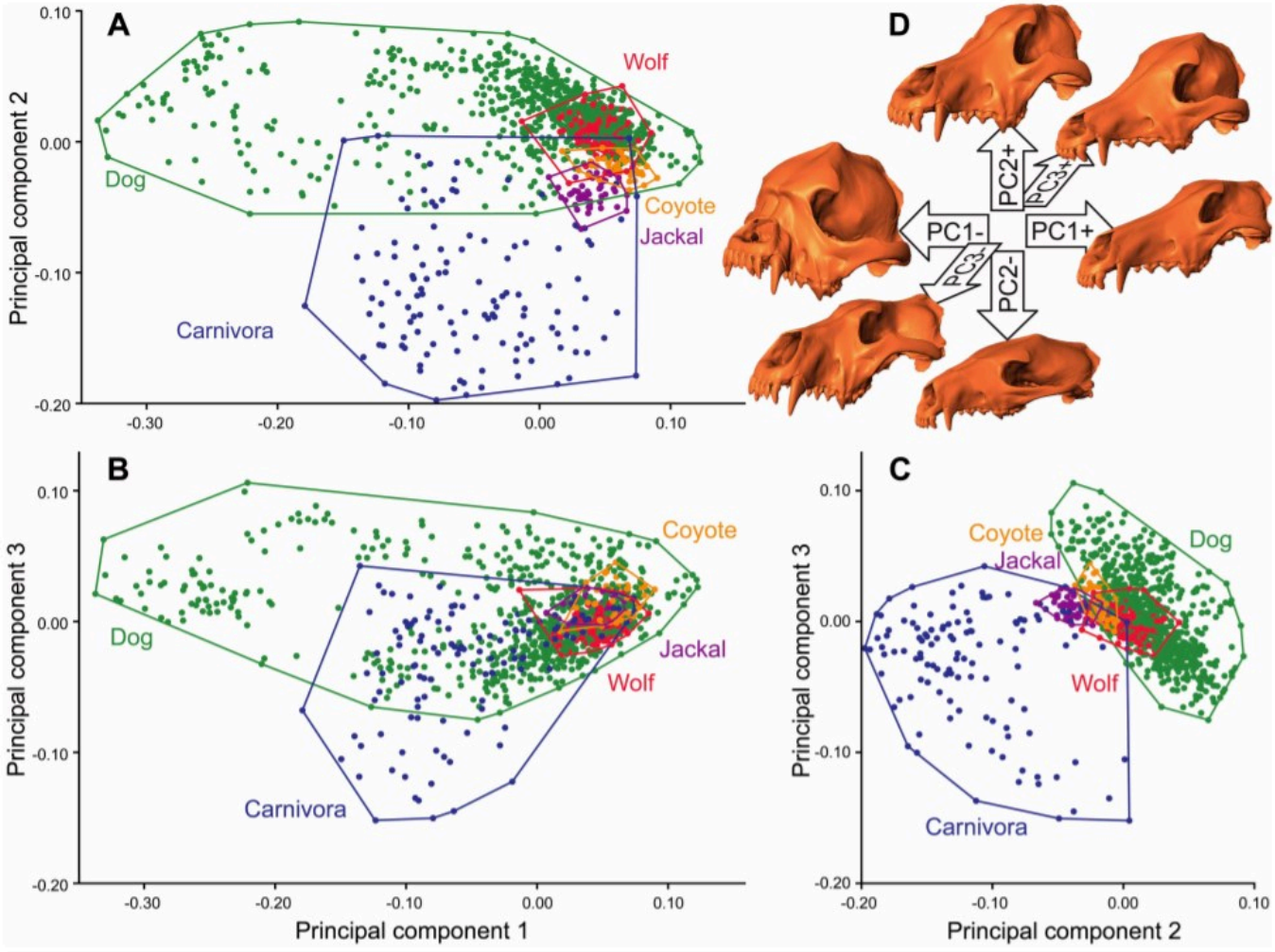

Figure 40. Variation in cranial shape in dogs, wild canids and other Carnivora. From Drake and Klingenberg, 2010

Numerous studies have examined the effects of domestication or recent selection on morphological variability, integration and modularity in canids. Some research has also explored the relationship between variability in dogs and the function of the masticatory apparatus (e.g. Ellis *et al.*, 2009, other studies will be cited in the next chapters). However, these

studies have often been focused on the cranium and rarely on the mandible. Only few papers have studied the integration between these two bony complexes.

Artificial selection targets more directly the cranium (since it is the cranium that contributes most to the general shape of the head). The shape of the mandible is more related to constraints that maintain the integrity of the system, and to mechanical constraints depending on muscle loads. This is particularly well illustrated in some hypertypes (e.g. very brachycephalic dogs such as bulldogs), for whom a decoupling between the upper and the lower jaw exists. One might therefore expect the mandible to be morphologically less variable than the skull, and that the relationships between the shape of the cranium and the shape of the mandible are less homogeneous and less strong in dogs than in canids not submitted to intensive artificial selection. For similar reasons, one would also expect the relationship between muscle or bite forces and skull (cranial and mandibular) shape to be less strong for dogs than for other commensal or wild species, particularly given that "strong selective pressure can cause a departure from patterns favored by developmental constraints" (Beldade, Koops and Brakefield, 2002; Renaud, Auffray and de la Porte, 2010). Furthermore, one may assume that the functional integration between muscle or bite force and skull shape is stronger for the mandible than for the cranium since the mandible is only involved in biting, unlike the cranium. However, these questions have not been explored to date.

The great morphological variability within the dog's head has had other repercussions, notably on the teeth. Some teeth may be missing (particularly the lower third molar or first premolar – this is called oligodonthia) or on the contrary, may be supernumerary (e.g. presence of a lower fourth molar or duplication of the lower first premolar). A reduction in the number of teeth is very frequently observed in brachycephalic breeds, due to the shortening of the face: the teeth do not have enough space to develop normally on the jaw.

The archaeozoological literature seems to suggest that before the Bronze Age humans did not select particular morphotypes of dogs other than on a size criterion, and that dogs had a rather commensal lifestyle (cf. Conclusion of Part 1: Formulation of the research problem). Modern dogs are therefore perhaps not the best models for studying ancient populations. However, as we do not have a very precise idea of the morphological variability that existed in the past (metric data are scattered, multivariate studies are scarce, and large-scale comparative studies use small samples and do not rely on 3D geometric morphometrics), we cannot exclude modern dogs from our reference sample *a priori*. These can provide points of comparison to understand and locate the variability of ancient dogs in relation to modern dogs. If ancient dogs prove to be included in the morphological variability of modern dogs, then these can provide useful keys to the understanding of the evolution of form and function in archaeological dogs. If significant relationships between the mandible and the other elements of the masticatory apparatus (cranium / muscles / bite force) are found (which are expected, even though they are expected to be weak), then mandibles can be used to make morphological and functional inferences for archaeological specimens. That is, from the shape of the mandible, one can predict the shape of the cranium, the associated musculature and possibly even the bite force.

KEY POINTS

In canids, the mandibular morphology and its variability within a population is likely the result of the **interplay between genetics, developmental constraints**, as well as **functional** or **ecological constraints**

This is likely driven by different processes including geographical isolation followed by genetic and morphological drift, natural selection (which is exerted on certain phenotypic variants more adapted to a particular context) or epigenetic processes ("any modification other than changes in DNA sequences affecting gene expression, whether those modifications have been shown to be stable or not", Herrel, Joly and Danchin, 2020), and, in the case of dogs, artificial selection for aesthetic or utilitarian reasons.

However, these effects have been, so far, incompletely described for the mandible of dogs and foxes.

2. Methodological tools to approach function and form

2.1. Methods to quantify the masticatory function

The masticatory function can be appreciated by the **bite force**.

In vertebrates, "Maximum voluntary bite force is an indicator of the functional state of the masticatory system", a "measure of whole organism performance that is associated with both cranial morphology and dietary ecology" (Koc, Dogan and Bek, 2010; Santana, 2016). "The level of maximum bite force results from the combined action of the jaw elevator muscles modified by jaw biomechanics and reflex mechanisms" (Koc, Dogan and Bek, 2010).

Bite force results from the sum of the forces exerted by the adductor muscles (masseter, temporal and pterygoid muscles). It is thus strongly dependent on **muscle architecture**, which consists of:

- the intrinsic strength that can be developed by each muscle (**Physiological Cross-Sectional Area, PCSA)** depending on:
    - the **volume** of the muscle;
    - the **arrangement of the muscle fibres** within these muscles: muscle fibers are rarely orientated parallel to the surface of the muscle in the axis of action of the muscle, which is called pennation. Pennation influences fibre length (Figure 41) and allows the packing of more fibres in parallel in a given muscle volume.
- the **points of attachment of each adductor muscle** on the skull which impact the orientation of the force exerted by the muscle and more importantly the moment arm of the muscle around the temporomandibular joint.
- Muscle stress or the intrinsic ability of a muscle to generate force. This reflects the muscle fibre types that make up a muscle.

So far, morpho-functional studies in dogs or foxes have relied on estimates of bite force based on linear skull measurements, either via estimation of muscle PCSA using predictive equations (**dry-skull method**, Ellis *et al.*, 2009; Forbes-Harper *et al.*, 2017), or by assimilating the mandible to a system of levers. However, these methods do not take into account the architecture of the masticatory muscles, i.e. their more complex decomposition into bundles, whose insertions, muscle fiber lengths and pennation angles can vary greatly from one individual to another. These anatomical variations can result in variations in the magnitude of the PCSA of each muscle (a muscle with long parallel fibres such as the digastricus produces less strength than a strongly pennate muscle with shorter fibres such as the temporal, see figure), and in the orientation of the muscle forces and thus the muscle moment arms. This can therefore result in considerable variation in bite force estimates. Accurate muscle measurements are then crucial to build accurate bite force models (Gröning *et al.*, 2013).

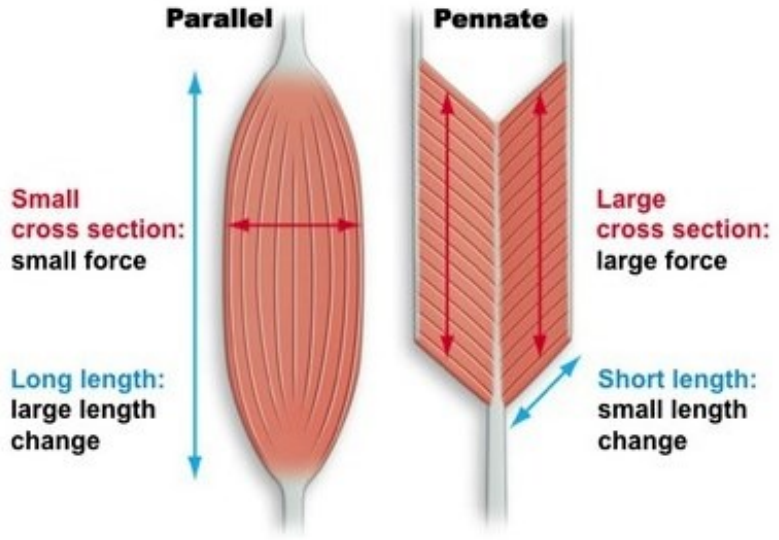

Figure 41. Influence of pennation and fibre length on the strength developed by the muscle. From https://quizlet.com/124308534/musculoskeletal-system-flash-cards/

So far, only a few studies have used muscle data obtained from **dissection** to estimate bite forces in canids and felids (Hartstone-Rose, Perry and Morrow, 2012; Penrose, Kemp and Jeffery, 2016; Penrose *et al.*, 2020). However, to date, no comprehensive dataset on the muscle architecture in dogs nor red foxes was available. Moreover, previous methods have not taken into account the geometry of the cranium, and even less that of the mandible. These gaps in the literature were among the principal motivations for the following chapters.

In this thesis we have dissected a large number of canid heads (around 150, further details about the sampling will be provided in section 3.1). After removing the skin, the masticatory muscles appear within their superficial connective tissue sheets. At this stage, the extraordinary development of the muscles in some dog breeds, such as the pit bull, was clearly noticeable (Figure 42). All the bundles of the masticatory muscles were dissected step by step to be isolated, removed and then measured (mass, fibre length and pennation angle), in order to calculate the PCSA. The coordinates of the points of attachment of the muscles were also recorded in order to deduce the orientation of the muscular forces.

Then the bones were boiled for several hours and scrubbed to remove the remaining flesh. They were dried in the open air for several days. Finally, a unique ID was assigned to each individual. This ID was written on the crania and the two mandibles, on the bag containing them and on a label in the bag. It was carefully preserved throughout the process to ensure that all available information (sex, age, location, body mass, etc.) was correctly assigned to an anatomical specimen.

The data on muscle architecture (PCSA and attachment coordinates) were injected into a **biomechanical model** based on the theory of levers. In this model, the mandible is considered as a 3-dimensional lever maintained in static equilibrium by the forces exerted on it and the forces it exerts on the external environment. This model allows us to estimate the value of the

bite force as a function of the opening angle of the jaws, for bites at different positions along the jaw (at the incisors, canines, or molars).

To be confident in the modelling results, models needed to be validated by experimental data. For this purpose, we measured ***in vivo* bite forces** on Malinois dogs trained for attack (in a dog defense club in Beauvais), and on silver foxes held in captivity (in a wildlife disease study centre, ANSES Nancy, Atton experimental station). Measurements were taken with a force sensor placed either on the incisor or the molar teeth. We also tried to record *in vivo* bite forces on small hunting dogs (fox terrier, Jack Russel), but to no avail because they were reluctant to bite the rabbit skin fixed on top of the sensor. In the future, we would like to adapt the device in order to extend experimental measurements to other dog breeds.

The methods reported in this paragraph will be explained in more detail in the articles of the following chapters.

For archaeological mandibles, we will use (in Part 3) a complementary approach. This consists of calculating the **mechanical potential** of each major muscle group (masseter, temporal and pterygoid muscles) from simple mandibular dimensions. This approach makes it possible to avoid using muscle data and also to appreciate the contribution of each functional group to the bite force. This will be discussed in more detail in Part 3.

Figure 42. The different steps of dissection and preparation of canid heads. Dig: Digastric; MS: M. masseter pars superficialis; MP: M. masseter pars profunda; ZMA: M. zygomaticomandibularis pars anterior; ZMP: zygomaticomandibularis pars posterior; SZ: M. temporalis pars suprazygomatica; TS: M. temporalis pars superficialis; TP: M. temporalis pars profunda; PM: M. pterygoideus medialis; PM: M. pterygoideus lateralis; PA: pennation angle; FL: fibre length.


A - SKINNING
B - DISSECTION
SZ
MS
Dig
TS
TP
ZMA
ZMP
Dig
PM
PL
C - PRELEVMENT OF EACH BUNDLE
Dig
MS
MP
ZMA
ZMP
SZ
TS
TP
PM
PL
D - MUSCLE DATA MEASUREMENT
after longitudinal section
FL
PA
E- BOILING
F- CLEANING
G - DRYING

Figure 43. Measurement of *in vivo* bite forces to validate biomechanical models. A: Malinois dogs trained for attack; B: unsuccessful trial on small hunting dogs; C: silver fox.

2.2. Describing shape variation using three-dimensional geometric morphometrics

In this thesis, we used three-dimensional **geometric morphometrics**. This statistical method allows us to describe quantitatively, as accurately and precisely as possible, the variations in the form of an object based on the 3D Cartesian coordinates of landmarks (Mitteroecker and Gunz, 2009). Unlike traditional morphometry (that uses linear measurements between anatomical landmarks), geometric morphometrics takes into account the spatial relationships between landmarks.

We chose to work in 3D for several reasons:

- it allows digital preservation, ensuring the continuity and conservation of anatomical material over time;
- it allows a more detailed description of variations in shape, which is particularly important for the mandible which has a "simpler" shape than the cranium and for which a study of the surface is particularly important to capture a functional signal;
- it offers better visualisation possibilities.

In this thesis we focused mainly on the mandible, but the cranium was studied in parallel in the framework of a master's thesis carried by Marilaine Merlin. In the following paragraphs, we will focus on the methodology used for the mandible. The few variants in the analysis of the cranium will be mentioned in the articles in the following chapters.

2.2.1. Photogrammetry

The first step was to build three-dimensional models of the mandibles (archaeological and modern) to enable their virtual manipulation and subsequent shape analyses. For this purpose, we chose the most economical and mobile technique: **photogrammetry**. Indeed, it would have been difficult, if not impossible, to take all the archaeological mandibles out of their storage space and scan it using high-end surface scanners. Photogrammetry allowed a direct on-site acquisition, thereby saving time and limiting the risks of dispersal of the material. This technique has been proven to be very efficient and useful in archaeozoology (Evin *et al.*, 2016).

We used a circular plate, covered with a coloured map (so as to contrast with the colour of the object and to provide numerous points that can be easily identified by the software used for the 3D reconstruction) and a scale (Figure 44). The mandible was placed in the centre of this plate, fixed by its ventral border with modeling clay. We then rotated the plate and took photos. We used the macro mode and focused either on the front of the mandible or its back, to ensure all the parts of the mandible are clearly photographed despite the relatively large depth of field. The photos were taken from 3 different angles and orientations, as in Evin *et al.* (2016). Approximately 15 photos were taken for each angle so as to cover the 360 degrees around the mandible. We also took some close-up photos to better visualize some fine or transparent reliefs on the back of the mandible. Then the mandible was turned over and the same protocol was applied to reconstruct the other side of the mandible. When taking the photos, we made sure that the lighting was diffused (neon, to avoid projected shadows) and that the object was far

enough away and contrasted from the background. In some cases, we had to increase the number of photos because the lighting conditions were not good.

The two batches of photos (each made up of 50 to 60 photos) were subsequently imported into commercial software allowing the 3D reconstruction: Agisoft Photoscan (now Metashape).

Each face of the mandible was reconstructed separately, which included a first step to align the photos, a second step to build the dense cloud, a third phase of triangulation between these points to obtain a 3D surface called a mesh, and finally the texture was calculated and projected on this mesh to render colour variations.

On one of the two textured hemi-models, the grid of the plate was used to scale the object (by placing reference points on either side of a 10mm tile).

Then the dense cloud of each hemi-model was cleaned to remove the plate and the modeling clay.

Next, a few landmarks were placed on strategic and common points of the texture of the two hemi-models, so as to align the two models. The two superimposed dense clouds were merged, and the resulting merged dense cloud was cleaned again (any points that protruded too much were removed). A new triangulation and texturing were performed to obtain the final textured 3D model. Finally, the scale was updated and the model exported in ply format.

Once the models were exported, they were cleaned and "repaired" with Geomagic (in case there were holes, as for some archaeological mandibles that were sampled for DNA analyses). Then the models were simplified (reduction of the number of nodes) and mirrored where needed (all mandibles were transformed into a right mandible) with Meshlab. The final mandibles were re-exported in ply format.

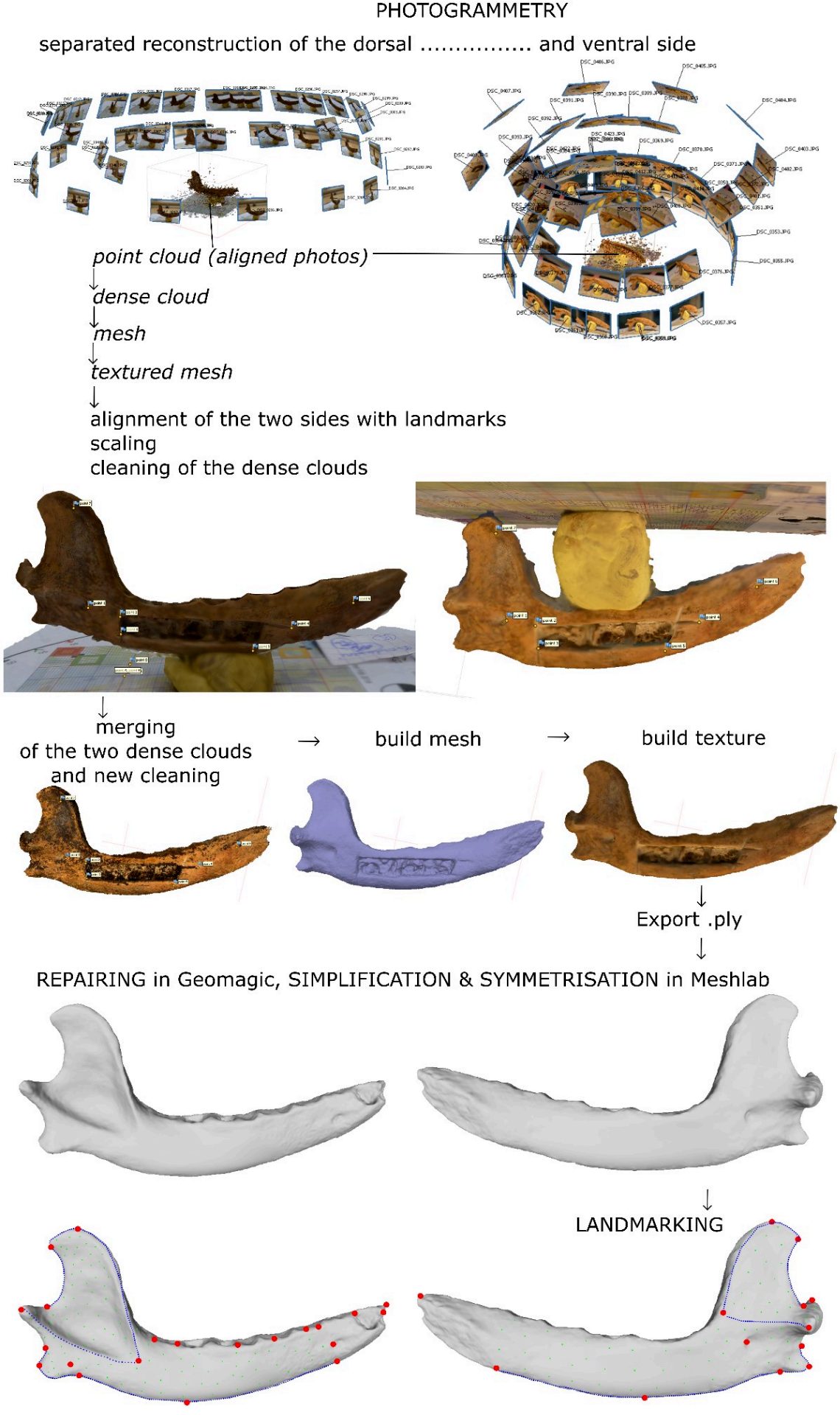

Figure 44. Acquisition of data on the mandibular form: from 3D reconstruction to landmarking.

2.2.2. Landmarking

The second step consists in placing points (**landmarks**) at strategic anatomical locations to represent the form. To do this we imported the 3D models in the "Landmark" software (IDAV).

The landmarks must be located on discrete anatomical points that are homologous in all individuals in the analysis (i.e. they can be regarded as the "same" point in each specimen in the study). They may be points of intersection between two sutures, foramina, maxima or minima of curvature (the latter being somewhat less robust). In particular the teeth are reliable landmarks that are interesting to capture. Care must be taken to ensure that the points are evenly distributed over the object, so that one region is not better represented than another.

These points must be easy to identify so that the capture of points can be repeated. We have conducted a repeatability test on the 25 landmarks chosen to represent the form of the mandible. To do this, we considered the mandibles of 3 red foxes (N-R9, N-R40 and N-R47) and placed the 25 landmarks 10 times on each specimen. We chose foxes because they are more homogeneous in terms of shape than dogs. We performed a Procrustes superimposition (see section 2.2.3), and then a Principal Component Analysis (PCA, see section 2.2.4). On the first two axes of this PCA (Figure 45), the 3 foxes are clearly distinguishable, and the intra-individual variability is much lower than the inter-individual variability, which confirms the repeatability of our protocol. Repeatability was estimated at 97.7% using the method of Claude (2008) which measures the measurement error as the ratio of intra-group variability to inter-group variability. Since all the landmarks were placed by the same operator, we did not test the repeatability between operators.

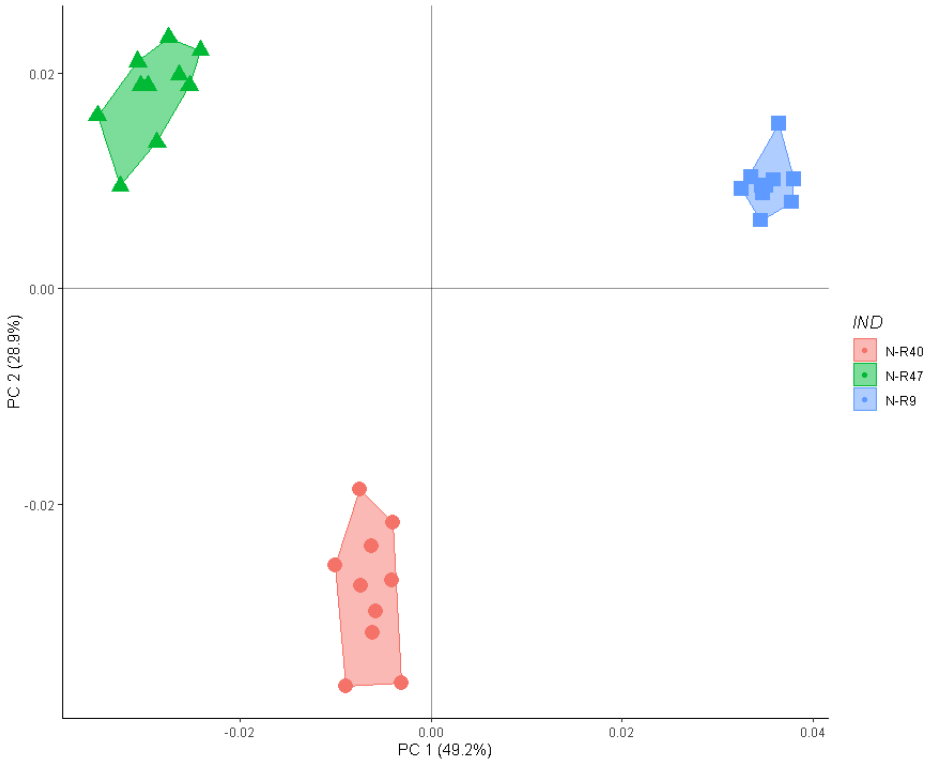

Figure 45. First two axes of the Principal Component Analyses performed on the 3D coordinates of the 25 anatomic landmarks used to describe mandibular shape, in three red foxes.

To describe the form even more precisely, in addition to these anatomical landmarks, sliding semi-landmarks were placed on curves and surfaces. The landmarks used to describe the surfaces were placed only once on a mesh that serves as a template (we chose the mandible of a fox, the surface landmarks (patch) from this template were projected onto the other mandibles through later informatic iterative procedures).

For each mandible, the 3D coordinates of the anatomical and curve landmarks were exported in pts format. These files were then imported into the R software.

R is an open source software allowing the statistical processing of the data. Functions are implemented in the form of specialised packages. Here, we mainly used the Morpho and geomorph packages. We also created our own functions, in particular to optimise data mining when using combined functions repeatedly.

In R, the pts files were compiled to create an object containing all the coordinates of all the individuals. This object, called an array, works like a spreadsheet with rows corresponding to landmarks, columns to coordinates along the x, y and z axes, and sheets to specimens.

Thanks to functions contained in the Morpho and geomorph packages, the surface landmarks of the template (patch) were projected and relaxed onto the mesh surface of all the other mandibles. The curve and surface landmarks were then made homologous by iterative sliding processes which minimized the overall bending energy. During these sliding procedures, the anatomical landmarks do not move. They are therefore very important and must be favoured. Let us note here that the procedure had to be performed on all the mandibles contained in our corpus (all species, modern and archaeological individuals).

The new coordinates obtained after this procedure were exported. They were used in all the statistical analyses carried out within the framework of this thesis.

2.2.3. Procrustes superimposition

In geometric morphometrics, the form of an object can be decomposed into two elements (Bookstein, 1991):

- size, called **centroid size**: it corresponds to the square root of the summed squared distances between all landmarks and their centroid (Mitteroecker *et al.*, 2013);
- **shape**, which represents the proportions of the object, based on the distances between the different landmarks.

We therefore have **FORM = SHAPE + SIZE** (Needham, 1950).

The centroid size may be considered as a proxy of the overall volume of the object. However, in some cases it can be misleading if one wishes to generalize to the size of the individual. Centroid size combines information related to the width, length and height of an object. However, a thin but elongated mandible may have the same centroid size than a short but thick mandible (Figure 46).

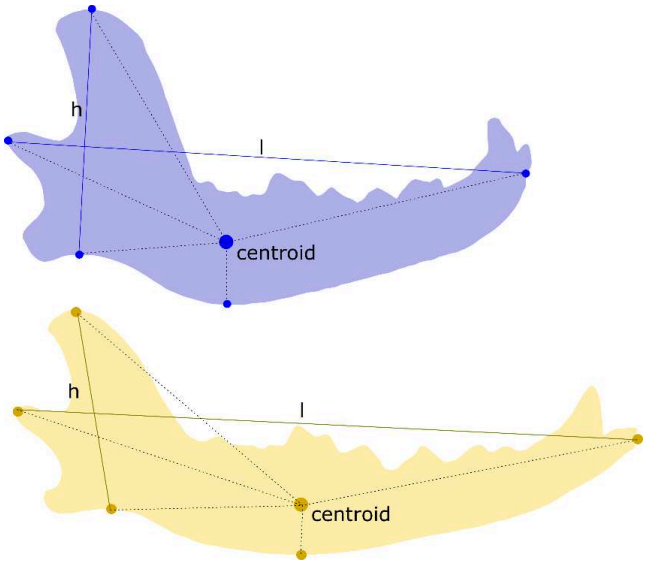

Figure 46. Example of two mandibles of dogs of about the same centroid size but with very different length (l) and height (h). We chose here a configuration of five landmarks with their centroid (i.e. the average landmark position). Centroid size is equal to the square root of the summed squared lengths of the dashed lines. Top: Rottweiller (Ny-C18); bottom: Colley (Ny-C11).

Shapes were obtained by using **Generalized Procrustes Alignment (GPA)**, or Procrustes superimposition. This statistical method consists of 3 steps: thanks to iterative processes, the objects undergo (1) scaling (normalisation by centroid size), (2) translation and (3) rotation to finally be aligned and placed in the same morphological space (Figure 47). Accordingly, "shape" consists in the geometric properties that are invariant to translation, rotation, and scaling, whereas "form" refers to the geometric properties invariant only to translation and rotation (Mitteroecker *et al.*, 2013). The calculation of GPA in geometric morphometrics is based on the raw Cartesian coordinates of the landmarks. At the end of this procedure, Procrustes coordinates are obtained, on which statistical analyses can be performed to visualise shape variation (see section 2.3.1.2), quantify them statistically and relate them to other

parameters (see section 2.3.2). It should be noted that the GPA needs to be repeated each time the sample changes (if some individuals are removed or added from an analysis, the analysis has to be performed on the GPA coordinates of exactly the same individuals than those falling within the scope of this test).

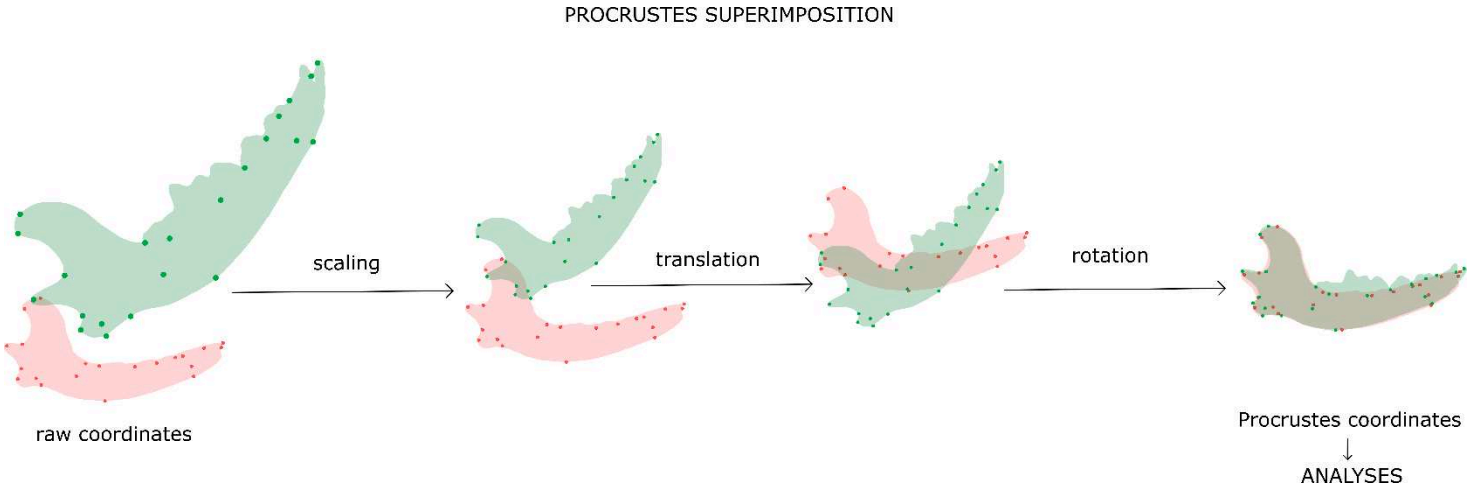

Figure 47. Steps of the Procrustes superimposition, illustrated with two mandibles of archaeological dogs.

Geometric morphometrics therefore allows to work on proportions only, but part of the conformation itself depends on the size, which is called allometry (Mitteroecker *et al.*, 2013), which has already been mentioned above. For example, the mandible of a newborn puppy will tend to have a more curved, round mandible, with small muscle insertion reliefs, than the mandible of adult dogs (see following chapters).

It is possible to remove this allometry effect to get the allometry-free shapes (via Procrustes ANOVAs, see below). However, their interpretation quickly becomes more complex. Size is an integral part of the final phenotype and, as such, is an intrinsic object of selection. This is why one will tend to keep the allometries in many of the following analyses, but analyses without allometry can also be carried out in a second phase to answer more specific questions.

More information on these concepts is available in Mitteroecker *et al.* (2013) and Klingenberg (2016).

2.2.4. Visualisation of variability from multivariate data: Principal Component Analyses (PCA)

The morphological variability in a sample can first be visualised. For this purpose, a **Principal Component Analysis (PCA)** is carried out. This is a multivariate statistical method that considers all the superimposed landmark coordinates (original variables) of all individuals, and decomposes the variance in the sample into new variables (axes or principal components, PC) in order to maximise the variance on the first axis. Subsequent axes are by definition perpendicular and thus independent. In this way, most of the information contained in the form can be summarised in one or two graphs.

Unlike bivariate graphs, the first two axes of a PCA graph will take into account many more variables, since each axis is a linear combination of all the original variables. Each axis is associated with a percentage of variance explained. On the graph, the closer the points, the more similar their morphology is. However, two individuals that are close together in one plane (PC1 and PC2 for example) can be distant in another plane (PC1 and PC3 for example) because they are only distinguished by some landmarks which are only represented in the PC3 axis and not in the PC1 nor PC2 axes. For this reason, several visualisations can be sometimes useful.

The PCA is generally performed on shape data (Procrustes coordinates after GPA), but it also possible to conduct analyses on a matrix that concatenates shape data with centroid size (in order to explore the variation in form).

This technique is unsupervised, i.e. there is no *a priori* on whether individuals belong to a group (e.g. males or females, different species, dogs from different sites). To distinguish between groups known *a priori*, there are other methods of visualisation, this time supervised. For example, the between-group PCA performs a PCA based on the groups' centres of gravity (in fact on the group mean covariance matrix).

Thanks to geometric morphometrics it is possible to visualize the theoretical shapes at the extremity of the PCA axes (what is not possible in traditional morphometry).

2.3. Statistical tools to explore variation in form: general presentation

In this section, we will explain some basic statistical tools that have been used in the rest of this thesis. The aim is not to be exhaustive but to give keys for understanding to readers not familiar with morphometrics.

Within the framework of this thesis, all the statistical analyses were carried out with the software R. We indicate the functions used when relevant.

First of all, it should be remembered that to explore variation in form, parallel analyses on both the shape and the centroid size should be performed.

2.3.1. Visualizing and comparing variability in form

2.3.1.1. *Centroid size*

A **boxplot** can be made to visualize the dispersion of the data (Figure 48). A boxplot is a standardized way of displaying the distribution of a quantitative variable, based on a five-number summary: “minimum”, first quartile (Q1: 25% of the values are under this threshold), median (50% of the values are under this threshold), third quartile (Q3: 75% of the values are under this threshold), and “maximum”. It can thus inform on the way data are grouped around the median, the presence of outliers, or the symmetry existing in the data.

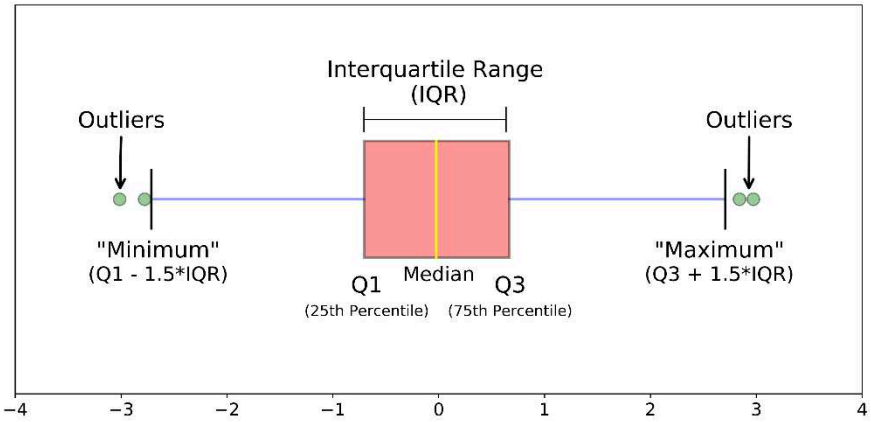

Figure 48. Example of a boxplot. From https://www.kdnuggets.com/2019/11/understanding-boxplots.html

In order to statistically compare the variance (= sum of squares of the deviations from the mean), an F-test of variance with 'var.test' can be performed.

2.3.1.2. *Shape*

PCA is a method for visualising morphological variability, but the observations that may emerge from it (e.g. separation of two groups according to a parameter) are only indications and have no direct statistical value. For example, on a plot representing the first two main components, if there is a clear separation of archaeological dogs and modern dogs and a greater dispersion (morphospace) for modern dogs, this tends to suggest that there is a significant difference between the mean shape of the two groups, and probably also differences in the variability (=disparity) of the two groups. However, to confirm this, statistical tests will need to be conducted.

In addition to visualisation with a PCA, the variabilities can be compared between groups with a **disparity test**. For this purpose, we used a function already implemented in the geomorph package: 'morphol.disparity'. This function estimates, for each group, the morphological disparity as the Procrustes variance within each group, the value being adjusted by the sample size for each group. This function also performs pairwise comparisons to identify differences among groups through permutation procedures.

2.3.2. Testing the relationship between the form, centroid size or bite force and other data

2.3.2.1. *Testing for covariation*

Covariation is a measure of dependence between variables. It simply indicates the extent to which variables vary together. In this thesis, it was particularly used to explore how muscle data covaried with the shape of the mandible or cranium. To do this, we used the **two-block partial least squares (2B-PLS)** method (function pls2b, Rohlf and Corti, 2000). The PLS method is particularly suitable for large datasets with more variables than individuals or when there are strong collinearities between variables. Somewhat like PCA, the method calculates

new axes and decomposes the covariance matrix (and not the variance matrix this time) to optimise the covariation between the two blocks on the first axes. Contrary to the PCA, the method of constructing the components in PLS has the advantage of coping well with the presence of missing data. After permutations, a P-value is provided, which indicates the significance of the covariation, and a correlation coefficient (r-PLS) which indicates the strength of the covariation. PLS regression is also used for predictive purposes.

2.3.2.2. *Testing for a correlation*

Correlation is a special case of covariance that can be obtained when the data are normalised. Correlation actually quantifies the extent to which one (or more) quantitative variable(s) is (are) explained and one (or more) quantitative or qualitative explanatory variable(s) are related. Correlation tests are generally accompanied by the performing of linear models in order to understand the linear relation between the models.

Linear models consist of explaining what proportion of the variation in the variable(s) is explained by the explanatory variable(s). These analyses provided a percentage of explained variation (R^2) and a p-value indicating the strength and significance of the relationship, respectively. The coefficients of the linear model are also provided.

In this thesis, simple correlation tests were used for testing the correlation between muscle masses or between bite force and centroid size for example (cor.test). But we mainly used ANOVAs (analysis of variance, followed by Tukey post-hoc tests) or even MANOVAs or MANCOVAS when the data to be explained were multivariate and/or when covariation factors were added to the models. For example, we sometimes tried to explain variation in bite force by variation in muscle data, size (covariate), and sex (fixed effect).

For the analysis of shape, we used **Procrustes ANOVAs** (function 'procD.lm'), a powerful tool that is adapted to the large number of variables in geometric morphometrics datasets (Goodall, 1991; Anderson, 2001; Anderson and Braak, 2003; Collyer, Sekora and Adams, 2015; Adams and Collyer, 2016, 2017). These analyses allow to quantify allometries, the links between muscle architecture and shape, or to account for shape differences between localities or between modern or archaeological canids for example. Shape changes can be visualized in case of correlation between shape and a unique quantitative variable (for example mandible shape and temperature).

We note that the order of the variables in the correlation models is important and is likely to change the results. There are tools for ANOVAs to choose the best model (the best order of variables), but few if any tools exist for multivariate analyses.

2.3.3. Quantifying shape differences between groups by discrimination analyses

Procrustes ANOVA can highlight the influence of a qualitative variable (e.g. sex) on the shape, but it does not allow to visualize the shape according to this variable. For this purpose, other techniques are used to quantify and maximise the differences between groups. We have

already mentioned above the between-group PCA which investigates patterns of between-group variation, without standardizing by the within-group variance. Instead, in this thesis we preferred to perform **Canonical Variate Analyses (CVA)**, which aims at looking for linear combinations of variables in order to separate the groups by maximizing the between-group to within-group variance ratio. However, while PCA and bgPCA tend to put the focus on the direction of the main variance as lines of least resistance to evolution, CVA by dampening the expression of this line of least resistance, has the potential to reveal other relevant patterns of differentiation that may otherwise be blurred (Renaud, Auffray and de la Porte, 2010).

The CVA also offers the possibility to apply decision rules established from a known sample on new unknown specimens. For example, it is possible to predict the species of archaeological remains using decision rules established on modern canids of various species. Of course, the efficiency of the model depends on the individuals used to build the decision rules (the same species must be present, and the variability within the sample must be equivalent).

We used the function 'CVA' (Campbell and Atchley, 1981; Klingenberg and Monteiro, 2005).

2.3.4. Classifying using non-supervised analyses

To explore the structure of a population without having any preconceived ideas about membership to a group, and maybe identify sub-populations characterised by differences in shape, we have used unsupervised clustering methods.

These were particularly useful for archaeological canids.

The advantage of these methods, contrary to simple visualisation on PCA plots, is that it is possible to consider the real distances between individuals (and not only in the first principal component axes, that only represent a small amount of the total variation in shape).

2.3.4.1. *Gaussian mixture models (GMMs)*

In Gaussian Mixture Models (GMMs), it is assumed that, within the array of Procrustes coordinates, there are a certain number of Gaussian distributions, and each of these distributions represent a population with a multivariate normal distribution. Hence, this method tends to group the individuals belonging to a single distribution together. We used the function 'Mclust' from package 'mclust'.

It is possible to force the algorithm by imposing a decomposition in a certain number of groups, but we preferred to follow the optimal number of groups provided by the software, based on a Bayesian information criterion (BIC). This criterion gives us an estimation on how good the GMM is in terms of predicting the data. The lower the BIC, the better the model in predicting the data, and by extension, the true, unknown, distribution.

This method thus provides an information on the morphological structuration of the sample.

2.3.4.2. *Hierarchical clustering*

To summarize on the same graph the proximity in shape between all the individuals in a sample we have built **classification trees**. We used the function "pvclust" from the package pvclust, and ggtree (Yu *et al.*, 2017) to display the trees.

First, a distance matrix is created. Here the distances are the Procrustes distances. The distance matrix thus represents the Euclidean distance between all the Procrustes coordinates of all the individuals.

Then, an ascending hierarchical clustering (AHC) is carried out in order to gather individuals that are similar in shape. This iterative method seeks to ensure that the individuals grouped within the same sub-groups are as similar as possible (intra-class homogeneity), while the sub-groups are as dissimilar as possible (inter-class heterogeneity). Classification is ascending because it starts from individual observations, and it is hierarchical because it produces increasingly larger sub-groups. To aggregate the individuals, we chose the Ward's method. This method seeks to minimise intra-class inertia and maximise inter-class inertia in order to obtain sub-groups that are as homogeneous as possible.

At the end of the procedure, a dendrogram or classification tree is produced. On these trees, the individuals are at the extreme end of branches whose length is proportional to the morphological distance between the individuals.

By cutting this tree to a certain chosen height, the desired partition is produced. There are also tools available to find out what the best partition is.

3. Questions investigated and reference sample

3.1. Sampling of extant canids

The functional approaches developed in this thesis required to establish a **reference sample** that included 160 modern canids consisting of the same species as the archaeological canids targeted in our research questions (see Conclusion of Part 1: Formulation of the research problem). Since the targeted animal models are the dog and the red fox, and since part of our work consists in comparing their evolutionary trajectories between the Mesolithic and the very early Bronze Age, our reference sample was made up of foxes of the *Vulpes vulpes* species (mainly red foxes but also some silver foxes), domestic dogs *Canis lupus familiaris*, some dingoes *Canis lupus dingo* and some grey wolves *Canis lupus*.

The different populations considered in this reference sample can be positioned along a human-canid proximity gradient (Figure 49). Following this gradient, natural and anthropic constraints have opposing influences. Wild commensal red foxes are placed to the left of this gradient, where natural constraints are stronger than anthropogenic constraints. Silver foxes, selected for their fur, are subject to stronger anthropogenic stresses, but since they are not domesticated, natural stresses remain predominant. Dogs belonging to hypertypes are on the opposite side of this gradient, on the right, where anthropogenic constraints and artificial selection are the strongest. Dogs not subject to drastic selection to meet breed criteria (stray dogs) or returned to the wild (dingoes), approach foxes along this gradient.

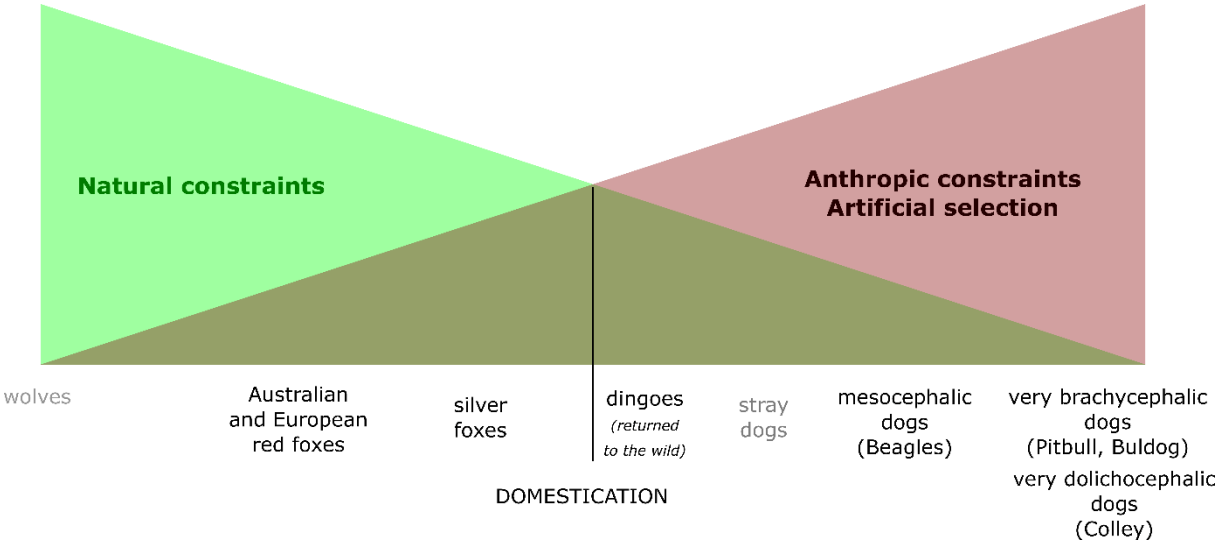

Figure 49. Positioning of the populations contained in our reference sample from the point of view of natural and anthropogenic constraints. The populations that could not be studied in this thesis are shown in grey.

The animals in our sample were provided by the veterinary school of Nantes (ONIRIS, C. Guintard), the ANSES of Nancy (E. Monchâtre-Leroy and J. Barrat), the School of Veterinary and Life Science, Murdoch University, Perth, Australia (T. Flemming), R. Triquet, the ONCFS (A. Larralle), the "Direction des Services Vétérinaires - DDCSP de la Dordogne", Périgueux, France (H. Garès) and the veterinary school of Alfort. A unique code has been assigned to each individual so that all available data can be traced.

Dogs

The sample of modern dogs contains 70 individuals of various breeds (37 breeds):

- Amstaff (1)
- Barzoi (2)
- Beagle (21)
- Belgian shepherd (2)
- Border collie (2)
- Boxer (2)
- Bull terrier (1)
- Bulldog (2)
- Cane Corso (1)
- Poodle (1)
- Chihuahua (1)
- Colley (1)
- Dachshund (1)
- Deerhound (1)
- Doberman (1)
- Fox terrier (1)
- German shepherd (1)
- Golden (1)
- Hunting dog (1)
- Husky (1)
- King Charles (1)
- Leonberg (1)
- Loulou (1)
- Mastiff (2)
- Papillon (1)
- Pitbull (1)
- Rottweiller (2)
- Shepherd dog (4)
- Shetland sheepdog (1)
- Sloughi (1)
- Long-hair dachshund (1)
- Tenerife dog / podengo (1)
- Wippeth (1)
- Yorkshire (3)

We included breeds that probably have no archaeological equivalent (Rottweiller, Chihuahua, Collie), in order to overcome the variability of ancient dogs, and with the aim of evaluating how the integration of the masticatory apparatus responded to the extreme morphological variability in this species.

The modern dog sample also contains a fairly large number of beagles. These dogs are easier to collect in comparison to other breeds as they are widely used for experimental purposes. Additionally, their morphology seems *a priori* relatively little modified and perhaps closer to ancient dogs. The beagles could therefore perhaps constitute good reference individuals for applying some tools developed on modern dogs to ancient dogs.

Unfortunately, our sample does not include commensally living stray dogs (e.g. North African pariah dogs) which might be subject to constraints closer to pre-Bronze Age than purebred dogs (less artificial selection and more natural constraints than for modern purebred dogs). Thus, they may be better models for comparison with archaeological dogs. However, we have not been able to access such specimens during this PhD project. This is an area for future improvement.

Grey wolves

We photographed the mandibles of 8 wolves from the MNHN collections, coming mostly from zoological parks (the species attribution is therefore certain, Table 13). However, we were not able to access fresh heads to dissect them during the course of this thesis.

Table 13. Origin of the modern wolves considered in shape analyses.

ID (this study)	Sex	ID MNHN	Age	Origin
loup1	F	2016-1672	11yo	Mercantour, St Martin-Vésubie, France
loup2		2018-2921	adult	Réserve de la Haute-Touche, France
loup3	F	1984-0,36	1yo+	Ménagerie
loup4	F	1959-181	8yo	Ménagerie
loup5	F	1973-3	4yo+	Ménagerie
loup6	F	1990-74	7yo	Ménagerie
loup7	F	1979-18	16yo	Birth in Zurich zoo en 1962, death at "la Ménagerie"
loup8		2016-1665	adult	Réserve de la Haute-Touche, France

Dingoes

We also dissected and reconstructed the cranium and mandible of 10 Australian dingoes (including 2 juveniles). The species assignment of each specimen was verified by a genetic test.

Foxes

The foxes in this study mainly come from the south west of France, although other French regions are also represented (65 red foxes and 4 silver foxes). We also photographed the mandibles of 3 Romanian foxes (especially for part 3, since our archaeological sample contains many mandibles from Romania), and we also photographed the mandibles of a large population of Australian foxes (>400) to answer some specific questions (see below). A few heads of Australian foxes (14) were also completely dissected.

The muscular data of some dogs and foxes could not be exploited because the specimens were preserved in formaldehyde. In this case, the bones were used for shape analyses only. Therefore, we do not have the same sample sizes in analyses focusing on muscle data and

analyses focusing on bone shape. Dissected dogs therefore represent less variability compared to all the dogs in our sample. Moreover, some crania being too damaged, it was sometimes not possible to study their shape. The number of individuals is therefore not the same in shape analyses based on the cranium or mandible.

The ages were estimated from the state of eruption of the teeth and cranial sutures (see articles in the following chapters). There are 10 juvenile canids (with non-erupted permanent teeth) that were removed from many shape analyses (in particular those with archaeological canids):

- 4 dogs: M8, Ny-C2, Ny-C29, Ny-C9;
- 4 red foxes: N-R11, N-R15, N-R25, N-R29;
- 2 dingoes: ND-Dog8, ND-Dog10

Detailed information about modern canids are given in the supplementary material of the articles of the following chapters.

3.2. Questions explored in the articles of the following chapters

In the following chapters, we address several questions to clarify the relationships between elements of the masticatory apparatus (skull/mandibular/muscles) and bite force, as well as the relations with developmental (size, age, sex, species) or environmental factors (climatic variation and diet) in canids.

The answers to these questions will be useful for the continuation of this work and will allow us to adapt our methods to the study of pre-Bronze Age canids.

1- *How do the shape of the mandible and skull co-vary in dogs and foxes?*
Can mandible morphology be linked to a specific cranial morphology, which could inform on the overall morphotype, especially in dogs?

2- *How do the shape of the mandible and the architecture of the muscles co-vary in dogs and foxes?*

3- *How do the shape of the mandible and the bite force co-vary in dogs and foxes?*

4- *Are the relations between shape and muscle data or bite force stronger for the mandible than for the cranium, as can be suspected given that the mandible is specialised only in chewing, unlike the cranium?*
This would validate the use of the mandible as an item of choice to functionally interpret morphological variation in archaeological canids.

5- *Has extreme artificial selection in dogs altered the functional integrative relationships between the skull, mandible, masticatory muscles and bite force?*

To answer this question, we compare the results obtained for domestic dogs and red foxes, and we may refer to the preliminary results obtained for dingoes (for which the sample size is limited).

The answer to this question will be crucial for the continuation of our work, as it will be an element in deciding whether modern dogs are good models for establishing predictive tools for making functional inferences about pre-Bronze Age canids. Indeed, if integration remains strong despite the extreme selection and morphological variability of modern dogs, it will be possible to interpret variation in form in functional terms. Of course, another condition for the application of these models will be that the variability of ancient dogs is included in the variability of modern dogs.

6- *To what other factors can the shape of the mandible and the bite force be related?*

a. What are the effects of size and age on the shape of the mandible?
b. Is there a sexual dimorphism in the form and bite force?
c. Does the form of the mandible or bite force vary with geographical or climatic parameters?
d. Does the form of the mandible or bite force vary with the degree of urbanism?
e. Are the form of the mandible and bite force related to diet?

To address these questions, we will focus (except for size) on red foxes, for which the factors mentioned above are easier to study as their effects are not masked by an intensive artificial selection. In addition, we could access a huge collection of mandibles of Australian red foxes for which a lot of information were available and published (age, sex, size, body mass, stomach contents, as well as climatic data: temperature, rainfall, geographical location, etc., Forbes-Harper *et al.*, 2017).

The following chapters are intended to address these questions. In Chapter 3 we will look at domestic dogs exclusively, and in Chapter 4 we will look at wild species (red fox and dingo) in a comparative approach. Finally, in Chapter 5 we will explore other factors (developmental or environmental) that may create variation in the shape of the mandible using Australian foxes as models.

At the beginning of each chapter, we will very briefly introduce the articles to explain the logical progression between sections, and we will summarise the key findings for the study of ancient canids in Part 3.

We will summarise the answers to the overall questions formulated above in the conclusion of Part 2 (see page 299).

Chapter 3.
The functional relations between mandibular shape, cranial shape, jaw muscles architecture and bite force in domestic dogs

In this chapter we describe and quantify the relationships between the different components of the masticatory apparatus in domestic dogs exclusively. The idea was to explore how the shape of the mandible, the shape of the cranium, the architecture of the masticatory muscles and bite force covary. These articles also provided an opportunity to describe the strong allometries in the mandibular and cranial shapes.

In article 1 (section 1, page 165), we focused on the relation between the shape of the mandible and muscle data obtained from dissections (volume and PCSA).

In article 2 (section 2, page 185), we compared these relationships to those observed for the cranium, and explored the covariations between the shape of the two bony complexes of the head.

In article 3 (section 3, page 203), we used the muscle PCSA obtained from dissection to estimate bite forces using a biomechanical model validated by *in vivo* measurements. We studied the involvement of the different muscles in the bite force, the mechanical impact of both the bite point (incisor or molar teeth) and jaw opening angle, as well as the relationship between bone shape and the absolute value of the bite force, or the value relative to size. We compared the results obtained for the cranium and the mandible. We also compared performance as a function of morphotype.

These articles show that in modern domestic dogs:

KEY POINTS

The shape of the mandible covaries strongly with that of the cranium, and is strongly impacted by the morphotype.

- ⇨ **The mandible of archaeological dogs is a good item for apprehending the overall shape of the head.**

There are strong relationships between the shape of the mandible and muscle data or even bite force, and variations affect the areas of muscle attachment, the robustness and curvature of the mandible.

- ⇨ **It is possible to make functional inferences.**

Brachycephalic dogs produce stronger bite forces for their size.

The functional links observed for the cranium are surprisingly not less strong than those observed for the mandible.

The shape of the mandible is strongly allometric (like the shape of the cranium).

1. The relationships between mandible shape and jaw muscle architecture in dogs.

Article 1 –
How Does Masticatory Muscle Architecture Covary with Mandibular Shape in Domestic Dogs?

Colline Brassard, Marilaine Merlin, Elodie Monchâtre-Leroy, Claude Guintard, Jacques Barrat, Cécile Callou, Raphaël Cornette, Anthony Herrel

Published in *Evolutionary Biology*, accepted: 10 March 2020

Evolutionary Biology
https://doi.org/10.1007/s11692-020-09499-6

RESEARCH ARTICLE

How Does Masticatory Muscle Architecture Covary with Mandibular Shape in Domestic Dogs?

Colline Brassard[1,2] · Marilaine Merlin[1] · Elodie Monchâtre-Leroy[3] · Claude Guintard[4,5] · Jacques Barrat[3] · Cécile Callou[2] · Raphaël Cornette[6] · Anthony Herrel[1]

Received: 27 September 2019 / Accepted: 10 March 2020

Abstract

Despite the considerable scientific interest in the variability and patterns of integration in the dog skull, how these patterns impact or are driven by function remains largely unexplored. Since the mandible is directly involved in mastication, it can be expected to be directly related to the development of the adductor and abductor muscles. Here, we explore whether variation in the architecture and size of the masticatory muscles is associated with the variation in mandibular shape in dogs. We obtained muscle data from the dissection of 48 dogs from different breeds and morphotypes to explore the architecture of the muscles and used 3D geometric morphometric approaches to quantify the shape of the mandible. Covariations between the masticatory muscles and mandibular shape were explored using two-block partial least square analyses (2B-PLS). Our results show there is a strong covariation between mandibular shape and masticatory muscles mass (rPLS from 0.70 to 0.74 for the first axis representing more than 90% of the total covariance) and physiological cross-sectional area (rPLS from 0.64 to 0.73 for the first axis representing more than 80% of the total covariance), irrespective of whether size is taken into account or not. These results suggest muscle size and thus attachment area requirements for individual muscles are likely drivers of mandibular shape. Moreover, mandible shape is likely to be a good predictor of muscle force. Finally, it appears that domestication of dogs has not resulted in a disuse phenotype characterized by a decoupling between form and function.

Keywords Dog · Geometric morphometrics · Jaw muscle · Mandible · Masticatory system

Electronic supplementary material The online version of this article (https://doi.org/10.1007/s11692-020-09499-6) contains supplementary material, which is available to authorized users.

✉ Colline Brassard
colline.brassard@mnhn.fr

[1] UMR 7179 Mécanismes Adaptatifs et Evolution (CNRS, MNHN), Muséum national d'Histoire naturelle, 55 rue Buffon, Paris, France

[2] Archéozoologie, archéobotanique : sociétés, pratiques et environnements (AASPE), Muséum national d'Histoire naturelle, CNRS, CP55, 57 rue Cuvier, Paris, France

[3] ANSES, Laboratoire de la rage et de la faune sauvage, Station expérimentale d'Atton, Malzéville, France

[4] Laboratoire d'Anatomie comparée, Ecole Nationale Vétérinaire, de l'Agroalimentaire et de l'Alimentation, Nantes Atlantique – ONIRIS, Nantes Cedex 03, France

[5] GEROM, UPRES EA 4658, LABCOM ANR NEXTBONE, Faculté de santé de l'Université d'Angers, Angers, France

[6] UMR 7205 Institut de Systématique, Evolution, Biodiversité (CNRS, MNHN, UPMC, EPHE), Muséum national d'Histoire naturelle, Paris, France

Introduction

As a consequence of several thousand years of artificial selection and inbreeding, the domestic dog has the highest variability in skull shape within the Carnivora (Drake and Klingenberg 2010; Selba et al. 2019) and encompasses over 400 breeds according to kennel clubs. The shapes extend beyond the variability of wild species (Drake and Klingenberg 2010), varying from elongated and narrow skull shapes (dolichocephalic) to short and wide (brachycephalic) skulls. This diversification is the result of a slight relaxation of natural and functional selection pressures (Drake et al. 2015, 2017; Curth et al. 2017), but more importantly, depends on anthropogenic selection pressures driven by aesthetic considerations or the selection of animals for particular skills such as hunting or defense (Drake and Klingenberg 2008).

The genetic mechanisms underlying this diversity are well known (Fondon and Garner 2004; Bannasch et al. 2010; Boyko et al. 2010; Marchant et al. 2017). For example, the mutation of BMP3 has been shown to be involved in

Published online: 19 March 2020

brachycephaly (Schoenebeck et al. 2012). Integration and modularity have also been extensively studied within the cranium and even the mandible (Drake and Klingenberg 2010; Meloro et al. 2011; Curth et al. 2017; Curth 2018; Machado et al. 2018; Selba et al. 2019). However, the functional impact of this extraordinary variability in shape has received less attention in dogs (but see Ström et al. 1988; Endo et al. 1999; Koch et al. 2003; Ellis et al. 2008, 2009). Given that artificial selection can have indirect functional consequences in wild canids such as the red fox (Trut 1999; Trut et al. 2009; Dugatkin 2018), and since these selection pressures are strong, the resulting morphological changes may have occurred extremely rapidly (Johnston and Selander 1964; Reznick et al. 1997; Hendry and Kinnison 1999; Huey et al. 2000; Grant and Grant 2006; Trut et al. 2009; Dugatkin 2018). In most vertebrates species variation in the shape of the cranium and mandible is linked to variation in the jaw adductor muscles (Watt and Williams 1951; He and Kiliaridis 2003; Cornette et al. 2013; Cornette, Tresset, Houssin, et al. 2015a, b; Fabre et al. 2018). Indeed, the jaw adductors and abductors and the skull and mandible are parts of the same functional unit with bones providing skeletal struts and levers that are moved by the forces generated by muscles (Frost and Schönau 2000; Herring et al. 2001; Frost 2003). In addition to the need for providing muscular attachment, bones are also modified due to the loads imposed by muscle contraction in addition to external forces such as bite and joint forces (Frost 2001, 2003; Schoenau 2005; Sharir et al. 2011; Brotto and Bonewald 2015). For the jaw system to function, the muscles and bones need to be coordinated to achieve effective mastication and biting. As such the system can be expected to be functionally integrated (Olson and Miller 1951; Van Valen 1965; Klingenberg 2014). The quantitative interplay between jaw muscles and the bones of the skull remains poorly described in domestic dogs (but see Liebman and Kussick, 1965), in contrast to other mammals (Crompton 1963; Weijs and Hillen 1986; Hylander et al. 1992, 1998; Herring et al. 2001; Lieberman et al. 2004; Ross and Metzger 2004; Ross et al. 2005; Herring 2007; Ravosa et al. 2007, 2016; Bourke et al. 2008; Cornette et al. 2013; Cornette, Tresset, and Herrel 2015a, b; Penrose et al. 2016; Fabre et al. 2018) rendering our understanding of the functional consequences of the tremendous morphological variation in the skull of domestic dogs limited.

Prior studies of in vivo bite forces and jaw-muscle electromyography in dogs (Lindner et al. 1995; Ellis et al. 2008; Kim et al. 2018), as well as estimations obtained from the dry skull method (Thomason 1991; Ellis et al. 2009) have suggested that differences in morphology are related to differences in bite force, mainly because of space constraints around the skull, and because of differences in the length of the in and out-levers of the masticatory apparatus. However, no study has focused on the architecture of the jaw muscles (fiber length, pennation angle or muscle mass) in domestic dogs rendering estimates of bite force difficult. In the dry skull method, the three-dimensional architecture of the jaw muscles is not incorporated (Schumacher 1961; Miller et al. 1965; Thomason 1991; Ellis et al. 2009), which can result in underestimates of maximal bite force.

The great morphological diversity present in the cranium of dogs provides a unique opportunity to understand the relationships between morphological variation and muscle development. Moreover, understanding these relationships would permit better inferences on the functional impact of selection in dogs. Here we focus on the mandible as this bone is implicated in a single function: mastication. We expect there to be a direct link between muscle attachment area and jaw shape, that means, in other words, significant covariations between jaw muscles architecture (mass and physiological cross-sectional area) and mandibular shape. However, as recent dog breeds have been selected largely for aesthetic reasons, we predict that these covariations are likely low. Finally, as the posterior part of the mandible both serves as the area for muscle insertion and is more strongly impacted by the need for muscle attachement, we expect patterns of covariation to be stronger for the mandibular ramus.

Materials and Methods

Specimens

Specimens were obtained from the Veterinary School of Nantes (France), the Veterinary School of Maisons Alfort (France), and the laboratory of rabies and wildlife disease studies in Nancy—Anses (France). The dataset is composed of the mandibles of 59 dogs (*Canis lupus familiaris*) from various breeds (Table 1, see Supplementary material Table S1 for details). The breeds were estimated based on their similarity to existing standards, but crossbreeding is important and as such these animals may not represent 'pure' breeds. Because accurate ages were unknown, we estimated ages based on tooth wear, bone texture, and the aspect of the cranial sutures (degree of closure). The two dogs in the group 'A' (a Beagle and a Bull terrier) represent the youngest individuals with molars still erupting, a very porous mandible and unclosed cranial sutures (4–6 months according to Barone 2010). The Beagle in group 'B' has its spenobasilar suture still open (< 8–10 months for the dog according to Barone 2010) and the mandible is still porous. The 22 individuals from the group 'D' are older, with a closed interfrontal suture and worn denture (> 3–4 years). The 33 other dogs, from the group 'C', are intermediate adults (from 10 months to 3 years). We chose to keep the youngest individuals in our analyses to increase the morphological variability in the sample. There is no geriatric dog.

Table 1 List of the material used in this study

Related breeds	n mdb n = 59	n mass n = 48	n PCSA n = 47
American Staffordshire terrier (Ams)	1	1	1
Beagle	21	10	10
Belgian shepherd—Tervueren (Bel)	2	2	2
Border collie (Bor)	2	2	2
Boxer (Box)	2	2	2
Bulldog (Buld)	2	2	2
Bull terrier (Bult)	1	1	1
Chihuahua (Chi)	1	1	1
Cane Corso (Can)	1	1	1
Cavalier King Charles Spaniel (Kin)	1	1	1
Collie (Col)	1	1	1
Continental Toy Spaniel Papillon (Pap)	1	1	1
Dachshund (Dac)	1	1	1
Deerhound (Dee)	1	1	1
Dobermann (Dob)	1	1	1
Fox terrier (Fox)	1	1	1
German shepherd (Ger)	1	1	1
Golden retriever (Gol)	1	1	1
Husky (Hus)	1	1	1
Leonberger (Leo)	1	1	1
Mastiff (Mas)	2	2	2
Pitbull (Pit)	1	1	1
Rottweiler (Rot)	2	2	2
Shetland sheepdog (She)	1	1	1
Non-breed dog	9	9	8

Where possible, equilibrated ratio of males and females were included and all ages are represented. See Supplementary material Table S1 for a complete list of the specimens used in the analyses

n mdb number of mandibles used to study shape variation, *n mass* number of individuals used for the 2B-PLS with muscle masses, *n PCSA* number of individuals used for the 2B-PLS with muscle PCSAs

Dissections

Specimens were either dissected when still fresh or frozen and then defrosted (48 dogs). If preserved in formol, the head was not dissected but directly prepared for shape analyses (an additional 11 Beagles). Dissection of the constituent bellies of the jaw adductor muscles were done in accordance with the description provided by Penrose et al. (2016), following the nomenclature of previous authors (Turnbull 1970; Ström et al. 1988; Tomo et al. 1993; Druzinsky et al. 2011). However the anterior and posterior parts of the zygomaticomandibularis were separated and the digastric was dissected as well. Since the lateral pterygoid is very small in carnivores (Turnbull 1970; Herring 2007; Penrose et al. 2016), we considered medial and lateral pterygoids as one single muscle mass.

The following muscles were removed layer by layer: the digastric (Dig), the superficial masseter (MS), the deep masseter (MP), the anterior part of the zygomaticomandibularis (ZMA), the posterior part of the zygomaticomandibularis (ZMP), the suprazygomatic part of the temporalis (SZ), the superficial temporalis (TS), the deep temporalis (TP), and the pterygoids (P). The origins and insertions of the nine muscle layers dissected are illustrated in Fig. 1 and described in Supplementary material Table S2.

Quantification of Jaw Muscles Architecture

After dissection, all muscle divisions were weighed using a digital scale (Mettler Toledo AE100). Fiber length and pennation angles were measured directly on the muscle after sectioning the muscles along their line of action. Several measurements were taken for each measurement at different location in the muscle, and we used the mean for our calculations. The reduced Physiological Cross-Section Area (PCSA), which represents a proxy of the intrinsic strength of the muscles, was calculated for each muscle muscle following the definition of Haxton (1944), and using a muscle density of 1.06 g/cm3 (Méndez and Keys 1960).

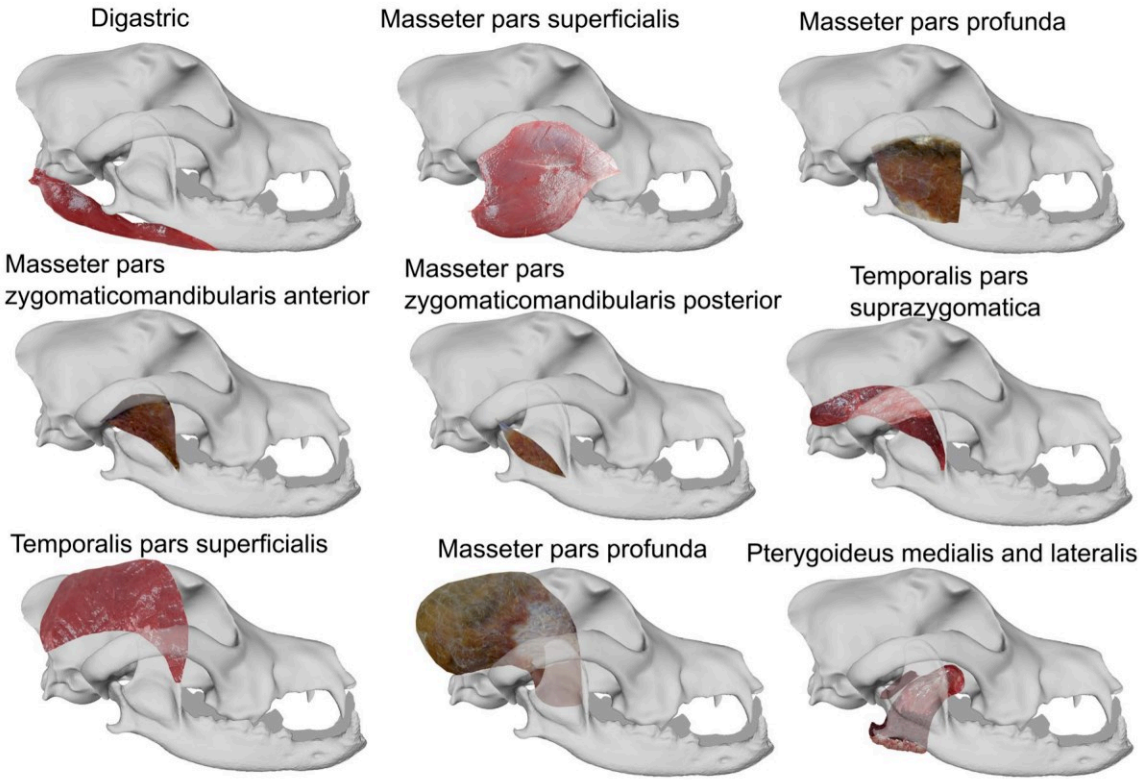

Fig. 1 Schematic illustration of the jaw muscles dissected in this study. Muscles in medial to mandible are rendered transparent

We used the following formula: $PCSA = \frac{mass(g)*\cos(angle\ of\ pennation\ (rad))}{1{,}06(g.cm^{-3})*fiber\ length\ (cm)}$.

Photogrammetry

After dissection, bones were cleaned and dried. One hundred photographs per right hemi-mandible were taken while turning around the specimen (Fau et al. 2016). Photos were taken using a Nikon D5500 Camera (24.2 effective megapixels) with a 60 mm lense. The Agisoft PhotoScan software (© 2014 Agisoft LLC, 27 Gzhatskaya st., St. Petersburg, Russia) was used for the 3D reconstructions of the mandibles.

Landmarking and Geometric Morphometrics

Geometric morphometric analysis was used to quantify patterns of morphological variation. Twenty-five homologous anatomical landmarks and 190 sliding semilandmarks on curves were placed on each specimen using the software Landmark version 3.0.0.6 (© IDAV 2002–2005; Wiley et al. 2005). Landmark locations are provided in Fig. 2 and Table 2.

A template was also created following the method of Cornette et al. (2013) to patch 185 slinding semilandmarks on the mandible surface of all specimens (Fig. 2). The three-dimensional coordinates for all sets of landmarks were then imported into R version 3.6.0 (2019–04-26). The Morpho package (version 2.7) implemented in R (Schlager 2013) was used for most of the following analyses. A 3D sliding semilandmark procedure (Bookstein 1997; Gunz et al. 2005) was performed. According to this iterative procedure, sliding semilandmarks on surfaces are projected from the template onto each specimen using a thin plate spline deformation (Klingenberg et al. 2002; Gunz et al. 2005; Schlager 2012, 2013). Next, landmarks are slid iteratively while minimizing the bending energy. All sliding semilandmarks were constrained by homologous landmarks (Gunz et al. 2005) and allowed to slide along the predefined curves and surfaces. The sliding semilandmarks are consequently transformed into spatially homologous landmarks. Landmarks coordinates of all specimens can then be compared using traditional geometric morphometric methods.

Variability in Mandibular Shape and Jaw Muscles

A Generalized Procrustes Analysis (GPA—Rohlf and Slice 1990) was performed using the function "procSym" (Klingenberg et al. 2002; Gunz et al. 2005; Dryden and Mardia 2016). The importance and significance of the correlations between mandibular shape and centroid size and between muscle morphology (PCSA and mass) and centroid size were explored using the function "cor.test". Allometry-free

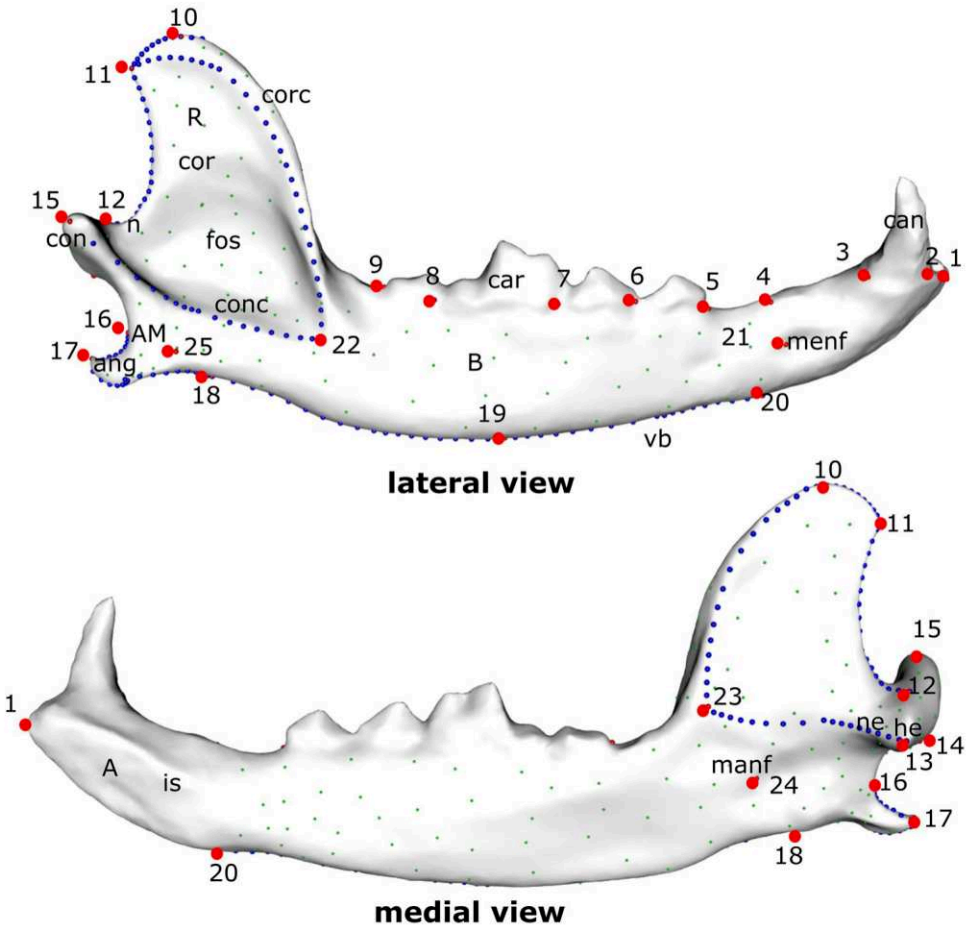

Fig. 2 Position of the landmarks used in this study and mandible features following Budras (2007), Barone (2010) and Evans and DeLahunta (2010). Anatomical landmarks are indicated in red, sliding semi-landmarks of curves are in blue and sliding semi-landmarks on the surface are in green. *AM* angle of mandible, *B* body of mandible, *R* ramus of mandible, *con* condyloid process, *cor* coronoid process, *ang* angular process, *is* intermandibular suture, *n* mandibular notch, *he* head of mandible, *ne* condylar neck, *vb* ventral border, *fos* masseteric fossa, *conc* condyloid crest, *corc* coronoid crest, *manf* mandibular foramen, *menf* main mental foramen, *can* canine, *car* carnassial (M1)

coordinates and visualisations were obtained using the functions "CAC" (Mitteroecker et al. 2004) and "showPC". Allometry-free coordinates of Log_{10}-transformed muscle data were calculated using the function "lm". Principal Component Analyses (PCA) were performed using the function "prcomp" based on the coordinates of all aligned specimens, on allometry-free coordinates, on the PCSA of all muscles, on the scaled PCSA of all muscles, on muscle mass and, on scaled muscle mass. The deformation of the mandible of a Beagle to the consensus of the GPA was used as a reference for all further visualisations. The Beagle was chosen because it was the dog that was closest to center of the PCA describing variation in mandibular shape.

Covariations Between Mandible Shape and Jaw Muscles

To explore the patterns of covariation between the mandibular shape and the PCSA or mass of the jaw muscles, we performed a two-block partial least square analyses (2B-PLS) with the function "pls2B" (Rohlf and Corti 2000). We did not consider phylogeny (Parker et al. 2004) in our analyses because we had no indication of pure race membership.

2B-PLS calculates singular values and creates new axes by looking for linear combinations in each block that maximise the covariance between blocks (the variation of PCSA or mass of all the muscles and mandibular shape). For each axis a PLS coefficient is generated (intensity of the covariation) and p values are calculated by comparing the singular value to those obtained from 1000 permuted blocks (significance of the covariation).

The mandibular ramus is likely to be more closely associated with space constraints related to the volume of jaw muscles than the mandibular body. To test whether the covariation was higher between muscles and the ramus of the mandible only, we explored both covariations with the complete mandible shape, and with a subset of landmarks and sliding semilandmarks of curves representing the posterior part of the mandible only.

A total of twelve 2B-PLS analyses were conducted: mandibular shape—PCSA, mandibular shape—scaled PCSA, allometry-free mandibular shape—scaled PCSA, ramus shape—PCSA, ramus shape—scaled PCSA, allometry-free ramus shape—scaled PCSA, mandibular shape—mass, mandibular shape—scaled mass, allometry-free mandibular shape—scaled mass, ramus shape—mass, ramus

Table 2 Definition of the landmarks of the mandible used in the geometric morphometric analyses

Landmark	Definition
1	Most rostromedial point of the mandiblular symphysis, at the base of the first incisor
2	Most rostral point of the canid, on the lateral side
3	Most caudal point of the canid, on the lateral side
4	Most rostral point of the second premolar, on the lateral side
5	Most rostral point of the third premolar, on the lateral side
6	Most rostral point of the fourth premolar, on the lateral side
7	Most caudal point of the fourth premolar, on the lateral side
8	Most caudal point of the carnassial, on the lateral side
9	Most caudal point of the second molar, on the lateral side
10	Highest point of the tip of the coronoid process
11	Most caudal point of the tip of the coronoid process
12	Most caudal point of the mandibular notch, at the intersection of the condyle and the coronoid process
13	Most medial point of the condyle (tip of the head of the mandible)
14	Most ventral point of the condyle
15	Most lateral point of the condyle
16	Most anterior point on the curve of the angle of mandible
17	Point at the tip of the angular process
18	Most elevated point on the inferior border of the ramus
19	Lowest point on the ventral border of the ramus, right under the carnassial
20	Most caudal and lowest point of the intermandibular suture on the medial side
21	Main mental foramen
22	Rostral point of intersection between the coronoid crest and the condyloid crest
23	Most rostral point of the edge joining the basis of the coronoid process and the condyle on the medial side
24	Most rostral point of the mandibular foramen
25	The most lateral point on the angle of mandible, at the beginning of the angular process

True landmarks are in red, sliding semi-landmarks of curves are in blue and sliding semi-landmarks of surface are in green

shape—scaled mass, allometry-free ramus shape—scaled mass.

A Z-score was finally calculated to compare PLS coefficients with the function "compare.pls" from the package geomorph.

Results

Variability in Mandibular Shape

Results of the Principal Component Analyses and correlation tests for exploring allometries are detailed in Supplementary material Table S3.

The first two axes of the PCA represents 46.1% of the variability in mandibular shape. The next axes each represent a very small part of the total variability (8.9% for axis 3). Only the morphological variations related to axis 1 and axis 2—that are the most informative—will therefore be described (Fig. 3). The mandibular shape varies greatly depending on the morphotype, and variation is also important within a single breed (Beagles). Especially noticeable is the variation in robustness, the shape of the coronoid process, and the ventral curvature of the mandibular body. Along the first axis of the PCA, the molossoid/brachycephalic dogs are generally opposed to dolichocephalic/lupoid dogs. The first axis is mainly explained by differences in size ($r = 0.51$; $P < 0.001$) with the biggest mandibles being positioned to right of the scatterplot. Mesocephalic and dolichocephalic dogs are not clearly distinguishable and overlap towards the left part of the scatterplot. Most of these morphological changes are explained by size, since allometry is moderately strong ($R^2 = 0.44$; $P < 0.001$, Fig. S1). Molossoid dogs—which most often correspond to large mandible sizes—have shorter and more robust and laterally curved mandibles, with more developed coronoid, condylar, and angular processes. The rostral part of the mandible is more ventrally curved and the condyle tends to be at a straight angle to the sagittal plane in molossoid dogs (Figs. 3a, S1). Variation along axis two is observed for dogs of the same breed, as is the case for the Beagle which occupies the entire upper left quadrant of the scatterplot. This variation is not related to size ($P > 0.05$) and describes the rostro-ventral curvature of the mandible and the orientation of the coronoid process. The two first axes

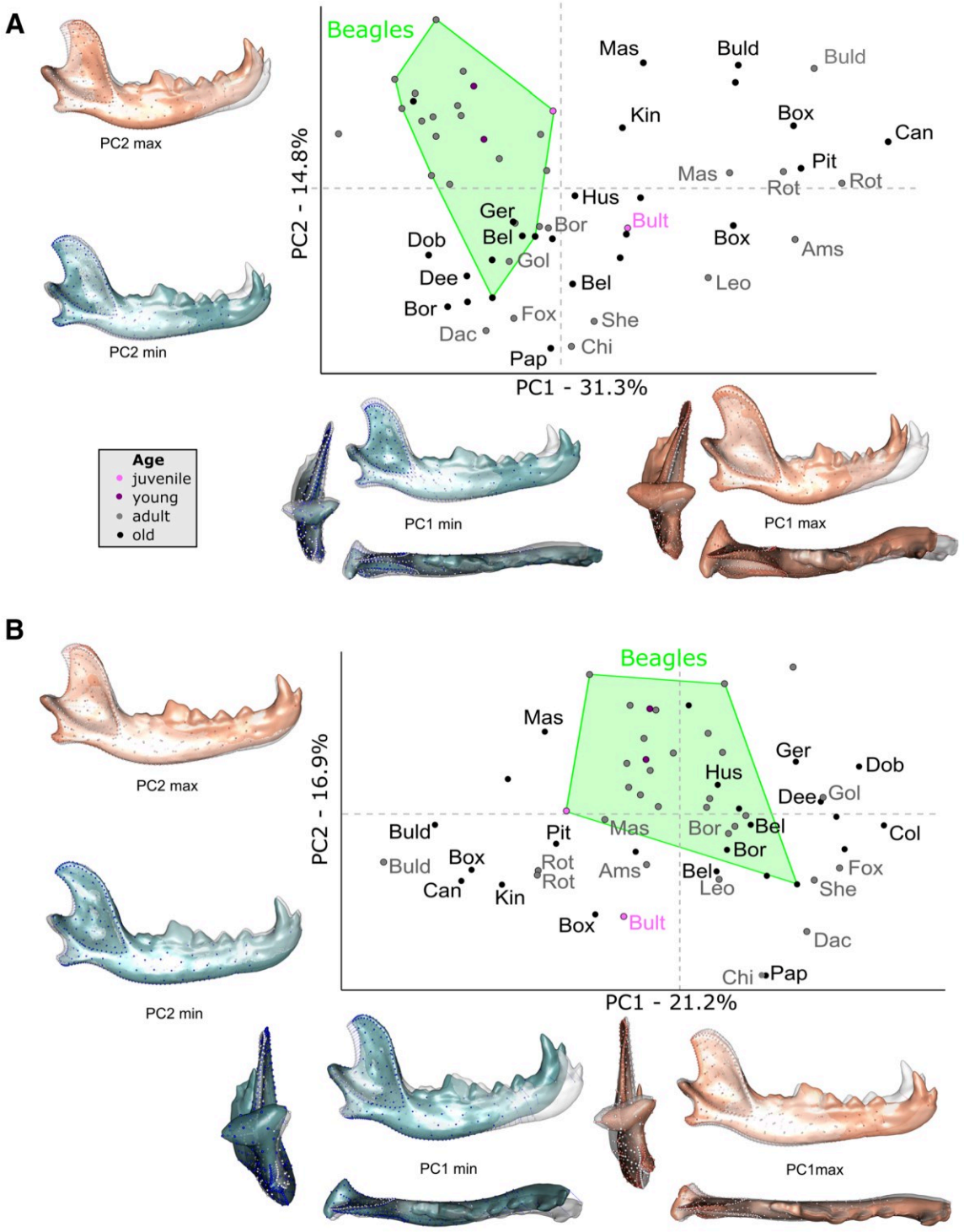

Fig. 3 First two axes of the PCA describing variation in: **a** mandibular shape; **b** allometry-free mandibular shape. The mesh of the consensus is represented in white. Illustrations represent the deformations from the consensus to the extreme of the axis in lateral, dorsal and caudal views for PC1 and in lateral view for PC2. Ages are indicated by colors. Beagles are in green and other breed names are indicated following Table 1

are not correlated with the age of the dogs ($P > 0.05$). The PCA performed on allometry-free shapes (Fig. 3b) show that dolichocephalic and brachycephalic dogs oppose themselves along the first axis with the mesocephalic dogs at the very center. The variation along this axis involves the ventral and lateral curvature of the mandibular body, the width of the

coronoid process and the relative size of the condyle and angular processes. The two youngest dogs are included in the same morphospace as the adults. Interestingly, the "juvenile" Bull terrier is located in the same part of the scatterplot as the other molossoid dogs when analyses are performed on allometry-free shapes (Fig. 3b). The "juvenile" Beagle remains positioned close to the adult Beagles.

Variability in Jaw Muscle Architecture

Muscle data are given in Supplementary material Table S1 and the results of the statistical analyses (PCA and correlation tests exploring allometries) are detailed in Supplementary material Table S3.

The angles of pennation are around 0° in the digastric, 30–40° in the temporalis and masseter and 40° in the pterygoids. Muscles from the temporal complex have very long muscle fibers (up to 60 mm; mean around 30 mm) compared to muscles from the masseteric and pterygoid complexes (up to 30 mm; mean around 15–20 mm). The temporal complex represents 64% (min = 55%; max = 71%) of the total volume and 50% (min = 40%; max = 61%) of the total PCSA of the adductor muscles. The masseteric complex represents 27% (min = 22%; max = 32%) of the total volume and 36% (min = 29%; max = 46%) of the total PCSA of the adductor muscles. The pterygoid complex represents only 9.6% (min = 6%; max = 13%) of the total volume and 14% (min = 6%; max = 24%) of the total PCSA of the adductor muscles. The mass of the lateral pterygoid muscles represents only around 7% of the mass of the pterygoid complex in the domestic dog (min = 2.5%; max = 20.4%) and 0.67% of the total mass of the adductor muscles (min = 0.20%; max = 2.4%).

Whereas the mass and PCSA of jaw muscles vary greatly depending on breeds, significant variation is also observed among Beagles. Their morphological space stretches along axis 1, but mainly along axis 2. Since similar results were observed for mass and PCSA, only the PCA with muscle PCSAs will be described here (Fig. 4). The PCA with muscle masses is available in the supplementary material (Supplementary Fig. S2).

The first axis of the PCA performed on the raw or scaled PCSA (representing 76.5% or 51.3% of the total variation, respectively) or mass data (91.7% for raw mass and 71.8% for scaled mass) loads strongly with the temporalis and masseter muscles. The second axis of the same analyses explains only a small amount of the total variation (PCSA: 5.5% for raw data and 10.5% for scaled data; mass: 2.3% for raw data and 7.5% for scaled data), and is driven by variation in the anterior part of the zygomaticomandibularis and the temporalis pars suprazygomatica, for our analyses of PCSA, or by variation in the masseter group (above all the anterior part of the zygomaticomandibularis) for the PCA on mass.

The PCAs with raw muscle data reflect differences in the size of the head. Molossoid dogs—most often with larger heads—have more powerful jaw muscles than most of the other dogs. On the opposite, dogs from the Toy group (Chihuahua, Papillon)—characterized by very small heads—have the smaller and less forceful muscles. Statistical analyses showed that the variation in muscle volume and force is strongly corelated to variation in mandibular size (mass: $r = 0.89$, $P < 0.001$; PCSA: $r = 0.83$, $P < 0.001$).

The PCAs performed on scaled PCSA and scaled mass show that the dogs with biggest and strongest jaw muscles for their size are large molossoid dogs, represented by a Leonberger, an American Staffordshire, Mastiffs, a Cane corso, and more markedly the two Rottweillers, the Pitbull and the two Bulldogs. Surprisingly, the Chihuahua in our sample also has very strong and voluminous muscles for its size and is positioned close to the Cane Corso, the Rottweiler and the American stafforshire. The hunting and shepherds dogs (including the German Shepherd), the Papillon and the Boxers of our sample have medium to low muscle masses and rather weak muscles for their size. The Cavalier King Charles has masticatory muscle masses that are larger than the average of our sample when corrected for differences in size (close to the Cane Corso) but muscle strength is not impacted. Although the small sample size and the low intra-breed diversity of our sample does not allow us to draw conclusions about breed-specific diversity our results suggest that this would a fruitful avenue for further research.

Covariation Between Mandibular Shape and Jaw Muscle Architecture

A summary of the results of the 2B-PLS is given in Table 3. Detailed results are available in Supplementary material Table S4. Only the main results are detailed below.

The covariation between mandibular shape and the masticatory muscles is highly significant, whether size is taken into account or not (Table 3). The coefficients of covariation are high, and they do not significantly differ between muscle masses and muscle PCSAs, and between scaled and raw muscle data. The coefficients of covariation obtained for the shape of the ramus only are not higher than the ones for the complete mandible.

Here we focus on the covariations between mandibular shape and the scaled muscle data, since the centroid size is an important driver of covariation (but see supplementary material for further visualisations and results for the raw data: Figs S3 to S6). The covariation between scaled PCSA and mandibular shape was significant (Fig. 5), for the first PLS axis (PCSA: PLS1 88% of the covariance, $rPLS1 = 0.64$, $P < 0.001$). Similar results were observed for scaled masses (PLS-1 95% of the covariance, $rPLS1 = 0.70$, $P < 0.001$, $Zscore = 0.75$; $P = 0.23$, Supplementary Fig. S7).

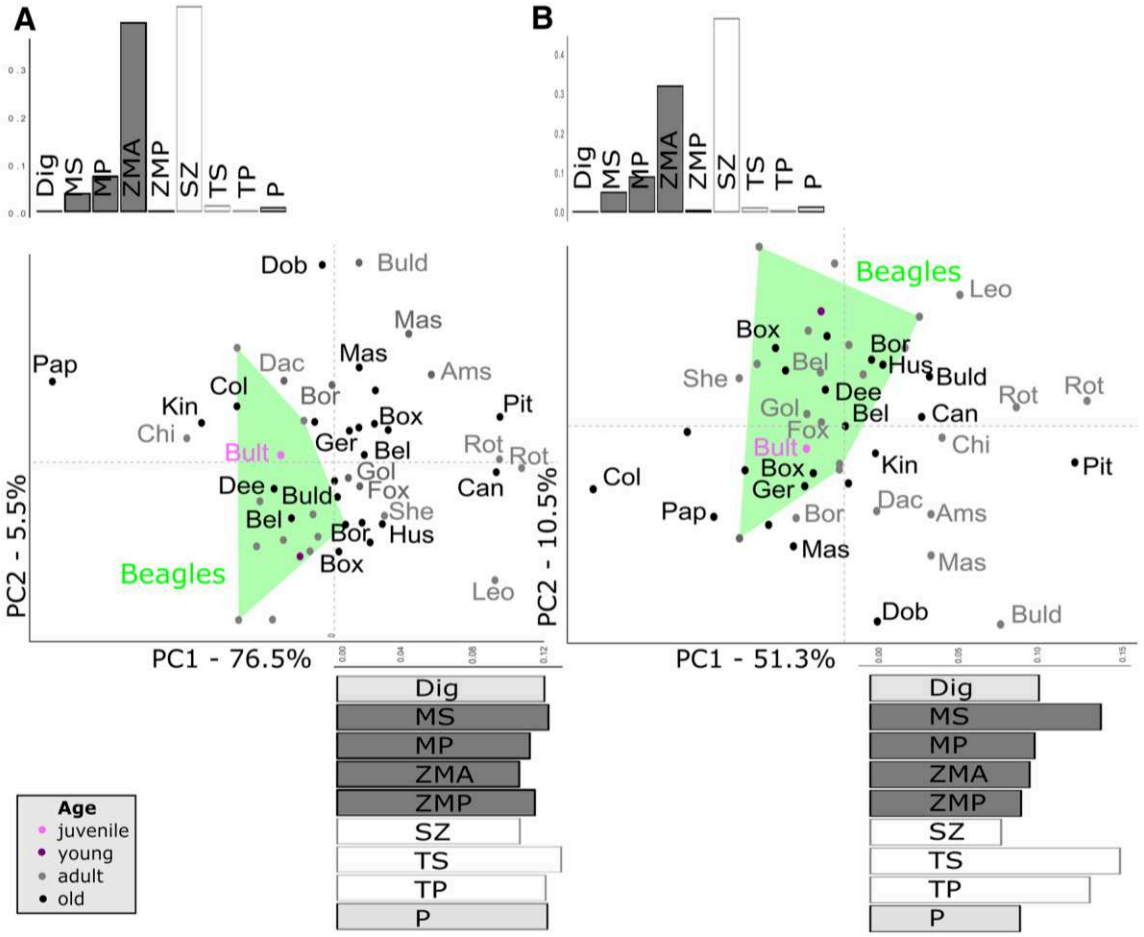

Fig. 4 PCA describing variation in **a** PCSA or **b** scaled PCSA of the jaw muscles. Histograms represent the loadings of the original variables on the axes. *Dig* digastric, *MS* masseter pars superficialis, *MP* masseter pars profunda, *ZMA* masseter pars zygomaticomandibularis anterior, *ZMP* masseter pars zygomaticomandibularis posterior, *SZ* temporalis pars suprazygomatica, *TS* temporalis pars superficialis, *TP* temporalis pars profunda, *P* pterygoids. Ages are indicated by colors. Beagles are in green and other breed names are indicated following Table 1

Table 3 Results of the 2B-PLS analyses comparing the mandibular shape (complete mandible or mandibular ramus only) against: (A) the Log10 of the mass of the jaw muscles; (B) the Log10 of the PCSA of the jaw muscles

A.	Shape–mass				Shape–scaled mass				Allometry-free shape–scaled mass			
Bone	Axe	%coVar	p-value	r-PLS	Axe	%coVar	p-value	r-PLS	Axe	%coVar	p-value	r-PLS
Complete mandible	PLS 1	99	< 0.001	**0.74**	PLS 1	95	< 0.001	**0.70**	PLS 1	92	< 0.001	**0.74**
					PLS 3	2.1	0.049	**0.52**				
Mandibular ramus	PLS 1	96	< 0.001	**0.68**	PLS 1	61	0.155	0.68	PLS 1	65	0.075	0.68
	PLS 2	2	0.05	0.54	PLS 2	21	0.003	**0.63**	PLS 2	16	0.022	**0.62**
B.	Shape–PCSA				Shape–scaled PCSA				Allometry-free shape–scaled PCSA			
Bone	Axe	%coVar	p-value	r-PLS	Axe	%coVar	p-value	r-PLS	Axe	%coVar	p-value	r-PLS
Complete mandible	PLS 1	97	< 0.001	**0.73**	PLS 1	88	< 0.001	**0.64**	PLS 1	82	< 0.001	**0.68**
Mandibular ramus	PLS1	89	< 0.001	**0.66**	PLS 1	44	0.411	0.65	PLS 1	47	0.290	0.65
					PLS 3	16	0.029	**0.52**				

%coVar indicates the percentage of covariation explained by the axis of interest. r-PLS indicates the coefficient of covariation between the two variables. Significant results are indicated in bold. Only the first and/or significant axes are reported. See supplementary material Table S4 for details

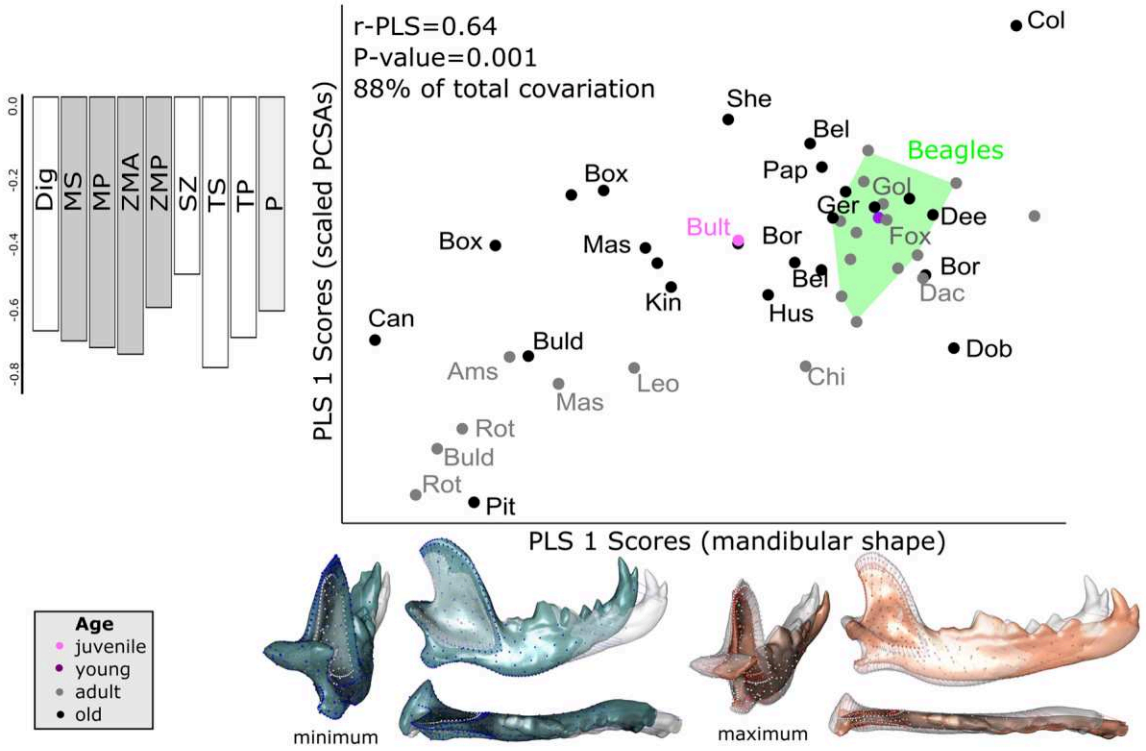

Fig. 5 2-Block Partial Least Square Analyses between mandibular shape and the scaled PCSA of jaw muscles, with muscle vectors and shapes at the minimum and maximum of the PLS axis. Illustrations represent the deformations from the consensus to the extreme of the axis in lateral, dorsal and caudal views. *Dig* digastric, *MS* masseter pars superficialis, *MP* masseter pars profunda, *ZMA* masseter pars zygomaticomandibularis anterior, *ZMP* masseter pars zygomaticomandibularis posterior, *SZ* temporalis pars suprazygomatica, *TS* temporalis pars superficialis, *TP* temporalis pars profunda, *P* pterygoids. Ages are indicated by colors. Beagles are in green and other breed names are indicated following Table 1

The first PLS axis (accounting for 88% of the covariance) shows that lupoid, graioid and bracoid dogs are situated at the positive part of the scatterplot and oppose molossoid breeds at the negative part of the scatterplot. All muscles strongly covary with mandibular shape. The positive part of the scatterplot corresponds to the breeds with a low PCSA of these muscles and a gracile mandible with a strait and flat body that curves outward, a higher ventral part of the ramus, a thin, reduced and slightly tilted outwards coronoid process with a shallow masseteric fossa, a small condyle and a small and straight angular process. Dogs at the negative part of the scatterplot have robust mandibles with a very ventrally curved and thick body, a lower ventral part of the ramus, a taller coronoid process with a deep masseteric fossa, and a large, medially and caudally extended and less medio-laterally oblique condyle.

The covariations between scaled muscle data and ramus shape are significant only on secondary axes, explaining less than 16% of the covariance. The 2B-PLS between the mandible ramus shape and the scaled masses of the jaw muscles (PLS-2 21% of covariation, r-PLS2 = 0.63, P = 0.006, Fig. 6) shows that dogs with more voluminous deep masseter muscles and less voluminous temporal muscles and superficial masseters for their size have a more curved coronoid process with a deeper masseteric fossa and a lower and less curved angular process (and vice versa). Similar results were observed for the third axis of the 2B-PLS between ramus shape and the scaled PCSA (Supplementary Fig. S8) and for the second axis of the 2B-PLS between allometry-free ramus shape and scaled masses (Supplementary Fig. S9).

Similar results were observed for allometry-free mandibular shape and scaled PCSA (Fig. 7) or scaled mass (Fig. S9). Changes in the body of the mandible along the first PLS axis are the same as those previously described except some more specific anatomical features for the coronoid process. For a given size of the coronoid process dogs with less forceful muscles have a more caudally curved and narrower coronoid process (with a shallower masseteric fossa) contrary to dogs with stronger muscles which have a wider and thicker coronoid process (with a deeper masseteric fossa).

Significant covariations between allometry-free shape of the mandible ramus and scaled masses show that a more caudally curved coronoid process and a less pronounced and curved angular process are related to proportionally more developed deep masseter muscles and a proportionally less developed superficial masseter muscle (Fig. S10).

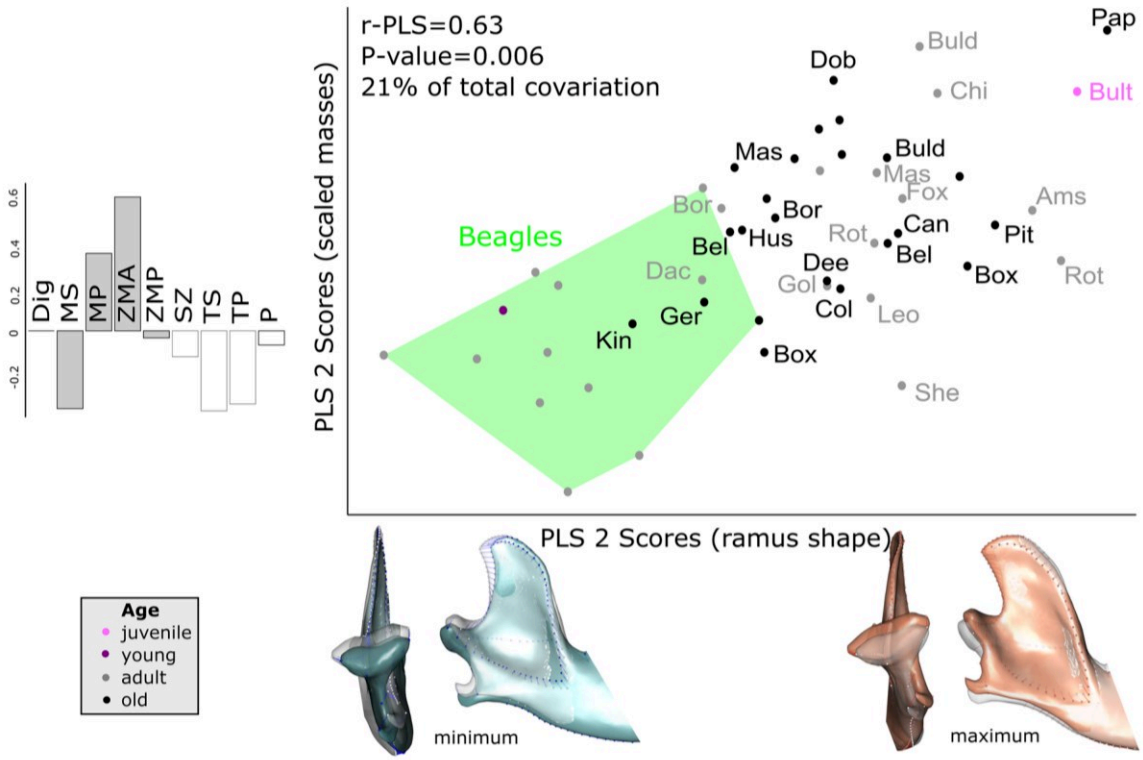

Fig. 6 2-Block Partial Least Square Analyses between the shape of the ramus and the scaled mass of jaw muscles, with muscle vectors and shapes at the minimum and maximum of the PLS axis. Illustrations represent the deformations from the consensus to the extreme of the axis in lateral, dorsal and caudal views. *Dig* digastric, *MS* masseter pars superficialis, *MP* masseter pars profunda, *ZMA* masseter pars zygomaticomandibularis anterior, *ZMP* masseter pars zygomaticomandibularis posterior, *SZ* temporalis pars suprazygomatica, *TS* temporalis pars superficialis, *TP* temporalis pars profunda, *P* pterygoids. Ages are indicated by colors. Beagles are in green and other breed names are indicated following Table 1

Discussion

Variations in Mandibular Shape and Masticatory Muscles

The general shape of the mandibular ramus and the relative importance of masticatory muscles in dogs reflects the specialization towards vertical movements as in other canids. Indeed, the condyle is cylinder-shaped, mediolaterally elongated, curved backwards, and at a right angle to the sagittal plane. Moreover, the temporal and masseteric complexes responsible for the vertical movements of the jaw are by far the most strongly developed in canids since they represent around 90% of the mass and intrinsic strength of the adductor muscles. This corroborates descriptions of previous authors (Schumacher 1961; Turnbull 1970; Noble 1973; Ström et al. 1988). The pterygoid muscles—that have a more medio-lateral line of action—are small and the shape of the condyle permits only limited medio-lateral rotational movements that function to bring the blades of the carnassials into close contact (Ström et al. 1988; Ewer 1998). The lateral pterygoid is very small (it represents less than 3% of the of the total mass of the adductor muscles) and its role is ambiguous because it could be involved in both mandibular protraction and adduction (Turnbull 1970; Tomo et al. 1993; Evans and DeLahunta 2010).

The proportions in volume and PCSA of the different muscles were not the same. For example, even though the pterygoid complex always represents less than 13% of the total mass of the adductor muscles, it can represents up to 24% of the total intrinsic strength of the adductor muscles, indicating that these muscles are optimized for force production. This is because muscles with longer fibers (temporal) are in proportion 'disadvantaged' compared to muscles with shorter fibers (pterygoids or masseter). This reflects an architectural trade-off between PCSA and fiber length: a muscle cannot be optimized for both force production and contraction velocity (Gans and Bock 1965; Taylor and Vinyard 2013). The PCSA data provided here are further of interest as they may provide better estimations of bite force than estimations obtained from models using the dry skull method (Thomason 1991; Ellis et al. 2009). However, muscle PCSAs are only general proxies of maximal intrinsic muscle force. Muscle loads on the mandible will also depend on the size

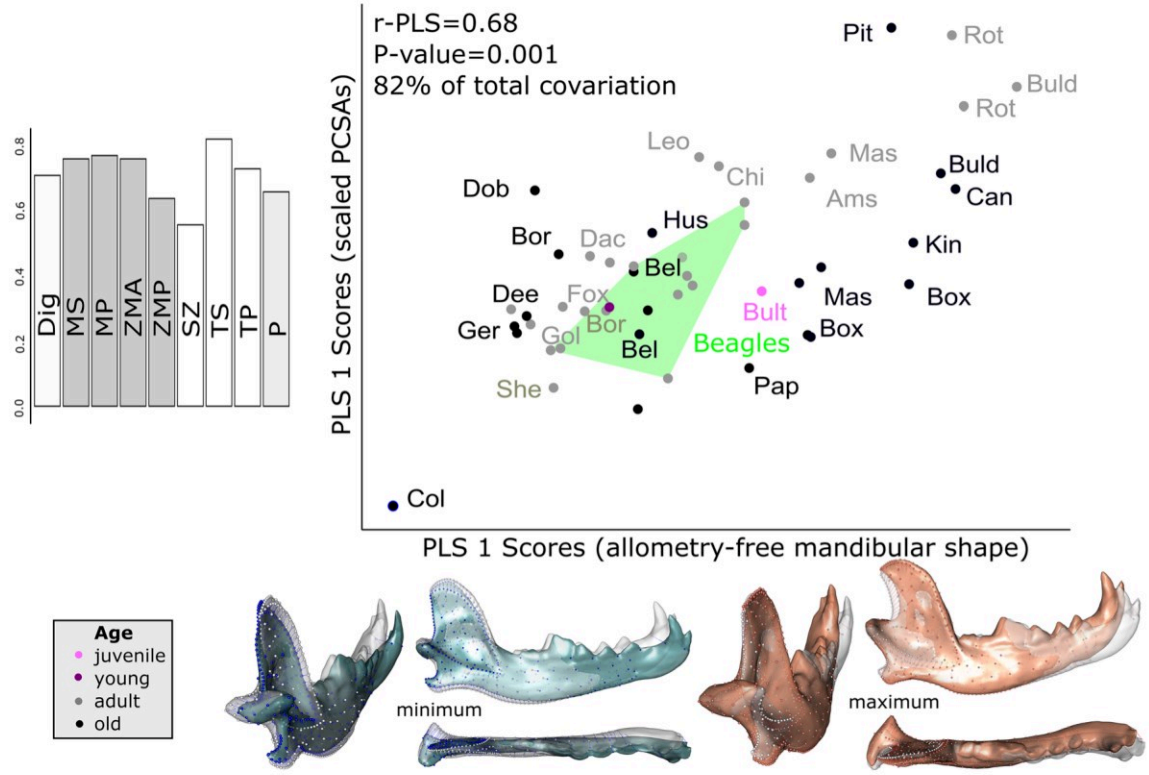

Fig. 7 2-Block Partial Least Square Analyses between allometry-free mandibular shape and the scaled PCSA of jaw muscles, with muscle vectors and shapes at the minimum and maximum of the PLS axis. Illustrations represent the deformations from the consensus to the extreme of the axis in lateral, dorsal and caudal views. *Dig* digastric, *MS* masseter pars superficialis, *MP* masseter pars profunda, *ZMA* masseter pars zygomaticomandibularis anterior, *ZMP* masseter pars zygomaticomandibularis posterior, *SZ* temporalis pars suprazygomatica, *TS* temporalis pars superficialis, *TP* temporalis pars profunda, *P* pterygoids. Ages are indicated by colors. Beagles are in green and other breed names are indicated following Table 1

and position of the attachment sites of the jaw muscles on the skull and mandible, on the unbalanced and uncomplete recruitment of the muscle during biting (Kim et al. 2018), and on the nature of the muscle fibers (Grünheid et al. 2009; Kim et al. 2018).

Extreme variation has already been demonstrated for the skull (Drake and Klingenberg 2010; Selba et al. 2019) and is generally considerd to be the result of intensive dog breeding and artificial selection for aesthetic reasons. Our study demonstrates that the masticatory muscles and the shape of the mandible also show important variation related to variation in the size of the individuals and the type of breed. Breeds represented by several individuals, such as Beagles, also showed unexpected levels of variation. Although we had too few young individuals to assess the effect of ontogeny this is also likely to contribute to the overall diversity in both mandible shape and muscle architecture.

The different muscle layers show an important diversity in mass, but also in intrinsic muscle strength due to the great variation in fiber length and pennation angles (Supplementary material Table S1), making the architecture of the jaw muscles complex. Our results indicate that the masticatory muscles scale isometrically relative to mandibular size, which corroborates the results of Penrose et al. (2016). The molossoid dogs of our sample generally have the strongest and most voluminous muscles. On the contrary, the dogs from the Toy group of our sample (the Chihuahua, the King Charles and the Papillon) have very small muscles, logically resulting in a lower intrinsic force generation capacity. However our analyses suggest that some dogs of very small breeds such as the Chihuahua—the smallest breed recognized by kennel clubs—tend to have muscles that are as imposing and as powerful as those of some specimens of Cane Corso, Rottweiller or American Staffordshire when size is taken into account. However, the low intrabreed diversity in our sample does not allow us to explicitly test for differences between breeds. Future studies are needed to explore this further. In our study, the only German Shepherd is included within the variability of the other shepherd dogs in our sample, with less voluminous and powerful muscles irrespective of variation in size. As stated above, our sample does not allow to draw conclusions on breed-specific diversity but it would be interesting to test whether German Shepherd dogs are grouped with other shepherd dogs or with

breeds dedicated to protection. Indeed, the German Shepherd is a very "multi-skilled" breed, that has been modified as an army or police dog but that was originally designed to be a working sheepherder (Parker et al. 2004).

Relations Between Mandibular Shape and the Development of Masticatory Muscles

As predicted, we found significant covariation between the shape of the mandible and the development of the masticatory muscles irrespective of whether size is taken into account or not. This study logically suggests that there is a strong association between muscle volume and mandibular form. The coefficient of covariation of the 2B-PLS with allometry-free shape and/or scaled muscle data is not different from the 2B-PLS on raw data and remains elevated. Therefore, size alone is not enough to explain the existing covariation. The dispersion of the individuals along the PLS axis for the 2B-PLS with scaled muscle data (Figs. 5, 6, 7, S7-S10) shows, however, that similar mandibular morphologies can correspond to different relative muscle volumes or strength. For example, among the three dogs from the Toy group of our sample, the Chihuahua and the Papillon have very similar mandibular shapes but the Chihuahua dog has much more powerful and voluminous muscles than the Papillon when size is removed. This suggests significant differences in muscle architecture among dogs with similar morphotypes.

Morphological changes that appear directly related to muscle volume and strength involve areas of insertion of the masticatory muscles: the size and shape of the coronoid process, the depth of the masseteric fossa and the size and curvature of the angular process. This suggests that the attachment area requirements for individual muscles likely drive mandibular shape. Muscle volume and strength are also related to changes in general features, such as the robustness of the mandible, the ventral and lateral curvature of the body and the size of the condyle. Surprisingly, covariations are not significantly different when considering the posterior part of the mandible only relative to the entire mandible. This suggests that the curvature and thickness of the body where no muscles attach and which bears the dental alveoli, also covaries with the shape of the ramus. Indeed, the body and the ramus together form an integrated system adapted to the mechanical constraints of biting and chewing. The shape associated with low (scaled or not scaled) muscle masses and PCSAs is characterised by a relatively long and flat body, a small coronoid process curved at its posterior tip, a shallow masseteric fossa, and a small and ventromedial oblique condyle. On the contrary, shapes related to large and strong muscles correspond to robust mandibles with a relatively large, wide coronoid process with a deep masseteric fossa, a laterally and ventrally curved ramus, and a (medially) long and large condyle. All these changes can be explained by muscle volume, conditioning the space available for those muscles and responses to loading of the mandible at the teeth. Accordingly, for dogs with big and strong muscles (mainly large brachycephalic dogs), the mandible is more curved in the medio-lateral plane. This temporomandibular joint axis rotation has been described by Curth et al. (2017) and interpreted as a result of reduced space availability in short-faced skulls. However, this could also be a mechanical adaptation to the volume occupied by the temporal and masseter muscles. An inclined mandible is more suite to allow large muscles to pass between the skull and the mandible and goes hand-in-hand with wider zygomatic arches in brachycephalic breeds. The slightly opposing orientations of the coronoid process and mandibular body (medially inclined condyle and body anteriorly curved outwards in dolichocephalic dogs) seem to reflect a compromise in shape to distribute the forces exerted on the mandible, allowing both muscle attachement and vertical opening/closing movements. Thus the change in the angle between the coronoid process and the condyle could be a mechanical response to the reaction forces and important for joint stabilisation.

All muscles covary together on the first axis of the 2B-PLS with the complete mandible (explaining more than 80% of the covariation; Figs. 5, 7, S3, S4, S7, S9) but the secondary axis of the 2B-PLS performed with the mandible ramus only (explaining up to 20% of the covariation; Figs. 6, S5, S6, S8, S10) allowed us to describe more specific variations. We observed that the more the superficial masseter, the temporal complex and the pterygoid muscles were developed, the straighter the coronoid process was. On the opposite, the bigger the deep masseter and zygomaticomandibularis, the more caudally curved the coronoid process. Liebman and Kussick (1965) described variation in the morphology of the mandible depending on the removal of the temporal or masseter on one side of the head of a dog. They report that the variation in shape of the angular process is likely to be due to variation in both the pterygoid and masseter muscles. Indeed, the angular process tended to be straight rather than curved when the masseter muscle was removed. This description is consistent with our observations (Figs. 6, S8, S10). For these authors, the shape of the coronoid process is more probably linked to the temporal muscle. They observed that the coronoid process tended to be straighter after removing the temporal muscle, whereas on the normal side the coronoid process was more caudally oriented. Our own observations, however, do not support these results (Figs. 6, S8, S10). This could be due to a balance between the masseteric and temporal complexes. Liebman and Kussick (1965) completely removed one of the two complexes so their observations do not take these interactions into account. In our 2B-PLS showing opposing

loadings (Figs. 6, S8, S10), both complexes play a role in the construction of the PLS-1 axis. The less developed the temporal complex is, the more developed the deep masseter, including the zygomaticomandibularis. As the zygomaticomandibularis anterior inserts mainly on the anterior part of the masseteric fossa to the tip of the coronoid process, a bigger muscle would involve a more important surface area. This could explain why we observed more caudally curved coronoid process in dogs with a relatively more imposing zygomaticomandibularis.

However, our study did not allow to explore the mechanical relations between mandible shape and muscle loading per se. Further investigations would be needed to explore the connection between bone resistance and muscle force through, for example, finite element analyses (e.g. Bourke et al. 2008; Kim et al. 2018; Penrose et al. *under review*). An interesting and complementary approach may be to investigate the link between mandible shape and bone cortical thickness and its degree of biomineralization to track functional variation according to load resistance (Ross et al. 2005; Kupczik et al. 2007; Rayfield 2007; Cox et al. 2015). Indeed, even though the shape of the mandible is the combined result of phylogeny and developmental constraints, its shape also depends on mechanical loading (Weijs and Hillen 1986; Wolff 1986; Hannam and Wood 1989; Raadsheer et al. 1999; Currey 2002, 2003; Daegling and Hotzman 2003; Mavropoulos et al. 2004; Ravosa et al. 2007; Sharir et al. 2011; Slizewski et al. 2013). Furthermore, it has been shown that the relationship between bone morphology and muscle force is reciprocal, as the shape of a bone determines the load that it can tolerate (Weiner and Wagner 1998; Frost 2001). As a result, the mandible is plastic: it is constantly modeled throughout life to be able to resist the changes in the mechanical environment, that is the muscle forces and external forces exerted upon it during chewing (Frost 2001; Currey 2002; Fabre et al. 2018). Accordingly, it has been demonstrated that increased physical activity affects the geometry and composition of bones, whereas decreased loads due to enforced rest or muscle dysfunctions result in thinner bones (Schoenau 2005; Ward et al. 2006). Among other external constraints, diet is likely to play a significant role in mandible shape. We had no information about the diet of the individuals in our sample, but further studies exploring the influence of food texture on mandible shape and the mechanical properties of the cortical bone of the mandible would be of interest. Indeed, it has been demonstrated that food mechanical properties influence cortical bone modelling and remodelling (Bouvier and Hylander 1981, 1984; Lieberman et al. 2004; Ionova-Martin et al. 2011; Scott et al. 2014a, b; Ravosa et al. 2015, 2016). The study of Scott et al (2014a) on rabbits lead them to suggest that mammals may be very plastic even at late life-history stages. All these elements might explain the observed differences among the different dogs in our study (Bouvier and Hylander 1981, 1984). Moreover it would be interesting to study how pathologies that impact muscle development (dysplasia and jaw locking) affect mandible shape (Robins and Grandage 1977; Johnson 1979; Thomas 1979; Hoppe and Svalastoga 1980; Ström et al. 1988). Indeed, according to He and Kiliaridis (2003), the alteration of masticatory muscle function can affect the morphology of certain regions of the skull and face in ferrets. Additionnaly, we could not explore the role of ontogeny because we had too few juveniles to test for the effect of age. Future studies could explore the evolution of the interplay between bone and jaw muscles in dogs through postnatal development, as it has been done in other mammals (Swiderski and Zelditch 2013). Indeed, muscle provides growth factors for bone tissue throughout postnatal development independently of forces imparted to bones. This can significantly impact bone formation at attachment areas and might thus be a source of the observed patterns of covariation between muscle size and the shape of the mandibular ramus.

Domestication and Integration in the Masticatory Apparatus

As predicted, jaw muscle architecture covaries with mandibular shape, but we did not expect such a strong covariation.

Integration is produced by the sharing of biological processes such as the same developmental origin or the implementation of the same function (Olson and Miller 1951, 1958, 1999). This strong integration makes sense given that bone is a living and plastically remodelled tissue, causing changes in the shape of the mandible in direct response to muscle and jaw loading. However we expected the extreme diversity in shapes due to artificial selection to interfere with this functional integration, as many domestic dogs are not under strong functional constraints for chewing or biting. This is even more surprinsing as a low integration has been documented in strepsirrhine primates, which are, on the contrary, subject to strong natural selection and dietary constraints (Fabre et al. 2018).

We suggest that this strong integration is perhaps determined by a strong interaction between genes responsible for the mandibular shape and genes responsible for the development of jaw muscles. Muscle development would therefore be intrinsically linked to bone development. Consequently, selection on morphology would therefore produce a correlated response in the functional abilities (Cheverud 1982; Klingenberg 2010, 2014). Muscles and bones indeed share common genetic determinants (Karasik and Kiel 2008; Blank 2014) and cells derive from a common mesenchymal precursor. Multiple loci overlapping between the two traits and several genes with possible pleiotropic effects on both bones and muscles

have been indentified (Kaji 2014). As a consequence, it is possible that some genes may trigger changes in bone anatomy, and as a result, affect muscle architecture (Karasik and Kiel 2008). It is also plausible that slight changes of systemic control factors occurs during development and impact both muscle and bone (e.g., small modulations of the growth hormone; Karasik and Kiel 2008). Genetic muscle disorders provide an opportunity to learn how muscle and bone interact. For example, a myostatin deficiency (*growth differentiation factor 8* [*GDF8*]) is observed in the whippet dog breed (Mosher et al. 2007) and results in a 'bully' whippet, with an approximate doubling of muscle mass and resulting in more robust bones. Observed allometries in muscle data and covariations between muscle data and shape supports the genetic influence on both bone and muscle, as well as integration (Karasik and Kiel 2010). However, more investigations on the genetic and molecular interplay between jaw muscles and the mandible are needed to better understand the drivers of variation in the masticatory apparatus.

Morover, our study seems to suggest that dogs show different patterns of integration according to their function. Breeds first selected for hunting or herding differ from the dogs that were first selected for human or herd protection. It seems that the selection for different biting abilities has resulted in different patterns of integration. Further studies focusing on a much larger sample are, however, needed to investigate whether dog breed selection is related to specialisations towards specific patterns of covariation between muscle and bones.

Our results raise the question of whether artificial selection produces a reorganization of the integration patterns in order to allow morphological traits to vary, as proposed by Hanot et al. (2018). Karasik and Kiel (2010) suggested that natural selection tends to favour alleles whose pleiotropic effects contribute to the attainment of appropriate proportions between muscles and bones, and the pattern of covariation is expected to evolve to match fitness demands. As a consequence, one would expect stronger integration among wild species since it responds to environmental selection pressures driving the jaw system towards an 'optimum' corresponding to the ecological context, and resulting in less morphological variability, especially for the wolf (Curth et al. 2017). We had no wolves in our sample which would be essential to test this hypothesis, but comparing our results with those non-domestic canids could help understand whether the phenotypic diversification of dogs is responsible for a change in integration pattern, and how integration may constrain changes in morphology or jaw muscle development.

Conclusion

Our study assessed the impact of the dramatic variation in mandible shape in domestic dogs on the development and architecture of the masticatory muscles. Our results suggest that jaw muscles and mandible shape form a highly integrated system in dogs. This could be the consequence of genes controlling both muscle and bone development, as well as epigenetic effects driving variation in muscles and bones (Iinuma et al. 1991) or the interaction between genetic mecanisms and plasticity (Hanot et al. 2017). Our results provide a better understanding of jaw function in dogs which despite its general interest remains rather poorly understood (Ellis et al. 2008, 2009). To further test whether mandibular form is driven by attachment area requirements and/or load resistance, finite element approaches may be of interest. The strong integration of the lower jaw offers the possibility to infer the functional consequences of morphological changes in fossil or archaeological specimens. Despite this strong integration, the question remains wether integration is stronger in wild or commensal canids, and whether domestication has lead to a disruption of the natural integration between form and function as suggested previously.

Acknowledgements We thank the Veterinary school ONIRIS-Nantes (France) and Anses (Nancy, France) for providing dog heads for dissection. We are grateful to Manuel Comte, Mickaël Godet and Frederic Lebatard for their help in managing specimens and their helpful discussions about the preparation of the skulls. We also thank Arnaud Delapré for his help with photogrammetry and Fabien Belhaoues for his constructive feedback on a first draft of this manuscript. We thank two anonymous reviewers who contributed to the improvement of an earlier version of this manuscript by their valuable comments and suggestions.

Funding This research was funded by the Ministère de l'Enseignement supérieur, de la Recherche et de l'Innovation.

Compliance with Ethical Standards

Conflict of interest The authors declare that they have no conflict of interest.

References

Bannasch, D., Young, A., Myers, J., Truvé, K., Dickinson, P., Gregg, J., et al. (2010). Localization of canine brachycephaly using an across breed mapping approach. *PLoS ONE, 5*(3), e9632. https://doi.org/10.1371/journal.pone.0009632.

Barone, R. (2010). *Anatomie comparée des mammifères domestiques : Tome 1, Ostéologie* (5th ed.). Paris: Vigot.

Blank, R. D. (2014). Bone and muscle pleiotropy: The genetics of associated traits. *Clinical Reviews in Bone and Mineral Metabolism, 12*(2), 61–65. https://doi.org/10.1007/s12018-014-9159-4.

Bookstein, F. L. (1997). *Morphometric tools for landmark data: Geometry and biology*. Cambridge: Cambridge University Press.

Bourke, J., Wroe, S., Moreno, K., McHenry, C., & Clausen, P. (2008). Effects of gape and tooth position on bite force and skull stress in the dingo (Canis lupus dingo) using a 3-dimensional finite element approach. *PLoS ONE, 3*(5), e2200. https://doi.org/10.1371/journal.pone.0002200.

Bouvier, M., & Hylander, W. L. (1981). Effect of bone strain on cortical bone structure in macaques (Macaca mulatta). *Journal of Morphology, 167*(1), 1–12. https://doi.org/10.1002/jmor.1051670102.

Bouvier, M., & Hylander, W. L. (1984). The effect of dietary consistency on gross and histologic morphology in the craniofacial region of young rats. *American Journal of Anatomy, 170*(1), 117–126. https://doi.org/10.1002/aja.1001700109.

Boyko, A. R., Quignon, P., Li, L., Schoenebeck, J. J., Degenhardt, J. D., Lohmueller, K. E., et al. (2010). A simple genetic architecture underlies morphological variation in dogs. *PLoS Biology, 8*(8), e1000451. https://doi.org/10.1371/journal.pbio.1000451.

Brotto, M., & Bonewald, L. (2015). Bone and muscle: Interactions beyond mechanical. *Bone, 80*, 109–114. https://doi.org/10.1016/j.bone.2015.02.010.

Budras, K.-D. (Ed.). (2007). *Anatomy of the dog* (5th rev ed.). Hannover: Schlüter.

Cheverud, J. M. (1982). Phenotypic, genetic, and environmental morphological integration in the cranium. *Evolution, 36*(3), 499–516. https://doi.org/10.1111/j.1558-5646.1982.tb05070.x.

Christiansen, P., & Adolfssen, J. S. (2005). Bite forces, canine strength and skull allometry in carnivores (Mammalia, Carnivora). *Journal of Zoology, 266*(2), 133–151. https://doi.org/10.1017/S0952836905006643.

Cornette, R., Baylac, M., Souter, T., & Herrel, A. (2013). Does shape co-variation between the skull and the mandible have functional consequences? A 3D approach for a 3D problem. *Journal of Anatomy, 223*(4), 329–336. https://doi.org/10.1111/joa.12086.

Cornette, R., Tresset, A., & Herrel, A. (2015a). The shrew tamed by Wolff's law: Do functional constraints shape the skull through muscle and bone covariation? *Journal of Morphology, 276*(3), 301–309. https://doi.org/10.1002/jmor.20339.

Cornette, R., Tresset, A., Houssin, C., Pascal, M., & Herrel, A. (2015b). Does bite force provide a competitive advantage in shrews? The case of the greater white-toothed shrew. *Biological Journal of the Linnean Society, 114*(4), 795–807. https://doi.org/10.1111/bij.12423.

Cox, P. G., Rinderknecht, A., & Blanco, R. E. (2015). Predicting bite force and cranial biomechanics in the largest fossil rodent using finite element analysis. *Journal of Anatomy, 226*(3), 215–223. https://doi.org/10.1111/joa.12282.

Crompton, A. W. (1963). The evolution of the mammalian jaw. *Evolution, 17*(4), 431–439. https://doi.org/10.2307/2407093.

Currey, J. D. (2002). *Bones: Structure and mechanics*. Princeton: Princeton University Press.

Currey, J. D. (2003). How well are bones designed to resist fracture? *Journal of Bone and Mineral Research, 18*(4), 591–598. https://doi.org/10.1359/jbmr.2003.18.4.591.

Curth, S. (2018). Modularity and Integration in the Skull of Canis lupus (Linnaeus 1758): A Geometric Morphometrics Study on Domestic Dogs and Wolves, p. 78.

Curth, S., Fischer, M. S., & Kupczik, K. (2017). Can skull form predict the shape of the temporomandibular joint? A study using geometric morphometrics on the skulls of wolves and domestic dogs. *Annals of Anatomy - Anatomischer Anzeiger, 214*, 53–62. https://doi.org/10.1016/j.aanat.2017.08.003.

Daegling, D. J., & Hotzman, J. L. (2003). Functional significance of cortical bone distribution in anthropoid mandibles: An in vitro assessment of bone strain under combined loads. *American Journal of Physical Anthropology, 122*(1), 38–50. https://doi.org/10.1002/ajpa.10225.

Drake, A. G., Coquerelle, M., & Colombeau, G. (2015). 3D morphometric analysis of fossil canid skulls contradicts the suggested domestication of dogs during the late Paleolithic. *Scientific Reports, 5*, 82–99. https://doi.org/10.1038/srep08299.

Drake, A. G., Coquerelle, M., Kosintsev, P. A., Bachura, O. P., Sablin, M., Gusev, A. V., et al. (2017). Three-dimensional geometric morphometric analysis of fossil canid mandibles and skulls. *Scientific Reports, 7*(1), 9508. https://doi.org/10.1038/s41598-017-10232-1.

Drake, A. G., & Klingenberg, C. P. (2008). The pace of morphological change: Historical transformation of skull shape in St Bernard dogs. *Proceedings of the Royal Society, 275*(1630), 71–76. https://doi.org/10.1098/rspb.2007.1169.

Drake, A. G., & Klingenberg, C. P. (2010). Large-scale diversification of skull shape in domestic dogs: Disparity and modularity. *The American Naturalist, 175*(3), 289–301. https://doi.org/10.1086/650372.

Druzinsky, R. E., Doherty, A. H., & De Vree, F. L. (2011). Mammalian masticatory muscles: Homology, nomenclature, and diversification. *Integrative and Comparative Biology, 51*(2), 224–234. https://doi.org/10.1093/icb/icr067.

Dryden, I. L., & Mardia, K. V. (2016). *Statistical shape analysis: With applications in R*. Hoboken: Wiley. https://doi.org/10.1002/9781119072492.

Dugatkin, L. A. (2018). The silver fox domestication experiment. *Evolution: Education and Outreach, 11*(1), 16. https://doi.org/10.1186/s12052-018-0090-x.

Ellis, J. L., Thomason, J. J., Kebreab, E., & France, J. (2008). Calibration of estimated biting forces in domestic canids: Comparison of post-mortem and in vivo measurements. *Journal of Anatomy, 212*(6), 769–780. https://doi.org/10.1111/j.1469-7580.2008.00911.x.

Ellis, J. L., Thomason, J., Kebreab, E., Zubair, K., & France, J. (2009). Cranial dimensions and forces of biting in the domestic dog. *Journal of Anatomy, 214*(3), 362–373. https://doi.org/10.1111/j.1469-7580.2008.01042.x.

Endo, H., Taru, H., Nakamura, K., Koie, H., Yamaya, Y., & Kimura, J. (1999). MRI examination of the masticatory muscles in the gray wolf (Canis lupus), with special reference to the M. temporalis. *Journal of Veterinary Medical Science, 61*(6), 581–586. https://doi.org/10.1292/jvms.61.581.

Evans, H. E., & DeLahunta, A. (2010). *Guide to the dissection of the dog* (7th ed.). St. Louis, MO: Saunders/Elsevier.

Ewer, R. F. (1998). *The carnivores*. Ithaca: Cornell University Press.

Fabre, A.-C., Perry, J. M. G., Hartstone-Rose, A., Lowie, A., Boens, A., & Dumont, M. (2018). Do muscles constrain skull shape evolution in strepsirrhines? *The Anatomical Record, 301*(2), 291–310. https://doi.org/10.1002/ar.23712.

Fau, M., Cornette, R., & Houssaye, A. (2016). Photogrammetry for 3D digitizing bones of mounted skeletons: Potential and limits. *Comptes Rendus Palevol, 15*(8), 968–977. https://doi.org/10.1016/j.crpv.2016.08.003.

Flahive, M. A. (2015). *Evaluating Muscle Fiber Architecture*. Master's thesis, University of South Carolina. https://scholarcommons.sc.edu/etd/3632.

Fondon, J. W., & Garner, H. R. (2004). Molecular origins of rapid and continuous morphological evolution. *Proceedings of the National Academy of Sciences, 101*(52), 18058. https://doi.org/10.1073/pnas.0408118101.

Frost, H. M. (2001). From Wolff's law to the Utah paradigm: Insights about bone physiology and its clinical applications. *The Anatomical Record, 262*(4), 398–419. https://doi.org/10.1002/ar.1049.

Frost, H. M. (2003). Bone's mechanostat: A 2003 update. *The Anatomical Record Part A, 275*(2), 1081–1101. https://doi.org/10.1002/ar.a.10119.

Frost, H. M., & Schönau, E. (2000). The" muscle-bone unit" in children and adolescents: A 2000 overview. *Journal of Pediatric Endocrinology and Metabolism, 13*(6), 571–590. https://doi.org/10.1515/JPEM.2000.13.6.571.

Gans, C., & Bock, W. J. (1965). The functional significance of muscle architecture—A theoretical analysis. *Ergebnisse Der Anatomie Und Entwicklungsgeschichte, 38*, 115–142.

Grant, P. R., & Grant, B. R. (2006). Evolution of character displacement in Darwin's finches. *Science (New York, N.Y.), 313*(5784), 224–226. https://doi.org/10.1126/science.1128374.

Grünheid, T., Langenbach, G. E. J., Korfage, J. A. M., Zentner, A., & van Eijden, T. M. G. J. (2009). The adaptive response of jaw muscles to varying functional demands. *European Journal of Orthodontics, 31*(6), 596–612. https://doi.org/10.1093/ejo/cjp093.

Gunz, P., Mitteroecker, P., & Bookstein, F. L. (2005). Semilandmarks in three dimensions. In D. E. Slice (Ed.), *Modern morphometrics in physical anthropology* (pp. 73–98). Boston, MA: Springer.

Hamrick, M. W., McNeil, P. L., & Patterson, S. L. (2010). Role of muscle-derived growth factors in bone formation. *Journal of Musculoskeletal & Neuronal Interactions, 10*(1), 64–70.

Hannam, A. G., & Wood, W. W. (1989). Relationships between the size and spatial morphology of human masseter and medial pterygoid muscles, the craniofacial skeleton, and jaw biomechanics. *American Journal of Physical Anthropology, 80*(4), 429–445. https://doi.org/10.1002/ajpa.1330800404.

Hanot, P., Herrel, A., Guintard, C., & Cornette, R. (2017). Morphological integration in the appendicular skeleton of two domestic taxa: The horse and donkey. *Proceedings of the Royal Society B, 284*(1864), 20171241. https://doi.org/10.1098/rspb.2017.1241.

Hanot, P., Herrel, A., Guintard, C., & Cornette, R. (2018). The impact of artificial selection on morphological integration in the appendicular skeleton of domestic horses. *Journal of Anatomy, 232*(4), 657–673. https://doi.org/10.1111/joa.12772.

Hartstone-Rose, A., Perry, J. M. G., & Morrow, C. J. (2012). Bite force estimation and the fiber architecture of felid masticatory muscles. *The Anatomical Record, 295*(8), 1336–1351. https://doi.org/10.1002/ar.22518.

Haxton, H. A. (1944). Absolute muscle force in the ankle flexors of man. *The Journal of Physiology, 103*(3), 267–273.

He, T., & Kiliaridis, S. (2003). Effects of masticatory muscle function on craniofacial morphology in growing ferrets (Mustela putorius furo). *European Journal of Oral Sciences, 111*(6), 510–517. https://doi.org/10.1111/j.0909-8836.2003.00080.x.

Hendry, A. P., & Kinnison, M. T. (1999). Perspective: The pace of modern life: Measuring rates of contemporary microevolution. *Evolution, 53*(6), 1637–1653. https://doi.org/10.2307/2640428.

Herring, S. W. (2007). Masticatory muscles and the skull: A comparative perspective. *Archives of Oral Biology, 52*(4), 296–299. https://doi.org/10.1016/j.archoralbio.2006.09.010.

Herring, S. W., Rafferty, K. L., Liu, Z. J., & Marshall, C. D. (2001). Jaw muscles and the skull in mammals: The biomechanics of mastication. *Comparative Biochemistry and Physiology Part A, 131*(1), 207–219. https://doi.org/10.1016/S1095-6433(01)00472-X.

Hoppe, F., & Svalastoga, E. (1980). Temporomandibular dysplasia in American Cocker Spaniels. *Journal of Small Animal Practice, 21*(12), 675–678. https://doi.org/10.1111/j.1748-5827.1980.tb05960.x.

Huey, R. B., Gilchrist, G. W., Carlson, M. L., Berrigan, D., & Serra, L. (2000). Rapid evolution of a geographic cline in size in an introduced fly. *Science, 287*(5451), 308. https://doi.org/10.1126/science.287.5451.308.

Hung, M.-L., Chou, C., Chen, C.-H., & Own, Z.-Y. (2010). Learner readiness for online learning: Scale development and student perceptions. *Computers & Education, 55*(3), 1080–1090. https://doi.org/10.1016/j.compedu.2010.05.004.

Hylander, W. L., Johnson, K. R., & Crompton, A. (1992). Muscle force recruitment and biomechanical modeling: An analysis of masseter muscle function during mastication in Macaca fascicularis. *American Journal of Physical Anthropology, 88*(3), 365–387. https://doi.org/10.1002/ajpa.1330880309.

Hylander, W. L., Ravosa, M. J., Ross, C. F., & Johnson, K. R. (1998). Mandibular corpus strain in primates: Further evidence for a functional link between symphyseal fusion and jaw-adductor muscle force. *American Journal of Physical Anthropology, 107*(3), 257–271. https://doi.org/10.1002/(SICI)1096-8644(199811)107:3%3c257:AID-AJPA3%3e3.0.CO;2-6.

Iinuma, M., Yoshida, S., & Funakoshi, M. (1991). Development of masticatory muscles and oral behavior from suckling to chewing in dogs. *Comparative Biochemistry and Physiology A, 100*(4), 789–794. https://doi.org/10.1016/0300-9629(91)90293-I.

Ionova-Martin, S. S., Wade, J. M., Tang, S., Shahnazari, M., Ager, J. W., Lane, N. E., et al. (2011). Changes in cortical bone response to high-fat diet from adolescence to adulthood in mice. *Osteoporosis International, 22*(8), 2283–2293. https://doi.org/10.1007/s00198-010-1432-x.

Johnson, K. A. (1979). Temporomandibular joint dysplasia in an Irish Setter. *Journal of Small Animal Practice, 20*(4), 209–218. https://doi.org/10.1111/j.1748-5827.1979.tb06708.x.

Johnston, R. F., & Selander, R. K. (1964). House sparrows: Rapid evolution of races in North America. *Science, 144*(3618), 548–550. https://doi.org/10.1126/science.144.3618.548.

Kaji, H. (2014). Interaction between muscle and bone. *Journal of Bone Metabolism, 21*(1), 29–40. https://doi.org/10.11005/jbm.2014.21.1.29.

Karasik, D., & Kiel, D. P. (2008). Genetics of the musculoskeletal system: A pleiotropic approach. *Journal of Bone and Mineral Research, 23*(6), 788–802. https://doi.org/10.1359/jbmr.080218.

Karasik, D., & Kiel, D. P. (2010). Evidence for pleiotropic factors in genetics of the musculoskeletal system. *Bone, 46*(5), 1226–1237. https://doi.org/10.1016/j.bone.2010.01.382.

Kim, S. E., Arzi, B., Garcia, T. C., & Verstraete, F. J. M. (2018). Bite forces and their measurement in dogs and cats. *Frontiers in Veterinary Science*. https://doi.org/10.3389/fvets.2018.00076.

Klingenberg, C. P. (2010). Evolution and development of shape: Integrating quantitative approaches. *Nature Reviews Genetics, 11*(9), 623–635. https://doi.org/10.1038/nrg2829.

Klingenberg, C. P. (2014). Studying morphological integration and modularity at multiple levels: Concepts and analysis. *Philosophical Transactions of the Royal Society B, 369*(1649), 20130249. https://doi.org/10.1098/rstb.2013.0249.

Klingenberg, C. P., Barluenga, M., & Meyer, A. (2002). Shape analysis of symmetric structures: Quantifying variation among individuals and asymmetry. *Evolution, 56*(10), 1909–1920. https://doi.org/10.1111/j.0014-3820.2002.tb00117.x.

Koch, D. A., Arnold, S., Hubler, M., & Montavon, P. M. (2003). Brachycephalic syndrome in dogs. *VetLearn.com, 25*(1), 48–55.

Kupczik, K., Dobson, C., Fagan, M., Crompton, R., Oxnard, C., & O'Higgins, P. (2007). Assessing mechanical function of the zygomatic region in macaques: Validation and sensitivity testing of finite element models. *Journal of Anatomy, 210*(1), 41–53. https://doi.org/10.1111/j.1469-7580.2006.00662.x.

Lieberman, D. E., Krovitz, G. E., Yates, F. W., Devlin, M., & Claire, M. S. (2004). Effects of food processing on masticatory strain and craniofacial growth in a retrognathic face. *Journal of Human Evolution, 46*(6), 655–677. https://doi.org/10.1016/j.jhevol.2004.03.005.

Liebman, F. M., & Kussick, L. (1965). An electromyographic analysis of masticatory muscle imbalance with relation to skeletal growth

in dogs. *Journal of Dental Research, 44*(4), 768–774. https://doi.org/10.1177/00220345650440042401.

Lindner, D., Marretta, S., Pijanowski, G., Johnson, A., & Smith, C. (1995). Measurement of bite force in dogs: A pilot study. *Journal of Veterinary Dentistry, 12*(2), 49–52.

Machado, F. A., Zahn, T. M. G., & Marroig, G. (2018). Evolution of morphological integration in the skull of Carnivora (Mammalia): Changes in Canidae lead to increased evolutionary potential of facial traits. *Evolution, 72*(7), 1399–1419. https://doi.org/10.1111/evo.13495.

Marchant, T. W., Johnson, E. J., McTeir, L., Johnson, C. I., Gow, A., Liuti, T., et al. (2017). Canine brachycephaly is associated with a retrotransposon-mediated missplicing of SMOC2. *Current Biology, 27*(11), 1573–1584.e6. https://doi.org/10.1016/j.cub.2017.04.057.

Mavropoulos, A., Kiliaridis, S., Bresin, A., & Ammann, P. (2004). Effect of different masticatory functional and mechanical demands on the structural adaptation of the mandibular alveolar bone in young growing rats. *Bone, 35*(1), 191–197. https://doi.org/10.1016/j.bone.2004.03.020.

Meloro, C., Raia, P., Carotenuto, F., & Cobb, S. N. (2011). Phylogenetic signal, function and integration in the subunits of the carnivoran mandible. *Evolutionary Biology, 38*(4), 465–475. https://doi.org/10.1007/s11692-011-9135-6.

Méndez, J. V., & Keys, A. (1960). Density and composition of mammalian muscle. *Metabolism-Clinical and Experimental, 9*, 184–188.

Miller, M. E., Christensen, G. C., & Evans, H. E. (1965). Anatomy of the dog. *Academic Medicine, 40*(4), 400.

Mitteroecker, P., Gunz, P., Bernhard, M., Schaefer, K., & Bookstein, F. L. (2004). Comparison of cranial ontogenetic trajectories among great apes and humans. *Journal of Human Evolution, 46*(6), 679–698. https://doi.org/10.1016/j.jhevol.2004.03.006.

Mosher, D. S., Quignon, P., Bustamante, C. D., Sutter, N. B., Mellersh, C. S., Parker, H. G., et al. (2007). A mutation in the myostatin gene increases muscle mass and enhances racing performance in heterozygote dogs. *PLoS Genetics, 3*(5), e79–e79. https://doi.org/10.1371/journal.pgen.0030079.

Noble, H. W. (1973). Comparative functional anatomy of temporomandibular joint. *Oral Sciences Reviews, 2*, 3–28.

Olson, E. C., & Miller, R. L. (1951). A mathematical model applied to a study of the evolution of species. *Evolution, 5*(4), 325–338. https://doi.org/10.2307/2405677.

Olson, E. C., & Miller, R. L. (1958). *Morphological integration*. Chicago: University of Chicago Press.

Olson, E. C., & Miller, R. L. (1999). *Morphological Integration*. Chicago: University of Chicago Press.

Parker, H. G., Kim, L. V., Sutter, N. B., Carlson, S., Lorentzen, T. D., Malek, T. B., et al. (2004). Genetic structure of the purebred domestic dog. *Science, 304*(5674), 1160–1164.

Penrose, F., Cox, P., Kemp, G., & Jeffery, N. (under review). Functional morphology of the jaw adductor muscles in the Canidae. *The Anatomical Record*.

Penrose, F., Kemp, G. J., & Jeffery, N. (2016). Scaling and accommodation of jaw adductor muscles in canidae. *The Anatomical Record, 299*(7), 951–966. https://doi.org/10.1002/ar.23355.

Raadsheer, M. C., van Eijden, T. M. G. J., van Ginkel, F. C., & Prahl-Andersen, B. (1999). Contribution of jaw muscle size and craniofacial morphology to human bite force magnitude. *Journal of Dental Research, 78*(1), 31–42. https://doi.org/10.1177/00220345990780010301.

Ravosa, M. J., Kunwar, R., Stock, S. R., & Stack, M. S. (2007). Pushing the limit: Masticatory stress and adaptive plasticity in mammalian craniomandibular joints. *Journal of Experimental Biology, 210*(4), 628–641. https://doi.org/10.1242/jeb.02683.

Ravosa, M. J., Menegaz, R. A., Scott, J. E., Daegling, D. J., & McAbee, K. R. (2016). Limitations of a morphological criterion of adaptive inference in the fossil record. *Biological Reviews of the Cambridge Philosophical Society, 91*(4), 883–898. https://doi.org/10.1111/brv.12199.

Ravosa, M. J., Scott, J. E., McAbee, K. R., Veit, A. J., & Fling, A. L. (2015). Chewed out: An experimental link between food material properties and repetitive loading of the masticatory apparatus in mammals. *PeerJ*. https://doi.org/10.7717/peerj.1345.

Rayfield, E. J. (2007). Finite element analysis and understanding the biomechanics and evolution of living and fossil organisms. *Annual Review of Earth and Planetary Sciences, 35*, 541–576. https://doi.org/10.1146/annurev.earth.35.031306.140104.

Reznick, D. N., Shaw, F. H., Rodd, F. H., & Shaw, R. G. (1997). Evaluation of the rate of evolution in natural populations of Guppies (Poecilia reticulata). *Science (New York, N.Y.), 275*(5308), 1934–1937. https://doi.org/10.1126/science.275.5308.1934.

Robins, G., & Grandage, J. (1977). Temporomandibular joint dysplasia and open-mouth jaw locking in the dog. *Journal of the American Veterinary Medical Association, 171*(10), 1072–1076.

Rohlf, F. J., & Corti, M. (2000). Use of two-block partial least-squares to study covariation in shape. *Systematic Biology, 49*(4), 740–753. https://doi.org/10.1080/106351500750049806.

Ross, C. F., & Metzger, K. A. (2004). Bone strain gradients and optimization in vertebrate skulls. *Annals of Anatomy - Anatomischer Anzeiger, 186*(5), 387–396. https://doi.org/10.1016/S0940-9602(04)80070-0.

Ross, C. F., Patel, B. A., Slice, D. E., Strait, D. S., Dechow, P. C., Richmond, B. G., et al. (2005). Modeling masticatory muscle force in finite element analysis: Sensitivity analysis using principal coordinates analysis. *The Anatomical Record Part A, 283*(2), 288–299. https://doi.org/10.1002/ar.a.20170.

Schlager, S. (2012). *Sliding semi-landmarks on symmetric structures in three dimensions*. Paper presented at the the 81st Annual Meeting of the American Association of Physical Anthropologists, Portland, OR, Anthropology, University of Freiburg, Germany.

Schlager, S. (2013). Soft-tissue reconstruction of the human nose : Population differences and sexual dimorphism.

Schoenau, E. (2005). From mechanostat theory to development of the 'Functional Muscle-Bone-Unit'. *Journal of Musculoskeletal and Neuronal Interactions, 3*, 232–238.

Schoenebeck, J. J., Hutchinson, S. A., Byers, A., Beale, H. C., Carrington, B., Faden, D. L., et al. (2012). Variation of BMP3 contributes to dog breed skull diversity. *PLoS Genetics, 8*(8), e1002849. https://doi.org/10.1371/journal.pgen.1002849.

Schumacher, G.-H. (1961). *Funktionelle Morphologie der Kaumuskulatur*. Jena: Fischer.

Scott, J. E., McAbee, K. R., Eastman, M. M., & Ravosa, M. J. (2014a). Teaching an old jaw new tricks: Diet-induced plasticity in a model organism from weaning to adulthood. *Journal of Experimental Biology, 217*(22), 4099–4107. https://doi.org/10.1242/jeb.111708.

Scott, J. E., McAbee, K. R., Eastman, M. M., & Ravosa, M. J. (2014b). Experimental perspective on fallback foods and dietary adaptations in early hominins. *Biology Letters, 10*(1), 20130789. https://doi.org/10.1098/rsbl.2013.0789.

Selba, M. C., Oechtering, G. U., Gan Heng, H., & DeLeon, V. B. (2019). The impact of selection for facial reduction in dogs: Geometric morphometric analysis of canine cranial shape. *The Anatomical Record, 303*(2), 330–346. https://doi.org/10.1002/ar.24184.

Sharir, A., Stern, T., Rot, C., Shahar, R., & Zelzer, E. (2011). Muscle force regulates bone shaping for optimal load-bearing capacity during embryogenesis. *Development, 138*(15), 3247–3259. https://doi.org/10.1242/dev.063768.

Slizewski, A., Schönau, E., Shaw, C., & Harvati, K. (2013). Muscle area estimation from cortical bone. *The Anatomical Record, 296*(11), 1695–1707. https://doi.org/10.1002/ar.22788.

Ström, D., Holm, S., Clemensson, E., Haraldson, T., & Carlsson, G. E. (1988). Gross anatomy of the craniomandibular joint and masticatory muscles of the dog. *Archives of Oral Biology, 33*(8), 597–604. https://doi.org/10.1016/0003-9969(88)90135-5.

Swiderski, D. L., & Zelditch, M. L. (2013). The complex ontogenetic trajectory of mandibular shape in a laboratory mouse. *Journal of Anatomy, 223*(6), 568–580. https://doi.org/10.1111/joa.12118.

Taylor, A. B., & Vinyard, C. J. (2013). The relationships among jaw-muscle fiber architecture, jaw morphology, and feeding behavior in extant apes and modern humans. *American Journal of Physical Anthropology, 151*(1), 120–134. https://doi.org/10.1002/ajpa.22260.

Thomas, R. E. (1979). Temporo-mandibular joint dysplasia and open-mouth jaw locking in a Bassett Hound: A case report. *The Journal of Small Animal Practice, 20*(11), 697–701. https://doi.org/10.1111/j.1748-5827.1979.tb06684.x.

Thomason, J. J. (1991). Cranial strength in relation to estimated biting forces in some mammals. *Canadian Journal of Zoology, 69*(9), 2326–2333. https://doi.org/10.1139/z91-327.

Tomo, S., Hirakawa, T., Nakajima, K., Tomo, I., & Kobayashi, S. (1993). Morphological classification of the masticatory muscles in dogs based on their innervation. *Annals of Anatomy - Anatomischer Anzeiger, 175*(4), 373–380. https://doi.org/10.1016/S0940-9602(11)80047-6.

Trut, L. (1999). Early Canid Domestication: The Farm-Fox Experiment: Foxes bred for tamability in a 40-year experiment exhibit remarkable transformations that suggest an interplay between behavioral genetics and development. *American Scientist, 87*(2), 160–169.

Trut, L., Oskina, I., & Kharlamova, A. (2009). Animal evolution during domestication: The domesticated fox as a model. *BioEssays, 31*(3), 349–360. https://doi.org/10.1002/bies.200800070.

Turnbull, W. D. (1970). Mammalian masticatory apparatus. *Geology, 18*(2), 149–356.

Van Valen, L. (1965). The study of morphological integration. *Evolution, 19*(3), 347–349. https://doi.org/10.1111/j.1558-5646.1965.tb01725.x.

Ward, K. A., Caulton, J. M., Adams, J., & Mughal, M. Z. (2006). Perspective: Cerebral palsy as a model of bone development in the absence of postnatal mechanical factors. *Journal of Musculoskeletal & Neuronal Interactions, 6*(2), 154–159.

Watt, D. G., & Williams, C. H. (1951). The effects of the physical consistency of food on the growth and development of the mandible and the maxilla of the rat. *American Journal of Orthodontics, 37*(12), 895–928.

Weijs, W. A., & Hillen, B. (1986). Correlations between the cross-sectional area of the jaw muscles and craniofacial size and shape. *American Journal of Physical Anthropology, 70*(4), 423–431. https://doi.org/10.1002/ajpa.1330700403.

Weiner, S., & Wagner, H. D. (1998). The material bone: Structure-mechanical function relations. *Annual Review of Materials Science, 28*(1), 271–298. https://doi.org/10.1146/annurev.matsci.28.1.271.

Wiley, D. F., Amenta, N., Alcantara, D. A., Ghosh, D., Kil, Y. J., Delson, E., et al. (2005). *Evolutionary morphing*. Presented at the VIS 05. IEEE Visualization. (pp. 431–438). https://doi.org/10.1109/VISUAL.2005.1532826.

Wolff, J. (1986). *The law of bone remodelling*. Berlin: Springer.

2. The relationships between cranial shape, mandible shape and jaw muscle architecture in dogs

Article 2 –
Interrelations between the cranium, the mandible and muscle architecture in modern domestic dogs

Colline Brassard, Marilaine Merlin, Elodie Monchâtre-Leroy, Claude Guintard, Jacques Barrat, Cécile Callou, Raphaël Cornette, Anthony Herrel

Published in *Evolutionary Biology*, accepted: 06 September 2020

Evolutionary Biology
https://doi.org/10.1007/s11692-020-09515-9

RESEARCH ARTICLE

Interrelations Between the Cranium, the Mandible and Muscle Architecture in Modern Domestic Dogs

Colline Brassard[1,2] · Marilaine Merlin[1] · Claude Guintard[3,4] · Elodie Monchâtre-Leroy[5] · Jacques Barrat[5] · Cécile Callou[2] · Raphaël Cornette[6] · Anthony Herrel[1]

Received: 17 March 2020 / Accepted: 7 September 2020

Abstract

Many studies have attested to the consequences of the recent and intense artificial selection on the morphological variability of the cranium and mandible in domestic animals. However, the functional relations of the cranium with other constituents of the masticatory apparatus (the mandibles and the adductor muscles) have rarely been explored. Previous work has demonstrated strong relationships between the overall shape of the mandible and muscle data, however, drastic artificial selection in dogs has led to frequent malocclusions, suggesting a possible decoupling between the cranium and the mandible. Moreover, the more complex role of the cranium suggests that it is likely less impacted by, and correlated with, the architecture of the jaw muscles than the mandible. We explored the covariations between cranial and mandibular shape and between cranial shape and the masticatory muscle architecture. Shape analyses were conducted on 58 dogs from various breeds and we used muscle data previously obtained from the dissection of 48 of these dogs. The shape of the cranium was quantified using 3D geometric morphometric approaches. Principal component analyses (PCA) and two-block partial least square analyses (2B-PLS) were used to quantify the variations in cranial shape and the covariations with mandible shape and muscle architecture, respectively. Interestingly, our results reveal strong covariations between cranial shape and mandibular shape and between cranial shape and masticatory muscles mass or physiological cross-sectional area, irrespective of whether size is taken into account or not. We conclude that the drastic artificial selection in domestic dogs has not tainted the integrity of the jaw system, which reinforces previous assumptions hypothesising that phenotypic variability in dogs may be limited by developmental factors.

Keywords Dog · Skull · Masticatory system · Jaw muscle architecture · Domestication · Geometric morphometrics

Introduction

Many studies have focused on the modularity and integration of the skull in carnivores and have attested to the consequences of domestication on the morphological variability

Colline Brassard and Marilaine Merlin are co-first authors.

Electronic supplementary material The online version of this article (https://doi.org/10.1007/s11692-020-09515-9) contains supplementary material, which is available to authorized users.

✉ Colline Brassard
colline.brassard@mnhn.fr

[1] UMR 7179 Mécanismes Adaptatifs et Evolution (CNRS, MNHN), Muséum national d'Histoire naturelle, 55 rue Buffon, Paris, France

[2] Archéozoologie, archéobotanique : sociétés, pratiques et environnements (AASPE), Muséum national d'Histoire naturelle, CNRS, 57 rue Cuvier, CP5575005 Paris, France

[3] Laboratoire d'Anatomie comparée, Ecole Nationale Vétérinaire, de l'Agroalimentaire et de l'Alimentation, Nantes Atlantique – ONIRIS, Nantes Cedex 03, France

[4] GEROM, UPRES EA 4658, LABCOM ANR NEXTBONE, Faculté de santé de l'Université d'Angers, Angers, France

[5] ANSES, Laboratoire de la rage et de la faune sauvage, Station expérimentale d'Atton, Malzéville, France

[6] UMR 7205, Institut de Systématique, Evolution, Biodiversité (CNRS, MNHN, UPMC, EPHE), Muséum national d'Histoire naturelle, Paris, France

Published online: 18 September 2020

of the cranium and mandible (Drake and Klingenberg 2008, 2010; Curth et al. 2017; Curth 2018; Machado et al. 2018; Selba et al. 2019). Over the last century, drastic artificial selection has led to huge variability in dog morphotypes (Drake and Klingenberg 2010). Domestic dogs are thus a good model to study the functional consequences of skull shape variation in canids. The great morphological diversity in the cranium of dogs raises questions, however, about the interplay between the jaw muscles and the bones of the head given that bones are known to model and remodel in relation to external forces like muscle forces (Frost 2001, 2003; Schoenau 2005; Sharir et al. 2011; Brotto and Bonewald 2015). Yet, to date our understanding of the interrelationships between bones, muscles, and bite force in dogs remains incomplete (but see Ellis et al. 2008, 2009; Kim et al. 2018; Brassard et al. 2020a, b). Historically, selective breeding was based on the requirement for specific morphological traits or performance without regard for genetic health and integrity. This intensive selection leads to frequently distorted dentitions, particularly in brachycephalic breeds (Bell 1965). The cranium is often too short (maxillary brachygnathism, e.g. in the Bulldog) or too long (mandibular brachygnathism, e.g. in the Bull terrier; Milella 2009) to accommodate all the teeth. These frequent malocclusions well illustrate the possible functional decoupling between the cranium and the mandible, and possibly between the jaw and its associated musculature.

Because dogs are no longer submitted to natural selection, one would expect a disruption in the functional integrity of the jaw. Interestingly, previous results have shown that the shape of the mandible strongly covaries with the architecture of the adductor muscles (Brassard et al. 2020a). This suggests that strong functional connections still exist in the head of dogs, despite intense artificial selection. However, whereas the mandible is involved in a single function (chewing) the cranium faces many other functional challenges as it also protects the sensory organs and the brain, for example. Moreover, selection for aesthetics reasons has often focused specifically on morphological traits of the cranium rather than on the mandible. As a consequence, it is possible that the functional links between the mandible and the cranium, and between jaw muscles and cranial shape, may be impacted by this selection. We thus expect the shape of the cranium to covary relatively little with mandible shape and to be less strongly driven by variation in jaw muscle volume or intrinsic muscle strength than the mandible.

The aims of the present study were to (1) explore the variability in cranial shape in a range of dogs of various sizes and morphotypes, (2) to test whether the shape of the cranium covaries with that of the mandible despite frequent malocclusion due to artificial selection, and (3) to test whether the shape of the cranium is related to the architecture of the jaw muscles and whether this covariation is less important than for the mandible. We predict that strong artificial selection will have resulted in a functional decoupling between the cranium and the mandible, resulting in little covariation between the shape of the cranium and that of the mandible, and possibly in a lower integration between the jaw muscle architecture and the shape of the cranium than between muscle architecture and mandible shape.

Materials and Methods

Materials

In this study, we studied the skull of 58 dogs from various breeds (see Table S1 for a complete list of the specimens used in the analyses). The cadavers were collected from a veterinary school (ONIRIS, Nantes, France) and from a wildlife disease study centre (ANSES in Nancy, France). Dogs were unlikely to be pure bred (membership to a standard was not known). Those that were morphologically close (in shape and color) to existing breeds were assigned as such to provide context for further discussions (see Table 1). Additionaly, for visualisation and discussion purposes, dogs were categorised into brachycephalic, mesocephalic or dolichocephalic, based on the cephalic index (CI = skull width/skull length * 100; Roberts et al. 2010). Skull length was measured from the anterior tip at the end of the suture of the nasal bones (landmark 2, Fig. 1) to the most posterior point on the occipital protuberance (landmark 14, Fig. 1). Skull width was measured between the two zygomatic arches (landmark 37 and the symmetric landmark to the sagittal plane, Fig. 1). Dogs with a cephalic index less than 0.70 were considered brachycephalic and dogs with an index less than 0.60 were considered dolichocephalic. The dogs with an index between 0.60 and 0.70 were considered mesocephalic. The boundary between groups was chosen to ensure that the three groups are similar in size, but specimens within the same breed can be classified in two adjacent morphotypes. Additionaly, the specimens were classified into four age groups depending on the degree of closure of the cranial sutures and dental eruption patterns. Group 'A' corresponds to the youngest individuals with permanent teeth still erupting (4–6 months according to Barone 2010), group 'B' to individuals with the sphenobasilar suture still open (< 8–10 months for the dog according to Barone 2010), group 'D' to dogs with a closed interfrontal suture and worn dentures (> 3–4 years), and group 'C' to intermediate adults (from 10 months to 3 years). We chose to keep the youngest individuals in our analyses to increase the morphological variability in the sample, but most of the dogs are adults or old adults. We did not include geriatric dogs in our sample.

Table 1 List of the specimens used in this study

Estimated breeds	Age groups				Morphotype	N		
	Juvenile	Young	Adult	Old		Cranium and mandible	PCSA	Mass
American Staffordshire terrier			1		Brachycephalic	1	1	1
Beagle	1	2	15	3	Mesocephalic	20	10	10
Belgian shepherd—Tervueren				2	1 mesocephalic 1 dolichocephalic			
Border collie			1	1	Dolichocephalic	2	2	2
Boxer				2	Brachycephalic	2	2	2
Bulldog			1	1	Brachycephalic	2	2	2
Bull terrier	1				Mesocephalic	1	1	1
Cane Corso			1		Brachycephalic	1	1	1
Cavalier King Charles Spaniel			1		Brachycephalic	1	1	1
Chihuahua				1	Brachycephalic	1	1	1
Collie				1	Dolichocephalic	1	1	1
Continental Toy Spaniel Papillon			1		Brachycephalic	1	1	1
Dachshund			1		Dolichocephalic	1	1	1
Deerhound				1	Dolichocephalic	1	1	1
Dobermann				1	Dolichocephalic	1	1	1
Fox terrier			1		Mesocephalic	1	1	1
German shepherd				1	Dolichocephalic	1	1	1
Golden retriever			1		Dolichocephalic	1	1	1
Husky			1		Dolichocephalic	1	1	1
Leonberger			1		Dolichocephalic	1	1	1
Mastiff			1	1	Mesocephalic	2	2	2
Pitbull				1	Brachycephalic	1	1	1
Rottweiler			2		Brachycephalic	2	2	2
Shetland sheepdog			1		Dolichocephalic	1	1	1
Non-estimated breed			3	6	2 mesocephalic 5 dolichocephalic 2 brachycephalic	9	9	8
Total	2	2	33	22		58	48	47

N number of specimens, represented by both their mandible and cranium. Note that the number of individuals is different for the study of the covariation between the cranium and mandible shape, and between muscle data and cranial shape. Estimated breeds refer to the assignment of the breed for each dog

Muscle fiber lengths, pennation angles, masses and physiological cross-sectional areas (PCSAs) were quantified for 48 and 47 of these dogs, respectively (Brassard et al. 2020a). Pennation angles and $\log_{10}$-transformed muscle fiber lengths, masses and reduced physiological cross-sectional area (PCSA) were calculated for the digastric (Dig) and the adductor muscles: the M. masseter pars superficialis (MS), the M. masseter pars profunda (MP), the M. zygomaticomandibularis pars anterior (ZMA), the M. zygomaticomandibularis pars posterior (ZMP), the M. temporalis pars suprazygomatica (SZ), the M. temporalis pars superficial (TS), the M. temporalis pars profunda (TP), and the M. pterygoideus (P). Since the M. pterygoideus pars lateralis attaches to the condyle (that is the fulcrum system), it is more an anterior translator than an adductor muscle. However, it is very small (it represents less than 1% of the total muscle volume; Brassard et al. 2020a) and difficult to clearly distinguish from the M. pterygoideus pars medialis. Accordingly, we considered both muscles as a single muscle mass.

Landmarking

Shape analyses were conducted using geometric morphometrics. Landmark locations are provided in Fig. 1 and Table 2. Because the crania were often broken, and because cranial shape is easily described with a relatively small number of landmarks, contrary to the mandible, different methods were used for landmarking the cranium and mandible.

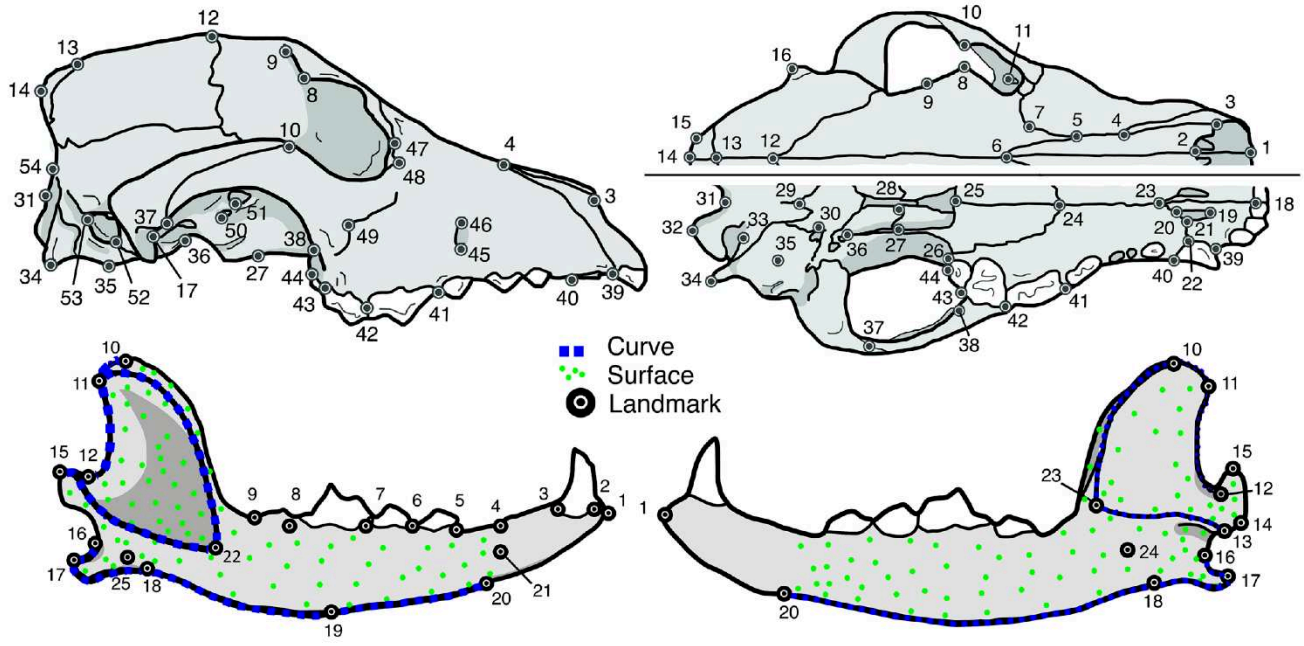

Fig. 1 Landmarks used in this study, illustrated in dorsal, lateral and ventral views of the cranium and mandible of a beagle. Anatomical landmarks are in black, landmarks on curves are in blue and surface landmarks are in green. We refer to Table 2 and Table S2 (Supplementary file 5) for the definitions of the landmarks on the cranium and mandible, respectively

To quantify cranial shape we recorded fifty-four 3D landmarks on one side using a MicroScribe MX (MicroScribe MX R", REVWARE). A mirror function was then applied to obtain the symmetrical landmarks relative to the sagittal plane using the function 'mirrorfill' from the package 'paleomorph'. This resulted in a total of 108 landmarks. For further visualisation of cranial shape, the cranium of a beagle (which shape is close to the mean shape of our sample) was photographed using a Nikon D5500 Camera (24,2 effective megapixels) with a 60 mm lens. One hundred and forty photographs were taken by turning around the dorsal and ventral views of the cranium (Fau et al. 2016). 3D models of the crania were obtained after merging the two sides, using the Agisoft PhotoScan software (© 2014 Agisoft LLC, 27 Gzhatskaya st., St. Petersburg, Russia).

The landmarks on the mandible were taken from a previous study (Brassard et al. 2020a). In brief, we obtained 3D reconstructions of the mandible using photogrammetry. To do so we used the same camera than the one mentioned above. One hundred photographs were taken by turning around the dorsal and ventral views of the mandible. A total of 400 landmarks (including 25 homologous anatomical landmarks, 190 sliding semilandmarks on curves and 185 sliding semilandmarks on the surface) were placed on the mandibles using the software Landmark, version 3.0.0.6 (© IDAV 2002–2005) (Wiley et al. 2005). A sliding semi-landmark procedure (Bookstein 1997; Gunz et al. 2005; Schlager 2012) was performed to obtain homologous landmarks. The 3D model of a beagle's right mandible (for the same reasons as stated above) was used to visualise variation in mandibular shape.

Shape Analyses with Geometric Morphometrics

Shape analyses were conducted using the packages 'Morpho' (version 2.7) and 'geomorph' (version 3.1.2) in R (version 3.6.0; 2019-04-26). All specimen were aligned, scaled and translated using a Generalized Procrustes Analysis (GPA—Rohlf and Slice 1990) using the function 'procSym' (Klingenberg et al. 2002; Gunz et al. 2005; Dryden and Mardia 2016). The theoric shape of the consensus of each GPA (on cranial or mandibular shapes) was obtained by deforming the reference beagle specimen to the mean shape of the GPA, using the function 'tps3d'. In order to perform analyses without size, we also obtained allometry-free shapes using the functions 'CAC' (Mitteroecker et al. 2004), and 'showPC'.

Principal component analyses (PCA) were performed based on the Procrustes coordinates using the function 'procSym'. We also performed a PCA on the allometry-free shapes using 'plotTangentSpace'. Visualisations at the minimum or maximum of the two first principal components were obtained using the functions 'plotTangentSpace', 'tps3d' and 'deformGrid3d'. We computed linear models to explain each PCA component by the size of the individuals. Sample sizes were too small and too different between sexes

Table 2 Definitions of the landmarks placed on the cranium and used in the geometric morphometric analyses, following the N.A.V. nomenclature

Landmark	Definition
1	Most rostral point of *Os incisivum*, between incisors I1 in dorsal view
2	Most rostral point of *Os nasale*, on the midline (*Sutura internasalis*)
3	Most rostral point on *Sutura nasoincisiva*
4	Point at the junction of *Os incisivum*, *Os nasale* and *Maxilla*
5	Point at the junction of *Os nasale*, *Maxilla* and *Os frontale*
6	Most rostral point of *Os temporale* and most caudal point of *Os nasale*, on the midline (*Sutura internasalis*)
7	Most posterior point of the *Maxilla* in dorsal view
8	Most lateral point of the *Processus zygomaticus* of *Os frontale*
9	Most medial point of the curvature corresponding to the *Linea temporalis*, most medial point at the postorbital constriction
10	*Processus frontalis* of *Os zygomaticum*
11	Most rostral point of the curvature of the lower edge of the *Fossa sacci lacrimalis*
12	Bregmatic fontanel, most medial point of the *Sutura coronalis*, on the midline
13	Most medial point on the *Sutura lambdoidea*
14	Inion, posterior end of *Os occipitale*
15	Point at the extreme convex curvature of the *Tuberculum nuchale*
16	Point at the extreme convex curvature of the *Crista supramastoidea*
17	*Fossa mandibularis*, on the *Sutura sphenoparietalis*
18	Central point of the *Sutura interincisiva* in ventral view, just posterior to the two incisors I1
19	Most rostral point of the *Fissura palatina*
20	Most caudal point of the *Fissura palatina*
21	Point on the *Fissura palatina* at the junction between *Os incisivum* and *Maxilla* in ventral view
22	Point between the *Canina* and the incisor I3 at the junction between *Os incisivum* and *Maxilla* in ventral view
23	Most rostral point of *Maxilla* in ventral view, on the midline
24	Most rostral point of the *Sutura palatomaxillaris*, on the midline
25	Most caudal point of *Os palatinum*, on the midline
26	Point near molar M2, on the *Sutura palatomaxillaris*
27	Ventral point on the *Sutura sphenopalatina*
28	Point on vomer, at the junction with *Os presphenoidale* (*Sutura vomerosphenoidalis*)
29	Most caudal point of the *Synchondrosis sphenooccipitalis*, on the midline
30	Most lateral point of the *Synchondrosis sphenooccipitalis*, rostrally to the *Bulla tympanica*
31	Most cranial point of the caudal curve of *Os occipitale* (*Foramen magnum*) in ventral view, on the midline
32	Most caudal point of the caudal curve of *Os occipitale* in ventral view
33	Point on the *Foramen lacerum*
34	*Processus paracondylaris*
35	Ventral tip of the *Bulla tympanica*
36	Most dorsal and caudal point of the curve of the *Foramen alare caudale*
37	Most ventral and posterior point at the junction of the *Pars squamosa* of *Os temporale* and *Os zygomaticum*, on the *Arcus zygomaticus*
38	Most caudal point at the junction between *Maxilla* and *Os zygomaticum*, near M2
39	Most cranial point of the alveolus of the *Canina*
40	Most caudal point of the alveolus of the *Canina*
41	Most cranial point of the alveolus of the upper carnassial P4
42	Point between the alveolus of P4 and M1
43	Point between the alveolus of M1 and M2
44	Most caudal point of *Maxilla* behind M2
45	Most dorsal point of the *Foramen infraorbitale*
46	Most ventral point of the *Foramen infraorbitale*
47	Point at the junction of *Maxilla*, *Os lacrimale* and *Os temporale*

Table 2 (continued)

Landmark	Definition
48	Point at the junction of *Maxilla*, *Os lacrimale* and *Os zygomaticum*
49	Most caudal point of curvature at the junction of *Maxilla* and *Os zygomaticum*
50	Most ventral and caudal point of the *Foramen alare rostrale*
51	Most ventral and caudal point of the *Fissura orbitalis*
52	Most rostral point of *Meatus acusticus externus* in lateral view
53	Most caudal point of *Meatus acusticus externus* in lateral view
54	Opisthion, dorsal and caudal border of the *Foramen magnum*, on the midline

We refer to Table S2 (Supplementary file 5) for the definitions of the landmarks on the mandible

(9 females and 23 males) and age groups (two juvenile and two young dogs only) to test for the effect of these variables (Tables 1, S1).

Relationships Between Cranial, Mandibular Shape and Muscle Data

To investigate the drivers of cranial and mandibular shape we performed non-parametric Procrustes ANOVA/regressions with permutation procedures on the shape coordinates and centroid size (of the cranium or mandible), residual muscle mass and PCSA data using the function 'procD.lm' with 1000 iterations (Goodall 1991; Anderson 2001; Anderson and Braak 2003; Collyer et al. 2015; Adams and Collyer 2016, 2017). We performed multiple and simple regressions (to better describe the amount of variation in shape explained by variation in a single explanatory variable) on the coordinates from the GPA (allometric shape) and on the coordinates of the allometry-free shape. We performed these analyses with the three main adductor complexes in order to increase statistical power: the masseter complex, the temporal complex, and the pterygoid complex. For each complex, fiber lengths were averaged while masses and PCSAs were summed. Data were $\log_{10}$-transformed. We used the 'shape.predictor' function and the 'Avizo 8.1.1.' software to visualize the effect of the variation in the PCSA of the temporal, masseter, and pterygoid muscles on the shape of the cranium and mandible.

Additionally, to test whether certain head-types differed significantly in muscle mass or PCSA for their size, we performed ANOVAs (function 'aov') and post-hoc tests (function 'TukeyHSD') to compare the residual muscle masses and muscle PCSAs for the three main adductor complexes between brachycephalic, mesocephalic and dolichocephalic dogs.

To understand the covariations between the shape of the cranium and that of the mandible and between cranial shape and the muscle data we performed two-block partial least squares analyses (2B-PLS) with the function 'pls2B' (Rohlf and Corti 2000). P-values (attesting to the significance of the covariations) were computed from 1000 permuted blocks. Because the dogs are from mixed breeds, we did not consider phylogeny (Parker et al. 2004) in our analyses. Because variation in the shape of the cranium and mandible and the muscle data is largely driven by size (Wayne 1986; Brassard et al. 2020a), we also quantified the covariation between residual muscle data and/or allometry-free shapes. Residual muscle data were calculated using the function 'lm', considering the $\log_{10}$-transformed centroid size of the cranium as our proxy of size. A total of thirteen 2B-PLS analyses were conducted: cranial shape—mandibular shape, allometry-free cranial shape—allometry-free mandibular shape, cranial shape—muscle mass, cranial shape—residual mass, allometry-free cranial shape—residual mass, cranial shape—PCSA, cranial shape—residual PCSA, allometry-free cranial shape—residual PCSA. Visualisations at the minimum or maximum of the PLS axes were obtained using the functions 'plsCoVar', 'tps3d' and 'deformGrid3D'. To compare PLS coefficients from this study and those from previous work (Brassard et al. 2020a), we calculated Z-scores using the function 'compare.pls'. Juveniles were excluded from the analyses of covariation between cranial and mandibular shape.

Results

We refer to the Supplementary file 6 for detailed results of the statistical analyses. Below we describe the main patterns only.

Variability in Cranial Shape

The first two axes of the PCA on cranial shape (Fig. 2a) represent 63.5% of the total variance (the first six axes explain 80% of the total variance). Linear models show that variation along PC1 is driven by variation in size (adjusted $R^2 = 0.23$, $P < 0.001$). PC2 is mostly related to variation in centroid size (adjusted $R^2 = 0.58$, $P < 0.001$). The first axis of the PCA with cranial shape (Fig. 2a) separates the brachycephalic (with short but wide crania) from the more dolichocephalic dogs

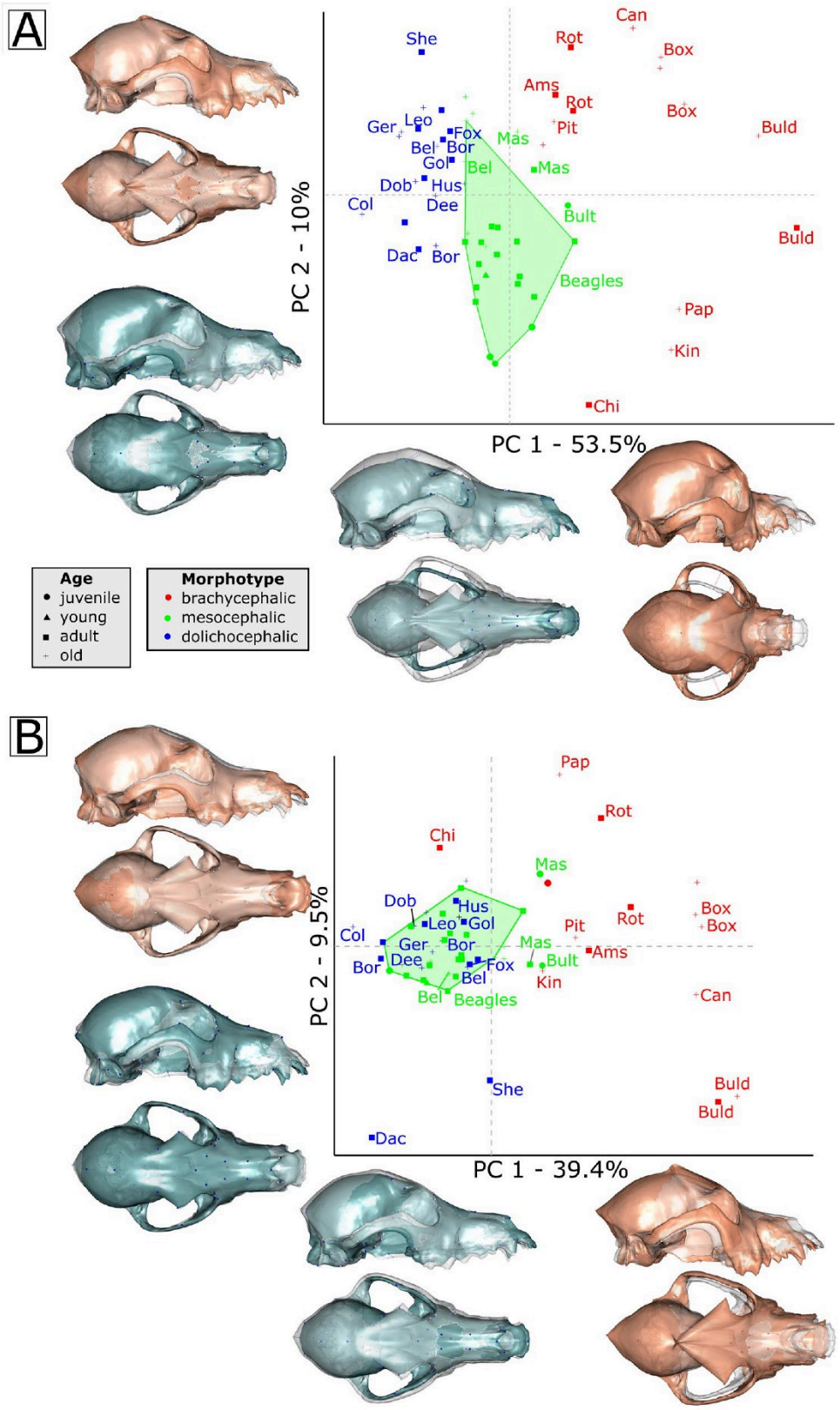

Fig. 2 Principal component analyses performed on cranial shapes (**a**) or allometry-free cranial shapes (**b**). The dorsal and lateral views of the shapes at the minimum of each axis are in blue. Shapes at the maximum of the axes are in red. Ages are indicated by different shapes and morphotypes are indicated by different colors. Beagles are located in the green area. *Ams* American Staffordshire terrier, *Box* Boxer, *Buld* Bulldog, *Bult* Bull terrier, *Chi* Chihuahua, *Can* Cane Corso, *Kin* Cavalier King Charles Spaniel, *Pap* Papillon, *Pit* Pitbull, *Rot* Rottweiler, *Mas* Mastiff, *Fox* Fox terrier, *Bel* Belgian Shepherd, *Bor* Border collie, *Col* Collie, *Dac* Dachshund, *Ger* German Shepherd, *Gol* Golden retriever, *Hus* Husky, *Leo* Leonberg, *She* Shetland sheepdog

(with long and narrow crania). Dogs on the right part of the scatterplot have crania with a very rounded and tall braincase, large zygomatic arches, and a short snout. They correspond mainly to molossoid dogs and to small brachycephalic dogs (Chihuahua, King Charles, and Papillon). Dogs to the left of the scatterplot have narrow crania with a lower braincase, a

Table 3 Results of the simple and multiple regressions performed on cranial shape (N = 47)

	Df	SS	MS	Rsq	F	Z	Pr(> SS)
Multiple regression							
Shape of the cranium (N = 47)							
Centroid size	1	0.10	0.11	**0.21**	21	3.7	0.001
Residual PCSA—temporal	1	0.050	0.050	**0.10**	10	3.3	0.001
Residual PCSA—masseter	1	0.037	0.037	**0.075**	7.6	3.0	0.005
Residual PCSA—pterygoid	1	0.026	0.026	**0.053**	5.3	2.7	0.001
Residual mass—temporal	1	0.034	0.034	**0.067**	6.8	3.7	0.001
Residual mass—masseter	1	0.044	0.044	**0.087**	8.8	4.5	0.001
Residual mass—pterygoid	1	0.011	0.011	**0.021**	2.1	2.4	0.036
Residuals	39	0.19	0.0050	0.39			
Allometry-free shape of the cranium (N = 47)							
Residual PCSA—temporal	1	0.028	0.028	**0.10**	6.6	4.2	0.001
Residual PCSA—masseter	1	0.018	0.018	**0.064**	4.2	3.3	0.005
Residual PCSA—pterygoid	1	0.016	0.016	**0.056**	3.7	3.2	0.002
Residual mass—temporal	1	0.020	0.020	**0.073**	4.8	3.9	0.001
Residual mass—masseter	1	0.026	0.026	**0.091**	6.0	4.6	0.001
Residual mass—pterygoid	1	0.0068	0.0068	0.024	1.6	1.5	0.076
Residuals	39	0.17	0.0042	0.59			
Shape of the mandible (N = 47)							
Centroid size	1	0.027	0.027	**0.091**	5.7	3.4	0.001
PCSA temporal	1	0.014	0.014	**0.048**	3.0	2.4	0.006
PCSA masseter	1	0.018	0.018	**0.060**	3.7	2.9	0.004
PCSA pterygoid	1	0.006	0.006	0.021	1.3	0.64	0.20
Mass temporal	1	0.012	0.012	**0.039**	2.4	2.2	0.016
Mass masseter	1	0.025	0.025	**0.085**	5.2	4.1	0.001
Mass pterygoid	1	0.0073	0.0073	0.025	1.5	1.6	0.10
Residuals	39	0.19	0.0048	0.63			
Allometry-free shape of the mandible (N = 47)							
PCSA temporal	1	0.0095	0.0095	**0.041**	2.2	2.1	0.018
PCSA masseter	1	0.013	0.013	**0.056**	3.0	3.0	0.003
PCSA pterygoid	1	0.0053	0.0053	0.023	1.2	0.61	0.27
Mass temporal	1	0.011	0.011	**0.047**	2.5	2.4	0.008
Mass masseter	1	0.015	0.015	**0.066**	3.5	3.5	0.002
Mass pterygoid	1	0.0066	0.0066	0.029	1.5	1.3	0.100
Residuals	39	0.17	0.0044	0.74			
Simple regressions							
Shape of the cranium							
Centroid size (N = 58)	1	0.11	0.11	**0.19**	13	4.2	0.001
Temporal, raw PCSA (N = 47)	1	0.028	0.028	0.056	2.7	1.8	0.051
Masseter, raw PCSA (N = 47)	1	0.027	0.027	0.053	2.5	1.6	0.069
Pterygoids, raw PCSA (N = 47)	1	0.031	0.031	**0.061**	2.9	1.9	0.045
Temporal, raw mass (N = 47)	1	0.033	0.033	**0.066**	3.2	2.0	0.043
Masseter, raw mass (N = 47)	1	0.034	0.034	**0.068**	3.3	2.0	0.038
Pterygoids, raw mass (N = 47)	1	0.036	0.036	**0.072**	3.5	2.1	0.027
Temporal, residual PCSA (N = 47)	1	0.050	0.050	**0.10**	5.0	2.8	0.004
Masseter, residual PCSA (N = 47)	1	0.079	0.079	**0.16**	8.4	3.4	0.001
Pterygoids, residual PCSA (N = 47)	1	0.093	0.093	**0.19**	10	3.6	0.001
Temporal, residual mass (N = 47)	1	0.10	0.10	**0.20**	12	3.7	0.001
Masseter, residual mass (N = 47)	1	0.14	0.14	**0.27**	17	4.2	0.001
Pterygoids, residual mass (N = 47)	1	0.15	0.15	**0.30**	20	4.4	0.001

Table 3 (continued)

	Df	SS	MS	Rsq	F	Z	Pr(> SS)
Allometry-free shape of the cranium							
Temporal, residual PCSA (N = 47)	1	0.028	0.028	**0.10**	5.0	3.6	0.001
Masseter, residual PCSA (N = 47)	1	0.038	0.038	**0.14**	7.1	4.2	0.001
Pterygoids, residual PCSA (N = 47)	1	0.047	0.047	**0.17**	9.0	4.7	0.001
Temporal, residual mass (N = 47)	1	0.053	0.053	**0.19**	11	5.0	0.001
Masseter, residual mass (N = 47)	1	0.066	0.066	**0.24**	14.3	5.5	0.001
Pterygoids, residual mass (N = 47)	1	0.075	0.075	**0.27**	17	6.1	0.001
Shape of the mandible							
Centroid size (N = 59)	1	0.037	0.037	**0.098**	6.2	4.2	0.001
Temporal, raw PCSA (N = 47)	1	0.033	0.033	**0.11**	5.6	3.8	0.001
Masseter, raw PCSA (N = 47)	1	0.043	0.043	**0.14**	7.5	4.3	0.001
Pterygoids, raw PCSA (N = 47)	1	0.038	0.038	**0.13**	6.7	4.1	0.001
Temporal, raw mass (N = 47)	1	0.040	0.040	**0.13**	7.0	4.1	0.001
Masseter, raw mass (N = 47)	1	0.049	0.049	**0.16**	8.8	4.5	0.001
Pterygoids, raw mass (N = 47)	1	0.045	0.045	**0.15**	8.1	4.3	0.001
Temporal, residual PCSA (N = 47)	1	0.014	0.014	**0.048**	2.3	2.1	0.029
Masseter, residual PCSA (N = 47)	1	0.027	0.027	**0.091**	4.5	3.4	0.001
Pterygoids, residual PCSA (N = 47)	1	0.023	0.023	**0.076**	3.7	3.1	0.001
Temporal, residual mass (N = 47)	1	0.027	0.027	**0.088**	4.5	3.3	0.001
Masseter, residual mass (N = 47)	1	0.043	0.043	**0.14**	7.6	4.4	0.001
Pterygoids, residual mass (N = 47)	1	0.045	0.045	**0.15**	8.0	4.5	0.001
Allometry-free shape of the mandible							
Temporal, residual PCSA (N = 47)	1	0.0095	0.0095	**0.041**	1.9	1.9	0.03
Masseter, residual PCSA (N = 47)	1	0.018	0.018	**0.076**	3.7	3.5	0.002
Pterygoids, residual PCSA (N = 47)	1	0.016	0.016	**0.067**	3.2	3.1	0.002
Temporal, residual mass (N = 47)	1	0.020	0.020	**0.082**	4.1	3.5	0.001
Masseter, residual mass (N = 47)	1	0.028	0.028	**0.12**	6.2	4.6	0.001
Pterygoids, residual mass (N = 47)	1	0.030	0.030	**0.13**	6.6	4.8	0.001

Significant results ($P < 0.05$) are indicated in bold

proportionally longer snout and narrow zygomatic arches. The beagles, represented by 20 crania, occupy the center of the scatter plot and extend along axis 2. This axis describes differences in size, the positioning of the zygomatic arches, and the width of the braincase, in particular the post-orbital constriction. In our sample, cranial shape is strongly allometric (Table 3, Fig. S1). The smallest dogs here correspond to small brachycephalic dogs: they have very rounded crania with wide zygomatic arches and a relatively short muzzle. The largest dogs of our sample have more dolichocephalic crania: they are relatively longer and narrower. However, these allometry patterns are strongly related to the constitution of our sample, because brachycephaly/mesocephaly/dolichocephaly do not depend on body size and each group may contain small, as well as medium or large breeds. The PCA performed on allometry-free shapes (Fig. 2b) still separated the brachycephalic (on the right) from the more dolichocephalic dogs (on the left). Molossoid dogs have wider zygomatic arches, a more voluminous neurocranium with more pronounced orbital processes, and a shorter snout, even for their size.

Drivers of Variation in Cranial Shape

The results of the Procrustes ANOVAs (Table 3) indicate that the shape of the cranium is driven by both centroid size and muscle architecture (the models explain 61% of the variation in cranial shape). According to the multiple regressions, 21% of the total variation in cranial shape is explained by size, while muscles explain 40.3% of the residual variation in shape. Both muscle masses and PCSAs are important drivers of cranial shape variation. The multiple Procrustes ANOVAs performed on allometry-free cranial shape and residual muscle masses and PCSAs (Table 3) also show significant result and muscles explain around 41% of the variation of non-allometric cranial shape.

The results of the simple regressions (whether on shape or allometry-free shapes) indicate that cranial shape is more strongly driven by muscle volume than by muscle PCSA. The relative mass of the temporal muscle explains 20% of the variation in cranial shape, while the relative volume of the masseter and pterygoid muscles explain 27 or 30% of

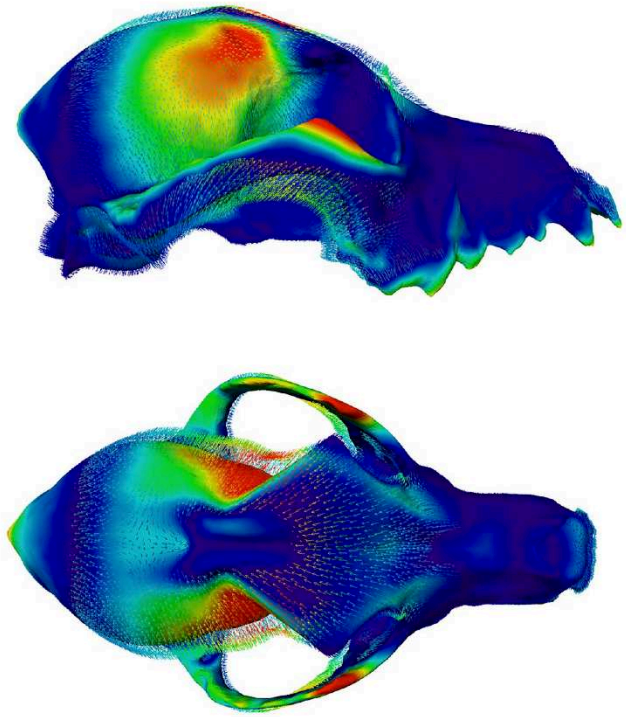

Fig. 3 Variation in cranial shape associated with variation in m. temporalis PCSA in lateral and dorsal views. The shape corresponding with the maximum of the PCSA is represented, and the arrows represent the deformation from the shape corresponding to the minimal PCSA to the shape corresponding to the maximal PCSA. Hotter colors indicate areas that show greater shape changes

the variation in cranial shape. Similar results and percentages are observed for the analysis with allometry-free cranial shape (Table 3). The visualisations highlight similar deformations associated with the temporal, masseter, and pterygoid muscles for both mass and PCSA. For all muscles, the zygomatic arches, the frontal bone, the sagittal crest, and the muzzle are the areas that are impacted the most (Fig. 3).

The ANOVAS and post-hoc tests performed on residual muscle data to compare brachycephalic, mesocephalic, and dolichocephalic dogs show that the masseter, temporal and pterygoid muscles are larger and more powerful in brachycephalic dogs than in meso or dolichocephalic dogs, relatively to their size ($P < 0.001$ for the masseter and pterygoid muscles; $P < 0.05$ for the temporal muscle). Differences between mesocephalic and dolichocephalic dogs were not significant.

Covariations Between Cranial and Mandibular Shape

The first PLS axis of the 2B-PLS between cranial and mandibular shape, accounting for 86% of the total covariance, is highly significant ($P < 0.001$) and indicates strong covariations (r-PLS = 0.82, Fig. 4a). The two axes are strongly dependent on the centroid sizes of the cranium and mandible, respectively (cranium: adjusted $R^2 = 0.15$, $P = 0.002$; mandible: adjusted $R^2 = 0.096$, $P = 0.012$). Molossoid dogs (large brachycephalic dogs) on the left part of the scatter plot have short and broad crania, with a short snout, a large neurocranium and wide zygomatic arches, associated to a ventrally curved mandibular body, with a large ramus and very developed coronoid, condylar and angular processes, and a deep masseteric fossa. On the opposite side of the scatterplot, we have the mesocephalic and dolichocephalic dogs. They have very elongated and narrow crania, with a smaller braincase, a longer snout and narrow zygomatic arches. This is associated with long and flat mandibles and smaller coronoid, condylar, and angular processes. The small brachycephalic dogs are located on the middle part of the scatterplot, the papillon being a little off-centre with respect to the main covariance axis. This covariation is not only linked with size variation, as the allometry-free shapes also show strong covariations (PLS 1 explains 79% of the total covariation, $P < 0.001$, r-PLS = 0.88, Fig. 4b). The deformations along the PLS axes are similar to those described for non allometry-free shapes, although the magnitude of the deformations is somewhat lower for the cranium.

Covariations Between Muscle Data and Cranial Shape

The results of the 2B-PLS are represented in Table 4. We observed significant covariations for all combinations. The covariations between cranial shape and raw PCSAs or between allometry-free cranial shape and residual PCSAs are stronger than the ones between cranial shape and residual PCSAs (shape: $Z = 1.97$, $P = 0.02$; allometry-free shape: $Z = 1.94$, $P = 0.03$). For the masses, the covariations are not significantly different. The visualisations are similar for the mass and the PCSA and the covariations are not significantly different ($P > 0.05$), although the coefficients tend to be higher for the 2B-PLS with masses.

Here we only describe the covariations between muscle masses and cranial shape. The scatterplots representing the first PLS axis reveals very strong covariations (mass: 96% of the total covariation, r-PLS = 0.9, $P = 0.025$; PCSA: 87% of the total covariation, r-PLS = 0.84, $P = 0.039$). All muscles loaded similarly reflecting the strong correlation between muscle groups. The covariatons between absolute muscle masses and the shape of the cranium (Fig. S2) are mainly driven by size (cranial shape: adjusted $R^2 = 0.58$, $P < 0.001$; muscle masses: adjusted $R^2 = 0.61$, $P < 0.001$). The covariations between shape and the residual masses (Fig. 5) indicate that molossoid dogs with a rounded neurocranium, larger zygomatic arches, shorter snouts, a more developed pterygoid process, and a more oblique cranium with more caudally located jugal teeth, have more developed muscles for

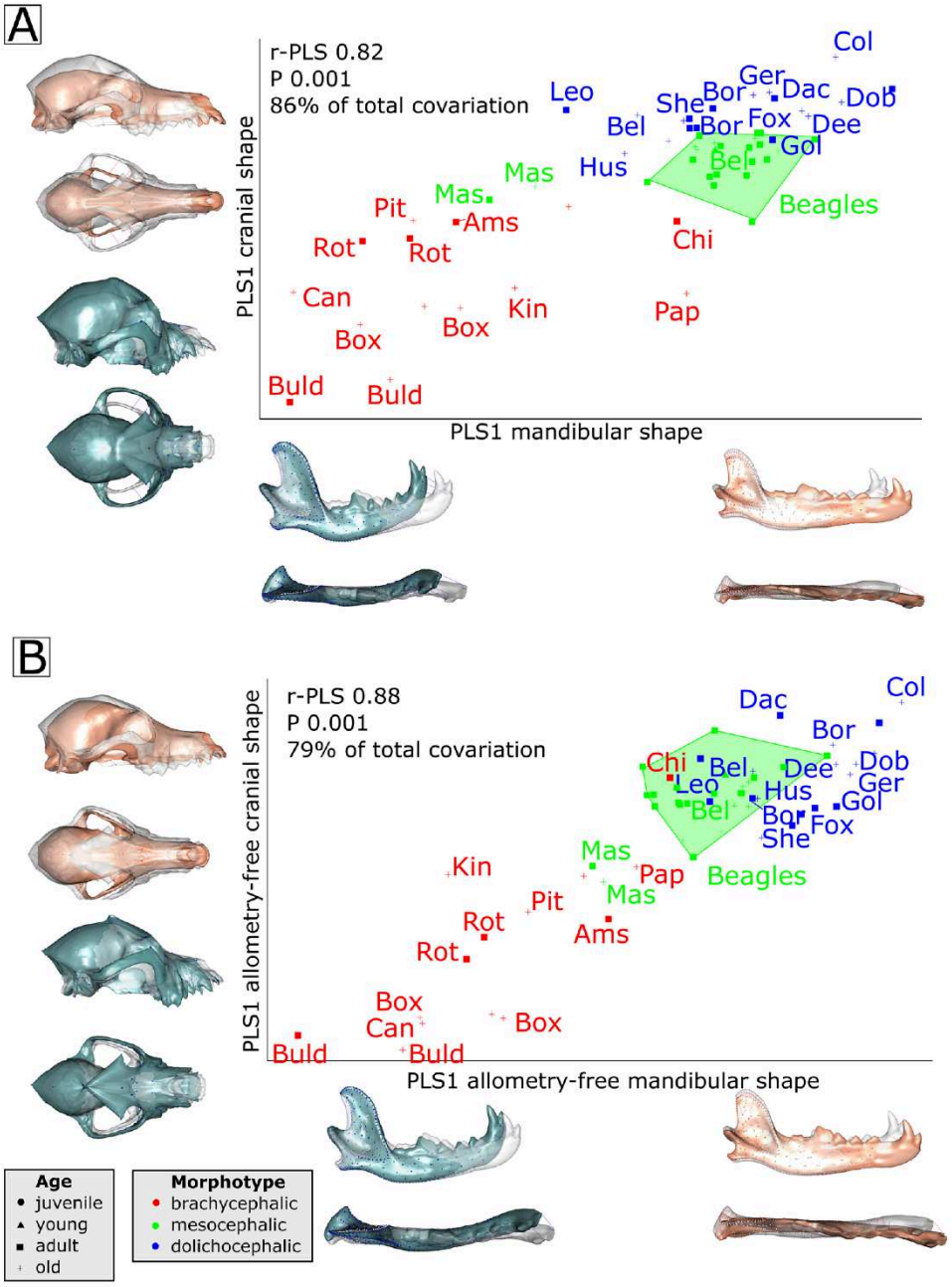

Fig. 4 2-Block Partial Least Square analyses between cranium and mandible shapes **(a)** or allometry-free cranium and mandible shapes **(b)**, with vectors and shapes at the minimum and maximum of the PLS axis. Illustrations represent the deformations from the consensus to the extreme of the axis in lateral and dorsal views. Ages are indicated by different shapes and morphotypes are indicated by different colors. Beagles are located in the green area. *Ams* American Staffordshire terrier, *Box* Boxer, *Buld* Bulldog, *Bult* Bull terrier, *Chi* Chihuahua, *Can* Cane Corso, *Kin* Cavalier King Charles Spaniel, *Pap* Papillon, *Pit* Pitbull, *Rot* Rottweiler, *Mas* Mastiff, *Fox* Fox terrier, *Bel* Belgian Shepherd, *Bor* Border collie, *Col* Collie, *Dac* Dachshund, *Ger* German Shepherd, *Gol* Golden retriever, *Hus* Husky, *Leo* Leonberg, *She* Shetland sheepdog

Table 4 Results of the 2B-PLS analyses on the shape of the cranium and the Log_{10}-transformed muscle mass or PCSA data

Muscle data	Shape–muscle data			Shape–residual data			Allometry-free shape–residual data		
	%CV	*P*	r-PLS	%CV	*P*	r-PLS	%CV	*P*	r-PLS
Mass	96	0.025	**0.90**	99	0.001	**0.74**	98	0.001	**0.83**
PCSA	87	0.039	**0.84**	96	0.001	**0.64**	93	0.001	**0.72**

Only the first PLS axis is reported. %coVar indicates the percentage of covariation explained by the axis of interest. r-PLS indicates the coefficient of covariation between the two variables. Significant results are indicated in bold

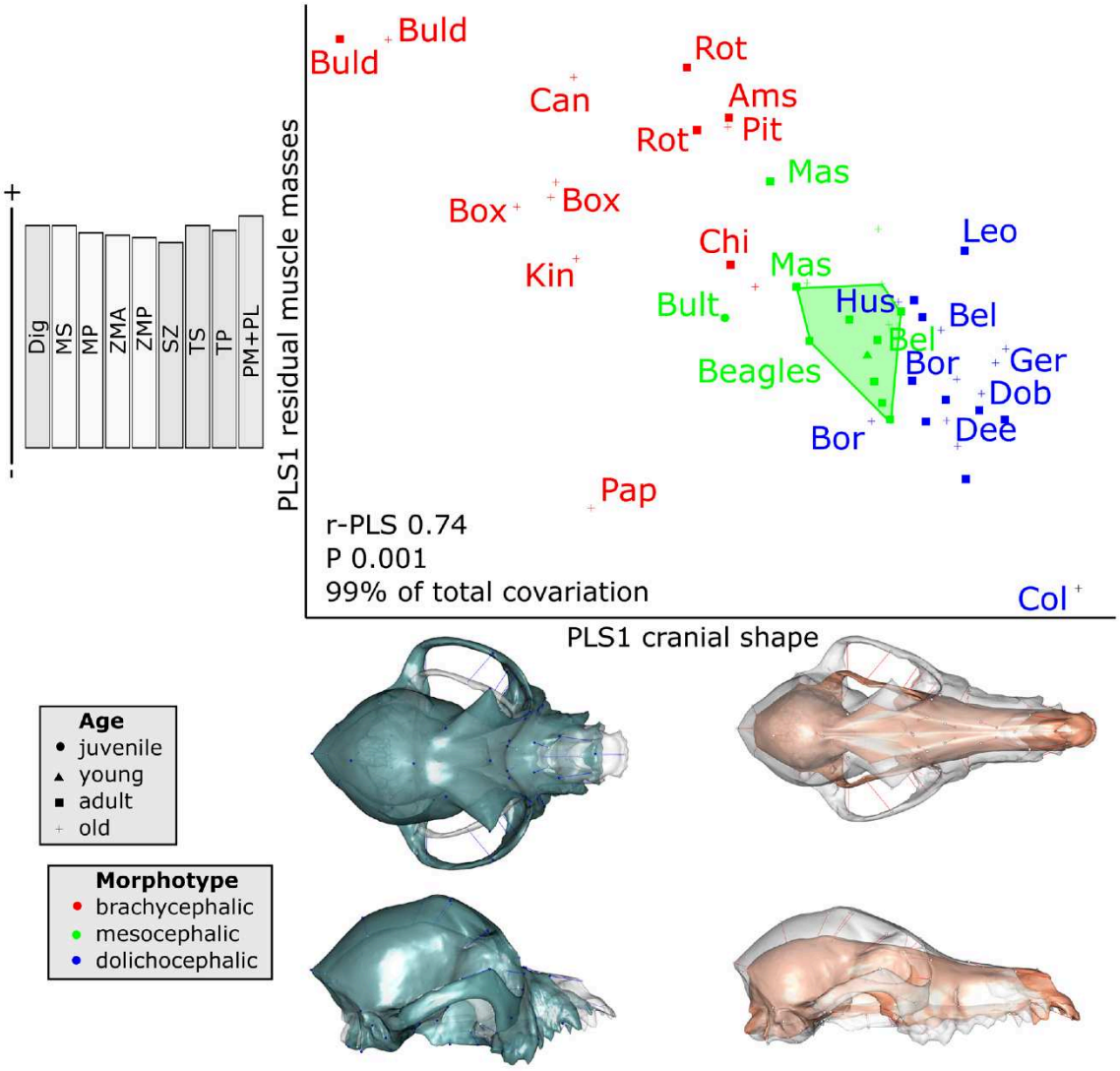

Fig. 5 2-Block Partial Least Square Analyses between cranial shape and the residual masses of the jaw muscles, with vectors and shapes at the minimum and maximum of the PLS axis. Illustrations represent the deformations from the consensus to the extreme of the axis in lateral and dorsal views. Ages are indicated by different shapes and morphotypes are indicated by different colors. Beagles are located in the green area. *Ams* American Staffordshire terrier, *Box* Boxer, *Buld* Bulldog, *Bult* Bull terrier, *Chi* Chihuahua, *Can* Cane Corso, *Kin* Cavalier King Charles Spaniel, *Pap* Papillon, *Pit* Pitbull, *Rot* Rottweiler, *Mas* Mastiff, *Fox* Fox terrier, *Bel* Belgian Shepherd, *Bor* Border collie, *Col* Collie, *Dac* Dachshund, *Ger* German Shepherd, *Gol* Golden retriever, *Hus* Husky, *Leo* Leonberg, *She* Shetland sheepdog, *Dig* M. digastricus, *MS* M. masseter pars superficialis, *MP* M. masseter pars profunda, *ZMA* M. zygomaticomandibularis pars anterior, *ZMP* M. zygomaticomandibularis pars posterior, *SZ* M. temporalis pars supra-zygomatica, *TS* M. temporalis pars superficialis, *TP* M. temporalis pars profunda, *PM+PL* M. pterygoideus pars medialis and lateralis

their size. More dolichocephalic dogs, on the right part of the scatterplot, which have straight, flat and narrow crania, with a long snout, a straight cranium, more cranially located jugal teeth and very small and narrow zygomatic arches, have less well-developed muscles. The beagles are grouped at the center of the scatterplot and the relations between cranial shape and the jaw muscles are rather homogenous. Visualisations of the 2B-PLS using allometry-free shape show similar patterns (Fig. S3).

Discussion

As previously observed (Drake et al. 2017) dog crania show an extraordinary variation in shape. Brachycephalic dogs with relatively big and rounded braincases, large zygomatic arches, and short snouts oppose dolichocephalic dogs that have long and narrow crania. Dogs from the same breed (beagles) also show variation in cranial shape but to a lesser degree. Yet, we found no significant effect of age which may be due to a bias in our sample and our age estimations. Males

and females did significantly differ in shape if we consider all breeds together. However, as our sample size is rather small (N = 32) and unbalanced we did not further explore the morphological traits related to sexual dimorphism. We did not have enough specimens of known sex (5) to test for sexual dimorphism in beagles specifically. In summary, cranial shape is allometric, and size explains more of the total variation in cranial shape ($R^2 = 0.21$) than mandible shape ($R^2 = 0.10$, Table 3).

We observed very strong covariations between mandible shape and cranial shape (rPLS = 0.81, $P = 0.001$; 85% of the total covariation, Fig. 4). We observed similar patterns of covariation as those previously described in the dog (Selba et al. 2019), other mammals (Cornette et al. 2013, 2015; Smith and Grosse 2016; Fabre et al. 2018; Penrose et al. 2020), and even in other tetrapods (Fabre et al. 2014). More robust and curved mandibles are associated with crania with a shorter snout and larger adductor chambers. The high coefficient of covariation is consistent with previously published data by Selba et al. (2019; r-PLS = 0.976; $P = 0.001$; 57 dogs). The slight differences are likely to be explained by the sample and to the lower number of landmarks used by Selba et al. (2019; 45 landmarks on the cranium and 17 on the mandible). This strong integration between the bony elements of the cranium suggests that the strong artificial selection upon morphological traits has not impacted the integrity of the jaw system. Possibly, the development of the overall system is under control of a limited set of key developmental genes assuring the integration between cranium and mandible. Moreover, Curth et al. (2017) showed that the greater skull shape diversity in dogs was not explained by less integrated skull modules and that the pattern of covariation in the cranium is similar to that observed in the wolf. Further studies focusing on the wolf and commensal canids might provide information about the impact of domestication in canids and test whether lower values of integration are associated with higher disparity across the modules in the cranium/mandible as has been documented in equids (Heck et al. 2018).

Cranial shape is also significantly impacted by the architecture of the muscles. Absolute muscle data explain less of the total variation in cranial shape than in mandibular shape (Table 3). This may be related to the implication of the cranium in numerous functions including the protection of the brain and the sensory organs, while the mandible is specialized towards mastication only. Unexpectedly, the covariations are stronger for the cranium compared to the mandible (mass: rPLS = 0.90 for the cranium and 0.74 for the mandible, Z-score = 2.45, $P = 0.007$; PCSA: r-PLS = 0.84 for the cranium and 0.73 for the mandible, Z-score = 2.02, $P = 0.02$). The covariations remain strong when the analyses are conducted on size-free data but the differences between the covariations between muscle architecture and the shape of the mandible and the cranium disappear (see also Brassard et al. 2020a; $P > 0.05$). The relative muscle data explain even more variation in cranial shape (40.3%) compared to mandible shape (22.4%, Table 3) and individual residual masses or PCSAs are better predictors of cranial shape than of mandibular shape. This may be explained by the differential contribution of the temporal and masseter muscle to the shape of the cranium and mandible and to their different contribution to the overall mass of the jaw adductors. The temporal muscle is the most voluminous muscle (Brassard et al. 2020a) and it covers the entire cranial vault while it inserts onto a small portion of the mandible (coronoid process). On the contrary, the masseter muscle is less voluminous, originates on a relatively small portion of the cranium (the lower portion of the zygomatic arch) but is attached to a large area on the mandibular ramus (the masseteric fossa). Both the masseter and temporal muscles may thus have distinct effects on the shape of the cranium or mandible, but it may be the attachment areas of the muscles that drive the covariations rather than the entire muscle mass per se. All this suggests that the cranium and the adductor muscles are a strongly integrated system.

Because of strong correlation between muscle masses/PCSAs, similar deformations are associated with all the muscles: the masseter, temporal, and pterygoid are acting jointly on overall cranial shape (Fig. 3). Dogs with the more voluminous or powerful muscles have a more caudally pronounced sagittal crest, a more marked postorbital constriction, and broader, stronger and more dorsally oriented zygomatic arches, bigger braincases, and reduced snouts (Figs. 5, S2, S3). The relative volume of the masseter explains 27% of the variation in cranial shape and impacts the shape of the zygomatic arch. The stiffness of the zygomatic arch in molossoid dogs suggests an adaptation to an increase in the relative proportion of applied muscle load due to the contraction of the more voluminous masseter muscle (Smith and Grosse 2016). The relative volume of the temporal drives the shape of the neurocranium, in particular the shape of the postorbital process and sagittal crest. The wide zygomatic arches determine the space available for the muscle to pass through.

Our results suggest that the mandible, the cranium, and the jaw adductors form a highly integrated system despite the intense artificial selection for very diverse head shapes. These strong connections are likely under genetic control, as suggested by studies on mice with muscle deficiencies. Vecchione et al. (2007, 2010) showed that mice with myostatin (a regulator of skeletal muscle growth) deficiency developed more brachycephalic craniofacial morphologies adapted to hypermuscularity, with significantly shorter and wider crania compared to controls (modifications in mandible shape were also observed). These modifications are consistent with our observations for the shape of the molossoid dogs that

have very voluminous muscles, even for their size. Spassov et al. (2017) also showed that mice with a congenital muscle dystrophy have a more flattened neurocranium with a more dorsally displaced foramen magnum. Our results also showed lower correlations and covariations of cranial shape with muscle PCSAs than with muscle mass. This suggests that volume constraints are likely the principal drivers of the observed covariation. The lower correlations between shape and PCSA may result from a decoupling between shape and bite force. Variation in PCSA (or bite force) may, in turn, correlate more to cortical bone thickness than to the overall shape of the cranium as demonstrated in other species or for other bones (Bouvier and Hylander 1981; Daegling and Hotzman 2003; Slizewski et al. 2013).

The low ratio of the number of individuals to the much higher number of variables is frequent in comparative morphology studies and may result in statistical biaises. It has been suggested that high correlations can possibly be observed in 2bPLS analyses even if the two blocks are completely independent when the sample size is smaller or similar to the number of variables (Mitteroecker and Bookstein 2007). However, more recent studies using simulated and empirical datasets have demonstrated that the potential issues related to the use of high-resolution three-dimensional data are unlikely to obscure genuine biological signal (Goswami et al. 2019). Moreover, to make sure that our results were not biased by the low sample size relative to the high number of landmarks, we performed parallel analyses with a subsample of 25 landmarks on the cranium and mandible. We obtained very similar results (in terms of *P*-values and coefficients of covariation) suggesting that our analyses are not biased by the number of landmarks used to describe shape variation.

Our study focused on the relations between the overall shape of the bones and muscles but did not allow to study the relations between muscle loads and bone histology, nor to evaluate the impact of changes in diet or muscle activity throughout life. The biomechanical interactions between muscle and bone have been investigated in some detail in mammals, showing that muscles act on bones throughout late ontogeny and adult life and that the bones of the cranium respond plastically to changes in masticatory function (Wolff 1986; Frost and Schönau 2000; Renaud et al. 2010; Herring 2011; Klingenberg and Navarro 2012; Blank 2014; Brotto and Bonewald 2015; Yamamoto et al. 2020). Diet is known to influence both muscle volume and cortical bone thickness in mammals (Bouvier and Hylander 1984; Herring 2011; Scott et al. 2014a, b) and even overall craniofacial shape (Stavros Kiliaridis et al. 1985; He and Kiliaridis 2003; Renaud et al. 2010; Anderson et al. 2014; Spassov et al. 2017). For example, rodents fed a soft food diet have a shorter and narrower face, and a shorter mandible with less pronounced bony processes compared to animals fed on a hard diet (Anderson et al. 2014; Kiliaridis et al. 1985). He and Kiliaridis (2003) further showed that ferrets fed a humid, soft diet have narrower crania with slenderer zygomatic arches and shorter and narrower coronoid process on the mandible, compared to ferrets fed with a dry, hard diet. Exercising also may have an influence on bone shape (Kiliaridis et al. 1995; Shirai et al. 2018; Thompson et al. 2001). Although few studies have focused on canids (but see Forbes-Harper et al. 2017; Liebman and Kussick 1965; Penrose et al. 2020; Wroe et al. 2007) these results suggest that diet may be an important driver of cranial shape variation in dogs as well, yet this remains to be investigated. Comparing domestic dogs with commensal or wild canids would further enable to better understand the impact of domestication on the interrelationships between muscles and bones of the jaw apparatus.

Conclusion

Our study assessed the impact of the extraordinary variation in cranial shape in domestic dogs on the interrelationships between bones and muscles. Our results show that the bony elements (cranium and mandible) and muscles form a highly integrated system in dogs. This supports the role of genes controlling both muscle and bone development, epigenetic effects driving the development of both muscles and bones (Iinuma et al. 1991), or the interaction between genetic mechanisms and plasticity. The strong integration of the masticatory apparatus consequently provides the possibility to infer the functional consequences of morphological changes in extinct taxa. Despite this strong integration, muscles explain relatively little of the overall shape variation in the cranium in domestic dogs. This raises the question of whether muscle architecture explains a higher proportion of the variation in shape in commensal or wild canids, and whether domestication has led to a change in the patterns of integration between form and function as suggested previously.

Acknowledgements We thank the Veterinary school ONIRIS-Nantes (France) and Anses (Nancy, France) for providing dog heads for dissection. We are grateful to Manuel Comte, Mickaël Godet and Frederic Lebatard for their help in managing specimens and their helpful discussions about the preparation of the skulls. We also thank Arnaud Delapré for his help with photogrammetry. We are very grateful to two anonymous reviewers for their comments and advice on an earlier version of the manuscript.

Funding This research was funded by the Ministère de l'Enseignement supérieur, de la Recherche et de l'Innovation.

Compliance with Ethical Standards

Conflict of interest The authors declare that they have no conflicts of interest.

References

Adams, D. C., & Collyer, M. L. (2016). On the comparison of the strength of morphological integration across morphometric datasets. *Evolution, 70*(11), 2623–2631. https://doi.org/10.1111/evo.13045.

Adams, D. C., & Collyer, M. L. (2017). Multivariate phylogenetic comparative methods: Evaluations, comparisons, and recommendations. *Systematic Biology, 67*(1), 14–31.

Anderson, M. J. (2001). A new method for non-parametric multivariate analysis of variance. *Austral Ecology, 26*(1), 32–46.

Anderson, M., & Braak, C. T. (2003). Permutation tests for multifactorial analysis of variance. *Journal of Statistical Computation and Simulation, 73*(2), 85–113.

Anderson, P. S., Renaud, S., & Rayfield, E. J. (2014). Adaptive plasticity in the mouse mandible. *BMC Evolutionary Biology, 14*(1), 1–9. https://doi.org/10.1186/1471-2148-14-85.

Barone, R. (2010). *Anatomie comparée des mammifères domestiques: Tome 1, Ostéologie* (5e édition.). Paris: Vigot.

Bell, A. F. (1965). Dental disease in the dog. *Journal of Small Animal Practice, 6*(6), 421–428. https://doi.org/10.1111/j.1748-5827.1965.tb04359.x.

Blank, R. D. (2014). Bone and muscle pleiotropy: The genetics of associated traits. *Clinical Reviews in Bone and Mineral Metabolism, 12*(2), 61–65. https://doi.org/10.1007/s12018-014-9159-4.

Bookstein, F. L. (1997). *Morphometric tools for landmark data: Geometry and biology*. Cambridge: Cambridge University Press.

Bouvier, M., & Hylander, W. L. (1981). Effect of bone strain on cortical bone structure in macaques (Macaca mulatta). *Journal of Morphology, 167*(1), 1–12. https://doi.org/10.1002/jmor.1051670102.

Bouvier, M., & Hylander, W. L. (1984). The effect of dietary consistency on gross and histologic morphology in the craniofacial region of young rats. *American Journal of Anatomy, 170*(1), 117–126. https://doi.org/10.1002/aja.1001700109.

Brassard, C., Merlin, M., Guintard, C., Monchâtre-Leroy, E., Barrat, J., Callou, C., et al. (2020a). How does masticatory muscle architecture covary with mandibular shape in domestic dogs? *Evolutionary Biology*. https://doi.org/10.1007/s11692-020-09499-6.

Brassard, C., Merlin, M., Guintard, C., Monchâtre-Leroy, E., Barrat, J., Bausmayer, N., et al. (2020b). Bite force and its relationship to jaw shape in domestic dogs. *Journal of Experimental Biology*. https://doi.org/10.1242/jeb.224352.

Brotto, M., & Bonewald, L. (2015). Bone and muscle: Interactions beyond mechanical. *Bone, 80*, 109–114. https://doi.org/10.1016/j.bone.2015.02.010.

Collyer, M. L., Sekora, D. J., & Adams, D. C. (2015). A method for analysis of phenotypic change for phenotypes described by high-dimensional data. *Heredity, 115*(4), 357.

Cornette, R., Baylac, M., Souter, T., & Herrel, A. (2013). Does shape co-variation between the skull and the mandible have functional consequences? A 3D approach for a 3D problem. *Journal of Anatomy, 223*(4), 329–336. https://doi.org/10.1111/joa.12086.

Cornette, R., Tresset, A., & Herrel, A. (2015). The shrew tamed by Wolff's law: Do functional constraints shape the skull through muscle and bone covariation? *Journal of Morphology, 276*(3), 301–309. https://doi.org/10.1002/jmor.20339.

Curth, S. (2018). Modularity and integration in the skull of *Canis lupus* (Linnaeus 1758): A geometric morphometrics study on domestic dogs and wolves, 78.

Curth, S., Fischer, M. S., & Kupczik, K. (2017). Patterns of integration in the canine skull: An inside view into the relationship of the skull modules of domestic dogs and wolves. *Zoology (Jena, Germany), 125*, 1–9. https://doi.org/10.1016/j.zool.2017.06.002.

Daegling, D. J., & Hotzman, J. L. (2003). Functional significance of cortical bone distribution in anthropoid mandibles: an in vitro assessment of bone strain under combined loads. *American Journal of Physical Anthropology, 122*(1), 38–50. https://doi.org/10.1002/ajpa.10225.

Drake, A. G., Coquerelle, M., Kosintsev, P. A., Bachura, O. P., Sablin, M., Gusev, A. V., et al. (2017). Three-dimensional geometric morphometric analysis of fossil canid mandibles and skulls. *Scientific Reports, 7*(1), 9508. https://doi.org/10.1038/s41598-017-10232-1.

Drake, A. G., & Klingenberg, C. P. (2008). The pace of morphological change: Historical transformation of skull shape in St Bernard dogs. *Proceedings. Biological sciences, 275*(1630), 71–76. https://doi.org/10.1098/rspb.2007.1169.

Drake, A. G., & Klingenberg, C. P. (2010). Large-scale diversification of skull shape in domestic dogs: Disparity and modularity. *The American Naturalist, 175*(3), 289–301. https://doi.org/10.1086/650372.

Dryden, I. L., & Mardia, K. V. (2016). *Statistical shape analysis: With applications in R*. New York: Wiley.

Ellis, J. L., Thomason, J. J., Kebreab, E., & France, J. (2008). Calibration of estimated biting forces in domestic canids: Comparison of post-mortem and in vivo measurements. *Journal of Anatomy, 212*(6), 769–780. https://doi.org/10.1111/j.1469-7580.2008.00911.x.

Ellis, J. L., Thomason, J., Kebreab, E., Zubair, K., & France, J. (2009). Cranial dimensions and forces of biting in the domestic dog. *Journal of Anatomy, 214*(3), 362–373. https://doi.org/10.1111/j.1469-7580.2008.01042.x.

Fabre, A.-C., Andrade, D. V., Huyghe, K., Cornette, R., & Herrel, A. (2014). Interrelationships between bones, muscles, and performance: biting in the lizard *Tupinambis merianae*. *Evolutionary Biology, 41*(4), 518–527. https://doi.org/10.1007/s11692-014-9286-3.

Fabre, A.-C., Perry, J. M. G., Hartstone-Rose, A., Lowie, A., Boens, A., & Dumont, M. (2018). Do muscles constrain skull shape evolution in strepsirrhines? *The Anatomical Record, 301*(2), 291–310. https://doi.org/10.1002/ar.23712.

Fau, M., Cornette, R., & Houssaye, A. (2016). Photogrammetry for 3D digitizing bones of mounted skeletons: Potential and limits. *Comptes Rendus Palevol, 15*(8), 968–977. https://doi.org/10.1016/j.crpv.2016.08.003.

Forbes-Harper, J. L., Crawford, H. M., Dundas, S. J., Warburton, N. M., Adams, P. J., Bateman, P. W., et al. (2017). Diet and bite force in red foxes: Ontogenetic and sex differences in an invasive carnivore. *Journal of Zoology, 303*(1), 54–63. https://doi.org/10.1111/jzo.12463.

Frost, H. M. (2001). From Wolff's law to the Utah paradigm: Insights about bone physiology and its clinical applications. *The Anatomical Record, 262*(4), 398–419. https://doi.org/10.1002/ar.1049.

Frost, H. M. (2003). Bone's mechanostat: a 2003 update. *The Anatomical Record Part A: Discoveries in Molecular, Cellular, and Evolutionary Biology: An Official Publication of the American Association of Anatomists, 275*(2), 1081–1101. https://doi.org/10.1002/ar.a.10119.

Frost, H. M., & Schönau, E. (2000). The" muscle-bone unit" in children and adolescents: a 2000 overview. *Journal of Pediatric Endocrinology and Metabolism, 13*(6), 571–590. https://doi.org/10.1515/JPEM.2000.13.6.571.

Goodall, C. (1991). Procrustes methods in the statistical analysis of shape. *Journal of the Royal Statistical Society: Series B (Methodological), 53*(2), 285–321.

Goswami, A., Watanabe, A., Felice, R. N., Bardua, C., Fabre, A.-C., & Polly, P. D. (2019). High-density morphometric analysis of shape and integration: The good, the bad, and the not-really-a-problem. *Integrative and Comparative Biology, 59*(3), 669–683. https://doi.org/10.1093/icb/icz120.

Gunz, P., Mitteroecker, P., & Bookstein, F. L. (2005). Semilandmarks in three dimensions. In D. E. Slice (Ed.), *Modern morphometrics in physical anthropology* (pp. 73–98). Boston: Springer.

He, T., & Kiliaridis, S. (2003). Effects of masticatory muscle function on craniofacial morphology in growing ferrets (*Mustela putorius* furo). *European Journal of Oral Sciences, 111*(6), 510–517. https://doi.org/10.1111/j.0909-8836.2003.00080.x.

Heck, L., Wilson, L. A. B., Evin, A., Stange, M., & Sánchez-Villagra, M. R. (2018). Shape variation and modularity of skull and teeth in domesticated horses and wild equids. *Frontiers in Zoology, 15*(1), 14. https://doi.org/10.1186/s12983-018-0258-9.

Herring, S. W. (2011). Muscle-bone interactions and the development of skeletal phenotype: Jaw muscles and the skull. *Epigenetics Linking Genotype and Phenotype in Development and Evolution., 13*, 201.

Iinuma, M., Yoshida, S., & Funakoshi, M. (1991). Development of masticatory muscles and oral behavior from suckling to chewing in dogs. *Comparative Biochemistry and Physiology. A, Comparative Physiology, 100*(4), 789–794. https://doi.org/10.1016/0300-9629(91)90293-l.

Kiliaridis, S., Engström, C., & Thilander, B. (1985). The relationship between masticatory function and craniofacial morphology: I. A cephalometric longitudinal analysis in the growing rat fed a soft diet. *The European Journal of Orthodontics, 7*(4), 273–283.

Kiliaridis, S., Tzakis, M. G., & Carlsson, G. E. (1995). Effects of fatigue and chewing training on maximal bite force and endurance. *American Journal of Orthodontics and Dentofacial Orthopedics: Official Publication of the American Association of Orthodontists, Its Constituent Societies, and the American Board of Orthodontics, 107*(4), 372–378. https://doi.org/10.1016/s0889-5406(95)70089-7.

Kim, S. E., Arzi, B., Garcia, T. C., & Verstraete, F. J. M. (2018). Bite forces and their measurement in dogs and cats. *Frontiers in Veterinary Science*. https://doi.org/10.3389/fvets.2018.00076.

Klingenberg, C. P., Barluenga, M., & Meyer, A. (2002). Shape analysis of symmetric structures: Quantifying variation among individuals and asymmetry. *Evolution, 56*(10), 1909–1920. https://doi.org/10.1111/j.0014-3820.2002.tb00117.x.

Klingenberg, C. P., & Navarro, N. (2012). Development of the mouse mandible. In J. Piálek, M. Macholán, P. Munclinger, & S. J. E. Baird (Eds.), *Evolution of the house mouse* (pp. 135–149). Cambridge: Cambridge University Press.

Liebman, F. M., & Kussick, L. (1965). An Electromyographic analysis of masticatory muscle imbalance with relation to skeletal growth in dogs. *Journal of Dental Research, 44*(4), 768–774. https://doi.org/10.1177/00220345650440042401.

Machado, F. A., Zahn, T. M. G., & Marroig, G. (2018). Evolution of morphological integration in the skull of Carnivora (Mammalia): Changes in Canidae lead to increased evolutionary potential of facial traits. *Evolution, 72*(7), 1399–1419. https://doi.org/10.1111/evo.13495.

Milella, L. (2009). Mandibular brachygnathism in dogs. *Companion. Animal, 14*(6), 29–35. https://doi.org/10.1111/j.2044-3862.2009.tb00382.x.

Mitteroecker, P., & Bookstein, F. (2007). The conceptual and statistical relationship between modularity and morphological integration. *Systematic Biology,56*(5), 818–836.

Mitteroecker, P., Gunz, P., Bernhard, M., Schaefer, K., & Bookstein, F. L. (2004). Comparison of cranial ontogenetic trajectories among great apes and humans. *Journal of Human Evolution, 46*(6), 679–698. https://doi.org/10.1016/j.jhevol.2004.03.006.

Parker, H. G., Kim, L. V., Sutter, N. B., Carlson, S., Lorentzen, T. D., Malek, T. B., et al. (2004). Genetic structure of the purebred domestic dog. *Science, 304*(5674), 1160–1164.

Penrose, F., Cox, P., Kemp, G., & Jeffery, N. (2020). Functional morphology of the jaw adductor muscles in the Canidae. *The Anatomical Record, 1*, 12. https://doi.org/10.1002/ar.24391.

Renaud, S., Auffray, J.-C., & de la Porte, S. (2010). Epigenetic effects on the mouse mandible: Common features and discrepancies in remodeling due to muscular dystrophy and response to food consistency. *BMC Evolutionary Biology, 10*, 28. https://doi.org/10.1186/1471-2148-10-28.

Roberts, T., McGreevy, P., & Valenzuela, M. (2010). Human induced rotation and reorganization of the brain of domestic dogs. *PLoS ONE, 5*(7), e11946. https://doi.org/10.1371/journal.pone.0011946.

Rohlf, F. J., & Corti, M. (2000). Use of two-block partial least-squares to study covariation in shape. *Systematic Biology, 49*(4), 740–753. https://doi.org/10.1080/106351500750049806.

Rohlf, F., & Slice, D. (1990). Extensions of the procrustes method for the optimal superimposition of landmarks. *Systematic Zoology, 39*, 40–59. https://doi.org/10.2307/2992207.

Schlager, S. (2012). *Sliding semi-landmarks on symmetric structures in three dimensions*. Présenté à the 81st annual meeting of the American Association of Physical Anthropologists, Portland, OR, Anthropology, University of Freiburg, Germany.

Schoenau, E. (2005). From mechanostat theory to development of the « Functional Muscle-Bone-Unit ». *Journal of Musculoskeletal and Neuronal Interactions, 3*, 232–238.

Scott, J. E., McAbee, K. R., Eastman, M. M., & Ravosa, M. J. (2014a). Teaching an old jaw new tricks: Diet-induced plasticity in a model organism from weaning to adulthood. *Journal of Experimental Biology, 217*(22), 4099–4107. https://doi.org/10.1242/jeb.111708.

Scott, J. E., McAbee, K. R., Eastman, M. M., & Ravosa, M. J. (2014b). Experimental perspective on fallback foods and dietary adaptations in early hominins. *Biology Letters, 10*(1), 20130789. https://doi.org/10.1098/rsbl.2013.0789.

Selba, M. C., Oechtering, G. U., Gan Heng, H., & DeLeon, V. B. (2019). The impact of selection for facial reduction in dogs: geometric morphometric analysis of canine cranial shape. *The Anatomical Record*. https://doi.org/10.1002/ar.24184.

Sharir, A., Stern, T., Rot, C., Shahar, R., & Zelzer, E. (2011). Muscle force regulates bone shaping for optimal load-bearing capacity during embryogenesis. *Development, 138*(15), 3247–3259. https://doi.org/10.1242/dev.063768.

Shirai, M., Kawai, N., Hichijo, N., Watanabe, M., Mori, H., Mitsui, S. N., et al. (2018). Effects of gum chewing exercise on maximum bite force according to facial morphology. *Clinical and Experimental Dental Research, 4*(2), 48–51. https://doi.org/10.1002/cre2.102.

Slizewski, A., Schönau, E., Shaw, C., & Harvati, K. (2013). Muscle area estimation from cortical bone. *The Anatomical Record, 296*(11), 1695–1707. https://doi.org/10.1002/ar.22788.

Smith, A. L., & Grosse, I. R. (2016). The biomechanics of zygomatic arch shape. *Anatomical Record, 299*(12), 1734–1752. https://doi.org/10.1002/ar.23484.

Spassov, A., Toro-Ibacache, V., Krautwald, M., Brinkmeier, H., & Kupczik, K. (2017). Congenital muscle dystrophy and diet consistency affect mouse skull shape differently. *Journal of Anatomy, 231*(5), 736–748. https://doi.org/10.1111/joa.12664.

Thompson, D. J., Throckmorton, G. S., & Buschang, P. H. (2001). The effects of isometric exercise on maximum voluntary bite forces and jaw muscle strength and endurance. *Journal of*

Oral Rehabilitation, 28(10), 909–917. https://doi.org/10.1111/j.1365-2842.2001.00772.x.

Vecchione, L., Byron, C., Cooper, G., Barbano, T., Hamrick, M. W., Sciote, J., et al. (2007). Craniofacial morphology in myostatin-deficient mice. *Journal of Dental Research, 86*(11), 1068–1072.

Vecchione, L., Miller, J., Byron, C., Cooper, G. M., Barbano, T., Cray, J., et al. (2010). Age-related changes in craniofacial morphology in GDF-8 (myostatin)-deficient mice. *The Anatomical Record: Advances in Integrative Anatomy and Evolutionary Biology, 293*(1), 32–41.

Wayne, R. K. (1986). Cranial morphology of domestic and wild canids: The influence of development on morphological change. *Evolution, 40*(2), 243–261. https://doi.org/10.1111/j.1558-5646.1986.tb00467.x.

Wiley, D. F., Amenta, N., Alcantara, D. A., Ghosh, D., Kil, Y. J., Delson, E., et al. (2005). Evolutionary morphing. In *VIS 05 IEEE visualization, 2005* (pp. 431-438). Présenté à VIS 05. IEEE Visualization. https://doi.org/10.1109/VISUAL.2005.1532826.

Wolff, J. (1986). *The law of bone remodelling*. Berlin: Springer.

Wroe, S., Clausen, P., McHenry, C., Moreno, K., & Cunningham, E. (2007). Computer simulation of feeding behaviour in the thylacine and dingo as a novel test for convergence and niche overlap. *Proceedings of the Royal Society B: Biological Sciences, 274*(1627), 2819–2828.

Yamamoto, M., Takada, H., Ishizuka, S., Kitamura, K., Jeong, J., Sato, M., et al. (2020). Morphological association between the muscles and bones in the craniofacial region. *PLoS ONE, 15*(1), e0227301. https://doi.org/10.1371/journal.pone.0227301.

3. The relationships between mandibular shape or cranial shape and bite force in dogs

Article 3 –

Bite force and its relationship to jaw shape in domestic dogs

Colline Brassard, Marilaine Merlin, Claude Guintard, Elodie Monchâtre-Leroy, Jacques Barrat, Nathalie Bausmayer, Adrien Bausmayer, Michel Beyer, André Varlet, Céline Houssin, Cécile Callou, Raphaël Cornette, Anthony Herrel

Published in *Journal of Experimental Biology*, accepted: 18 June 2020

© 2020. Published by The Company of Biologists Ltd | Journal of Experimental Biology (2020) 223, jeb224352. doi:10.1242/jeb.224352

RESEARCH ARTICLE

Bite force and its relationship to jaw shape in domestic dogs

Colline Brassard[1,2,*], Marilaine Merlin[1], Claude Guintard[3,4], Elodie Monchâtre-Leroy[5], Jacques Barrat[5], Nathalie Bausmayer[6,7], Stéphane Bausmayer[6,7], Adrien Bausmayer[6,7], Michel Beyer[6,7], André Varlet[7], Céline Houssin[8], Cécile Callou[2], Raphaël Cornette[8] and Anthony Herrel[1]

ABSTRACT

Previous studies based on two-dimensional methods have suggested that the great morphological variability of cranial shape in domestic dogs has impacted bite performance. Here, we used a three-dimensional biomechanical model based on dissection data to estimate the bite force of 47 dogs of various breeds at several bite points and gape angles. *In vivo* bite force for three Belgian shepherd dogs was used to validate our model. We then used three-dimensional geometric morphometrics to investigate the drivers of bite force variation and to describe the relationships between the overall shape of the jaws and bite force. The model output shows that bite force is rather variable in dogs and that dogs bite harder on the molar teeth and at lower gape angles. Half of the bite force is determined by the temporal muscle. Bite force also increased with size, and brachycephalic dogs showed higher bite forces for their size than mesocephalic dogs. We obtained significant covariation between the shape of the upper or lower jaw and absolute or residual bite force. Our results demonstrate that domestication has not resulted in a disruption of the functional links in the jaw system in dogs and that mandible shape is a good predictor of bite force.

KEY WORDS: Skull, Mandible, Jaw muscles, Masticatory system, *Canis familiaris*, Lever model

INTRODUCTION

The constituents of the masticatory system have been described in some detail in the domestic dog (Barone, 2010; Budras, 2007; Curth et al., 2017; Evans and DeLahunta, 2010; Hoppe and Svalastoga, 1980; Johnson, 1979; Miller et al., 1965; Penrose et al., 2016; Robins and Grandage, 1977; Thomas, 1979; Tomo et al., 1993). During mastication, the lower jaws (i.e. the mandibles) move up or down relative to the upper jaw (here we use this term to refer to the cranium and face, following the Nomina Anatomica Veterinaria nomenclature; International Committee on Veterinary Gross Anatomical Nomenclature, 2017) by rotation about the temporomandibular joint that receives the condylar process of the mandible. These movements are driven by contractions of the jaw adductors. Acting like a lever, the forces are transmitted to the teeth, generating the bite force (Kim et al., 2018). The macroscopic arrangement of muscle fibres (i.e. muscle architecture) directly determines muscle force production. A good overall measure of this architecture is the physiological cross-sectional area (PCSA), which takes into account muscle volume, fibre length, fibre type and pennation angle (Haxton, 1944).

The extraordinary variability in the size and shape of the head (Brassard et al., 2020; Coppinger and Coppinger, 2001; Drake and Klingenberg, 2010; Miller et al., 1965; Selba et al., 2019; Wayne, 1986, 2001), and jaw muscle architecture (Brassard et al., 2020) between dog breeds raises questions about the impact of this variability on the function of the masticatory system and bite performance. Differences in skull shape between breeds have been suggested to be associated with differences in jaw strength (Case, 2013) and bite force (Ellis et al., 2008, 2009) as the shape of the neurocranium drives the size of the jaw muscles and the length and shape of the jaws determine the out- and in-lever arms of the system.

A few studies have investigated bite force in domestic dogs using the dry-skull method or *in vivo* measurements (Ellis et al., 2008, 2009; Kim et al., 2018; Lindner et al., 1995). However, quantitative data on muscle architecture that could be used to improve these models are scarce. Ellis et al. (2008, 2009) used two-lever models or multivariate regression modelling to estimate bite forces (Ellis et al., 2008, 2009; Kim et al., 2018; Lindner et al., 1995). The jaw is modelled as a two-lever system: jaw muscle cross-sectional area of the major jaw-adducting muscles, and the moment arms (the perpendicular distance between the point of application of the force and the temporomandibular joint) of the muscles (in-levers) and of bite points about the temporomandibular joint (out-levers) are approximated from skull dimensions taken from photographs. Skull length and skull width are then considered as a proxy of shape and size. Estimations obtained using the equations provided by Kiltie (1984) and Thomason (1991) were used and adjusted by values recorded *in vivo* on 20 dogs of various breeds during stimulation of the m. temporalis and m. masseter under general anaesthesia (Ellis et al., 2008). Ellis et al. (2008, 2009) also established an equation from multivariate regression analysis to estimate bite force independently of any lever model, using cranial measurements and the body mass of the same dogs for which bite force was recorded *in vivo*. However, the authors did not consider the muscle cross-sectional area and the effective moment arms of the forces in their equations. Moreover, in these two dimensional (2D) methods, the PCSA of the temporal muscle is often underestimated, while that of the m. masseter and m. pterygoideus is overestimated (Davis et al., 2010). The regression model using body mass was based on only 20 dogs of different breeds. Using these equations, negative bite forces were obtained for small brachycephalic dogs (with a

[1]Mécanismes Adaptatifs et Evolution (MECADEV), Muséum National d'Histoire Naturelle, CNRS, 55 rue Buffon, 75005 Paris, France. [2]Archéozoologie, Archéobotanique: Sociétés, Pratiques et Environnements (AASPE), Muséum National d'Histoire Naturelle, CNRS, CP55, 57 rue Cuvier, 75005 Paris, France. [3]ANSES, Laboratoire de la Rage et de la Faune Sauvage, Station Expérimentale d'Atton, CS 40009 54220 Malzéville, France. [4]Laboratoire d'Anatomie Comparée, Ecole Nationale Vétérinaire, de l'Agroalimentaire et de l'Alimentation, Nantes Atlantique – ONIRIS, Nantes Cedex 03, France. [5]GEROM, UPRES EA 4658, LABCOM ANR NEXTBONE, Faculté de Santé de l'Université d'Angers, 49933 Angers Cedex, France. [6]Club de Chiens de Défense de Beauvais, avenue Jean Rostand, 60 000 Beauvais, France. [7]Société Centrale Canine, 155 Avenue Jean Jaurès, 93300 Aubervilliers, France. [8]Institut de Systématique, Evolution, Biodiversité (ISYEB), CNRS, Muséum National d'Histoire Naturelle, Sorbonne Université, Ecole Pratique des Hautes Etudes, Université des Antilles, CNRS, CP 50, 57 rue Cuvier, 75005 Paris, France.

*Author for correspondence (colline.brassard@mnhn.fr)

C.B., 0000-0002-9789-2708; J.B., 0000-0002-7426-0249; C.C., 0000-0002-8540-8114; R.C., 0000-0003-4182-4201; A.H., 0000-0003-0991-4434

Received 28 February 2020; Accepted 18 June 2020

short and wide skull), which demonstrates that the equation is not appropriate when applied outside of the range of values for which it was developed. However, no studies to date have explored the covariation between bite force and bone shape.

In the present paper, we aimed to explore the diversity of bite force in dogs as well as the relationships between the three dimensional (3D) shape of the upper and lower jaws and bite force. To do so, we used a biomechanical model based on 3D lever mechanics using muscle data (fibre length, pennation angle, muscle mass and PCSA) and the 3D coordinates of origin and insertion of jaw adductor muscles obtained from dissection of 47 dogs of various breeds. We also report *in vivo* measurements recorded from three trained Belgian shepherd dogs (Malinois) to validate the output of our bite model. We used a combination of geometric morphometric techniques and comparative methods to: (1) assess the variability in bite force in dogs and test for differences between morphotypes; (2) test which components of the jaw adductor system are the best predictors of bite force; and (3) describe the pattern of covariation with the overall shape of the upper and lower jaws.

Dogs can be classified based on the shape of their head by using the cephalic index, a ratio between skull width and length (Helton, 2011; Koch et al., 2003). There are three morphotypes: dolichocephalic (relatively long skulls) are opposed to brachycephalic (broad skulls) dogs, and mesocephalic (moderate skulls) dogs are intermediate. As a result of selection determined by standards (Fédération Cynologique Internationale, FCI; http://www.fci.be/en/Presentation-of-our-organisation-4.html), different breeds contain animals with specific traits/metrics that can therefore be assigned to one of these three morphotypes. Excessive artificial selection has resulted in some 'hypertypes' (where some characters within a dog breed are developed to excess; Triquet, 1999; Guintard and Class, 2017) among brachycephalic or dolichocephalic groups, showing exaggerated morphotypes. Given that our sample is small and gathers non-pure-breed dogs, we here focused on the impact of the morphotype (Roberts et al., 2010) only and compared brachycephalic with mesocephalic and dolichocephalic dogs. As previously stated by numerous authors (Ellis et al., 2008, 2009; Kim et al., 2018; Lindner et al., 1995), the combined variability in size and morphology – pertaining to both skull shape and jaw muscle architecture – among morphotypes probably significantly explains the variability in estimated bite force. For example, as suggested by Ellis et al. (2009), we expected bite forces to be higher in large brachycephalic dogs than in other morphotypes. Here, we aimed to describe the relationships between the overall morphology and bite force.

Moreover, we expected intensive breeding for aesthetic reasons or functional ability to potentially have perturbed the functional relationships between the different components of the feeding system as diet no longer imposes constraints on the jaw system. Indeed, the domestication of dogs has led to a release from ecological constraints, which may have increased the diversity in a large array of genes as aberrant phenotypes were no longer selected against (Björnerfeldt et al., 2006). Recent dog breeds largely feed on processed food requiring little or no chewing. Given that bite force is usually a good indicator of dietary diversity as it directly determines prey size and feeding ecology (Aguirre et al., 2002; Cornette et al., 2013, 2015; Dollion et al., 2017; Felice et al., 2019; Firmat et al., 2018; Forbes-Harper et al., 2017; Herrel and Holanova, 2008; Herrel et al., 2001, 2005; Huber et al., 2009; Kerr et al., 2017; Maestri et al., 2016; Marcé-Nogué et al., 2017; Nogueira et al., 2009; Sagonas et al., 2014; Santana et al., 2010; Van Daele et al., 2009; Verwaijen et al., 2002; Young and Badyaev, 2010), one would expect a disruption between bite force and bone shape, resulting in low coefficients of covariation (or possibly non-significant coefficients) across dogs as a whole.

MATERIALS AND METHODS

Materials

The dataset is composed of 47 dog heads (Table 1). Breeds were estimated based on morphological similarities with dogs from existing standards. Beagles are the most represented, with 10 specimens. Given that most of the breeds are represented by only one specimen and that most of the dogs are likely to be cross-breeds, our sample does not allow any conclusion at the breed level.

To test for the effect of the morphotype (brachycephalic, mesocephalic or dolichocephalic), the cephalic index (CI) was calculated following Roberts et al. (2010): skull width/skull length×100 (Fig. 1). Skull width was measured between the two zygomatic arches (landmark 37 and the symmetric landmark to the sagittal plane), and skull length was measured from the anterior tip at the end of the suture of the nasal bones (landmark 2) to the most posterior point on the occipital protuberance (landmark 14). The brachycephalic dogs have the most elevated values of CI, the dolichocephalic dogs have the lowest values, and the mesocephalic dogs have intermediate values. Given that there is no clear consensus on the boundary between groups (Roberts et al., 2010), we chose limits to ensure that the three groups were similar in size.

Table 1. List of specimens used in this study, showing related breed, morphotype and age estimations

Morphotype and related breeds	*N*	Age	CI
Brachycephalic dogs (*n*=16)			
American Staffordshire terrier	1	1C	73
Boxer	2	2D	80–84
Bulldog	2	1C–1D	85–93
Bull terrier	1	1A	70
Chihuahua	1	1C	72
Cane corso	1	1D	81
Cavalier King Charles spaniel	1	1D	81
Continental toy spaniel papillon	1	1C	83
Pitbull	1	1D	74
Rottweiler	2	2C	70–77
Mastiff	1	1C	70
Other (non-estimated)	2	2D	72–78
Mesocephalic dogs (*n*=15)			
Beagles	10	1B–8C–1D	62–69
Fox terrier	1	1D	63
Belgian shepherd – Tervueren	1	1D	67
Mastiff	1	1D	66
Other (non-estimated)	2	2D	61–63
Dolichocephalic dogs (*n*=16)			
Belgian shepherd – Tervueren	1	1D	58
Border collie	2	1C–1D	59–59
Collie	1	1D	46
Dachshund	1	1C	55
Deerhound	1	1D	57
Dobermann	1	1D	59
German shepherd	1	1D	52
Golden retriever	1	1C	59
Husky	1	1C	59
Leonberger	1	1C	58
Shetland sheepdog	1	1C	50
Other (non-estimated)	4	1C–3D	54–59
Total	47	1A–1B–22C–23D	

CI, minimal and maximal cephalic index calculated for each breed, following Roberts et al. (2010). A, juveniles; B, young adults; C, adults; D, old adults. See Table S1 for a complete list of the specimens used in the analyses.

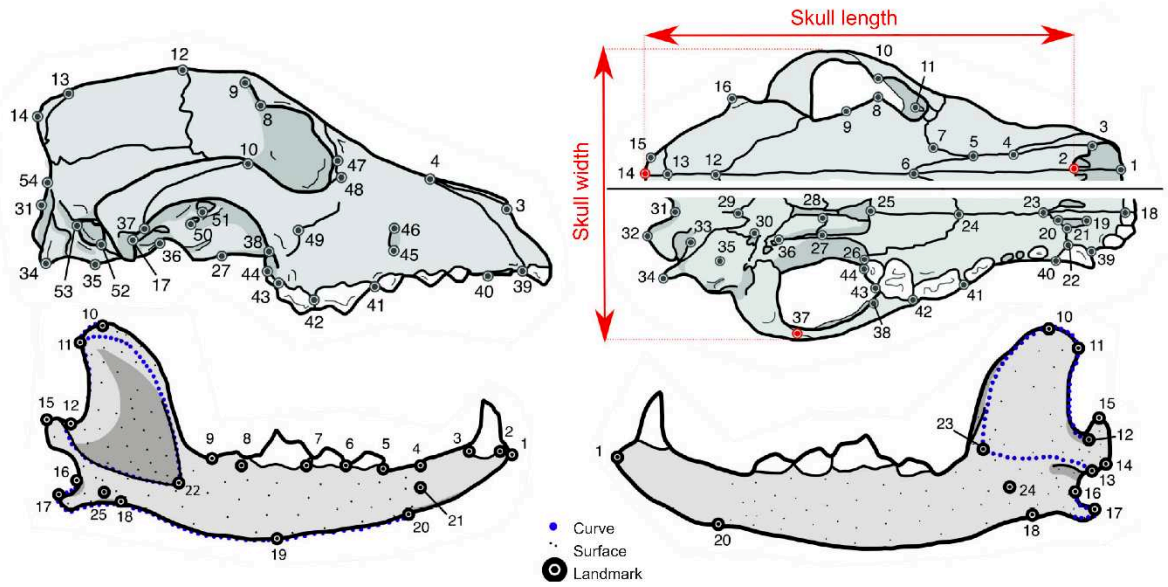

Fig. 1. Landmarks considered in this study for the geometric morphometrics analysis. True landmarks are in black or red, sliding semi-landmarks of curves are in blue and sliding semi-landmarks of surface are in grey. The landmarks in red were used to calculate skull length and width, which were used to estimate the cephalic index. Detailed definitions of the landmarks are provided in Table S2.

Specimens within the same breed can thus be classified into two adjacent morphotypes because they fall on either side of a morphotype boundary. This may be linked to age-related changes that can push skulls from one type to another. Dogs with a CI <0.70 were considered brachycephalic and the dogs with a CI <0.60 were considered dolichocephalic; dogs with an intermediate CI were mesocephalic.

Age was estimated based on the aspect of the cranial sutures (degree of closure), tooth wear and bone texture. Group A corresponds to dogs with molar teeth still erupting, a very porous mandible (minute interstices were observable with the naked eye) and unclosed cranial sutures (4–6 months according to Barone, 2010). Group B corresponds to dogs with the basispheno-basioccipital suture still open (<8–10 months according to Barone, 2010) and a still-porous mandible. Group D corresponds to old dogs with a closed interfrontal suture and worn denture (>3–4 years). Group C corresponds to intermediate adults (from 10 months to 3 years). We chose to keep the youngest individuals in our analyses to increase the morphological variability in the sample but they are far under-represented (only one dog in group A and one dog in group B) More detailed information about the sample is given in Table S1.

Muscle data

We focused on the adductor muscles of the jaw only, because they are involved in mouth closing and bite force generation. The m. pterygoideus medialis and lateralis were considered together because the m. pterygoideus lateralis is very small and difficult to clearly distinguish (Brassard et al., 2020). We considered the constituent bellies of the following jaw adductor muscles (following Penrose et al., 2016): m. masseter pars superficialis (MS), m. masseter pars profunda (MP), m. zygomaticomandibularis anterior (ZMA), m. zygomaticomandibularis posterior (ZMP), m. temporalis pars suprazygomatica (SZ), m. temporalis pars superficialis (TS), m. temporalis pars profunda (TP) and m. pterygoideus (P). The mass and the PCSA were measured from dissections (Brassard et al., 2020). In a previous study, we measured muscle mass using a digital scale (Mettler Toledo AE100) and then we sectioned the muscle along its long axis to measure fibre lengths and pennation angles directly on the muscle. With these data, we calculated the reduced PCSA (Haxton, 1944), using a density of 1.06 g cm^{-3} (Mendez and Keys, 1960) and the mean of five measurements of the pennation angle and fibre length taken on different parts of the muscle. We used the following formula:

$$\text{PCSA} = \frac{\text{mass} \times \cos(\text{angle of pennation})}{1.06 \times \text{fibre length}}, \quad (1)$$

where mass is in g, pennation angle is in rad and fibre length is in cm.

Shape of the upper and lower jaws

3D geometric morphometric analysis was used to describe the patterns of morphological variation. R version 3.6.0 (2019-04-26; http://www.R-project.org/) was used for all statistical analyses.

For the lower jaw, we considered 25 landmarks, 190 sliding semi-landmarks on curves and 185 sliding semi-landmarks on surfaces that were placed on 3D reconstructions of the lower jaw obtained using photogrammetry (Brassard et al., 2020; the 3D models of the mandibles are available on request from the corresponding author). A 3D sliding semi-landmark procedure was performed to transform all the landmarks into spatially homologous landmarks (Bookstein, 1997; Gunz et al., 2005). For the upper jaw, 54 landmarks were recorded on one side (left or right) of the upper jaw using a MicroScribe MX (Revware). A mirror function was then applied to obtain the symmetrical landmarks relative to the sagittal plane using the function 'mirrorfill' from the package 'paleomorph'. This resulted in a total of 108 landmarks. Fewer landmarks were used for the upper jaw because the shapes are more easily quantified with a smaller number of landmarks. The landmarks are represented in Fig. 1 and described in Table S2.

For further visualization of shape changes, we used the 3D models of the upper and lower jaws of a beagle, obtained using photogrammetry. One-hundred and forty photographs were taken using a Nikon D5500 Camera (24.2 effective megapixels) with a 60 mm lens, by turning around the dorsal and ventral views of the

upper jaw (Fau et al., 2016). One-hundred photographs per side were taken for the lower jaw. 3D models of the jaws were obtained after merging the two sides of each jaw, using the Agisoft PhotoScan software (©2014 Agisoft LLC, St Petersburg, Russia).

A generalized Procrustes analysis (GPA; Rohlf and Slice, 1990) was performed to obtain the Procrustes shape of each jaw using the function 'procSym' (Dryden and Mardia, 2016; Gunz et al., 2005; Klingenberg et al., 2002). The centroid sizes of each jaw were used as an estimation of size.

In vivo bite force measurements

In vivo bite force data were recorded for three pure-breed Belgian shepherd dogs (Malinois) from a training club for defence dogs (Beauvais, France). The dogs are trained to bite for competitions and shows. These dogs are thus expected to bite relatively hard as a result of artificial selection by breeders for this purpose. We used a piezoelectric isometric Kistler force transducer (9311B, range ±5000 N; Kistler Inc., Winterthur, Switzerland) linked to a charge amplifier (type 5058A5, Kistler Inc.) similar to the one used for large turtles in Herrel et al. (2002). The transducer was mounted in a custom set-up and fixed on a wooden stick and covered by hessian fabric to protect the teeth of the dog and to provide a known bite substrate (see Movie 1). We performed several consecutive trials (at least 4) for each animal. The dogs did not all bite at exactly the same position on the transducer, so we had to correct the recorded bite force for each trial by taking into account the distance between the real location of the bite that we recorded *in vivo* and the sensor (corrected BF=recorded BF×distance between the sensor and the bite plates of the transducer/distance between the location of the bite and the sensor). For this purpose, we filmed each trial so we could extract the location of the bite relative to the sensor. The dogs bit at a gape angle of about 40–45 deg while grabbing the hessian cover with the last premolar teeth. We retained the maximal corrected bite force recorded across all trials for analyses. Head length and width were measured from photographs. The obtained values were used to validate the model output for shepherd dogs of a similar size biting on the first lower molar tooth at 40 deg.

Bite model

To estimate bite force, we used a 3D lever model similar to that described by Herrel et al. (1998a,b). The movement of the lower jaw near occlusion is mainly rotational so we did not consider any translational movement. All bite points then rotate in an arc for which the radius corresponds to the shortest distance from the condylar process of the mandible to the point of application of the bite force.

At static force equilibrium, for each side (left or right), the sum of the moments of the external forces is zero (positive moments of all the muscles on one side plus negative moments of the bite force on one side). The moment is a vector that corresponds to the vectorial product of the moment arm and the force. The magnitude of the moment thus corresponds to the product of force magnitude and the shortest distance between the centre of the system and the line of action of the force. The muscular forces were established by multiplying the reduced PCSA by a conservative muscle stress estimate of 30 N cm^{-2} (Herzog, 1994). The maximal bite forces were then deduced from the sum of the muscle moments for each side, and doubled, considering that the adductor muscles on both sides are contracting maximally during maximal effort biting.

We can then estimate the resulting maximal bite force as follows:

$$\sum_{i=1}^{8} \overrightarrow{M_{\text{muscles}_{\text{one side}}}} + \overrightarrow{M_{\text{BF}_{\text{one side}}}} + \overrightarrow{M_{\text{JF}_{\text{one side}}}} = \vec{0}$$

$$\Leftrightarrow \sum_{i=1}^{8} \overrightarrow{F_{\text{muscles}_{\text{one side}}}} \Lambda \overrightarrow{\text{id}} = \overrightarrow{\text{BF}_{\text{one side}}} \Lambda \overrightarrow{\text{od}}$$

$$\Leftrightarrow \text{BF}_{\text{two sides}} = 2 \times \left(\frac{\sum_{i=1}^{8} \text{PCSA} \times 30 \times \text{eid}}{\text{eod}} \right), \quad (2)$$

where eid is the length representing the effective in-lever arms:

$$\text{eid} = \text{id} \times \sin\theta, \quad (3)$$

and eod is the length representing the effective out-lever arms:

$$\text{eod} = \text{od} \times \sin\theta', \quad (4)$$

where $\vec{M}$ represents the moment of the corresponding force, $\overrightarrow{\text{BF}}$ represents the vector of bite force, BF is the norm of the bite force, $\overrightarrow{\text{JF}}$ is the vector of the joint force, $\overrightarrow{\text{id}}$ and $\overrightarrow{\text{od}}$ are the vectors of the in-lever and out-lever arm, respectively, θ is the angle between $\overrightarrow{F_{\text{muscles}}}$ and $\overrightarrow{\text{id}}$, and θ' is the angle between $\overrightarrow{\text{BF}}$ and $\overrightarrow{\text{od}}$.

To calculate the effective length of the lever arm for all the muscle moments, we used the 3D coordinates of origin and insertion of each muscle (Fig. S1) that we recorded with a microscribe. We first chose a reference frame with a centre located at the right temporomandibular joint (Fig. 2). The *x*-axis runs through the

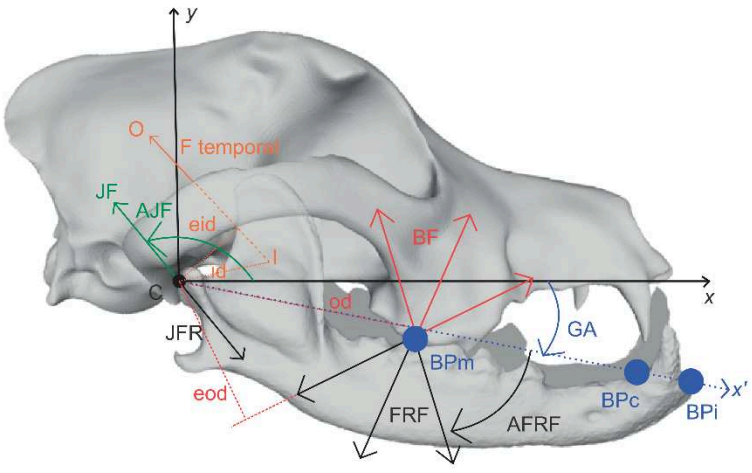

Fig. 2. Schematic illustration of the 3D lever model for bite force estimation. Solid lines represent the *x*- and *y*-axes for a 0 deg gape angle. The dotted line represents the *x*-axis for a non-zero gape angle. For the adductor muscle forces, only the force exerted by the m. temporalis pars profunda is represented. C, centre of rotation of the system; GA, gape angle; BF, bite force; FRF, food reaction force; AFRF, angle of food reaction force; JF, joint force; JFR, joint force reaction; AJF, angle of joint force; BPi, bite point on the incisor teeth; BPc, bite point on the canine tooth; BPm, bite point on the carnassial tooth; F temporal, force exerted by the m. temporalis pars profunda; O, origin of the m. temporalis pars profunda; I, insertion of the m. temporalis pars profunda; id, vector of the in-lever arm of the m. temporalis pars profunda; od, vector of the out-lever arm; eid, distance of the effective in-lever arm of the m. temporalis pars profunda; eod, distance of the effective out-lever arm.

rostral border of the right mandible, just medially to the first incisor, and the *y*-axis is directed towards the top of the skull and perpendicular to *x*. The approximate centroid of the origin and insertion areas of the muscles were used, based on observations from our dissections (Brassard et al., 2020). We also recorded the 3D coordinates of three possible points of application of the food reaction force: at the incisor teeth, at the lower canine tooth and at the lower carnassial tooth (point between the fourth upper premolar tooth P^4 and the first lower molar tooth M_1). We chose these locations as they are important during feeding in canids. The first point is at the first incisor tooth (BPi in Fig. 2), the second one is just behind the lower canine tooth (BPc in Fig. 2) and the last one is located on the caudal part of the lower carnassial tooth, which corresponds to the contact area between P^4 and M_1 (BPm in Fig. 2). The last two points are compatible with the bite points chosen by Ellis et al. (2008, 2009).

The bite force vector is opposed to the food reaction force. Given that we do not know the direction of the food reaction force (which may depend upon the shape, texture and position of the food item as well as the shape and position of the teeth; Herrel et al., 1998b; Cleuren et al., 1995), we calculated the moment of the food reaction force for a large range of angles thereof (set to vary between −40 and −140 deg with respect to the lower jaw). We calculated the bite forces for several mouth opening angles (0, 20 and 40 deg). The magnitude and orientation of the joint forces were estimated as well because, at static equilibrium, the sum of the external forces (muscle and bite forces) is zero.

The input for the model, therefore, consists of the PCSA of the jaw muscles, muscle origins and insertions, mouth opening angle, and the point of application of the bite force. Model output consists of the magnitude of the bite forces, the magnitude of the joint forces, and the orientation of the joint forces at any given orientation of the food reaction forces. An R script for the calculation of the bite force is available on request from the corresponding author.

Bite force drivers

As previously suggested for muscle data, bite force is expected to be highly dependent on size (Brassard et al., 2020). To test whether skull length or the centroid size of the jaws is a driver of bite force, we performed linear regressions on bite force and $\log_{10}$ of skull length or $\log_{10}$ of centroid size of the upper or lower jaw using the function 'lm'. The importance and significance of the correlation between bite force and the centroid size of the bone were explored using the function 'cor.test'. The residuals of these two regressions are further considered as 'residual bite forces'.

To test for differences in bite force between morphotypes (brachycephalic, dolichocephalic and mesocephalic), an ANOVA and a linear model were calculated on residual bite forces using the functions 'anova' and 'lm'. *Post hoc* tests were performed using the function 'TukeyHSD'.

To investigate the muscular drivers of bite force (to determine which muscle contributed the most to the variation in bite force among the muscle bundles we dissected), we performed a linear regression of the bite force on the mandibular centroid size and main muscle mass, fibre length, pennation angle and PCSA using the function 'lm'. For this analysis only, we considered the three main adductor complexes to increase statistical power and avoid noise in the data: the masseter complex, the temporal complex and the pterygoid complex. Among each complex, fibre length and pennation angle were averaged while mass and PCSA were summed. Data were $\log_{10}$-transformed before analyses. We considered the calculated bite force for a food reaction force orientation of 90 deg and a gape angle of 20 deg. The best-fitted models were obtained from stepwise model selection by AIC using the function 'stepAIC' from the package 'MASS'. To compare the contribution of each bundle to the bite force, we calculated the ratio of the moment exerted by each muscle and the moment exerted by the bite force at the lower carnassial tooth. We performed Friedman tests and *post hoc* tests using the functions 'friedman.test' and 'posthoc.friedman.nemenyi.test' from the package 'PMCMRplus' to compare the contribution of each bundle for the four gape angles and to compare the contribution of the three main muscular complexes for a gape angle of 0 deg.

To test whether the shape of the upper or lower jaws is a driver of bite force, we performed Procrustes ANOVA on jaw shape and bite force or residual bite force using the function 'procD.lm' from the package 'geomorph' (Adams and Collyer, 2016, 2017; Anderson, 2001; Anderson and Braak, 2003; Collyer et al., 2015; Goodall, 1991).

Covariation between bite force and the shape of the jaws

We explored the covariations between bite force (block 1) and the Procrustes coordinates of the upper or lower jaw (block 2). The patterns of covariation were explored using two-block partial least square (2B-PLS) analysis with the function 'pls2B' from the package 'Morpho' (Rohlf and Corti, 2000). The 2B-PLS method constructs pairs of variables that are linear combinations of the variables within each of the two blocks and that maximize the covariance between blocks (Rohlf and Corti, 2000). With this method, PLS coefficients and *P*-values are generated. PLS coefficients are the coefficient of correlation between PLS scores (between blocks) and thus reflect the intensity of the covariation (we refer to these coefficients as coefficients of covariation, r-PLS, below). *P*-values reflect the significance of the covariation for each new axis. They are calculated by comparing the singular value with those obtained from 10,000 permuted blocks. We did not consider phylogeny (Parker et al., 2004) in our analyses because we had no indication of a pure breed membership.

For these analyses, bites force and muscle data were $\log_{10}$-transformed. 2B-PLS analysis was thus conducted between the shape of the upper or lower jaw and bite force or residual bite force. We also performed analysis for brachycephalic dogs only, and for mesocephalic/dolichocephalic dogs only. As differences in the number of variables and the number of individuals influence the PLS coefficient, a *Z*-score was calculated to compare the levels of functional integration between different types of dogs with the function 'compare.pls' from the package 'geomorph' (Adams and Collyer, 2016). The deformation of the mandible of a beagle to the consensus of the GPA was used as a reference for all visualizations. The beagle was chosen because it was the dog that was closest to the centre of the PCA describing variation in mandibular shape in our previous study (Brassard et al., 2020).

RESULTS

The model outputs for all specimens are detailed in Table S1. Although the small sample size did not allow us to describe the intra-breed variability, except for beagles, we have indicated the breeds in the Results so that future studies can expand upon our results.

Biomechanical model output and variation in bite force

The magnitude of the bite force ranged widely depending on the gape angle, bite point and orientation of the food reaction force (Table 2, Fig. 3). Mean bite force decreased when the gape angle

Table 2. Summary of calculated bite force at different gape angles for a 90 deg angle of food reaction force

Bite point	Gape (deg)	BF (N)	JF (N)	AJF (deg)
Incisor teeth	40	412±228	1065±500	131±4
	20	480±264	1042±489	134±4
	0	531±292	1018±473	139±5
Canine tooth	40	478±264	1040±487	132±4
	20	557±306	1015±474	136±4
	0	617±338	990±459	141±5
Carnassial tooth	40	846±435	912±429	140±4
	20	986±504	880±413	146±5
	0	1091±559	863±402	154±6

BF, bite force; JF, joint force; AJF, angle joint force. Table data are means±s.d.

increased. Moreover, the mean bite force estimated on the carnassial tooth was more elevated than that estimated on the canine tooth or incisor teeth. For example, for an angle of the food reaction force of 90 deg, mean bite force ranged from 412 to 531 N at the incisor teeth, from 478 to 617 N at the canine tooth and from 846 to 1091 N at the carnassial tooth, for a gape angle ranging from 40 to 0 deg. A shift of the food reaction force away from the perpendicular axis caused an increase in bite force. Contrary to mean bite force, mean joint force increased when the gape angle increased (Table 2), for all orientations of the food reaction force. For example, for an angle of the food reaction force of 90 deg, it ranged from 1018 to 1065 N at the incisors, from 990 to 1040 N at the canine tooth and from 863 to 912 N at the carnassial tooth for a gape angle ranging from 40 to 0 deg. The angle of the joint force decreased when the gape angles increased (Table 2), ranging from 131 to 139 deg for incisors, from 132 to 141 deg for the canine tooth and from 140 to 154 deg for the carnassial tooth.

For a given gape angle and bite point, a great variation in bite force exists among dogs (Fig. 4). We observed similar patterns of variation for all gape angles. To merge *in vivo* measurements recorded on the Malinois shepherd dogs with the bite forces estimated from dissection in the following descriptions, we focused on the model outputs obtained for a gape angle of 40 deg and we considered an angle of the food reaction force of 90 deg. Estimated bite force ranged from 100 to 1092 N on the incisor teeth, from 116 to 1268 N on the canine teeth and from 214 to 2172 N on the carnassial tooth. The three *in vivo* measurements were included in the overall variability of the predicted bite force. *In vivo* values were relatively close to our estimations for other dogs that are similar in shape (dog 1: 1094 N, dog 2: 688 N, dog 3: 903 N). The *in vivo* measurements thus validate our model. The dogs with the highest bite forces in our sample were the largest brachycephalic dogs, such as the rottweiler (2172 N on the carnassial tooth for one individual) and the pitbull (2051 N). The dogs with the lowest bite forces were the smallest dogs, belonging to the toy group. If we consider the 10 beagles we dissected, calculated bite forces ranged from 262 to 466 N on the incisor teeth (mean: 359 N), 302 to 481 N on the canine tooth (mean: 375 N) and 501 to 902 N on the carnassial tooth (mean: 709 N). Bite force was correlated to the length of the skull (R^2=0.33, P<0.001), as well as to the mandibular centroid size (R^2=0.54, P<0.001) and that of the upper jaw (R^2=0.41, P<0.001). Brachycephalic dogs produced higher bite forces than dolichocephalic and mesocephalic dogs when scaled to the same skull length (P<0.05 when testing for differences between brachycephalic and mesocephalic or dolichocephalic dogs), which suggests that the shape of the upper jaw is an important driver of bite force and that brachycephalic dogs produce higher bite forces. However, the Leonberger dog from our sample seems to break this trend, as it produced a bite force that was as high as that of large brachycephalic dogs. There was no significant difference between mesocephalic and dolichocephalic dogs (P>0.05).

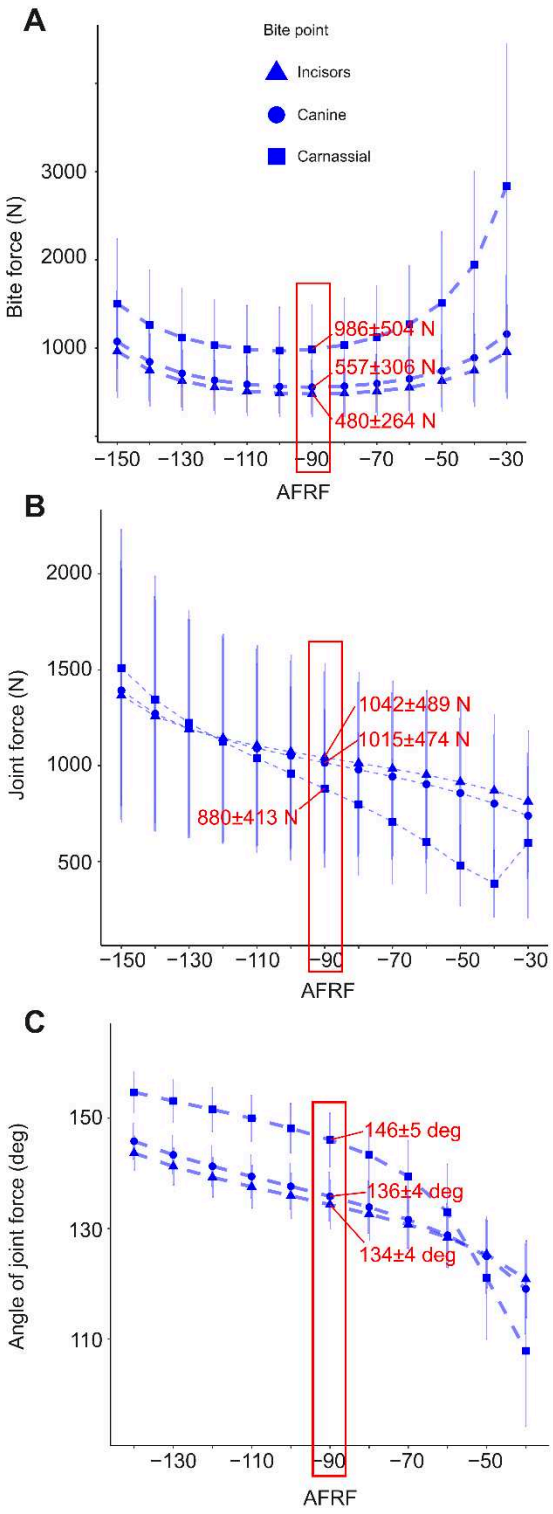

Fig. 3. Graphs representing the model output for a given range of food reaction force orientations at a gape angle of 20 deg. (A) Bite force, (B) joint force and (C) angle of the joint force for all bite points plotted against angle of the food reaction force (AFRF). Different bite points are represented by different shapes. Mean±s.d. values for all bite points at an AFRF of 90 deg are indicated in red.

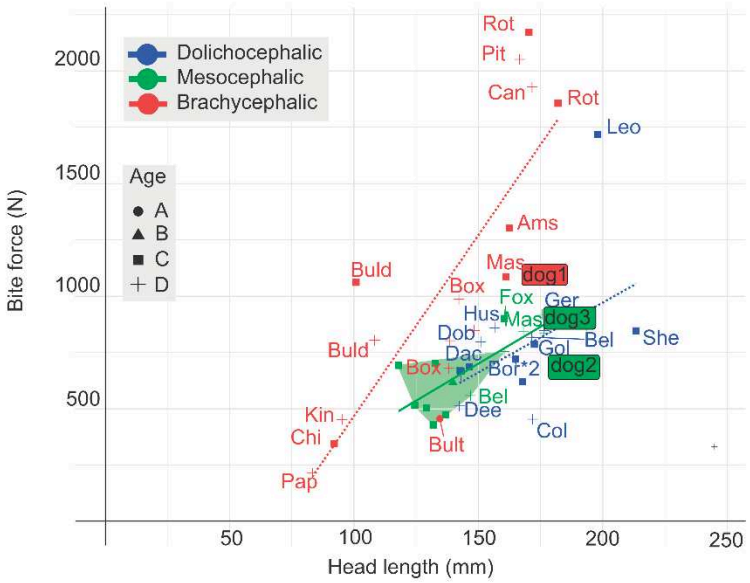

Fig. 4. Scatterplot representing the bite force on the carnassial tooth for a 90 deg angle of food reaction force and a 40 deg gape angle. Regression lines between bite force and head length are shown for the three morphotypes, which are represented by different colours. Different ages are indicated by different symbols. Rectangles indicate the three trained Belgian shepherd dogs (Malinois) from which *in vivo* bite force data were obtained to validate the output of our bite model. Ams, American Staffordshire terrier; Box, boxer; Buld, bulldog; Bult, bull terrier; Chi, chihuahua; Can, cane corso; Kin, cavalier King Charles spaniel; Pap, papillon; Pit, pitbull; Rot, rottweiler; Mas, mastiff; Fox, fox terrier; Bel, Belgian shepherd; Bor, border collie; Col, collie; Dac, dachshund; Ger, German shepherd; Gol, golden retriever; Hus, husky; Leo, Leonberger; She: Shetland sheepdog. Beagles are in the green polygon.

Functional determinants of bite force

The contributions of each adductor muscle to the total moment of the bite force are indicated in Table 3 and Fig. 5. The muscles that contributed the most to bite force are the m. temporalis pars superficialis (TS; 22%) and m. temporalis pars profunda (TP; 25%). The moment exerted by the temporal complex (SZ, TS and TP) was, on average, responsible for 50% of the moment of the bite force, while the m. masseter (MS, MP, ZMA and ZMP) was responsible for around 37% and the pterygoid (P) 13% (P<0.001 between all muscle groups according to the *post hoc* tests). We noticed that the more important the angle of mouth opening, the higher the contribution of the m. temporalis pars profunda (TP) and m. zygomaticomandibularis anterior (ZMA), and the lower the contribution of the m. masseter pars superficialis (MS) and m. temporalis pars suprazygomatica (SZ), which was supported by significant results of the *post hoc* tests after a Friedman test (P<0.05). The contribution of the m. pterygoideus (P) remained almost unchanged. The contributions of the m. temporalis pars superficialis (TS), m. masseter pars profunda (MP) and m. zygomaticomandibularis posterior (ZMP) did not significantly differ.

The centroid size of both the upper and lower jaw is a driver of bite force (upper jaw: R^2=0.41, P<0.001; lower jaw: R^2=0.54, P<0.001).

Stepwise multiple regressions with calculated bite forces at the carnassial tooth as a dependent variable and muscle mass, fibre length and PCSA as independent variables retained a significant model with mandible size (β=−0.40, P=0.02), m. masseter mass (β=0.62, P<0.001), m. temporalis (β=−0.18, P=0.08), m. pterygoideus (β=0.18, P=0.09) and m. masseter fibre length (β=−0.35, P<0.001), m. pterygoideus fibre length (β=−0.19, P=0.002), m. temporalis PCSA (β=0.44, P<0.001), m. masseter pennation angle (β=−0.10, P<0.2) and m. pterygoideus pennation angle (β=−0.10, P=0.04) as best predictors (R^2=0.97; P<0.001).

The Procrustes ANOVA showed that the shape of the upper jaw was not correlated to the absolute bite force, while the absolute bite force explained 16% of the variation in the shape of the lower jaw (P<0.001). However, the residual bite force was significantly correlated to the shape of both the upper jaw (R^2=0.17, P<0.001) and the lower jaw (R^2=0.11, P<0.001).

Covariation between bite force and jaw shape

A summary of the results of the 2B-PLS analysis is given in Table 4. Only the main results will be described further. Further visualizations are presented in Fig. S2.

We observed significant covariation between the shape of the upper and lower jaws and absolute bite force (Table 4; Fig. S2). Significant covariation with high coefficient of covariation was also observed between residual bite force and bone shape (r-PLS=0.65 for the lower jaw versus 0.62 for the upper jaw; Fig. 6). A comparison of the Z-scores indicated that there was no significant difference in the level of covariation between the upper and lower jaws and between absolute and residual bite force (P>0.05). The covariation remained significant if we distinguished brachycephalic from mesocephalic/dolichocephalic dogs in the analyses with absolute bite force, but was no longer significant in the analyses with residual bite force. This suggests that size and the diversity in shape are important drivers of the covariation.

For all analyses, the first axis of the 2B-PLS explained more than 99% of the total covariance. The large brachycephalic dogs

Table 3. Contribution of the different constituent bellies of the jaw muscles to the moment of bite force for different gape angles

Gape angle (deg)	MS	MP	ZMA	ZMP	SZ	TS	TP	P
0	13.37±2.8	10.10±3.13	8.14±3.52	5.87±2.03	3.38±1.27	21.72±3.74	24.60±4.81	12.81±3.49
20	13.18±2.78	9.94±3.09	8.37±3.57	5.84±2.02	3.02±1.15	21.79±3.75	24.92±4.99	12.94±3.59
30	13.02±2.77	9.90±3.08	8.52±3.61	5.84±2.02	2.87±1.12	21.87±3.78	25.07±5.08	12.91±3.63
40	12.80±2.75	9.86±3.07	8.70±3.66	5.84±2.02	2.77±1.14	21.98±3.83	25.22±5.19	12.82±3.67

Table data are mean±s.d. percentage contribution. MS, m. masseter pars superficialis; MP, m. masseter pars profunda; ZMA, m. zygomaticomandibularis anterior; ZMP, m. zygomaticomandibularis posterior; SZ, m. temporalis pars suprazygomatica; TS, m. temporalis pars superficialis; TP, m. temporalis pars profunda; P, m. pterygoideus (medialis and lateralis).

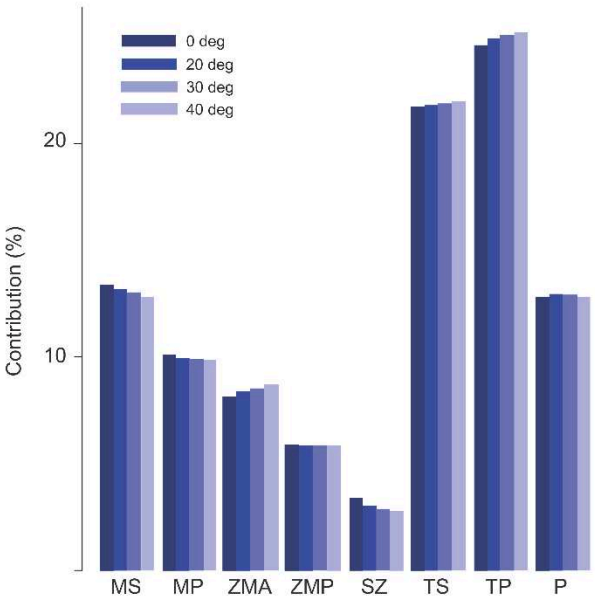

Fig. 5. Contribution of the different constituent bellies of the jaw muscles to the moment of the bite force for different gape angles. MS, m. masseter pars superficialis; MP, m. masseter pars profunda; ZMA, m. zygomaticomandibularis anterior; ZMP, m. zygomaticomandibularis posterior; SZ, m. temporalis pars suprazygomatica; TS, m. temporalis pars superficialis; TP, m. temporalis pars profunda; P, m. pterygoideus (medialis and lateralis).

occupied the left part of the scatterplot and were related to high (or relatively high) bite forces. The distinction between brachycephalic and mesocephalic/dolichocephalic dogs along the first PLS axis was even clearer for the PLS with residual bite force. This reinforces the idea that the ability of large brachycephalic dogs to produce high bite forces is related to the specific shape of both the upper and lower jaws. The beagles occupied a small part of the scatterplot, even though a small variability in the covariation was observed. Age did not seem to drive the observed covariation.

Below we describe only the covariation between bone shape and the residual bite force (Fig. 6), and we refer to Fig. S2 for covariation with the absolute bite force. Dogs that produce a low bite force for their size have an elongated, flat and straight mandibular body in the sagittal plane, a small and narrow coronoid process with a shallow masseteric fossa, a medially short and small condylar process of the mandible and a weak angular process (Fig. 6A). The upper jaw is fox-like (Fig. 6B): it is elongated, with a proportionally long, flat and narrow snout, and a reduced braincase. The zygomatic process of the frontal bone and the post-orbital constriction are not very pronounced and the zygomatic arches are narrower. The perpendicular plate of the palatal bone is reduced and the retro-articular process of the temporal bone is reduced. In contrast, the dogs that can produce a high bite force for their size have a very robust mandible with a relatively large, coronoid process with a deep masseteric fossa, a shortened, ventrally and laterally curved mandibular body, a big, medially extended and caudally curved condylar process of the mandible, and a more pronounced angular process. The upper jaw is more massive, with a proportionally shorter, wider and laterally very marked snout, and a bigger and more rounded braincase. The zygomatic arches are much larger and more distant from the cranium, and the area that bears the frontal process of the zygomatic bone is more craniodorsally elevated. The perpendicular plate of the palatal bone and the retro-articular process of the temporal bone are well developed. For both the upper and lower jaws, the cheek teeth (premolar and molar teeth) are more cranially located for the dogs that produce the highest bite forces.

DISCUSSION

The objectives of this study were: (1) to assess the variability in bite force in the domestic dog considering a wide range of breeds/morphotypes; (2) to test which components of the jaw adductor system are the best predictors of bite force; and (3) to describe the pattern of covariation between bone shape and bite force.

Bite force variability assessed by the biomechanical model

In this study, we used a biomechanical model to explore the effect of the great variation in size and shape of the jaw on bite force in dogs. We provide the first estimations of bite force using individual PCSA and 3D coordinates of attachment of the jaw adductors obtained from dissection in a sample of domestic dogs of various breeds. These data are complementary and consistent with those already available in the scientific literature (values recorded *in vivo* or under anaesthesia, estimation using the dry-skull method or regression methods calibrated by measurements obtained under anaesthesia; Ellis et al., 2008, 2009; Lindner et al., 1995). For comparative purposes, we here focus on estimates for a gape angle of 30 deg. We estimated bite forces from 124 to 1380 N (mean: 520 N) on the canine tooth and from 229 to 2364 N (mean: 919 N) on the lower carnassial tooth. The strongest biters in our sample were the rottweiler and pitbull, with values exceeding 2000 N at the carnassial tooth. Lindner et al. (1995) provided *in vivo* measurements on 22 dogs of various breeds ranging from 13 to 1394 N (there is no mention of the bite point). Ellis et al. (2008) measured values under anaesthesia on 20 dogs of various breeds ranging from 147±6.9 to 926±8.1 N on the canine tooth and from 574±83.2 to 3417±43.1 N on the lower carnassial tooth. Ellis et al.

Table 4. Results of two-block partial least square (2B-PLS) analysis comparing the shape of the lower and upper jaws against log_{10} bite force

	Shape–BF				Shape–residual BF			
Bone	Axis	% CV	*P*	r-PLS	Axis	% CV	*P*	r-PLS
Lower jaw								
All (*n*=47)	PLS 1	100	0.001	**0.75**	PLS 1	100	0.001	**0.65**
Brachycephalic (*n*=16)	PLS 1	100	0.001	**0.95**	PLS 1		>0.05	0.65
Other (*n*=31)	PLS 1	100	0.001	**0.74**	PLS 1		>0.05	0.67
Upper jaw								
All (*n*=47)	PLS 1	99	0.036	**0.68**	PLS 1	100	0.001	**0.62**
Brachycephalic (*n*=16)	PLS 1	100	0.022	**0.86**	PLS 1		>0.05	0.68
Other (*n*=31)	PLS 1	100	0.007	**0.63**	PLS 1		>0.05	0.49

BF, bite force; % CV, percentage of covariation explained by the axis of interest; r-PLS, coefficient of covariation between the two variables. Significant results are in bold.

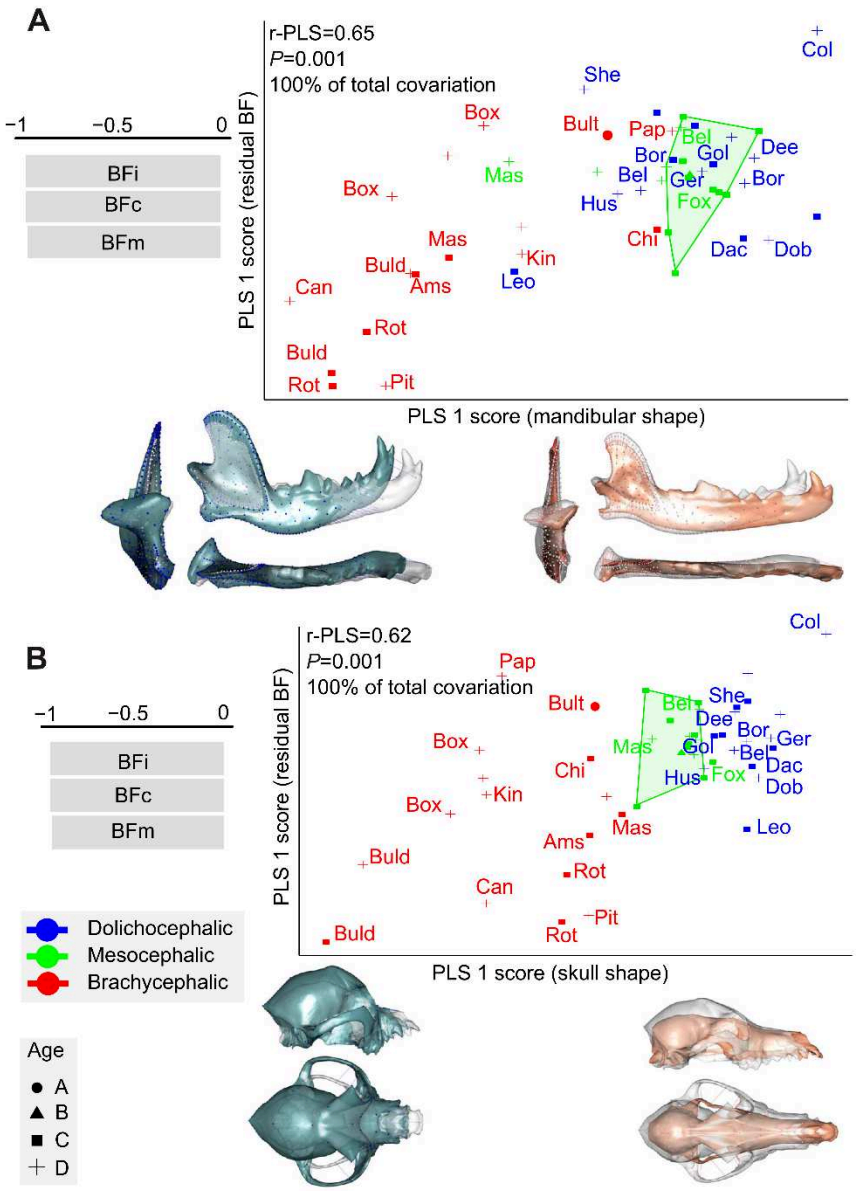

Fig. 6. Two-block partial least square (2B-PLS) analysis of the shape of the jaw versus residual bite force (BF). Bite force vectors and shapes at the minimum and maximum of the PLS axis are shown. (A) Lower jaw. (B) Upper jaw. Illustrations represent deformations from the consensus to the extreme of the axis in lateral, dorsal and caudal views. Different morphotypes are indicated by different colours and ages are indicated by different symbols. r-PLS, coefficient of covariation between the two variables. BFi, bite force at the incisor teeth; BFc, bite force at the canine tooth; BFm, bite force at the molar tooth. Ams, American Staffordshire terrier; Box, boxer; Buld, bulldog; Bult, bull terrier; Chi, chihuahua; Can, cane corso; Kin, cavalier King Charles spaniel; Pap, papillon; Pit, pitbull; Rot, rottweiler; Mas, mastiff; Fox, fox terrier; Bel, Belgian shepherd; Bor, border collie; Col. collie; Dac, dachshund; Ger, German shepherd; Gol, golden retriever; Hus, husky; Leo, Leonberger; She, Shetland sheepdog. Beagles are in the green polygon.

(2009) estimated bite forces up to 4468 N on the lower carnassial tooth with their regression models and up to 3338 N with the dry-skull method as described by Thomason (1991). It is difficult to ascertain whether our estimates are more accurate than those of Ellis et al. (2008, 2009). Their studies were based on a simple 2D analysis of bite force supported by experimental determination of bite force on 20 dogs of a range of shapes and breeds. The present work included the muscle architecture and craniomandibular shape, combined with *in vivo* measurements of bite force from individuals of one breed (Malinois). Our results demonstrated excellent correspondence for dogs of similar size and shape, thus validating our model. Similar validation for other breeds is needed, however, to be able to confirm that our model provides reliable results irrespective of breed or shape.

Determinants of bite force

The m. temporalis was found to contribute to half of the estimated bite force. Its contribution even tended to increase when the gape angle increased, which is related to the significantly increasing contribution of its deep bundle, and shows that it provides a performance advantage at large gapes. This is consistent with the need for carnivores to produce high bite forces at large gapes (Herrel et al., 2008; Turnbull, 1970). As demonstrated for other species (Herrel et al., 1998b; Bourke et al., 2008; Cleuren et al., 1995; Dumont and Herrel, 2003; Herrel et al., 2008; Kerr et al., 2017), the bite force and angle of reaction force in the joint (relative to the upper jaw) decrease as the mouth opening angle increases, and as food reaction forces move away from the orthogonal to the lower jaw. The reaction force, in contrast, increases.

Our results show that bite force is extremely variable in dogs and that it increases as size increases, as expected. However, we found significant differences in the residual bite force between brachycephalic dogs and the two other morphotypes. These results are consistent with the results of Ellis et al. (2009) and are coherent with lever mechanics. A short out-lever transmits a high

force for a small movement: breeds with a shorter lower jaw will produce a relatively higher bite force (Slater et al., 2009). Conversely, a long lever arm (related to a longer lower jaw, as in dolichocephalic dogs) transmits a lower force but the amplitude of its movement is larger. We found no significant difference between the mesocephalic and dolichocephalic dogs, but this is probably due to our sample which contained very few extreme dolichocephalic dogs. The limits between the groups are further somewhat arbitrary and depend on the definitions used by different authors (Ellis et al., 2009; Miller et al., 1965; Roberts et al., 2010). To make homogeneous groups, we chose a relatively high value of the cephalic index of 0.6 to distinguish mesocephalic and dolichocephalic dogs. However, Miller et al. (1965) stated that the mean value was 0.39 for dolichocephalic dogs versus 0.52 for mesocephalic dogs and 0.81 for brachycephalic dogs. This could explain why we did not find a difference between these two groups. It would be interesting to add some graioid dogs (greyhounds) and other large dolichocephalic dogs (Leonberger) in future analyses.

The huge diversity in bite force observed can be expected to be related to the use of the dogs and the task they have been bred for. The distinction between the large brachycephalic dogs and the other dogs (small brachycephalic, mesocephalic and dolichocephalic dogs) in our sample might indeed be the result of different selection practices. Most of the large brachycephalic dogs are historically dedicated to the protection of humans (such as the rottweiler), whereas small brachycephalic dogs are dedicated to companionship, and mesocephalic or dolichocephalic dogs are dedicated to herding or hunting. For skills such as protection or attacking, breeders try to improve biting or gripping ability. Thus, it is not surprising to observe relatively higher bite forces in large brachycephalic dogs that were bred for defence/attack rather than dogs bred for herding or hunting, which are more commonly dolichocephalic. Previously, trade-offs between these two functions have been demonstrated in the musculoskeletal system (Cameron et al., 2013; Helton, 2011), suggesting that running/scent hound dogs are likely to be poor biters. Interestingly, the Leonberger, despite being dolichocephalic, is classified in group 2 of the FCI, with molossoid breeds and mountain-type dogs such as the rottweiler and cane corso. The breed is derived from a mixture of a Newfoundland, a grand St Bernhard and a Pyrenean mountain dog. It is thus not surprising that this dog produces bite forces as elevated as those of the other large brachycephalic dogs in our sample. To investigate the influence of inbreeding and genetic heritage on the functional abilities of the masticatory apparatus, a much bigger sample, including at the intra-breed level is, however, required.

A high intra-breed variability was also observed. If we consider the 10 beagles we dissected, calculated bite forces ranged from 262 to 466 N on the incisor teeth (mean: 359 N), 301 to 543 N on the canine tooth (mean: 418 N) and 559 to 1018 N on the carnassial tooth (mean: 790 N). Age, size and sex are probably important drivers of this variability. Moreover, changes throughout life may also influence bite force, as mammals are very plastic even at late life-history stages (Scott et al., 2014). Differences related to pathologies may further influence cortical bone modelling or muscle architecture. Diet and training probably also influence muscle development and bone shape and need to be taken into account to understand the intra-breed variability in bite force. The influence of training is a fundamental issue that would be worth exploring further. Indeed, exercise can improve masticatory function (Bourke et al., 2008; He et al., 2013; Kiliaridis et al., 1995; Kim et al., 2018; Lindner et al., 1995; Shirai et al., 2018; Thompson et al., 2001) but few studies have investigated this in detail.

Shape predictors of bite force

The shape of the upper and lower jaws is significantly related to the absolute or residual bite force. The 2B-PLS analysis indicated that the curvature of the mandibular body, the relative size of the coronoid process and its processes, as well as the shape of the zygomatic arches relative to that of the neurocranium (which determines the space that is available for the adductor muscles to pass through) influence bite force variation. Overall, the presence of hypertypes with malocclusion between the lower and upper jaws (frequent in the small brachycephalic dogs), did not seem to alter the patterns of covariation much. However, there was significant variability in the data and caution is needed when interpreting the functionality of specific shapes, in particular with regard to the small brachycephalic dogs. In the 2B-PLS analysis with absolute bite force (Fig. S2), these dogs slightly diverged from the overall pattern. The shape of the upper or lower jaw alone can therefore lead to an overestimation of the absolute bite force in these small dogs, hence the need to take into account size in the estimates. The visualizations provided by the 2B-PLS analysis with residual bite force and the shape of the upper jaw show that similar shapes along axis 1 can produce very different relative bite forces, especially in brachycephalic dogs (e.g. the papillon dog versus the cane corso dog; Fig. 6): the small brachycephalic dogs produce much lower relative bite forces compared with other dogs of similar shape along axis 1. This supports previous observations by Ellis et al. (2009). The authors suggest that there is an interaction between shape and size for bite force and that shape may not be a significant factor in determining bite force in small brachycephalic dogs. Further studies including more hypertypes (small brachycephalic dogs) would be necessary to confirm that domestication did not completely disrupt the patterns of integration. Finally, it would be interesting to compare the coefficients with those of wild or commensal canids (wolves, dingoes) to test whether domestication has led to a decrease in the functional integration in the masticatory apparatus.

The shape of the lower jaw appears to be a better predictor of absolute bite force than the shape of the upper jaw (i.e. the results for the upper jaw are not significant for the Procrustes ANOVA; the variability of the point cloud along axis 1 of the 2B-PLS of the upper jaw is greater). This is consistent with the specialization of the lower jaw towards a single function (mastication), while the upper jaw has to cope with many functional demands related to the sensory organs, protection of the brain, etc. The strong relationship observed between the lower jaw and bite force should enable us to make predictions of bite force based on bone remains from the fossil record. Our study focused on the relationships between the overall shape of the bones and bite force, but did not allow us to explore the relationships between bone structure and the loads imposed during mastication. Finite element analysis may be an interesting complementary approach for this purpose (Bourke et al., 2008; Kim et al., 2018; Penrose et al., 2020; Wroe et al., 2007). Moreover, exploring the link between bone cortical thickness and bite force may be of interest to track functional variation according to load resistance (Cox et al., 2015; Kupczik et al., 2007; Rayfield, 2007; Ross et al., 2005).

Conclusions

The use of data on the muscle architecture obtained from dissections enabled us to describe the functional links between the muscular and bony components of the jaw system. The extreme variability in bite force in dogs is related to the extreme variability in size and shape, with brachycephalism conferring a mechanical advantage, as well as a great variation in muscle architecture (PCSA). Overall, it seems

that the masticatory system is strongly integrated in dogs and that the strong relationships between the lower jaw and bite force observed are promising in terms of predictions using the 3D shape of the mandible only (which may be interesting, for example, in archaeology).

Acknowledgements
We thank Manuel Comte, Mickaël Godet and Frederic Lebatard for their help in managing specimens and their helpful discussions about the preparation of the skulls. We also thank Marie-France Varlet, member of the Société Centrale Canine and President of the Belgian Shepherd Dog Club (France). We also thank Arnaud Delapré for his help with photogrammetry. We are very grateful to the two anonymous reviewers for their comments and their valuable contribution to the manuscript.

Competing interests
The authors declare no competing or financial interests.

Author contributions
Conceptualization: C.B., C.C., R.C., A.H.; Methodology: C.B., M.M., C.C., R.C., A.H.; Software: C.B., M.M., R.C.; Validation: C.B., M.M.; Formal analysis: C.B., M.M.; Investigation: C.B., M.M., N.B., S.B., A.B., M.B., A.V., C.H., R.C., A.H.; Resources: C.G., E.M.-L., J.B., N.B., S.B., A.B., M.B., A.V., A.H.; Data curation: C.B., M.M.; Writing - original draft: C.B., A.H.; Writing - review & editing: C.B., C.G., E.M.-L., R.C., A.H.; Visualization: C.B.; Supervision: R.C., A.H.; Project administration: C.C., R.C., A.H.; Funding acquisition: A.H.

Funding
This research was funded by the Ministère de l'Enseignement supérieur, de la Recherche et de l'Innovation.

Supplementary information
Supplementary information available online at
https://jeb.biologists.org/lookup/doi/10.1242/jeb.224352.supplemental

References

Adams, D. C. and Collyer, M. L. (2016). On the comparison of the strength of morphological integration across morphometric datasets. *Evolution* **70**, 2623-2631. doi:10.1111/evo.13045
Adams, D. C. and Collyer, M. L. (2017). Multivariate phylogenetic comparative methods: evaluations, comparisons, and recommendations. *Syst. Biol.* **67**, 14-31. doi:10.1093/sysbio/syx055
Aguirre, L. F., Herrel, A., Van Damme, R. and Matthysen, E. (2002). Ecomorphological analysis of trophic niche partitioning in a tropical savannah bat community. *Proc. R. Soc. Lond. B Biol. Sci.* **269**, 1271-1278. doi:10.1098/rspb.2002.2011
Anderson, M. J. (2001). A new method for non-parametric multivariate analysis of variance. *Austral. Ecol.* **26**, 32-46. doi:10.1046/j.1442-9993.2001.01070.x
Anderson, M. and Braak, C. T. (2003). Permutation tests for multi-factorial analysis of variance. *J. Stat. Comput. Simul.* **73**, 85-113. doi:10.1080/00949650215733
Barone, R. (2010). *Anatomie comparée des mammifères domestiques : Tome 1, Ostéologie*, 5th edn. Paris: Vigot.
Björnerfeldt, S., Webster, M. T. and Vilà, C. (2006). Relaxation of selective constraint on dog mitochondrial DNA following domestication. *Genome Res.* **16**, 990-994. doi:10.1101/gr.5117706
Bookstein, F. L. (1997). *Morphometric Tools for Landmark Data: Geometry and Biology*. Cambridge University Press.
Bourke, J., Wroe, S., Moreno, K., McHenry, C. and Clausen, P. (2008). Effects of gape and tooth position on bite force and skull stress in the dingo (Canis lupus dingo) using a 3 dimensional finite element approach. *PLoS ONE* **3**, e2200. doi:10.1371/journal.pone.0002200
Brassard, C., Merlin, M., Monchâtre-Leroy, E., Guintard, C., Barrat, J., Callou, C., Cornette, R. and Herrel, A. (2020). How does masticatory muscle architecture covary with mandibular shape in domestic dogs? *Evol. Biol.* **47**, 133-151. doi:10.1007/s11692-020-09499-6
Budras, K.-D. (ed.) (2007). *Anatomy of the Dog*, 5. rev. edn. Hannover: Schlüter.
Cameron, S. F., Wynn, M. L. and Wilson, R. S. (2013). Sex-specific trade-offs and compensatory mechanisms: bite force and sprint speed pose conflicting demands on the design of geckos (Hemidactylus frenatus). *J. Exp. Biol.* **216**, 3781-3789. doi:10.1242/jeb.083063
Case, L. P. (2013). *The Dog: Its Behavior, Nutrition, and Health*. John Wiley & Sons.
Cleuren, J., Aerts, P. and De Vree, F. (1995). Bite and joint force analysis in Caiman crocodilus. *Belg. J. Zool.* **125**, 79-94.
Collyer, M. L., Sekora, D. J. and Adams, D. C. (2015). A method for analysis of phenotypic change for phenotypes described by high-dimensional data. *Heredity* **115**, 357. doi:10.1038/hdy.2014.75
Coppinger, R. and Coppinger, L. (2001). *Dogs: A Sartling New Understanding of Canine Origin, Behavior & Evolution*. Simon and Schuster.
Cornette, R., Baylac, M., Souter, T. and Herrel, A. (2013). Does shape co-variation between the skull and the mandible have functional consequences? A 3D approach for a 3D problem. *J. Anat.* **223**, 329-336. doi:10.1111/joa.12086
Cornette, R., Tresset, A. and Herrel, A. (2015). The shrew tamed by Wolff's law: do functional constraints shape the skull through muscle and bone covariation? *J. Morphol.* **276**, 301-309. doi:10.1002/jmor.20339
Cox, P. G., Rinderknecht, A. and Blanco, R. E. (2015). Predicting bite force and cranial biomechanics in the largest fossil rodent using finite element analysis. *J. Anat.* **226**, 215-223. doi:10.1111/joa.12282
Curth, S., Fischer, M. S. and Kupczik, K. (2017). Can skull form predict the shape of the temporomandibular joint? A study using geometric morphometrics on the skulls of wolves and domestic dogs. *Ann. Anat. Anat. Anz.* **214**, 53-62. doi:10.1016/j.aanat.2017.08.003
Davis, J. L., Santana, S. E., Dumont, E. R. and Grosse, I. R. (2010). Predicting bite force in mammals: two-dimensional versus three-dimensional lever models. *J. Exp. Biol.* **213**, 1844-1851. doi:10.1242/jeb.041129
Dollion, A. Y., Measey, G. J., Cornette, R., Carne, L., Tolley, K. A., Silva, J. M. da, Boistel, R., Fabre, A.-C. and Herrel, A. (2017). Does diet drive the evolution of head shape and bite force in chameleons of the genus Bradypodion? *Funct. Ecol.* **31**, 671-684. doi:10.1111/1365-2435.12750
Drake, A. G. and Klingenberg, C. P. (2010). Large-scale diversification of skull shape in domestic dogs: disparity and modularity. *Am. Nat.* **175**, 289-301. doi:10.1086/650372
Dryden, I. L. and Mardia, K. V. (2016). *Statistical Shape Analysis: With Applications in R*. John Wiley & Sons.
Dumont, E. R. and Herrel, A. (2003). The effects of gape angle and bite point on bite force in bats. *J. Exp. Biol.* **206**, 2117-2123. doi:10.1242/jeb.00375
Ellis, J. L., Thomason, J. J., Kebreab, E. and France, J. (2008). Calibration of estimated biting forces in domestic canids: comparison of post-mortem and in vivo measurements. *J. Anat.* **212**, 769-780. doi:10.1111/j.1469-7580.2008.00911.x
Ellis, J. L., Thomason, J., Kebreab, E., Zubair, K. and France, J. (2009). Cranial dimensions and forces of biting in the domestic dog. *J. Anat.* **214**, 362-373. doi:10.1111/j.1469-7580.2008.01042.x
Evans, H. E. and DeLahunta, A. (2010). *Guide to the Dissection of the Dog*, 7th edn. St. Louis, MO: Saunders/Elsevier.
Fau, M., Cornette, R. and Houssaye, A. (2016). Photogrammetry for 3D digitizing bones of mounted skeletons: potential and limits. *Comptes Rendus Palevol* **15**, 968-977. doi:10.1016/j.crpv.2016.08.003
Felice, R. N., Tobias, J. A., Pigot, A. L. and Goswami, A. (2019). Dietary niche and the evolution of cranial morphology in birds. *Proc. R. Soc. B Biol. Sci.* **286**, 20182677. doi:10.1098/rspb.2018.2677
Firmat, C., Gomes Rodrigues, H., Renaud, S., Hutterer, R., Garcia-Talavera, F. and Michaux, J. (2018). Mandible morphology, dental microwear, and diet of the extinct giant rats Canariomys (Rodentia: Murinae) of the Canary Islands (Spain). *Biol. J. Linn. Soc.* **101**, 28-40. doi:10.1111/j.1095-8312.2010.01488.x
Forbes-Harper, J. L., Crawford, H. M., Dundas, S. J., Warburton, N. M., Adams, P. J., Bateman, P. W., Calver, M. C. and Fleming, P. A. (2017). Diet and bite force in red foxes: ontogenetic and sex differences in an invasive carnivore. *J. Zool.* **303**, 54-63. doi:10.1111/jzo.12463
Goodall, C. (1991). Procrustes methods in the statistical analysis of shape. *J. R. Stat. Soc. Ser. B Methodol.* **53**, 285-321. doi:10.1111/j.2517-6161.1991.tb01825.x
Guintard, C. and Class, A.-M. (2017). Hypertypes et standards de races chez le chien : Une histoire d'équilibre. *Bull. Académie Vét. Fr* **170**. doi:10.4267/2042/67199
Gunz, P., Mitteroecker, P. and Bookstein, F. L. (2005). Semilandmarks in three dimensions. In *Modern Morphometrics in Physical Anthropology* (ed. D. E. Slice), pp. 73-98. Boston, MA: Springer.
Haxton, H. A. (1944). Absolute muscle force in the ankle flexors of man. *J. Physiol.* **103**, 267-273. doi:10.1113/jphysiol.1944.sp004075
He, T., Stavropoulos, D., Hagberg, C., Hakeberg, M. and Mohlin, B. (2013). Effects of masticatory muscle training on maximum bite force and muscular endurance. *Acta Odontol. Scand.* **71**, 863-869. doi:10.3109/00016357.2012.734411
Helton, W. S. (2011). Performance constraints in strength events in dogs (Canis lupus familiaris). *Behav. Processes* **86**, 149-151. doi:10.1016/j.beproc.2010.07.019
Herrel, A. and Holanova, V. (2008). Cranial morphology and bite force in Chamaeleolis lizards–adaptations to molluscivory? *Zool. Jena Ger.* **111**, 467-475. doi:10.1016/j.zool.2008.01.002
Herrel, A., Aerts, P. and De Vree, D. (1998a). Static biting in lizards: functional morphology of the temporal ligaments. *J. Zool.* **244**, 135-143. doi:10.1111/j.1469-7998.1998.tb00015.x
Herrel, A., Aerts, P. and De Vree, F. (1998b). Ecomorphology of the lizard feeding apparatus: a modelling approach. *Neth. J. Zool.* **48**, 1-25. doi:10.1163/156854298X00183
Herrel, A., De Grauw, E. and Lemos-Espinal, J. A. (2001). Head shape and bite performance in xenosaurid lizards. *J. Exp. Zool.* **290**, 101-107. doi:10.1002/jez.1039
Herrel, A., O'Reilly, J. C. and Richmond, A. M. (2002). Evolution of bite performance in turtles. *J. Evol. Biol.* **15**, 1083-1094. doi:10.1046/j.1420-9101.2002.00459.x

Herrel, A., Podos, J., Huber, S. K. and Hendry, A. P. (2005). Evolution of bite force in Darwin's finches: a key role for head width. *J. Evol. Biol.* **18**, 669-675. doi:10.1111/j.1420-9101.2004.00857.x

Herrel, A., De Smet, A., Aguirre, L. F. and Aerts, P. (2008). Morphological and mechanical determinants of bite force in bats: do muscles matter? *J. Exp. Biol.* **211**, 86-91. doi:10.1242/jeb.012211

Herzog, W. (1994). Muscle. In *Biomechanics of the Musculoskeletal System* (ed. B. M. Nigg and W. Herzog), pp. 154-187. John Wiley & Sons.

Hoppe, F. and Svalastoga, E. (1980). Temporomandibular dysplasia in American Cocker Spaniels. *J. Small Anim. Pract.* **21**, 675-678. doi:10.1111/j.1748-5827.1980.tb05960.x

Huber, D. R., Claes, J. M., Mallefet, J. and Herrel, A. (2009). Is extreme bite performance associated with extreme morphologies in sharks? *Physiol. Biochem. Zool. PBZ* **82**, 20-28. doi:10.1086/588177

International Committee on Veterinary Gross Anatomical Nomenclature (2017). *Nomina Anatomica Veterinaria*, 6th edn. Hanover, Germany; Ghent, Belgium; Columbia, MO, USA; Rio de Janeiro, Brazil: Editorial Committee.

Johnson, K. A. (1979). Temporomandibular joint dysplasia in an Irish Setter. *J. Small Anim. Pract.* **20**, 209-218. doi:10.1111/j.1748-5827.1979.tb06708.x

Kerr, E., Cornette, R., Gomes Rodrigues, H., Renaud, S., Chevret, P., Tresset, A. and Herrel, A. (2017). Can functional traits help explain the coexistence of two species of Apodemus? *Biol. J. Linn. Soc.* **122**, 883-896. doi:10.1093/biolinnean/blx099

Kiliaridis, S., Tzakis, M. G. and Carlsson, G. E. (1995). Effects of fatigue and chewing training on maximal bite force and endurance. *Am. J. Orthod. Dentofac. Orthop. Off. Publ. Am. Assoc. Orthod. Its Const. Soc. Am. Board Orthod.* **107**, 372-378. doi:10.1016/S0889-5406(95)70089-7

Kiltie, R. A. (1984). Size ratios among sympatric neotropical cats. *Oecologia* **61**, 411-416. doi:10.1007/BF00379644

Kim, S. E., Arzi, B., Garcia, T. C. and Verstraete, F. J. M. (2018). Bite forces and their measurement in dogs and cats. *Front. Vet. Sci.* **5**, 76. doi:10.3389/fvets.2018.00076

Klingenberg, C. P., Barluenga, M. and Meyer, A. (2002). Shape analysis of symmetric structures: quantifying variation among individuals and asymmetry. *Evolution* **56**, 1909-1920. doi:10.1111/j.0014-3820.2002.tb00117.x

Koch, D. A., Arnold, S., Hubler, M. and Montavon, P. M. (2003). Brachycephalic syndrome in dogs. *VetLearn.com* **25**, 48-55.

Kupczik, K., Dobson, C. A., Fagan, M. J., Crompton, R. H., Oxnard, C. E. and O'Higgins, P. (2007). Assessing mechanical function of the zygomatic region in macaques: validation and sensitivity testing of finite element models. *J. Anat.* **210**, 41-53. doi:10.1111/j.1469-7580.2006.00662.x

Lindner, D., Marretta, S., Pijanowski, G., Johnson, A. and Smith, C. (1995). Measurement of bite force in dogs: a pilot study. *J. Vet. Dent.* **12**, 49-52. doi:10.1177/089875649501200202

Maestri, R., Patterson, B. D., Fornel, R., Monteiro, L. R. and de Freitas, T. R. O. (2016). Diet, bite force and skull morphology in the generalist rodent morphotype. *J. Evol. Biol.* **29**, 2191-2204. doi:10.1111/jeb.12937

Marcé-Nogué, J., Püschel, T. A. and Kaiser, T. M. (2017). A biomechanical approach to understand the ecomorphological relationship between primate mandibles and diet. *Sci. Rep.* **7**, 1-12. doi:10.1038/s41598-017-08161-0

Mendez, J. and Keys, A. (1960). Density and composition of mammalian muscle. *Metabolism* **9**, 184-188.

Miller, M. E., Christensen, G. C. and Evans, H. E. (1965). Anatomy of the Dog. *Acad. Med.* **40**, 400.

Nogueira, M. R., Peracchi, A. L. and Monteiro, L. R. (2009). Morphological correlates of bite force and diet in the skull and mandible of phyllostomid bats. *Funct. Ecol.* **23**, 715-723. doi:10.1111/j.1365-2435.2009.01549.x

Parker, H. G., Kim, L. V., Sutter, N. B., Carlson, S., Lorentzen, T. D., Malek, T. B., Johnson, G. S., DeFrance, H. B., Ostrander, E. A. and Kruglyak, L. (2004). Genetic structure of the purebred domestic dog. *Science* **304**, 1160-1164. doi:10.1126/science.1097406

Penrose, F., Kemp, G. J. and Jeffery, N. (2016). Scaling and accommodation of jaw adductor muscles in Canidae. *Anat. Rec.* **299**, 951-966. doi:10.1002/ar.23355

Penrose, F., Cox, P., Kemp, G. and Jeffery, N. (2020). Functional morphology of the jaw adductor muscles in the Canidae. *Anat. Rec.* doi:10.1002/ar.24391

Rayfield, E. J. (2007). Finite element analysis and understanding the biomechanics and evolution of living and fossil organisms. *Annu. Rev. Earth Planet. Sci.* **35**, 541-576. doi:10.1146/annurev.earth.35.031306.140104

Roberts, T., McGreevy, P. and Valenzuela, M. (2010). Human induced rotation and reorganization of the brain of domestic dogs. *PLoS ONE* **5**, e11946. doi:10.1371/journal.pone.0011946

Robins, G. and Grandage, J. (1977). Temporomandibular joint dysplasia and open-mouth jaw locking in the dog. *J. Am. Vet. Med. Assoc.* **171**, 1072-1076.

Rohlf, F. J. and Corti, M. (2000). Use of two-block partial least-squares to study covariation in shape. *Syst. Biol.* **49**, 740-753. doi:10.1080/106351500750049806

Rohlf, F. and Slice, D. (1990). Extensions of the Procrustes method for the optimal superimposition of landmarks. *Syst. Zool.* **39**, 40-59. doi:10.2307/2992207

Ross, C. F., Patel, B. A., Slice, D. E., Strait, D. S., Dechow, P. C., Richmond, B. G. and Spencer, M. A. (2005). Modeling masticatory muscle force in finite element analysis: sensitivity analysis using principal coordinates analysis. *Anat. Rec. Part Discov. Mol. Cell. Evol. Biol. Off. Publ. Am. Assoc. Anat.* **283A**, 288-299. doi:10.1002/ar.a.20170

Sagonas, K., Pafilis, P., Lymberakis, P., Donihue, C. M., Herrel, A. and Valakos, E. D. (2014). Insularity affects head morphology, bite force and diet in a Mediterranean lizard. *Biol. J. Linn. Soc.* **112**, 469-484. doi:10.1111/bij.12290

Santana, S. E., Dumont, E. R. and Davis, J. L. (2010). Mechanics of bite force production and its relationship to diet in bats. *Funct. Ecol.* **24**, 776-784. doi:10.1111/j.1365-2435.2010.01703.x

Scott, J. E., McAbee, K. R., Eastman, M. M. and Ravosa, M. J. (2014). Teaching an old jaw new tricks: diet-induced plasticity in a model organism from weaning to adulthood. *J. Exp. Biol.* **217**, 4099-4107. doi:10.1242/jeb.111708

Selba, M. C., Oechtering, G. U., Gan Heng, H. and DeLeon, V. B. (2019). The impact of selection for facial reduction in dogs: geometric morphometric analysis of canine cranial shape. *Anat. Rec.* **17**. doi:10.1002/ar.24184

Shirai, M., Kawai, N., Hichijo, N., Watanabe, M., Mori, H., Mitsui, S. N., Yasue, A. and Tanaka, E. (2018). Effects of gum chewing exercise on maximum bite force according to facial morphology. *Clin. Exp. Dent. Res.* **4**, 48-51. doi:10.1002/cre2.102

Slater, G. J., Dumont, E. R. and Van Valkenburgh, B. (2009). Implications of predatory specialization for cranial form and function in canids. *J. Zool.* **278**, 181-188. doi:10.1111/j.1469-7998.2009.00567.x

Thomas, R. E. (1979). Temporo-mandibular joint dysplasia and open-mouth jaw locking in a Bassett Hound: a case report. *J. Small Anim. Pract.* **20**, 697-701. doi:10.1111/j.1748-5827.1979.tb06684.x

Thomason, J. J. (1991). Cranial strength in relation to estimated biting forces in some mammals. *Can. J. Zool.* **69**, 2326-2333. doi:10.1139/z91-327

Thompson, D. J., Throckmorton, G. S. and Buschang, P. H. (2001). The effects of isometric exercise on maximum voluntary bite forces and jaw muscle strength and endurance. *J. Oral Rehabil.* **28**, 909-917. doi:10.1046/j.1365-2842.2001.00772.x

Tomo, S., Hirakawa, T., Nakajima, K., Tomo, I. and Kobayashi, S. (1993). Morphological classification of the masticatory muscles in dogs based on their innervation. *Ann. Anat. - Anat. Anz.* **175**, 373-380. doi:10.1016/S0940-9602(11)80047-6

Triquet, R. (1999). *Dictionnaire Encyclopédique des Termes Canins*. Éd. Maradi.

Turnbull, W. D. (1970). Mammalian masticatory apparatus. *Fieldiana: Geology* **18**, 149-356.

Van Daele, P. A. A. G., Herrel, A. and Adriaens, D. (2009). Biting performance in teeth-digging African mole-rats (Fukomys, Bathyergidae, Rodentia). *Physiol. Biochem. Zool. PBZ* **82**, 40-50. doi:10.1086/594379

Verwaijen, D., van Damme, R. and Herrel, A. (2002). Relationships between head size, bite force, prey handling efficiency and diet in two sympatric lacertid lizards. *Funct. Ecol.* **16**, 842-850. doi:10.1046/j.1365-2435.2002.00696.x

Wayne, R. K. (1986). Cranial morphology of domestic and wild canids: the influence of development on morphological change. *Evolution* **40**, 243-261. doi:10.1111/j.1558-5646.1986.tb00467.x

Wayne, R. K. (2001). Consequences of domestication: morphological diversity of the dog. In *The Genetics of the Dog* (ed. A. Ruvinsky and J. Sampson), pp. 43-60. CAB international.

Wroe, S., Clausen, P., McHenry, C., Moreno, K. and Cunningham, E. (2007). Computer simulation of feeding behaviour in the thylacine and dingo as a novel test for convergence and niche overlap. *Proc. R. Soc. B Biol. Sci.* **274**, 2819-2828. doi:10.1098/rspb.2007.0906

Young, R. L. and Badyaev, A. V. (2010). Developmental plasticity links local adaptation and evolutionary diversification in foraging morphology. *J. Exp. Zoolog. B Mol. Dev. Evol.* **314B**, 434-444. doi:10.1002/jez.b.21349

Summary: Variation in bite force in dogs is driven by their extreme morphological variation. The covariation with skull shape suggests strong functional relationships within the masticatory system despite strong artificial selection.

Chapter 4.
Comparison with other commensal canids: the dingo and the red fox

1. The red fox *Vulpes vulpes*

In article 4, we studied the relationships between the shape of the cranium, the shape of the mandible, masticatory muscle architecture (volume, PCSA) and bite force in European foxes (red and some silver), using the same methodological tools as those previously used in Chapter 3 for dogs. The results obtained were compared with those obtained for the dog in Chapter 3.

The following key points emerge from this article:

KEY POINTS

Mandible shape is as variable in commensal foxes as in domestic dogs, whereas the cranium is much more variable in domestic dogs.

⇨ **Human artificial selection has less impacted the morphological variability of the mandible compared to the cranium.**

Mandible shape is related to size and age and a sexual dimorphism exists.

Strong functional relationships are observed between the shape of the mandible and that of the cranium, or between the shape of the mandible and muscle data and bite force, but surprisingly no more than in dogs. Co-variation patterns are broadly similar (though less distinct) than those described in dogs.

⇨ **Intensive artificial selection does not appear to have disturbed the integrity of the masticatory system in dogs.**

Bite force is more correlated to the shape of the mandible than to the shape of the cranium.

⇨ **The mandible is a better item for making functional inferences in terms of bite force for commensal canids submitted to natural constraints.**

Article 4 –
Masticatory system integration in a commensal canid: interrelationships between bones, muscles, and bite force in the red fox.

Colline Brassard, Marilaine Merlin, Elodie Monchâtre-Leroy, Claude Guintard, Jacques Barrat, Hélène Garès, Arnaud Larralle, Raymond Triquet, Céline Houssin, Cécile Callou, Raphaël Cornette, Anthony Herrel

In revision for *Journal of Experimental Biology*

Masticatory system integration in a commensal canid: interrelationships between bones, muscles, and bite force in the red fox.

Colline Brassard[1,2*], Marilaine Merlin[1], Elodie Monchâtre-Leroy[3], Claude Guintard[4,5], Jacques Barrat[3], Hélène Garès[6], Arnaud Larralle[7], Raymond Triquet[8], Céline Houssin[9], Cécile Callou[1], Raphaël Cornette[9], Anthony Herrel[1].

[1] Mécanismes Adaptatifs et Evolution (MECADEV), Muséum national d'Histoire naturelle, CNRS ; 55 rue Buffon 75005 Paris, France.

[2] Archéozoologie, archéobotanique : sociétés, pratiques et environnements (AASPE), Muséum national d'Histoire naturelle, CNRS ; CP55, 57 rue Cuvier 75005 Paris, France.

[3] ANSES, Laboratoire de la rage et de la faune sauvage, Station expérimentale d'Atton, Malzéville, France.

[4] Laboratoire d'Anatomie comparée, Ecole Nationale Vétérinaire, de l'Agroalimentaire et de l'Alimentation, Nantes Atlantique – ONIRIS, Nantes Cedex 03, France.

[5] GEROM, UPRES EA 4658, LABCOM ANR NEXTBONE, Faculté de santé de l'Université d'Angers, France.

[6] Direction des Services Vétérinaires –D.D.C.S.P.P. de la Dordogne, Périgueux, France.

[7] ONCFS, 24210 Brouchaud, France

[8] Université de Lille III, France

[9] Institut de Systématique, Evolution, Biodiversité (ISYEB), CNRS, Muséum national d'Histoire naturelle, Sorbonne Université, Ecole Pratique des hautes Etudes, Université des Antilles, CNRS ; CP 50, 57 rue Cuvier 75005 Paris, France.

Corresponding author: colline.brassard@mnhn.fr

Key words

red fox; skull; mandible; jaw muscle architecture; geometric morphometrics; domestication

Summary statement

Strong interrelationships between the components of the masticatory system in red foxes suggest that it is strongly integrated, but not more so than dogs. Yet, the components of the masticatory system are less variable in foxes compared to dogs.

1.1. Abstract

The jaw system in canids is essential for defence and prey acquisition. However, how it varies in wild species in comparison with domestic species remains poorly understood, yet is of interest to understand the impact of artificial selection. Here we compare the interrelationships between the upper and lower jaws, muscle architecture, and bite force in the red fox (*Vulpes vulpes*) with data previously obtained for dogs (*Canis familiaris*). We performed dissections and used 3D geometric morphometric approaches to quantify shape in 68 foxes. We used a static lever model and bite force estimates were compared with *in vivo* measurements of ten silver foxes. Our results show that foxes and dogs differ in skull shape and muscle physiological cross-sectional areas (PCSA). They show a similar amount of morphological variation in muscle PCSA and mandible shape, but lower variation in cranial shape. In foxes, a strong relationship between the bony and muscle components of the jaw system exists, confirming their strong integration. However, the patterns of covariation are not stronger than in dogs, suggesting that domestication did not lead to a disruption of the functional links of the jaw system. Shape correlated with size, age, sex, and is impacted by muscle architecture. Finally, the functional links between shape and bite force are stronger for the mandible, which likely reflects its greater specialisation towards biting.

1.2. Introduction

Skull morphology has been demonstrated to be the complex product of phylogeny, development, mechanical processes, compromises produced by competing demands, and epigenetic constraints (Smith, 1993; Bels and Herrel, 2019). The head is involved in many fundamental functions in vertebrates (protection of the sensory organs and brain, and functioning of the digestive and respiratory tracts; Santagati and Rijli, 2003), and has thus been the subject of many studies. In particular, the relationships between the mechanical components of the jaw have been a subject of major interest as it contributes to the understanding of the evolutionary processes that have driven variation in the jaw system (Cornette et al., 2015). The mandibles rotate up or down relative to the cranium, the movements being driven by the contractions of the jaw adductors, thus generating the bite force, which is an excellent indicator the performance of the jaw system (Dessem and Druzinsky, 1992; Binder and Valkenburgh, 2000; Anderson et al., 2008; Nogueira et al., 2009). Numerous studies have documented the biomechanics of the jaws in a variety of organisms and attempted to link this to prey capture mode, dietary specialisation, competition or non-feeding and environmental variables (e.g. Bels, 2006; Bels and Herrel, 2019; Bels et al., 2012; Cornette et al., 2015b; Fabre et al., 2018; Gueldre and Vree, 1990; Hannam and Wood, 1989; Hartstone-Rose et al., 2012; Herrel and Aerts, 2004; Herrel et al., 1998b, 2008; Herring et al., 2001; Nogueira et al., 2009; Perry et al., 2011; Slater and Van Valkenburgh, 2009; Tseng and Flynn, 2015a, 2015b, 2015c, 2018).

Previous studies focusing on canids have documented the functional relations of the cranium with the adductor muscles (Penrose et al., 2016, 2020) and the mandible (Curth et al., 2017; Curth, 2018). The relations between these structures and bite force have often been explored using bite force estimations based on skull measurements (i.e. dry skull method: Ellis et al., 2008, 2009; Forbes-Harper et al., 2017; Thomason, 1991). Yet, this approach does not take into

account the macroscopic arrangement of muscle fibres (i.e. muscle architecture: muscle volume, fibre length, fibre type and pennation angle). A good overall measure of this architecture is the physiological cross-sectional area (PCSA; Haxton, 1944). Moreover, differences in bone shape and lever arms may change the relative arrangement of muscles on the skull with respect to the teeth or the temporomandibular joint which will also influence bite force (Taylor and Vinyard, 2013). As such, the inclusion of data on muscle architecture and the position of the muscles on the skull may influence estimates of the magnitude of the bite force and jaw-closing speed (Penrose et al., 2020). Muscle dissections hence enable better estimations of bite force. Previous studies have further shown good correspondence between *in vivo* data and results from biomechanical models based on dissection data (Herrel et al., 1999, 2008; Meyers et al., 2018). Other studies have used finite element analyses (Wroe et al., 2007; Bourke et al., 2008; Penrose et al., 2020) to explore possible adaptations to predation (Radinsky, 1981; Van Valkenburgh and Koepfli, 1993; Slater, Dumont and Van Valkenburgh, 2009).

Unfortunately, direct *in vivo* measurements of bite force in canids are scarce. Ellis et al. (2008) recorded bite force data under anaesthesia for 20 dogs of various breeds, and Lindner et al. (1995) recorded *in vivo* data on 22 dogs of various breeds *in vivo*. To date there is no *in vivo* data for bite forces in other canids such as red foxes. Contrary to dogs (*Canis familairis*) and despite their commensal nature across a large part of the range, phenotypic variation in the red fox is mostly driven by natural selection. Consequently, they are an excellent model to compare to domestic dogs where phenotypic differences are almost exclusively the result of artificial (intentional) selection. As the jaw system plays a major role in feeding and predation, it is likely to be a highly integrated system that is submitted to natural selection pressures. Wild species are only rarely compared to domestic dogs although many studies have attested to the consequences of domestication on the morphological variability of the cranium and mandible (Curth, 2018; Curth et al., 2017; Drake and Klingenberg, 2008, 2010; Machado et al., 2018; Sánchez-Villagra et al., 2016; Selba et al., 2019). Consequently, our understanding of how domestication may impact the functional properties of the jaw system remains limited.

Foxes (*Vulpes vulpes*) are the most widespread wild canids in the world (Schipper et al., 2008). The success of the red foxes in a wide variety of ecological contexts suggests that they present functional adaptations to diverse environments and resources. Foxes are opportunists that feed mostly on small prey. As a result, they have long and narrow jaws (Van Valkenburgh and Koepfli, 1993), allowing the jaws to close quickly (Herring and Herring, 1974; Slater, Dumont and Van Valkenburgh, 2009; Perry, Hartstone-Rose and Logan, 2011; Hartstone-Rose, Perry and Morrow, 2012; Santana, 2016). This is made possible by a longer out-lever that should logically result in a decrease in bite force at the tip of the jaw (Radinsky, 1981; Christiansen and Wroe, 2007) unless the size and orientation of the jaw musculature compensate (Jaslow, 1987). Yet, the morphological and functional variability of this species has only been briefly described. Previous studies suggested age- and sex-related differences, geographic variation and differences between wild and farm-bred or even domesticated populations of foxes (Bisaillon and DeRoth, 1979; Thomason, 1991; Cavallini, 1995; Szuma, 2004; Trut, Oskina and Kharlamova, 2009; Csanády, 2013; Forbes-Harper et al., 2017; Zatoń-Dobrowolska et al., 2017). Variation in the shape of the head as well as in the architecture of

the adductor muscles likely results in variation in bite force. Forbes-Harper et al. (2017) estimated bite forces ranging from 170 to 342 N (mean: 239 N) at the canine tooth, using the dry-skull method for a population of over 300 Australian red foxes. Surprisingly, no previous studies have explored the variation in muscle architecture in the red fox, and how the 3D shape variation in the cranium or mandible is related to jaw muscle morphology and consequently bite force. Further, no *in vivo* bite force measurements are available in the literature, yet these are essential to validate any biomechanical model used to calculate bite force.

Here, we explore the morphological variability in the shape of the cranium (skull without the mandible) and mandible of 68 foxes *Vulpes vulpes* from France using 3D geometric morphometrics. We further quantify the jaw muscle architecture (PCSA, mass) of 65 of these animals by means of dissection. We then estimate bite force to assess the functional impact of the variability in shape and muscle architecture. We use a 3D static biomechanical model based on the origin and insertion of the adductor muscles and the PCSAs obtained from dissection to estimate bite force and compared its output using *in vivo* measurements. We then characterise the interrelationships between the components of the masticatory system by testing the correlations and covariations between the shape of the cranium, the shape of the mandible, muscle architecture, and bite force. We compared these results to results obtained previously for domestic dogs (Brassard et al., 2020a,b,c, articles 1 to 3). Our aim is to [1] document the variability in cranial and mandible shape and jaw muscle architecture in the red fox and to compare it with the domestic dog; [2] study the relationships between shape, muscle architecture, and bite force; and [3] compare the patterns of integration between the domestic dog and the commensal red fox. We predict that the variability in cranial and mandibular shape will be lower in the red fox compared to domestic dogs based on previous studies (Drake and Klingenberg, 2010). We also expect stronger correlations and covariations between bone shape and muscles or bite force in the red fox as its jaw system is principally under the influence of natural selection. This study should thus contribute to a better understanding of the evolutionary processes that drive jaw biomechanics in wild canids and the modifications induced by artificial selection in the domestic dog.

1.3. Materials and methods

1.3.1. Specimens

The dataset is composed of the heads of 68 fresh-frozen *Vulpes vulpes*, including 64 red foxes from the wild and four silver foxes from a wildlife virology testing centre. Silver foxes are a melanistic form of the red fox and belong to the same genus and species *Vulpes vulpes* (Trut, 1999). Detailed information on the sample is available in supplementary Table S1. Sixty-five of these heads were dissected. Three heads were not dissected but directly prepared for shape analyses because they were preserved in formaldehyde which may impact muscle architecture data. Fifty-eight crania and sixty-eight mandibles were well-preserved enough to be used for shape analyses, after cleaning and drying. Foxes were classified in several age groups depending on the aspect of the cranial sutures. Four foxes are juveniles with deciduous teeth, a very porous mandible and unclosed cranial sutures. Young foxes represent foxes for which the basispheno-basioccipital suture is still open (<8-10 months for dogs according to

Barone, 2010) and the mandible is still porous. Old foxes represent foxes with a closed interfrontal suture and worn dentures (>3-4 years). The other foxes are intermediate adults.

1.3.2. Dissections of the jaw muscles

Following the description provided by Penrose et al. (2016) and Brassard et al. (2020a, article 1), we dissected the M. digastricus (Dig), the M. masseter pars superficialis (MS), the M. masseter pars profunda (MP), the M. zygomaticomandibularis anterior (ZMA), the M. zygomaticomandibularis posterior (ZMP), the M. temporalis pars suprazygomatica (SZ), the M. temporalis pars superficialis (TS), the M. temporalis pars profunda (TP), and the M. pterygoideus (P, combining the M. pterygoideus medialis and M. pterygoideus lateralis) when the heads were still fresh or frozen and defrosted (Fig. 1A). Fibre lengths and pennation angles were measured directly on the muscle after sectioning the muscle along its long axis. We considered the mean of five measurements taken on different parts of the muscle. Muscle mass was measured using a digital scale (Mettler Toledo AE100). We calculated the reduced PCSA (Haxton, 1944) using a density of 1.06 g cm−3 (Mendez and Keys, 1960). We used the following formula:

$$PCSA = \frac{mass\ (g) * \cos(angle\ of\ pennation\ (rad))}{1.06\ (g.cm^{-3}) * fiber\ length\ (cm)}$$

Muscle masses could be recorded for 65 foxes and muscle PCSAs for 63 foxes.

The proportions of the masseter, temporal and pterygoid muscles (sum of the masses of all the bundles belonging to a functional group) to the total mass of the adductor muscles were compared between dogs and foxes using Welch's two-sample t-tests.

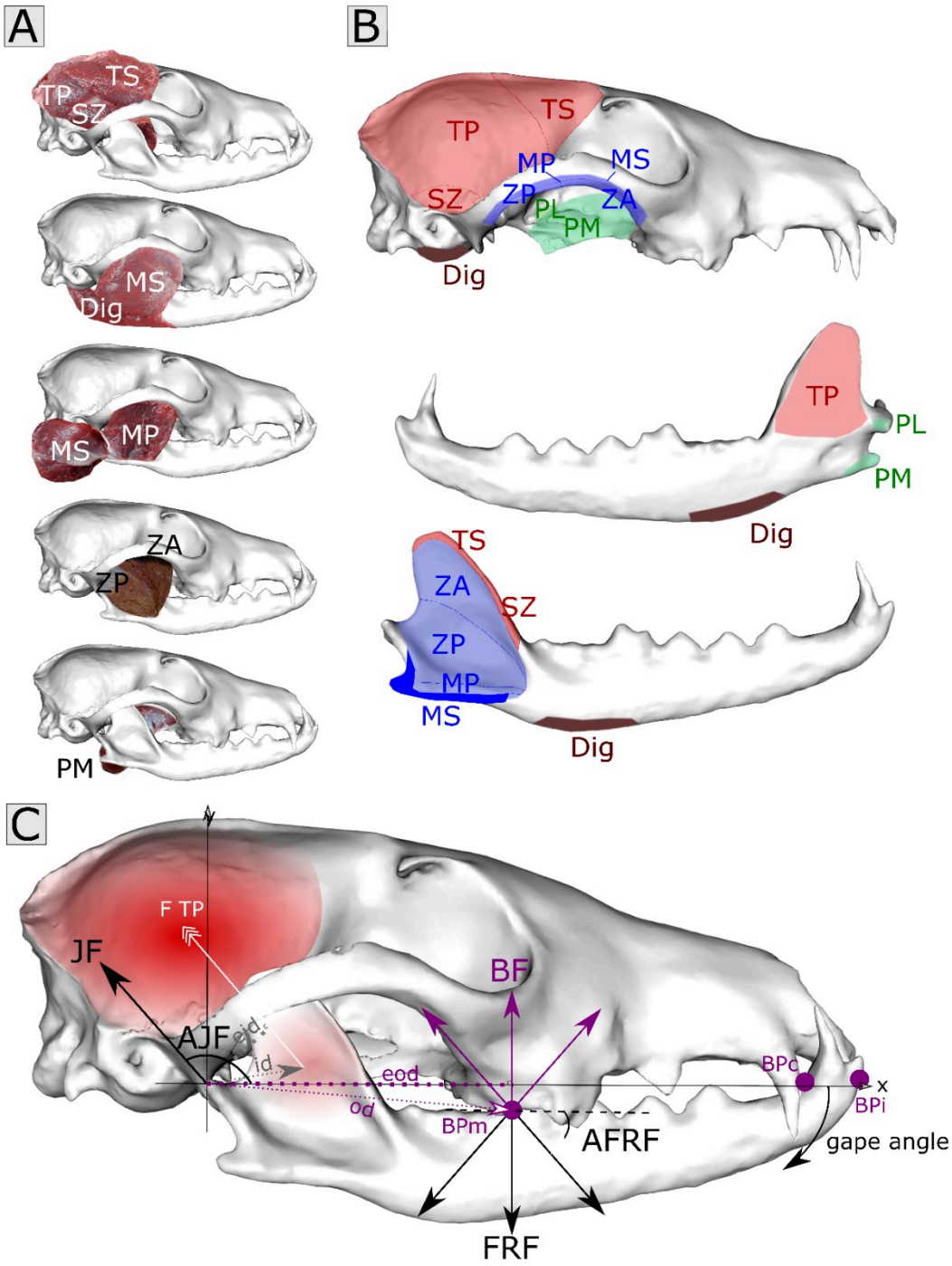

Fig. 1. Jaw muscles and force production in the red fox. A: Jaw muscles dissected in this study; B: attachment area on the skull; C: biomechanical model. Dig: M. digastricus; MS: M. masseter pars superficialis; MP: M. masseter pars profunda; ZA: M. zygomaticomandibularis pars anterior; ZP: M. zygomaticomandibularis pars posterior; SZ: M. temporalis pars suprazygomatica; TS: M. temporalis pars superficialis; TP: M. temporalis pars profunda; PM: M. pterygoideus pars mfedialis; PL: M. pterygoideus pars lateralis; BF: estimated bite force; FRF: food reaction force; AFRF: angle of the food reaction force with respect to axe x; JF: joint force; AJF: angle of the joint force; F TP: force exerted by the M. temporalis pars profunda; eid: effective in-lever arm of the force exerted by the M. temporalis pars profunda; eod: effective out-lever arm exerted by the estimated bite force or the food reaction force; BPi: bite point at the incisor teeth; BPc: bite point at the canine tooth; BPm: bite point at the carnassial tooth; gape angle: angle of opening of the lower jaw with respect to the upper jaw. In the illustration, only the moment arm of the M. temporalis pars profunda is represented. The attachment area of the masseter bundles is indicated in blue, that of the temporal muscles in red, the pterygoids in green, and digastric in brown.

1.3.3. Geometric morphometrics analyses

All statistical analyses were run in 'R' version 3.6.0 (2019-04-26). The patterns of morphological variation and covariation with muscle data or estimated bite force were explored using geometric morphometric analyses. Three-dimensional models of all the mandibles and one cranium were obtained from photogrammetry using the 'Agisoft PhotoScan' software (© 2014 Agisoft LLC, 27 Gzhatskaya st., St. Petersburg, Russia). Twenty-five landmarks, 190 sliding semi-landmarks on curves and 185 sliding semi-landmarks on surfaces were placed on the mandible of each specimen (Fig. 2, Table S1) using the software 'Landmark' version 3.0.0.6 (© IDAV 2002-2005; Wiley et al., 2005). The landmarks were slid and transformed into spatially homologous landmarks using a sliding semi-landmark procedure implemented in the 'Morpho' package (version 2.7) in R (Bookstein, 1991; Gunz, Mitteroecker and Bookstein, 2005; Schlager, 2013). Fifty-four landmarks were placed on one side of the cranium, using a microscribe (Fig. 2, Table S1). A mirror was then applied to obtain the symmetric landmarks compared to the sagittal plane, using the function 'mirrorfill' from the package 'paleomorph', and leading to a total of 108 landmarks.

Generalised Procrustes Analyses (GPA – Rohlf & Slice, 1990) were performed using the function 'procSym' (Klingenberg, Barluenga and Meyer, 2002; Gunz, Mitteroecker and Bookstein, 2005; Dryden and Mardia, 2016) from the package 'Morpho'. Allometries in bone shape and muscle morphology (PCSA and mass) were explored using the function 'procD.lm' (Goodall, 1991; Anderson, 2001; Anderson and Braak, 2003; Collyer, Sekora and Adams, 2015; Adams and Collyer, 2016, 2017) from the package 'geomorph'. Allometry-free coordinates were calculated using the function 'CAC' (Mitteroecker et al., 2004) and 'showPC'. Residual muscle data and residual estimated bite forces were obtained from the regression of the Log10-transformed muscle or estimated bite force data on the Log10-transformed centroid size of the mandible (or cranium whenever appropriate for the further 2B-PLS analyses), using the function 'lm'.

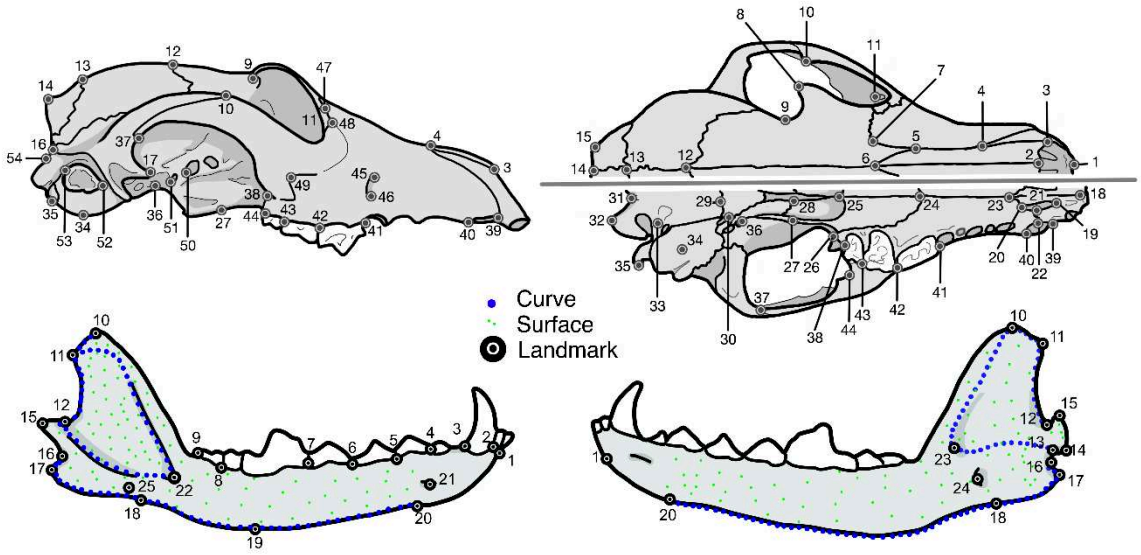

Fig. 2. Landmarks used in this study illustrated on the dorsal, lateral and ventral views of the cranium and mandible of a red fox. Definitions of the landmarks are provided in Table S1.

1.3.4. Exploration of the variability in cranial shape, mandibular shape, muscle PCSA and muscle mass

Principal Component Analyses (PCA) were performed using the function 'procSym' from the package 'Morpho' based on the mandibular or cranial coordinates of all aligned specimens, on allometry-free coordinates, on the PCSA of all muscles, on the residual PCSA of all muscles, on muscle mass and on residual muscle mass. The deformation of the mandible or cranium to the consensus of the GPA was used as a reference for all further visualisations. To compare the variability in cranial and mandible shape between dogs and foxes, we performed a PCA on the Procrustes coordinates of the merged coordinates from this study and that of previous studies using the same landmarking protocol (Brassard et al., 2020a,b,c, articles 1 to 3). To compare the level of morphological variation between the two species (called disparity), we used the function 'morphol.disparity' from the package 'geomorph' (Foote, 1993; Zelditch, Swiderski and Sheets, 2012). Morphological disparity is estimated as the Procrustes variance in each species, using residuals of a linear model fit (the sum of the diagonal elements of the group covariance matrix is divided by the number of observations in the group). The differences between species are statistically evaluated through 1000 permutations, where the vectors of residuals are randomised among groups.

1.3.5. Cranial and mandibular shape determinants

To investigate the drivers of cranial and mandibular shape variation, we performed Procrustes ANOVAs with permutation procedures on the coordinates from the GPA using the function 'procD.lm' from the package 'geomorph'. We considered the mass of the three main adductor muscle groups, their fibre lengths, pennation angles, PCSA, and the centroid size (of the cranium or mandible) as explanatory variables, to increase statistical power. For each muscle complex, we considered the sum of the masses or PCSAs and the mean of the fibre lengths or pennation angles of the constituent bellies. Data were Log10-transformed. We performed Procrustes ANOVAs using the function 'procD.lm' from the package 'geomorph'. We performed several multiple or simple regressions with Log10-transformed centroid size, age, sex and muscle data as explanatory variables. For these analyses, we considered the three main muscle complexes (masseter, temporalis and pterygoid). We used the 'shape.predictor' function and the 'Avizo 8.1.1.' software to visualise the effect of the variation in the PCSA of the temporal, masseter and pterygoids on the shape of the cranium and mandible.

To explore the patterns of covariation, we used two-block partial least-squares analyses (2B-PLS) with the function 'pls2B' (Rohlf and Corti, 2000). P-values were calculated based on 1000 permutations. We tested the covariation between shapes or allometry-free shapes and raw or residual muscle masses or PCSAs. Z-scores were finally calculated to compare the PLS coefficients with the function 'compare.pls' from the package 'geomorph'. To test whether the integration was greater in foxes than in dogs, we also compared the PLS coefficients obtained for the red fox with those obtained for dogs (Brassard et al., 2020a,c, articles 1 and 3).

1.3.6. Bite model

The cranium, mandible and the jaw adductor muscles act jointly to produce jaw motion and estimated bite force. We used a similar biomechanical model to the one described by Herrel et al. (1998a,b) and that takes into account the 3D coordinates of origin and insertion and the PCSA of the jaw muscles to calculate the moments exerted by each muscle and to deduce the estimated bite force, the joint force, and the angle of the joint force (Fig. 1C).

The cranium is positioned in a reference frame whose centre is located at the right temporomandibular joint, whose x-axis runs through the long axis of the mandible to the first incisor tooth, and whose y-axis is directed towards the top of the cranium and perpendicular to X. The Z-axis runs from the midline outwards perpendicular to the other two axes. In this reference frame, the 3D coordinates of origin and insertion of the adductor muscles were recorded using a microscribe. We approximated the centroid of the origin and insertion areas of the muscles based on observations from our dissections. The 3D coordinates of three bite points (point of application of estimated bite force, which is the opposite of the food reaction force) were also recorded. The first point is at the first incisor tooth (BPi in Fig. 1), the second one is just behind the lower canine tooth (BPc in Fig. 1) and the last one is located on the caudal part of the lower carnassial tooth, which corresponds to the contact area between P^4 and M_1 (BPm in Fig. 1). These locations were chosen because they are essential during feeding in canids.

In this three-dimensional lever model, the lower jaw rotates around the condylar process of the mandible (the centre of the system) following a gape angle of 0 to 40°. We do not take into account translational movements as they are negligible. All bite points then rotate in an arc for which the radius corresponds to the shortest distance from the condylar process of the mandible to the point of application of the estimated bite force. At static force equilibrium, the sum of the moments of the external forces (force in the joint, force at the bite point and force exerted by each muscle) is zero. In other words, the sum of the vectorial products of the in-lever moment arms and the adductor muscles forces (for both sides, which are considered symmetric) is equal to the vectorial product of the out-lever moment arm and the estimated bite force. The magnitude of each moment corresponds to the numeric product of force magnitude and the shortest distance between the centre of the system and the line of action of the force (i.e. the effective lever arm or moment arm). The magnitude of the muscular forces were established by multiplying the reduced PCSA by a conservative muscle stress estimate of 30 $N.cm^{-2}$ (Herzog, 1994). The effective lever arms were calculated from the recorded coordinates.

We can then deduce the maximal estimated bite force as follows, considering that the adductor muscles on both sides are contracting maximally and symmetrically during maximal effort biting:

$$BF_{\ two\ sides} = 2 * \left(\frac{\sum_{i=1}^{8} PCSA * 30 * id}{eod} \right)$$

Where BF represents the norm of the bite force, eid the length of the effective in-lever arms for each adductor muscle and eod the length of the effective out-lever arm at the bite point, respectively.

Given that we do not know the direction of the estimated bite force (opposite to the food reaction force, which may depend upon the shape, texture and position of the food item as well as the shape and position of the teeth; Cleuren et al., 1995; Aerts et al., 1997), we calculated the effective out-lever arm for a large range of angles thereof (set to vary between -40 and -140 degrees with respect to the lower jaw; indicated as 'AFRF' in Fig. 1C). We calculated the estimated bite forces for several mouth opening angles (0°, 20° and 40°; indicated as 'gape angle' in Fig. 1C). The magnitude and orientation of the forces in the joint (indicated as 'JF' in Fig. 1C) were estimated as well since, at static equilibrium, the sum of the external forces (muscle and estimated bite forces) is zero.

The input for the model, therefore, consists of the PCSA of the jaw muscles, muscle origins and insertions, mouth opening angle, and the point of application of the estimated bite force. Model output consists of the magnitude of the estimated bite forces, the magnitude of the joint forces, and the orientation of the joint forces at any given orientation of the food reaction forces. An R script for the calculation of the estimated bite force is available on request. Only the estimated bite forces of the foxes with a well enough preserved cranium were estimated (60 individuals).

1.3.7. In vivo bite force measurements

In vivo bite force data were recorded on ten awake restrained silver foxes (five males and five females) at the Laboratory for Rabies and Wildlife in Nancy (France). We used a piezoelectric isometric Kistler force transducer (9203, range ± 500 N; Kistler Inc., Winterthur, Switzerland) linked to a charge amplifier (type 5995A, Kistler Inc.), similar to the set-up presented in Herrel et al. (1999) and Aguirre et al. (2002). The distance between the two steel bite plates was adjusted so that the foxes bit at a gape angle of about 20° when biting at the front of the jaw and 30° when biting at the molars. The tips of the bite plates were covered with a thin medical cloth tape (which was changed between each animal) to avoid direct contact of the teeth with the metal. The foxes were placed on a table and manually restrained and the transducer place either at the level of the incisor teeth or behind the major cusps of the carnassial teeth and therefore made contact with upper premolar tooth P^4 and molar tooth M_1, and lower molar teeth M_1 and M_2. We performed five consecutive trials for each animal and retained the maximal bite force recorded across the trials for analyses. One-sided Welch's tests were performed to compare the mean of the *in vivo* bite forces with the mean of the bite forces estimated using the biomechanical model for a gape angle of 20° and 30°, for the two bite points (on the incisor and molar teeth).

1.3.8. Muscular and morphological drivers of estimated bite force

To identify the relative contribution of the moment exerted by each of the adductor muscles on the moment of the estimated bite force, we calculated the mean and standard deviation of this ratio for each bundle and four gape angles (0°, 20°, 30° and 40°). We compared the contributions between dogs and foxes using bilateral two-sample Welch's test.

To identify the main drivers of estimated bite force variation we performed multiple linear regressions using the function 'lm' with the masses, fibre lengths, pennation angles and PCSAs of the main muscles, and the centroid size of the mandible as explanatory variables. We considered the estimated bite force for a food reaction force orientation of 90° and a gape angle of 20°. The data were Log_{10}-transformed. For this analysis, we considered the three main muscular complexes (masseter, temporal, pterygoid) to increase statistical power. For each complex, we considered the sum of the masses or PCSAs of the constituent bellies and the mean of the fibre lengths or pennation angles. The best-fitted model was obtained from stepwise model selection by AIC using the function 'stepAIC' from the package 'MASS'. In another analysis, we look for the best model to explain bite force by mandibular centroid size, age and sex.

To test whether mandible or cranial shape are correlated to estimated bite force, we performed Procrustes ANOVAs. The patterns of covariation between mandibular or cranial shape (block 1) and estimated bite force at the three bite points (block 2) were explored using 2B-PLS analyses. We calculated Z-scores to compare the results with those obtained previously for dogs (Brassard et al., 2020a,c, articles 1 and 3).

1.4. Results

Model outputs are detailed in the supplementary Table S1.

1.4.1. Variability in cranial and mandibular shape

The PCAs describing the variation in cranial and mandibular shape for both dogs and the foxes from this study shows that dogs and foxes are clearly separated along the first PC axis (accounting for 32% of the total variance for the mandible and 54.6% for the cranium; Fig. 3). Almost all the foxes are located on the right part of the scatterplot. They have straight and flat mandibles, with a small and triangular coronoid process, and a low, long and straight cranium in contrast to dogs which have a more curved body and a more rounded and larger cranium, with a reduced snout. The segregation is stronger for the cranium than for the mandible since a few foxes are very close or even overlap the morphological space of dogs in terms of mandible shape. In particular, the Dobermann, a relatively dolichocephalic dog, has a 'fox-like' mandible. The results of the disparity tests indicate that the shape disparity of the cranium is greater in dogs compared to red foxes (Procrustes variance: 0.0062 in dogs versus 0.0022 in foxes, $P < 0.001$). However, there is no significant difference in the disparity of mandibular shape between dogs and foxes ($P = 0.067$).

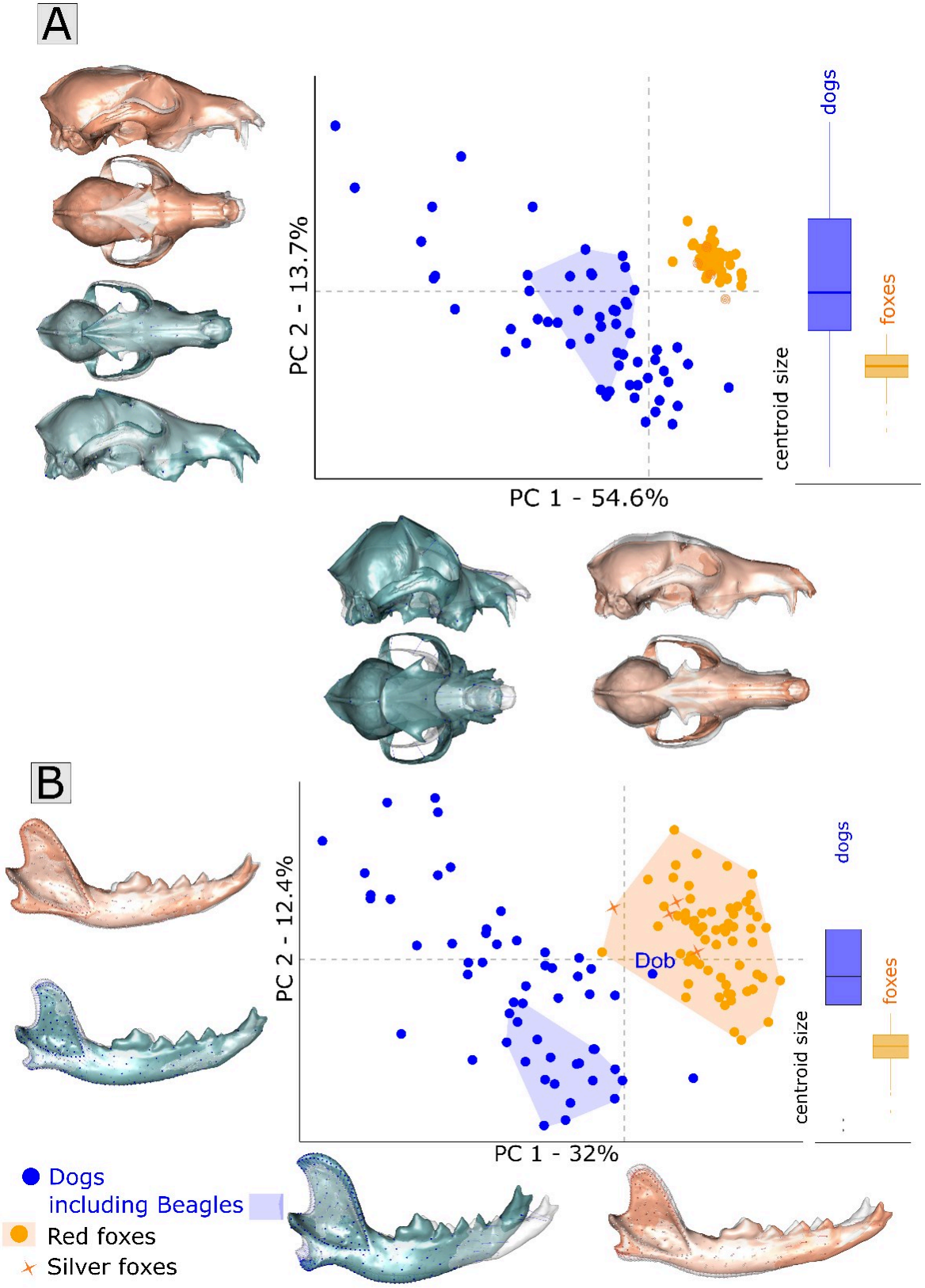

Fig. 3. PCA analyses of cranial (A) and mandibular (B) shape in dogs and red foxes with shapes at the maximum and minimum of the PCA axis and boxplots representing the centroid size in both species. Illustrations represent deformations from the consensus (white) to the extreme of the axis in lateral view. Dogs are in blue and foxes are in orange. Beagles are located in the blue polygon. B: The Doberman (Dob) is located in the area of variation of the red foxes.

Further visualisations of the variability in cranial or mandibular shape in red foxes are provided in the supplementary material (Fig. S1). The width of the zygomatic arches, the height of the cranium, the size of the braincase, the orientation and size of the snout vary among red foxes. Some of these changes are related with size (cranium: $R^2 = 0.061$, $P < 0.001$; mandible: $R^2 = 0.055$, $P = 0.002$). Bigger individuals have a longer snout, a lower and smaller braincase, a more marked postorbital constriction, narrower but thicker and more anteriorly oriented zygomatic arches (Fig. S2A), more developed coronoid, condylar and angular processes on the mandibular ramus, and a straighter ventral border of the mandibular body (Fig. S2B). On the contrary, the smaller the individuals, the more rounded the cranium, the shorter the snout (Fig. S2A), the more ventrally curved the body of the mandible, and the smaller the mandibular ramus. (Fig. S2B). The Procrustes ANOVAs (Table 1) show that variation in cranial shape is also explained by age ($R^2 = 0.097$, $P = 0.002$) and sex ($N = 51$, $R^2 = 0.03$, $P = 0.041$), whereas there is no significant effect of either age nor sex on mandible shape.

Table 1. Results of the Procrustes Analyses performed on overall cranial and mandible shape. Sample sizes are indicated for each parameter. Significant results are in bold.

	Df	SS	MS	R^2	F	Z	Pr(>SS)
Cranium							
Multiple regressions (N=49)							
Size	1	0.0044	0.0044	**0.067**	3.4	4.8	0.001
Age	3	0.0049	0.0016	0.074	1.3	1.3	0.12
Sex	1	0.0022	0.0022	**0.033**	1.7	2.6	0.009
PCSA temporalis	1	0.0011	0.0011	0.016	0.81	-0.24	0.59
PCSA masseter	1	0.0015	0.0015	0.023	1.2	1.3	0.090
PCSA pterygoids	1	0.0010	0.0010	0.015	0.78	-0.15	0.56
Mass temporalis	1	0.0011	0.0011	0.017	0.89	0.43	0.33
Mass masseter	1	0.0010	0.0010	0.016	0.81	0.45	0.11
Mass pterygoid	1	0.0011	0.0011	0.016	0.82	0.30	0.39
Residuals	37	0.048	0.0013	0.72			
Simple regressions							
Size (N=58)	1	0.0052	0.0052	**0.061**	3.66	4.9	0.001
Age (N=58)	3	0.0082	0.0027	**0.097**	1.93	3.1	0.002
Sex (N=51)	1	0.0052	0.0052	**0.061**	3.7	5.0	0.001
Estimated bite force (N=54)	1	0.0018	0.0018	0.024	1.3	1.1	0.13
Residual estimated bite force (N=54)	1	0.0013	0.0013	0.017	0.91	-0.26	0.6
PCSA temporalis (N=54)	1	0.0029	0.0029	**0.037**	2.0	2.8	0.005
Residual PCSA temporalis (N=54)	1	0.0012	0.0012	0.016	0.84	-0.57	0.71
PCSA masseter (N=54)	1	0.0025	0.0025	**0.032**	1.7	2.3	0.012
Residual PCSA masseter (N=54)	1	0.0021	0.0021	0.027	1.5	1.6	0.059
PCSA pterygoid (N=54)	1	0.0021	0.0021	**0.027**	1.4	1.7	0.044
Residual PCSA pterygoid (N=54)	1	0.0020	0.0020	0.026	1.4	1.4	0.084
Mass temporalis (N=56)	1	0.0047	0.0047	**0.059**	3.4	4.7	0.001
Residual mass temporalis (N=56)	1	0.0028	0.0028	**0.035**	1.9	2.6	0.008
Mass masseter (N=56)	1	0.0040	0.0040	**0.05**	2.8	4.1	0.001
Residua mass masseter (N=56)	1	0.0025	0.0025	**0.031**	1.7	2.1	0.023
Mass pterygoid (N=56)	1	0.0039	0.0039	**0.048**	2.7	4.05	0.001
Residual mass pterygoid (N=56)	1	0.0021	0.0021	0.026	1.4	1.6	0.071
	Df	**SS**	**MS**	**R^2**	**F**	**Z**	**Pr(>SS)**

Mandible							
Multiple regressions (N=58)							
Size	1	0.011	0.011	**0.049**	3.1	2.9	0.006
Age	3	0.022	0.0073	**0.097**	2.1	2.9	0.005
Sex	1	0.0039	0.0039	0.017	1.1	0.60	0.27
PCSA temporalis	1	0.0022	0.0022	0.0099	0.63	-0.75	0.76
PCSA masseter	1	0.0039	0.0039	0.018	1.2	0.71	0.23
PCSA pterygoids	1	0.0036	0.0036	0.016	1.0	0.53	0.28
Mass temporalis	1	0.0051	0.0051	0.023	1.5	1.4	0.089
Mass masseter	1	0.0030	0.0030	0.014	0.86	0.17	0.42
Mass pterygoid	1	0.0075	0.0075	**0.034**	2.1	2.6	0.009
Residuals	46	0.16	0.0035	0.72			
Simple regressions							
Size (N=68)	1	0.015	0.015	**0.055**	3.9	3.6	0.002
Age (N=68)	3	0.011	0.0037	0.041	0.92	-0.26	0.60
Sex (N=60)	1	0.0035	0.0034	0.015	0.87	-0.16	0.54
Estimated bite force (N=60)	1	0.016	0.016	**0.069**	4.4	3.7	0.001
Residual estimated bite force (N=60)	1	0.015	0.015	**0.062**	3.8	3.4	0.001
PCSA temporalis (N=60)	1	0.015	0.015	**0.061**	4.0	3.6	0.001
Residual PCSA temporalis (N=60)	1	0.0092	0.0092	**0.037**	2.3	2.3	0.015
PCSA masseter (N=63)	1	0.014	0.014	**0.054**	3.5	3.3	0.001
Residual PCSA masseter (N=63)	1	0.0089	0.0089	0.036	2.3	2.2	0.019
PCSA pterygoid (N=63)	1	0.0093	0.0093	0.037	2.4	2.3	0.015
Residual PCSA pterygoids (N=63)		0.0072	0.0072	0.029	1.8	1.6	0.066
Mass temporalis (N=63)	1	0.021	0.021	**0.081**	5.5	4.5	0.001
Residual mass temporalis (N=63)	1	0.014	0.014	**0.054**	3.6	3.4	0.001
Mass masseter (N=65)	1	0.019	0.019	**0.073**	4.9	4.2	0.001
Residual mass masseter (N=65)	1	0.013	0.013	**0.049**	3.28	3.1	0.002
Mass pterygoid (N=65)	1	0.011	0.011	**0.044**	2.9	3.0	0.006
Residual mass pterygoid (N=65)	1	0.0048	0.0048	0.019	1.2	0.71	0.247

1.4.2. Covariations between mandible and cranial shape in the red fox

The shape of the cranium strongly covaries with that of the mandible (PLS-1: 30% of total covariance, *r*-PLS = 0.78, *P* = 0.02, Fig. 4; PLS-2: 19% of total covariance, *r*-PLS = 0.69, *P* < 0.001; PLS-3: 14% of total covariance, *r*-PLS = 0.73, *P* < 0.001; PLS-4: 9% of total covariance, *r*-PLS = 0.74, *P* = 0.002; PLS-5: 6% of the total covariance, *r*-PLS = 0.61, *P* = 0.003). A mandible with a body that narrows and bends up towards the anterior end with a more anteriorly inclined coronoid process and a bigger angular process is associated with a shorter and higher cranium, lower and slightly larger zygomatic arches, a larger braincase, more anteriorly positioned orbital processes, and a more oblique snout (Fig. 4). On the contrary, a mandible with a straighter and rostrally taller body is related to a lower cranium, a smaller braincase with more caudal and laterally extended orbital processes, a straighter snout, a reduced palatine bone, more rostrally oriented mastoid processes and basioccipital foramen, and more elevated but slightly smaller zygomatic arches. These patterns of covariation match our observation of the deformations along the allometric slopes (Fig. S2). Indeed, linear regressions performed on the PLS1 scores of each block and the log10 of the centroid size indicate that covariations are driven by the centroid size of the mandible (R^2 = 0.09, *P* = 0.02) and cranium (R^2 = 0.13, *P* = 0.003).

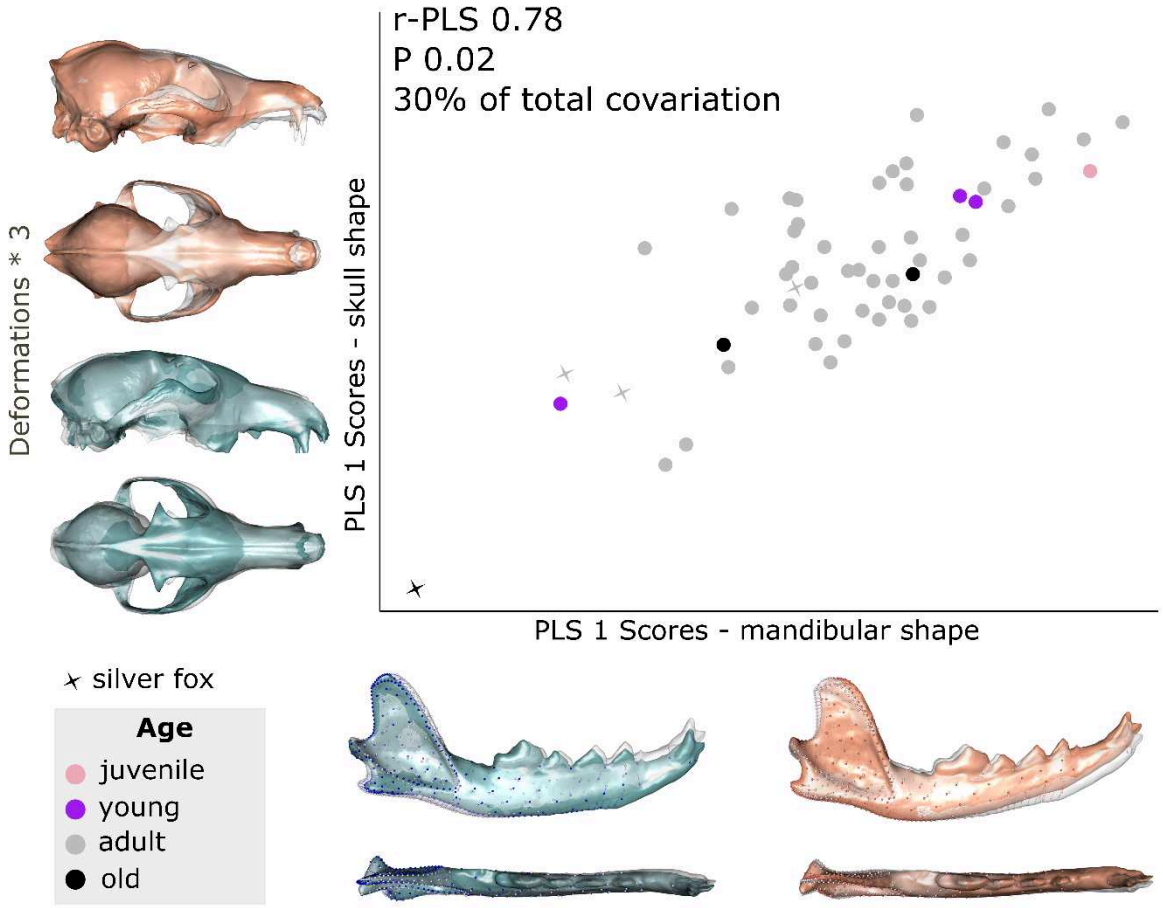

Fig. 4. 2-Block Partial Least Square Analyses between mandibular and cranial shapes in the red fox. Shapes at the minimum and maximum of the PLS axis are illustrated. Illustrations represent the deformations from the consensus to the extreme of the axis in lateral and/or dorsal views. Deformations were magnified by a factor three for the cranium. Different ages are represented by different colours.

1.4.3. Variability in muscle morphology

The pennation angles range from 0° in the digastric over 30-40° in the temporalis and masseter to 40° in the pterygoids. Muscles from the temporalis complex have very long muscle fibres (up to 50 mm, mean 24 mm) compared to muscles from the masseteric and pterygoid groups that have shorter fibres (11-15 mm). The mass of the lateral pterygoid muscles represents only around 9% of the mass of the pterygoid complex (from 0 to 25%) and 0.77% of the total mass of the adductor muscles (from 0 to 2.5%). The proportions of the masseter, temporalis and pterygoid muscles to the total mass of the adductor muscle are similar in foxes and dogs (in foxes: respectively 27 ± 4, 64 ± 8, 9 ± 3 %; dogs: 27 ± 5, 63 ± 10, 10 ± 3 %; $P_{Welch's\ t\text{-}tests} > 0.10$ for each muscle group). Muscle masses are strongly correlated ($r > 0.8$ for all groups).

The first two axes of the PCA describing variation in raw jaw muscle mass (Fig. S3A) account for 80.8% of the total variability, while the two first axes explain 62.5% of the variation in scaled mass (Fig. S3B). The first two axes of the PCA describing variation in absolute jaw muscle PCSA (Fig. S3C) account for 61.9% of the total variability while the two first axes explain 48.9% of the variation in scaled PCSA (Fig. S3D). The second axis of the PCAs with

muscle masses (Figs S3A,B) is determined by variation in the suprazygomatic part of the temporalis and the anterior zygomaticomandibularis muscle. The pterygoids, the zygomaticomandibularis (anterior and posterior), the suprazygomatic part of the temporalis and the deep temporalis drive the second axis of the PCA with muscle PCSAs (Figs S3C,D). The first axes are strongly correlated with mandible centroid size, age, and sex ($P < 0.001$ in all cases, $N = 58$). Silver foxes are included within the variability of the red foxes. However, it can be noticed that they plot with the youngest red foxes, on the left part of the scatterplots with the scaled masses (Fig. S3B) and scaled PCSAs (Fig. S3D). This suggests that these four adult/old silver foxes have smaller MS, TS, TP, P than the average of all the foxes of our sample.

MANOVAs show that there is a difference in the PCSA of the adductor muscles of the foxes compared to dogs, which is mostly explained by size ($P < 0.001$ on raw data, $P > 0.05$ on residuals). The first axis of the PCA combining data for dogs and foxes shows that the variability in muscle architecture of foxes clearly overlaps with that of dogs. Values in the red fox are similar to those for small dogs and beagles (Fig. S4A). The disparity tests indicate that there is no difference in disparity between the two species ($P > 0.05$). Residual volume and residual PCSA (residuals of the regression with the log10 of the mandibular centroid size) cover the same area in foxes as described by dogs which suggests a great variability in the relative importance and strength of the jaw muscles in red foxes despite a lower shape variability (Figs S3B and S4B).

1.4.4. Covariation between mandible or cranial shape and muscle PCSAs and masses

The Procrustes ANOVAs between mandible or cranial shape and centroid size, age, sex muscle PCSAs and muscle masses showed significant correlations (Table 1). In these analyses, size, age and sex explain 17.4% of the variation in cranial shape and 16.3% of the variation in mandible shape, while muscle PCSAs and masses explained 10.3% of the variation in cranial shape and 11.5% of the variation in mandible shape. The results of the simple regressions indicate that cranial shape is more closely associated with the relative volume occupied by the temporalis and masseter muscles. Muscle PCSA did not predict variation in cranial shape, however. On the contrary, mandible shape is associated with both the volume and PCSA of the temporalis and masseter muscles.

Because muscle data are strongly correlated, an increase in the PCSA of the masseter, temporal, or pterygoid muscles is associated with a similar variation in shape for the upper jaw as well as for the lower jaw (Fig. 5). The PCSA of the masseter, temporalis, and pterygoid muscles are all related to the area of insertion of the three muscles: the dorsal tip of the coronoid process, the deep masseteric fossa, and the angular process. The shape of the braincase seems to be more related to variation in the PCSA of the temporalis muscle. An increase in the PCSA is related to a change in the convexity of the temporal bones and the shape of the sagittal crest. The PCSA of the masseter drives the shape of the zygomatic arch more specifically, although the shape of the braincase is also impacted. The pterygoid bone does not seem to be impacted much by the PCSA of the three main adductor muscle groups.

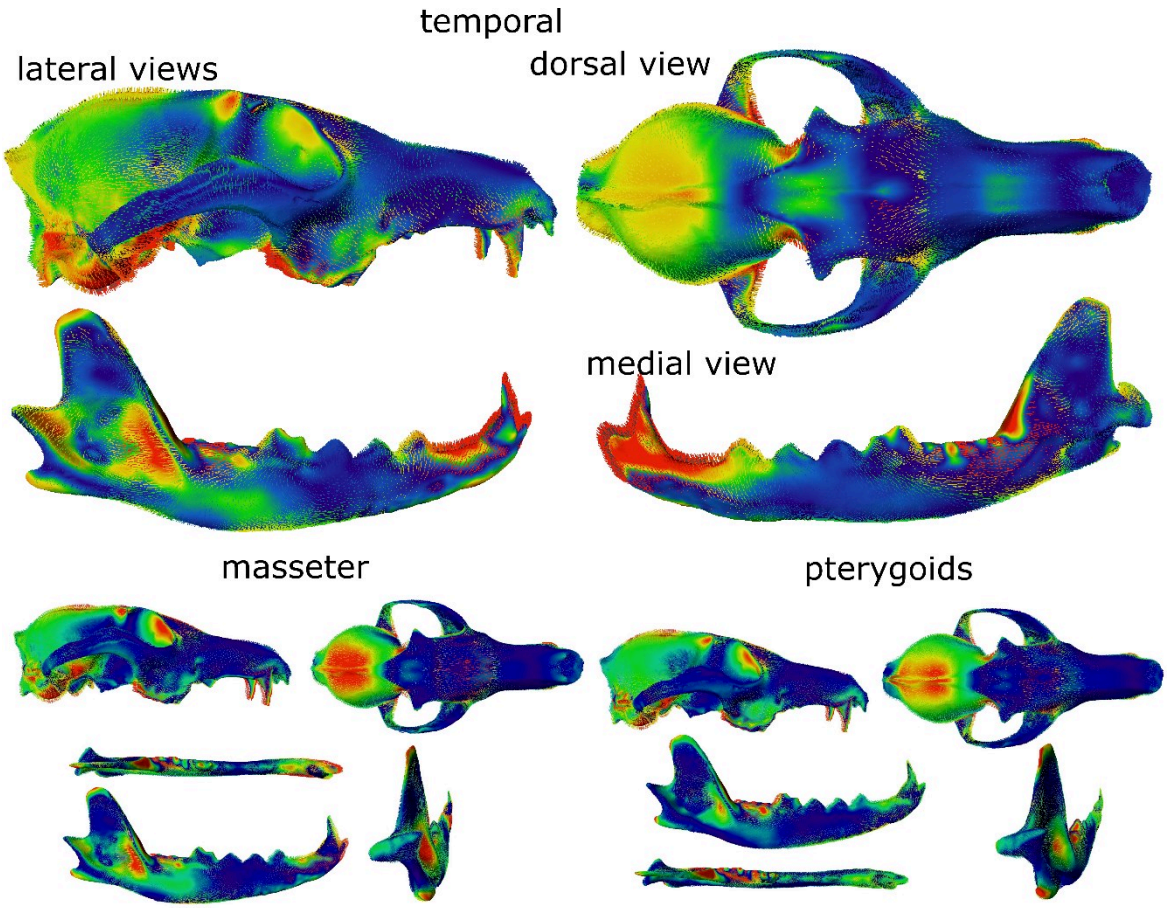

Fig. 5. Illustrations of the deformations associated with variation in the PCSA of the temporalis, masseter and pterygoid muscles. Hotter colours indicate areas that show greater shape changes. The shape corresponding to the maximum muscle PCSA is represented. The vectors from the minimum to the maximum are represented according to the distance between the two shapes.

Additionally, the 2B-PLS shows significant covariations between muscle data (scaled or not) and the shape of the mandible, and irrespective of whether allometries are taken into account or not (Table 2). The same observations can be made for the covariations between muscle volume and the shape of the cranium. However, there is no significant covariation between raw muscle PCSA and cranial shape, but the covariations are significant for scaled PCSA and/or allometry-free shape. Ontogeny/age seems to play a major role in the intensity of the covariations. However, even after removing the youngest individuals (4 foxes classified as age juveniles), covariations remain significant and strong. The covariations are significantly less important between muscle data and the ramus of the mandible only than with the complete mandible (mass: $Z = 2.07$, $P = 0.02$; PCSA: $Z = 1.17$, $P = 0.01$). There is no significant difference between the covariations obtained for the mandible and those for the cranium ($P > 0.05$ in all cases). The covariations drastically decrease when shape and/or muscle data are scaled, which suggests the strong importance of size in the patterns of integration.

Table 2. Results of the 2B-PLS analyses conducted on muscle data (PCSA and mass) or estimated bite force and mandible or cranial shape. The results are given with or without the four juvenile foxes. %coVar: percentage of covariance explained by PLS 1; r-PLS: coefficient of covariation; p-PLS: p-value of the 2B-PLS; p-Z: p-value associated with the Z-score comparing r-PLS obtained for dogs and foxes. See supplementary material 3 for further details.

	Shape – mass /PCSA/bite force				Shape – residual mass/PCSA/bite force			Allometry-free shape – residual mass/PCSA/bite force		
	%	r-PLS	p-PLS	p-Z	%	r-PLS	p-PLS	%	r-PLS	p-PLS
Mass (N=65)										
Mandible	93%	**0.77**	0.001	0.46	73%	**0.56**	0.005	73%	**0.51**	0.009
Mandible without juveniles	86%	**0.74**	0.001		64%	0.60	0.052	68%	**0.56**	0.018
Cranium	85%	**0.84**	0.001	<0.001	54%	0.66	0.07	55%	**0.65**	0.047
Cranium without juveniles	77%	**0.81**	0.014		65%	**064**	0.034	70%	**0.61**	0.019
PCSA (N=63)										
Mandible	84%	**0.69**	0.001	0.21	70%	**0.54**	0.006	68%	**0.51**	0.006
Mandible without juveniles	62%	**0.64**	0.032		61%	0.54	0.056	61%	**0.54**	0.024
Cranium	61%	0.76	0.24	<0.001	61%	**0.76**	0.006	51%	**0.69**	0.032
Cranium without juveniles	57%	0.55	0.12		61%	**0.53**	0.053	63%	0.54	0.056
Bite force (N=60)										
Mandible	100	**0.63**	0.001	0.002	100%	**0.55**	0.001	100%	0.55	0.001
Mandible without juveniles	100	**0.53**	0.053		100%	**0.50**	0.009	100%	0.51	0.003
Cranium	99	0.66	0.13		98%	0.55	0.4	99%	0.66	0.4
Cranium without juveniles	98	0.71	0.75		98%	0.55	0.38	99%	0.66	0.51

1.4.5. In vivo bite forces

A comparison of bite force estimated on the incisor and carnassial teeth at a gape angle of 20-30° (and for an AFRF of 90°) with the *in vivo* data shows good correspondence (Fig. 6, Table S1). On the incisor teeth, the mean bite forces estimated for a gape angle of 20° (206 ± 55 N) is not significantly inferior to the mean of the *in vivo* bite forces (243 ± 67 N; $P_{Welch's\ unilateral\ test}$ = 0.06), whereas model outputs for a gape angle of 30° (191 ± 53 N) slightly underestimate the *in vivo* bite forces ($P_{Welch's\ unilateral\ test}$ = 0.02). The mean of the *in vivo* bite forces at the carnassial teeth (337 ± 86 N with a maximum of 484 N *in vivo*) is significantly lower than the mean of the model outputs for a gape angle of 20° (434 ± 111 N; $P_{Welch's\ unilateral\ test}$ = 0.003) and for a gape angle of 30° (403 ± 107 N; $P_{Welch's\ unilateral\ test}$ = 0.02). However, we could not compare both methods for the same individuals, except for the specimen Ny-R5, which was included both in the model and the *in vivo* measurements and further showed that estimated bite forces are very close to the maximal forces recorded *in vivo* (incisor teeth: 183 N *in vivo* and 192 N in our model estimations; molar teeth: 435 N *in vivo* and 408 N in our model estimation for a gape angle of 20° and an AFRF of 90°). This suggests that the model output gives a reliable estimate of *in vivo* data.

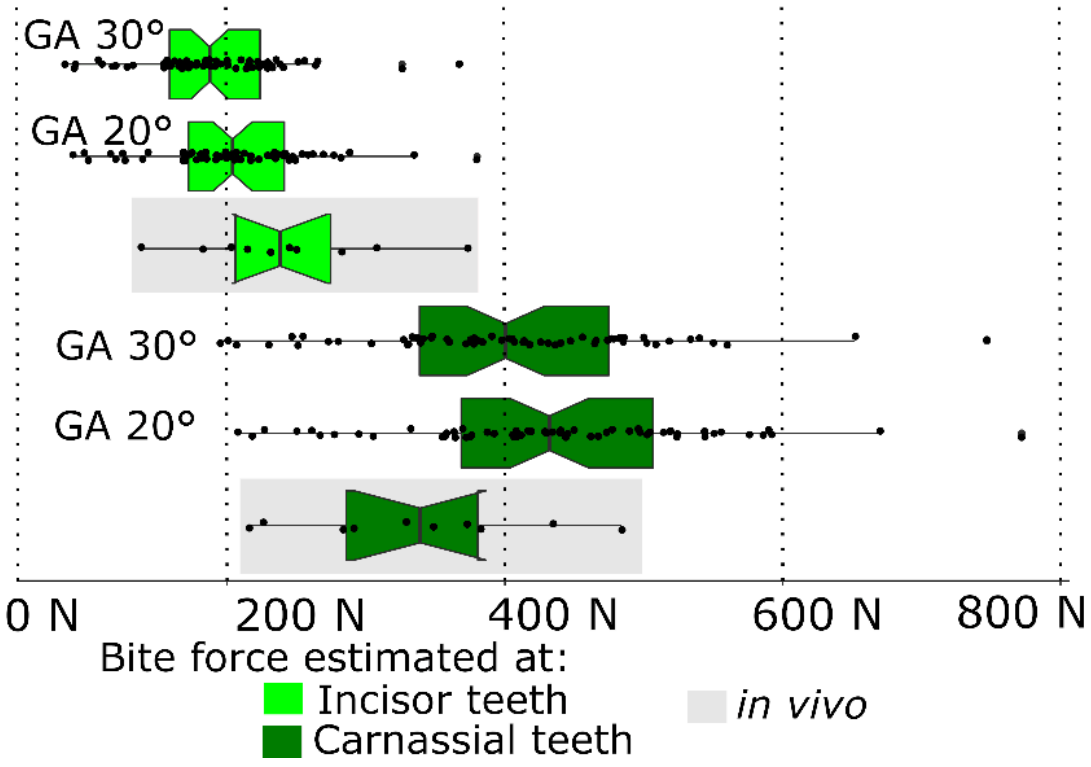

Fig. 6. Comparison of *in vivo* (N = 10) and estimated (N = 60) bite forces for a gape angle of 20° and an angle of the food reaction force of 90°.

1.4.6. Estimated bite forces

As expected, the mean bite force estimated at the carnassial tooth is higher than the one estimated on the canine or incisor teeth (Table 3, Fig. S3). For example, at a gape angle of 0° for an angle of the food reaction force of 90°, mean estimated bite force ranges from 174 (gape angle 40°) to 230 N (gape angle 0°) at the incisor teeth, from 198 to 261 N at the canine tooth and from 368 to 486 N at the carnassial tooth. For a given AFRF, mean bite force decreases when gape angle increases (Table 3). A shift of the food reaction forces away from the perpendicular axis causes an increase in bite force (Fig. S3), which is consistent with previous observations (Dumont and Herrel, 2003). On the contrary, the mean joint force increases when the gape angle increases and when the point of application of the food reaction forces get closer to the incisor teeth, ranging from 534 ± 123N on the incisor teeth and 463 ± 109N on the carnassial tooth for a gape angle of 0°, to 553 ± 128N on the incisor teeth and 484 ± 114N on the carnassial tooth for a gape angle of 40° (Table 3). The more elevated the angle of the food reaction force, the more elevated the force in the joint (Fig. S5). The angle of the joint force decreases when the gape angles increases and when the point of application of the food reaction force gets closer to the incisor teeth, ranging from 140 ± 5° on the incisor teeth and 152 ± 7° on the carnassial tooth for a gape angle of 0°, to 131 ± 3° on the incisor teeth and 138±4° on the carnassial tooth for a gape angle of 40° (Table 3). This aligns the joint force more with the orientation of the joint capsule. The more elevated the angle of the food reaction force, the more elevated the force in the joint. These patterns are similar to the ones described previously in dogs (Fig. S5).

Table 3. Summary of the outputs of the biomechanical model, for an angle of the food reaction forces of 90°.

	Bite force (N)			Joint Force (N)			Angle of the Joint Force (°)		
Gape angle	**0**	**20**	**40**	**0**	**20**	**40**	**0**	**20**	**40**
Bite Point									
Incisor teeth	230±60	205±55	174±50	534±123	541±125	553±128	140±5	134±4	131±3
Canine tooth	261±67	233±62	198±57	524±121	531±123	544±126	141±5	135±4	131±3
Carnassial tooth	486±120	434±111	368±101	463±109	467±110	484±114	152±7	144±5	138±4

1.4.7. Drivers of variation in estimated bite force

The outputs of the biomechanical model show that the masseter represents around 40% of the total moment of the estimated bite force, the temporalis 50%, the masseter 40% and the pterygoid 10% (Table S1). When the gape angle increases, the contribution of the masseter decreases, while that of the pterygoid (and the temporalis) increases. Detailed contributions of all muscle bundles and for several gape angles are reported in Table S1. For example, for a gape angle of 0°, M. masseter superficialis contributes to 16% of the moment of the bite force, while M. temporalis superficialis contributes to 24%. The M. masseter superficialis and M. temporalis superficialis contribute proportionally more to the bite force in the red fox than in dogs (for a gape angle of 0°, for the M. masseter superficialis: 16% in the fox, 13% in dogs, $P_{\text{bilateral Welch t-}}$

$_{test}$ < 0.001; for the M. temporalis superficialis: 24% in the red fox, 22% in dogs, $P_{bilateral\ Welch\ t\text{-}test}$ < 0.01).

The best model explaining variation in estimated bite force with mandibular centroid size and muscle data (PCSA, masses, fibre length, pennation angle of the three main muscle groups) is the model that considers the PCSA of the masseter (0.40), the PCSA of the temporalis (0.40) and the PCSA of the pterygoids (0.14) and the pennation angle of the masseter muscle (0.12, adjusted $R^2 = 0.82$, $P < 0.001$).

The centroid size of the mandible and age are also important drivers of estimated bite force as suggested by the results of the linear regression of bite force with size and age ($R^2 = 0.60$, $P < 0.001$). Moreover, males have significantly higher estimated bite forces (Welch two-sample t-test: $P = 0.025$) than females, probably because of their larger size. The Procrustes ANOVAs (Table 1) show that 6-7% of the variation in mandible shape is related to estimated bite force or residual estimated bite force ($P < 0.001$).

We also observe significant covariations between mandibular shape and estimated bite force (r-PLS = 0.64, $P < 0.001$) or residual estimated bite force (r-PLS = 0.56, $P = 0.002$) and between the allometry-free mandible shape and the residual estimated bite force (r-PLS = 0.56, $P <$ 0.002, Table 2). Once the juvenile foxes are removed, the covariations with residual estimated bite force are still significant but lower (r-PLS = 0.50, $P < 0.01$, Table 2). Calculation of the Z-scores shows that the covariation between mandible shape and estimated bite force is significantly lower in foxes compared to dogs (foxes: r-PLS = 0.63; dogs: r-PLS = 0.75; P associated with the Z-score ($P_Z = 0.002$). The same is observed with residual estimated bite forces (foxes: r-PLS = 0.55; dogs: r-PLS = 0.65; $P_Z = 0.035$) and allometry-free shapes (foxes: r-PLS = 0.55; dogs: r-PLS = 0.69; $P_Z = 0.02$). The first PLS axis of the 2B-PLS between mandible shape and estimated bite force (Fig. 7) is strongly related to the size of the individuals ($P < 0.001$), and consequently also the age of the individuals ($P < 0.001$). Foxes that occupy the right part of the scatterplot (smaller and/or younger) have a proportionally shorter ramus and a longer body, which is more ventrally rounded, a smaller and straighter coronoid process, a small angular process, and a thick body under the carnassial tooth. These foxes have low estimated bite forces. Foxes with high bites forces, on the left part of the scatter plot, have a proportionally large coronoid process and a reduced body, a more caudally oriented coronoid process with a deeper masseteric fossa, bigger angular and condylar processes, and a more angular and ventral border of the body. In contrast, the Procrustes ANOVAs and 2B-PLS analyses performed with cranial shape and estimated or residual estimated bite force show that there is no significant correlation either covariation between them (Tables 1, 2).

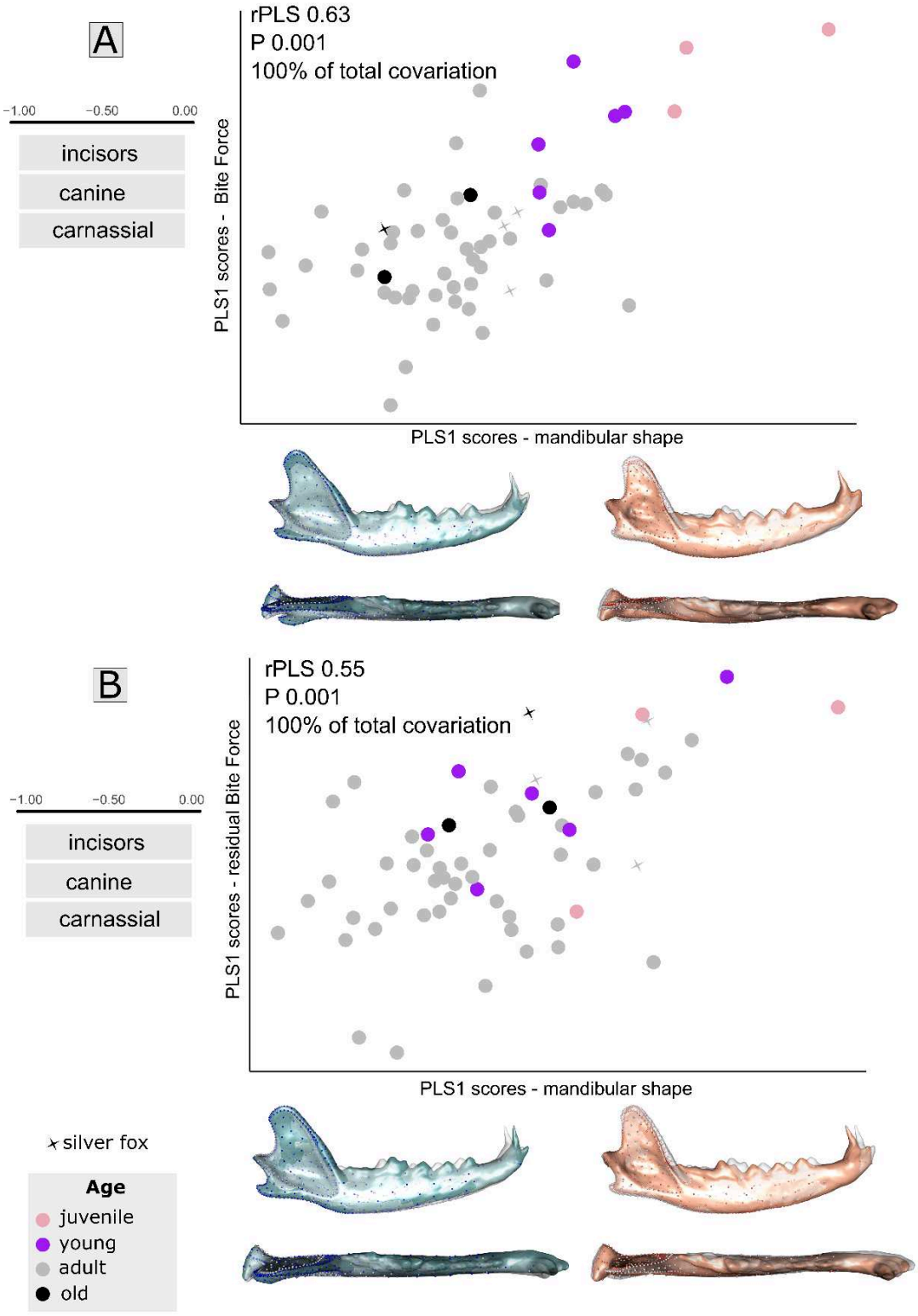

Fig. 7. 2-Block Partial Least Square Analyses between mandibular shape and estimated bite force (A) or residual estimated bite force (B) with estimated bite force vectors for different bite points and shapes at the minimum and maximum of the PLS axis. Illustrations represent the deformations from the consensus to the extreme of the axis in lateral and dorsal views. Different ages are represented by different colours.

1.5. Discussion

In this study, we describe the overall relations between the upper jaw, the lower jaw and muscle architecture in red foxes by using three-dimensional geometric morphometrics and by estimating bite forces using a 3D static biomechanical model based on dissection data. We predicted that the variability in skull shape would be lower in the red fox compared to domestic dogs based on previous studies (Drake and Klingenberg, 2010). We also expected stronger correlations and covariations between bone shape and muscle morphology or bite force in the red fox as its jaw system is principally under the influence of natural selection.

1.5.1. Comparison of the morphological variability between foxes and dogs

Dogs and foxes clearly differ in both cranial and mandibular shape and size. Moreover, the disparity in shape is much lower in the fox than in dogs, in particular for the cranium. This is consistent with previous results showing that domestication has resulted in an increase in shape variability for dogs (Darwin, 1868; Drake and Klingenberg, 2010; Heck et al., 2018). The increased variability in mandibular shape is less obvious, however (Fig. 3). Both mandible and cranial shape depend on size, and our results indicate a significant effect of age and sex on the shape of the cranium. The effects of age and sex were not significant for the mandible. This suggests that the observed sexual dimorphism may not be related to feeding but rather to other functions as the cranium also protects the sensory organs and the brain for example (Radinsky, 1981; Santagati and Rijli, 2003; Figueirido et al., 2011; Fabre et al., 2014). However, analyses including additional juvenile foxes would be necessary to investigate the influence of age more exhaustively. As expected, cranial and mandibular shape strongly covary (r-PLS 0.78) but the covariations are not significantly stronger than those observed for dogs (r-PLS 0.81), in contrast to our predictions. Overall, we observe patterns of covariation that are similar to those for dogs and that are possibly driven by muscle constraints: curved mandibles with more pronounced muscle insertions are associated with shorter and more rounded crania. This covariation is likely driven by the muscles that link the upper and lower jaws, which is supported by the results of the Procrustes ANOVAs (Fig. 5). This supports the hypothesis that the masticatory apparatus is strongly integrated in canids, and that domestication did not lead to a disruption of the functional links of the jaw system despite the increased variability in shape and the commonly observed malformations in dogs.

Interestingly, foxes represent a similar variability in muscle architecture (masses and PCSA) compared to dogs. Moreover, the jaw muscle architecture is very similar and nearly spans in the same morphological range as in dogs. The lateral pterygoid represents, on average, 1% of the total volume, which is consistent with previous observations (Penrose et al., 2020: 0.27% for one individual only). The proportions of the masseter, temporalis and pterygoid muscles are similar to what was observed in dogs (Brassard et al., 2020a, article 1).

1.5.2. Relevance of the biomechanical model, variability in bite force

Our biomechanical model showed excellent correspondence with the *in vivo* measurements, especially for the specimen where we had both *in vivo* and model data. Several parameters may account for the slight differences we observed between the means of model outputs and the mean of the *in vivo* bite forces. The *in vivo* bite forces were recorded for silver foxes and not red foxes. Further, we could not precisely control the gape angle (between 20 and 30°). This highlights the inter-individual differences that exist and the importance of deriving individual-specific models based on dissection data to be able to accurately estimate bite forces (Gröning et al., 2013). Foxes bite less hard than dogs on average, but this is mostly the result of their smaller size and the long out-lever due to their relatively longer jaws. The estimated bite force ranges from 200 N on the incisor teeth to 450 N on the carnassial tooth for a gape angle of 20° and an AFRF of 90°. Higher estimated bite forces are recorded/calculated on the carnassial tooth, as a result of the shorter out-lever arm (because the bite point is positioned more closely to the attachment sites of the adductors; Dumont and Herrel, 2003; Ellis et al., 2008; Ellis et al., 2009; Greaves, 2000; Greaves, 2002; Herrel et al., 2008; Spencer, 1998). The higher the gape angle, the lower the estimated bite force and the angle of the joint force, and the higher the joint force. The same has been observed for dogs and other species of mammals (Dumont and Herrel, 2003; Herrel et al., 2008; Santana, 2016; Kerr et al., 2017). There is no *in vivo* data available in the literature for wild red foxes, unfortunately. Forbes-Harper et al. (2017) estimated bite forces in Australian red foxes using dry skulls only and found forces ranging from 170 to 342 N (mean: 239 N). Whereas our estimations are in the same range, differences between populations are likely, especially when comparing invasive with native populations. Future studies are needed to compare estimations obtained with the dry skull method and those obtained using muscle data obtained from dissections.

1.5.3. Relationships between muscles and bite force

As expected, most of the variation in estimated bite force (81%) is explained by muscle data, that were used for the construction of the biomechanical model rather than variation in lever arms driven by the shape of the bony elements. Size and age are also important drivers of bite force (alone, they explain 60% of the total variation). Size, age, sex and muscle architecture, however, explain relatively little of the total variation in both cranial and mandible shape. However, males produce significantly higher estimated bite forces, likely due to their larger size. This was demonstrated previously with a sample of over 300 Australian red foxes (Forbes-Harper et al., 2017). These results are not surprising considering that low coefficients of correlation are typically found in mammals, including humans (Toro-Ibacache, Zapata Muñoz and O'Higgins, 2016). This suggests that other factors – possibly developmental factors – constrain the shape of the cranium and mandible (Wayne, 1986; Drake and Klingenberg, 2010).

As for dogs, the muscles that contribute most to estimated bite force are the temporalis (50%) and then the masseter (40%). The fact that foxes tend to have the largest moment about the temporomandibular joint axis produced by the temporalis is consistent with the fact that, like other carnivores, they need to produce high bite forces at high gape angles (Greaves, 1985;

Slater, Dumont and Van Valkenburgh, 2009). Interestingly, the contributions of the muscles to bite force do not reflect the contribution in muscle masses, since the masseter contributes relatively more to bite force for its volume compared to the temporalis. This is due to muscle architecture: the M. temporalis underperforms because of its longer muscle fibres, while the M. masseter overperforms thanks to shorter fibres. This is consistent with the observations of Penrose et al. (2020) across different species of canids. The fact that the superficial layers of M. masseter and M. temporalis are more developed and contribute more to the bite force in the red fox than in dogs is consistent with the necessity of a small prey hunter to close the jaws quickly. This is also in line with the long muscle fibres of the temporalis, allowing fast jaw closure. The important volume of the M. digastricus (9% of the total volume) is probably associated with the need for a fast jaw opening during prey capture (Curtis and Santana, 2018).

1.5.4. Relations between shape and bite force and comparison with dogs

Estimated bite force is explained by mandible and cranial shape, but these factors explain relatively little of total shape variation (7% and 2%, respectively), different from what has previously been shown in studies on shrews (Cornette, Tresset and Herrel, 2015) and other vertebrates (Fabre et al., 2014; Dollion et al., 2017). Despite the reduced variability in bone shape in foxes compared to dogs, the 2B-PLS analyses and Procrustes ANOVAs provided further insights into the relations between skull shape, muscle architecture, and bite force. As all muscles are strongly correlated, the deformations associated with the PCSA of all the muscular groups or estimated bite force are similar and involve the area of origin or insertion of the muscles on the bone. In particular, deformations involve the tip of the coronoid process (insertion of the M. temporalis superficialis), the rostral border of the angular process (insertion of the m. temporalis suprazygomatica), the masseteric fossa (M. masseter pars profunda and M. zygomaticomandubularis), the angular process (M. pterygoideus medialis) and, on the cranium, the sagittal crest, the temporal fossa, and the post orbital constriction (M. temporalis). Areas of mechanical constraints are also highlighted (between the orbital processes and on the snout at the midline, and the ventral curvature of the mandible) which is consistent with observations of the distribution of stress related to intrinsic loads, as described for other canids (Slater, Dumont and Van Valkenburgh, 2009).

Correlations between cranial shape and residual PCSAs were not significant, contrary to the correlations between cranial shape and residual masses (Table 1). Thus, skull shape seems to be more closely related to space constraints than to reflect the modelling of the bones to mechanical constraints imposed by the external muscle loadings contrary to the mandible. The coefficients of covariation between muscle mass and shape are more elevated for the cranium than for the mandible. The same observation has previously been made for dogs and strepsirrhines (Fabre et al., 2018). Moreover, the covariations with estimated bite force (or raw PCSA) are significant for the mandible only, contrary to what has been observed in dogs. This supports the hypothesis that, in foxes, the cranium presents a lesser degree of functional plasticity compared to the mandible, probably because it has to cope with additional functional demands, such as the protection of the sensory systems and brain (Figueirido et al., 2011; Fabre

et al., 2014). The mandible is thus a better predictor of functional demands and estimated bite force than the cranium. It is also possible that there are stronger correlations between internal bone structure and cranium and muscle PCSA or estimated bite force because cortical thickness may be a better proxy of external loads than the overall shape (Bouvier and Hylander, 1981; Daegling and Hotzman, 2003; Slizewski et al., 2013), yet this remains to be tested.

Since food mechanical properties are known to influence cortical bone modelling and remodelling (Bouvier and Hylander, 1981; Lieberman et al., 2004; Ionova-Martin et al., 2011; Scott et al., 2014a, 2014b; Ravosa et al., 2015, 2016), diet is another parameter that is worth taking into account. Unfortunately, we had no information about the diet of the specimens we dissected, so we could not test whether it impacts bone shape or estimated bite force. The relations between diet and cranial shape and bite force were investigated for Australian foxes using the dry-skull method (Forbes-Harper et al., 2017) and showed that diet does impact cranial morphology but only to a small degree. As the foxes used in this study were mostly from the countryside in South-Western France, we could not test for differences between urban or more rural foxes. These parameters would be of interest to explore in future studies.

1.6. Conclusion

Our study showed that the cranium, the mandible, and the jaw muscles form a highly integrated system in the red fox. Despite much greater variation in bone shape in domestic dogs, variation in muscle architecture was equally great in foxes and dogs and we observed similar patterns of covariation. The mandible appears more plastic than the cranium. Differences in shape and muscle architecture result in a wide range of estimated bite forces that probably offer different possibilities of adaptation according to the ecological context (e.g. more or less commensal). Future research is needed to investigate in greater detail the effect of the environmental variation on shape, muscles, and estimated bite force in domestic, commensal and wild canids.

1.7. References

Adams, D. C. and Collyer, M. L. (2016). On the comparison of the strength of morphological integration across morphometric datasets. *Evolution* **70**, 2623–2631.

Adams, D. C. and Collyer, M. L. (2017). Multivariate phylogenetic comparative methods: evaluations, comparisons, and recommendations. *Syst. Biol.* **67**, 14–31.

Aerts, P., Vree, F. D. and Herrel, A. (1997). Ecomorphology of the Lizard Feeding Apparatus: a Modelling Approach. *Neth. J. Zool.* **48**.

Aguirre, L. F., Herrel, A., Van Damme, R. and Matthysen, E. (2002). Ecomorphological analysis of trophic niche partitioning in a tropical savannah bat community. *Proc. R. Soc. Lond. B Biol. Sci.* **269**, 1271–1278.

Anderson, M. J. (2001). A new method for non-parametric multivariate analysis of variance. *Austral Ecol.* **26**, 32–46.

Anderson, M. and Braak, C. T. (2003). Permutation tests for multi-factorial analysis of variance. *J. Stat. Comput. Simul.* **73**, 85–113.

Anderson, R. A., Mcbrayer, L. D. and Herrel, A. (2008). Bite force in vertebrates: opportunities and caveats for use of a nonpareil whole-animal performance measure. *Biol. J. Linn. Soc.* **93**, 709–720.

Barone, R. (2010). *Anatomie comparée des mammifères domestiques : Tome 1, Ostéologie*. 5e édition. Paris: Vigot.

Bels, V. L. (2006). *Feeding in Domestic Vertebrates: From Structure to Behaviour*. CABI.

Bels, V. and Herrel, A. (2019). Feeding, a Tool to Understand Vertebrate Evolution Introduction to "Feeding in Vertebrates." In *Feeding in Vertebrates: Evolution, Morphology, Behavior, Biomechanics* (ed. Bels, V.) and Whishaw, I. Q.), pp. 1–18. Cham: Springer International Publishing.

Bels, V. L., Aerts, P., Chardon, M., Vandewalle, P., Berkhoudt, H., Crompton, A., de Vree, F., Dullemeijer, P., Ewert, J. and Frazzetta, T. (2012). *Biomechanics of feeding in vertebrates*. Springer Science & Business Media.

Binder, W. J. and Valkenburgh, B. V. (2000). Development of bite strength and feeding behaviour in juvenile spotted hyenas (Crocuta crocuta). *J. Zool.* **252**, 273–283.

Bisaillon, A. and DeRoth, L. (1979). Morphology and morphometry of the appendicular skeleton of the red fox (Vulpes vulpes). *Can. J. Zool.* **57**, 2089–2099.

Bookstein, F. L. (1991). *Morphometric Tools for Landmark Data: Geometry and Biology*. Cambridge University Press.

Bourke, J., Wroe, S., Moreno, K., McHenry, C. and Clausen, P. (2008). Effects of gape and tooth position on bite force and skull stress in the dingo (Canis lupus dingo) using a 3 dimensional finite element approach. *PLoS One* **3**, e2200.

Bouvier, M. and Hylander, W. L. (1981). Effect of bone strain on cortical bone structure in macaques (Macaca mulatta). *J. Morphol.* **167**, 1–12.

Brassard, C., Merlin, M., Monchâtre-Leroy, E., Guintard, C., Barrat, J., Callou, C., Cornette, R. and Herrel, A. (2020a). How Does Masticatory Muscle Architecture Covary with Mandibular Shape in Domestic Dogs? Evol Biol 47, 133–151.

Brassard, C., Merlin, M., Guintard, C., Monchâtre-Leroy, E., Barrat, J., Bausmayer, N., Bausmayer, S., Bausmayer, A., Beyer, M., Varlet, A., et al. (2020b). Bite force and its relationship to jaw shape in domestic dogs. Journal of Experimental Biology 223.

Brassard, C., Merlin, M., Guintard, C., Monchâtre-Leroy, E., Barrat, J., Callou, C., Cornette, R. and Herrel, A. (2020c). Interrelations Between the Cranium, the Mandible and Muscle Architecture in Modern Domestic Dogs. Evol Biol.

Cavallini, P. (1995). Variation in the body size of the red fox. *Ann. Zool. Fenn.* **32**, 421–427.

Christiansen, P. and Wroe, S. (2007). Bite forces and evolutionary adaptations to feedinge ecology in Carnivores. *Ecology* **88**, 347–358.

Cleuren, J., Aerts, P. and De Vree, F. (1995). Bite and joint force analysis in Caiman crocodilus. *Belg. J. Zool.* **125**, 79–94.

Collyer, M. L., Sekora, D. J. and Adams, D. C. (2015). A method for analysis of phenotypic change for phenotypes described by high-dimensional data. *Heredity* **115**, 357.

Cornette, R., Tresset, A. and Herrel, A. (2015a). The shrew tamed by Wolff's law: do functional constraints shape the skull through muscle and bone covariation? *J. Morphol.* **276**, 301–309.

Cornette, R., Tresset, A., Houssin, C., Pascal, M. and Herrel, A. (2015b). Does bite force provide a competitive advantage in shrews? The case of the greater white-toothed shrew. *Biol. J. Linn. Soc.* **114**, 795–807.

Csanády, A. (2013). Variability of the baculum in the red fox (Vulpes vulpes) from Slovakia. *Zool. Ecol.* **23**,.

Curth, S. (2018). Modularity and Integration in the Skull of Canis lupus (Linnaeus 1758): A Geometric Morphometrics Study on Domestic Dogs and Wolves. 78.

Curth, S., Fischer, M. S. and Kupczik, K. (2017). Patterns of integration in the canine skull: an inside view into the relationship of the skull modules of domestic dogs and wolves. *Zool. Jena Ger.* **125**, 1–9.

Curtis, A. A. and Santana, S. E. (2018). Jaw-Dropping: Functional Variation in the Digastric Muscle in Bats. *Anat. Rec.* **301**, 279–290.

Daegling, D. J. and Hotzman, J. L. (2003). Functional significance of cortical bone distribution in anthropoid mandibles: an in vitro assessment of bone strain under combined loads. *Am. J. Phys. Anthropol.* **122**, 38–50.

Darwin, C. (1868). *The variation of animals and plants under domestication*.

Dessem, D. and Druzinsky, R. E. (1992). Jaw-muscle activity in ferrets, Mustela putorius furo. *J. Morphol.* **213**, 275–286.

Dollion, A. Y., Measey, G. J., Cornette, R., Carne, L., Tolley, K. A., Silva, J. M. da, Boistel, R., Fabre, A.-C. and Herrel, A. (2017). Does diet drive the evolution of head shape and bite force in chameleons of the genus Bradypodion? *Funct. Ecol.* **31**, 671–684.

Drake, A. G. and Klingenberg, C. P. (2008). The pace of morphological change: historical transformation of skull shape in St Bernard dogs. *Proc. Biol. Sci.* **275**, 71–76.

Drake, A. G. and Klingenberg, C. P. (2010). Large-scale diversification of skull shape in domestic dogs: disparity and modularity. *Am. Nat.* **175**, 289–301.

Dryden, I. L. and Mardia, K. V. (2016). *Statistical Shape Analysis: With Applications in R*. John Wiley & Sons.

Dugatkin, L. A. (2018). The silver fox domestication experiment. *Evol. Educ. Outreach* **11**, 16.

Dumont, E. R. and Herrel, A. (2003). The effects of gape angle and bite point on bite force in bats. *J. Exp. Biol.* **206**, 2117–2123.

Ellis, J. L., Thomason, J. J., Kebreab, E. and France, J. (2008). Calibration of estimated biting forces in domestic canids: comparison of post-mortem and in vivo measurements. *J. Anat.* **212**, 769–780.

Ellis, J. L., Thomason, J., Kebreab, E., Zubair, K. and France, J. (2009). Cranial dimensions and forces of biting in the domestic dog. *J. Anat.* **214**, 362–373.

Fabre, A.-C., Andrade, D. V., Huyghe, K., Cornette, R. and Herrel, A. (2014). Interrelationships Between Bones, Muscles, and Performance: Biting in the Lizard Tupinambis merianae. *Evol. Biol.* **41**, 518–527.

Fabre, A.-C., Perry, J. M. G., Hartstone-Rose, A., Lowie, A., Boens, A. and Dumont, M. (2018). Do Muscles Constrain Skull Shape Evolution in Strepsirrhines? *Anat. Rec.* **301**, 291–310.

Figueirido, B., Macleod, N., Krieger, J., De Renzi, M., Pérez-Claros, J. and Palmqvist, P. (2011). Constraint and adaptation in the evolution of carnivoran skull shape. *Paleobiology* **37**, 490–518.

Foote, M. (1993). Contributions of Individual Taxa to Overall Morphological Disparity. *Paleobiology* **19**, 403–419.

Forbes-Harper, J. L., Crawford, H. M., Dundas, S. J., Warburton, N. M., Adams, P. J., Bateman, P. W., Calver, M. C. and Fleming, P. A. (2017). Diet and bite force in red foxes: ontogenetic and sex differences in an invasive carnivore. *J. Zool.* **303**, 54–63.

Goodall, C. (1991). Procrustes methods in the statistical analysis of shape. *J. R. Stat. Soc. Ser. B Methodol.* **53**, 285–321.

Greaves, W. (1985). The generalised carnivore jaw. *Zool. J. Linn. Soc.* **85**, 267–274.

Greaves, W. S. (2000). Location of the vector of jaw muscle force in mammals. *J. Morphol.* **243**, 293–299.

Greaves, W. S. (2002). Modeling the distance between the molar tooth rows in mammals. *Can. J. Zool.* **80**, 388–393.

Gröning, F., Jones, M. E. H., Curtis, N., Herrel, A., O'Higgins, P., Evans, S. E. and Fagan, M. J. (2013). The importance of accurate muscle modelling for biomechanical analyses: a case study with a lizard skull. *J. R. Soc. Interface* **10**, 20130216.

Gueldre, G. and Vree, F. (1990). Biomechanics of the masticatory apparatus of *Pteropus giganteus* (Megachiroptera). *J. Zool.* **220**, 311–332.

Gunz, P., Mitteroecker, P. and Bookstein, F. L. (2005). Semilandmarks in Three Dimensions. In *Modern Morphometrics in Physical Anthropology* (ed. Slice, D. E.), pp. 73–98. Boston, MA: Springer US.

Hannam, A. G. and Wood, W. W. (1989). Relationships between the size and spatial morphology of human masseter and medial pterygoid muscles, the craniofacial skeleton, and jaw biomechanics. *Am. J. Phys. Anthropol.* **80**, 429–445.

Hartstone-Rose, A., Perry, J. M. G. and Morrow, C. J. (2012). Bite Force Estimation and the Fiber Architecture of Felid Masticatory Muscles. *Anat. Rec.* **295**, 1336–1351.

Haxton, H. A. (1944). Absolute muscle force in the ankle flexors of man. *J. Physiol.* **103**, 267–273.

Heck, L., Wilson, L. A. B., Evin, A., Stange, M. and Sánchez-Villagra, M. R. (2018). Shape variation and modularity of skull and teeth in domesticated horses and wild equids. *Front. Zool.* **15**, 14.

Herrel, A. and Aerts, P. (2004). Biomechanical Studies of Food and Diet Selection. In *eLS*, p. American Cancer Society.

Herrel, A., Aerts, P. and De Vree, F. (1998a). Ecomorphology of the lizard feeding apparatus: a modelling approach. *Neth. J. Zool.* **48**, 1–25.

Herrel, A., Aerts, P. and De Vree, D. (1998b). Static biting in lizards: functional morphology of the temporal ligaments. *J. Zool.* **244**, 135–143.

Herrel, A., Spithoven, L., Van Damme, R. and DE Vree, F. (1999). Sexual dimorphism of head size in Gallotia galloti: testing the niche divergence hypothesis by functional analyses. *Funct. Ecol.* **13**, 289–297.

Herrel, A., De Smet, A., Aguirre, L. F. and Aerts, P. (2008). Morphological and mechanical determinants of bite force in bats: do muscles matter? *J. Exp. Biol.* **211**, 86–91.

Herring, S. W. and Herring, S. E. (1974). The superficial masseter and gape in mammals. *Am. Nat.* **108**, 561–576.

Herring, S. W., Rafferty, K. L., Liu, Z. J. and Marshall, C. D. (2001). Jaw muscles and the skull in mammals: the biomechanics of mastication. *Comp. Biochem. Physiol. A. Mol. Integr. Physiol.* **131**, 207–219.

Herzog, W. (1994). Muscle. In *Biomechanics of the musculoskeletal system*, pp. 154–187. B.M. Nigg & W. Herzog.

Hulme-Beaman, A., Dobney, K., Cucchi, T. and Searle, J. B. (2016). An Ecological and Evolutionary Framework for Commensalism in Anthropogenic Environments. *Trends Ecol. Evol.* **31**, 633–645.

Ionova-Martin, S. S., Wade, J. M., Tang, S., Shahnazari, M., Ager, J. W., Lane, N. E., Yao, W., Alliston, T., Vaisse, C. and Ritchie, R. O. (2011). Changes in cortical bone response to high-fat diet from adolescence to adulthood in mice. *Osteoporos. Int. J. Establ. Result Coop. Eur. Found. Osteoporos. Natl. Osteoporos. Found. USA* **22**, 2283–2293.

Jaslow, C. R. (1987). Morphology and digestive efficiency of red foxes (Vulpes vulpes) and grey foxes (Urocyon cinereoargenteus) in relation to diet. *Can. J. Zool.* **65**, 72–79.

Kerr, E., Cornette, R., Gomes Rodrigues, H., Renaud, S., Chevret, P., Tresset, A. and Herrel, A. (2017). Can functional traits help explain the coexistence of two species of Apodemus? *Biol. J. Linn. Soc.* **122**, 883–896.

Klingenberg, C. P., Barluenga, M. and Meyer, A. (2002). Shape analysis of symmetric structures: quantifying variation among individuals and asymmetry. *Evolution* **56**, 1909–1920.

Lieberman, D. E., Krovitz, G. E., Yates, F. W., Devlin, M. and St. Claire, M. (2004). Effects of food processing on masticatory strain and craniofacial growth in a retrognathic face. *J. Hum. Evol.* **46**, 655–677.

Lindner, D., Marretta, S., Pijanowski, G., Johnson, A. and Smith, C. (1995). Measurement of bite force in dogs: a pilot study. *J. Vet. Dent.* **12**, 49–52.

Machado, F. A., Zahn, T. M. G. and Marroig, G. (2018). Evolution of morphological integration in the skull of Carnivora (Mammalia): Changes in Canidae lead to increased evolutionary potential of facial traits. *Evolution* **72**, 1399–1419.

Mendez, J. and Keys, A. (1960). Density and composition of mammalian muscle. *Metabolism* **9**, 184–188.

Meyers, J. J., Nishikawa, K. C. and Herrel, A. (2018). The evolution of bite force in horned lizards: the influence of dietary specialisation. *J. Anat.* **232**, 214–226.

Mitteroecker, P., Gunz, P., Bernhard, M., Schaefer, K. and Bookstein, F. L. (2004). Comparison of cranial ontogenetic trajectories among great apes and humans. *J. Hum. Evol.* **46**, 679–698.

Nogueira, M. R., Peracchi, A. L. and Monteiro, L. R. (2009). Morphological correlates of bite force and diet in the skull and mandible of phyllostomid bats. *Funct. Ecol.* **23**, 715–723.

Penrose, F., Kemp, G. J. and Jeffery, N. (2016). Scaling and Accommodation of Jaw Adductor Muscles in Canidae. *Anat. Rec.* **299**, 951–966.

Penrose, F., Cox, P., Kemp, G. and Jeffery, N. (2020). Functional morphology of the jaw adductor muscles in the Canidae. *Anat. Rec.* **n/a**,.

Perry, J. M. G., Hartstone-Rose, A. and Logan, R. L. (2011). The Jaw Adductor Resultant and Estimated Bite Force in Primates. *Anat. Res. Int.*

Radinsky, L. B. (1981). Evolution of skull shape in carnivores: 1. Representative modern carnivores. *Biol. J. Linn. Soc.* **15**, 369–388.

Ravosa, M. J., Scott, J. E., McAbee, K. R., Veit, A. J. and Fling, A. L. (2015). Chewed out: an experimental link between food material properties and repetitive loading of the masticatory apparatus in mammals. *PeerJ* **3**,.

Ravosa, M. J., Menegaz, R. A., Scott, J. E., Daegling, D. J. and McAbee, K. R. (2016). Limitations of a morphological criterion of adaptive inference in the fossil record. *Biol. Rev. Camb. Philos. Soc.* **91**, 883–898.

Rohlf, F. J. and Corti, M. (2000). Use of two-block partial least-squares to study covariation in shape. *Syst. Biol.* **49**, 740–753.

Rohlf, F. and Slice, D. (1990). Extensions of the Procrustes Method for the Optimal Superimposition of Landmarks. *Syst. Zool.* **39**,.

Sánchez-Villagra, M. R., Geiger, M. and Schneider, R. A. (2016). The taming of the neural crest: a developmental perspective on the origins of morphological covariation in domesticated mammals. *R. Soc. Open Sci.* **3**, 160107.

Santagati, F. and Rijli, F. M. (2003). Cranial neural crest and the building of the vertebrate head. *Nat. Rev. Neurosci.* **4**, 806–818.

Santana, S. E. (2016). Quantifying the effect of gape and morphology on bite force: biomechanical modelling and in vivo measurements in bats. *Funct. Ecol.* **30**, 557–565.

Schipper, J., Chanson, J. S., Chiozza, F., Cox, N. A., Hoffmann, M., Katariya, V., Lamoreux, J., Rodrigues, A. S., Stuart, S. N. and Temple, H. J. (2008). The status of the world's land and marine mammals: diversity, threat, and knowledge. *Science* **322**, 225–230.

Schlager, S. (2013). Soft-tissue reconstruction of the human nose : population differences and sexual dimorphism.

Scott, J. E., McAbee, K. R., Eastman, M. M. and Ravosa, M. J. (2014a). Experimental perspective on fallback foods and dietary adaptations in early hominins. *Biol. Lett.* **10**, 20130789.

Scott, J. E., McAbee, K. R., Eastman, M. M. and Ravosa, M. J. (2014b). Teaching an old jaw new tricks: diet-induced plasticity in a model organism from weaning to adulthood. *J. Exp. Biol.* **217**, 4099–4107.

Selba, M. C., Oechtering, G. U., Gan Heng, H. and DeLeon, V. B. (2019). The impact of selection for facial reduction in dogs: geometric morphometric analysis of canine cranial shape. *Anat. Rec.* 17.

Slater, G. J. and Van Valkenburgh, B. (2009). Allometry and performance: the evolution of skull form and function in felids. *J. Evol. Biol.* **22**, 2278–2287.

Slater, Gj., Dumont, E. and Van Valkenburgh, B. (2009). Implications of predatory specialisation for cranial form and function in canids. *J. Zool.* **278**, 181–188.

Slizewski, A., Schönau, E., Shaw, C. and Harvati, K. (2013). Muscle area estimation from cortical bone. *Anat. Rec.* **296**, 1695–1707.

Smith, K. K. (1993). The form of the feeding apparatus in terrestrial vertebrates: studies of adaptation and constraint. *The skull* **3**, 150–196.

Spencer, M. A. (1998). Force production in the primate masticatory system: electromyographic tests of biomechanical hypotheses. *J. Hum. Evol.* **34**, 25–54.

Szuma, E. (2004). Evolutionary implications of morphological variation in the lower carnassial of red foxVulpes vulpes. *Acta Theriol. (Warsz.)* **49**, 433–447.

Taylor, A. B. and Vinyard, C. J. (2013). The relationships among jaw-muscle fiber architecture, jaw morphology, and feeding behavior in extant apes and modern humans. *Am. J. Phys. Anthropol.* **151**, 120–134.

Thomason, J. J. (1991). Cranial strength in relation to estimated biting forces in some mammals. *Can. J. Zool.* **69**, 2326–2333.

Toro-Ibacache, V., Zapata Muñoz, V. and O'Higgins, P. (2016). The relationship between skull morphology, masticatory muscle force and cranial skeletal deformation during biting. *Ann. Anat. - Anat. Anz.* **203**, 59–68.

Trut, L. (1999). Early Canid Domestication: The Farm-Fox Experiment: Foxes bred for tamability in a 40-year experiment exhibit remarkable transformations that suggest an interplay between behavioral genetics and development. *Am. Sci.* **87**, 160–169.

Trut, L., Oskina, I. and Kharlamova, A. (2009). Animal evolution during domestication: the domesticated fox as a model. *Bioessays* **31**, 349–360.

Tseng, Z. J. and Flynn, J. J. (2015a). Convergence analysis of a finite element skull model of Herpestes javanicus (Carnivora, Mammalia): implications for robust comparative inferences of biomechanical function. *J. Theor. Biol.* **365**, 112–148.

Tseng, Z. J. and Flynn, J. J. (2015b). Are cranial biomechanical simulation data linked to known diets in extant taxa? A method for applying diet-biomechanics linkage models to infer feeding capability of extinct species. *PLoS One* **10**,.

Tseng, Z. J. and Flynn, J. J. (2015c). An integrative method for testing form–function linkages and reconstructed evolutionary pathways of masticatory specialisation. *J. R. Soc. Interface* **12**, 20150184.

Tseng, Z. J. and Flynn, J. J. (2018). Structure-function covariation with nonfeeding ecological variables influences evolution of feeding specialisation in Carnivora. *Sci. Adv.* **4**,.

Van Valkenburgh, B. and Koepfli, K. (1993). Cranial and dental adaptations to predation in canids.pp. 15–37.

Wayne, R. K. (1986). Cranial Morphology of Domestic and Wild Canids: The Influence of Development on Morphological Change. *Evolution* **40**, 243–261.

Wiley, D. F., Amenta, N., Alcantara, D. A., Ghosh, D., Kil, Y. J., Delson, E., Harcourt-Smith, W., Rohlf, F. J., John, K. S. and Hamann, B. (2005). Evolutionary morphing. In *VIS 05. IEEE Visualization, 2005.*, pp. 431–438.

Wroe, S., Clausen, P., McHenry, C., Moreno, K. and Cunningham, E. (2007). Computer simulation of feeding behaviour in the thylacine and dingo as a novel test for convergence and niche overlap. *Proc. R. Soc. B Biol. Sci.* **274**, 2819–2828.

Zatoń-Dobrowolska, M., Moska, M., Mucha, A., Wierzbicki, H. and Dobrowolski, M. (2017). Variation in fur farm and wild populations of the red fox, Vulpes vulpes (Carnivora: Canidae). Part II: Craniometry. *Can. J. Anim. Sci.*

Zelditch, M. L., Swiderski, D. L. and Sheets, H. D. (2012). *Geometric Morphometrics for Biologists: A Primer*. Academic Press.

2. The dingo Canis lupus dingo

2.1. Allometries in mandibular and cranial shape

Following the same methodology as in the previous articles, we explored allometries in mandible (n=10) and cranial (n=7) shape in dingoes. The sample size is lower for the cranium because one adult and two juveniles had their cranium too damaged to be included. The better preservation of mandibles after the boiling process offers an opportunity to visualise the (strong) growth allometries (Figure 50A). Allometries remain important even without the juveniles (Figure 50B,C).

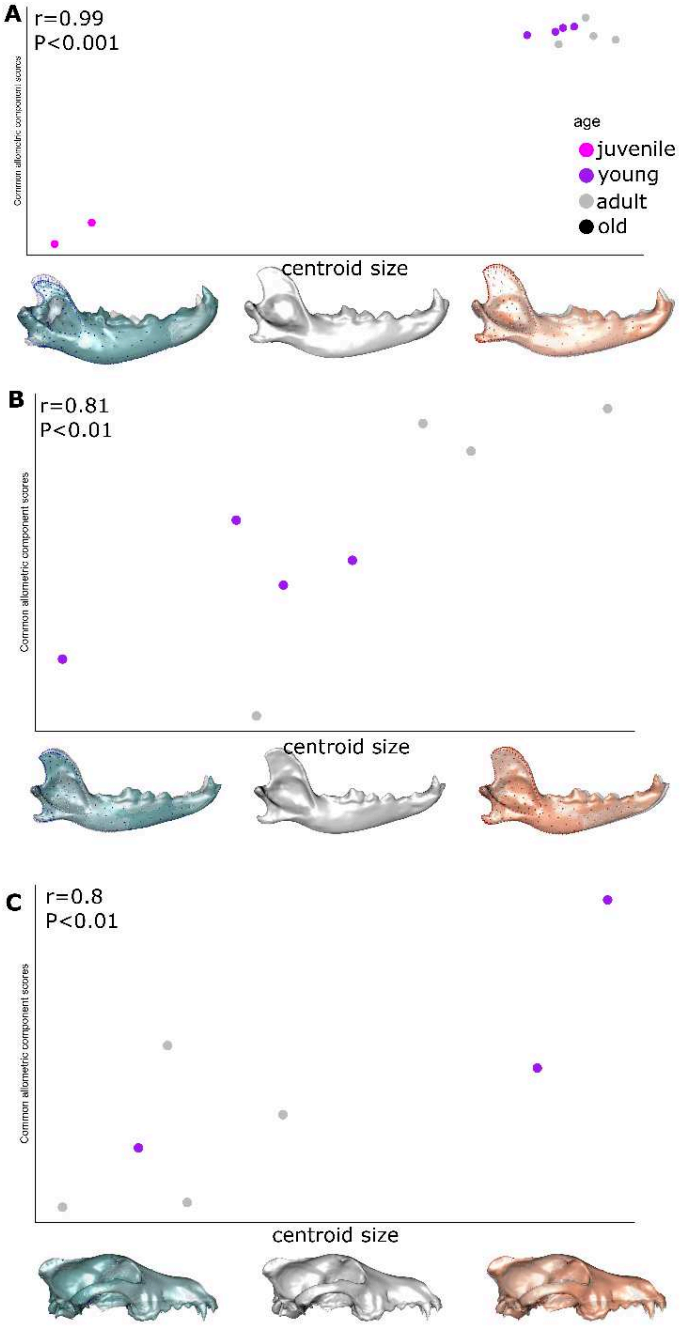

Figure 50. Visualisation of the deformations along the allometry slope. A: mandible shape with juvenile dingoes included in the analysis; B: mandible shape with juvenile dingoes excluded from the analysis; C: skull shape with juvenile dingoes excluded from the analysis.

2.1. Covariations between mandibular and cranial shapes

Following the same methodology as in the previous articles, we explored the covariations between the shape of the mandible and cranium or between the allometry-free shapes in dingoes (n=7). Given their small number, these results are very preliminary and should be considered with caution. Although not significant given the small sample size, the results tend to indicate very strong covariations with deformations similar to those previously described in Chapter 3 for dogs (Figure 51).

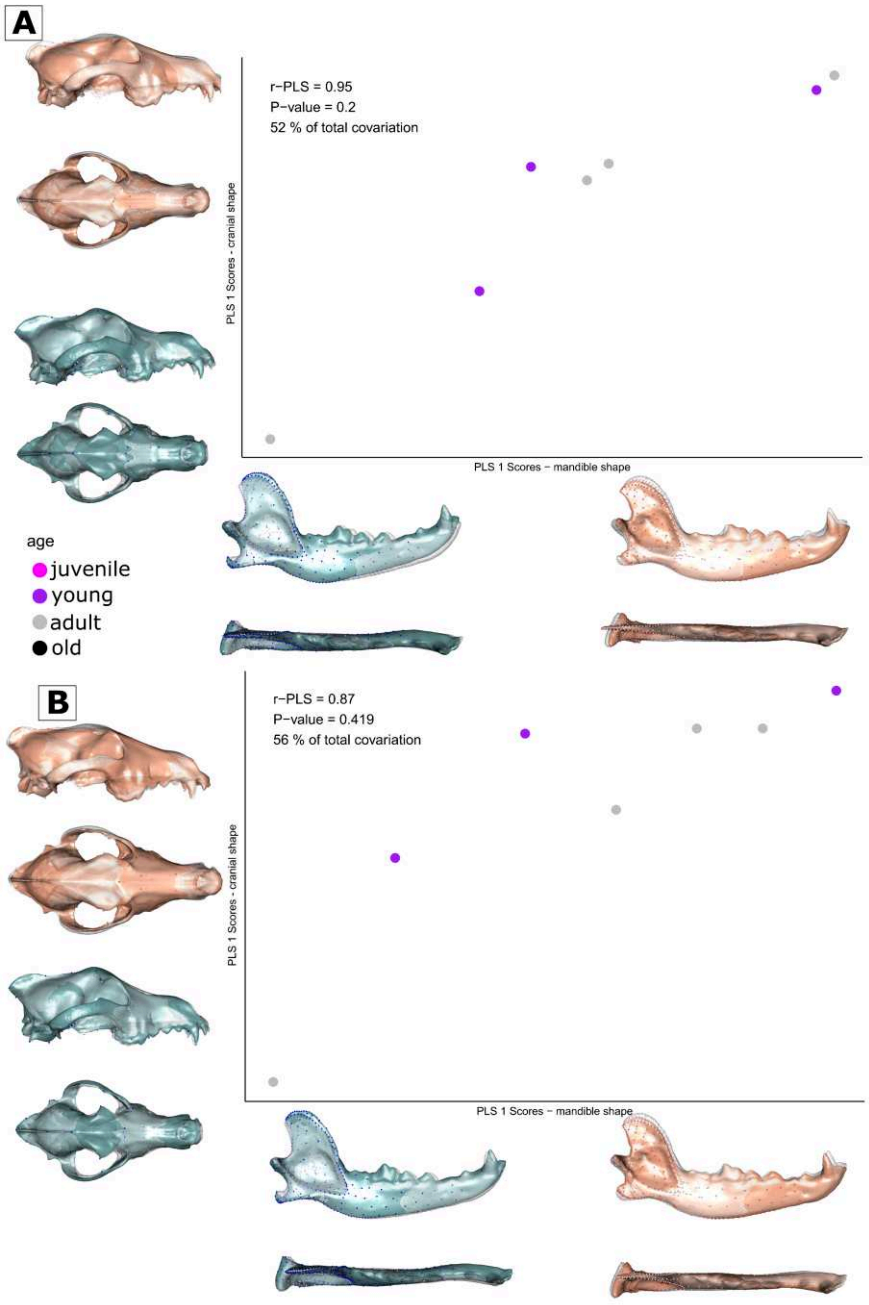

Figure 51. 2-Block Partial Least Square analyses between the shapes of the mandible and cranium (A) or between the allometry-free shapes (B), with vectors and shapes at the minimum and maximum of the PLS axis. Illustrations represent the deformations from the consensus to the extreme of the axis in lateral and dorsal views. Ages are indicated by different colors.

2.2. Covariations between muscle mass and skull shape

Following the same methodology as in articles 1, 2 and 4, we explored the covariations between the shape of the mandible (n=8) or cranium (n=7) and the mass or PCSA of the main muscle groups (digastric, masseter and temporal) in non-juvenile dingoes. Given their small number, these results are very preliminary and should be considered with caution.

However, the results tend to indicate very strong covariations between the shape of the mandible or skull and the muscle architecture data (Table 14, Figure 52). As in the dog, the covariation coefficients tend to be higher for the skull. The P-values are not significant which is related to the low number of individuals. The deformations associated with variation in muscle data are similar to those previously described in Chapter 3 for dogs (aspect of the coronoid process, curvature and robustness of the mandible).

As the dingoes stayed on site (veterinary school of life science, Murdoch university) and we did not have a microscribe, we did not estimate bite forces.

Detailed data about the dingo sample are provided in the appendices (page 618).

Table 14. Results of the 2B-PLS analyses performed between muscle masses and mandibular or cranial shape in dingoes.

Shape	r-PLS	P	PLS1
MASS			
Mandibular shape – mass	0.85	0.24	97%
Mandibular shape – scaled mass	0.88	0.20	89%
Allometry-free mandibular shape – scaled mass	0.88	0.051	92%
Cranial shape - mass	0.92	0.21	95%
Cranial shape – scaled mass	0.92	0.21	95%
Cranial shape – scaled mass	0.92	0.21	95%
Allometry-free cranial shape – scaled mass	0.91	0.076	95%
PCSA			
Mandibular shape – PCSA	0.84	0.29	86%
Mandibular shape – scaled PCSA	0.88	0.19	87%
Allometry-free mandibular shape – scaled PCSA	0.8	0.04	87%
Cranial shape - PCSA	0.92	0.22	87%
Cranial shape – scaled PCSA	0.92	0.21	88%
Allometry-free cranial shape – scaled PCSA	0.92	0.1	88%

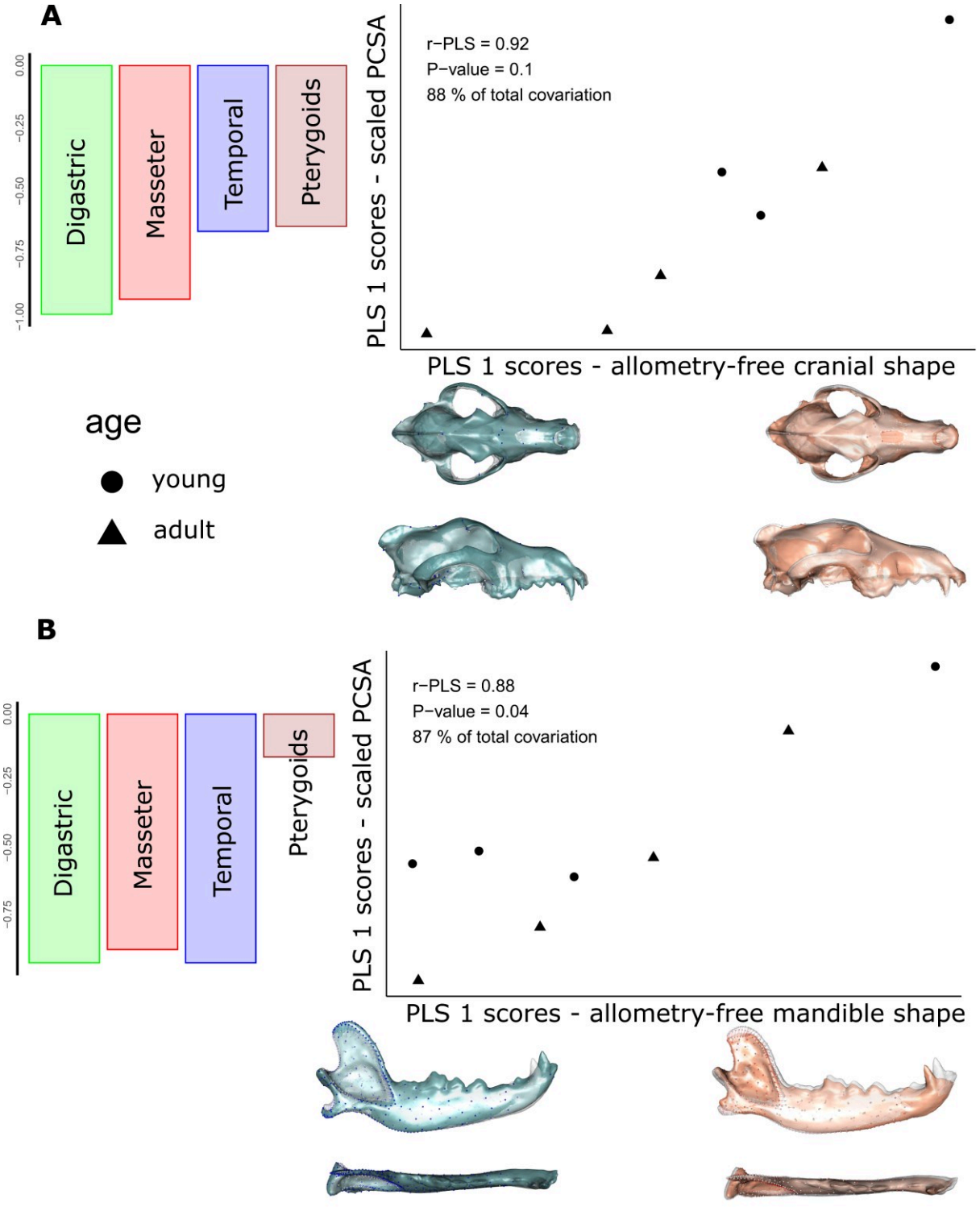

Figure 52. 2-Block Partial Least Square analyses between the residual PCSA and the allometry-free cranial (A) or mandibular (B) shapes, with vectors and shapes at the minimum and maximum of the PLS axis. Illustrations represent the deformations from the consensus to the extreme of the axis in lateral and dorsal views. Ages are indicated by different shapes.

Chapter 5.
Developmental, environmental or dietary factors driving morphological and functional variability in the lower jaw of red foxes

In this chapter, we explored how some developmental and environmental factors may drive the shape of the mandible in commensal canids. To do this, we studied a large population of Australian foxes (>400 individuals) for which these types of data were available (Forbes-Harper *et al.*, 2017). Based on the results of article 4, which suggests that the shape of the mandible covaries strongly with bite force, we established a predictive model of bite force based on the form of the mandible. This model was applied to Australian red foxes and the bite force estimates were compared with those obtained using the dry-skull method or dissection data.

In a first step (article 5), we explored the relationship between mandible shape or bite force and developmental (age, sex, and body mass) and environmental data given by the geographical location of individuals. From the geographical locations, we were able to assess the impact of climatic factors (precipitation, temperature) and the proximity between commensal foxes and human settlements (based on demographics). We also compared the morphological variability within this Australian population to that within our European corpus, in order to assess the effect of introduction into a novel environment.

In a second step (article 6), information on stomach contents of these red foxes allowed us to study the relationship between mandibular shape or bite force and diet.

From the two articles the following key points emerge:

KEY POINTS

In red foxes, the shape of the mandible and bite force are strongly related to size and age, and a strong sexual dimorphism exists (males bite stronger than females, which is related to differences in size between the two sexes).

Australian foxes differ from European foxes in terms of average shape and size and bite force. There are also significant differences between geographical regions in Australia. In addition, climatic variations (temperature, rainfall) are accompanied by morphological variations.

Morphological differeeces between urban and rural contexts are subtle and need further research.

⇨ **In archaeological canids, morphological and functional differences between geographical regions are to be expected, especially as they are far apart and are characterized by different climates (e.g. South-Eastern and Western Europe, Northern and Southern France). Differences among regions through the Neolithic period may also be linked to the growing anthropization of the environment with the multiplication of permanent villages (which influences the living environment for canids and leads to functional adaptations or a relaxation of certain selection pressures).**

Variations in diet do not appear to be strongly related to variations in the shape of the mandible but a little more to variation in bite force. However, the relationships are weak and tend to be related to age and sex differences in diet: The increase of carrion (sheep) in the diet of young animals and adult males is accompanied by a decrease in bite force, even relative to size. The increase in the consumption of small preys (rodents), particularly by adult females, is accompanied by a relative increase in bite force.

⇨ **Variation in the shape of the mandible in archaeological canids cannot be interpreted directly in terms of differences in diet, and one should be very cautious when interpreting variations in bite force in terms of changes in diet.**

1. Non-feeding factors driving variation in mandibular shape in red foxes

Article 5 –
How do non-feeding constraints shape the mandible in red foxes?

Colline Brassard, Jesse L. Forbes-Harper, Heather M. Crawford, John-Michael Stuart, Natalie M. Warburton, Michael C. Calver, Peter Adams, Elodie Monchâtre-Leroy, Jacques Barrat, Claude Guintard, Hélène Garès, Arnault Larralle, Raymond Triquet, Marilaine Merlin, Raphaël Cornette, Anthony Herrel, Patricia A. Fleming

How do non-feeding constraints shape the mandible in red foxes?

Colline Brassard[1,*], Forbes-Harper[2] , Crawford[3] , Dundas[3], Warburton[3], Elodie Monchâtre-Leroy[4], Jacques Barrat[4], Claude Guintard[5,6], Hélène Garès[7], Arnault Larralle, Raymond Triquet, Marilaine Merlin[1], Raphaël Cornette[8], Anthony Herrel[1] & Trish Fleming[2]

[1] UMR 7179 Mécanismes Adaptatifs et Evolution (CNRS, MNHN), Muséum national d'Histoire naturelle, Paris, France.

[2] School of Veterinary & Life Sciences, Murdoch University, Murdoch, WA, Australia

[3] Department of Environment and Agriculture, Curtin University, Bentley, WA, Australia

[4] ANSES, Laboratoire de la rage et dela faune sauvage, Station expérimentale d'Atton, Malzéville, France.

[5] Laboratoire d'Anatomie comparée, Ecole Nationale Vétérinaire, de l'Agroalimentaire et de l'Alimentation, Nantes Atlantique – ONIRIS, Nantes Cedex 03, France.

[6] GEROM, UPRES EA 4658, LABCOM ANR NEXTBONE, Faculté de santé de l'Université d'Angers, France.

[7] Direction des Services Vétérinaires –D.D.C.S.P.P. de la Dordogne, Périgueux, France.

[8] UMR 7205 Institut de Systématique, Evolution, Biodiversité (CNRS, MNHN, UPMC, EPHE), Muséum national d'Histoire naturelle, Paris, France.

* Corresponding author: colline.brassard@mnhn.fr

1.1. Abstract

The red fox is one of the most common and widespread species of carnivore suggesting that it can rapidly adapt to differences in ecological context. However, the morphological variability of this canid, although a major element that likely accounts for this adaptability, remains poorly studied. We describe the variability in mandible shape and jaw muscle architecture (physiological cross-sectional area, mass) and test whether these differ between native and invasive populations. Next, we explore the developmental or environmental parameters that may impact this variability. For this purpose, we used three dimensional geometric morphometric analyses on the mandibles of 433 Australian and 69 French foxes of the species *Vulpes vulpes*, and we dissected fourteen Australian red foxes to compare the muscle architecture with data previously obtained for French foxes. We explored the impact of age, sex, body mass, as well as location (GPS coordinates, degree of urbanism), temperature or rainfall through Procrustes ANOVAs for the invasive population. Our results showed that Australian and French foxes significantly differ in mandibular shape with French foxes show greater variability. In the Australian foxes, all parameters tested show significantly impacted mandibular shape. Visualisations of the deformation along the regression axes highlighted functionally important areas of the mandible, suggesting that changes in non-feeding variables impact the function of the mandible.

1.2. Introduction

The factors driving morphological variation in the vertebrate skull are not fully understood and are very complex (e.g. Van Valkenburgh & Koepfli 1993; Wroe & Milne 2007; Figueirido et al. 2011; Schoenebeck & Ostrander 2013). It has previously been demonstrated based on studies using geometric morphometrics and finite element analysis that cranial shape depends on more than just feeding ecology (Tseng and Flynn, 2018). Indeed, size, age and sex are known to influence cranial shape. Moreover, environmental constraints also play a fundamental role in driving skull shape evolution since locally varying selective pressures (e.g., competition, available resources, sexual selection, climate) will favour advantageous variants and cause them to become more common (Darwin, 1909; Gittleman, 1985; Meiri et al., 2004; Meloro et al., 2011).

Given the complexity of the cranial system these are difficult questions to address. However, invasive populations often provide excellent study systems as animals are transferred by humans into radically divergent habitats allowing one to test for differences in morphology in relation to external variables. Moreover, focusing on the mandible may be of interest as this structure is specialized towards biting and thus likely reflects direct selection on function. To address these questions, we here focus on a commensal canid, the red fox, that not only has a wide distribution area but also has been introduced in many areas around the world thus providing an excellent opportunity to investigate the drivers of variation in mandibular shape. Indeed, *Vulpes vulpes* is one of the most widespread species of carnivores on the planet (Schipper et al., 2008). It has colonised the entire Holarctic and the European red fox has been successfully introduced into the South-east of Australia in 1855 (Rolls, 1969; Saunders et al., 2010) for recreational hunting and hunting control (Cox, 2004). The species has since spread across the continent with the exception of tropical areas at North (Forsyth, 2004; Statham et al., 2014) and some off-shore islands.

Accordingly, the red fox has colonised and likely adapted to many different habitats, ranging from tundra to deserts to cities. Indeed, it has successfully invaded urban environments in many parts of the world (Artois, 1989; Debuf, 1987; Doncaster and Macdonald, 1997; Gloor et al., 2001; Wandeler et al., 2003). In urban environments, red foxes find more favourable conditions to survive and spread, likely related to increased food accessibility. In Australia, human activity provides foxes with dead livestock, kangaroos and abundant shelter (Hulme-Beaman et al., 2016). Consequently, urban foxes have reduced home ranges compared with foxes of rural populations (Hulme-Beaman et al., 2016). This widely distributed and thus highly adaptable species, thus provides a unique opportunity to investigate functional and morphological responses to climatic variation (Schipper et al., 2008; Statham et al., 2014) or to anthropic constraints and urbanisation. In particular, these different natural and artificial selection pressures may induce phenotypic variation in different traits of *Vulpes Vulpes* (Melero et al. 2012; Zatoń-Dobrowolska et al. 2016).

Surprisingly, relatively few studies have explored the morphological variability within the species. Most of the studies have focused on the teeth (Gingerich & Winkler 1979; Pengilly

1984; Szuma 2004), the baculum (Čanády, 2013) or the skull (Aubry, 1983; Churcher, 1959; Forbes-Harper et al., 2017; Hartová-Nentvichová et al., 2010; Hell et al., 1989; Huson and Page, 1980; Jojić et al., 2017; Sacks et al., 2010). Variation in the morphology may reflect both genetic determinism and phenotypic plasticity. Phenotypic plasticity (i.e. "the ability of a single genotype to produce more than one alternative form of morphology, physiological state, and/or behavior in response to environmental condition", West-Eberhard 1989) may have played a key role in the success of the species because it could explain how it can quickly morphologically or functionally adapt to different environmental conditions. However, local adaptation is also likely to occur (Edwards et al., 2012; Sacks et al., 2010). Indeed, geographical variation of the morphology in red foxes has been previously reported (Churcher, 1959; Huson and Page, 1980; Jojić et al., 2017; Sacks et al., 2010; Stepkovitch et al., 2019). Churcher (1959) conducted a morphometric study of North American and Eurasian red foxes and found that some dental and cranial measurements varied between the continents. Surprisingly, the morphology of red foxes has never been compared between the invasive Australian and the native European population. Huson & Page (1980) identified variation in skull measurements between six counties in Wales, probably in response to adaptations to local environmental conditions. Jojić et al. (2017) used geometric morphometric techniques and found that cranial shape of Serbian red foxes varies geographically, as well as depending on proportion of agricultural habitats. Specimen from Northern regions (with higher proportions of agricultural areas) have more robust crania with shorter snouts and maxillae, larger palatine bones accompanied with anteriorly moved posterior edges of the canine alveolus and laterally expanded zygomatic arches. The authors suggested that these shape changes are related to dietary differences. Stepkovitch et al. (2019) found that urban red foxes had larger body mass and skeletal measurements than foxes living in more natural habitats in a sample of 135 red foxes of Sydney region. They hypothesised that the urban environment provided favourable conditions for foxes to increase in size, enabling them to hunt a wider range of prey. Other evidence of significant craniometric and dental between wild and farm populations variation have been reported, for example in red foxes from the Czech Republic (Zatoń-Dobrowolska et al., 2017). In a morphometric study on 540 red foxes from Western Australia, Forbes-Harper et al. (2017) found that most of the variation in cranial shape was driven by age, but sex also had an influence. Our goal here was to explore the variation in the same population of Australian red foxes (Forbes-Harper et al., 2017), focusing on the mandible and the jaw muscles. We first test whether Australian foxes have developed different morphologies compared to red foxes from France (including, size, shape and jaw muscle architecture). Second, we explore the developmental drivers of mandible shape variation (body mass, centroid size, sex, age) and finally test how mandible shape is associated with variation in ecological context (geographic location, urbanism, temperatures or rainfall).

1.3. Material and methods

1.3.1. Sample and information

The dataset is composed of the mandibles of 502 foxes *Vulpes vulpes* used for shape analyses. Sixty-nine of the mandibles belong to European foxes (65 red foxes and 4 silver foxes). The others mandibles (433) belong to Australian foxes. Fourteen of them, similar in size, were dissected in this study. For most of the 419 other Australian foxes, information about their body mass, age, sex, and provenance are available (see Forbes-Harper et al., 2017). Because very few foxes were over 4 years old, we considered four groups: foxes of 1, 2, 3 or 4 and more years old. Fourteen different localities in Western Australia (Fig. 1) are represented. Most of the sites are located in very rural areas (with a very low number of inhabitants), however, some foxes are from bigger cities, which enable us to construct a rural to urban gradient. In Australia, the home ranges of foxes in rural environments are about 500 ha (Queensland government, 2019). We chose to consider the number of inhabitants within a 5km radius area using the NASA SEDAC Population Estimator. Rural foxes ('R') correspond to areas with less than 100 inhabitants and urban foxes ('U') correspond to areas where the number of humans exceeds 1000 inhabitants. Two intermediate groups represent values between 100 and 350 inhabitants ('SR1') and between 350 and 1000 inhabitants ('SR2'). The limits between groups were arbitrarily defined to represent equally all categories. We also extracted climatic data using the function 'getData' from the package 'raster' in R version 3.6.0 (2019-04-26). Climatic data are extracted from WorldClim version 2 (Fick and Hijmans, 2017), a database of global interpolated climate data. Monthly climate data are averaged for minimum (bio6 variable) and maximum temperature (bio5), and for precipitation (bio12) for the period from 1970 to 2000. Detailed information about the sample are reported in Table 1 and Table S1.

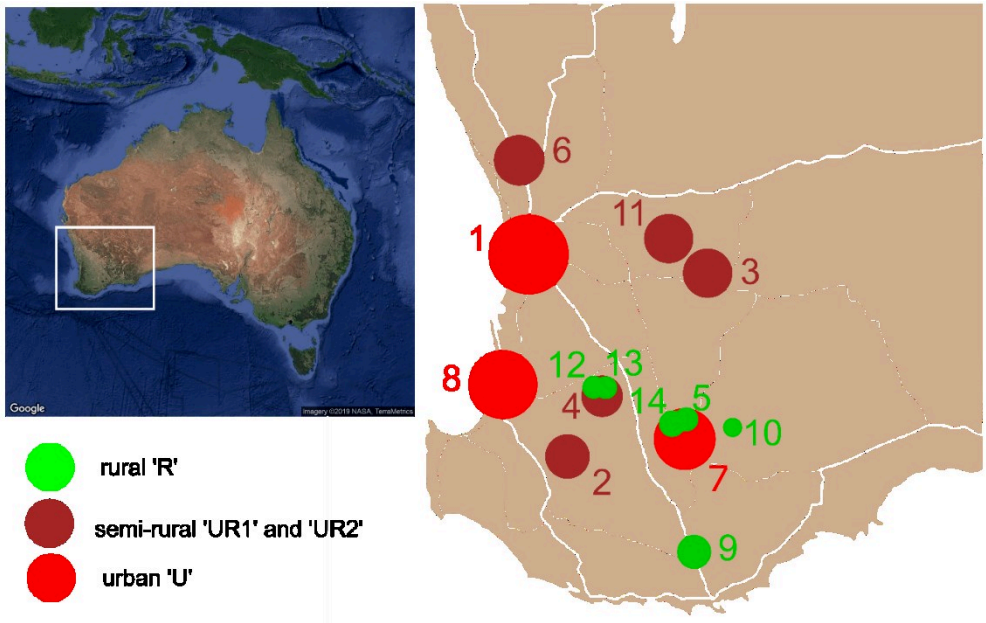

Fig. 1. Locations of the Australian foxes considered in this study.
1: Armadale; 2: Boyup Brook; 3: Corrigin; 4: Darkan; 5: Dumbleyung; 6: Gingin; 7: Katanning; 8: Kemerton; 9: Mt. Baker; 10: Nyabing; 11: Quairading; 12: Quindanning-Darkan; 13: Williams-Darkan; 14: Woodanilling. Colors indicate the degree of urbanism: rural foxes 'R' are illustrated in green, 'UR1' and 'UR2' are in brown, and urban foxes 'U' are illustrated in red. Point sizes are proportional to the number of inhabitants in a radius of 5 km around the city.

Table 1. Specimens used in this study and sample sizes.
Diss: specimens dissected; Shape: shape analyses were performed; F: female; M: male; A1: 1 year old; A2: 2 years old; A3: 3 years old; A4+: more than 4 years old; R: 'rural'; SR1: 'semirural 1'; SR2: 'semirural 2'; U: 'urban'. Report to Table S1 for details.

Geographic location	Diss	Shape	Bodymass	Age	Sex	urbanism	
France	65 (mass) – 63 (PCSA)	69			23F 38M		
Australian-dissected	14	14					
Armadale		3	3	3A1	2F 1M	3	U
Boyup Brook		51	51	36A1 11A2 1A3 3A4+	23F 28M	51	SR1
Corrigin		15	15	4A1 4A2 2A3 5A4+	8F 7M	15	SR2
Darkan		138	137	100A1 22A2 7A3 2A4+	63F 75M	138	SR1
Dumbleyung		11	11	3A1 6A2 1A3 1A4+	6F 5M	11	R
Gingin		14	14	4A1 7A2 3A4+	6F 8M	14	SR2
Katanning		49	49	25A1 14A2 7A3 3A4+	24F 24M	49	U
Kemerton		1	1		1F	1	U
Mt. Baker		50	50	26A1 9A2 8A3 7A4+	17F 33M	50	R
Nyabing		20	20	11A1 4A2 2A3 3A4+	12F 8M	20	R
Quairading		26	26	14A1 7A2 1A3 4A4+	16F 10M	26	SR2
Quindanning-Darkan		4	4		1F 3M	4	U
Williams-Darkan		4	4	1A1	2	4	U
Woodanilling		33	33	16A1 10A2 4A3 3A4+	14	33	R
Total		**502**	**418**	**404 (243A1 94A2 33A3 34A4+)**	**479**	**419**	**122R 189SR1 55SR2 53U**

1.3.2. Dissections

We dissected the digastric, superficial masseter, deep masseter, zygomaticomandibularis, suprazygomatic, superficial temporal, deep temporal, medial pterygoid and lateral pterygoid, following the descriptions provided by Tomo et al. (1993), Penrose et al. (2016) and Brassard et al. (under review, article 4). Muscle mass was measured using a digital scale (Mettler Toledo AE100). Pennation angle and fiber lengths were recorded directly on the muscle after cross longitudinal section of each belly without acid dissection, and we considered the mean of five measurements taken on different parts of the muscle.

We calculated the reduced PCSA (Haxton, 1944) of each belly following the formula: $RPCSA = \frac{mass\ (g) * \cos(angle\ of\ pennation\ (rad))}{1{,}06\ (g.cm^{-3}) * fiber\ length\ (cm)}$ and using a density of 1.06 g cm−3 (Mendez and Keys, 1960), which is a reliable estimate for use in the RPCSA in the red fox (Penrose et al., under review).

To increase statistical power (because we dissected only 14 red foxes), we considered the mean of fiber lengths, the mean of pennation angles, the sum of muscle masses, and the sum of muscle PCSAs for each muscular group (masseter, temporal and pterygoids).

We used geometric morphometrics to explore the patterns of variation in mandibular shape. We used photogrammetry and the 'Agisoft PhotoScan' software (© 2014 Agisoft LLC, 27

Gzhatskaya st., St. Petersburg, Russia) to build 3D models of all mandibles. The models were cleaned with Geomagic v. 11 (Geomagic, Research Triangle Park, NC, USA) and Meshlab version 2016.12 (Cignoni et al., 2008). Twenty-five homologous anatomical landmarks, 190 sliding semi-landmarks on curves and 185 sliding semi-landmarks of surface were placed on the mandibles of each specimen using the 'Landmark' software, version 3.0.0.6 (© IDAV 2002-2005; Wiley et al., 2005, Fig. 2). The landmarks were changed into homologous landmarks using a sliding semi-landmark procedure implemented in the 'Morpho' package (version 2.7) implemented in R (Bookstein, 1991; Gunz et al., 2005; Schlager, 2013).

Generalized Procrustes Analyses (GPA – Rohlf & Slice, 1990) and Principal Component Analyses (PCA) were performed using the function procSym (Dryden and Mardia, 2016; Gunz et al., 2005; Klingenberg et al., 2002). The deformation of the mandible of a French fox to the consensus of the GPA was used as a reference for all visualisations.

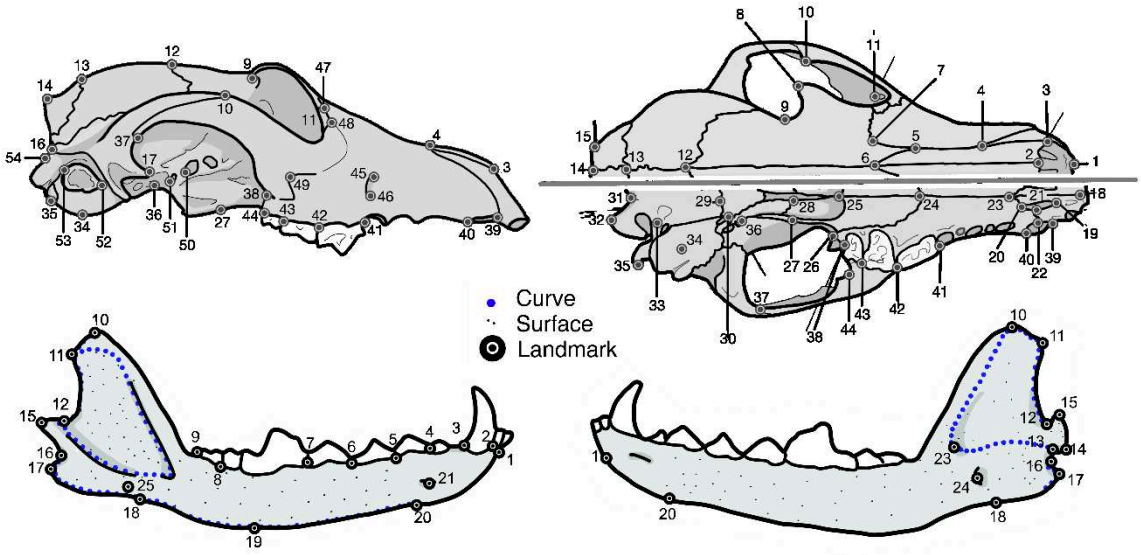

Fig. 2. Landmarks used in this study. Detailed definitions of the landmarks are reported in Table S2.

1.3.3. Statistical analyses

All statistical analyses were run in R version 3.6.0 (2019-04-26) and R studio version 1.2.1335.

To test for differences in muscle architecture between Australian and French foxes we performed multivariate analyses of variance using the function 'manova' on Log10-transformed muscle masses and PCSAs (or residual muscle data obtained from the regression by the Log10 of the mandibular centroid size, using the function 'lm'). The covariations between muscle architecture (PCSA and mass) and shape were assessed using two-blocks partial least-squares analyses with the function 'pls2b' from the package 'Morpho' (Rohlf and Corti, 2000).

To test whether Australian and French foxes differ in size and shape, we performed a t-test and Procrustes analyses of variance using the function 'procD.lm' from the geomorph package

(Hand and Taylor, 1987; Krzanowski, 1988). Disparity tests were conducted using the function 'morphol.disparity' from the geomorph package (Foote, 1993; Zelditch et al., 2012) which performs pairwise comparisons among groups and calculates p-values after 999 iterations.

Differences in shape related to the (Log10-transformed) centroid size, bodymass, sex, age, location, degree of urbanism, minimal or maximal average temperatures and rainfall were assessed with Procrustes ANOVA. Shapes at the minimum or maximum of the regression analyses were obtained using the function 'shape.predictor' on the results of the Procrustes ANOVAs. We used Canonical Variate Analyses, performed with the function 'CVA' (Campbell and Atchley, 1981; Klingenberg and Monteiro, 2005), to identify mean shapes of groups. Visualisations of the shape deformation were obtained from the 'Avizo 8.1.1.' software.

To investigate the drivers of mandibular centroid size, we performed linear regression using the function 'lm', ANOVAs using 'aov' and post-hoc tests using the function 'TukeyHSD'.

1.4. Results

Detailed results of the statistical analyses are in the electronic supplementary material. The results of the Procrustes ANOVAs are summarised in Table 2. The results of the linear regression explaining the centroid size are reported in Table 3.

1.4.1. Comparison of Australian and French red foxes

The MANOVAs show that muscle masses significantly differ between French and Australian foxes ($P < 0.001$, 14 Australian red foxes and 64 French red foxes). Australian foxes tend to have proportionally more voluminous pterygoid muscles than French foxes ($P = 0.032$, supplementary Fig. S2). However, these differences are balanced by the other parameters of muscle architecture (pennation angle and fiber length) since the PCSAs show no significant differences ($P = 0.2$; N = 14 Australian red foxes and 63 French red foxes).

The same foxes also differ in mandibular shape between France and Australia (Procrustes ANOVAs: $P < 0.001$) but not in mandibular size (t-test: $P = 0.50$). The CVA resulted in an excellent success rate (97%) and showed that the Australian red foxes we dissected have a more robust mandibular body, a much more caudally oriented and curved coronoid process and a more pronounced angular process than the dissected French foxes (Fig. 3B).

However, the 14 Australian foxes we dissected represent only a small amount of the total variation in shape in the Australian foxes of our sample (Fig. 3A). When all the foxes are considered in the analyses, Australian and French foxes still significantly differ in mandibular shape (Procrustes ANOVAs: $P < 0.001$) but not in mandibular size (t-test: $P = 0.80$). The CVA still easily distinguished the two populations (success rate of the cross-validation: 97%). French foxes have relatively longer mandibles, with a more triangular coronoid process, a deeper masseteric fossa, a bigger angular process and condyle. The mandibular body is longer, thinner but lower just under the carnassial and the most cranial part of the ventral border is more elevated in French foxes (Fig. 3). Disparity tests show that variances are significantly lower, however, for Australian foxes (Procrustes variance 0.0034) than for European foxes (Procrustes variance = 0.0045, $P < 0.001$).

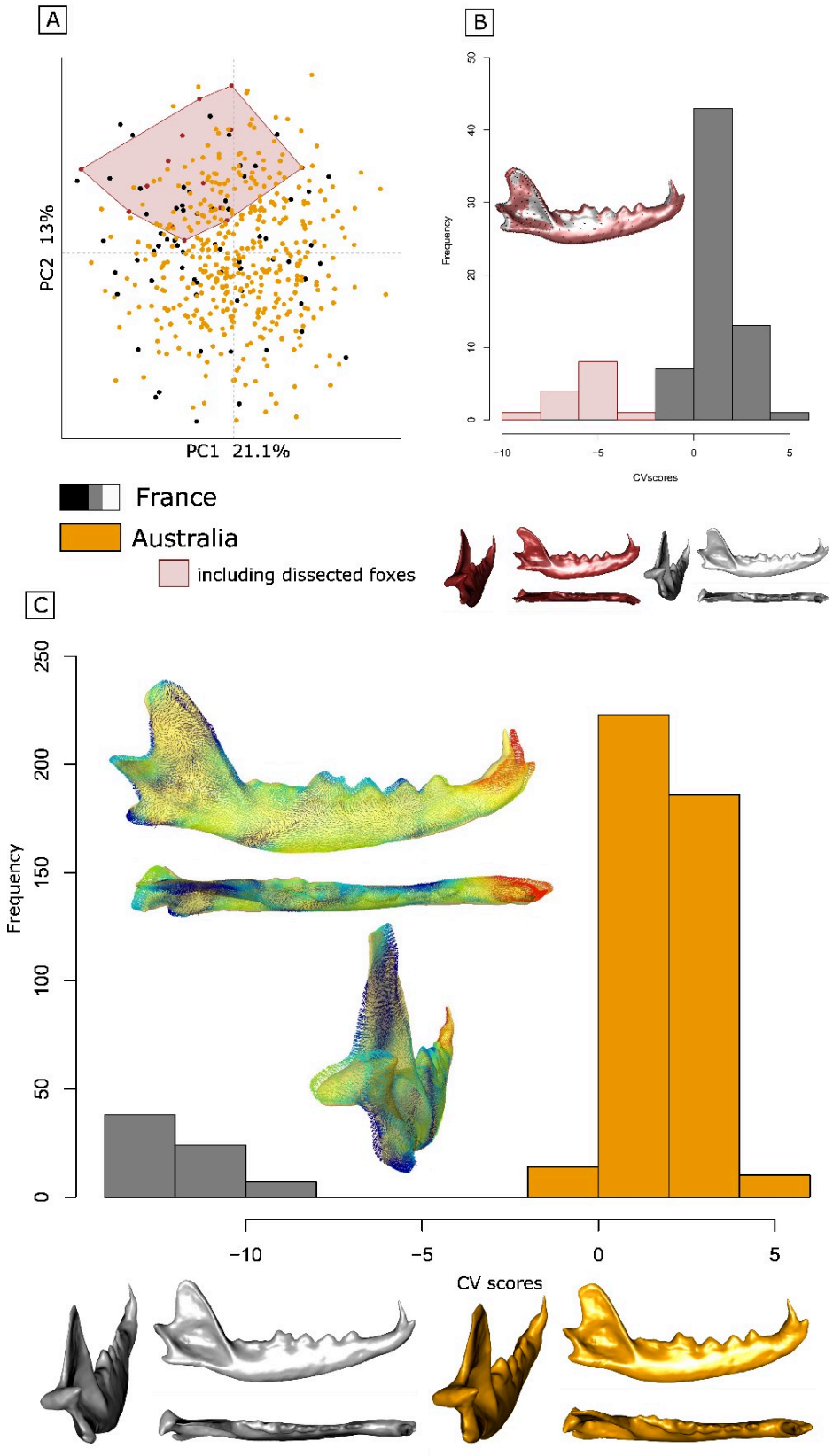

Fig. 3. Mandibular shape variation in Australian and French red foxes. A: First two axes of the PCA; B: Results of the CVA with the dissected specimen only; C: Results of the CVA with all foxes. The vectors of deformation to the mean shape of Australian red foxes to the mean shape of French red foxes are represented, as well as the mean shape of each group, the deformations from the consensus being amplified by three.

1.4.2. Muscular drivers of shape in Australian red foxes

The Procrustes ANOVAs (Table 2) show that the shape of the mandible is driven by the architecture of the masseter and pterygoid muscles. There is no significant correlation with the mass/PCSA of the temporalis. The results of the 2B-PLS analyses are not significant (Table 3). However, since covariations are strong visualisations provide interesting insights in the interplay between muscles and shape. All muscle masses are acting jointly on mandibular shape, contrary to muscle PCSAs (Fig. 4, S1). The more developed the muscles, the more robust the mandible: the wider and caudally oriented the coronoid process, the larger the angular process, the straighter the condyle in the sagittal plane, the deeper the masseteric fossa and the dorsoventrally thicker the mandibular ramus.

The more powerful the muscles, the more developed the mandibular ramus, the more elevated the height of the mandibular body under the carnassial (which gives the impression that the body is more curved under the carnassial; Fig. 4). The scatterplot representing the first axis of the 2B-PLS on muscle PCSAs (Fig. 4A) show that the more powerful the pterygoids, the more curved the angular process in the sagittal plane, and the more powerful the digastricus, the shorter and ventrally curved the mandibular body, the part just behind the carnassial being thicker and the most anterior part being more elevated. The masseteric fossa is deeper and the coronoid process on the right part of the scatterplot, which is probably related to the PCSA of the masseter. The scatterplot representing the second axis of the 2B-PLS (Fig. 4B) show that the more powerful the masseter and the temporal, the wider the coronoid process and the deeper the masseteric fossa.

Table 2. Results of the Procrustes ANOVAs performed on mandibular shape.

Factor and sample size (N)	Df	SS	MS	R2	F	Z	Pr (>SS)
Centroid size and muscle mass (n=14)							
Centroid size	1	0.0049	0.0049	0.11	1.6	1.1	0.15
Mass of the masseter	1	0.0053	0.0054	**0.12**	1.7	1.7	0.036
Mass of the temporalis	1	0.0016	0.0016	0.036	0.52	-1.3	0.90
Mass of the pterygoids	1	0.0048	0.0048	**0.11**	1.5	1.8	0.026
Residuals	9	0.0282	0.0031	0.63			
Centroid size and muscle PCSA (n=14)							
Centroid size	1	0.0049	0.0049	0.11	1.7	1.1	0.15
PCSA of the masseter	1	0.0058	0.0058	**0.13**	2.0	1.8	0.024
PCSA of the temporalis	1	0.0039	0.0039	0.087	1.3	1.23	0.10
PCSA of the pterygoids	1	0.0042	0.0042	**0.09**	1.4	1.6	0.053
Residuals	9	0.0262	0.0029	0.58			
Intrinsic parameters							
Centroid size (N=502)	1	0.10	0.10	**0.057**	30	9.2	0.001
Body mass (N=418)	1	0.076	0.076	**0.054**	24	8.2	0.001
Sex (N=479)	1	0.012	0.012	**0.0074**	3.5	3.6	0.002
Age (N=404)	3	0.087	0.029	**0.065**	9.2	9.1	0.001
External parameters							
Urbanism (N=419)	3	0.034	0.011	**0.024**	3.5	5.6	0.001
Location (N=419)	13	0.11	0.0083	**0.077**	2.6	8.1	0.001
Minimal temperature (bio6) (N=419)	1	0.019	0.019	**0.014**	5.8	5.0	0.001
Maximal temperature (bio5) (N=419)	1	0.013	0.013	**0.0090**	3.8	3.9	0.001

Table 3. Results of the 2B-PLS analyses.

	PLS axis	% of total covariation	r-PLS	P-value
Mass (n=14)	PLS1	83	0.73	0.28
Residual mass	PLS1	66	0.79	0.32
PCSA (n=14)	PLS1	63	0.85	0.097
Residual PCSA	PLS1	62	0.85	0.090

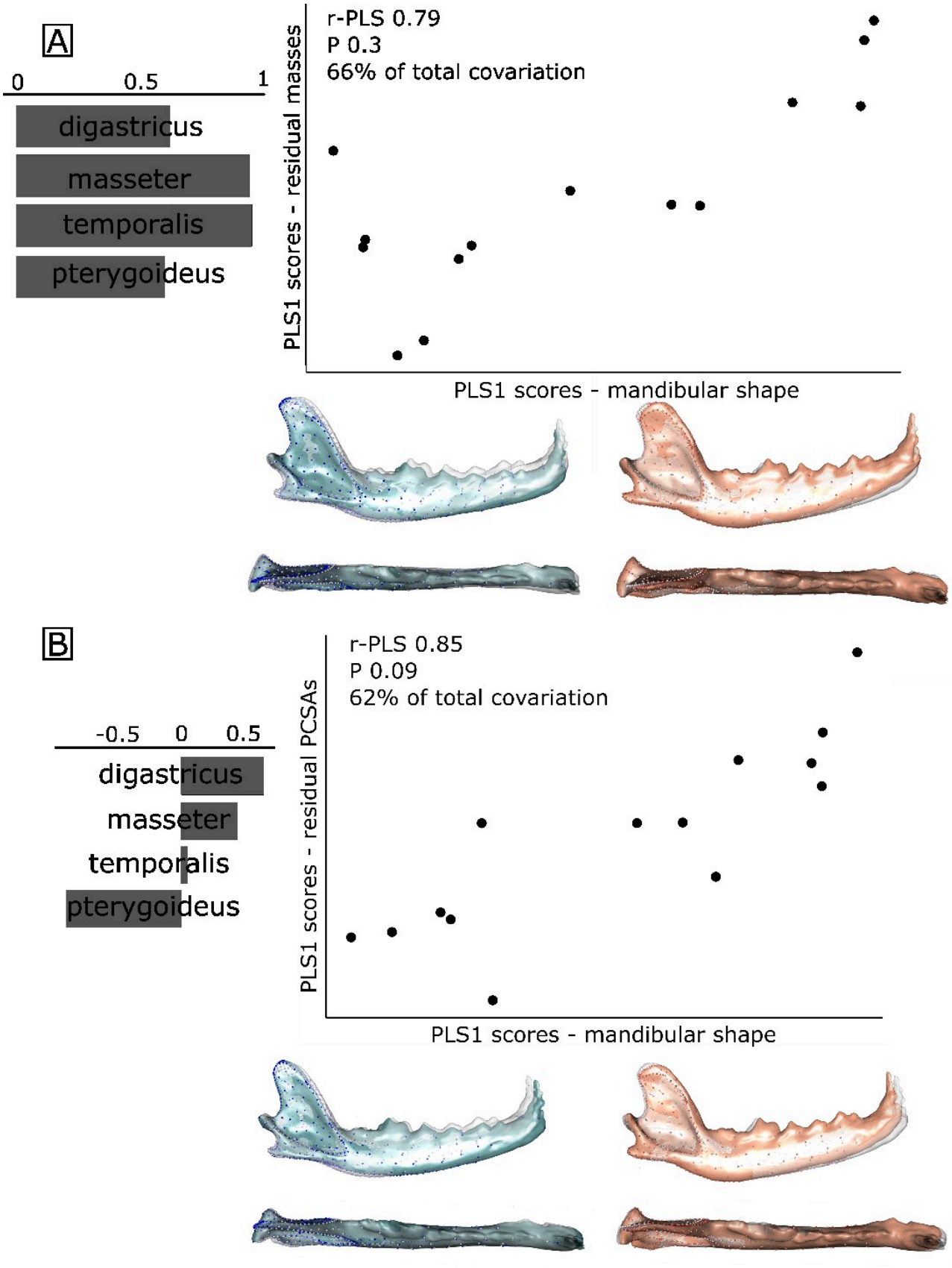

Fig. 4. Visualisation of the results of the 2B-PLS analyses on mandible shape and residual muscle masses (A) or PCSAs (B) with loadings on the first PLS axis. The deformations from the consensus to the minimum (in blue) and maximum (in red) are represented on lateral, dorsal and cauda views.

1.4.3. Intrinsic drivers of mandibular shape (body mass, age and sex)

We refer to Table 2 for the results of the Procrustes ANOVAs to investigate shape drivers and to Table 3 to investigate the drivers of size.

Table 4. Results of the regression analyses to explain the centroid size

Factor	Slope sign	Pr (>t)	Rsq
Body mass (N=418)	+	<2e-16	0.61
Sex (N=479)		< 2e-16	0.17
Age (N=404)		< 2e-16	0.26
Urbanism (N=419)		0.67	-0.0035
Location (N=419)		1e-06	0.092
Minimal temperature (bio6) (N=419)	+	0.00037	0.028
Maximal temperature (bio5) (N=419)	-	0.0093	0.014
Rainfall (bio12) (N=419)	+	0.0046	0.0077

Males and females significantly differ in shape (P = 0.002) and size (t-test: $P < 0.001$). Males are bigger and have a wider coronoid process, a deeper masseteric fossa with a lower condyloid ridge (Fig. 5). In males, the angular process is more curved and the condyle is bigger. In females, the mandibular is more regularly curved on its ventral side, while in males it is more irregular, the anterior part being lower, and the angular process being straighter under the coronoid process. Sixty-four percent of the Australian red foxes were correctly classified as males or females in the CVA.

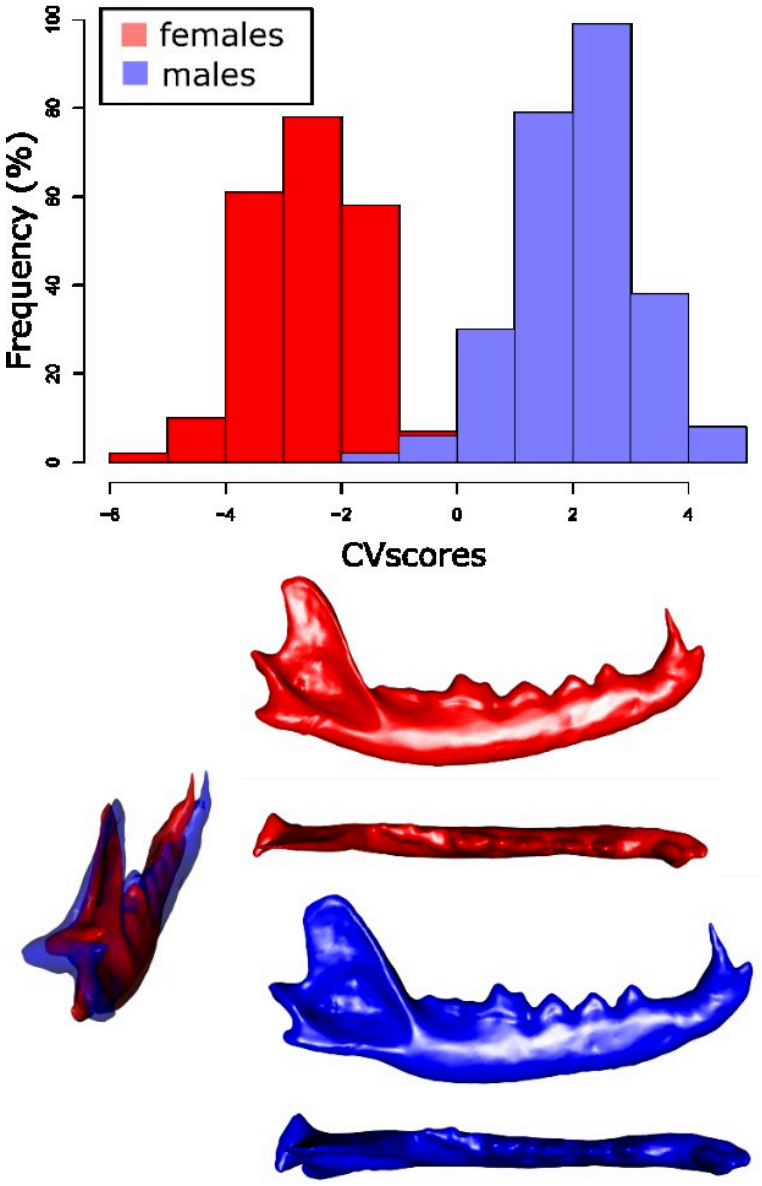

Fig. 5. Results of the CVA with mean shapes of females and males on lateral, dorsal and caudal views. The deformation from the consensus to the mean of each sex was amplified by ten.

Age is also a significant driver of mandibular shape (R^2 = 0.065; P < 0.001) and size (R^2 = 0.26; P < 0.001). The cross-validation of the CVA results in a success rate of 72%. Shape differences are located at the area of insertion of the jaw adductor muscles and on the ventral curvature of the mandibular body (Fig. 6B). The first axis of the CVA distinguishes the youngest individuals of maximum 1 year old from the older foxes (Fig. 6A). The youngest foxes have a proportionally much smaller coronoid process and very rounded mandibular body. The second axis mainly separates the 2 years old from the 3 and more years old. The older the fox, the more developed and caudally oriented the coronoid process, and the straighter and more robust the mandibular body, especially at the level of the carnassial. Only foxes younger than one year have significantly smaller centroid sizes (Fig. 6C, $P_{post\text{-}hoc\ tests}$<0.001).

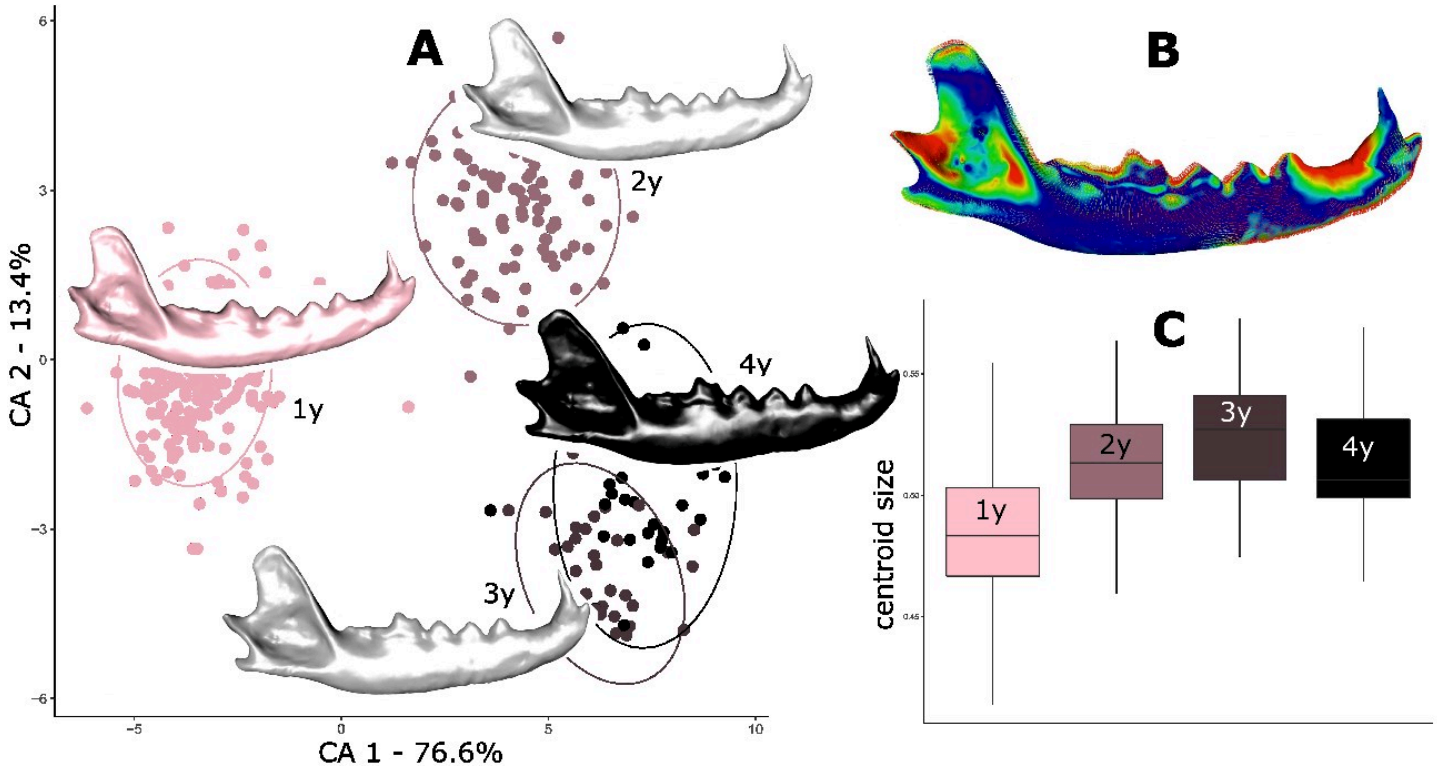

Fig. 6. Impact of age on mandible shape and size. A: Results of the CVA distinguishing foxes by their age with lateral views of the mean shapes of each group. Ellipses correspond to the 95% confidence intervals. Colors represent the distance between the mean shape and the mean shape of each group; B: Shape deformation from 1 year old to 2 years old. Hottest colors are used to represent maximum differences; C: Boxplot representing the centroid size.

As expected, the shape of the mandible is allometric (R^2 = 0.057; P < 0.001) and dependant on body mass (R^2 = 0.054; P < 0.001, Fig. 9).

1.4.4. External drivers of mandibular shape and size

We also observe significant differences in shapes between Australian sites ($R^2 = 0.077$; $P = 0.001$) as well as differences in size ($R^2 = 0.09$, $P < 0.001$). The post-hoc tests indicate that differences occur between Quindanning-Darkan-Armadale ($P = 0.017$), Darkan-Boyup Brook ($P = 0.04$), Quindanning-Darkan-Boyup Brook ($P < 0.001$), Quindanning-Darkan-Corrigin ($P < 0.001$), Mt. Baker-Darkan ($P < 0.04$), Quindanning-Darkan-Darkan ($P < 0.001$), Quindanning-Darkan-Gingin ($P < 0.001$), Quindanning-Darkan-Katanning ($P < 0.001$), Quindanning-Darkan-Kemerton ($P = 0.03$), Quindanning-Darkan-Mt. Baker ($P < 0.001$), Quindanning-Darkan-Nyabing ($P < 0.001$), Quindanning-Darkan-Quairading ($P < 0.001$), Williams-Darkan-Quindanning-Darkan ($P < 0.001$), Woodanilling-Quindanning-Darkan ($p<0.001$).

The degree of urbanism drives variation in shape ($R^2 = 0.024$; $P = 0.001$) but not size ($P = 0.7$). The success rate of the classification performed by the CVA is low (51%), suggesting that the differences are subtle and separations between groups not very clear. The groups that are most appropriately identified are the rural foxes and the foxes from the 'SR1' group. Only 34% of the urban foxes are correctly identified while 66% of the SR1 foxes are well identified. The foxes from the 'urban' group have relatively longer mandibles with a straighter mandibular body, a smaller angular process and a wider coronoid process with a deeper masseteric fossa (Fig. 7). Foxes from the 'rural' group have a shorter and more curved mandibular body, the part under the carnassial being higher, a more developed angular process, and a narrower coronoid process with a shallower masseteric fossa. Foxes from the 'SR2' group have a bigger and more robust mandibular body than the average, including under the carnassial and a less developed angular process. There is no gradual evolution of the shape throughout the rural-urban gradient. Differences are thus likely related to other parameters, such as geographic variation or different composition of each group with respect to body size or age, for example. Indeed, 75% of the foxes from group 'SR1' are less than 1 year old and consequently show a juvenile morphology - they have a less developed coronoid process, a smaller angular process, a straighter curved mandible.

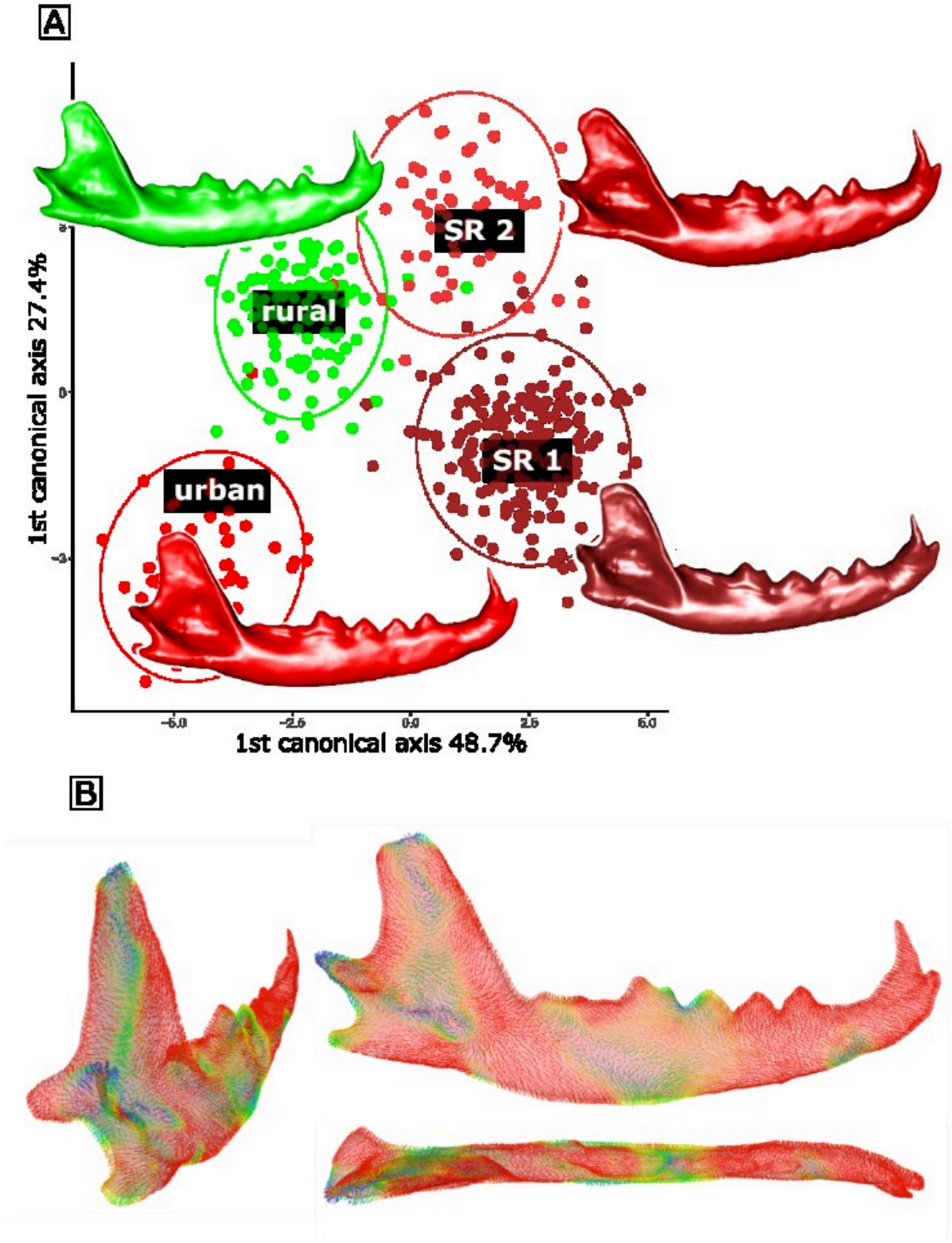

Fig. 7. Results of the CVA to distinguish urban and rural foxes. A: Scatterplot with ellipses corresponding to the 95% confidence intervals and lateral views of the mean shape for each group (the deformations from the consensus are amplified by five). B: shape of the 'rural' red foxes and vector of deformation from the 'urban' to 'rural' foxes. Colors represent the distance between the two shapes. Hottest colors are used to represent the maximum differences.

All the climatic parameters we tested are significant drivers of mandible shape. Deformations in shape are mainly located on the coronoid process and the ventral curvature of the mandibular body (Fig. 8).

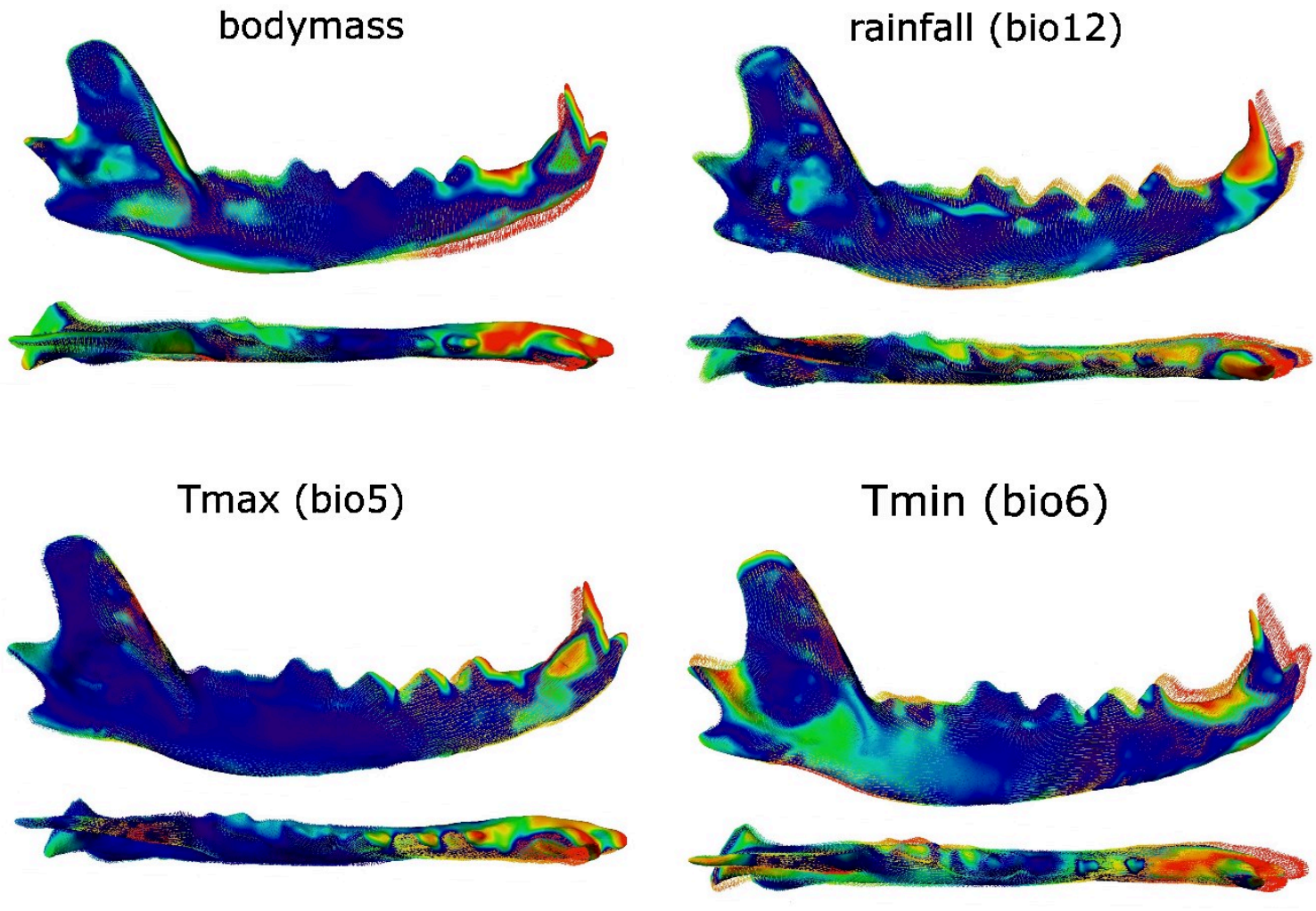

Fig. 8. Shape deformations from the minimum to the maximum shapes determined from the multivariate regression of mandible shape by the body mass, rainfall (bio12), the averaged maximal temperature (Tmax, bio5) and the averaged minimal temperature (Tmin, bio6). The shapes at the maximum are represented. Vectors indicate the direction of the deformation from the minimum to the maximum. Hottest colours correspond to the most important distances between the shapes at the minimum and maximum.

1.5. Discussion

Here we tested whether Australian and European red foxes differ in mandibular shape, size or in muscle architecture, and explore whether non-feeding variables (body mass, centroid size, sex, age, geographic location, urbanism, temperatures, rainfall) are related to variation in mandibular shape and size.

1.5.1. Differences in morphology between Australian and French foxes

The disparity of the Australian foxes was lower than that observed for the French red foxes, despite the lower sample size for the latter. This is consistent with a founder effect. Given that the population of the Australian red foxes was established by a very small number of European red foxes from a larger population their morphology likely had a disproportionate impact on the variation observed in the population (Allendorf and Lundquist, 2003), resulting in a lower disparity. Previous studies have documented founder effects and genetic drift in Australian red foxes although little loss of alleles by genetic drift appeared to have occurred (Lade et al., 1996).

Interestingly, we found that the mandible shape of Australian foxes is variable but very different from that of French foxes. In contrast, there is no significant difference in size. The success rate of the reclassification based on mandible shape is excellent (97%), suggesting a high differentiation between native European and invasive Australian populations. Australian red foxes tend to have more 'dog-like' mandibles, with a more robust mandibular body and a more rectangular coronoid process. Interestingly, the morphological differences concentrate on the area of insertion of the jaw muscles, which suggests functional differences between native and invasive foxes. Future studies should investigate the consequences of these differences in shape between the continents on bite force (see Forbes-Harper et al. 2017) to explore this further.

Muscle PCSAs were not significantly different between Australian and French red foxes. However, only 14 Australian red foxes were dissected in this study, and these foxes only represent a small amount of the total shape variation in the Australian foxes in our sample (Fig. 3). Other dissections are needed to test further whether the architecture of the jaw muscles differs significantly between France and Australia. However, the results of the analyses of covariance (Fig. 4) and correlation analyses (Table 2) suggest that the masseter and pterygoid muscles drive variation in mandibular shape. Moreover, the bony deformations associated with variation in muscle architecture are similar to those describe in French foxes (Brassard et al., under review, article 4). However, the first axis of the 2B-PLS showed different patterns compared to those observed in red foxes from France (Brassard et al., under review, article 4). These patterns highlight the functional link between the angular process and the strength of the pterygoid muscles. The more powerful the muscles, the more curved the angular process. This is suggestive of functional differences between invasive and native foxes, yet remains to explored further. Overall, our results suggest differences in the mandible and jaw adductor muscles in an invasive population of red foxes. Whether these reflect local adaptation to diet or other factors or are the result of a strong founder effect remains to be explored.

1.5.2. Impact of non-feeding variables on mandibular shape

The population divergence in morphology between European and Australian foxes could reasonably be related to both genetic drift and divergent selection acting upon different functional adaptations to very different environments. The very different climate conditions (including temperature, precipitation, elevation and topography) and community composition potentially drive variation in mandibular shape (Fischer and Still, 2007; Funk et al., 2016; Spalding et al., 2007). Because the sample of French red foxes is rather small and we did not have detailed information on all specimens we could not investigate the impact of environmental for this sample.

Interestingly, although the non-feeding related ecological variables we tested (geographic location, urbanism, minimal or maximal temperature and rainfall) explain relatively little of the total variation in shape (Table 2), we do find significant correlations. One of the most important drivers of mandibular shape seems to be the geographic location (which explain almost 8% of the variation in mandible shape). Interestingly, we also observed morphological differences along the rural-urban gradient. We found differences in shape in the areas of insertion of the jaw muscle, suggesting functional differences. The most urban foxes, that tend to have less robust mandibles with a wider coronoid process and a deeper masseteric fossa (Fig. 7), may have a proportionally more developed masseter muscle while foxes from the 'rural' group have a more developed angular process, providing an expanded insertion area for the pterygoid muscle. These variations in shape do not show a continuum across the urban-rural gradient, suggesting that the impact of other variables may be more important (geographic location, age, sex) than the proximity to humans. Our observations are in accordance with that of Jojić et al. (2017), who observed that foxes from more agricultural areas of Serbia have more robust crania with a shorter snout (we found shorter and more robust mandibles in the 'rural' group). As hypothesised by the authors, these differences may be related to dietary differences, although genetic diversification cannot be excluded as a possible contributing factor. We also found significant correlations between the centroid size and environmental data. However, the constitution of the sample and non-equilibrated age classes or sex ratios for each site may partly impact our results.

Mandibular shape was significantly correlated to all the intrinsic parameters we tested (body mass, age and sex). However, these again explain little of the total variation (maximum 6%). The related anatomical changes are likely to have functional consequences, however. The centroid size is, in comparison, much more strongly explained by variation in body mass, age and sex. First, as expected, the bigger/older the fox, the less rounded the mandible and the proportionally more developed the coronoid process. Age mostly distinguishes the less than 1-year old foxes from the older ones. Sexual dimorphism is very clear (as previously reported by Jojić et al., 2017) and involves mainly muscular insertion areas, suggesting that males can produce higher bite forces (since they have more robust mandibles with a proportionally much bigger coronoid process). Moreover, males are also bigger (Jojić et al., 2017).

Tseng and Flynn found that cranial shape significantly correlates to non-feeding ecological variables (as well as to feeding variables), and that the covariation generates significant masticatory performance gradients, suggesting that "mechanisms of obligate shape covariation with non-feeding variables can produce performance changes resembling those arising from feeding adaptations in Carnivora". It is possible that we here observe similar trends in the mandible of these Australian red foxes. Yet, the mandible is more directly specialised towards mastication (more so than the skull). It is thus likely that diet explains more of the variation in shape than the non-feeding variables we tested. Future studies investigating the relation between diet and the 3D morphology of the mandible would be of interest. Given that environmental constraints (geographic location, temperature, rainfall and urbanism) could drive differences in food availability it is possible that similar patterns of covariation/correlation with both feeding and non-feeding variables would be observed.

1.6. Conclusion

Our results highlighted morphological differences between Australiana and French red foxes. Our results further showed significant correlations between environmental and developmental variables and mandibular shape. The analyses of shape suggest mechanical adaptations to local living conditions and selective pressures. Future studies are needed to investigate the relation between mandibular shape and diet in red foxes, and to compare the effect of non-feeding or feeding variables on French and Australian foxes.

Acknowledgements

We thank the School of Veterinary medicine and life Science of Murdoch University for providing fox heads for dissection.

Competing interests

The authors declare that they have no conflicts of interest.

Funding

This research was funded by the Ministère de l'Enseignement supérieur, de la Recherche et de l'Innovation.

1.7. References

Allendorf, F.W., Lundquist, L.L., 2003. Introduction: population biology, evolution, and control of invasive species. Conserv. Biol. 17, 24–30.

Artois, M., 1989. Encyclopédie des Carnivores de France. Vol. 3. Le renard roux. Soc. Francaise Pour L'Etude Prot. Mammiferes Bourges.

Aubry, K.B., 1983. The Cascade red fox: distribution, morphology, zoogeoraphy and ecology.

Bookstein, F.L., 1991. Morphometric tools forl andmark data: geometry and biology. Cambridge University Press.

Brassard, C., Merlin, M., Guintard, C., Monchâtre-Leroy, E., Barrat, J., Callou, C., Cornette, R., Herrel, A., 2020a. How does masticatory muscle architecture covary with mandibular shape in domestic dogs? Evol. Biol. https://doi.org/10.1007/s11692-020-09499-6

Brassard, C., Merlin, M., Monchâtre-Leroy, E., Guintard, C., Barrat, J., Garès, H., Laralle, A., Triquet, R., Houssin, C., Callou, C., Cornette, R., Herrel, A., under review. Masticatory system integration in a commensal canid: interrelationships between bones, muscles, and bite force in the red fox.

Campbell, N.A., Atchley, W.R., 1981. The geometry of canonical variate analysis. Syst. Zool. 30, 268–280. https://doi.org/10.2307/2413249

Čanády, A., 2013. Variability of the baculum in the red fox (Vulpes vulpes) from Slovakia. Zool. Ecol. 23, 165–170. https://doi.org/10.1080/21658005.2013.832848

Churcher, C.S., 1959. The specific status of the New World red fox. J. Mammal. 40, 513–520.

Cignoni, P., Callieri, M., Corsini, M., Dellepiane, M., Ganovelli, F., Ranzuglia, G., 2008. MeshLab: an Open-Source Mesh Processing Tool. The Eurographics Association. http://dx.doi.org/10.2312/LocalChapterEvents/ItalChap/ItalianChapConf2008/129-136

Cox, G.W., 2004. Alien species and evolution: the evolutionary ecology of exotic plants, animals, microbes, and interacting native species. Island Press.

Darwin, C., 1909. The origin of species. PF Collier & son New York.

Debuf, J.-M., 1987. Contribution à l'étude du renard urbain en région parisienne.

Doncaster, C.P., Macdonald, D.W., 1997. Activity patterns and interactions of red foxes (Vulpes vulpes) in Oxford city. J. Zool. 241, 73–87. https://doi.org/10.1111/j.1469-7998.1997.tb05500.x

Dryden, I.L., Mardia, K.V., 2016. Statistical Shape Analysis: With Applications in R. John Wiley & Sons.

Edwards, C.J., Soulsbury, C.D., Statham, M.J., Ho, S.Y.W., Wall, D., Dolf, G., Iossa, G., Baker, P.J., Harris, S., Sacks, B.N., Bradley, D.G., 2012. Temporal genetic variation of the red fox, Vulpes vulpes, across Western Europe and the British Isles. Quat. Sci. Rev. 57, 95–104. https://doi.org/10.1016/j.quascirev.2012.10.010

Fick, S.E., Hijmans, R.J., 2017. WorldClim 2: new 1-km spatial resolution climate surfaces for global land areas. Int. J. Climatol. 37, 4302–4315. https://doi.org/10.1002/joc.5086

Figueirido, B., Macleod, N., Krieger, J., De Renzi, M., Pérez-Claros, J., Palmqvist, P., 2011. Constraint and adaptation in the evolution of carnivoran skull shape. Paleobiology 37, 490–518. https://doi.org/10.2307/23014735

Fischer, D.T., Still, C.J., 2007. Evaluating patterns of fog water deposition and isotopic composition on the California Channel Islands. Water Resour. Res. 43.

Foote, M., 1993. Contributions of Individual Taxa to Overall Morphological Disparity. Paleobiology 19, 403–419.

Forbes-Harper, J.L., Crawford, H.M., Dundas, S.J., Warburton, N.M., Adams, P.J., Bateman, P.W., Calver, M.C., Fleming, P.A., 2017. Diet and bite force in red foxes: ontogenetic and sex differences in an invasive carnivore. J. Zool. 303, 54–63. https://doi.org/10.1111/jzo.12463

Forsyth, T., 2004. Critical political ecology: the politics of environmental science. Routledge.

Frati, F., Hartl, G.B., Lovari, S., Delibes, M., Markov, G., 1998. Quaternary radiation and genetic structure of the red fox Vulpes vulpes in the Mediterranean Basin, as revealed by allozymes and mitochondrial DNA. J. Zool. 245, 43–51. https://doi.org/10.1111/j.1469-7998.1998.tb00070.x

Funk, W.C., Lovich, R.E., Hohenlohe, P.A., Hofman, C.A., Morrison, S.A., Sillett, T.S., Ghalambor, C.K., Maldonado, J.E., Rick, T.C., Day, M.D., Polato, N.R., Fitzpatrick, S.W., Coonan, T.J., Crooks, K.R., Dillon, A., Garcelon, D.K., King, J.L., Boser, C.L., Gould, N., Andelt, W.F., 2016. Adaptive divergence despite strong genetic drift: genomic analysis of the evolutionary mechanisms causing genetic differentiation in the island fox (Urocyon littoralis). Mol. Ecol. 25, 2176–2194. https://doi.org/10.1111/mec.13605

Gingerich, P.D., Winkler, D.A., 1979. Patterns of Variation and Correlation in the Dentition of the Red Fox, Vulpes vulpes. J. Mammal. 60, 691–704. https://doi.org/10.2307/1380186

Gittleman, J., 1985. Functions of communal care in mammals.

Gloor, S., Bontadina, F., Hegglin, D., Deplazes, P., BU 2001. The rise of urban fox populations in Switzerland. Mamm. Biol. 66, 155–164.

Gunz, P., Mitteroecker, P., Bookstein, F.L., 2005. Semilandmarks in Three Dimensions, in: Slice, D.E. (Ed.), Modern Morphometrics in Physical Anthropology, Developments in Primatology: Progress and Prospects. Springer US, Boston, MA, pp. 73–98. https://doi.org/10.1007/0-387-27614-9_3

Hand, D.J., Taylor, C.C., 1987. Multivariate analysis of variance and repeated measures: A practical approach for behavioural scientists, Multivariate analysis of variance and repeated measures: A practical approach for behavioural scientists. Chapman & Hall/CRC, Boca Raton, FL. https://doi.org/10.1007/978-94-009-3143-5

Hartová-Nentvichová, M., Anděra, M., Hart, V., 2010. Cranial ontogenetic variability, sex ratio and age structure of the Red fox. Cent. Eur. J. Biol. 5, 894–907. https://doi.org/10.2478/s11535-010-0093-2

Haxton, H.A., 1944. Absolute muscle force in the ankle flexors of man. J. Physiol. 103, 267–273.

Hell, P., Paule, L., Sevcenko, L.S., Danko, S., Panigaj, L., Vitaz, V., 1989. Craniometrical investigation of the red fox (Vulpes vulpes) from the Slovak Carpathians and adjacent lowlands. Craniometrical Investig. Red Fox Vulpes Vulpes Slovak Carpathians Adjac. Lowl. 38, 139–155.

Hulme-Beaman, A., Dobney, K., Cucchi, T., Searle, J.B., 2016. An Ecological and Evolutionary Framework for Commensalism in Anthropogenic Environments. Trends Ecol. Evol. 31, 633–645. https://doi.org/10.1016/j.tree.2016.05.001

Huson, L.W., Page, R.J.C., 1980. Multivariate geographical variation of the Red fox (Vulpes vulpes) in Wales. J. Zool. 191, 453–459. https://doi.org/10.1111/j.1469-7998.1980.tb01477.x

Johnson, M.T., Munshi-South, J., 2017. Evolution of life in urban environments. Science 358, eaam8327.

Jojić, V., Porobić, J., Ćirović, D., 2017. Cranial variability of the Serbian red fox. Zool. Anz. 267, 41–48. https://doi.org/10.1016/j.jcz.2017.02.001

Klingenberg, C.P., Barluenga, M., Meyer, A., 2002. Shape Analysis of Symmetric Structures: Quantifying Variation Among Individuals and Asymmetry. Evolution 56, 1909–1920. https://doi.org/10.1111/j.0014-3820.2002.tb00117.x

Klingenberg, C.P., Monteiro, L.R., 2005. Distances and Directions in Multidimensional Shape Spaces: Implications for Morphometric Applications. Syst. Biol. 54, 678–688. https://doi.org/10.1080/10635150590947258

Krzanowski, W.J. (Ed.), 1988. Principles of Multivariate Analysis: A User's Perspective. Oxford University Press, Inc., New York, NY, USA.

Lade, J.A., Murray, N.D., Marks, C.A., Robinson, N.A., 1996. Microsatellite differentiation between Phillip Island and mainland Australian populations of the red fox Vulpes vulpes. Mol. Ecol. 5, 81–87. https://doi.org/10.1111/j.1365-294X.1996.tb00293.x

Manel, S., Holderegger, R., 2013. Ten years of landscape genetics. Trends Ecol. Evol. 28, 614–621.

McDonnell, M.J., Pickett, S.T.A., 1990. Ecosystem Structure and Function along Urban-Rural Gradients: An Unexploited Opportunity for Ecology. Ecology 71, 1232–1237. https://doi.org/10.2307/1938259

Meiri, S., Dayan, T., Simberloff, D., 2004. Carnivores, biases and Bergmann's rule. Biol. J. Linn. Soc. 81, 579–588.

Meloro, C., Raia, P., Carotenuto, F., Cobb, S.N., 2011. Phylogenetic signal, function and integration in the subunits of the carnivoran mandible. Evol. Biol. 38, 465–475. https://doi.org/10.1007/s11692-011-9135-6

Mendez, J., Keys, A., 1960. Density and composition of mammalian muscle. Metabolism 9, 184–188.

NASA SEDAC Population Estimator, [WWW Document]. URL https://sedac.ciesin.columbia.edu/mapping/popest/pes-v3/ (accessed 11.5.19).

Niemelä, J., 1999. Is there a need for a theory of urban ecology? Urban Ecosyst. 3, 57–65.

Pengilly, D., 1984. Developmental versus Functional Explanations for Patterns of Variability and Correlation in the Dentitions of Foxes. J. Mammal. 65, 34–43. https://doi.org/10.2307/1381197

Penrose, F., Cox, P., Kemp, G., Jeffery, N., 2020. Functional morphology of the jaw adductor muscles in the Canidae. Anat. Rec.

Penrose, F., Kemp, G.J., Jeffery, N., 2016. Scaling and Accommodation of Jaw Adductor Muscles in Canidae. Anat. Rec. 299, 951–966. https://doi.org/10.1002/ar.23355

Queensland government, 2019. European fox Vulpes vulpes.

Rohlf, F., Slice, D., 1990. Extensions of the Procrustes Method for the Optimal Superimposition of Landmarks. Syst. Zool. 39. https://doi.org/10.2307/2992207

Rohlf, F.J., Corti, M., 2000. Use of two-block partial least-squares to study covariation in shape. Syst. Biol. 49, 740–753. https://doi.org/10.1080/106351500750049806

Rolls, E.C., 1969. They all ran wild.

Sacks, B.N., Statham, M.J., Perrine, J.D., Wisely, S.M., Aubry, K.B., 2010. North American montane red foxes: expansion, fragmentation, and the origin of the Sacramento Valley red fox. Conserv. Genet. 11, 1523–1539.

Saunders, G.R., Gentle, M.N., Dickman, C.R., 2010. The impacts and management of foxes Vulpes vulpes in Australia. Mammal Rev. 40, 181–211. https://doi.org/10.1111/j.1365-2907.2010.00159.x

Schipper, J., Chanson, J.S., Chiozza, F., Cox, N.A., Hoffmann, M., Katariya, V., Lamoreux, J., Rodrigues, A.S., Stuart, S.N., Temple, H.J., 2008. The status of the world's land and marine mammals: diversity, threat, and knowledge. Science 322, 225–230.

Schlager, S., 2013. Soft-tissue reconstruction of the human nose : population differences and sexual dimorphism.

Schoenebeck, J.J., Ostrander, E.A., 2013. The Genetics of Canine Skull Shape Variation. Genetics 193, 317–325. https://doi.org/10.1534/genetics.112.145284

Spalding, M.D., Fox, H.E., Allen, G.R., Davidson, N., Ferdaña, Z.A., Finlayson, M., Halpern, B.S., Jorge, M.A., Lombana, A., Lourie, S.A., 2007. Marine ecoregions of the world: a bioregionalization of coastal and shelf areas. BioScience 57, 573–583.

Statham, M.J., Murdoch, J., Janecka, J., Aubry, K.B., Edwards, C.J., Soulsbury, C.D., Berry, O., Wang, Z., Harrison, D., Pearch, M., Tomsett, L., Chupasko, J., Sacks, B.N., 2014. Range-wide multilocus phylogeography of the red fox reveals ancient continental divergence, minimal genomic exchange and distinct demographic histories. Mol. Ecol. 23, 4813–4830. https://doi.org/10.1111/mec.12898

Statham, M.J., Sacks, B.N., Aubry, K.B., Perrine, J.D., Wisely, S.M., 2012. The origin of recently established red fox populations in the United States: translocations or natural range expansions? J. Mammal. 93, 52–65. https://doi.org/10.1644/11-MAMM-A-033.1

Stepkovitch, B., Martin, J.M., Dickman, C.R., Welbergen, J.A., 2019. Urban lifestyle supports larger red foxes in Australia: an investigation into the morphology of an invasive predator. J. Zool. 309, 287–294. https://doi.org/10.1111/jzo.12723

Szuma, E., 2004. Evolutionary implications of morphological variation in the lower carnassial of red foxVulpes vulpes. Acta Theriol. (Warsz.) 49, 433–447. https://doi.org/10.1007/BF03192588

Tomo, S., Hirakawa, T., Nakajima, K., Tomo, I., Kobayashi, S., 1993. Morphological classification of the masticatory muscles in dogs based on their innervation. Ann. Anat. - Anat. Anz. 175, 373–380. https://doi.org/10.1016/S0940-9602(11)80047-6

Tseng, Z.J., Flynn, J.J., 2018. Structure-function covariation with nonfeeding ecological variables influences evolution of feeding specialization in Carnivora. Sci. Adv. 4. https://doi.org/10.1126/sciadv.aao5441

Van Valkenburgh, B., Koepfli, K., 1993. Cranial and dental adaptations to predation in canids. Presented at the Symposium of the Zoological Society of London, pp. 15–37.

Wandeler, P., Funk, S.M., Largiadèr, C.R., Gloor, S., Breitenmoser, U., 2003. The city-fox phenomenon: genetic consequences of a recent colonization of urban habitat. Mol. Ecol. 12, 647–656. https://doi.org/10.1046/j.1365-294x.2003.01768.x

West-Eberhard, M.J., 1989. Phenotypic plasticity and the origins of diversity. Annu. Rev. Ecol. Syst. 20, 249–278.

Wiley, D.F., Amenta, N., Alcantara, D.A., Ghosh, D., Kil, Y.J., Delson, E., Harcourt-Smith, W., Rohlf, F.J., John, K.S., Hamann, B., 2005. Evolutionary morphing, in: VIS 05. IEEE Visualization, 2005. Presented at the VIS 05. IEEE Visualization, 2005., pp. 431–438. https://doi.org/10.1109/VISUAL.2005.1532826

Wroe, S., Milne, N., 2007. Convergence and remarkably consistent constraint in the evolution of carnivore skull shape. Evol. Int. J. Org. Evol. 61, 1251–1260.

Zatoń-Dobrowolska, M., Moska, M., Mucha, A., Wierzbicki, H., Dobrowolski, M., 2017. Variation in fur farm and wild populations of the red fox, Vulpes vulpes (Carnivora: Canidae). Part II: Craniometry. Can. J. Anim. Sci. https://doi.org/10.1139/CJAS-2017-0015

Zelditch, M.L., Swiderski, D.L., Sheets, H.D., 2012. Geometric Morphometrics for Biologists: A Primer. Academic Press.

Ziege, M., Theodorou, P., Jüngling, H., Merker, S., Plath, M., Streit, B., Lerp, H., 2020. Population genetics of the European rabbit along a rural-to-urban gradient. Sci. Rep. 10, 1–12. https://doi.org/10.1038/s41598-020-57962-3

2. Relationship between diet and mandibular shape or bite force in red foxes

Article 6 – Does diet drive mandibular shape and bite force in an invasive population of red foxes?

Colline Brassard, Jesse L. Forbes-Harper, Heather M. Crawford, John-Michael Stuart, Natalie M. Warburton, Michael C. Calver, Peter Adams, Elodie Monchâtre-Leroy, Jacques Barrat, Claude Guintard, Hélène Garès, Arnault Larralle, Raymond Triquet, Marilaine Merlin, Raphaël Cornette, Anthony Herrel, Patricia A. Fleming

Does diet drive mandibular shape and bite force in an invasive population of red foxes?

Colline Brassard[1,2,*], Forbes-Harper[1], Crawford[1] , Dundas[1], Warburton[1] , Adams[1] , Bateman[2], Calver[1], Elodie Monchâtre-Leroy[3], Claude Guintard[4,5], Jacques Barrat[3], Hélène Garès[6], Arnault Larralle, Raymond Triquet, Marilaine Merlin, Raphaël Cornette, Anthony Herrel & Trish Fleming

[1] UMR 7179 Mécanismes Adaptatifs et Evolution (CNRS, MNHN), Muséum national d'Histoire naturelle, Paris, France.

[2] Archéozoologie, archéobotanique : sociétés, pratiques et environnements (AASPE), Muséum national d'Histoire naturelle, CNRS, CP55, 57 rue Cuvier 75005 Paris, France
[3] ANSES, Laboratoire de la rage et dela faune sauvage, Station expérimentale d'Atton, Malzéville, France.

[4] Laboratoire d'Anatomie comparée, Ecole Nationale Vétérinaire, de l'Agroalimentaire et de l'Alimentation, Nantes Atlantique – ONIRIS, Nantes Cedex 03, France.

[5] GEROM, UPRES EA 4658, LABCOM ANR NEXTBONE, Faculté de santé de l'Université d'Angers, France.

[6] Direction des Services Vétérinaires –D.D.C.S.P.P. de la Dordogne, Périgueux, France.

[7] UMR 7205 Institut de Systématique, Evolution, Biodiversité (CNRS, MNHN, UPMC, EPHE), Muséum national d'Histoire naturelle, Paris, France.

1 School of Veterinary & Life Sciences, Murdoch University, Murdoch, WA, Australia
2 Department of Environment and Agriculture, Curtin University, Bentley, WA, Australia
* Corresponding author: colline.brassard@mnhn.fr

2.1. Materials and methods

All statistical analyses were run in 'R' version 3.6.0 (2019-04-26).

2.1.1. Sample information

The dataset is composed of the mandibles of 451 red foxes (Table 1).

Table 1. Information about the sample used in this study. y: year old; 2+: foxes over 2 years old; F: female; M:male; Gdt: urban-rural gradient; BF FH: bite forces estimated in Forbes-Harper et al. (2017); NA: missing data. Detailed information about all individuals are available in the supplementary material Table S1.

	Total	Age		Sex		Gdt
Type/Location		**1y**	**2+y**	**F**	**M**	
France - dissected	**60**			23	38	
Australia - dissected	**14**					
Australia – not dissected:	**387**					
Armadale	2	2	0	2	0	Urban
Boyup Brook	46	32	14	19	27	SR 1
Corrigin	15	4	11	8	7	SR 2
Darkan	131	92	29	60	71	SR 1
Dumbleyung	11	3	8	6	5	Rural
6: Gingin	14	4	10	6	8	SR 2
7: Katanning	45	23	22	22	23	Urban
8: Kemerton	1	NA	NA	0	1	Urban
9: Mt. Baker	47	24	23	17	30	Rural
10: Nyabing	19	11	8	12	7	Rural
11: Quairading	21	12	9	13	8	SR 2
12: Quindanning-Darkan	2	NA	NA	1	1	Rural
13: Williams-Darkan	3	>1	NA	2	1	Rural
14: Woodanilling	30	15	15	12	18	Rural

Sixty of these foxes are from France and were dissected previously to estimate bite forces (Brassard et al., under review, article 4).

The other red foxes are from an invasive population from South Western Australia (Fig. 1 supplementary material Table S1). The jaw muscles of fourteen of these foxes were dissected (see article 5). For the 387 remaining Australian red foxes, individual information about the age, sex, bodymass, GPS location and stomach content are available (see Forbes-Harper et al., 2017).

Detailed information about the sample is reported in Table 1 and Table S1.

Age was established from the cranial sutures and microscopic analysis of the canine tooth dentine lamina (Forbes-Harper et al., 2017). Because previous studies have shown that age-related differences in shape mainly differentiate foxes younger than one year of age from the others (article 5), we here considered two age classes: foxes up to one year old, and older foxes.

Following previous studies (article 5), we separated the different localities depending on their degree of urbanism (approximated based on the number of inhabitants in a 5 km radius). Locations with fewer than 100 inhabitants in a 5 km radius are considered rural areas ('R'), while those with more than 1000 inhabitants are considered urban ('U'). SR1 and SR2 refer to sites with an intermediate degree of urbanism (SR1: between 100 and 350 inhabitants; SR2:

between 350 and 1000 inhabitants). The limits between groups were arbitrary defined to represent equally all categories.

We used WorldClim version 2 (Fick and Hijmans, 2017), a database of global interpolated climate data, using the function 'getData' from the package 'raster' in R, to extract climatic data from the GPS coordinates. We retained average minimal temperature (bio6), average maximal temperature (bio5), and average precipitation (bio12).

2.1.2. Diet analyses

We retained in the analyses the following food items: sheep, rodent (rat and house mouse), rabbit, marsupials (brushtail possum), bird, reptile/frog, invertebrates, plant (deliberately consumed plant matter including grass, figs, grapes, mulberries, corn, grains), other mammals (cattle, unknown mammal, cat hair, fox hair), other (incidental plant matter: dead grass, leaves, twigs, bark, that were generally in low proportion and that were probably partly present on/in other food items; gastro-intestinal worms; maggots, other).

Forbes-Harper and colleagues (2017) identified age and sex differences in diet but performed analyses on a larger sample of foxes (473 foxes). To check that the same trends were observed in our subsample (387 foxes), we performed similar non-parametric analyses. We ran a two-way Permutational Multivariate Analysis of Variance (PERMANOVA) for sex (male and female) and age (two age categories: 1 and 2 + years old) cohorts, using the function 'adonis2' from the package 'vegan' and performed pairwise comparisons using the function 'calc_pairwise_permanovas' from the package package 'mctoolsr'. These analyses were performed on a dissimilarity matrix using the raw proportions of stomach contents, using the function 'dist' from the package 'vegan' (calculus are based on the Euclidean distance). We also performed Similarity Percentage (SIMPER) analysis to determine the food categories that contributed to significant diet differences. We used similar analyses to test for the effect of bodymass, longitude and latitude, climatic data (bio 5, bio 6, bio 12) and urbanism on diet. Differences were visualized using non-metric multidimensional scaling analysis (N-M MDS) of the proportions of each food item (arcsine-square root transformed proportions of the total stomach contents). We tested the correlation between the two first axis of the N-M MDS with Kruskal-Wallis rank sum tests, using the function 'kruskal.test'.

2.1.3. Geometric morphometrics

Three dimensional geometric morphometric analyses were used to explore the patterns of morphological variation and covariation/correlation with diet. We used the three-dimensional coordinates of landmarks placed on 3D models derived from a previous study (Brassard et al. 2020a, article 1, Fig. 2, Table S2). The models were obtained using photogrammetry ('Agisoft PhotoScan' software © 2014 Agisoft LLC, 27 Gzhatskaya st., St. Petersburg, Russia) and the landmarks were placed on the mandible of each specimen using the software 'Landmark' version 3.0.0.6 (© IDAV 2002-2005; Wiley et al., 2005). We considered 25 homologous anatomical landmarks, 190 sliding semi-landmarks on curves and 185 sliding semi-landmarks on surfaces that were slid and transformed into spatially homologous landmarks using a sliding

semi-landmark procedure implemented in the 'Morpho' package (version 2.7) in R (Bookstein, 1991 On the necropolis of Van-Yoncatepe, in Eastern Anatolia (first millennium BC), the remains of five foxes were discovered associated with human skeletal remains (Onar, Belli and Owen, 2005).

Four foxes (as well as a large number of dogs) have been found in Can Roqueta (Barcelona) and Minferri (Lleida), in graves from the Early-Middle Bronze Age. As stated above (see section 2.3.1), isotopes analyses have revealed shared diets between humans, dogs and foxes, suggesting a controlled feeding by humans (Grandal-d'Anglade *et al.*, 2019).

; Gunz et al., 2005; Schlager, 2013). To isolate size and shape, we performed a Generalized Procrustes Analysis (GPA – Rohlf & Slice, 1990) using the function 'procSym' (Dryden and Mardia, 2016; Gunz et al., 2005; Klingenberg et al., 2002) from the package 'Morpho'. We used the function 'tps3d' to deform the mandible of a red fox to the mean shape of the GPA for further visualisations.

We explored the covariations between the proportions of food items (arcsine-square root transformed proportions of the total stomach contents) and mandibular shape with two-block partial least-squares analyses (2B-PLS), using the function 'pls2B' from the package 'Morpho' (Rohlf and Corti, 2000). P-values were calculated based on 1000 permutations. To investigate whether proportions of diet are drivers of mandibular shape, we performed Procrustes ANOVAs with permutation procedures on the coordinates from the GPA using the function 'procD.lm' from the package 'geomorph'. We considered the proportion of food items as explanatory variables. The 'shape.predictor' function and the 'Avizo 8.1.1.' software were used to visualize the effect of the variation in food proportions on the shape of the mandible.

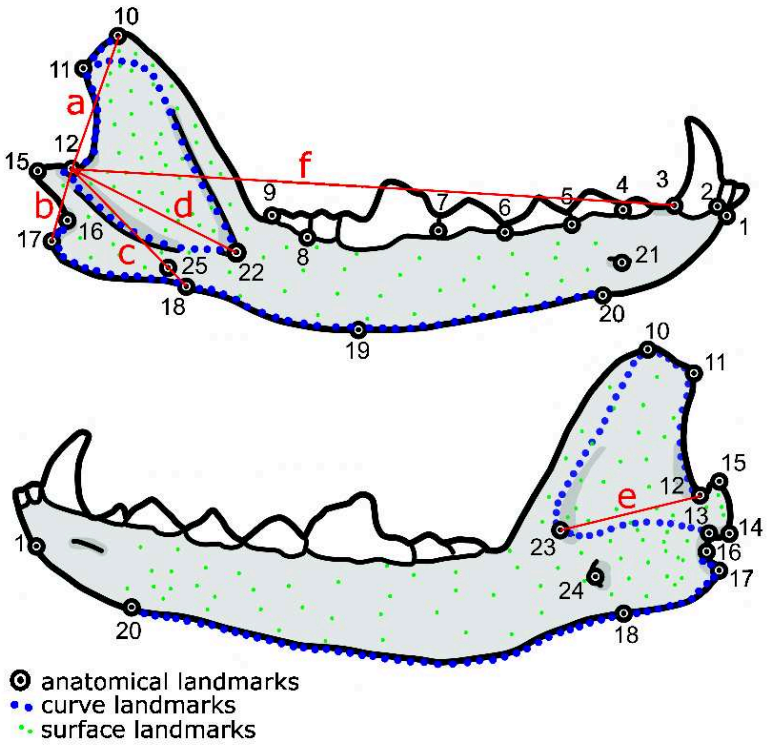

Fig. 1. Landmarks used in this study illustrated on the lateral and medial views of the mandible of a red fox. Definitions of the landmarks are provided in Table S2. The landmarks and distances that are used for bite force prediction in Model 2 are illustrated in red. They correspond to the (non-effective) in-lever arm of the M. superficial temporalis (a), M. masseter superficialis (b), M. masseter pars profunda (c), M. masseter pars suprazygomatica (d), M. temporalis pars profunda (e), and to the out-lever arm exerted by the resultant bite force at the canine tooth (f).

2.1.4. Bite force estimations

Forbes-Harper and colleagues (2017) previously estimated bite forces at the canine using the dry skull method. However, this method estimates the PCSA from dimensions taken on the skull, which does not reflect the architecture of the muscles per se. Here, we developed two alternative predictive models to estimate the bite force at the canine using the shape of the mandible only. We used the function 'plsR' from the package 'plsRglm' (Meyer et al., 2010). Model 1 uses the Procrustes coordinates and log10-transformed centroid size. Model 2 uses only a few landmarks that correspond roughly to the point of insertion of the adductor muscles on the lower jaw, the centre of rotation of the mandible (condyle), and the point of application of the bite force (on the canine tooth). The lengths of the in-lever (euclidean distances between the point of insertion of the muscle and centre of rotation) and out-levers (euclidean distances between the canine tooth and centre of rotation) were calculated based on the coordinates of these points. As we cannot know the orientation of the muscle force vectors of the individuals, we could not use the muscle moment arms. The second method provides the advantage of not needing a GPA. The problem with the method 1 is indeed that the decision rules of the model need to be established each time new individuals are added to the sample (because all the individuals, even the ones used for the prediction need to be superimposed with the same GPA).

To establish the decision rules of the models, we used data previously obtained for 60 French *Vulpes vulpes* (Brassard et al., under review, Article 4). Bite forces were estimated using individual muscle architecture and they show strong correlation with mandibular shape. Here we considered the log10-transformed bite force at the canine for a gape angle of 20° and an orientation of the force perpendicular to the mandible.

The accuracy of each model was assessed using leave-one-out cross validations and further correlation tests (with the function 'cor.test') or linear regressions (function 'lm'). We compared the model outputs (predicted bite force) with the inputs (bite force from dissections) for the French foxes, and for the 14 Australian foxes that were dissected (cf article 5). To estimate the bite forces of these 14 red foxes from the Australian population we used a simplified model of the one described in Brassard et al. (2020b, article 3). Since we could not use a microscribe during the dissection of these foxes, and because the skulls were damaged we recorded the 3D coordinates of attachment of the main muscular groups only (masseter, temporalis and pterygoid) – without distinguishing all the bundles –, and those of three possible points of application of the bite force (at the incisors BPi, at the canine BPc and at the carnassial BPm). To do so we used photographs of the dorsal and lateral view of the skull. In order to compare the accuracy of this simplified model with the one that uses all muscle bundles, we performed a correlation test ('cor.test') between the outputs of both models when applied to the 60 French red foxes for which we had both data sets. We also compared the two models' outputs with estimations obtained previously from the dry skull method (Forbes-Harper et al., 2017).

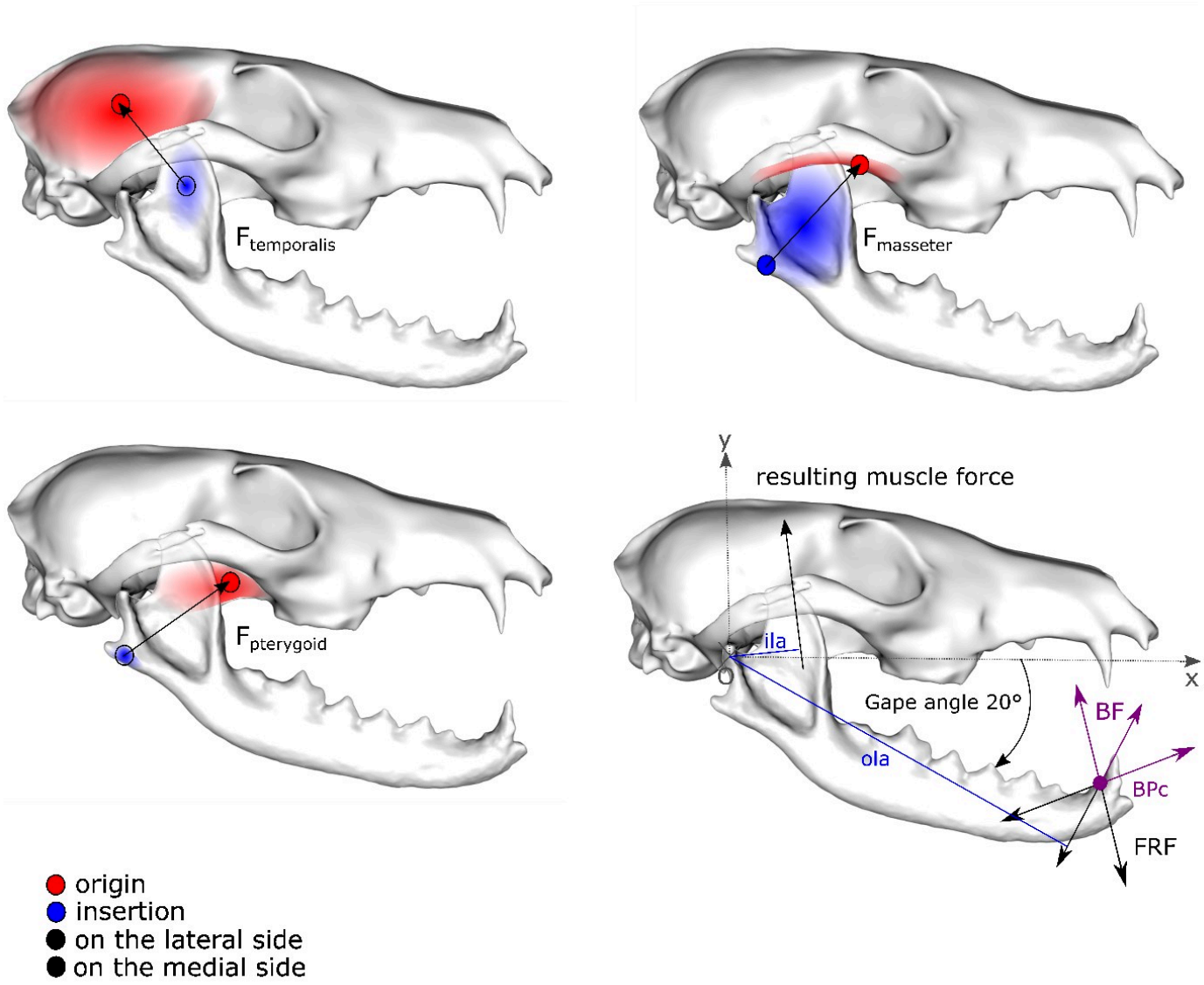

Fig. 2. Simplified biomechanical model used in this study to predict bite force using the individual architecture of the jaw muscles in the dissected Australian foxes. For each muscle complex, the attachment area on the skull are represented in red and those on the mandible are in blue. The landmarks corresponding to muscle attachment for the calcul of muscle moments are represented in transparent when on the medial side. BF: bite force; FRF: food reaction force; Ftemporalis, Fmasseter and Fpterygoid: forces calculated from attachment coordinates and PCSA of the jaw adductors; ila: in-lever arm; ola: out-lever arm; BPc: bite point at the canine.

2.1.5. Determinants of bite force

We compared the variation in bite force between the French red foxes and the Australian red foxes with a t-test ('t.test' function on the log10-bite force). To explore the drivers of variation (or residual bite force variation) in bite force in the Australian red foxes we performed several multiple or simple regressions and (m)ANOVAs with sex, age, Log10-transformed body mass, average maximal temperature (bio5), average minimal temperature (bio6), average precipitation (bio12) and the proportions of food items eaten as explanatory variables, using the function 'lm' or 'aov'. We also performed post-hoc tests using the function 'TukeyHSD' to test between young and adult males or females, or foxes according to the degree of urbanism. The relations between the scaled bite force and mandibular shape in the 14 dissected Australian foxes were explored using 2B-PLS analyses and Procrustes ANOVAs. Residual bite forces were obtained from the regression of the Log_{10}-transformed bite forces on the Log_{10}-transformed centroid size of the mandible, using the function 'lm'.

2.2. Results

Detailed results of the statistical analyses and all model outputs are provided in the supplementary material.

2.2.1. Estimation of bite force in Australian red foxes using muscle architecture

Estimations provided by the simplified biomechanical model estimating bite force from muscle architecture of the main muscle groups only are very close to the estimations obtained using the more complex biomechanical model that uses all muscle bundles (r = 0.89). This method thus provides a good approximation of the maximal bite force in the 14 Australian red foxes in comparison with the full model developed in Brassard et al. (under review, article 4). Bite forces of the dissected Australian foxes ranged from 136 to 246 N (mean = 196 ± 35 N).

2.2.2. Validation of the predictive models of bite force using mandibular shape only and comparison with the dry skull method

Bite force was predicted from the PLS regression analyses using either the complete shape and centroid size of the mandible (model 1) or dimensions on the mandible (model 2). Predicted (predBF) and calculated bite force (BF) show good correspondence for both models in the 60 French red foxes that were used to establish the decision rules (r = 0.82 for model 1 and r = 0.74 for model 2, $P < 0.001$).

Table X. Correspondence between calculated (BF) and predicted bite forces (predBF) for the two alternative models.

		Calculated BF (dissection) vs model predictions		Model predictions BF vs dry-skull predictions
Sample		60 French foxes	14 Australian foxes	300 Australian foxes
Model 1	P	< 0.001	0.06	< 0.001
	r	0.82	0.51	0.69
	Eq	$\log_{10}(BF) = 0.19 * \log_{10}(predBF) - 0.078$		$\log_{10}(predBF_{this\ study}) = 1.02 * \log_{10}(predBF_{dry\ skull\ method}) - 0.26$
	Intercept	> 0.05		> 0.05
Model 2	P	< 0.001	0.08	< 0.001
	r	0.74	0.09	0.78
	Eq	$\log_{10}(BF) = 0.19 * \log_{10}(predBF) - 0.078$		$\log_{10}(predBF_{this\ study}) = 1.02 * \log_{10}(predBF_{dry\ skull\ method}) - 0.23$
	intercept	>0.05		> 0.05

These models do not work well when applied to the 14 Australian red foxes that we dissected (model 1: r = 0.51, *P* = 0.06; model 2: r = 0.09, P = 0.8). However, the results suggest that better results are obtained with the first model that uses more accurate shape information, even for the Australian red foxes.

Bite forces predicted from the two PLS regression models are strongly correlated with estimations obtained previously by the dry skull method (n=300 Australian red foxes; $predBF_{dry\ skull\ method}$ was extracted from Forbes-Harper et al., 2017, Table X). Interestingly, the correlation is better with model 2 which uses simple Euclidean distances, possibly as it is more similar to the simplified dry skull method.

The validation of these models on the 14 Australian red foxes we dissected is significant but rather poor, in particular with regards to model 1 (model 1: *r* = 0.51, *P* = 0.06; model 2: *r* = 0.09, *P* = 0.08).

We estimated significantly lower BF using model 1 than using the dry skull method, in Australian red foxes (T-test: n=300, P<0.001, mean $BF_{dry\ skull}$= 236±32N, mean BF_{model1}= 201±40N). The bite forces predicted with model 2 are higher than those predicted using model 1 (mean $BF_{model\ 2}$ = 210±38N; P<0.001) but remain significantly lower than those predicted with the dry skull method (P<0.001). In all further analyses, we consider the predicted bite forces obtained using model 1 for all the Australian red foxes as this provided a better estimate of the bite forces. Australian red foxes have significantly lower bite forces (n=387, mean $predBF_{model1}$ = 197±41N) than French red foxes (n=60, $BF_{dissection}$ = 233±62N, $predBF_{model1}$ = 230±46 N, $P_{T\text{-}test}$<0.001,). The same foxes differ in mandibular shape ($P_{Procrustes\ ANOVA}$ = 0.001, R^2 = 0.023), but not in centroid size ($P_{T\text{-}test}$ = 0.6), as previously demonstrated on a bigger sample (Brassard et al., article 5).

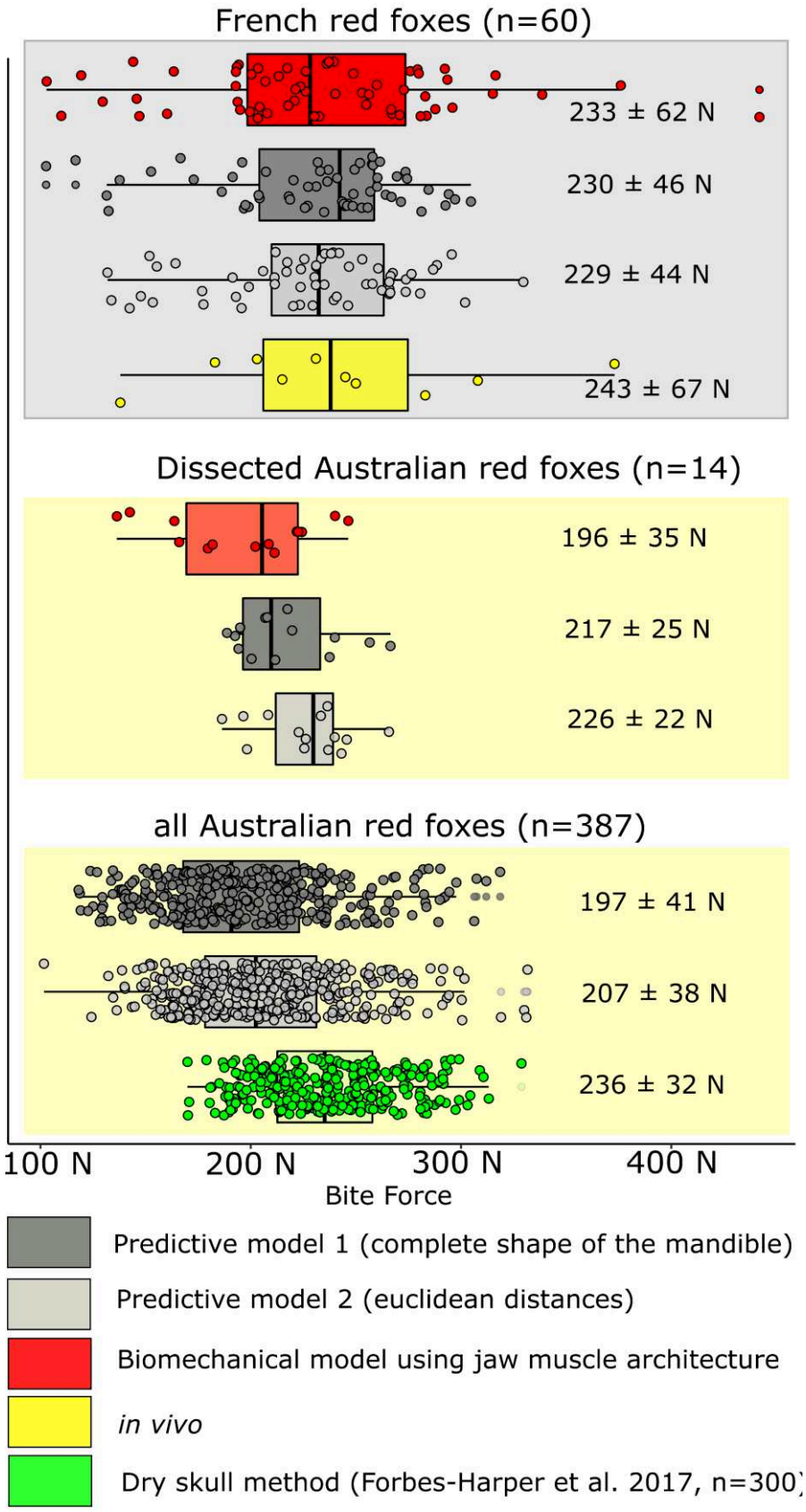

Fig. 3. Bite forces in Australian and French red foxes, estimated from the different methods used in this study. Different methods are indicated by different colors. The mean value ± standard deviation is indicated for each group and method. Although log-transformed values were used for statistical analyses, raw data are shown for clarity.

2.2.3. Diet analyses

Table 3. Mean diet proportions and bite forces according to age and sex or to urbanism. *these means are not significantly different (Tukey post-hoc test).

N=375	Female 1y N=105	Female 2+y N=66	Male 1y N=121	Male 2+y N=83	Rural N=112	SR1 N=177	SR2 N=50	Urban N=48
Mean BF	171±26 N*	215±28 N	177±26 N*	245±31 N	209±40 N*	187±40 N	200±34 N*	206±41 N*
Food item proportions (%)								
Sheep	61	50	64	61	65	61	44	57
Rodent	6.3	12	6.0	8.2	7.8	4.3	16	8.0
Rabbit	3.3	1.4	3.6	0.0	1.2	4.2	0.0	0.0
Marsupial	0.62	1.1	0.84	1.3	1.0	0.58	0.0	2.7
Other mammal	0.067	0.10	0.26	0.036	0.089	0.085	0.0	0.46
Bird	4.1	1.9	5.5	2.9	2.1	5.3	1.8	3.6
Reptile/frog	2.0	1.8	0.36	0.77	0.23	1.5	1.3	1.6
Invertebrate	9.8	19	8.9	4.5	7.4	11	22	3.6
Plant	9.1	10	9.5	16	11	9.3	11	17
other	3.4	2.1	2.4	4.8	4.2	2.8	4.5	6.1

As already demonstrated for a larger sample (Forbes-Harper et al., 2017, n=540), we recorded significant sex and age-related differences in diet (n=375, $P_{PERMANOVA} = 0.026$). Sheep carrion comprised 50-64% of diet volume (47–65% in Forbes-Harper et al., 2017). Adult females showed a tendency to consume sheep to a lower degree (50%) than adult males ($P = 0.08$) or juveniles of both sexes ($P < 0.03$, detailed results of the statistical analyses are provided in the supplementary material). In contrast, adult females had more invertebrates (19%) and slightly more rodents (12%) in their diet. Young foxes have similar diets regardless of their sex. Adult males eat more plants (16%) than other foxes (~9%).

Diet is strongly correlated with the geographic provenance of the foxes ($P < 0.01$, n=387, $R_{latitude}^2 = 0.0093$, $R_{longitude}^2 = 0.012$). The lower the latitude, the higher the proportion of sheep, rabbit, marsupials, bird, other mammal, plant and other. The lower the longitude, the higher the proportion of sheep, rabbit, birds, reptiles/frogs, invertebrates and other. We also found significant differences related to urbanism ($P < 0.001$, $R^2 = 0.027$) although the differences are not continuous along the urban-rural gradient. Foxes from the SR2 group eat significantly fewer sheep than foxes from the SR1 group ($P < 0.01$) or the 'rural' group ($P < 0.01$). However the difference between the 'SR1' or the 'rural' group or for urban foxes is not significant. Foxes from the SR2 group also eat more rodents and invertebrates than both urban and rural foxes, $P < 0.05$), which suggests that differences in diet are more likely related to the exact locality than the proximity to humans. Urban foxes eat significantly more plants than foxes in the three other groups ($P < 0.05$). We found no significant correlation between diet and climatic data such as average maximal temperature (bio5, $P = 0.10$), average minimal temperature (bio6, $P = 0.48$) or average precipitation (bio12, $P = 0.13$).

2.2.4. Bite force determinants in the Australian red foxes

The visualisations of the first axis of the 2B-PLS between bite force or scaled bite force and mandibular shape in the dissected Australian red foxes suggest strong covariations (rPLS = 0.80 or 0.77, respectively), despite the low sample size (resulting in non-significant results, $P = 0.6$). The results of the Procrustes ANOVAs show a similar trend ($P = 0.15$).

ANOVAs show that the absolute bite force significantly increases with body mass ($R^2 = 0.42$, $P < 0.001$, n= 386). It also depends on sex ($R^2 = 0.034$, $P<0.001$, n = 387) and age ($R^2 = 0.47$, $P< 0.0001$, n=375), whether ther are considered separately or together (together they explain 51% of the variation in bite force). Post-hoc tests show that young foxes produce similar absolute bite forces, regardless of their sex ($P_{adjusted} = 0.2$). However, young males produce relatively higher bite forces than young females ($P_{adjusted} = 0.017$). Adults produce greater bite forces than young foxes ($P_{adjusted} < 0.001$), even for their size ($P_{adjusted} < 0.001$). Adult males produce greater absolute bite forces than adult females ($P_{adjusted} < 0.001$), which is related to their bigger size (there is no difference in scaled bite forces, $P_{adjusted} = 0.8$). There are also significant differences depending on the geographic area. The bite force is significantly lower in SR1 areas than in rural ($P_{adjusted} < 0.001$), urban ($P_{adjusted} < 0.01$) or SR2 areas ($P_{adjusted} = 0.06$). Bite force is also significantly negatively correlated with average maximal temperature (bio5, $P = 0.03$, $R^2 = 0.0098$, n = 387), positively correlated with average minimal temperature (bio6, $P < 0.0001$, $R^2 = 0.045$, n = 387). There is no significant correlation with average precipitation (bio12, $P = 0.5$, n= 387). The scaled bite force is correlated with average minimal temperature only ($P = 0.003$, $R^2 = 0.02$, n = 387).

The results of the 2B-PLS between mandibular shape and food proportions is not significant ($P_{2B\text{-}PLS}>0.10$ for all PLS axes, n= 387). The multiple Procrustes ANOVA show significant correlation with the proportion of rodents ($P = 0.022$) but this explain only 0.52% of the variation in shape. The 2B-PLS between diet and bite force or scaled bite force are significant (PLS1 explain 100% of the total covariation, $P < 0.001$) but the coefficient of covariation is low (bite force: $rPLS_{BF}= 0.15$, scaled bite force: rPLSscaledBF = 0.16). Higher absolute bite forces are associated with lower proportions of sheep, rabbit and invertebrates, and higher proportions of rodents, plants, and other prey. Higher relative bite forces are associated with lower proportions of sheep, rodent and other, and with higher proportions of rabbits, invertebrates and birds.

The results of the multivariate regression with all food items are not significant ($P = 0.09$ for absolute bite force and $P = 0.11$ for scaled bite forces). The best fitted models are obtained with the proportions of ‘rabbit’ and ‘other’ only ($P < 0.01$, $R2 = 0.021$ for absolute bite forces and 0.025 for scaled bite forces). Higher proportions of rabbit are associated with lower bite forces ($R2 = 0.0084$, $P = 0.04$).

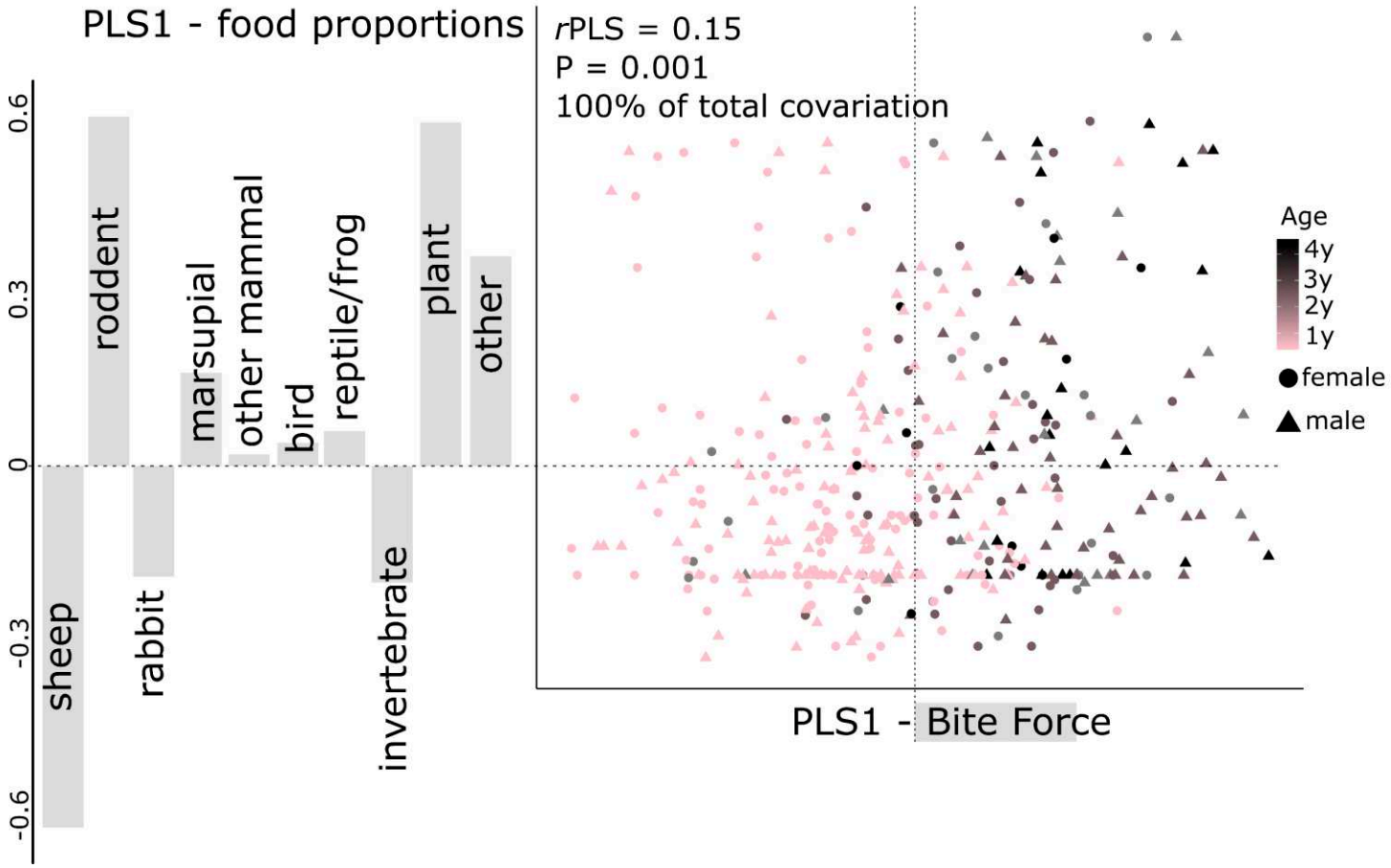

Fig. 4. 2-Block Partial Least Square Analyses between mandibular shape and food proportions in stomach content of the Australian red foxes (n = 387) with vectors along PLS axis. Different ages are represented by colours and males and females are distinguished by different shapes.

Conclusion and discussion of Part 2 and perspectives for Part 3

Strong relationships between the bony and muscular components of the masticatory apparatus despite drastic artificial selection

In this part, we highlighted strong architectural and functional relationships within the masticatory apparatus of canids. Surprisingly, these links are as strong in modern dogs that are artificially hyper-selected, as in the red fox, a commensal canid more submitted to natural constraints. Thus, the integration between bones and muscles is very strong and maintained despite drastic artificial selection.

However, we lacked muscle data for very dolichocephalic dogs (Afghan greyhound type). In the future, we would like to increase the sample by including more dolichocephalic and brachycephalic hypertypes, in order to compare the integration of structures in these two canine typologies. Our dingo sample was too small and calls for future enrichment with new specimens to provide reliable results comparable with dogs. In the same perspective, studying a population of stray dogs (e.g. North African pariah dogs) in order to enrich our natural-artificial constraint gradient (Figure 49) with domesticated but commensal dogs (that are less genetically isolated than dingoes) would be of interest. In the framework of this thesis, we were unable to access wolf heads to dissect them. This is also a perspective for future research. Gathering large poulations of stray dogs, dingoes and wolves (yet a long-term effort), would allow to go further in the exploration of the effects of domestication and artificial selection on the functional integration of the masticatory apparatus.

The possibility of inferring function in archaeological canids

The strong integration observed is very promising to allow functional inferences in archaeological dogs (and red foxes). Variation in the shape of the mandible can be interpreted in terms of variation in muscle development and in terms of bite strength (absolute or relative to size).

These inferences should be made on the condition that archaeological canids are included in the variability of the modern canids with estimated bite force. Given that we have dissected dogs of a wide variety of breeds, and that before the Bronze Age, dogs are unlikely to display such (extraordinary) diversity in form, this is highly plausible. But it will have to be ascertained.

As seen in Part 1, prehistoric humans are unlikely to have selected very particular morphotypes (selection would have been more based on size criteria). These dogs can be expected to be closer in shape to small wolves, small dingoes, or Beagles (their shape is fairly average as seen on the PCAs in the previous chapters). Preliminary results obtained for the dingo tend to suggest that the covariation patterns between muscles and the shape of the

mandible for this subspecies are comparable to those observed in domestic dogs. Thus, since we have dissected a reasonable number of beagles (likely the closest in mean shape to archaeological canids), and since we expect to have extended this variability beyond the variability of pre-Bronze Age canids (which will have to be verified in Part 3), our dissected modern dog sample could be quite relevant for interpreting variations in shape in archaeological canids in terms of muscle development (especially in areas of muscular attachment, robustness, or curvature).

Furthermore, our results showed that the shape covaried and was strongly correlated with bite force (in a commensal canid such as the red fox, the mandible is even a better indicator than the cranium). Variations in shape can therefore be interpreted in terms of variation in bite force. It is even conceivable to construct a linear predictive model to provide each mandible of our archaeological corpus with an estimated bite force. Once again, this will only be possible on the condition that the variability of archaeological dogs is included in the variability of modern dogs whose bite force was calculated from dissection data. This verification will be an important step in part 3.

The mandible is indicative of the overall morphotype and function of dogs.

The strong relationship observed between the shape of the mandible and cranium, even in modern dogs, confirms one of our basic hypotheses (see Conclusion of Part 1: Formulation of the research problem): the shape of the mandible is indicative of the overall shape of the head. This is interesting because human intentional artificial selection is more likely to target directly the cranium than the mandible. Accordingly, if very particular mandibular shapes reminiscent of certain modern hypertypes are observed in archaeological canids (although this is unlikely *a priori* given the state of the art), we may suspect intentional human selection for a particular morphotype.

On the same principle as for bite force, it is conceivable to predict the shape of the cranium from the shape of the mandible for archaeological dogs and foxes. This requires two things: that the variability of archaeological dogs is included in the variability of the modern dogs with cranium and mandible that we have studied, and that the integration between these two structures has not changed over time.

Furthermore, the selection for certain morphotypes for particular functions (such as defense or herding) may be related to variations in jaw strength. Indeed, we saw in chapter 3 that brachycephalic dogs are more efficient in biting than dolichocephalic dogs, which is partly related to the function of the dogs in our corpus. In our reference sample, brachycephalic dogs are indeed mainly dogs dedicated to defense (towards humans) or attack (bite force abilities are important) whereas the dolichocephalic dogs are mainly dogs dedicated to protection (towards herds, running ability and therefore speed tend to be preferred over biting).

Evolution of integration, modularity and allometric patterns over time: effects of anthropisation in foxes and wolves and of artificial selection in dogs.

Bite forces will have to be predicted from the model established from the dissection of the modern canids of our sample, using a predictive model based on the shape of the mandible. This means that the results are likely to be biased if the integration between the elements of the masticatory apparatus has changed over time.

We will not be able to study the evolution of the relationship between the shape of the skull and the shape of the mandible over time because of the lack of cranial remains. Nor will we be able to follow the evolution of the integration between muscles or bite force and the shape of the mandible, due to the absence of muscle data for archaeological canids. However, we can follow the evolution of the modularity within the mandible, which can provide indications on a part of the masticatory apparatus. Is modularity the same in dogs before the Bronze Age as in modern dogs? If the relationship between the front and back of the mandible changes over time, it is quite possible that the relationships between the mandible and the muscles or cranium and therefore the bite force have changed as well, and therefore the predictive model of bite force may be biased. We will also be able to compare the evolution of modularity over time, in particular between commensal (foxes) and domestic (dogs) species.

Finally, it is also possible that the relationship between shape and size has changed over time, especially in dogs for which artificial selection may have altered the allometric patterns. In particular, if dogs before the Bronze Age looked like "little wolves" or "little dingoes", similar allometries should be observed to those found in ancient and modern wild canids. This will allow us to compare the effect of size on conformation in modern and pre-Bronze Age dogs, and compare with red foxes, wolves and dingoes.

Adapting models to fragmentation

In this section we have studied complete mandibles. However, in an archaeological context, complete mandibles are relatively rare due to taphonomic processes. In order not to reduce our archaeological sample too drastically, and to exploit a maximum of mandibles, we will have to adapt our models to fragmentation and check their reliability (especially for small fragments). To what degree of mandibular fragmentation is it possible to describe accurately, without risk of confusion, the size, morphological variability, or estimate bite force (or even the shape of the cranium)? What are the limits of the use of these patterns?

Interpreting shape variations from a developmental and ecological or anthropic point of view

The study of Australian foxes demonstrated the multifactorial and complex relationships between mandible shape and developmental (age, sex, size) and environmental (geographical and climatic parameters, degree of urbanisation) factors. We were unable to make a similar study in modern dogs due to their highly modified lifestyle. Once again, the ideal would be to study, in the same way as we did for the fox, stray dogs subjected to a less artificial lifestyle

than current dogs, or even dingoes. However, it is highly likely that the more commensal archaeological canids responded in a similar way to modern foxes to the types of constraints we have studied. This is all the more likely as we saw in Part 1 that dogs and foxes respond with the same morphological, physiological and behavioural modifications to similar selection pressures (see Part 1 – 1.3.3).

Inferring a diet: a utopia?

The study of Australian foxes showed a low correlation between bite force and the stomach contents. The differences in diet are mainly related to age-related diet differences in our sample. In addition, this diet reflects dietary resources that are quite different from those available to dogs prior to Bronze Age in Europe, so it will be difficult to transpose these results and great care must be taken when interpreting variations in bite strength in terms of diet.

KEY POINTS

It emerges from this part of the thesis that **the mandible is a very good model for monitoring the morphological evolution of canids** (in terms of overall form of the head), **tracing their masticatory abilities and linking the variations observed with geographical or temporal variations**, depending on **anthropisation** or even the possible **intentional selection** of particular morphotypes to perform certain functions.

Interpretations in terms of diet will have to be conducted with great caution.

Within the same population, variability should be considered in relation to the age of the individuals and the possibility of sexual dimorphism.

The question of whether modern dogs are good models for interpreting ancient dogs cannot yet be fully answered, as it requires a comparison of morphological variability and modularity within the mandible in the present and in the past.

Part 3
Morpho-functional study of canids prior to the Bronze Age

The purpose of this third part is to adapt and apply the methodologies used on modern canids to the archaeological mandibles. Given the exploratory aspect of the results obtained in this part and the complexity and diversity of questions explored, the part will be presented so as to reflect the strategic progression of our reflections in the processing of the data.

First, in Chapter 6, the archaeological corpus will be presented. The size and constitution of the archaeological sample will justify the questions that will be more precisely addressed in the following chapters.

Based on the results obtained on modern mandibles (cf. Part 2) we develop, in Chapter 8, predictive methods for interpreting variations in the shape of archaeological mandibles in terms of function. As already mentioned in the conclusion of part 2, it is necessary to verify that ancient canids are included in the variability of modern canids, before building predictive models whith decision rules based on modern canids. We will thus first compare modern and ancient canids, in Chapter 7, to make sure that modern dogs and foxes are good models for interpreting ancient dogs. We will make some methodological choices and will discuss limitations based on these results. Additionnaly, the degree of information loss related to fragmentation when describing mandible shape and size will be investigated.

Then, in the following chapters, we apply the methods to the archaeological remains of dogs (Chapter 9) and red foxes (Chapter 10). We will proceed from the most general to the most detailed question. First, we will compare dogs in Eastern and Western Europe. Then, for each geographical area, we will look at the evolution of form and function from the Mesolithic to the pre-Bronze Age. We will compare two Middle Neolithic cultures in Western Europe (Chasséen and Cortaillod), and two cultures in Eastern Europe (Hamangia III/Boian and Gumelnița). Then, we will focus on the Middle Neolithic site of Twann in Western Europe to explore the diversity within this site during the Cortaillod culture over a fairly long and well-documented period of time. Finally, we will compare the dogs of Borduşani and Hârşova to compare two contemporary and similar sites of the Gumelnița culture in Eastern Europe. The chapter on the application to the remains of archaeological foxes is more succinct as the small amount of material does not allow us to explore most of the questions mentioned above.

At the end of each chapter, key results will be pointed out and discussed.

In the conclusion of this part 3, we will summarize the main findings provided by the study of ancient canids and discuss future perspectives.

Chapter 6.
Archaeological sampling

The aim of this chapter is to present the archaeological corpus considered in this thesis. A brief description of the sites considered as well as the results of the observations made on canid mandibles are given. The strategy to collect data, the adaptation of the geometric morphometric protocol to fragmentation and the classification of specimens into chrono-cultural and geographical groups are also explained.

1. Strategy for the collection of archaeological material

Based on the preliminary list of sites containing canid remains between the Mesolithic and pre-Bronze Age in Europe (cf section 2.2 Non-exhaustive occurrence of canid remains in the archaeological record from the Mesolithic to the early Bronze Age), we contacted the archaeozoologists who studied the the faunal assemblages. After ascertaining the presence of dog or fox mandibles and the accessibility of the material, we contacted the persons in charge of the storage in order to access the remains. A list of the archaeological sites whose material has been studied in the scope of this thesis is given in Table 15. The corresponding sites are represented on the maps in Figure 53 and Figure 54. Further details about these sites will be provided in section 3.

We have collected a large sample of dog mandibles, roughly equal numbers originating from Western Europe (France, Germany, Switzerland: around 360 mandibles) and South-Eastern Romania (around 250 mandibles). We report in Table 15 the available information for the dogs from these sites (archaeological context, dating, and mitochondrial DNA).

The collection was more limited for the red fox (Western Europe: just under 60 mandibles; Eastern Europe: less than 10 mandibles), although the sampling strategy was the same as for the dog. This is likely related to several things. First, to the low number of remains in the faunal assemblages. Red foxes are often represented only by their teeth, and mandibles are quite rare. Moreover, contrary to dogs, the fox has not been the subject of any large-scale comparative study involving the progressive collection of material. We therefore started from scratch, whereas the field was well prepared for dogs. However, this material collection is a long-term effort, impossible in only three years. This is why our study of the red fox, provided in this thesis as a comparison with dogs, must remain preliminary and needs to be completed in the future.

The aim of this study is not to focus on domestication, but when it was possible, we also included a few wolf skulls from sites where we collected dogs or red foxes. The aim is to use these pre-Bronze Age wolves as outgroups in all further analyses. Accordingly, only the wolves of which the subspecies attribution was absolutely certain were used. This represents 8 wolves from the Late Neolithic of Chalain 4 or from the Chalcolithic (Gumelnița B1) in Vităneşti.

Identification was based mainly on a size criterion and on the presence of many other wild species in the site under consideration. Wolf remains are scarce in sites from the Neolithic to the Bronze Age, which explains the low number of confirmed specimens in our sample.

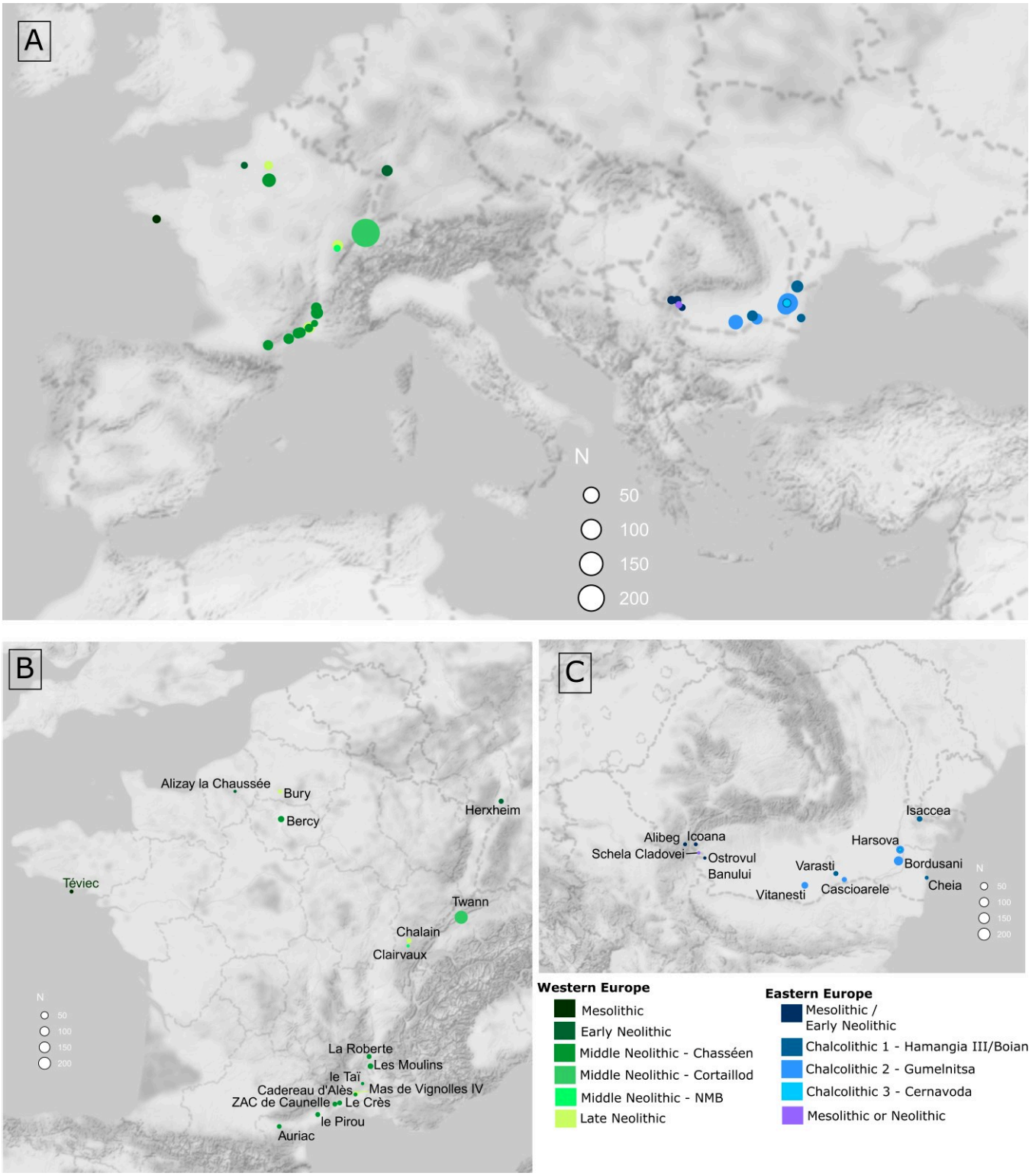

Figure 53. Location of the archaeological sites with dog mandibles considered in this thesis. Dot size is proportional to the number of mandibles studied in geometric morphometric analyses (see Table 18). A: Europe; B: Western Europe; C: Eastern-Europe: Romania.

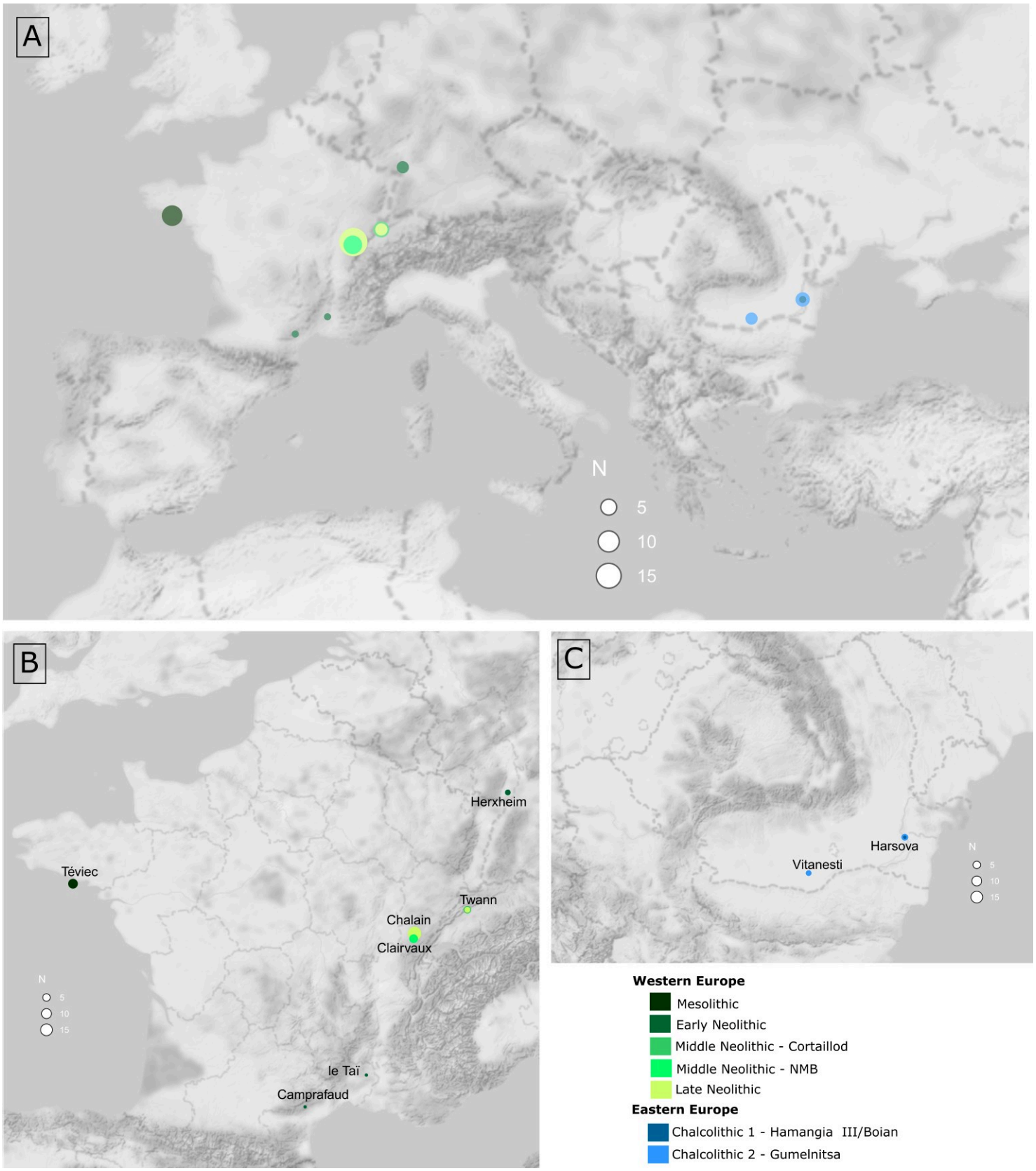

Figure 54. Location of the archaeological sites with red fox mandibles considered in this thesis. Dot size is proportional to the number of mandibles studied in geometric morphometric analyses (see Table 19). A: Europe; B: Western Europe; C: Eastern-Europe: Romania.

2. Data acquisition

All the mandibles were first observed to record some morphological criteria (section 2.2). Then, the mandibles were photographed for photogrammetric reconstruction (section 2.3).

2.1. Species identification

Species identification was already done by zooarchaeologists. We only had to confirm them, on the basis of the pathognomonic dental formula of canids and overall size and form criteria. The distinction between *Canis* and *Vulpes* is usually obvious. The distinction between dogs and wolves was made by visual appreciation of size (wolves being much larger than dogs during the period considered in this thesis, as previously reported in the literature, see Part 1). However, fragmentation may have led us to question the identification of some individuals. For example, some fragments of the mandibular body (without teeth) led us to doubt between wolf and dog or dog and fox, or even between dog or fox and badger, the latter being well represented at some sites included in our corpus (Chalain, Herxheim).

We therefore verified our attributions for the fragments before morphometric analyses, by carrying out a quantitative analysis of the centroid size and shape of the mandible (see Appendix 8: Part 3 – Chapter 6. Verification of species identification for fragmented archaeological mandibles).

2.2. Morphological traits

Morphological traits were previously recorded for most of the dog mandibles (data were recorded and provided by S. Bréhard, A. Bălăşescu, A. Tresset and M. Pionnier). We completed this referencing for the newly acquired dog mandibles, and for the fox mandibles.

The morphological traits observed consist of:

- The **stage of eruption of the teeth** for juveniles, and the **aspect of the bone** and the **state of tooth wear of the lower first molar**, in non-juvenile individuals, as described by Horard-Herbin (2000, Figure 55). We thus considered 4 age groups:
  - **Juveniles**: individuals with the first molar not erupted or still erupting;
  - Subadults: the first molar tooth is erupted but the first or second premolar tooth are still erupting;
  - **Young**: the mandible is still porous but all teeth are erupted;
  - **Adult**;
  - **Old**: tooth wear over stage E

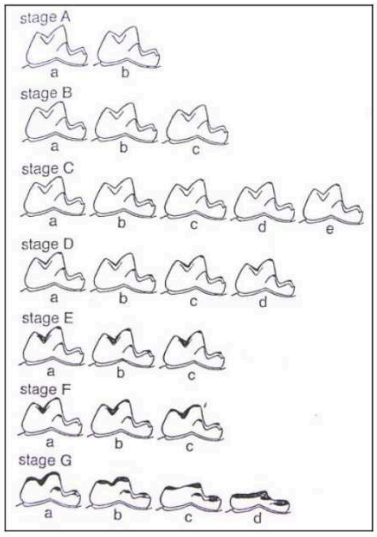

Age (mois)	6-10	10-15	15-24	24-36	36-48	48-72	>72
Stade A	46%		12%				
Stade B	23%		16%				
Stade C	31%		20%	17%			
Stade D			48%	17%			
Stade E			4%	67%	25%		
Stade F					75%		
Stade G						100%	100%

Figure 55. Stages of enamel wear on the lower first molar tooth in dogs, lingual view (left) and relations with the absolute age of the animal (right). From Horard-Herbin, 2000.

- The existence of **dental anomalies** (absence of a tooth or presence of supernumerary teeth);

- The presence of **cut marks** (Binford, 1981; Vigne and Marinval-Vigne, 1983) in areas where the skin or muscles are strongly attached:
  - **Skinning marks**: incisions located towards the front of the mandible, under the canine or incisor teeth;
  - **Filleting marks**: located on the lingual (medial) or ventral side of the mandible, possibly indicative of tongue retraction.
  - **Dismembering marks**: located on the mandibular ramus.

    Anthropogenic marks must be distinguished from taphonomic processes related to post-depositional events. We were looking for incisions that are often multiple, parallel, thin, with a “V” rather than a “U” cross section.

    Butchering marks were not always observable due to the preservation state of the bone surface or fragmentation. In this case we indicated "not observable".

- The presence of localized **burn marks** on the front of the mandible, characterized by the disintegration of the enamel of incisor, canine and first premolar teeth and by a coloration of the dentine. Only this criterion was considered truly diagnostic, but we also noted when other teeth seemed burned or when the appearance of the bone, eroded, suggested that the mandible may have been burned). Special caution is needed in the case of lakeside settlements (Twann, Chalain, Clairvaux), where humidity may have dark colored the dentine, and the alternance between humid and dry conditions may have weaken the enamel (Denys and Patou-Mathis, 2014). Under these conditions, only the criteria we mentioned first will be considered as truly diagnostic. These marks, located in areas where the bone is less or not protected by the flesh, result from cooking and thus attest to the consumption of the animal (Vigne, 1988; Bréhard, 2007).

2.3. Adaptation of the photogrammetry protocol

The **photogrammetry** protocol was globally the same as the one used for modern specimens. Sometimes, the mandible was caught in a concretion coating with the skull still connected. In these cases, the entire block was reconstructed to preserve the information related to the anatomical connection. Whenever possible, the mandibles were isolated and cleaned before being reconstructed alone. When the mandible was broken into several remountable pieces, these were glued together using PRIMAL glue.

The two mandibles of an individual may have been photographed, in particular when their state of fragmentation was not the same, in order to increase the representation of these individuals in subsequent analyses.

A unique ID was assigned to each of the archaeological remains that was reconstructed using photogrammetry. This ID is composed of the first 3 or 4 letters of the site (to avoid confusion) followed by a number.

618 three-dimensional models of different mandibles of non-juvenile canids were reconstructed over the course of this thesis. Two of them were still connected to the cranium and surrounded by the concretion coatings and could not be photographed separately: Pir5, Mas2, Mas10 (Neolithic). In this corpus, there are only three subadult dogs (Bor23, Bor36 and Bor92: Chalcolithic, Gulmenitsa A2) and 2 subadult foxes (Vit23, Chalcolithic 2, Gulmenitsa; Her15 Early Neolithic, LBK). We also reconstructed the mandibles of two juvenile dogs (Twa86: Middle Neolithic, Cortaillod; Her11: Early Neolithic LBK) and two juvenile foxes (Cla3: Middle Neolithic, NM; Cla8: Middle Neolithic NMB).

Additionally, 3D models of 9canid crania (skull without mandibles) were built given their relatively good state of preservation.

We also reconstructed 49 mandibles of mustelids (badger, mink, weasel, marten) from the sites of Chalain and Herxheim, and 8 mandibles of wolves from the sites of Chalain 4 (5, early Clairvaux, Late Neolithic) and Vităneşti (3, Chalcolithic), for preliminary analyses allowing to verify the species identification (see Appendix 8: Part 3 – Chapter 6. Verification of species identification for fragmented archaeological mandibles).

3. General description of the archaeological sites

In this section we provide a very brief description of the sites considered in this thesis. We recall the culture(s) and date(s) of occupation, the originality of the site and the place of dogs among faunal remains. The results of previous observations on the long bones are mentioned when relevant. The overall number of mandibles observed (not all of them are used in the geometric morphometric analyses) as well as the results of my own observations or those of S. Bréhard (cut and cooking marks and dental peculiarities) are given.

3.1.1. Sites in South-Eastern Europe

3.1.1.1. *Alibeg*

In Alibeg (Pescari village, Coronini commune, Caraș-Severin county, South-Eastern Romania), two occupations have been identified: at the end of the Mesolithic and during the Early Neolithic (Starcevo-Criș culture; Boroneanț, 2000; Boroneanț, Bălășescu and Radu, 2012). The the number of faunal remains is very limited (only 115 remains for the Mesolithic, including 85 NISP, and 15 for the Neolithic, including 11 NISP; Bălășescu, unpublished). Dogs represent around 3% of the NISP. Two dogs included in our corpus come from the levels situated at the limit between Mesolithic and Early Neolithic occupations (at the turn between the 7th and the 6th millennium cal. BC; Boroneanț, 2000), and a mandible from the Mesolithic period. All show burn marks (observations: S. Bréhard, C. Brassard).

Figure 56. Burn marks on the canine of aLate Mesolithic or early Neolithic dog in Alibeg.

3.1.1.2. *Icoana*

Icoana (Caraș Severin county, South-Eastern Romania) is an open-air site in the upper gorge of the Iron Gates region, located on a narrow slip of land along the Danube (Boroneanț, 2000; Boroneanţ, Bălăşescu and Radu, 2012; Bonsall *et al.*, 2015). The site is pluristratified, with the upper layers almost completely washed away by the Danube prior to excavation, leaving traces of the Early Neolithic Starčevo-Criș culture (mainly pit features and sunken huts) and Mesolithic occupation (trapeze and rectangular-shaped dwellings). The faunal remains originated mainly from the identified features rather than the so-called cultural layers.

8 mandibles were observed in the present thesis. Only one was dated to the early Neolithic (Ico4), the others were stratigraphically assigned to the Mesolithic. Recent radiocarbon dates on 18 pig bones suggest that the main occupation of the site occurred between 9,100-7,500 cal. BC, only one date indicating an occupation at the very end of the 7th millennium cal. BC (Boric, 2011). No anthropogenic marks or teeth abnormalities were evidenced (observations: S. Bréhard); however, the high fragmentation of the material prevents most of the observations (Figure 57).

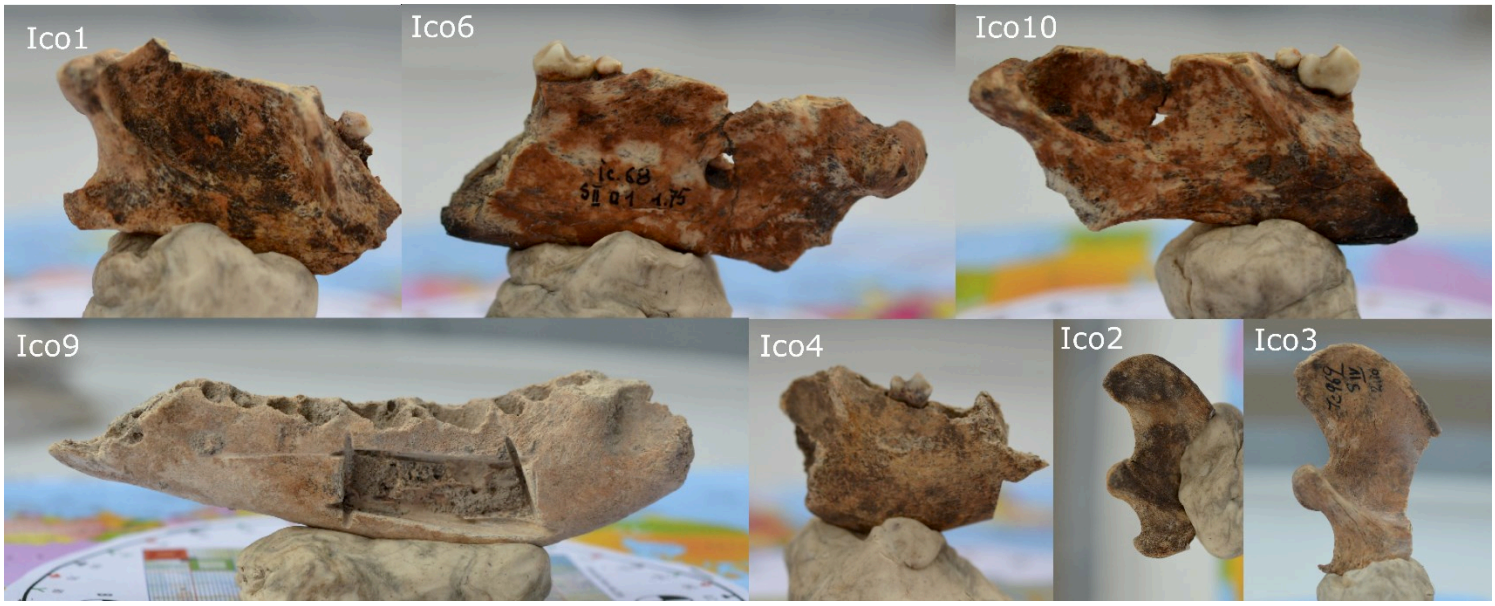

Figure 57. Fragmentation of dog remains from the Mesolithic (Ico1,2,3,6,9,10) and Early Neolithic (Ico4) of Icoana.

3.1.1.3. *Ostrovul Banului*

In Ostrovul Banului (Gura village Văii, Mehedinți county, South-Eastern Romania), several cultural levels have been identified: Mesolithic, Early Neolithic (Starcevo culture-Criș), Bronze Age, Romano-Byzantine Hallstatt and Middle Ages. The Mesolithic was dated by 14C between 7,478 and 6,228 cal. BC (Mărgărit, Boroneanț and Bonsall, 2017, 40) The Mesolithic fauna includes 308 NISP, and the dog is the only domestic animal, with a percentage of 22.7% (70 remains, Bălăşescu and Radu, 2012).

Our corpus contains one dog mandible dated to the Mesolithic (Ost2, Figure 58). The fourth premolar shows burn marks.

Figure 58. Burn marks on a dog mandible from the Mesolithic of Ostrovul Banului.

3.1.1.1. *Cheia*

Cheia (Gradina, Constanta county, South-Eastern Romania) was occupied during the Hamangia III culture of the Chalcolithic (5,200-4,850 cal. BC, Voinea and Neagu, 2008; Balasse *et al.*, 2014) The site has provided the largest number of animal remains for the Hamangia culture. The archaeozoological study has shown that more than 85% of the spectrum consists of domestic species (domestic cattle, sheep, goats, dogs), which suggests that livestock farming plays a very important role for the community of Cheia. Hunting is a secondary occupation to complement the meat diet (Bălăşescu, 2008).

Our corpus contains two dog mandibles from the Hamangia III culture. The third molar is missing and the second premolar is rotated in one of them (Che2). No butchering or burn marks were evidenced (observations: S. Bréhard and C. Brassard).

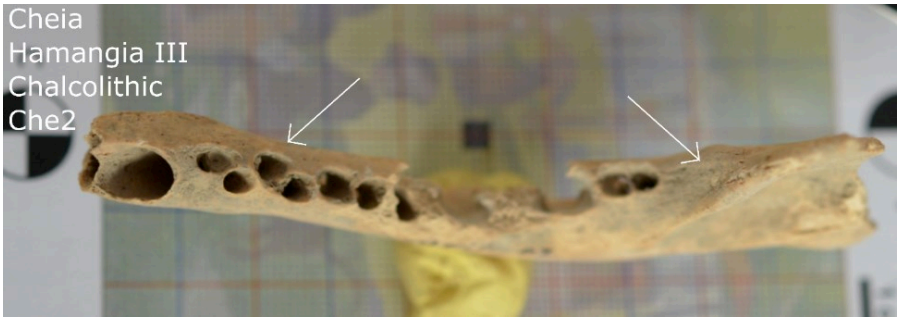

Figure 59. Dental anomalies in a dog from Hamangia III occupation in Cheia

3.1.1.2. *Isaccea*

Isaccea (Tulcea county, South-Eastern Romania) is situated on the lower terrace of the Danube and is dated to early Chalcolithic (Boian culture, Giulești phase, last part of the 6th millennium cal. BC, Micu, 2000; Bălăşescu and Radu, 2004).

Faunal remains came from refuse pits. Domestic mammals were predominant (67% of NISP). Dogs were skinned and eaten on this site (Bréhard and Bălăşescu, 2012).

Our corpus contains 13 mandibles belonging to 12 different dogs dated to the Boian Giulești. No bruning marks were evidenced but this criterion was rarely measurable due to fragmentation and absence of teeth. Skinning (Isa9), dismembering (Isa3, Isa8) and filleting (Isa8) marks have been evidenced (observations: S. Bréhard, Figure 60).

Some dental anomalies have been observed: absence of the first premolar (Isa8), or third molar (Isa1 left and right, Isa11), rotation of the second premolar (Isa2), third root on the fourth premolar (Isa7).

Figure 60. Dismembering and filleting marks and dental anomalies in dogs from the Gumelnița culture in Isaccea.

3.1.1.3. *Vărăşti*

At Vărăști (Vărăşti municipality, Călăraşi county, South-Eastern Romania), the fauna comes from a Boian culture establishment (Vidra phase). There is no absolute dating, but the site was dated by relative chronology between 4,700-4,500 BC (Bălăşescu, *pers. comm.*). The fauna is not very numerous (366 remains, including 260 remains of mammals, Bolomey, 1966). Dogs represent only 2.7% of the NISP.

Our corpus contains 8 dog mandibles dated to the Boian Vidra culture. One mandible (Var1) shows skinning marks, and another one (Var5) shows dismembering marks.

The first premolar teeth are sometimes missing (in three mandibles, e.g. Var6), as well as the third molar (in one mandible, Var8). The second premolar is rotated in Var7.

Figure 61. Dismembering marks and dental anomalies on dog mandibles from the Boian Vidra culture in Varasti.

3.1.1.4. *Hârşova-tell*

The site Hârşova-tell (Constanța county, South-Eastern Romania) was occupied during the Boian Spanţov culture (first half of the 5th millennium cal. BC, 4,702-4,547 cal. BC, Bréhard and Bălăşescu, 2012) but mainly during the Gumelniţa culture , phase A (Gumelniţa phase A2 is the main occupation: 4,350-4,050 BC, Bréhard and Bălăşescu, 2012). It was also occupied during the Cernavoda culture (3,700-3,300 BC). Domestic cattle and sheep/goats were the main species exploited during the Boian occupation while sheep/goats and pigs dominate during the Gumelniţa A2 occupation (Bălăşescu and Radu, 2004; Bălăşescu, Moise and Radu, 2005; Bréhard and Bălăşescu, 2012). During the Gumelniţa A2 occupation, dogs represented 17% of the identified remains and they were skinned and eaten (Lazăr, Mărgărit and Bălăşescu, 2016).

Our corpus contains 79 dog mandibles (4 from the Boian Spantov, 17 from Gumelnița A, 57, including 6 juveniles) from Gumelnița A2.

Dental anomalies are frequent in dogs dated to the Gumelnița culture. The third molar is missing in 18 mandibles (e.g. Har5). This is often associated with other anomalies (the second premolar is missing in 9 mandibles and the fourth premolar is missing in 4 cases). The second premolar is rotated in 2 mandibles from the Gumelnița and in one from the Cernavoda culture (Har73).

Numerous butchering marks have been evidenced, for all cultures (observations: S. Bréhard and C. Brassard). Anthropogenic marks were visible on juveniles as well. Skinning marks were observable on 2 mandibles from the Boian Spantov and 32 from the Gumelnița (e.g. Har48). Dismembering marks were clearly observable on the mandible from the Cernavoda culture (Har73) and on 12 mandibles from the Gumelnița. Burn marks were attested on 6 mandibles from the Gumelnița culture (e.g. Har39). Long bones also present butchering marks (Pionnier-Capitan, 2010, Figure 62).

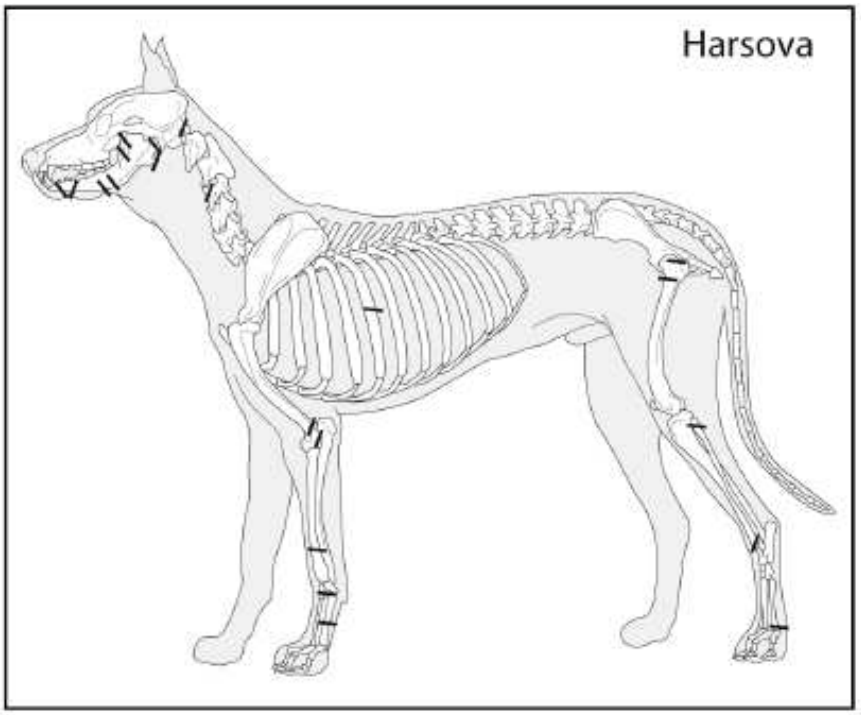

Figure 62. Location of cut marks on the Chalcolithic dog remains of Hârşova (from Pionnier-Capitan, 2010).

Our corpus also contains the mandibles of 5 red foxes (1 from the Boian Spantov occupation, 3 from the Gumelnița A2 occupation and 1 is dated to the chalcolithic without more details). No anomalies or anthropogenic marks were evidenced on these mandibles.

Figure 63. Butchering and burn marks and dental anomalies in dogs from Hârşova tell.

3.1.1.5. *Vitănești-Măgurice*

In Vitănești-Măgurice (hereafter Vitănești, Teleorman County, South-Eastern Romania), two phases of Chalcolithic occupation were identified – separated by an abandonment phase. The first belonged to the early phase of the Gumelnița culture A1 and the second to Gumelnița A2 and B1(Andreescu, Mirea and Apope, 2003). The Gumelnița A2 level was dated to the second half of the 5th millennium cal. BC (4,449-4162 cal. BC, Balasse *et al.*, 2016). During the Gumelnița, hunting was very important (wild taxa represent 84% of the NISP), as in Cascioarele (Bălăşescu and Radu, 2003; Bălăşescu, Radu and Moise, 2005).

I observed 35 mandibles of dogs, 2 of red foxes and 3 of wolves, from the Gumelnița (mainly from the Gumelnița A2). I observed skinning marks on 3 dog mandibles (e.g. Vit26), and dismembering marks in one wolf (Vit1) and 9 dogs (e.g. Vit19). Burn marks are observable on two wolf mandibles (Vit1, Vit3) and 4 dog mandibles (e.g. Vit19). Some dogs show dental anomalies. The third molar is missing in 2 dogs (e.g. Vit25). The first and/or second premolar teeth are missing in 5 dogs (e.g. Vit10, Vit15). The shape of the fourth premolar is abnormal in Vit15. A fourth molar is present in Vit34. The second premolar is rotated in two mandibles (e.g. Vit34).

Figure 64. Butchering and burn marks and dental anomalies in dogs from the Gumelnița culture in Vitănești.

3.1.1.6. *"Ostrovel" Căscioarele*

Căscioarele "Ostrovel" (Călăraşi county, South-Eastern Romania) was occupied during the Boian Spantov culture (4,790-4,368cal. BC, Bălăşescu, Radu and Moise, 2005) but mainly during the Gumelniţa B1 (first half of the 4th millennium BC, Bălăşescu, Radu and Moise, 2005). Căscioarele is a unique case in the Gumelnita culture: everyday activities coexisted with unusual practices: an annex with statuettes, bone figurines, anthropomorphic and zoomorphic pottery vessels and miniature chairs has been excavated (Marinescu-Bîlcu, 2001). Moreover, hunting (mainly of red deer and wild boar) occupied an essential place in the socio-economic system (Bălăşescu, Moise and Radu, 2005; Bréhard and Bălăşescu, 2012).

Our corpus contains 10 mandibles of dogs dated to the Gumelnița B occupation.

Only a mandible revealed skinning marks (Cas4, observations: S. Bréhard). On the same mandible, the second premolar and third molar are missing. The third molar is likely missing in another mandible (Cas3).

Figure 65. Absence of the third molar in two dog mandibles from the Gumelnița B in Cascioarele.

3.1.1.7. *Popina-Borduşani*

Borduşani-Popină (Ialomița county, South-Eastern Romania) is located on the large island of Balta Ialomiței on the Danube River. There were two main phases of human occupation: Late Chalcolithic (Gumelniţa culture, A2 phase, *circa* 4,500-4,250 cal. BC; Bréhard *et al.*, 2014) and Iron Age. As in Hârșova, the importance of husbandry during the Chalcolithic is highlighted by the clear predominance of domestic animals (>70 % of mammal remains identified to species): pigs were predominant, followed by domestic cattle, sheep/goats and dogs (Bălăşescu, Moise and Radu, 2005). During the Gumelniţa A2 occupation, dogs represented 14% of the identified remains and they were skinned and eaten (Lazăr, Mărgărit and Bălăşescu, 2016).

Our corpus contains 96 dog mandibles from this culture (including 9 of juveniles).

Skinning (55 mandibles, including juveniles), dismembering (7) and burn marks (3 mandibles) have been evidenced (e.g. Bor25, observations: S. Bréhard and C. Brassard). Long bones also present butchering marks (Pionnier-Capitan, 2010, Figure 66).

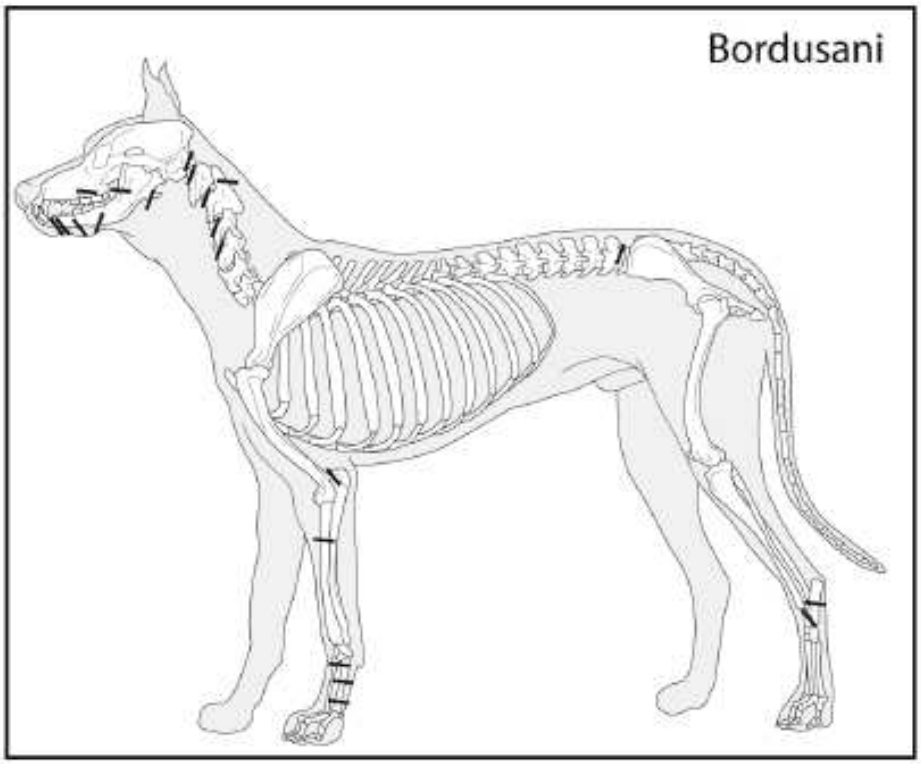

Figure 66. Location of cut marks on the Chalcolithic dog remains of Borduşani (from Pionnier-Capitan, 2010).

As in Hârşova tell, dental anomalies are frequent. The third molar is missing in 13 mandibles (e.g. Bor8, Bor47), the second premolar is missing in 8 mandibles (e.g. Bor8) and it is rotated in 4 mandibles (e.g. Bor47).

Figure 67. Butchering marks and dental anomalies in Gumelnița dogs from Popina-Bordușani.

3.1.1.8. *Taraschina*

In Taraschina (Tulcea county, Doubroudja region) is mainly occupied during the Gumelnița culture, phase A, dated to *circa* 4,600-4,300 cal. BC (Carozza *et al.*, 2013; Danu *et al.*, 2019). The study of the fauna (more than 6500 remains, including 965 NISP for mammals) from the last levels of the Gumlenița occupation have shown an open environment, formed by a mosaic of landscapes (Bălăşescu and Radu, 2011; Carozza *et al.*, 2013). Dogs represent 6.7% and the anthropogenic marks identified on the bones show the consumption of this species (Lazăr, Mărgărit and Bălăşescu, 2016).

Our corpus contains the mandible of one red fox from the Gumelnița A. I observed no butchering mark or dental anomalies (Figure 68).

Figure 68. Fox mandible from the Gumelnița culture of Taraschina.

3.1.2. Sites in Western Europe

3.1.2.1. *Téviec*

Téviec (Morbihan, Brittany, North-Western France) is one of the most famous Mesolithic sites in Atlantic France (Péquart *et al.*, 1937). It has been dated to the mid-8th millennium cal. BP (5,200 cal. BC with reservoir correction, Schulting and Richards, 2001).

The site is a large shell midden in which several structures, hearths and graves constituting a small cemetery, were embedded. Animals and deceased persons were intimately connected, and animals have been assigned different statuses: food waste, decorative element of the tomb, offering, and ornament (Fontan, 2019).

Dog remains, disarticulated and broken, were found among the domestic refuse and it is likely that dogs were eaten at that site (Ollivier *et al.*, 2018, supplementary data).

The mandibles of dogs (3) and foxes (12) are very fragmented and their surface is very poorly preserved, which greatly limited the observation of anthopogenic marks.

I evidenced no obvious traces, except a dubious cutmark of dismembering on the mandible of a red fox (Tev5) and possibly on a dog (Tev15), and a burn mark on the fourth premolar of a fox (Tev3, Figure 69). A certain number of dental anomalies were noticed: absence of the third molar in a dog (Tev14), healing of the alveoli of some premolars in red foxes (Tev2, Tev3, Tev9, Figure 69).

Figure 69. Dubious cutmark of dismembering (Tev5, Tev15) and burn mark (Tev3, Tev14) and tooth anomalies (Tev2, Tev9) in dogs and red foxes from Téviec.

3.1.2.1. *Le Taï*

"Le Taï" (Remoulins, Gard department, Languedoc region, Southern France) is a site that presents a long stratigraphic sequence from the Early to Late Neolithic period (Manen *et al.*, 2002, 2019).

The main cultural facies in the site is the Epicardial (5,300-5,000 cal. BC, Caro and Manen, 2012; Manen *et al.*, 2019). The faunal assemblage is characterised by a high proportion of domestic sheep, goats and cattle. Suids and wild carnivores do not appear to play an important role in the economic system of the site (Tornero *et al.*, 2020, Bréhard and Vigne, *in press*). In our corpus, we have a fox mandible attributed to this culture. No anthropogenic marks nor dental abnormalities have been evidenced.

The second major phase of use of the site took place during the Chasséen culture, in the first half of the 4th millennia BC (Manen, *in press*), Domestic ruminants remain the base of the socio-economic system (Bréhard *et al.*, *in press*). In our corpus, a dog mandible is attributed to this culture, and anthropogenic marks attest to its consumption (dismembering and burn marks on the canine tooth, observation by S. Bréhard).

Figure 70. Dsmembering (left) and burn (right) marks on the dog mandible from the Chasséen of "Le Tai".

3.1.2.1. *Camprafaud*

The Camprafaud Cave (Ferrières-Poussarou, Hérault, south France) has a wide stratigraphic sequence, comprising occupations ranging from the Early Neolithic to the Bell Beaker culture. The large faunal accumulation of the early Neolithic is indicative of hunting activities and the presence of domestic animals (Rodriguez, 1984). Our corpus contains a fox mandible from layer c.19, which is related to the Epicardial cultural facies (Early Neolithic) and dated to around 5,230 cal BC(Manen *et al.*, 2019). The mandible showed dismembering marks, and localized burn marks were observed on the second premolar tooth as well as on the top of the mandibular body (observation by S. Bréhard, Figure 71). This fox has thus been prepared and eaten.

Figure 71. Dismembering (left) and burn (right) marks on the fox mandible from the early Neolithic of Camprafaud C19.

3.1.2.1. *Herxheim*

Herxheim (Rhineland-Palatinate, Southern Germany) was occupied during the Early Neolithic (LBK culture), around 5,350 to 5,000 cal. BC. Settlements were organized within an area surrounded by a ditch, which had been built juxtaposed to pre-established pits. These structures produced abundant goods such as ceramic fragments, lithic tools and innumerable bone remains from both humans and animals (Arbogast, 2009; Jeunesse, Boulestin and Zeeb-Lanz, 2009; Zeeb-Lanz *et al.*, 2009). This site represents the largest dog bone series from the Early Neolithic in Western Europe. More than 250 dog remains, coming from a limited number of individuals, were found mixed with the remains of other animals and humans in a collective burial. Dog bones are notably complete, and evidence many cut and burn marks (Figure 72), showing that dogs were prepared following various procedures for consumption (carving in quarters, cooking by roasting). Human remains were systematically and extensively fragmented and exhibited numerous marks of dislocation, meat carving and scraping. Dog meat consumption therefore seems to have taken place in a collective context and was associated with cannibalism.

Our corpus includes 2 foxes and 12 dogs (including a juvenile). On some dog mandibles, I clearly observed dismembering marks (Her5 and Her13), as well as filleting marks (Her10, Figure 72). No anthropogenic mark was evidenced on red foxes. No dental abnormalities were noticed in either dogs or red foxes.

Figure 72. Dismembering (Her5, Her13) and skinning (Her10) marks on mandibles, and burn marks on the upper teeth (Arbogast, 2018) of dogs from the LBK in Herxheim.

3.1.2.2. *Alizay la Chaussée*

In “Alizay la Chaussée” (Eure department, Northern France), the evidence of human occupation begins during the Early Neolithic, around 5,000 cal. BC, and ends with the Antic period (C. Bémilli, *pers. comm*). The faunal remains related to the Neolithic period are distributed in 12 different structures and represent 2081 vertebrate remains (23.8 kg). Structure 506 is the richest, since it contains slightly more than half of the remains (1338 remains, 10.2kg). The domestic triad represents almost all of the remains, with two dogs and one aurochs remains associated with it. The material is quite altered by vermiculation stigmas. Some traces of chewing by dogs have been evidenced. The structure has also yielded bone industry and ornaments on shells.

Our corpus contains a dog mandible dated to the VSG culture (early Neolithic) from structure 506. The surface was too damaged to observe butchering marks, but the second and third premolar show burn marks (observation by S. Bréhard, Figure 73).

Figure 73. Burn marks on the second premolar tooth of an Early Neolithic dog in Alizay-la-Chaussée.

3.1.2.3. *ZAC de Caunelle*

"ZAC de Caunelle" (Juvignac, Hérault, Southern France) is a site occupied mainly during the Late Neolithic, but that yielded two pits dated to the early Chasséen. In this thesis, we studied the dog mandibles coming from the pit 42, dated to the end of the 5th millennium cal. BC (unpublished ^{14}C date), which, in addition to the largely anthropised filleting sediments, contained the disturbed and badly preserved remains of at least nine canids, most probably in connection (Convertini *et al.*, 2014). No evidence of butchering or burn marks was found, but the poorly preserved surface of the bones strongly limited the observations (observation by S. Bréhard).

There are some dental abnormalities. The alveolus of the second premolar is resorbed for Cau3, and the dental alveoli of the third and fourth premolars are resorbed for Cau6.

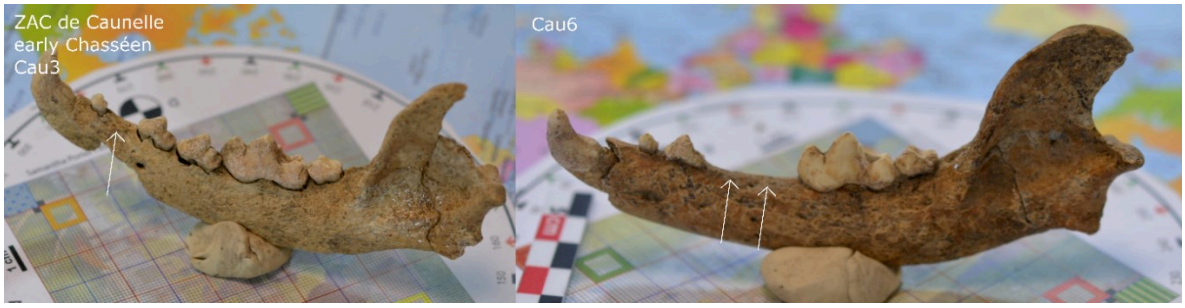

Figure 74. Oligodontia in dog mandibles from ZAC de Caunelle.

3.1.2.4. *Cadereau d'Alès*

"Cadereau d'Alès" (Gard, Southern France) is a site which has revealed numerous domestic structures and 20 tombs dating mainly from the Chasséen and the Late Neolithic. In the 1094 pit, dated to the early Chasséen, two dog skeletons have been discovered on a level of heated stone, one lying on its left side, its limbs bent in a resting position, the other lying on its right side, its hind limbs in a resting position and its fore limbs in hyperflexion (Hasler and Noret, 2004, Figure 21). According to archaeologists, some bones bear burn marks, but given that none was observed on teeth and that skeletons were more or less in connection, these are likely to result from the deposit on still hot stones rather than from cooking.

Our corpus comprises the mandibles of these two dogs as well as a cranium. The dogs are old (given the stage of enamel wear and the general aspect of the mandible with well-defined muscular insertion reliefs). I observed no anthropogenic mark on these remains. The most likely hypothesis is the deposit of complete dogs, without dismembering. However, skinning cannot be excluded given the poor preservation of bone surfaces.

Figure 75. Cranium and mandible of one of the dogs from the early Chasséen of Cadereau d'Alès.

3.1.2.5. *Le Crès*

"Le Crès" (Hérault, Southern France) revealed a large number of domestic structures and funerary deposits dating from the early Chasséen, between 4,350-4,000 cal. BC (Loison and Schmitt, 2009). The preliminary archaeozoological study (Forest in Loison, Fabre and Villemeur, 2003) indicates that domestic species were predominant and mostly represented by ruminants. Dogs were also well represented on the site.

This site is characterised by the presence of several dog burials. Some animals were buried in pits adjacent to those of humans, in single and double deposits (Amt4: two dog burials arranged head to tail opposite each other; Amt73: exclusive deposits of 2 dogs). However, in two cases the dogs were associated with human remains in the same grave (Amt7-SP 13 and Amt79-SP 23). In SP13, the bodies of a human and a dog were placed head to foot opposite to each other, raising the issue of "accompanying deaths". In SP23, there is evidence of the probably successive deposition of two anatomically complete dogs and two isolated human remains corresponding to two distinct individuals (a fragment of immature skull cap and a mature premolar). Some of these dogs benefited from the same practices as humans (packing, empty space). According to Loison and Schmitt (2009), the fact that tools have been found associated with dog burials (Amt 4, 73 and 79) seems to support the fact that they may have been burials.

In order to better understand the diet of humans, a stable isotope analysis was conducted, based on a sampling carried out by V. Forest for the faunal remains, consisting of 16 individuals of different species and diet, including mainly cattle, sheep, goats and dogs (Le Bras-Goude *et al.*, 2006). Dogs are distinguished from the rest of the fauna by higher $\delta^{15}N$ values, which is related to the greater importance of meat in their diet compared to other animals, but the values obtained suggest that their diet was more omnivorous than strictly carnivorous (Le Bras-Goude *et al.*, 2006).

Our corpus includes the mandibles of the 7 dogs mentioned above. I also photographed the cranium still in connection with one of the mandibles before we isolated it (Figure 76). I observed no cut mark nor burn mark. One of the dogs presents oligodontia: the dental alveoli of the second and third premolars are filled (agenesis?).

Figure 76. Cranium and mandible of one of the early Chasséen dogs from Le Crès, with the mandible showing absence of two premolar teeth.

3.1.2.6. *Le Pirou*

"Le Pirou" (Valros, Hérault, Southern France) was mainly occupied during the early Chasséen culture (middle Neolithic), during the second half of the 5th millennium cal. BC (unpublished ^{14}C dates (Gandelin, 2015). The site is similar to Le Crès, with funerary pits discovered in a habitat context. Besides pits with human remains, 10 pits with complete (or almost complete) dog skeletons have been excavated. Apart from these dogs, the faunal assemblage is dominated by domestic cattle and sheep/goats (Gandelin, 2015). We had access to the mandible of 6 different dogs from Amt 229 (Can1), 273 (Can9), 291, 316, 413 (Can4) and 431. We also photographed the cranium of a dog from Amt 103. As the cranium and mandible were often caught in a concretion coating, we photographed and reconstructed the whole before isolating the mandible. No obvious butchering or burn marks have been evidenced on the bones of the complete dogs mentioned above. In contrast, in Amt103 (Pir12), where only a skull fragment has been identified for the dog, some teeth bearing burn marks (left and right third incisor and canine, left second premolar) show that, in this unique case, the head was cooked (observations by S. Bréhard, Figure 77).

Figure 77. Cranium and mandible (top), and burn marks (bottom) on two early Chasséen dogs from Le Pirou.

3.1.2.7. *Mas de Vignoles IV*

The site of "Mas de Vignoles IV" (Nîmes, Hérault, Southern France) revealed numerous occupations from the Neolithic to the Middle Ages. Several dog skeletons were excavated, but most of them are poorly dated (Jallot, 2004). I studied the mandibles of 8 different dogs, but only three of them could be related to a Neolithic period/culture.

Pit 8443, attributed to the Chasséen culture (Middle Neolithic), contained slaughter rejects (cattle skulls), and the subcomplete skeleton of a dog. It was roughly in anatomical connection and rested on its right side. A baculum was found between the two femurs, demonstrating it was a male. The mandible (Mas10) was still in anatomical connection with the cranium and could not be removed from the concretion coatings (Figure 78). I observed no butchering nor burn mark.

Pit FS1029, dated to the Late Neolithic (Fontbouisse culture), contained the complete skeleton of a dog in strict connection resting on its right side, with the forelegs bent. The left mandible (Mas1) revealed no anthropogenic mark or dental abnormalities. Tooth wear (stage G) suggests that this was a relatively old specimen.

Pit FS3165, dated to the Late Neolithic (undetermined culture), contained the skeleton of a complete dog (ribs and vertebrae are missing because of sedimentary dissolution) lying on its left side, the right foreleg in caudal hyperextension. The left mandible (Mas4) revealed no anthropogentic mark nor anomalies. Tooth wear (stage G) also suggests that it was an old animal.

Figure 78. Dog remains from Mas de Vignolles IV dated to the early Chasséen, Middle Neolithic (top) or to the Late Neolithic (bottom).

3.1.2.8. *Auriac*

Auriac (Carcassonne, Aude, Southern France) is a large open-air settlement with an enclosureditch, controlling a passage on the Aude river. It has yielded one of the most important series of artefacts in the classic Chasséen of Languedoc, during the two first centuries of the 4th millennium BC (Vaquer and Remicourt, 2010; Vaquer and Gandelin, 2018). The fauna list is dominated by domestic cattle and sheep/goats (Bréhard, 2011). The remains of dogs were scattered mostly in the ditch. Our corpus contains 6 mandibles of young dogs and adults, and a skull fragment. Dismembering and burn marks on different mandibles show that dogs were consumed (observations by S. Bréhard, Figure 79).

Figure 79. Dismembering (left) and burn marks (right) on the dog mandible from the classic Chasséen of Auriac

3.1.2.9. *Les Moulins*

“Les Moulins” (Saint Paul-Trois-Châteaux, Drôme, Southern France) is a large open-air settlement dated to the late Chasséen culture (Middle Neolithic), between 3,950 and 3,700 cal. BC. Only pits are preserved. The site accommodated a wide variety of activities, probably related to its use as a central place in the regional territory. The faunal assemblage is largely dominated by domestic animals. Dog bones represent 25% of the identified mammal specimens (NISP) and skinning, dismembering, filleting and bunning marks have been previously observed (Bréhard, 2007; Bréhard, Beeching and Vigne, 2010, Figure 81).

Our corpus contains the mandibles of 8 different individuals (and 1 juvenile). One mandible reveals the absence of the first premolar (Mou1). Six of these individuals (including the juvenile), bear dismembering marks (Mou1, Mou2, Mou3, Mou4, Mou5, Mou7, Mou12). Burn marks are visible on the two canines of one individual (Mou4 and Mou7, SPM-132) and on the incisors, canines and premolars of the two mandibles of another dog (Mou8, Mou13, SPM157, Figure 81).

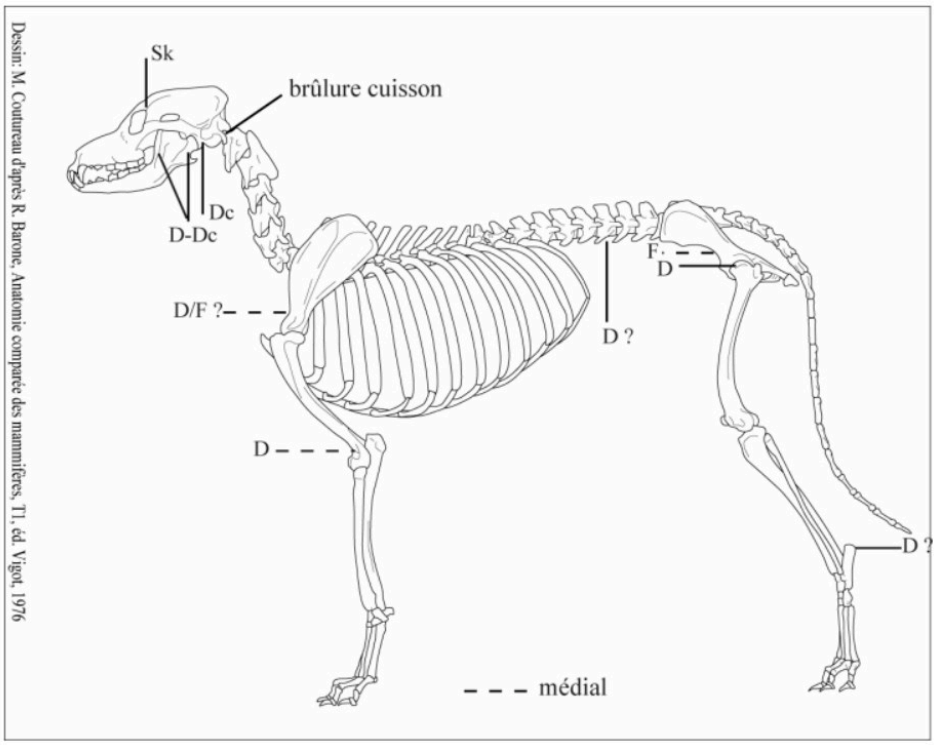

Figure 80. Anthropogenic marks on dog remains from the Late Chasséen of "Les Moulins". D: dismembering; F: filleting; Sk: skinning. From Bréhard (2007).

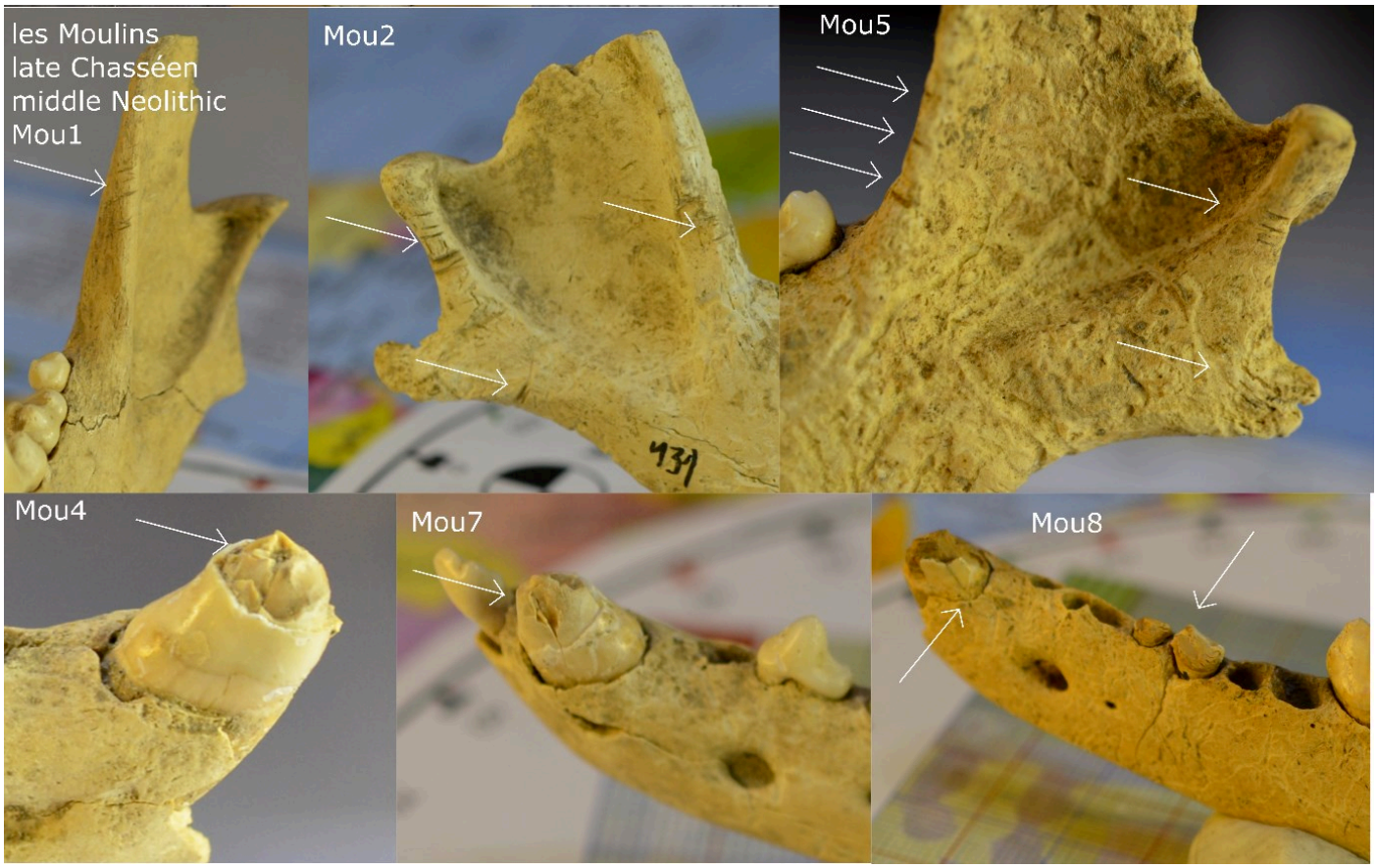

Figure 81. Dismembering (top) and burn marks (bottom) on dog mandibles from the Late Chasséen of "Les Moulins".

3.1.2.10.*La Roberte*

Like “Les Moulins”, “La Roberte” (Châteauneuf-du-Rhône, Drôme, Southern France) is located on an alluvial terrace, on the Eastern bank of the Rhône River. Only pits are preserved. Pits are dated to the late Chasséen culture (Middle Neolithic), approximately between 3,950 and 3,700 cal. BC. The site accommodated a wide variety of activities, probably linked to its use as a central place in the regional territory. The faunal assemblage is greatly dominated by domestic animals, mainly cattle and sheep/goats. Dog remains were scattered in pits. They represent 12% of the identified mammal specimens (NISP). Many skinning, filleting and dismembering marks have been previously observed (Bréhard, 2007; Bréhard, Beeching and Vigne, 2010, Figure 82).

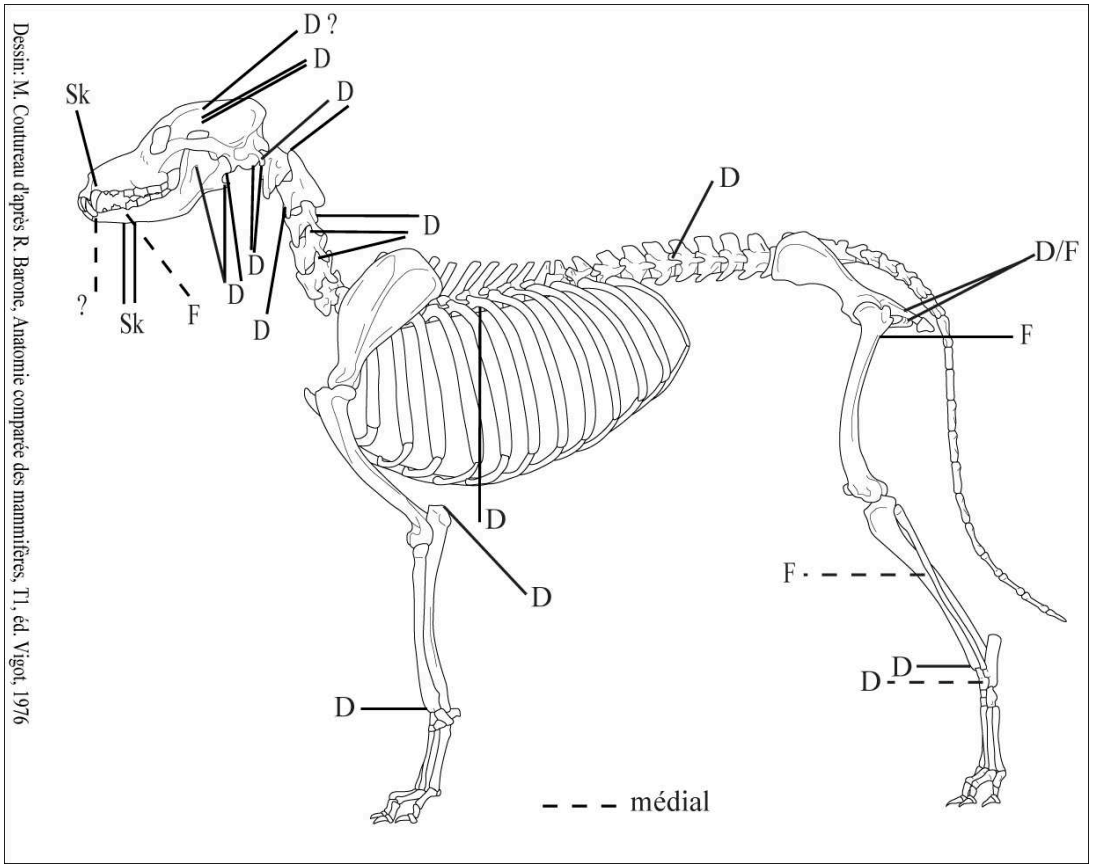

Figure 82. Anthropogenic marks on dog remains from the Late Chasséen of “La Roberte”. D: dismembering; F: filleting; Sk: skinning. From Bréhard (2007).

In this thesis, we observed the mandibles of 8 different dogs (one was a juvenile and 7 were from young/adults), some of them showing skinning (Rob1, Rob6) and dismembering marks (Rob1, Rob2). In one individual (Rob7), the third and fourth premolars and the ventral border of the mandible are burnt (Figure 83).

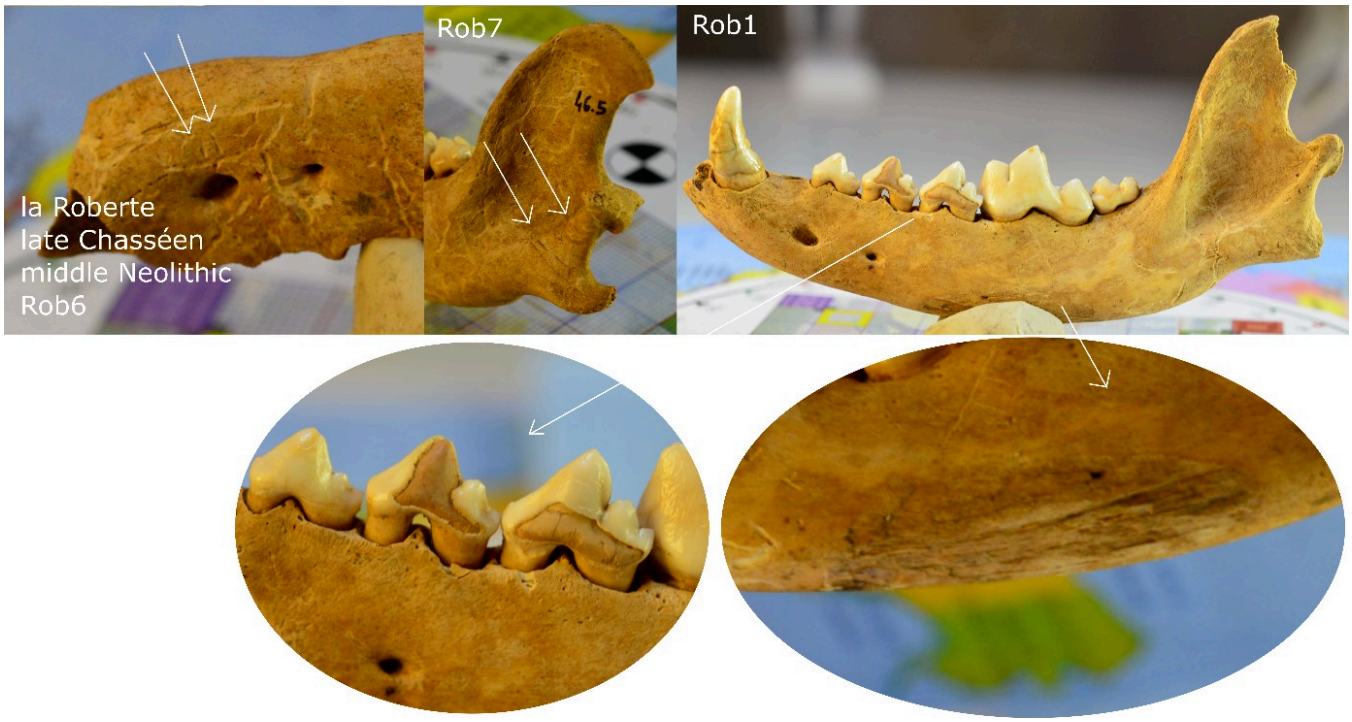

Figure 83. Skinning (top left), dismembering (top middle) and burn marks (top right and bottom) on dog mandibles from the late Chassén of "La Roberte".

3.1.2.1. *Bercy*

Bercy (Paris, Northern France) corresponds to a settlement set on the river bank, whose main occupation belongs to the Northern Chasséen (middle Neolithic) and was dated to around 4,000 cal. BC. In this cultural horizon, the faunal assemblage is dominated by domesticated animals and dogs account for less than 2% of the identified mammal bones (Tresset, 1996). Dog remains were scattered in garbage layers. They show no obvious marks of dismembering. The absence of teeth on the mandibles (and the fact that very few isolated teeth are available) prevent the observation of burn marks resulting from cooking. However, cut marks have been observed on long bones (observations by S. Bréhard). They are similar in dimension to the dogs from Chalain (Pionnier-Capitan, 2010). Our corpus contains 22 dog mandibles. Some mandibles show abnomalies in the number of teeth. For three mandibles (Ber1, Ber9 and Ber15) the third molar is missing (Figure 84). The alveolus of the first premolar is filled in Ber17.

Figure 84. Absence of the third molar (left, middle) and filleting of the alveolus of the first premolar (right) on dog mandibles from the Northern Chasséen of Bercy.

3.1.2.2. *Twann*

Twann (Bern Canton, Switzerland) is a waterlogged site corresponding to a Neolithic hamlet located on the Western bank of Lake Bienne (Becker and Johansson, 1981). It was inhabited during the 4th millennium BC, in a period encompassing the Cortaillod (~ 4,000-3,500 BC) and Horgen (~3,500-3,000 BC) cultures. The chronology of occupation is known with great precision thanks to dendrology, which will be detail further in Chapter 9 section 3.2.2, Figure 149.

The site of Twann is a good illustration that the mandibles are much better preserved than the crania, despite the outstanding preservation of the material at this site (Figure 98).

Figure 85. Study of dog mandibles from Twann.

Our corpus contains a very large number of dog mandibles from this site (233).

Almost all (232) are related to the Cortaillod horizon, dated to the first part of the 4th millennium BC (Arbogast *et al.*, 2005), except one which is attached to the Horgen horizon.

Among the 232 Cortaillod mandibles, 2 belong to juveniles, 42 to young individuals, and most to adults (168). Only 15 individuals seem rather old considering tooth wear. On many mandibles, I observed skinning (5), filleting (5) and obvious dismembering marks (59, including one juvenile Twa86, Figure 86). I also observed burn marks that often extend over many teeth and even to the bone (138, Figure 86). Anthropogenic marks have been previously evidenced on other bones (Pionnier-Capitan, 2010, Figure 87). In addition, many long bones (humerus and femur) show helical diaphysis breaks, suggesting extraction of bone marrow (Pionnier-Capitan, 2010).

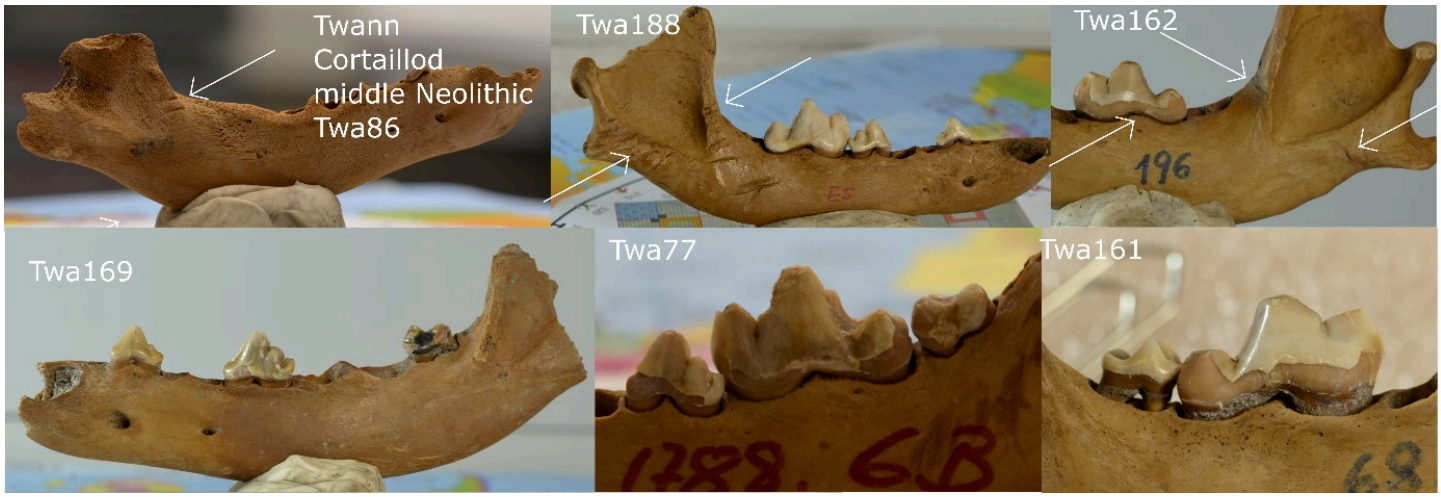

Figure 86. Cut and burn marks on dog mandibles dated to the Cortaillod of Twann.

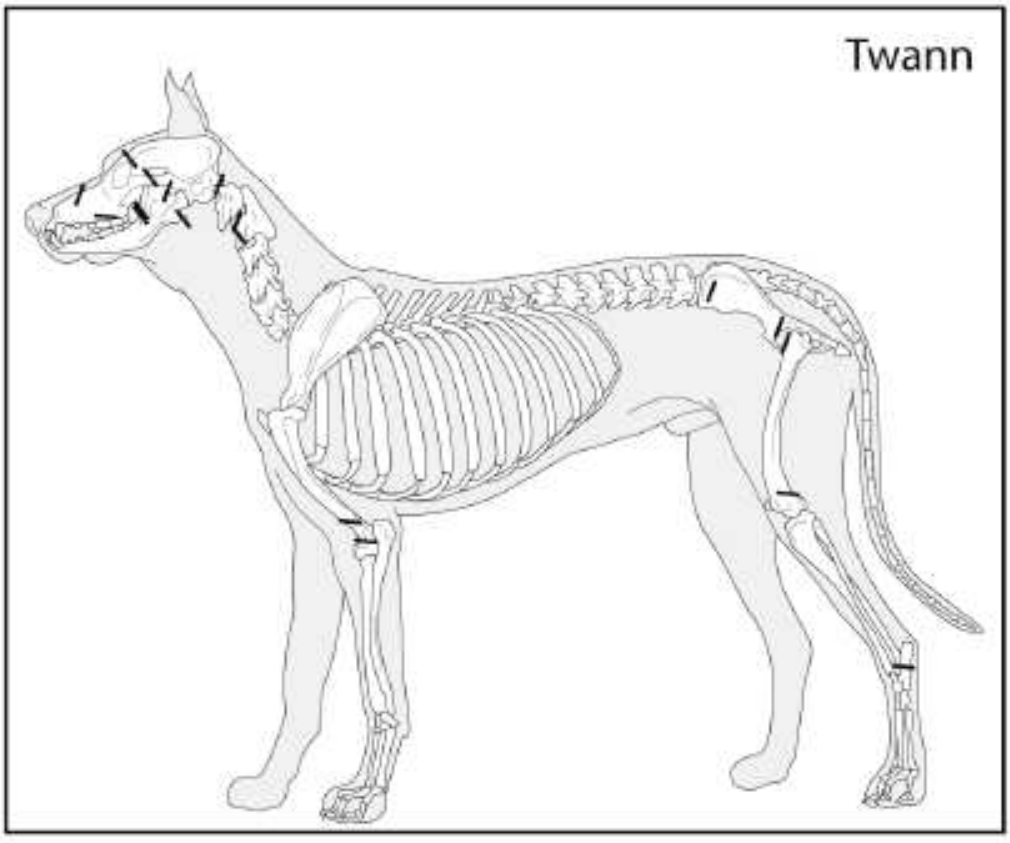

Figure 87. Location of cut marks on the remains of Twann's dogs. From Pionnier-Capitan, 2010

I also observed some dental anomalies (Figure 88). These included the absence of the first premolar in 2 individuals (Twa178, Twa193), the absence of the third molar in 5 dogs and the presence of a fourth (supernumerary) molar in 3 dogs. There was also a rotation of the second premolar in 3 dogs. These anomalies therefore remain infrequent in the population.

Figure 88. Dental anomalies in dog mandibles from the Cortaillod of Twann.

The single dog mandible related to the Horgen culture did not reveal any butchering or burn mark nor any dental abnormality.

I have also studied the mandibles of 6 red foxes (4 are related to the Cortaillod culture, 2 to the Horgen culture, Figure 89). More mandibles were expected according to the publication of Becker and Johansson (1981), but after opening all the boxes containing faunal remains, I did not find more. The red fox mandibles of the Cortaillod show skinning (Twa176), dismembering (Twa84, Twa15) and filleting marks (Twa175, Twa176). No clear cut mak was evidenced on the fox mandibles from the Horgen culture, but in two mandibles (Twa 68, Twa69), the appearance of the enamel and bone suggests that the animal was burned. Two mandibles also show dental abscesses (Twa184, Twa15).

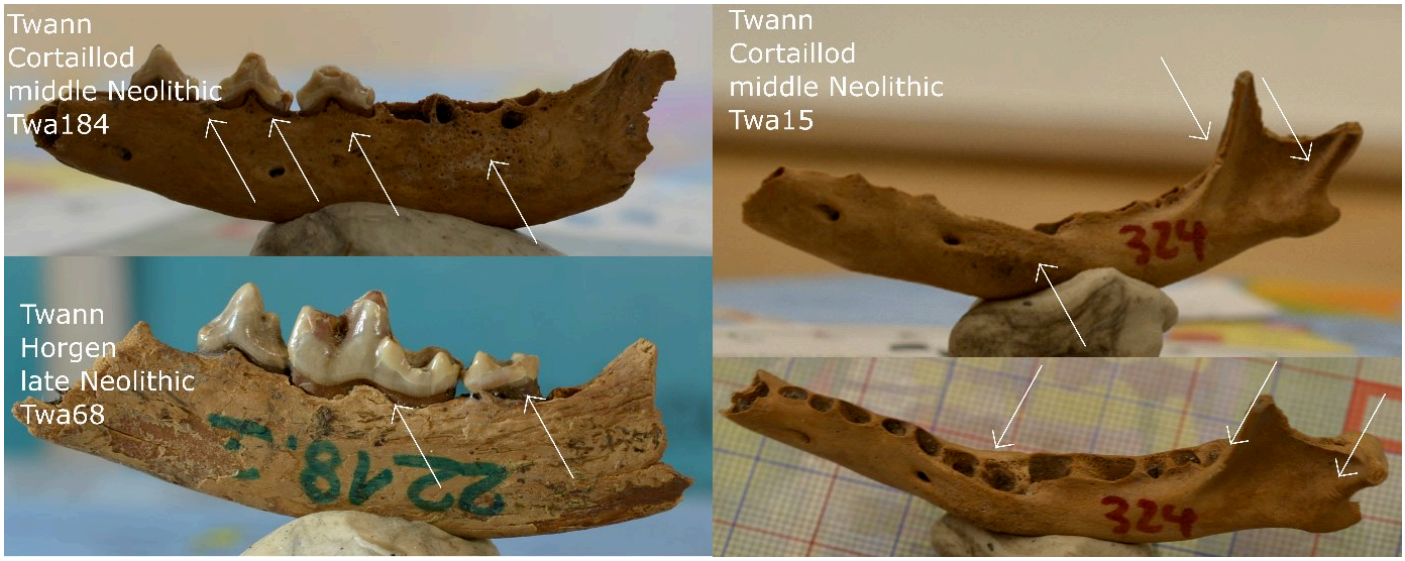

Figure 89. Butchering marks and abscesses in red foxes from Twann.

3.1.2.1. *Chalain and Clairvaux*

Chalain and Clairvaux (Jura, France) are two lacustrine sites located west of the Chalain and Clairvaux lakes, at 500 m a.s.l., which constitutes the upper limit of the extension of cereal agriculture, and are a prime example of the adaptation of Neolithic civilisations to a harsh climate. In these sites, bones are exceptionally well preserved, presumably because they were quickly covered by a layer of lacustrine chalk and preserved under anoxic conditions, either covered by water or below the groundwater (Pétrequin *et al.*, 1998, 2002). These sites were inhabited during a period encompassing the NMB (Middle Neolithic) and Horgen and Clairvaux cultures (Late Neolithic, Pétrequin *et al.*, 2002; Arbogast *et al.*, 2005; Arbogast, 2008, p. 5).

Our corpus contains 1 mandible of dog and 8 of foxes (including 2 juveniles) from Clairvaux XIV and dated to the Middle Neolithic NMB (3,650 BC), as well as the mandibles of dogs and foxes from Chalain 2, 3, 4, 19:

- 8 mandibles of dogs and 2 mandibles of foxes related to the Horgen culture (3,200-3,120 BC);
- 10 mandibles of dogs related to the early Clairvaux culture (3,035-2,990 BC, Arbogast, 2008, p. 5)

We also examined the crania of a dog (Cha19, Figure 90) and a red fox (Cha24) from Chalain 4 and dated to early Clairvaux, and this of a dog dated to the middle Clairvaux in “la Motte aux Magnins” (Cla1, Figure 90, around 2,960 BC, Arbogast, 2008, p. 5).

Figure 90. 3D models of dog crania from early Clairvaux (Late Neolithic) in Chalain 4 (left, Cha19) and middle Clairvaux (late Neolithic) in Clairvaux La Motte aux Magnins (right, Cla1).

I observed skinning marks on 2 fox mandibles from the Late Neolithic (early Clairvaux) of Chalain 19 (e.g. Cha48) and one mandible from the NMB of Clairvaux XIV (Cla6). I also noticed obvious dismembering marks on the mandible of a fox dated to the NMB (Cla8). Filleting marks were visible on 4 red foxes from the Late Neolithic of Chalain 19 (e.g. Cha48). Additionnaly, I observed burn marks on a large number of mandibles of dogs and foxes from the Middle and Late Neolithic. However, these are dubious, as I observed marks on the molar teeth, which are far from the anterior part of the mandible (e.g. talonid of the M1 in Cha9). The canine and premolar teeth were rarely present to confirm. No butchering marks were noticeable on the mandibles of dogs but I observed dismembering marks on the distal end of a femur from the Middle Neolithic NMB (Cla4 NMB cl14). No dental anomalies were observed.

As in Twann, many long bones (humerus and femur) show helical diaphyseal breaks, suggesting voluntary extraction of bone marrow (Pionnier-Capitan, 2010).

Figure 91. Butchering and burn marks in dogs and red foxes from Chalain and Clairvaux.

We also photographed 2 crania and 6 mandibles of wolves from Chalain 4 (early Clairvaux, Late Neolithic). On of them has its first and fourth premolar missing (Cha12). No cut marks were evidenced but all show burn marks on the teeth.

3.1.2.2. ***Bury***

Bury (Picardy Region, Northern France) is a funerary monument consisting of a gallery grave. Most of the graves date back to the end of the Neolithic (Salanova *et al.*, 2017).

Our corpus comprises three dogs dating back to the Late Neolithic (first half of the 3rd millennium cal. BC) and to the very beginning of the Bronze Age (one dog was radiocarbon dated to the turn from the 3rd to the 2nd millennium cal. BC, between 2,150 and 1,950 cal. BC ; Salanova *et al.*, 2017: GrA-23275). The Late Neolithic dog (Bur2) comes from layers predating the closure events, and may correspond to ritual practices though not funerary activity. The two other ones come from archaeological structures post-dating the closure of the burial chamber, and for which interpretion is difficult. Two dogs (Bur1, Bur2) were complete and partly in anatomical connection, and one (Bur3) is represented by scattered remains. No anthropogenic mark or dental anomalies were evidenced on the corresponding mandibles (observation: A. Tresset and S. Bréhard, Figure 92).

Figure 92. Dog mandibles from the Late Neolithic (Bur2) and very early Bronze Age (Bur1, Bur3) of Bury.

4. Classification into geographical and chrono-cultural groups and overall sample size

The sites have been classified into several groups, according to their geographical location (Western Europe or Eastern Europe, i.e. South-Eastern Romania) and the cultural attribution of the material (Table 15).

It is possible to draw an initial assessment of the representativeness of our sample for the different cultures. The trends described below will be quantified more accurately in the section where we detail sample sizes of individuals submitted to geometric morphometric analyses. (cf Table 17, Table 18, Table 19, Table 20 and Figure 94 in section 5.3).

4.1. Dogs

In Western Europe, the only Mesolithic site that could be included is the site of Téviec. The Neolithic was split into three groups: Early Neolithic, Middle Neolithic and Late Neolithic (see Part 1 section Table 3 for details about the cultures included in these groups). The dogs of the Early Neolithic come from Alizay la Chaussée and mostly from Herxheim. However, these periods are very poorly represented, which is related to the rarity of archaeological material (see Part 1 section 2.2). We also have very few dog mandibles from the Late Neolithic in our sample.

The Middle Neolithic is largely over-represented, and was thus divided into 3 groups, according to the cultures Chasséen, Cortaillod and NMB. We will therefore be able to follow the evolution of the form during this period and to provide comparisons between the Chasséen and Cortaillod culture, which are the most represented. However, it is worth pointing out that Twann is the only site in our corpus for the Cortaillod culture, whereas the Chasséen is represented by 10 different sites from Northern and Southern France. This is likely to have an impact on the variability among these groups.

A large part of the dog mandibles of Western Europe comes from a single site, Twann (233 dog mandibles and 6 fox mandibles), which will allow us to conduct an intra-site study to provide insights into regional morphological variation during the Cortaillod culture in Switzerland.

In South-Eastern Europe, Mesolithic and Early Neolithic were grouped together. Mesolithic dogs are rare (they come from Alibeg, Icoana and Ostrovul Banului) and we have no other Neolithic dog in the corpus than the two mandibles of Alibeg, whose occupation (Mesolithic or Early Neolithic) could not even be clearly attributed. This corresponds to the state of research since no dog/fox mandible have been reported from Neolithic sites in South-Eastern Romania (see Part 1 section 2.2.3). Thus, in South-Eastern Europe, we switch directly from the Mesolithic/Early Neolithic to the Chalcolithic, which was divided into 3 groups according to culture: Hamangia III/Boian, Gumelnița and Cernavoda. The Cernavoda is only represented by one dog. Although we have a consistent number of mandibles from the Hamangia III/Boian culture, the culture which is far from the most represented is the Gumelniţa (represented by the

sites of Căscioarele, Borduşani, Hârşova, Taraschina and Vităneşti). Within this culture, the sites of Borduşani and Hârşova are located very close geographically from each other (Figure 53) and were occupied roughly at the same time based on radiocarbon dating (during the Gumelnița A). Additionally, the faunal lists are similar. Each has yielded a great number of mandibles, allowing comparisons. Comparing these sites should provide insights into intra-regional morphological variation during Gumelnița A in South-Eastern Romania.

The differences in sample sizes will be illustrated later in the manuscript, when we detail the samples sizes for geometric morphometrics analyses (see section 5.3, Figure 94).

The most important sampes in Western Europe (i.e. Middle Neolithic) and Eastern Europe (i.e. Chalcolithic Gumelnița) are far apart in terms of socio-economic evolution, but the time elapsed since the diffusion of the Neolithic package is roughtly the same in both areas (*circa* 5,800 and 4,500 cal. BC for the Chasséen in Southern France; *circa* 6,000 and 4,500 cal. BC for the Gumelniţa in South-Eastern Romania; see Part 1 section 0, Table 2, Table 3). As a reminder, in 1,500/1,300 years, there is a total replacement of the European maternal lineage by an exogenous lineage of Near Eastern dogs in Eastern Europe, whereas a clear predominance of the European lineage persists in Western Europe and is accompanied by a greater diversity in haplogroups (see Part 1 section 2.4.2.3.5, Table 12). It will therefore be interesting and relevant to compare the mandible forms between these two poles.

4.2. Red foxes

Our corpus illustrates an archaeological reality: the remains of foxes are rare whatever the period (cf Part 1 section 2.2, Table 19, Table 20).

In our corpus, red foxes mostly come from Western Europe (51 mandibles). Eastern Europe is too poorly represented to enable comparisons with Western Europe.

In Western Europe, the Middle Neolithic (Twann, Clairvaux) and Late Neolithic (Chalain, Twann) are the most represented periods but there are enough mandibles from the Mesolithic (Téviec) and early Neolithic (Le Taï, Camprafaud, Herxheim) to provide preliminary insights into the evolution of the morphology and function from the Mesolithic to the Late Neolithic in Western Europe.

Table 15. List of the archaeological sites with cultural grouping and total number of dog and red fox mandibles observed in the course of this thesis.
Published information about coat color or starch digestion from mitochondrial DNA are reported.
Dating: C: relative, derived from cultural attribution (BC); D: radiocarbon dates from dog bones (cal. BC); O: radiocarbon dates from other bones or plant remains (cal. BC); W: dendrochronology (BC)
The site of Schela Cladovei (Sch) is not reported here as the dog mandibles cannot be clearly attributed to the Mesolithic or Neolithic period.

	Group	Archaeological site	Code	Culture	Dating (references in section 3)	Hypothethical coat color (Ollivier *et al.*, 2013)	AMY2B gene copy number (Ollivier *et al.*, 2016)	Haplogroups (Pionnier-Capitan, 2010; Ollivier *et al.*, 2018)	N dogs	N foxes	Eaten
Eastern Europe	Mesolithic or Early Neolithic	Alibeg	Ali		/				3		Yes
		Icoana	Ico		9,100-7,500 cal. BC [O]	Black (CH1120)		C	8		No?
		Ostrovul Banului	Ost		7,478-6,228 cal. BC [O]				4		Yes
	Chalcolithic 1	Cheia	Che	Hamangia III	5,200-4,850 cal. BC [O]				2		No
		Isaccea	Isa	Boian Giulesti	4,543-4,354 cal. BC [O]	Black (CH767)	2 (CH767) 6 (CH766)	C-D	20		Yes
		Varasti	Var	Boian Vidra	4,700-4,500 BC [C]				8		Yes
		Hârșova	Har	Boian Spantov	4,702-4,547 cal. BC [O]			D	4	1	Yes
	Chalcolithic 2	Vitănești	Vit	Gulmenita A2 + B1	4,449-4162 cal. BC (A2) [O] 4,100-3,900 BC (B1) [C]				35	2	Yes
		Căscioarele	Cas	Gulmenita B	first half of the 4th millennia BC				10		Yes?
		Hârșova	Har	Gulmenita A + A2	4,350-4,050 BC (A2) [O]	Black (CH771)	2 (CH768)	D	74	3	Yes
		Bordușani	Bor	Gulmenita A2	4,500-4,250 cal. BC (A2) [O]		12-20 (CH1585)	D	96		Yes
		Taraschina	Tar	Gulmenita A	4,600-4,300 cal. BC [O]					1	No?
	Chalcolithic 3	Hârșova	Har	Cernavoda	3,700-3,300 BC [C]				1		
Western Europe	Mesolithic	Téviec	Tev		5,200 cal. BC [O]			C	3	12	Yes
	Early Neolithic	le Taï	Tai	Early Epicardial	5,300-5,000 cal. BC [O]					1	Yes
		Camprafaud	Cam	Early Epicardial	5,230 cal. BC [O]					1	Yes
		Herxheim	Her	LBK	5,350-5,000 cal. BC [O]	Yellow (CH1042)		C-C-D	12	2	Yes, cannibalism
		Alizay la Chaussée	Ali	VSG	5,000 cal. BC o				1		Yes
	Middle Neolithic – Chasséen	ZAC des Caunelle	Cau	Early Chassén	end of the 5th millennium cal. BC				11		No
		Cadereau d'Alès	Cad	Early Chasséen	/				2		No
		Le Crès	Cre	Early Chasséen	4,350-4,000 cal. BC [O]				8		No
		Le Pirou	Pir	Early Chasséen	second half of the 5th millennium cal. BC				7		No
		Mas de Vignolles IV	Mas	Early Chasséen	/				1		No
		Auriac	Aur	Classic Chasséen	4,000-3,800 cal. BC [O]				6		Yes
		Les Moulins	Mou	Late Chasséen	3,950-3,700 cal. BC [O]			C-B	14		Yes
		La Roberte	Rob	Late Chasséen	3,950-3,700 cal. BC [O]				8		Yes
		Le Taï	Tai	Chasséen	first half of the 4th millennia BC				1		Yes
		Bercy	Ber	Northern Chasséen	~ 4,000 cal. BC [O]		2	C	22		Yes
	Middle Neolithic – Cortaillod	Twann	Twa	Cortaillod	~3,500-3,000 BC [W]		2-4 (CH1055)	C-C-C-D-D	232	4	Yes
	Middle Neolithic – NMB	Clairvaux	Cla	NMB (Middle Neolithic in Burgundy)	~3,650 BC [W]				1	8	Yes
	Late/Final Neolithic	Chalain-Clairvaux	Cha, Cla	early Clairvaux, Horgen	3,200-2,990 BC [W]			D-A	15	29	Yes
		Twann	Twa	Horgen	~3,500-3,000 BC [W]				1	2	Yes?
		Mas de Vignoles IV	Mdv		/				2		No
		Bury	Bur		2,900-2,650 cal. BC [O] 2,150-1,950 cal. BC [D]	Yellow (CH735) Black (CH734)	4-12 (CH735) 8-16 (CH734)	C-D	3		No
								Total	**618**	**66**	

5. Geometric morphometric analyses: adaptation of the protocol and sample size

5.1. Selection of non-juvenile canids

The form (both size and shape) of the mandible is strongly impacted by age, and juveniles show morphological traits that are very different from adults (see Part 2). Accordingly, juveniles (first molar tooth not erupted) were not considered in our shape analyses. Subadults (first molar already erupted but first and second premolar teeth still erupting) were included in the analyses and grouped with young dogs (mandible still porous but all teeth erupted) because of the difficulty to identify the affiliation to the subadult group for small fragmentation patterns.

Sexual dimorphism may also be an important parameter to consider when exploring the variation in form, however this information is extremely rarely available. Sexual dimorphism has been reported in the 3D shape of the mandible in red foxes (see Part 2 Chapter 5 section 1). It could not be tested in our sample of modern dogs but previous work on linear dimensions has suggested the existence of an overall dimorphism in modern breeds that was however too slight to enable predictions in the archaeological record (Brassard and Callou, 2020).

5.2. Adaptation of the landmarking protocol to fragmentation

Although they are among the most robust bones, mandibles are relatively rarely complete, hence the need to adapt our shape analyses to the **patterns of fragmentation** observed. In order to analyse the shape of a maximum of these mandibles, 10 different templates were used (Figure 93).

The most complete template (template A) is almost the same as the one used for the modern canids. The only difference is that the landmark at the incisor tooth has been removed because the proximal part of the mandible is too often broken. The other templates consist of subsamples of some of the anatomical landmarks and landmarks on curves or on the surface of template A. Surface patches were used for all templates except for templates G, I and J. The mandibular ramus (where the adductor muscles insert) is very precisely described by templates A and F. Templates B, H and J reflect the height of the coronoid process but not its precise shape and deepness. The angular process (where the pterygoid muscle inserts) is precisely described by templates A, C, F and H. The mandibular ramus is completely described by templates A, B and C. Templates D, E only describe the most anterior part of the mandibular ramus (where no adductor muscles insert). Templates G and I are the smallest and they do not describe any of these reliefs. However, they descrive the ventral curvature under the coronoid process and reflect the thickness of the mandible.

Given that the different templates do not represent the same regions, they will not provide access to the same information (as regards the shape of the complete mandible or function). However, if the integration (modularity) between the different parts of the mandible is strong enough, we can expect even small fragments to represent the overall shape of the complete mandible and to carry a functional signal. However, fragmentation may have altered this information, more or less importantly depending on the fragmentation pattern (number and nature of landmarks and area on the mandible). We will therefore have to quantify this modularity and the loss of information linked to these templates.

Only 32 mandibles of the 618 models of canid mandibles we reconstructed could not be included in any of the 10 templates. 95% of the mandibles (586/618) could therefore be analyzed using geometric morphometrics and the loss of information due to fragmentation is under 5%. Of the 32 mandibles that did not enter any of the fragmentation patterns, 9 date back to the Mesolithic period (4 dog mandibles from Icoana, 4 dog mandibles and 1 fox mandible from Téviec) and 2 date back to the early Neolithic of Western Europe (2 dog mandibles from Herxheim). The material from these periods is indeed often extremely fragmented, which raises the question of a methodological bias. These periods will be less well represented due to the scarcity of material and its great fragmentation, which makes it difficult to consider for shape analyses.

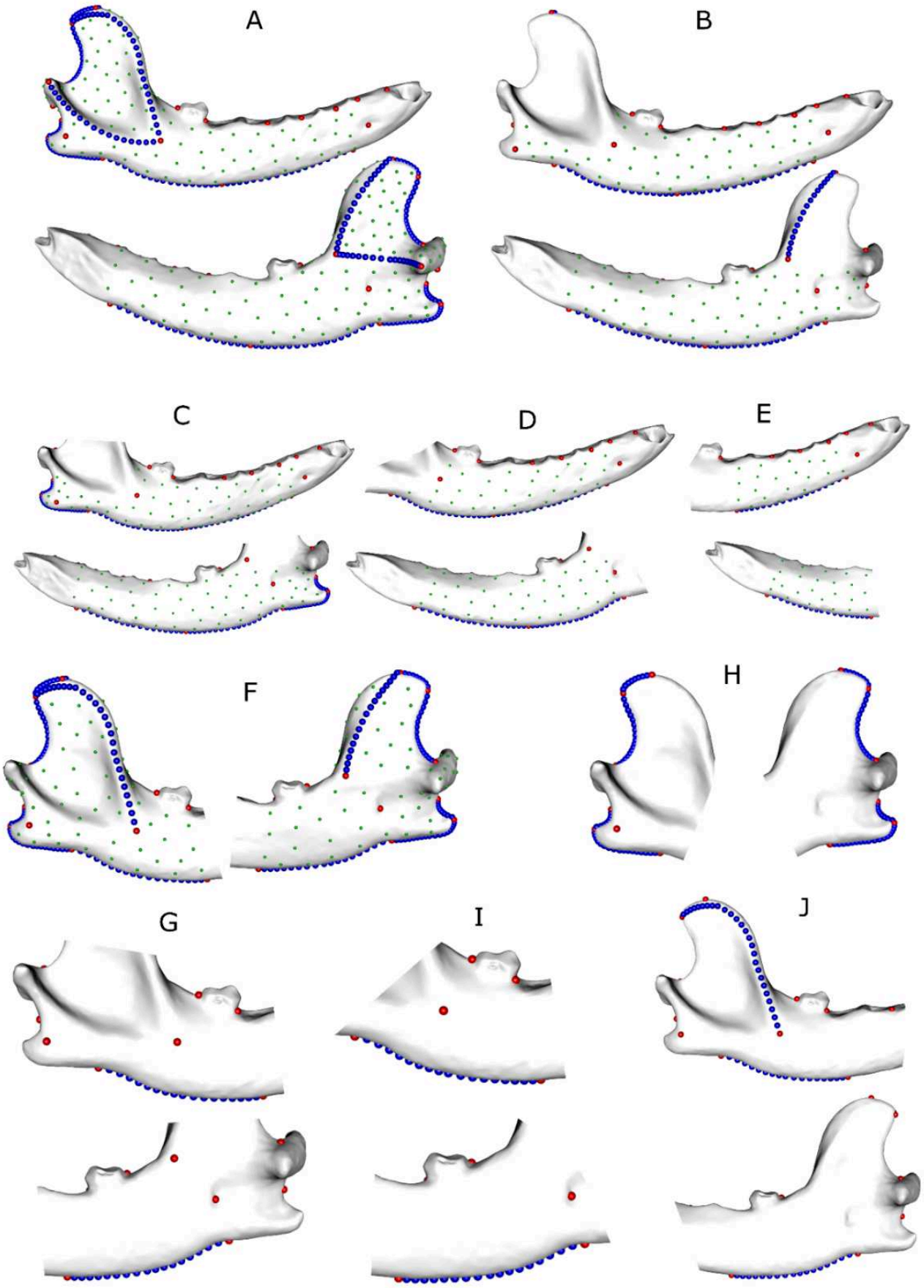

Figure 93. Templates used for the geometric morphometric analyses with the archaeological mandibles.

5.3. Sample size and representativeness by species, geographic area, archaeological site and chrono-cultural context, for each fragmentation pattern

The 586 canid mandibles considered in the shape analyses include 528 dogs, 50 foxes and 8 wolves (Table 16).

Table 16. Sample size per template and species. We also reported the number of mustelids used for the preliminary verification of species identification for the small fragments (see Appendix 9).

Template	Dogs		Red foxes		Wolves	Mustelids
	N	%	N	%		
A	127	24%	8	16%	4	21
B	228	43%	13	26%	4	23
C	217	41%	10	20%	4	27
D	395	75%	22	44%	6	38
E	440	83%	32	64%	7	40
F	155	29%	14	28%	5	25
G	389	74%	25	50%	6	45
H	160	30%	14	28%	5	25
I	491	93%	40	80%	7	47
J	215	41%	18	36%	5	25
All mandibles	**528**	**100%**	**50**	**100%**	**8**	**49**

5.3.1. Dogs

Among the 528 dog mandibles, even if the complete mandibles are relatively numerous (127 dogs), but template A still represents a small part (24%, Table 16). The second most complete template (template B) enables to almost double the sample size (228 – 43%, Table 16). The most representative template as regards sample size are the templates E (83%) and I (93%, Table 16).

We highlight here that the few Mesolithic or early Neolithic dogs from Eastern or Western Europe are mostly represented by the smallest templates (E, G and I, Table 17). Similarly, the few mandibles dated to the Late Neolithic in Western Europe and those dated to the Hamangia III/Boian cultures in South-Eastern Romania are mostly represented by templates D, E, G and I (Table 17). "Small" fragmentation patterns/templates are thus particularly important to represent mandibles from these groups.

In chapters 8 and 9, we removed from the analyses the mandibles that were not clearly attributed to one of the cultural groups defined in section 4:

- the dog mandible from Schela Cladovei which were dated to the Mesolithic or Neolithic, without more precise cultural context;
- the dog mandibles from Mas de Vignolles IV that could not be clearly attributed to the early Chasséen or Late Neolithic (Mas2, 3, 5, 6, 7, 8, 9)
- a fox mandible that was dated to the Chalcolithic without more precision (Har78).

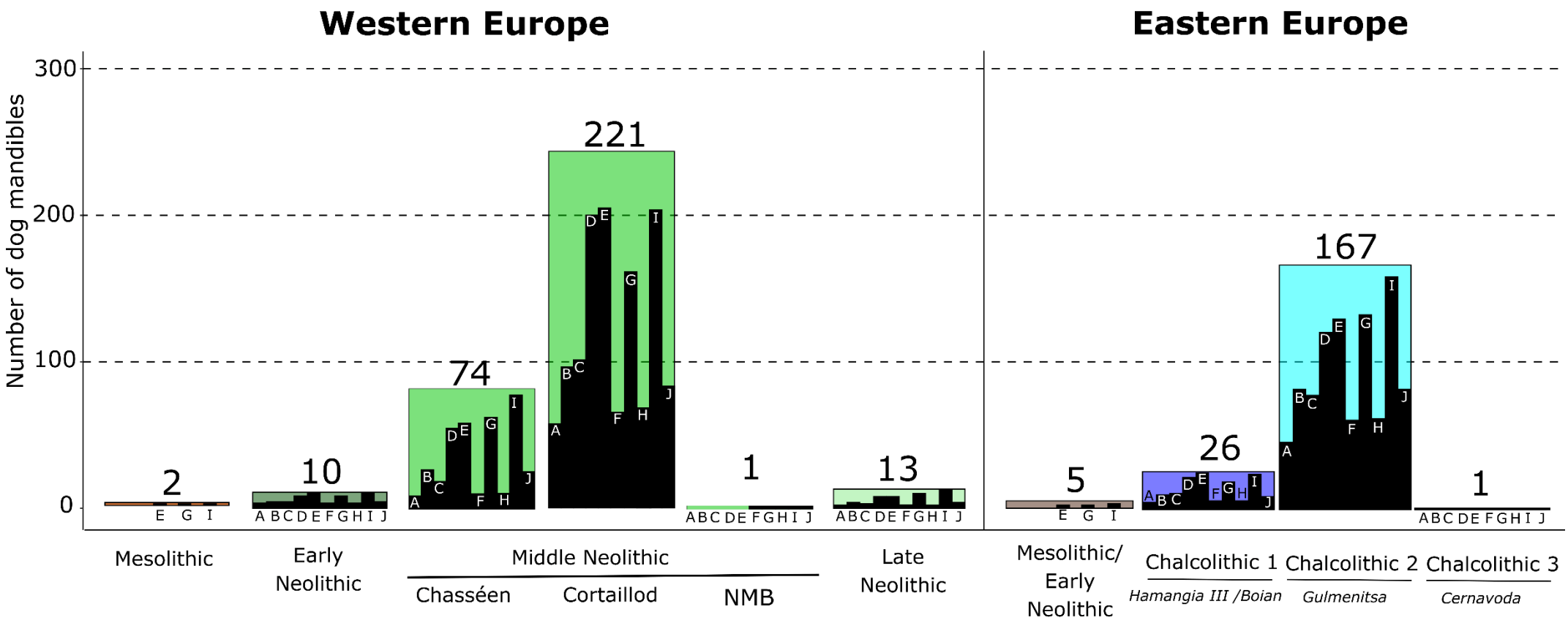

Figure 94. Sample size for each template and chrono-cultural context for the ancient dogs.

Table 17. Sample size per template and chrono-cultural context for pre-Bronze Age dogs. N: dog mandibles from Mas de Vignolles IV which attribution to a specific Neolithic culture was unclear; M/N: dog mandible from Schela Cladovei which attribution to the Mesolithic or Neolithic period was unclear. Chalco: Chalcolithic.

	Western Europe							Eastern Europe					
	Mesolithic	Early Neolithic	Middle Neolithic Chasséen	Middle Neolithic Cortaillod	Middle Neolithic NMB	Late Neolithic	N	Mesolithic/ Early Neolithic	M/N	Chalco 1	Chalco 2	Chalco 3	all
A	0	3	8	62	0	2	0	0	0	5	46	1	**127 (24%)**
B	0	4	29	97	0	4	1	0	0	10	82	1	**228 (43%)**
C	0	4	20	99	0	3	0	0	1	11	78	1	**217 (41%)**
D	0	8	50	180	0	8	4	0	1	22	121	1	**395 (75%)**
E	1	9	56	203	0	8	4	2	1	25	130	1	**440 (83%)**
F	0	3	11	70	1	2	0	0	0	6	61	1	**155 (29%)**
G	1	7	58	150	1	10	6	2	1	19	133	1	**389 (74%)**
H	0	3	11	73	1	2	1	0	0	6	62	1	**160 (30%)**
I	1	9	70	202	1	13	7	3	1	24	159	1	**491 (93%)**
J	0	5	26	86	1	4	2	0	0	9	81	1	**215 (41%)**
All	**2**	**10**	**74**	**221**	**1**	**13**	**7**	**5**	**1**	**26**	**167**	**1**	**528 (100%)**

Table 18. Sample size per template and archaeological site for pre-Bronze Age dogs.

	Period and archaeological site	A	B	C	D	E	F	G	H	I	J	All mandibles
Western Europe												
	Mesolithic											
	Téviec	0	0	0	0	1	0	1	0	1	0	**2**
	Early Neolithic											
	Herxheim	2	3	3	7	8	2	6	2	8	4	**9**
	Alizay la chaussée	1	1	1	1	1	1	1	1	1	1	**1**
	Middle Neolithic - Chasséen											
	Auriac	0	1	0	2	3	0	2	0	6	0	**6**
	Bercy	1	12	3	17	18	1	18	1	21	8	**22**
	ZAC de Caunelle	0	1	0	2	2	1	5	1	7	1	**7**
	Cadereau d'Alès	2	2	2	2	2	2	2	2	2	2	**2**
	Le Crès	2	3	2	4	5	2	6	2	6	4	**7**
	Le Pirou	0	2	1	4	6	0	5	0	6	3	**7**
	Les Moulins	2	5	6	12	12	4	12	4	14	7	**14**
	Mas de Vignoles IV	0	0	0	0	0	0	1	0	1	0	**1**
	Le Taï	0	0	1	1	1	0	1	0	1	0	**1**
	La Roberte	1	3	5	6	7	1	6	1	6	1	**7**
	Middle Neolithic - Cortaillod											
	Twann	62	97	99	180	203	70	150	73	202	86	**221**
	Middle Neolithic - NMB											
	Clairvaux XIV	0	0	0	0	0	1	1	1	1	1	**1**
	Late Neolithic											
	Mas de Vignoles IV	0	0	0	0	0	0	1	0	2	1	**2**
	Bury	0	1	1	3	3	0	3	0	3	0	**3**
	Chalain 19	1	1	1	2	2	1	3	1	4	1	**4**
	Chalain 2	0	1	0	2	2	0	2	0	3	1	**3**
	Chalain 3	1	1	1	1	1	1	1	1	1	1	**1**
	Neolithic											
	Mas de Vignoles IV	0	1	0	4	4	0	6	1	7	2	**7**
Eastern Europe												
	Mesolithic / Early Neolithic											
	Alibeg	0	0	0	0	1	0	1	0	1	0	**2**
	Icoana	0	0	0	0	0	0	1	0	2	0	**2**
	Ostrovul Banului	0	0	0	0	1	0	0	0	0	0	**1**
	Chalcolithic 1											
	Isaccea	3	7	5	11	12	3	11	3	12	6	**13**
	Varasti	1	2	4	7	8	2	5	2	8	2	**8**
	Cheia	0	0	0	1	2	0	0	0	1	0	**2**
	Hârşova tell	1	1	2	3	3	1	3	1	3	1	**3**
	Chalcolithic 2 – Gumelnița											
	Vitănești	2	5	7	14	16	7	18	7	27	7	**29**
	Căscioarele	2	3	4	6	6	5	6	5	9	5	**9**
	Popina-Borduşani	28	50	43	66	70	31	67	31	77	46	**79**
	Hârşova tell	14	24	24	35	38	18	42	19	46	23	**50**
	Chalcolithic 3 – Cernavoda											
	Hârşova tell	1	1	1	1	1	1	1	1	1	1	**1**
	Mesolithic / Neolithic											
	Schela Cladovei	0	0	1	1	1	0	1	0	1	0	**1**
	Total	**127**	**228**	**217**	**395**	**440**	**155**	**389**	**160**	**491**	**215**	**528**

5.3.2. Red foxes

Sample sizes of red foxes submitted to geometric morphometric analyses are provided in Table 19 and Table 20.

Most of the 50 mandibles of red foxes in the total archaeological sample are represented by template E (69%) and I (80%), as a result of the high fragmentation of the material (Table 19).

In chapters 8 and 9, we removed the mandible Har78 from the analyses (since it is date back to the Chalcolithic, without having a more precise cultural context).

Table 19. Sample size per template and site for pre-Bronze Age foxes.

Period	Site	A	B	C	D	E	F	G	H	I	J	All mandibles
Western Europe												
	Mesolithic											
	Téviec	0	0	0	3	5	0	0	0	6	0	**8**
	Early Neolithic											
	Camprafaud	0	0	0	0	1	0	0	0	0	0	**1**
	Herxheim	1	1	2	2	2	1	2	1	2	1	**2**
	Le Taï	0	1	0	1	1	0	1	0	1	1	**1**
	Middle Neolithic - Cortaillod											
	Twann	0	0	0	0	3	0	1	0	1	0	**4**
	Middle Neolithic - NMB											
	Clairvaux XIV	3	5	3	6	6	3	6	3	6	5	**6**
	Late Neolithic											
	Chalain 3	0	0	0	1	1	0	1	0	2	1	**2**
	Chalain 4	1	2	1	3	4	2	3	2	5	3	**6**
	Chalain 19	1	1	1	1	2	6	7	6	9	5	**10**
	Twann	0	0	0	0	0	0	0	0	2	0	**2**
Eastern Europe												
	Chalcolithic 1 – Boian Spantov											
	Hârşova tell	0	0	0	0	0	0	0	0	1	0	**1**
	Chalcolithic 2 – Gumelniţa											
	Hârşova tell	2	2	2	2	3	2	2	2	2	2	**3**
	Taraschina	0	0	0	1	1	0	0	0	1	0	**1**
	Vităneşti	0	1	0	1	2	0	1	0	1	0	**2**
	Chalcolithic – undetermined culture – Hârşova tell	0	0	1	1	1	0	1	0	1	0	**1**
	Total	**8**	**13**	**10**	**22**	**32**	**14**	**25**	**14**	**40**	**18**	**50**

Table 20. Sample size per template and chrono-cultural period for pre-Bronze Age foxes. Chalco: Chalcolithic; C: fox mandible from the Chalcolithic of Hârşova without more precision on the cultural context.

	Western Europe					Eastern Europe			
	Mesolithic	**Early Neolithic**	**Middle Neolithic - Cortaillod**	**Middle Neolithic - NMB**	**Late Neolithic**	**Chalco1**	**Chalco2**	**C**	**Total**
A	0	1	0	3	2	0	2	0	**8**
B	0	2	0	5	3	0	3	0	**13**
C	0	2	0	3	2	0	2	1	**10**
D	3	3	0	6	5	0	4	1	**22**
E	5	4	3	6	7	0	6	1	**32**
F	0	1	0	3	8	0	2	0	**14**
G	0	3	1	6	11	0	3	1	**25**
H	0	1	0	3	8	0	2	0	**14**
I	6	3	1	6	18	1	4	1	**40**
J	0	2	0	5	9	0	2	0	**18**
All	**8**	**4**	**4**	**6**	**20**	**1**	**6**	**1**	**50**

5.3.3. Wolves

Sample sizes of wolves submitted to geometric morphometric analyses (from Chalain 4 and Vitănești) are provided in Table 21 and Table 22.

Table 21. Sample size per template and site for pre-Bronze Age wolves.

Site	A	B	C	D	E	F	G	H	I	J	All mandibles
Chalain 4	4	4	4	5	5	4	5	4	5	4	5
Vitănești	0	0	0	1	2	1	1	1	2	1	3

Table 22. Sample size per template and chrono-cultural period for pre-Bronze Age wolves.

	Late Neolithic	Chalcolithic 2 - Gumelnița	Total
A	4	0	4
B	4	0	4
C	4	0	4
D	5	1	6
E	5	2	7
F	4	1	5
G	5	1	6
H	4	1	5
I	5	2	7
J	4	1	5

Conclusion

From the presentation of the archaeological sample, the following key points emerge:

KEY POINTS

The corpus contains few remains from the Mesolithic or Early Neolithic. In order to represent these phases in the analyses, the smallest patterns of fragmentation will be of major importance.

This raises the question of the interest of these patterns to describe the complete shape of the mandible and the masticatory function. What is the loss of information due to fragmentation?

The balanced sample of dogs from the west and east of Europe will allow global comparison between these two areas, which are characterized by very different neolithisatiion histories. The two main groups within these areas (Midlle Neolithic for Western Europe, and Chalcolithic Gumelnița for Eastern Europe) can be compared as the time elapsed between the beginning of the Neolithic and the beginning of the Middle Neolithic or Gumelnița (respectively) is similar.

In both areas, it will be possible to follow the evolution from the Mesolithic to the early Bronze Age, but the small number of individuals in the earlier and latter phases should lead to caution in the interpretions.

In Western Europe, we can compare Middle Neolithic dogs from the Chasséen (represented by several sites) with those from the Cortaillod (however represented by a single site) cultures.

The very numerous dog mandibles from Cortaillod culture of Twann offer the possibility to study the morphological and functional variability that existed within a single site, during the same culture but over a relatively long and precisely known period of time.

In Eastern Europe, the large number of dogs from the sites of Harsova and Borduşani will offer the possibility to describe and compare the morphological and functional variability that existed in two contemporaryand very close sites of the Gumelnița culture.

The fox sample is very small. The comparative study will therefore only be very preliminary. The sample will not allow a comparison between Eastern and Western Europe

The following chapters will explore these questions.

Chapter 7.
Comparison of modern and ancient canids and the efficiency of each fragmentation pattern to describe variation in size and shape

The aim of this chapter is to provide a comparison between modern and ancient canids. This is of interest for several reasons. First, it will help position pre-Bronze Age canids relative to modern canids, providing a framework for comparison. Additionally, if ancient canids are included within the variability of modern canids, we may conclude that extant modern dogs and red foxes are good models for interpreting features on the mandible of ancient dogs.

We recall here that the exploration of variation in form implies a combined study of centroid size and conformation (shape), and that it is possible to compare average shapes/sizes as well as their variability (cf Part 2 Chapter 2 section 2.3).

In this chapter we will try to answer the following questions:

- *Where do pre-Bronze Age dogs and wolves stand in relation to modern dogs and wolves?*
- *Is there a risk of confusion between ancient wolves and modern dogs?*
- *Do pre-Bronze Age dogs (or foxes) lie within the variability of modern dogs (or foxes)?*
- *Do modern dogs (or foxes) and ancient dogs (or foxes) show the same variability/disparity?*
- *To which morphotypes/current breeds are pre-Bronze Age dogs most closely related?*
- *Do modern and ancient dogs (or foxes) differ in terms of size and average shape?*
- *Are the allometric patterns the same in modern and archaeological dogs (or foxes)?*
- *Is the modularity between the different parts of the mandible the same in modern and archaeological dogs (or foxes)?*

Since the preliminary analyses conducted to verify species attribution for small mandible fragments (see appendix 9) suggested that templates A, B, C, F and J were the most insightful to differenciate species and describe the overall shape of the mandible, we focused our following analyses mainly on these templates. This enabled us to take into account 323 specimens of ancient *Canis* (318 dogs and 5 wolves) and 22 specimens of ancient foxes. Given that these analyses also demonstrated that *Vulpes* and *Canis* specimens were clearly different in shape (there is no risk of confusion). Consequently, we performed separate analyses for *Vulpes* and *Canis* in the following sections. All modern juveniles were excluded from the following analyses.

1. Comparison of modern and ancient *Canis*

In the following section, modern dog breeds are abbreviated by their first three letters (Table 23).

Table 23. Correspondance between abbreviations and modern dog breeds used in this section.

Abbreviation	Modern dog breed
Ams	American Staffordshire terrier
Bar	Barzoï
	Beagles
Bel	Belgian shepherd - Tervueren
Bor	Border collie
Box	Boxer
Buld	Bulldog
Bult	Bull terrier
Chi	Chihuahua
Can	Cane Corso
Col	Cavalier King Charles Spaniel
Kin	Collie
Pap	Continental Toy Spaniel Papillon
Poo	Poodle
Dac	Dachshund
Dee	Deerhound
Dob	Dobermann
Fox	Fox terrier
Ger	German shepherd
Leo	Leonberg
Lou	Loulou
Gol	Golden retriever
Hus	Husky
Leo	Leonberg
Mas	Mastiff
Pit	Pitbull
Poo	Poodle
Rot	Rottweiler
Ten	Teneriffe
She	Shetland sheepdog
Slo	Sloughi
Yor	Yorkshire
Wip	Wippeth

1.1. Comparison of centroid size between modern and ancient *Canis*

1.1.1. Efficiency of each template to describe the overall size of the mandible

First, we tested the correlation between the centroid sizes obtained for the complete mandible (template A) with those obtained for all the other templates, in order to appreciate to what extent the centroid sizes of the different templates were reliable proxies of the overall size of the mandible and what degree of information was lost for each fragmentation pattern.

We used the function "cor.test" on the log10 centroid size. We performed analyses on the 67 modern dogs of our sample (juveniles were excluded from the analyses, Table 24) and on the 127 ancient dogs with complete mandibles (Table 25).

The correlation is excellent in all cases. Surprisingly, lower correlations are observed for template I in ancient dogs (compared to modern dogs). This tends to suggest that this portion of the mandible covaries differently with the rest of the mandible in modern and ancient dogs. However, this remains quite acceptable. Template I can therefore be used to compare centroid sizes with a large number of individuals but differences in size may be flattened.

Table 24. Results of the correlation tests between centroid sizes, for 67 modern dogs (juveniles were excluded).

Template	**B**	**C**	**D**	**E**	**F**	**G**	**H**	**I**	**J**
Correlation (r)	1	0.99	0.97	0.94	0.98	0.97	0.97	0.94	0.98
P-value	***	***	***	***	***	***	***	***	***

Table 25. Results of the correlation tests between centroid sizes, for the 127 ancient dogs with complete mandibles.

Template	**B**	**C**	**D**	**E**	**F**	**G**	**H**	**I**	**J**
Correlation (r)	0.98	0.99	0.95	0.80	0.98	0.88	0.92	0.78	0.97
P-value	***	***	***	***	***	***	***	***	***

1.1.2. Comparison of centroid size between modern and ancient *Canis*

To test whether modern and ancient *Canis* species (dogs, wolves and dingoes) differ in centroid size, we performed ANOVAs and Tukey post-hoc tests using the functions “aov” and “TukeyHSD” (we performed analyses on the log10-transformed centroid size but plotted the results on the absolute values, Figure 95).

The results indicate that **both modern and ancient wolves are significantly bigger than both archaeological and modern dogs**, and that **ancient dogs tend to be smaller than modern dogs** ($P < 0.001$ for all templates). Additionally, **modern dogs are more variable in size than ancient dogs** (Bartlett test: $P < 0.001$ for the five templates). Dingoes have intermediate sizes.

The differences are less obvious with template I, which is likely related to the fact that differences in size are underestimated with this template (see above) and that much more archaeological mandibles are included in the analyses, thus inevitably increasing the variability. Accordingly, a dog mandible from Icoana (Ico9, only represented by template I) has a centroid size that is included in the variability of both modern and ancient wolves with this template. Given that this is a very small fragment and we lack perspective on the variability that existed in dogs during the Mesolithic period (this will be detailed in the next chapters), it cannot be completely excluded that this mandible belongs to a wolf rather than to a dog.

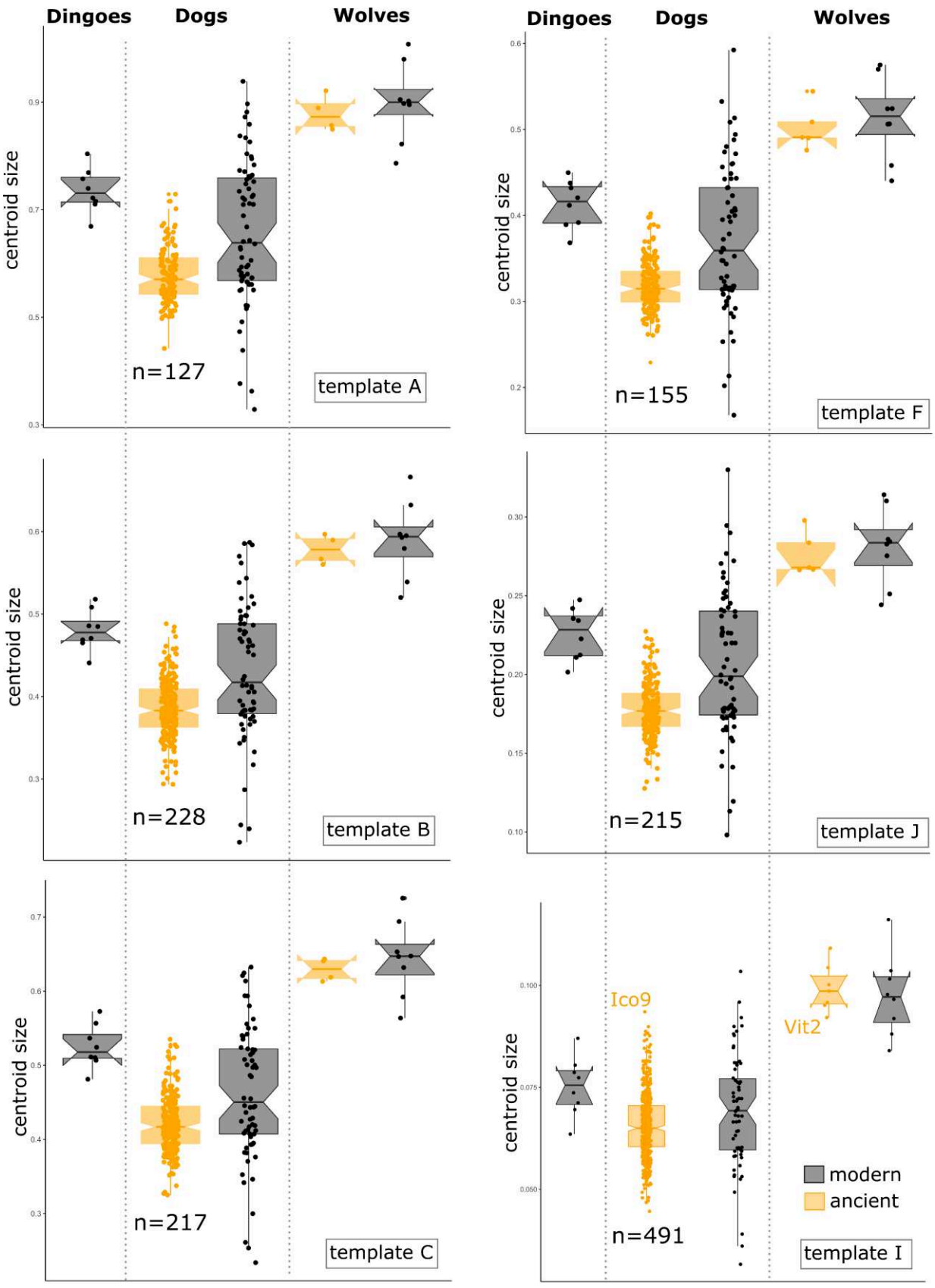

Figure 95. Boxplot of the centroid sizes of modern and ancient canids. Dingoes n=8; Modern dogs n=67; modern wolves n=8; sample size for ancient dogs are reported directly on the graph.

1.2. Comparison of mandibular shapes between modern and ancient *Canis*

1.2.1. Preliminar observation: Principal Component Analyses

We performed a Principal Component Analyses (PCA) on the Procrustes coordinates based on all the archaeological and modern dogs, modern dingoes and ancient and modern wolves (Figure 96). The first two axes represent only 34.7% of the total variation in shape. The first principal component (PC1) is strongly correlated with the centroid size ($R^2 = 0.23$, $P < 0.001$), as well as PC2 ($R^2 = 0.06$, $P < 0.001$). The smallest dogs are on the left part of the scatterplot and the biggest dogs tend to be on the right part (except the two barzoï that are in the middle).

Modern dogs occupy a more important part of the scatterplot, suggesting they are more variable than ancient dogs. Some modern breeds are not overlapping with the point cloud of ancient dogs, in particular large brachycephalic breeds (such as rottweilers, pitbulls, bulldogs, leonberger, boxer, mastiff), **extremely dolichocephalic dogs** (such as barzoï) and **small toy dogs** (papillon, chihuahua, dachshund). However, **ancient dogs seem to overlap modern normocephalic breeds**. **The area of variation of beagles along PC1 and PC2 is clearly overlap the area of variation of the ancient dogs**.

Interestingly, **ancient dogs appear to occupy a private part of morphospace not occupied by modern canids**, as they do not overlap any of the modern dogs on the negative part of PC1.

Wild canids (wolves and dingoes) are at the centre of the scatterplot, suggesting that they have intermediate shapes. They are included in the morphospace of modern dogs in PC1 and PC2. They **partly overlap with ancient dogs** but they tend to be differenciated along PC1. Interestingly, **modern wolves tend to group together with pre-Bronze Age dogs**, as has already been pointed out by previous authors (Benecke, 1987, 1994; Vigne and Marinval-Vigne, 1988). This could be explained by the fact that modern wolves included in the analyses are from zoological parks, and their captivity may have resulted in rapid bone changes mimicking the morphology of dogs.

Visualisation along axes PC3 and PC4 does not provide any additional information, so no additional figure is shown here.

These observations are confirmed when the sample size is increased by conducting the same analyses with template B (Figure 97).

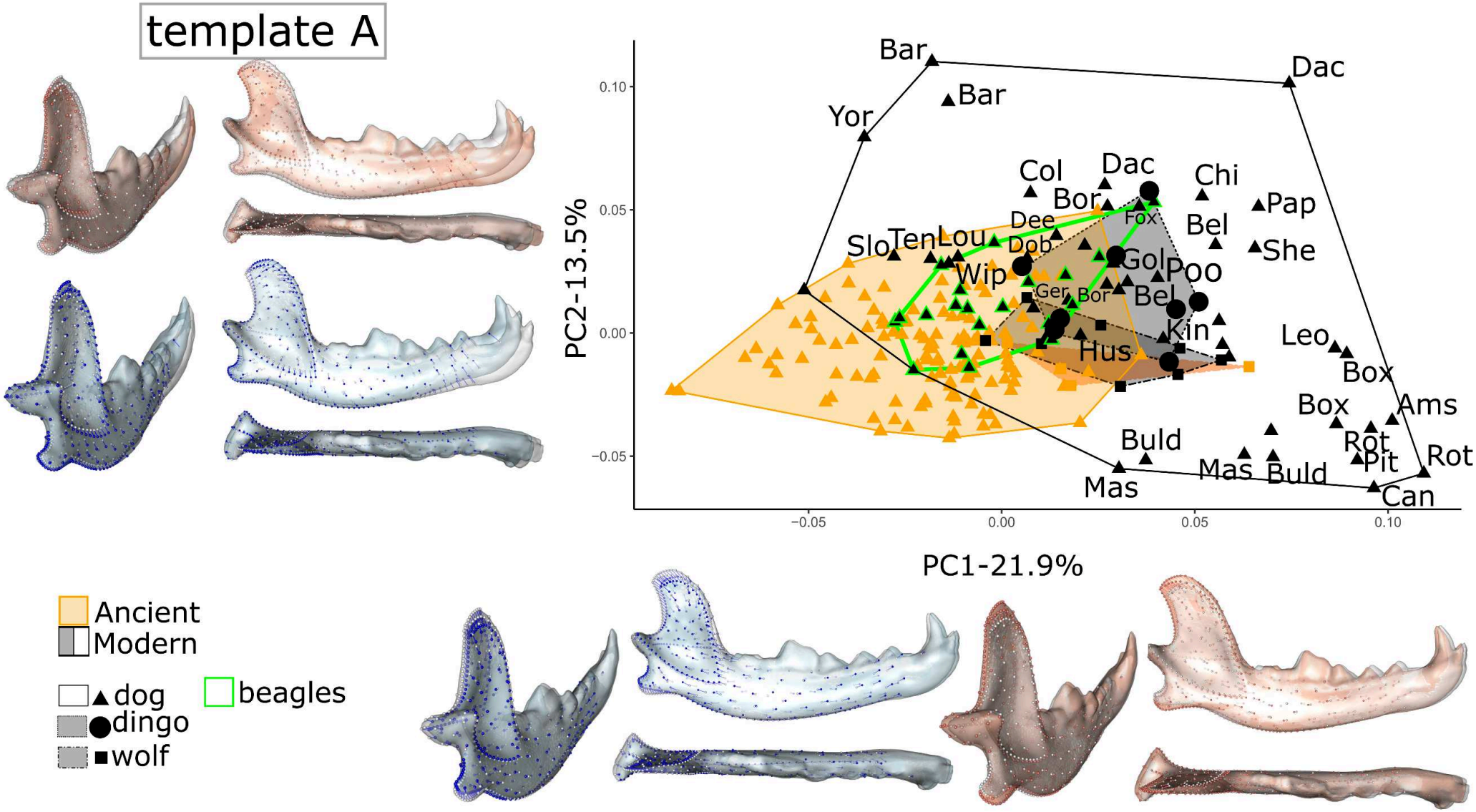

Figure 96. PCA on modern and ancient specimens of *Canis* with template A (66 modern dogs, 8 modern dingoes, 8 modern wolves, 127 ancient dogs and 4 ancient wolves).

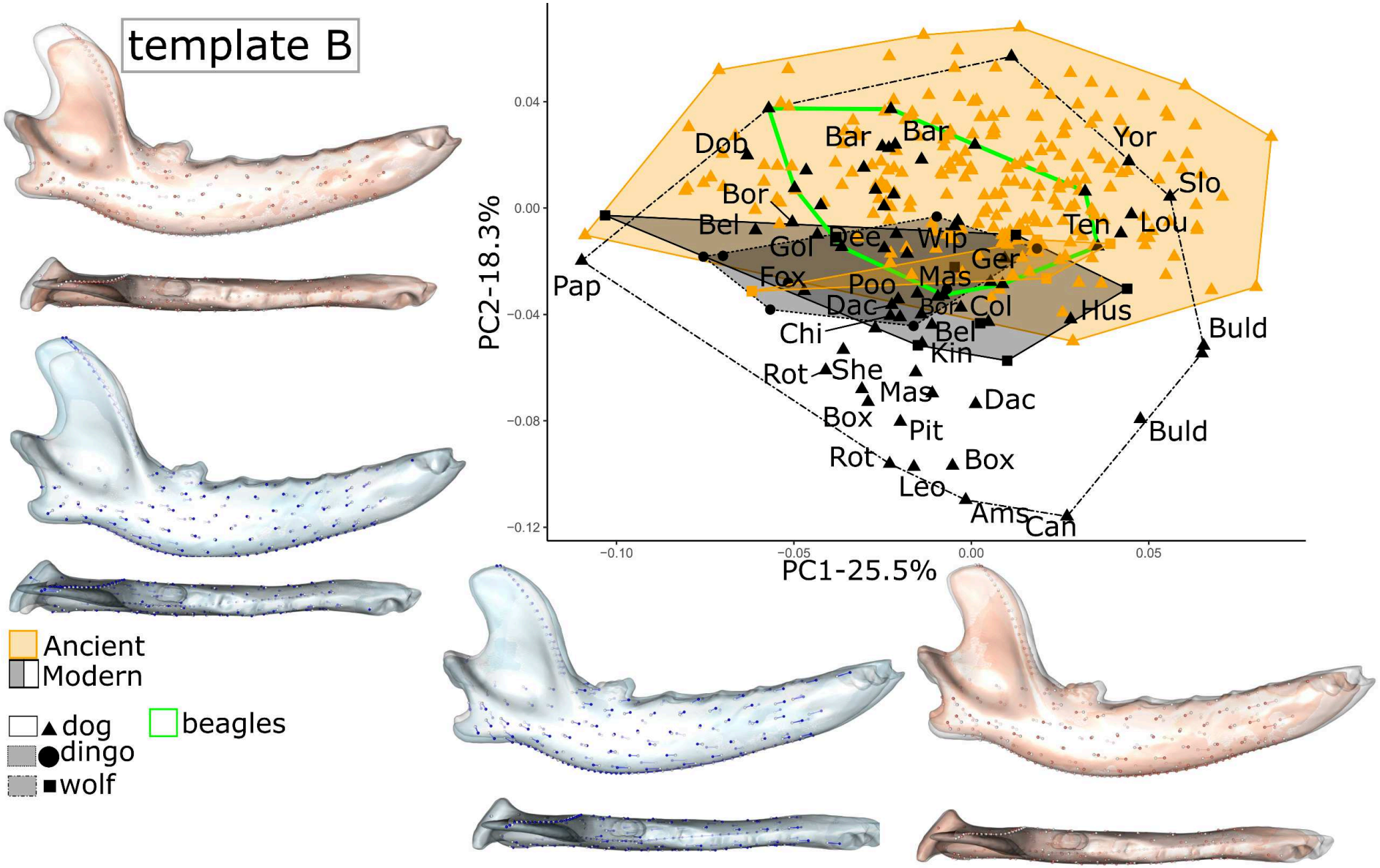

Figure 97. PCA on modern and ancient specimens of Canis with template A (66 modern dogs, 8 modern dingoes, 8 modern wolves, 228 ancient dogs and 4 ancient wolves).

1.2.2. Proximities between ancient dog morphotypes and modern dog breeds: classification tree

The PCA in the previous section suggested that some modern dogs have no equivalent among pre-Bronze Age dogs, and *vice versa*, but this analysis only represents a small amount of the total variation in shape.

To go further, and consider the real morphological distances between individuals, we computed classification trees based on the Procrustes distances between all ancient and modern canids.

We first performed a GPA using the function "procSym", then we calculated a distance matrix using the function "dist" (we used the Euclidean distance), and we performed hierarchical clustering using the function "pvclust" (we used the Ward D2 method for cluster aggregation). The function "pvclust" conducts multiscale bootstrap resampling (1000 boots) to calculate P-values for each cluster, thus assessing the uncertainty in hierarchical cluster analysis. The P-value of a cluster is a value between 0 and 1, which indicates how strong the cluster is supported by data. On the graph, we reported the AU (Approximately Unbiased) P-values, which are computed by multiscale bootstrap resampling, and are thus better approximations to unbiased P-value than BP (Bootstrap Probability) values computed by normal bootstrap resampling. Finally we ploted the results with "ggtree". To project the P-values on the tree we used the code which is available here: http://www.jafy.eu/posts/2019/06/pvclust-nodevalues-in-ggtree.md/

```
## 1. Make pvclust object e.g.
hclust_boot <- pvclust::pvclust(otu_matrix,
                  method.hclust = selected_method,
                  method.dist = "euclidean",
                  nboot = 1000,
                  parallel = T)

## 2. Set modified fastbaps function
as.phylo.pvclust.node.attributes <- function(x, attribute)
{
  N <- dim(x$merge)[1]
  edge <- matrix(0L, 2*N, 2)
  edge.length <- numeric(2*N)
  ## `node' gives the number of the node for the i-th row of x$merge
  node <- integer(N)
  node[N] <- N + 2L
  node.attributes <- rep(NA, N)
  cur.nod <- N + 3L
  j <- 1L
  for (i in N:1) {
    edge[j:(j + 1), 1] <- node[i]
    for (l in 1:2) {
      k <- j + l - 1L
      y <- x$merge[i, l]
      if (y > 0) {
        edge[k, 2] <- node[y] <- cur.nod
        cur.nod <- cur.nod + 1L
```

```
        edge.length[k] <- x$height[i] - x$height[y]
        node.attributes[edge[k, 1] - (N + 1)] <- attribute[i]
      } else {
        edge[k, 2] <- -y
        edge.length[k] <- x$height[i]
        node.attributes[edge[k, 1] -  (N + 1)] <- attribute[i]
      }
    }
    j <- j + 2L
  }

  if (is.null(x$labels))
    x$labels <- as.character(1:(N + 1))

  ## MODIFICATION: clean up node.attributes so they are in same format in
  ## pvclust plots
  node.attributes <- as.character(round(node.attributes * 100, 0))
  node.attributes[1] <- NA

  obj <- list(edge = edge, edge.length = edge.length / 2,
              tip.label = x$labels, Nnode = N, node.label = node.attributes)
  class(obj) <- "phylo"
  stats::reorder(obj)
}

## 3. Use the modified fastbaps function by accessing the hclust object in first
## position, and the corresponding au values from the edges list entry.
hclust_boot_phylo <- as.phylo.pvclust.node.attributes(hclust_boot$hclust,
                                                      hclust_boot$edges$au)


## 4. Display the values on the tree with ggtree
ggtree(hclust_boot_phylo  aes(x, y)) +
    geom_text2(aes(subset = !isTip, label = label))
```

First, we performed analyses with template A for all modern and ancient dogs, dingoes, and wolves (Figure 98). Three main groups can be observed. **Most of the dingoes and modern and ancient wolves are grouped on the same branch in group B**. The ancient dog Har24 is grouped with these dingoes and wolves but its centroid size is compatible with dogs only (0.54, Figure 98). Two dingoes and two modern wolves are with other dogs in group A.

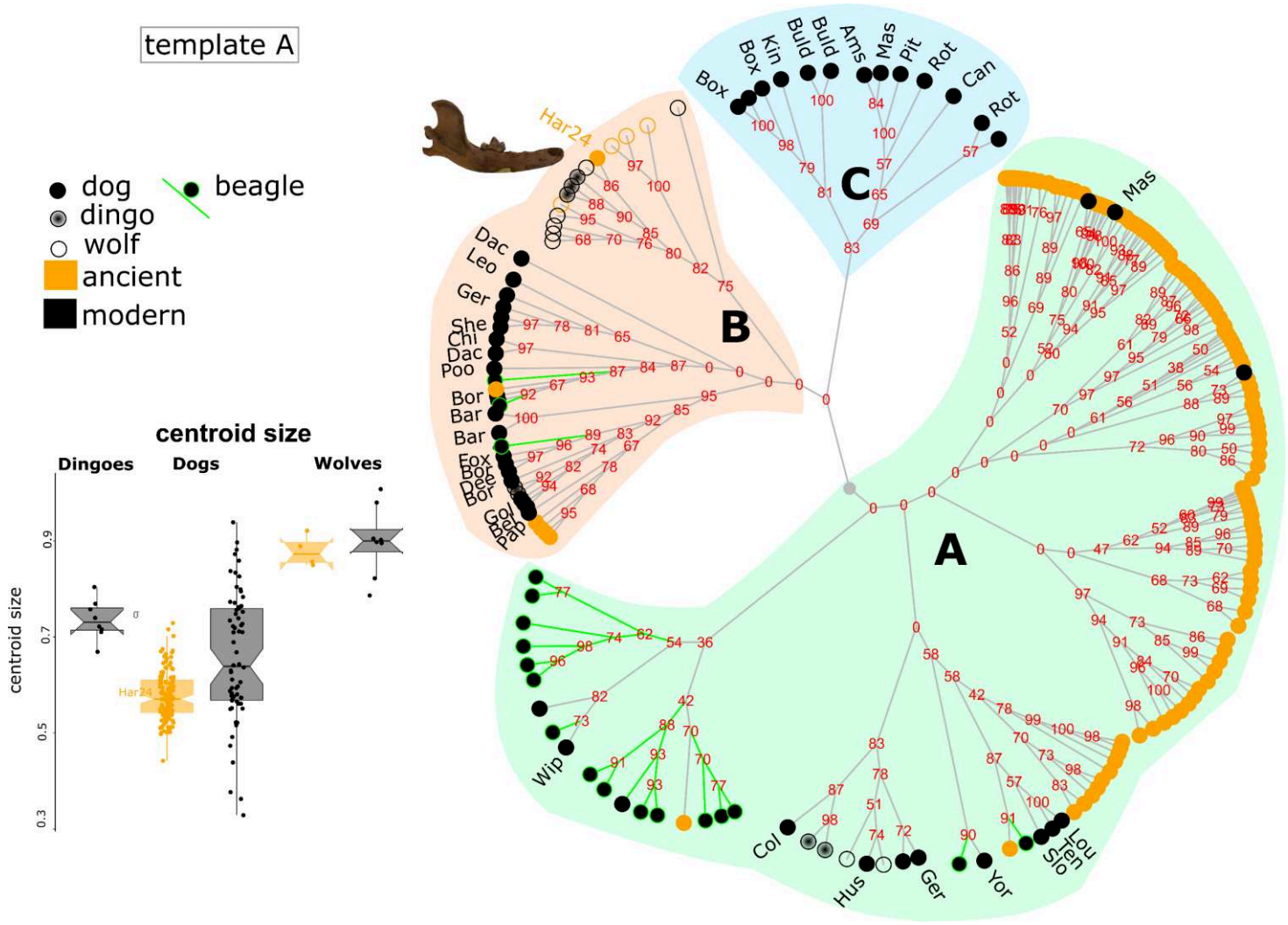

Figure 98. Classification tree performed on the complete mandibles (template A) of modern and ancient *Canis* specimens (66 modern dogs, 8 modern dingoes, 8 modern wolves, 127 ancient dogs and 4 ancient wolves). The AU p-values (in %) for each cluster from pvclust are reported in red. Centroid sizes are given to the left.

Next, we focused on modern and ancient dogs only. We performed similar analyses based on the Procrustes coordinates of templates A (Figure 99) and B (Figure 100).

In both analyses, **one group (C and C') contains only modern dogs: the largest or more brachycephalic ones** (plus the leonberg, which was not in this group in analyses with template A). The two other groups are very different when crossing the classifications obtained for the two templates. This likely related to the fact that template B describes less precisely the shape of the coronoid process, which is of major importance in the overall shape of the complete mandible. We will therefore mainly focus our interpretations on the graph obtained using template A. **Modern and ancient dogs tend to be on separate branches** (which is still true for the graph obtained with template B). **Some modern breeds seem quite close to ancient dogs**, as they are closer in shape to ancient dogs than to other modern dogs. This is the case of the mastiff, husky, loulou, teneriffe, sloughi and beagles. **The beagles are indeed mainly all grouped together on the same branch, in the middle of the ancient dogs** in group A and B'.

We focused only on these templates because they are the best to describe the overall shape of the mandible.

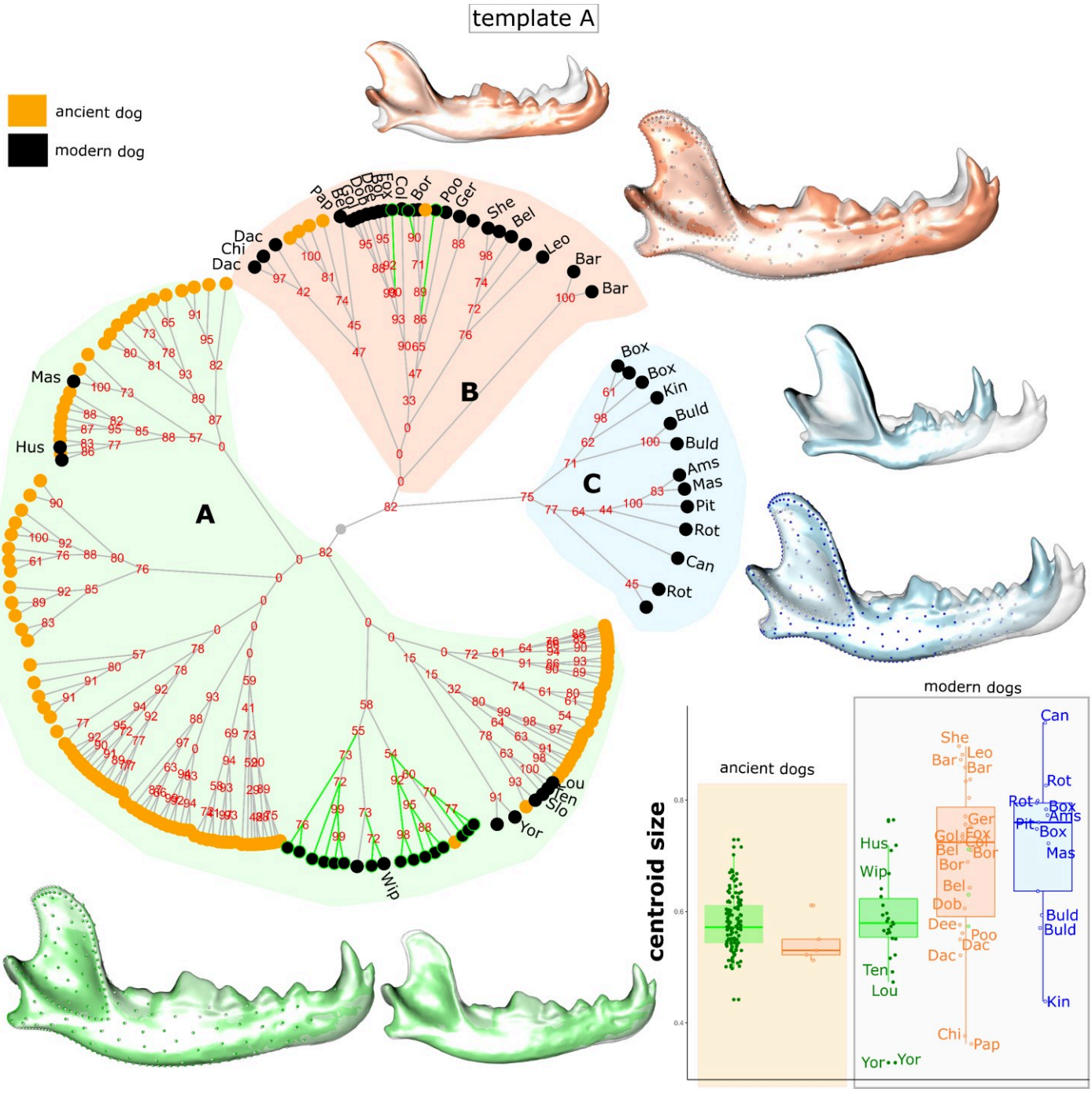

Figure 99. Classification tree on modern (66) and ancient (127) dogs based on coordinates from template A. The AU p-values (in %) for each cluster from pvclust are reported in red.

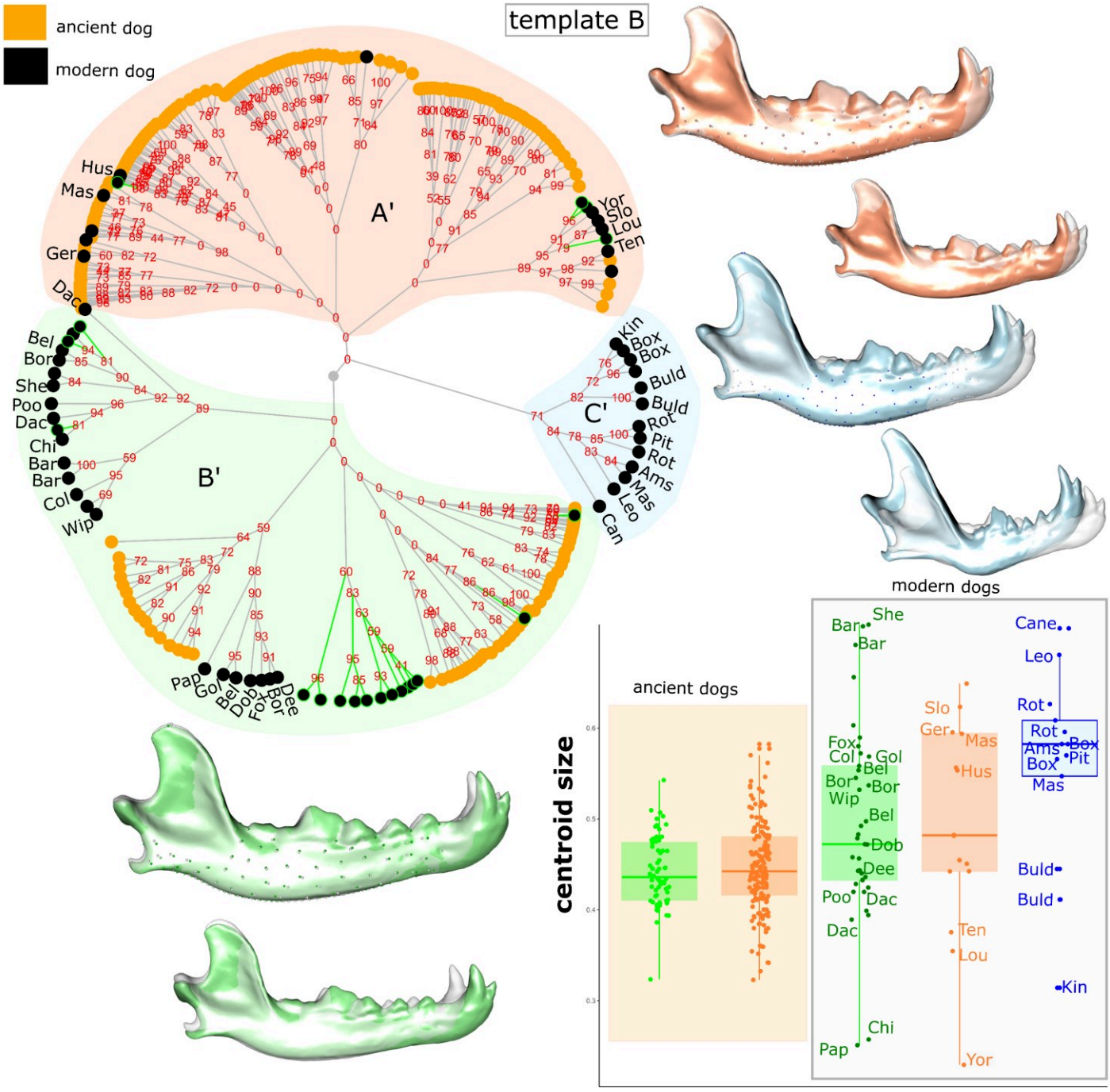

Figure 100. Classification tree on modern (66) and ancient (228) dogs based on coordinates from template B. The AU p-values (in %) for each cluster from pvclust are reported in red

To include as many mandibles as possible in the analysis, we tried to conduct the same analysis with template I.

First, we tested whether this small portion of the mandible carried sufficient information to obtain a tree similar to the one obtained with template A. To do this, we conducted the analysis on the Procrustes coordinates of template I, but only for the 127 complete mandibles that are described by template A. Therefore, if template I was also relevant for describing global variations in the morphotype, we should obtain a tree similar to the Figure 99. Unfortunately, the tree obtained is very different (Figure 101). There is no longer a clear distinction between modern and ancient dogs. **The fragmentation pattern I therefore does not allow to describe global variations in the morphotype.**

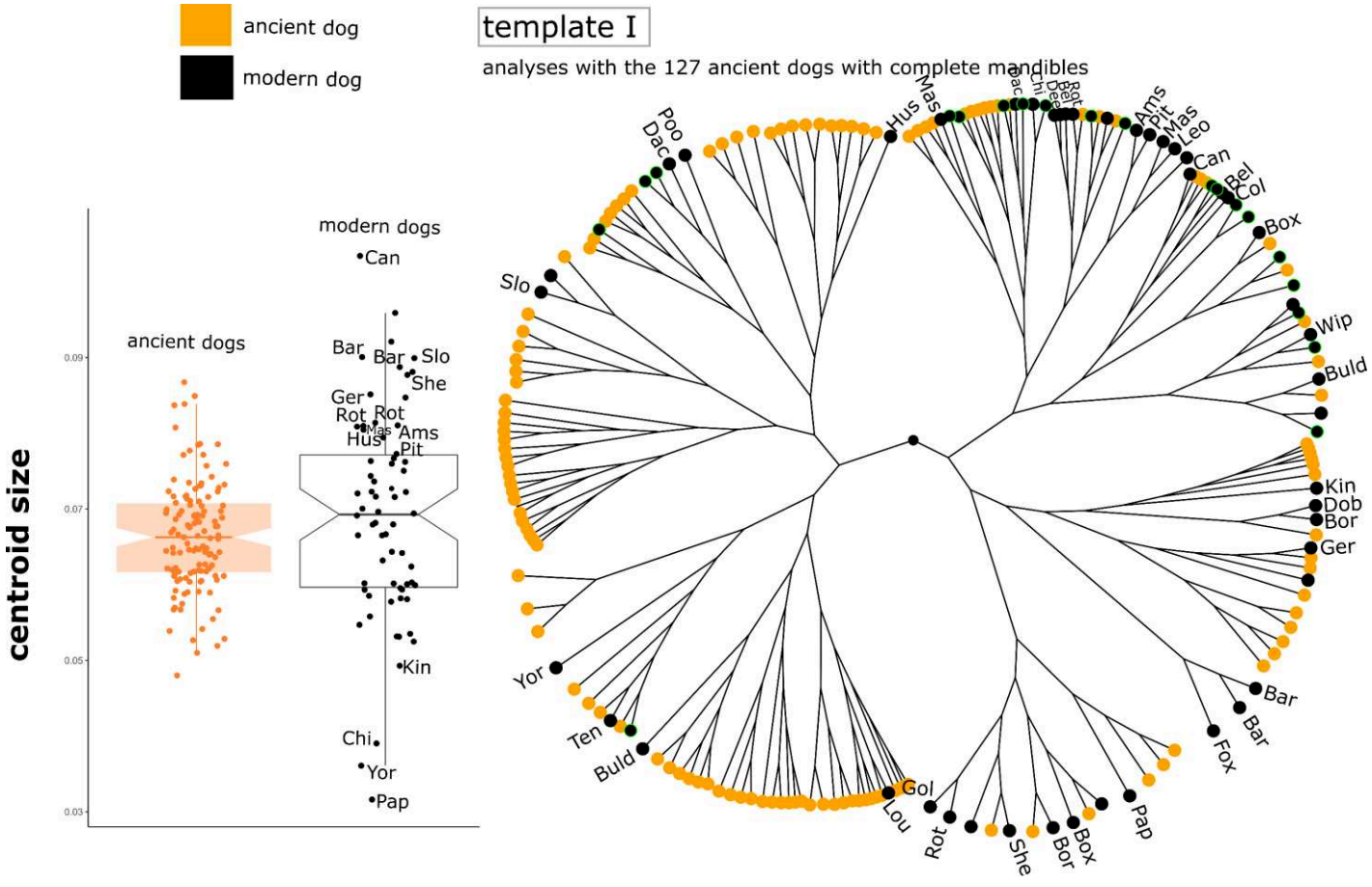

Figure 101. Classification tree on modern dogs (66) and ancient dogs with complete mandibles (127) based on coordinates from template I. The AU p-values (in %) for each cluster from pvclust are reported in red.

Not surprisingly, the analyses conducted on all (491) archaeological dogs described by template I lead to a tree without clear architecture, which can not be interpreted in terms of the overall morphotype (Figure 105). On this graph, large brachycephalic dogs tend to be grouped together at the top of the tree (with a few ancient dogs). On some branches, ancient dogs are isolated without modern equivalent (branches in the upper left corner, next to the papillon). This thus tends to confirm what has been previously described with templates A and B.

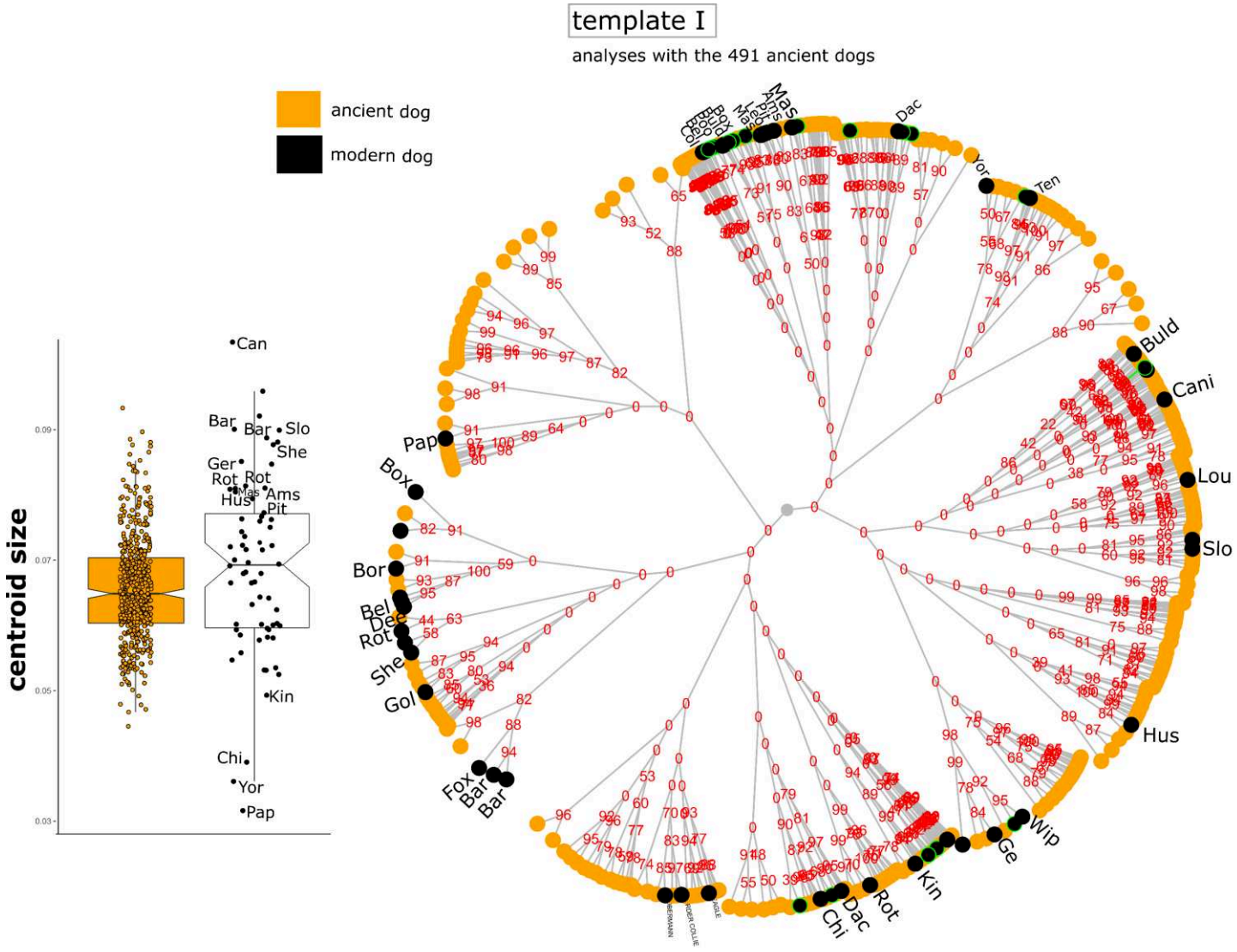

Figure 102. Classification tree on modern (66) and all ancient dogs (491) based on coordinates from template I. The AU p-values (in %) for each cluster from pvclust are reported in red.

1.2.3. Comparison of the variability: disparity test

To test whether morphological variability (i.e. disparity) differs between modern and ancient dogs, we performed a **disparity test** on the Procrustes coordinates obtained from a GPA on modern and ancient dogs with template A (66 modern dogs, 127 ancient dogs). We used the function "morphol.disparity" from the package "geomorph". This function estimates morphological disparity and performs pairwise comparisons among groups. Morphological disparity is estimated as the Procrustes variance for groups (modern dogs, ancient dogs) using residuals of a linear model fit.

The results indicate that ancient dogs (Procrustes variance = 0.0039) are much less variable than modern dogs (Procrustes variance = 0.0069, $P < 0.001$). This is confirmed by the results obtained for template B (Procrustes variance of modern dogs = 0.0069, Procrustes variance of ancient dogs = 0.0039, $P < 0.001$), template C (Procrustes variance of modern dogs = 0.0054, Procrustes variance of ancient dogs = 0.0034, $P = 0.002$), template F (Procrustes variance of modern dogs = 0.0076, Procrustes variance of ancient dogs = 0.0062, $P = 0.013$) and template J (Procrustes variance of modern dogs = 0.0058, Procrustes variance of ancient dogs = 0.0044, $P < 0.001$). Analyses performed on template I lead to no significantly different disparities between modern and ancient dogs (P = 0.95). This is not surprising considering that this part of the mandible is not representative of the complete morphotype, as stated above. We also obtained significant results for the analyses that used the predicted complete shapes of the 491 mandibles with template I (using 2B-PLS predictions; Procrustes variance of modern dogs = 0.0082, Procrustes variance of ancient dogs = 0.0046, $P < 0.001$).

The sample size was too small to test for differences in disparity compared to wolves.

We also performed a disparity test on the Procrustes coordinates of template A to compare the variability in mandibular shape between modern and ancient dogs and foxes. The results indicate that ancient dogs (n = 127, Procrustes variance = 0.0039) are as variable as modern foxes (n=68, Procrustes variance = 0.0046, $P = 0.6$) or ancient foxes (n = 8, Procrustes variance = 0.0035, $P = 0.7$).

1.2.4. Comparison of mean shapes: Procrustes ANOVA and CVA

To compare the mean mandibular conformations of modern and ancient dogs, we performed a Procrustes ANOVA, using the function "procD.lm" from the package "Morpho".

The results suggest that **ancient dogs significantly differ from modern dogs in shape** ($R^2_{\text{template A}} = 0.12$, $R^2_{\text{template B}} = 0.090$, $R^2_{\text{template C}} = 0.079$, $R^2_{\text{template F}} = 0.088$, $R^2_{\text{template J}} = 0.11$, $P < 0.001$).

The small sample size did not allow to explore the differences between modern and ancient foxes neither with wolves.

To describe more precisely what differs in the mandibular shape between modern and ancient dogs, we performed Canonical Variate Analyses (CVA) using the function "CVA" from the package "Morpho".

The CVA performed on template A leads to a classification rate of 99.5% (only 1 modern yorkshire was classified as an ancient dog). This reinforces the idea that ancient and modern dogs differ in shape. Pre-**Bronze Age dogs seem to have more robust (the mandibular ramus is taller under the carnassial) and curved mandibles** (Figure 103). **The coronoid process is straighter, the angular process is more developed and the masseteric fossa is shallower in ancient dogs.** These differences may thus result in differences in bite force production.

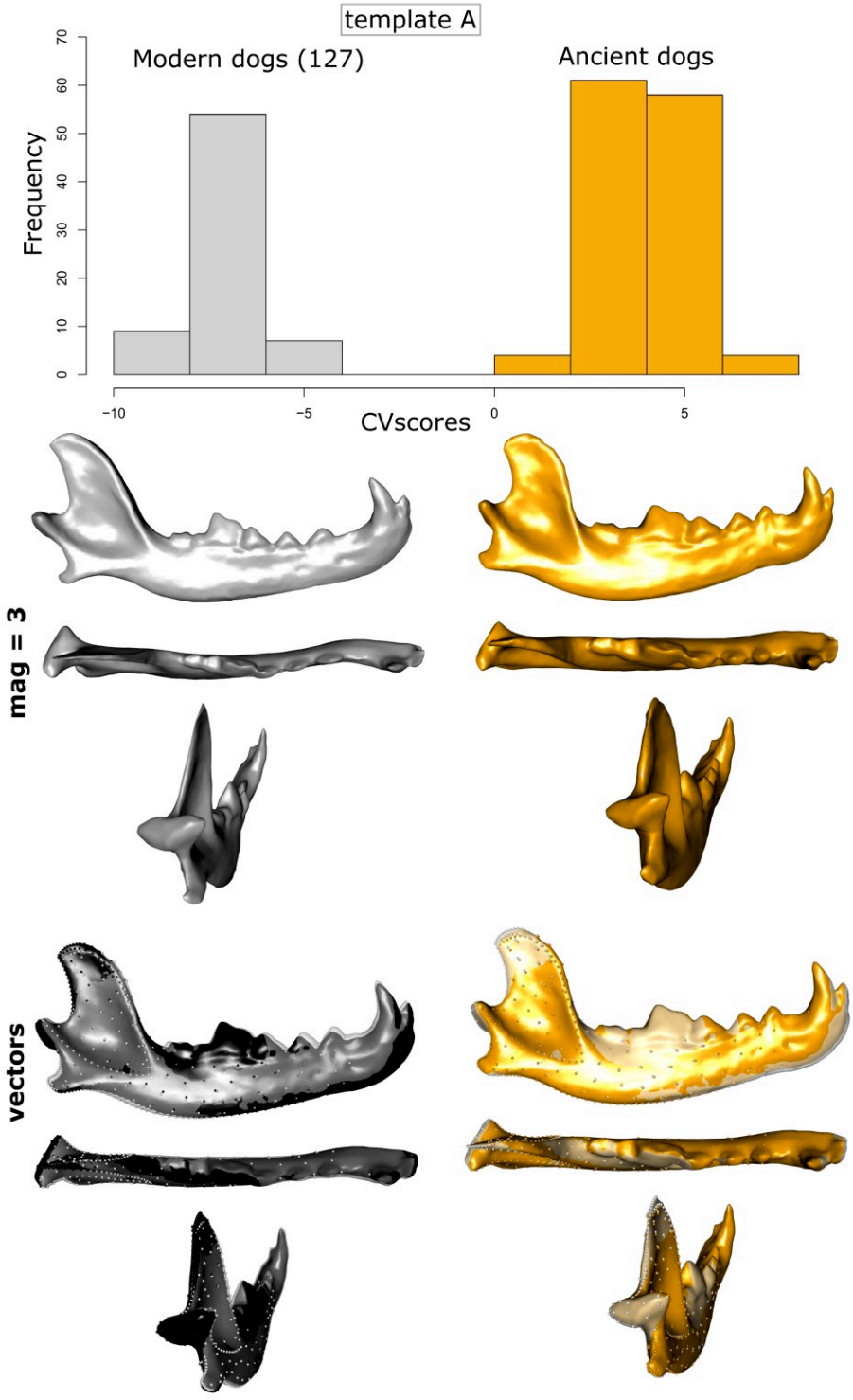

Figure 103. CVA performed on modern and ancient dogs with template A. Shapes at the minimum and maximum of CV scores are magnified by 3 (top) or superposed to the mean shape of the CVA and vectors of deformations between the two shapes are represented (bottom).

These differences are confirmed by analyses conducted on coordinates from templates B, C, F and J (Figure 104).

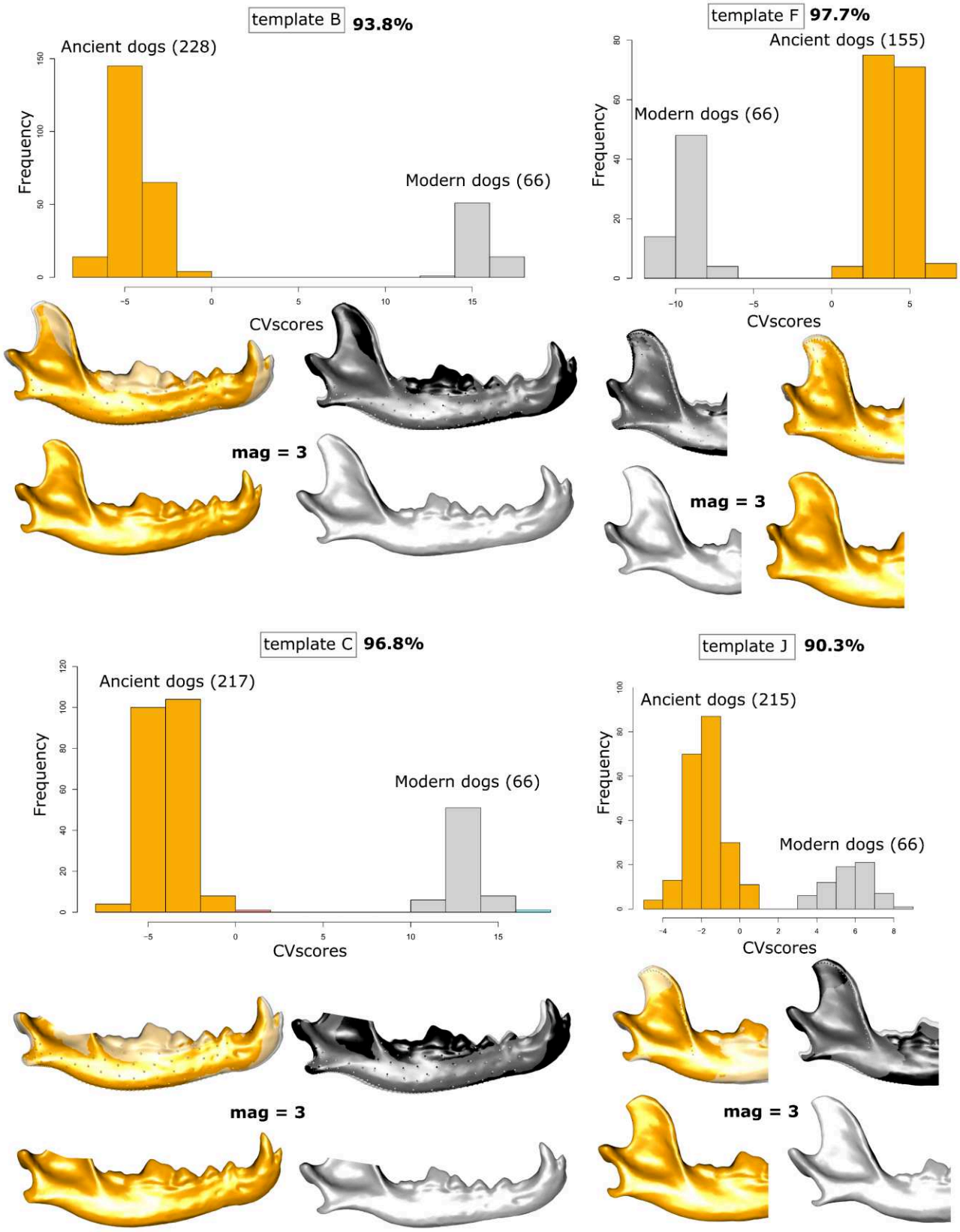

Figure 104. CVA performed on modern and Neolithic dogs with templates B, C, F and J, with shapes at the minimum and maximum of CV scores.

1.2.5. Comparison of allometry patterns between modern and ancient dogs and wolves

Based on the observation that ancient dogs are less variable than modern dogs and closer in shape to wild *Canis* (modern dingoes and modern and ancient wolves), we expected the allometry patterns to be different between modern and ancient dogs. We expected the extreme artificial selection to have upset the allometry patterns, while in ancient dogs, small individuals would not be very different in shape from large ones and would look like small wolves/dingoes.

To explore this possibility, we performed a Procrustes ANOVA on the shape coordinates and the log10 of the centroid size. We also calculated the common allometric components to visualise allometric trajectories (Mitteroecker *et al.*, 2004). We used the functions "CAC" and "showPC".

We first performed analyses for modern and ancient dogs separately. For modern dogs, analyses were performed on template A, while for ancient dogs, analyses were performed on both templates A and B to increase the sample size.

The results indicate that the centroid size explains 8.7% of the variation in shape in modern dogs while it explains only 1.2% of the variation in shape in ancient dogs ($P < 0.001$ in both cases). **Mandible shape is thus more allometric in modern dogs**. **The deformations due to allometry are, however, similar in modern and ancient dogs** (Figure 105).

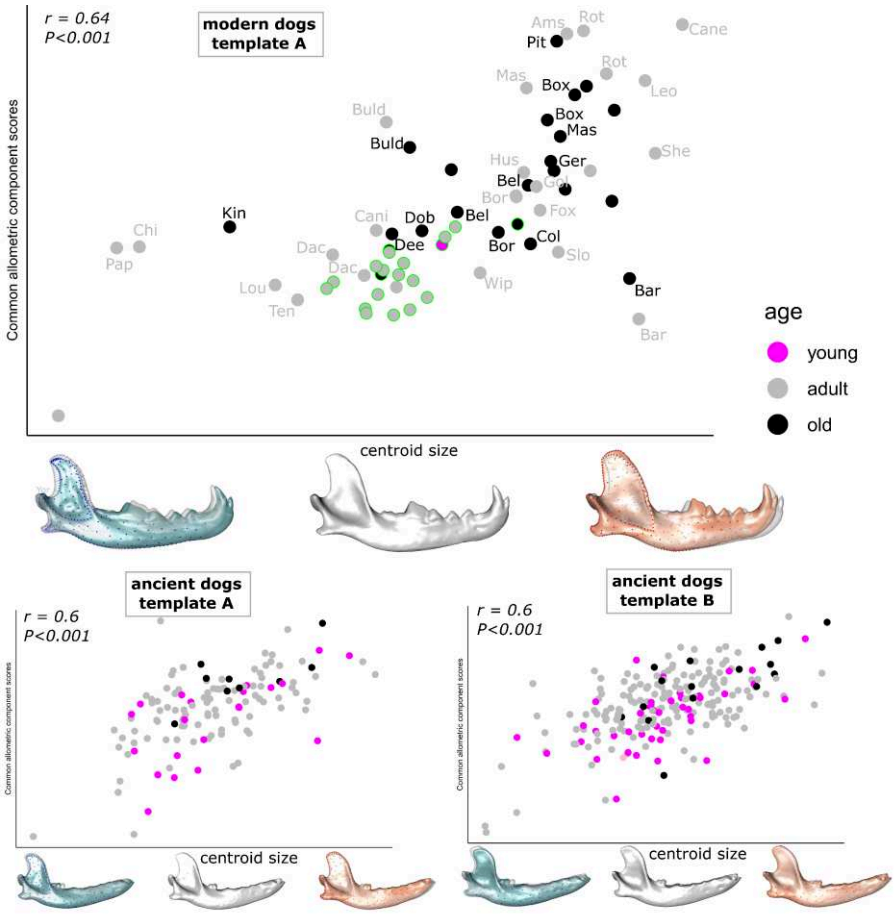

Figure 105. Deformations along the allometry slope in modern and ancient dogs.

Next, we performed analyses on modern and ancient dogs together. The results show that centroid size explains 7.3% of the variation in shape ($P < 0.001$), and the period (modern or ancient) explains 9.3% of the residual difference in shape (in other words of the allometry-free shape, $P < 0.001$). The interaction between these parameters (size and period) is not significant ($P > 0.5$). It thus suggests that **allometries are not different between modern and ancient dogs.** The **allometric trajectories are actually parallel** (the slope is the same but the intercepts are different), and the **dispersion around the regression line is more important in modern dogs** (Figure 106A). Similar results were obtained with template B (size and time explain 5.1% and 7.7% of the variation in shape, respectively)

In other analyses, we added modern dingoes and modern and ancient wolves (Figure 106B). The results show that centroid size explains 8.5% of the variation in shape ($P < 0.001$), the species explains 2.7% of the allometry-free shape, and the period 8%. The interaction parameter between size and time is still not significant ($P = 0.086$) which suggests similar trajectories between periods. **Modern wolves have a parallel trajectory to both modern and archaeological dogs, but the intercept is closer to that of archaeological dogs. Modern dingoes have a different trajectory to modern and ancient dogs** (in terms of both slope and intercept).

These results overall tend to suggest that **ancient dogs show allometric patterns that are similar to those of modern wolves, and similar to those of modern dogs** as the slopes are the same. The differences between modern and ancient dogs in terms of intercept reflects the differences in mean shapes between groups. However, the sample of wolves (both ancient and modern) is small and calls for additional data to be able to compare the trajectories between ancient dogs and wolves as well as between ancient and modern wolves.

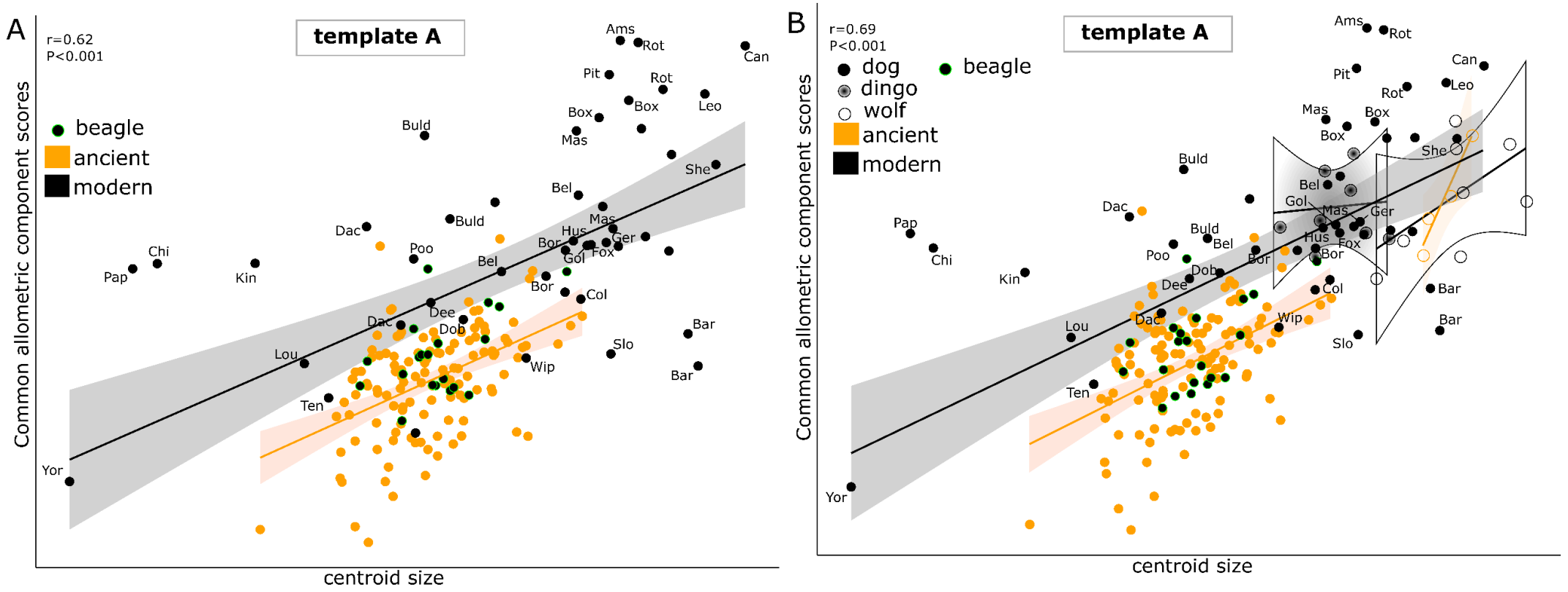

Figure 106. Allometry slope in modern and ancient dogs (A) or in all modern and ancient dogs, dingoes and wolves (B). Analyses performed on template A.

We also performed preliminary analyses for modern and ancient wolves, in order to explore whether the deformations associated with allometry involve overall similar features compared to those observed in dogs. The results of the analyses are not significant because of the small sample sizes but the visualisation suggests strong patterns of correlation (Figure 107). The centroid size explains 13.6% of the variation in shape in modern wolves (n = 8, $P = 0.45$) while it explains 50% of the variation in shape in ancient wolves (but n = 4, $P = 0.11$). The deformations involve the same deformations as in modern or ancient dogs (Figure 109) or modern dingoes (Figure 50 in Part 2 Chapter 4 section 2.1).

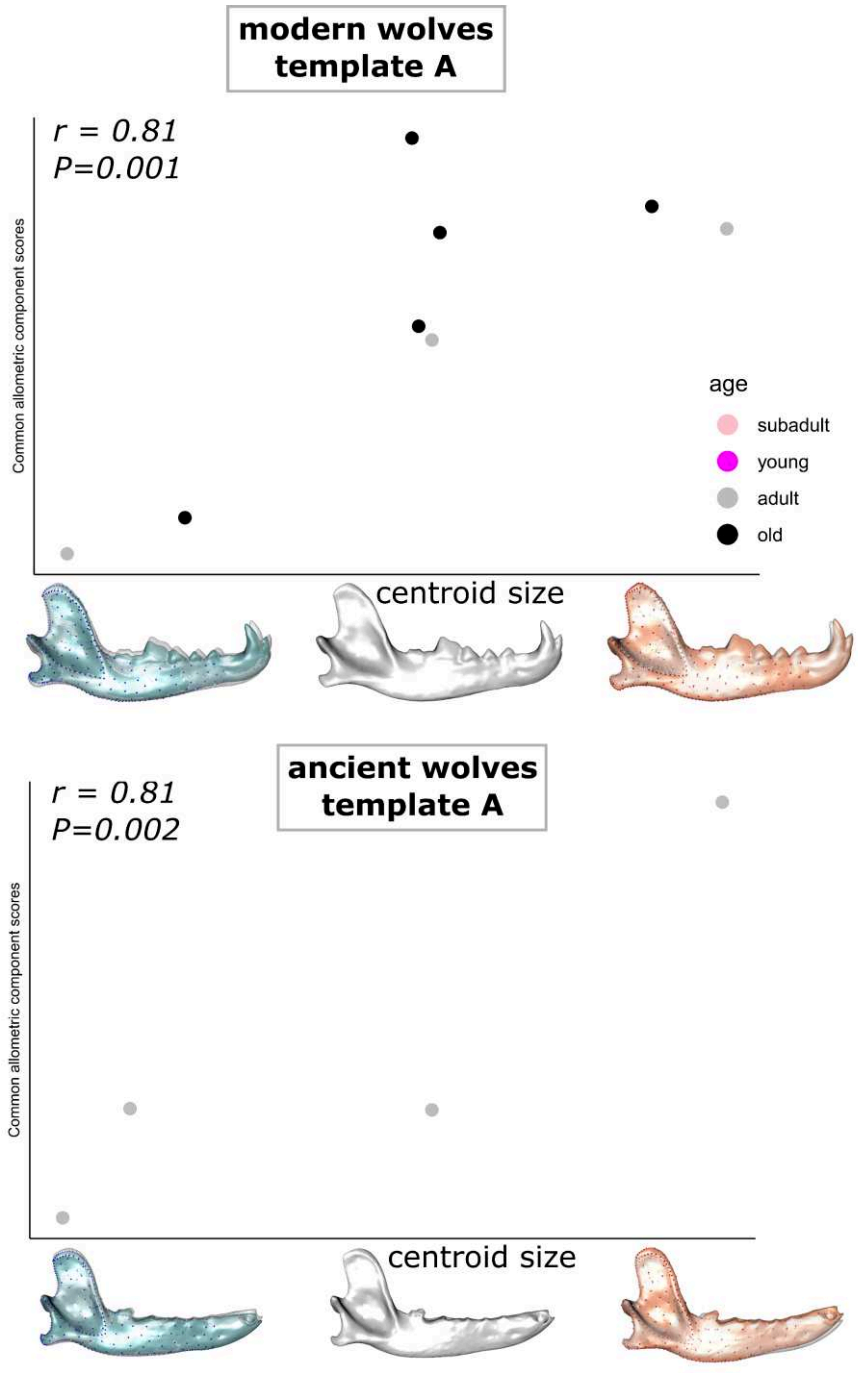

Figure 107. Deformations along the allometry slope in modern and ancient wolves.

1.2.6. Comparison of integration and modularity patterns

Morphological integration is the coordinated variation of different parts, while **modularity** refers to the formation of internally cohesive units (i.e. modules) marked by the strong interconnection among their parts and relative independence from others (Segura *et al.*, 2020; see Part 2 Chapter 2 section 1.1).

1.2.6.1. *Modularity between the anterior and posterior parts of the mandible in dogs and wolves*

While the effects of domestication on modularity have already been widely studied within the cranium (Drake and Klingenberg, 2010; Curth, Fischer and Kupczik, 2017; Curth, 2018), data are almost inexistent for the mandible. Segura *et al.* (2020) have explored modularity in many extant and extinct canid species but without looking at the effect of domestication. One point that has been mentioned, but not really explored, is the modularity between the front and back of the mandible. However, it is possible that the intensive artificial selection in modern dogs has led to a decoupling between these different parts. In other words, it is more likely that the different regions of the mandible are more highly integrated and covary stronger in ancient dogs than in modern dogs, for which the different regions may behave like separate modules.

We therefore carried out additional tests to compare modularity in the different subspecies of modern canids considered in this thesis. To quantifiy the degree of modularity between the anterior (module 1) and posterior (module 2) part of the mandible (that constitute two distinct modules), we performed a modularity test using the function "modularity.test" from package "geomorph" based on the Procrustes coordinates of template A (module 1: 150 landmarks; module 2: 30 landmarks, we did not consider surface landmarks). We performed separate analyses for the 67 modern dogs and for the 127 ancient dogs with complete mandibles. The function calculates a covariation ratio (CR) coefficient to quantify the degree of modularity and then compares it to a distribution of values obtained by randomly assigning landmarks into subsets after 1000 permutations (Adams, 2016; Adams and Collyer, 2019). Thus, the CR coefficient is a "ratio of the overall covariation between modules relative to the overall covariation within modules" (Adams, 2016).

Interestingly, our results show that **the CR coefficient is higher in modern dogs** (0.91, $P < 0.001$) **compared to ancient dogs** (0.67, $P < 0.001$). **The CR of modern dogs is not different from that of modern** (n = 8, CR = 0.93, $P < 0.001$) **or ancient wolves** (n = 4, CR = 0.93, $P < 0.002$). **The CR of modern dingoes** (n = 8, 0.79, $P < 0.001$) **is intermediate** between the CR of ancient dogs and modern dogs and wolves.

These results suggest a different modularity within the mandible of ancient dogs.

1.2.6.2. *Efficiency of each fragmentation pattern to predict the overall shape of the mandible*

The objective here is to quantify to what extent a small fragment is informative of the complete shape of the mandible. Accordingly, we explored the covariations between the shape of the complete mandible (template A) and that of all the other templates (B, C, D, E, F, G, H, I and J). The approach is different from that of the previous section given that here we look at the covariation between blocks which are not exclusive: the information related to shape and contained in block 2 (small fragment) is also completely contained in block 1 (complete template A). We performed separate covariation (2B-PLS) analyses for the 66 modern dogs (Table 26), and for the 127 ancient dogs with complete mandibles (Table 27).

The coefficients of covariation are similar in ancient and modern dogs; however, they tend to be higher in ancient dogs for the smaller fragments. This suggests that recent the artificial selection of modern breeds has altered the integration within the mandible of dogs to some degree. The patterns of covariation are overall the same in ancient and modern dogs, but the dispersion is more important for modern dogs (Figure 108, Figure 109).

The strong covariation patterns evidenced in ancient dogs also allow to make predictions of the complete shape of the mandible, based on the shape of small areas of the mandible. In a preliminary exploration of our results, we conducted parallel analyses on the predicted complete mandible, based on coordinates of template I, using the decision rules established on the three first axes of the 2B-PLS performed on ancient dogs (which represents 95% of the overall covariation). We used template I to predict the overall shape of a maximum of dog mandibles (491). However, the comparison between the results obtained from these predicted Procrustes coordinates and the real Procrustes coordinates, for the dogs with complete mandibles revealed a methodological biais that prevent us to use these predictions to infer biological meaningful results from our sample (see appendix 9 for more details).

Table 26. Results of the 2B-PLS analyses performed between the Procrustes coordinates of each template and the Procrustes coordinates of template A for the 66 modern dogs (juveniles were excluded).

Template	B	C	D	E	F	G	H	I	J
Correlation (r)	0.98	0.95	0.92	0.73	0.89	0.82	0.71	0.77	0.88
P-value	***	***	***	***	***	***	***	***	***

Table 27. Results of the 2B-PLS analyses performed between the Procrustes coordinates of each template and the Procrustes coordinates of template A for the 127 ancient dogs.

Template	B	C	D	E	F	G	H	I	J
Correlation (r)	0.98	0.98	0.97	0.81	0.97	0.94	0.89	0.91	0.96
P-value	***	***	***	***	***	***	***	***	***

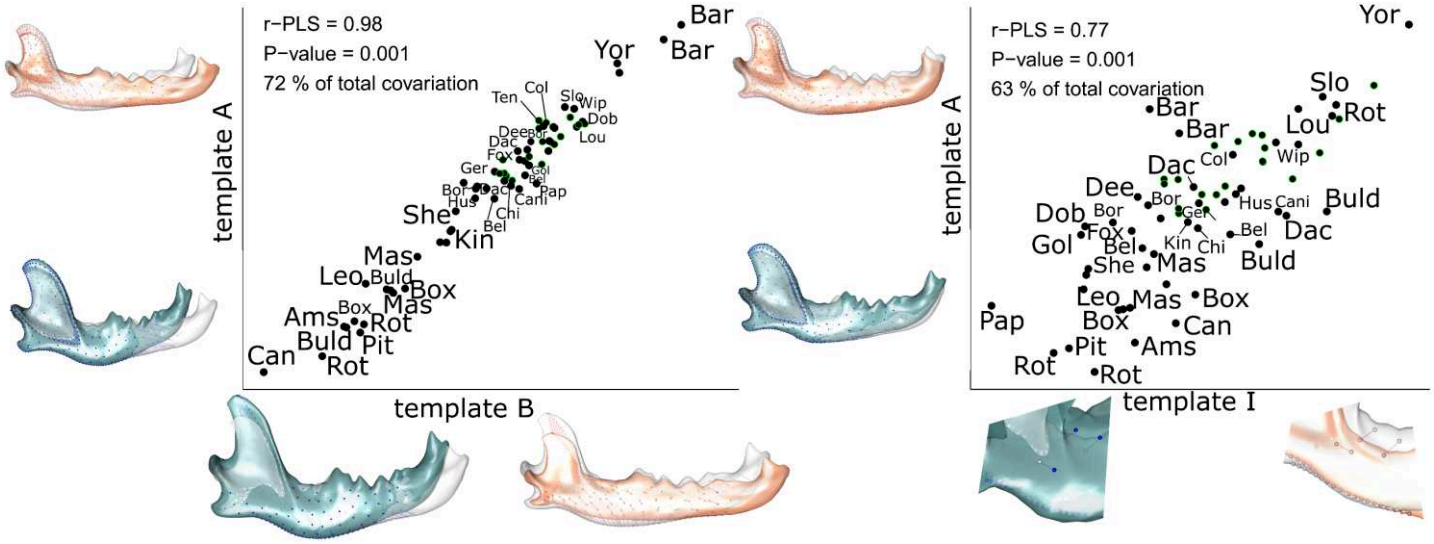

Figure 108. Visualisation of the scores and shape deformations along the first PLS axis from the 2B-PLS analyses performed on the Procrustes coordinates of template B or I and those of template A for the 66 modern dogs.

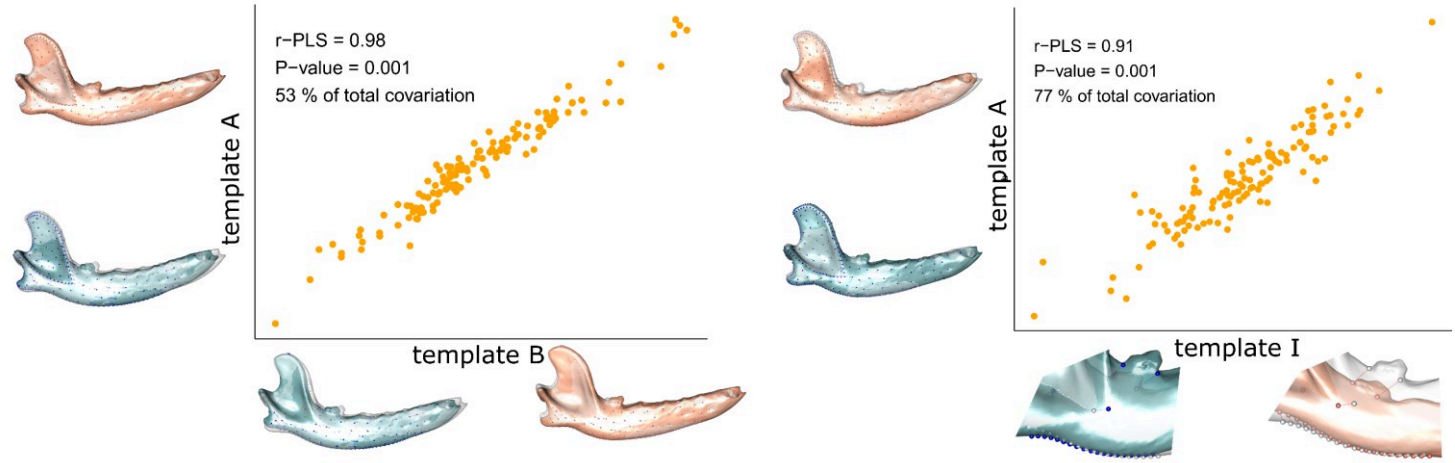

Figure 109. Visualisation of the scores and shape deformations along the first PLS axis from the 2B-PLS analyses performed on the Procrustes coordinates of template B or I and those of template A for the 127 ancient dogs.

1.2.6.3. *Efficiency of each fragmentation pattern to predict the overall shape of the cranium*

In part 2 we found strong covariations between the shape of the cranium and that of the mandible in modern dogs (Chapter 3 section 2), dingoes (Chapter 4 section 2.1) and red foxes (Chapter 4 section 1), demonstrating that the shape of the mandible is informative of the shape of the entire skull, which is of great interest for the description of morphotypes. We previously discussed the possibility of predicting cranial shape based on mandible shape. To go further in the exploitation of small fragments, we conducted exploratory analyses to study the covariations between the different fragmentation patterns and the shape of the cranium in modern dogs and dingoes. We used pls regression to build predictive models which were then applied to a few archaeological dogs for which we had reconstructed the mandible and the associated cranium using photogrammetry. **We were therefore able to compare the predicted shape with the real shape of the cranium.** For the calculation of the decision rules, we either used all the modern dogs of our corpus (to take into account the largest morphological variability possible), or we have excluded the modern dogs that are the more distant from archaeological dogs in terms of size and/or conformation based on size boxplots and classification trees build from templates A and B. **The predictions seem to be better when considering all modern dogs.** We will return to this point of methodological discussion in Chapter 8. Given the exploratory methodological aspect of this investigation, a little outside of the main objectives of this thesis, the detailed results are reported in appendix 10.

2. Comparison of modern and ancient *Vulpes*

Analyses similar to those carried out in the previous sections were performed to compare modern and ancient red foxes. The analyses were conducted for all the templates. However, considering the important fragmentation of the archaeological material, only templates E and I allow us to compare samples with fairly consistent numbers (n=32 and 40, respectively). However, **these templates only allow us to describe a small part of the mandible**. The results should therefore be interpreted with caution.

2.1. Variations in size, shape and function

The results are reported in Table 28. They indicate that **there is no significant difference in shape variability** (except for template E) **nor size variability** (except for templates E and H which is not comforted by other templates). Interestingly, **for all templates mean shapes significantly differ between the two groups**. **Differences in mean centroid sizes are significant only for templates C, E, F, H and J. This is accompanied by significant differences in absolute bite force: ancient foxes bite less strong than modern foxes. The differences in residual bite force are accompanied by a much greater variability in modern red foxes**.

Table 28. Results of the statistical performed to compare the modern and ancient red foxes.

Template	N	N	Shape		Centroid size		Bite force	
	arch	modern	Differences	Disparity	Differences (t-test)	Variance	absolute	residual
A	8	68	R2 = 0.04, P < 0.001	0.3	0.083	0.046	Modern > Ancient 0.03	Modern > Ancient 0.02
B	13	68	R2 =0.098, P<0.001	0.11	0.085	0.11	Modern > Ancient 0.003	Modern > Ancient <0.001
C	10	68	R2= 0.061, P=0.005	0.94	Modern> Ancient 0.048	0.26	Modern > Ancient 0.03	Modern > Ancient 0.07
D	22	68	R2=0.11, P<0.001	0.7	0.051	0.12	Modern > Ancient <0.001	Modern > Ancient 0.009
E	32	68	R2=0.11, P<0.001	0.01 (Arch: 0.021, Modern: 0.014)	Modern> Ancient <0.001	0.0087	Modern > Ancient <0.001	0.5
F	14	68	R2=0.04902, P<0.001	0.6	Modern> Ancient 0.0037	0.14	Modern> Ancient 0.002	0.3
G	25	68	R2=0.17888, P<0.001	0.2813	0.7	0.3	Modern > Ancient <0.001	Modern > Ancient <0.001
H	14	68	R2=0.07786, P<0.001	0.2	Modern > Ancient 0.0025	0.020	Modern > Ancient <0.001	0.08
I	40	68	R2=0.11, P<0.001	0.18	0.5	1	Modern > Ancient <0.001	Modern > Ancient <0.001
J	18	68	R2=0.10913, P<0.001	0.81	Modern > Ancient 0.0037	0.2	Modern > Ancient <0.001	Modern > Ancient 0.02

The PCAs based on template A (Figure 110), B (Figure 111), E (Figure 112) and I (Figure 113) suggest that **some ancient foxes have mandibular shapes that extend beyond the variability existing in modern European red foxes**.

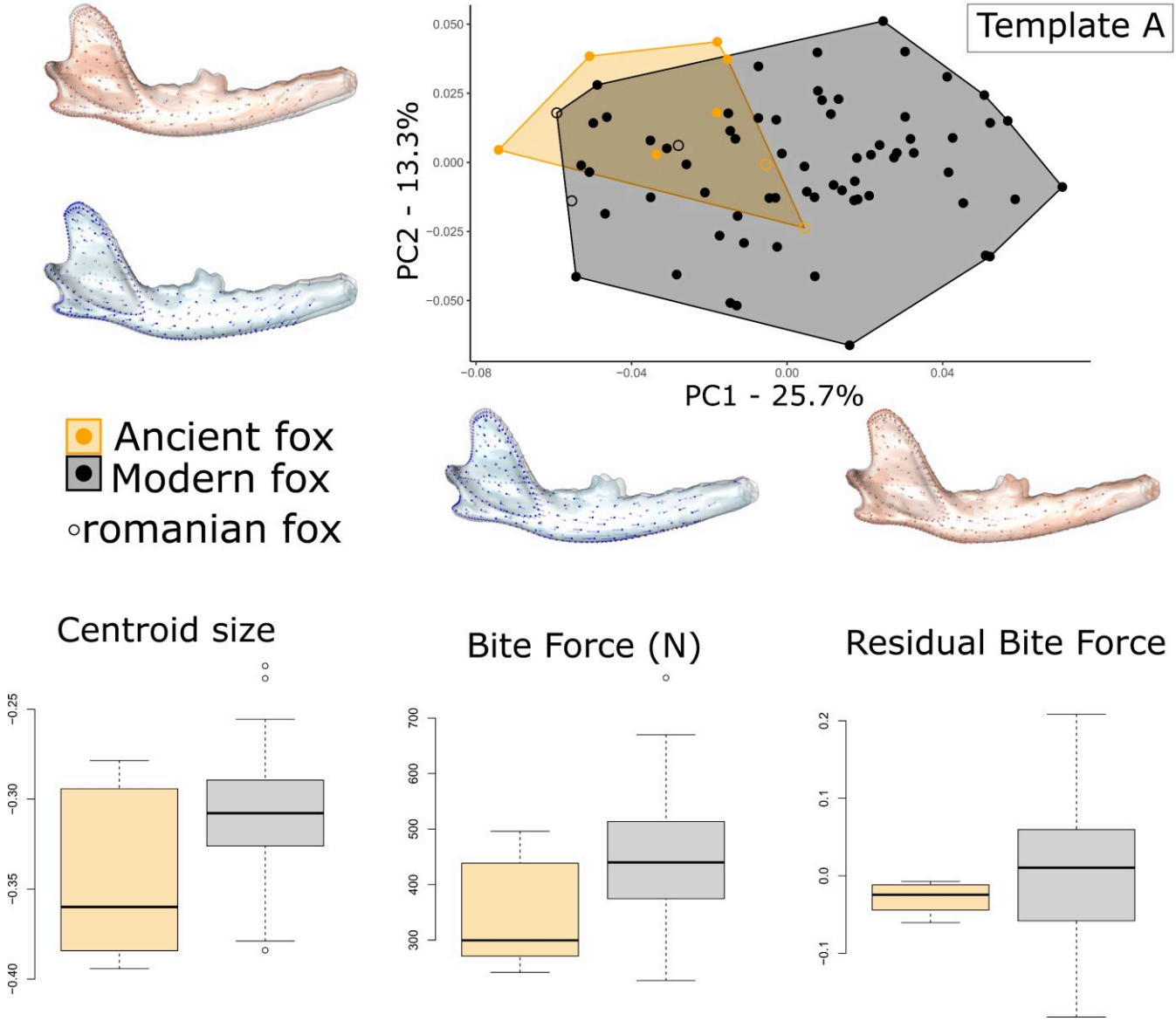

Figure 110. Comparison between modern and ancient red foxes. Analyses are performed on template A. Top: PCA; bottom: boxplot of the centroid size, bite force and residual bite force.

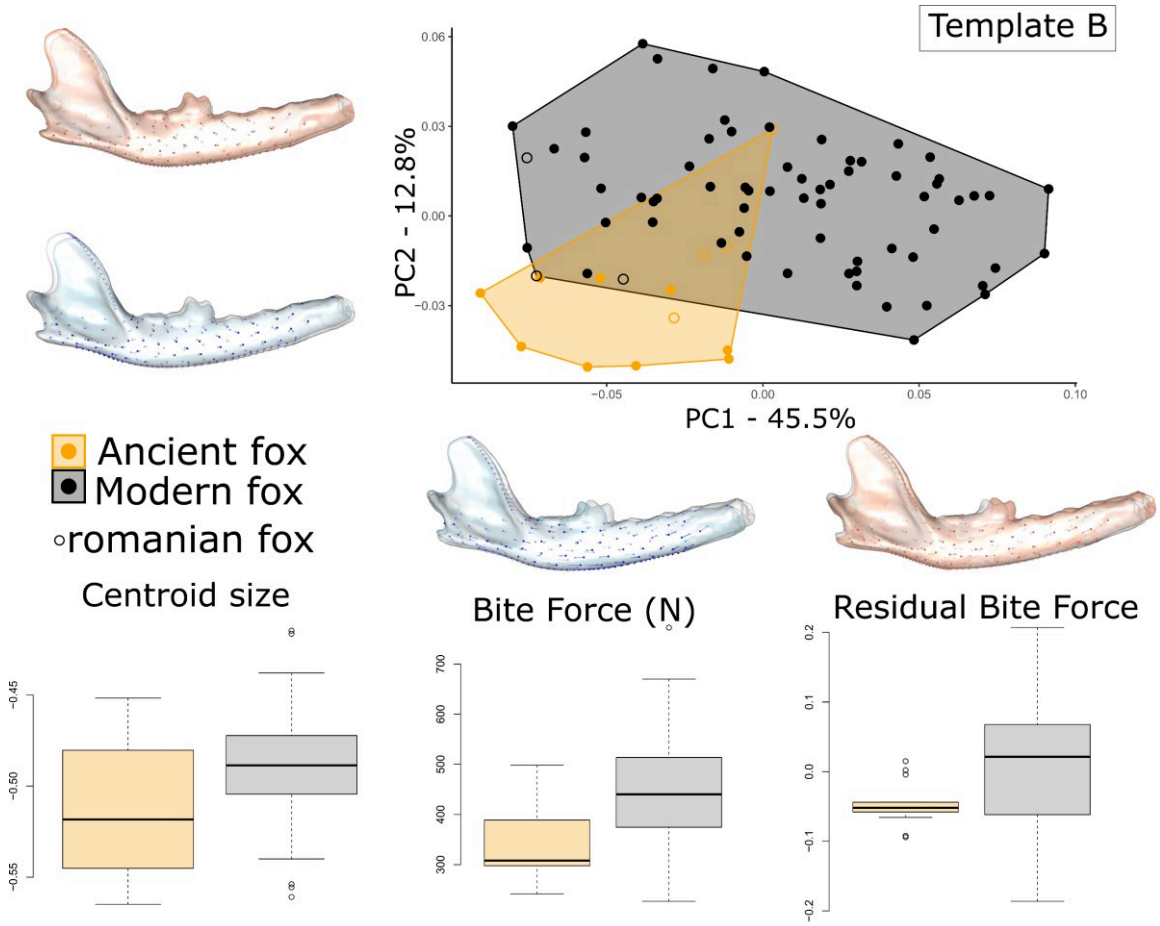

Figure 111. Comparison between modern and ancient red foxes. Analyses are performed on template B. Top: PCA; bottom: boxplot of the centroid size, bite force and residual bite force.

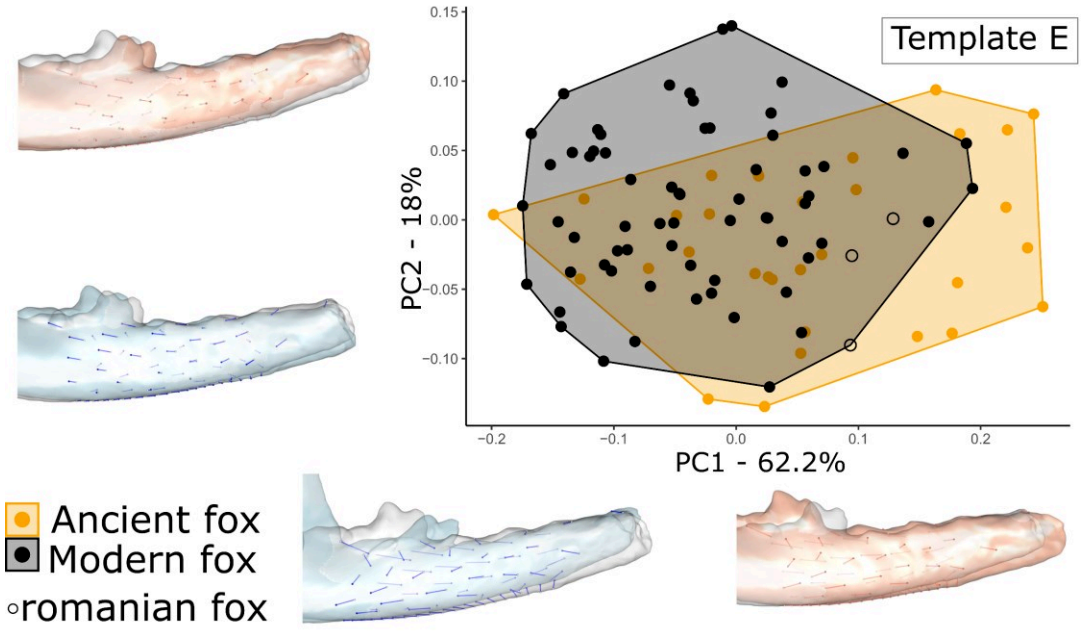

Figure 112. Comparison between modern and ancient red foxes. Analyses are performed on template E. Top: PCA; bottom: boxplot of the centroid size, bite force and residual bite force.

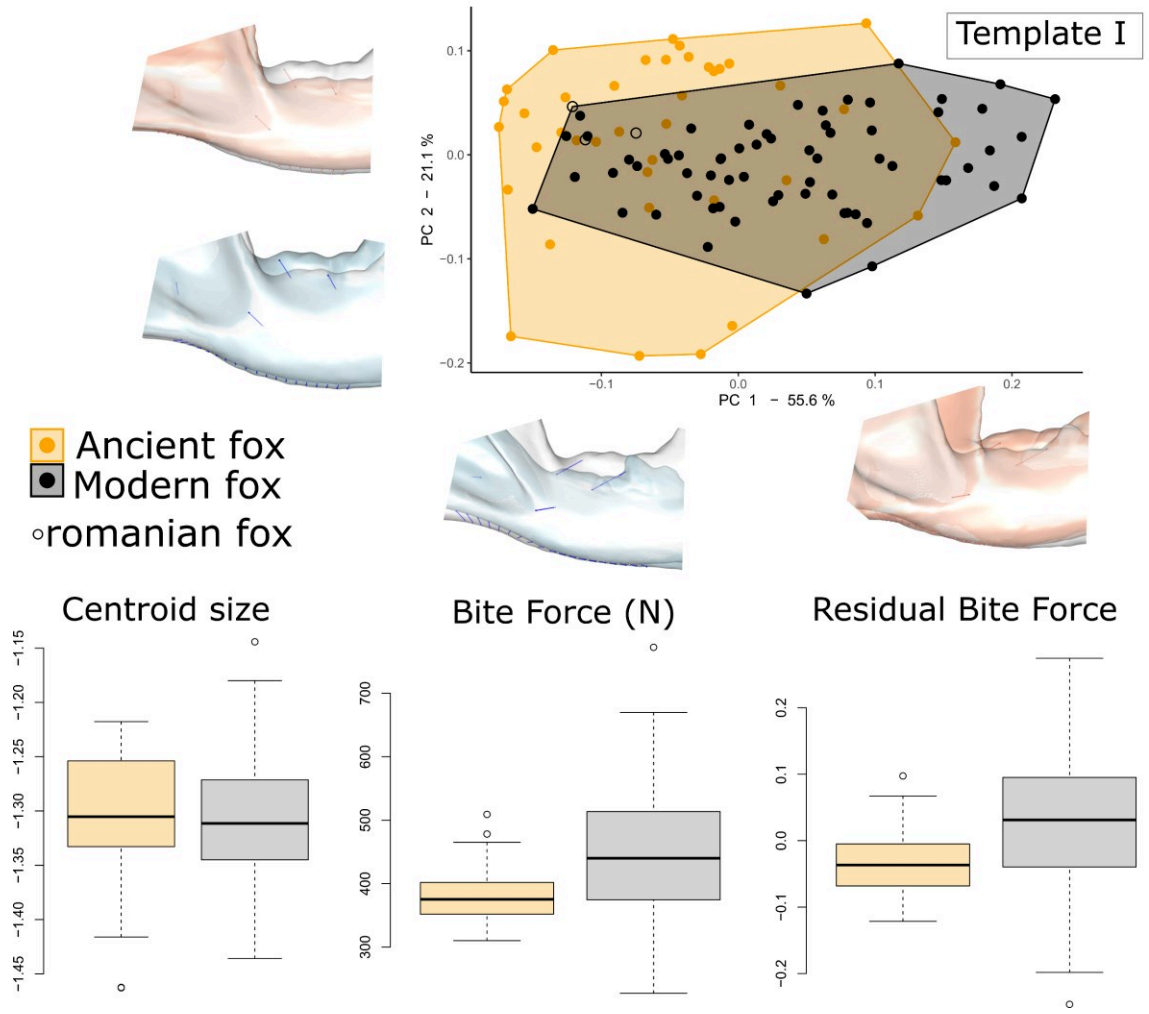

Figure 113. Comparison between modern and ancient red foxes. Analyses are performed on template I. Top: PCA; bottom: boxplot of the centroid size, bite force and residual bite force.

The CVAs based on data from templates A, B (Figure 114), E and I (Figure 115) all tend to suggest that **ancient foxes have less robust and shorter mandibles, with less pronounced muscle insertion reliefs, a shallower masseteric fossa, a shorter coronoid process, and a less marked ventral border**. These differences are consistent with the functional differences highlighted above.

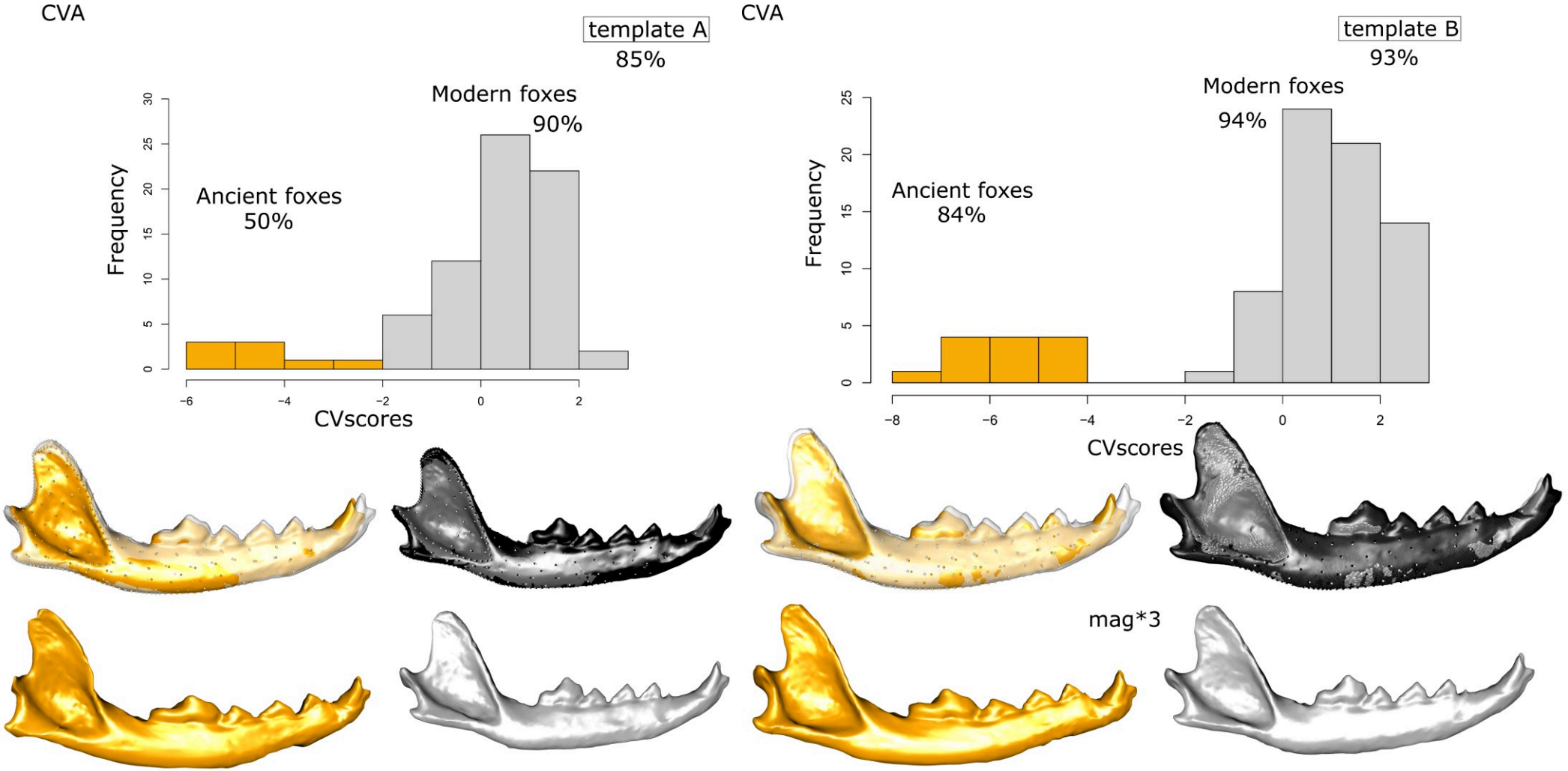

Figure 114. CVA performed on modern and ancient red foxes with template A (left) or B (right). Shapes at the minimum and maximum of CV scores are magnified by 3 (bottom) or superposed to the mean shape of the CVA and vectors of deformations between the two shapes are represented (top).

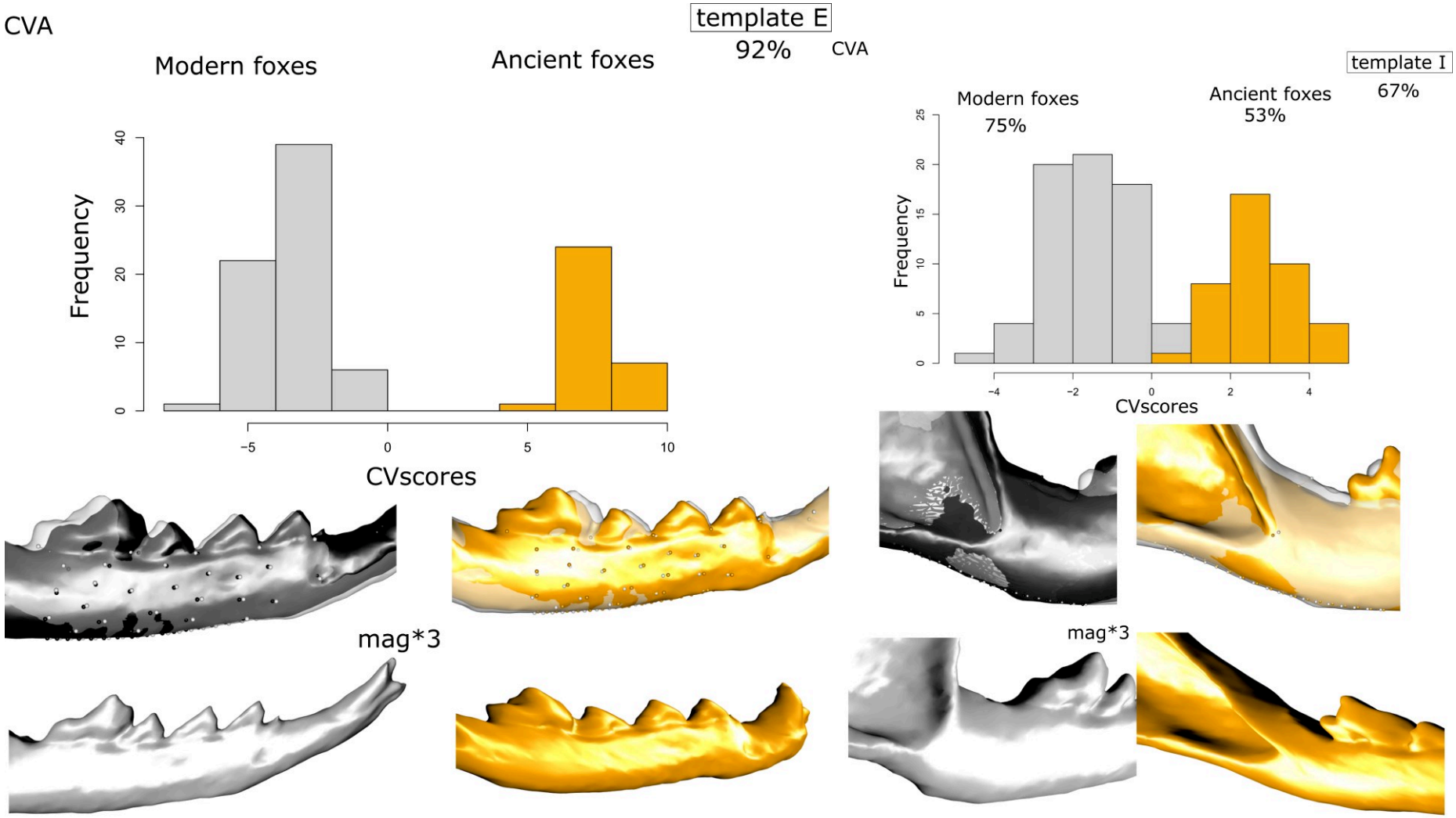

Figure 115. CVA performed on modern and ancient red foxes with template E (left) or I (right). Shapes at the minimum and maximum of CV scores are magnified by 3 (bottom) or superposed to the mean shape of the CVA and vectors of deformations between the two shapes are represented (top).

2.2. Allometries

The allometric slopes obtained for templates A and B suggest **slight differences between modern and ancient red foxes in both the slope and intercept** but these results have to be considered with caution given the low sample size (Figure 117). The deformations along the allometric trajectory are reported in Figure 116 for information purposes.

2.3. Modularity and integration within the mandible

Modularity tests based on Procrustes coordinates from template A show that **the CR coefficient of ancient red foxes** (n = 8, CR = 0.88, $P < 0.001$) **is relatively similar to that of modern red foxes** (CR = 0.79, $P < 0.001$). **The CR of modern red foxes is intermediate between the CR of ancient and modern dogs, and close to the CR of dingoes**.

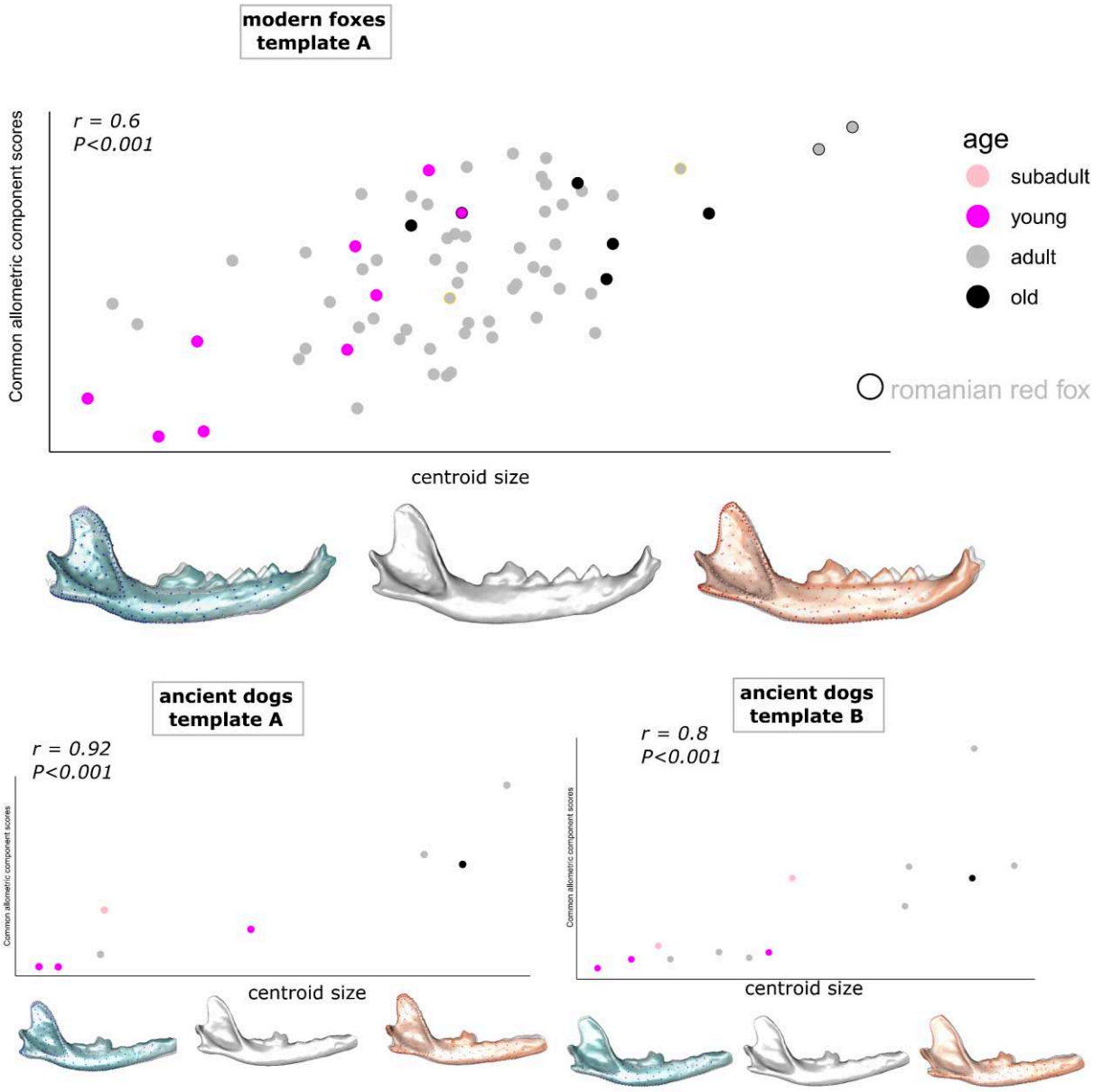

Figure 116. Deformations along the allometry slope in modern and ancient red foxes.

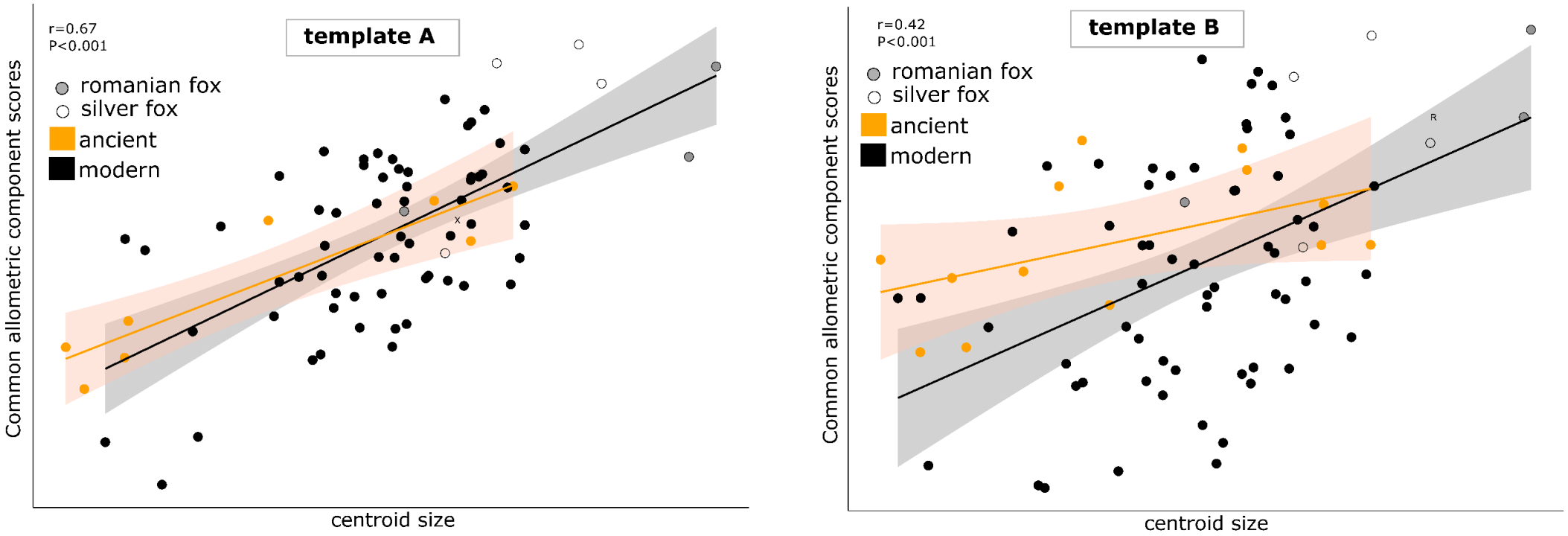

Figure 117. Allometry slope in modern and ancient red foxes. Analyses performed on template A (left) or B (right).

Conclusion

So far, we performed several analyses that provide insights into the degradation of information related to size or conformation depending on the fragmentation pattern. The following key points emerge:

KEY POINTS

All templates can be used to describe the centroid size, but templates G and I carry slightly degraded information (differences will therefore be blurred).

- ⇨ Whilst exploring archaeological data, the boxplots representing the centroid size for the 10 templates for the same individuals (the 127 complete archaeological mandibles) are compared to ensure the comparability of the results, before interpreting the boxplots obtained with template I, which has the largest sample size.

All the fragmentation patterns carry information on the complete shape of the mandible, or even that of the cranium and therefore of the morphotype (see appendix 10). However, the signal is degraded for small fragment and the use of predicted Procrustes coordinates raises methodological biases that prevent us from using them in parallel analyses.

- ⇨ Template A should be used first to describe the shape. Templates B, C, F and J provide a broadly similar picture (even though the significancy of the results may be lower) and they can be used to validate the results obtained with template A in order to increase the sample size.

- ⇨ Template A provides more accurate information about the whole morphotype, but the other templates may reflect local convergences in shape, reflecting functional convergences.

From the comparison of modern and ancient canids, the following key points emerge:

KEY POINTS

Unsurprisingly, modern dogs have mandibular forms that are more variable than dogs prior to the Bronze Age, in terms of both size and conformation.

The mandible of the ancient dogs, however, shows a rather important variability, both in terms of size and conformation (the variability in the latter being close to that of modern foxes).

The variability of ancient dogs is largely included in the variability of modern dogs and primitive and little modified breeds (loulou, husky, mastiff, beagles, podenco) are the closest to archaeological dogs.

Some morphologies of pre-Bronze Age dogs have no equivalent in our sample of modern dogs, although covering a large variability. On the contrary, some hyper brachycephalic mandibles of modern dogs have no equivalent in the archaeological sample.

We observe significant differences in the average shape of modern and ancient dogs, as well as between modern and ancient foxes, in areas suggesting functional differences.

The allometric patterns in mandible shape of ancient and modern dogs (and modern wolves) are similar, suggesting that it has not been altered by extreme artificial selection.

The relationship between the shape of the mandibular ramus and that of the body in pre-Bronze Age dogs appears to be surprisingly more relaxed than in foxes or dingoes, and even more so than in modern dogs and wolves (held in captivity) for which there appears to be a high degree of integration.

All these results lead to questions as to the relevance of using models established on modern canids to interpret animals prior to the Bronze Age.

This is a point we explored briefly in Appendix 11 “Part 3 – Chapter 7. A consequence of differences between modern and ancient canids: the inadequacy of supervised learning for species prediction”. In this appendix we show that the use of modern dogs/foxes/dingos to predict the species of ancient canids by means of CVA leads to many erroneous identifications.

Since predictive models are based on morphological variability and consider architectural relationships within the mandible, the accuracy of the predictive models may be altered when applied to specimens that are outside this variability. An additional question is to decide whether it is better to keep all modern dogs in the construction of decision rules, to increase the variability considered by the model, or whether it is preferable to exclude individuals without archaeological equivalent and adapt the model by calculating it on the canids that are morphologically closest to ancient dogs. This is a point that we discuss in Appendix 10 “Efficiency of each template to predict cranial shape” and that will need to be explored in the next chapter when adaptating the functional tools to quantify jaw function. In Appendix 10 it seems that better results are obtained when considering the maximum variability observed accross modern dogs.

Chapter 8.
Adaptation of the functional approach to the fragmentation

In this Chapter, based on results obtained in Part 2 when exploring the relations between bite force and mandible shape in modern dogs (Chapter 3 section 3) or red foxes (Chapter 4 section 1), we propose different methods to quantify the functional capacities of the jaw depending on the state of preservation of the bones.

We have used two different methods.

The first one consists in creating predictive models of the absolute bite force based on PLS regression, using data on the shape, size and muscle architecture obtained from the dissection of modern canids. This method allows prediction even for small pieces where there is no muscular attachment. However, this method only provided an absolute value of the bite force and does not provide any indication of the direction of the muscle forces.

The second method consists in estimating the mechanical potential using simple metric ratios. This method is simple and does not require any comparison with modern animals as the architecture of the jaw muscles is not precisely taken into account. However, it provides complementary information to the first method, as it provides insights on the relative contribution of the main adductors (M. temporalis, M. masseter, M. pterygoideus) to the overall force exerted by the jaw.

1. Prediction of the absolute bite force based on mandibular form for different fragmentation patterns, using data on the muscle architecture

1.1. General method

Previously, we estimated the bite forces of 47 modern dogs (Chapter 3 section 3) and 60 red and silver foxes (Chapter 4 section 1), using data on the muscle architecture (PCSA, attachment area on the skull) obtained from dissections. We showed that the mandibular shape strongly correlates and strongly covaries with bite force (or residual bite force), suggesting that shape is a good predictor of bite performance and that it could be use to infer function from archaeological remains. Here, we test whether the different fragments are good predictors of bite force. We use two-blocks partial least squares regressions to predict the bite force based on the Procrustes coordinates of the landmarks for each template.

Different models were established for dogs and foxes, for each template and to predict the bite force at two different bite points (at the canine tooth or at the carnassial tooth). A total of 40 models were thus established (10 templates * 2 species * 2 bite points).

For each bite point, each template and each species, we proceeded in 2 steps:

- Step 1: construction of the decision rules on modern canids for which bite forces were estimated from jaw muscle architecture (PCSA, attachment arear on the cranium and mandible) by means of dissections.
- Step 2: application of the decision rules to archaeological remains of the same species.

Considering that we did not include any juvenile canids (the carnassial is not erupted) in our sampling of archaeological dogs, we removed the modern canids for which the carnassial tooth was not erupted (dog Ny-C9). The foxes N-R11, N-R25 and N-R29 that were classified as juveniles in the previous chapter correspond to subadults in the classification we considered for the study of archaeological canids. They were thus included in the following analyses.

For foxes, considering that ancient foxes are included in the variability of modern foxes with regard to both shape and size, the model was established on the same 60 modern red/silver foxes (of all ages without juvenile at the preM1 stage) that we considered in article 4 in chapter 8 (see page 217). We did not use the muscular data we obtained on Australian red foxes because bite forces were estimated using a slightly different method (no microscribe, the 3D coordinates were estimated from 2D photographs, cf article 6 in Chapte 5 section 2 page 285).

The classification trees with modern and ancient dogs provided us information about the proximity between ancient dogs and modern breeds (see Chapter 7 section 1.2.2). The tree obtained with template A and B indicated that some modern breeds are morphologically distant from ancient dogs (in particular large brachycephalic dogs such as Rottweilers, Am staff, Pitbull, Boxer, Bulldog, King Charles, Cane Corso, Mastiff, and the large dolichocephalic Leonberg according to analyses with template B). Moreover, the Chihuahua and the Papillon of our modern sample are much smaller than the smallest ancient dog and the Shetland sheepdog is much larger than the largest ancient dog.

Following the discussion in the previous Chapter (see page 393), we wondered whether it was better to use all modern dogs to increase the variability in shape and muscle data considered by the model or to exclude the modern canids that have no equivalent in the archaeological record, in order to provide the most suited models for the archaeological canid sample of this thesis. We thus conducted parallel analyses, either on all adult modern dogs (46) or only on some modern adult specimens that are the closest in age, shape and size to the ancient canids, by excluding the 17 specimens cited above (N-C5, N-C16, N-C17, N-C21, N-C23, Ny-C4, Ny-C8, Ny-C14, Ny-C16, Ny-C18, Ny-C20, Ny-C21, Ny-C28, Ny-C15, N-C20, Ny-C19, Ny-C22) from the calculation of the decision rules.However, it should be noted that the modern canids with estimated bite forces represent only a reduced part of the total variation represented by all the modern canids in our sample. This is especially true for dogs as it was not possible to estimate the bite force of some beagles, nor of the barzois, podenco, yorkshires, etc. The reference sample used for the construction of the model thus covers only a part of the variability of shapes described by the archaeological dogs, as shown by PCAs performed on Procrustes coordinates of templates A and B (Figure 118).

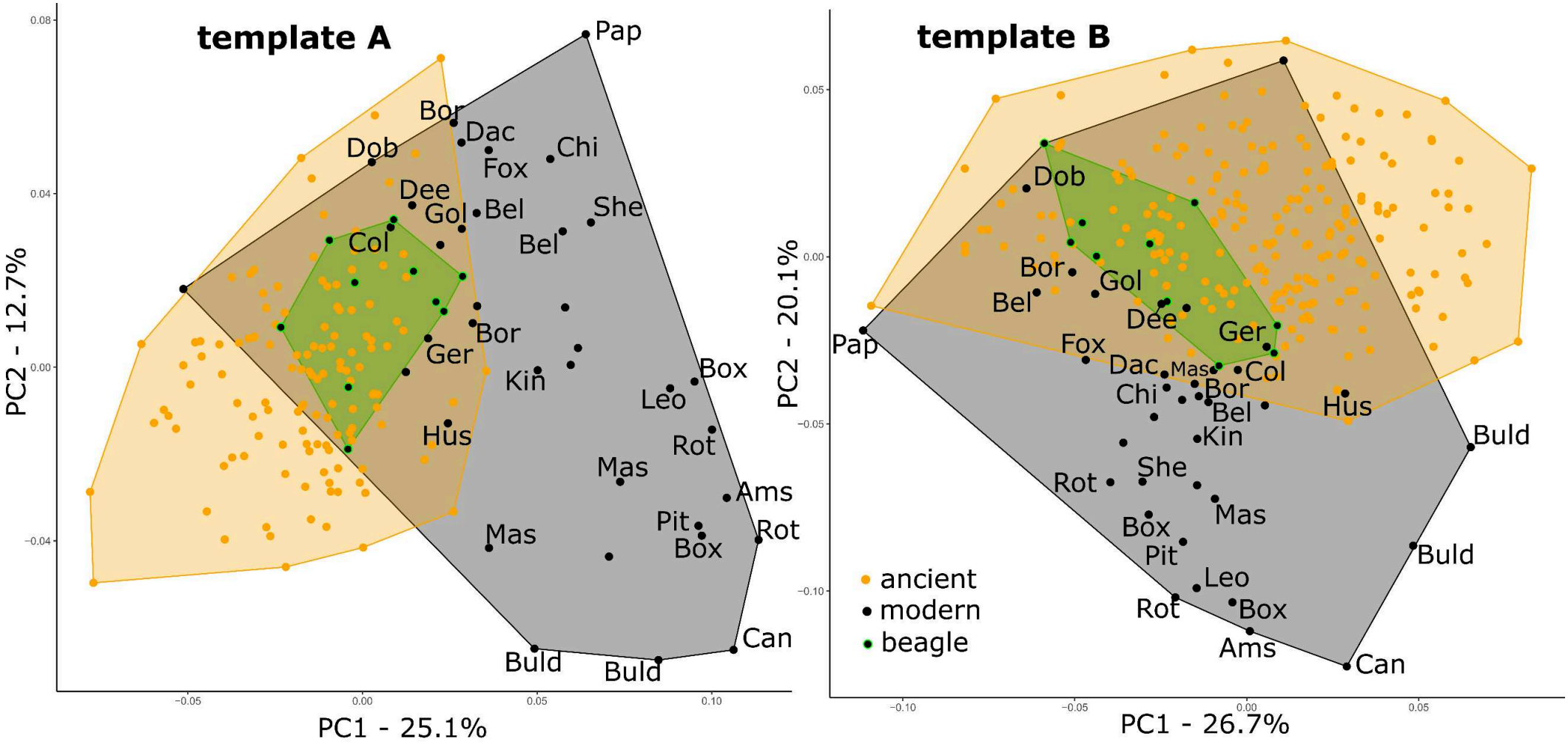

Figure 118. Principal Component Analysis performed on mandible shape for all dissected dogs (n= 46, black) and ancient dogs (orange) included in template A (n=147) and B (n= 228). Beagles are circled in green.

The PCAs performed on the Procrustes coordinates of template I show that a lot of variability is lost and a large part of the archaeological shapes is no longer described by the modern dogs when reducing the reference sample of modern dogs to 29 dogs (Figure 119). Given this, it may be more interesting to retain as many individuals as possible. Furthermore, not all the information in form contributes to bite force (the relevant information is given by the covariation axis), and another more relevant selection criterion might be to ensure that archaeological dogs are included in the area of covariation (between conformation and bite force) of modern dogs. We will explore this point in the next paragraph by projecting the archaeological individuals into the 2B-PLS covariation graphs.

Considering that the aim is to apply the model to the ancient canids, we could not use the raw landmark coordinates. All the mandibles needed to be in the same reference frame. We thus conducted a GPA to superimpose all specimens (modern and archaeological canids). Consequently, a new GPA needs to be performed each time a new archaeological specimen is added to the sample. This means that the decision rules depend on the sample. We showed in article 6 (chapter 5 section 2) that the Euclidean distance between landmarks that correspond to in or out-lever arms can be used, but this method leads to less accurate predictions. To take into account size in our predictive model, we concatenated the Procrustes coordinates (gpa$rotated) and the log10 of the centroid size (gpa$size). The models to predict the bite force (BF) were calculated using the function “pls2B” from the package “Morpho”, as follows:

```
Model <- pls2B (log10(BF) ~ cbind (two.d.array(gpa$rotated, log10(gpa$size) )
```

Bite force and size were log-transformed to normalize the data. The 2B-PLS analyses results in only one PLS axis, given that there is a single variable in bloc 2 (bite force).

To make predictions, we used the function “predictPLSfromData” from the package “Morpho”. This function returns a vector of predicted bite forces (in log10). The absolute bite force can be deduced from the log10 of the predicted bite forces as $10^{\text{predicted BF}}$.

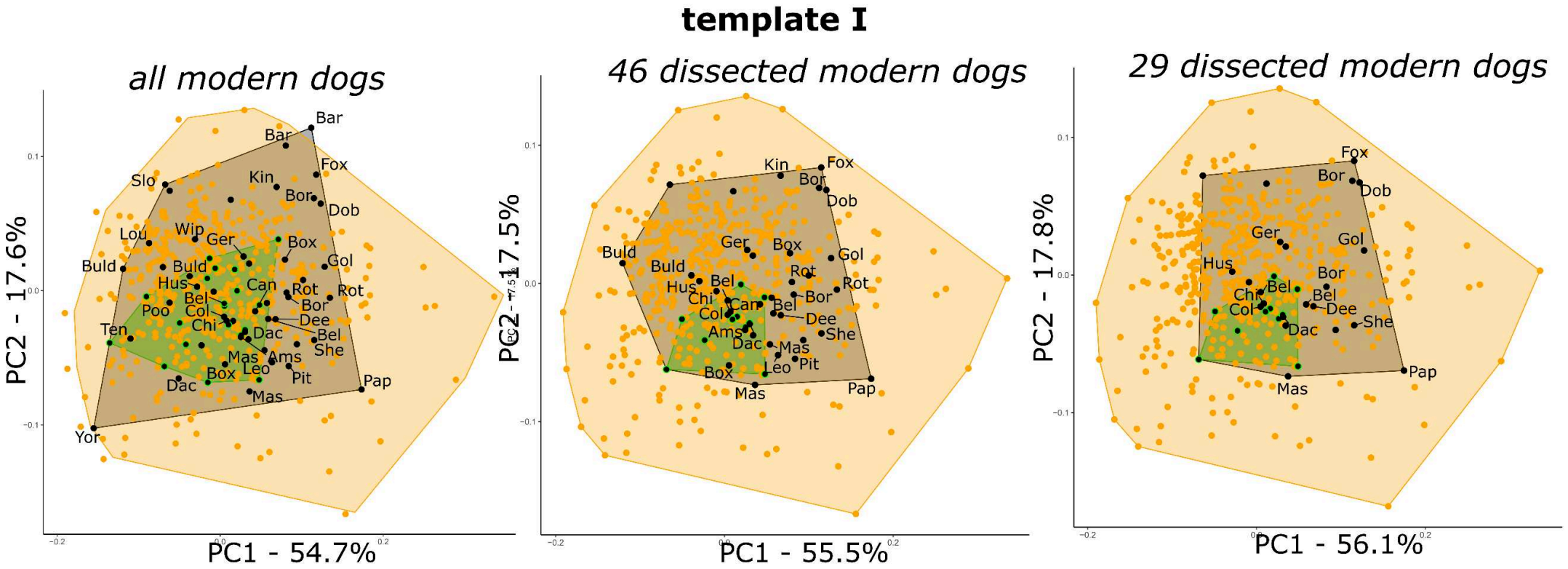

Figure 119. Principal Component Analysis performed on mandible shape for all modern dogs of our corpus, or on the 46 dogs with estimated bite forces, or on a reduce sample of 29 modern dogs, and on ancient dogs included in template I (n=491). Modern dogs are in black and archaeological dogs are in orange. Beagles are in the green polygon.

1.2. Results

In order to evaluate the functional interest of each template in modern dogs and foxes, we looked at the coefficient of covariation between the form (shape and size) and the bite force, and the corresponding P-value computed after 1000 permutations. This coefficient reflects the accuracy of the predictions for each template in comparison with bite forces estimated from dissection. Indeed, it corresponds to the coefficient of correlation between model inputs (bite force estimated from dissection) and outputs (PLS predictions) for each model for the same individuals that were used to establish the decision rules (30 modern dogs for the model with dogs and 60 foxes for the model with foxes).

PLS scores were plotted and shape deformations along the PLS axis of block 1 were calculated. The function "getPLSscores" was used to project the new PLS1 scores of block 1 (mandible shape) and block 2 (bite force) for all new (archaeological) individuals in this plot. The aim was to visualise whether ancient canids are included in the area of covariation occupied by modern canids.

1.2.1. Covariation between the form (size and shape) and bite force

The results of the 2B-PLS are reported in Table 29, Table 30 and Table 31.

Covariations are significant for all templates for both foxes and dogs.

For dogs, the covariations are stronger when all the dogs are considered (likely because more variation in size is included in the model and covariations are mainly driven by size). When only 29 dogs are used to build the model, template E appears not to be a good predictor of bite force.

Additionally, Figure 120 shows that archaeological dogs are included in the covariation area of modern dogs only when the 46 modern dogs are used for the construction of the model. When 29 dogs are used for the construction of the model, ancient dogs extend far beyond on the left part of the graph.

For this reason, it seems more appropriate to base our predictive model on the maximum number of modern dogs for which we have been able to estimate bite force (46).

In foxes, the covariation is significant but relatively low for templates E and I, that enable to describe a maximum number of the ancient foxes. The archaeological foxes project in the area of variation of modern foxes in the PLS regression (Figure 121).

Table 29. Coefficients of covariation obtained in the 2B-PLS analyses performed between the bite force and the form (shape and size) for the 60 modern foxes. Significant results are written in blue.

		A	B	C	D	E	F	G	H	I	J
Canine	r-PLS	0.78	0.76	0.77	0.62	0.48	0.79	0.62	0.71	0.47	0.71
	P	<0.001	<0.001	<0.001	<0.001	<0.001	<0.001	<0.001	<0.001	0.004	<0.001
Carnassial	r-PLS	0.78	0.76	0.77	0.62	0.48	0.78	0.61	0.71	0.45	0.71
	P	<0.001	<0.001	<0.001	<0.001	<0.001	<0.001	0.003	<0.001	0.009	<0.001

Table 30. Coefficients of covariation obtained in the 2B-PLS analyses performed between the bite force and the form (shape and size) for the 29 modern dogs. Significant results are written in blue.

		A	B	C	D	E	F	G	H	I	J
Canine	r-PLS	0.68	0.67	0.66	0.70	0.55	0.69	0.69	0.68	0.70	0.67
	P	<0.001	<0.001	<0.001	<0.001	0.034	<0.001	<0.001	<0.001	<0.001	<0.001
Carnassial	r-PLS	0.61	0.59	0.59	0.63	0.50	0.63	0.63	0.61	0.63	0.59
	P	<0.001	0.002	0.002	<0.001	0.063	<0.001	0.005	<0.001	0.003	0.004

Table 31. Coefficients of covariation obtained in the 2B-PLS analyses performed between the bite force and the form (shape and size) for the 46 modern dogs. Significant results are written in blue.

		A	B	C	D	E	F	G	H	I	J
Canine	r-PLS	0.82	0.81	0.78	0.76	0.76	0.82	0.79	0.82	0.78	0.80
	P	<0.001	<0.001	<0.001	<0.001	<0.001	<0.001	<0.001	<0.001	<0.001	<0.001
Carnassial	r-PLS	0.81	0.80	0.77	0.75	0.74	0.81	0.75	0.81	0.77	0.79
	P	<0.001	<0.001	<0.001	<0.001	<0.001	<0.001	<0.001	<0.001	<0.001	<0.001

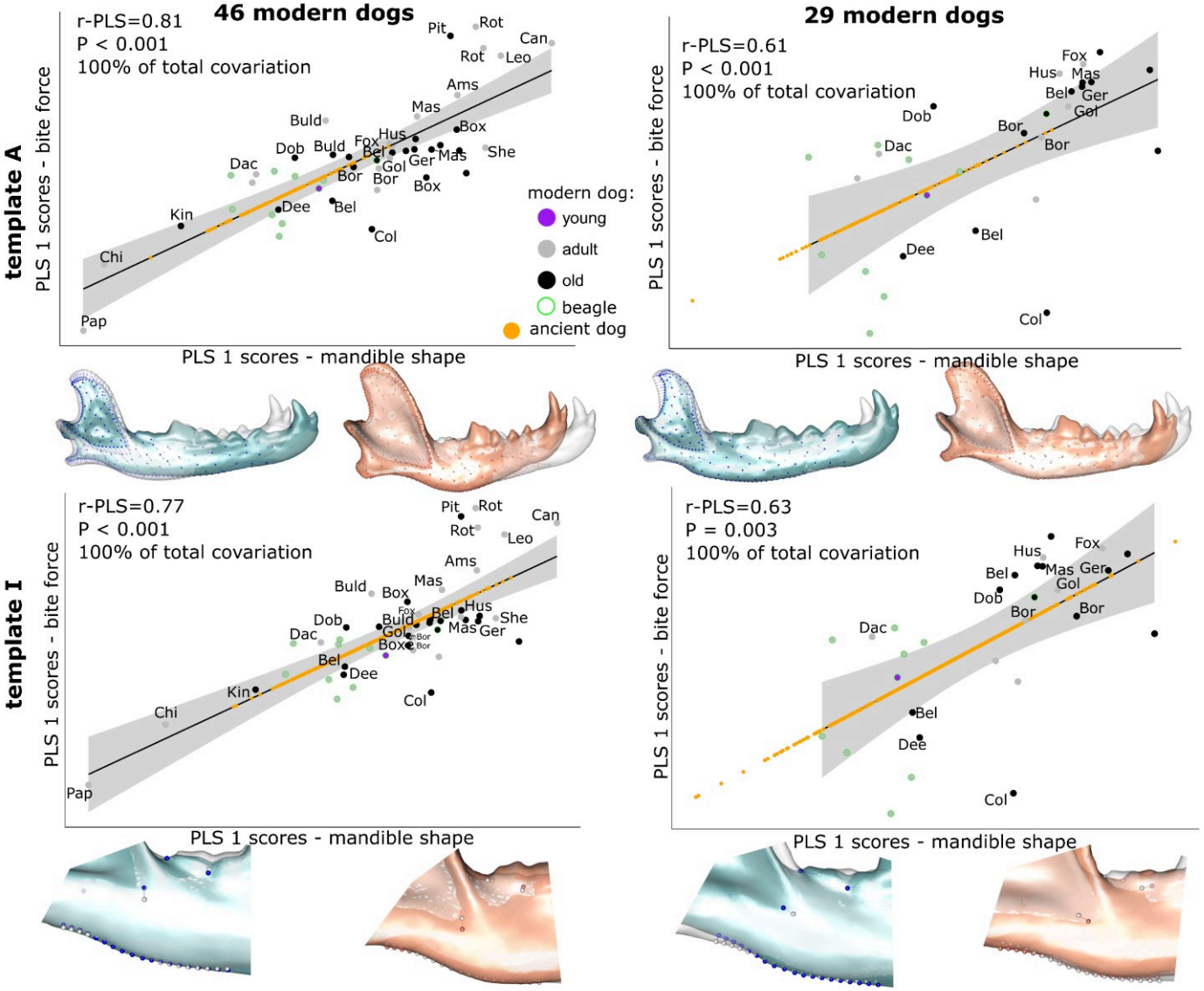

Figure 120. 2-Block Partial Least Square analyses between mandibular form (shape and centroid size) and bite force at the carnassial teeth with visualisation of shape deformation along the PLS axis in modern dogs and projection of archaeological dogs (n=147 for template A and n= 491 for template I).

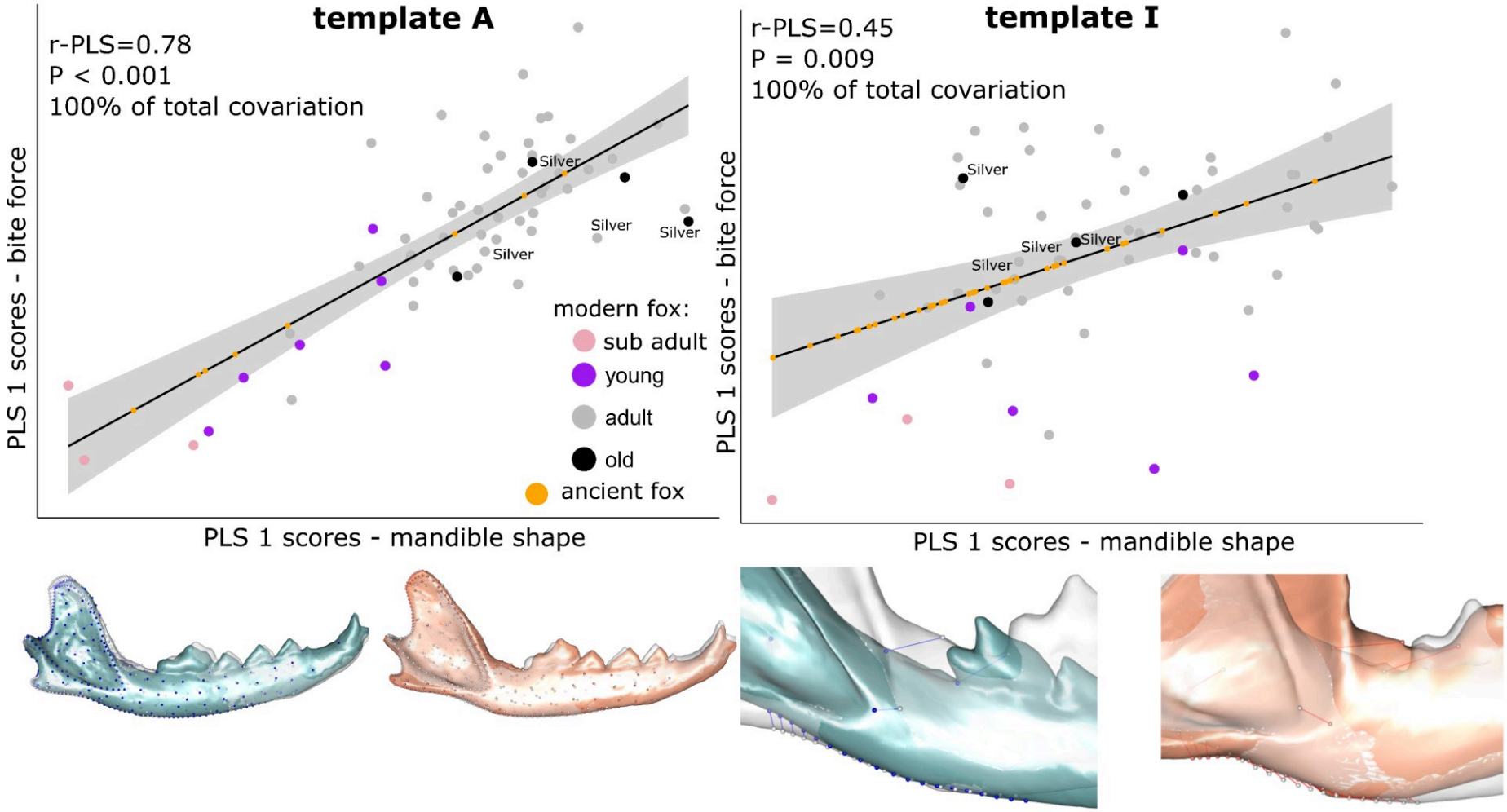

Figure 121. 2-Block Partial Least Square analyses between mandibular form (shape and centroid size) and bite force at the carnassial teeth with visualisation of shape deformation along the PLS axis in modern foxes and projection of archaeological foxes (n=8 for template A and n= 41 for template I).

To further explore the functional relations between shape and bite force, we performed 2B-PLS between analyses without size. The following results helped determine the reliability of each fragment type to predict bite force.

1.2.2. Covariation between shape and bite force

The results of the 2B-PLS are reported in Table 32 and Table 34.

For foxes, results are similar to those including shape plus size but the covariations are lower.

Once again, the results are much better when all dogs are taken into account in the construction of the model because size drives the covariations. Here we notice that the shape of template I (without centroid size) is not relevant to predict the absolute bite force. When only 29 dogs are considered, only the complete mandibles (template A) predict the bite force correctly.

Table 32. Coefficients of covariation obtained in the 2B-PLS analyses performed between the bite force and the shape for the 60 modern foxes. Significant results are written in blue.

		A	B	C	D	E	F	G	H	I	J
Canine	r-PLS	0.62	0.47	0.46	0.38	0.37	0.60	0.44	0.53	0.38	0.41
	P	0.001	0.009	0.013	0.024	0.015	0.001	0.001	0.007	0.008	0.004
Carnassial	r-PLS	0.61	0.47	0.44	0.36	0.36	0.59	0.42	0.53	0.36	0.41
	P	0.001	0.009	0.019	0.023	0.013	0.001	0.002	0.007	0.013	0.005

Table 33. Coefficients of covariation obtained in the 2B-PLS analyses performed between the bite force and the shape for the 29 modern dogs. Significant results are written in blue.

		A	B	C	D	E	F	G	H	I	J
Canine	r-PLS	0.68	0.61	0.65	0.76	0.37	0.65	0.53	0.58	0.43	0.53
	P	0.01	0.07	0.04	0.2	0.3	0.07	0.07	0.1	0.09	0.03
Carnassial	r-PLS	0.66	0.58	0.64	0.74	0.34	0.66	0.52	0.57	0.412	0.52
	P	0.02	0.2	0.1	0.3	0.4	0.09	0.06	0.2	0.1	0.06

Table 34. Coefficients of covariation obtained in the 2B-PLS analyses performed between the bite force and the shape for the 46 modern dogs. Significant results are written in blue.

		A	B	C	D	E	F	G	H	I	J
Canine	r-PLS	0.77	0.78	0.77	0.76	0.74	0.66	0.50	0.62	0.53	0.57
	P	0.001	0.001	0.001	0.001	0.01	0.001	0.007	0.001	0.2	0.01
Carnassial	r-PLS	0.74	0.74	0.74	0.73	0.70	0.64	0.48	0.60	0.51	0.55
	P	0.001	0.001	0.001	0.001	0.009	0.004	0.03	0.005	0.26	0.01

1.2.3. Covariation between shape and residual bite force

The results of the 2B-PLS are reported in Table 35, Table 36 and Table 37.

In red foxes, the shape of all fragments (except D and E) are informative of the bite force relative to the centroid size.

Once again, the results are much better when all dogs are considered in the construction of the model. In the model built with 46 modern dogs, all templates (except F, G and J) are informative of the bite force relative to the centroid size. Template I seems to be relevant to predict the residual bite force, however the covariation coefficient is relatively low (0.50 for the carnassial) and P-values are barely significant.

Table 35. Coefficients of covariation obtained in the 2B-PLS analyses performed between the residual bite force and the shape on the 60 modern foxes. Significant results are written in blue.

		A	B	C	D	E	F	G	H	I	J
Canine	r-PLS	0.55	0.46	0.45	0.29	0.28	0.58	0.63	0.48	0.53	0.53
	P	0.001	0.002	0.002	0.1	0.4	0.001	0.001	0.01	0.001	0.001
Carnassial	r-PLS	0.54	0.45	0.44	0.28	0.29	0.59	0.61	0.49	0.51	0.51
	P	0.001	0.001	0.001	0.1	0.2	0.001	0.001	0.01	0.001	0.001

Table 36. Coefficients of covariation obtained in the 2B-PLS analyses performed between the residual bite force and the shape on the 29 modern dogs. Significant results are written in blue.

		A	B	C	D	E	F	G	H	I	J
Canine	r-PLS	0.70	0.57	0.53	0.57	0.28	0.70	0.61	0.57	0.50	0.55
	P	0.6	0.9	0.7	0.8	0.4	0.27	0.021	0.13	0.027	0.2
Carnassial	r-PLS	0.70	0.55	0.53	0.54	0.25	0.72	0.61	0.57	0.48	0.56
	P	0.5	0.8	0.6	0.7	0.7	0.23	0.041	0.13	0.037	0.15

Table 37. Coefficients of covariation obtained in the 2B-PLS analyses performed between the residual bite force and the shape on the 46 modern dogs. Significant results are written in blue.

		A	B	C	D	E	F	G	H	I	J
Canine	r-PLS	0.66	0.67	0.63	0.74	0.61	0.69	0.55	0.64	0.51	0.61
	P	0.001	0.001	0.001	0.001	0.001	0.1	0.07	0.001	0.03	0.3
Carnassial	r-PLS	0.61	0.62	0.58	0.70	0.58	0.67	0.54	0.59	0.50	0.58
	P	0.001	0.001	0.001	0.001	0.001	0.1	0.08	0.004	0.04	0.3

1.2.4. Applicability to ancient dogs

We have demonstrated that ancient dogs extend beyond the range of morphological variation of modern dogs, in particular those for wich we have predicted bite forces. Extrapolating the model to a range of variation initially not anticipated by the model may cause problem while applying the decision rules to ancient dogs and may lead to distorted results.

In order to check whether estimations obtained using the PLS models are equivalent for all templates in ancient dogs (if this is not the case it suggests that morphological differences impact the reliability of the model), we compared the estimations obtained for the 10 templates for the 127 dogs with the most complete mandibles (and for the modern dogs that were used to establish the decision rules of the models). We performed ANOVAs and post-hoc tests using the functions “aov” and “TukeyHSD”.

Results are represented in Figure 122 and Figure 123. As expected, there is no difference in means for the modern dogs that participated in the construction of the model. As for ancient dogs, we found significant differences between template A and templates C, D, G and I when the model is based on 46 modern dogs and between templates A and templates C, D, E, G and I when the model is based on 29 modern dogs. These templates tend to overestimate the bite force in comparison with estimations provided by template A. As a consequence, the predicted bite force obtained using the different templates cannot be grouped together in the same analyses to interpret ancient dogs. Separate analyses must be performed for each template. However, the trends observed within the same analyses with each template can be compared since the predicted bite force using the different templates are correlated. The dispersion around the regression line is more important for template I.

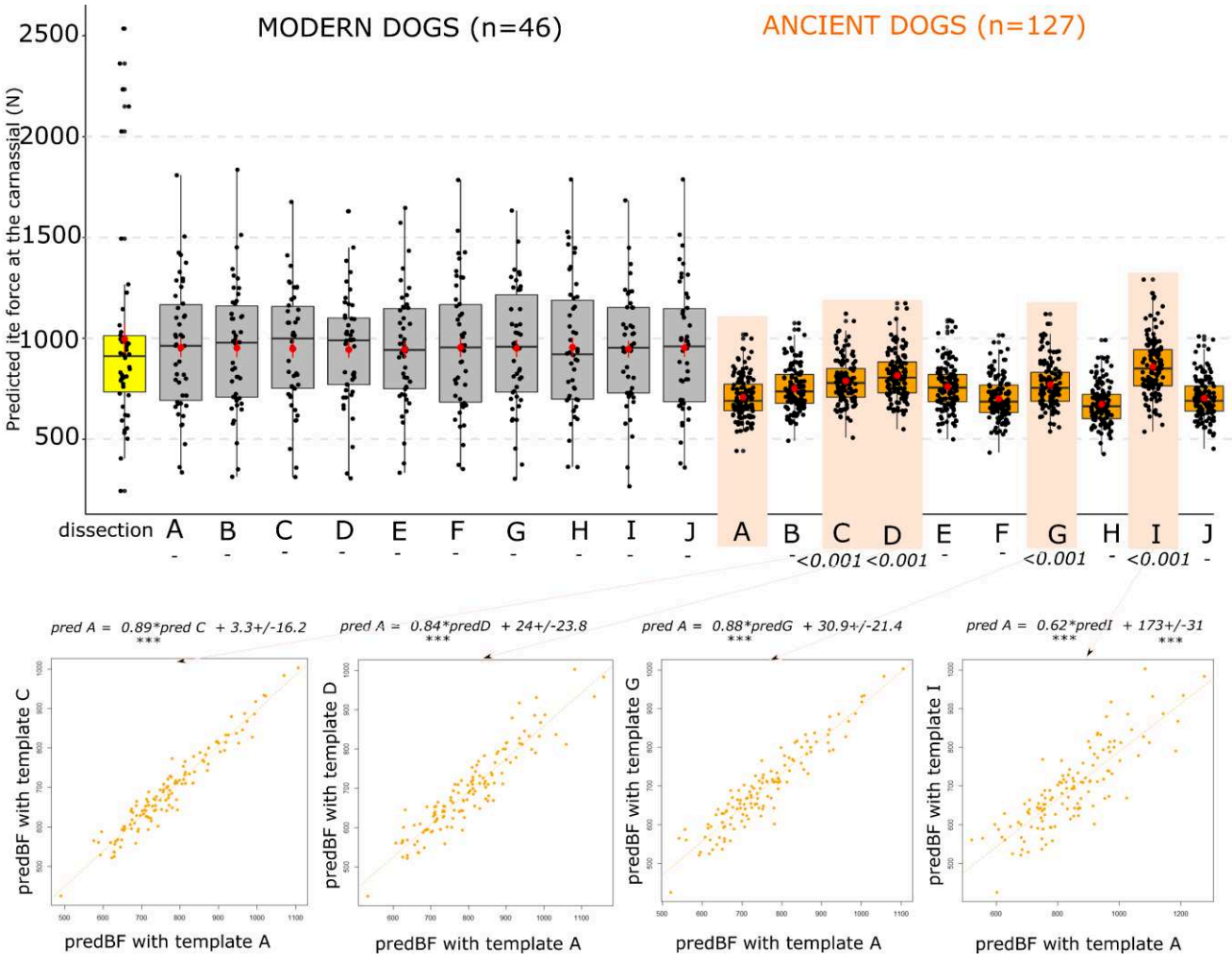

Figure 122. Comparison of the predicted bite force using the 2B-PLS models for all templates in the 46 modern dogs used to build the models and the 127 ancient dogs with complete mandibles. ***: adjusted P-value of the Tukey HSD test < 0.001.

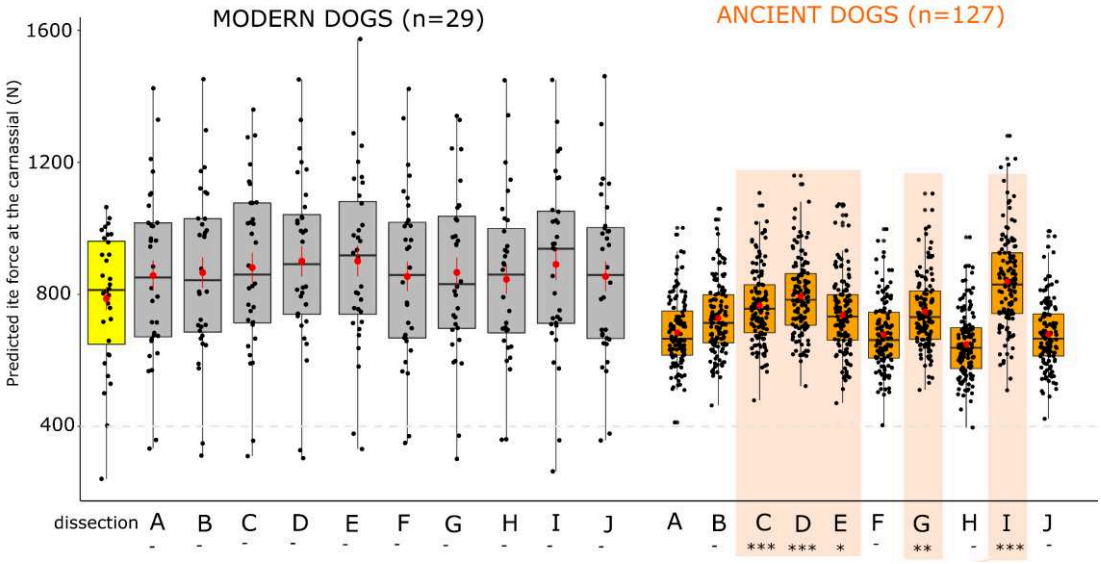

Figure 123. Comparison of the predicted bite force using the 2B-PLS models for all templates in the 29 modern dogs used to build the models and the 127 ancient dogs with complete mandibles. ***: adjusted P-value of the Tukey HSD test < 0.001.

2. Mechanical potential

This approach brings complementary information to the predicted absolute bite force. The calculation of the **mechanical potential** allows to account for the relative contribution of different muscles to the bite force. More precisely, the mechanical potential of each muscle corresponds to the ratio of the moment arm of the force exerted by the muscle over the lever arm of the resulting bite force at a given bite point (outlever).

Our method is based on that of Carraway *et al.* (1996), who calculated the mechanical potential of a muscle as the ratio of the in-lever (distance between the point of application of the muscle force and the centre of rotation of the system) and the out-lever arm (distance between the point of application of the bite force and the centre of rotation of the system). Carraway and colleagues did not consider, however, the muscle moment arm (that is to say the shortest or perpendicular distance between the centre of rotation of the system and the force vector.

In the present thesis, we used an adaptation of this method to take into account the muscle moment arms in the calculations, as previously performed by Kouvari, Herrel and Cornette (*under review*) and Cornette *et al.* (2012) in shrews.

We calculated the mechanical potential (MP) of the temporalis (MPtemp), of the masseter (MPmass) and of the pterygoideus (MPpter). For this purpose, we approximated the direction of the force exerted by each muscle from a few key landmarks whose raw coordinates (without Procrustes superimposition because we do not want to scale the bones, size matters) were extracted from the templates A, F and J (Figure 124). Not all templates could thus be exploited.

To represent the force exerted by the temporal muscle, we created a vector that takes its origin at the mid-point between landmark 2 and the middle between landmarks 3 and 4 (m2), and who's direction is given by the midpoint between landmarks 3 and 4 (m1). The perpendicular between this vector and the centre of rotation (landmark 5, il) corresponds to the the moment arm of the temporal muscle. This assumes no variation in the origin of the muscle on the cranium. The moment arm thus depends on the inclination of the coronoid process relative to the axis of the mandible.

We considered that the out-lever arm was the distance between the centre of rotation of the system (landmark 5) and the caudal border of the alveolus of the carnassial tooth (landmark 1, olm) or that of the canine tooth (landmark 1', olc). It is therefore assumed that the bite force is oriented perpendicular to this line.

The mechanical potential at the carnassial was calculated for the mandibles included in templates A, F or J as follows:

$$MP_{temp} = \frac{\mathrm{ilFt}}{\mathrm{olBFm}}$$

Additionally, we calculated the mechanical potential at the canine for the mandibles included in template A:

$$MP_{temp} = \frac{\mathrm{ilFt}}{\mathrm{olBFc}}$$

We also calculated the angle between the force exerted by each muscle and the bite force (at the canine or carnassial tooth):

$$FA_{temp} = 90 - \left(\widehat{\vec{il}, \vec{olm}}\right)$$

The same way, the moment arm of the masseter muscle was calculated by creating a vector that takes its origin at the landmark 6 and whose direction is given by the midpoint between m1 and m2 (m3). The moment arm of the pterygoid muscle was calculated by creating a vector that takes its origin at the landmark 6 and whose direction is given by the midpoint between landmark 2 and m2 (m4). The moment arms of the masseter and pterygoid muscles thus depend on the shape of both the angular and coronoid processes.

For all analyses we used the log10 of the mechanical potential values.

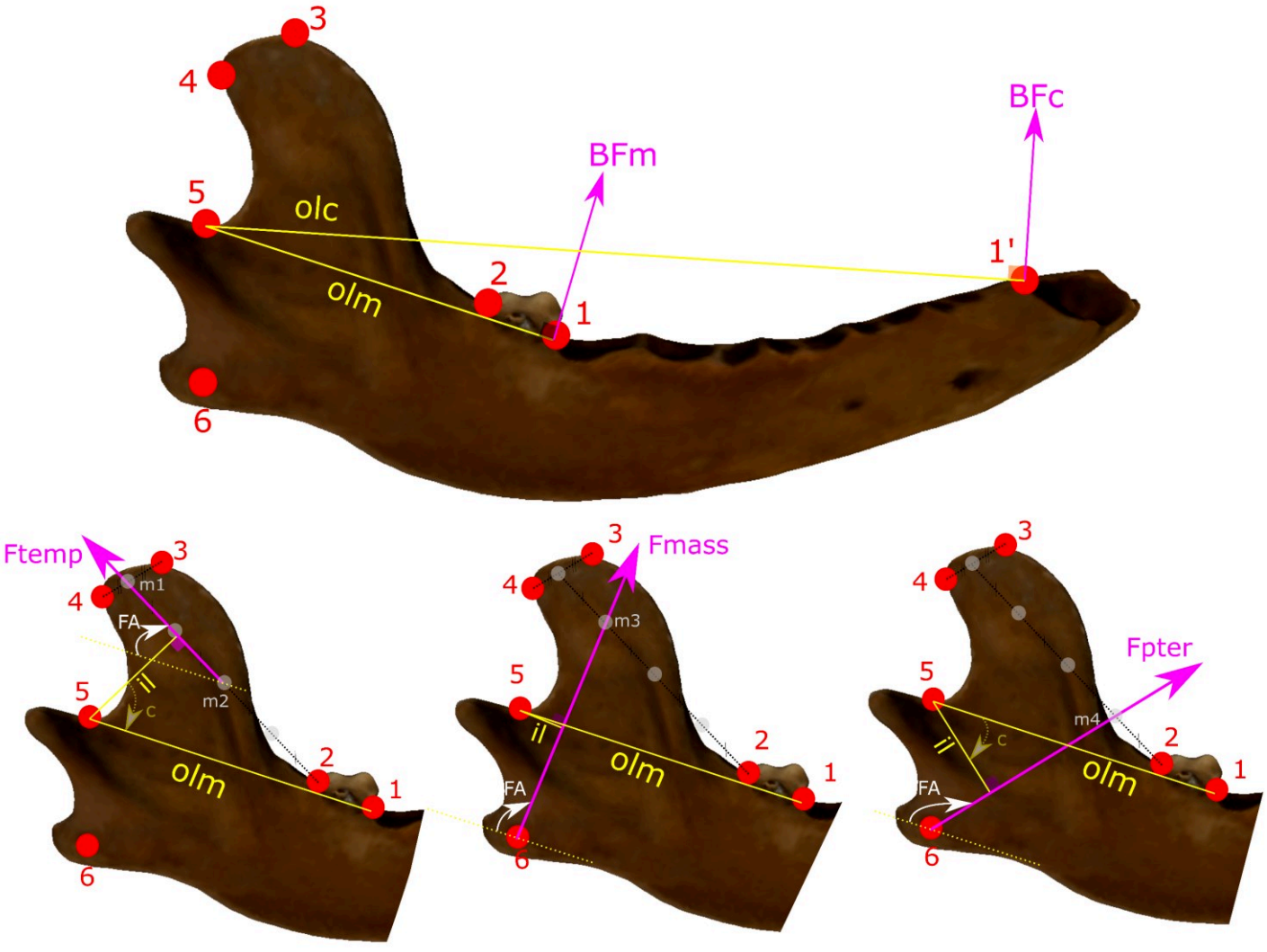

Figure 124. Landmarks used to calculate the mechanical potential of the temporal, masseter and pterygoid muscles. Ftemp: force exerted by M. temporalis, Fmass: Force exerted by M. masseter, Fpter: force exerted by M. pterygoideus, BFc: bite force at the canine; BFm: bite force at the carnassial; il: in-lever arm of the force exerted by the corresponding muscle; olc: out-lever arm of the force exerted by the bite force at the canine; olm: out-lever arm of the force exerted by the bite force at the carnassial; FA: angle of the force exerted by the corresponding muscle with respect to the bite force at the carnassial tooth.

Conclusion

KEY POINTS

To estimate the bite force of ancient dogs we used two different methods.

1- We created **predictive models of the absolute bite force** based on PLS regressions using data on the shape, size, and muscle architecture obtained from the dissection of modern canids.

Better and more applicable covariations are obtained when all the **46 modern dogs are used to build the model**, likely because the large and small dogs drive the covariations and because the **ancient dogs are included within the area of covariation** of the modern dogs. We thus chose to keep all the individuals in the construction of the model.

Better predictions are obtained when using the size in the predictions and the covariations tested without size inform that the best templates to infer function are templates A, B, C, D, E, H and I in dogs and templates A, B, C, F, G, H, I and J in foxes. Predictions obtained from these different templates cannot be mixed but they can be compared.

Template I is particularly interesting as it enables to study a maximum of archaeological mandibles, but the **predictions with template I are less accurate given the relatively low covariation in both dogs and foxes**, which could erase the differences between certain groups.

- ⇨ Whilst exploring archaeological data, the boxplots representing the absolute or residual bite force for the 10 templates for the same individuals (the 127 complete archaeological mandibles) will be compared to ensure the comparability of the results before interpreting the boxplots obtained with template I, as previously suggested for the centroid size.

This method allows prediction even for small pieces where there is no muscular attachment. However, this method only provided an absolute value of the bite force and does not provide any indication of the direction of the muscle forces.

2- We estimated the **mechanical potential** using simple metric ratios, which do not require any comparison with modern animals and provides **complementary insights into the relative contribution of the M. temporalis, M. masseter and M. pterygoideus** to the bite force.

Chapter 9.
Exploring the form and function of the jaw in dogs prior to the Bronze Age in Europe

The aim of this chapter is to apply the methods developed in the previous chapters to the study of form and function of archaeological dogs.

This chapter is composed of four sections, each addressing one of the questions raised while formulating the research questions at the end of the first part. We proceed from the most general to the most specific questions.

In the first section, we compare dogs from Eastern and Western Europe prior to the Bronze Age. Since the two areas show different Neolithisation histories and that the respective dog poulations have inherently different evolutionary histories, we expect to observe differences in the shape and/or size of the mandibles.

In the second section, we compare dogs from the Mesolithic to the pre-Bronze Age separately in Eastern and Western Europe. If differences are detected, they can be related to chrono-cultural differences (especially in Eastern Europe where all sites are located in the same geographical region, Mesolithic sites excepted) but possibly also to geographical variation (in Western Europe in particular, where a great diversity of sites in different geographic regions are considered).

In the third section, we focus on dogs from the site of Twann, which will provide insights into the variability existing within the same site during the same cultural phase (Cortaillod, Middle Neolithic) and the evolution of this diversity over a long and well-calibrated period of time.

Finally, in the fourth section, we compare two populations of dogs from the sites of Hârşova and Borduşani, both located close to the Danube River, in South-Eastern Romania. The comparison of these populations in sites that are geographically close and similar in absolute chronology and culture, will provide insights into the regional variations existing at a given period and culture.

The organisation of each section is similar. We detail the methodology in section 1 and then simply present the results in the other sections. We study the differences in the variability in size and shapes, in the mean sizes and shapes, and in the mean and general trend of absolute or relative bite force in relation to centroid size, as well as the mechanical potential (which provides roughly similar information as the residual bite force) and the differences in the contribution of the different adductors to the bite force. The results of the statistical analyses

are summarised in a table at the beginning of the section and then results are commented point by point.

Considering the conclusions of Chapter 8, bite forces of ancient dogs were predicted using the full sample of modern dogs we dissected (46 dogs). Considering the points of discussion in this chapter, as some templates may represent a loss of information, it is necessary to ensure that the variation patterns give access to the same information before interpreting the data for all the templates. Thus, in each sub-section, prior to analysis of all specimens, we compared the centroid sizes and absolute and residual bite forces for the 127 complete mandibles for the 10 templates, to ensure the transferability of the results. This allow us to know, for each question, the degree of confidence to be given to each template.

At the end of each section, the major key points raised are summarized and discussed in light of our knowledge regarding the genetic and cultural context as specified in Chapter 6. The link between the different sections and further discussion will be made in the general discussion of this thesis.

1. General comparison of dogs from Eastern and Western Europe prior to the Bronze Age

1.1. Statistical tests and table of results

In order to compare mandibular shape and size between dogs from Eastern and Western Europe, we performed Procrustes ANOVAs on the shape coordinates for each template (or on the allometry-free shapes) and Welch two-sample t-tests on the log-10 centroid sizes. When appropriate, shape differences were explored using CVA. We also compared the variance in shape and size using disparity and variance tests, respectively.

We performed parallel analyses on the predicted shapes of the complete mandibles based on the Procrustes coordinates of template I (cf Chapter 7 section 1.2.6.2 page 382). We performed analyses on 2 sets of predictions: the first one uses only the 3 first PLS axes (that represent 96% of the total covariations), and the second set uses the 15 first axes that show significant levels of covariation. The results are indicated in Table 38 and discussed in Appendix 9.2.

In order to test whether Eastern and Western dogs differ in predicted bite force, we performed two-sided t-tests on the log-10 of the absolute or residual (residuals of the linear regression of the predicted bite force on the log10 of the centroid size) predicted bite force at the molar teeth. Bite forces were predicted using the 46 modern dogs, following the methodology explained in Chapter 8 section 1.2.2.1. We compared the total mechanical potential at the molar teeth between 124 dogs from Western Europe and 93 dogs from Eastern Europe, and then we compared the relative mechanical potential of each of the three main jaw muscles, using two-sided Welch two-sample t-tests.

Table 38. Results of the analyses performed to compare ancient dogs from Eastern and Western Europe. Bite force were predicted using 2B-PLS analyses based on 46 modern dogs. Significant results are indicated in blue.

	SHAPE					CENTROID SIZE		BITE FORCE			
	Disparity	Mean - Procrustes ANOVA			Mean - CVA	Variance – f-test	Mean – t-test				
		On raw shape	on allometry-free shapes					Absolute		Residual	
		Geolgraphic pole	Size	Bloc				carnassial	canine	carnassial	canine
A	0.6	$R^2 = 0.036$ $P < 0.001$	$R^2 = 0.027$ $P < 0.001$	$R2 = 0.037$ $P < 0.001$	82%	0.7	0.016	0.058	0.0059	0.022	0.027
B	0.08	$R^2 = 0.025$ $P < 0.001$	$R^2 = 0.030$ $P < 0.001$	$R^2 = 0.024$ $P < 0.001$	86%	0.2	< 0.001	0.0001	0.0011	0.038	0.045
C	0.1	$R^2 = 0.040$ $P < 0.001$	$R^2 = 0.030$ $P < 0.001$	$R^2 = 0.040$ $P < 0.001$	81%	0.1	< 0.001	< 0.001	< 0.001	0.49	0.43
D	0.4	$R^2 = 0.020$ $P < 0.001$	$R^2 = 0.035$ $P < 0.001$	$R^2 = 0.017$ $P < 0.001$	86%	0.2	< 0.001	< 0.001	< 0.001	0.0089	0.0064
E	0.9	$R^2 = 0.00052$ $P = 0.074$	$R^2 = 0.015$ $P < 0.001$	$R^2 = 0.0072$ $P = 0.011$	80%	0.9	0.020	0.0075	0.0074	0.15	0.15
F	0.7	$R^2 = 0.0038$ $P < 0.001$	$R^2 = 0.021$ $P < 0.001$	$R^2 = 0.039$ $P < 0.001$	84%	0.5	0.026	0.084	0.083	< 0.001	< 0.001
G	0.5	$R^2 = 0.021$ $P < 0.001$	$R^2 = 0.047$ $P < 0.001$	$R^2 = 0.018$ $P < 0.001$	74%	0.4	< 0.001	0.037	0.0042	< 0.001	< 0.001
H	0.6	$R^2 = 0.053$ $P < 0.001$	$R^2 = 0.0099$ $P = 0.10$	$R^2 = 0.056$ $P < 0.001$	66%	1	0.27	0.50	0.51	< 0.001	< 0.001
I	0.5	$R^2 = 0.0094$ $P = 0.009$	$R^2 = 0.11$ $P < 0.001$	$R^2 = 0.0092$ $P = 0.004$	76%	0.5	< 0.001	< 0.001	< 0.001	< 0.001	< 0.001
J	0.5	$R^2 = 0.023$ $P < 0.001$	$R^2 = 0.027$ $P < 0.001$	$R^2 = 0.024$ $P < 0.001$	72%	0.1	< 0.001	< 0.001	< 0.001	< 0.001	< 0.001
I➔A (127)		$R^2 = 0.070$ $P < 0.001$	/	/	70%	/	/	/	/	/	/
I➔ A (all)		$R^2 = 0.023$ $P < 0.001$	/	/	67%	/	/	/	/	/	/

1.2. Results and interpretation

1.2.1. Differences in mandible shape and size

The analyses show significant differences in mean shape, mean allometry-free shape, and mean centroid size. Results are similar for all templates (except template H), suggesting a strong biological signal (that is maintained whatever the number of variables and individuals) and **significant morphological differences between Eastern and Western Europe**.

Template A provides the most reliable visualisations of the differences between dogs from Eastern and Western Europe (Figure 125). Visualisations for templates B, C, F and J (that are relevant to discuss about the morphotype) show similar patterns (Figure 126). The CVA has a success rate of 82% (81% for Eastern Europe, n=52 and 83% for dogs from Western Europe, n=75). **Dogs from Eastern Europe have smaller (in centroid size) but thicker and ventrally straighter mandibles, with a wider angular process, and a straighter coronoid process with a deeper masseteric fossa.** Dogs from Western Europe tend to have larger but thiner mandibles and more ventrally curved mandibles, with a more curved backwards coronoid process.

The classification tree suggests that there are 3 main groups in ancient dogs (analyses performed with template A). The composition of the groups between Eastern and Western Europe significantly differs, as evidenced by a Chi-square test performed on the results of the classification and the geographical pole (East or West; X^2=14.3, df = 2, $P < 0.001$). Group 2 contains more dogs from Eastern Europe (26/52, 50%) than from Western Europe (14/75, 18%), while Groups 1 and 3 contain more dogs from Western Europe (Group 1: 37/75, 49%, Group 3:24/75, 32%) than from Eastern Europe (Groupe1: 14/52 or 26%, Group3: 12/52, 23%). However, the statistic robustess of these groups is not significant and it would be preferable to consider smaller branches. **It is therefore difficult to identify clearly different morphotypes using this unsupervised method.**

Groups obtained with template B are not the same as those obtained with template A when analyses are performed on the same 127 complete mandibles (Table 39), because template B uncompletely describes mandible shape (in particular as regards the coronoid process).

Table 39. Cross table of the classifications obtained in the trees based on templates A and B for the 127 complete mandibles of ancient dogs.

		Classification tree with template A		
		1	2	**3**
With Template B	**1**	11	9	3
	2	29	13	12
	3	11	18	21

Interestingly**, no significant difference in size or shape variability was evidenced** for any of the templates. The diversity in size and shape is thus important in both areas based on the comparison between pre-Bronze Age and modern dogs (see Chapter 7 section 1, Figure 96, Figure 98).

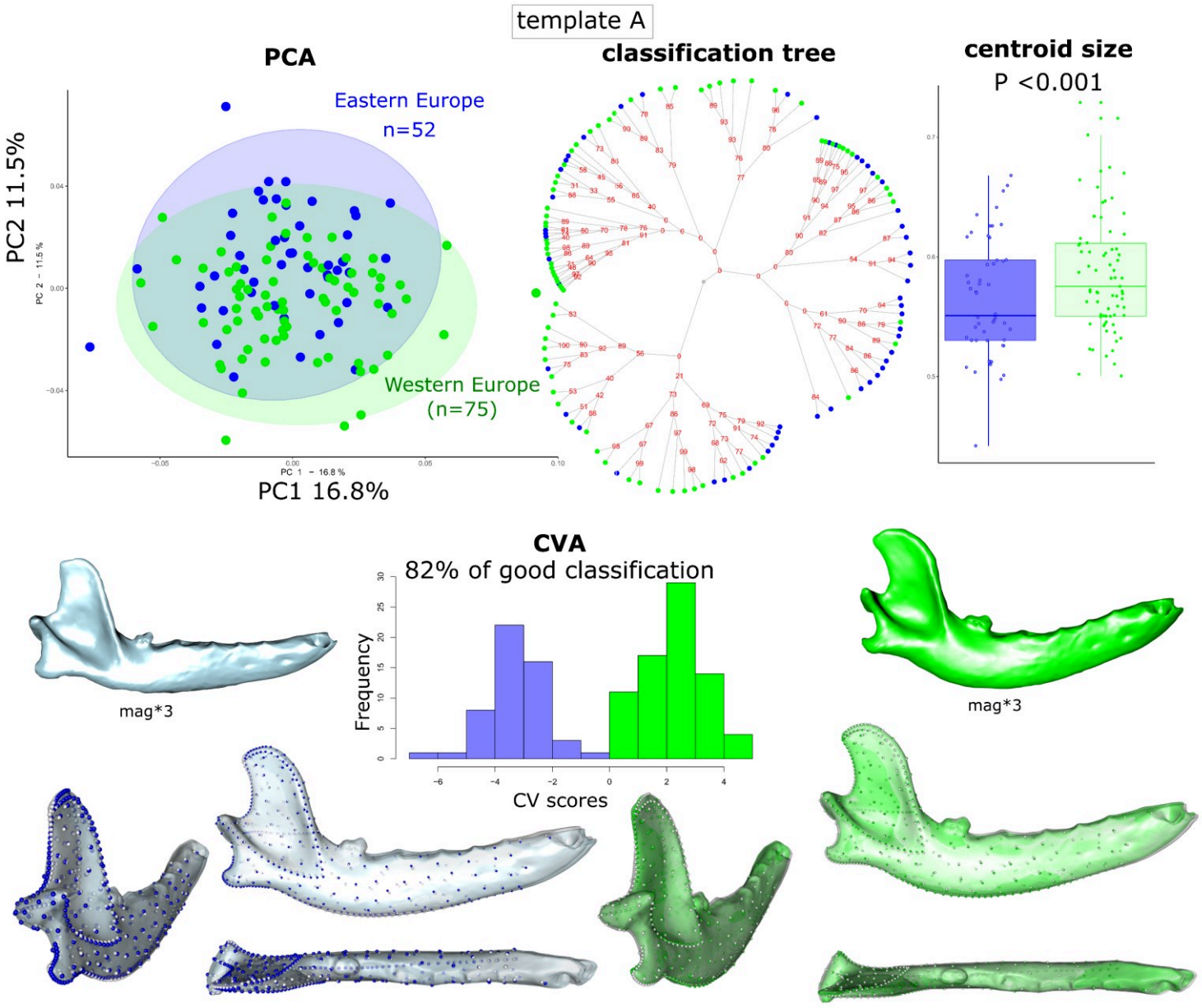

Figure 125. Visualisation of differences in mandible form between ancient dogs from Eastern and Western Europe. Analyses based on template A. mag: magnification of the differences by 3.

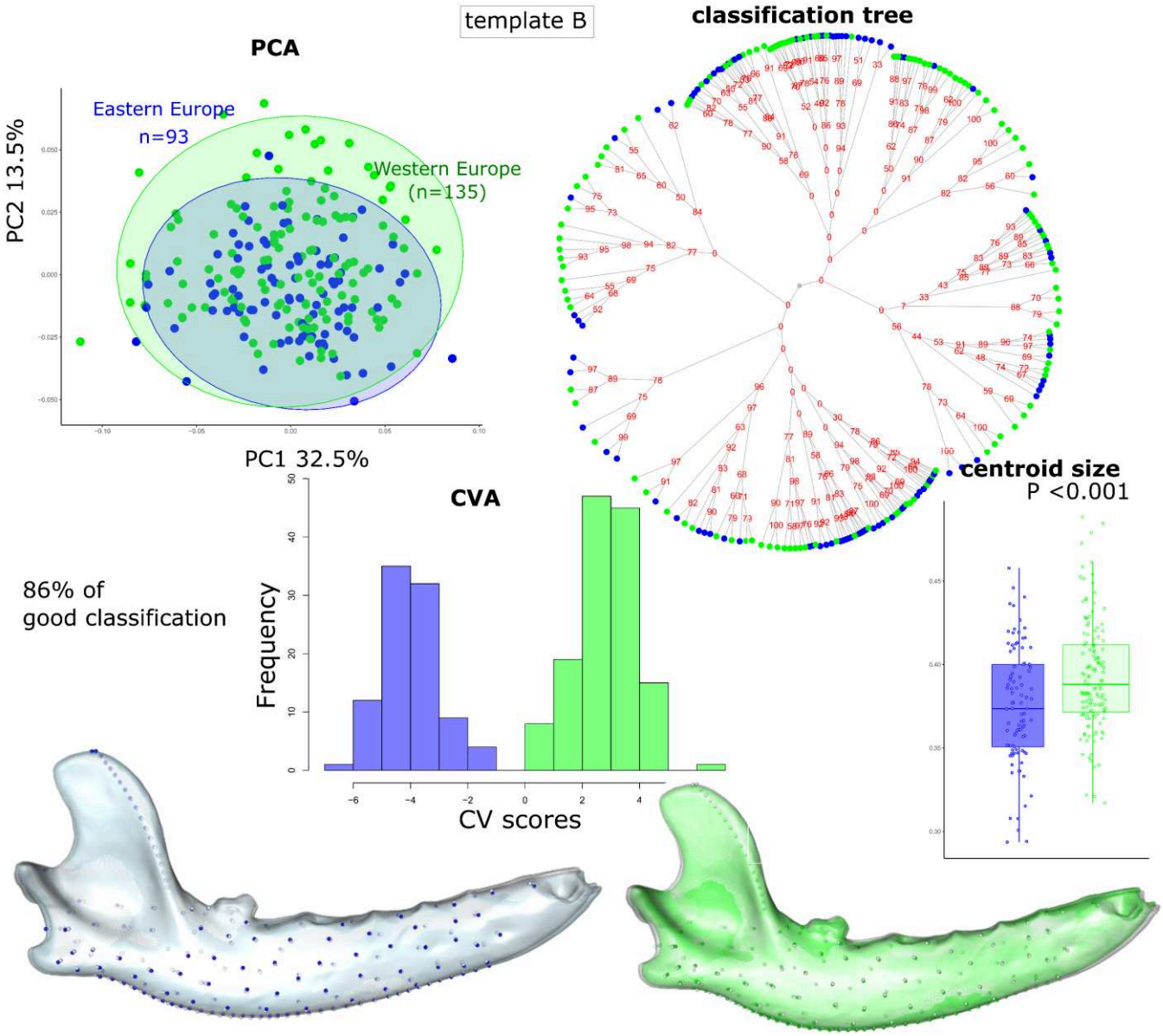

Figure 126. Visualisation of differences in mandible form between ancient dogs from Eastern and Western Europe. Analyses based on template B. mag: magnification of the differences by 3.

1.2.2. Differences in function

1.2.2.1. *Predicted bite forces*

The differences observed in shape between Eastern and Western Europe suggest functional differences.

To ensure that all templates provide comparable information, we first compared bite forces between all templates but only based on the same 127 complete mandibles. We should observe similar trends and statistical results for all templates.

For these 127 complete mandibles, the mean of the residual bite force tends to be either equal or higher in dogs from Eastern Europe than in dogs from Western Europe (Figure 127). The slight significant difference with template A ($P = 0.02$) is smoothed and no longer significant with templates B and C. With templates D and E, the difference is not significant and we almost observe the opposite trend. The difference is significant and even emphasized with templates H, I and J. We thus have to be cautious with results of templates B, C, D and E for further interpretations with all the ancient dogs of each template. For this analysis, we will thus focus more on templates A, F, G, H, I and J.

When performing analyses on all the individuals of each template (Table 38, Figure 128), **the absolute bite forces tend to be higher in Western Europe because of the larger centroid size of the dogs** (see above). Additionally, **templates A, F, G, H, I and J suggest that dogs from Eastern Europe tend to have higher bite forces relative to their size**.

We also performed similar analyses using predictions based on the 29 modern dogs that are the closest to ancient dogs (Table 40). The differences in residual bite force are no longer significant, which reinforces the idea that the model using 46 modern dogs is better appropriate.

Table 40. Predicted bite forces and p-values of the comparison t-tests between Eastern and Western Europe. Bite force were predicted using 2B-PLS analyses on 29 modern dogs.

	t-test absolute BF		t-test residual BF	
Template	**carnassial tooth**	**canine tooth**	**carnassial tooth**	**canine tooth**
A	0.030	0.028	0.40	0.40
B	0.0011	0.0011	0.038	0.042
C	0.0022	0.0018	0.054	0.15
D	< 0.001	< 0.001	0.10	0.36
E	0.063	0.041	0.59	0.80
F	0.038	0.035	0.70	0.72
G	< 0.001	< 0.001	0.68	0.87
H	0.33	0.37	0.37	0.11
I	< 0.001	0.0075	0.62	0.76
J	< 0.001	0.067	0.36	0.28

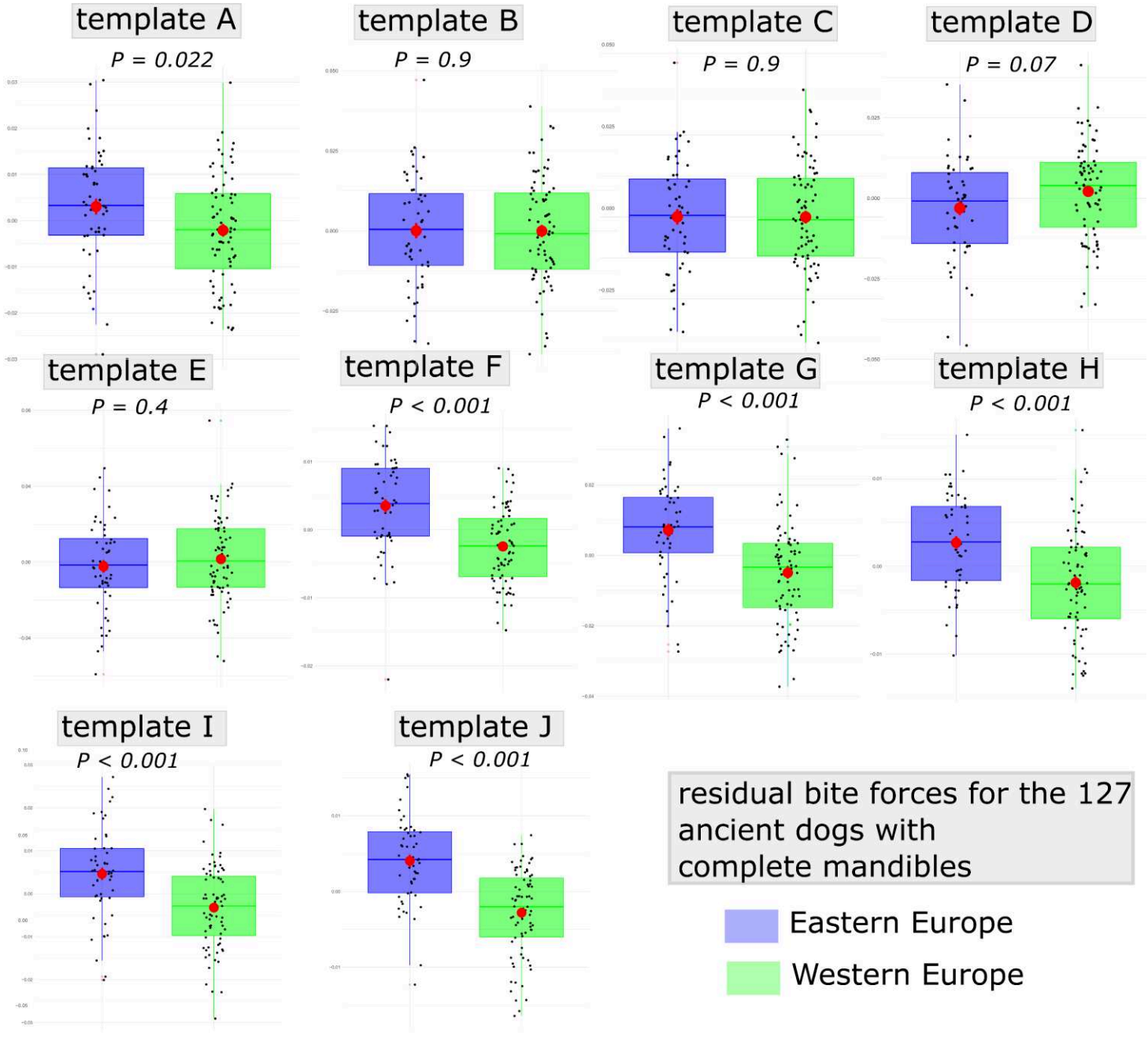

Figure 127. Residual predicted bite forces at the carnassial teeth and p-values of the t-tests between Eastern and Western Europe for the 127 dogs with complete mandibles. Bite force were predicted using 2B-PLS analyses on 46 modern dogs.

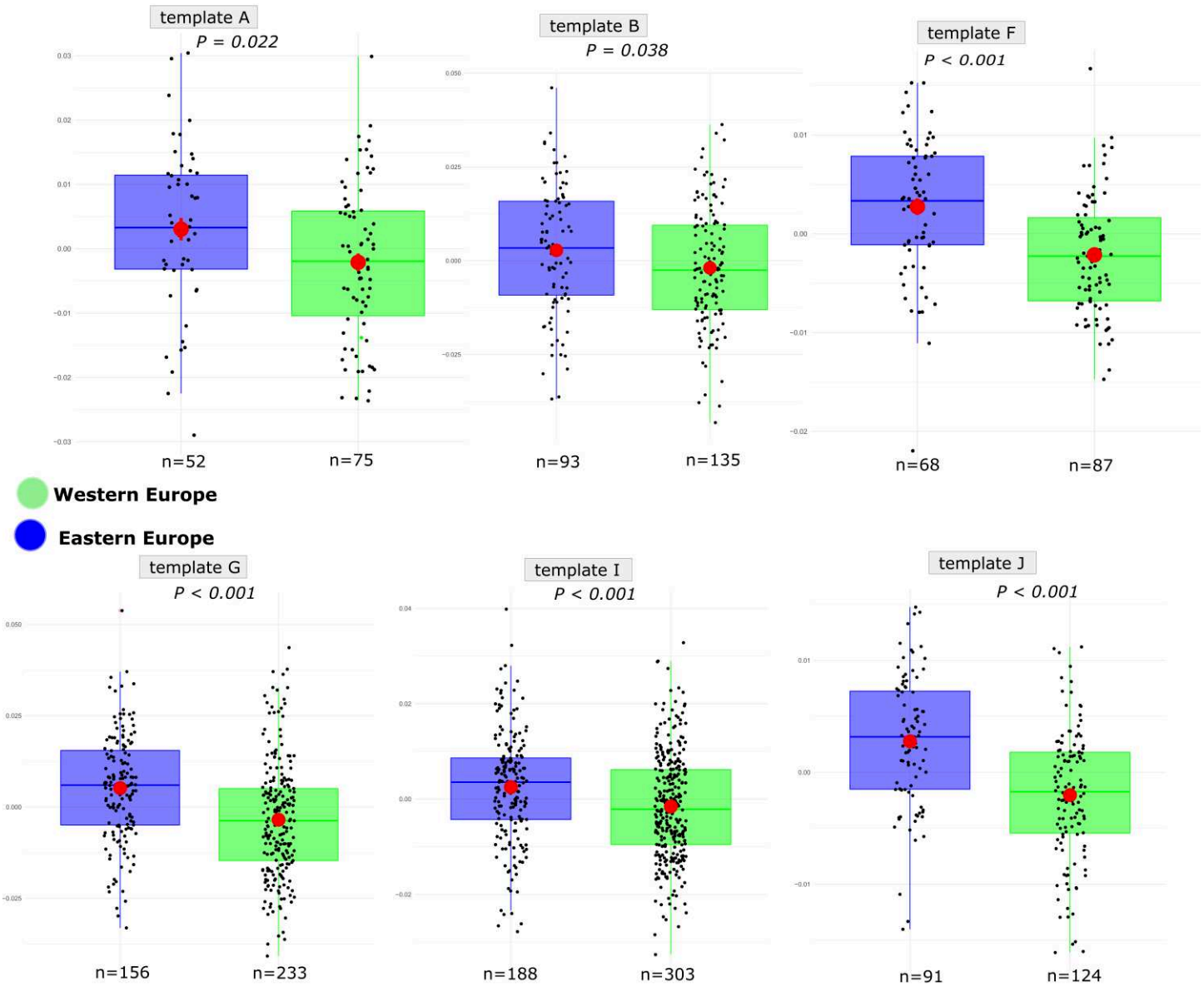

Figure 128. Residual predicted bite forces at the carnassial teeth and p-values of the t-tests between Eastern and Western Europe for templates A, B, F, G, I and J. Bite force were predicted using 2B-PLS analyses on 46 modern dogs.

1.2.2.2. *Mechanical potential*

The total mechanical potential is higher in dogs from Eastern Europe, despite their smaller size (Figure 129), which is consistent with the previous results suggesting that relative bite forces are higher in dogs from Eastern Europe. **The masseter contributes more to the bite force in dogs from Eastern Europe than in dogs from Western Europe while the pterygoid muscle contributes relatively more to the bite force in dogs from Western Europe ($P < 0.001$)**. These results are consistent with the differences in shape between the two locations, considering the results of the covariation analyses conducted on modern dogs in this thesis. This suggests that **dogs from Western Europe have jaws more adapted to lateral movements while dogs from Eastern Europe tend to have jaws more adapted for vertical chewing at low gapes**.

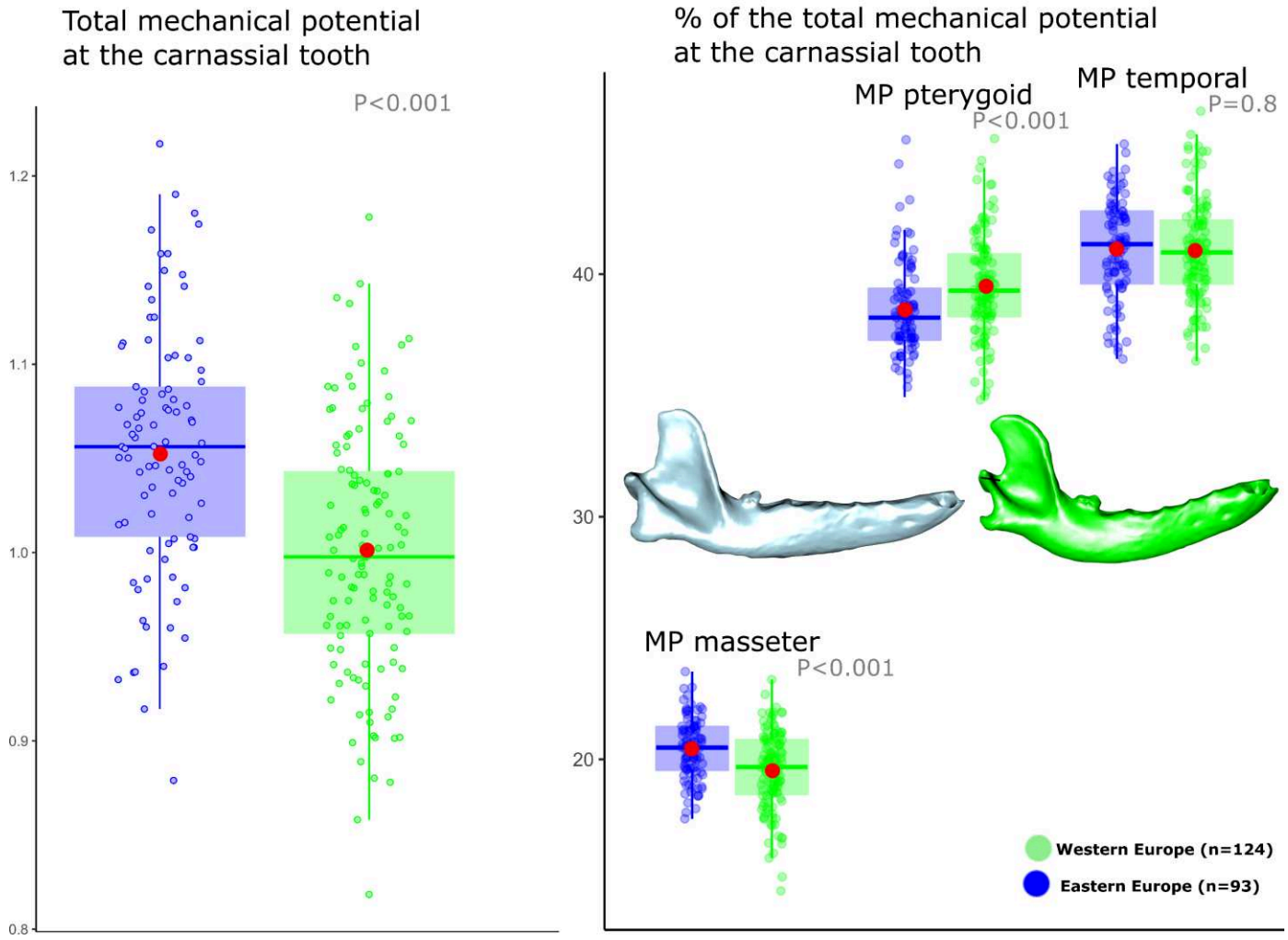

Figure 129. Mechanical potential (MP) in dogs from Eastern and Western Europe. The p-values from the t tests and the associated (magnified by 3) shapes at the minimum and maximum of the CVA based on Procrustes coordinates of template A (Figure 125) are reported.

Conclusion

From the comparison of dogs prior to the Bronze Age in Eastern and Western Europe, the following key points emerge:

KEY POINTS

We compared two sets of ancient dog mandibles mostly represented by the Middle Neolithic in Western Europe and the Chalcolithic in Eastern Europe, which represents overall the same amount of time spent since the diffusion of the Neolithic package (5,800 and 4,500 cal. BC for the Chasséen in Southern France; 6,000 and 4,500 cal. BC for the Gumelnița in south-Eastern Romania, see Part 1 section 0, Table 2, Table 3).

Dogs from Eastern and Western Europe differ in the mean shape and size of the mandible which is accompanied by functional differences. Dogs from Eastern Europe are smaller and the mandible is more fox-like, however they are suggested to bite harder for their size (which is to be related to the greater implication of the masseter muscle and the deeper masseteric fossa) compared to dogs from Western Europe. Accordingly, the jaw of dogs from Eastern Europe is more adapted to vertical movements at low gapes than the mandible of dogs from Western Europe that is best fitted for horizontal chewing.

These results are consistent with the fact that dog populations have very different histories in Eastern and Western Europe. The neolithisation processes and the composition of dog populations in genetic terms are indeed not the same in these two areas (see Part 1 section 2.4.2.3.5, Table 12). In 1,500/1,300 years, there was a total replacement of the European maternal lineage by an exogenous lineage (probably coming from the Near-East) in Eastern Europe (haplogroup C ➔ Hg D), whereas a clear predominance of the European maternal lineage (Hg C) persisted in Western Europe at least until the end of the Middle Neolithic, and was accompanied by a greater diversity in haplogroups (Hg C, D, A and B are attested during the Middle Neolithic).

Considering the greatest diversity in haplogroups in Western Europe, one might have expected to observe greater morphological variability in Western Europe, but it is not the case.

⇨ These results demonstrate that the **analyses of the variations in form and function from the Mesolithic to the pre-Bronze Age need to be conducteded separately in Eastern and Western Europe**.

2. Evolution of dogs from the Mesolithic to the very early Bronze-Age in Eastern and Western Europe

In this section, we wanted to explore whether the shape of the mandible and its function changed through time in each of the European areas studied.

2.1. Statistical tests and table of results

As dogs have different histories in Eastern and Western Europe, their evolution through time should be interepreted separately. We thus performed separate analyses for dogs from Eastern and Western Europe. However, to facilitate the general discussion, the evolution in size and bite forces in Eastern and Western Europe on the same graphs.

In Eastern Europe, we compared dogs from the Mesolithic – early Neolithic (MesoEarly Neo), Chalcolithic 1 – Hamangia III/Boian cultures (Chalco1), Chalcolithic2 – Gumelnița cultures (Chalco2) and Chalcolithic3 – Cernavoda culture (Chalco3).

In Western Europe, we compared dogs from the Mesolithic (Meso), Early Neolithic (Early), Middle Neolithic – Chasséen culture (Chas), Middle Neolithic – Cortaillod culture (Cort), Late Neolithic (Late).

In each geographical area (Eastern or Western Europe), and for each template, we performed the same analyses as the ones conducted in the previous section (section 1.1 Statistical tests and table of results, page 414)

Given that we mostly have dogs from the Hamangia III/Boian and Gumelnița cultures in Eastern Europe, and dogs from the Chasséen and Cortaillod cultures in Western Europe, we also performed Procrustes ANOVAs (and CVA where differences in shape can be identified) on these groups more specifically.

The results of the statistical analyses are reported in Table 41 for dogs from Eastern Europe and in Table 42 for dogs from Western Europe. We will interpret them progressively in the next sections.

Table 41. Results (P-values) of the analyses performed to compare dogs between groups in easern Europe. Bite force were predicted using 2B-PLS analyses on 46 modern dogs. Significant results are written in blue. P-values for groups with only one specimen are not reported. Chalco1: Hamangia III/Boian cultures, Chalco2: Gumelnița culture, Chalco3: Cernavoda culture.

	SHAPE			**CENTROID SIZE**		**BITE FORCE**	
	Disparity	**Mean - Procrustes ANOVA Chalco1/Chalco2**	**Mean – CVA Chalco1/ Chalco2**	**Variance – f-test Chalco1/ Chalco 2**	**Mean – t-test**	**mean – t-test**	
						Absolute	**Residual**
A	> 0.05	0.027	88%	0.9	>0.05	Chalco1 > Chalco2 0.014	Chalco1 > Chalco2 0.02
B	Chalco2 > Chalco 1 0.033	0.002	82%	1	Chalco1 > Chalco2 0.001	Chalco1> Chalco2 <0.001	Chalco1 > Chalco2 <0.001
C	> 0.07	0.49	/	0.5	Chalco1 > Chalco2 0.0042	Chalco1 > Chalco2 0.0044	> 0.05
D	> 0.08	0.07	/	0.4	Chalco1 > Chalco2 <0.001	Chalco1 > Chalco2 <0.001	Chalco1 > Chalco2 0.0035
E	> 0.05	0.32	/	0.8	Chalco1 > Chalco2 <0.001	Chalco1 > Chalco2 <0.001 MesoEarly > Chalco2 0.0094	Chalco1 > Chalco2 0.042 MesoEarly > Chalco2 0.0034
F	> 0.05	0.28	/	0.4	> 0.05	Chalco1 > Chalco2 0.056	> 0.05
G	> 0.05	0.95	/	0.6	MesoEarly > Chalco2 0.043 Chalco1 > Chalco2 <0.001	Chalco1 > Chalco2 <0.001 MesoEarly > Chalco2 0.0042	Chalco1 > Chalco2 0.053 MesoEarly > Chalco2 0.074
H	> 0.05	0.36	/	0.2	> 0.05	Chalco1> Chalco2 0.079	> 0.05
I	> 0.05	0.82	/	0.3	MesoEarly > Chalco2 0.0032 Chalco1 > Chalco2 <0.001	Chalco1 > Chalco2 <0.001 MesoEarly > Chalco2 0.0023	> 0.05
J	> 0.05	0.12	/	0.7	Chalco1 > Chalco2 <0.001	Chalco1 > Chalco2 < 0.001	> 0.05

Table 42. Results (P-values) of the analyses performed to compare dogs between groups in Western Europe. Bite force were predicted using 2B-PLS analyses on 46 modern dogs. Significant results are written in blue. P-values for groups with only one specimen are not reported. Chas: Chasséen culture, Cort: Cortaillod culture.

	SHAPE				CENTROID SIZE		BITE FORCE	
	Disparity All groups	Mean - Procrustes ANOVA All groups	 Chas-Cort	Mean - CVA Chas-Cort	Variance – f-test Chas-Cort	Mean – t-test	mean – t-test Absolute	 Residual
A	Cort > Late 0.024 Chas > Late 0.043	0.026	0.012	91%	Chas > Cort 0.001	Early > Cort 0.013 Chas > Cort 0.057	Early > Cort 0.017 Chas > Cort 0.050	>0.05
B	Chas > Cort 0.006	0.001	< 0.001	81%	Chas > Cort 0.05	>0.05	>0.05	>0.05
C	Chas > Cort 0.002	0.001	< 0.001	/	Chas > Cort 0.003	Early > Chas 0.015 Early > Cort 0.0019	Early > Chas 0.0084 Early > Cort 0.0031	>0.05
D	>0.05	0.001	< 0.001	/	Chas > Cort 0.003	Early > Chas 0.039 Early > Cort <0.001 Late > Cort 0.0085	Early > Chas 0.051 Early > Cort 0.0041 Late > Cort 0.022	>0.05
E	Ancient > Cort 0.035	0.001	< 0.001	/	Chas > Cort 0.001	Early > Chas 0.056 Early > Cort <0.001 Chas > Cort <0.001 Late > Cort 0.0086	Early > Chas 0.062 Early > Cort <0.001 Chas > Cort <0.001 Late > Cort 0.019	Chas > Cort 0.012
F	>0.05	>0.05	0.013	/	Chas > Cort 0.004	Early > Cort 0.019	Early > Cort 0.019 Chas > Cort 0.054	>0.05
G	>0.05	0.001	< 0.001	/	Chas > Cort <0.001	>0.05	Late > Cort 0.057	Early > Cort 0.012 Chas > Cort <0.001 Late > Cort 0.0041
H	>0.05	0.001	0.017	/	Chas > Cort 0.02	Early > Cort 0.032	Early > Cort 0.017	>0.05
I	>0.05	0.001	< 0.001	/	Chas > Cort <0.001	>0.05	>0.05	Early > Cort <0.001 Chas > Cort <0.001 Late > Cort <0.001
J	>0.05	0.001	< 0.001	/	Chas > Cort 0.02	>0.05	Chas > Cort 0.043	Chas > Cort 0.0019

2.2. Results and interpretation

2.2.1. Reliability of all templates to reflect the size of the complete mandible

Previously (see Chapter 7 section 1.1.1), we have shown that the centroid size is correlated between templates but the coefficient of correlation is lower for some templates such as template I, suggesting that this template can be misleading when interpreting centroid size (the differences between groups can be reduced relative to comparison with other templates). Thus, before interpreting the results of this section, we wanted to ensure that the centroid size of each template brings similar information to compare the chronological evolution from the Mesolithic to the early Neolithic in Eastern and Western Europe. For this purpose, we compared the centroid sizes given by each of the 10 templates based on the 127 complete mandibles (Figure 133). It turns out that template I shows a slighltly different pattern: differences in size between groups are indeed reduced. **Results witht template I should thus be considered with caution in this section.**

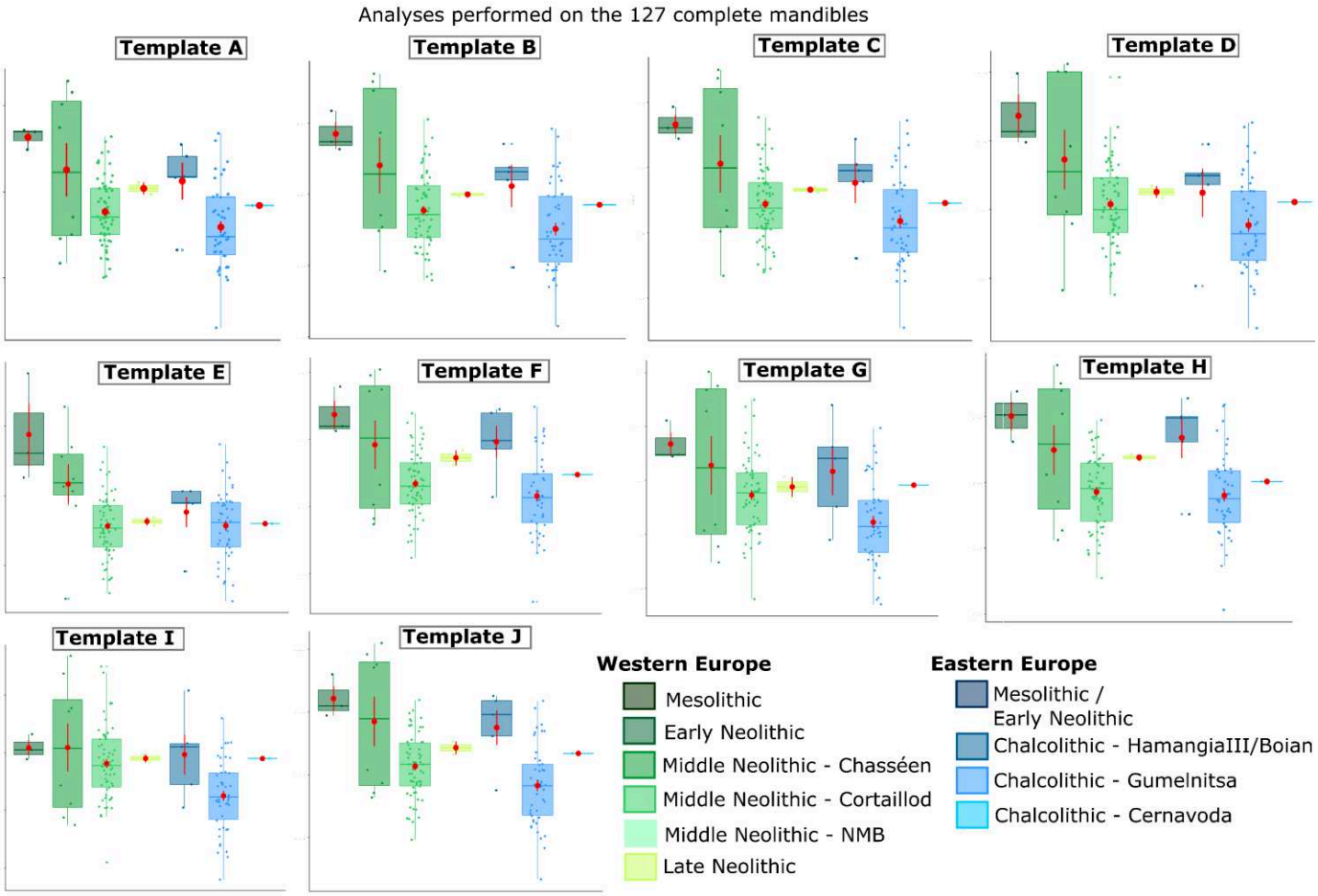

Figure 130. Centroid size of the 127 complete mandibles of ancient dogs, obtained from the Procrustes analyses performed on coordinates from the 10 templates. Red dots correspond to the mean.

2.2.2. Reliability of all templates to reflect the absolute or residual bite force of the complete mandible

We followed the same procedure as in the previous section for the predicted bite forces or for the residual bite forces (which is more indicative of the relative performance of the jaw).

For the absolute bite forces, the same trends are observed for all templates, but the **differences between groups are lower for templates C, D and I** (Figure 131). **Templates E tends to amplify the differences.**

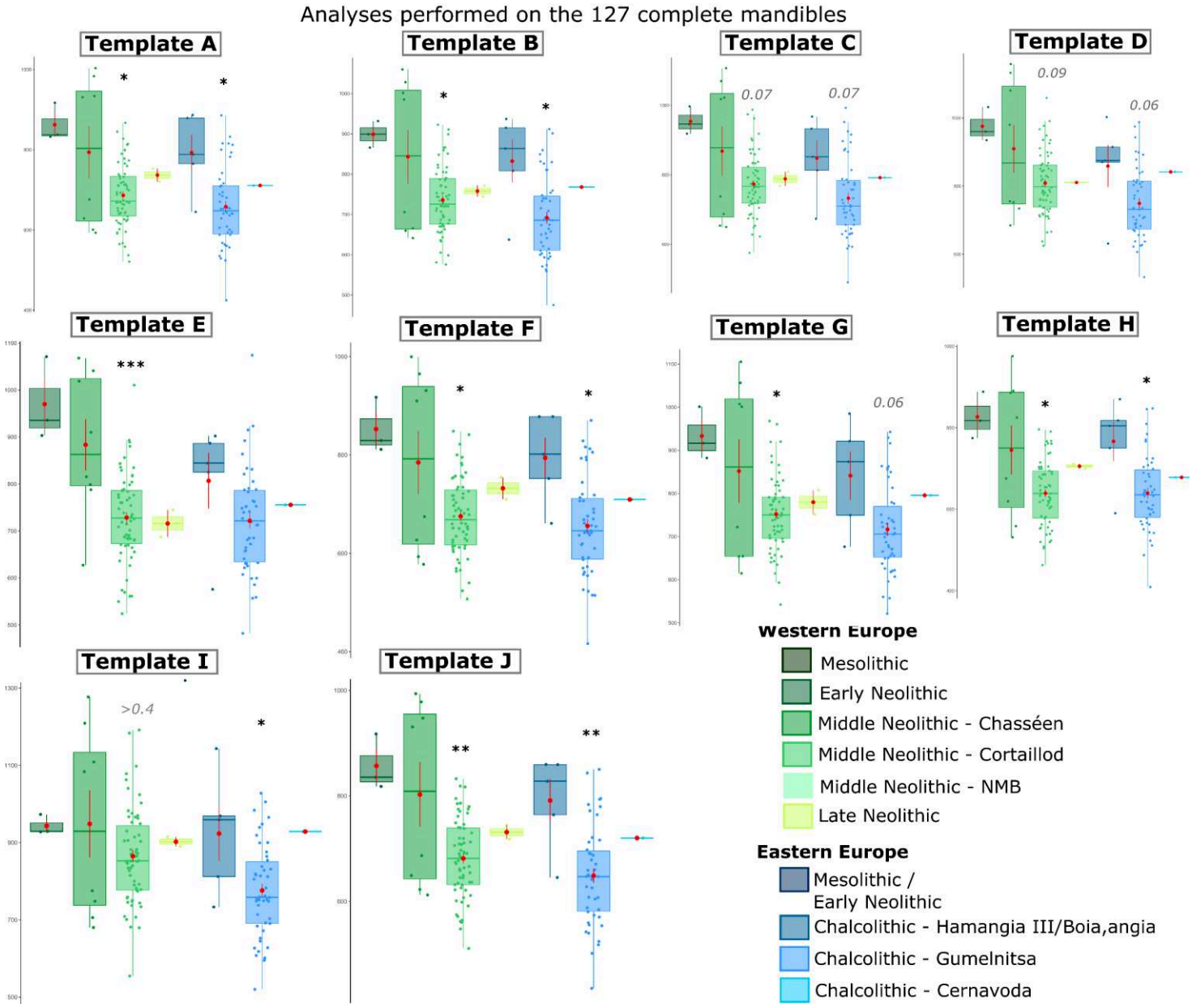

Figure 131. Absolute bite force of the 127 complete mandibles of ancient dogs, obtained from the Procrustes analyses performed on coordinates from the 10 templates. The * indicates the significance of the post-hoc tests. Red dots correspond to the mean.

For the residual bite forces, templates A, B, D show similar trends between groups. **With templates E, F, G, H, I and J, artificial differences appear between groups in Western Europe (but not in Eastern Europe).** This is likely related to the different levels of modularity in the shape of the mandible in dogs from Eastern and Western Europe. These templates are thus misleading to answer the question addressed in this section (Figure 132).

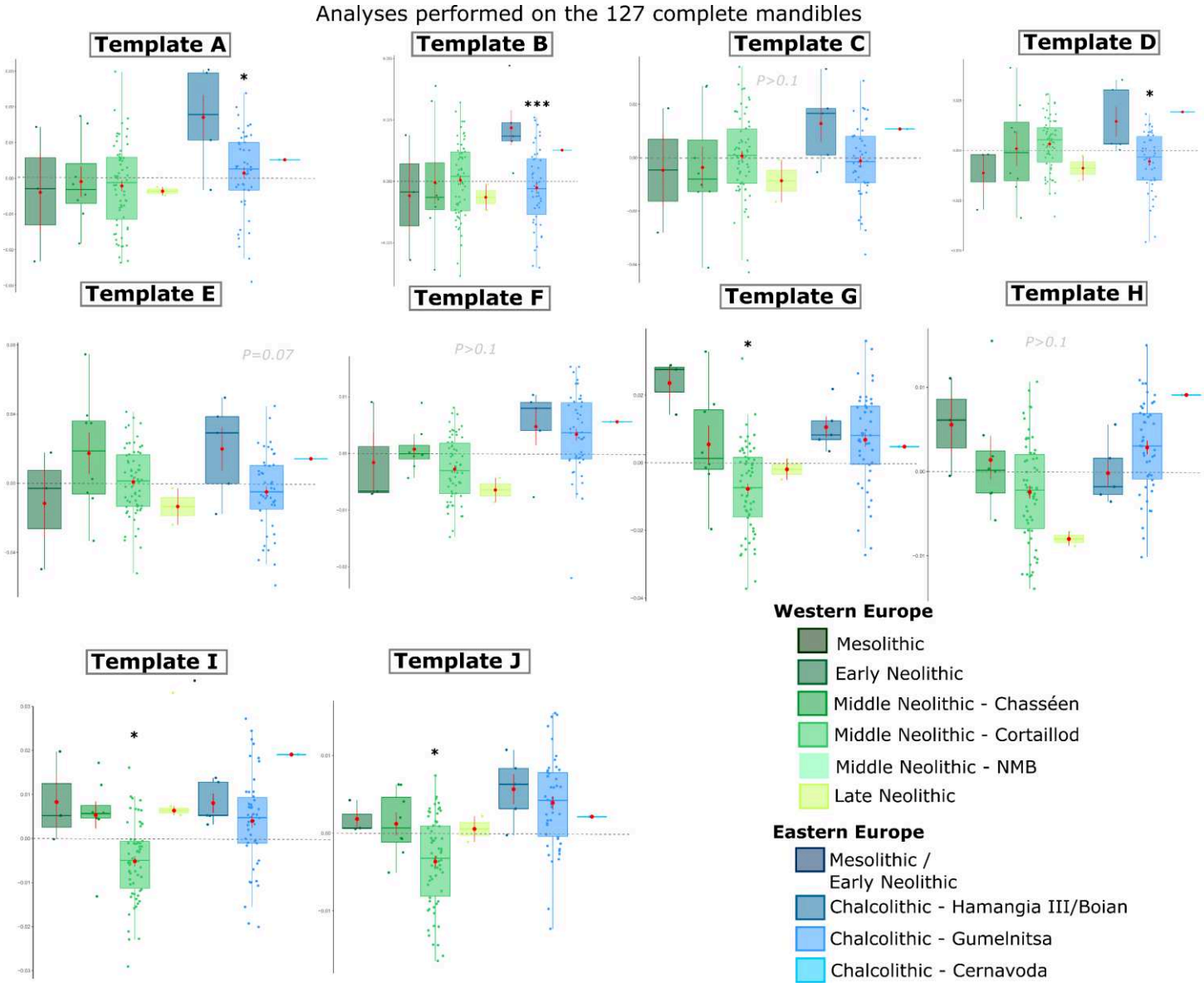

Figure 132. Residual bite force of the 127 complete mandibles of ancient dogs, obtained from the Procrustes analyses performed on coordinates from the 10 templates. The * indicates the significance of the post-hoc tests. Red dots correspond to the mean. Red dots correspond to the mean.

2.2.3. Evolution in Eastern Europe

2.2.3.1. *Centroid size*

The results are represented in Figure 133. There is huge variability in each group of Eastern Europe and two of them (Mesolithic-Early Neolithic and Chalcolithic 3-Cernavoda) are very poorly represented. Given this, the following results need to be taken with caution.

In Eastern Europe, **the size of the dogs tends to decrease from the Mesolithic to the Gumelnița culture.** Statistically, **the difference is highly significant between the Hamangia III/Boian III and Gumelnița cultures for many templates** (B, C, D, E, G, I, J), thus reinforcing the strength of the biological signal. Additionnally, **templates G and I show significant differences between the Mesolithic-Early Neolithic and the Gumelnița culture** (despite the fact that template I tends to reduce differences between groups). **Small dogs are more represented in later periods (in particular during the Gumelnița culture). There are no differences in the variability of sizes between the Hamangia III/Boian and the Gumelnița cultures.**

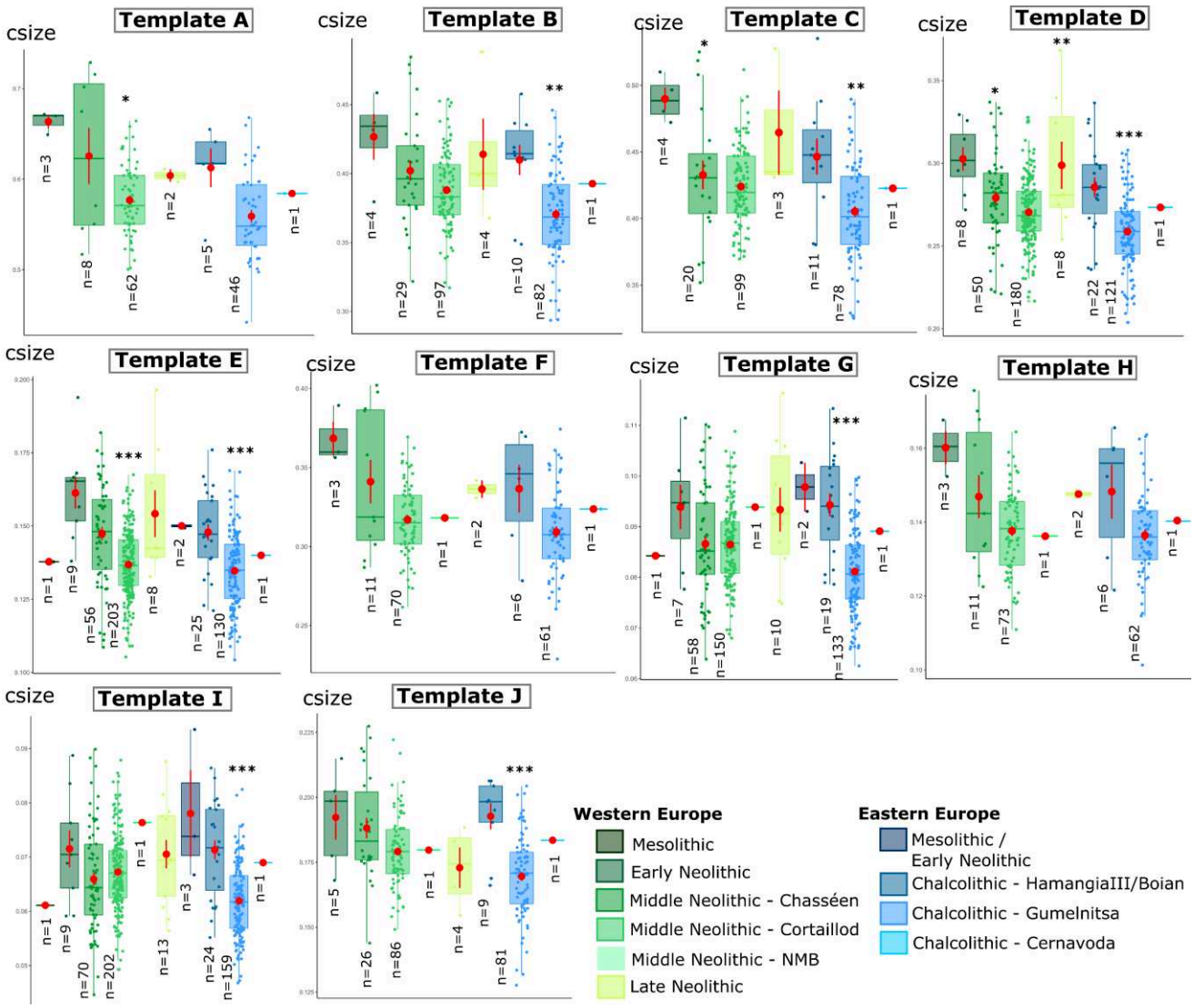

Figure 133. Centroid size of all mandibles of ancient dogs for the 10 templates.
The * indicate the significance of the post-hoc tests. Red dots correspond to the mean.

2.2.3.2. *Variability in shape*

Disparity

In Eastern Europe, variability in shape seems rather stable through time. In particular, there is no significant difference in shape variability between the Hamangia III/Boian and Gumelnița cultures, except in analyses performed with template B, which suggest that variability was greater during the Gumelnița than during the Hamangia III/Boian, however the much lower sample size in this group must be taken into account.

Principal Component Analyses

We provide visualisation of the morphological variation in dogs prior to the Bronze Age in Eastern Europe for templates A (Figure 134), B (Figure 135), C (Figure 136), F (Figure 137) and J (Figure 138) for information.

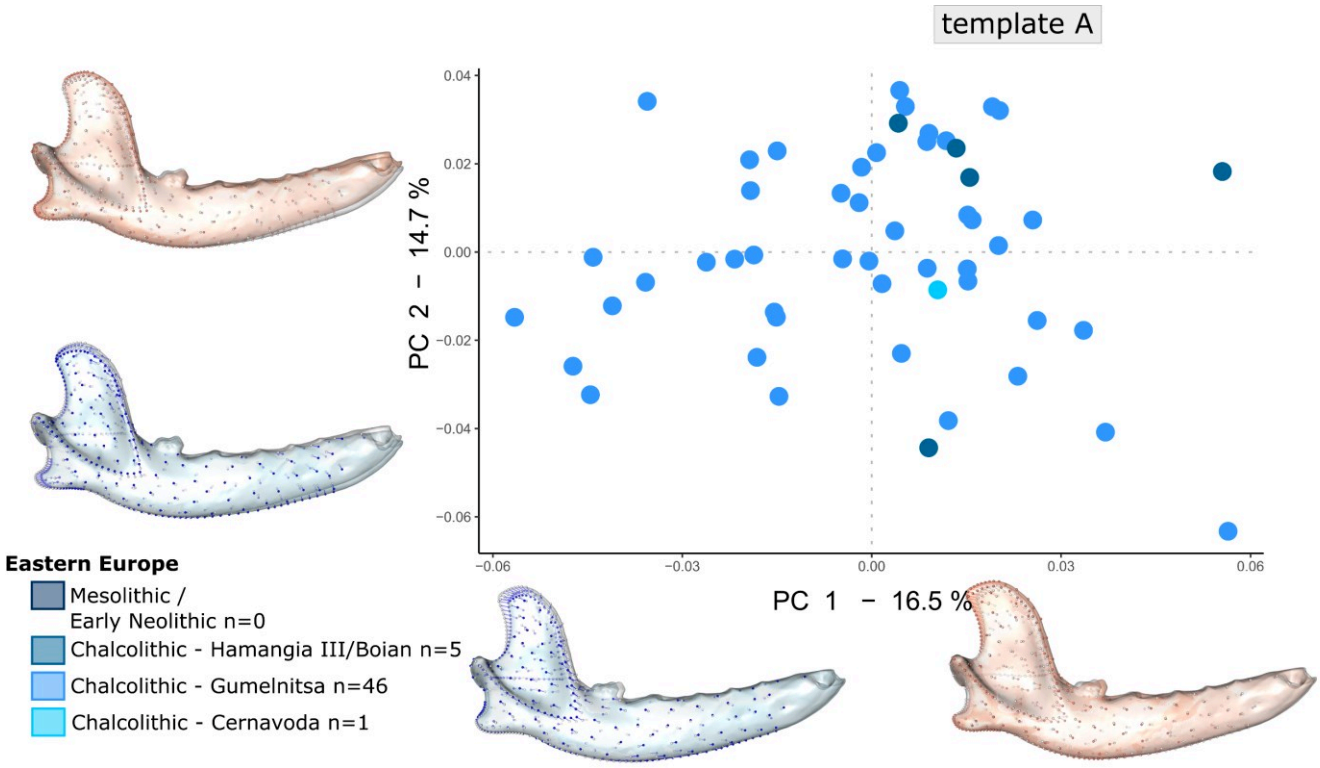

Figure 134. Visualisation of the two first axes of the Principal Component Analyses performed on the prorustes coordinates of template A for all ancient dogs from Eastern Europe.

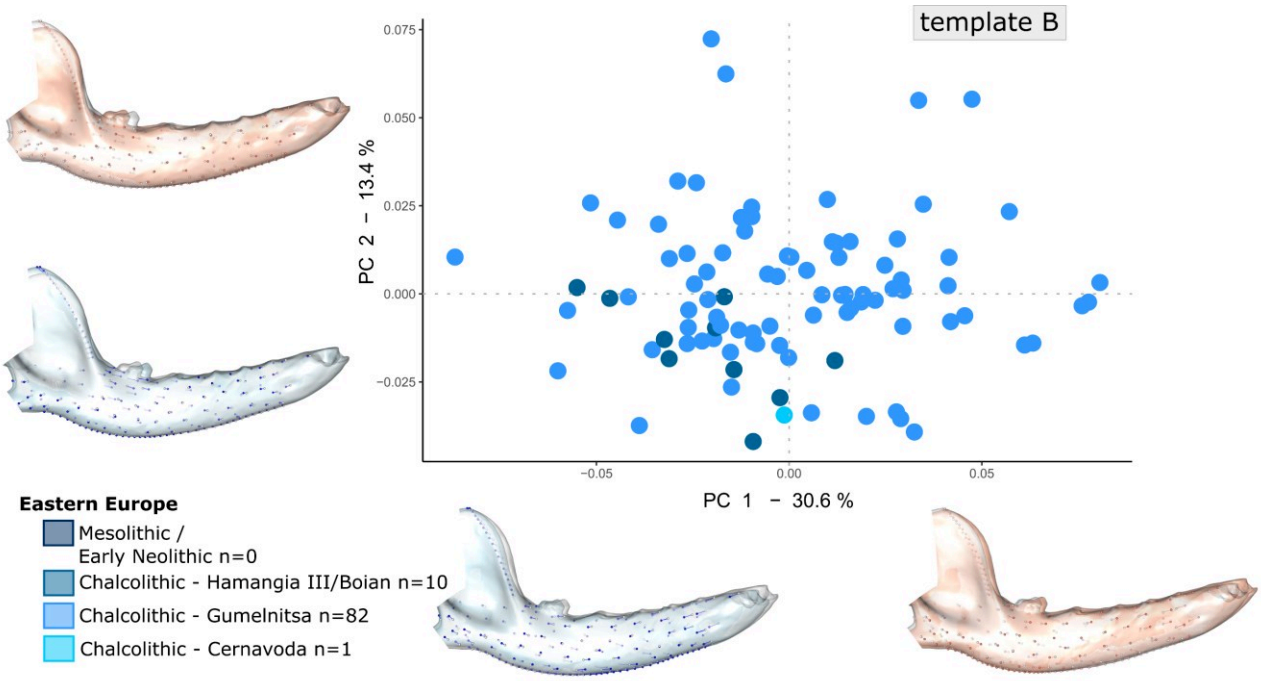

Figure 135. Visualisation of the two first axes of the Principal Component Analyses performed on the prorustes coordinates of template B for all ancient dogs from Eastern Europe.

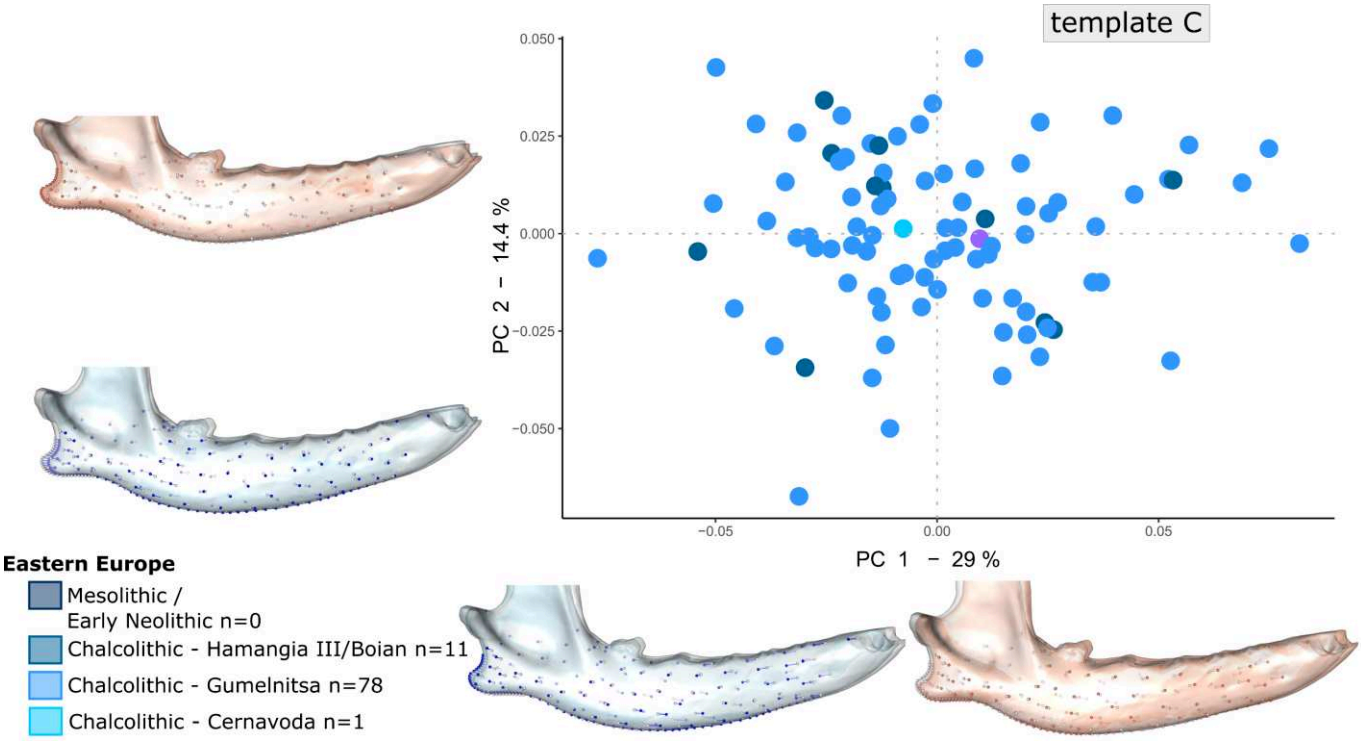

Figure 136. Visualisation of the two first axes of the Principal Component Analyses performed on the prorustes coordinates of template C for all ancient dogs from Eastern Europe.

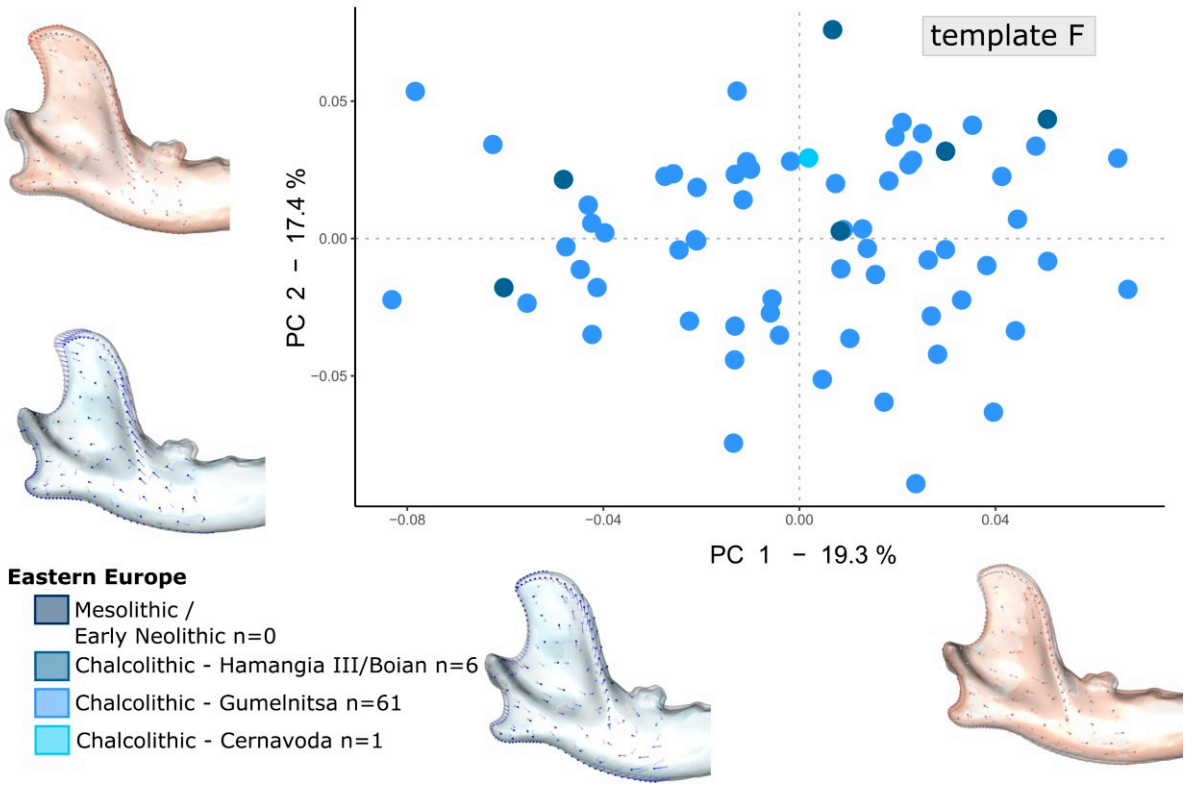

Figure 137. Visualisation of the two first axes of the Principal Component Analyses performed on the prorustes coordinates of template F for all ancient dogs from Eastern Europe.

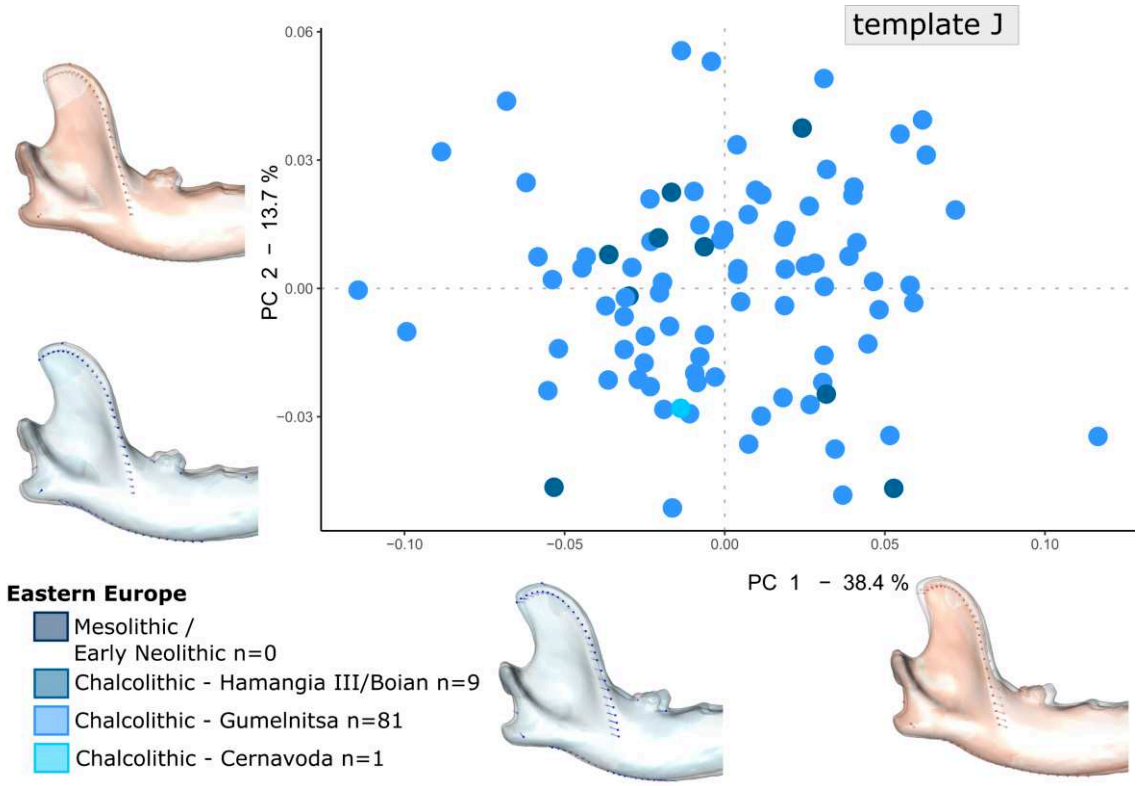

Figure 138. Visualisation of the two first axes of the Principal Component Analyses performed on the prorustes coordinates of template J for all ancient dogs from Eastern Europe.

2.2.3.3. *Shape difference between dogs from the Hamangia III/Boian and Gumelnița cultures – Canonical Variate Analyses*

Procrustes ANOVAs performed on templates A and B revealed **significant differences in the mean shapes of mandibles dated to the Hamangia III/Boian or Gumelnița cultures**.

The CVAs performed on template B (for template A there are too few specimens from the Boian/Hamngia cultures, Figure 139) allowed to describe further how mandible shape differs between the cultures. The cross validation is good only for dogs from the Gumelnița culture, which is to be related to their (likely) higher variability in shape. **It is likely that shapes of the Hamangia III/Boian cultures persist into the Late Chalcolithic and that new shapes appear during the Late Chalcolithic.**

Mandibles from the Hamangia III/Boian cultures are more robust, they have a more ventrally curved ramus, a more oriented backwards and higher coronoid process with a deeper masseteric fossa. The differences as regard the angular process are unclear in analyses based on template B, and the sample size in dogs from the Hamangia III/Boian group in analyses based on template A is too low to conclude. **Dogs from the Gumelnița culture have more "fox-like" mandibles** (the ramus is straighter and the ramus is very small in proportion).

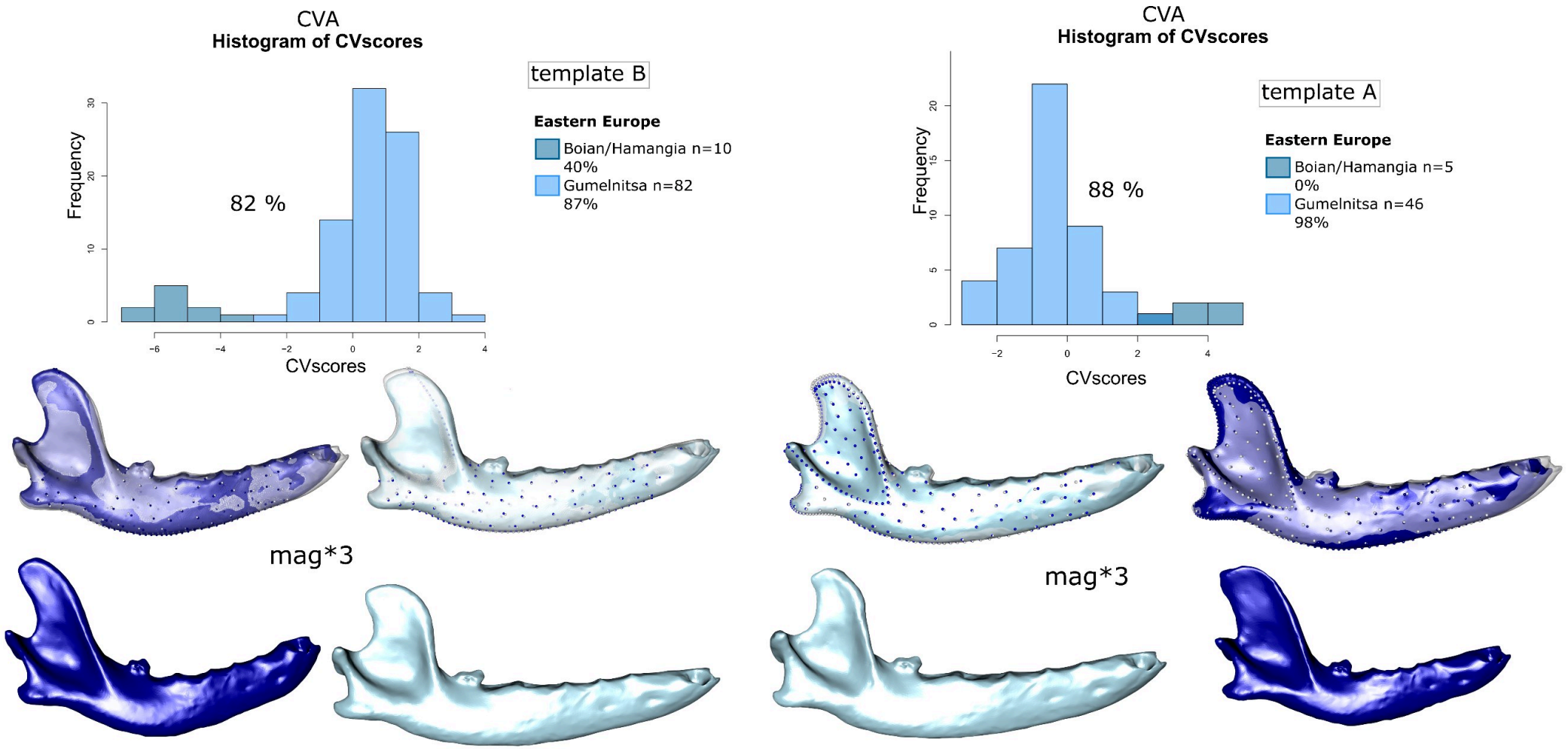

Figure 139. Results of the CVA performed on mandibles from the Hamangia III/Boian and Gumelnița cultures in Eastern Europe – analyses performed with template B and A. Analyses performed on coordinated from template A are reported for information purposes because the sample size is too low. mag: deformations are magnified by 3.

Absolute bite force

Variations in the absolute bite force are represented in Figure 140. **Dogs from the Hamangia III/Boian culture bite harder than dogs from the Gumelnița culture** as suggested by all templates. Templates E (misleading) G and I tend to suggest that **Mesolithic-Early Neolithic dogs bite harder than dogs from the Chalcolithic**, however, there are very few remains dated to the Mesolithic.

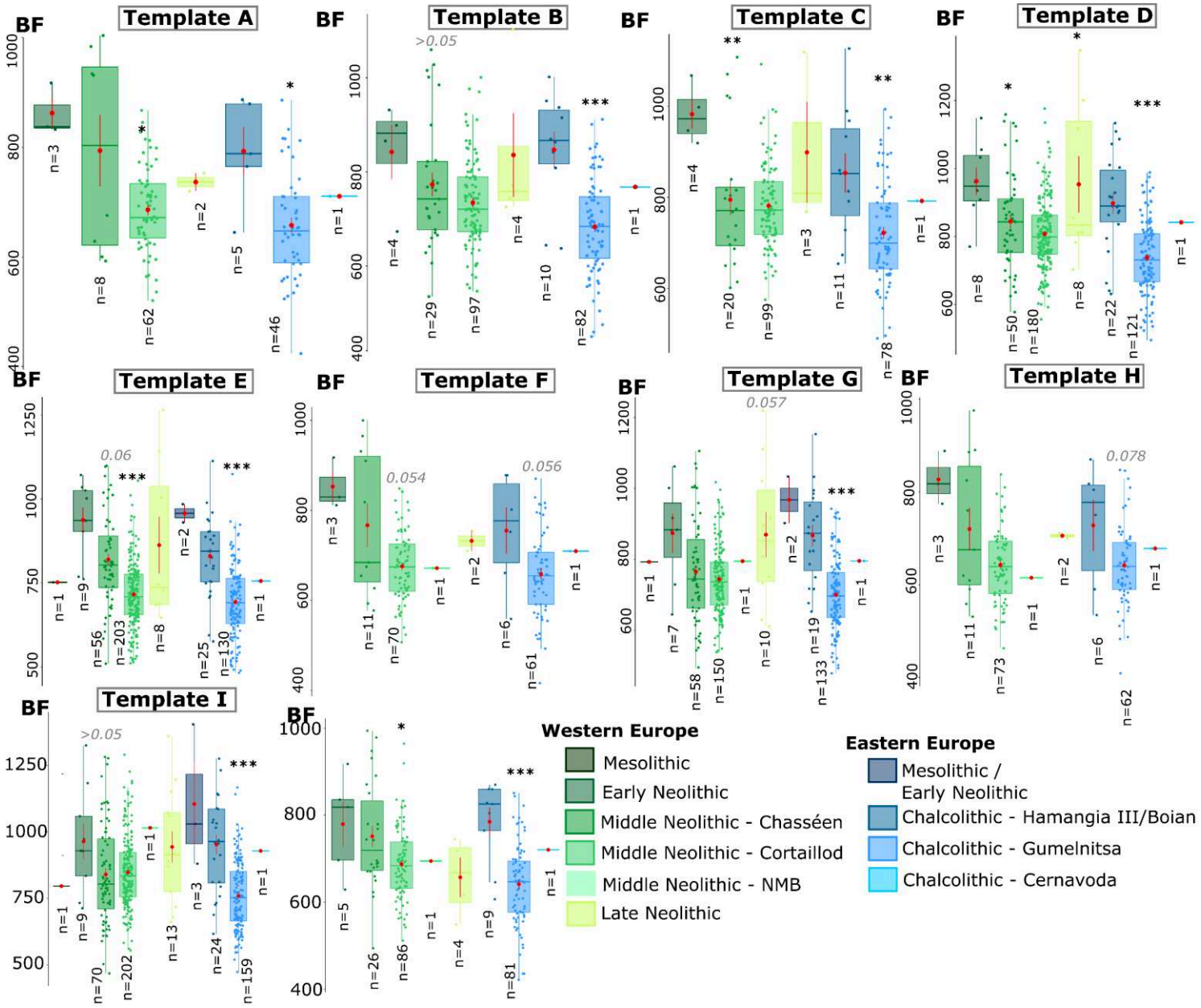

Figure 140. Absolute predicted bite force of ancient dogs from the Mesolithic to the early-Bronze Age in Europe for the 10 templates. Red dots correspond to the mean.

Residual bite force

Residual bite forces are represented on Figure 141. In Eastern Europe, **dogs dated to the Hamangia III/Boian culture bite relatively harder than dogs dated to the Gumelnița culture** (results are significant for templates A, B, D, E but template E is less relevant as regards size). **Dogs dated to the Mesolithic-Early Neolithic of Eastern Europe bite relatively harder than dogs from the Chalcolithic** according to templates E (misleading) and I.

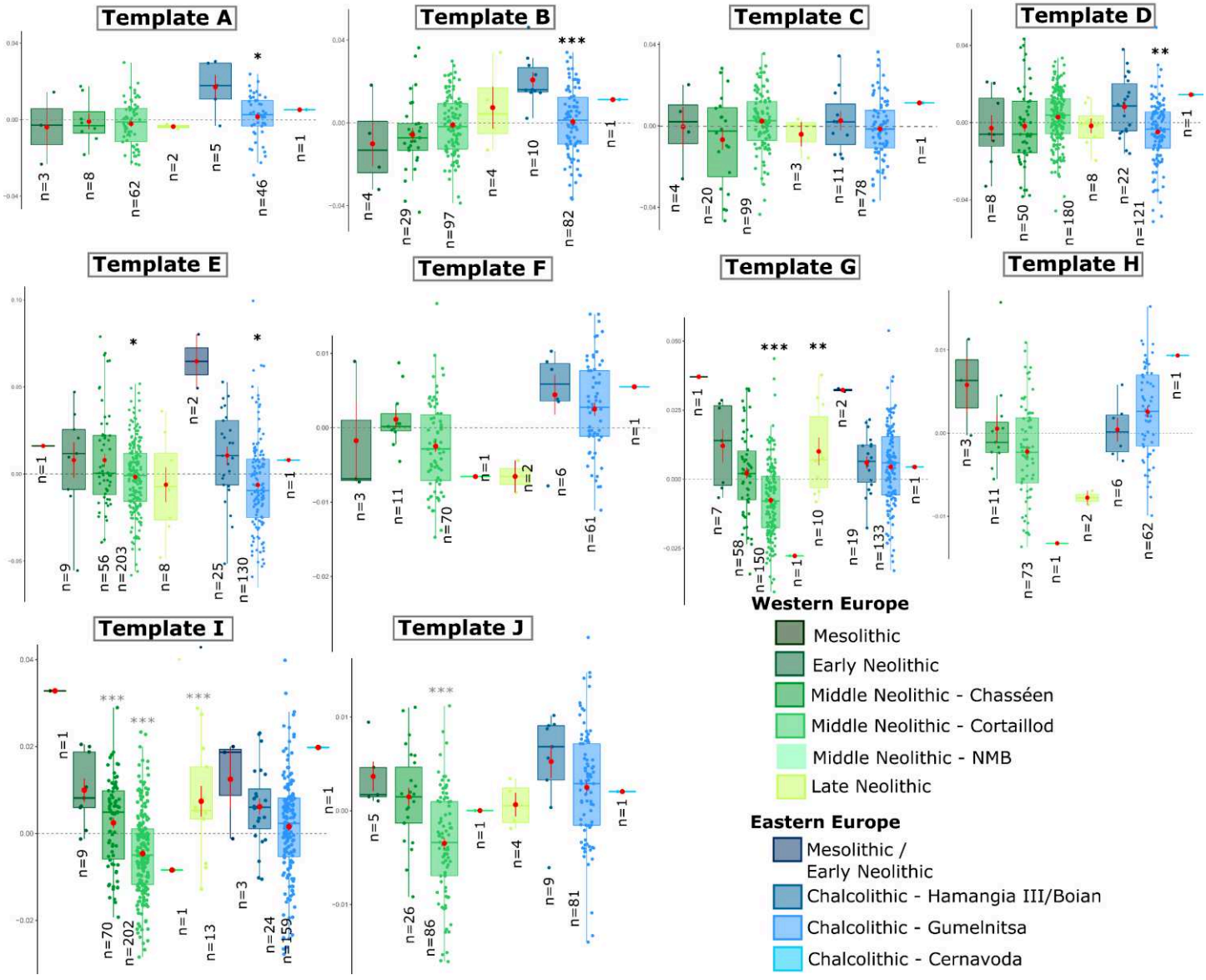

Figure 141. Residual predicted bite force of ancient dogs from the Mesolithic to the early-Bronze Age in Europe for the 10 templates. Red dots correspond to the mean. Sample sizes are indicated in Table 42.

Mechanical potential

Mechanical potentials are represented in Figure 142. There is no significant variation in the mechanical potential of dogs from Eastern Europe through time. We had no Mesolithic/early Neolithic dog to compare with the Chalcolithic dogs. In dogs dated to the Hamangia III/Boian cultures, the pterygoid muscle tends to contribute slightly more and the temporal and masseter tend to contribute slightly less to the overall bite force, but the results are not significant because of the high variability in dogs from the Gumelnița culture and the low sample size in dogs from the Hamangia III/Boian culture (n=9).

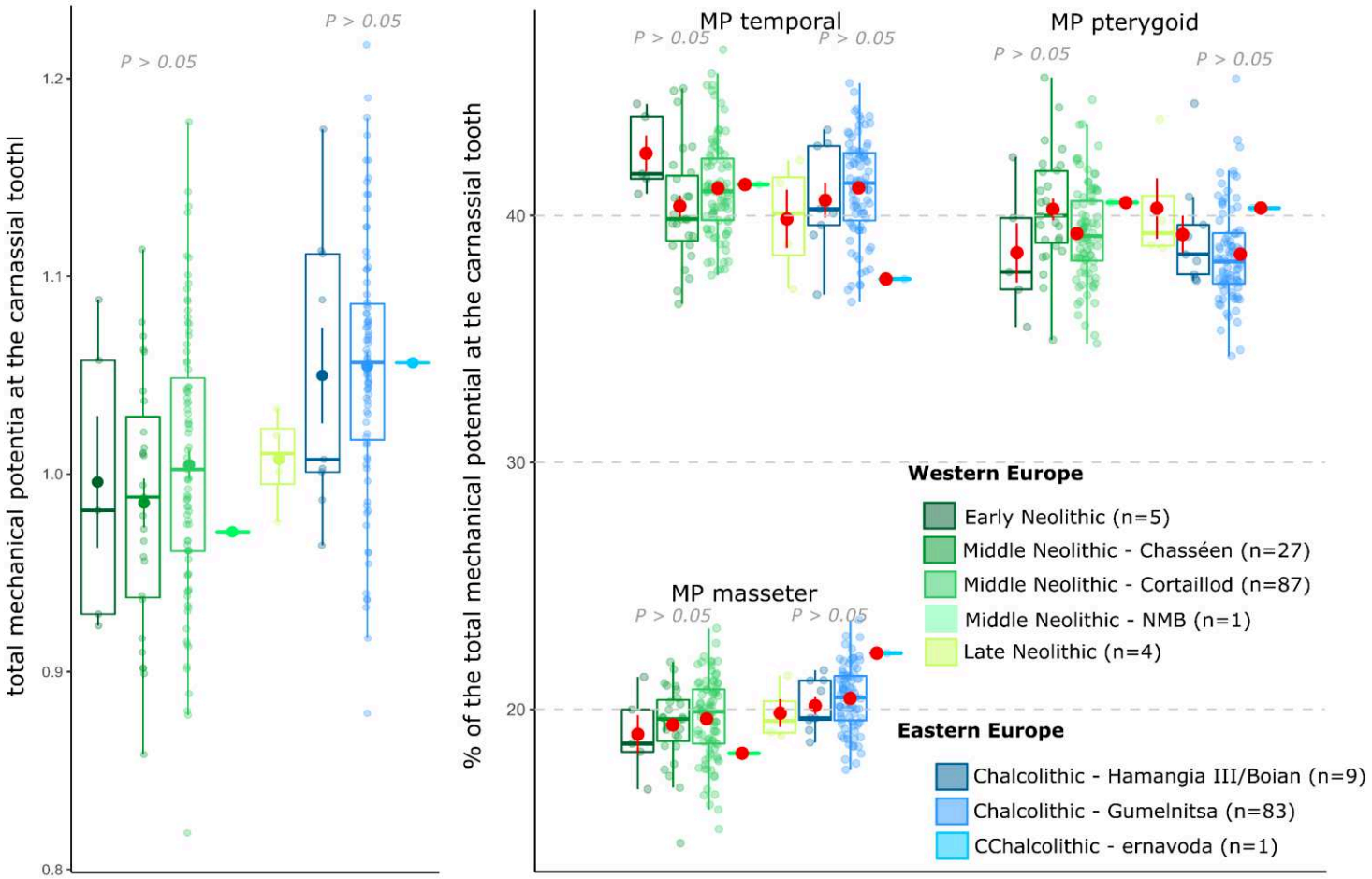

Figure 142. Mechanical potential of ancient dogs from the Mesolithic to the end of the Neolithic in Europe. Red dots correspond to the mean.

2.2.1. Evolution in Western Europe

2.2.1.1. *Centroid size*

We refer to Figure 133. There is huge variability in each group and some groups are poorly represented (Mesolithic, Early Neolithic and Late Neolithic). The following results thus must be interpreted with caution.

In Western Europe, **Early Neolithic dogs are relatively large** (as large as the largest dogs of the Middle Neolithic) and **small dogs tend to be more frequent during the Chasséen culture and even more during the Cortaillod culture**. Accordingly, **the mean size of dogs significantly decreases from the Early Neolithic to the Middle Neolithic**. Statistically, the differences are highly significant between the Early Neolithic and the Cortaillod culture for 6 of the 10 templates (A, C, D, E, F and H), highlighting the strength of the biological signal. Dogs from the Late Neolithic are relatively large compared to those of the Middle Neolithic, however the difference is only significant for template D (this is likely due to the small sample size in Late Neolithic dogs).

Centroid sizes are also more variable during the Chasséen culture than during the Cortaillod culture, for all templates. **Chasséen dogs are significantly bigger than Cortaillod** dogs only for templates A, D, E, but not for templates G and I. These results are more likely explained by differences in shape of some parts of the mandible than to differences in the overall size.

2.2.1.2. *Variability in shape*

Disparity

In Western Europe, we have too few Mesolithic and Early Neolithic dogs to be sure that the diversity in the Mesolithic and early Neolithic is correctly represented.

The variability in shape is greater during the Chasséen culture than during the Cortaillod culture according to analyses with template B (P = 0.006), but more specimens from the Cortaillod culture (n = 97) than from the Chasséen culture (n = 29) were analysed. The results are thus not due to the lower sample size in the Chassean group. The results are confirmed by analyses with template C (P = 0.002). However, the Cortaillod is represented by a single site (Twann), while the Chasséen is represented by eight different sites. It is therefore not surprising to observe a greater variability in this group.

Principal component analyses

We performed Principal Component Analyses for templates A and B (Figure 183), C, F and J (Figure 184) to visualize the morphological variation described by ancient dogs in Western Europe. Visualisations of shape deformations at the extremities of the principal components provide information on the existing range of variation. The morphospaces occupied by the Cortaillod and Chasséen dogs partially overlap but they tend to differ in all templates, suggesting differences in mean shapes. However, this analysis does not allow to clearly visualise the separation between groups.

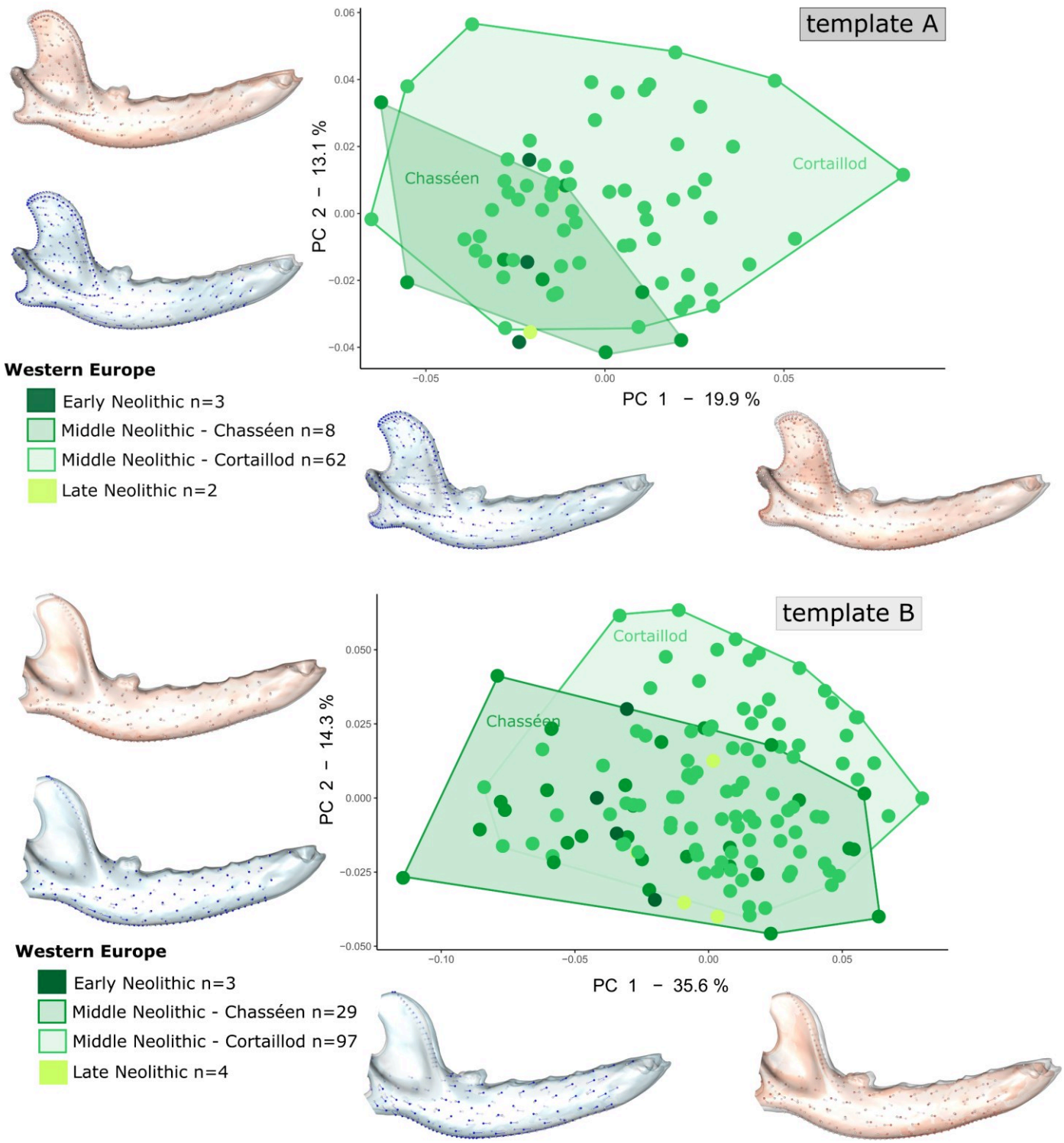

Figure 143. Visualisation of the two first axes of the Principal Component Analyses performed on the Procrustes coordinates of template A and B for all ancient dogs from Western Europe.

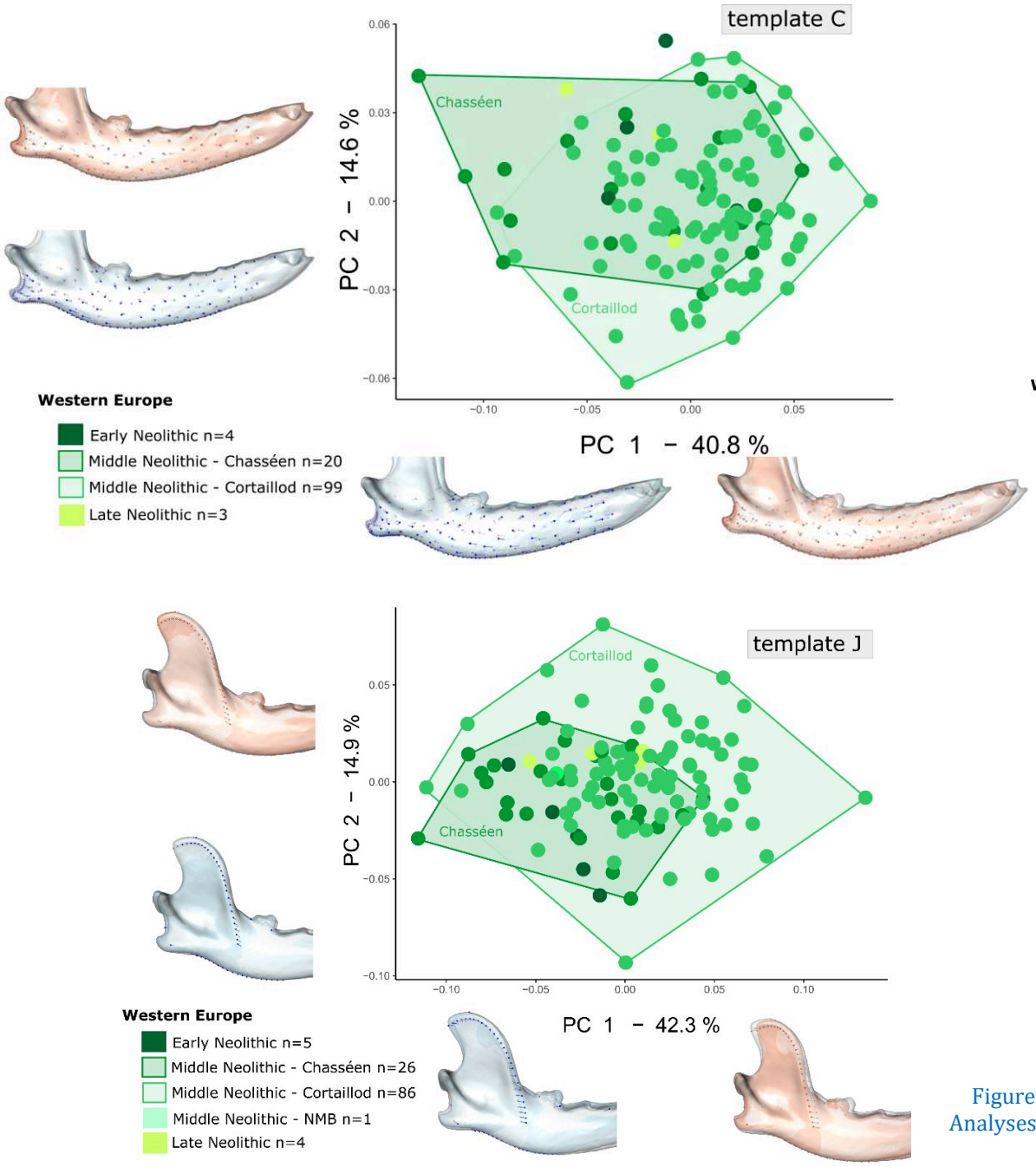

Figure 144. Visualisation of the two first axes of the Principal Component Analyses performed on the prorustes coordinates of template C, F and J for all ancient dogs from Western Europe.

2.2.1.3. *Shape difference between dogs from the Chasséen and Cortaillod cultures – Canonical Variate Analyses*

The results of the Procrustes ANOVAs show that **the mean shape of the mandible in dogs from the Chasséen culture significantly differs from that of dogs from the Cortaillod culture**. We obtained significant results for all templates.

The CVAs performed for templates A, B (Figure 145), C, F (Figure 146), I and J (Figure 147) allowed to describe further how mandible shape differs between the two cultures. **Dogs from the Chasséen have a straighter mandibular ramus** (templates A, B and C) **but a more robust mandibular branch** (A, B, C, F and J), **with a lower angular process and a more pronounced curvature under this process** (A, C, F), a **more backwards oriented coronoid process** (A, B, F, J) **and a likely shallower masseteric fossa** (A, F).

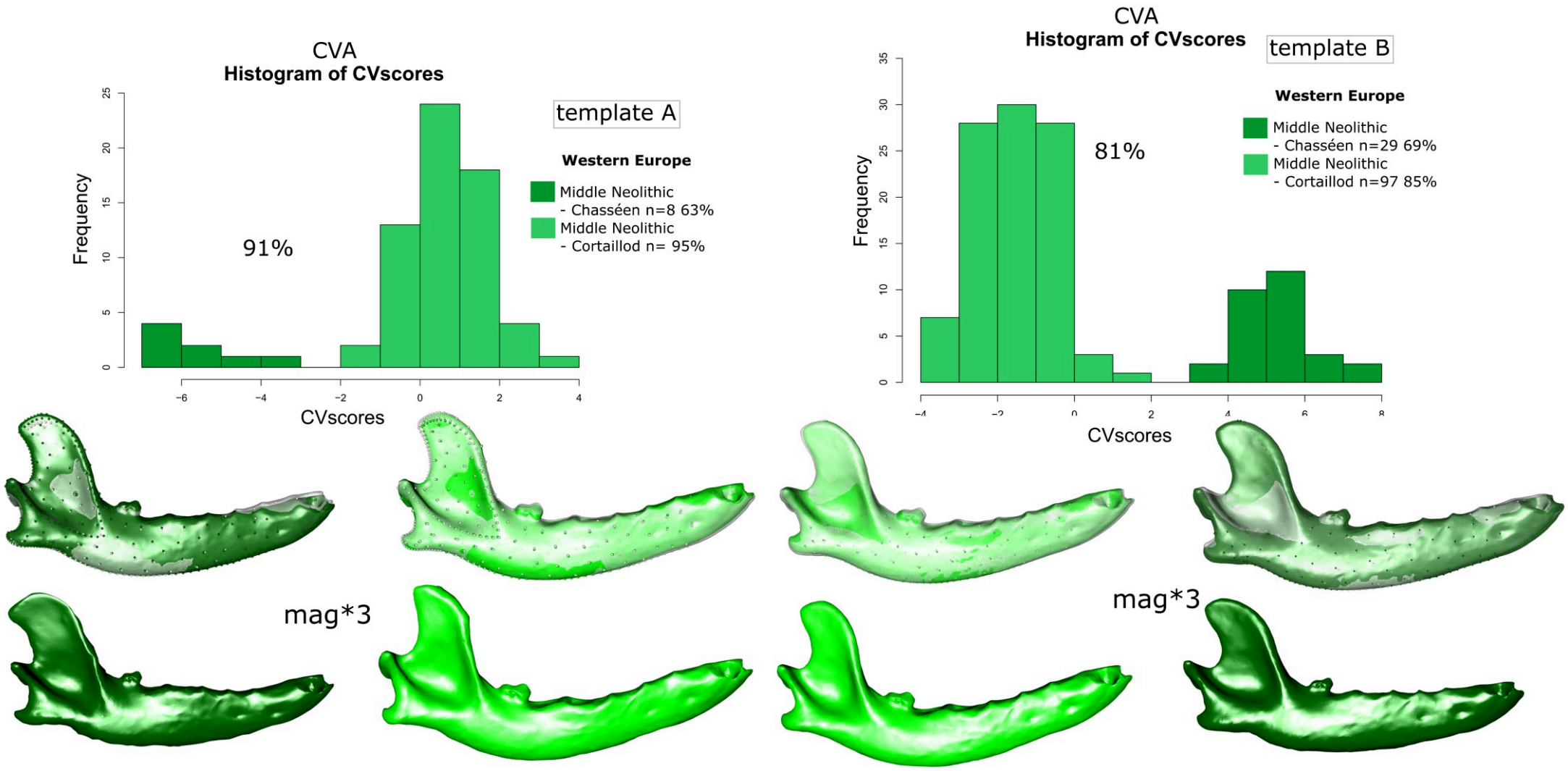

Figure 145. Results of the CVA performed on mandibles from the Chasséen and Cortaillod cultures in Western Europe – analyses performed with templates A and B. mag: deformations are magnified by three.

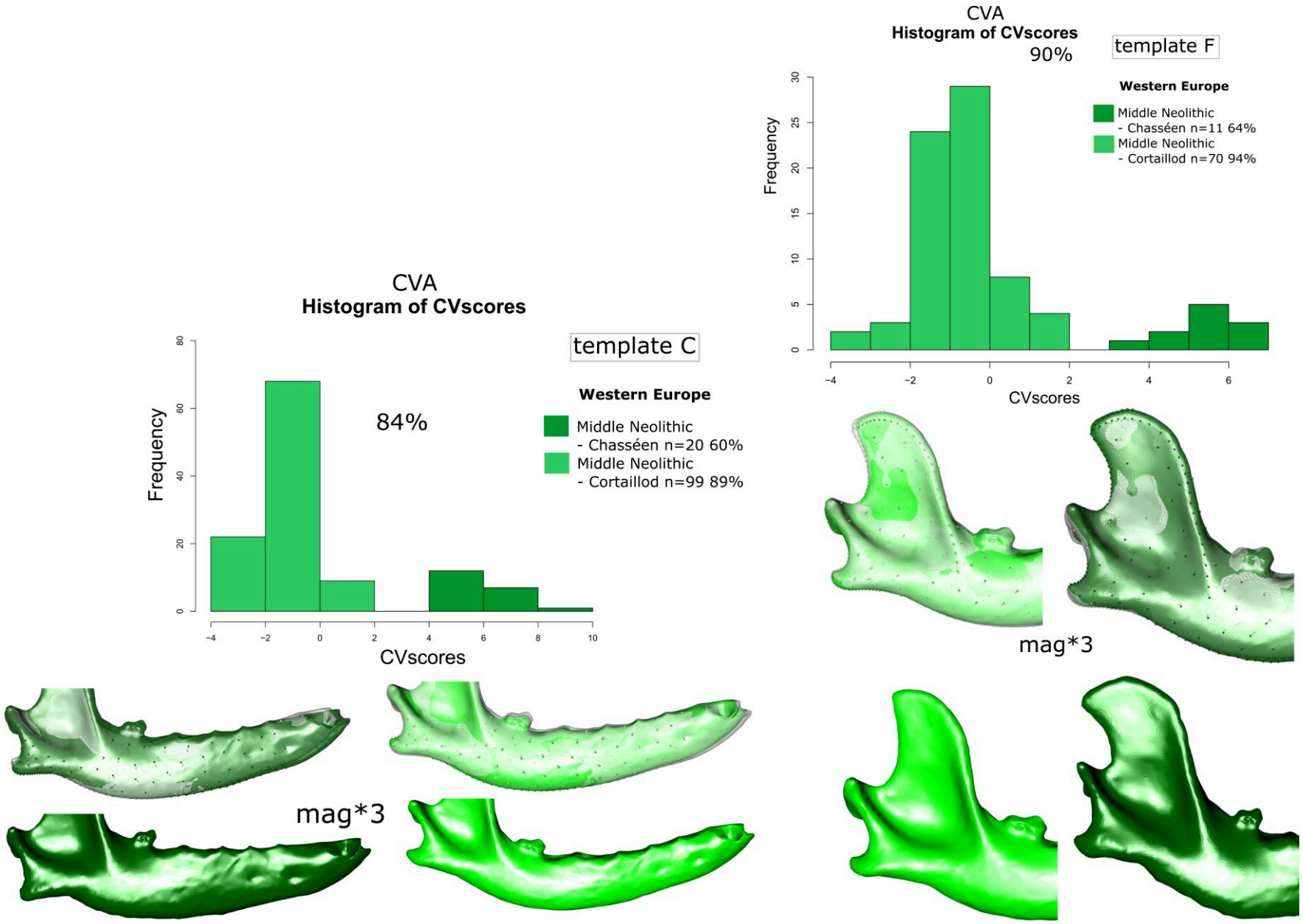

Figure 146. Results of the CVA performed on mandibles from the Chasséen and Cortaillod cultures in Western Europe – analyses performed with templates C and F. mag: deformations are magnified by three.

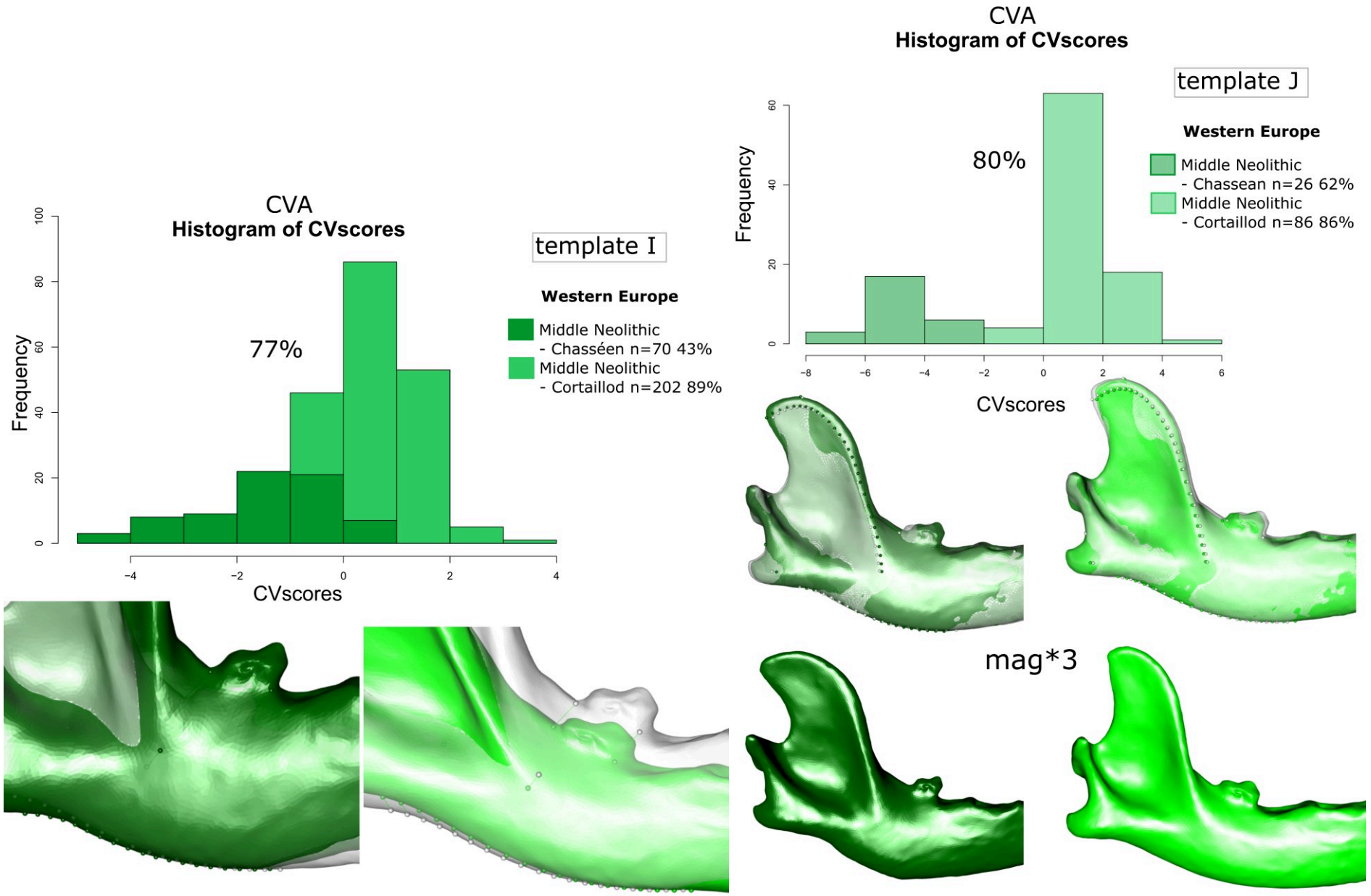

Figure 147. Results of the CVA performed on mandibles from the Chassean and Cortaillod in Western Europe – analyses performed with templates I and J. mag: deformations are magnified by three.

2.2.1.4. *Bite force*

Absolute bite force

We refer to Figure 140. Variation in bite force is mostly driven by variation in size. As expected, larger remains are associated with higher values of the predicted bite force and the graphs of predicted bite force are symmetric to the graphs of centroid sizes (Figure 140). Accordingly, **dogs dated to the early Neolithic tend to bite harder on average than dogs from the Middle Neolithic**. We indeed observed significant differences between the Early Neolithic and the Chasséen culture (template C) and above all highly significant differences between the Early Neolithic and the Cortaillod culture (templates A, C, D, E, F, H). **There is no clear difference between dogs from the Chasséen and Cortaillod cultures** (the p-values for templates A, F and J indicate almost significant results for an alpha risk of 5%), except for template E ($P < 0.001$) but as it amplifies differences, we do not take it into account.

Residual bite force

We refer to Figure 141. Only results obtained with templates A, B, C and D are reliable enough considering section 2.2.2. Accordingly, **we observe no significant difference in residual bite force from the early Neolithic to the end of the Neolithic in Western Europe.** The boxplot for template B seems to suggest that the mean residual bite force tends to increases over time, but this is not significant and the tendency is not confirmed by templates A, C and D.

Mechanical potential

We refer to Figure 142. There is no significant variation in the mechanical potential of dogs from Western Europe through time (according to ANOVAs performed on the total mechanical potential neither the mechanical potential of each jaw muscle, Figure 142). **Dogs dated to the Early Neolithic tend to have a slightly higher contribution of the temporal muscle and a lower contribution of the pterygoid muscle to the bite force**, however the statistical results are not significant because of the low sample size in Early Neolithic dogs and the high variability in Middle Neolithic dogs. In dogs dated to the Chasséen, the pterygoid muscle tends to contribute slightly more and the temporal muscle tends to contribute slightly less to the bite force than in Cortaillod dogs but the difference is unclear because of the high variability in the two groups. Besides, results are not significant.

Conclusion

We interpreted the evolution through time in Eastern and Western Europe separately. Because we had few and mostly fragmented dog mandibles from the Mesolithic, early Neolithic, Late Neolithic or Cernavoda culture, our conclusions are more robust when comparing dogs from the Chasséen and Cortaillod cultures in the Middle Neolithic of Western Europe and the Hamangia III/Boian and Gumelnița cultures in the Chalcolithic of Eatern Europe.

From the comparison of dogs from the Mesolithic to the very early Bronze Age in Eastern Europe, the following key points emerge:

KEY POINTS – Eastern Europe

- **An overall decrease in the mean centroid size from the Mesolithic to the end of the Chalcolithic**, with highly significant differences between the Hamangia III/Boian and Gumelnița cultures. This is related to the **presence of very small dogs during the Gumelnița**;

- **The residual bite force decreases from the Mesolithic to the Gumelnița culture**;

- The overall variability in shape and size does not change much over time. Tests indicate that **dogs from the Gumelnița tend to be significantly more variable in shape than dogs from the Hamangia III/Boian**. The CVA additionnaly suggest that during the Gumelnița, **shapes from the Hamangia III/Boian cultures are still attested and new shapes appear**. However, the sample size is relatively low for the Hamangia III/Boian group and requires a future enrichment. If confirmed this might be related to the almost complete replacement of local dogs from haplogroup C by exogenous dogs of haplogroup D, probably coming from the Near East (see Table 12);

- **These new shapes (more "fox-like")** are characterized by a straighter mandibular body and a lower coronoid process which may be related to a **slightly higher contribution of the temporal muscle and the likely but not significant lower contribution of the pterygoid muscle**.

- **Dogs dated to the Hamangia III/Boian cultures have a more robust and ventrally curved mandible with a more voluminous coronoid process, angular process and a deeper masseteric fossa, which is to be related to higher residual bite forces.**

From the comparison of dogs from the Mesolithic to the very early Bronze Age in Western Europe, the following key points emerge:

KEY POINTS – Western Europe

- The mean **centroid size significantly decreases between the Early Neolithic and the Middle Neolithic** (the results are very highly significant for the Cortaillod). This is related to the appearance of **small dogs in the Chasséen culture and to their growing importance in dog populations during the Cortaillod culture**;

- The decrease in the variability in shape between the Chasséen and Cortaillod cultures likely results from the constitution of the sample, as the Cortaillod group contains only one site (Twann). This result, if confirmed, would not be consistent with the fact that, in Western Europe, local dogs are maintained and accompanied by new exogenous dogs (one should observe an increase in the variability through time). This requires a future enrichment for the Cortaillod group with dogs coming from other sites;

- **No significant change in bite force relative to size** (nor the mechanical potential) from the Early Neolithic to the end of the Neolithic, but **dogs from the Early Neolithic tend to use more their temporal muscle and less their pterygoid muscle in comparison to dogs from the Middle Neolithic** (but the results are not significant).

- **Dogs from the Chasséen and Cortaillod cultures significantly differ in shape.**
  - ⇨ This might be related to the different composition of the populations in genetic terms (Chasséen: haplogroups C, A, D, B; Cortaillod: haplogroups C, D, see Table 12).
  - ⇨ It also can be related to differences in the contribution of muscles to the bite force. Dogs from the Chasséen have a straighter mandibular ramus but a more robust mandibular branch (these two aspects compensate each other, explaining the lack of difference in relative bite forces), with a more developed angular process and a more pronounced curvature under this process (**the pterygoid muscle thus tends to contribute more to the bite force**) and a more backwards oriented coronoid process (however the temporal muscle tends to contribute less). The differences in the contribution of the adductors to the bite force are not significant but are reminiscent of similar trends as those observed between the Hamangia III/Boian and the Gumelnița cultures in Eastern Europe;

- Our corpus of Late Neolithic dogs is smaller than for the previous period but no small dogs are attested, resulting in an overall increase in size.

3. Exploration of the morphological and functional variability existing in the jaw of dogs from the site of Twann (Middle Neolithic – Cortaillod culture)

Now we have explored the chronological evolution in Western Europe, we focus in the following section on the analyses of the 221 dog mandibles from Twann included in the geometric morphometric analyses, all being dated to the Cortaillod culture (Middle Neolithic). This waterlogged site is dated with great precision thanks to dendrochronology. This site therefore offers the unique opportunity to study the evolution of the morphological and functional variability of the dogs on the same site within a well known period of time.

3.1. Preliminar exploration of the variability in shape within the site of Twann in comparison to other sites of Western Europe

The **dogs from Twann occupy a wide range of morphological variation in comparison to other dogs from Western Europe** (Figure 148). They are also **less variable** as suggested by disparity tests based on template B (Twann: n = 97 and Procrustes variance = 0.0034, other sites from Western Europe: n = 38 and Procrustes variance = 0.0044, $P = 0.01$), and as suggested in the previous section – see section 1.1). **Their centroid size is in the low average of Western European dogs.**

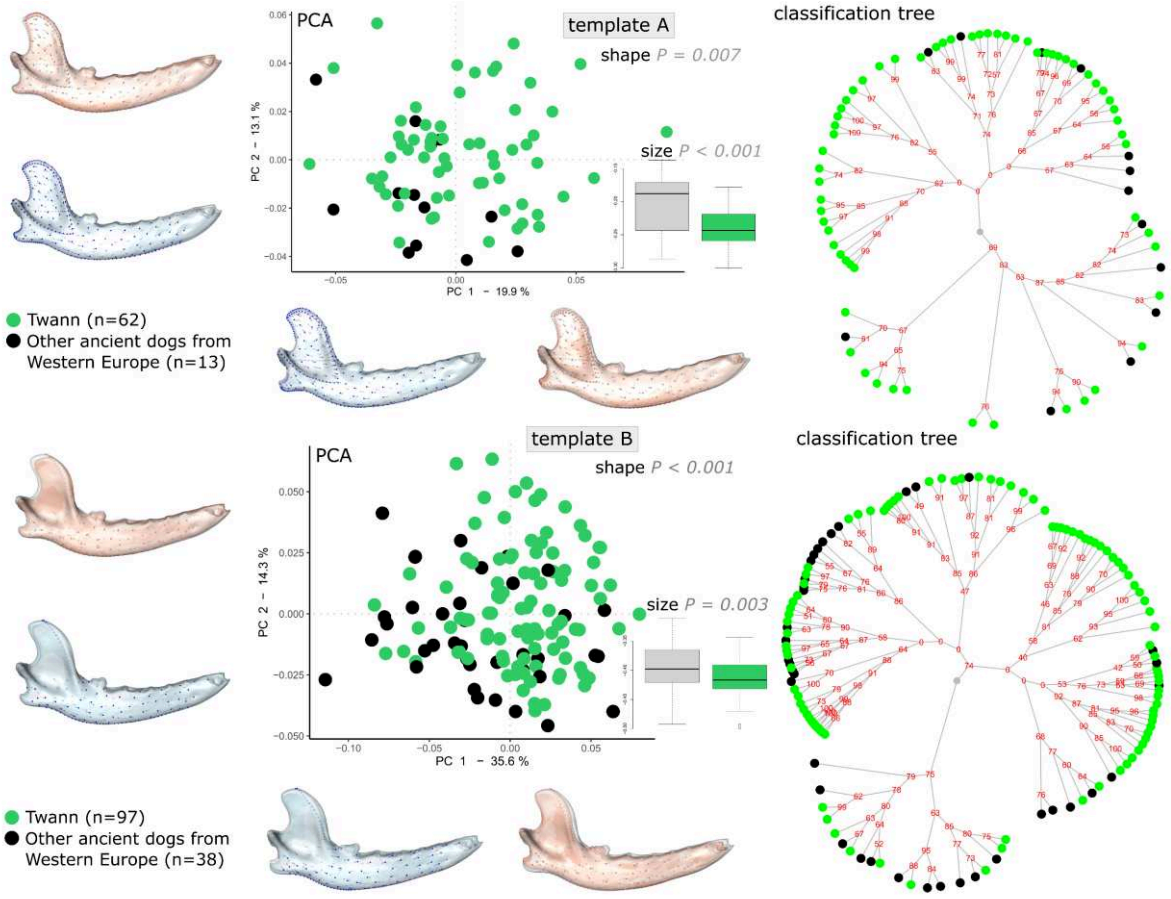

Figure 148. Visualisation of the morphological variability existing in dogs from Twann (middle Neolithic, Cortaillod) in comparison to the other ancient dogs from Western Europe.

3.2. Methodology and chronology

The stratigraphy of this site is relatively complex and requires to synthetise the available information. Three publications provided us with information on the chronology that we summarized in Figure 149 (Schibler and Suter, 1990; Burri-Wyser and Jammet-Reynal, 2014; Stöckli, 2018).Twann is a multistratified settlement. For the Cortaillod culture (~ 4,000-3,500BC), there are several levels (the "Schichtpaket") based on arbitrary subdivisions: US (untere Schicht: lower levels), MS (mittlere Schicht: intermediate level) and OS (Obere Schicht: upper level). In the same timeframe, some occupation levels are more precisely described and dated (levels E1 to E10). There are also later occupations related to the Late Neolithic Horgen culture (UH, MH and OH, ~ 3,500-3,000 BC), where canid remains are rare: we do not have any dog remains from this culture, only red foxes.

3.2.1. Data registration

During data registration, I noted the information that were written on the mandibles, on the bags and on the storage boxes. On the bones, inventory numbers or sometimes the layer OS, US, MS, or even the occupation (E1, E2, etc.) were indicated. In this case, the information was considered a very reliable and recorded as a chronological variable.

I noticed that a special colour coding was used (as mentioned in Stöckli, 2018). The colour blue was used for the US layer, red for the MS layer and black for the OS colour. This reinforced the attributions, but sometimes the colour was present without the layer being mentioned either on the bones or on the container. For example, in box 145 (A 6/7), in the "Hund??" bag, the mandible number 1137.7 was written in red, without any mention of the MS layer. In this case I put "MS?". If the number was written in red and the layer was not written on the mandible but on the bag or box and this information matched the colour, the colour and the layer were considered to assign a time group to the mandible.

When the colour was not especially suggestive (black, which is likely to be used by default), the layer reported on the bag or box was used. Sometimes this layer was uncertain, for example in box 181, the mandibles were written in black and the box mentioned that the dogs belong to the US (MS?) layer 4. I recorded them as US/MS.

If there was no mention, no group was assigned (this was the case for mandibles in box 212 A2-4; A16, where there was nothing more written on the mandibles than an inventory number).

In box 94, I was confronted with dubious mentions. Box 94 was marked as US1, but it contained mandibles with the mention OS written in black (the OS attribution is kept), or with the mention E2-E3 or MS written in red (the E2-E3 or MS attribution were kept, respectively), or mandibles with just an ID written in black, red or white (in this case I recorded them as US?).

In box 95 (US1 zt (i.e. including) MS) mandibles were attribute to "US" when the writings were in black color and to “US/MS” when the mandibles were written in red (in two bags, one having a red hallmark and being clearly attributed to US/MS).

Sometimes the layer and the E occupation (e.g. MS-E5) were mentioned, but sometimes only one or the other of these informations was available.

Some bags reported slightly mixed attribution (MS/OS or OS/US).

In an unnamed box there was a bag written "A 6/7 OS-MS Hund (nicht vesmessene Knochen)" where the mandibles 927.1 and 39D 689.4 were assigned to the MS/OS group.

Figure 149. Chronology of Twann. Synthesis of available information and groups considered in this thesis. C. : Cortaillod

3.2.2. Simplified classification in chrono-groups

To sum up, once all this information was noted, we obtained the following:

E10	E2-E3	E3	E5	E6	E7	E8	E9	MS	MS/OS	MS?	OS	OS/US	US	US/MS	US?
2	1	2	8	3	3	11	12	15	2	7	49	1	15	38	40

Due to the heterogeneity of the information available when collecting the material, the first step was to cross-check as much information as possible to provide chronological groups as homogeneous as possible in terms of size and time period.

We chose two different simplified classifications: one considers two large chronological groups (T1a and T1b), and the other is more precise as regards chronology, with three chrono-groups, but contains fewer specimens (Table 43). Two batches of analyses were therefore conducted and the results will be compared to make sure that they are not completely different.

Our sample contains a lot of mandibules with a likely but not 100% sure attribution to layers “US” or “MS”. We thus conducted analyses with and without the mandibles reported as “US?”, “MS?” or “E2/E3” and compared the results. If compatible results are obtained, only the results from the analyses including all the mandibles are considered. Accordingly, for each batch, we performed analyses on two samples (sample 1 considers only the mandibles with a reliable attribution and sample 2 considers also mandibles with a likely but slightly doubtful attribution, Table 43).

The constitution of each batch and sampling is reported in Table 43 and Figure 150.

In the first batch of analyses, more mandibles are represented, especially with the sampling 2 (in this case only 2 MS/OS and 1 OS/US mandibles are left out), but the chronology is less precisely described. In the second batch of analyses, 38 US/MS mandibles are lost, which is not negligible, but it allows to go further in the exploration of the chronological changes.

Dog mandibles are well preserved but the preservation is less good for the more recent phases (T1b). Accordingly, to explore the evolution through time the templates A and B will be of minor interest, as we will be limited by the small sample size (less than 25 dogs for templates A, B, C F and J in T1b and T2b groups). Smaller templates will be more helpful.

If only individuals whose attribution to a chrono-group is absolutely certain are considered, the sample size for groups T2a and T2abis is too low. As a consequence, the second batch of analyses with sampling 1 makes little sense.

Table 43. Sampling methods for the analyses of Twann dogs.

Batch 1		
Chrono-group	**Sampling 1**	**Sampling 2**
T1a	US	US
	US/MS	US/MS
	MS	MS
		E2-E3
	E3	E3
	E5	E5
		40US?
		7MS?
	N=79	N=126
T1b	E6-E7-E8-E89-E10-OS	
	N=80	

Batch 2		
Chrono-group	**Sampling 1**	**Sampling 2**
T2a	US	US
		US?
	N= 15	N=55
T2abis	E3	E3
	E5	E5
	MS	MS
		MS?
	N=25	N=32
T2 b	E6-E7-E8-E89-E10-OS	
	N=80	

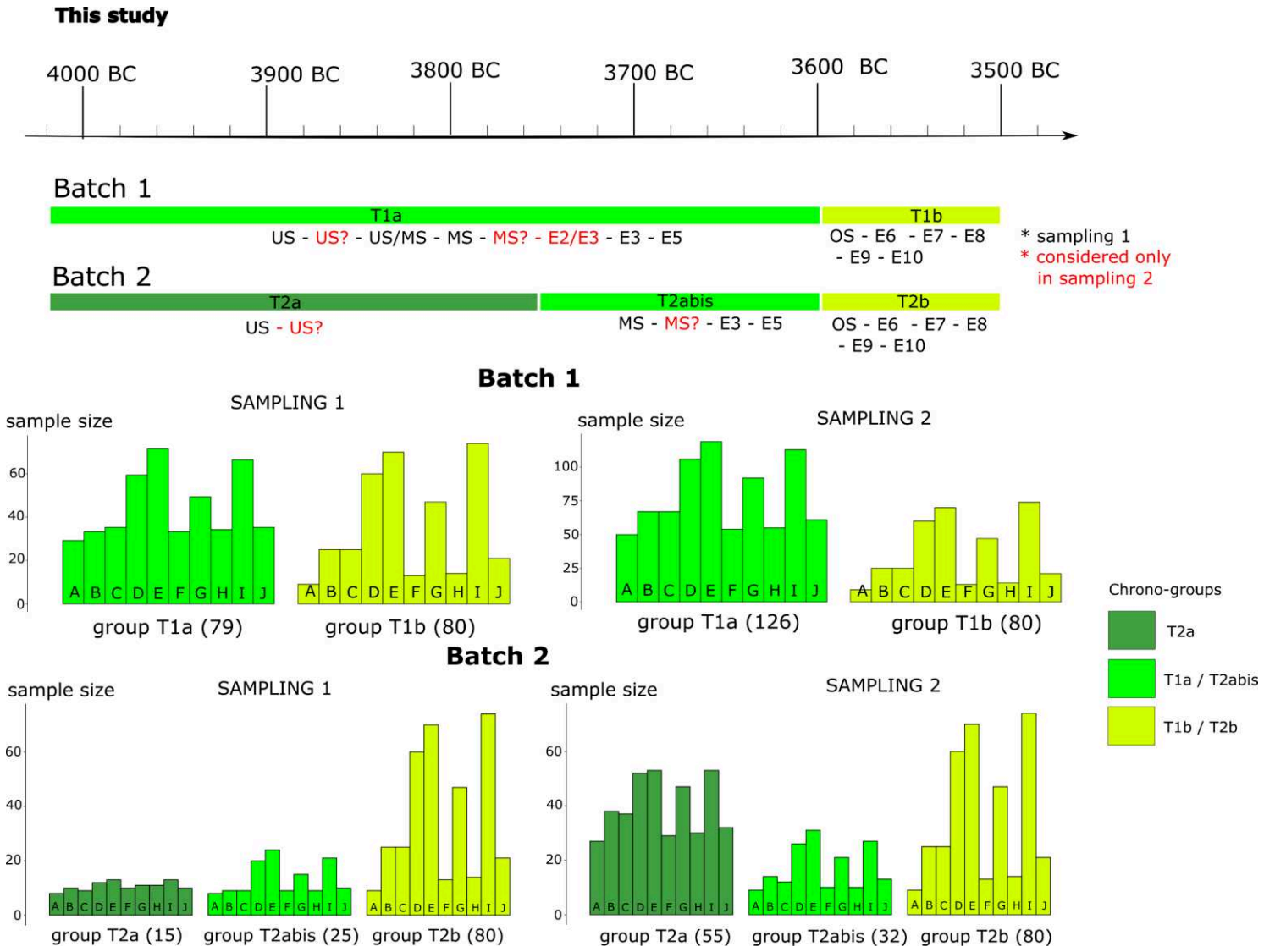

Figure 150. Constitution of the chrono-groups considered for the analyses of dogs from Twann and sample size for each batch and sampling method.

3.3. Results

We performed the same analyses than the ones conducted in the previous section (section 1.1 Statistical tests and table of results, page 414)

3.3.1. Results of the first batch of analyses with two chrono-groups

The results of the statistical analyses are reported in Table 44.

Table 44. Results of the first batch of analyses conducted on sampling 2 of dog mandibles from Twann. Significant results are written in blue.

	Sample size			Shape		Centroid size		BF	
	T1a	T1b	Other	Mean	Disparity	Mean	Variance	Absolute	Residual
A	50	9	1	0.2	0.5	0.5	0.8	0.5	0.7
B	67	25	1	0.8	0.5	0.064	0.13	0.049	0.5
C	67	25	1	0.6	0.2	0.12	0.6	0.093	0.5
D	106	60	3	0.039	0.2	T1a>T1b <0.001	0.018	0.0011	0.9
E	119	70	3	0.023	0.9	T1a>T1b <0.001	0.18	<0.001	0.5
F	54	13	1	0.048	0.15	0.7	0.6	0.8	0.13
G	92	47	1	0.7	0.9	T1a>T1b 0.031	0.9	0.025	0.54
H	55	14	1	0.4	0.1	0.3	0.17	0.3	0.2
I	113	74	3	0.4	1	T1a>T1b 0.006	0.9	0.003	0.077
J	61	21	1	0.6	0.8	0.2	0.6	0.3	0.1

There is no difference in variability between groups, neither in shape nor centroid size (except for template D).

For the templates with a sufficient number of dogs in the chrono-group Tb (D, E, G and I), the **centroid size is significantly bigger in the early phase (T1a) and smaller in the most recent phase (T1b**, Figure 153). As expected, the same holds for the absolute bite force.

Significant differences in shape were evidenced for templates D, E and F, without any repercussion on the residual bite force. The CVAs for templates D, E (Figure 151) and F (Figure 152) show that in the early phase (T1a) the mandibular body is higher, more curved and robust and the coronoid and angular processes are more imposing (but the masseteric fossa is shallower). The success rates of the CVAs are quite low, suggesting that overlap between groups is important (which is consistent with the low significance of the p-value in Procrustes ANOVAs).

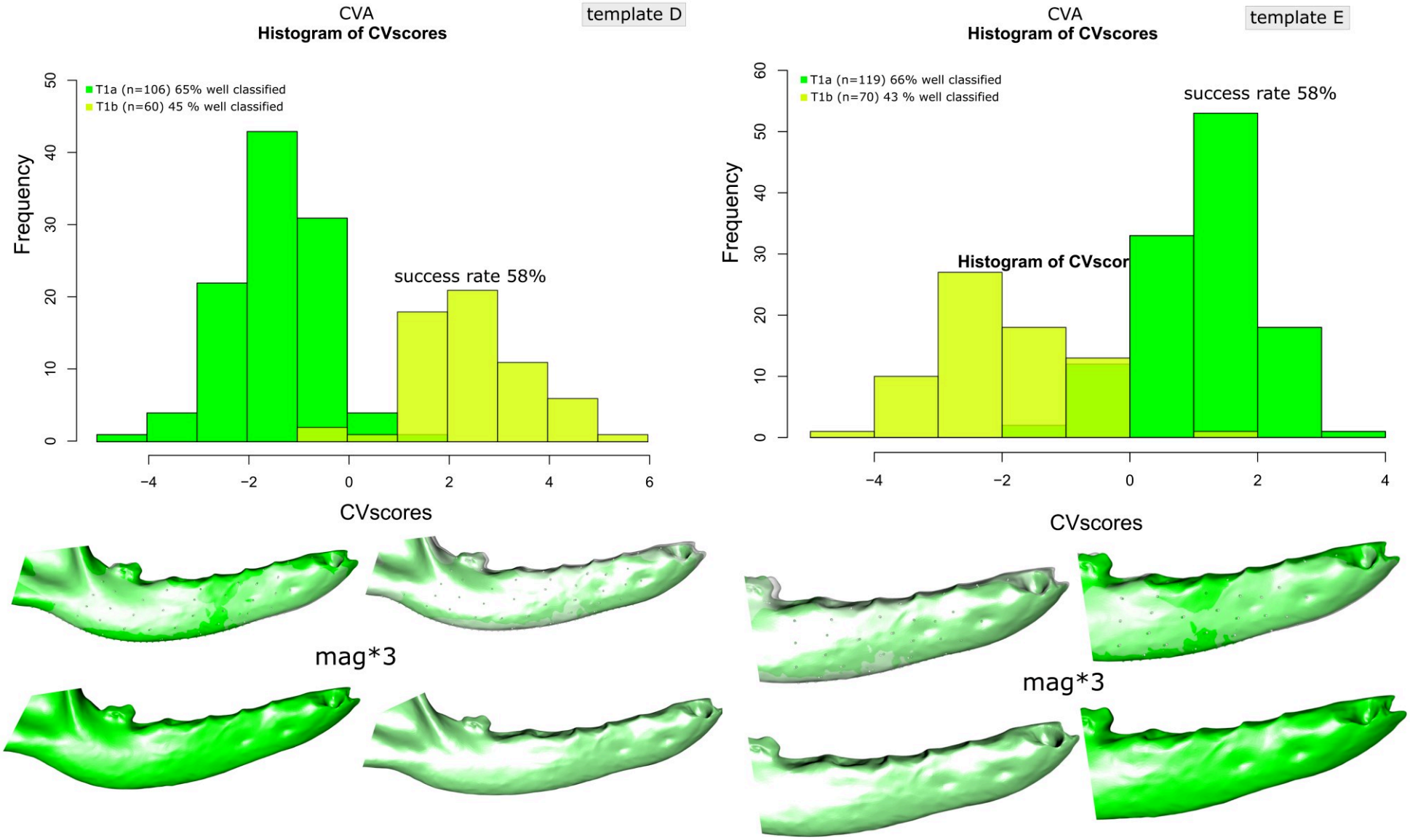

Figure 151. CVA performed on dogs from Twann – batch 1 – sampling – templates B and D.

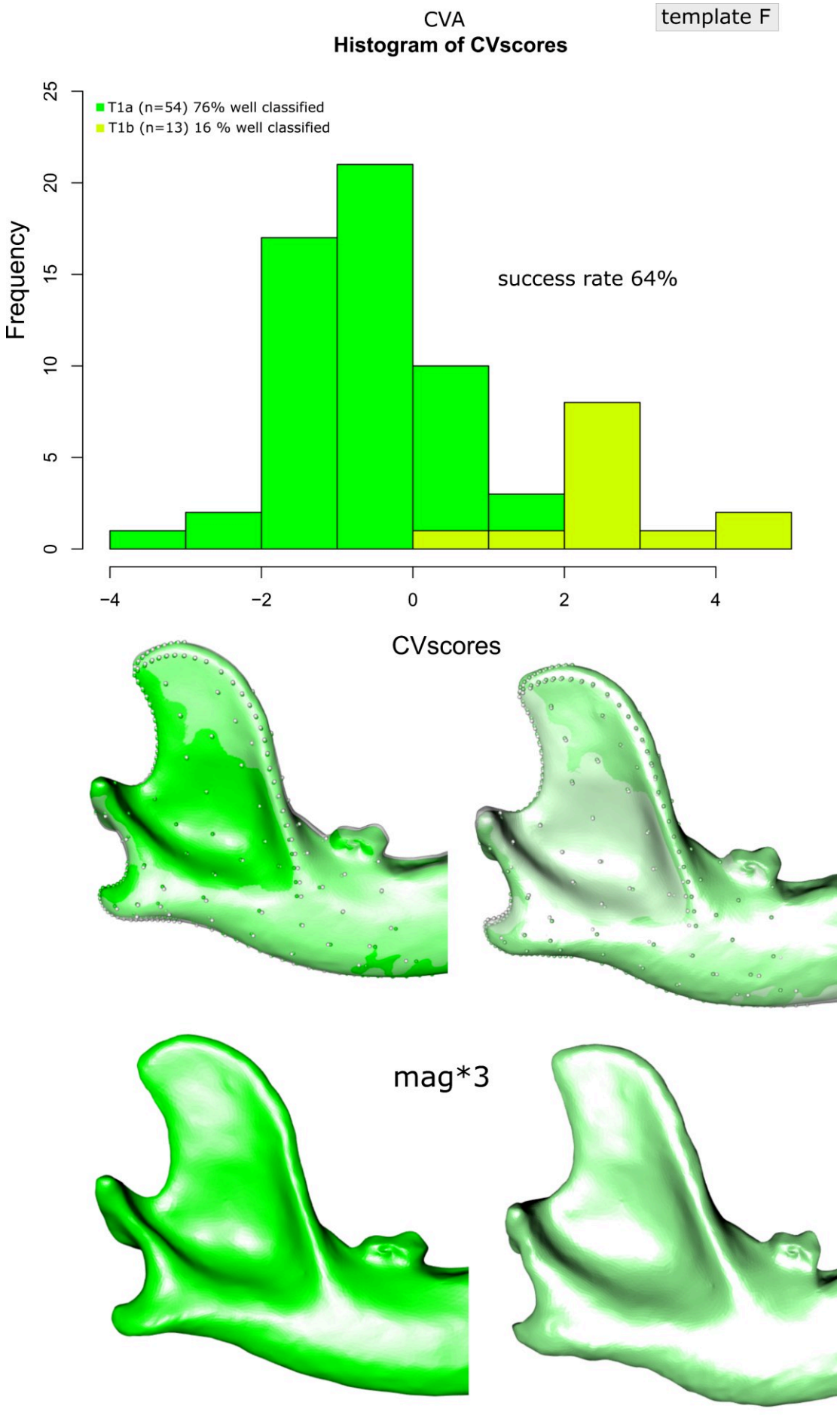

Figure 152. CVA performed on dogs from Twann – batch 1 – sampling 2– template F.

In the analyses carried out on sampling 1 (Table 45), the **differences in centroid size and absolute bite force are still significant, but the differences in shape are no longer significant** (the P value for template E, which has the largest sample size in both groups, indicates an almost significant result, with $P = 0.054$). As these results are consistent with those obtained with sampling 2, we maintain the conclusions obtained from the previous analyses.

Table 45. Results of the first batch of analyses conducted on sampling 1 of dog mandibles from Twann. Significant results are written in blue.

	Sample size			Shape		Centroid size		BF	
	T1a	T1b	Other	Mean	Disparity	Mean	Variance	Absolute	Residual
A	30	9	21	0.9	0.6	0.9	0.9	1	0.7
B	34	25	34	0.2	0.7	0.4	0.2	0.2	0.2
C	36	25	32	0.6	0.1	0.6	0.8	0.5	0.5
D	60	60	49	0.2	0.7	T1a>T1b 0.03	0.041	T1a>T1b 0.03	0.8
E	72	70	50	0.054	0.9	T1a>T1b 0.02	0.3	T1a>T1b 0.02	0.7
F	34	13	21	0.073	0.2	0.8	0.7	0.7	0.2
G	50	47	43	0.9	1	0.15	0.7	0.11	0.4
H	35	14	21	0.7	0.2	0.13	0.2	0.13	0.7
I	67	74	49	0.8	1	T1a>T1b 0.032	0.8	T1a>T1b 0.026	0.5
J	36	21	26	0.3	0.7	0.6	0.7	0.8	T1a>T1b 0.034

3.3.2. Results of the second batch of analyses with three chrono-groups

The results of the second batch of analyses peformed on sampling 2 (Table 46) suggest that the **differences are more precisely located between the oldest (US - T2a) and latest (OS - T2b) mandibles**. **Centroid size and absolute bite force are higher in T2a than in T2b** based on templates D, E, G and I. Template E further suggests that this decrease in centroid size and bite force is confirmed between T2a, T2abis and T2b (Figure 153). There is still no difference in the residual bite force (which is consistent with the results of batch 1). Differences in shape are significant for template D only.

Table 46. Results of the second batch of analyses conducted on sampling 2 of dog mandibles from Twann. Significant results are written in blue.

	Sample size				Shape		Centroid size	BF	
	T2a	T2abis	T2b	Other	Mean	Disparity	Mean	Absolute	Residual
A	27	9	9	15	0.14	>0.1	0.6	0.7	0.9
B	38	14	25	16	0.6	>0.1	0.09	0.08	0.5
C	37	12	25	19	0.5	>0.1	0.17	0.14	0.6
D	52	25	60	31	0.044	>0.1	T2a>T2b 0.0014	T2a>T2b 0.0017	0.9
E	53	31	70	38	0.12	>0.1	T2a>T2b 0.0010 T2abis>T2b 0.074	T2a>T2b 0.0015 T2abis>T2b 0.024	0.24
F	29	10	13	16	0.083	>0.1	0.8	0.9	0.4
G	47	21	47	25	0.17	>0.1	T2a>T2b 0.029	T2a>T2b 0.038	0.3
H	30	10	14	16	0.2	T2a<T2b 0.04	0.9	0.8	0.09
I	53	27	74	36	0.21	>0.1	T2a>T2b 0.017	T2a>T2b 0.0071	0.09
J	32	13	21	17	0.6	>0.1	0.2	0.3	0.1

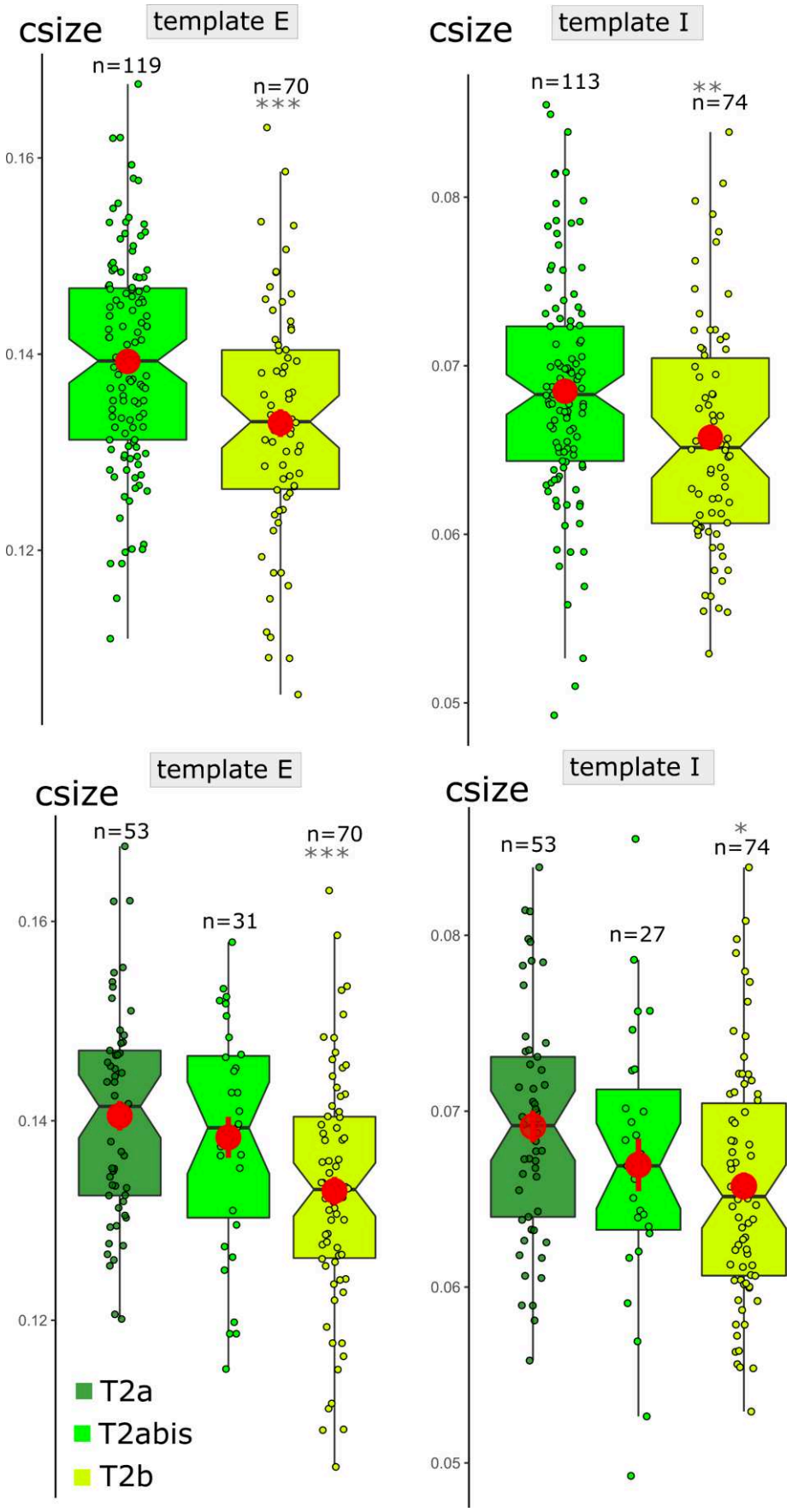

Figure 153. Centroid size of dogs from Twann based on templates E and I and the two batch of analyses on sampling 2. Red dots correspond to the mean.

The CVA based on template D has a low success rate, highligthing the strong overlap in shapes between groups (Figure 154). The CVA mainly distinguishes the mandibles of the T2a group, to the left of axis 1 of the CVA. The mandibles of this group are more curved overall, which is in line with our observations with previous analyses.

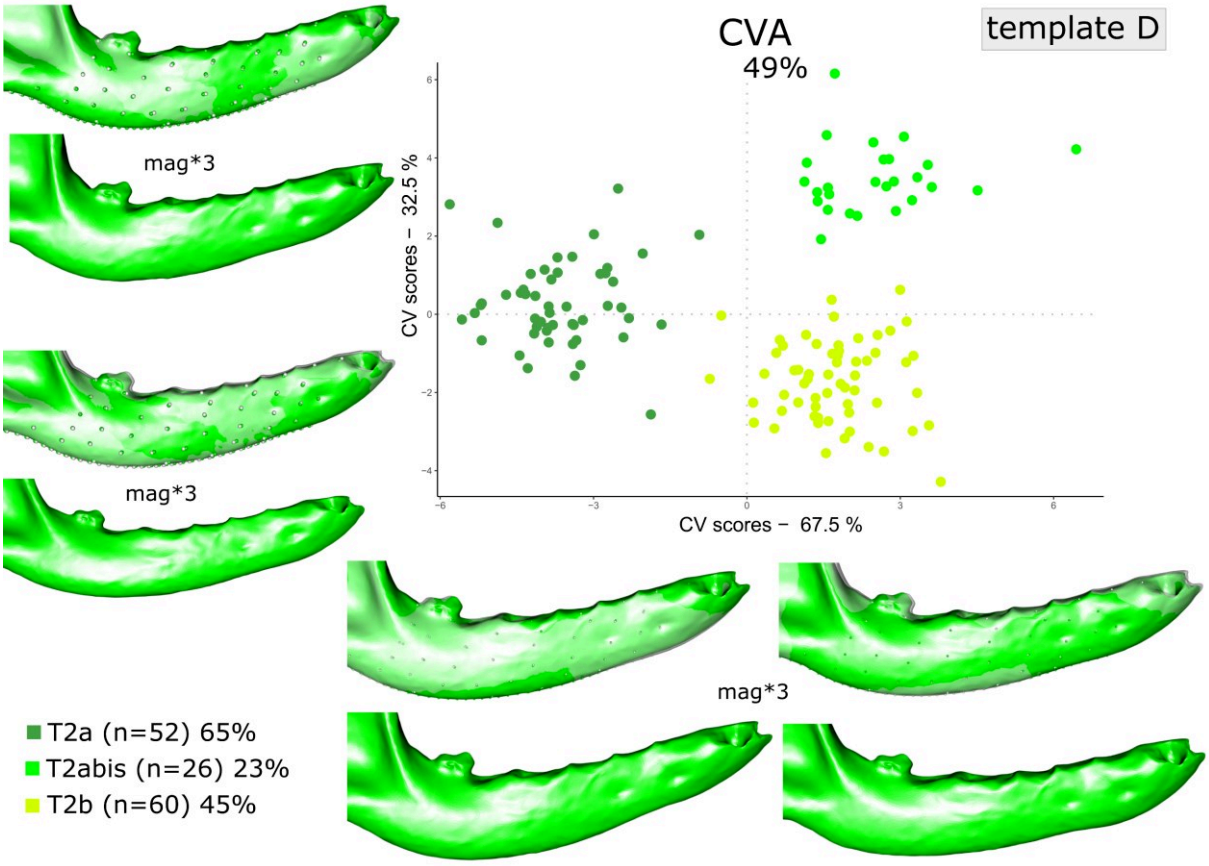

Figure 154. CVA performed on dogs from Twann – batch 2 – sampling 2 – template D.

In analyses performed on sampling 1 we no longer observe any significant result, but the sample size is low in group T2a (between 8 and 13, Table 47).

Table 47. Results of the second batch of analyses conducted on sampling 1 of dog mandibles from Twann.

	Sample size				Shape		Centroid size	BF	
	T2a	T2abis	T2b	Other	Mean	Disparity	Mean	Absolute	Residual
A	8	8	9	35	0.3	NA	0.8	0.8	1
B	10	9	25	49	0.6	NA	0.7	0.4	0.2
C	9	9	25	50	0.5	NA	0.8	0.8	0.4
D	12	20	60	70	0.5	NA	0.2	0.2	0.8
E	13	24	70	85	0.4	NA	0.3	0.1	0.3
F	10	9	13	36	0.3	T2a>T2abis 0.054	0.9	0.9	0.7
G	11	15	47	67	0.3	NA	0.5	0.6	0.2
H	11	9	14	36	0.5	NA	0.6	0.5	0.7
I	13	21	74	82	0.3	NA	0.4	0.3	0.4
J	10	10	21	42	0.6	NA	0.8	0.8	0.9

3.3.3. Mechanical potential

We observed no significant difference in the total mechanical potential (which is consistent with the absence of significance for residual bite forces) nor in the relative contribution of the muscles to the bite force because of the great variability in groups, for the batches of analyses conducted on sampling 2 (Figure 155).

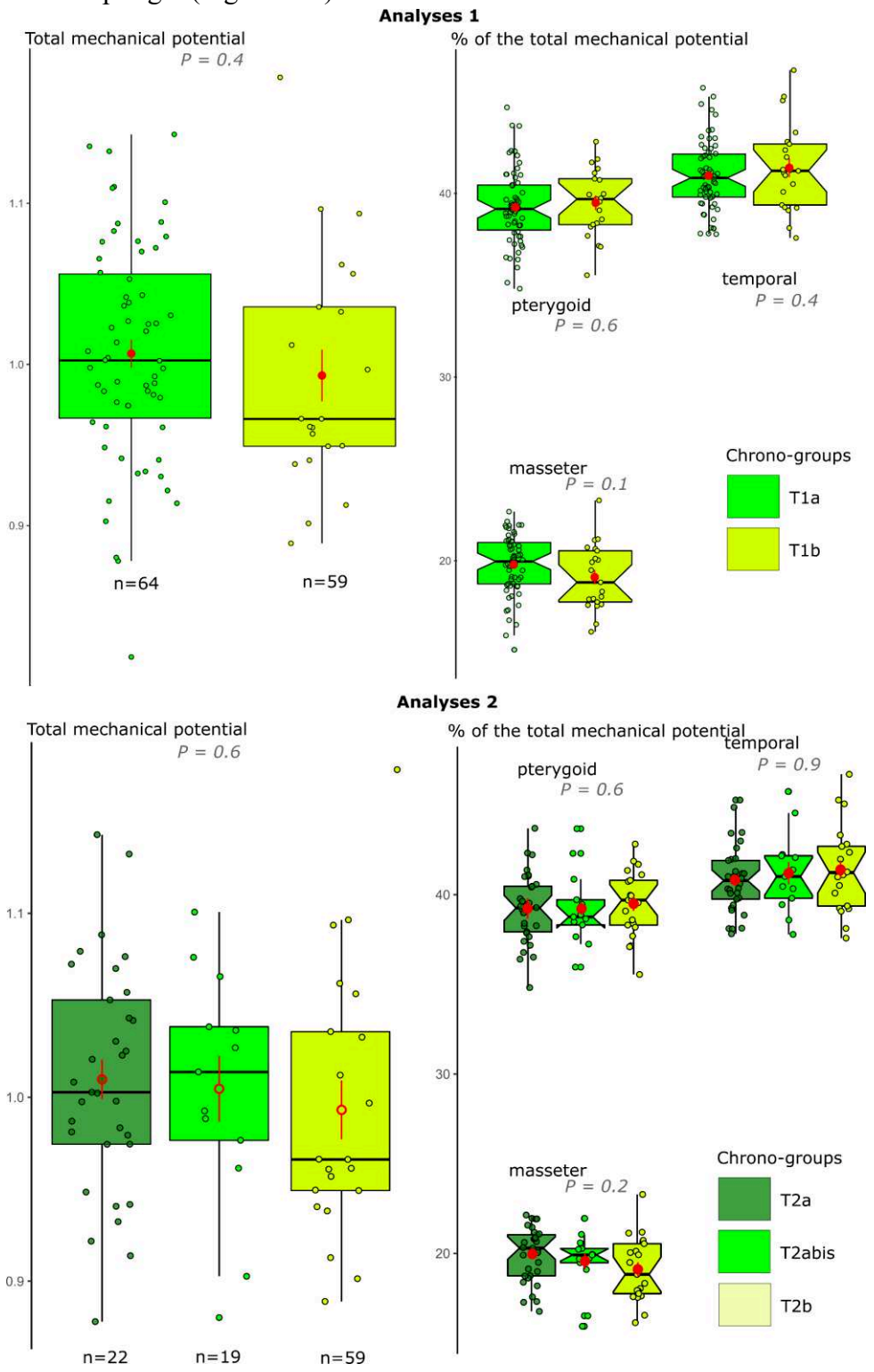

Figure 155. Mechanical potential in dogs from Twann. Red dots correspond to the mean.

Conclusion

From the study of dogs related to the Cortaillod culture of Twann, the following key points emerge:

KEY POINTS – Twann

- **The mean mandibular centroid size and bite force of dogs significantly decreases through time** (from *c.* 4,020 to *c.* 3,500 BC). **The shape of the mandible also changes, but there is strong overlap between periods. The variability (in size and shape) does not change.**

- The latest dogs (from *c.* 3,600 to *c.* 3,500 BC) and the earliest dogs (4,020-3,750 cal. BC) are those that differ the most, as regards size, bite force and shape. The latest dogs are on average smaller and the mandible is less robust with a less well-defined coronoid process, a less pronounced angular process but a deeper masseteric fossa. **The earliest dogs have more robust mandibles with a more curved mandibular body and a larger coronoid process with a larger angular process but a shallower masseteric fossa**.

- **These differences are not related to differences in the bite force relative to size nor the contribution of the muscles**.

- **Twann's dogs show a great variability in size and shape**, in comparison to all the mandibles of Western European dogs included in our corpus**. Some shapes are reminiscent of dog mandibles from other Western European periods**, but **some shapes are quite peculiar, perhaps reflecting regional or cultural particularities**. However, we had too few dogs from the neighbouring lakeside settlements of Chalain and Clairvaux (Late Neolithic) to compare with those of Twann (Middle Neolithic). In the future it might be interesting to compare Twann's dogs with other dogs from the Cortaillod culture.

4. Comparison of dogs from two similar and contemporary sites of the Chalcolithic 2 in Eastern Europe: Hârşova tell and Popina-Borduşani

In this section, we compared the mandibles of dogs from two subcontemporary Romanian sites: Popina-Borduşani and Hârşova tell. These sites are close from each and were attributed to the same culture (Gumelnița - phase A). In both sites, the socio-economic system relies on herding, dogs were eaten (see Chapter 6 sections 3.1.1.4 and 3.1.1.7) and only the haplogroup D is attested on both sites (see Table 12). Additionally, the distribution of age classes (estimated based on the first molar tooth, see Chapter 6 section 2.2) are similar in both sites (as confirmed by a Chi-squared test performed on the dogs included in template I: 3 subadults and 4 young adults in Borduşani, 7 young adults in Borduşani, 39 adults in Hârşova and 70 in Borduşani, $P = 0.08$).

We performed the same kind of analyses than in the previous sections.

The results of the statistical analyses are reported in Table 48 and illustrated on Figure 156 to Figure 159.

Table 48. Results of the statistical tests to compare the shape, size and bite force in dogs dated to the Gumelnița culture in Hârşova (Har) and Borduşani (Bor). Bite force were predicted using 2B-PLS analyses on 46 modern dogs. Significant results are written in blue.

	Sample size		SHAPE			CENTROID SIZE		BITE FORCE	
	H arsova tell	Popina Borduşani	Disparity	Mean - Procrustes ANOVA	Mean - CVA	Mean t-test	Variance	mean – t-test Absolute	mean – t-test Residual
A	14	28	>0.1	R2 = 0.059 P<0.004	67%	0.09	0.28	0.07	0.68
B	24	50	>0.1	R2 = 0.076 P<0.001	68%	0.0046 Har>Bor	0.068	0.022 Har>Bor	0.12
C	24	43	>0.1	R2 = 0.035 P=0.018	73%	0.53	0.68	0.67	0.47
D	35	66	>0.1	R2 = 0.034 P=0.007	73%	0.054	0.48	0.17	0.078
E	38	70	>0.1	R2 = 0.020 P=0.067	73%	0.0048 Har>Bor	0.45	0.11	0.027 Bor>Har
F	18	31	>0.1	R2 = 0.051 P=0.003	73%	0.27	0.30	0.21	0.22
G	42	67	>0.1	R2 = 0.046 P=0.003	61%	1	0.74	0.56	0.010 Har>Bor
H	19	31	>0.1	P=0.12	61%	0.38	0.064	0.38	1
I	46	77	>0.1	R2 = 0.056 P<0.001	61%	0.78	0.81	0.81	0.00042 Har>Bor
J	23	46	>0.1	R2 = 0.10 P<0.001	80%	0.053	0.12	0.033 Har>Bor	0.036 Har>Bor

Significant differences in the centroid size are obtained only with templates B and E, and in a lesser degree with templates D and J ($P < 0.06$), **dogs from Borduşani having a more variable centroid size with very small dogs being present that are not found in Hârşova**. The same holds for the absolute bite forces.

There is no significant difference in shape variability between the two sites, but it is likely due to the small and low sample size for Hârşova in comparison to Borduşani, for the templates that best represent shape (templates A, B, C, F and J, n<24). **All templates (except templates E and H) indicate significant differences in mean shape**, thus highlighting the strength of the biological signal. However, the success rates of the CVA are low and are greater for dogs from Borduşani. This is possibly because most of the dogs from Hârşova have equivalents in the population of Borduşani, but **the population of Borduşani contains some specific morphologies (in both shape and size**). This is supported by the classification trees, which show some branches gathering only dogs from Borduşani, while others contain dogs from both sites.

The CVAs reported in Figure 156, Figure 157 and Figure 158 indicate that **dogs from Borduşani have a taller mandibular body than in Hârşova, with a ventral border of the mandibular body more regularly curved** (in dogs from Hârşova, there is a pronounced curvature right under the carnassial tooth and then the body goes straight upwards, recalling the mandibular body of a fox), **the coronoid process is more vertical and smaller** (it is more oriented backwards and taller in dogs from Hârşova), **and the angular process is lower and larger.**

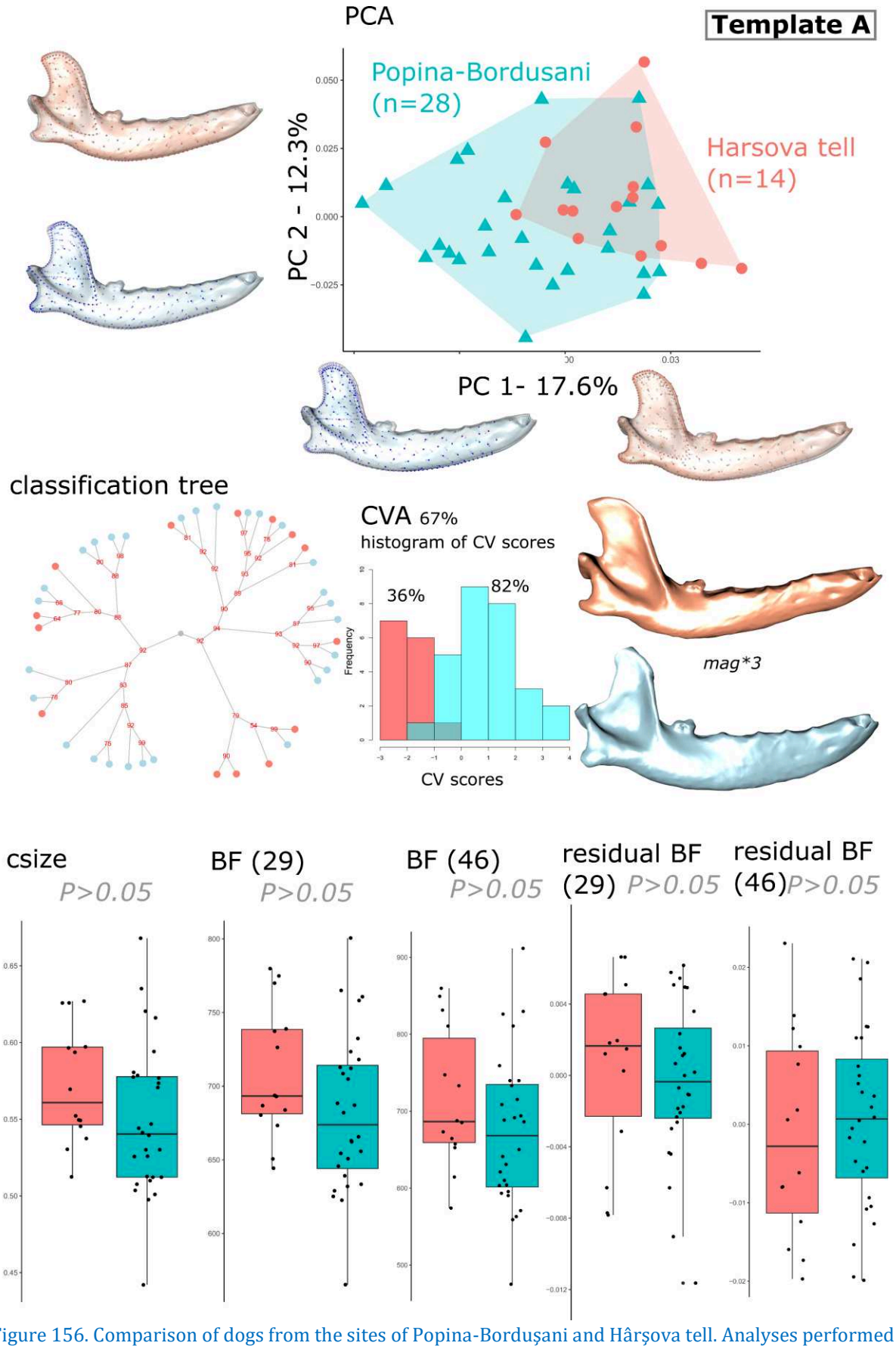

Figure 156. Comparison of dogs from the sites of Popina-Borduşani and Hârşova tell. Analyses performed with template A. BF: bite force.

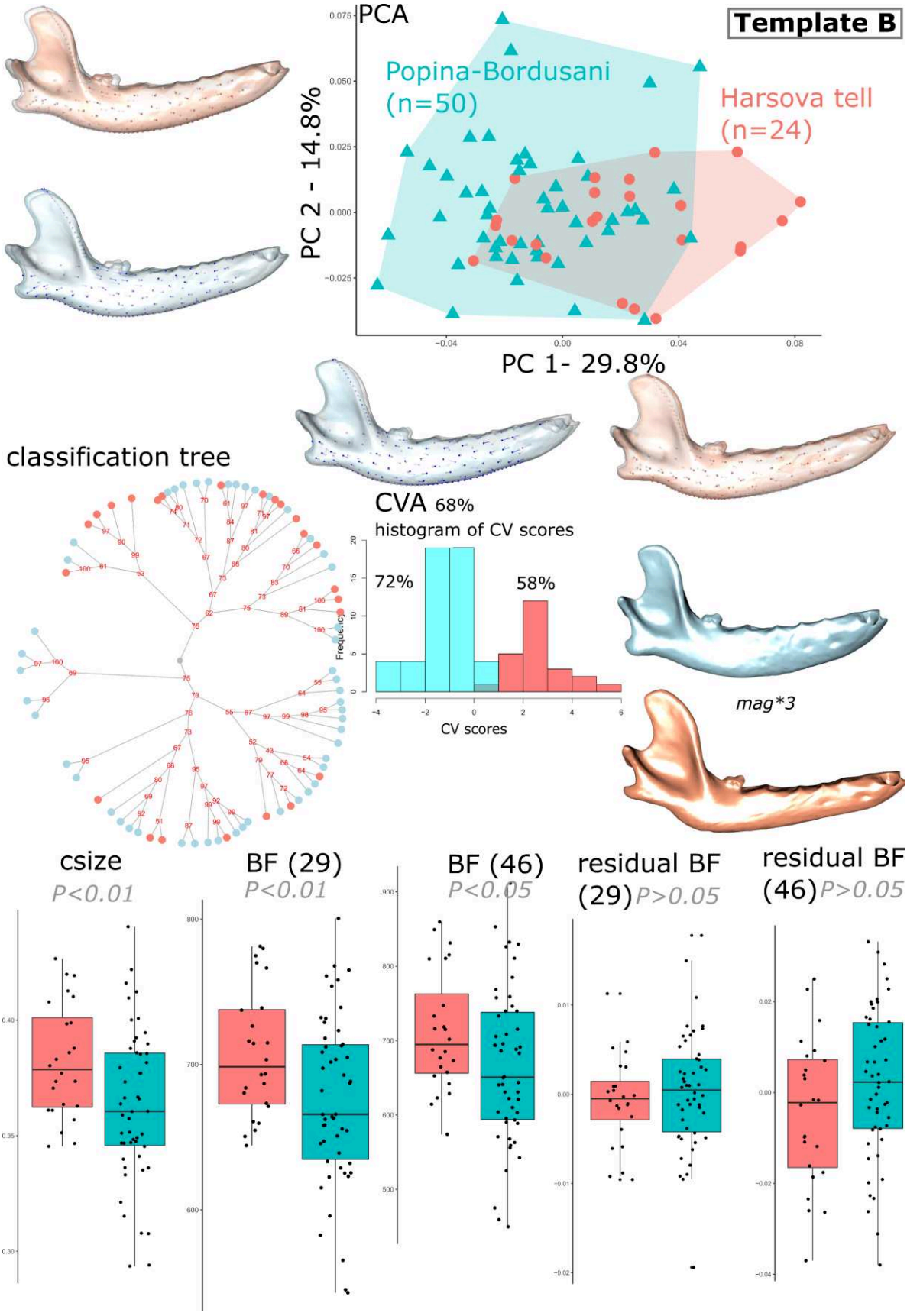

Figure 157. Comparison of dogs from the sites of Popina-Borduşani and Hârşova tell. Analyses performed with template B. BF: bite force.

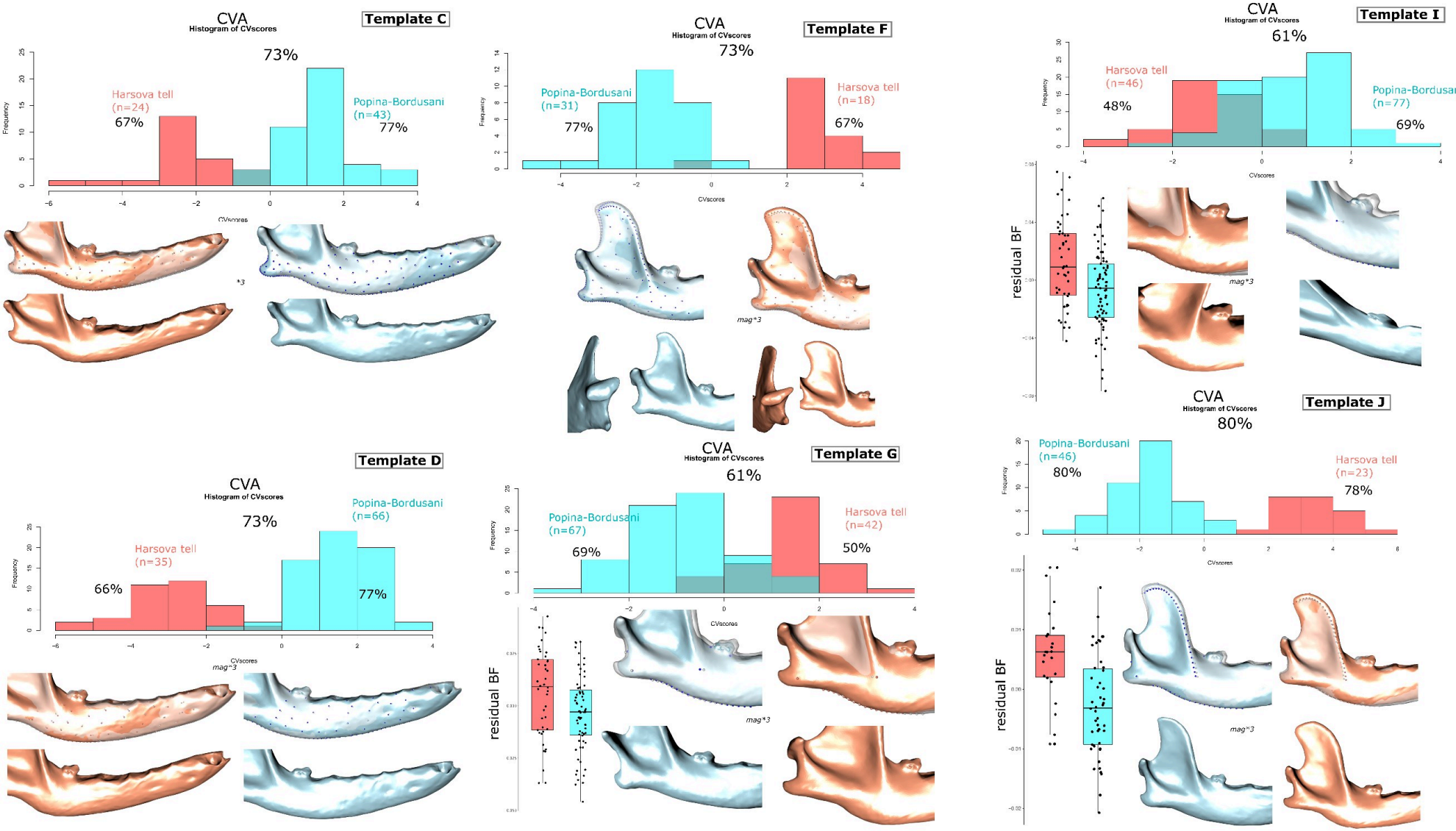

Figure 158. Comparison of dogs from the sites of Popina-Borduşani and Hârşova tell. Analyses performed with template C, D, E, F, G, I and J. Residual BF: residual bite force.

These differences in shape have no strong consequence on the residual bite force nor on the mechanical potential or contribution of the different muscles (Figure 159). Dogs from Hârşova tend to have higher mean bite forces for their size only for templates G, I and J, but not for template B, although the constitution of the sample is almost the same for templates B and J. Additionnaly, the variability is very important.

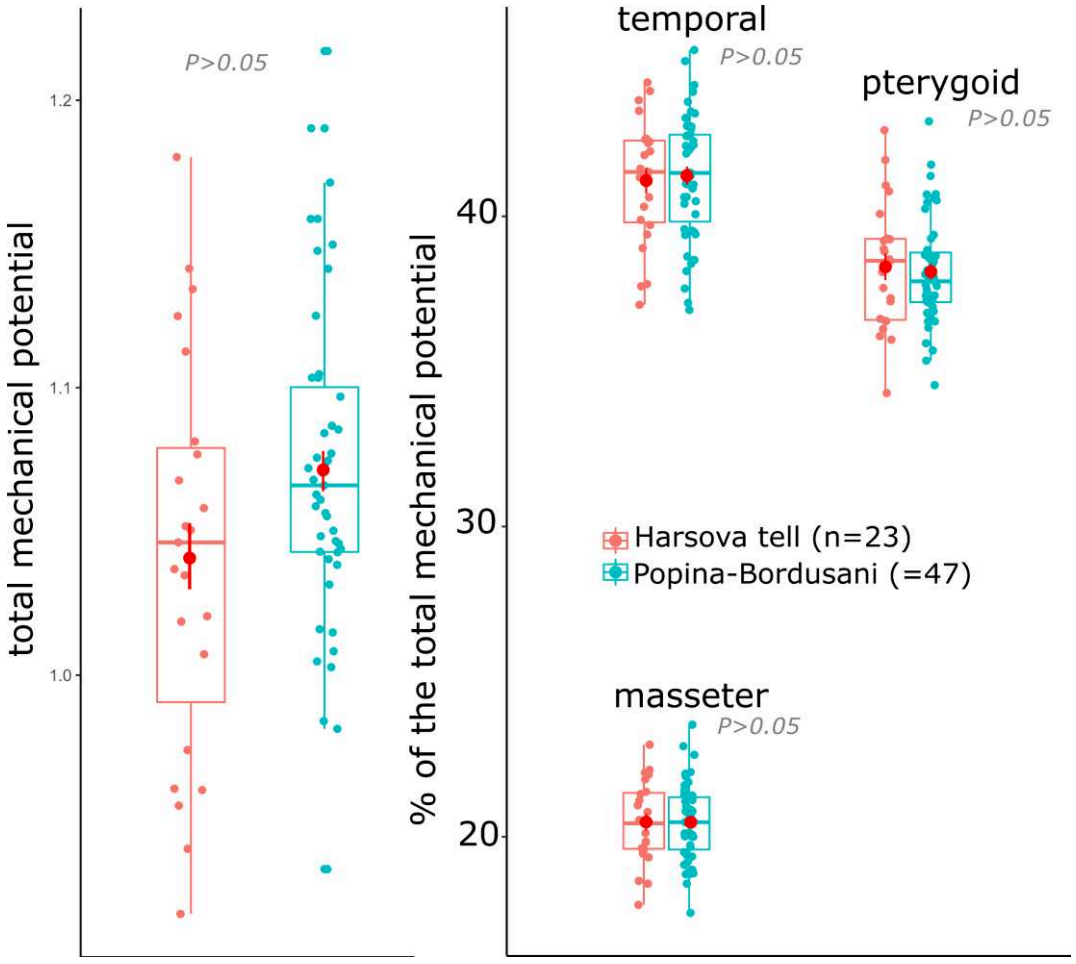

Figure 159. Comparison of the mechanical potential of dogs from the sites of Popina-Bordușani and Hârșova tell.

Conclusion

Thus, from the comparison of two dog populations from two sites of the same culture (Gumelnița phase A), sharing similar characteristics and located close from each other, the following key points emerge:

KEY POINTS

- **Dogs from Borduşani are more variable than dogs from Hârşova** (results are statistically significant for the centroid size) however they belong to the same haplogroup (D, Table 15).

- Most of the dogs from Hârşova have equivalents in the population of Borduşani, but **in Borduşani we also found smaller dogs with specific mandible shapes** (characterized by a regularly curved and taller mandibular ramus, a small and vertical coronoid process and a larger and lower angular process).

- Accordingly, dogs from Hârşova have mean bite forces that are higher than dogs from Borduşani, but **the residual bite forces do not differ on average, nor the mean contribution of the adductor muscles.**

    ⇨ These local differences suggest that the **inhabitants of Borduşani and Hârşova did not exchange their dogs much. Each village seemed to have its own population of dogs.**

Chapter 10.
Exploring the form and function of the jaw in red foxes prior to the Bronze Age in Europe

The aim of this chapter is to apply the methods developed in the previous chapters for the study of form and function exclusively to ancient red foxes and to compare the results with those obtained in Chapter 9 for dogs.

Because the archaeological corpus is small (50 mandibles) and the mandibles often very fragmented (cf Chapter 6 section 5.3.2, Table 19 and Table 20), the analyses will be limited in scope. Therefore, we cannot explore the same questions as for dogs in Chapter 9. This part is therefore preliminary and exploratory. The results are provided as a guide for further research.

1. Methodology and questions investigated

We had too few mandibles from Eastern Europe to compare foxes from Eastern and Western Europe. No statistical analysis will include data on foxes from Eastern Europe but data will be reported in the graphs.

We will focus on comparing the centroid sizes, shapes, and bite forces between the chrono-cultural groups, using the same analyses as in Chapter 8 (correspond to the section 2). However, the chronological parameter is accompanied by strong geographical and environmental differences. All the Mesolithic foxes come from the French Atlantic coast (Britanny, Téviec), those of the Early Neolithic from the French Mediterranean areas (Camprafaud, le Taï) and Germany (Herxheim, contemporary of Téviec), and those of the Middle and Late Neolithic from Swiss and French lakeside settlements, between the Alps and Jura (cf Chapter 6 section 4.2).

Chalain provided a third of our corpus, with 18 mandibles dated to the Late Neolithic (early Clairvaux culture and 1 fox from the Horgen culture). We can therefore explore the variability existing in this site in comparison with other sites in Western Europe. We do not have enough mandibles from Late Neolithic other sites (2 from Twann) to compare foxes within the same chrono-cultural phase.

In this chapter, we will focus on templates E and I, which are the only ones that allow considering a sufficient number of mandibles. However, these templates have proved to be poorer indicators of bite force, especially template E (see Chapter 8, section 1.2).

2. Table of results of the statistical analyses

Results of the statistical analyses are reported in Table 49.

Table 49. Results of the analyses performed to compare ancient foxes from the Mesolithic to the end of the Neolithic in Western Europe. Bite force were predicted using 2B-PLS analyses on 60 modern foxes. Significant results are written in blue. PV: Procrustes variance.

	Sample size	SHAPE			CENTROID SIZE	BITE FORCE	
		Disparity	Mean – Procrustes ANOVA	Mean – CVA	Mean – t-test	mean – t-test Absolute	mean – t-test Residual
E	N=25	Cortaillod (PV 0.0063) < Late Neolithic (PV 0.020) $P = 0.052$ Cortaillod < Early Neolithic (PV 0.020), $P = 0.1$	$P = 0.26$		Mesolithic > Cortaillod $P = 0.045$	$P = 0.41$	NMB > Mesolithic $P = 0.020$
I	N=34	Mesolithic (PV 2.5e-02) > NMB (PV 7.9e-03), $P = 0.009$ Mesolithic > Early Neolithic (PV 5.4e-03), $P = 0.017$ Mesolithic > Late Neolithic (PV 1.4e-02), $P = 0.027$	$P = 0.031$		Early Neolithic > Cortaillod $P = 0.046$ NMB > Cortaillod $P = 0.069$	$P = 0.75$	$P = 0.60$
I without Twa15		Mesolithic > NMB $P = 0.010$ Mesolithic > Late Neolithic $P = 0.033$	$P = 0.009$		$P = 0.69$	$P = 0.64$	$P = 0.56$

3. Results and interpretation

3.1. Centroid size

3.1.1. Correlation between the centroid sizes of the different patterns of fragmentation

In order to quantify the loss of information related to template I for the centroid size, a correlation test was carried out between the centroid size based on templates A and I for the 8 complete mandibles of ancient foxes. **The correlation coefficient is quite low (r = 0.6) for template I**. In other words, the centroid size of template I explains only 34% of the centroid size of the complete mandible ($R^2 = 0.34$). **The correlation is better for template E** ($r = 0.85$, $R^2 = 0.72$). This difference can possibly be explained by the modularity within the mandible, the portion related to template I being more variable and the portion related to template E being more integrated with the rest of the mandible. **Template E is thus the best fragmentation pattern to explore differences in centroid size.**

3.1.2. Comments

Differences between groups are observable in Figure 160 and Figure 161. In analyses with template E, **foxes from the Mesolithic (Téviec) and early Neolithic (Herxheim, Camprafaud and Le Taï) are relatively bigger than foxes from the Cortaillod (Twann).** These last foxes tend to be smaller than foxes from the middle Neolithic NMB of Clairvaux XIV or even foxes from the Late Neolithic of Chalain, but the results are not significant due to the low sample size. **These differences may be related to both geographic and chronological differences. Foxes from the French and Swiss lakes tend to be smaller than foxes from other regions**, which may be related to the geographical constraints that may have impacted on size, as discussed in Article 5 in Part 2. In particular, we demonstrated that the smaller the minimal temperature, the smaller the size. The climate must have been cooler in the Alpine and Jura regions (i.e. French and Swiss lakes) than in other regions, which may explain, among other factors, the lower centroid size of these foxes.

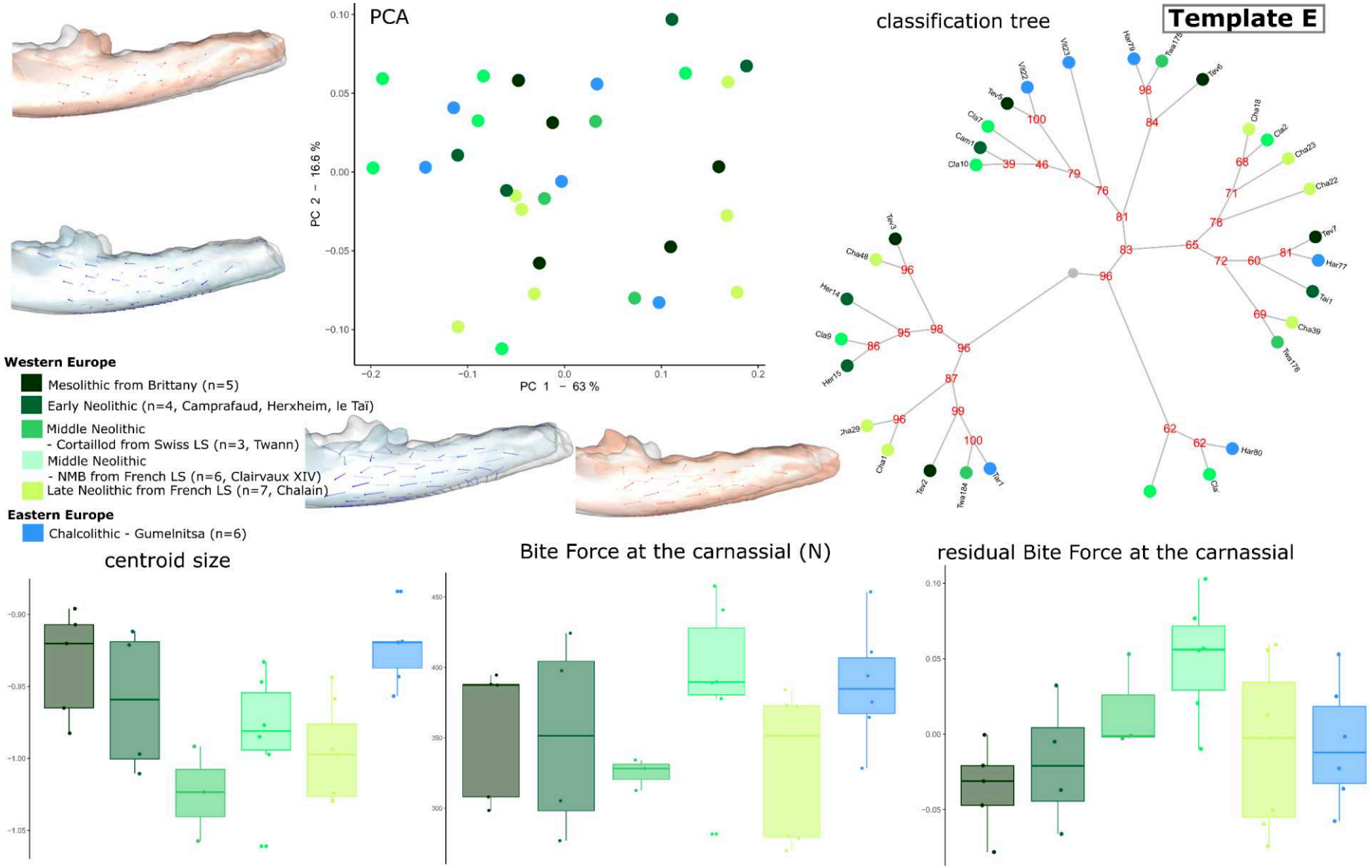

Figure 160. Visualisation of shapes, sizes and bite forces of foxes from the Mesolithic to the very early Bronze Age in Europe – analyses performed on template E. LS: lakeside settlements.

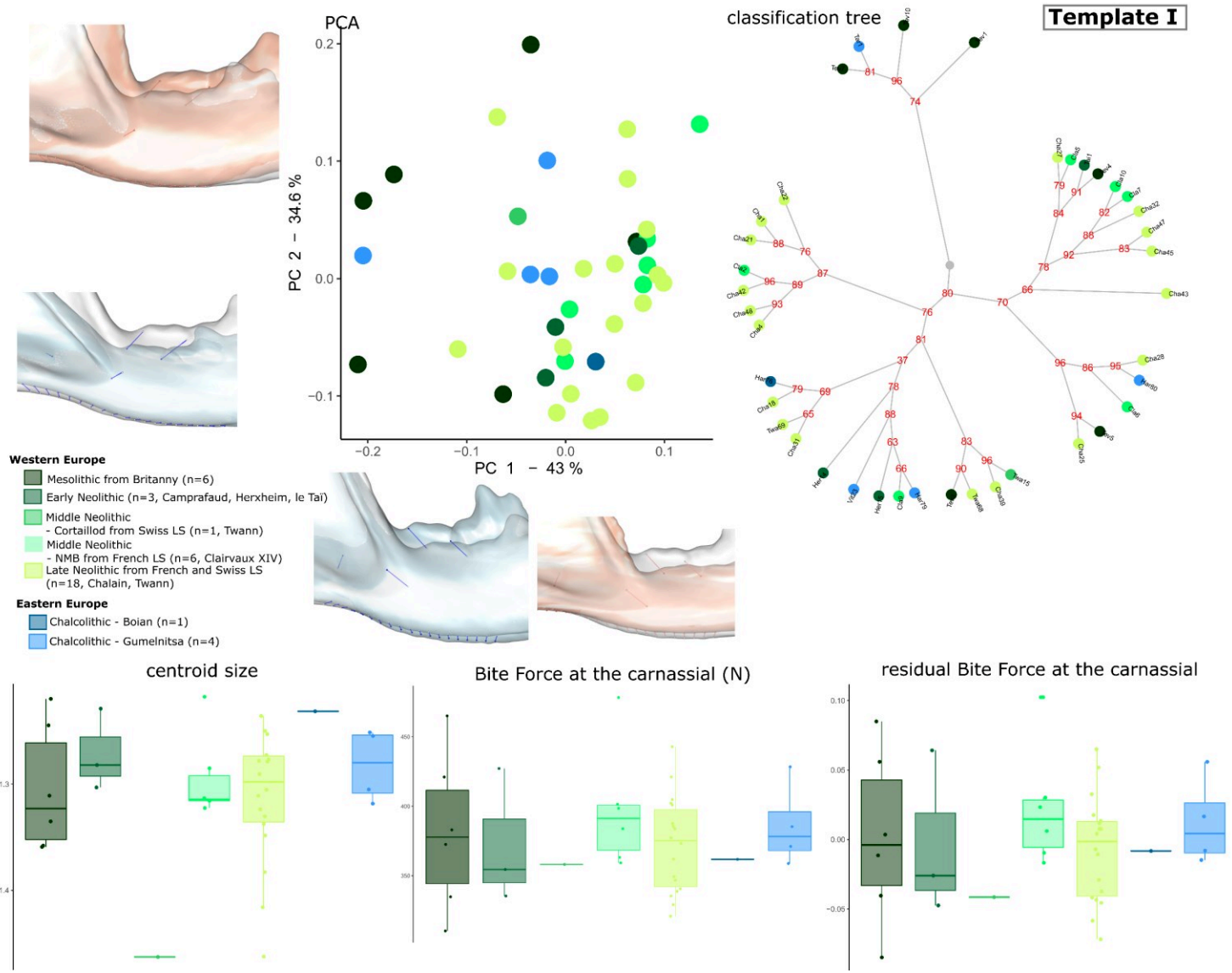

Figure 161. Visualisation of shapes, sizes and bite forces of foxes from the Mesolithic to the very early Bronze Age in Europe – analyses performed on template I. LS: lakeside settlements.

3.1. Shape

PCAs do not show any clear distinction in conformation between chrono-cultural groups, and Eastern European foxes are not particularly distinguishable on the first two axes of the PCA with templates E and I, and they are not isolated on particular branches in classification trees (Figure 160 and Figure 161). Only **template I shows significant differences between the average shapes of the different groups in Western Europe**, alhough this is not the best template to explore overall variations in the morphotype. It appears that **Mesolithic foxes from Brittany are more robust than those from the Early Neolithic and above all, than those from Middle Neolithic NMB** (first axis of the CVA, Figure 162). The **Late Neolithic foxes can be distinguished on the second axis by their slenderer mandibles.** However, the percentage of good classifications is very low (15%) which leads us to limit our interpretations.

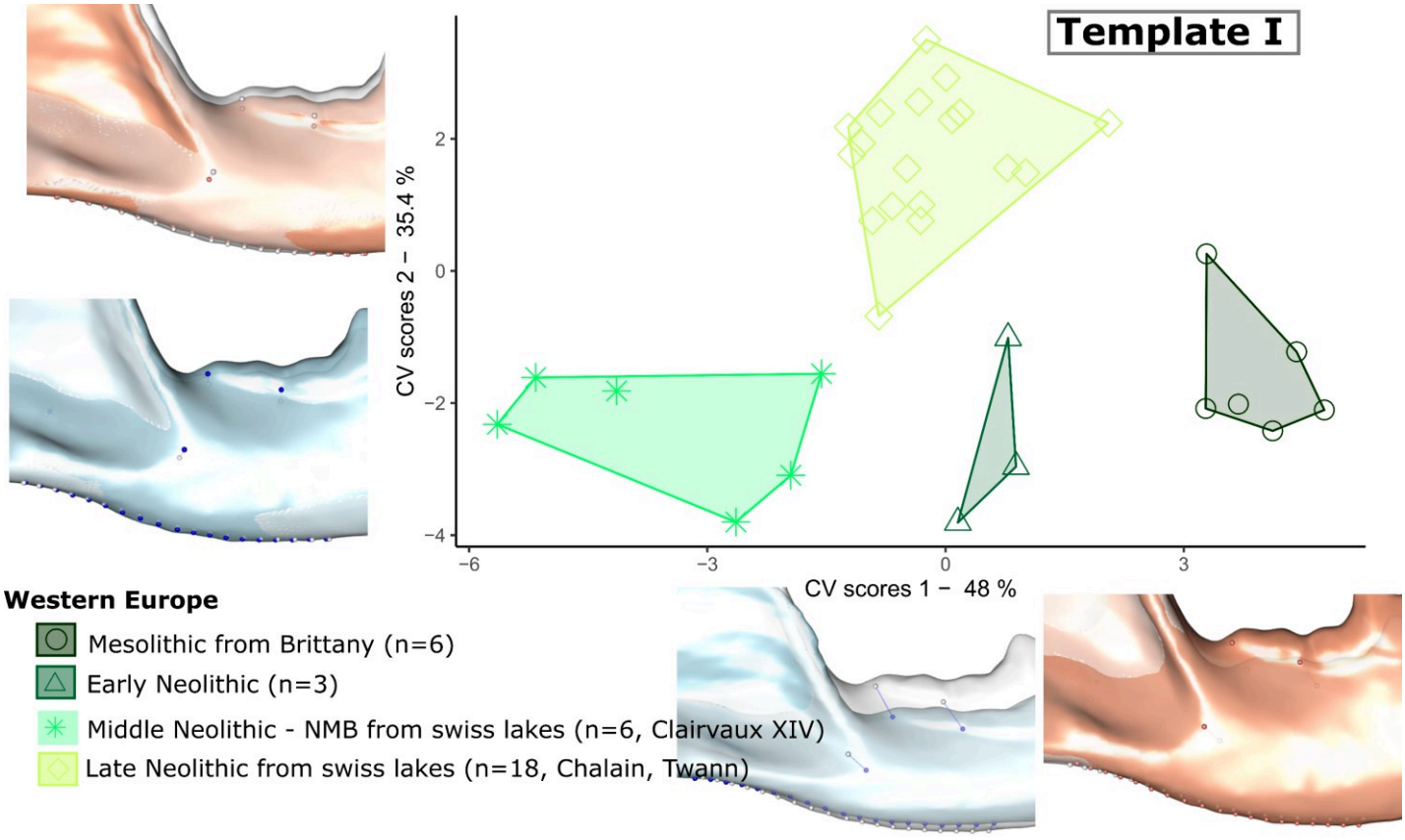

Figure 162. Visualisation of shape changes along the axes of the CVA performed on ancient foxes with template I. For this CVA we removed the only fox dated to the Cortaillod culture in Twann. LS: lakeside settlements.

Surprisingly, **disparity seems greater in the Mesolithic of Téviec than in the Early Neolithic**, although several sites are included in the latter group (Herxheim, Camprafaud, the Taï). The **disparity is also higher in the Mesolithic than in the Late Neolithic of Chalain**. Thus, the Mesolithic foxes of Téviec seem to show a great diversity of shapes (but not as regards size, as they remain rather large).

3.1. Bite force

Both the mechanical potential and the residual bite force of template E seem to indicate that the performance of the jaw increased from the Mesolithic to the end of the Neolithic (the differences being mainly located between the Early Neolithic and the Middle Neolithic) **in Western Europe** (Figure 160**,** Figure 163). **The contribution of the masseter muscle seems to increase between the Early Neolithic and the Middle/Late Neolithic, while that of the pterygoid muscle tends to decrease** (but the results are not significant, Figure 163). However, once again, geographic and environmental differences may play an important role in the observed variations.

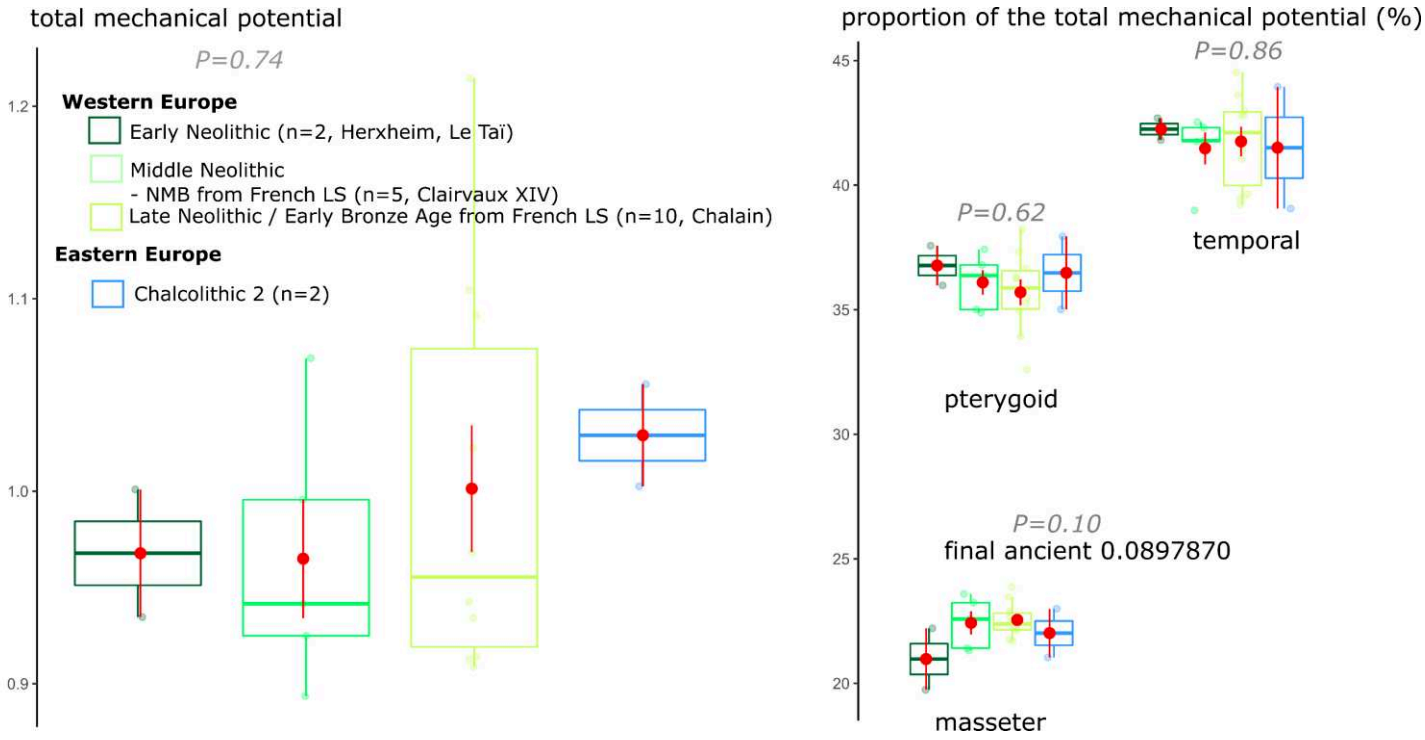

Figure 163. Mechanical potential of the foxes from the Mesolithic to the very early Bronze Age in Europe. LS: lakeside settlements.

Conclusion

Thus, from the exploration of the variability existing in the lower jaw of red foxes from the Mesolithic to the very early Bronze Age in Europe, the following key points emerge:

KEY POINTS

- **A certain variability existed in this commensal species prior to the Bronze Age**, which is, given our data, probably more related to environmental constraints rather than to anthropogenic constraints.

- Analyses are strongly limited by the high fragmentation and the low number of fox remains which are available prior to the Bronze Age.

- To go further in the analyses, it is necessary to increase the sample size, both geographically and chronologically, and to focus on the same region in order to study diachronic variability in the same environmental context.

Synthesis and discussion:
new insights into the diversity of dogs and red foxes in the first agricultural societies

Archaeological data provide information on the great diversity of status types of dogs in Europe from the Mesolithic to the very early Bronze Age. These status types varied depending on regions and periods. Dogs were widely eaten (in South-Eastern Romania only this status is attested to date), either in a limited (family) or collective context, and their skin and bones were occasionally used for the manufacturing of ornaments. Sometimes, they may have been the subject of more symbolic considerations, as attested by the burial of complete bodies in more or less close association with human burials (especially in Western Europe, but also in Central Europe or the Iron Gates), sometimes following the same process as for human bodies. It is more difficult to demonstrate their role as assistant for hunting or for the protection of camps or villages, but their presence in settlements is an indication. Dogs were most likely free-ranging and closer to a commensal lifestyle, as observed in some extant tribes of hunter-gatherers (the Sentinels), sharing human food resources (which has been confirmed by isotope analyses at some sites).

Accordingly, as they were strongly integrated into human societies, dogs are likely to be a marker of the transition from foraging to farming in human societies and of the evolution of the first agricultural societies.

While paleogenetic data inform us on the evolutionary history of dog populations in Europe and about their functional adaptations (acquisition of the ability to digest starch) in response to the development of agriculture during the Neolithic, data on the morphological diversity of dogs have remained scattered and rather uninformative. Indeed, available information on the morphology of dogs prior to the Bronze Age was limited to information about the stature (size) or overall robustness of the bones through linear measurements, and multivariate analyses have only rarely been used. The only attempts of doing two-dimensional geometric morphometrics are reported in unpublished PhD or master theses, and these studies were based either on the teeth (the shape of which is rather conservative, and therefore not able to document rapid changes) or on a limited number of dog mandibles.

Red foxes were living more distant from humans, yet they may have been impacted by the profound changes that occurred during the Neolithic transition (as they may have benefited from easier access to food resources by feeding on human refuse or small rodents attracted by Neolithic storages). Archaeological data inform us on the rather uniform status granted to this commensal canid: it was most often eaten and also likely used for its fur (during the Epipaleolithic, Mesolithic and Early Neolithic humans probably exploited its presence around the settlements rather than selectively hunting foxes). Foxes were exceptionally buried, yet many of these cases date to late periods (Bronze Age) compared to dog burials and many cases are dubious. To date, no study has explored its morphological diversity, mainly because remains

are scarce irrespective of the period (as demonstrated by our review on fox occurrences in Western Europe and South-Eastern Romania from the Mesolithic to the Bronze Age). Consequently, collecting a consistent series of bones is a time-consuming process. However, as foxes – which live further from human groups compared to dogs – can develop the same morphological adaptations to anthropic changes as dogs, they are a good model to compare a wild commensal canid with a domestic one. This comparison aimed to provide insights into the impact of the proximity between humans and canids in the first agricultural societies.

In the course of this PhD thesis, I used for the first time 3D geometric morphometrics on a vast sample of more than 550 mandibles of European canids from the Mesolithic to the very Early Bronze Age. Dogs being largely the most represented (more than 500 mandibles), my study was therefore mainly based on this species. The fine analysis of shape has helped to fill some gaps in our knowledge about the morphological diversity of dogs prior to the Bronze Age. The data produced in this thesis provide new information that enriches our knowledge on the morphological diversity of canids prior to the Bronze Age. In particular, these data provide elements to answer to the questions raised in the conclusion of the first part (page 119).

1. Methodological prerequisites: adaptation of the exploration of form to fragmentation, and the validity of the interpretations

To study the largest number of mandibles as possible, I performed analyses on 10 different fragment types in order to be able to consider even the smallest fragments (that were more frequent in the earliest periods). Template A (with landmarks on all curves and the surface) was used primarily to explore the variability in morphotypes (i.e. the overall mandible size and shape) because it is the one that most completely describes the shape, since the entire bone surface is represented. The information is still present but degraded (to different degrees) for the other fragment types. The analyses performed on fragment types B, C, F and J were used to strengthen the results obtained with the complete mandibles. The analyses performed on the other, smaller fragments were able to highlight more localized shape variations. All of the templates provided information on the size, but not all the fragments are as precisely informed on the size of the complete mandible (in particular templates E, G and I).

2. Modern versus pre-Bronze Age canids

First, we used a reference sample of modern canids consisting of about 60 dogs of various breeds and 80 European foxes (France and Romania), as well as a few wolves. Unfortunately, we had no access to stray dogs (e.g. pariah dogs that live commensally in North Africa). These could be interesting to consider as they are less subjected to artificial selection constraints, and potentially closer in shape to ancient dogs. We were, however, able to include some (eight) dingoes in our analyses, which allowed us to represent a case of domesticated dogs returned to the wild.

The use of a modern reference sample first provided us with a comparative framework to apprehend the diversity in the past, and it enabled us to answer the following question:

Q.1: What was the morphological variability in dogs before the Bronze Age compared to modern canids?

It clearly emerged from our analyses that **the diversity in pre-Bronze Age dogs was very important, although less important than in modern dogs**. Indeed, a **great diversity in both size** and shape was demonstrated. In pre-Bronze Age dogs, mandible size varies from sizes similar to some modern small dogs such as the loulou or dachshund, to sizes compatible with some modern large dogs such as the husky, golden, or German shepherd, although the size is always much smaller than that of wolves and **on average corresponds rather to that of modern** beagles. **Some ancient shapes are close to wild shapes** (of ancient or modern wolves or modern dingoes), others are more similar to **modern meso-dolichocephalic dogs** (e.g. beagles, sloughi, podenco, loulou, mastiff, shepherd dogs), but **most of them are clearly different from modern dog breeds**. **No extreme form** was evidenced: the very **brachycephalic** (pitbull, amstaff, boxer, bulldog etc.) **and very dolichocephalic (barzoi) modern dogs have no equivalent** in Pre-Bronze Age dogs. This suggests that **early European farmers did not select for very marked morphotypes**, at least not in terms of shape. These results support the hypothesis we formulated in the conclusion of part 1, which proposed that **some shapes may have disappeared** and that **the variability may have been much greater than previously thought**.

These results are based on a large number of ancient mandibles (227), based on templates A and B, and tend to be confirmed with the smaller templates, which reinforces the strength of the biological signal. As these results are mainly based on the most complete templates, and considering the state of the material and the constitution of our sample, **the conclusions are valid for the Middle Neolithic in Western Europe and the Chalcolithic in South-Eastern Romania**. Indeed, we had no complete/sub-complete Mesolithic dog mandibles from Western Europe, and very few mandibles from the Early or Late Neolithic in Western Europe or for the Mesolithic and Neolithic in South-Eastern Romania. It is possible that during these periods other forms existed, but we do not have them in our sample.

The fact that pre-Bronze Age and modern dogs are found in distinct areas of morphological space allowed us to highlight the **inapplicability of CVA-based predictive methods to assign the species (or subspecies) of ancient canids based on modern canids** (see appendix 11).

In red foxes, we also evidenced significant differences in size and shape between modern and pre-Bronze Age specimens for all the templates (thus reinforcing the strength of the morphological signal). However, our sample of foxes remains small and needs further enrichment to ascertain our results.

Moreover, the data suggested that the **mandible was more modular in ancient dogs than in modern captive dogs and wolves** (subjected to strong anthropic constraints), but also (to a lesser extent) compared **to modern commensal canids (dingoes and foxes)** subjected to constraints that are still predominantly natural. This is evidence by a less strong integration

between the shape of the front and back of the mandible in pre-Bronze Age dogs. This tends to support the hypothesis that **early farmers did not exert very strong selection pressures on dogs for aesthetic or utilitarian reasons** that might have constrained the anatomy (and modularity) of the mandible.

Finally, by demonstrating that the **mandible is strongly integrated within the masticatory apparatus in modern canids** (see part 2), we **developed promising predictive models to infer cranial shape** (see appendix 10) **and bite force**, based on PLS regression. The differences observed in the morphological space and in the modularity within the mandible between modern and ancient dogs could suggest that the integration patterns between the cranium and the mandible or the bite force were different in the past, making our predictive models invalid. However, only a part of the shape carries information on bite force (obtained using decomposition of the covariance through the PLS method). We found that the variability in the part of the shape that covaries with bite force in modern dogs used for the construction of the model was more important and included that of pre-Bronze Age dogs. This is why we chose to keep all breeds, even the most modified. Thus, we used our model to make interpolations rather than extrapolations (even though the morphospace of the two groups is distinct). One possibility would have been to use only beagles (provided that we could dissect more of them), which appear relatively similar in shape to ancient dogs, but in this case some shapes within the pre-Bronze Age dogs would not have been included in the variability of the sample. Another model was built for foxes.

The predictive models of bite force I developed in this thesis (by PLS regression) allowed functional inferences even from very small fragments, by taking into account fine variations in the shape, size, and associated architecture of the adductor muscles, based on data for modern dogs or foxes. However, the loss of information in estimates of size and bite force due to fragmentation accumulate when exploring residual bite force. Thus, depending on the samples analyzed and the questions raised, not all fragments proved to be equally reliable in estimating residual bite force in relation to the complete size of the mandible (which is considered to be a proxy of the overall size). This model allowed to quantify the masticatory function, alongside the calculation of mechanical potential allowing to estimate the relative contributions of the M. temporalis, M. masseter and M. pterygoideus to bite force.

This **method could be used for archaeological remains of dogs and foxes from other periods or geographical regions**, assuming that the variation (in ancient dogs, or foxes) in the part of the mandible that carries the functional information is included in that of the modern dogs used to build the model.

3. Cross-referencing of data from geometric morphometrics with other data already available in pre-Bronze Age dogs

In a second step, we studied the morphological variability within pre-Bronze Age dogs, and we applied the models developed on modern canids to make functional inferences. We thus produced many new data that enrich the set of data available on dogs from the first European agricultural societies (archaeological context, haplogroups, starch digestion capacity, coat color). It then becomes possible to link/confront these data, to better understand how the profound changes in human societies were accompanied by changes in the constitution of canid populations. In particular, we provided some elements in response to the questions formulated in the conclusion of part 1 (page 125).

Q.2: Are there different morphotypes in Eastern and Western Europe?

The global comparison of dogs from Western (mostly represented by the Middle Neolithic, Chasséen and Cortaillod cultures) and Eastern Europe (mostly represented by the Late Chalcolithic) enabled to **demonstrate strong differences between these dog populations**. Our analyses revealed strong differences in **mean mandible shape and size, which are accompanied by functional differences.** These results are consistent with the fact that dog populations have **very different histories in Eastern and Western Europe**, as the neolithisation processes and the composition of dog populations in genetic terms are not the same in both areas (see Part 1 section 2.4.2.3.5, Table 12). Indeed, in the 1,300/1,500 years since the beginning of neolithisation, there was a total replacement of the European maternal lineage by an exogenous lineage in South-Eastern Europe (probably coming from the Near-East, Hg C ➔ Hg D), whereas in Western Europe a clear predominance of the European maternal lineage (Hg C) persisted at least until the end of the Middle Neolithic, and was accompanied by a greater diversity in haplogroups (Hg C, D, A and B are attested during the Middle Neolithic).

Nevertheless, one might have expected to observe greater morphological variability in Western Europe, but **no significant difference in disparity nor in centroid size variance** was evidenced. This is not related to the constitution of our sample, since more sites are included in the sample of Western European dogs, and these sites are more distant from each other than the sites from Eastern Europe. However, the **variability of the mandible, which is great in both areas, may have been limited by mostly natural constraints** exerted on dogs at that time (if humans had intentionally selected very specific morphotypes, likely not the same in both areas, one might have observed clearer differences in the disparity).

Q.3: Can we understand the temporal and cultural variations in form for a same region (Eastern or Western Europe)?

In both areas, we followed the evolution from the Mesolithic to the very early Bronze Age. Our sample contained few individuals for the earliest (Mesolithic and Early Neolithic, which were mainly represented by small fragments) and latest periods (Late Neolithic in Western Europe and Late Chalcolithic Cernavoda in Eastern Europe), which greatly limited our appreciation of the diversity at these times and thus our interpretations. It was thus not possible to ascertain whether the variability in size and shape really increased from the Mesolithic onwards in both areas. In Western Europe, we mainly compared Middle Neolithic dogs from the Chasséen and Cortaillod cultures. In Eastern Europe, we mainly compared Chalcolithic dogs from the Hamangia III/Boian and Gumelnița cultures.

Size

In both areas, we evidenced **a significant decrease in mean size through time** (between the **Early Neolithic and the Middle Neolithic Cortaillod** in Western Europe; between the **Mesolithic/Early Neolithic and Gumelnița** or between the **Hamangia III/Boian and Gumelnița** cultures in Eastern Europe). This is related to the presence of **very small dogs during the Chasséen** and above all during the **Cortaillod** in Western Europe, and similarly during the **Gumelnița** culture in Eastern Europe. However, this is likely not the result of the same phenomena. Indeed, in Western Europe, local dogs remained predominant, making the hypothesis of a local evolution in resident Mesolithic dogs more likely. In Eastern Europe, however, it is not possible to decide between a local evolution and the arrival of new dogs of smaller size into the local populations. Additionally, **at the end of the Neolithic in Western Europe**, these small dogs no longer appear in our assemblage, resulting in an **increase in mean size**. Further enrichment for the late Neolithic and for the early phases would enable to explore the variability at these periods further. It is possible that small dogs are also represented in the Late Neolithic and that the diversity at this time increases, prefiguring the important variability of dogs documented as early as the Bronze Age and that exploded during the Roman era (Belhaoues, 2018).

Diversity in shapes in Western Europe

In Western Europe, we had no complete mandible from the Mesolithic and too few complete/subcomplete mandibles from the Early Neolithic to compare shapes between the Early and Middle Neolithic. We thus could not assess the variability in shape at these periods.

We evidenced that **dogs from the Middle Neolithic Chasséen and the Cortaillod of Twann significantly differ in shape**, which may reflect the **different genetic composition of the populations** (Chasséen: haplogroups C, A, D, B; Cortaillod: Hg C, D, see Table 12) as well as geographic differences (Figure 15). The hypothesis of a **complete replacement of the existing population in Western Europe** is not supported by the low success rates of the CVAs for the Chasséen group, suggesting that the **native morphotypes persisted and that the populations (ancestral and exogenous) mixed**. This is consistent with the results from paleogenetics.

We expected the variability to be greater in the Chasséen than in the Cortaillod based on the more varied haplogroup composition. This was not the case and we even obtained opposite results. However, the lower variability observed within the Cortaillod compared to the Chasséen probably results from the fact that the first group includes only one site (Twann), while the latter contains the dogs of 10 sites from different geographical areas (Mediterranean area, Rhône Valley, Paris Basin). If the lower variability during the Cortaillod is confirmed even when enriching our corpus of Cortaillod dogs with other sites, this would not be consistent with the persistence of local dogs and the incoming of new exogenous dogs.

Diversity in shapes in Eastern Europe

In Eastern Europe, **dogs from the Gumelnița tend to be significantly more variable in shape than dogs from the Hamangia III/Boian: shapes from the Hamangia III/Boian cultures are still present, yet new shapes appear**. All the dogs come from the same geographical area (close to the Danube River in South-Eastern Romania). However, the sample size is relatively low for the Hamangia III/Boian group and requires a future enrichment. If confirmed, this suggests **cultural differences rather than geographical differences**, and this may be related to the **almost complete replacement of local dogs** (from haplogroup C) **by exogenous dogs** (of Hg D, probably coming from the Near East), attested in the Gumelnița culture (see Table 12).

Q4: Can the different haplogroups be linked to significant morphological differences?

In an attempt to characterize the different haplogroups based on shapes, we compared the most specific shapes of the Hamangia III/Boian and Gumelnița cultures in Eastern Europe with those of the Chasséen and Cortaillod cultures in Western Europe, based on the results of the CVA (see sections 2.2.3.3 and 2.2.1.3, Figure 164).

If each haplogroup was related to a specific shape, the most specific shapes of the Gumelnița dogs would correspond to the shape characteristic of Hg D, the only one to be present in this culture (small, fox-like with a small and vertical coronoid process).

The differences of the most specific shape of Hamangia III/Boian (Hg C and D) with this of the Gumelnița should thus be indicative of haplogroup C since it is also present in this culture (large and curved mandible with a large and backward oriented coronoid process).

In Western Europe, Chasséen dogs (Hg C, D, A and B) are vary varied, complexifying our understanding of the link between shape and Hg. It is thus not possible to use the specific shape of the Chasséen dogs to investigate the link between mandible shape and the haplogroup.

The most characteristic shape of Cortaillod dogs from Twann (Hg C, D) show mixed features: a coronoid process compatible with haplogroup D and a mandibular ramus compatible with Hg C. Hence, **the most characteristic shapes of the Cortaillod from Twann in Western Europe are reminiscent of the most characteristic shapes of the Hamangia III/Boian in Eastern Europe**. This supports the idea that **in Western Europe, the inlux of dogs with Hg D resulted in the appearance of new morphotypes reminiscent of dogs from Eastern Europe with Hg D** (yet probably modified by genetic interbreeding with local European males, given the great distance in both time and geography).

The specific mandible shapes related to haplogroups we mentioned above also support the morphological differences we observed between Eastern and Western Europe (Figure 164). Due to the composition of our sample, the differences between the two areas are mainly related to the comparison of Gumelnița dogs (Hg D) in Eastern Europe and Cortaillod (from Twann: Hg C, D) and Chasséen dogs (Hg C, D, A and B) in Western Europe. Accordingly, the more "fox-like" mandibles observed in dogs from Eastern Europe are related to the predominance of the Gumelnița dogs with Hg D in the corpus of Eastern dogs. The larger and more curved but thinner dog mandibles from Western Europe may be related to the stronger mixing between haplogroups in this region.

However, haplogroups provide only one element of reflection, and things are probably much more complicated, given that mandibular morphology is the complex product of many factors: genetics, developmental, functional, and ecological constraints. It is possible to observe convergence in mandible shape due to similar functional or ecological constraints, for example, all the more so as the mandible is highly plastic during development (we mentioned this possibility to explain the strong proximity in shape of some mandible fragments in dogs and badgers, see Appendix 8, page 676). Unravelling all this is very complex and will require further study. To go further in our understanding of the link between mandibular form and haplogroups, and of the original geographical differences that existed between the two populations, it would be necessary to compare the dogs of the Mesolithic and early Neolithic periods in Eastern and Western Europe. The same haplogroup (Hg C) was present in both areas, but it is, however, likely that differences in mandible form already existed at these very early phases, based on the great geographical distance that separated these two populations.

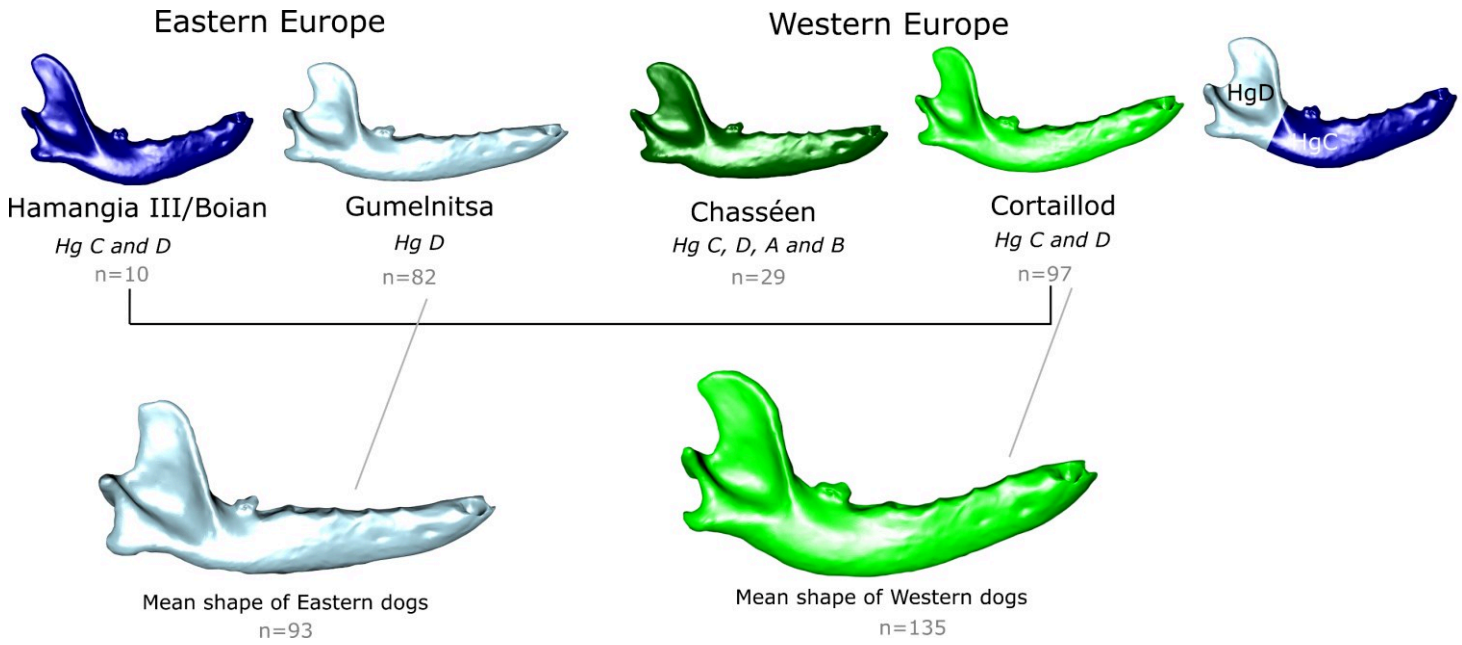

Figure 164. Proposed correspondence between haplogroups and mandibular shape. Sample sizes and shapes are from the CVAs performed on template B.

Q. 6: Has the appearance of the ability to digest starch been accompanied by changes in mandibular morphology, which could result in changes in masticatory abilities over time, in both Eastern and Western Europe?

While formulating our research problems, we suggested that dogs may have different mandible shapes and bite forces relative to their size depending on their diet, which may be related to their ability to digest starch (i.e. their copy number of the AMY2B gene). However, based on a population of 387 Australian foxes with known diet (Part 2), we showed that there was no significant direct link between the stomach content and mandible shape. We found significant but weak relations between the bite force relative to size and the diet, these relations being likely more related to prey availability and age and sex differences in the diet than to differences in performance. We found that lower absolute bite forces are associated with higher proportions of sheep, rabbit and invertebrates, and lower proportions of rodents, plants, and other prey. Lower relative bite forces are associated with higher proportions of sheep, rodents and other prey, and with higher proportions of rabbits, invertebrates and birds. Of course, the diet of pre-Bronze Age dogs was probably different (but item size categories were probably similar) and these results cannot be projected directly to ancient dogs. These results may suggest that the lower the absolute or residual bite force, the higher the proportion of anthropogenic food (in study of Australian foxes, it correspond to carrion: although it is not household garbage, the presence of sheep is directly related to a human activity of breeding).

In parallel to changes in size, we observed **an overall decrease in the absolute bite force through time, in both Eastern and Western Europe**. This was mostly statistically asserted **between the Early Neolithic and the Cortaillod** culture in Western Europe, **between the Hamangia III/Boian and the Gumelnița cultures and to some degree even between the Mesolithic-Early Neolithic and the Chalcolithic** in Eastern Europe. Based on the results from the study of Australian foxes, this would suggest that dogs had a more and more anthropogenic diet in both areas. However, the **changes in bite force relative to size show different patterns in both geographic areas.** In **Eastern Europe, the residual bite force decreases from the Mesolithic/Early Neolithic to the Gumelnița** culture (the results were highly significant only between the **Hamangia III/Boian and Gumelnița** cultures). This result thus tends to confirm our previous assumption (dogs switched to a more anthropogenic diet), but this need to be confirmed with more Mesolithic and Neolithic dogs. On the contrary, **in Western Europe, from the Early Neolithic to the Middle Neolithic Cortaillod, the residual bite force does not seem to change**. However, our corpus of dogs from Western Europe gathers sites from different regions, and the differences in food resources may not have been related to time only, but also to geography, rendering the pattern more complex. In Eastern Europe, as all Chalcolithic dogs come from the same region, the evolution is more likely related to time (as well as to the replacement of female dogs during the Gumelnița).

Additionally, we could not identify significant differences in the contribution of the muscles to the bite force (based on the mechanical potential) due to strong variability and overlaps between groups. Yet, the **contribution of the temporal muscle tends to decrease while that of the pterygoid tends to increase between the Early and Middle Neolithic in Western**

Europe. This suggests that **in Western Europe, dogs from the first agricultural societies developed mandibles that are more adapted to bite at low gapes and that execute more horizontal movements**. However, the sample sizes for the Mesolithic and early Neolithic dogs are too small to conclude. In Eastern Europe, we had no mechanical potential estimations for Mesolithic/early Neolithic dogs to compare with Chalcolithic dogs.

These results thus support the idea that in the first agricultural societies, dogs adapted their morphology to the new human subsistence model. Through the Neolithic transition, **dogs had access to more anthropogenic food**, causing **functional changes in the mandible. With a likely softer diet (based on the increasing part of prepared cereal and pulses or more or less prepared meat), dogs likely do not need to produce high bite forces to capture living prey, but needed to chew more.** This is all the more likely as game hunting activities decreased during this transition, which must have changed the functional constraints that were exerted on the mandible of dogs, given their likely key role as hunting auxiliaries. Indeed, during the Mesolithic, dogs were expected to play a key role in capturing and killing large prey to hunt game for human groups. Even though they probably fed on the products of the hunt[m], hunting activities likely required high bite forces at high gape angles: the jaws had to be closed fast to capture, bite hard to kill, and at wide gapes because the preys were large (wild ruminants rather than small rodents). However, we had too few Mesolithic specimens to explore this hypothesis further.

However, the relation between diet and bite force is weak in modern commensal foxes, and the tendencies suggested by the use of mechanical potential are not significant; this hypothesis thus needs to be considered with caution, and requires for further research. As highlighted in Part 2, it is possible that cortical thickness is a better indicator of food mechanical properties and thus of the diet. This is an avenue for further research. Additionally, it would be better to compare dogs with an anthropogenic diet (constituted partly of cereals and pulses) and dogs fed on a more carnivorous diet with similar preys that pre-Bronze Age dogs were likely to feed on.

[m] If not, it is unlikely they would have hunted only for humans, they must have taken advantage of the situation.

Q. 5: Can particular morphotype be linked to particular status/use?

In Western Europe dogs had a more varied status. In South-Eastern Romania, they were almost exclusively eaten in the sites we studied, and the deposit or burial of complete animals is, to date, not attested. In Western Europe, we included some dogs found complete and in connection (from Southern France in particular) that attested to their different status. The observed differences in mean shape between the two European areas raises the question whether prehistoric humans selected specific shapes/sizes for these different functions (which would be particularly visible in Western Europe). It is possible that humans favored more massive dogs for company or protection (of herds or settlements) and that these dogs were more likely to be buried than eaten. It is also possible that prehistoric humans favored small dogs with more fox-like morphologies for meat consumption. **Testing this hypothesis calls for further analyses to check whether buried dogs differed in shape and/or size compared to the dogs that were eaten in Western Europe.** As this requires new specimens to increase the sample size, we did not test it in this PhD. If confirmed, this may also contribute to explain the anatomical features that differ between Eastern and Western European dogs. In particular, dogs are on average larger in Western Europe than in Eastern Europe, the largest dogs being found in the Chasséen and Late Neolithic group, where dogs were both eaten and buried, and the smallest dogs being found in the Cortaillod group (Twann), where dogs were extensively eaten, and in the Chasséen group. The great diversity in size observed during the Chasséen group may be related to this diversity of status types.

We observed no greater diversity in mandible shape or size in dogs from Western Europe compared to Eastern Europe, which suggests that a great variability existed in the Eastern population even though the dogs in our sample were exclusively eaten. It is possible that prehistoric humans encouraged the breeding of small dogs but that the cross-breeding was so important (because dogs were commensal) that larger dogs persisted, resulting in an apparent great variability.

Additionally, based on estimations of the bite force or relative contribution of muscles to the bite force (mechanical potential), **we suggested that Eastern dogs had mandibles more adapted to produce strong vertical bites (relative to size) at low gapes compared to dogs from Western Europe**. We deduced that **Eastern dogs were likely best adapted for the capture of live prey** (the jaw needs to close fast and strong to capture and kill the prey) **than dogs from Western** Europe (which were more adapted for horizontal chewing). Accordingly, a hypothesis is that **Eastern dogs were more free-ranging and had to hunt live prey by themselves to feed**, whereas **Western dogs likely more easily fed on garbage or were even fed intentionally with more or less prepared food** (the jaws do not "need" to close fast but they need to chew). This difference in food acquisition may illustrate the difference in dog status.

Q.7: Can we understand the temporal and cultural variations in form or masticatory function within a single site providing material over a long and rich chrono-stratigraphic period (e.g. Twann)?

The very numerous dog mandibles from the Cortaillod culture in Twann offered the possibility to study the morphological and functional variability that existed within a single site, during the same culture but over a relatively long and precisely known period of time (*c.* 4,020 to *c.* 3,500 BC). We demonstrated that **the variability in size and shape was important in comparison to the overall sample of dog mandibles from Western Europe**. **Some shapes are reminiscent of dog mandibles from earlier Western European** periods, but **some shapes are quite peculiar, perhaps reflecting regional or cultural particularities**. However, we had too few dogs from the neighboring lakeside settlements of Chalain and Clairvaux (Late Neolithic) to compare with those of Twann (Middle Neolithic).

We observed a significant decrease in the mean centroid size and bite force of dogs through time, as well as slight changes in mandible shape (less robust with a less well-defined coronoid process, a less pronounced angular process but a deeper masseteric fossa) but with no change in the variability. **These changes are thus more likely related to a local evolution of dogs through time than to the arrival of new exogenous dogs.** All these dogs being dated to the Cortaillod (and thus late in the Neolithic process), it is not surprising we did not evidence changes in the bite force relative to size or the relative contribution of the muscles. This suggests that the changes in diet occurred earlier than 4,000 BC in this region (and dogs were thus already adapted to an anthropogenic diet, as suggested by their lower relative bite force compared to other dogs from earlier phases in Western Europe).

Q. 8: For contemporary and similar sites with regard to food acquisition strategy (e.g. Hârşova and Borduşani), are there differences in shape between dog populations?

We compared dogs from the two contemporary sites of the Gumelnița (phase A) of Hârşova and Borduşani, these sites sharing similar characteristics and are located close to each other. We demonstrated that **the two dog populations significantly differ, both in terms of size and shape**. **Dogs from Borduşani appear more variable** than dogs from Hârşova. Most of the dogs from Hârşova have equivalents in the population of Borduşani, but **in Borduşani we also found smaller dogs with a specific mandible shape**. Interestingly, **mandible shapes found in Hârşova are reminiscent of dogs from the Hamangia III/Boian**, whereas **some shapes found in Borduşani are very specific** (with a taller mandibular ramus, and a small and vertical coronoid process and a lower and larger angular process). **These differences are not accompanied by functional differences relative to size**. These differences would more likely result from anthropic constraints (e.g. selection for aesthetics or functional purposes, strong endogamy) than from natural constraints. We thus propose that t**wo distinct dog populations evolved separately in both villages, without much exchange between populations.** This is the first evidence that **two contemporary human groups located in a geographically close area each possessed their own dogs**.

4. Comparison of pre-Bronze Age dogs and red foxes in the first European agricultural societies

Q. 9: What can be learned from the comparison of the results obtained for dogs and red foxes?

This PhD is the first study that has explored the morphological variability existing in the red fox prior to the Bronze Age. However, the sample collected was small and highly fragmented, which greatly limited our exploration of the existing diversity at the time of the first agricultural societies. Our comparison between a domestic canid (the dog) and a commensal one (the red fox) has thus remained limited. This has prevented us from comparing their evolutionary trajectories and from evaluating the impact of the proximity between humans and canids on their morphological and functional adaptations.

However, our study revealed **that a certain variability existed in this commensal species prior to the Bronze Age**, which is, given our data, probably **more related to environmental constraints rather than to anthropogenic constraints**. In particular, **foxes from Swiss and French lakeside settlements (located in colder regions) are of smaller size** compared to foxes from other regions, which may be the result of climatic constraints in these cooler climates and mountainous regions. It was not possible to compare foxes from Eastern and Western Europe.

In Western Europe, **the bite force tends to increase relative to size from the Mesolithic to the end of the Neolithic** and **the contribution of the masseter tends to increase while that of the pterygoid tends to decrease from the Early Neolithic to the Middle/Late Neolithic**, suggesting that **foxes get more adapted to vertical bites at low gapes** (results are, however, not significant). If confirmed with a more important sample, this would suggest an opposite result compared to dogs. Indeed, if we infer results from the study of Australian foxes, this would suggest that through time, the diet of pre-Bronze Age foxes got richer in small rodents and less rich in large meet and carrion. However, the significance of food items in modern Australian foxes and pre-Bronze Age foxes is not the same. In modern Australian foxes, small rodents are more a “natural” item compared to sheep carrion, but in ancient foxes, small rodents are likely a sign of increasing anthropogenic pressures, as they are attracted by human storage or open green spaces surrounding the settlements. Thus, it is possible that foxes were more attracted by the small rodents around the settlements than by the food garbage (all the more so as there were already dogs that took advantage of human garbage, so dogs and foxes would have entered in competition). However, as highlighted above, these results are only very preliminary and await larger sample sizes before firm conclusions can be drawn.

The absence of previous studies, which would have laid the foundation for this research (as for dogs), is partly responsible for the small sample size. In three years, it was not possible to collect as much remains as in 30 years of studies on dogs. This first approach therefore calls for future enrichment with new specimens of diverse regions and periods and to further explore the diachronic variability in the same environmental context. However, the small sample also results from the rare presence of foxes in sites prior to the Bronze Age, and to the state of archaeological excavations. Even in the future, the sample may never be large enough to enable to explore the same questions as for dogs. We will be limited to very general questions, but we may extend to more recent periods (Bronze Age, Iron Age, Middle Age) to compare the variability over a longer time period.

Perspectives

In this thesis we used an advanced technique that has never been used before to document the variability in mandible shape in pre-Bronze Age dogs. Although 3D geometric morphometrics is the most accurate method to study shape variation, it is also time consuming and it requires access to the mandibles even though they have been studied before. However, some bones are no longer available and the linear dimensions are the last remaining testament of this material. Given that many data are already available and will continue to be produced, in order to make the work of previous archaeozoologists profitable (and not to lose information on remains that are no longer accessible), it could be interesting to adapt the methods we developed here to linear measurements. This would require to conduct similar analyses on both modern and ancient canids but using multivariate analyses adapted to linear dimensions (log-shape ratio for example). If the approach is successful, much more material could be considered. Alternatively, archaeozoologists may need to adopt the reflex of using 3D reconstruction methods (which nowadays are fast and cheap) to provide a permanent and complete record of the remains recovered from archaeological sites.

The mandible provides a good indication of the overall shape of the head, but the head only represents a small amount of information on the overall appearance of the dogs. In the future, it would be interesting to use a similar methodology on long bones. Archaeological series would be less common but would provide other, complementary, information. Indeed, the study of long bones has only been used to estimate wither heights, based on equations established on modern dogs whose proportions between the different segments of the skeleton (integration) are probably not the same as in the past. A 3D morphometric study on long bones should allow a further, more detailed exploration of shape variability. In particular, one can ask whether the small dogs found in the Romanian Chalcolithic or the Swiss Cortaillod sites show deformed long bones, following a chondrodysplasia characteristic of small modern dog breeds (dachshund) and already documented in ancient Egypt? Moreover, it would probably be possible to make functional inferences and discuss the mobility of dogs, as it has been done in for pigs (Harbers *et al.*, in press). However, there are no data on the architecture of dog limbs that consider the variety of extant breeds. The same work as done in this thesis, but on long bones, would therefore be an interesting perspective. In particular, it could be interesting to compare the relationships between bones and muscles in dogs of the same breed (beagles for example), kept in captivity, or on the contrary involved in intensive physical activity (hunting). If differences in shape were to be found on certain bone parts, inferences could be made in the archaeological record, thus providing information on the degree of free-ranging of the dogs.

References

Adams, D. C. (2016) 'Evaluating modularity in morphometric data: challenges with the RV coefficient and a new test measure', *Methods in Ecology and Evolution*, 7(5), pp. 565–572.

Adams, D. C. and Collyer, M. L. (2016) 'On the comparison of the strength of morphological integration across morphometric datasets', *Evolution*, 70(11), pp. 2623–2631. doi: 10.1111/evo.13045.

Adams, D. C. and Collyer, M. L. (2017) 'Multivariate phylogenetic comparative methods: evaluations, comparisons, and recommendations', *Systematic Biology*, 67(1), pp. 14–31.

Adams, D. C. and Collyer, M. L. (2019) 'Comparing the strength of modular signal, and evaluating alternative modular hypotheses, using covariance ratio effect sizes with morphometric data', *Evolution*, 73(12), pp. 2352–2367.

Albizuri, S. *et al.* (2019) 'Dogs in funerary contexts during the Middle Neolithic in the northeastern Iberian Peninsula (5th–early 4th millennium BCE)', *Journal of Archaeological Science: Reports*, 24, pp. 198–207. doi: 10.1016/j.jasrep.2019.01.004.

Altuna, J., Baldeón, A. and Mariezkurrena, K. (1985) *Cazadores magdalenienses en Erralla:(Cestona, País Vasco)*. Sociedad de Ciencias Aranzadi.

Altuna, J. and Marsan, G. (1986) 'Le gisement préhistorique de la grotte du Bignalats à Arudy (Pyrénées-Atlantiques). Première partie: Présentation des fouilles et étude de la faune de mammifères', *Archéologie des Pyrénées Occidentales et des Landes*, 6, pp. 53–73.

Anderson, M. and Braak, C. T. (2003) 'Permutation tests for multi-factorial analysis of variance', *Journal of statistical computation and simulation*, 73(2), pp. 85–113.

Anderson, M. J. (2001) 'A new method for non-parametric multivariate analysis of variance', *Austral ecology*, 26(1), pp. 32–46.

Andreescu, R., Mirea, P. and Apope, S. (2003) 'Cultura Gumelniţa în vestul Munteniei. Aşezarea de la Vităneşti, jud. Teleorman', *Cercetări Arheologice*, 12, pp. 71–87.

Ansermet, S. (1999) 'La faune du Néolithique final et du Bronze ancien de la grotte du Gardon (Ain): étude préliminaire'.

Arbogast, R. (inédit) *grotte des Perrats, Agris (Charente).* Rapport d'étude.

Arbogast, R. (1991) 'La faune des structures rubanées du site de Bischoffsheim "Le village" (Bas-Rhin).', *Cahiers Alsaciens pour la promotion de la recherche archéologique en Alsace*, (7), pp. 59–63.

Arbogast, R. M. (unpublished) *Ay-sur-Moselle (Moselle)*. Rapport d'étude.

Arbogast, R. M., Jeunesse, C. and Schibler, J. (2001) *Rôle et statut de la chasse dans le Néolithique ancien danubien (5500–4900 av. J.-C.)/Rolle und Bedeutung der Jagd während*

des Frühneolithikums Mitteleuropas (Linearbandkeramik 5500–4900 v. Chr.). Premieres rencontres danubiennes, Strasbourg 20 et 21 novembre 1996, Actes de la premiere table-ronde (Internationale Archäologie: Arbeitsgemeinschaft, Symposium, Tagung, Kongress Band 1). Rahden/Westfalia: Marie Leidorf.

Arbogast, R.-M. (1989) 'IV. Les animaux domestiques des fosses-silos', *Gallia Préhistoire*, 31(1), pp. 139–158.

Arbogast, R.-M. *et al.* (1989) 'Le cerf et le chien dans les pratiques funéraires de la seconde moitié du Néolithique du Nord de la France', *Anthropozoologica*, 3, pp. 37–42.

Arbogast, R.-M. (1993) 'Les vestiges osseux d'animaux du site VSG de Trosly-Breuil "Les Obeaux" (Oise) : campagnes de fouilles 1983 et 1984', *Revue archéologique de Picardie*, 3(1), pp. 31–40. doi: 10.3406/pica.1993.1664.

Arbogast, R.-M. (1994) *Premiers élevages néolithiques du Nord-Est de la France.* Liège (ERAUL).

Arbogast, R.-M. (1995) 'Les faunes du groupe de Villeneuve-Saint-Germain de la vallée de l'Oise et leur contexte en Bassin Parisien', *Bulletin de la Société préhistorique française*, 92(3), pp. 322–331. doi: 10.3406/bspf.1995.10033.

Arbogast, R.-M. (1997) *La grande faune de Chalain 3*. Verlag nicht ermittelbar.

Arbogast, R.-M. *et al.* (2005) 'Du loup au «chien des tourbières». Les restes de canidés sur les sites lacustres entre Alpes et Jura', *Revue de Paléobiologie*, 10, pp. 171–183.

Arbogast, R.-M. (2008) *Caractéristiques, organisation et limites de l'exploitation des ressources animales dans l'économie des sites lacustres du Néolithique final de Chalain et de Clairvaux (Jura, France)*. Université de Franche-Comté.

Arbogast, R.-M. (2009) 'Les vestiges de faune associés au site et structrures d'enceinte du site rubané de Herxheim (Rhénanie-Palatinat, Allemagne.)', in *Krisen, Kulturwandel-Kontinuitäten. Zum Ende der Bandkeamik in Mitteleuropa. Beiträge der Internationalen Tagung in Herxheim bei Landau (Pfalz) vom 17-17.06-07*. Verlag Marie Leidorf GmbH. Rahden/westf, p. xxx. Available at: https://halshs.archives-ouvertes.fr/halshs-00593529 (Accessed: 9 September 2020).

Arbogast, R.-M. *et al.* (2013) 'Les dépôts d'animaux en fosse circulaire du Néolithique récent dans la plaine du Rhin superieur: les données des fouilles récentes', *G. Auxiette i P. Méniel, Les dépôts d'ossements animaux en France, de la fouille à l'interpretation, Montagnac, França*, pp. 191–200.

Arbogast, R.-M. (2018) 'Une vie de chien auprès des premiers éleveurs agriculteurs du Néolithique ancien en Europe occidentale', in Costamagno, S. et al. (eds) *Animal symbolisé, animal exploité : du Paléolithique à la Protohistoire*. Paris: Éditions du Comité des travaux historiques et scientifiques (Actes des congrès nationaux des sociétés historiques et scientifiques), pp. 234–248. Available at: http://books.openedition.org/cths/4659 (Accessed: 30 September 2020).

Arbogast, R.-M. (2019) 'Analysis of the faunal assemblages of the LBK site of Herxheim: the larger mammals', in *Ritual Destruction in the Early Neolithic - The Exceptional Site of*

Herxheim. (Forschungen zur Pfälzischen Archäologie), pp. 139–232. Available at: https://hal.archives-ouvertes.fr/hal-02785545 (Accessed: 16 August 2020).

Arbogast, R.-M. and Pétrequin, P. (1993) 'La chasse du cerf au Néolithique dans le Jura: gestion d'une population animale sauvage', in *Exploitation des animaux sauvagesa travers le temps. XIII◦ rencontres Internationales d'Archéologie et d'Histoire d'Antibes, IV◦ colloque international de l'Homme et l'Animal, Société de Recherche Interdisciplinaire, Ed. APDCA, Juan-Les-Pins*, pp. 221–232.

Ardalan, A. *et al.* (2011) 'Comprehensive study of mtDNA among Southwest Asian dogs contradicts independent domestication of wolf, but implies dog–wolf hybridization', *Ecology and Evolution*, 1(3), pp. 373–385. doi: 10.1002/ece3.35.

Arendt, M. *et al.* (2016) 'Diet adaptation in dog reflects spread of prehistoric agriculture', *Heredity*, 117(5), pp. 301–306. doi: 10.1038/hdy.2016.48.

Arias, P. *et al.* (2015) 'CHAPTER TWENTY-TWO AT THE EDGE OF THE MARSHES: NEW APPROACHES TO THE SADO VALLEY MESOLITHIC (SOUTHERN PORTUGAL)', *Muge 150th: The 150th Anniversary of the Discovery of Mesolithic Shellmiddens: Volume 1*, 1, p. 301.

Balasescu, A. (2008) 'CONSIDERATII CU PRIVIRE LA EXPLOATAREA MAMIFERELOR IN AŞEZAREA HAMANGIA III DE LA CHEIA', *Pontica (Constanţa)*, 41, pp. 49–56.

Bălăşescu, A., Moise, D. and Radu, V. (2005) 'The palaeoeconomy of Gumelniţa communities on the territory of Romania', *Culturã si Civilizaţie la Dunãrea de Jos*, 22, pp. 167–200.

Bălăşescu, A. and Radu, V. (2003) 'Studiul materialului faunistic descoperit în tell-ul de la Vităneşti (jud. Teleorman): nivelul Gumelniţa B1', *Cercetări arheologice*, 12, pp. 375–387.

Bălăşescu, A. and Radu, V. (2004) *Oamenii şi animale. Strategii şi resurse la comunităţile preistorice Hamangia şi Boian.* Editura Cetatea de Scaun. Bucuresti (In Biblioteca Muzeului Naţional, Seria Cercetări Pluridisciplinare).

Balasescu, A. and Radu, V. (2004) *Omul si animalele: strategii si resurse la Comunitatile Hamangia si Boian*. Editura Cetatea de Scaun.

Balasescu, A. and Radu, V. (2011) 'Paléo-économie animalière et reconstitution de l'environnement', in Carozza, L., Bem, C., and Micu, C. (eds) *Société et environnement dans la zone du Bas Danube durant le 5ème millénaire avant notre ère, seconde partie*. editura Universitatii Alex I. Cuza (Recherches archeologiques autour de Taraschina), pp. 385–408. Available at: https://www.researchgate.net/publication/244483526_Paleo-economie_animaliere_et_reconstitution_de_l'environnement (Accessed: 21 September 2020).

Bălăşescu, A. and Radu, V. (2012) 'Fauna de la Ostrovul Banului, sector D', in Boroneanț, A., *Aspecte ale tranziţiei de la mezolitic la neoliticul timpuriu în zona Porţile de Fier/ Aspects of the Mesolithic- Early Neolithic transition in the Iron Gates region*. edition Mega. Cluj Napoca, pp. 164–169.

Bălăşescu, A., Radu, V. and Moise, D. (2005) *Omul şi mediul animal între mileniile VII-IV Î. E. N. La Dunărea de Jos*. Cetatea de Scaun.

Balasse, M. *et al.* (2014) 'Cattle and Sheep Herding at Cheia, Romania, at the Turn of the Fifth Millennium cal BC', in Whittle, A. and Bickle, P. (eds) *Proceedings of the British Academy. Early Farmers. The View from Archaeology and Science.*, Oxford: Oxford University Press, pp. 115–42.

Balasse, M. *et al.* (2016) 'Wild, domestic and feral? Investigating the status of suids in the Romanian Gumelniţa (5th mil. cal BC) with biogeochemistry and geometric morphometrics', *Journal of Anthropological Archaeology*, 42, pp. 27–36. doi: 10.1016/j.jaa.2016.02.002.

Bánffy, E. (2017) 'Neolithic Eastern and Central Europe', in *The Oxford Handbook of Prehistoric Figurines*, pp. 705–728.

Barone, R. (2010) *Anatomie comparée des mammifères domestiques : Tome 1, Ostéologie*. 5e édition. Paris: Vigot.

Bartosiewicz, L. (2018) '" Forever young" neoteny and design', *Annalen des Naturhistorischen Museums in Wien. Serie A für Mineralogie und Petrographie, Geologie und Paläontologie, Anthropologie und Prähistorie*, 120, pp. 19–30.

Baudais, D. *et al.* (1993) 'L'abri de Roche-Chêvre à Bretonvillers (Doubs): campements de chasse du Néolithique Moyen et de l'Age du Bronze', *Revue Archéologique de l'Est et du Centre-est*, 44(2), pp. 261–292.

Becker, C. and Johansson, F. (1981) *Die neolitischen Ufersiedlungern von Twann. Tierknochenfunde. Zweiter Bericht*. Bern, Staatlicher Lehrmittelverlag.

Bedault, L. (2012) *L'exploitation des ressources animales dans la société du Néolithique ancien du Villeneuve-Saint-Germain en Bassin parisien: synthèse des données archéozoologiques.*

Beeching, A. and Crubézy, E. (1998) 'Les sépultures chasséennes de la vallée du Rhône', *Sépultures d'Occident et genèses des mégalithismes (9000-3500 avant notre ère), Séminaire du Collège de France, Paris, Errance*, pp. 147–164.

Beldade, P., Koops, K. and Brakefield, P. M. (2002) 'Developmental constraints versus flexibility in morphological evolution', *Nature*, 416(6883), pp. 844–847.

Belhaoues, F. (2018) *Variabilité morpho-anatomique et statuts des chiens entre âge du Bronze et Antiquité: référentiel et applications archéologiques en Méditerranée nord occidentale*. Montpellier 3.

Bémilli, C. (2005) *La Faune Néolithique de la Route de Varreddes à Meaux*. Rapport d'étude, p. 9.

Benecke, N. (1987) 'Studies on early dog remains from Northern Europe', *Journal of Archaeological Science*, 14(1), pp. 31–49.

Benecke, N. (1994) 'Der Mensch und seine Haustiere', *Stuttgart: Theiss*, pp. 353–5.

Benecke, N. (1999) 'Die Tierreste aus bandkeramischen Siedlungen von Dresden-Cotta', *PRATSCH, A.: Die linien-und stichbandkeramische Siedlung in Dresden-Cotta. Eine frühneolithische Siedlung im Dresdener Elbkessel.–Beiträge zur Ur-und Frühgeschichte Mittel europas*, 17, pp. 137–171.

Bernabò Brea, M. *et al.* (2010) 'Testimonianze funerarie della gente dei Vasi a Bocca Quadrata in Emilia occidentale: archeologia e antropologia', *Testimonianze funerarie della gente dei Vasi a Bocca Quadrata in Emilia occidentale: archeologia e antropologia*, pp. 63–126.

Beyneix, A. (2003) *Traditions funéraires néolithiques en France méridionale: 6000-2200 avant J.-C.* Editions Errance.

Billard, C., Guillon, M. and Verron, G. (2010) 'Les sépultures collectives du Néolithique récent-final de Val-de-Reuil et Porte-Joie (Eure, France)', *Liège, universtié de Liège (ERAUL, 123)*.

Binder, D. (2002) *Abri Pendimoun (Castellar)*. Rapport de fouilles programmées. UMR6130 Valbonne Sophia-Antipolis, SRA PACA.

Binford, L. R. (1981) *Bones : Ancient Men and Modern Myth*. University of Mexico: Academic Press (Department of Anthropology). Available at: https://www.persee.fr/doc/nda_0242-7702_1983_num_11_1_2398_t1_0094_0000_2 (Accessed: 30 September 2020).

Blaise, E. (2009) *Economie animale et gestion des troupeaux au Néolithique final en Provence: approche archéozoologique et contribution des analyses isotopiques de l'émail dentaire*. These de doctorat. Aix-Marseille 1.

Blaise, E. *et al.* (2009) 'L'élevage du Néolithique moyen 2 au Néolithique final dans le midi méditerranéen de la France: état des données archéozoologiques', in *Actes de la table ronde Quatrième millénaire, du Néolithique moyen au Néolithique final dans le sud-est de la France et les régions voisines*. Aix-en-Provence, 2005: Monographies d'Archéologie Méditerranéenne.

Blouet, V. *et al.* (1984) 'Le Michelsberg en Lorraine', *Revue archéologique de Picardie*, 1(1), pp. 125–145. doi: 10.3406/pica.1984.1408.

Boelicke, U. and Aniol, R. W. (1988) *Der bandkeramische Siedlungsplatz Langweiler 8: Gemeinde Aldenhoven, Kreis Düren*. Rheinland-Verlag.

Bökönyi, S. (1959) *Die frühalluviale Wirbeltierfauna Ungarns von Neolithikum bis zur La Tène-Zeit*. Akadémiai Kiadó.

Bökönyi, S. (1974) *History of domestic mammals in Central and Eastern Europe*. Akademiae Kiado. Budapest: Akademiai kiado.

Bökönyi, S. (1978) 'The vertebrate fauna of Vlasac', *Vlasac. A Mesolithic Settlement in the Iron Gates*, 2, pp. 35–65.

Bökönyi, S. (1984) 'Die neolithische Wirbeltierfauna von Battonya-Gödrösök', *Battonya-Gödrösök, eine neolithische Siedlung in Südost-Ungarn*, pp. 119–69.

Bökönyi, S. (1988) *History of domestic mammals in central and eastern Europe*. Budapest: Akadémiai Kiadó.

Bökönyi, S. and Bartosiewicz, L. (1999) 'IX. Analyse de la faune (Diconche)', *Les enceintes néolithiques de Diconche à Saintes (Charente-Maritime). Société Préhistorique Française, Mémoire XXV*, 1, pp. 147–166.

Bolomey, A. (1966) ‘Fauna neolitica din asezarea Boian A de la Varasti’, *Studii si cercetari de antropologie*, 3(1), pp. 27–34.

Bolomey, A. (1973) ‘present stage of knowledge of mammal exploitation during the Epipalaeolithic and the earliest Neolithic on the terr itory of romania’, in *Domestikationsforschung und Geschichte der Haustiere Inteernationales Symposium in Budapest*.

Bonsall, C. *et al.* (2015) ‘New AMS 14C dates for human remains from Stone Age sites in the Iron Gates reach of the Danube, Southeast Europe’, *Radiocarbon*, 57(1), pp. 33–46.

Bookstein, F. L. (1991) *Morphometric Tools for Landmark Data. Geometry and Biology*. Cambridge University Press. (Bookstein).

Boric, D. (2011) ‘Adaptations and transformations of the Danube Gorges foragers (c. 13,000–5500 cal. BC): an overview’.

Boroneanţ, A. E., Bălăşescu, A. and Radu, V. (2012) ‘Aspecte ale tranziţiei de la mezolitic la neoliticul timpuriu în zona Porţile de Fier. Aspects of the Mesolithic–Early Neolithic transition in the Iron Gates region.’, in. Cluj-Napoca: Editura Mega.

Boroneanţ, V. (2000) *Paleolithique superieur et epipaleolithique dans la zone des Portes de Fer*. Bucureşti: Silex.

Bostyn, F. *et al.* (2016) ‘L’apport du site d’habitat de Conty «ZAC Dunant»(Somme) à la connaissance de la culture de Cerny’, *Bulletin de la Société préhistorique française*, pp. 291–332.

Bostyn, F., Hachem, L. and Lanchon, Y. (1991) ‘Le site néolithique de “la Pente de Croupeton” à Jablines (Seine-et-Marne). Premiers résultats.’, in. *15è colloque interrégional sur le Néolithique. (oct 1988).*, Châlons-sur-Marne, pp. 45-81.

Boudadi-Maligne, M. *et al.* (2012) ‘Magdalenian dog remains from Le Morin rock-shelter (Gironde, France). Socio-economic implications of a zootechnical innovation’, *PALEO. Revue d’archéologie préhistorique*, (23), pp. 39–54. doi: 10.4000/paleo.2465.

Boudadi-Maligne, M. *et al.* (2020) ‘The earliest double dog deposit in the Palaeolithic record: The case of the Azilian level of Grotte-abri du Moulin (Troubat, France)’, *International Journal of Osteoarchaeology*, 30(3), pp. 382–394. doi: 10.1002/oa.2857.

Boudadi-Maligne, M. and Escarguel, G. (2014) ‘A biometric re-evaluation of recent claims for Early Upper Palaeolithic wolf domestication in Eurasia’, *Journal of Archaeological Science*, 45, pp. 80–89. doi: 10.1016/j.jas.2014.02.006.

Boyko, A. R. *et al.* (2009) ‘Complex population structure in African village dogs and its implications for inferring dog domestication history’, *Proceedings of the National Academy of Sciences*, 106(33), pp. 13903–13908.

Braguier, S. (1997) *Economie alimentaire et gestion des troupeaux au Néolithique récent/final, dans les zones d’occupation des faciès culturels Matignons, Peu-Richard et Artenac: bilan des connaissances actuelles et définition des problématiques*. Mémoire de DEA : Anthropologie sociale et historique de l’Europe. Toulouse 2 : Ecole des Hautes Etudes en Sciences Sociales.

Braguier, S. (1999a) ‘Étude de la faune néolithique de l’enceinte de Temps-Perdu à Migné-Auxances (Vienne)’, *Bulletin de la Société préhistorique française*, 96(3), pp. 363–365.

Braguier, S. (1999b) ‘La faune du Rocher à Villedoux (Charente-Maritime) et de Champ-Durand à Nieul-sur-l’Autize (Vendée)’, *Bulletin de la Société préhistorique française*, 96(3), pp. 409–418.

Braguier, S. (2000) *Economie alimentaire et gestion des troupeaux au Néolithique récent/final dans le centre-ouest de la France*. These de doctorat. Toulouse 2. Available at: https://www.theses.fr/2000TOU20049 (Accessed: 11 October 2020).

Braguier, S. (2009) ‘Exploitation du milieu continental V. Etude diachronique de la faune provenant de trois sites appartenant à la fin du Néolithique, sur l’île d’Oléron’, in Laporte, L. (ed.) *Des premiers paysans aux premiers métallurgistes sur la façade atlantique de la France (3500-2000 av. J.C.).* (Association des Publications Chauvignoises, Chauvigny. Mémoire XXXIII), pp. 622–641.

Brassard, C. (2018) ‘Le chien en Egypte ancienne : approche archéozoologique et apports de la craniologie’, *Paleobios*, (20). Available at: http://www.laboratoiredanthropologieanatomiqueetdepaleopathologiedelyon.fr/PALEOBIOS%202018%20Colline%20Brossard%20Le%20chien%20en%20Egypte%20Ancienne.pdf.

Brassard, C. and Callou, C. (2020) ‘Sex determination of archaeological dogs using the skull: evaluation of morphological and metric traits on various modern breeds’, *Journal of Archaeological Science: Reports*, 31, p. 102294. doi: 10.1016/j.jasrep.2020.102294.

Bréhard, S. (2007) *Contribution archéozoologique à la connaissance de la fonction des grands sites de terrasse du Chasséen récent (début du 4e millénaire avant J.-C.) de la moyenne vallée du Rhône, dans leur contexte de Méditerranée nord-occidentale*. These de doctorat. Paris, Muséum national d’histoire naturelle.

Bréhard, S. (2011) ‘Le complexe chasséen vu par l’archéozoologie : révision de la dichotomie Nord-Sud et confirmation de la partition fonctionnelle au sein des sites méridionaux’, *Bulletin de la Société préhistorique française*, 108(1), pp. 73–92. doi: 10.3406/bspf.2011.13994.

Bréhard, S. *et al.* (2014) ‘L’exploitation du chien, trait culturel chasséen ou caractère des sociétés européennes au tournant des 5e/4e millénaires?’ *Colloque international Le Chasséen, des Chasséens. Retour sur une culture nationale et ses parallèleSepulcres de fossa, Cortaillod, Lagozza*, Paris, 18 November.

Bréhard, S. and Bălăşescu, A. (2012) ‘What’s behind the tell phenomenon? An archaeozoological approach of Eneolithic sites in Romania’, *Journal of Archaeological Science*, 39(10), pp. 3167–3183. doi: 10.1016/j.jas.2012.04.054.

Bréhard, S., Beeching, A. and Vigne, J.-D. (2010) ‘Shepherds, cowherds and site function on middle Neolithic sites of the Rhône valley: An archaeozoological approach to the organization of territories and societies’, *Journal of Anthropological Archaeology*, 29(2), pp. 179–188.

Bréhard, S. and Vigne, J. D. (in press) ‘Le Taï (Remoulins – Gard). Premières sociétés agropastorales du Languedoc rhodanien (6e-3e millénaire avant notre ère).’, in. Toulouse (Archives d’Ecologie Préhistorique).

Bridault, A. (1993) *Les économies de chasse épipaléolithiques et mésolithiques dans le nord et l'est de la France*. These de doctorat. Paris 10. Available at: http://www.theses.fr/1993PA100124 (Accessed: 9 October 2020).

Bridault, A. and Bautista, A. (1993) 'La grotte" à la peinture" à Larchant (Seine-et-Marne), lieu-dit Les Dégoûtants à Ratard. La faune (Mésolithique, Bronze final et Gallo-Romain)'.

Brown, S. K. *et al.* (2011) 'Phylogenetic distinctiveness of Middle Eastern and Southeast Asian village dog Y chromosomes illuminates dog origins', *PloS one*, 6(12), p. e28496.

Brunet, P. *et al.* (2020) 'La fosse 264 du Néolithique récent de Vignely, la Noue-Fénard (Seine-et-Marne)', in Cottiaux, R. and Salanova, L. (eds) *La fin du IVe millénaire dans le bassin parisien : Le Néolithique récent entre Seine, Oise et Marne (3500-2900 avant notre ère)*. Dijon: ARTEHIS Éditions (Suppléments à la Revue archéologique de l'Est), pp. 93–136. Available at: http://books.openedition.org/artehis/16686 (Accessed: 17 August 2020).

Brunet, V. *et al.* (2006) 'Saint-Julien-lès-Metz (Moselle)«Ferme de Grimont»: Site d'habitat Groβgartach/épi-Roëssen'.

Brunnacker, M. *et al.* (1967) 'Neolithische Fundschicht mit Harpunen-Fragmenten im Travertin von Stuttgart-Bad Cannstatt', *Fundberichte Schwaben NF*, 18, pp. 43–60.

Buffat, L. *et al.* (2008) *Au coeur du vignoble de l'ager baeterrensis: Fermes et plantations du Gasquinoy à Béziers, futur centre pénitentaire*. Rapport final d'opération. SRA Languedoc-Roussillon, INRAP, OPTIMEP 4, groupe EIFFAGE.

Burnez, C. (1986) 'Echiré – Les loups', *Gallia Préhistoire, Informations archéologiques*, 29(2), p. 463.

Burri-Wyser, E. and Jammet-Reynal, L. (2014) 'La seconde partie du Néolithique moyen de Suisse occidentale (4000-3350 BC) : essai de synchronisation des cultures rhodaniennes et lacustres', in *Chronologie de la Préhistoire récente dans le Sud de la France*. Toulouse (Archives d'Ecologie Préhistorique), pp. 75–86.

Campbell, N. A. and Atchley, W. R. (1981) 'The geometry of canonical variate analysis', *Systematic Zoology*, 30(3), pp. 268–280. doi: 10.2307/2413249.

Caro, J. and Manen, C. (2012) 'Les productions céramiques du Néolithique ancien du Taï (Remoulins, Gard). Approche spatiale, caractérisation typo-technologique et attribution culturelle', in.

Carozza, L. *et al.* (2013) *LE TELL SUBMERGÉ CHALCOLITHIQUE DE TARASCHINA ET L'ÉVOLUTION INTERNE DU DELTA DU DANUBE-REGARDS CROISÉS A PARTIR DES DONNÉES ARCHÉOLOGIQUES ET GÉO-ARCHÉOLOGIQUES*.

Carraway, L. N. *et al.* (1996) 'A search for age-related changes in bite force and diet in shrews', *American Midland Naturalist*, pp. 231–240.

Carré, A. (2004) *Etude archéozoologique d'un site du Néolithique ancien dans l'Yonne : Etigny 'Le Brassot-Est'.* Mémoire de Maîtrise d'Ethnologie et Préhistoire. Université Paris X Nanterre.

Carrère, I. (1986) ‘Le Gisement Chasséen de la Fosse de la Toronde à Cavanac (Aude), II La faune’, *Gallia Préhistoire*, 29(1), pp. 187–190.

Carrère, I. and Forest, V. (2003) ‘Les Vautes et l’alimentation animale. Archéozoologie du Néolithique final au Bronze ancien en Languedoc oriental in’, *Les Vautes (Saint Gély du Fesc, Hérault) et le Néolithique final du Languedoc oriental, Archives d’Ecologie Préhistorique, Centre d’Anthropologie, Toulouse, INRAP, DRAC Languedoc-Roussillon*, pp. 307–333.

Cauliez, J. *et al.* (2005) ‘Rapport de fouille de sauvetage nécessitée par l’urgence absolue, Le Limon-Raspail Lieu dit Le Limon (Bédoin, Vaucluse), Aix-en-Provence’.

Cauwe, N. *et al.* (2007) *Le néolithique en Europe*. Armand Colin.

Célérier, G. and Delpech, F. (1978) ‘Un chien dans l’Azilien de «pont d’Ambon»’, *Bulletin de la Société préhistorique française*, 75(7), pp. 212–215.

Célérier, G., Tisnerat, N. and Valladas, H. (1999) ‘Données nouvelles sur l’âge des vestiges de chien à Pont d’Ambon, Bourdeilles (Dordogne)/New data on the age of Canis remains at Pont d’Ambon, Bourdeilles (Dordogne, France)’, *Paléo, Revue d’Archéologie Préhistorique*, 11(1), pp. 163–165.

Chaix, L. (1976) *La faune néolithique du Valais (Suisse): ses caractères et ses relations avec les faunes néolithiques des régions proches*. Doctoral thesis. University of Geneva. doi: 10.13097/archive-ouverte/unige:104428.

Chaix, L. (1988) ‘La faune de l’habitat Néolithique moyen du Petit-Chasseur I (Sion, Valais)’, *Jahrbuch der Schweizerischen Gesellschaft für Ur-und Frühgeschichte*, 71, pp. 103–105.

Chaix, L. (2000) ‘A preboreal dog from the northern Alps (Savoie, France)’.

Chaix, L. (2013) ‘Cynophagy at Zamostje 2 (Russia)(Mesolithic and Neolithic)’, in Lozovski, V., Lozovskaya, O., and Clemente, I. (eds) *Zamostje 2. Lake Settlement of the Mesolithic and Neolithic Fisherman in Upper Volga Region*. St. Petersbourg, pp. 231–237.

Chenevoy, M. and Chaix, L. (1985) ‘Les faunes des sites littoraux de Chalain et de Clairvaux conservées au Musée de Lons-le-Saunier’, in *Néolithique Chalain-Clairvaux. Fouilles anciennes. Présentation des collections du Musée de Lons-le-Saunier.* Lons-leSaunier (Musée d’archéologie), pp. 105–119.

Chiquet, P. (2012) *La faune du Néolithique moyen: analyse des modes d’exploitation des ressources animales et contribution à l’interprétation de l’espace villageois.* Lausanne: Cahiers d’archéologie romande (Cahiers d’archéologie romande, 4).

Chiquet, P. A. (2013) ‘La faune du Néolithique moyen II de la grotte du Gardon’, *La grotte du Gardon (Ain), volume II. Du Néolithique moyen II au Bronze ancien (couches 46 à 33)*, pp. 195–228.

Christiansen, P. and Wroe, S. (2007) ‘Bite forces and evolutionary adaptations to feedinge ecology in Carnivores’, *Ecology*, 88(2), pp. 347–358. doi: 10.1890/0012-9658(2007)88[347:BFAEAT]2.0.CO;2.

Clark, K. M. (2006) 'Dogs and wolves in the Neolithic of Britain', *Animals in the Neolithic of Britain and Europe*, 7, p. 32.

Claude, J. (2008) *Morphometrics with R*. Springer Science & Business Media.

Claudet, K. (2003) *Les restes fauniques de l'enceinte néolithique de Vignely « La Noue Fénard » (Seine-et-Marne)*. Mémoire de maîtrise. Université Paris 1, Panthéon-Sorbonne.

Clutton-Brock, JULIET (1989) 'Introduction to domestication', *The walking larder. Patterns of domestication, pastoralism, and predation. Unwin Hyman, London*, pp. 7–9.

Clutton-Brock, Juliet (ed.) (1989) *The Walking Larder: Patterns of Domestication Pastoralism and Predation*. London ; Boston: Unwin Hyman.

Clutton-Brock, J. (1995) 'Origins of the dog: domestication and early history', in *The Domestic Dog, its Evolution, Behavior and Interactions With People*. Serpell J (eds). Cambridge: Cambridge University Press, pp. 7–20.

Clutton-Brock, J. (1999) *A natural history of domesticated mammals*. Cambridge University Press.

Cockin, G. and Furestier, R. (2009) *A8 Saint-Maximin/Chemin de Barjols à Saint-Maximin-la-Sainte-Baume (Var).* Rapport final d'opération. Aix en provence: Service Régional de l'Archéologie, p. 413.

Collonge, J. (2000) *Etude de la faune de La Baume Layrou (Gard, France): approche de la vie pastorale à la fin du Néolithique en Languedoc Oriental*. Mémoire de maîtrise. Université de Paris I-Panthéon La Sorbonne.

Collyer, M. L., Sekora, D. J. and Adams, D. C. (2015) 'A method for analysis of phenotypic change for phenotypes described by high-dimensional data', *Heredity*, 115(4), p. 357.

Convertini, F. *et al.* (2004) 'Le Mas de Vignoles IV à Nîmes (Gard): résultats préliminaires des fouilles du fossé à occupation campaniforme', in *Actes du Colloque de Clermont-Ferrand «Ve Rencontres méridionales de la Préhistoire récente». Préhistoire du Sud-Ouest, Cressensac*, pp. 493–507.

Convertini, F. *et al.* (2014) 'ZAC de Caunelle à Juvignac (Hérault) : résultats préliminaires de la fouille d'un site de plein air stratifié', in *Chronologie de la Préhistoire récentedans le Sud de la France Actualité de la recherche*. *Actes des 10 e Rencontres méridionales de Préhistoire récente 18 au 20 octobre 2012*, Porticcio: Archives d'Écologie Préhistorique.

Coppinger, R. and Schneider, R. (1995) *The evolution of working dogs. In 'The Domestic Dog: Its Evolution, Behaviour and Interactions with People'.(Ed. J. Serpell.) pp. 21–47*. Cambridge University Press: New York.

Corbett, L. K. (1995) *The dingo in Australia and Asia*. Sydney, University of New South Wales Press.

Cornette, R. *et al.* (2012) 'Rapid morpho-functional changes among insular populations of the greater white-toothed shrew', *Biological Journal of the Linnean Society*, 107(2), pp. 322–331. doi: 10.1111/j.1095-8312.2012.01934.x.

Cornette, R. *et al.* (2015) 'Does bite force provide a competitive advantage in shrews? The case of the greater white-toothed shrew', *Biological Journal of the Linnean Society*, 114(4), pp. 795–807. doi: 10.1111/bij.12423.

Crégut-Bonnoure, E. (1988) 'Les Mammifères néolithiques de la grotte de Saint-Marcel (Bidon, Ardèche).', *Ardèche Archéologie*, (5), pp. 49–50.

Crégut-Bonnoure, E. (2008) '18,000 ans d 'évolution de la faune mammalienne en Vaucluse', *Bull. Archéol. Provence*, pp. 5–6.

Crockford, S. J. and Kuzmin, Y. V. (2012) 'Comments on Germonpré et al., Journal of Archaeological Science 36, 2009 "Fossil dogs and wolves from Palaeolithic sites in Belgium, the Ukraine and Russia: osteometry, ancient DNA and stable isotopes", and Germonpré, Lázkičková-Galetová, and Sablin, Journal of Archaeological Science 39, 2012 "Palaeolithic dog skulls at the Gravettian Předmostí site, the Czech Republic"', *Journal of Archaeological Science*, 39(8), pp. 2797–2801.

Croutsch, C. *et al.* (2007) *Entzheim-Geispolsheim (Alsace, Bas-Rhin) Aéroparc (Lidl-CUS). Vol. 2: Les occupations néolithiques*. Rapport de fouille préventive, PAIR/SRA Alsace.

Crubézy, E. (1991) 'Les pratiques funéraires dans le Chasséen de la moyenne vallée du Rhône', *Mémoires du Musée de préhistoire d'Ile-de-France*, (4), pp. 393–398.

Cupillard, C. *et al.* (2000) 'Les occupations mésolithiques de la grotte de la Baume de Montandon à Sainte-Hippolyte (Doubs, France)'.

Curth, S. (2018) 'Modularity and Integration in the Skull of Canis lupus (Linnaeus 1758): A Geometric Morphometrics Study on Domestic Dogs and Wolves', p. 78.

Curth, S., Fischer, M. S. and Kupczik, K. (2017) 'Patterns of integration in the canine skull: an inside view into the relationship of the skull modules of domestic dogs and wolves', *Zoology (Jena, Germany)*, 125, pp. 1–9. doi: 10.1016/j.zool.2017.06.002.

D'Anna, A. (1993) 'L'habitat en plein air : recherches récentes', in *Le Néolithique au quotidien. Actes du XVIe colloque interrégional sur le Néolithique*. Maison des Sciences de l'Homme, Paris, 5-6 novembre 1989: Documents d'Archéologie Française, pp. 72–84.

Danu, M. *et al.* (2019) 'Phytolith evidence of cereal processing in the Danube Delta during the Chalcolithic period', *Quaternary International*, 504, pp. 128–138.

Davis, S. J. and Valla, F. R. (1978a) 'Evidence for domestication of the dog 12,000 years ago in the Natufian of Israel', *Nature*, 276(5688), pp. 608–610.

Davis, S. J. and Valla, F. R. (1978b) 'Evidence for domestication of the dog 12,000 years ago in the Natufian of Israel', *Nature*, 276(5688), pp. 608–610.

Deckers, M. *et al.* (2009) *'Rue Jean Bernier, les Lauréades', Valenciennes (Nord), 02/05/2006 - 31/08/2006 et 02/04/2007 - 31/08/2007.* Rapport de fouille préventive. Service Archéologique de Valenciennes, SRA Nord-Pas-de-Calais.

Demoule, J.-P. (2007) *La révolution néolithique en France*. La Découverte. (Archéologie de la France). Available at: https://livre.fnac.com/a1929974/Jean-Paul-Demoule-La-revolution-neolithique-en-France (Accessed: 26 September 2020).

Denys, C. and Patou-Mathis, M. (2014) *Manuel de taphonomie*. Errance.

Deschler-Erb, S. and Marti-Grädel, E. (2004) 'Viehhaltung und Jagd. Ergebnisse der Untersuchung der handaufgelesenen Tierknochen', *Die jungsteinzeitliche Seeufersiedlung Arbon Bleiche*, 3, pp. 158–252.

Detry, C. and Cardoso, J. L. (2010) 'On some remains of dog (Canis familiaris) from the Mesolithic shell-middens of Muge, Portugal', *Journal of Archaeological Science*, 37(11), pp. 2762–2774.

Digard, J. P. (2006) 'Essai d'ethno-archéologie du chien', *Ethnozootechnie*, (78), pp. 33–40.

Dimitrijević, V. and Vuković, S. (2015) 'Was the Dog Locally Domesticated in the Danube Gorges? Morphometric Study of Dog Cranial Remains From Four Mesolithic–Early Neolithic Archaeological Sites by Comparison With Contemporary Wolves', *International Journal of Osteoarchaeology*, 25(1), pp. 1–30. doi: 10.1002/oa.2260.

Döhle, H.-J. (1994) *Die linienbandkeramischen Tierknochen von Eilsleben, Bördekreis: ein Beitrag zur neolithischen Haustierhaltung und Jagd in Mitteleuropa*. na.

Doumerc, J. O. (2016) *Analyse ostéo-archéologique d'une stratigraphie néolithique.* Mémoire de Master 2. EHESS-Université Toulouse Jean Jaurès.

Drake, A. G., Coquerelle, M. and Colombeau, G. (2015) '3D morphometric analysis of fossil canid skulls contradicts the suggested domestication of dogs during the late Paleolithic', *Scientific Reports*, 5, pp. 82–99. doi: 10.1038/srep08299.

Drake, A. G. and Klingenberg, C. P. (2010) 'Large-scale diversification of skull shape in domestic dogs: disparity and modularity.', *The American Naturalist*, 175(3), pp. 289–301. doi: 10.1086/650372.

Druzhkova, A. S. *et al.* (2013) 'Ancient DNA Analysis Affirms the Canid from Altai as a Primitive Dog', *PLoS ONE*, 8(3). doi: 10.1371/journal.pone.0057754.

Dubois, J. *et al.* (1998) *'Le Parc du Château', Auneau (Eure-et-Loir). Le site mésolithique et néolithique. Rapport intermédiaire 1998-2000.* Rapport de fouilles programmées. SRA Centre, Association ARCHEA (CRICA).

Ducos, P. (1958) 'Le gisement de Châteauneuf-lès-Martigues (Bouches-du-Rhône): les mammifères et le problème de la domestication', *Bulletin du Musée d'Anthropologie préhistorique de Monaco*, 5, pp. 119–33.

Ducos, P. (1968) *L'Origine des animaux domestiques en Palestine, Bordeaux, CNRS*. thèse, mémoire.

Dufresnes, C. *et al.* (2018) 'Howling from the past: historical phylogeography and diversity losses in European grey wolves', *Proceedings of the Royal Society B: Biological Sciences*, 285(1884), p. 20181148. doi: 10.1098/rspb.2018.1148.

Durrenmath, G. *et al.* (2003) *Le Collet-Redon*. Rapport de fouilles programmée. Martigues (Bouches-du-Rhône): SRA PACA, UMR 6636.

Edwards, C. J. *et al.* (2012) 'Temporal genetic variation of the red fox, Vulpes vulpes, across western Europe and the British Isles', *Quaternary Science Reviews*, 57, pp. 95–104. doi: 10.1016/j.quascirev.2012.10.010.

Ellis, J. L. *et al.* (2009) 'Cranial dimensions and forces of biting in the domestic dog', *Journal of Anatomy*, 214(3), pp. 362–373. doi: 10.1111/j.1469-7580.2008.01042.x.

Encyclopedia of Ecology | ScienceDirect (no date). Available at: https://www.sciencedirect.com/referencework/9780080454054/encyclopedia-of-ecology (Accessed: 2 September 2020).

Endicott, P. *et al.* (2003) 'The Genetic Origins of the Andaman Islanders', *American Journal of Human Genetics*, 72(1), pp. 178–184.

Erroux, J. and Poulain, T. (1984) 'II. Faune et céréales de la grotte 1 de Sargel à Saint-Rome-de-Cernon (Aveyron)', *Gallia Préhistoire*, 27(1), pp. 211–228.

Ersmark, E. *et al.* (2016) 'From the past to the present: wolf phylogeography and demographic history based on the mitochondrial control region', *Frontiers in Ecology and Evolution*, 4, p. 134.

Evin, A. *et al.* (2016) 'The use of close-range photogrammetry in zooarchaeology: Creating accurate 3D models of wolf crania to study dog domestication', *Journal of Archaeological Science: Reports*, 9, pp. 87–93. doi: 10.1016/j.jasrep.2016.06.028.

Fan, Z. *et al.* (2016) 'Worldwide patterns of genomic variation and admixture in gray wolves', *Genome Research*, 26(2), pp. 163–173. doi: 10.1101/gr.197517.115.

Favrie, T. (2003) *Etude archéozoologique du niveau à bovidés de la Grotte Chazelles (Saint-André-de-Cruzières, Ardèche), couche VI-Néolithique final*. Mémoire de DEA. Université Lyon II, Lumière.

Filippo, A. (2017) *Exploration de la diversité morphologique de la mandibule chez les chiens d'Europe et du Proche et Moyen Orient de l'Epipaléolithique à l'Age du Bronze Aspects morpho-fonctionnels liés aux changements alimentaires induits par l'Homme*. Mémoire de Master 2. Muséum national d'Histoire naturelle.

Fontaine, A. (2002) *Analyse de l'assemblage faunique du puits chasséen de Villeneuve-Tolosane (Haute-Garonne)*. Mémoire de DEA. Université Paris 1-Panthéon Sorbonne.

Fontan, P. (2019) 'Une réflexion épistémologique sur les interprétations des relations Homme-animal dans les sépultures préhistoriques issues de fouilles anciennes : l'exemple de la nécropole mésolithique de Téviec (Saint-Pierre-Quiberon, Morbihan)', in Costamagno, S. et al. (eds) *Animal symbolisé, animal exploité : du Paléolithique à la Protohistoire*. Paris: Éditions du Comité des travaux historiques et scientifiques (Actes des congrès nationaux des sociétés historiques et scientifiques), pp. 279–298. Available at: http://books.openedition.org/cths/4679 (Accessed: 2 August 2020).

Fontana, L. (2000) *Les Baraquettes: Étude archéozoologique*.

Forbes-Harper, J. L. *et al.* (2017) 'Diet and bite force in red foxes: ontogenetic and sex differences in an invasive carnivore', *Journal of Zoology*, 303(1), pp. 54–63. doi: 10.1111/jzo.12463.

Forest, V. and Rodet-Belarbi, I. (2018) 'Loups et chiens au Néolithique et au Moyen Âge en France méditerranéenne', in Costamagno et al. (eds) *animal symbolisé - Animal exploité. Du Paléolithique à la Protohistoire*. (Actes des Congrès des sociétés historiques et scientifiques), pp. 198–206. Available at: https://hal.archives-ouvertes.fr/hal-02195997 (Accessed: 22 August 2020).

Fosse, P. (1988) *Zooarchéologie du renard en France du Mésolithique au Chalcolithique*. Mémoire de maîtrise. Université de Paris 1.

Fowler, C., Harding, J. and Hofmann, D. (2015) 'The Oxford Handbook of Neolithic Europe: an introduction', *The Oxford Handbook of Neolithic Europe*.

Frantz, L. A. F. *et al.* (2016) 'Genomic and archaeological evidence suggest a dual origin of domestic dogs', *Science*, 352(6290), pp. 1228–1231. doi: 10.1126/science.aaf3161.

Frati, F. *et al.* (1998) 'Quaternary radiation and genetic structure of the red fox Vulpes vulpes in the Mediterranean Basin, as revealed by allozymes and mitochondrial DNA', *Journal of Zoology*, 245(1), pp. 43–51. doi: 10.1111/j.1469-7998.1998.tb00070.x.

Freedman, A. H. *et al.* (2014) 'Genome Sequencing Highlights the Dynamic Early History of Dogs', *PLOS Genetics*, 10(1), p. e1004016. doi: 10.1371/journal.pgen.1004016.

Freedman, A. H. and Wayne, R. K. (2017) 'Deciphering the Origin of Dogs: From Fossils to Genomes', *Annual Review of Animal Biosciences*, 5(1), pp. 281–307. doi: 10.1146/annurev-animal-022114-110937.

Gandelin, M. (Dir.) (2015) *Autoroute A75 - Section Béziers – Pézenas. Hérault, Montblanc et Valros. Aire de Repos de Valros. Les occupations du Néolithique et du Bronze ancien.* Rapport final d'opération. Inrap Méditerranée. Service Régional de l'Archéologie de Languedoc-Roussillon, p. 4 volumes.

García-Moncó, C. (2005) 'El perro en la Prehistoria de la Península Ibéric', *Estudio crítico de la documentación arqueozoológica anterior al Calcolítico en su contexto euroasiático. Trabajo de Investigación de Tercer Ciclo. Universidad de Cantabria, Santander*.

Geddès, D. (1980) 'De la chasse au troupeau en Méditerranée occidentale. Les débuts de l'élevage dans le bassin de l'Aude', *Archives d'Ecologie Préhistorique Toulouse*, (5), pp. 1–145.

Geddes, D. (1984) 'La faune néolithique de Leucate-Corrège dans son contexte méditerranéen occidental. Perspectives économiques', *Leucate-Corrège, habitat noyé du Néolithique cardial*, pp. 235–249.

Geddès, D. (1993) 'La faune de l'abri de Dourgne: paléontologie et paléoéconomie', *Dourgne. Derniers chasseurs-collecteurs et premiers éleveurs de la Haute Vallée de l'Aude*, pp. 365–397.

Georjon, C. *et al.* (2007) *'Le Lagarel, Autoroute A 750', Saint-André-de-Sangonis (Hérault), 15/09/2004 - 15/01/2005.Question de vie et de mort sur les rives du Lagarel*. Rapport final d'opération. INRAP, SRA Languedoc-Roussillon.

Germond, G., Bizard, M. and Guinot, Y. (1987) 'Le tumulus A du Montiou à Sainte-Soline (Deux-Sèvres) Dolmens, inhumations, mobilier', *Bulletin de la Société préhistorique française*, pp. 139–154.

Germonpré, M. *et al.* (2013) 'Palaeolithic dogs and the early domestication of the wolf: a reply to the comments of', *Journal of Archaeological Science*, 40(1), pp. 786–792.

Germonpré, M. *et al.* (2015) 'Palaeolithic dogs and Pleistocene wolves revisited: a reply to', *Journal of Archaeological Science*, 54, pp. 210–216.

Germonpré, M. B. *et al.* (2019) 'Traditional Morphometric Evidence for the Beginning of the Dog Domestication Process during the Early Upper Palaeolithic', in *JOURNAL OF MORPHOLOGY*. WILEY 111 RIVER ST, HOBOKEN 07030-5774, NJ USA, pp. S5–S5.

Germonpré, M., Lázničková-Galetová, M. and Sablin, M. V. (2012) 'Palaeolithic dog skulls at the Gravettian Předmostí site, the Czech Republic', *Journal of Archaeological Science*, 39(1), pp. 184–202. doi: 10.1016/j.jas.2011.09.022.

Ghesquière, E. and Marchand, G. (2010) *Le Mésolithique en France*. La Découverte. (Archéologie de la France).

Gompper, M. E. (2014) 'The dog-human-wildlife interface: assessing the scope of the problem', *Free-ranging dogs and wildlife conservation*, pp. 9–54.

Goodall, C. (1991) 'Procrustes methods in the statistical analysis of shape', *Journal of the Royal Statistical Society: Series B (Methodological)*, 53(2), pp. 285–321.

Grandal-d'Anglade, A. *et al.* (2019) 'Dogs and foxes in Early-Middle Bronze Age funerary structures in the northeast of the Iberian Peninsula: human control of canid diet at the sites of Can Roqueta (Barcelona) and Minferri (Lleida)', *Archaeological and Anthropological Sciences*, 11(8), pp. 3949–3978. doi: 10.1007/s12520-019-00781-z.

Gröning, F. *et al.* (2013) 'The importance of accurate muscle modelling for biomechanical analyses: a case study with a lizard skull', *Journal of The Royal Society Interface*, 10(84), p. 20130216. doi: 10.1098/rsif.2013.0216.

Guilaine, J. (2003) *De la vague à la tombe. La conquête néolithiue de la Méditerrannée.* Seuil. Paris.

Guilbert, R. *et al.* (2003) *'Gramari', Méthamis (Vaucluse). Un gisement mésolithique de plein air.* Rapport de fouilles programmées. Conseil général de Vaucluse.

Guiry, E. J. (2012) 'Dogs as analogs in stable isotope-based human paleodietary reconstructions: a review and considerations for future use', *Journal of Archaeological Method and Theory*, 19(3), pp. 351–376.

Guthmann, É., Lefranc, P. and Arbogast, R.-M. (2016) 'Un dépôt de renard roux (Vulpes vulpes) du 4e Millénaire av. J.-C. à Entzheim « Les Terres de la Chapelle » (Bas-Rhin) : offrande ou sépulture animale ?', *Revue archéologique de l'Est*, (tome 65), pp. 257–268.

Haak, W. *et al.* (2015) 'Massive migration from the steppe was a source for Indo-European languages in Europe', *Nature*, 522(7555), pp. 207–211. doi: 10.1038/nature14317.

Hachem, L. (1987) *La faune de l'enceinte Michelsberg de Bazoches-sur-Vesle, le bois de Muisemont (Aisne): étude préliminaire*. Mémoire de DEA. Université Paris.

Hachem, L. (1989) 'La faune et l'industrie osseuse de l'enceinte Michelsberg de Maisy (Aisne): approche économique, spatiale et régionale', *Revue archéologique de Picardie*, 1–2, pp. 67–108.

Hachem, L. (1996) *La faune rubanée de Cuiry-les-Chaudardes (Aisne, France): essai sur la place de l'animal dans la première sociéte néolithique du bassin parisien*. Paris 1.

Hachem, L. (2009) *La faune du site Néolithique moyen de Pont-sur-Seine 'Ferme de l'Ile' (Aube)*. Rapport final d'opération. SRA Champagne-Ardennes.

Hachem, L. (2011) 'Les faunes du Néolithique moyen dans le nord de la France: bilan et pistes de recherches', *Revue archéologique de Picardie*, 28(1), pp. 313–329.

Hachem, Lamys *et al.* (2002) 'La faune du site Néolithique moyen de Maisons-Alfort "Zac d'Alfort" (Val-de-Marne)', in *Maisons Alfort ZAC d'Alfort (Val-de-Marne), sauvetages urgents 1998-2001, Document Final de Synthèse, Inrap, Saint-Denis, 2 vol.,*. Inrap. Saint-Denis (Maisons Alfort ZAC d'Alfort (Val-de-Marne), sauvetages urgents 1998-2001, Document Final de Synthèse), p. 133.

Haimovici, S. (1987) 'L'Étude de la faune découverte dans l'établissement mésolithique de Ostrovul Corbului (culture Schela Cladovei)', *Chirica V La genèse et l'évolution des cultures paléolithiques sur le territoire de la Roumania. Iasi: Bibliotheca Archaeologica Iassiensis II*, pp. 123–138.

Hainard, R. and Perrot, J. L. (1961) *Mammifères sauvages d'Europe: Précédes d'une partie générale de Jean-Louis Perrot*. Delachaux & Niestlé.

Hameau, H. *et al.* (1994) 'La Baume Saint-Michel Mazaugues (Var)', *Bulletin archéologique de Provence*, (23), pp. 3–42.

Harbers, H. *et al.* (in press) 'The mark of captivity: plastic responses in the ankle bone of a wild ungulate (Sus scrofa)', *Royal Society Open Science*.

Hartstone-Rose, A., Perry, J. M. G. and Morrow, C. J. (2012) 'Bite Force Estimation and the Fiber Architecture of Felid Masticatory Muscles', *The Anatomical Record*, 295(8), pp. 1336–1351. doi: 10.1002/ar.22518.

Hasler, A. *et al.* (2011) *Languedoc-Roussillon, Manduel, Gard: Fumérian, Zac multi-sites: occupations néolithiques et de l'Age du fer*. Rapport final d'opération. INRAP.

Hasler, A. and Noret, C. (2004) 'Habitats et structures funéraires néolithiques sur le tracé du cadereau d'Alès à Nîmes (Gard) : premiers résultats', in. *Paysages et peuplements. Aspects*

culturels et chronologiques en France méridionale. Actualité de la recherche. Available at: https://hal-inrap.archives-ouvertes.fr/hal-01472202 (Accessed: 10 August 2020).

Helmer, D. (1991b) 'Étude de la faune', *ROUDIL J.-L. & SAUMADE H.(éds), La Grotte de Combe Obscure à Lagorce, Ardèche. Chez les auteurs, Montpellier*, pp. 125–147.

Helmer, D. (1979) *Recherches sur l'économie alimentaire et l'origine des animaux domestiques d'aprés l'étude des mammifères post-paléolithiques (du Mésolithique à l'âge du Bronze) en Provence*. Université des Sciences et Techniques du Languedoc.

Helmer, D. (1991) 'La faune mammalienne', *Une économie de chasse au Néolithique ancien. La Grotte Lombard à Saint-Vallier-de-Thiey (Alpes-Maritimes). Ed. CNRS, Paris*, pp. 115–139.

Helmer, D. (1992) *La domestication des animaux par les hommes préhistoriques*. FeniXX.

Helmer, D. (2004) 'Un chantier archéologique à la loupe: Villa Giribaldi', in Binder, D. et al., *Catalogue d'exposition 23 octobre 2004-4 janvier 2005]*. Nice: Nice-Musées.

Hofmanová, Z. *et al.* (2016) 'Early farmers from across Europe directly descended from Neolithic Aegeans', *Proceedings of the National Academy of Sciences*, 113(25), pp. 6886–6891. doi: 10.1073/pnas.1523951113.

Horard-Herbin, M. P. and Vigne, J. D. (2005) *Prélèvement, échantillonnage, traitement et analyse des vestiges fauniques*. Errance.

Horard-Herbin, M.-P. (2000) 'Dog management and use in the late Iron age: The evidence from the Gallic site of Levroux, France', *BAR International Series*, 889, pp. 115–122.

Horard-Herbin, M.-P. (2014) 'La viande de chien à l'âge du Fer: Quels individus pour quelles consommations?', *Gallia*, pp. 69–87.

Horard-Herbin, M.-P., Tresset, A. and Vigne, J.-D. (2014) 'Domestication and uses of the dog in western Europe from the Paleolithic to the Iron Age', *Animal Frontiers*, 4(3), pp. 23–31. doi: 10.2527/af.2014-0018.

Hulme-Beaman, A. *et al.* (2016) 'An Ecological and Evolutionary Framework for Commensalism in Anthropogenic Environments', *Trends in Ecology & Evolution*, 31(8), pp. 633–645. doi: 10.1016/j.tree.2016.05.001.

Hüster-Plogmann, H. and Schibler, J. (1997) 'Archäozoologie', *Okonomie und Okologie neolithischer und bronzezeitlicher Ufersiedlungen am Zürichsee*, pp. 40–121.

Jallot, L. (2004) *Mas de Vignoles IV à Nîmes (Gard) : rapport de fouilles*. Rapport de fouilles. Nîmes: Inrap MED, p. 11 volumes.

Janssens, L. *et al.* (2019) 'An evaluation of classical morphologic and morphometric parameters reported to distinguish wolves and dogs', *Journal of Archaeological Science: Reports*, 23, pp. 501–533. doi: 10.1016/j.jasrep.2018.10.012.

Jeunesse, C. (2001) 'Les animaux dans les pratiques funéraires autochtones de la Préhistoire récente de l'Europe. Le cas du Mésolithique.'

Jeunesse, C., Boulestin, B. and Zeeb-Lanz, A. (2009) 'Cannibalisme de masse au Néolithique.'

Joachim, W. (1984) *Stuttgart-Münster*. Fundberichte aus Baden-Württemberg, pp. 603–608.

Kannegaard Nielsen, E. *et al.* (1993) 'Grave, mennesker og hunde', *Da klinger i muld*, 25, pp. 76–81.

Klaus Schmidt (2010) 'Göbekli Tepe – the Stone Age Sanctuaries. New results of ongoing excavations with a special focus on sculptures and high reliefs', *Documenta Praehistorica*, 37(0). doi: 10.4312/dp.37.21.

Klingenberg, C. P. (2014) 'Studying morphological integration and modularity at multiple levels: concepts and analysis', *Philosophical Transactions of the Royal Society B: Biological Sciences*, 369(1649), p. 20130249. doi: 10.1098/rstb.2013.0249.

Klingenberg, C. P. (2016) 'Size, shape, and form: concepts of allometry in geometric morphometrics', *Development Genes and Evolution*, 226(3), pp. 113–137. doi: 10.1007/s00427-016-0539-2.

Klingenberg, C. P. and Monteiro, L. R. (2005) 'Distances and Directions in Multidimensional Shape Spaces: Implications for Morphometric Applications', *Systematic Biology*, 54(4), pp. 678–688. doi: 10.1080/10635150590947258.

Koc, D., Dogan, A. and Bek, B. (2010) 'Bite Force and Influential Factors on Bite Force Measurements: A Literature Review', *European Journal of Dentistry*, 4(2), p. 223.

Kotova, N. S. (2003) *Neolithization in Ukraine*. British Archaeological Reports Ltd.

Koungoulos, L. and Fillios, M. (2020) 'Hunting dogs down under? On the Aboriginal use of tame dingoes in dietary game acquisition and its relevance to Australian prehistory', *Journal of Anthropological Archaeology*, 58, p. 101146. doi: 10.1016/j.jaa.2020.101146.

Kouvari, M., Herrel, A. and Cornette, R. (under review) 'Rapid functional morphological changes in the mandible of Suncus etruscus in historical times in Corsica: the impact of humans and climate', *Journal of Archaeological Science*.

Kovačiková, L. (2011) 'Archeozoologie neolitu Čech'.

Kratochvíl, Z. (1973) 'Der Fund von Equus (hydruntinus) hydruntinus (Regalia, 1907) und anderer Säuger aus dem südmährischen Neolithikum', *Slovenská archeológia*, 21(1), pp. 195–210.

Kruska, D. (1988) 'Effects of domestication on brain structure and behavior in mammals', *Human Evolution*, 3(6), pp. 473–485. doi: 10.1007/BF02436333.

Kuhnle, G. *et al.* (1999) 'Le site Michelsberg et Munzingen de Holtzheim (Bas-Rhin)', *Revue archéologique de l'Est et du centre-Est*, 50, pp. 3–51.

Kulczycka-Leciejewiczowa, A. and Romanow, J. (1985) 'Wczesnoneolityczne osiedla w Gniechowicach i Starym Zamku (Les habitats du début du Néolithique de Gniechowice et de Stary Zamek)', *Silesia Antiqua*, 27, pp. 9–68.

Lanchon, Y. *et al.* (2008) 'Le Néolithique ancien dans la basse vallée de la Marne: L'habitat de Changis-sur-Marne «les Pétreaux» (Seine-et-Marne)', *Revue Archéologique d'Île-de-France*, 1, pp. 43–94.

Larson, G. *et al.* (2012) 'Rethinking dog domestication by integrating genetics, archeology, and biogeography', *Proceedings of the National Academy of Sciences*, 109(23), p. 8878. doi: 10.1073/pnas.1203005109.

Larsson, L. (1990) 'Late Mesolithic settlements and cemeteries at Skateholm, southern Sweden', in *The Mesolithic in Europe. International Symposium. 3*, pp. 367–378.

Larsson, L. (1994) 'MORTUARY PRACTICES AND DOG GRAVES IN MESOLITHIC SOCIETIES OF SOUTHERN SCANDINAVIA', *ANTHROPOLOGIE*, 98(4), pp. 562–575.

Lazăr, C., Mărgărit, M. and Bălăşescu, A. (2016) 'Dogs, jaws, and other stories: Two symbolic objects made of dog mandibles from southeastern Europe', *Journal of Field Archaeology*, 41(1), pp. 101–117.

Le Bras-Goude, G. *et al.* (2006) 'Contribution des méthodes isotopiques pour l'étude de l'alimentation humaine au Néolithique moyen méridional: le cas du site Chasséen ancien du Crès (Béziers, Hérault, France)', *Antropo*, 11, pp. 167–75.

Le Bras-Goude, G., Herrscher, E. and Vaquer, J. (2013) 'Funeral practices and foodstuff behaviour: What does eat meat mean? Stable isotope analysis of Middle Neolithic populations in the Languedoc region (France)', *Journal of Anthropological Archaeology*, 32(3), pp. 280–287.

Leathlobhair, M. N. *et al.* (2018) 'The evolutionary history of dogs in the Americas', *Science*, 361(6397), pp. 81–85.

Lefranc, P. *et al.* (1998) 'L'habitat Rubané final de Westhouse Ziegelhof (Bas-Rhin).', *Cahiers de l'Association pour la promotion de la recherche archéologique en Alsace*, (14), pp. 5–43.

Lefranc, P. *et al.* (2015) 'Vendenheim (Bas-Rhin), Aux portes du Kochersberg', *Enceinte, habitats et systèmes de fentes néolithiques (Roessen, Bruebach-Oberbergen et Michelsberg) et camps d'entrainement romain*.

Lefranc, P., Arbogast, R. M. and Boës, E. (2007) 'L'habitat néolithique récent de Rosheim" Leimen"', *Cahiers alsaciens d'archeologie, d'art et d'histoire*, (50), pp. 11–26.

Lehnebach, C. (2003) *La grotte du Phare (Biarritz, Pyrénées atlantiques). Origine des assemblages fauniques du Néolithique récent/final au Premier Age du Fer. Etude archéozoologique.* Mémoire de Maîtrise. Université de Paris I, Panthéon-Sorbonne.

Lenneis, E. (1977) 'Siedlungsfunde aus Poigen und Frauenhofen bei Horn: Prähistorische Forschungen'.

Leonard, J. A. *et al.* (2007) 'Megafaunal extinctions and the disappearance of a specialized wolf ecomorph', *Current Biology*, 17(13), pp. 1146–1150.

Lepetz, S. (1996) 'Les animaux dans les pratiques funéraires', *Revue archéologique de Picardie*, 12(1), pp. 148–153.

Lequatre, P. (1994) ‘La faune des grands vertébrés’, *Gallia Préhistoire*, 36(1), pp. 197–204.

Leroi-Gourhan, A. and Bernot, L. (1988) *André Leroi-Gourhan: ou Les Voies de l’homme: actes du Colloque du CNRS, mars 1987*. Editions Albin Michel.

Lescureux, N. and Linnell, J. D. C. (2014) ‘Warring brothers: The complex interactions between wolves (Canis lupus) and dogs (Canis familiaris) in a conservation context’, *Biological Conservation*, 171, pp. 232–245. doi: 10.1016/j.biocon.2014.01.032.

Lichardus, J. and Lichardus-Itten, M. (1985) ‘Diffusion de la civilisation néolithique en Europe et évolution historico-culturelle jusqu’à la fin du Chalcolithique’, *La protohistoire de l’Europe: Le Néolithique et le Chalcolithique entre la Méditerranée et la mer Baltique*, pp. 207–515.

Lindblad-Toh, K. *et al.* (2005) ‘Genome sequence, comparative analysis and haplotype structure of the domestic dog’, *Nature*, 438(7069), pp. 803–19. doi: 10.1038/nature04338.

Loison, G., Fabre, V. and Villemeur, I. (2003) ‘Structures domestiques et aménagements funéraires sur le site chasséen du Crès à Béziers (Hérault)’, *Archéopages*, 10, pp. 33–9.

Loison, G. and Schmitt, A. (2009) ‘Diversité des pratiques funéraires et espaces sépulcraux sectorisés au Chasséen ancien sur le site du Crès à Béziers (Hérault). Croisements de données archéologiques et anthropologiques’, *Gallia Préhistoire*, 51(1), pp. 245–272.

Loog, L. *et al.* (2018) ‘Modern wolves trace their origin to a late Pleistocene expansion from Beringia’, *bioRxiv*, p. 370122. doi: 10.1101/370122.

Lord, K. A. *et al.* (2020) ‘The History of Farm Foxes Undermines the Animal Domestication Syndrome’, *Trends in Ecology & Evolution*, 35(2), pp. 125–136. doi: 10.1016/j.tree.2019.10.011.

Lorenzen, E. D. *et al.* (2011) ‘Species-specific responses of Late Quaternary megafauna to climate and humans’, *Nature*, 479(7373), pp. 359–364. doi: 10.1038/nature10574.

Louboutin, C., Burnez, C. and Braguier, S. (2003) ‘Authon-Ébéon, Le Chemin Saint-Jean (Charente-Maritime): une nouvelle enceinte Vienne-Charente en Centre-Ouest. Campagne de fouilles 2003’, *Antiquités nationales (Saint-Germain-en-Laye)*, (35), pp. 215–236.

Louwe Kooijmans, L. P. (2011) ‘Archeologie in de Betuweroute. Hardinxveld-Giessendam Polderweg. Een mesolithisch jachtkamp in het rivierengebied (5500-5000 v. Chr.)’. doi: 10.17026/DANS-ZPK-4G4A.

Macdonald, D. W. and Sillero-Zubiri, C. (2004) *The Biology and Conservation of Wild Canids*. OUP Oxford.

Maher, L. A. *et al.* (2011) ‘A Unique Human-Fox Burial from a Pre-Natufian Cemetery in the Levant (Jordan)’, *PLOS ONE*, 6(1), p. e15815. doi: 10.1371/journal.pone.0015815.

Mallye, J.-B. (2007) *Les restes de blaireau en contexte archéologique: taphonomie, archéozoologie et éléments de discussion des séquences préhistoriques*. Bordeaux 1.

Manen, A. (2005) *‘Le Taï’, Remoulins (Gard). Rapport intermédiaire 2005*. Rapport de fouilles programmées. AFAN, URA 1415.

Manen, C. *et al.* (2002) 'Nouvelles données sur le Néolithique ancien gardois: résultats des campagnes de fouille 2001-2002 de la grotte du Taï (Remoulins)', in.

Manen, C. *et al.* (2019) 'The Neolithic transition in the western Mediterranean: A complex and non-linear diffusion process—the radiocarbon record revisited', *Radiocarbon*, 61(2), pp. 531–571.

Maréchal, D. *et al.* (1998) 'II. Les parures du Néolithique final à Chalain et Clairvaux', *Gallia préhistoire*, 40(1), pp. 141–203.

Mărgărit, M., Boroneanț, A. and Bonsall, C. (2017) 'Analiza morfologică și funcțională a pieselor din materii dure animale din situl mezolitic de la Ostrovul Banului (jud. Mehedinți)(Morphological and functional analyze of animal hard substances finds from Ostrovul Banului Mesolithic site (Mehedinți County))', *Banatica*, 27(1).

Margarit, X., Durrenmath, G. and Gilabert, C. (2002) *'Ponteau-Gare', Martigues (Bouches-du-Rhône). Synthèse 2000-2001-2002*. Rapport de fouilles programmées. SRA PACA, UMR 6636.

Marinescu-Bîlcu, S. (2001) 'O civilizaţie necunoscută: Gumelniţa. Colecţia Patrimoniu Cultural'.

Marti-Grädel, E. and Stopp, B. (1997) 'Late Neolithic economy at lakeside settlements in Western Switzerland', *Anthropozoologica*, 25(26), pp. 495–504.

Martín Cólliga, A. *et al.* (2005) 'Indices miniers et métallurgie ancienne dans la Catalogne sub-pyrénéenne', *Mémoires de la Société préhistorique française*, 37, pp. 211–216.

Martin, L. *et al.* (2008) *'Chemin d'Aix', Saint-Maximin-la-Sainte-Baume (Var). Occupations du Chasséen réccent, Rhône-Ouvèze, premier âge du Fer et haut Moyen Age*. Rapport final d'opération. NRAP, SRA PACA.

Meixner, D. (2009) 'Ausnahme oder Regel–zum Phänomen der Münchshöfener bestattungen', *Vorträge des*, 27, pp. 91–144.

Meloro, C. *et al.* (2011) 'Phylogenetic signal, function and integration in the subunits of the carnivoran mandible', *Evolutionary Biology*, 38(4), pp. 465–475. doi: 10.1007/s11692-011-9135-6.

Méniel, P. (1984a) 'Contribution à l'histoire de l'élevage en Picardie. Du Néolithique à la fin de l'Age du Fer', *Revue archéologique de Picardie*, 3(1), pp. 1–56.

Méniel, P. (1984b) 'Les faunes rubanées de Berry-au-Bac et Menneville (Aisne)', *Revue archéologique de Picardie*, 1(1), pp. 87–93.

Méniel, P. (1984c) 'Les mammifères domestiques en Picardie du néolithique à l'Âge du fer. Annexes', *Revue archéologique de Picardie*, 3(1), pp. 1–177.

Méniel, P. (1987) 'Essai de reconstitution de la découpe des animaux du site néolithique de Boury–en-Vexin (Oise)', *Anthropozoologica*, (1), pp. 115–119.

Meunier, K., Sidéra, I. and Arbogast, R.-M. (2003) 'Rubané et groupe d'Entzheim à Pfulgriesheim" Langgarten" et" Buetzel"(Bas-Rhin)', *Bulletin de la Société préhistorique française*, pp. 267–292.

Micu, C. (2000) 'Aşezarea neoliticā de la Isaccea, punctul Suhat, jud. Tulcea', in *Istro-Pontica, Muzeul tulcean la a 50-a aniversare 1950-2000 (omagiu lui Simion Gavrilă la 45 de ani de activitate 1955-2000)*. Tulcea, pp. 5–53.

Miklósi, Á. (2014) *Dog behaviour, evolution, and cognition*. oUp Oxford.

Mitteroecker, P. *et al.* (2004) 'Comparison of cranial ontogenetic trajectories among great apes and humans', *Journal of Human Evolution*, 46(6), pp. 679–698. doi: 10.1016/j.jhevol.2004.03.006.

Mitteroecker, P. *et al.* (2013) 'A brief review of shape, form, and allometry in geometric morphometrics, with applications to human facial morphology', *Hystrix, the Italian Journal of Mammalogy*, 24(1), pp. 59–66. doi: 10.4404/hystrix-24.1-6369.

Mitteroecker, P. and Gunz, P. (2009) 'Advances in Geometric Morphometrics', *Evolutionary Biology*, 36(2), pp. 235–247. doi: 10.1007/s11692-009-9055-x.

Morel, P. *et al.* (1997) *Un campement magdalénien au bord du lac de Neuchâtel: étude archéozoologique (secteur 1)*. Musée cantonal d'archéologie.

Morey, D. F. (2006) 'Burying key evidence: the social bond between dogs and people', *Journal of Archaeological Science*, 33(2), pp. 158–175. doi: 10.1016/j.jas.2005.07.009.

Morey, D. F. (2014) 'In search of Paleolithic dogs: a quest with mixed results', *Journal of Archaeological Science*, 52, pp. 300–307.

Mosimann, J. E. (1970) 'Size allometry: size and shape variables with characterizations of the lognormal and generalized gamma distributions', *Journal of the American Statistical Association*, 65(330), pp. 930–945. doi: 10.1080/01621459.1970.10481136.

Mougne, C. (2006) *Etude archéozoologique du site de Roucadour du Néolithique final au premier âge du Fer*. Mémoire de Maîtrise.

Muller, A. *et al.* (1986) 'Le gisement de plein air chalcolithique de la Plaine-des-Blancs à Courthézon, Vaucluse', *Bulletin de la Société préhistorique française*, 83. doi: 10.3406/bspf.1986.8722.

Müller, H. (1964) 'Die Haustiere der mitteldeutschen Bandkeramiker.-Naturwiss', *Beiträge zur Vor-und Frühgeschichte I. Schriften der Sektion für Vor-und Frühgeschichte*, 17, p. 181.

NAV, N. A. V. (2017) 'The International Committee on Veterinary Gross Anatomical Nomenclature', *Published by the Editorial Committee Hannover (Germany), Columbia, MO (USA), Ghent (Belgium), Sapporo (Japan), 6th edition (Revised version)*.

Needham, A. E. (1950) 'The form-transformation of the abdomen of the female pea-crab, Pinnotheres pisum Leach', *Proceedings of the Royal Society of London. Series B - Biological Sciences*, 137(886), pp. 115–136. doi: 10.1098/rspb.1950.0027.

Ollivier, M. *et al.* (2013) 'Evidence of Coat Color Variation Sheds New Light on Ancient Canids', *PLOS ONE*, 8(10), p. e75110. doi: 10.1371/journal.pone.0075110.

Ollivier, M. *et al.* (2016) 'Amy2B copy number variation reveals starch diet adaptations in ancient European dogs', *Royal Society Open Science*, 3(11), p. 160449. doi: 10.1098/rsos.160449.

Ollivier, M. *et al.* (2018) 'Dogs accompanied humans during the Neolithic expansion into Europe', *Biology Letters*. doi: 10.1098/rsbl.2018.0286.

Onar, V., Belli, O. and Owen, P. R. (2005) 'Morphometric Examination of Red Fox (Vulpes vulpes) from the Van-Yoncatepe Necropolis in Eastern Anatolia', *International Journal of Morphology*, 23(3), pp. 253–260. doi: 10.4067/S0717-95022005000300011.

Osztás, A. *et al.* (2016) 'Coalescent community at Alsónyék: The timings and duration of Lengyel burials and setdement', *Bericht der Romisch-Germanischen Kommission*, 94, pp. 179–282.

Ott, M. *et al.* (2008) *'ZAC Saint-Antoine - tranche 3' Saint-Aunès (Hérault), 09/06/2008 - 23/06/2008*. Rapport de diagnostic archéologique. INRAP, SRA Languedoc-Roussillon.

Otte, M. (1984) *Les Fouilles de la place Saint-Lambert à Liège*. 18. Liège.

Ovodov, N. D. *et al.* (2011) 'A 33,000-year-old incipient dog from the Altai Mountains of Siberia: evidence of the earliest domestication disrupted by the Last Glacial Maximum', *PloS one*, 6(7), p. e22821.

Pang, J.-F. *et al.* (2009) 'mtDNA data indicate a single origin for dogs south of Yangtze River, less than 16,300 years ago, from numerous wolves', *Molecular biology and evolution*, 26(12), pp. 2849–2864.

Pearson, J. A. *et al.* (2015) 'Stable carbon and nitrogen isotope analysis and dietary reconstruction through the life course at Neolithic Çatalhöyük, Turkey', *Journal of Social Archaeology*, 15(2), pp. 210–232.

Pechenkina, E. A. *et al.* (2005) 'Reconstructing northern Chinese Neolithic subsistence practices by isotopic analysis', *Journal of archaeological Science*, 32(8), pp. 1176–1189.

Penrose, F. *et al.* (2020) 'Functional morphology of the jaw adductor muscles in the Canidae', *The Anatomical Record*, n/a(n/a). doi: 10.1002/ar.24391.

Penrose, F., Kemp, G. J. and Jeffery, N. (2016) 'Scaling and accommodation of jaw adductor muscles in Canidae', *The Anatomical Record*, 299(7), pp. 951–966. doi: 10.1002/ar.23355.

Péquart, M. *et al.* (1937) *Téviec, station-nécrolopole mésolithique du Morbihan*. Masson et Cie.

Perri, A. (2016) 'A wolf in dog's clothing: Initial dog domestication and Pleistocene wolf variation', *Journal of Archaeological Science*, 68, pp. 1–4. doi: 10.1016/j.jas.2016.02.003.

Perry, G. H. *et al.* (2007) 'Diet and the evolution of human amylase gene copy number variation', *Nature Genetics*, 39(10), pp. 1256–1260. doi: 10.1038/ng2123.

Peške, L. (1991) ‘Archeologický výzkum neolitického sídliště v Roztokách’, *Muzeum a současnost*, 10(2), pp. 271–293.

Pétrequin, P. *et al.* (1998) ‘Demographic growth, environmental changes and technical adaptations: responses of an agricultural community from the 32nd to the 30th centuries BC’, *World Archaeology*, 30(2), pp. 181–192.

Pétrequin, P. *et al.* (2002) ‘Le mythe de la stabilité: déséquilibres et réajustements d’une communauté agricole néolithique dans le Jura français, du 32ème au 30ème siècle av. J.-C’, in *ANNALES LITTERAIRES-UNIVERSITE DE BESANCON*. DIALOGUES D’HISTOIRE ANCIENNE, pp. 175–190.

Pilot, M. *et al.* (2010) ‘Phylogeographic history of grey wolves in Europe’, *BMC Evolutionary Biology*, 10, p. 104. doi: 10.1186/1471-2148-10-104.

Pilot, M. *et al.* (2019) ‘Global Phylogeographic and Admixture Patterns in Grey Wolves and Genetic Legacy of An Ancient Siberian Lineage’, *Scientific Reports*, 9(1), p. 17328. doi: 10.1038/s41598-019-53492-9.

Pionnier-Capitan, M. (2010) *La domestication du chien en Eurasie: étude de la diversité passée, approches ostéoarchéologiques, morphométriques et paléogénétiques*. Lyon, Ecole normale supérieure.

Pionnier-Capitan, M. *et al.* (2011) ‘New evidence for Upper Palaeolithic small domestic dogs in South-Western Europe’, *Journal of Archaeological Science*, 38(9), pp. 2123–2140. doi: 10.1016/j.jas.2011.02.028.

Pires, A. E. *et al.* (2019) ‘The curious case of the Mesolithic Iberian dogs: An archaeogenetic study’, *Journal of Archaeological Science*, 105, pp. 116–129. doi: 10.1016/j.jas.2019.03.002.

Poplin, F. (1975) ‘La faune danubienne d’Armeau (Yonne, France): ses données sur l’activité humaine’, *Archaeozoological studies*, pp. 179–192.

Poulain, T. (1964) ‘Appendice I. Abri tardenoisien de la Chambre des Fées Coincy (Aisne). Étude de la faune’, *Gallia Préhistoire*, 7(1), pp. 93–94. doi: 10.3406/galip.1964.2186.

Poulain, T. (1971) ‘Etude des vestiges osseux de la grotte" C" de Baudinard (Var)’, *Bulletin de la Société préhistorique française. Études et travaux*, 68(Fasc. 2), pp. 562–566.

Poulain, T. (1972) ‘Le site archéologique du dolmen de Villaine à Sublaines (Indre-et-Loire). Première partie (Néolithique, Âge du Bronze). IV : étude de la faune’, *Gallia Préhistoire*, 15(1), pp. 131–135.

Poulain, T. (1974) ‘L’habitat campaniforme de Saint-Côme-et-Maruejols (Gard)(suite). II. Étude de la faune’, *Gallia préhistoire*, 17(1), pp. 215–217.

Poulain, Thérèse (1979) ‘Dolmen de Pierre-Levée Nieul-sur-l’Autize (Vendée)’, *Bulletin de la Société préhistorique française*, pp. 157–160.

Poulain, T. (1979) ‘Etude de la faune de l’abri Jean Cros’, *L’abri Jean Cros, essai d’approche d’un groupe humain du Néolithique ancien dans son environnement. Toulouse: CNRS*, pp. 291–306.

Poulain, T. (1984a) ‘A study of the fauna in the deposit at Rouffach-Gallbuhl (Haut-Rhin)’, *Revue archéologique de l’est et du centre-est*, 35(1–2), pp. 34–39.

Poulain, T. (1984b) ‘La domestication des animaux en France à l’époque Néolithique’, *Die Anfänge des Neolithikums IX vom Orient bis Nordeuropa. Der Beginn der Haustierhaltung in der “Alten Welt”. Böhlau, Köln*.

Poulain, T. (1984c) ‘Le camp chasséen du mont d’Huette à Jonquières (Oise). IV. La faune’, in. *Actes du colloque inter-régional sur le Néolithique du Nord de la France.*, Revue Archéologique de Picardie, pp. 257–264.

Poulain, T. (1985) ‘La faune’, in Rodriguez, F., *La grotte de Camprafaud*. Fédération archéologique de l’Hérault. Montpellier, pp. 251–356.

Poulain, T. (1989) ‘La faune ; Annexe 3.’, *Revue Archéologique de l’Est et du Centre-Est*, 40(1), pp. 39–45.

Poulain, Thérèse (1992) ‘La faune de l’Abri du Roc Troué (Sainte-Eulalie-de-Cernon, Aveyron)’, *Bulletin de la Société préhistorique française*, 89(7), pp. 219–223.

Poulain, T (1992) ‘La faune du camp de la Vergentière (fouilles de 1976 à 1985)’, in *La Vergentière (camp et nécropole) à Cohons (Haute-Marne) du Néolithique moyen au Bronze final, Langres*. Société archéologique champenoise (Mémoire 6), pp. 285–306.

Poulain, T. (2003a) ‘Etude de la faune, Châtelet-d’Étaules’, in *L’habitat fortifié pré- et protohistorique en Côte- d’Or : les camps de Myard à Vitteaux et du Châtelet-d’Étaules dans le contexte archéologique régional (du V e millénaire au IV e siècle avant J.-C.), Dijon*. Société archéologique de l’Est (Revue archéologique de l’Est supplément 19), pp. 223–234.

Poulain, T. (2003b) ‘Étude de la faune, camp de Myard’, in *L’habitat fortifié pré- et protohistorique en Côte-d’Or : les camps de Myard à Vitteaux et du Châtelet-d’Étaules dans le contexte archéologique régional (du V e millénaire au IV e siècle avant J.-C.), Dijon*. Société archéologique de l’Est (Revue archéologique de l’Est sup-plément 19), pp. 213–222.

Poulain, T. (2005) ‘La faune des niveaux néolithiques de la Redoute au camp de Chassey’, in *Le camp de Chassey (Chassey- le-Camp, Saône et Loire) : les niveaux néolithiques du camp de la Redoute, Dijon*. Éd. Société archéologique de l’Est (Revue archéologique de l’Est supplément 22), pp. 387–413.

Poulain, T., Thévenin, A. and Sainty, J. (1979) ‘Etude de la faune’, in *Nouveaux sites rubanés et données récentes sur la séquence chronologique Néolithique ancien-Néolithique moyen dans le Bas-Rhin. Le rubané d’Alsace et de Lorraine, Etat de la recherche.*

Poulain-Josien, T. (1957) ‘Etude de la Faune des stations chalcolithiques de Gimel et de la Paillade: Commune de Grabels (Hérault)’, *Bulletin de la Société préhistorique de France*, pp. 757–762.

Poulain-Josien, Thérèse (1965a) ‘Etude de la faune du gisement de Soubérac Gensac-la-Pallue (Charente)’, *Bulletin de la Société préhistorique française. Études et travaux*, 62(Fasc. 2), pp. 316–327.

Poulain-Josien, T (1965) ‘Gisement de Beaussement. Etude de la faune’, *Cahiers Rhodaniens*, pp. 33–40.

Poulain-Josien, Thérèse (1965b) ‘L’ossuaire néolithique d’Eteauville, commune de Lutz-en-Dunois (Eure et Loir). VI : Etude de la faune.’, *Bulletin de la Société Préhistorique Française*, 63(3), pp. 576–648.

Poulain-Josien, T. (1966) ‘Etude de la faune du gisement Néolitique de Matignons’, *Commune de Juillac-le-Coq (Charente). Gallia(préhist.)*, 9, pp. 210–241.

Poulain-Josien, T. (1972) ‘L’abri sous roche de Saint-Etienne-de-Gourgas (Hérault)’, *Gallia Préhistoire*, 15(2), pp. 309–322.

Poulain-Josien, T. (1978) ‘Le site néolithique de Reichstett (Bas Rhin). Etude de la faune.’, *Revue Archéologique de l’Est et du Centre Est*, 1–2(29), pp. 45–46.

Pucher, E. (1998) ‘Die Tierknochen des linearbandkeramischen Siedlungsplatzes Brunn am Gebirge (Niederösterreich)’, *Man and the Animal World. Studies in Archaeozoology, Archaeology, Anthropology and Palaeolinguistics in memoriam Sándor Bökönyi*, pp. 465–479.

Remicourt, M. *et al.* (2012) ‘Les occupations pré et protohistoriques du Clos de Roque, a Saint-Maximin-la-Sainte-Baume (Var)’.

Remicourt, M. *et al.* (2014) ‘Les occupations pré- et protohistoriques du Clos de Roque à Saint-Maximin-la-Sainte-Baume dans le Var’, in *Chronologie de la Préhistoire récente dans le Sud de la France. Acquis 1992-2012. Actualité de la recherche. Actes des 10e Rencontres Méridionales de Préhistoire Récente*. Archives d’Écologie Préhistorique, p. 523. Available at: https://archive-ouverte.unige.ch/unige:40877 (Accessed: 5 October 2020).

Renaud, S., Auffray, J.-C. and de la Porte, S. (2010) ‘Epigenetic effects on the mouse mandible: common features and discrepancies in remodeling due to muscular dystrophy and response to food consistency’, *BMC Evolutionary Biology*, 10, p. 28. doi: 10.1186/1471-2148-10-28.

Rillardon, M. (2010) *Environnement et subsistance des derniers chasseurs-cueilleurs dans la basse vallée du Rhône et ses marges du Pléniglaciaire supérieur (20 ka BP) à l’Optimum climatique (8 Ka BP)*.

Rivière, J. (2006) *Approche archéozoologique des occupations du Mésolithique moyen et final des Escabasses (Thémines, Lot). Campagnes 1993-2002*. Mémoire de master.

Rodriguez, G. (1984) ‘La grotte de Camprafaud: contribution à l’étude du Néolithique en Languedoc central, Montpellier’, *Office régional de la culture du Languedoc-Roussillon*.

Rohlf, F. J. and Corti, M. (2000) ‘Use of two-block partial least-squares to study covariation in shape’, *Systematic Biology*, 49(4), pp. 740–753. doi: 10.1080/106351500750049806.

Rozoy, J.-G. (1978) *Les derniers chasseurs: l’Epipaléolithique en France et en Belgique: essai de synthèse*. J.-G. Rozoy.

Ruttkay, E. (1971) ‘Neolithische und bronzezeitliche Siedlungsreste in Schwechat, pB Wien-Umgebung, NÖ’, *Archaeologia Austriaca*, 50, pp. 21–67.

Sablin, M. V. and Khlopachev, G. A. (2002) 'The Earliest Ice Age Dogs: Evidence from Eliseevichi 1', *Current Anthropology*, 43(5), pp. 795–799. doi: 10.1086/344372.

Saetre, P. *et al.* (2004) 'From wild wolf to domestic dog: gene expression changes in the brain', *Molecular brain research*, 126(2), pp. 198–206.

Salanova, L. (2007) 'Bury–Saint-Claude, 202 rue de la Plaine', *ADLFI. Archéologie de la France-Informations. une revue Gallia*.

Salanova, L. *et al.* (2017) 'From one ritual to another: the long-term sequence of the Bury gallery grave (northern France, fourth–second millennia BC)', *Antiquity*, 91(355), pp. 57–73. doi: 10.15184/aqy.2016.256.

San, E. D. L. (2002) 'Socialité, territorialité et dispersion chez le blaireau européen (Meles meles): état des connaissances, hypothèses et besoins de recherche', in *L'étude et la conservation des carnivores*. Société Française pour l'Etude et la Protection des Mammifères Paris, pp. 74–86.

Santana, S. E. (2016) 'Quantifying the effect of gape and morphology on bite force: biomechanical modelling and in vivo measurements in bats', *Functional ecology*, 30(4), pp. 557–565.

Savolainen, P. *et al.* (2002) 'Genetic evidence for an East Asian origin of domestic dogs', *Science*, 298(5598), pp. 1610–1613.

Savolainen, P. *et al.* (2004) 'A detailed picture of the origin of the Australian dingo, obtained from the study of mitochondrial DNA', *Proceedings of the National Academy of Sciences*, 101(33), pp. 12387–12390.

Schibler, J. (1981) *Die neolithischen Ufersiedlungen von Twann. Band 17: Typologische Untersuchungen der cortaillodzeitlichen Knochenartefakte*. Staatlicher Lehrmittelverlag Bern 1981.

Schibler, J. and Suter, P. J. (1990) 'Archäozoologische Ergebnisse datierter neolithischer Ufersiedlungen des schweizerischen Mittellandes', *Festschrift für Hans R. Stampfli*, pp. 205–240.

Schietzel, K. and Stampfli, H. (1965) 'Müddersheim, eine Ansiedlung der jüngeren Bandkeramik', *Rheinland, Böhlau Verlag Köln Graz*.

Schmitzberger, M. (2010) *Die linearbandkeramische Fauna von Mold bei Horn, Niederösterreich*. na.

Schulting, R. J. and Richards, M. P. (2001) 'Dating Women and Becoming Farmers: New Palaeodietary and AMS Dating Evidence from the Breton Mesolithic Cemeteries of Téviec and Hoëdic', *Journal of Anthropological Archaeology*, 20(3), pp. 314–344. doi: 10.1006/jaar.2000.0370.

Séara, F., Rotillon, S. and Cupillard, C. (2002) *Campements mésolithiques en Bresse jurassienne: Choisey et Ruffey-sur-Seille*.

Segura, V. *et al.* (2020) 'Integration or Modularity in the Mandible of Canids (Carnivora: Canidae): a Geometric Morphometric Approach', *Journal of Mammalian Evolution*. doi: 10.1007/s10914-020-09502-z.

Seidel, U. *et al.* (2008) *Michelsberger Erdwerke im Raum Heilbronn: Neckarsulm-Obereisesheim" Hetzenberg", Ilsfeld" Ebene", Landkreis Heilbronn und Heilbronn-Klingenberg" Schlossberg", Stadtkreis Heilbronn. Bd 3, Osteologische Beiträge*. Theiss.

Shipman, P. (2015a) 'How do you kill 86 mammoths? Taphonomic investigations of mammoth megasites', *Quaternary International*, 359, pp. 38–46.

Shipman, P. (2015b) *The invaders: how humans and their dogs drove Neanderthals to extinction*. Harvard University Press.

Šiška, S. (1989) 'Kultúra s východnou lineárnou keramikou na Slovensku (The Eastern Linear Pottery Culture in Slovakia)', *Bratislava, Veda*, 189.

Skoglund, P. *et al.* (2015) 'Ancient wolf genome reveals an early divergence of domestic dog ancestors and admixture into high-latitude breeds', *Current Biology*, 25(11), pp. 1515–1519.

Slater, Gj., Dumont, E. and Van Valkenburgh, B. (2009) 'Implications of predatory specialization for cranial form and function in canids', *Journal of Zoology*, 278(3), pp. 181–188.

Sobociński, M. (1981) 'Szczątki kostne zwierzęce z osady neolitycznej w Łagiewnikach', *Roczniki Akademii Rolniczej w Poznaniu*, 131, pp. 75–95.

Sobocinski, M. (1984) 'Zwierzece szczatki kostne z obiektow kultury ceramiki wstegowel rytej w Zalecinie i Zukowie, wojewodztwo Szczecinskie', *Roczniki Akademii Rolniczej w Poznaniu*, 154, pp. 87–99.

Sobocinski, M. (1985) 'Szczatki kostne zwierzat z osady Ludnosci w Lagiewnikach', *Roczniki Akademii Rolniczej w Poznaniu*, 131, pp. 75–93.

Sommer, R. and Benecke, N. (2005) 'Late-Pleistocene and early Holocene history of the canid fauna of Europe (Canidae)', *Mammalian Biology*, 70(4), pp. 227–241. doi: 10.1016/j.mambio.2004.12.001.

Statham, M. J. *et al.* (2012) 'The origin of recently established red fox populations in the United States: translocations or natural range expansions?', *Journal of Mammalogy*, 93(1), pp. 52–65. doi: 10.1644/11-MAMM-A-033.1.

Stöckli, W. E. (2018) *Twann. Ausgrabungen 1974–1976, Auswertungen 1976–1982, Schlussbericht von 1981/82, Kommentar von 2017*. Erziehungsdirektion des Kantons Bern, Archäologischer Dienst des Kantons Bern.

Stork, M. (1993) 'Tierknochenfunde aus neolithischen Gruben in der Gemeinde Ammerbuch, Kr. Tubingen', *Zeitschrift für Archäologie*, 27(1993), pp. 91–104.

Studer, T. (1901) *Die praehistorischen Hunde in ihrer Beziehung zu den gegenwärtig lebenden'Rassen*. Druck von Zürcher and Furrer.

Tchérémissinoff, Y. *et al.* (2005) 'Les sépultures chasséennes du site de Narbons Montesquieu-de-Lauragais (Haute-Garonne)', *Bulletin de la Société préhistorique française*, 97(4), pp. 663–665.

Tchernov, E. and Valla, F. F. (1997) 'Two new dogs, and other Natufian dogs, from the southern Levant', *Journal of Archaeological Science*, 24(1), pp. 65–95.

Teichert, M. (1987) 'Brachymel dogs', *Archaeozoologia*, 1(1), pp. 69–75.

Thalmann, O. *et al.* (2013) 'Complete mitochondrial genomes of ancient canids suggest a European origin of domestic dogs', *Science (New York, N.Y.)*, 342(6160), pp. 871–874. doi: 10.1126/science.1243650.

Thévenin, A. (1981) 'Lorraine', *Gallia Préhistoire*, 24(2), pp. 477–499.

Thévenin, A., Sainty, J. and Poulain, T. (1977) 'Fosses et sépultures Michelsberg, sablière Maetz à Rosheim (Bas-Rhin)', *Bulletin de la Société préhistorique française*, 74(2), pp. 608–621. doi: 10.3406/bspf.1977.8470.

Tornero, C. *et al.* (2020) 'Early evidence of sheep lambing de-seasoning in the Western Mediterranean in the sixth millennium BCE', *Scientific Reports*, 10(1), p. 12798. doi: 10.1038/s41598-020-69576-w.

Tresset, A. (1996b) *Le rôle des relations homme/animal dans l'évolution économique et culturelle des sociétés des Ve-IVe millénaires en Bassin Parisien : approche ethno-zootechnique fondée sur les ossements animaux*, *http://www.theses.fr*. Paris 1. Available at: http://www.theses.fr/1996PA010638 (Accessed: 11 October 2020).

Tresset, A. (1988) 'La faune néolithique de Noyen-sur-Seine', *Anthropozoologica*, (8), pp. 12–14.

Tresset, A. (1996) *Quelques aspects de l'approvisionnement carné en contexte Chasséen septentrionnal à Bercy*. Unpublished report. SRA Ile de France.

Tresset, A. (2005) 'Élevage, chasse et alimentation carnée', in *Un site néolithique moyen en zone humide : Louviers-la Villette (Eure), Rennes*. Association pour la diffusion des recherches archéo-logiques dans l'ouest de la France (Documents archéologiques de l'Ouest). [" Revue archéologique de l'Ouest"], pp. 249–262.

Tresset, A. and Vigne, J. (2011) 'Last hunter-gatherers and first farmers of Europe', *Comptes rendus biologies*, 334(3), pp. 182–189.

Trut, L. (1999) 'Early Canid Domestication: The Farm-Fox Experiment: Foxes bred for tamability in a 40-year experiment exhibit remarkable transformations that suggest an interplay between behavioral genetics and development', *American Scientist*, 87(2), pp. 160–169.

Trut, L. N., Plyusnina, I. Z. and Oskina, I. N. (2004) 'An experiment on fox domestication and debatable issues of evolution of the dog', *Russian Journal of Genetics*, 40(6), pp. 644–655.

Trut, L., Oskina, I. and Kharlamova, A. (2009) 'Animal evolution during domestication: the domesticated fox as a model', *Bioessays*, 31(3), pp. 349–360. doi: 10.1002/bies.200800070.

Trut, L., Oskina, I. N. and Kharlamova, A. V. (2012) 'Experimental studies of early canid domestication', *The Genetic of the Dog/Eds EA Ostrander, A. Ruvinsky. 2nd ed. CAB International*, pp. 12–37.

Uerpmann, M. (2001) *Animaux sauvages et domestiques du Rubané "le plus ancien"(LBK 1) en Allemagne*. na.

Valdeyron, N. (1998) 'Le gisement de la grotte des Escabasses à Thémines (Lot) et la séquence Mésolithique en Aquitaine', in. *Les derniers chasseurs-cueilleurs d'Europe occidentale (13000–5500 av. J.-C.). Actes du colloque international de Besançon*, pp. 151–159.

Van Valkenburgh, B. (1989) 'Carnivore dental adaptations and diet: a study of trophic diversity within guilds', in *Carnivore behavior, ecology, and evolution*. Springer, pp. 410–436.

Van Valkenburgh, B. and Koepfli, K. (1993) 'Cranial and dental adaptations to predation in canids', in. *Symposium of the Zoological Society of London*, pp. 15–37.

Vaquer, J. (1998) 'Les sépultures du Néolithique moyen en France méditerranéenne', *Sépultures d'occident et genèse des magalithismes (9500–3500). Errance, Paris*, pp. 167–186.

Vaquer, J. and Gandelin, M. (2018) 'Auriac à Carcassonne (Aude). Une enceinte du Chasséen méridional', in Gandelin, M. (Dir.), *Les sites ceinturés de la Préhistoire récente*. Toulouse (Archives d'Ecologie Préhistorique), pp. 33–54.

Vaquer, J. and Remicourt, M. (2010) 'Rythmes et modalité s d'ap-provisionnement en silex blond bédoulien dans le Chassé en du bassin de l'Aude. Le cas d'Auriac, Carcassonne (Aude)', *É conomie et socié té à la fin de la Préhistoire. Lyon: ALPARAA, Publications de la Maison de l'Orient et de la Mé diterrané e (DARA 34)*, pp. 39–56.

Verjux, C. (2004) 'Sépultures mésolithiques de France et d'Europe', *Cahier des thèmes transversaux ArScAn*, IV, pp. 107–118.

Vignaud, A. (2003) 'Les Jardins de Vert Parc (Castelnau-le-Lez, Hérault): un habitat néolithique moyen de culture chasséenne', in *Temps et espaces culturels: du 6e au 2e millénaire en France du Sud, actes des rencontres méridionales de Préhistoire récente (Nîmes, 2000)*. ADAL Lattes, pp. 397–400.

Vigne, J. D. (2007) 'Exploitation des animaux et néolithisation en Méditerranée nord-occidentale', *Pont de Roque-Haute (Portiragnes, Hérault). Nouveaux regards sur la néolithisation de la France méditerranéenne*, pp. 181–214.

Vigne, J.-D. (1988) *Les mammifères post-glaciaires de Corse. Étude archéozoologique*, *Gallia Préhistoire*. Paris: CNRS (Gallia Préhistoire). Available at: https://www.persee.fr/doc/galip_0072-0100_1988_sup_26_1 (Accessed: 30 September 2020).

Vigne, J.-D. *et al.* (2004) 'Early taming of the cat in Cyprus', *Science*, 304(5668), pp. 259–259.

Vigne, J.-D. (2005) 'L'humérus de chien magdalénien de Erralla (Gipuzkoa, Espagne) et la domestication tardiglaciaire du loup en Europe', *Munibe*, 51, pp. 279–287.

Vigne, J.-D. (2011) 'The origins of animal domestication and husbandry: a major change in the history of humanity and the biosphere', *Comptes rendus biologies*, 334(3), pp. 171–181.

Vigne, J.-D. (2012) *Les débuts de l'élevage*. Le Pommier.

Vigne, J.-D. and Guilaine, J. (2004) 'Les premiers animaux de compagnie, 8500 ans avant notre ère ? ou comment j'ai mangé mon chat, mon chien et mon renard', *Anthropozoologica*, 39(1), pp. 249–273.

Vigne, J.-D. and Marinval-Vigne, M.-C. (1983) 'Méthode pour la mise en évidence de la consommation du petit gibier', *Animals and archaeology*, 1, pp. 239–242.

Vigne, J.-D. and Marinval-Vigne, M.-C. (1988) 'Quelques réflexions préliminaires sur les Canidés mésolithiques de Noyen-sur-Seine (France) et sur la domestication du Chien en Europe occidentale', *Archaeozoologica II (1e2), 153e164*.

Vilà, C. *et al.* (1997) 'Multiple and ancient origins of the domestic dog', *Science*, 276(5319), pp. 1687–1689.

Villalba, M. J. (1999) 'Las sepulturas neolíticas del complejo de Can Tintorer y el modelo social de la población minera', *Revista d'arqueologia de Ponent*, (9), pp. 41–73.

Voinea, V. and Neagu, G. (2008) 'Archaeological research at Hamangia III settlement from Cheia (2004-2008)', *Pontica (Constanţa)*, 41, pp. 9–34.

Von den Driesch, A. (1976) *A guide to the measurement of animal bones from archaeological sites: as developed by the Inst. für Palaeoanatomie, Domestikationsforschung u. Geschichte d. Tiermedizin of the Univ. of Munich*. Peabody Museum Press.

Vonholdt, B. M. *et al.* (2010) 'Genome-wide SNP and haplotype analyses reveal a rich history underlying dog domestication', *Nature*, 464(7290), pp. 898–902. doi: 10.1038/nature08837.

Vretemark, M. and Sten, S. (2010) 'Skeletal manipulations of dogs at the Bronze Age site of Százhalombatta-Földvár in Hungary'.

Wang, G. *et al.* (2013) 'The genomics of selection in dogs and the parallel evolution between dogs and humans', *Nature communications*, 4(1), pp. 1–9.

Wang, G.-D. *et al.* (2016) 'Out of southern East Asia: the natural history of domestic dogs across the world', *Cell research*, 26(1), pp. 21–33.

Wang, X. *et al.* (2004) 'Evolutionary history, molecular systematics, and evolutionary ecology of Canidae', *Biology and conservation of wild canids (DW Macdonald and C. Sillero-Zubiri, eds.). Oxford University Press, Oxford, United Kingdom*, pp. 39–54.

Wang, X., Tedford, R. H. and Antón, M. (2010) *Dogs: their fossil relatives and evolutionary history*. New York: Columbia University Press.

Wayne, R. K. (1986) 'Cranial Morphology of Domestic and Wild Canids: The Influence of Development on Morphological Change', *Evolution*, 40(2), pp. 243–261. doi: 10.1111/j.1558-5646.1986.tb00467.x.

Wayne, R. K., Benveniste, R. E. and O'Brien, S. J. (1989) 'Phylogeny and evolution of the Carnivora and carnivore families (pp 465–494)', *Carnivore behavior, ecology and evolution. Cornell University Press, Ithaca, NY*.

Willcox, G. (2013) ‘The roots of cultivation in southwestern Asia’, *Science*, 341(6141), pp. 39–40.

Wolff, P. (1980) ‘Das Tierknochenmaterial von Pulkau’, *TRNKA, G.: Siedlungsreste der jüngeren Linienbandkeramik aus Pulkau, p. B. Hollabrunn, Niederösterreich.–Archaeologia Austriaca*, 64, pp. 106–107.

Yu, G. *et al.* (2017) ‘ggtree: an r package for visualization and annotation of phylogenetic trees with their covariates and other associated data’, *Methods in Ecology and Evolution*, 8(1), pp. 28–36. doi: 10.1111/2041-210X.12628.

Zalai-Gaál, I. *et al.* (2011) ‘Ins Jenseits Begleitend“: Hundemitbestattungen der Lengyel-Kultur von Alsónyék-Bátaszék’, *Acta Archaeologica*, 62, pp. 29–74. doi: 10.1556/AArch.62.2011.1.2.

Zeder, M. A. (2008) ‘Domestication and early agriculture in the Mediterranean Basin: Origins, diffusion, and impact’, *Proceedings of the national Academy of Sciences*, 105(33), pp. 11597–11604.

Zeder, M. A. (2012) ‘Pathways to animal domestication’, *Biodiversity in agriculture: domestication, evolution, and sustainability*, pp. 227–259.

Zeeb-Lanz, A. *et al.* (2009) ‘The Lbk settlement with pit enclosure at Herxheim near Landau (Palatinate)–first results’, *Creating communities: new advances in central European Neolithic research*, pp. 202–19.

Zeuner, F. E. (1963) *A History of Domesticated Animals*. Hutchinson.

Ziegler, R. (1985) ‘Neolithische Tierreste aus Straubing-Lerchenhaid (Niederbayern)’, *Bericht der Bayerischen Bodendenkmalpflege*, (26–27), pp. 7–32.

Zrzavý, J. *et al.* (2018) ‘Phylogeny of the Caninae (Carnivora): Combining morphology, behaviour, genes and fossils’, *Zoologica Scripta*, 47(4), pp. 373–389. doi: 10.1111/zsc.12293.

List of the Figures

List of the Tables

Index

Appendices

1. Part 2 – script to calculate the bite force from dissection data

```
######### Fonction to calculate the bite force, for given gape angles, attachment
area coordinates and PCSAs
BFcanid <- function ( angle_ouv, coordarray, pcsa ) {
```

Coordarray has this form:

			x	y	z
1	O	Centre of rotation			
2	DIG_o	Origin on the cranium of the M. digastricus			
3	DIG_i	Insertion on the mandible of M. digastricus			
4	MS_o	Origin on the cranium of the M. masseter pars superficialis			
5	MS_i	Insertion on the mandible of M. masseter pars superficialis			
6	MP_o	Origin on the cranium of the M. masseter pars profunda			
7	MP_i	Insertion on the mandible of M. masseter pars profunda			
8	ZA_o	Origin on the cranium of the M. zygomaticomandibularis anterior			
9	ZA_i	Insertion on the mandible of M. zygomaticomandibularis anterior			
10	ZP_o	Origin on the cranium of the M. zygomaticomandibularis posterior			
11	ZP_i	Insertion on the mandible of M. zygomaticomandibularis posterior			
12	SZ_o	Origin on the cranium of the M. temporalis pars suprazygomatica	3D Coordinates in centimeters		
13	SZ_i	Insertion on the mandible of M. temporalis pars suprazygomatica			
14	TS_o	Origin on the cranium of the M. temporalis pars superficialis			
15	TS_i	Insertion on the mandible of M. temporalis pars superficialis			
16	TP_o	Origin on the cranium of the M. temporalis pars profunda			
17	TP_i	Insertion on the mandible of M. temporalis pars profunda			
18	PM_o	Origin on the cranium of the M. pterygoideus pars medialis			
19	PM_i	Insertion on the mandible of M. temporalis pars medialis			
20	I	Bite point at the incisor teeth			
21	C	Bite point at the canine tooth			
22	M1	Bite point at the lower carnassial (M1) tooth			

And PCSA has this form:

	Individual 1	Individual 2	Individual 3
Dig			
MS			
MP			
ZA			
ZP		PCSA in N.cm^{-2}	
TS			
TP			
P			

```
  force<-pcsa*30
  BF <- list()
  # Conversion of mouth opening angles in negative values
angle_ouv[angle_ouv==abs(angle_ouv)] <- -angle_ouv[angle_ouv==abs(angle_ouv)]

  for (k in 1 : length(angle_ouv)) {
    # coordinates after mouth opening with an angle of "angle_ouv"

    coordouv <- array(data=NA, dim=dim(coordarray))
    dimnames(coordouv)=dimnames(coordarray)
    coordouv_o <- coordarray[c(4,6,8,10,12,14,16,18),,]
    coordouv_i <- coordarray[c(5,7,9,11,13,15,17,19),,]
    coordouv_bp <- coordarray[c(20:22),,]

    for (i in 1: dim(coordarray)[3])  {
      x_ouv <- cos(deg2rad(angle_ouv[k]))*coordouv_i[,1,i]-
sin(deg2rad(angle_ouv[k]))*coordouv_i[,2,i]
```

```
      y_ouv <-
sin(deg2rad(angle_ouv[k]))*coordouv_i[,1,i]+cos(deg2rad(angle_ouv[k]))*coordouv_i[
,2,i]
      z_ouv <- coordouv_i[,3,i]
      coordouv_i[,,i] <-cbind(x_ouv,y_ouv,z_ouv)

      x_ouv_bp <- cos(deg2rad(angle_ouv[k]))*coordouv_bp[,1,i]-
sin(deg2rad(angle_ouv[k]))*coordouv_bp[,2,i]
      y_ouv_bp <-
sin(deg2rad(angle_ouv[k]))*coordouv_bp[,1,i]+cos(deg2rad(angle_ouv[k]))*coordouv_b
p[,2,i]
      z_ouv_bp <- coordouv_bp[,3,i]
      coordouv_bp[,,i] <-cbind(x_ouv_bp,y_ouv_bp,z_ouv_bp)
    }

    # Calculation of the effective lever arms
    d=CI=OI=OC<-vector()
    for (i in 1: dim(coordouv)[3])  {
      CI <- sqrt(coordouv_i[,1,i]^2 + coordouv_i[,2,i]^2 +coordouv_i[,3,i]^2 )
      OI <- sqrt(   (coordouv_i[,1,i]-coordouv_o[,1,i]) ^2 +
                     (coordouv_i[,2,i]-coordouv_o[,2,i]) ^2 +
                     (coordouv_i[,3,i]-coordouv_o[,3,i]) ^2 )
      OC <- sqrt ( coordouv_o [,1,i]^2 + coordouv_o[,2,i]^2 + coordouv_o[,3,i]^2)

      d <- cbind(d,sqrt ( CI^2 - ((OI^2-OC^2+CI^2) / (2*OI))^2))
    }
    dimnames(d)[1] <- list( substr( unlist(dimnames(coordouv_o)[1]), 1,
                                    nchar(unlist(dimnames(coordouv_o)[1]))-2))
    dimnames(d)[2]<-dimnames(coordouv_o)[3]

    # Calculation of the moments
    m <- matrix(nrow = dim(d)[1], ncol=dim(d)[2])
    for (i in 1: dim(d)[2])  {
      for (j in 1:dim(d)[1]) {
        m[j,i] <- d[j,i]*force[j+1,i]
      }
    }
    dimnames(m)[1] <- dimnames(d)[1]
    dimnames(m)[2] <- dimnames(d) [2]
    m_total =apply(m,2,sum)
    pc_m <- round(m/m_total*100, 2)

    # Angle of the bite force
    angle_force <- vector()
    force_x <-array(dim=c(8,dim(coordouv_o)[3]))
    force_y <-array(dim=c(8,dim(coordouv_o)[3]))
    for (i in 1: dim(coordouv)[3])  {
      angle_force_i <- rad2deg(pi-atan(abs(coordouv_o[,2,i]-coordouv_i[,2,i]) /
                                         abs(coordouv_o[,1,i]-coordouv_i[,1,i])))
      angle_force <- cbind(angle_force, angle_force_i)
      for (j in 2:9) {
        force_y[j-1,i] <- sin(deg2rad(angle_force_i[j-1]))*force[j,i]
        force_x[j-1,i] <- cos(deg2rad(angle_force_i[j-1]))*force[j,i]
      }
    }
    dimnames(angle_force)[1]=dimnames(d)[1]
    dimnames(angle_force)[2]=dimnames(d)[2]
    dimnames(force_x)[2]=dimnames(d)[2]
    dimnames(force_y)[2]=dimnames(d)[2]
```

```
    dimnames(force_x)[1]=dimnames(d)[1]
    dimnames(force_y)[1]=dimnames(d)[1]

    # Calculation of the bite force for different gape angles
    BF_angle=c(0,10,20,30,40,50,60,70)
    rBP=array(dim=c(dim(coordouv_bp)[1],length(BF_angle),dim(coordouv_bp)[3]))
    BF_k <- array(dim=c(dim(coordouv_bp)[1],length(BF_angle),dim(coordouv_bp)[3]))
    for (i in 1: dim(coordouv_bp)[3])  {
      for (j in 1: length(BF_angle))  {
        rBPi = sqrt(coordouv_bp[,3,i]^2 +
                      (coordouv_bp[,1,i] * sin(deg2rad(BF_angle[j]))-
coordouv_bp[,2,i]*cos(deg2rad(BF_angle[j])))^2)
        rBP[,j,i]<-rBPi
        BF_k[,j,i]<- 2*m_total[i]/rBP[,j,i]
      }
    }
    dimnames(rBP) [3] = dimnames(BF_k) [3] = dimnames(coordouv_bp)[3]
    dimnames(rBP) [2] = dimnames(BF_k) [2] = list(as.character(BF_angle))
    dimnames(rBP) [1] = dimnames(BF_k) [1] = dimnames(coordouv_bp) [1]

    BF [[k]] <- BF_k
    names(BF) [k] <- paste("BF - mouth opening ",k," degrees")
  }

  return (BF)
}

###############
```

2. Part2 – Chapter 3 – Article 1 – supplementary material

2.1. Table S1.

Details of the specimen used in this study including raw jaw muscles data and PCSA.

							Digastric					Masseter superficialis				
ID	BREED	AGE	BIRTHDATE	SEX	BODY MASS (	formol	muscle length (mm)	fiber length (mm)	angle (°)	mass (g)	PCSA (N/cm2)	muscle length (mm)	fiber length (mm)	angle (°)	mass (g)	PCSA (N/cm2)
BEAGLE1	BEAGLE	adult				yes										
BEAGLE2	BEAGLE	adult				yes										
M1	BEAGLE	adult				yes										
M2	BEAGLE	adult				yes										
M3	BEAGLE	adult				yes										
M4	BEAGLE	old				yes										
M5	BEAGLE	adult				yes										
M6	BEAGLE	adult				yes										
M8	BEAGLE	juvenile				yes										
Ma-1	BEAGLE	old				yes										
N-C1	BEAGLE	adult				no										
N-C10	BEAGLE	adult				no	77,39	31,27	0,00	8,80	2,66	69,58	14,32	45,00	14,40	6,71
N-C11	COLLEY	old				no	85,66	37,16	0,00	6,00	1,52	71,32	17,89	47,50	10,80	3,85
N-C12	BEAGLE	adult				no	84,44	38,65	0,00	7,50	1,83	59,52	22,28	40,00	7,80	2,53
N-C13	BEAGLE	adult				no	92,89	35,79	0,00	11,10	2,93	73,18	19,30	45,00	14,70	5,08
N-C14	SHEPHERD DOG	old				no	112,46	44,85	0,00	17,00	3,58	78,85	27,33	37,50	15,00	4,11
N-C15	SHEPHERD DOG	old				no	101,36	37,02	0,00	13,40	3,42	77,27	12,46	45,00	13,40	7,18
N-C16	HUNTING DOG	old				no	100,85	35,87	0,00	9,00	2,37	70,87	14,34	40,00	9,80	4,94
N-C17	BOXER	old				no	124,32	46,10	0,00	23,30	4,77	87,16	25,26	45,00	21,30	5,63
N-C18	BELGIAN SHEPHERD	old				no	97,75	35,50	0,00	14,90	3,96	71,76	18,79	55,00	19,40	5,59
N-C19	GOLDEN	adult	10/04/2007	female	19	no	97,12	44,98	0,00	12,90	2,71	61,39	15,02	50,00	14,20	5,73
N-C2	BEAGLE	young		male	11	no	78,30	35,77	0,00	8,97	2,37	61,30	16,73	40,00	13,30	5,74
N-C20	PAPILLON	adult	30/09/2002	male	4	no	59,85	24,97	0,00	3,60	1,36	35,26	13,20	37,50	1,60	0,91
N-C21	KING CHARLES	old	17/05/2005	male	7	no	58,36	26,64	0,00	4,80	1,70	56,53	13,06	45,00	7,70	3,93
N-C22		old	14/03/2007	male	26	no	105,34	33,21	0,00	30,50	8,66	69,70	29,12	35,00	26,70	7,09
N-C23		old	21/10/2009	neutered fem	35	no	135,31	59,43	0,00	23,90	3,79	78,84	30,61	50,00	21,50	4,26
N-C3	BEAGLE	adult				no	88,70	49,15	0,00	8,00	1,54	60,90	15,43	35,00	11,00	5,51
N-C4	BEAGLE	adult				no	89,30	41,53	0,00	8,00	1,82	70,10	15,93	35,00	9,00	4,37
N-C5	BULLDOG	adult	12years old	neutered male		no	72,00	38,55	0,00	13,13	3,21	70,50	17,23	53,33	15,18	4,96
N-C6	BEAGLE	adult		female	8	no	75,00	39,40	0,00	6,75	1,62	56,40	15,10	27,50	9,40	5,21
N-C7	BEAGLE	adult		female	9	no	78,90	39,40	0,00	8,72	2,09	59,70	17,23	30,00	12,34	5,85
N-C8	BEAGLE	adult		male	11	no	83,70	37,35	0,00	10,81	2,73	62,70	17,78	32,50	13,67	6,12
N-C9	SHEPHERD DOG	adult				no	71,79	31,26	0,00	6,80	2,05	53,10	18,76	42,50	11,20	4,15
Ny-C1		adult	2 years old	female		no	100,80	46,05	0,00	19,40	3,97	90,20	23,80	35,00	26,70	8,67
Ny-C10	GERMAN SHEPHERD	old		female		no	98,00	37,50	0,00	15,80	3,97	62,00	33,00	35,00	23,30	5,46
Ny-C11	MASTIFF	old		male		no	103,00	47,00	0,00	22,10	4,44	87,00	30,00	42,50	24,00	5,56
Ny-C12	FOX TERRIER	adult		male		no	99,00	48,00	0,00	19,60	3,85	77,00	24,00	47,50	19,50	5,18
Ny-C13	HUSKY	adult		female		no	90,00	30,00	0,00	16,49	5,19	80,00	25,00	40,00	21,60	6,24
Ny-C14	CANE CORSO	adult		male		no	100,00	60,00	5,00	32,80	5,14	110,00	23,00	65,00	52,00	9,01
Ny-C15	LEONBERGER	adult		male		no	110,00	44,00	0,00	33,10	7,10	100,00	22,00	40,00	46,60	15,31
Ny-C16	BULLDOG	old		male		no	90,00	35,00	0,00	13,97	3,77	80,00	26,00	45,00	20,60	5,29
Ny-C17	BORDER COLLIE	old		male		no	75,00	26,00	0,00	11,27	4,09	70,00	16,50	35,00	17,82	8,35
Ny-C18	ROTTWEILLER	adult		male		no	12,00	39,50	10,00	46,60	10,96	105,00	30,67	47,50	55,70	11,58
Ny-C19	CHIHUAHUA	adult		male		no	60,00	22,50	0,00	2,59	1,09	42,00	8,67	50,00	4,11	2,88
Ny-C20	PITBULL	old		male		no	105,00	36,25	0,00	33,20	8,64	95,00	25,00	35,00	49,30	15,24
Ny-C21	BOXER	old		male		no	115,00	46,00	0,00	23,40	4,80	95,00	22,00	42,50	26,20	8,28
Ny-C22	SHETLAND SHEEPDOG	adult		male		no	110,00	39,50	0,00	23,30	5,56	70,00	27,50	37,50	25,01	6,81
Ny-C23	BELGIAN SHEPHERD	old		male		no	90,00	36,00	0,00	10,04	2,63	70,00	15,00	45,00	15,38	6,84
Ny-C24	DEERHOUND	old		female		no	70,00	40,00	0,00	7,11	1,68	65,00	15,00	45,00	10,27	4,57
Ny-C25		adult		male		no	75,00	27,50	0,00	8,96	3,07	60,00	12,50	40,00	9,02	5,21
Ny-C26	DOBERMANN	old		male		no	70,00	31,50	0,00	7,49	2,24	60,00	19,50	25,00	9,21	4,04
Ny-C27	BORDER COLLIE	adult		female		no	80,00	33,00	0,00	10,69	3,06	60,00	14,50	42,50	9,63	4,62
Ny-C28	ROTTWEILLER	adult		male		no	110,00	45,00	0,00	47,70	10,00	110,00	26,50	32,50	62,10	18,65
Ny-C3	DACHSHUND	adult	6 years old	female		no	56,40	33,13	0,00	6,68	1,90	60,00	11,67	45,00	9,55	5,46
Ny-C4	MASTIFF	adult		male		no	113,00	36,50	0,00	26,70	6,90	84,00	26,50	40,00	29,70	8,10
Ny-C5	BEAGLE	old		male		no	101,00	37,50	0,00	16,70	4,20	81,00	26,00	47,50	25,00	6,13
Ny-C6	SHEPHERD DOG	old		male		no	112,00	46,00	0,00	21,40	4,39	92,00	29,50	35,00	27,40	7,18
Ny-C8	AMSTAFF	adult		?		no	115,00	50,50	0,00	35,10	6,56	106,00	31,50	52,50	55,80	10,17
Ny-C9	BULL TERRIER	juvenile		?		no	93,00	35,50	0,00	10,40	2,76	60,00	21,00	32,50	11,10	4,21
						MEAN				**16,26**	**3,85**	**73,48**	**20,70**	**41,53**	**20,42**	**6,43**
						MIN						**35,26**	**8,67**	**25,00**	**1,60**	**0,91**
						MAX						**110,00**	**33,00**	**65,00**	**62,10**	**18,65**

	Masseter profundus					Zygomaticomandibularis pars anterior					Zygomaticomandibularis pars posterior				
ID	muscle length (mm)	fiber length (mm)	angle (°)	mass (g)	PCSA (N/cm2)	muscle length (mm)	fiber length (mm)	angle (°)	mass (g)	PCSA (N/cm2)	muscle length (mm)	fiber length (mm)	angle (°)	mass (g)	PCSA (N/cm2)
BEAGLE1															
BEAGLE2															
M1															
M2															
M3															
M4															
M5															
M6															
M8															
Ma-1															
N-C1															
N-C10	37,14	5,81	50,00	4,60	4,80	19,34	15,37	25,00	1,10	0,61	29,18	8,46	45,00	3,70	2,92
N-C11	30,39	9,51	35,00	2,40	1,95	49,16	12,75	30,00	2,40	1,54	28,69	16,40	27,50	1,60	0,82
N-C12	41,70	16,16	35,00	5,10	2,44	34,79	22,10	30,00	2,50	0,92	31,50	11,70	20,00	1,90	1,44
N-C13	25,40	24,85	30,00	2,30	0,76	30,24	11,94	20,00	1,20	0,89	22,45	11,94	50,00	1,90	0,96
N-C14	82,58	26,69	30,00	14,30	4,38	84,34	30,66	27,50	5,80	1,58	56,26	12,59	35,00	6,20	3,81
N-C15	72,85	19,27	40,00	8,00	3,00	59,91	15,13	27,50	4,50	2,49	46,27	11,74	22,50	5,30	3,93
N-C16	67,82	15,34	35,00	6,00	3,02	44,63	17,24	40,00	4,50	1,89	39,37	9,05	35,00	2,80	2,39
N-C17	42,52	12,76	37,50	6,90	4,05	68,55	35,81	35,00	5,30	1,14	52,94	17,24	35,00	6,40	2,87
N-C18	61,65	31,16	32,50	9,30	2,37	58,33	13,49	27,50	5,40	3,35	38,22	9,96	35,00	4,10	3,18
N-C19	63,91	19,65	35,00	8,30	3,26	60,56	19,12	35,00	3,90	1,58	51,72	11,79	30,00	3,70	2,57
N-C2	25,70	12,03	20,00	3,57	2,63	27,40	15,60	35,00	2,12	1,05	26,70	12,05	32,50	1,62	1,07
N-C20	22,68	10,17	37,50	0,80	0,59	23,62	6,08	27,50	0,30	0,41	34,30	5,65	20,00	0,30	0,47
N-C21	33,32	10,94	50,00	2,90	1,61	18,44	8,29	30,00	0,80	0,79	26,92	13,62	30,00	1,00	0,60
N-C22	47,30	21,43	35,00	11,00	3,97	66,24	35,38	30,00	10,20	2,36	45,97	10,87	35,00	6,30	4,48
N-C23	55,62	22,89	30,00	15,40	5,50	52,96	33,54	25,00	10,40	2,65	68,51	23,29	25,00	6,10	2,24
N-C3	19,00	9,90	2,50	3,00	2,86	30,50	14,55	5,00	3,00	1,94	31,00	13,85	27,50	5,00	3,02
N-C4	24,10	6,00	42,50	2,00	2,32	20,60	10,47	10,00	2,00	1,78	37,30	13,05	60,00	2,00	0,72
N-C5	24,60	12,12	23,75	8,36	5,96	41,00	11,75	37,50	6,60	4,20	40,80	9,95	42,50	4,08	2,85
N-C6	27,50	9,27	20,00	2,81	2,69	26,00	9,30	10,00	0,88	0,88	22,60	9,40	30,00	1,36	1,18
N-C7	43,90	9,60	20,00	3,22	2,97	28,20	11,70	35,00	1,50	0,99	27,00	10,25	45,00	1,31	0,85
N-C8	29,40	13,17	15,00	5,26	3,64	30,00	13,40		1,88	1,32	34,10	9,53	42,50	2,81	2,05
N-C9	26,70	15,94	30,00	3,10	1,59	36,29	17,17	20,00	1,30	0,67	29,63	9,14	40,00	3,00	2,37
Ny-C1	31,60	13,15	15,00	9,01	6,24	46,00	16,45		7,00		56,70	10,50	35,00	7,58	5,58
Ny-C10	54,00	19,50	32,50	6,30	2,57	46,00	24,00	12,50	5,40	2,07	49,00	10,50	27,50	6,20	4,94
Ny-C11	60,00	10,00	35,00	10,60	8,19	62,00	29,00	15,00	8,00	2,51	57,00	17,00	40,00	7,50	3,19
Ny-C12	54,00	13,50	37,50	8,70	4,82	67,00	42,50	30,00	6,30	1,21	49,00	10,50	35,00	5,10	3,75
Ny-C13	35,00	10,00	45,00	6,70	4,47	45,00	20,00	45,00	5,75	1,92	40,00	10,00	35,00	5,10	3,94
Ny-C14	65,00	25,00	35,00	37,50	11,59	70,00	21,00	45,00	16,50	5,24	55,00	10,15	32,50	10,37	8,13
Ny-C15	50,00	15,00	37,50	19,30	9,63	60,00	20,00	40,00	10,57	3,82	55,00	10,00	42,50	9,28	6,45
Ny-C16	40,00	16,00	35,00	7,02	3,39	40,00	20,00	42,50	5,65	1,96	40,00	10,00	52,50	4,00	2,30
Ny-C17	40,00	15,00	30,00	5,26	2,86	60,00	15,00	50,00	5,13	2,07	40,00	8,00	35,00	3,18	3,07
Ny-C18	47,00	20,00	37,50	13,27	4,97	70,00	20,30	30,00	21,04	8,47	52,00	12,13	47,50	9,05	4,76
Ny-C19	36,00	11,00	35,00	1,80	1,26	20,00	9,00	30,00	1,09	0,99	22,00	4,50	40,00	0,94	1,51
Ny-C20	70,00	11,00	22,50	15,10	11,96	70,00	18,50	35,00	14,95	6,24	55,00	12,00	40,00	10,07	6,06
Ny-C21	35,00	11,00	35,00	8,25	5,80	40,00	15,00	45,00	5,73	2,55	35,00	12,00	32,50	3,57	2,37
Ny-C22	40,00	20,00	30,00	6,44	2,63	50,00	20,00	45,00	7,64	2,55	50,00	15,00	32,50	6,00	3,18
Ny-C23	30,00	10,00	37,50	3,45	2,58	40,00	31,00	35,00	4,15	1,03	35,00	15,00	25,00	3,22	1,84
Ny-C24	30,00	16,00	25,00	2,47	1,32	30,00	13,00	37,50	2,29	1,32	25,00	7,00	30,00	1,64	1,91
Ny-C25	30,00	13,00	40,00	4,19	2,33	40,00	15,00	30,00	3,55	1,93	40,00	12,00	25,00	2,67	1,90
Ny-C26	40,00	7,00	20,00	3,70	4,69	40,00	7,50	27,50	4,76	5,31	30,00	10,00	27,50	2,30	1,92
Ny-C27	35,00	12,00	30,00	5,62	3,83	50,00	13,00	40,00	3,93	2,18	30,00	7,00	42,50	2,72	2,70
Ny-C28	80,00	22,50	35,00	24,80	8,52	60,00	17,00	40,00	16,03	6,81	55,00	11,00	42,50	9,42	5,96
Ny-C3	27,50	9,40	35,00	2,20	1,81	29,80	9,40	35,00	2,24	1,84	27,00	7,40	35,00	2,00	2,09
Ny-C4	59,00	12,50	37,50	8,90	5,33	84,00	15,50	32,50	12,60	6,47	54,00	15,00	35,00	6,70	3,45
Ny-C5	46,00	20,00	35,00	7,10	2,74	56,00	30,00	27,50	5,00	1,39	49,00	10,50	37,50	4,90	3,49
Ny-C6	47,00	18,00	27,50	10,80	5,02	75,00	34,00	35,00	11,90	2,70	56,00	11,50	30,00	6,70	4,76
Ny-C8	55,00	22,50	42,50	17,10	5,29	90,00	21,50	37,50	15,90	5,54	53,00	16,50	37,50	8,60	3,90
Ny-C9	50,00	18,00	32,50	4,80	2,12	63,00	23,50	27,50	4,00	1,42	40,00	7,50	25,00	3,30	3,76
	43,60	**15,12**	**32,21**	**7,90**	**4,01**	**48,23**	**18,79**	**31,14**	**5,93**	**2,44**	**41,07**	**11,34**	**35,10**	**4,47**	**2,99**
	19,00	**5,81**	**2,50**	**0,80**	**0,59**	**18,44**	**6,08**	**5,00**	**0,30**	**0,41**	**22,00**	**4,50**	**20,00**	**0,30**	**0,47**
	82,58	**31,16**	**50,00**	**37,50**	**11,96**	**90,00**	**42,50**	**50,00**	**21,04**	**8,47**	**68,51**	**23,29**	**60,00**	**10,37**	**8,13**

	Temporalis par suprazgomatica					Temporal pars superficialis					Temporalis pars profunda					
ID	muscle length (mm)	fiber length (mm)	angle (°)	mass (g)	PCSA (N/cm2)	muscle length (mm)	fiber length (mm)	angle (°)	mass (g)	PCSA (N/cm2)	muscle length (mm)	fiber length (mm)	angle (°)	mass (g)	PCSA (N/cm2)	muscle length (mm)
BEAGLE1																
BEAGLE2																
M1																
M2																
M3																
M4																
M5																
M6																
M8																
Ma-1																
N-C1																
N-C10	93,33	24,18	25,00	5,30	1,87	100,25	29,38	32,50	20,20	5,47	87,83	28,66	25,00	32,60	9,73	32,74
N-C11	76,74	22,72	27,50	3,20	1,18	105,60	24,93	20,00	12,80	4,55	88,60	22,68	32,50	17,60	6,17	83,11
N-C12	86,42	16,24	25,00	5,60	2,95	111,94	31,45	25,00	19,40	5,27	91,39	34,42	40,00	29,40	6,17	52,11
N-C13	84,54	20,56	30,00	5,90	2,34	108,74	47,27	27,50	20,00	3,54	87,26	39,87	30,00	34,30	7,03	82,79
N-C14	127,90	30,48	25,00	8,40	2,36	133,43	39,42	35,00	22,50	4,41	138,72	37,17	40,00	47,00	9,14	79,15
N-C15	85,37	17,47	30,00	9,00	4,21	127,74	20,08	45,00	20,40	6,78	108,12	27,09	37,50	32,90	9,09	70,31
N-C16	84,30	31,81	30,00	6,00	1,54	118,14	27,20	32,50	21,90	6,41	93,06	29,52	37,50	26,60	6,74	71,45
N-C17	93,86	38,95	25,00	12,90	2,83	123,54	52,44	27,50	31,80	5,07	113,09	38,41	40,00	45,90	8,64	78,09
N-C18	99,10	30,70	20,00	9,60	2,77	117,01	36,31	35,00	34,30	7,30	116,36	29,85	35,00	50,00	12,95	75,13
N-C19	91,94	29,51	17,50	7,40	2,26	123,04	27,29	32,50	39,90	11,64	103,64	30,27	35,00	39,60	10,11	78,12
N-C2	92,80	20,15	30,00	6,32	2,56	103,10	21,90	30,00	17,15	6,40	94,50	27,23	35,00	29,40	8,34	66,00
N-C20	37,21	12,98	17,50	0,50	0,35	70,72	9,65	22,50	1,70	1,54	56,25	10,59	37,50	3,00	2,12	44,98
N-C21	73,86	24,22	25,00	2,20	0,78	96,19	19,43	37,50	12,60	4,85	90,12	21,90	40,00	16,90	5,58	48,26
N-C22	126,50	55,65	20,00	13,30	2,12	143,53	44,09	37,50	65,60	11,14	128,81	48,70	45,00	70,40	9,64	88,82
N-C23	104,51	19,29	35,00	8,40	3,37	135,23	45,86	20,00	44,00	8,51	123,96	45,03	37,50	58,30	9,69	98,74
N-C3	66,70	11,95	15,00	2,00	1,53	106,20	28,20	45,00	22,00	5,20	99,10	28,20	40,00	42,00	10,76	74,90
N-C4	64,90	21,10	15,00	2,00	0,86	118,30	28,95	40,00	18,00	4,49	95,40	33,70	45,00	27,00	5,34	69,40
N-C5	75,20	24,80	15,00	3,09	1,14	118,40	25,17	22,50	21,76	7,54	100,00	20,80	45,00	36,51	11,71	68,70
N-C6	78,00	14,85	0,00	2,45	1,56	95,90	26,75	25,00	15,24	4,87	75,60	24,20	25,00	20,84	7,36	52,70
N-C7	92,60	20,25	30,00	5,57	2,25	93,10	20,90	40,00	15,46	5,35	87,20	24,93	40,00	27,35	7,93	66,00
N-C8	85,60	20,30	30,00	6,63	2,67	99,30	33,40	35,00	23,31	5,39	89,25	28,38	32,50	32,03	8,98	73,80
N-C9	91,01	10,67	25,00	3,50	2,80	94,85	28,03	22,50	17,20	5,35	87,17	24,21	20,00	27,00	9,89	66,91
Ny-C1	108,40	31,10	25,00	12,83	3,53	121,50	33,37	25,00	38,90	9,97	105,80	20,87	52,50	60,10	16,54	98,80
Ny-C10	99,00	42,00	10,00	8,40	1,86	121,00	38,50	27,50	57,50	12,50	75,00	18,50	32,50	28,10	12,09	107,00
Ny-C11	114,00	44,00	30,00	9,80	1,82	140,00	53,00	37,50	43,60	6,16	109,00	32,50	37,50	39,40	9,07	99,00
Ny-C12	91,00	34,00	27,50	8,70	2,14	120,00	32,00	37,50	36,80	8,61	112,00	27,50	40,00	50,60	13,30	89,00
Ny-C13	97,50	15,00	40,00	7,24	3,49	110,00	25,00	50,00	26,93	6,53	120,00	25,00	47,50	51,30	13,08	90,00
Ny-C14	135,00	30,00	35,00	28,20	7,26	160,00	40,00	41,67	89,61	15,79	150,00	35,00	45,00	131,80	25,12	100,00
Ny-C15	135,00	12,20	55,00	22,30	9,89	145,00	42,50	37,50	77,90	13,72	140,00	36,00	45,00	95,30	17,66	110,00
Ny-C16	90,00	20,00	30,00	7,63	3,12	130,00	25,00	50,00	29,34	7,12	110,00	32,00	50,00	41,69	7,90	80,00
Ny-C17	110,00	17,00	27,50	6,22	3,06	125,00	29,00	35,00	26,40	7,04	120,00	25,00	37,50	40,80	12,21	90,00
Ny-C18	150,00	40,00	35,00	33,70	6,51	165,00	40,00	42,50	95,70	16,64	140,00	40,00	40,00	149,90	27,08	105,00
Ny-C19	60,00	15,00	35,00	2,02	1,04	86,00	15,00	30,00	5,53	3,01	85,00	13,50	40,00	12,39	6,63	40,00
Ny-C20	110,00	25,00	25,00	13,85	4,74	140,00	36,00	35,00	77,11	16,55	120,00	39,00	45,00	104,00	17,79	80,00
Ny-C21	90,00	20,00	42,50	6,60	2,30	120,00	46,00	30,00	50,84	9,03	110,00	48,50	40,00	58,14	8,66	90,00
Ny-C22	110,00	30,00	30,00	12,74	3,47	125,00	45,00	37,50	52,30	8,70	120,00	42,50	37,50	76,76	13,52	100,00
Ny-C23	85,00	35,00	30,00	6,99	1,63	75,00	35,00	40,00	21,70	4,48	95,00	30,00	50,00	32,80	6,63	70,00
Ny-C24	85,00	16,00	35,00	3,14	1,52	80,00	21,50	30,00	14,17	5,38	85,00	20,00	37,50	29,03	10,86	65,00
Ny-C25	80,00	17,00	37,50	6,04	2,66	100,00	25,00	38,33	14,05	4,16	110,00	21,00	45,00	25,10	7,97	70,00
Ny-C26	80,00	22,00	25,00	4,00	1,55	90,00	18,00	37,50	16,30	6,78	100,00	20,00	37,50	26,20	9,80	55,00
Ny-C27	90,00	25,00	35,00	4,79	1,48	105,00	26,00	40,00	22,45	6,24	80,00	20,00	40,00	33,66	12,16	60,00
Ny-C28	130,00	30,00	27,50	22,96	6,40	175,00	40,00	35,00	118,40	22,87	140,00	47,50	45,00	145,10	20,38	100,00
Ny-C3	60,60	17,40	35,00	2,26	1,00	77,10	15,60	50,00	16,17	6,29	87,40	13,17	27,50	21,69	13,78	63,90
Ny-C4	103,00	44,50	27,50	12,40	2,33	141,00	43,00	37,50	51,60	8,98	126,00	46,50	35,00	72,80	12,10	94,00
Ny-C5	79,00	31,50	20,00	8,40	2,36	129,00	44,50	35,00	37,40	6,49	114,00	41,00	37,50	63,20	11,54	67,00
Ny-C6	116,00	44,00	27,50	8,80	1,67	119,00	37,50	47,50	40,90	6,95	124,00	46,00	45,00	71,10	10,31	102,00
Ny-C8	115,00	59,00	20,00	17,20	2,58	143,00	50,50	35,00	72,70	11,13	144,00	41,50	50,00	117,00	17,10	93,00
Ny-C9	86,00	29,00	20,00	5,10	1,56	75,00	33,00	27,50	20,00	5,07	107,00	28,00	40,00	18,30	4,72	78,00
	94,21	**26,34**	**27,08**	**8,57**	**2,65**	**115,87**	**32,46**	**34,58**	**34,82**	**7,65**	**105,93**	**30,55**	**39,06**	**48,81**	**10,86**	**77,48**
	37,21	**10,67**	**0,00**	**0,50**	**0,35**	**70,72**	**9,65**	**20,00**	**1,70**	**1,54**	**56,25**	**10,59**	**20,00**	**3,00**	**2,12**	**32,74**
	150,00	**59,00**	**55,00**	**33,70**	**9,89**	**175,00**	**53,00**	**50,00**	**118,40**	**22,87**	**150,00**	**48,70**	**52,50**	**149,90**	**27,08**	**110,00**

	Pterygoideus medialis				Pterygoideus lateralis											
ID	fiber length (mm)	angle (°)	mass (g)	PCSA (N/cm2)	muscle length (mm)	fiber length (mm)	angle (°)	mass (g)	PCSA (N/cm2)		% digastricus mass	mass of adductors	% temporal mass	%masseter mass	%pterygoid mass	%PL
BEAGLE1																
BEAGLE2																
M1																
M2																
M3																
M4																
M5																
M6																
M8																
Ma-1																
N-C1																
N-C10	18,06	20,00	7,00	9,58	4,22	30,00	0,20	7,20	3,53		**8,39**	89,10	65,21	26,71	8,08	0,22
N-C11	16,57	25,00	6,30	9,38	4,75	35,00	0,20	6,50	3,35		**8,62**	57,30	58,64	30,02	11,34	0,35
N-C12	13,70	20,00	5,10	8,04			0,20	5,30	3,43		**8,37**	77,00	70,65	22,47	6,88	0,26
N-C13	20,94	47,50	7,90	10,71	0,50	30,00	0,50	8,40	2,56		**10,31**	88,70	67,87	22,66	9,47	0,56
N-C14	14,63	45,00	15,20	17,09	11,42	27,50	1,30	16,50	7,52		**10,13**	135,70	57,41	30,43	12,16	0,96
N-C15	13,13	22,50	9,90	22,25	9,20	20,00	2,50	12,40	8,23		**10,37**	105,90	58,83	29,46	11,71	2,36
N-C16	11,12	25,00	9,40	19,15	9,37	20,00	1,40	10,80	8,30		**8,43**	88,40	61,65	26,13	12,22	1,58
N-C17	17,24	30,00	10,90	24,19	9,01	25,00	2,80	13,70	6,49		**13,06**	144,20	62,83	27,67	9,50	1,94
N-C18	17,60	37,50	15,40	20,50	8,46	27,50	1,10	16,50	7,02		**8,33**	148,60	63,19	25,71	11,10	0,74
N-C19	14,46	22,50	10,70	16,39	6,75	32,50	0,70	11,40	6,87		**8,49**	128,40	67,68	23,44	8,88	0,55
N-C2	8,27	50,00	7,22	17,70	7,95	40,00	0,67	7,89	5,79		**9,19**	81,37	64,97	25,33	9,70	0,82
N-C20	8,07	37,50	1,10	8,46	2,84	25,00	0,10	1,20	1,11		**25,53**	9,40	55,32	31,91	12,77	1,06
N-C21	16,20	20,00	3,30	12,05	7,54	30,00	0,30	3,60	1,97		**8,60**	47,70	66,46	26,00	7,55	0,63
N-C22	27,19	35,00	18,20	13,52	7,92	15,00	1,10	19,30	5,49		**11,23**	222,80	67,01	24,33	8,66	0,49
N-C23	26,18	47,50	14,60	17,04	15,09	25,00	1,20	15,80	3,85		**10,94**	179,90	61,53	29,68	8,78	0,67
N-C3	15,73	15,00	6,00	51,00	10,40	25,00	1,00	7,00	4,05		**7,34**	95,00	69,47	23,16	7,37	1,05
N-C4	14,25	32,50	5,00	23,60	11,65	37,50	1,00	6,00	3,35		**9,88**	68,00	69,12	22,06	8,82	1,47
N-C5	10,15	42,50	10,44	19,40	7,30	20,00	0,71	11,15	7,64		**10,08**	106,73	57,49	32,06	10,45	0,67
N-C6	8,50	50,00	4,48	16,50	7,30		0,28	4,76	3,40		**9,79**	57,74	66,73	25,03	8,24	0,48
N-C7	9,95	27,50	5,28	18,60	3,80	50,00	0,39	5,67	4,77		**10,09**	72,42	66,80	25,37	7,83	0,54
N-C8	12,67	45,00	8,01	19,50	5,00		1,04	9,05	4,77		**9,53**	94,64	65,48	24,96	9,56	1,10
N-C9	10,39	50,00	4,20	10,59	5,94	45,00	0,20	4,40	2,57		**8,32**	70,70	67,47	26,31	6,22	0,28
Ny-C1	13,20	55,00	18,24	28,00	8,45	25,00	1,34	19,58	8,03		**8,84**	181,70	61,55	27,68	10,78	0,74
Ny-C10	25,50	47,50	15,70	10,00	6,50	30,00	0,94	16,64	4,16		**8,62**	151,84	61,91	27,13	10,96	0,62
Ny-C11	29,00	32,50	20,00	17,00	11,50	40,00	1,20	21,20	5,82		**10,72**	164,10	56,55	30,53	12,92	0,73
Ny-C12	14,50	47,50	13,50	16,00	6,00	25,00	1,10	14,60	6,42		**10,69**	150,30	63,94	26,35	9,71	0,73
Ny-C13	11,00	37,50	10,70	20,00	7,00	40,00	0,81	11,51	7,83		**10,10**	136,13	62,79	28,76	8,46	0,60
Ny-C14	22,00	45,00	40,30	22,00	10,00	50,00	2,20	42,50	12,89		**6,81**	408,48	61,11	28,49	10,40	0,54
Ny-C15	15,00	47,50	26,60	25,00	10,00	50,00	1,63	28,23	11,99		**8,97**	309,48	63,17	27,71	9,12	0,53
Ny-C16	15,00	45,00	11,43	15,00	0,70		0,52	11,95	5,31		**9,11**	127,88	61,51	29,14	9,34	0,41
Ny-C17	13,50	42,50	9,15	15,00	5,50	40,00	0,50	9,65	4,97		**8,36**	114,46	64,14	27,42	8,43	0,44
Ny-C18	22,20	45,00	34,20	25,00	12,00	50,00	3,00	37,20	11,18		**9,39**	415,56	67,21	23,84	8,95	0,72
Ny-C19	15,00	40,00	2,29	6,00	4,00	30,00	0,06	2,35	1,13		**7,38**	30,23	65,96	26,27	7,77	0,20
Ny-C20	16,00	40,00	24,60	17,00	7,50	40,00	0,77	25,37	11,46		**9,03**	309,75	62,94	28,87	8,19	0,25
Ny-C21	17,50	42,50	16,43	15,00	10,00		0,52	16,95	6,73		**10,83**	176,28	65,57	24,82	9,61	0,29
Ny-C22	20,00	45,00	21,90	15,00	7,00	40,00	0,95	22,85	7,62		**9,14**	209,74	67,61	21,50	10,89	0,45
Ny-C23	11,00	50,00	9,59	10,00	0,50	50,00	0,30	9,89	5,45		**8,57**	97,58	63,01	26,85	10,14	0,31
Ny-C24	10,00	45,00	5,56	12,00	5,00	42,50	0,20	5,76	3,84		**8,73**	68,77	67,38	24,24	8,38	0,29
Ny-C25	8,50	50,00	9,32	15,00	6,70	50,00	0,42	9,74	6,95		**9,67**	74,36	60,77	26,13	13,10	0,56
Ny-C26	12,00	45,00	6,22	12,00	7,00	50,00	0,16	6,38	3,55		**8,65**	72,85	63,83	27,41	8,76	0,22
Ny-C27	12,00	40,00	8,60	15,00	8,00	50,00	0,55	9,15	5,51		**9,61**	91,95	66,23	23,82	9,95	0,60
Ny-C28	17,20	50,00	33,20	20,00	20,00	40,00	3,00	36,20	12,76		**9,25**	435,01	65,85	25,83	8,32	0,69
Ny-C3	11,80	62,50	5,55	13,80	12,80		0,36	5,91	2,18		**9,00**	62,02	64,69	25,78	9,53	0,58
Ny-C4	21,00	42,50	18,40	17,00	7,50	27,50	1,40	19,80	6,56		**10,29**	214,50	63,78	26,99	9,23	0,65
Ny-C5	23,00	35,00	16,30	10,00	6,00	30,00	0,70	17,00	5,71		**8,31**	168,00	64,88	25,00	10,12	0,42
Ny-C6	22,00	40,00	23,00	15,00	5,50	20,00	0,90	23,90	7,85		**8,70**	201,50	59,95	28,19	11,86	0,45
Ny-C8	24,50	40,00	23,60	26,00	10,00	30,00	1,90	25,50	7,52		**9,03**	329,80	62,73	29,53	7,73	0,58
Ny-C9	17,00	37,50	8,10	14,00	4,50	32,50	0,50	8,60	3,79		**11,10**	75,20	57,71	30,85	11,44	0,66
	15,92	**39,53**	**12,88**	**16,90**	**7,58**	**34,35**	**0,93**	**13,81**	**5,90**	**MEAN**	**9,66**		**63,72**	**26,67**	**9,61**	**0,67**
	8,07									**MIN**	**6,81**		**55,32**	**21,50**	**6,22**	**0,20**
	29,00									**MAX**	**25,53**		**70,65**	**32,06**	**13,10**	**2,36**

ID	% PL/P	PCSA of adductors	% temporal PCSA	% masseter PCSA	% pterygoid PCSA
BEAGLE1					
BEAGLE2					
M1					
M2					
M3					
M4					
M5					
M6					
M8					
Ma-1					
N-C1					
N-C10	2,78	35,65	47,89	42,19	9,91
N-C11	3,08	23,41	50,85	34,82	14,33
N-C12	3,77	25,16	57,22	29,15	13,63
N-C13	5,95	23,17	55,75	33,21	11,04
N-C14	7,88	37,31	42,64	37,20	20,17
N-C15	20,16	44,91	44,71	36,96	18,33
N-C16	12,96	35,24	41,69	34,74	23,57
N-C17	20,44	36,72	45,05	37,27	17,68
N-C18	6,67	44,54	51,69	32,55	15,76
N-C19	6,14	44,01	54,53	29,86	15,61
N-C2	8,49	33,58	51,52	31,25	17,23
N-C20	8,33	7,50	53,40	31,75	14,85
N-C21	8,33	20,11	55,75	34,46	9,80
N-C22	5,70	46,27	49,49	38,66	11,85
N-C23	7,59	40,06	53,83	36,57	9,60
N-C3	14,29	34,87	50,17	38,21	11,63
N-C4	16,67	23,23	46,06	39,52	14,42
N-C5	6,37	46,00	44,31	39,08	16,61
N-C6	5,88	27,15	50,80	36,69	12,51
N-C7	6,88	30,96	50,14	34,46	15,40
N-C8	11,49	34,94	48,77	37,59	13,64
N-C9	4,55	29,39	61,38	29,89	8,74
Ny-C1	6,84				
Ny-C10	5,65	45,64	57,93	32,95	9,11
Ny-C11	5,66	42,32	40,28	45,97	13,74
Ny-C12	7,53	45,43	52,93	32,94	14,13
Ny-C13	7,04	47,50	48,63	34,89	16,49
Ny-C14	5,18	95,04	50,69	35,75	13,56
Ny-C15	5,77	88,48	46,64	39,80	13,56
Ny-C16	4,35	36,39	49,84	35,56	14,61
Ny-C17	5,18	43,64	51,13	37,48	11,39
Ny-C18	8,06	91,18	55,09	32,65	12,26
Ny-C19	2,55	18,46	57,89	35,97	6,13
Ny-C20	3,04	90,05	43,40	43,88	12,73
Ny-C21	3,04	45,72	43,72	41,55	14,73
Ny-C22	4,16	48,48	52,99	31,29	15,72
Ny-C23	3,03	30,49	41,80	40,32	17,88
Ny-C24	3,47	30,73	57,82	29,68	12,50
Ny-C25	4,31	33,12	44,66	34,36	20,98
Ny-C26	2,51	37,64	48,18	42,40	9,42
Ny-C27	6,01	38,73	51,34	34,43	14,23
Ny-C28	8,29	102,35	48,51	39,02	12,47
Ny-C3	6,09	34,46	61,16	32,50	6,33
Ny-C4	7,07	53,32	43,91	43,79	12,30
Ny-C5	4,12	39,87	51,16	34,51	14,33
Ny-C6	3,77	46,45	40,77	42,33	16,90
Ny-C8	7,45	63,22	48,73	39,38	11,90
Ny-C9	5,81	26,65	42,60	43,20	14,21
	6,88		**49,78**	**36,44**	**13,79**
	2,51		**40,28**	**29,15**	**6,13**
	20,44		**61,38**	**45,97**	**23,57**

2.2. Table S2.

Origin and insertion of the jaw muscles dissected in this study, after a synthesis of the nomenclature proposed by Schumacher (1961), Turnbull (1970), Ström et al. (1988), Tomo et al. (1993), Christiansen and Adolfssen (2005), Budras (2007), Barone (2010), Evans and DeLahunta (2010), Hung et al. (2010), Druzinsky et al. (2011), Hartstone-Rose et al. (2012), Flahive (2015), Penrose et al. (2016).

Muscle	Origin and insertion	Function
Digastric	Origin: jugular process. Insertion: caudal part of the ventral border of the body of the mandible.	Abduction
M. masseter, pars superficialis	Origin: facial crest on the lateral edge of the zygomatic process and maxillar bone. Insertion: angle of the mandible.	Adduction
M. masseter, pars profunda	Origin: lower ventro-lateral part of the zygomatic arch. Insertion: ventro-lateral margin of the masseteric fossa.	Adduction
M. masseter, pars zygomaticomandibularis anterior	Origin: anteromedial part of the zygomatic arch. Insertion: anterolateral surface of the masseteric fossa on the mandibular ramus.	Adduction
M. masseter, pars zygomaticomandibularis posterior	Origin: posteroriomedial part of the zygomatic arch. Insertion: posterolateral surface of the masseteric fossa on the mandibular ramus.	Adduction
M. temporalis, pars suprazygomatica	Origin: posteroventral surface of the temporal, just after the caudal end of the zygomatic arch Insertion: rostrolateral border of the coronoid process.	Adduction
M. temporalis, pars superficialis	Origin: circumference of the temporal fossa on the parietal bone along the sagittal crest, posterior surface of the frontal bone along the orbital ligament, the external frontal crest, and the medial side of the zygomatic arch. Insertion: rostral border of the coronoid process.	Adduction
M. temporalis, pars profunda posterior	Origin: base of the temporal fossa on the surface of the parietal and temporal bones, until the pteygoidian crest. Insertion: Medial surface and dorsal edge of the coronoid process.	Adduction
M. pterygoideus medialis	Origin: lateral edge of the pterygoid, palatine and sphenoid bones. Insertion: medial and ventral surfaces of the angular process anteriorly to the insertion of the temporal.	Adduction and lateral movements if unilateral contraction
M. pterygoideus lateralis	Origin: small fossa on the ventro-lateral edge of the sphenoid, underneath the orbital foramen and the foramen rotundum. Insertion: medial edge of the neck and the head of the condyle, and in the anteromedial part of the disc.	Indeterminate, used as an adductor or protractor muscle

2.3. Table S3.

Results of the statistical analyses exploring allometries (sheet 1) and the variability (sheet 2) in mandibular shape and muscle data.

Results of the correlation tests exploring allometries

Shapes

Global allometries using the function CAC

```
        Pearson's product-moment correlation

data:  cac$CACscores and cac$size
t = 6, df = 46, p-value = 2e-07
alternative hypothesis: true correlation is not equal to 0
95 percent confidence interval:
 0.477 0.802
sample estimates:
 cor
0.67
```

Allometries along PC1

```
        Pearson's product-moment correlation

data:  pca$pc.scores[, 1] and gpa$size
t = 4, df = 57, p-value = 5e-05
alternative hypothesis: true correlation is not equal to 0
95 percent confidence interval:
 0.286 0.674
sample estimates:
  cor
0.505
```

Allometries along PC2

```
        Pearson's product-moment correlation

data:  pca$pc.scores[, 2] and gpa$size
t = -1, df = 57, p-value = 0.2
alternative hypothesis: true correlation is not equal to 0
95 percent confidence interval:
 -0.4010  0.0986
sample estimates:
   cor
-0.162
```

Muscle masses

```
        Pearson's product-moment correlation

data:  pca$x[, 1] and size
t = 13, df = 46, p-value <2e-16
alternative hypothesis: true correlation is not equal to 0
95 percent confidence interval:
 0.807 0.936
sample estimates:
  cor
0.888
```

Muscle PCSAs

```
        Pearson's product-moment correlation

data:  pca$x[, 1] and size
t = 10, df = 45, p-value = 4e-13
alternative hypothesis: true correlation is not equal to 0
95 percent confidence interval:
 0.717 0.904
sample estimates:
  cor
0.833
```

Statistics related to the Principal Component Analyses

PCA on muscle mass

	eigenvalue	percentage of variance	cumulative percentage of variance
comp 1	8.2531	91.701	91.7
comp 2	0.2061	2.290	94.0
comp 3	0.1515	1.684	95.7
comp 4	0.1011	1.124	96.8
comp 5	0.0906	1.007	97.8
comp 6	0.0846	0.940	98.7
comp 7	0.0516	0.573	99.3
comp 8	0.0326	0.362	99.7
comp 9	0.0288	0.320	100.0

PCA on scaled muscle masses

	eigenvalue	percentage of variance	cumulative percentage of variance
comp 1	8.2531	91.701	91.7
comp 2	0.2061	2.290	94.0
comp 3	0.1515	1.684	95.7
comp 4	0.1011	1.124	96.8
comp 5	0.0906	1.007	97.8
comp 6	0.0846	0.940	98.7
comp 7	0.0516	0.573	99.3
comp 8	0.0326	0.362	99.7
comp 9	0.0288	0.320	100.0

PCA on muscle PCSAs

	eigenvalue	percentage of variance	cumulative percentage of variance
comp 1	6.883	76.48	76.5
comp 2	0.496	5.51	82.0
comp 3	0.392	4.35	86.3
comp 4	0.323	3.59	89.9
comp 5	0.289	3.21	93.1
comp 6	0.212	2.35	95.5
comp 7	0.175	1.95	97.4
comp 8	0.128	1.42	98.9
comp 9	0.103	1.14	100.0

PCA on scaled muscle PCSAs

	eigenvalue	percentage of variance	cumulative percentage of variance
comp 1	4.613	51.25	51.3
comp 2	0.943	10.48	61.7
comp 3	0.846	9.40	71.1
comp 4	0.673	7.47	78.6
comp 5	0.641	7.12	85.7

comp 6	0.431	4.79	90.5
comp 7	0.382	4.25	94.8
comp 8	0.265	2.94	97.7
comp 9	0.206	2.29	100.0

PCA on mandibular shapes

	PC1	PC2	PC3	PC4	PC5	
Standard deviation	4.501929e-02	3.097517e-02	2.405685e-02	2.136623e-02	1.718276e-02	1.578
Proportion of Variance	3.133500e-01	1.483400e-01	8.948000e-02	7.058000e-02	4.565000e-02	3.854
Cumulative Proportion	3.133500e-01	4.617000e-01	5.511800e-01	6.217600e-01	6.674100e-01	7.059
	PC9	PC10	PC11	PC12	PC13	
Standard deviation	1.200500e-02	1.127413e-02	1.094126e-02	1.002182e-02	9.337408e-03	9.046
Proportion of Variance	2.228000e-02	1.965000e-02	1.851000e-02	1.553000e-02	1.348000e-02	1.265
Cumulative Proportion	7.873000e-01	8.069600e-01	8.254600e-01	8.409900e-01	8.544700e-01	8.671
	PC17	PC18	PC19	PC20	PC21	
Standard deviation	7.616498e-03	7.407778e-03	7.076374e-03	6.621546e-03	6.362937e-03	6.172
Proportion of Variance	8.970000e-03	8.480000e-03	7.740000e-03	6.780000e-03	6.260000e-03	5.890
Cumulative Proportion	8.981900e-01	9.066700e-01	9.144200e-01	9.211900e-01	9.274500e-01	9.333
	PC25	PC26	PC27	PC28	PC29	
Standard deviation	5.301239e-03	5.141720e-03	5.039989e-03	5.011082e-03	4.567138e-03	4.344
Proportion of Variance	4.350000e-03	4.090000e-03	3.930000e-03	3.880000e-03	3.220000e-03	2.920
Cumulative Proportion	9.478500e-01	9.519400e-01	9.558700e-01	9.597500e-01	9.629800e-01	9.658
	PC33	PC34	PC35	PC36	PC37	
Standard deviation	3.930825e-03	3.868031e-03	3.799922e-03	3.540325e-03	3.390280e-03	3.205
Proportion of Variance	2.390000e-03	2.310000e-03	2.230000e-03	1.940000e-03	1.780000e-03	1.590
Cumulative Proportion	9.736500e-01	9.759600e-01	9.781900e-01	9.801300e-01	9.819100e-01	9.835
	PC41	PC42	PC43	PC44	PC45	
Standard deviation	2.870565e-03	2.793988e-03	2.747930e-03	2.621358e-03	2.505817e-03	2.411
Proportion of Variance	1.270000e-03	1.210000e-03	1.170000e-03	1.060000e-03	9.700000e-04	9.000
Cumulative Proportion	9.877400e-01	9.889500e-01	9.901100e-01	9.911800e-01	9.921500e-01	9.930
	PC49	PC50	PC51	PC52	PC53	
Standard deviation	2.207218e-03	2.085626e-03	2.039715e-03	1.973595e-03	1.892561e-03	1.832
Proportion of Variance	7.500000e-04	6.700000e-04	6.400000e-04	6.000000e-04	5.500000e-04	5.200
Cumulative Proportion	9.954000e-01	9.960700e-01	9.967200e-01	9.973200e-01	9.978700e-01	9.983
	PC57	PC58				
Standard deviation	1.544630e-03	1.499448e-03	4.563354e-17			
Proportion of Variance	3.700000e-04	3.500000e-04	0.000000e+00			
Cumulative Proportion	9.996500e-01	1.000000e+00	1.000000e+00			

PC6	PC7	PC8
898e-02	1.442129e-02	1.319452e-02
000e-02	3.215000e-02	2.692000e-02
500e-01	7.381000e-01	7.650200e-01
PC14	PC15	PC16
835e-03	8.854641e-03	8.030741e-03
000e-02	1.212000e-02	9.970000e-03
300e-01	8.792500e-01	8.892200e-01
PC22	PC23	PC24
072e-03	5.932597e-03	5.527198e-03
000e-03	5.440000e-03	4.720000e-03
400e-01	9.387900e-01	9.435100e-01
PC30	PC31	PC32
354e-03	4.302303e-03	4.022437e-03
000e-03	2.860000e-03	2.500000e-03
900e-01	9.687600e-01	9.712600e-01
PC38	PC39	PC40
643e-03	3.178351e-03	3.016997e-03
000e-03	1.560000e-03	1.410000e-03
000e-01	9.850600e-01	9.864700e-01
PC46	PC47	PC48
578e-03	2.318973e-03	2.233513e-03
000e-04	8.300000e-04	7.700000e-04
500e-01	9.938800e-01	9.946500e-01
PC54	PC55	PC56
621e-03	1.716730e-03	1.676363e-03
000e-04	4.600000e-04	4.300000e-04
900e-01	9.988500e-01	9.992800e-01

2.4. Table S4.

Results of the 2-Block Partial Least Square Analyses (sheet 1) and P-values and Z-scores of the comparison tests (sheet 2). S: shape of the mandible; rS: shape of the ramus; a: allometry-free (shape or shape of the ramus); M: mass; PCSA: PCSA; s: scaled (mass or PCSA). Sigificant results (p-value < 0.05) are indicated in bold.

Sheet 1

Results of the 2B-PLS analyses

- **2B-PLS between shape and PCSA for the complete mandible**

Covariance explained by the singular values

singular value	% total covar.	Corr. coefficient	p-value
0.020637	96.7282	0.734	0.001
0.002495	1.4141	0.612	0.598
0.001888	0.8100	0.574	0.419
0.001356	0.4175	0.610	0.711
0.001005	0.2296	0.517	0.933
0.000795	0.1437	0.621	0.975
0.000769	0.1343	0.549	0.555
0.000580	0.0763	0.526	0.754
0.452	0.0464	0.491	0.730

- **2B-PLS between shape and mass for the complete mandible**

Covariance explained by the singular values

singular value	% total covar.	Corr. coefficient	p-value
0.029561	98.7778	0.739	0.001
0.002257	0.5757	0.585	0.300
0.001479	0.2474	0.480	0.392
0.001186	0.1590	0.493	0.250
0.000878	0.0871	0.566	0.482
0.000776	0.0680	0.552	0.199
0.000607	0.0416	0.560	0.277
0.000516	0.0301	0.631	0.107
0.343	0.0133	0.541	0.617

- **2B-PLS between shape and scaled PCSA for the complete mandible**

Covariance explained by the singular values

singular value	% total covar.	Corr. coefficient	p-value
0.009985	87.818	0.636	0.001
0.002448	5.278	0.598	0.523
0.001788	2.815	0.613	0.495
0.001369	1.652	0.604	0.586
0.001027	0.929	0.504	0.844
0.000819	0.590	0.549	0.913
0.000707	0.440	0.642	0.802
0.000581	0.297	0.530	0.685
0.453	0.180	0.489	0.679

- **2B-PLS between shape and scaled mass for the complete mandible**

Covariance explained by the singular values

singular value	% total covar.	Corr. coefficient	p-value
0.013189	94.5879	0.698	0.001
0.002367	3.0463	0.578	0.178
0.001276	0.8850	0.499	0.790
0.000886	0.4270	0.557	0.970
0.000832	0.3765	0.543	0.622
0.000780	0.3310	0.552	0.144
0.000595	0.1923	0.544	0.278
0.000455	0.1128	0.603	0.305
0.000275	0.0412	0.429	0.900

- **2B-PLS between allometry-free shape and scaled PCSA for the complete mandible**

Covariance explained by the singular values

singular value	% total covar.	Corr. coefficient	p-value
0.007648	81.745	0.676	0.001
0.002387	7.965	0.610	0.308
0.001730	4.181	0.647	0.308
0.001346	2.532	0.607	0.363
0.000966	1.305	0.530	0.842
0.000772	0.832	0.616	0.908
0.000701	0.687	0.650	0.578
0.000578	0.468	0.525	0.440
0.000451	0.285	0.495	0.498

- **2B-PLS between allometry-free shape and scaled mass for the complete mandible**

Covariance explained by the singular values

singular value	% total covar.	Corr. coefficient	p-value
0.010363	92.1662	0.735	0.001
0.002198	4.1457	0.611	0.080
0.001267	1.3785	0.493	0.537
0.000880	0.6641	0.550	0.881
0.000832	0.5942	0.543	0.343
0.000775	0.5152	0.554	0.039
0.000595	0.3035	0.545	0.108
0.000454	0.1771	0.619	0.153
0.000254	0.0555	0.630	0.934

- **2B-PLS between shape and PCSA for the posterior part of the mandible**

Covariance explained by the singular values

singular value	% total covar.	Corr. coefficient	p-value
0.013949	89.329	0.657	0.001
0.003050	4.270	0.698	0.424
0.002314	2.458	0.545	0.457
0.001712	1.345	0.565	0.757
0.001583	1.150	0.523	0.314
0.001119	0.575	0.484	0.841
0.000997	0.457	0.504	0.557
0.000752	0.260	0.509	0.698
0.000585	0.157	0.489	0.684

- **2B-PLS between shape and mass for the posterior part of the mandible**

Covariance explained by the singular values

singular value	% total covar.	Corr. coefficient	p-value
0.020439	95.7775	0.684	0.001
0.003004	2.0693	0.535	0.050
0.001836	0.7730	0.562	0.351
0.001458	0.4876	0.631	0.340
0.001233	0.3483	0.580	0.205
0.001005	0.2315	0.538	0.180
0.000806	0.1491	0.502	0.191
0.000728	0.1216	0.525	0.015
0.000429	0.0421	0.518	0.692

- **2B-PLS between shape and scaled PCSA for the posterior part of the mandible**

Covariance explained by the singular values

singular value	% total covar.	Corr. coefficient	p-value
0.004475	43.890	0.648	0.411
0.003090	20.922	0.625	0.247
0.002693	15.898	0.520	0.029
0.001850	7.506	0.584	0.357
0.001587	5.521	0.529	0.187
0.001116	2.728	0.486	0.755
0.000824	1.487	0.537	0.956
0.000741	1.205	0.547	0.690
0.000621	0.844	0.449	0.426

- **2B-PLS between shape and scaled mass for the posterior part of the mandible**

singular value	% total covar.	Corr. coefficient	p-value
0.005560	61.130	0.683	0.155
0.003242	20.781	0.627	0.003
0.001859	6.833	0.549	0.226
0.001469	4.265	0.638	0.217
0.001117	2.465	0.485	0.443
0.001036	2.123	0.632	0.074
0.000783	1.213	0.483	0.197
0.000676	0.903	0.489	0.048
0.000381	0.287	0.456	0.732

Results of the 2-Blocks Partial Least Square Analyses (2BPLS)

- **2B-PLS between allometry-free shape and scaled PCSA for the posterior part of the mandible**

Covariance explained by the singular values

singular value	% total covar.	Corr. coefficient	p-value
0.004475	47.292	0.648	0.290
0.003029	21.674	0.698	0.136
0.002234	11.785	0.559	0.195
0.001699	6.819	0.609	0.415
0.001566	5.793	0.529	0.063
0.001115	2.937	0.488	0.501
0.000823	1.601	0.535	0.874
0.000738	1.287	0.537	0.504
0.000586	0.812	0.508	0.428

- **2B-PLS between allometry-free shape and scaled mass for the posterior part of the mandible**

Covariance explained by the singular values

singular value	% total covar.	Corr. coefficient	p-value
0.005536	65.248	0.677	0.075
0.002738	15.961	0.615	0.022
0.001854	7.317	0.557	0.099
0.001452	4.488	0.638	0.077
0.001052	2.357	0.568	0.429
0.000989	2.083	0.572	0.053
0.000774	1.276	0.489	0.095
0.000676	0.972	0.490	0.010
0.000374	0.297	0.502	0.620

Sheet 2

Comparison tests of the 2B-PLS

P-values

			Mass						PCSA					
			complete mdb			ramus			complete mdb			ramus		
			S-M	S-sM	aS-sM	rS-M	rS-sM	arS-sM	S-PCSA	S-sPCSA	aS-sPCSA	rS-PCSA	rS-sPCSA	arS-sPCSA
Mass	complete mdb	S-M	1.00000											
		S-sM	0.35826	1.0000										
		aS-sM	0.30590	0.4485	1.0000									
	ramus	rS-M	0.07729	0.1396	0.1552	1.0000								
		rS-sM	0.06379	0.1197	0.1324	0.4752	1.0000							
		arS-sM	**0.04839**	0.0933	0.1022	0.4114	0.4331	1.0000						
PCSA	complete mdb	S-PCSA	0.48316	0.3755	0.3234	0.0856	0.0713	0.0545	1.0000					
		S-sPCSA	0.13803	0.2275	0.2545	0.3781	0.3519	0.2971	0.1496	1.000				
		aS-sPCSA	0.30590	0.4485	0.5000	0.1552	0.1324	0.1022	0.3234	0.255	1.0000			
	ramus	rS-PCSA	**0.03668**	0.0717	0.0779	0.3431	0.3607	0.4240	**0.0415**	0.243	0.0779	1.0000		
		rS-sPCSA	**0.01178**	**0.0261**	**0.0266**	0.1980	0.2071	0.2622	0.0139	0.127	**0.0266**	0.3377	1.0000	
		arS-sPCSA	0.00913	**0.0206**	**0.0207**	0.1689	0.1760	0.2266	0.0109	0.107	**0.0207**	0.2982	0.4524	1.00000

S shape of the complete mandible
rS ramus shape
a allometry-free (shape or ramus shape)
M mass
PCSA PCSA
s scaled (mass or PCSA)

Z scores

			Mass						PCSA					
			complete mdb			ramus			complete mdb			ramus		
			S-M	S-sM	aS-sM	rS-M	rS-sM	arS-sM	S-PCSA	S-sPCSA	aS-sPCSA	rS-sPCSA	rS-sPCSA	arS-SPCSA
Mass	complete mdb	S-M	0.0000											
		S-sM	0.3631	0.000										
		aS-sM	0.5075	0.129	0.000									
	ramus	rS-M	1.4235	1.082	1.014	0.0000								
		rS-sM	1.5237	1.176	1.115	0.0622	0.0000							
		arS-sM	**1.6607**	1.321	1.269	0.2239	0.1685	0.000						
PCSA	complete mdb	S-PCSA	0.0422	0.317	0.458	1.3684	1.4658	1.602	0.0000					
		S-sPCSA	1.0892	0.747	0.660	0.3103	0.3802	0.533	1.0383	0.000				
		aS-sPCSA	0.5075	0.129	0.000	1.0144	1.1150	1.269	0.4581	0.660	0.000			
	ramus	rS-PCSA	**1.7906**	1.463	1.419	0.4041	0.3565	0.192	**1.7332**	0.698	1.419	0.000		
		rS-sPCSA	**2.2643**	**1.941**	**1.933**	0.8487	0.8167	0.637	2.1999	1.139	**1.933**	0.419	0.000	
		arS-sPCSA	2.3604	**2.041**	**2.040**	0.9584	0.9307	0.750	2.2956	1.243	**2.040**	0.529	0.120	0.000

S shape of the complete mandible
rS ramus shape
a allometry-free (shape or ramus shape)
M mass
PCSA PCSA
s scaled (mass or PCSA)

2.5. Fig. S1.

Distribution of the specimens with a visualisation of the differences between large and small specimens relative to consensus shape. Ages are indicated by colors. Beagles are in green and other breed names are indicated following Table 1.

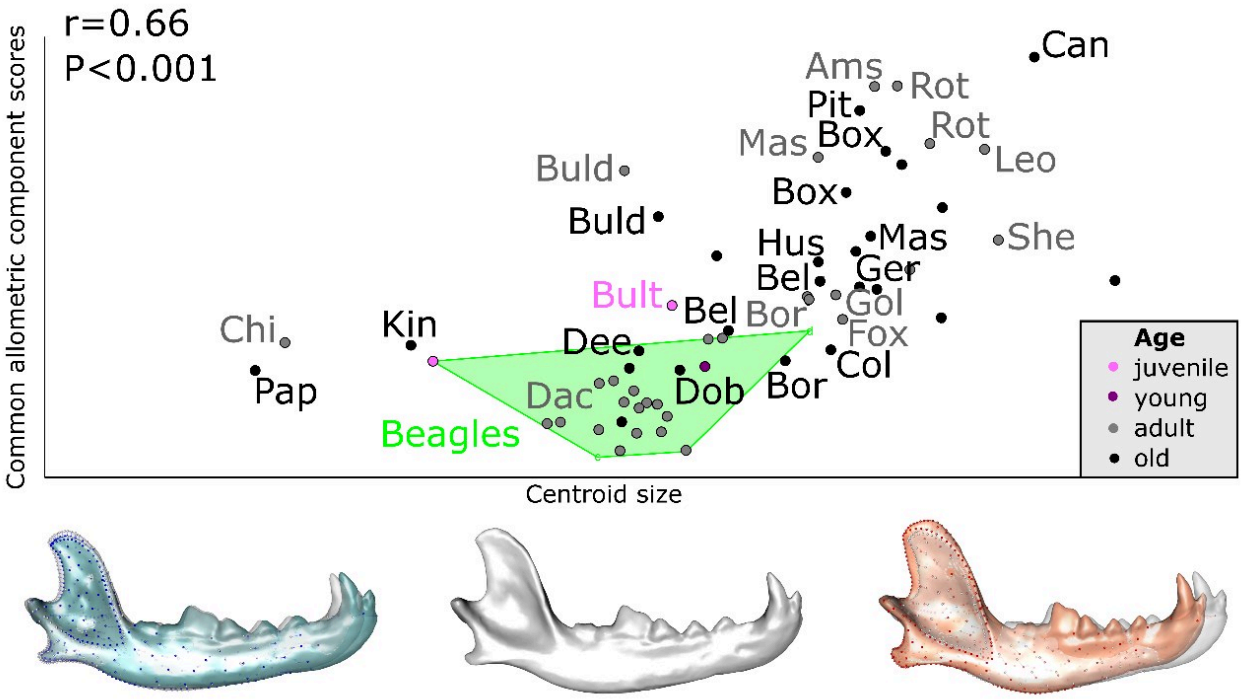

2.6. Fig. S2.

PCA describing variation in A) mass or B) scaled mass of the jaw muscles. Histograms represent the loadings of the original variables on the axes. Dig: Digastric; MS: masseter pars superficialis; MP: masseter pars profunda; ZMA: masseter pars zygomaticomandibularis anterior; ZMP: masseter pars zygomaticomandibularis posterior; SZ: temporalis pars suprazygomatica; TS: temporalis pars superficialis; TP: temporalis pars profunda; P: pterygoids. Ages are indicated by colors. Beagles are in green and other breed names are indicated following Table 1.

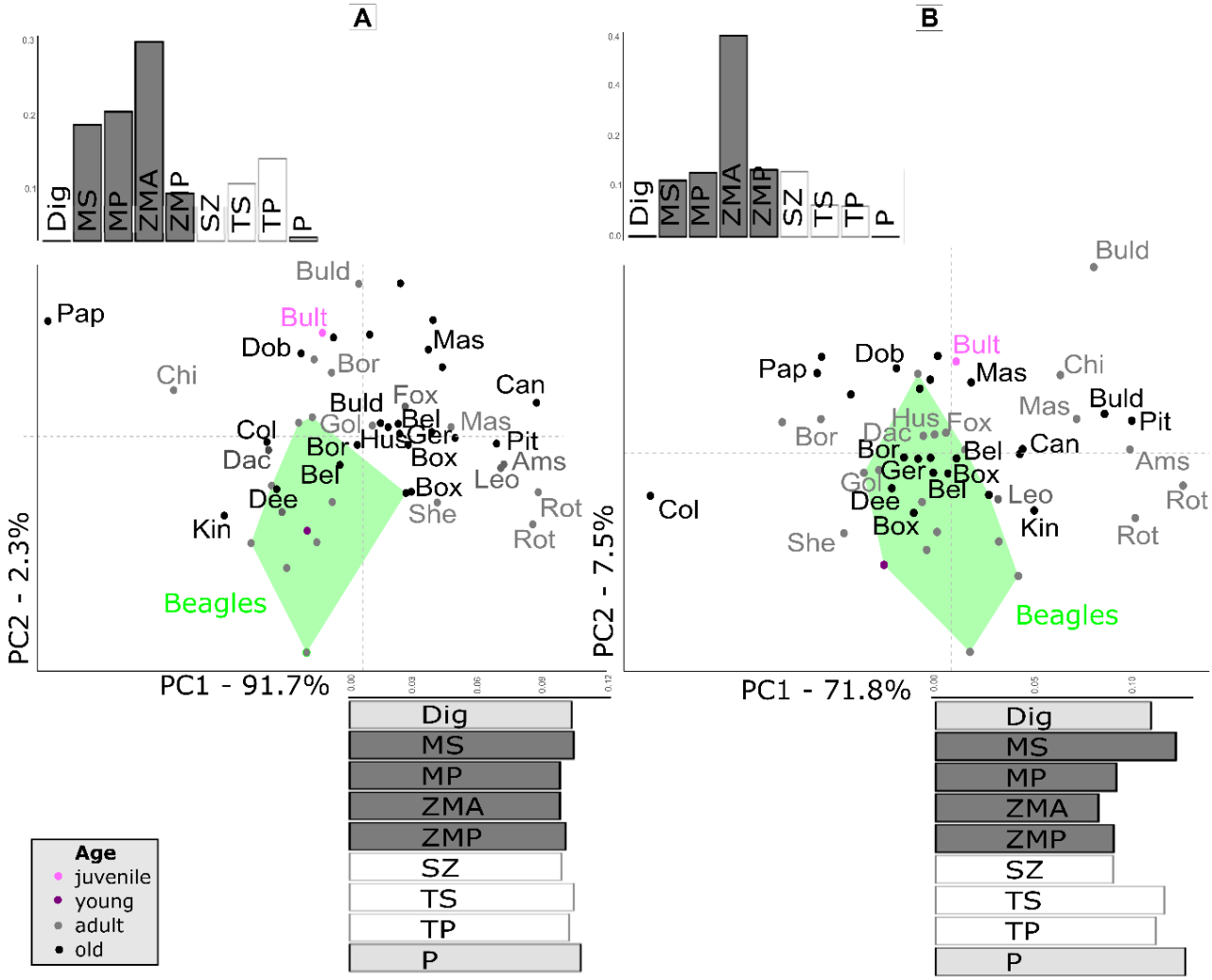

2.7. Fig. S3.

2-Block Partial Least Square Analyses between mandibular shape and the PCSA of jaw muscles, with muscle vectors and shapes at the minimum and maximum of the PLS axis. Illustrations represent the deformations from the consensus to the extreme of the axis in lateral, dorsal and caudal views. Dig: Digastric; MS: masseter pars superficialis; MP: masseter pars profunda; ZMA: masseter pars zygomaticomandibularis anterior; ZMP: masseter pars zygomaticomandibularis posterior; SZ: temporalis pars suprazygomatica; TS: temporalis pars superficialis; TP: temporalis pars profunda; P: pterygoids. Ages are indicated by colors. Beagles are in green and other breed names are indicated following Table 1.

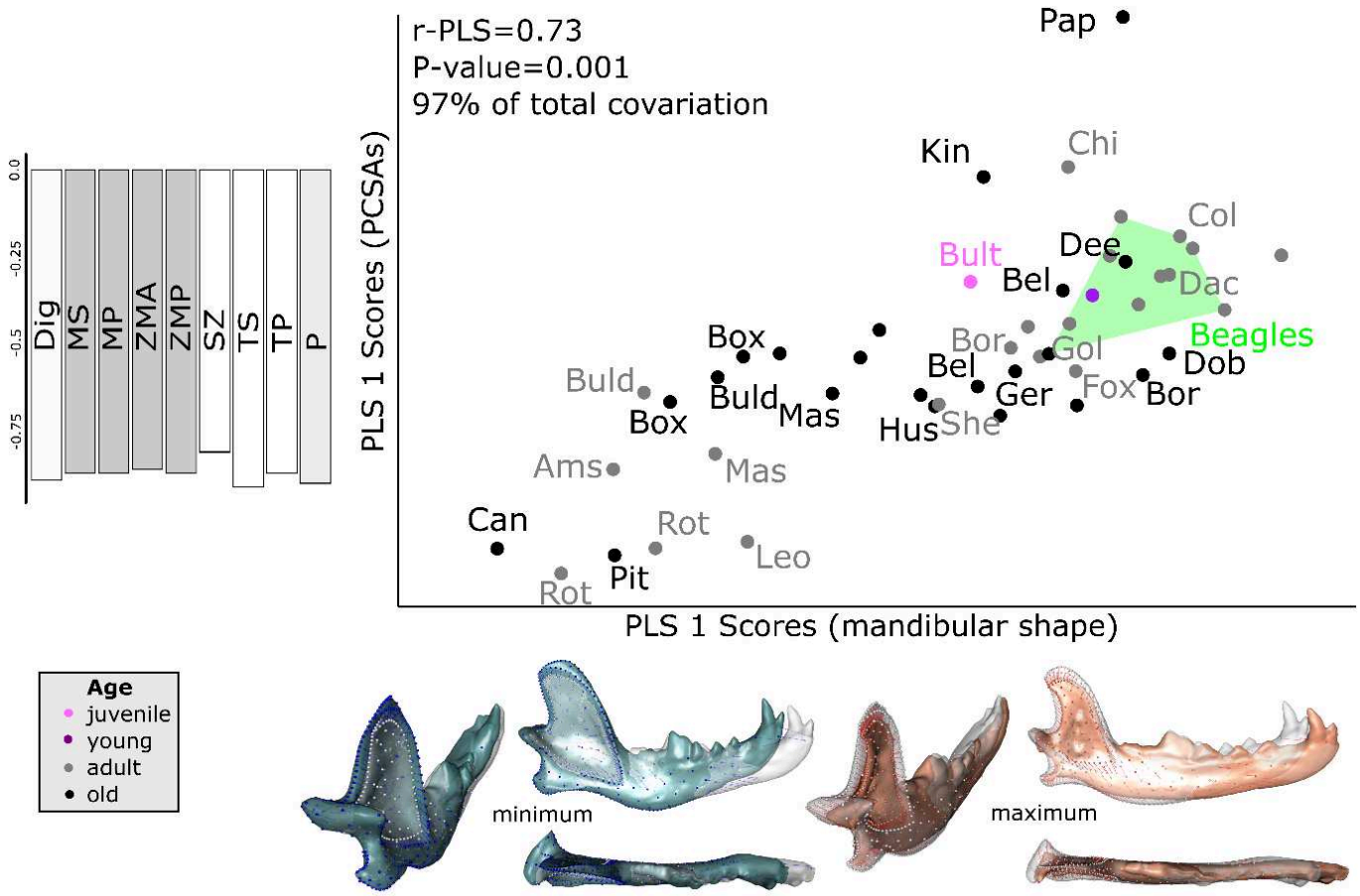

2.8. Fig. S4.

2-Block Partial Least Square Analyses between mandibular shape and the mass of jaw muscles, with muscle vectors and shapes at the minimum and maximum of the PLS axis. Illustrations represent the deformations from the consensus to the extreme of the axis in lateral, dorsal and caudal views. Dig: Digastric; MS: masseter pars superficialis; MP: masseter pars profunda; ZMA: masseter pars zygomaticomandibularis anterior; ZMP: masseter pars zygomaticomandibularis posterior; SZ: temporalis pars suprazygomatica; TS: temporalis pars superficialis; TP: temporalis pars profunda; P: pterygoids. Ages are indicated by colors. Beagles are in green and other breed names are indicated following Table 1.

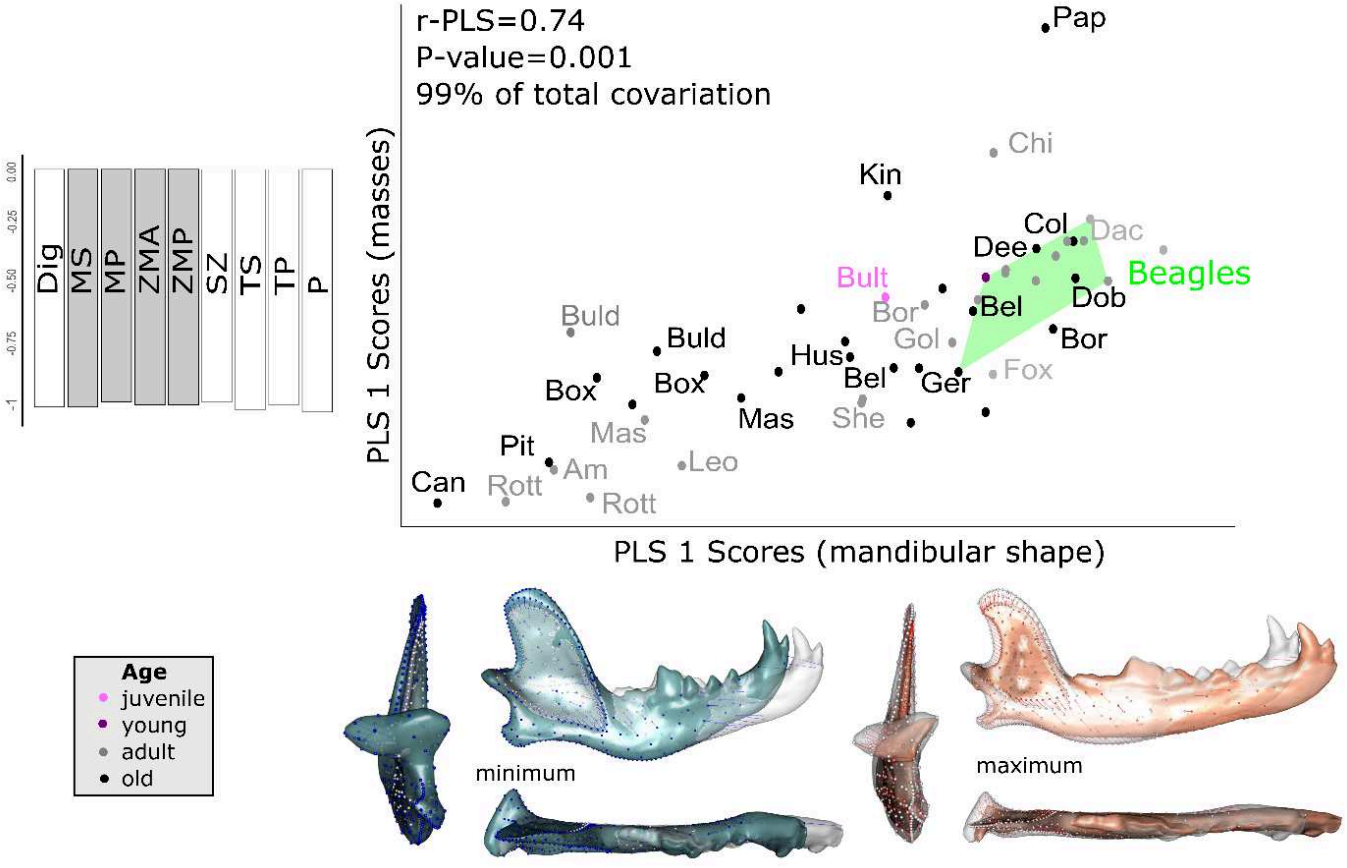

2.9. Fig. S5.

2-Block Partial Least Square Analyses between the shape of the ramus and the PCSA of jaw muscles, with muscle vectors and shapes at the minimum and maximum of the PLS axis. Illustrations represent the deformations from the consensus to the extreme of the axis in lateral, dorsal and caudal views. Dig: Digastric; MS: masseter pars superficialis; MP: masseter pars profunda; ZMA: masseter pars zygomaticomandibularis anterior; ZMP: masseter pars zygomaticomandibularis posterior; SZ: temporalis pars suprazygomatica; TS: temporalis pars superficialis; TP: temporalis pars profunda; P: pterygoids. Ages are indicated by colors. Beagles are in green and other breed names are indicated following Table 1.

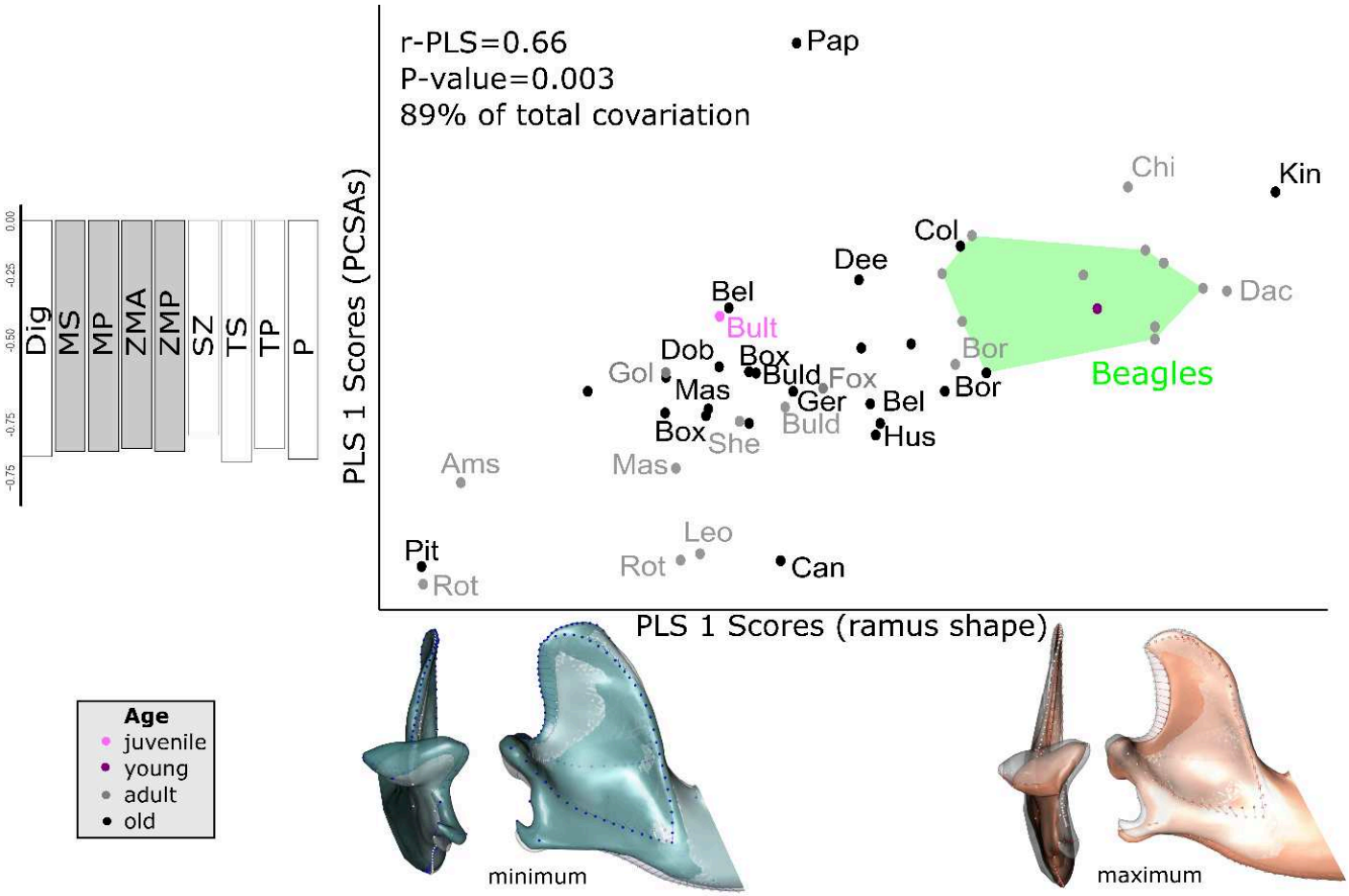

2.10. Fig. S6.

2-Block Partial Least Square Analyses between the shape of the ramus and the mass of jaw muscles, with muscle vectors and shapes at the minimum and maximum of the PLS axis. Illustrations represent the deformations from the consensus to the extreme of the axis in lateral, dorsal and caudal views. Dig: Digastric; MS: masseter pars superficialis; MP: masseter pars profunda; ZMA: masseter pars zygomaticomandibularis anterior; ZMP: masseter pars zygomaticomandibularis posterior; SZ: temporalis pars suprazygomatica; TS: temporalis pars superficialis; TP: temporalis pars profunda; P: pterygoids. Ages are indicated by colors. Beagles are in green and other breed names are indicated following Table 1.

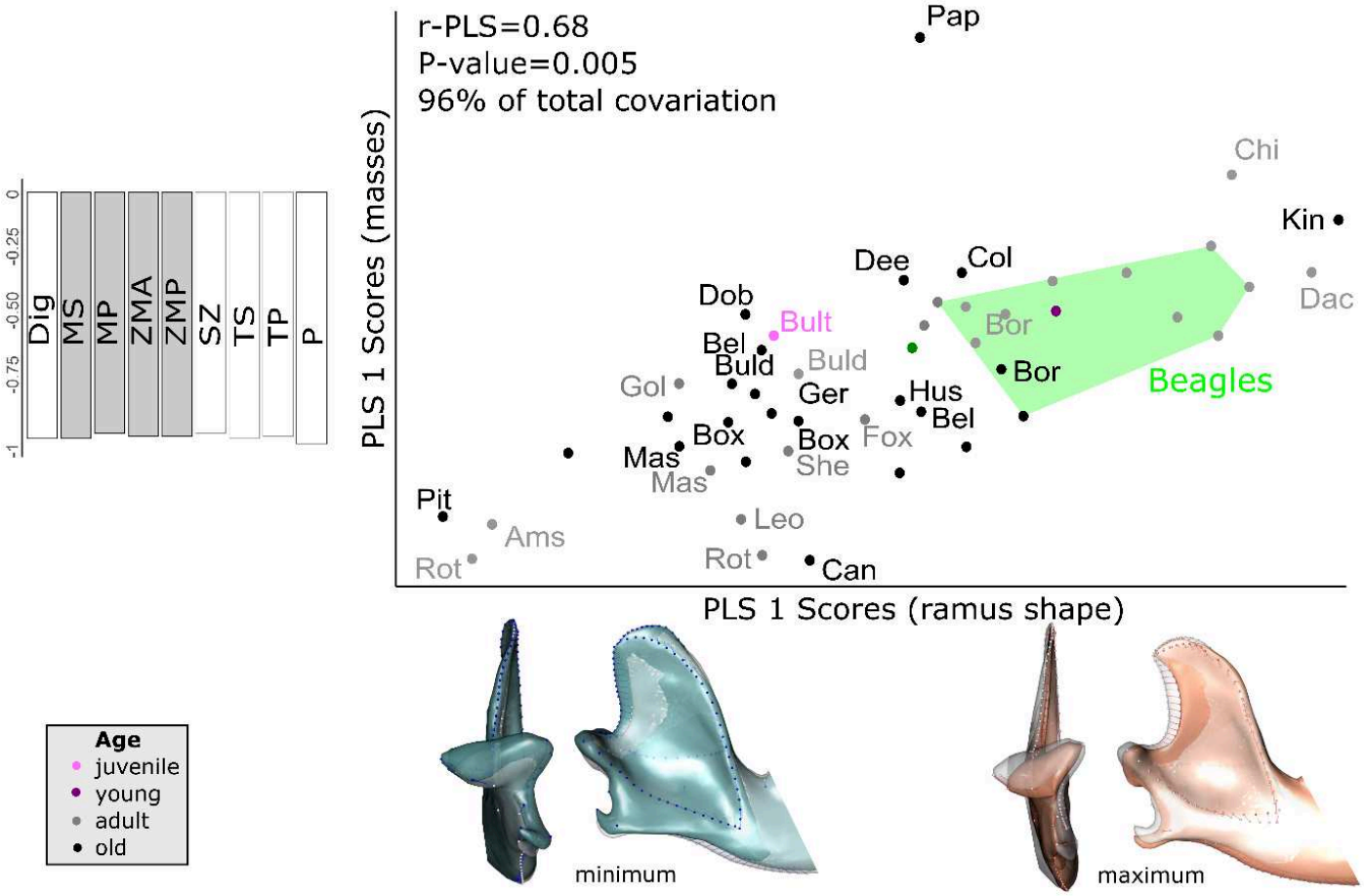

2.11. Fig. S7.

2-Block Partial Least Square Analyses between mandibular shape and the scaled mass of jaw muscles, with muscle vectors and shapes at the minimum and maximum of the PLS axis. Illustrations represent the deformations from the consensus to the extreme of the axis in lateral, dorsal and caudal views. Dig: Digastric; MS: masseter pars superficialis; MP: masseter pars profunda; ZMA: masseter pars zygomaticomandibularis anterior; ZMP: masseter pars zygomaticomandibularis posterior; SZ: temporalis pars suprazygomatica; TS: temporalis pars superficialis; TP: temporalis pars profunda; P: pterygoids. Ages are indicated by colors. Beagles are in green and other breed names are indicated following Table 1.

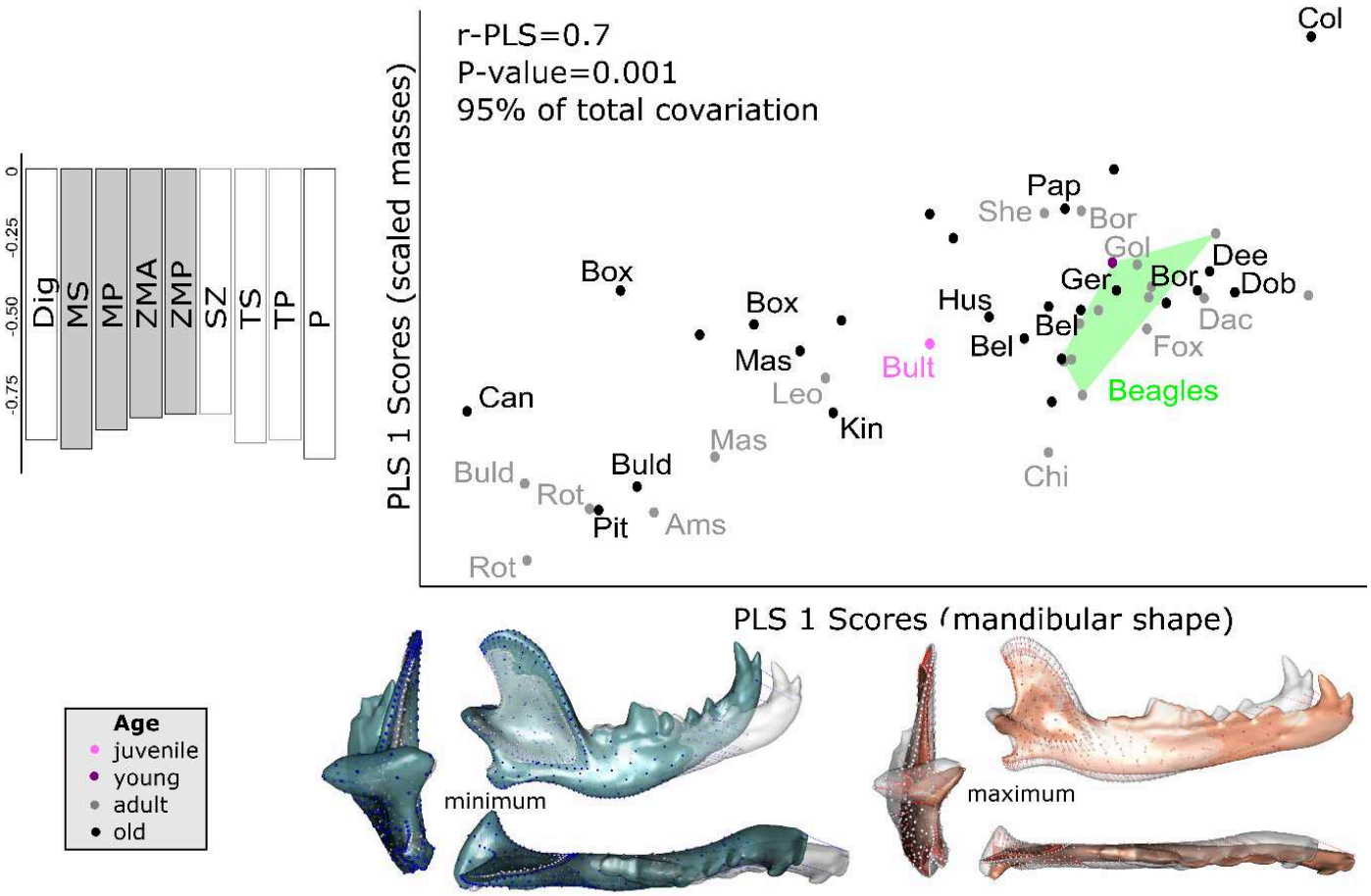

2.12. Fig. S8.

2-Block Partial Least Square Analyses between the shape of the ramus and the scaled PCSA of jaw muscles, with muscle vectors and shapes at the minimum and maximum of the PLS axis. Illustrations represent the deformations from the consensus to the extreme of the axis in lateral, dorsal and caudal views. Dig: Digastric; MS: masseter pars superficialis; MP: masseter pars profunda; ZMA: masseter pars zygomaticomandibularis anterior; ZMP: masseter pars zygomaticomandibularis posterior; SZ: temporalis pars suprazygomatica; TS: temporalis pars superficialis; TP: temporalis pars profunda; P: pterygoids. Ages are indicated by colors. Beagles are in green and other breed names are indicated following Table 1.

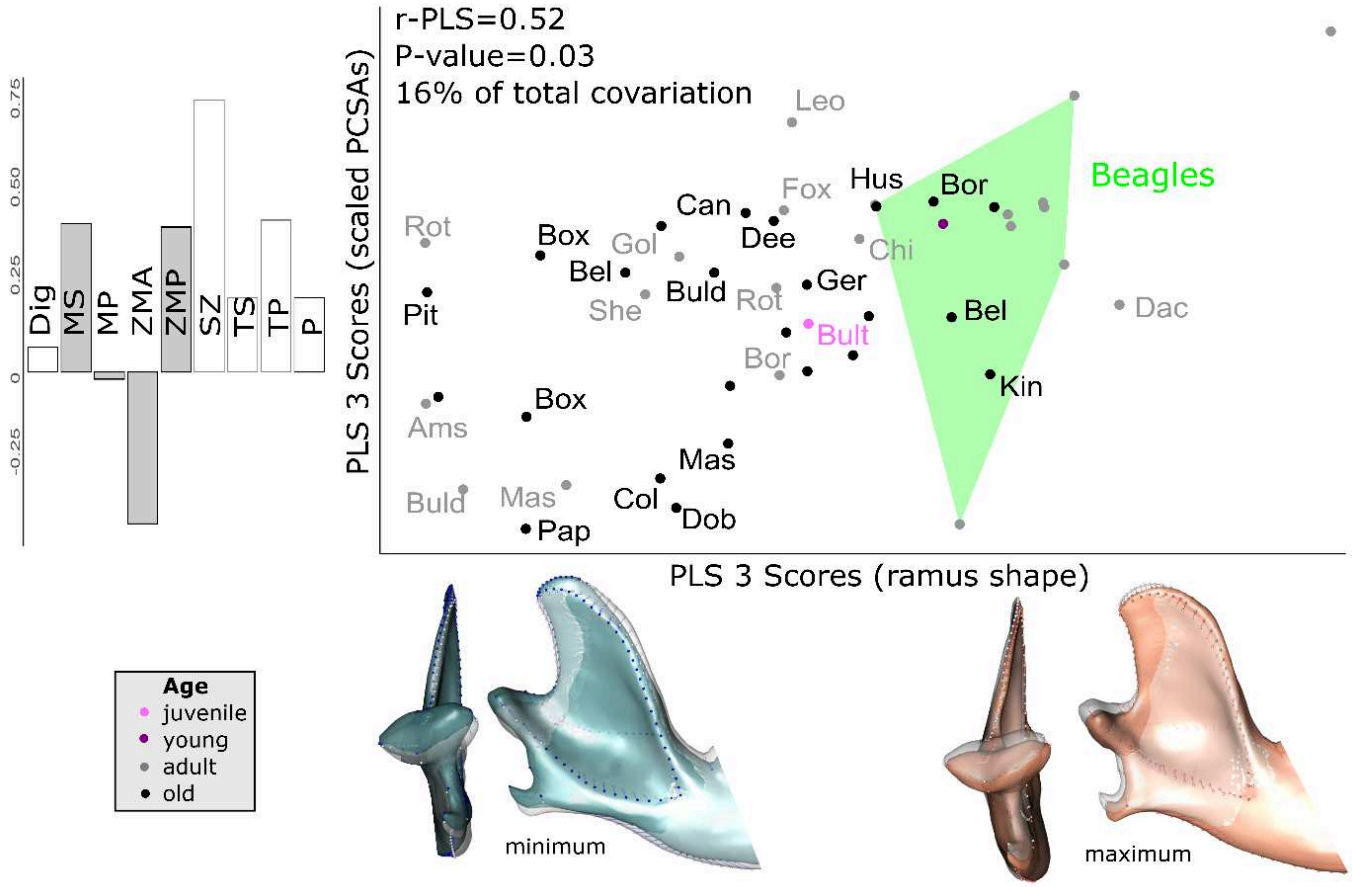

2.13. Fig. S9.

2-Block Partial Least Square Analyses between between allometry-free mandibular shape and the scaled mass of jaw muscles, with muscle vectors and shapes at the minimum and maximum of the PLS axis. Illustrations represent the deformations from the consensus to the extreme of the axis in lateral, dorsal and caudal views. Dig: Digastric; MS: masseter pars superficialis; MP: masseter pars profunda; ZMA: masseter pars zygomaticomandibularis anterior; ZMP: masseter pars zygomaticomandibularis posterior; SZ: temporalis pars suprazygomatica; TS: temporalis pars superficialis; TP: temporalis pars profunda; P: pterygoids. Ages are indicated by colors. Beagles are in green and other breed names are indicated following Table 1.

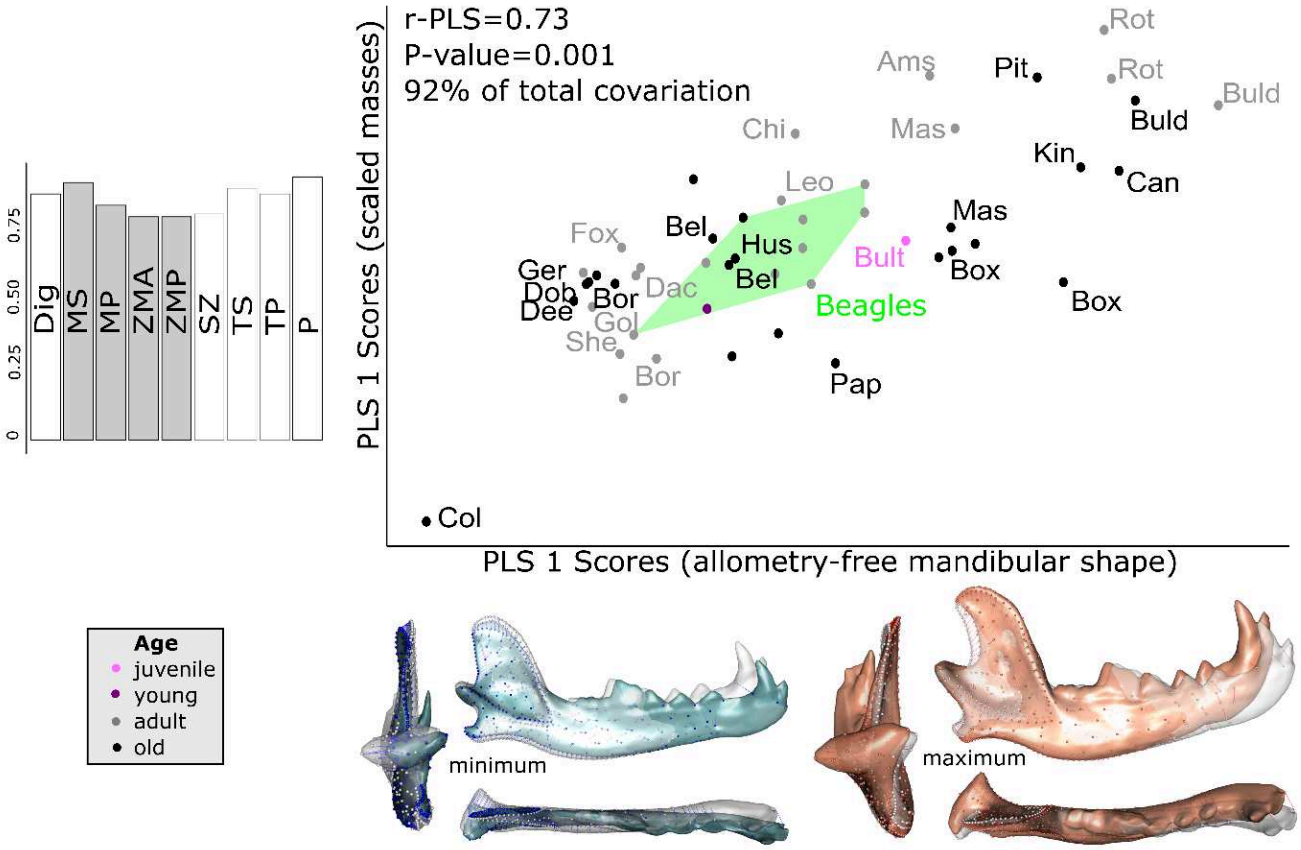

2.14. Fig. S10.

2-Block Partial Least Square Analyses between the allometry-free shape of the ramus and the scaled mass of jaw muscles, with muscle vectors and shapes at the minimum and maximum of the PLS axis. Illustrations represent the deformations from the consensus to the extreme of the axis in lateral, dorsal and caudal views. Dig: Digastric; MS: masseter pars superficialis; MP: masseter pars profunda; ZMA: masseter pars zygomaticomandibularis anterior; ZMP: masseter pars zygomaticomandibularis posterior; SZ: temporalis pars suprazygomatica; TS: temporalis pars superficialis; TP: temporalis pars profunda; P: pterygoids. Ages are indicated by colors. Beagles are in green and other breed names are indicated following Table 1.

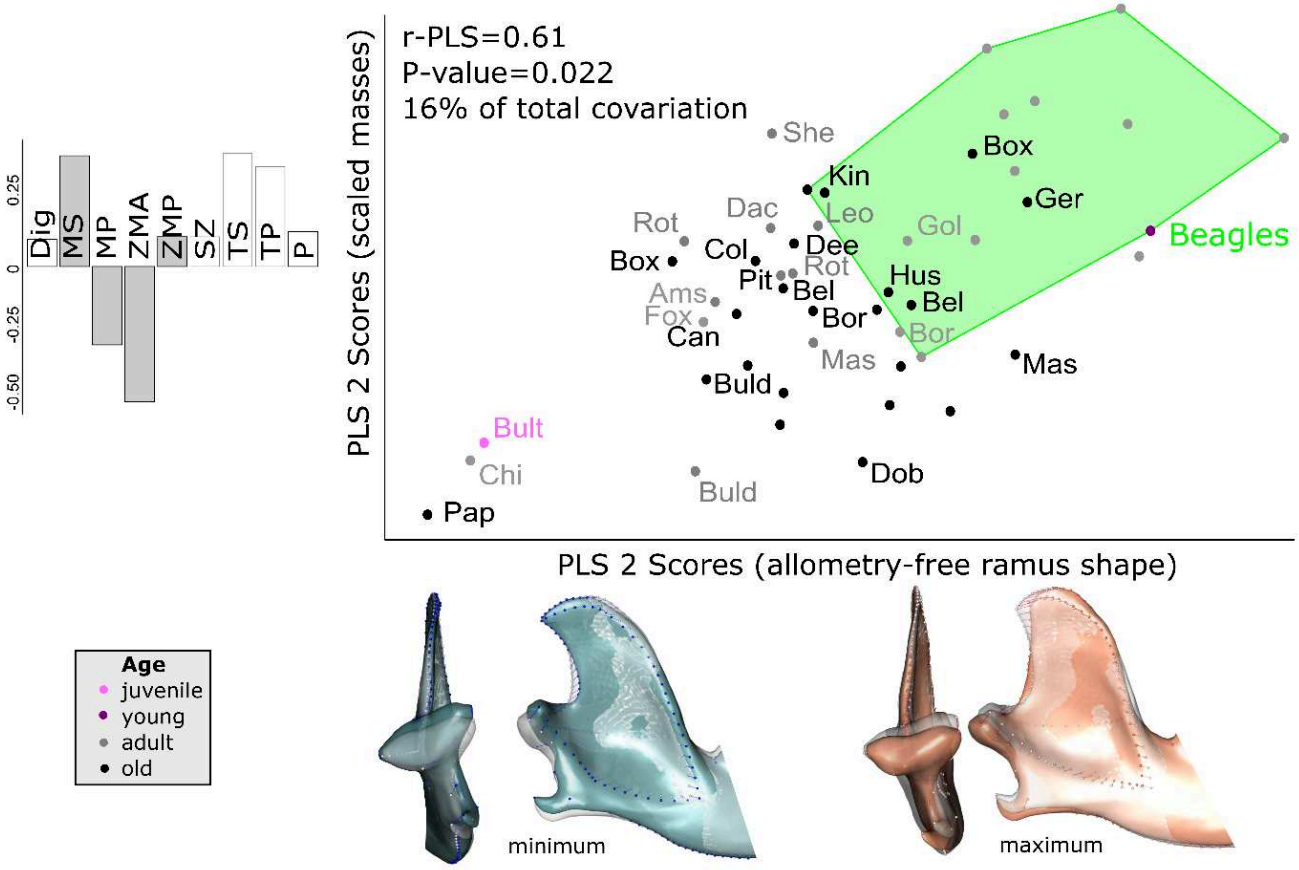

3. Part2 – Article 2 – supplementary material

3.1. Table S1.

Details of the specimen used in this study including raw jaw muscles masses, pennation angles, fiber lengths and PCSAs.

Sheet 1 Sample data, including muscle masses, fiber lengths, pennation angles and PCSAs

Morphotypes:

D dolichocephalic
M mesocephalic
B brachycephalic

headl head length
headw head width
ci cephalic index

Sheet 3

Age	Female	Male	neutered female	neutered male	unknown	Total
juvenile					2	2
young		1			1	2
adult	7	11		1	14	33
old	2	11	1		8	22
Total	9	23	1	1	25	59

Sheet 2 Sample size according to age and sex

													Digastric					
ID	BREED	AGE	BIRTHDATE	SEX	headl	headw	ci	Morphotype	BODY MASS (kg)	mandible	skull	formol	muscle length (mm)	fiber length (mm)	angle (°)	mass (g)	PCSA (N/cm2)	muscle length (mm)
BEAGLE1	BEAGLE	adult			131,5	88	67 M			yes	yes	yes						
BEAGLE2	BEAGLE	adult			135,2	91	67 M			yes	yes	yes						
M1	BEAGLE	young			120,9	83	69 M			yes	yes	yes						
M2	BEAGLE	adult			126,4	80	63 M			yes	yes	yes						
M3	BEAGLE	adult			138,7	98	71 B			yes	yes	yes						
M4	BEAGLE	old			139,3	88	63 M			yes	yes	yes						
M5	BEAGLE	adult			116,8	87	74 B			yes	yes	yes						
M6	BEAGLE	adult			120,7	83	69 M			yes	yes	yes						
M8	BEAGLE	juvenile			122,6	74	60 M			yes	yes	yes						
Ma-1	BEAGLE	old			130,9	80	61 M			yes	yes	yes						
N-C1	BEAGLE	adult			/ /	/ /				yes	no	no						
N-C10	BEAGLE	adult			133	82	62 M			yes	yes	no	77,39	31,27	0,00	8,80	2,66	69,58
N-C11	COLLEY	old			172	79	46 D			yes	yes	no	85,66	37,16	0,00	6,00	1,52	71,32
N-C12	BEAGLE	adult			129	84	65 M			yes	yes	no	84,44	38,65	0,00	7,50	1,83	59,52
N-C13	BEAGLE	adult			132	91	69 M			yes	yes	no	92,89	35,79	0,00	11,10	2,93	73,18
N-C14	SHEPHERD DOG	old			196	116	59 D			yes	yes	no	112,46	44,85	0,00	17,00	3,58	78,85
N-C15	SHEPHERD DOG	old			176	111	63 M			yes	yes	no	101,36	37,02	0,00	13,40	3,42	77,27
N-C16	HUNTING DOG	old			139	99	72 B			yes	yes	no	100,85	35,87	0,00	9,00	2,37	70,87
N-C17	BOXER	old			138	116	84 B			yes	yes	no	124,32	46,10	0,00	23,30	4,77	87,16
N-C18	BELGIAN SHEPHERD	old			171	99	58 D			yes	yes	no	97,75	35,50	0,00	14,90	3,96	71,76
N-C19	GOLDEN	adult	10/04/2007	female	173	102	59 D		19	yes	yes	no	97,12	44,98	0,00	12,90	2,71	61,39
N-C2	BEAGLE	young		male	140	92	66 M		11	yes	yes	no	78,30	35,77	0,00	8,97	2,37	61,30
N-C20	PAPILLON	adult	30/09/2002	male	83	69	83 B		4	yes	yes	no	59,85	24,97	0,00	3,60	1,36	35,26
N-C21	KING CHARLES	old	17/05/2005	male	95	77	81 B		7	yes	yes	no	58,36	26,64	0,00	4,80	1,70	56,53
N-C22		old	14/03/2007	male	176	108	61 M		26	yes	yes	no	105,34	33,21	0,00	30,50	8,66	69,70
N-C23		old	21/10/2009	neutered female	148	116	78 B		35	yes	yes	no	135,31	59,43	0,00	23,90	3,79	78,84
N-C3	BEAGLE	adult			143	96	67 M			yes	yes	no	88,70	49,15	0,00	8,00	1,54	60,90
N-C4	BEAGLE	adult			137	86	63 M			yes	yes	no	89,30	41,53	0,00	8,00	1,82	70,10
N-C5	BULLDOG	adult	12years old	neutered male	101	86	85 B			yes	yes	no	72,00	38,55	0,00	13,13	3,21	70,50
N-C6	BEAGLE	adult		female	124	79	63 M		8	yes	yes	no	75,00	39,40	0,00	6,75	1,62	56,40
N-C7	BEAGLE	adult		female	118	79	67 M		9	yes	yes	no	78,90	39,40	0,00	8,72	2,09	59,70
N-C8	BEAGLE	adult		male	143	94	66 M		11	yes	yes	no	83,70	37,35	0,00	10,81	2,73	62,70
N-C9	SHEPHERD DOG	adult			143	82	57 D			yes	yes	no	71,79	31,26	0,00	6,80	2,05	53,10
Ny-C1		adult	2 years old	female	185,5	108	58 D			yes	yes	no	100,80	46,05	0,00	19,40	3,97	90,20
Ny-C10	GERMAN SHEPHERD	old		female	177	92	52 D			yes	yes	no	98,00	37,50	0,00	15,80	3,97	62,00
Ny-C11	MASTIFF	old		male	168	112	66 M			yes	yes	no	103,00	47,00	0,00	22,10	4,44	87,00
Ny-C12	FOX TERRIER	adult		male	160	102	63 M			yes	yes	no	99,00	48,00	0,00	19,60	3,85	77,00
Ny-C13	HUSKY	adult		female	157	93	59 D			yes	yes	no	90,00	30,00	0,00	16,49	5,19	80,00
Ny-C14	CANE CORSO	adult		male	172	140	81 B			yes	yes	no	100,00	60,00	5,00	32,80	5,14	110,00
Ny-C15	LEONBERG	adult		male	198	115	58 D			yes	yes	no	110,00	44,00	0,00	33,10	7,10	100,00
Ny-C16	BULLDOG	old		male	108	100	93 B			yes	yes	no	90,00	35,00	0,00	13,97	3,77	80,00
Ny-C17	BORDER COLLIE	old		male	164	99	59 D			yes	yes	no	75,00	26,00	0,00	11,27	4,09	70,00
Ny-C18	ROTTWEILLER	adult		male	182	128	70 B			yes	yes	no	12,00	39,50	10,00	46,60	10,96	105,00
Ny-C19	CHIHUAHUA	adult		male	92	66	72 B			yes	yes	no	60,00	22,50	0,00	2,59	1,09	42,00
Ny-C20	PITBULL	old		male	167	123	74 B			yes	yes	no	105,00	36,25	0,00	33,20	8,64	95,00
Ny-C21	BOXER	old		male	142	114	80 B			yes	yes	no	115,00	46,00	0,00	23,40	4,80	95,00
Ny-C22	SHETLAND SHEEPDOG	adult		male	213	108	50 D			yes	yes	no	110,00	39,50	0,00	23,30	5,56	70,00
Ny-C23	BELGIAN SHEPHERD	old		male	147	99	67 M			yes	yes	no	90,00	36,00	0,00	10,04	2,63	70,00
Ny-C24	DEERHOUND	old		female	142	81	57 D			yes	yes	no	70,00	40,00	0,00	7,11	1,68	65,00
Ny-C25		adult		male	168	90	54 D			yes	yes	no	75,00	27,50	0,00	8,96	3,07	60,00
Ny-C26	DOBERMANN	old		male	151	89	59 D			yes	yes	no	70,00	31,50	0,00	7,49	2,24	60,00
Ny-C27	BORDER COLLIE	adult		female	165	98	59 D			yes	yes	no	80,00	33,00	0,00	10,69	3,06	60,00
Ny-C28	ROTTWEILLER	adult		male	170	131	77 B			yes	yes	no	110,00	45,00	0,00	47,70	10,00	110,00
Ny-C3	DACHSHUND	adult	6 years old	female	146	81	55 D			yes	yes	no	56,40	33,13	0,00	6,68	1,90	60,00
Ny-C4	MASTIFF	adult		male	161	112	70 M			yes	yes	no	113,00	36,50	0,00	26,70	6,90	84,00
Ny-C5	BEAGLE	old		male	160	101	63 M			yes	yes	no	101,00	37,50	0,00	16,70	4,20	81,00
Ny-C6	SHEPHERD DOG	old		male	193	109	56 D			yes	yes	no	112,00	46,00	0,00	21,40	4,39	92,00
Ny-C8	AMSTAFF	adult			162	118	73 B			yes	yes	no	115,00	50,50	0,00	35,10	6,56	106,00
Ny-C9	BULL TERRIER	juvenile			135	94	70 M			yes	yes	no	93,00	35,50	0,00	10,40	2,76	60,00
												MEAN				**16,26**	**3,85**	**73,48**
												MIN						**35,26**
												MAX						**110,00**

	Masseter superficialis				Masseter profundus					Zygomaticomandibularis pars anterior					Zygomaticomandibularis pars po:		
ID	fiber length (mm)	angle (°)	mass (g)	PCSA (N/cm2)	muscle length (mm)	fiber length (mm)	angle (°)	mass (g)	PCSA (N/cm2)	muscle length (mm)	fiber length (mm)	angle (°)	mass (g)	PCSA (N/cm2)	muscle length (mm)	fiber length (mm)	angle (°)
BEAGLE1																	
BEAGLE2																	
M1																	
M2																	
M3																	
M4																	
M5																	
M6																	
M8																	
Ma-1																	
N-C1																	
N-C10	14,32	45,00	14,40	6,71	37,14	5,81	50,00	4,60	4,80	19,34	15,37	25,00	1,10	0,61	29,18	8,46	45,00
N-C11	17,89	47,50	10,80	3,85	30,39	9,51	35,00	2,40	1,95	49,16	12,75	30,00	2,40	1,54	28,69	16,40	27,50
N-C12	22,28	40,00	7,80	2,53	41,70	16,16	35,00	5,10	2,44	34,79	22,10	30,00	2,50	0,92	31,50	11,70	20,00
N-C13	19,30	45,00	14,70	5,08	25,40	24,85	30,00	2,30	0,76	30,24	11,94	20,00	1,20	0,89	22,45	11,94	50,00
N-C14	27,33	37,50	15,00	4,11	82,58	26,69	30,00	14,30	4,38	84,34	30,66	27,50	5,80	1,58	56,26	12,59	35,00
N-C15	12,46	45,00	13,40	7,18	72,85	19,27	40,00	8,00	3,00	59,91	15,13	27,50	4,50	2,49	46,27	11,74	22,50
N-C16	14,34	40,00	9,80	4,94	67,82	15,34	35,00	6,00	3,02	44,63	17,24	40,00	4,50	1,89	39,37	9,05	35,00
N-C17	25,26	45,00	21,30	5,63	42,52	12,76	37,50	6,90	4,05	68,55	35,81	35,00	5,30	1,14	52,94	17,24	35,00
N-C18	18,79	55,00	19,40	5,59	61,65	31,16	32,50	9,30	2,37	58,33	13,49	27,50	5,40	3,35	38,22	9,96	35,00
N-C19	15,02	50,00	14,20	5,73	63,91	19,65	35,00	8,30	3,26	60,56	19,12	35,00	3,90	1,58	51,72	11,79	30,00
N-C2	16,73	40,00	13,30	5,74	25,70	12,03	20,00	3,57	2,63	27,40	15,60	35,00	2,12	1,05	26,70	12,05	32,50
N-C20	13,20	37,50	1,60	0,91	22,68	10,17	37,50	0,80	0,59	23,62	6,08	27,50	0,30	0,41	34,30	5,65	20,00
N-C21	13,06	45,00	7,70	3,93	33,32	10,94	50,00	2,90	1,61	18,44	8,29	30,00	0,80	0,79	26,92	13,62	30,00
N-C22	29,12	35,00	26,70	7,09	47,30	21,43	35,00	11,00	3,97	66,24	35,38	30,00	10,20	2,36	45,97	10,87	35,00
N-C23	30,61	50,00	21,50	4,26	55,62	22,89	30,00	15,40	5,50	52,96	33,54	25,00	10,40	2,65	68,51	23,29	25,00
N-C3	15,43	35,00	11,00	5,51	19,00	9,90	2,50	3,00	2,86	30,50	14,55	5,00	3,00	1,94	31,00	13,85	27,50
N-C4	15,93	35,00	9,00	4,37	24,10	6,00	42,50	2,00	2,32	20,60	10,47	10,00	2,00	1,78	37,30	13,05	60,00
N-C5	17,23	53,33	15,18	4,96	24,60	12,12	23,75	8,36	5,96	41,00	11,75	37,50	6,60	4,20	40,80	9,95	42,50
N-C6	15,10	27,50	9,40	5,21	27,50	9,27	20,00	2,81	2,69	26,00	9,30	10,00	0,88	0,88	22,60	9,40	30,00
N-C7	17,23	30,00	12,34	5,85	43,90	9,60	20,00	3,22	2,97	28,20	11,70	35,00	1,50	0,99	27,00	10,25	45,00
N-C8	17,78	32,50	13,67	6,12	29,40	13,17	15,00	5,26	3,64	30,00	13,40		1,88	1,32	34,10	9,53	42,50
N-C9	18,76	42,50	11,20	4,15	26,70	15,94	30,00	3,10	1,59	36,29	17,17	20,00	1,30	0,67	29,63	9,14	40,00
Ny-C1	23,80	35,00	26,70	8,67	31,60	13,15	15,00	9,01	6,24	46,00	16,45		7,00		56,70	10,50	35,00
Ny-C10	33,00	35,00	23,30	5,46	54,00	19,50	32,50	6,30	2,57	46,00	24,00	12,50	5,40	2,07	49,00	10,50	27,50
Ny-C11	30,00	42,50	24,00	5,56	60,00	10,00	35,00	10,60	8,19	62,00	29,00	15,00	8,00	2,51	57,00	17,00	40,00
Ny-C12	24,00	47,50	19,50	5,18	54,00	13,50	37,50	8,70	4,82	67,00	42,50	30,00	6,30	1,21	49,00	10,50	35,00
Ny-C13	25,00	40,00	21,60	6,24	35,00	10,00	45,00	6,70	4,47	45,00	20,00	45,00	5,75	1,92	40,00	10,00	35,00
Ny-C14	23,00	65,00	52,00	9,01	65,00	25,00	35,00	37,50	11,59	70,00	21,00	45,00	16,50	5,24	55,00	10,15	32,50
Ny-C15	22,00	40,00	46,60	15,31	50,00	15,00	37,50	19,30	9,63	60,00	20,00	40,00	10,57	3,82	55,00	10,00	42,50
Ny-C16	26,00	45,00	20,60	5,29	40,00	16,00	35,00	7,02	3,39	40,00	20,00	42,50	5,65	1,96	40,00	10,00	52,50
Ny-C17	16,50	35,00	17,82	8,35	40,00	15,00	30,00	5,26	2,86	60,00	15,00	50,00	5,13	2,07	40,00	8,00	35,00
Ny-C18	30,67	47,50	55,70	11,58	47,00	20,00	37,50	13,27	4,97	70,00	20,30	30,00	21,04	8,47	52,00	12,13	47,50
Ny-C19	8,67	50,00	4,11	2,88	36,00	11,00	35,00	1,80	1,26	20,00	9,00	30,00	1,09	0,99	22,00	4,50	40,00
Ny-C20	25,00	35,00	49,30	15,24	70,00	11,00	22,50	15,10	11,96	70,00	18,50	35,00	14,95	6,24	55,00	12,00	40,00
Ny-C21	22,00	42,50	26,20	8,28	35,00	11,00	35,00	8,25	5,80	40,00	15,00	45,00	5,73	2,55	35,00	12,00	32,50
Ny-C22	27,50	37,50	25,01	6,81	40,00	20,00	30,00	6,44	2,63	50,00	20,00	45,00	7,64	2,55	50,00	15,00	32,50
Ny-C23	15,00	45,00	15,38	6,84	30,00	10,00	37,50	3,45	2,58	40,00	31,00	35,00	4,15	1,03	35,00	15,00	25,00
Ny-C24	15,00	45,00	10,27	4,57	30,00	16,00	25,00	2,47	1,32	30,00	13,00	37,50	2,29	1,32	25,00	7,00	30,00
Ny-C25	12,50	40,00	9,02	5,21	30,00	13,00	40,00	4,19	2,33	40,00	15,00	30,00	3,55	1,93	40,00	12,00	25,00
Ny-C26	19,50	25,00	9,21	4,04	40,00	7,00	20,00	3,70	4,69	40,00	7,50	27,50	4,76	5,31	30,00	10,00	27,50
Ny-C27	14,50	42,50	9,63	4,62	35,00	12,00	30,00	5,62	3,83	50,00	13,00	40,00	3,93	2,18	30,00	7,00	42,50
Ny-C28	26,50	32,50	62,10	18,65	80,00	22,50	35,00	24,80	8,52	60,00	17,00	40,00	16,03	6,81	55,00	11,00	42,50
Ny-C3	11,67	45,00	9,55	5,46	27,50	9,40	35,00	2,20	1,81	29,80	9,40	35,00	2,24	1,84	27,00	7,40	35,00
Ny-C4	26,50	40,00	29,70	8,10	59,00	12,50	37,50	8,90	5,33	84,00	15,50	32,50	12,60	6,47	54,00	15,00	35,00
Ny-C5	26,00	47,50	25,00	6,13	46,00	20,00	35,00	7,10	2,74	56,00	30,00	27,50	5,00	1,39	49,00	10,50	37,50
Ny-C6	29,50	35,00	27,40	7,18	47,00	18,00	27,50	10,80	5,02	75,00	34,00	35,00	11,90	2,70	56,00	11,50	30,00
Ny-C8	31,50	52,50	55,80	10,17	55,00	22,50	42,50	17,10	5,29	90,00	21,50	37,50	15,90	5,54	53,00	16,50	37,50
Ny-C9	21,00	32,50	11,10	4,21	50,00	18,00	32,50	4,80	2,12	63,00	23,50	27,50	4,00	1,42	40,00	7,50	25,00
	20,70	**41,53**	**20,42**	**6,43**	**43,60**	**15,12**	**32,21**	**7,90**	**4,01**	**48,23**	**18,79**	**31,14**	**5,93**	**2,44**	**41,07**	**11,34**	**35,10**
	8,67	**25,00**	**1,60**	**0,91**	**19,00**	**5,81**	**2,50**	**0,80**	**0,59**	**18,44**	**6,08**	**5,00**	**0,30**	**0,41**	**22,00**	**4,50**	**20,00**
	33,00	**65,00**	**62,10**	**18,65**	**82,58**	**31,16**	**50,00**	**37,50**	**11,96**	**90,00**	**42,50**	**50,00**	**21,04**	**8,47**	**68,51**	**23,29**	**60,00**

	terior		Temporalis par suprazgomatica					Temporal pars superficialis					Temporalis pars profunda				
ID	mass (g)	PCSA (N/cm2)	muscle length (mm)	fiber length (mm)	angle (°)	mass (g)	PCSA (N/cm2)	muscle length (mm)	fiber length (mm)	angle (°)	mass (g)	PCSA (N/cm2)	muscle length (mm)	fiber length (mm)	angle (°)	mass (g)	PCSA (N/cm2)
BEAGLE1																	
BEAGLE2																	
M1																	
M2																	
M3																	
M4																	
M5																	
M6																	
M8																	
Ma-1																	
N-C1																	
N-C10	3,70	2,92	93,33	24,18	25,00	5,30	1,87	100,25	29,38	32,50	20,20	5,47	87,83	28,66	25,00	32,60	9,73
N-C11	1,60	0,82	76,74	22,72	27,50	3,20	1,18	105,60	24,93	20,00	12,80	4,55	88,60	22,68	32,50	17,60	6,17
N-C12	1,90	1,44	86,42	16,24	25,00	5,60	2,95	111,94	31,45	25,00	19,40	5,27	91,39	34,42	40,00	29,40	6,17
N-C13	1,90	0,96	84,54	20,56	30,00	5,90	2,34	108,74	47,27	27,50	20,00	3,54	87,26	39,87	30,00	34,30	7,03
N-C14	6,20	3,81	127,90	30,48	25,00	8,40	2,36	133,43	39,42	35,00	22,50	4,41	138,72	37,17	40,00	47,00	9,14
N-C15	5,30	3,93	85,37	17,47	30,00	9,00	4,21	127,74	20,08	45,00	20,40	6,78	108,12	27,09	37,50	32,90	9,09
N-C16	2,80	2,39	84,30	31,81	30,00	6,00	1,54	118,14	27,20	32,50	21,90	6,41	93,06	29,52	37,50	26,60	6,74
N-C17	6,40	2,87	93,86	38,95	25,00	12,90	2,83	123,54	52,44	27,50	31,80	5,07	113,09	38,41	40,00	45,90	8,64
N-C18	4,10	3,18	99,10	30,70	20,00	9,60	2,77	117,01	36,31	35,00	34,30	7,30	116,36	29,85	35,00	50,00	12,95
N-C19	3,70	2,57	91,94	29,51	17,50	7,40	2,26	123,04	27,29	32,50	39,90	11,64	103,64	30,27	35,00	39,60	10,11
N-C2	1,62	1,07	92,80	20,15	30,00	6,32	2,56	103,10	21,90	30,00	17,15	6,40	94,50	27,23	35,00	29,40	8,34
N-C20	0,30	0,47	37,21	12,98	17,50	0,50	0,35	70,72	9,65	22,50	1,70	1,54	56,25	10,59	37,50	3,00	2,12
N-C21	1,00	0,60	73,86	24,22	25,00	2,20	0,78	96,19	19,43	37,50	12,60	4,85	90,12	21,90	40,00	16,90	5,58
N-C22	6,30	4,48	126,50	55,65	20,00	13,30	2,12	143,53	44,09	37,50	65,60	11,14	128,81	48,70	45,00	70,40	9,64
N-C23	6,10	2,24	104,51	19,29	35,00	8,40	3,37	135,23	45,86	20,00	44,00	8,51	123,96	45,03	37,50	58,30	9,69
N-C3	5,00	3,02	66,70	11,95	15,00	2,00	1,53	106,20	28,20	45,00	22,00	5,20	99,10	28,20	40,00	42,00	10,76
N-C4	2,00	0,72	64,90	21,10	15,00	2,00	0,86	118,30	28,95	40,00	18,00	4,49	95,40	33,70	45,00	27,00	5,34
N-C5	4,08	2,85	75,20	24,80	15,00	3,09	1,14	118,40	25,17	22,50	21,76	7,54	100,00	20,80	45,00	36,51	11,71
N-C6	1,36	1,18	78,00	14,85	0,00	2,45	1,56	95,90	26,75	25,00	15,24	4,87	75,60	24,20	25,00	20,84	7,36
N-C7	1,31	0,85	92,60	20,25	30,00	5,57	2,25	93,10	20,90	40,00	15,46	5,35	87,20	24,93	40,00	27,35	7,93
N-C8	2,81	2,05	85,60	20,30	30,00	6,63	2,67	99,30	33,40	35,00	23,31	5,39	89,25	28,38	32,50	32,03	8,98
N-C9	3,00	2,37	91,01	10,67	25,00	3,50	2,80	94,85	28,03	22,50	17,20	5,35	87,17	24,21	20,00	27,00	9,89
Ny-C1	7,58	5,58	108,40	31,10	25,00	12,83	3,53	121,50	33,37	25,00	38,90	9,97	105,80	20,87	52,50	60,10	16,54
Ny-C10	6,20	4,94	99,00	42,00	10,00	8,40	1,86	121,00	38,50	27,50	57,50	12,50	75,00	18,50	32,50	28,10	12,09
Ny-C11	7,50	3,19	114,00	44,00	30,00	9,80	1,82	140,00	53,00	37,50	43,60	6,16	109,00	32,50	37,50	39,40	9,07
Ny-C12	5,10	3,75	91,00	34,00	27,50	8,70	2,14	120,00	32,00	37,50	36,80	8,61	112,00	27,50	40,00	50,60	13,30
Ny-C13	5,10	3,94	97,50	15,00	40,00	7,24	3,49	110,00	25,00	50,00	26,93	6,53	120,00	25,00	47,50	51,30	13,08
Ny-C14	10,37	8,13	135,00	30,00	35,00	28,20	7,26	160,00	40,00	41,67	89,61	15,79	150,00	35,00	45,00	131,80	25,12
Ny-C15	9,28	6,45	135,00	12,20	55,00	22,30	9,89	145,00	42,50	37,50	77,90	13,72	140,00	36,00	45,00	95,30	17,66
Ny-C16	4,00	2,30	90,00	20,00	30,00	7,63	3,12	130,00	25,00	50,00	29,34	7,12	110,00	32,00	50,00	41,69	7,90
Ny-C17	3,18	3,07	110,00	17,00	27,50	6,22	3,06	125,00	29,00	35,00	26,40	7,04	120,00	25,00	37,50	40,80	12,21
Ny-C18	9,05	4,76	150,00	40,00	35,00	33,70	6,51	165,00	40,00	42,50	95,70	16,64	140,00	40,00	40,00	149,90	27,08
Ny-C19	0,94	1,51	60,00	15,00	35,00	2,02	1,04	86,00	15,00	30,00	5,53	3,01	85,00	13,50	40,00	12,39	6,63
Ny-C20	10,07	6,06	110,00	25,00	25,00	13,85	4,74	140,00	36,00	35,00	77,11	16,55	120,00	39,00	45,00	104,00	17,79
Ny-C21	3,57	2,37	90,00	20,00	42,50	6,60	2,30	120,00	46,00	30,00	50,84	9,03	110,00	48,50	40,00	58,14	8,66
Ny-C22	6,00	3,18	110,00	30,00	30,00	12,74	3,47	125,00	45,00	37,50	52,30	8,70	120,00	42,50	37,50	76,76	13,52
Ny-C23	3,22	1,84	85,00	35,00	30,00	6,99	1,63	75,00	35,00	40,00	21,70	4,48	95,00	30,00	50,00	32,80	6,63
Ny-C24	1,64	1,91	85,00	16,00	35,00	3,14	1,52	80,00	21,50	30,00	14,17	5,38	85,00	20,00	37,50	29,03	10,86
Ny-C25	2,67	1,90	80,00	17,00	37,50	6,04	2,66	100,00	25,00	38,33	14,05	4,16	110,00	21,00	45,00	25,10	7,97
Ny-C26	2,30	1,92	80,00	22,00	25,00	4,00	1,55	90,00	18,00	37,50	16,30	6,78	100,00	20,00	37,50	26,20	9,80
Ny-C27	2,72	2,70	90,00	25,00	35,00	4,79	1,48	105,00	26,00	40,00	22,45	6,24	80,00	20,00	40,00	33,66	12,16
Ny-C28	9,42	5,96	130,00	30,00	27,50	22,96	6,40	175,00	40,00	35,00	118,40	22,87	140,00	47,50	45,00	145,10	20,38
Ny-C3	2,00	2,09	60,60	17,40	35,00	2,26	1,00	77,10	15,60	50,00	16,17	6,29	87,40	13,17	27,50	21,69	13,78
Ny-C4	6,70	3,45	103,00	44,50	27,50	12,40	2,33	141,00	43,00	37,50	51,60	8,98	126,00	46,50	35,00	72,80	12,10
Ny-C5	4,90	3,49	79,00	31,50	20,00	8,40	2,36	129,00	44,50	35,00	37,40	6,49	114,00	41,00	37,50	63,20	11,54
Ny-C6	6,70	4,76	116,00	44,00	27,50	8,80	1,67	119,00	37,50	47,50	40,90	6,95	124,00	46,00	45,00	71,10	10,31
Ny-C8	8,60	3,90	115,00	59,00	20,00	17,20	2,58	143,00	50,50	35,00	72,70	11,13	144,00	41,50	50,00	117,00	17,10
Ny-C9	3,30	3,76	86,00	29,00	20,00	5,10	1,56	75,00	33,00	27,50	20,00	5,07	107,00	28,00	40,00	18,30	4,72
	4,47	**2,99**	**94,21**	**26,34**	**27,08**	**8,57**	**2,65**	**115,87**	**32,46**	**34,58**	**34,82**	**7,65**	**105,93**	**30,55**	**39,06**	**48,81**	**10,86**
	0,30	**0,47**	**37,21**	**10,67**	**0,00**	**0,50**	**0,35**	**70,72**	**9,65**	**20,00**	**1,70**	**1,54**	**56,25**	**10,59**	**20,00**	**3,00**	**2,12**
	10,37	**8,13**	**150,00**	**59,00**	**55,00**	**33,70**	**9,89**	**175,00**	**53,00**	**50,00**	**118,40**	**22,87**	**150,00**	**48,70**	**52,50**	**149,90**	**27,08**

	Pterygoideus medialis (PM)					Pterygoideus lateralis (PL)									Contributions	
ID	muscle length (mm)	fiber length (mm)	angle (°)	mass (g)	PCSA (N/cm2)	muscle length (mm)	fiber length (mm)	angle (°)	mass (g)	PCSA (N/cm2)	total mass of adductors	% temporal mass	%masseter mass	%pterygoid mass	%PL	% PL/(PL+PM)
BEAGLE1																
BEAGLE2																
M1																
M2																
M3																
M4																
M5																
M6																
M8																
Ma-1																
N-C1																
N-C10	32,74	18,06	20,00	7,00	9,58	4,22	30,00	0,20	7,20	3,53	89,10	65,21	26,71	8,08	0,22	2,78
N-C11	83,11	16,57	25,00	6,30	9,38	4,75	35,00	0,20	6,50	3,35	57,30	58,64	30,02	11,34	0,35	3,08
N-C12	52,11	13,70	20,00	5,10	8,04			0,20	5,30	3,43	77,00	70,65	22,47	6,88	0,26	3,77
N-C13	82,79	20,94	47,50	7,90	10,71	0,50	30,00	0,50	8,40	2,56	88,70	67,87	22,66	9,47	0,56	5,95
N-C14	79,15	14,63	45,00	15,20	17,09	11,42	27,50	1,30	16,50	7,52	135,70	57,41	30,43	12,16	0,96	7,88
N-C15	70,31	13,13	22,50	9,90	22,25	9,20	20,00	2,50	12,40	8,23	105,90	58,83	29,46	11,71	2,36	20,16
N-C16	71,45	11,12	25,00	9,40	19,15	9,37	20,00	1,40	10,80	8,30	88,40	61,65	26,13	12,22	1,58	12,96
N-C17	78,09	17,24	30,00	10,90	24,19	9,01	25,00	2,80	13,70	6,49	144,20	62,83	27,67	9,50	1,94	20,44
N-C18	75,13	17,60	37,50	15,40	20,50	8,46	27,50	1,10	16,50	7,02	148,60	63,19	25,71	11,10	0,74	6,67
N-C19	78,12	14,46	22,50	10,70	16,39	6,75	32,50	0,70	11,40	6,87	128,40	67,68	23,44	8,88	0,55	6,14
N-C2	66,00	8,27	50,00	7,22	17,70	7,95	40,00	0,67	7,89	5,79	81,37	64,97	25,33	9,70	0,82	8,49
N-C20	44,98	8,07	37,50	1,10	8,46	2,84	25,00	0,10	1,20	1,11	9,40	55,32	31,91	12,77	1,06	8,33
N-C21	48,26	16,20	20,00	3,30	12,05	7,54	30,00	0,30	3,60	1,97	47,70	66,46	26,00	7,55	0,63	8,33
N-C22	88,82	27,19	35,00	18,20	13,52	7,92	15,00	1,10	19,30	5,49	222,80	67,01	24,33	8,66	0,49	5,70
N-C23	98,74	26,18	47,50	14,60	17,04	15,09	25,00	1,20	15,80	3,85	179,90	61,53	29,68	8,78	0,67	7,59
N-C3	74,90	15,73	15,00	6,00	51,00	10,40	25,00	1,00	7,00	4,05	95,00	69,47	23,16	7,37	1,05	14,29
N-C4	69,40	14,25	32,50	5,00	23,60	11,65	37,50	1,00	6,00	3,35	68,00	69,12	22,06	8,82	1,47	16,67
N-C5	68,70	10,15	42,50	10,44	19,40	7,30	20,00	0,71	11,15	7,64	106,73	57,49	32,06	10,45	0,67	6,37
N-C6	52,70	8,50	50,00	4,48	16,50	7,30		0,28	4,76	3,40	57,74	66,73	25,03	8,24	0,48	5,88
N-C7	66,00	9,95	27,50	5,28	18,60	3,80	50,00	0,39	5,67	4,77	72,42	66,80	25,37	7,83	0,54	6,88
N-C8	73,80	12,67	45,00	8,01	19,50	5,00		1,04	9,05	4,77	94,64	65,48	24,96	9,56	1,10	11,49
N-C9	66,91	10,39	50,00	4,20	10,59	5,94	45,00	0,20	4,40	2,57	70,70	67,47	26,31	6,22	0,28	4,55
Ny-C1	98,80	13,20	55,00	18,24	28,00	8,45	25,00	1,34	19,58	8,03	181,70	61,55	27,68	10,78	0,74	6,84
Ny-C10	107,00	25,50	47,50	15,70	10,00	6,50	30,00	0,94	16,64	4,16	151,84	61,91	27,13	10,96	0,62	5,65
Ny-C11	99,00	29,00	32,50	20,00	17,00	11,50	40,00	1,20	21,20	5,82	164,10	56,55	30,53	12,92	0,73	5,66
Ny-C12	89,00	14,50	47,50	13,50	16,00	6,00	25,00	1,10	14,60	6,42	150,30	63,94	26,35	9,71	0,73	7,53
Ny-C13	90,00	11,00	37,50	10,70	20,00	7,00	40,00	0,81	11,51	7,83	136,13	62,79	28,76	8,46	0,60	7,04
Ny-C14	100,00	22,00	45,00	40,30	22,00	10,00	50,00	2,20	42,50	12,89	408,48	61,11	28,49	10,40	0,54	5,18
Ny-C15	110,00	15,00	47,50	26,60	25,00	10,00	50,00	1,63	28,23	11,99	309,48	63,17	27,71	9,12	0,53	5,77
Ny-C16	80,00	15,00	45,00	11,43	15,00	0,70		0,52	11,95	5,31	127,88	61,51	29,14	9,34	0,41	4,35
Ny-C17	90,00	13,50	42,50	9,15	15,00	5,50	40,00	0,50	9,65	4,97	114,46	64,14	27,42	8,43	0,44	5,18
Ny-C18	105,00	22,20	45,00	34,20	25,00	12,00	50,00	3,00	37,20	11,18	415,56	67,21	23,84	8,95	0,72	8,06
Ny-C19	40,00	15,00	40,00	2,29	6,00	4,00	30,00	0,06	2,35	1,13	30,23	65,96	26,27	7,77	0,20	2,55
Ny-C20	80,00	16,00	40,00	24,60	17,00	7,50	40,00	0,77	25,37	11,46	309,75	62,94	28,87	8,19	0,25	3,04
Ny-C21	90,00	17,50	42,50	16,43	15,00	10,00		0,52	16,95	6,73	176,28	65,57	24,82	9,61	0,29	3,04
Ny-C22	100,00	20,00	45,00	21,90	15,00	7,00	40,00	0,95	22,85	7,62	209,74	67,61	21,50	10,89	0,45	4,16
Ny-C23	70,00	11,00	50,00	9,59	10,00	0,50	50,00	0,30	9,89	5,45	97,58	63,01	26,85	10,14	0,31	3,03
Ny-C24	65,00	10,00	45,00	5,56	12,00	5,00	42,50	0,20	5,76	3,84	68,77	67,38	24,24	8,38	0,29	3,47
Ny-C25	70,00	8,50	50,00	9,32	15,00	6,70	50,00	0,42	9,74	6,95	74,36	60,77	26,13	13,10	0,56	4,31
Ny-C26	55,00	12,00	45,00	6,22	12,00	7,00	50,00	0,16	6,38	3,55	72,85	63,83	27,41	8,76	0,22	2,51
Ny-C27	60,00	12,00	40,00	8,60	15,00	8,00	50,00	0,55	9,15	5,51	91,95	66,23	23,82	9,95	0,60	6,01
Ny-C28	100,00	17,20	50,00	33,20	20,00	20,00	40,00	3,00	36,20	12,76	435,01	65,85	25,83	8,32	0,69	8,29
Ny-C3	63,90	11,80	62,50	5,55	13,80	12,80		0,36	5,91	2,18	62,02	64,69	25,78	9,53	0,58	6,09
Ny-C4	94,00	21,00	42,50	18,40	17,00	7,50	27,50	1,40	19,80	6,56	214,50	63,78	26,99	9,23	0,65	7,07
Ny-C5	67,00	23,00	35,00	16,30	10,00	6,00	30,00	0,70	17,00	5,71	168,00	64,88	25,00	10,12	0,42	4,12
Ny-C6	102,00	22,00	40,00	23,00	15,00	5,50	20,00	0,90	23,90	7,85	201,50	59,95	28,19	11,86	0,45	3,77
Ny-C8	93,00	24,50	40,00	23,60	26,00	10,00	30,00	1,90	25,50	7,52	329,80	62,73	29,53	7,73	0,58	7,45
Ny-C9	78,00	17,00	37,50	8,10	14,00	4,50	32,50	0,50	8,60	3,79	75,20	57,71	30,85	11,44	0,66	5,81
	77,48	**15,92**	**39,53**	**12,88**	**16,90**	**7,58**	**34,35**	**0,93**	**13,81**	**5,90**	**MEAN**	**63,72**	**26,67**	**9,61**	**0,67**	**6,88**
	32,74	**8,07**									**MIN**	**55,32**	**21,50**	**6,22**	**0,20**	**2,51**
	110,00	**29,00**									**MAX**	**70,65**	**32,06**	**13,10**	**2,36**	**20,44**

ID	PCSA of adductors	% temporal PCSA	% masseter PCSA	% pterygoid PCSA
BEAGLE1				
BEAGLE2				
M1				
M2				
M3				
M4				
M5				
M6				
M8				
Ma-1				
N-C1				
N-C10	35,65	47,89	42,19	9,91
N-C11	23,41	50,85	34,82	14,33
N-C12	25,16	57,22	29,15	13,63
N-C13	23,17	55,75	33,21	11,04
N-C14	37,31	42,64	37,20	20,17
N-C15	44,91	44,71	36,96	18,33
N-C16	35,24	41,69	34,74	23,57
N-C17	36,72	45,05	37,27	17,68
N-C18	44,54	51,69	32,55	15,76
N-C19	44,01	54,53	29,86	15,61
N-C2	33,58	51,52	31,25	17,23
N-C20	7,50	53,40	31,75	14,85
N-C21	20,11	55,75	34,46	9,80
N-C22	46,27	49,49	38,66	11,85
N-C23	40,06	53,83	36,57	9,60
N-C3	34,87	50,17	38,21	11,63
N-C4	23,23	46,06	39,52	14,42
N-C5	46,00	44,31	39,08	16,61
N-C6	27,15	50,80	36,69	12,51
N-C7	30,96	50,14	34,46	15,40
N-C8	34,94	48,77	37,59	13,64
N-C9	29,39	61,38	29,89	8,74
Ny-C1				
Ny-C10	45,64	57,93	32,95	9,11
Ny-C11	42,32	40,28	45,97	13,74
Ny-C12	45,43	52,93	32,94	14,13
Ny-C13	47,50	48,63	34,89	16,49
Ny-C14	95,04	50,69	35,75	13,56
Ny-C15	88,48	46,64	39,80	13,56
Ny-C16	36,39	49,84	35,56	14,61
Ny-C17	43,64	51,13	37,48	11,39
Ny-C18	91,18	55,09	32,65	12,26
Ny-C19	18,46	57,89	35,97	6,13
Ny-C20	90,05	43,40	43,88	12,73
Ny-C21	45,72	43,72	41,55	14,73
Ny-C22	48,48	52,99	31,29	15,72
Ny-C23	30,49	41,80	40,32	17,88
Ny-C24	30,73	57,82	29,68	12,50
Ny-C25	33,12	44,66	34,36	20,98
Ny-C26	37,64	48,18	42,40	9,42
Ny-C27	38,73	51,34	34,43	14,23
Ny-C28	102,35	48,51	39,02	12,47
Ny-C3	34,46	61,16	32,50	6,33
Ny-C4	53,32	43,91	43,79	12,30
Ny-C5	39,87	51,16	34,51	14,33
Ny-C6	46,45	40,77	42,33	16,90
Ny-C8	63,22	48,73	39,38	11,90
Ny-C9	26,65	42,60	43,20	14,21
		49,78	**36,44**	**13,79**
		40,28	**29,15**	**6,13**
		61,38	**45,97**	**23,57**

3.2. Table S2.

Definitions of the landmarks placed on the mandible and used in the geometric morphometric analyses, following the N.A.V. nomenclature.

Landmark	Definition
1	Most rostromedial point of the *Synchondrosis intermandibularis*, at the base of the first incisor
2	Most rostral point of the *Canina*, on the lateral side
3	Most caudal point of the *Canina*, on the lateral side
4	Most rostral point of the second premolar, on the lateral side
5	Most rostral point of the third premolar, on the lateral side
6	Most rostral point of the fourth premolar, on the lateral side
7	Most caudal point of the fourth premolar, on the lateral side
8	Most caudal point of the carnassial, on the lateral side
9	Most caudal point of the second molar, on the lateral side
10	Highest point of the tip of the *Processus coronoideus*
11	Most caudal point of the tip of the *Processus coronoideus*
12	Most caudal point of the *Incisura mandibulae*, at the intersection of the *Processus condylaris* and the *Processus coronoideus*
13	Most medial point of the *Processus condylaris* (tip of the Caput mandibulae)
14	Most ventral point of the *Processus condylaris*
15	Most lateral point of the *Processus condylaris*
16	Most anterior point on the curve of the *Angulus mandibulae*
17	Point at the tip of the *Processus angularis*
18	Most elevated point on the inferior border of the *Ramus mandibulae*
19	Lowest point on the ventral border of the *Ramus mandibulae*, right under the carnassial
20	Most caudal and lowest point of the *Synchondrosis intermandibularis* on the medial side
21	*Foramen mentale*
22	Most rostroventral point of the *Fossa masseterica* (intersection between the coronoid crest and the condyloid crest)
23	Most rostral point of the edge joining the basis of the *Processus coronoideus* and the *Processus condylaris* on the medial side.
24	Most rostral point of the *Foramen mandibulae*
25	The most lateral point on the *Angulus mandibulae*, at the beginning of the *Processus angularis*

3.3. Supplementary material 3.

Results of the statistical analyses.

Supplementary material 3 Results of the statistical analyses

1. Comparison of residual muscle data between morphotypes

- Mass – masseter muscle

```
> summary(aov(tab$mass.m~type))
            Df Sum Sq Mean Sq F value   Pr(>F)
type         2 0.8725  0.4363    19.8 7.38e-07 ***
Residuals   44 0.9697  0.0220
---
Signif. codes:  0 ‘***’ 0.001 ‘**’ 0.01 ‘*’ 0.05 ‘.’ 0.1 ‘ ’ 1
> TukeyHSD(aov(tab$mass.m~type))
  Tukey multiple comparisons of means
    95% family-wise confidence level

Fit: aov(formula = tab$mass.m ~ type)

$type
           diff        lwr        upr     p adj
D-B -0.32155306 -0.4488551 -0.1942510 0.0000007
M-B -0.22741193 -0.3568183 -0.0980056 0.0003047
M-D  0.09414113 -0.0352652  0.2235475 0.1933787
```

- Mass – temporal muscle

```
> summary(aov(tab$mass.t~type))
            Df Sum Sq Mean Sq F value   Pr(>F)
type         2 0.6803  0.3401   12.73 4.35e-05 ***
Residuals   44 1.1760  0.0267
---
Signif. codes:  0 ‘***’ 0.001 ‘**’ 0.01 ‘*’ 0.05 ‘.’ 0.1 ‘ ’ 1
> TukeyHSD(aov(tab$mass.t~type))
  Tukey multiple comparisons of means
    95% family-wise confidence level

Fit: aov(formula = tab$mass.t ~ type)

$type
           diff         lwr         upr     p adj
D-B -0.2907929 -0.43098881 -0.15059707 0.0000256
M-B -0.1646470 -0.30716034 -0.02213371 0.0201577
M-D  0.1261459 -0.01636739  0.26865924 0.0920683
```

- Mass – pterygoid muscle

```
> summary(aov(tab$mass.p~type))
            Df Sum Sq Mean Sq F value   Pr(>F)
type         2 0.7517  0.3758   22.77 1.63e-07 ***
Residuals   44 0.7263  0.0165
---
Signif. codes:  0 ‘***’ 0.001 ‘**’ 0.01 ‘*’ 0.05 ‘.’ 0.1 ‘ ’ 1
> TukeyHSD(aov(tab$mass.p~type))
  Tukey multiple comparisons of means
    95% family-wise confidence level

Fit: aov(formula = tab$mass.p ~ type)

$type
           diff        lwr         upr     p adj
D-B -0.30107060 -0.41124822 -0.19089298 0.0000001
M-B -0.20148875 -0.31348761 -0.08948989 0.0002216
M-D  0.09958184 -0.01241702  0.21158071 0.0902255
```


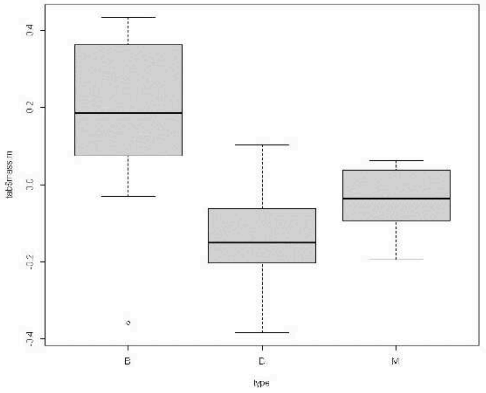

- PCSA – masseter muscle

```
> summary(aov(tab$pcsa.m~type))
            Df Sum Sq Mean Sq F value   Pr(>F)
type         2 0.3441 0.17205   9.676 0.000329 ***
Residuals   44 0.7824 0.01778
---
Signif. codes:  0 ‘***’ 0.001 ‘**’ 0.01 ‘*’ 0.05 ‘.’ 0.1 ‘ ’ 1
> TukeyHSD(aov(tab$pcsa.m~type))
  Tukey multiple comparisons of means
    95% family-wise confidence level

Fit: aov(formula = tab$pcsa.m ~ type)

$type
           diff         lwr         upr     p adj
D-B -0.20000969 -0.31435851 -0.08566087 0.0003244
M-B -0.14855925 -0.26479826 -0.03232024 0.0092658
M-D  0.05145044 -0.06478857  0.16768945 0.5352935
```

- PCSA – temporal muscle

```
> summary(aov(tab$pcsa.t~type))
            Df Sum Sq Mean Sq F value Pr(>F)
type         2 0.1556 0.07782   4.459 0.0172 *
Residuals   44 0.7678 0.01745
---
Signif. codes:  0 ‘***’ 0.001 ‘**’ 0.01 ‘*’ 0.05 ‘.’ 0.1 ‘ ’ 1
> TukeyHSD(aov(tab$pcsa.t~type))
  Tukey multiple comparisons of means
    95% family-wise confidence level

Fit: aov(formula = tab$pcsa.t ~ type)

$type
           diff        lwr          upr     p adj
```

```
D-B -0.119140939 -0.2324229 -0.005858991 0.0373203
M-B -0.123762550 -0.2389171 -0.008608046 0.0326545
M-D -0.004621611 -0.1197761  0.110532892 0.9947900
```

- PCSA – pterygoid muscle

```
> summary(aov(tab$pcsa.p~type))
             Df Sum Sq Mean Sq F value  Pr(>F)
type          2 0.2767 0.13833   6.817 0.00264 **
Residuals    44 0.8929 0.02029
---
Signif. codes:  0 ‘***’ 0.001 ‘**’ 0.01 ‘*’ 0.05 ‘.’ 0.1 ‘ ’ 1
> TukeyHSD(aov(tab$pcsa.p~type))
  Tukey multiple comparisons of means
    95% family-wise confidence level

Fit: aov(formula = tab$pcsa.p ~ type)

$type
           diff         lwr          upr     p adj
D-B -0.18331228 -0.30546867 -0.061155891 0.0020245
M-B -0.11934651 -0.24352215  0.004829125 0.0618636
M-D  0.06396577 -0.06020987  0.188141404 0.4310402
```

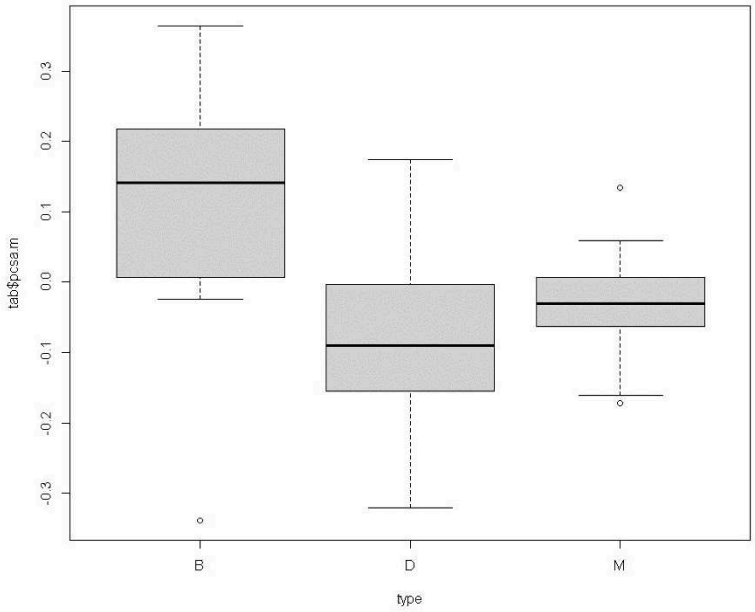

2. PCA on skull shapes: PC1 and PC 2 drivers

- PC1 - linear regression using 'lm' - size

```
Residuals:
     Min       1Q   Median       3Q      Max
-0.0917 -0.0360 -0.0204  0.0306  0.1689
Coefficients:
                Estimate Std. Error t value Pr(>|t|)
(Intercept)        1.289      0.304    4.24  8.5e-05 ***
log10(gpa$size)   -0.468      0.110   -4.24  8.4e-05 ***
---
Signif. codes:
0 ‘***’ 0.001 ‘**’ 0.01 ‘*’ 0.05 ‘.’ 0.1 ‘ ’ 1
Residual standard error: 0.063 on 56 degrees of freedom
Multiple R-squared:  0.243,   Adjusted R-squared:  0.23
F-statistic:   18 on 1 and 56 DF,  p-value: 8.41e-05
```

- PC1 - ANOVA - age

```
               Df Sum Sq Mean Sq F value Pr(>F)
cont$`AGE MDB`  3 0.0034 0.00114    0.21   0.89
Residuals      54 0.2899 0.00537
```

- PC1 - ANOVA - sex

```
            Df Sum Sq Mean Sq F value Pr(>F)
cont$SEXE    1 0.0209 0.02091    4.12  0.051 .
Residuals   30 0.1521 0.00507
---
Signif. codes:
0 ‘***’ 0.001 ‘**’ 0.01 ‘*’ 0.05 ‘.’ 0.1 ‘ ’ 1
26 observations deleted due to missingness
```

- PC1 - linear regression using 'lm' - sex

```
Residuals:
      Min       1Q   Median       3Q      Max
-0.09963 -0.04717 -0.00882  0.03599  0.18362
Coefficients:
             Estimate Std. Error t value Pr(>|t|)
(Intercept)  -0.0440     0.0237   -1.85    0.073 .
cont$SEXEM    0.0569     0.0280    2.03    0.051 .
---
Signif. codes:
0 ‘***’ 0.001 ‘**’ 0.01 ‘*’ 0.05 ‘.’ 0.1 ‘ ’ 1
Residual standard error: 0.0712 on 30 degrees of freedom
  (26 observations deleted due to missingness)
Multiple R-squared:  0.121,   Adjusted R-squared:  0.0915
F-statistic: 4.12 on 1 and 30 DF,  p-value: 0.0513
```

- PC2 - linear regression using 'lm' - size

```
Residuals:
      Min       1Q   Median       3Q      Max
-0.04191 -0.01134 -0.00126  0.00840  0.05293
```

```
Coefficients:
                Estimate Std. Error t value Pr(>|t|)
(Intercept)      -0.8693     0.0966      -9  1.8e-12 ***
log10(gpa$size)   0.3158     0.0351       9  1.8e-12 ***
---
Signif. codes:
0 '***' 0.001 '**' 0.01 '*' 0.05 '.' 0.1 ' ' 1
Residual standard error: 0.02 on 56 degrees of freedom
Multiple R-squared:  0.591,   Adjusted R-squared:  0.584
F-statistic:   81 on 1 and 56 DF,  p-value: 1.8e-12
```

- PC2 - ANOVA - age

```
              Df Sum Sq  Mean Sq F value Pr(>F)
cont$`AGE MDB`  3 0.0087 0.002886    3.37  0.025 *
Residuals      54 0.0462 0.000856
---
Signif. codes:
0 '***' 0.001 '**' 0.01 '*' 0.05 '.' 0.1 ' ' 1
```

- PC2 - linear regression using 'lm' - age

```
Residuals:
    Min      1Q  Median      3Q     Max
-0.0673 -0.0188 -0.0016  0.0187  0.0594
Coefficients:
                Estimate Std. Error t value Pr(>|t|)
(Intercept)     -0.03146    0.02068   -1.52    0.134
cont$`AGE MDB`b  0.00353    0.03583    0.10    0.922
cont$`AGE MDB`c  0.02377    0.02136    1.11    0.271
cont$`AGE MDB`d  0.04431    0.02150    2.06    0.044 *
---
Signif. codes:
0 '***' 0.001 '**' 0.01 '*' 0.05 '.' 0.1 ' ' 1
Residual standard error: 0.0293 on 54 degrees of freedom
Multiple R-squared:  0.158,   Adjusted R-squared:  0.111
F-statistic: 3.37 on 3 and 54 DF,  p-value: 0.0249
```

- PC2 - ANOVA - sex

```
            Df Sum Sq  Mean Sq F value Pr(>F)
cont$SEXE    1 0.0009 0.000921    0.86   0.36
Residuals   30 0.0323 0.001077
26 observations deleted due to missingness
```


3. Covariations between skull shape and mandible shape

3.1. Results of the 2B-PLS

Covariance explained by the singular values

singular value	% total covar.	Corr. coefficient	p-value
2.38e-03	8.50e+01	0.812	0.001
7.55e-04	8.54e+00	0.750	0.001
4.11e-04	2.53e+00	0.720	0.001
3.23e-04	1.57e+00	0.662	0.001
2.09e-04	6.55e-01	0.790	0.048
1.52e-04	3.44e-01	0.646	0.513
1.35e-04	2.75e-01	0.747	0.333
1.17e-04	2.04e-01	0.622	0.403
1.01e-04	1.54e-01	0.643	0.550
7.90e-05	9.36e-02	0.703	0.994
7.28e-05	7.94e-02	0.716	0.990
7.08e-05	7.51e-02	0.759	0.882
6.49e-05	6.31e-02	0.684	0.876
5.58e-05	4.67e-02	0.690	0.994
5.23e-05	4.10e-02	0.738	0.991
4.91e-05	3.61e-02	0.707	0.984
4.65e-05	3.25e-02	0.716	0.954
4.53e-05	3.08e-02	0.715	0.723
4.38e-05	2.88e-02	0.712	0.383
4.02e-05	2.42e-02	0.779	0.564
3.84e-05	2.21e-02	0.794	0.347
3.36e-05	1.69e-02	0.780	0.936
3.13e-05	1.47e-02	0.695	0.958
2.96e-05	1.32e-02	0.792	0.943
2.79e-05	1.16e-02	0.768	0.956
2.62e-05	1.03e-02	0.745	0.965
2.53e-05	9.60e-03	0.770	0.873
2.19e-05	7.22e-03	0.760	1.000
2.12e-05	6.74e-03	0.753	0.999
2.06e-05	6.36e-03	0.749	0.991
2.02e-05	6.14e-03	0.752	0.880
1.81e-05	4.91e-03	0.727	0.999
1.74e-05	4.55e-03	0.713	0.993
1.72e-05	4.44e-03	0.732	0.870
1.52e-05	3.46e-03	0.776	0.998
1.48e-05	3.30e-03	0.747	0.998
1.42e-05	3.03e-03	0.760	0.988
1.41e-05	2.97e-03	0.794	0.785
1.30e-05	2.54e-03	0.769	0.943
1.26e-05	2.37e-03	0.803	0.842
1.19e-05	2.13e-03	0.751	0.843
1.17e-05	2.06e-03	0.797	0.415
1.05e-05	1.65e-03	0.762	0.964
9.89e-06	1.46e-03	0.785	0.976
9.45e-06	1.34e-03	0.785	0.939
8.67e-06	1.13e-03	0.752	0.996
8.36e-06	1.05e-03	0.835	0.974
8.07e-06	9.75e-04	0.782	0.887
7.33e-06	8.06e-04	0.727	0.982
7.23e-06	7.82e-04	0.814	0.798
6.69e-06	6.70e-04	0.766	0.883
6.61e-06	6.55e-04	0.808	0.392
5.82e-06	5.08e-04	0.814	0.873
5.39e-06	4.36e-04	0.799	0.867

```
5.17e-06       4.00e-04            0.811   0.614
4.44e-06       2.95e-04            0.830   0.940
4.12e-06       2.54e-04            0.803   0.764
```

3.2. PLS1 drivers

- Centroid size and mandibular shape (PLS1)

```
Residuals:
    Min      1Q  Median      3Q     Max
-0.1149 -0.0274  0.0154  0.0239  0.0599
Coefficients:
                                          Estimate Std. Error t value
Pr(>|t|)
(Intercept)                                0.0787     0.0283    2.78
0.0074 **
corr.m.s.chiens.raw$res.prepPLS$gpa.mdb$size  -0.1165     0.0412   -2.83
0.0065 **
---
Signif. codes:  0 '***' 0.001 '**' 0.01 '*' 0.05 '.' 0.1 ' ' 1
Residual standard error: 0.0398 on 56 degrees of freedom
Multiple R-squared:  0.125,   Adjusted R-squared:  0.109
F-statistic:    8 on 1 and 56 DF,  p-value: 0.00647
```

- Centroid size and skull shape (PLS1)

```
Residuals:
    Min      1Q  Median      3Q     Max
-0.1746 -0.0317  0.0212  0.0352  0.0948
Coefficients:
                                           Estimate Std. Error t value
Pr(>|t|)
(Intercept)                               -0.157498   0.052315   -3.01
0.0039 **
corr.m.s.chiens.raw$res.prepPLS$gpa.skull$size  0.000274   0.000090    3.05
0.0035 **
---
Signif. codes:  0 '***' 0.001 '**' 0.01 '*' 0.05 '.' 0.1 ' ' 1
Residual standard error: 0.065 on 56 degrees of freedom
Multiple R-squared:  0.143,   Adjusted R-squared:  0.127
F-statistic: 9.31 on 1 and 56 DF,  p-value: 0.00348
```


4. Drivers of skull shape

4.1. Results of the Procrustes analyses to test for the effect of size, age and sex

- size (N=58)

```
          Df      SS      MS     Rsq      F      Z Pr(>SS)
size       1 0.10530 0.10530 0.19187 13.295 4.2716   0.001 **
Residuals 56 0.44352 0.00792 0.80813
Total     57 0.54882
---
Signif. codes:  0 '***' 0.001 '**' 0.01 '*' 0.05 '.' 0.1 ' ' 1

Call: procD.lm(f1 = coords ~ size, RRPP = T, data = gdfsize)
```

- age (N=58)

```
          Df      SS        MS     Rsq      F       Z Pr(>SS)
age        3 0.02731 0.0091017 0.04975 0.9424 0.16701   0.406
Residuals 54 0.52151 0.0096577 0.95025
Total     57 0.54882

Beagles only:
          Df      SS        MS     Rsq      F      Z Pr(>SS)
age        3 0.012401 0.0041338 0.22274 1.5284 1.5422    0.06 .
Residuals 16 0.043274 0.0027046 0.77726
Total     19 0.055675
---
Signif. codes:  0 '***' 0.001 '**' 0.01 '*' 0.05 '.' 0.1 ' ' 1
```

- sex (N=32)

```
          Df      SS        MS     Rsq      F      Z Pr(>SS)
sex        1 0.02470 0.024697 0.07602 2.4684 1.7798   0.063 .
Residuals 30 0.30016 0.010005 0.92398
Total     31 0.32486

Beagles only: 5 beagles only
```

4.2. Muscular drivers of skull shape (N=47)

- Size and all muscle masses and raw PCSA

```
Analysis of Variance, using Residual Randomization
Permutation procedure: Randomization of null model residuals
Number of permutations: 1000
Estimation method: Ordinary Least Squares
Sums of Squares and Cross-products: Type I
Effect sizes (Z) based on SS distributions

          Df      SS       MS     Rsq       F      Z Pr(>SS)
size       1 0.10539 0.105387 0.21070 21.2550 3.7388   0.001 **
pcsa.t     1 0.05001 0.050008 0.09998 10.0858 3.2716   0.003 **
pcsa.m     1 0.03744 0.037437 0.07485  7.5505 3.0464   0.004 **
pcsa.p     1 0.02635 0.026354 0.05269  5.3152 2.6772   0.005 **
mass.t     1 0.03353 0.033533 0.06704  6.7632 3.6564   0.001 **
```

```
mass.m     1 0.04359 0.043594 0.08715  8.7922 4.5160   0.001 **
mass.p     1 0.01050 0.010503 0.02100  2.1183 2.3637   0.015 *
Residuals 39 0.19337 0.004958 0.38660
Total     46 0.50019
---
Signif. codes:  0 '***' 0.001 '**' 0.01 '*' 0.05 '.' 0.1 ' ' 1

Call: procD.lm(f1 = coords ~ size + pcsa.t + pcsa.m + pcsa.p + mass.t +
    mass.m + mass.p, RRPP = T, data = gdf)

residual data:
          Df      SS       MS     Rsq       F      Z Pr(>SS)
size       1 0.10539 0.105387 0.21070 21.2550 3.7388   0.001 **
pcsa.t     1 0.05001 0.050008 0.09998 10.0858 3.2716   0.003 **
pcsa.m     1 0.03744 0.037437 0.07485  7.5505 3.0464   0.004 **
pcsa.p     1 0.02635 0.026354 0.05269  5.3152 2.6772   0.005 **
mass.t     1 0.03353 0.033533 0.06704  6.7632 3.6564   0.001 **
mass.m     1 0.04359 0.043594 0.08715  8.7922 4.5160   0.001 **
mass.p     1 0.01050 0.010503 0.02100  2.1183 2.3637   0.015 *
Residuals 39 0.19337 0.004958 0.38660
Total     46 0.50019
---
Signif. codes:  0 '***' 0.001 '**' 0.01 '*' 0.05 '.' 0.1 ' ' 1

Call: procD.lm(f1 = coords ~ size + pcsa.t + pcsa.m + pcsa.p + mass.t +
    mass.m + mass.p + fl.m + fl.t + fl.p, RRPP = T, data = gdf)
```

- PCSA of the masseter only

```
          Df      SS       MS    Rsq      F      Z Pr(>SS)
pcsa.m     1 0.02656 0.026558 0.0531 2.5233 1.6467   0.069 .
Residuals 45 0.47363 0.010525 0.9469
Total     46 0.50019

Residual:
          Df      SS       MS     Rsq      F      Z Pr(>SS)
pcsa.m     1 0.07877 0.078768 0.15748 8.411 3.4411   0.001 **
Residuals 45 0.42142 0.009365 0.84252
Total     46 0.50019
```

- PCSA of the temporal only

```
          Df      SS       MS     Rsq      F      Z Pr(>SS)
pcsa.t     1 0.02798 0.027975 0.05593 2.6659 1.7694   0.051 .
Residuals 45 0.47221 0.010494 0.94407
Total     46 0.50019

Residual:
          Df      SS       MS     Rsq      F      Z Pr(>SS)
pcsa.t     1 0.05001 0.050008 0.09998 4.9988 2.8195   0.004 **
Residuals 45 0.45018 0.010004 0.90002
Total     46 0.50019
```

- PCSA of the pterygoids only

```
          Df      SS       MS     Rsq      F      Z Pr(>SS)
pcsa.p     1 0.03065 0.030651 0.06128 2.9376 1.8689   0.045 *
Residuals 45 0.46954 0.010434 0.93872
Total     46 0.50019

Residual:
          Df      SS       MS     Rsq      F      Z Pr(>SS)
pcsa.p     1 0.09284 0.092840 0.18561 10.256 3.6289   0.001 **
```



```
Residuals 45 0.40735 0.009052 0.81439
Total     46 0.50019
```

- mass of the masseter only

```
          Df      SS       MS     Rsq      F      Z Pr(>SS)
mass.m     1 0.03416 0.034158 0.06829 3.2983 2.0283   0.038 *
Residuals 45 0.46603 0.010356 0.93171
Total     46 0.50019

Residual:
          Df      SS       MS     Rsq      F      Z Pr(>SS)
mass.m     1 0.13548 0.135480 0.26822 16.861 4.2066   0.001 **
Residuals 46 0.36962 0.008035 0.73178
Total     47 0.50510
```

- mass of the temporal only

```
          Df      SS       MS     Rsq      F      Z Pr(>SS)
mass.t     1 0.03311 0.033105 0.06619 3.1895 1.9812   0.043 *
Residuals 45 0.46708 0.010380 0.93381
Total     46 0.50019

Residual:
          Df      SS       MS     Rsq      F      Z Pr(>SS)
mass.t     1 0.10334 0.103342 0.2046 11.832 3.6666   0.001 **
Residuals 46 0.40176 0.008734 0.7954
Total     47 0.50510
```

- mass of the pterygoids only

```
          Df      SS       MS     Rsq      F      Z Pr(>SS)
mass.p     1 0.03599 0.035994 0.07196 3.4893 2.0965   0.027 *
Residuals 45 0.46419 0.010315 0.92804
Total     46 0.50019

Residual:
          Df      SS       MS     Rsq      F      Z Pr(>SS)
mass.p     1 0.15395 0.153954 0.3048 20.168 4.4086   0.001 **
Residuals 46 0.35115 0.007634 0.6952
Total     47 0.50510
```

4.3. Correlations in muscle masses

```
          mass.m    mass.t    mass.p
mass.m 1.0000000 0.9771350 0.9746071
mass.t 0.9771350 1.0000000 0.9542957
mass.p 0.9746071 0.9542957 1.0000000
```

4.4. Correlations in muscle PCSAs

```
          pcsa.m    pcsa.t    pcsa.p
pcsa.m 1.0000000 0.9096788 0.8535938
pcsa.t 0.9096788 1.0000000 0.7771239
pcsa.p 0.8535938 0.7771239 1.0000000
```

4.5. Covariations between muscle architecture and skull shape

- 2B-PLS mass - skull shape

Covariance explained by the singular values

singular value	% total covar.	Corr. coefficient	p-value
0.025846	95.7662	0.898	0.025
0.004667	3.1219	0.549	0.015
0.002105	0.6352	0.530	0.019
0.001184	0.2009	0.447	0.384
0.000949	0.1290	0.595	0.360
0.000672	0.0646	0.633	0.798
0.000612	0.0538	0.586	0.327
0.000343	0.0169	0.507	1.000
0.000282	0.0114	0.581	0.992

- 2B-PLS PCSA – skull shape

Covariance explained by the singular values

singular value	% total covar.	Corr. coefficient	p-value
0.016699	86.5191	0.843	0.039
0.005538	9.5147	0.456	0.022
0.002468	1.8899	0.691	0.057
0.001756	0.9565	0.561	0.099
0.001180	0.4318	0.615	0.615
0.000881	0.2408	0.577	0.890
0.000818	0.2075	0.516	0.475
0.000707	0.1550	0.525	0.208
0.000523	0.0848	0.559	0.357

- 2B-PLS residual mass – skull shape

Covariance explained by the singular values

singular value	% total covar.	Corr. coefficient	p-value
0.031813	98.94950	0.735	0.001
0.002560	0.64071	0.739	0.453
0.001278	0.15962	0.480	0.869
0.001044	0.10648	0.557	0.767
0.000751	0.05518	0.496	0.941
0.000619	0.03743	0.567	0.923
0.000567	0.03140	0.539	0.525
0.000335	0.01099	0.256	0.997
0.000298	0.00868	0.584	0.891

- 2B-PLS residual PCSA-skull

Covariance explained by the singular values

singular value	% total covar.	Corr. coefficient	p-value
0.020751	96.238	0.643	0.001
0.002730	1.665	0.726	0.700
0.002017	0.909	0.608	0.414
0.001284	0.368	0.403	0.926
0.001174	0.308	0.622	0.559
0.000879	0.173	0.577	0.839

0.000818	0.150	0.562	0.373
0.000749	0.125	0.429	0.049
0.000531	0.063	0.516	0.284

- 2B-PLS residual mass - allometry-free skull shape

Covariance explained by the singular values

singular value	% total covar.	Corr. coefficient	p-value
0.022420	97.9480	0.828	0.001
0.002553	1.2705	0.750	0.117
0.001277	0.3176	0.480	0.573
0.001009	0.1986	0.615	0.497
0.000712	0.0988	0.637	0.904
0.000617	0.0742	0.579	0.709
0.000554	0.0598	0.655	0.321
0.000298	0.0173	0.584	1.000
0.000279	0.0152	0.626	0.902

- 2B-PLS residual PCSA - allometry-free skull shape

Covariance explained by the singular values

singular value	% total covar.	Corr. coefficient	p-value
0.014416	92.706	0.719	0.001
0.002719	3.298	0.744	0.307
0.002009	1.800	0.616	0.080
0.001188	0.630	0.577	0.867
0.001160	0.600	0.641	0.235
0.000877	0.343	0.580	0.563
0.000799	0.285	0.587	0.180
0.000695	0.216	0.554	0.049
0.000522	0.122	0.560	0.169

- Linear regression between PLS1 (skull shape) and the centroid size

```
Residuals:
     Min       1Q   Median       3Q      Max
-0.03476 -0.01317 -0.00187  0.01112  0.04784
Coefficients:
                                        Estimate Std. Error t value
Pr(>|t|)
(Intercept)                            -1.41e-01   1.76e-02   -8.02  2.8e
10 ***
pls_chiens_skull_p$prep_PLS$gpa.size.p  2.40e-04   2.95e-05    8.13  1.9e
10 ***
---
Signif. codes:  0 ‘***’ 0.001 ‘**’ 0.01 ‘*’ 0.05 ‘.’ 0.1 ‘ ’ 1
Residual standard error: 0.02 on 46 degrees of freedom
Multiple R-squared:  0.59,    Adjusted R-squared:  0.581
F-statistic: 66.1 on 1 and 46 DF,  p-value: 1.91e-10
```

- Linear regression between PLS1 (muscle masses) and the centroid size

```
Residuals:
    Min      1Q  Median      3Q     Max
-1.2864 -0.3566 -0.0353  0.1910  1.2207
```

```
Coefficients:
                                    Estimate Std. Error t value
Pr(>|t|)
(Intercept)                        -4.349363   0.513723   -8.47  6.1e-
11 ***
pls_chiens_skull_p$prep_PLS$gpa.size.p  0.007399   0.000862    8.58  4.2e-
11 ***
---
Signif. codes:  0 '***' 0.001 '**' 0.01 '*' 0.05 '.' 0.1 ' ' 1
Residual standard error: 0.584 on 46 degrees of freedom
Multiple R-squared:  0.616,   Adjusted R-squared:  0.607
F-statistic: 73.7 on 1 and 46 DF,  p-value: 4.15e-11
```


5. Drivers of mandible shape

5.1. Results of the Procrustes analyses to test for the effect of size, age and sex

- size (N=59)

```
          Df      SS        MS     Rsq      F      Z Pr(>SS)
size       1 0.03692 0.036920 0.09842 6.2221 4.1912   0.001 **
Residuals 57 0.33822 0.005934 0.90158
Total     58 0.37514
---
Signif. codes:  0 '***' 0.001 '**' 0.01 '*' 0.05 '.' 0.1 ' ' 1

Call: procD.lm(f1 = coords ~ size, data = gdf)
```

- sex (N=32)

```
 Df       SS        MS     Rsq      F      Z Pr(>SS)
sex        1 0.012877 0.0128772 0.06921 2.2307 1.8912   0.043 *
Residuals 30 0.173180 0.0057727 0.93079
Total     31 0.186057
---
Signif. codes:  0 '***' 0.001 '**' 0.01 '*' 0.05 '.' 0.1 ' ' 1

Call: procD.lm(f1 = coords ~ sex, data = gdf2)
```

- age (n=59)

```
          Df      SS        MS     Rsq     F     Z Pr(>SS)
age        3 0.03009 0.0100316 0.08022 1.599 1.792   0.036 *
Residuals 55 0.34504 0.0062735 0.91978
Total     58 0.37514
---
Signif. codes:  0 '***' 0.001 '**' 0.01 '*' 0.05 '.' 0.1 ' ' 1

Call: procD.lm(f1 = coords ~ age, data = gdf)
```

5.2. Muscular drivers of mandible shape (N=47)

- Size and all muscle masses and PCSAs

```
          Df      SS        MS     Rsq      F      Z Pr(>SS)
          Df      SS        MS     Rsq      F      Z Pr(>SS)
size       1 0.027216 0.0272162 0.09171 5.6732 3.3707   0.002 **
pcsa.t     1 0.014260 0.0142600 0.04805 2.9725 2.3701   0.020 *
pcsa.m     1 0.017728 0.0177275 0.05973 3.6953 2.8905   0.004 **
pcsa.p     1 0.006365 0.0063648 0.02145 1.3267 0.6416   0.264
mass.t     1 0.011643 0.0116432 0.03923 2.4270 2.1855   0.019 *
mass.m     1 0.025176 0.0251765 0.08483 5.2480 4.1207   0.001 **
mass.p     1 0.007287 0.0072867 0.02455 1.5189 1.5980   0.059 .
Residuals 39 0.187096 0.0047973 0.63044
Total     46 0.296771

---
Signif. codes:  0 '***' 0.001 '**' 0.01 '*' 0.05 '.' 0.1 ' ' 1
```

```
Call: procD.lm(f1 = coords ~ size + pcsa.t + pcsa.m + pcsa.p + mass.t +
mass.m + mass.p, RRPP = T, data = gdf)

Residual:
          Df       SS        MS     Rsq      F      Z Pr(>SS)
size       1 0.027216 0.0272162 0.09171 5.6732 3.3707   0.002 **
pcsa.t     1 0.014260 0.0142600 0.04805 2.9725 2.3701   0.020 *
pcsa.m     1 0.017728 0.0177275 0.05973 3.6953 2.8905   0.004 **
pcsa.p     1 0.006365 0.0063648 0.02145 1.3267 0.6416   0.264
mass.t     1 0.011643 0.0116432 0.03923 2.4270 2.1855   0.019 *
mass.m     1 0.025176 0.0251765 0.08483 5.2480 4.1207   0.001 **
mass.p     1 0.007287 0.0072867 0.02455 1.5189 1.5980   0.059 .
Residuals 39 0.187096 0.0047973 0.63044
Total     46 0.296771
---
Signif. codes:  0 '***' 0.001 '**' 0.01 '*' 0.05 '.' 0.1 ' ' 1

Call: procD.lm(f1 = coords ~ size + pcsa.t + pcsa.m + pcsa.p + mass.t +
    mass.m + mass.p, RRPP = T, data = gdf)
```

- PCSA of the masseter only

```
          Df       SS        MS     Rsq      F      Z Pr(>SS)
pcsa.m     1 0.042529 0.042529 0.14331 7.5276 4.2682   0.001 **
Residuals 45 0.254241 0.005650 0.85669
Total     46 0.296771

Residual PCSA:
          Df       SS        MS     Rsq      F      Z Pr(>SS)
pcsa.m     1 0.026863 0.026863 0.09052 4.4787 3.4201   0.001 **
Residuals 45 0.269908 0.005998 0.90948
Total     46 0.296771
```

- PCSA of the temporal only

```
          Df       SS        MS     Rsq      F      Z Pr(>SS)
pcsa.t     1 0.032737 0.032737 0.11031 5.5795 3.7692   0.001 **
Residuals 45 0.264034 0.005867 0.88969
Total     46 0.296771

Residual PCSA:
          Df       SS        MS     Rsq      F      Z Pr(>SS)
pcsa.t     1 0.01426 0.014260 0.04805 2.2714 2.0907   0.029 *
Residuals 45 0.28251 0.006278 0.95195
Total
```

- PCSA of the pterygoids only

```
    Df      SS        MS     Rsq      F      Z Pr(>SS)
pcsa.p     1 0.03831 0.038310 0.12909 6.6701 4.0855   0.001 **
Residuals 45 0.25846 0.005744 0.87091
Total     46 0.29677

Residual PCSA:
          Df       SS        MS     Rsq      F      Z Pr(>SS)
pcsa.p     1 0.022501 0.0225007 0.07582 3.6917 3.0482   0.001 **
Residuals 45 0.274270 0.0060949 0.92418
Total     46 0.296771
```

- mass of the masseter only


```
          Df       SS        MS     Rsq      F      Z Pr(>SS)
mass.m     1 0.048736 0.048736 0.16422 8.8421 4.4778   0.001 **
Residuals 45 0.248035 0.005512 0.83578
Total     46 0.296771

Residual mass:
          Df       SS        MS     Rsq      F      Z Pr(>SS)
mass.m     1 0.042822 0.042822 0.14151 7.5826 4.3999   0.001 **
Residuals 46 0.259780 0.005647 0.85849
Total     47 0.302602
```

- mass of the temporal only

```
          Df       SS        MS    Rsq      F      Z Pr(>SS)
mass.t     1 0.039739 0.039739 0.1339 6.9573 4.0974   0.001 **
Residuals 45 0.257032 0.005712 0.8661
Total     46 0.296771
Residual temporal:
          Df       SS        MS     Rsq      F      Z Pr(>SS)
mass.t     1 0.026747 0.0267475 0.08839 4.4603 3.2584   0.001 **
Residuals 46 0.275855 0.0059968 0.91161
Total     47 0.302602
```

- mass of the pterygoids only

```
          Df       SS        MS     Rsq      F      Z Pr(>SS)
mass.p     1 0.045283 0.045283 0.15259 8.1027 4.3298   0.001 **
Residuals 45 0.251488 0.005589 0.84741
Total     46 0.296771

Residual mass:
          Df       SS        MS     Rsq      F      Z Pr(>SS)
mass.p     1 0.044804 0.044804 0.14806 7.9945 4.4855   0.001 **
Residuals 46 0.257799 0.005604 0.85194
Total     47 0.302602
```

Simple regressions

Skull							
Size (N=58)	1	0.11	0.11	**0.19**	13	4.2	0.001
Age (N=48)	3	0.022	0.0073	0.073	1.2	0.61	0.27
Sex (N=32)	1	0.013	0.013	**0.069**	2.2	1.9	0.043
PCSA temporal (N=47)	1	0.028	0.028	0.056	2.7	1.8	0.051
Temporal, Residual PCSA		0.028	0.028	0.056	2.7	1.8	0.046
PCSA masseter (N=47)	1	0.027	0.027	0.053	2.5	1.6	0.069
Masseter, residual PCSA	1	0.027	0.027	0.053	2.5	1.7	0.064
PCSA pterygoid (N=47)	1	0.031	0.031	**0.061**	2.9	1.9	0.045
Pterygoids, residual PCSA		0.030	0.030	0.061	2.9	1.9	0.044
Mass temporal (N=47)	1	0.033	0.033	**0.066**	3.2	2.0	0.043
Temporal, residual mass		0.033	0.034	0.066	3.3	2.1	0.034
Mass masseter (N=47)	1	0.034	0.034	**0.068**	3.3	2.0	0.038
Masseter, residual mass		0.0342	0.034	0.068	3.3	2.1	0.031
Mass pterygoid (N=47)	1	0.036	0.036	**0.072**	3.5	2.1	0.027
Pterygoids - residual mass		0.036	0.036	**0.072**	3.6	2.2	0.022
Mandible							
Size (N=59)	1	0.037	0.037	**0.098**	6.2	4.2	0.001
Age (N=59)	3	0.031	0.010	**0.080**	1.6	1.8	0.036
Sex (N=32)	1	0.013	0.013	**0.069**	2.2	1.9	0.043
PCSA temporal (N=47)	1	0.033	0.033	**0.11**	5.6	3.8	0.001
Residual PCSA - temporal	1	0.014	0.014	0.048	2.3	2.1	0.029
PCSA masseter (N=47)	1	0.043	0.043	**0.14**	7.5	4.3	0.001
Residual PCSA - masseter	1	0.027	0.027	0.091	4.5	3.4	0.001
PCSA pterygoid (N=47)	1	0.038	0.038	**0.13**	6.7	4.1	0.001

Residual PCSA - pterygoid	1	0.023	0.023	0.076	3.7	3.1	0.001
Mass temporal (N=47)	1	0.040	0.040	**0.13**	7.0	4.1	0.001
Residual mass - temporal	1	0.027	0.027	0.088	4.5	3.3	0.001
Mass masseter (N=47)	1	0.049	0.049	**0.16**	8.8	4.5	0.001
Residual mass - masseter	1	0.043	0.043	0.14	7.6	4.4	0.001
Mass pterygoid (N=47)	1	0.045	0.045	**0.15**	8.1	4.3	0.001
Residual mass- pterygoid	1	0.045	0.045	0.15	8.0	4.5	0.001

3.4. Fig. S1.

Distribution of the specimens with a visualisation of the differences between large and small specimens relative to consensus shape. Ages are indicated by different shapes and morphotypes are indicated by different colors. Beagles are located in the green area. Ams: American Staffordshire terrier; Box: Boxer; Buld: Bulldog; Bult: Bull terrier; Chi: Chihuahua; Can: Cane Corso; Kin: Cavalier King Charles Spaniel; Pap: Papillon; Pit: Pitbull; Rot: Rottweiler; Mas: Mastiff; Fox: fox terrier; Bel: Belgian Shepherd; Bor: Border collie; Col: Collie; Dac: Dachshund; Ger: German Shepherd; Gol: Golden retriever; Hus: Husky; Leo: Leonberg; She: Shetland sheepdog.

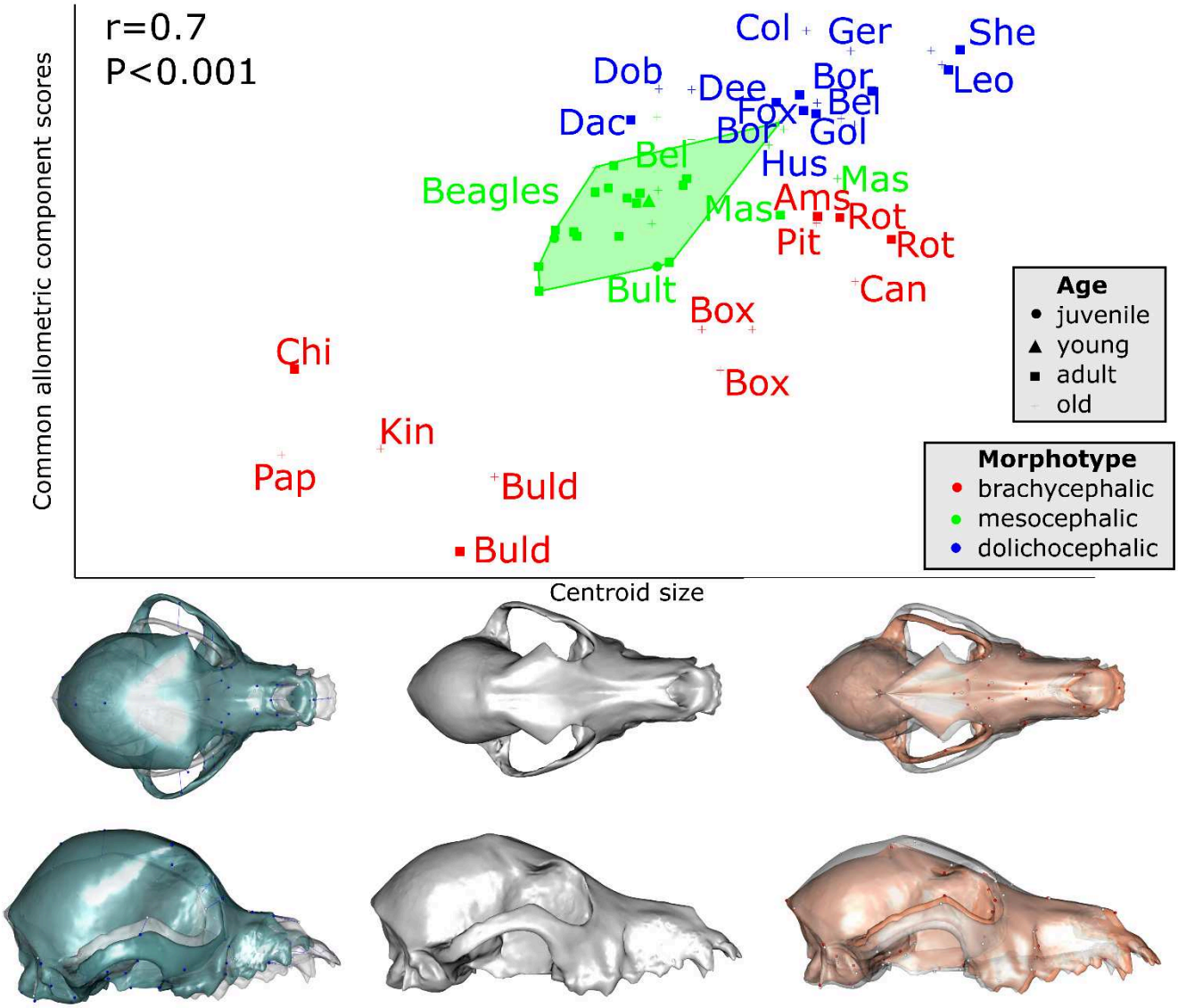

3.5. Fig. S2.

2-Block Partial Least Square Analyses between cranial shape and the masses of the jaw muscles, with vectors and shapes at the minimum and maximum of the PLS axis. Illustrations represent the deformations from the consensus to the extreme of the axis in lateral and dorsal views. Ages are indicated by different shapes and morphotypes are indicated by different colors. Beagles are located in the green area. Ams: American Staffordshire terrier; Box: Boxer; Buld: Bulldog; Bult: Bull terrier; Chi: Chihuahua; Can: Cane Corso; Kin: Cavalier King Charles Spaniel; Pap: Papillon; Pit: Pitbull; Rot: Rottweiler; Mas: Mastiff; Fox: fox terrier; Bel: Belgian Shepherd; Bor: Border collie; Col: Collie; Dac: Dachshund; Ger: German Shepherd; Gol: Golden retriever; Hus: Husky; Leo: Leonberg; She: Shetland sheepdog. Dig: M. digastricus; MS: M. masseter pars superficialis; MP: M. masseter pars profunda; ZMA: M. zygomaticomandibularis pars anterior; ZMP: M. zygomaticomandibularis pars posterior; SZ: M. temporalis pars suprazygomatica; TS: M. temporalis pars superficialis; TP: M. temporalis pars profunda; PM+PL: M. pterygoideus pars medialis and lateralis.

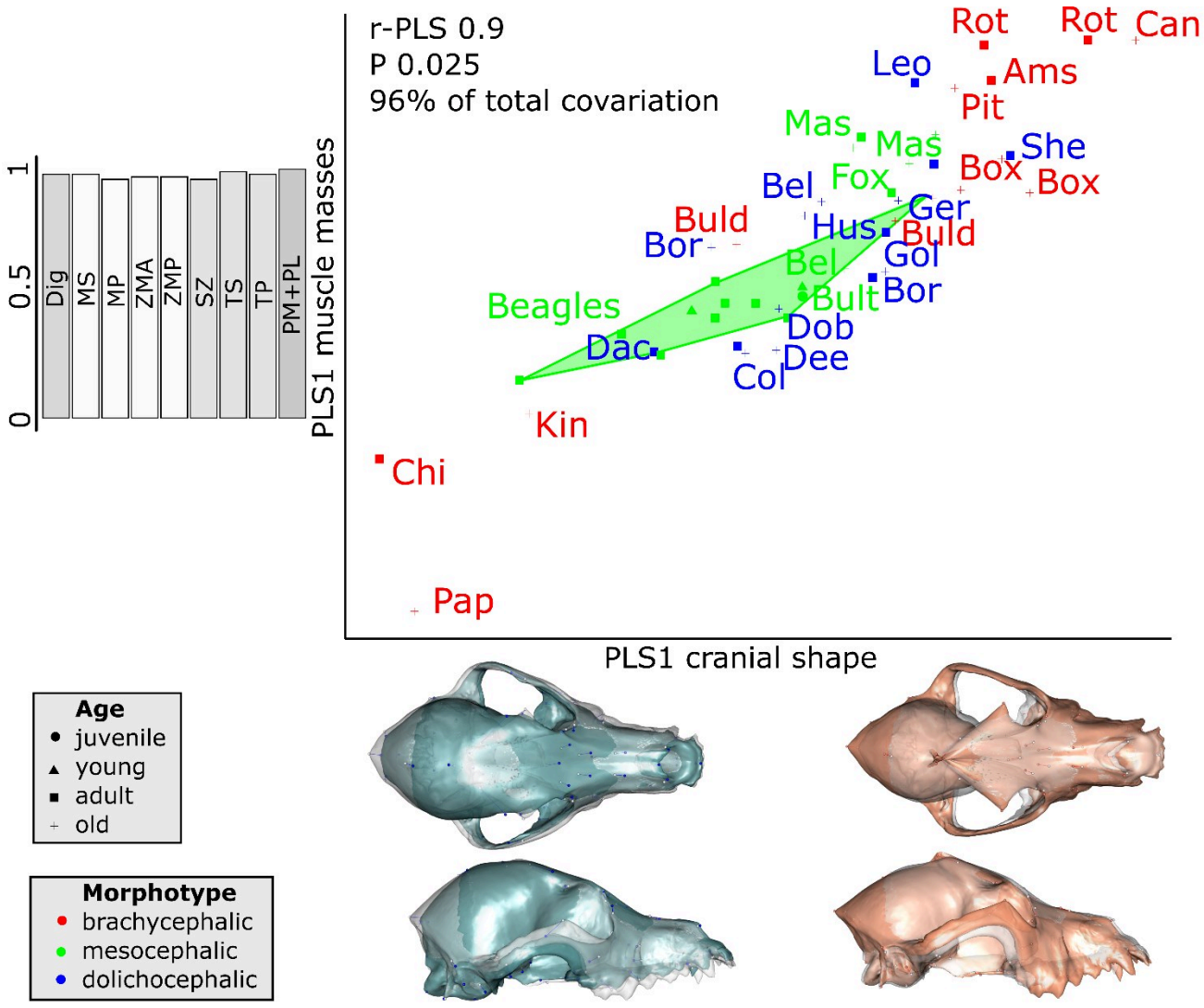

3.6. Fig. S3.

2-Block Partial Least Square Analyses between the allometry-free cranial shape and the residual masses of the jaw muscles, with vectors and shapes at the minimum and maximum of the PLS axis. Illustrations represent the deformations from the consensus to the extreme of the axis in lateral and dorsal views. Ages are indicated by different shapes and morphotypes are indicated by different colors. Beagles are located in the green area. Ams: American Staffordshire terrier; Box: Boxer; Buld: Bulldog; Bult: Bull terrier; Chi: Chihuahua; Can: Cane Corso; Kin: Cavalier King Charles Spaniel; Pap: Papillon; Pit: Pitbull; Rot: Rottweiler; Mas: Mastiff; Fox: fox terrier; Bel: Belgian Shepherd; Bor: Border collie; Col: Collie; Dac: Dachshund; Ger: German Shepherd; Gol: Golden retriever; Hus: Husky; Leo: Leonberg; She: Shetland sheepdog. Dig: M. digastricus; MS: M. masseter pars superficialis; MP: M. masseter pars profunda; ZMA: M. zygomaticomandibularis pars anterior; ZMP: M. zygomaticomandibularis pars posterior; SZ: M. temporalis pars suprazygomatica; TS: M. temporalis pars superficialis; TP: M. temporalis pars profunda; PM+PL: M. pterygoideus pars medialis and lateralis.

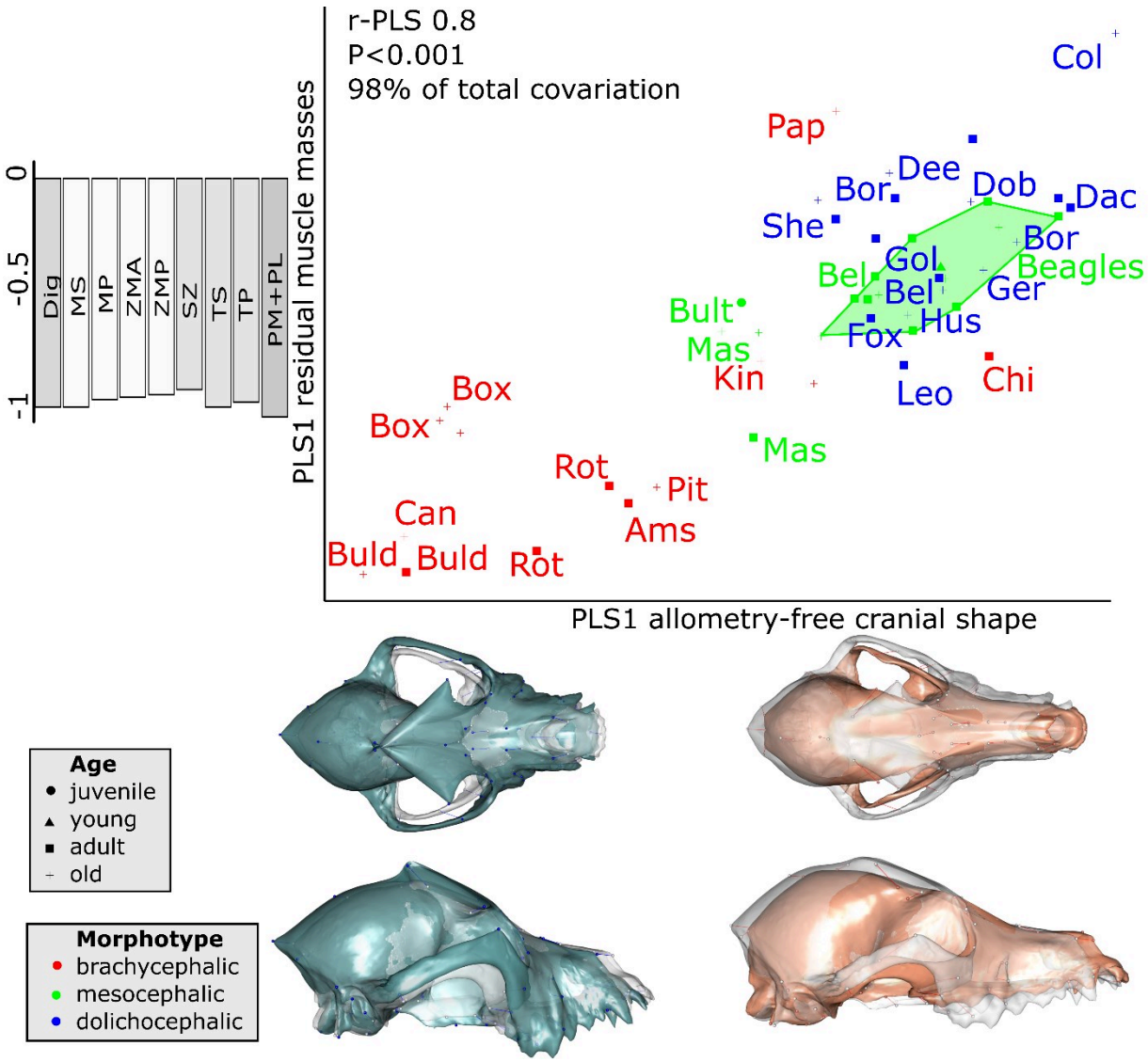

4. Part2 – Article 3 – supplementary material

4.1. Table S1.

Details of the specimen used in this study, including raw jaw muscles data and PCSA and the outputs of the biomechanical model for all individuals.

Table S1. Details of the specimen used in this study including raw jaw muscles data and PCSA and the outputs of the biomechanical model for all individuals.

ID	identification number
BREED	
LEGEND	Corresponding legend in the figures
Morphotype	B: brachycephalic; M: mesocephalic; D: dolichocephalic
age	age following suture closing
BF	Bite force in newtons
JF	Joint force in newtons
AJF	angle of the joint force in degrees
I	incisors
C	canine
M1	carnassial
MS	m. masseter pars superficialis
MP	m. masseter pars profunda
ZA	m. masseter pars zygomaticomandibularis anterior
ZP	m. masseter pars zygomaticomandibularis posterior
SZ	m. temporalis pars suprazygomatica
TS	m. temporalis pars superficialis
TP	m. temporalis pars profunda
PM	m. pterygoideus pars medialis
LM	muscle length
FL	fiber length
A	pennation angle
mass	mass of the muscle

										GAPE ANGLE = O°																
										BF			JF			AJF			Contribution to the total moment of the BF (%							
ID	BREED	BREED LEGEND	headl	headw	ci	Morphotype	age	sex		I	C	M1	I	C	M1	I	C	M1	MS	MP	ZA	ZP	SZ	TS	TP
N-C10	BEAGLE		133	82	62	M	C	NA		404	472	926	854	830	698	136	138	152	15,54	15,66	2,54	7,63	3,73	19,94	26,62
N-C11	COLLEY	COL	172	79	46	D	D	NA		271	316	586	571	558	496	144	146	159	15,42	9,29	9,66	2,93	2,46	22,35	25,56
N-C12	BEAGLE		129	84	65	M	C	NA		299	343	660	619	606	523	140	142	156	9,06	10,85	5,56	4,06	5,57	26,06	25,94
N-C13	BEAGLE		132	91	69	M	C	NA		262	301	559	576	564	497	142	143	155	21,81	3,46	6,29	3,49	5,19	18,55	29,53
N-C14	SHEPHERD DOG		196	116	59	D	D	NA		453	520	911	886	865	764	141	143	155	10,2	13,4	6,69	9,36	3,54	14,18	22,92
N-C15	SHEPHERD DOG		176	111	63	M	D	NA		508	623	1089	1123	1089	976	143	145	157	14,14	8,33	8,86	7,5	4,94	18,67	19,42
N-C16	HUNTING DOG		139	99	72	B	D	NA		481	567	1012	833	805	685	138	140	155	12,9	9,25	7,59	6,38	2,49	20,95	18,57
N-C17	BOXER	BOX	138	116	84	B	D	NA		420	492	870	909	889	800	145	147	158	13,03	13,06	4,76	7,11	3,94	18,48	25,11
N-C18	BELGIAN SHEPHERD	BEL	171	99	58	D	D	NA		539	616	1064	1083	1061	957	145	147	158	11	6,5	11,6	5,94	3,12	20,35	26,63
N-C19	GOLDEN	GOL	173	102	59	D	C	F		490	556	1021	1100	1081	964	143	145	156	11,8	8,02	5,75	5,42	3,09	31,51	21,34
N-C2	BEAGLE	BEA	140	92	66	M	B	M		385	449	803	819	797	694	137	139	150	15,93	9,81	4,94	3,16	4	23,1	22,67
N-C20	PAPILLON	PAP	83	69	83	B	C	M		118	137	253	169	162	129	134	136	155	10,29	8,1	7,44	4,79	3,24	24,95	26,95
N-C21	KING CHARLES	KIN	95	77	81	B	D	M		292	343	608	463	442	343	124	126	139	19,52	9,25	5,53	2,74	2,01	25,98	23,82
N-C22			176	108	61	M	D	M		565	649	1173	1122	1098	975	144	146	159	11,96	10,11	7,81	8,35	2,62	28,49	19,63
N-C23			148	116	78	B	D	neutered F		545	620	1062	944	918	785	135	137	149	8,69	13,68	8,81	3,63	5,52	26,02	23,95
N-C3	BEAGLE		143	96	67	M	C	NA		399	463	894	848	824	684	132	133	146	13,86	8,89	9,05	8,56	2,35	18,28	28,13
N-C4	BEAGLE		137	86	63	M	C	NA		287	333	610	556	540	459	136	138	151	16,98	11,11	11,48	2,37	1,64	22,84	20,28
N-C5	BULLDOG	BULD	101	86	85	B	C	neutered M		791	900	1349	1000	957	796	127	129	140	10,1	12,99	12,47	5,57	1,48	18,41	23,25
N-C6	BEAGLE		124	79	63	M	C	F		301	348	695	669	652	550	136	137	151	15,15	11,81	4,67	3,49	4,11	22,64	25,74
N-C7	BEAGLE		118	79	67	M	C	F		407	479	883	744	722	624	141	144	159	13,53	10,25	4,12	2,29	5,37	22,43	31,05
N-C8	BEAGLE		143	94	66	M	C	M		385	448	854	856	836	730	141	142	155	14,69	11,27	5,17	4,96	4,32	21,13	27,21
N-C9	SHEPHERD DOG		143	82	57	D	C	NA		362	414	805	733	720	647	149	151	166	11,5	6,13	3,31	6,48	4,66	26,99	36,48
Ny-C10	GERMAN SHEPHERD	GER	177	92	52	D	D	F		524	610	1062	1126	1106	1024	151	153	164	10,48	6,46	7,03	9,13	2,01	32,19	23,69
Ny-C11	MASTIFF	MAS	168	112	66	M	D	M		508	605	1089	999	965	817	134	136	149	11,68	20,29	9,11	5,34	2,4	17,7	19,48
Ny-C12	FOX TERRIER	FOX	160	102	63	M	C	M		531	632	1120	1083	1053	940	144	146	159	10,69	12,58	4,02	7,07	2,19	23,18	27,05
Ny-C13	HUSKY	HUS	157	93	59	D	C	F		532	610	1118	1159	1135	1004	142	143	155	11,38	11,5	6,62	7,32	3,45	18	26,42
Ny-C14	CANE CORSO	CAN	172	140	81	B	C	M		1354	1556	2479	2193	2125	1849	136	138	149	9,35	13,57	8,29	8,12	4,1	19,25	23,96
Ny-C15	LEONBERG	LEO	198	115	58	D	C	M		1027	1196	2271	2139	2092	1852	145	147	161	15,09	11,73	6,92	5,72	7,75	19,52	20,27
Ny-C16	BULLDOG	BUD	108	100	93	B	D	M		535	635	1050	839	804	679	134	137	150	13,25	10,58	7,81	6,45	4,58	21,96	19,29
Ny-C17	BORDER COLLIE	BOR	164	99	59	D	D	M		485	551	952	1071	1049	933	139	140	149	17,73	8,03	7,7	7,38	3,92	18,74	25,37
Ny-C18	ROTTWEILLER	ROT	182	128	70	B	C	M		1206	1388	2369	2156	2099	1839	140	142	154	9,99	5,85	13,42	4,68	4	22,42	28,14
Ny-C19	CHIHUAHUA	CHI	92	66	72	B	C	M		194	226	440	454	443	379	136	137	149	11,71	8,62	8,7	7,6	3,25	20,32	34,12
Ny-C20	PITBULL	PIT	167	123	74	B	D	M		1289	1515	2615	2076	2007	1740	141	144	159	15,52	15,15	10,57	5,57	2,45	21,41	19,05
Ny-C21	BOXER	BOX	142	114	80	B	D	M		633	699	1263	1057	1033	861	135	136	149	15,53	12,55	7,9	4,52	3,34	23,63	18,67
Ny-C22	SHETLAND SHEEPDOG	SHE	213	108	50	D	C	M		565	656	1115	1154	1127	1010	142	144	155	12,35	5,95	8,32	4,72	3,2	23,17	25,9
Ny-C23	BELGIAN SHEPHERD	BEL	147	99	67	M	D	M		321	383	734	759	739	641	138	140	152	18,12	9,2	5,14	5,03	3,11	18,81	22,54
Ny-C24	DEERHOUND	DEE	142	81	57	D	D	F		314	365	698	781	766	688	145	146	158	14,27	5,49	6,91	5,62	2,39	22,43	31,25
Ny-C25			168	90	54	D	C	M		384	454	782	799	781	715	148	150	162	14,52	7,88	8,34	5,03	4,09	15,32	27,4
Ny-C26	DOBERMANN	DOB	151	89	59	D	D	M		476	542	1010	867	843	701	134	136	150	10,65	14,03	21,79	5,25	1,96	19,29	19,37
Ny-C27	BORDER COLLIE	BOR	165	98	59	D	C	F		452	521	942	941	919	803	139	141	153	11,28	10,25	8,53	5,79	2,14	18,13	30,28
Ny-C28	ROTTWEILLER	ROT	170	131	77	B	C	M		1416	1644	2817	2389	2308	1949	134	136	149	16,03	9,37	10,2	5,14	3,91	26,01	16,92
Ny-C3	DACHSHUND	DAC	146	81	55	D	C	F		388	460	904	842	821	714	142	144	159	13,49	6,16	7,58	5,64	1,8	23,19	36,16
Ny-C4	MASTIFF	MAS	161	112	70	M	C	M		702	819	1407	1242	1203	1039	138	140	152	12,63	9,49	17,5	5,24	2,63	20,38	21,77
Ny-C5	BEAGLE		160	101	63	M	D	M		466	543	1018	978	954	830	140	142	155	13,89	7,81	5,29	7,33	3,51	20,09	28,28
Ny-C6	SHEPHERD DOG		193	109	56	D	D	M		539	634	1127	1118	1086	943	137	139	150	14,98	12,64	9,14	9,42	1,81	17,61	18,43
Ny-C8	AMSTAFF	AMS	162	118	73	B	C	NA		836	983	1636	1495	1448	1267	139	141	152	12,54	9,28	13,56	4,91	2,34	21,55	25,08
Ny-C9	BULL TERRIER	BULT	135	94	70	M	A	NA		317	369	595	640	623	552	135	137	146	14,22	9,13	8,32	11,75	3,23	24,22	16,36

		GAPE ANGLE = 2O°																	GAPE ANGLE = 3O°												
	ś)	BF			JF			AJF			Contribution to the total moment of the BF (%)								BF			JF			AJF			Contribution to the total mom				
ID	PM	I	C	M1	I	C	M1	I	C	M1	MS	MP	ZA	ZP	SZ	TS	TP	PM	I	C	M1	I	C	M1	I	C	M1	MS	MP	ZA	ZP	SZ
N-C10	8,32	362	423	830	880	857	725	133	134	145	15,12	15,25	2,65	7,33	3,38	20,6	27,56	8,12	336	392	769	892	871	742	131	132	142	14,85	15,08	2,72	7,2	3,19
N-C11	12,33	245	286	529	590	576	505	138	139	150	15,44	9,3	10,19	2,98	2,13	22,59	25,18	12,2	228	267	494	599	586	515	136	137	146	15,36	9,33	10,49	2,99	1,95
N-C12	12,9	268	307	591	622	608	514	132	133	144	9,38	10,84	5,77	4,21	4,73	25,59	25,8	13,68	249	285	549	631	617	523	129	130	139	9,46	10,86	5,9	4,27	4,4
N-C13	11,67	234	269	501	585	573	502	136	137	147	21,74	3,39	6,58	3,45	4,98	18,45	29,5	11,92	218	250	466	591	579	508	133	134	143	21,51	3,34	6,74	3,41	5,12
N-C14	19,71	406	466	817	915	895	787	136	138	147	9,89	13,2	6,93	9,33	3,3	14,27	23,21	19,87	377	432	758	927	908	802	134	136	144	9,67	13,11	7,08	9,27	3,23
N-C15	18,15	458	562	982	1130	1095	974	138	140	149	14,1	8,36	9,14	7,65	4,44	18,25	19,7	18,35	426	523	913	1139	1106	986	136	138	146	14,01	8,42	9,36	7,75	4,31
N-C16	21,87	441	518	926	853	826	704	135	137	149	12,83	9,13	7,78	6,18	2,17	21,03	19,24	21,63	413	486	868	862	836	716	134	136	147	12,79	9,12	7,91	6,14	1,99
N-C17	14,51	382	446	790	929	908	809	139	140	150	12,92	12,9	5,1	7,16	3,28	18,52	24,73	15,38	356	417	737	937	916	816	136	137	146	12,8	12,87	5,25	7,21	2,99
N-C18	14,85	485	554	958	1118	1096	980	139	141	150	10,79	6,51	12,06	6,15	2,52	20,12	27,3	14,54	451	516	891	1135	1113	998	137	138	146	10,65	6,54	12,36	6,28	2,22
N-C19	13,08	442	501	920	1102	1082	953	136	138	147	11,99	7,76	5,94	5,3	2,74	30,95	21,63	13,69	411	466	856	1113	1093	964	134	135	143	12,02	7,65	6,07	5,23	2,58
N-C2	16,38	348	406	725	840	820	717	134	136	145	16	9,74	5,04	3,17	3,52	22,9	22,87	16,77	323	377	674	848	828	729	133	134	142	15,99	9,76	5,13	3,19	3,3
N-C20	14,24	113	130	241	169	162	127	130	132	149	10,08	7,68	7,38	4,74	2,7	26,01	26,7	14,72	107	124	229	170	163	127	128	129	145	10	7,57	7,44	4,74	2,47
N-C21	11,14	260	306	542	474	455	363	123	124	135	18,74	9,13	5,82	2,65	1,75	26,34	24,41	11,17	240	282	500	479	461	375	122	123	133	18,31	9,14	6	2,62	1,62
N-C22	11,01	512	588	1064	1141	1115	976	138	139	150	11,89	9,91	7,99	8,16	2,51	28,28	20,08	11,18	479	550	995	1148	1123	982	135	136	145	11,7	9,81	8,1	8,05	2,52
N-C23	9,69	499	568	973	956	929	788	130	131	141	8,17	13,31	9,12	3,66	5,05	25,61	25,46	9,62	469	534	914	970	944	806	128	129	138	7,88	13,16	9,28	3,66	4,88
N-C3	10,89	356	413	798	862	840	702	128	129	139	13,89	8,91	9,39	8,44	1,97	18,6	27,89	10,91	329	382	737	875	854	723	127	128	137	13,84	8,95	9,64	8,43	1,77
N-C4	13,31	260	302	553	568	552	469	132	133	144	17,16	10,87	11,81	2,36	1,39	22,95	19,92	13,54	242	282	516	575	561	479	130	132	141	17,16	10,79	12,05	2,36	1,26
N-C5	15,73	719	819	1227	1007	965	804	122	124	132	10,19	13	12,75	5,62	1,32	18,1	22,94	16,08	673	766	1148	1026	986	833	122	123	130	10,27	13,13	12,99	5,7	1,23
N-C6	12,39	268	310	618	686	670	570	133	134	145	14,39	11,76	4,85	3,47	3,68	23,17	25,73	12,94	247	285	569	693	678	582	132	133	142	13,9	11,8	4,99	3,46	3,45
N-C7	10,96	370	436	803	759	738	633	137	139	152	13,38	10,15	4,25	2,23	4,83	22,71	31,43	11,03	346	408	751	769	748	643	135	137	148	13,29	10,15	4,32	2,21	4,53
N-C8	11,26	348	406	773	879	859	748	136	138	148	14,29	11,02	5,29	4,81	3,93	21,18	27,5	11,99	325	379	722	886	867	758	134	136	145	13,9	10,89	5,37	4,7	3,84
N-C9	4,46	341	390	759	742	728	642	144	146	159	11,29	5,85	3,25	6,27	3,58	25,68	39,72	4,35	322	368	717	745	730	639	141	142	155	11,16	5,78	3,26	6,24	3,07
Ny-C10	9	479	558	970	1140	1115	1001	140	142	151	10,19	6,24	7,11	9	1,81	32,93	23,48	9,25	450	524	912	1143	1118	996	136	137	145	9,93	6,12	7,16	8,87	1,74
Ny-C11	14	458	545	981	1040	1008	863	132	133	143	11,27	19,97	9,44	5,49	2,23	17,94	19,81	13,86	427	508	915	1049	1019	878	131	132	141	10,97	19,85	9,64	5,58	2,18
Ny-C12	13,23	488	582	1031	1108	1076	945	137	139	150	11,06	12,22	4,08	6,91	1,94	23,74	26,57	13,5	460	548	970	1122	1091	957	135	136	145	11,14	12,08	4,12	6,87	1,81
Ny-C13	15,31	479	549	1005	1186	1162	1023	136	138	147	11,37	11,26	6,75	7,46	3,2	18,04	26,55	15,37	445	511	935	1193	1170	1032	134	135	144	11,32	11,16	6,85	7,53	3,13
Ny-C14	13,36	1221	1403	2237	2244	2175	1884	130	132	140	9,16	13,4	8,49	8,29	3,82	19,01	24,84	13	1141	1310	2089	2272	2206	1920	128	129	137	9,06	13,38	8,62	8,39	3,71
Ny-C15	13,01	918	1068	2028	2225	2178	1919	140	142	153	14,53	11,51	7,14	5,74	7,16	19,76	21,41	12,74	850	990	1879	2256	2210	1952	138	140	150	14,09	11,4	7,28	5,74	6,96
Ny-C16	16,07	480	569	941	856	822	693	129	131	141	13,81	10,75	8,16	6,59	3,89	21,74	18,87	16,18	446	529	876	869	836	711	128	129	138	14,15	10,94	8,4	6,73	3,49
Ny-C17	11,12	437	496	857	1099	1078	960	134	135	143	17,92	7,99	7,98	7,37	3,44	18,38	25,66	11,27	406	461	796	1112	1091	975	132	133	140	17,93	8	8,17	7,38	3,23
Ny-C18	11,5	1095	1261	2152	2223	2166	1898	136	138	148	9,57	5,66	13,47	4,58	3,54	22,5	29,42	11,27	1024	1179	2011	2249	2194	1928	135	136	145	9,33	5,59	13,55	4,56	3,31
Ny-C19	5,67	178	207	403	465	455	392	134	135	145	10,81	8,4	8,86	7,31	2,8	21,07	35,53	5,23	166	193	376	470	460	398	132	133	142	10,35	8,34	9,01	7,24	2,69
Ny-C20	10,28	1165	1370	2365	2137	2065	1759	134	136	148	15,58	15,12	10,86	5,66	2,27	21,3	19,07	10,15	1091	1283	2214	2175	2104	1797	132	134	144	15,6	15,17	11,03	5,72	2,21
Ny-C21	13,87	573	633	1144	1097	1075	910	133	134	146	15,08	12,22	8,16	4,47	3,16	24,1	19,28	13,53	536	592	1069	1108	1088	929	132	133	144	14,79	12,1	8,34	4,46	3,11
Ny-C22	16,39	504	586	995	1197	1170	1045	137	138	147	11,7	5,94	8,65	4,83	3,11	23,18	26,19	16,41	468	544	924	1219	1192	1068	134	136	143	11,27	5,94	8,84	4,87	3,16
Ny-C23	18,05	289	344	659	778	759	663	136	137	147	17,61	9,11	5,34	4,98	2,76	18,95	23,12	18,15	268	319	611	785	767	674	135	136	145	17,2	9,1	5,47	4,99	2,61
Ny-C24	11,62	277	322	616	796	782	698	139	141	150	14,26	5,49	7,18	5,63	2,15	22,79	30,72	11,78	255	296	566	802	788	705	137	138	146	14,15	5,51	7,37	5,64	2,07
Ny-C25	17,42	352	416	717	827	807	726	141	143	152	14,3	7,68	8,42	5,06	3,51	15,06	27,61	18,35	330	390	672	836	816	733	138	140	148	14,1	7,62	8,52	5,06	3,27
Ny-C26	7,66	434	494	920	885	862	710	128	129	140	10,78	13,58	22,11	5,08	1,72	19,22	19,8	7,71	406	463	862	908	886	738	127	128	137	10,77	13,37	22,36	5	1,6
Ny-C27	13,6	406	468	847	968	946	824	134	136	145	11,47	10,05	8,72	5,76	1,99	17,57	30,46	13,98	377	435	787	980	958	839	132	133	142	11,49	9,98	8,87	5,75	1,92
Ny-C28	12,42	1276	1482	2539	2449	2374	2023	132	133	144	15,52	9,24	10,5	5,13	3,69	25,91	17,89	12,12	1189	1380	2364	2462	2390	2051	131	132	141	15,16	9,2	10,7	5,13	3,66
Ny-C3	5,98	347	412	810	859	838	722	137	139	151	12,93	5,93	7,82	5,47	1,65	23,79	36,42	5,99	322	382	751	872	851	735	135	136	147	12,53	5,82	7,98	5,39	1,58
Ny-C4	10,37	632	737	1267	1274	1236	1063	133	135	145	12,04	9,19	17,98	5,15	2,48	20,81	22,19	10,16	589	687	1181	1304	1268	1101	132	133	142	11,67	9,06	18,27	5,09	2,44
Ny-C5	13,8	413	481	902	994	970	835	134	135	146	13,83	7,84	5,56	7,48	3,08	20,46	27,37	14,38	380	443	831	1005	982	850	131	133	142	13,76	7,9	5,74	7,62	2,83
Ny-C6	15,98	485	571	1015	1137	1105	954	131	133	142	14,88	12,49	9,37	9,38	1,71	17,77	18,06	16,32	452	531	945	1151	1121	974	129	131	139	14,74	12,44	9,53	9,34	1,7
Ny-C8	10,73	764	898	1495	1539	1492	1304	135	136	146	12,15	8,97	13,62	4,76	2,13	21,82	25,98	10,56	717	843	1404	1560	1514	1329	133	134	143	11,92	8,84	13,7	4,7	2,06
Ny-C9	12,77	286	332	536	651	633	561	130	132	139	14,01	9,01	8,52	11,76	2,81	24,25	16,43	13,2	266	309	498	652	636	565	128	129	135	13,82	8,99	8,68	11,75	2,62

				GAPE ANGLE = 4O°																											
	ent of the BF (%)			BF			JF			AJF			Contribution to the total moment of the BF (%)								Digastricus				MS				MP		
ID	TS	TP	PM	I	C	M1	I	C	M1	I	C	M1	MS	MP	ZA	ZP	SZ	TS	TP	PM	ML	FL	A	mass	ML	FL	A	mass	ML	FL	A
N-C10	21,02	28,01	7,94	307	359	703	903	883	761	129	130	139	15	15	3	7	3	22	29	8	77,39	31,27	0,00	8,80	69,58	14,32	45,00	14,40	37,14	5,81	50,00
N-C11	22,77	25,04	12,06	210	245	454	606	593	524	133	135	143	15	9	11	3	2	23	25	12	85,66	37,16	0,00	6,00	71,32	17,89	47,50	10,80	30,39	9,51	35,00
N-C12	25,38	25,77	13,97	229	262	505	636	623	531	126	127	135	9	11	6	4	4	25	26	14	84,44	38,65	0,00	7,50	59,52	22,28	40,00	7,80	41,70	16,16	35,00
N-C13	18,43	29,5	11,95	200	231	429	594	582	513	131	132	140	21	3	7	3	6	18	30	12	92,89	35,79	0,00	11,10	73,18	19,30	45,00	14,70	25,40	24,85	30,00
N-C14	14,39	23,43	19,83	345	396	694	935	917	815	133	134	141	9	13	7	9	3	15	24	20	112,46	44,85	0,00	17,00	78,85	27,33	37,50	15,00	82,58	26,69	30,00
N-C15	18,04	19,76	18,36	391	479	837	1144	1112	997	134	136	144	14	9	10	8	4	18	20	18	101,36	37,02	0,00	13,40	77,27	12,46	45,00	13,40	72,85	19,27	40,00
N-C16	21,14	19,52	21,4	382	449	803	868	844	728	133	134	144	13	9	8	6	2	21	20	21	100,85	35,87	0,00	9,00	70,87	14,34	40,00	9,80	67,82	15,34	35,00
N-C17	18,63	24,6	15,64	328	384	680	940	920	823	134	135	142	13	13	5	7	3	19	24	16	124,32	46,10	0,00	23,30	87,16	25,26	45,00	21,30	42,52	12,76	37,50
N-C18	20,04	27,64	14,27	414	473	818	1148	1127	1014	135	136	143	10	7	13	6	2	20	28	14	97,75	35,50	0,00	14,90	71,76	18,79	55,00	19,40	61,65	31,16	32,50
N-C19	30,76	21,78	13,9	378	428	786	1120	1101	976	131	132	139	12	8	6	5	2	31	22	14	97,12	44,98	0,00	12,90	61,39	15,02	50,00	14,20	63,91	19,65	35,00
N-C2	22,84	22,92	16,89	296	345	617	854	836	741	131	132	139	16	10	5	3	3	23	23	17	78,30	35,77	0,00	8,97	61,30	16,73	40,00	13,30	25,70	12,03	20,00
N-C20	26,37	26,54	14,87	100	116	214	172	165	130	126	128	141	10	7	8	5	2	27	26	15	59,85	24,97	0,00	3,60	35,26	13,20	37,50	1,60	22,68	10,17	37,50
N-C21	26,49	24,64	11,19	217	256	453	483	467	388	121	123	130	18	9	6	3	2	27	25	11	58,36	26,64	0,00	4,80	56,53	13,06	45,00	7,70	33,32	10,94	50,00
N-C22	28,29	20,37	11,16	443	508	919	1168	1145	1007	133	134	142	11	10	8	8	3	28	21	11	105,34	33,21	0,00	30,50	69,70	29,12	35,00	26,70	47,30	21,43	35,00
N-C23	25,5	26,1	9,54	435	495	847	979	955	822	126	128	135	8	13	9	4	5	25	27	9	135,31	59,43	0,00	23,90	78,84	30,61	50,00	21,50	55,62	22,89	30,00
N-C3	18,85	27,68	10,84	299	347	670	886	867	745	127	128	135	14	9	10	8	2	19	27	11	88,70	49,15	0,00	8,00	60,90	15,43	35,00	11,00	19,00	9,90	2,50
N-C4	23,09	19,76	13,54	223	259	474	580	566	489	129	130	138	17	11	12	2	1	23	20	13	89,30	41,53	0,00	8,00	70,10	15,93	35,00	9,00	24,10	6,00	42,50
N-C5	17,89	22,65	16,14	622	708	1062	1048	1012	870	122	123	130	10	13	13	6	1	18	22	16	72,00	38,55	0,00	13,13	70,50	17,23	53,33	15,18	24,60	12,12	23,75
N-C6	23,53	25,68	13,18	223	258	515	697	684	593	130	131	139	13	12	5	3	3	24	26	13	75,00	39,40	0,00	6,75	56,40	15,10	27,50	9,40	27,50	9,27	20,00
N-C7	22,92	31,61	10,96	319	376	693	776	756	654	134	135	145	13	10	4	2	4	23	32	11	78,90	39,40	0,00	8,72	59,70	17,23	30,00	12,34	43,90	9,60	20,00
N-C8	21,29	27,74	12,28	301	351	668	892	874	768	133	134	142	13	11	5	5	4	21	28	13	83,70	37,35	0,00	10,81	62,70	17,78	32,50	13,67	29,40	13,17	15,00
N-C9	25,29	40,94	4,27	300	343	667	747	732	638	138	139	150	11	6	3	6	3	25	42	4	71,79	31,26	0,00	6,80	53,10	18,76	42,50	11,20	26,70	15,94	30,00
Ny-C10	33,41	23,48	9,29	418	487	847	1142	1117	992	132	133	140	10	6	7	9	2	34	24	9	98,00	37,50	0,00	15,80	62,00	33,00	35,00	23,30	54,00	19,50	32,50
Ny-C11	18,12	19,99	13,67	393	468	842	1050	1021	889	130	131	139	11	20	10	6	2	18	20	13	103,00	47,00	0,00	22,10	87,00	30,00	42,50	24,00	60,00	10,00	35,00
Ny-C12	24,08	26,41	13,5	427	509	901	1132	1101	968	132	133	141	11	12	4	7	2	24	26	13	99,00	48,00	0,00	19,60	77,00	24,00	47,50	19,50	54,00	13,50	37,50
Ny-C13	18,1	26,64	15,28	410	470	860	1195	1173	1038	132	133	140	11	11	7	8	3	18	27	15	90,00	30,00	0,00	16,49	80,00	25,00	40,00	21,60	35,00	10,00	45,00
Ny-C14	18,89	25,27	12,69	1053	1210	1928	2291	2228	1952	126	127	133	9	13	9	9	4	19	26	12	100,00	60,00	5,00	32,80	110,00	23,00	65,00	52,00	65,00	25,00	35,00
Ny-C15	19,97	22	12,55	778	905	1719	2276	2232	1981	136	138	146	13	11	7	6	7	20	23	12	110,00	44,00	0,00	33,10	100,00	22,00	40,00	46,60	50,00	15,00	37,50
Ny-C16	21,55	18,56	16,19	410	486	804	880	849	730	126	128	135	15	11	9	7	3	21	18	16	90,00	35,00	0,00	13,97	80,00	26,00	45,00	20,60	40,00	16,00	35,00
Ny-C17	18,27	25,77	11,26	372	422	729	1123	1104	994	130	131	137	18	8	8	7	3	18	26	11	75,00	26,00	0,00	11,27	70,00	16,50	35,00	17,82	40,00	15,00	30,00
Ny-C18	22,6	29,99	11,08	945	1088	1856	2277	2225	1967	133	134	142	9	6	14	5	3	23	31	11	12,00	39,50	10,00	46,60	105,00	30,67	47,50	55,70	47,00	20,00	37,50
Ny-C19	21,37	36,03	4,98	152	178	346	473	463	405	131	132	140	10	8	9	7	3	22	36	5	60,00	22,50	0,00	2,59	42,00	8,67	50,00	4,11	36,00	11,00	35,00
Ny-C20	21,22	19,07	9,97	1011	1189	2051	2197	2130	1829	130	132	141	16	15	11	6	2	21	19	10	105,00	36,25	0,00	33,20	95,00	25,00	35,00	49,30	70,00	11,00	22,50
Ny-C21	24,32	19,6	13,27	494	546	986	1125	1106	957	132	133	142	14	12	9	4	3	25	20	13	115,00	46,00	0,00	23,40	95,00	22,00	42,50	26,20	35,00	11,00	35,00
Ny-C22	23,21	26,34	16,36	429	498	847	1234	1208	1088	132	133	140	11	6	9	5	3	23	27	16	110,00	39,50	0,00	23,30	70,00	27,50	37,50	25,01	40,00	20,00	30,00
Ny-C23	19,09	23,42	18,13	245	291	559	788	772	683	134	135	143	17	9	6	5	3	19	24	18	90,00	36,00	0,00	10,04	70,00	15,00	45,00	15,38	30,00	10,00	37,50
Ny-C24	23,04	30,48	11,74	231	268	513	808	795	715	135	136	143	14	6	8	6	2	23	30	12	70,00	40,00	0,00	7,11	65,00	15,00	45,00	10,27	30,00	16,00	25,00
Ny-C25	15,02	27,83	18,58	305	360	621	845	826	744	136	137	145	14	8	9	5	3	15	28	19	75,00	27,50	0,00	8,96	60,00	12,50	40,00	9,02	30,00	13,00	40,00
Ny-C26	19,26	19,98	7,65	376	428	797	932	911	771	126	127	135	11	13	23	5	1	19	20	8	70,00	31,50	0,00	7,49	60,00	19,50	25,00	9,21	40,00	7,00	20,00
Ny-C27	17,34	30,59	14,06	345	398	720	988	968	853	130	131	138	11	10	9	6	2	17	31	14	80,00	33,00	0,00	10,69	60,00	14,50	42,50	9,63	35,00	12,00	30,00
Ny-C28	25,89	18,33	11,94	1092	1268	2172	2489	2423	2106	130	132	140	15	9	11	5	4	26	19	12	110,00	45,00	0,00	47,70	110,00	26,50	32,50	62,10	80,00	22,50	35,00
Ny-C3	24,18	36,56	5,97	294	349	686	883	863	750	132	134	143	12	6	8	5	2	25	37	6	56,40	33,13	0,00	6,68	60,00	11,67	45,00	9,55	27,50	9,40	35,00
Ny-C4	21,11	22,39	9,97	542	632	1087	1326	1292	1134	131	132	140	11	9	19	5	2	21	23	10	113,00	36,50	0,00	26,70	84,00	26,50	40,00	29,70	59,00	12,50	37,50
Ny-C5	20,68	26,9	14,55	345	402	754	1013	991	863	129	130	138	14	8	6	8	3	21	26	15	101,00	37,50	0,00	16,70	81,00	26,00	47,50	25,00	46,00	20,00	35,00
Ny-C6	17,93	17,98	16,34	416	488	869	1164	1136	996	128	129	136	15	12	10	9	2	18	18	16	112,00	46,00	0,00	21,40	92,00	29,50	35,00	27,40	47,00	18,00	27,50
Ny-C8	22,01	26,38	10,39	666	782	1303	1573	1530	1350	131	133	140	12	9	14	5	2	22	27	10	115,00	50,50	0,00	35,10	106,00	31,50	52,50	55,80	55,00	22,50	42,50
Ny-C9	24,37	16,46	13,32	244	283	456	658	642	576	127	128	133	14	9	9	12	2	25	17	13	93,00	35,50	0,00	10,40	60,00	21,00	32,50	11,10	50,00	18,00	32,50

Muscle architecture

		ZA				ZP				SZ				TS				TP				PM				PL			
ID	mass	ML	FL	A	mass	ML	FL	A	mass	ML	FL	A	mass	ML	FL	A	mass	ML	FL	A	mass	ML	FL	A	mass	ML	FL	A	mass
N-C10	4,60	19,34	15,37	25,00	1,10	29,18	8,46	45,00	3,70	93,33	24,18	25,00	5,30	100,25	29,38	32,50	20,20	87,83	28,66	25,00	32,60	32,74	18,06	20,00	7,00	9,58	4,22	30,00	0,20
N-C11	2,40	49,16	12,75	30,00	2,40	28,69	16,40	27,50	1,60	76,74	22,72	27,50	3,20	105,60	24,93	20,00	12,80	88,60	22,68	32,50	17,60	83,11	16,57	25,00	6,30	9,38	4,75	35,00	0,20
N-C12	5,10	34,79	22,10	30,00	2,50	31,50	11,70	20,00	1,90	86,42	16,24	25,00	5,60	111,94	31,45	25,00	19,40	91,39	34,42	40,00	29,40	52,11	13,70	20,00	5,10	8,04	NA	NA	0,20
N-C13	2,30	30,24	11,94	20,00	1,20	22,45	11,94	50,00	1,90	84,54	20,56	30,00	5,90	108,74	47,27	27,50	20,00	87,26	39,87	30,00	34,30	82,79	20,94	47,50	7,90	10,71	0,50	30,00	0,50
N-C14	14,30	84,34	30,66	27,50	5,80	56,26	12,59	35,00	6,20	127,90	30,48	25,00	8,40	133,43	39,42	35,00	22,50	138,72	37,17	40,00	47,00	79,15	14,63	45,00	15,20	17,09	11,42	27,50	1,30
N-C15	8,00	59,91	15,13	27,50	4,50	46,27	11,74	22,50	5,30	85,37	17,47	30,00	9,00	127,74	20,08	45,00	20,40	108,12	27,09	37,50	32,90	70,31	13,13	22,50	9,90	22,25	9,20	20,00	2,50
N-C16	6,00	44,63	17,24	40,00	4,50	39,37	9,05	35,00	2,80	84,30	31,81	30,00	6,00	118,14	27,20	32,50	21,90	93,06	29,52	37,50	26,60	71,45	11,12	25,00	9,40	19,15	9,37	20,00	1,40
N-C17	6,90	68,55	35,81	35,00	5,30	52,94	17,24	35,00	6,40	93,86	38,95	25,00	12,90	123,54	52,44	27,50	31,80	113,09	38,41	40,00	45,90	78,09	17,24	30,00	10,90	24,19	9,01	25,00	2,80
N-C18	9,30	58,33	13,49	27,50	5,40	38,22	9,96	35,00	4,10	99,10	30,70	20,00	9,60	117,01	36,31	35,00	34,30	116,36	29,85	35,00	50,00	75,13	17,60	37,50	15,40	20,50	8,46	27,50	1,10
N-C19	8,30	60,56	19,12	35,00	3,90	51,72	11,79	30,00	3,70	91,94	29,51	17,50	7,40	123,04	27,29	32,50	39,90	103,64	30,27	35,00	39,60	78,12	14,46	22,50	10,70	16,39	6,75	32,50	0,70
N-C2	3,57	27,40	15,60	35,00	2,12	26,70	12,05	32,50	1,62	92,80	20,15	30,00	6,32	103,10	21,90	30,00	17,15	94,50	27,23	35,00	29,40	66,00	8,27	50,00	7,22	17,70	7,95	40,00	0,67
N-C20	0,80	23,62	6,08	27,50	0,30	34,30	5,65	20,00	0,30	37,21	12,98	17,50	0,50	70,72	9,65	22,50	1,70	56,25	10,59	37,50	3,00	44,98	8,07	37,50	1,10	8,46	2,84	25,00	0,10
N-C21	2,90	18,44	8,29	30,00	0,80	26,92	13,62	30,00	1,00	73,86	24,22	25,00	2,20	96,19	19,43	37,50	12,60	90,12	21,90	40,00	16,90	48,26	16,20	20,00	3,30	12,05	7,54	30,00	0,30
N-C22	11,00	66,24	35,38	30,00	10,20	45,97	10,87	35,00	6,30	126,50	55,65	20,00	13,30	143,53	44,09	37,50	65,60	128,81	48,70	45,00	70,40	88,82	27,19	35,00	18,20	13,52	7,92	15,00	1,10
N-C23	15,40	52,96	33,54	25,00	10,40	68,51	23,29	25,00	6,10	104,51	19,29	35,00	8,40	135,23	45,86	20,00	44,00	123,96	45,03	37,50	58,30	98,74	26,18	47,50	14,60	17,04	15,09	25,00	1,20
N-C3	3,00	30,50	14,55	5,00	3,00	31,00	13,85	27,50	5,00	66,70	11,95	15,00	2,00	106,20	28,20	45,00	22,00	99,10	28,20	40,00	42,00	74,90	15,73	15,00	6,00	51,00	10,40	25,00	1,00
N-C4	2,00	20,60	10,47	10,00	2,00	37,30	13,05	60,00	2,00	64,90	21,10	15,00	2,00	118,30	28,95	40,00	18,00	95,40	33,70	45,00	27,00	69,40	14,25	32,50	5,00	23,60	11,65	37,50	1,00
N-C5	8,36	41,00	11,75	37,50	6,60	40,80	9,95	42,50	4,08	75,20	24,80	15,00	3,09	118,40	25,17	22,50	21,76	100,00	20,80	45,00	36,51	68,70	10,15	42,50	10,44	19,40	7,30	20,00	0,71
N-C6	2,81	26,00	9,30	10,00	0,88	22,60	9,40	30,00	1,36	78,00	14,85	0,00	2,45	95,90	26,75	25,00	15,24	75,60	24,20	25,00	20,84	52,70	8,50	50,00	4,48	16,50	7,30	NA	0,28
N-C7	3,22	28,20	11,70	35,00	1,50	27,00	10,25	45,00	1,31	92,60	20,25	30,00	5,57	93,10	20,90	40,00	15,46	87,20	24,93	40,00	27,35	66,00	9,95	27,50	5,28	18,60	3,80	50,00	0,39
N-C8	5,26	30,00	13,40	NA	1,88	34,10	9,53	42,50	2,81	85,60	20,30	30,00	6,63	99,30	33,40	35,00	23,31	89,25	28,38	32,50	32,03	73,80	12,67	45,00	8,01	19,50	5,00	NA	1,04
N-C9	3,10	36,29	17,17	20,00	1,30	29,63	9,14	40,00	3,00	91,01	10,67	25,00	3,50	94,85	28,03	22,50	17,20	87,17	24,21	20,00	27,00	66,91	10,39	50,00	4,20	10,59	5,94	45,00	0,20
Ny-C10	6,30	46,00	24,00	12,50	5,40	49,00	10,50	27,50	6,20	99,00	42,00	10,00	8,40	121,00	38,50	27,50	57,50	75,00	18,50	32,50	28,10	107,00	25,50	47,50	15,70	10,00	6,50	30,00	0,94
Ny-C11	10,60	62,00	29,00	15,00	8,00	57,00	17,00	40,00	7,50	114,00	44,00	30,00	9,80	140,00	53,00	37,50	43,60	109,00	32,50	37,50	39,40	99,00	29,00	32,50	20,00	17,00	11,50	40,00	1,20
Ny-C12	8,70	67,00	42,50	30,00	6,30	49,00	10,50	35,00	5,10	91,00	34,00	27,50	8,70	120,00	32,00	37,50	36,80	112,00	27,50	40,00	50,60	89,00	14,50	47,50	13,50	16,00	6,00	25,00	1,10
Ny-C13	6,70	45,00	20,00	45,00	5,75	40,00	10,00	35,00	5,10	97,50	15,00	40,00	7,24	110,00	25,00	50,00	26,93	120,00	25,00	47,50	51,30	90,00	11,00	37,50	10,70	20,00	7,00	40,00	0,81
Ny-C14	37,50	70,00	21,00	45,00	16,50	55,00	10,15	32,50	10,37	135,00	30,00	35,00	28,20	160,00	40,00	41,67	89,61	150,00	35,00	45,00	131,80	100,00	22,00	45,00	40,30	22,00	10,00	50,00	2,20
Ny-C15	19,30	60,00	20,00	40,00	10,57	55,00	10,00	42,50	9,28	135,00	12,20	55,00	22,30	145,00	42,50	37,50	77,90	140,00	36,00	45,00	95,30	110,00	15,00	47,50	26,60	25,00	10,00	50,00	1,63
Ny-C16	7,02	40,00	20,00	42,50	5,65	40,00	10,00	52,50	4,00	90,00	20,00	30,00	7,63	130,00	25,00	50,00	29,34	110,00	32,00	50,00	41,69	80,00	15,00	45,00	11,43	15,00	0,70	NA	0,52
Ny-C17	5,26	60,00	15,00	50,00	5,13	40,00	8,00	35,00	3,18	110,00	17,00	27,50	6,22	125,00	29,00	35,00	26,40	120,00	25,00	37,50	40,80	90,00	13,50	42,50	9,15	15,00	5,50	40,00	0,50
Ny-C18	13,27	70,00	20,30	30,00	21,04	52,00	12,13	47,50	9,05	150,00	40,00	35,00	33,70	165,00	40,00	42,50	95,70	140,00	40,00	40,00	149,90	105,00	22,20	45,00	34,20	25,00	12,00	50,00	3,00
Ny-C19	1,80	20,00	9,00	30,00	1,09	22,00	4,50	40,00	0,94	60,00	15,00	35,00	2,02	86,00	15,00	30,00	5,53	85,00	13,50	40,00	12,39	40,00	15,00	40,00	2,29	6,00	4,00	30,00	0,06
Ny-C20	15,10	70,00	18,50	35,00	14,95	55,00	12,00	40,00	10,07	110,00	25,00	25,00	13,85	140,00	36,00	35,00	77,11	120,00	39,00	45,00	104,00	80,00	16,00	40,00	24,60	17,00	7,50	40,00	0,77
Ny-C21	8,25	40,00	15,00	45,00	5,73	35,00	12,00	32,50	3,57	90,00	20,00	42,50	6,60	120,00	46,00	30,00	50,84	110,00	48,50	40,00	58,14	90,00	17,50	42,50	16,43	15,00	10,00	NA	0,52
Ny-C22	6,44	50,00	20,00	45,00	7,64	50,00	15,00	32,50	6,00	110,00	30,00	30,00	12,74	125,00	45,00	37,50	52,30	120,00	42,50	37,50	76,76	100,00	20,00	45,00	21,90	15,00	7,00	40,00	0,95
Ny-C23	3,45	40,00	31,00	35,00	4,15	35,00	15,00	25,00	3,22	85,00	35,00	30,00	6,99	75,00	35,00	40,00	21,70	95,00	30,00	50,00	32,80	70,00	11,00	50,00	9,59	10,00	0,50	50,00	0,30
Ny-C24	2,47	30,00	13,00	37,50	2,29	25,00	7,00	30,00	1,64	85,00	16,00	35,00	3,14	80,00	21,50	30,00	14,17	85,00	20,00	37,50	29,03	65,00	10,00	45,00	5,56	12,00	5,00	42,50	0,20
Ny-C25	4,19	40,00	15,00	30,00	3,55	40,00	12,00	25,00	2,67	80,00	17,00	37,50	6,04	100,00	25,00	38,33	14,05	110,00	21,00	45,00	25,10	70,00	8,50	50,00	9,32	15,00	6,70	50,00	0,42
Ny-C26	3,70	40,00	7,50	27,50	4,76	30,00	10,00	27,50	2,30	80,00	22,00	25,00	4,00	90,00	18,00	37,50	16,30	100,00	20,00	37,50	26,20	55,00	12,00	45,00	6,22	12,00	7,00	50,00	0,16
Ny-C27	5,62	50,00	13,00	40,00	3,93	30,00	7,00	42,50	2,72	90,00	25,00	35,00	4,79	105,00	26,00	40,00	22,45	80,00	20,00	40,00	33,66	60,00	12,00	40,00	8,60	15,00	8,00	50,00	0,55
Ny-C28	24,80	60,00	17,00	40,00	16,03	55,00	11,00	42,50	9,42	130,00	30,00	27,50	22,96	175,00	40,00	35,00	118,40	140,00	47,50	45,00	145,10	100,00	17,20	50,00	33,20	20,00	20,00	40,00	3,00
Ny-C3	2,20	29,80	9,40	35,00	2,24	27,00	7,40	35,00	2,00	60,60	17,40	35,00	2,26	77,10	15,60	50,00	16,17	87,40	13,17	27,50	21,69	63,90	11,80	62,50	5,55	13,80	12,80	NA	0,36
Ny-C4	8,90	84,00	15,50	32,50	12,60	54,00	15,00	35,00	6,70	103,00	44,50	27,50	12,40	141,00	43,00	37,50	51,60	126,00	46,50	35,00	72,80	94,00	21,00	42,50	18,40	17,00	7,50	27,50	1,40
Ny-C5	7,10	56,00	30,00	27,50	5,00	49,00	10,50	37,50	4,90	79,00	31,50	20,00	8,40	129,00	44,50	35,00	37,40	114,00	41,00	37,50	63,20	67,00	23,00	35,00	16,30	10,00	6,00	30,00	0,70
Ny-C6	10,80	75,00	34,00	35,00	11,90	56,00	11,50	30,00	6,70	116,00	44,00	27,50	8,80	119,00	37,50	47,50	40,90	124,00	46,00	45,00	71,10	102,00	22,00	40,00	23,00	15,00	5,50	20,00	0,90
Ny-C8	17,10	90,00	21,50	37,50	15,90	53,00	16,50	37,50	8,60	115,00	59,00	20,00	17,20	143,00	50,50	35,00	72,70	144,00	41,50	50,00	117,00	93,00	24,50	40,00	23,60	26,00	10,00	30,00	1,90
Ny-C9	4,80	63,00	23,50	27,50	4,00	40,00	7,50	25,00	3,30	86,00	29,00	20,00	5,10	75,00	33,00	27,50	20,00	107,00	28,00	40,00	18,30	78,00	17,00	37,50	8,10	14,00	4,50	32,50	0,50

4.2. Table S2.

Definition of the landmarks used in the geometric morphometric analyses following the Nomina Anatomica Veterinaria nomenclature (NAV, 2017).

Landmark	Definition
Lower jaw: Mandibula	
1	Most rostromedial point of the Synchondrosis intermandibularis, at the base of the first incisor tooth
2	Most rostral point of the canine tooth, on the lateral side
3	Most caudal point of the canine tooth, on the lateral side
4	Most rostral point of the second premolar tooth, on the lateral side
5	Most rostral point of the third premolar tooth, on the lateral side
6	Most rostral point of the fourth premolar tooth, on the lateral side
7	Most caudal point of the fourth premolar tooth, on the lateral side
8	Most caudal point of the carnassial tooth, on the lateral side
9	Most caudal point of the second molar tooth, on the lateral side
10	Highest point of the tip of the Processus coronoideus
11	Most caudal point of the tip of the Processus coronoideus
12	Most caudal point of the Incisura mandibulae, at the intersection of the Processus condylaris and the Processus coronoideus
13	Most medial point of the Processus condylaris
14	Most ventral point of the Processus condylaris
15	Most lateral point of the Processus condylaris
16	Most anterior point on the curve of the Angulus mandibulae
17	Point at the tip of the Processus angularis
18	Most elevated point on the inferior border of the Ramus mandibulae
19	Lowest point on the ventral border of the Ramus mandibulae, right under the carnassial tooth
20	Most caudal and lowest point of the Synchondrosis intermandibularis on the medial side
21	Foramen mentale
22	Most rostral and ventral point of the Fossa masseterica
23	Most rostral point of the edge joining the basis of the Processus condylaris and Processus condylaris on the medial side.
24	Most rostral point of the Foramen mandibulae
25	The most lateral point on the Angulus mandibulae, at the beginning of the Processus angularis
Upper jaw	
1	Most rostral point of Os incisivum, between incisor teeth I1 in dorsal view
2	Most rostral point of Os nasale, on the midline (Sutura internasalis)
3	Most rostral point on Sutura nasoincisiva
4	Point at the junction of Os incisivum, Os nasale and Maxilla
5	Point at the junction of Os nasale, Maxilla and Os frontale
6	Most rostral point of Os temporale and most caudal point of Os nasale, on the midline (Sutura internasalis)
7	Most posterior point of the Maxilla in dorsal view
8	Most lateral point of the Processus zygomaticus of Os frontale
9	Most medial point of the curvature corresponding to the Linea temporalis, most medial point at the postorbital constriction
10	Processus frontalis of Os zygomaticum
11	Most rostral point of the curvature of the lower edge of the Fossa sacci lacrimalis
12	Bregmatic fontanel, most medial point of the Sutura coronalis, on the midline
13	Most medial point on the Sutura lambdoidea
14	Inion, posterior end of Os occipitale
15	Point at the extreme convex curvature of the Tuberculum nuchale
16	Point at the extreme convex curvature of the Crista supramastoidea
17	Fossa mandibularis, on the Sutura sphenoparietalis
18	Central point of the Sutura interincisiva in ventral view, just posterior to the two incisors teeth
19	Most rostral point of the Fissura palatina

20	Most caudal point of the Fissura palatina
21	Point on the Fissura palatina at the junction between Os incisivum and Maxilla in ventral view
22	Point between the Canina and the incisor tooth I3 at the junction between Os incisivum and Maxilla in ventral view
23	Most rostral point of Maxilla in ventral view, on the midline
24	Most rostral point of the Sutura palatomaxillaris, on the midline
25	Most caudal point of Os palatinum, on the midline
26	Point near molar tooth M2, on the Sutura palatomaxillaris
27	Ventral point on the Sutura sphenopalatina
28	Point on vomer, at the junction with Os presphenoidale (Sutura vomerosphenoidalis)
29	Most caudal point of the Synchondrosis sphenooccipitalis, on the midline
30	Most lateral point of the Synchondrosis sphenooccipitalis, rostrally to the Bulla tympanica
31	Most cranial point of the caudal curve of Os occipitale (Foramen magnum) in ventral view, on the midline
32	Most caudal point of the caudal curve of Os occipitale in ventral view
33	Point on the Foramen lacerum
34	Processus paracondylaris
35	Ventral tip of the Bulla tympanica
36	Most dorsal and caudal point of the curve of the Foramen alare caudale
37	Most ventral and posterior point at the junction of the Pars squamosa of Os temporale and Os zygomaticum, on the Arcus zygomaticus
38	Most caudal point at the junction between Maxilla and Os zygomaticum, near the molar tooth M2
39	Most cranial point of the alveolus of the canine tooth
40	Most caudal point of the alveolus of the canine tooth
41	Most cranial point of the alveolus of the upper carnassial tooth P4
42	Point between the alveolus of P4 and M1 teeth
43	Point between the alveolus of M1 and M2 teeth
44	Most caudal point of Maxilla behind tooth M2
45	Most dorsal point of the Foramen infraorbitale
46	Most ventral point of the Foramen infraorbitale
47	Point at the junction of Maxilla, Os lacrimale and Os temporale
48	Point at the junction of Maxilla, Os lacrimale and Os zygomaticum
49	Most caudal point of curvature at the junction of Maxilla and Os zygomaticum
50	Most ventral and caudal point of the Foramen alare rostrale
51	Most ventral and caudal point of the Fissura orbitalis
52	Most rostral point of Meatus acusticus externus in lateral view
53	Most caudal point of Meatus acusticus externus in lateral view
54	Opisthion, dorsal and caudal border of the Foramen magnum, on the midline

4.3. Movie S1.

Video showing *in vivo* bite force recording in a Malinois dog.

4.4. Fig. S1

Position of origin (in blue) and insertion (red) of the jaw adductors. MS: M. masseter par superficialis; MP: M. masseter pars profunda; ZA: M. zygomaticomandibularis pars anterior; ZP: M. zygomaticomandibularis pars posterior; SZ: M. temporalis pars suprazygomatica; TS: M. temporal pars superficialis; TP: M. temporal pars profunda; PM: M. pterygoideus medialis.

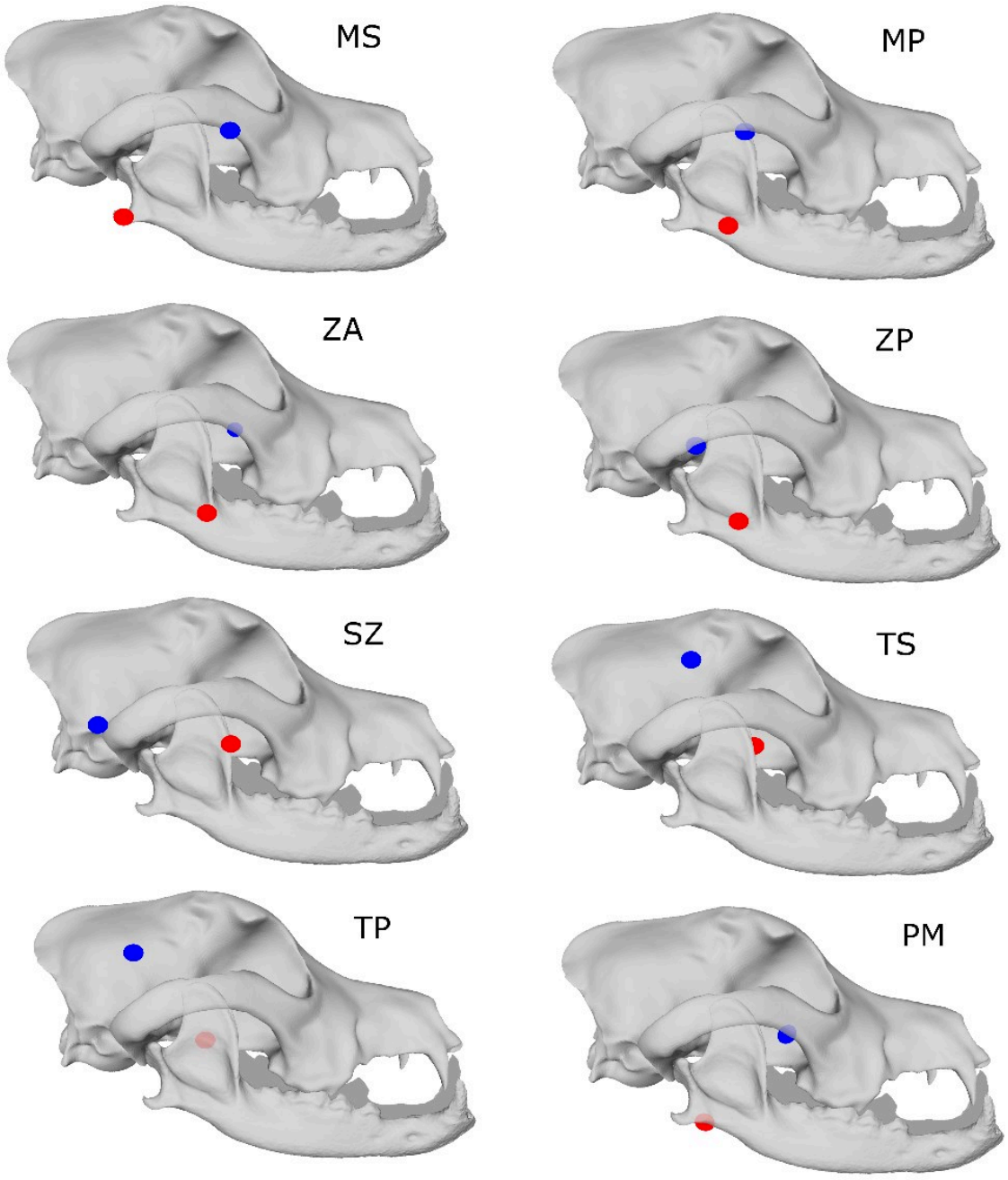

4.5. Fig. S2.

2-Block Partial Least Square Analyses between the shape of the upper jaw (A) or the shape of the lower jaw (B) and bite force (BF), with bite force vectors and shapes at the minimum and maximum of the PLS axis. Illustrations represent the deformations from the consensus to the extreme of the axis in lateral, dorsal and caudal views. Different morphotypes are indicated by different colors, and ages are indicated by different shapes. Ams: American Staffordshire terrier; Box: Boxer; Buld: Bulldog; Bult: Bull terrier; Chi: Chihuahua; Can: Cane Corso; Kin: Cavalier King Charles Spaniel; Pap: Papillon; Pit: Pitbull; Rot: Rottweiler; Mas: Mastiff; Fox: fox terrier; Bel: Belgian Shepherd; Bor: Border collie; Col: Collie; Dac: Dachshund; Ger: German Shepherd; Gol: Golden retriever; Hus: Husky; Leo: Leonberg; She: Shetland sheepdog. The right part of the scatterplots corresponds to the dogs with low bite forces, and that have a relatively elongated, flat and straight mandibular body in the sagittal plane, a small, narrow and posteriorly curved coronoid process with a shallow masseteric fossa, a medially short and small condylar process of the mandible and weak angular and coronoid processes. The braincase is lower in the lateral view, and the zygomatic arches are narrower. In contrast, the left part of the scatterplot corresponds to large brachycephalic dogs with a high bite and these have a very robust mandible with a relatively large, wide coronoid process with a deep masseteric fossa, a shorten, ventrally and laterally curved mandibular body, a big, medially extended and caudally curved condylar process of the mandible and a bigger angular process. The braincase is taller, and the zygomatic arches are wider in the dorsal view.

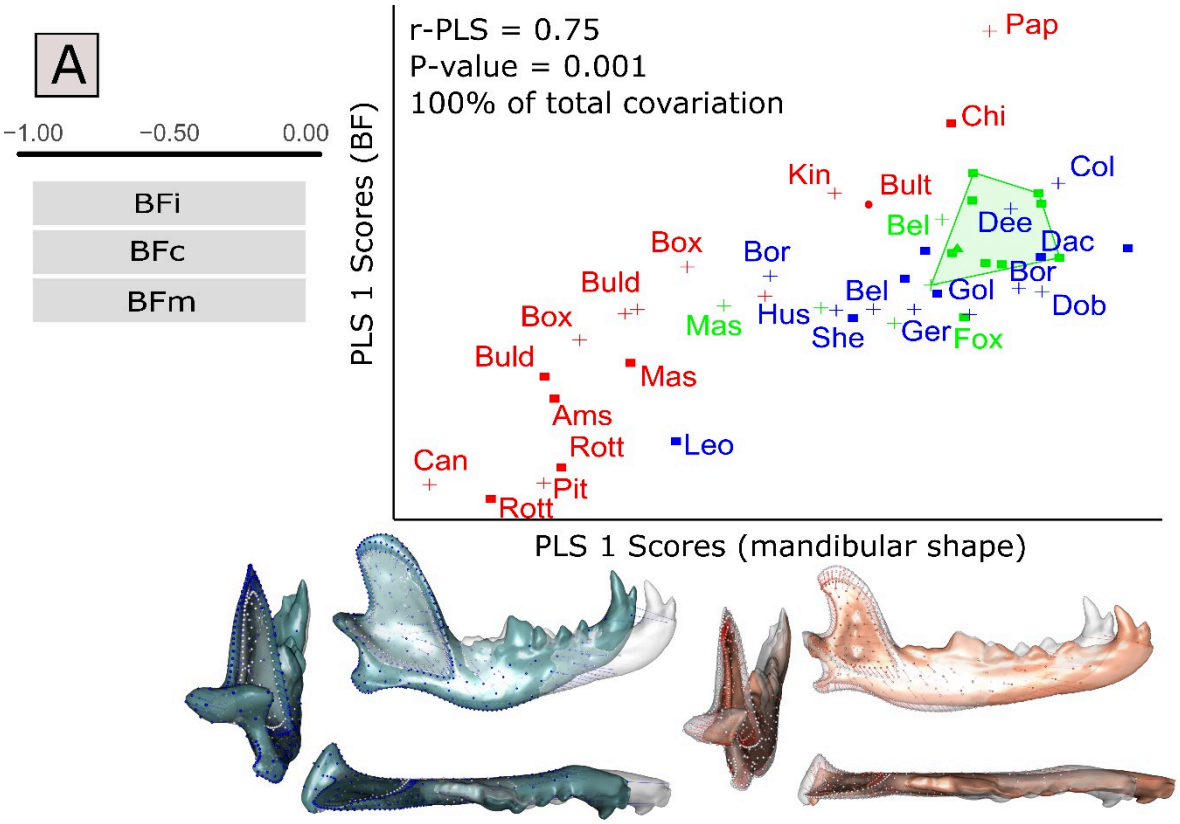
A
−1.00
−0.50
0.00
BFi
BFc
BFm
r-PLS = 0.75
P-value = 0.001
100% of total covariation
PLS 1 Scores (BF)
PLS 1 Scores (mandibular shape)
Pap
Chi
Kin
Bult
Col
Bel
Dee
Dac
Box
Bor
Buld
Gol
Dob
Hus
She
Ger
Fox
Mas
Ams
Rott
Leo
Can
Pit

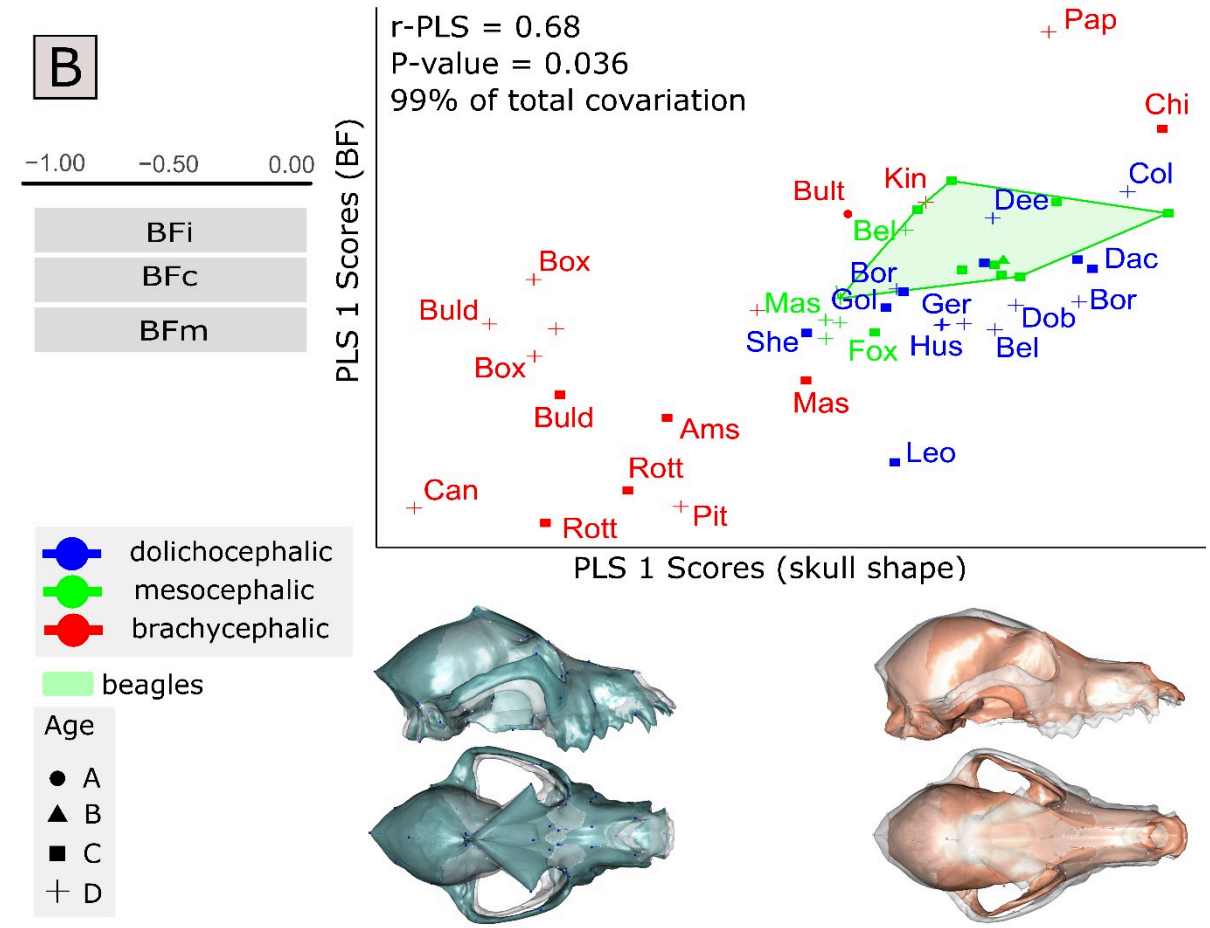
B
−1.00
−0.50
0.00
BFi
BFc
BFm
r-PLS = 0.68
P-value = 0.036
99% of total covariation
PLS 1 Scores (BF)
PLS 1 Scores (skull shape)
Pap
Chi
Bult
Kin
Col
Dee
Bel
Box
Dac
Bor
Buld
Mas
Gol
Ger
Dob
Bor
She
Fox
Hus
Bel
Box
Mas
Buld
Ams
Leo
Rott
Can
Pit
Rott
dolichocephalic
mesocephalic
brachycephalic
beagles
Age
A
B
C
D

4.1. Detailed results of the statistical analyses.

Results of the statistical analyses

1. Bite Force and size

1.1. Linear regression between skull length and Bite Force (in log10).

```
> summary(lm(log10(dt$bf)~log10(dt$lg)))

Call:
lm(formula = log10(dt$bf) ~ log10(dt$lg))

Residuals:
     Min       1Q   Median       3Q      Max
-0.30882 -0.09002 -0.03525  0.05523  0.37610

Coefficients:
             Estimate Std. Error t value Pr(>|t|)
(Intercept)  -0.01103    0.58957  -0.019    0.985
log10(dt$lg)  1.33190    0.27126   4.910 1.24e-05 ***
---
Signif. codes:  0 '***' 0.001 '**' 0.01 '*' 0.05 '.' 0.1 ' ' 1

Residual standard error: 0.1611 on 45 degrees of freedom
Multiple R-squared:  0.3488, Adjusted R-squared:  0.3344
F-statistic: 24.11 on 1 and 45 DF,  p-value: 1.241e-05
```

1.2. Linear regression between mandibular centroid size and bite force (in log10).

```
> summary(stepAIC(lm(bf~size.mdb,data=tab)))
Start:  AIC=-187.24
bf ~ size.mdb

            Df Sum of Sq     RSS     AIC
<none>                   0.80352 -187.24
- size.mdb  1   0.97964 1.78315 -151.77

Call:
lm(formula = bf ~ size.mdb, data = tab)

Residuals:
     Min       1Q   Median       3Q      Max
-0.29193 -0.07880 -0.02715  0.08102  0.33171

Coefficients:
            Estimate Std. Error t value Pr(>|t|)
(Intercept)  3.22376    0.04197  76.812  < 2e-16 ***
size.mdb     1.63898    0.22127   7.407 2.55e-09 ***
---
Signif. codes:  0 '***' 0.001 '**' 0.01 '*' 0.05 '.' 0.1 ' ' 1

Residual standard error: 0.1336 on 45 degrees of freedom
Multiple R-squared:  0.5494,   Adjusted R-squared:  0.5394
F-statistic: 54.86 on 1 and 45 DF,  p-value: 2.549e-09
```

1.3. Linear regression between cranial centroid size and bite force (in log10).

```
> summary(stepAIC(lm(bf~size.skull,data=tab)))
Start:  AIC=-175.22
bf ~ size.skull

             Df Sum of Sq    RSS     AIC
<none>                    1.0378 -175.22
- size.skull  1    0.7454 1.7832 -151.77

Call:
lm(formula = bf ~ size.skull, data = tab)

Residuals:
     Min       1Q   Median       3Q      Max
-0.29754 -0.08025 -0.03322  0.06319  0.35485

Coefficients:
             Estimate Std. Error t value Pr(>|t|)
(Intercept)  -1.5123     0.7849  -1.927   0.0604 .
size.skull    1.6156     0.2842   5.685 9.13e-07 ***
---
Signif. codes:  0 '***' 0.001 '**' 0.01 '*' 0.05 '.' 0.1 ' ' 1

Residual standard error: 0.1519 on 45 degrees of freedom
Multiple R-squared:  0.418,    Adjusted R-squared:  0.4051
F-statistic: 32.32 on 1 and 45 DF,  p-value: 9.134e-07
```

2. Comparison of muscle contributions to the moment of the Bite Force

```
> friedman.test(m0_c)

        Friedman rank sum test

data:  m0_c
Friedman chi-squared = 271.33, df = 7, p-value < 2.2e-16

> posthoc.friedman.nemenyi.test(m0_c)

        Pairwise comparisons using Nemenyi multiple comparison test
           with q approximation for unreplicated blocked data

data: m0_c

   MS      MP      ZA      ZP      SZ      TS      TP
MP 0.26232 -       -       -       -       -       -
ZA 0.00710 0.91232 -       -       -       -       -
ZP 1.7e-07 0.01295 0.35793 -       -       -       -
SZ 4.1e-13 2.5e-06 0.00115 0.55444 -       -       -
TS 0.00229 9.8e-09 1.4e-12 9.3e-14 < 2e-16 -       -
TP 3.5e-05 1.7e-11 7.9e-14 7.4e-14 < 2e-16 0.98360 -
PM 1.00000 0.38421 0.01497 6.0e-07 1.9e-12 0.00096 1.2e-05


> apply(m0_c2,2,summary)
                M        T        P
Min.    27.42000 37.84000  4.46000
1st Qu. 34.34000 45.21000 10.98500
Median  37.05000 49.77000 12.90000
Mean    37.49064 49.69872 12.80979
3rd Qu. 40.43000 52.96500 14.68000
Max.    51.72000 68.13000 21.87000
> apply(m0_c2,2,sd)
       M        T        P
4.974299 6.168395 3.490542
> # Comapraison de k éch appariés : Friedman
> friedman.test(m0_c2)

        Friedman rank sum test

data:  m0_c2
Friedman chi-squared = 85.064, df = 2, p-value < 2.2e-16

> posthoc.friedman.nemenyi.test(m0_c2)

        Pairwise comparisons using Nemenyi multiple comparison test
           with q approximation for unreplicated blocked data

data: m0_c2

  M       T
T 4e-04   -
P 2.4e-07 3.5e-14

P value adjustment method: none
```

3. Differences between Brachycephalic/mesocephalic and dolichocephalic dogs

3.1. Raw Bite Forces (log10)

```
> anova(lm(log10(dt$bf)~as.factor(dt$gpe_ci)))
```

```
Analysis of Variance Table

Response: log10(dt$bf)
                    Df Sum Sq Mean Sq F value Pr(>F)
as.factor(dt$gpe_ci)  2   0.13  0.0648    1.72   0.19
Residuals            44   1.66  0.0378
> TukeyHSD(aov(log10(dt$bf)~as.factor(dt$gpe_ci)))
  Tukey multiple comparisons of means
    95% family-wise confidence level

Fit: aov(formula = log10(dt$bf) ~ as.factor(dt$gpe_ci))

$`as.factor(dt$gpe_ci)`
                                    diff    lwr    upr p adj
dolichocephalic-brachycephalic -0.0670 -0.234 0.0997 0.596
mesocephalic-brachycephalic    -0.1293 -0.299 0.0402 0.165
mesocephalic-dolichocephalic   -0.0623 -0.232 0.1072 0.648

> summary(lm(log10(dt$bf)~as.factor(dt$gpe_ci)))

Call:
lm(formula = log10(dt$bf) ~ as.factor(dt$gpe_ci))

Residuals:
     Min       1Q   Median       3Q      Max
-0.6142 -0.0772  0.0099  0.0709  0.3914

Coefficients:
                                      Estimate Std. Error t value Pr(>|t|)
(Intercept)                            2.9455     0.0486   60.61   <2e-16 ***
as.factor(dt$gpe_ci)dolichocephalic   -0.0670     0.0687   -0.97    0.335
as.factor(dt$gpe_ci)mesocephalic      -0.1293     0.0699   -1.85    0.071 .
---
Signif. codes:  0 '***' 0.001 '**' 0.01 '*' 0.05 '.' 0.1 ' ' 1

Residual standard error: 0.194 on 44 degrees of freedom
Multiple R-squared:  0.0723,            Adjusted R-squared:  0.0302
F-statistic: 1.72 on 2 and 44 DF,  p-value: 0.192
```

3.3. Residual bite forces, using head length as a proxy of size

```
> anova(lm(dt2$bf~as.factor(dt2$gpe_ci)))
Analysis of Variance Table

Response: dt2$bf
                    Df Sum Sq Mean Sq F value Pr(>F)
as.factor(dt2$gpe_ci)  2  0.172  0.0862    5.95 0.0052 **
Residuals             44  0.638  0.0145
---
Signif. codes:  0 '***' 0.001 '**' 0.01 '*' 0.05 '.' 0.1 ' ' 1
> TukeyHSD(aov(dt2$bf~as.factor(dt2$gpe_ci)))
  Tukey multiple comparisons of means
    95% family-wise confidence level

Fit: aov(formula = dt2$bf ~ as.factor(dt2$gpe_ci))

$`as.factor(dt2$gpe_ci)`
                                    diff     lwr     upr p adj
dolichocephalic-brachycephalic -0.1366 -0.2399 -0.0334 0.007
mesocephalic-brachycephalic    -0.1159 -0.2208 -0.0109 0.028
mesocephalic-dolichocephalic    0.0208 -0.0842  0.1257 0.881

> summary(lm(dt2$bf~as.factor(dt2$ci)))

Call:
lm(formula = dt2$bf ~ as.factor(dt2$ci))

Residuals:
      Min       1Q   Median       3Q      Max
-0.21229 -0.00742  0.00000  0.00363  0.17488

Coefficients:
                 Estimate Std. Error t value Pr(>|t|)
(Intercept)       -0.292      0.100   -2.90  0.00909 **
as.factor(dt2$ci)50   0.125      0.142    0.88  0.38885
as.factor(dt2$ci)52   0.245      0.142    1.72  0.10119
as.factor(dt2$ci)54   0.155      0.142    1.09  0.28876
as.factor(dt2$ci)55   0.381      0.142    2.68  0.01478 *
as.factor(dt2$ci)56   0.185      0.142    1.31  0.20725
as.factor(dt2$ci)57   0.284      0.123    2.31  0.03234 *
as.factor(dt2$ci)58   0.354      0.123    2.87  0.00970 **
as.factor(dt2$ci)59   0.242      0.108    2.23  0.03814 *
as.factor(dt2$ci)61   0.266      0.142    1.88  0.07611 .
as.factor(dt2$ci)62   0.368      0.142    2.59  0.01788 *
as.factor(dt2$ci)63   0.245      0.110    2.23  0.03788 *
as.factor(dt2$ci)65   0.234      0.142    1.65  0.11591
as.factor(dt2$ci)66   0.249      0.116    2.15  0.04468 *
as.factor(dt2$ci)67   0.300      0.116    2.59  0.01801 *
as.factor(dt2$ci)69   0.145      0.142    1.02  0.31943
as.factor(dt2$ci)70   0.350      0.116    3.02  0.00704 **
as.factor(dt2$ci)72   0.348      0.123    2.83  0.01065 *
as.factor(dt2$ci)73   0.419      0.142    2.95  0.00824 **
as.factor(dt2$ci)74   0.628      0.142    4.43  0.00029 ***
as.factor(dt2$ci)77   0.621      0.142    4.37  0.00033 ***
as.factor(dt2$ci)78   0.209      0.142    1.47  0.15819
as.factor(dt2$ci)80   0.289      0.142    2.03  0.05616 .
as.factor(dt2$ci)81   0.407      0.123    3.31  0.00371 **
as.factor(dt2$ci)83   0.171      0.142    1.21  0.24264
as.factor(dt2$ci)84   0.161      0.142    1.13  0.27183
as.factor(dt2$ci)85   0.547      0.142    3.85  0.00108 **
as.factor(dt2$ci)93   0.398      0.142    2.80  0.01135 *
---
Signif. codes:  0 '***' 0.001 '**' 0.01 '*' 0.05 '.' 0.1 ' ' 1

Residual standard error: 0.1 on 19 degrees of freedom
Multiple R-squared:  0.764,             Adjusted R-squared:  0.428
F-statistic: 2.27 on 27 and 19 DF,  p-value: 0.0339
```

3.4. Residual bite forces, using mandible centroid size as a proxy of size

```
> anova(lm(dt3$bf~as.factor(dt$gpe_ci)))
Analysis of Variance Table

Response: dt3$bf
                    Df Sum Sq Mean Sq F value Pr(>F)
as.factor(dt$gpe_ci)  2  0.172  0.0862    5.95 0.0052 **
Residuals            44  0.638  0.0145
---
Signif. codes:  0 '***' 0.001 '**' 0.01 '*' 0.05 '.' 0.1 ' ' 1
> TukeyHSD(aov(dt3$bf~as.factor(dt$gpe_ci)))
  Tukey multiple comparisons of means
    95% family-wise confidence level

Fit: aov(formula = dt3$bf ~ as.factor(dt$gpe_ci))

$`as.factor(dt$gpe_ci)`
                                    diff     lwr     upr p adj
dolichocephalic-brachycephalic -0.1366 -0.2399 -0.0334 0.007
mesocephalic-brachycephalic    -0.1159 -0.2208 -0.0109 0.028
mesocephalic-dolichocephalic    0.0208 -0.0842  0.1257 0.881

> summary(lm(dt3$bf~as.factor(dt$ci)))

Call:
lm(formula = dt3$bf ~ as.factor(dt$ci))

Residuals:
      Min       1Q   Median       3Q      Max
-0.21229 -0.00742  0.00000  0.00363  0.17488

Coefficients:
                 Estimate Std. Error t value Pr(>|t|)
(Intercept)       -0.292      0.100   -2.90  0.00909 **
as.factor(dt$ci)50   0.125      0.142    0.88  0.38885
as.factor(dt$ci)52   0.245      0.142    1.72  0.10119
as.factor(dt$ci)54   0.155      0.142    1.09  0.28876
as.factor(dt$ci)55   0.381      0.142    2.68  0.01478 *
as.factor(dt$ci)56   0.185      0.142    1.31  0.20725
as.factor(dt$ci)57   0.284      0.123    2.31  0.03234 *
as.factor(dt$ci)58   0.354      0.123    2.87  0.00970 **
as.factor(dt$ci)59   0.242      0.108    2.23  0.03814 *
as.factor(dt$ci)61   0.266      0.142    1.88  0.07611 .
as.factor(dt$ci)62   0.368      0.142    2.59  0.01788 *
as.factor(dt$ci)63   0.245      0.110    2.23  0.03788 *
as.factor(dt$ci)65   0.234      0.142    1.65  0.11591
as.factor(dt$ci)66   0.249      0.116    2.15  0.04468 *
as.factor(dt$ci)67   0.300      0.116    2.59  0.01801 *
as.factor(dt$ci)69   0.145      0.142    1.02  0.31943
as.factor(dt$ci)70   0.350      0.116    3.02  0.00704 **
as.factor(dt$ci)72   0.348      0.123    2.83  0.01065 *
as.factor(dt$ci)73   0.419      0.142    2.95  0.00824 **
as.factor(dt$ci)74   0.628      0.142    4.43  0.00029 ***
as.factor(dt$ci)77   0.621      0.142    4.37  0.00033 ***
as.factor(dt$ci)78   0.209      0.142    1.47  0.15819
as.factor(dt$ci)80   0.289      0.142    2.03  0.05616 .
as.factor(dt$ci)81   0.407      0.123    3.31  0.00371 **
as.factor(dt$ci)83   0.171      0.142    1.21  0.24264
as.factor(dt$ci)84   0.161      0.142    1.13  0.27183
as.factor(dt$ci)85   0.547      0.142    3.85  0.00108 **
as.factor(dt$ci)93   0.398      0.142    2.80  0.01135 *
---
Signif. codes:  0 '***' 0.001 '**' 0.01 '*' 0.05 '.' 0.1 ' ' 1

Residual standard error: 0.1 on 19 degrees of freedom
Multiple R-squared:  0.764,             Adjusted R-squared:  0.428
F-statistic: 2.27 on 27 and 19 DF,  p-value: 0.0339
```

3.5. Residual bite forces, using skull centroid size as a proxy of size

```
> anova(lm(dt3$bf~as.factor(dt$gpe_ci)))
Analysis of Variance Table

Response: dt3$bf
                    Df Sum Sq Mean Sq F value  Pr(>F)
as.factor(dt$gpe_ci)  2  0.340  0.1698    10.5 0.00018 ***
Residuals            44  0.709  0.0161
---
Signif. codes:  0 '***' 0.001 '**' 0.01 '*' 0.05 '.' 0.1 ' ' 1


> TukeyHSD(aov(dt3$bf~as.factor(dt$gpe_ci)))
  Tukey multiple comparisons of means
    95% family-wise confidence level

Fit: aov(formula = dt3$bf ~ as.factor(dt$gpe_ci))

$`as.factor(dt$gpe_ci)`
                                    diff     lwr     upr p adj
dolichocephalic-brachycephalic -0.1900 -0.2989 -0.0811 0.000
mesocephalic-brachycephalic    -0.1655 -0.2762 -0.0548 0.002
mesocephalic-dolichocephalic    0.0245 -0.0862  0.1351 0.854

> summary(lm(dt3$bf~as.factor(dt$ci)))

Call:
lm(formula = dt3$bf ~ as.factor(dt$ci))

Residuals:
      Min       1Q   Median       3Q      Max
-0.23266 -0.00636  0.00000  0.00846  0.18746

Coefficients:
                 Estimate Std. Error t value Pr(>|t|)
(Intercept)       -0.2971     0.1105   -2.69  0.01454 *
as.factor(dt$ci)50   0.1460     0.1562    0.93  0.36193
as.factor(dt$ci)52   0.2347     0.1562    1.50  0.14950
as.factor(dt$ci)54   0.1422     0.1562    0.91  0.37424
as.factor(dt$ci)55   0.3215     0.1562    2.06  0.05360 .
as.factor(dt$ci)56   0.1800     0.1562    1.15  0.26352
as.factor(dt$ci)57   0.2308     0.1353    1.71  0.10437
as.factor(dt$ci)58   0.3554     0.1353    2.63  0.01662 *
as.factor(dt$ci)59   0.2328     0.1193    1.95  0.06603 .
as.factor(dt$ci)61   0.2774     0.1562    1.78  0.09180 .
as.factor(dt$ci)62   0.3452     0.1562    2.21  0.03965 *
```

```
as.factor(dt$ci)63   0.2326     0.1210    1.92  0.06978 .
as.factor(dt$ci)65   0.2054     0.1562    1.31  0.20420
as.factor(dt$ci)66   0.2569     0.1276    2.01  0.05840 .
as.factor(dt$ci)67   0.2826     0.1276    2.22  0.03914 *
as.factor(dt$ci)69   0.1261     0.1562    0.81  0.42974
as.factor(dt$ci)70   0.3553     0.1276    2.78  0.01181 *
as.factor(dt$ci)72   0.3330     0.1353    2.46  0.02359 *
as.factor(dt$ci)73   0.4482     0.1562    2.87  0.00984 **
as.factor(dt$ci)74   0.6452     0.1562    4.13  0.00057 ***
as.factor(dt$ci)77   0.6514     0.1562    4.17  0.00052 ***
as.factor(dt$ci)78   0.3154     0.1562    2.02  0.05784 .
as.factor(dt$ci)80   0.4064     0.1562    2.60  0.01755 *
as.factor(dt$ci)81   0.4647     0.1353    3.43  0.00278 **
as.factor(dt$ci)83   0.0982     0.1562    0.63  0.53722
as.factor(dt$ci)84   0.2588     0.1562    1.66  0.11412
as.factor(dt$ci)85   0.6496     0.1562    4.16  0.00053 ***
as.factor(dt$ci)93   0.4989     0.1562    3.19  0.00479 **
---
Signif. codes:  0 '***' 0.001 '**' 0.01 '*' 0.05 '.' 0.1 ' ' 1

Residual standard error: 0.11 on 19 degrees of freedom
Multiple R-squared:  0.779,     Adjusted R-squared:  0.465
F-statistic: 2.48 on 27 and 19 DF,  p-value: 0.0221
```

```
Analysis of Variance, using Residual Randomization
Permutation procedure: Randomization of null model residuals
Number of permutations: 1000
Estimation method: Ordinary Least Squares
Sums of Squares and Cross-products: Type I
Effect sizes (Z) based on SS distributions

          Df       SS       MS     Rsq      F      Z Pr(>SS)
size.mdb   1 0.027216 0.027216 0.09171 5.0599 3.3707   0.002 **
bf         1 0.032888 0.032888 0.11082 6.1144 4.2248   0.001 **
Residuals 44 0.236667 0.005379 0.79747
Total     46 0.296771
---
Signif. codes:  0 '***' 0.001 '**' 0.01 '*' 0.05 '.' 0.1 ' ' 1

Call: procD.lm(f1 = mdb ~ size.mdb + bf, iter = 999, data = gdf)
```

```
Analysis of Variance, using Residual Randomization
Permutation procedure: Randomization of null model residuals
Number of permutations: 1000
Estimation method: Ordinary Least Squares
Sums of Squares and Cross-products: Type I
Effect sizes (Z) based on SS distributions

           Df       SS       MS     Rsq      F      Z Pr(>SS)
size.skull  1 0.017229 0.017229 0.05805  3.3689 2.3685   0.013 *
bf          1 0.054521 0.054521 0.18371 10.6609 5.1694   0.001 **
Residuals  44 0.225021 0.005114 0.75823
Total      46 0.296771
---
Signif. codes:  0 '***' 0.001 '**' 0.01 '*' 0.05 '.' 0.1 ' ' 1

Call: procD.lm(f1 = mdb ~ size.skull + bf, iter = 999, data = gdf)
```

4. 2B-PLS analyses

4.1. Mandible shape - BF

```
> plot.pls.chiens.mdb$res2bPLS
 Covariance explained by the singular values

 singular value % total covar. Corr. coefficient p-value
     1.19e-02     99.94271          0.753  0.001
     2.82e-04      0.05595          0.615  0.068
     4.38e-05      0.00135          0.511  0.820
```

4.1. Mandible shape – scaled BF

```
> plot.pls.chiens.rbf.mdb$res2bPLS
 Covariance explained by the singular values

 singular value % total covar. Corr. coefficient p-value
     6.83e-03     99.82904          0.649  0.001
     2.79e-04      0.16685          0.587  0.070
     4.38e-05      0.00411          0.515  0.799
```

4.1. allometry-free mandible shape – scaled BF

```
> plot.pls.chiens.rbf.rsh.mdb$res2bPLS
 Covariance explained by the singular values

 singular value % total covar. Corr. coefficient p-value
     5.40e-03     99.73643          0.694  0.001
     2.74e-04      0.25701          0.612  0.012
     4.38e-05      0.00656          0.509  0.674
```

4.1. allometries in shape

```
> plot.pls.chiens.rbf.rsh.mdb$allom.shapes.results$cor

        Pearson's product-moment correlation

data:  cac$CACscores and cac$size
t = 6, df = 45, p-value = 9e-07
alternative hypothesis: true correlation is not equal to 0
95 percent confidence interval:
 0.443 0.788
sample estimates:
  cor
0.648
```

4.1. Allometries in bite force

```
> plot.pls.chiens.rbf.rsh.mdb$allom.muscles.results
Response I :

Call:
lm(formula = I ~ log10(gpa$size))

Residuals:
   Min     1Q Median     3Q    Max
-0.3123 -0.0793 -0.0245 0.0657 0.3465

Coefficients:
             Estimate Std. Error t value Pr(>|t|)
(Intercept)    2.9250     0.0444  65.82  < 2e-16 ***
log10(gpa$size)  1.7622     0.2343   7.52  1.7e-09 ***
---
Signif. codes:  0 '***' 0.001 '**' 0.01 '*' 0.05 '.' 0.1 ' ' 1

Residual standard error: 0.141 on 45 degrees of freedom
Multiple R-squared:  0.557,     Adjusted R-squared:  0.547
F-statistic: 56.6 on 1 and 45 DF,  p-value: 1.73e-09

Response C :

Call:
lm(formula = C ~ log10(gpa$size))

Residuals:
   Min     1Q Median     3Q    Max
-0.3100 -0.0795 -0.0283 0.0655 0.3422

Coefficients:
             Estimate Std. Error t value Pr(>|t|)
(Intercept)    2.9893     0.0444  67.37  < 2e-16 ***
log10(gpa$size)  1.7568     0.2339   7.51  1.8e-09 ***
```

```
---
Signif. codes:  0 ‘***’ 0.001 ‘**’ 0.01 ‘*’ 0.05 ‘.’ 0.1 ‘ ’ 1

Residual standard error: 0.141 on 45 degrees of freedom
Multiple R-squared:  0.556,     Adjusted R-squared:  0.546
F-statistic: 56.4 on 1 and 45 DF,  p-value: 1.8e-09


Response M1 :

Call:
lm(formula = M1 ~ log10(gpa$size))

Residuals:
   Min     1Q Median     3Q    Max
-0.2919 -0.0788 -0.0272  0.0810  0.3317

Coefficients:
             Estimate Std. Error t value Pr(>|t|)
(Intercept)     3.224      0.042   76.81  < 2e-16 ***
log10(gpa$size)   1.639      0.221    7.41  2.5e-09 ***
---
Signif. codes:  0 ‘***’ 0.001 ‘**’ 0.01 ‘*’ 0.05 ‘.’ 0.1 ‘ ’ 1

Residual standard error: 0.134 on 45 degrees of freedom
Multiple R-squared:  0.549,     Adjusted R-squared:  0.539
F-statistic: 54.9 on 1 and 45 DF,  p-value: 2.55e-0
```

En séparant les Brachy des autres

```
> plot.pls.chiens.mdb.brachy$res2bPLS
  Covariance explained by the singular values

 singular value % total covar. Corr. coefficient p-value
       2.19e-02       99.94607              0.946   0.001
       5.01e-04        0.05198              0.766   0.065
       3.69e-05        0.00195              0.834   0.472
> plot.pls.chiens.mdb.autres$res2bPLS
  Covariance explained by the singular values

 singular value % total covar. Corr. coefficient p-value
       4.70e-03        99.8398              0.739   0.001
       1.79e-04         0.1444              0.590   0.374
       5.92e-05         0.0158              0.706   0.380
> plot.pls.chiens.mdb.brachy.sbf$res2bPLS
  Covariance explained by the singular values

 singular value % total covar. Corr. coefficient p-value
       6.02e-03        99.2943              0.648   0.271
       4.99e-04         0.6829              0.749   0.062
       9.12e-05         0.0228              0.735   0.491
> plot.pls.chiens.mdb.autres.sbf$res2bPLS
  Covariance explained by the singular values

 singular value % total covar. Corr. coefficient p-value
       1.98e-03        99.6974              0.668   0.307
       9.63e-05         0.2367              0.480   0.981
       5.08e-05         0.0659              0.673   0.642
> plot.pls.chiens.skull.brachy$res2bPLS
  Covariance explained by the singular values

 singular value % total covar. Corr. coefficient p-value
       0.022508        99.86005              0.859   0.022
       0.000834         0.13701              0.736   0.012
       0.000122         0.00294              0.682   0.398
> plot.pls.chiens.skull.autres$res2bPLS
  Covariance explained by the singular values

 singular value % total covar. Corr. coefficient p-value
       4.20e-03         99.881              0.629   0.007
       1.36e-04          0.104              0.602   0.816
       5.15e-05          0.015              0.465   0.576
> plot.pls.chiens.skull.brachy.sbf$res2bPLS
  Covariance explained by the singular values

 singular value % total covar. Corr. coefficient p-value
       0.010139        99.6586              0.679   0.117
       0.000579         0.3252              0.675   0.153
       0.000129         0.0162              0.646   0.323
>
> plot.pls.chiens.skull.autres.sbf$res2bPLS
  Covariance explained by the singular values

 singular value % total covar. Corr. coefficient p-value
       1.45e-03         99.373              0.489   0.776
       1.03e-04          0.507              0.485   0.899
       5.01e-05          0.119              0.510   0.604
> plot.pls.chiens.skull.brachy.sbf.ash$res2bPLS
  Covariance explained by the singular values

 singular value % total covar. Corr. coefficient p-value
       0.007206        99.8243              0.556   0.228
       0.000282         0.1524              0.657   0.884
       0.000110         0.0233              0.436   0.290
> plot.pls.chiens.skull.autres.sbf.ash$res2bPLS
  Covariance explained by the singular values

 singular value % total covar. Corr. coefficient p-value
       1.73e-03         99.3858              0.635   0.238
       1.27e-04          0.5410              0.683   0.259
       4.69e-05          0.0732              0.487   0.456
> plot.pls.chiens.mdb.brachy.sbf.ash$res2bPLS
  Covariance explained by the singular values

 singular value % total covar. Corr. coefficient p-value
       4.89e-03         98.9381              0.875   0.316
       4.99e-04          1.0297              0.757   0.005
       8.82e-05          0.0323              0.765   0.273
> plot.pls.chiens.mdb.autres.sbf.ash$res2bPLS
  Covariance explained by the singular values

 singular value % total covar. Corr. coefficient p-value
       1.94e-03         99.6939              0.704   0.121
       9.48e-05          0.2378              0.518   0.935
       5.08e-05          0.0683              0.673   0.447
```

Comparaison raw BF et mdb shape entre Brachy et Meso/Doli

```
> compare.pls(plot.pls.chiens.mdb.autres$res2bPLSgeomorph, plot.pls.chiens.mdb.brachy$res2bPLSgeomorph)

Effect sizes

plot.pls.chiens.mdb.autres$res2bPLSgeomorph plot.pls.chiens.mdb.brachy$res2bPLSgeomorph
                                       2.28                                        3.48

Effect sizes for pairwise differences in PLS effect size

                                            plot.pls.chiens.mdb.autres$res2bPLSgeomorph
plot.pls.chiens.mdb.autres$res2bPLSgeomorph                                       0.000
plot.pls.chiens.mdb.brachy$res2bPLSgeomorph                                       0.939
                                            plot.pls.chiens.mdb.brachy$res2bPLSgeomorph
plot.pls.chiens.mdb.autres$res2bPLSgeomorph                                       0.939
plot.pls.chiens.mdb.brachy$res2bPLSgeomorph                                       0.000

P-values

                                            plot.pls.chiens.mdb.autres$res2bPLSgeomorph
plot.pls.chiens.mdb.autres$res2bPLSgeomorph                                       1.000
plot.pls.chiens.mdb.brachy$res2bPLSgeomorph                                       0.174
                                            plot.pls.chiens.mdb.brachy$res2bPLSgeomorph
plot.pls.chiens.mdb.autres$res2bPLSgeomorph                                       0.174
plot.pls.chiens.mdb.brachy$res2bPLSgeomorph                                       1.000
```

Comapraison residual BF et mdb shape entre Brachy et Meso/Doli

```
> summary(compare.pls(plot.pls.chiens.mdb.autres.sbf$res2bPLSgeomorph, plot.pls.chiens.mdb.brachy.sbf$res2bPLSgeomorph))

Effect sizes

plot.pls.chiens.mdb.autres.sbf$res2bPLSgeomorph plot.pls.chiens.mdb.brachy.sbf$res2bPLSgeomorph
                                           1.47                                         -0.25

Effect sizes for pairwise differences in PLS effect size

                                                plot.pls.chiens.mdb.autres.sbf$res2bPLSgeomorph
plot.pls.chiens.mdb.brachy.sbf$res2bPLSgeomorph                                            0.00
plot.pls.chiens.mdb.autres.sbf$res2bPLSgeomorph                                            1.17
                                                plot.pls.chiens.mdb.brachy.sbf$res2bPLSgeomorph
plot.pls.chiens.mdb.brachy.sbf$res2bPLSgeomorph                                            1.17
plot.pls.chiens.mdb.autres.sbf$res2bPLSgeomorph                                            0.00

P-values

                                                plot.pls.chiens.mdb.autres.sbf$res2bPLSgeomorph
plot.pls.chiens.mdb.brachy.sbf$res2bPLSgeomorph                                            1.00
plot.pls.chiens.mdb.autres.sbf$res2bPLSgeomorph                                            0.12
                                                plot.pls.chiens.mdb.brachy.sbf$res2bPLSgeomorph
plot.pls.chiens.mdb.brachy.sbf$res2bPLSgeomorph                                            0.12
plot.pls.chiens.mdb.autres.sbf$res2bPLSgeomorph                                            1.00
```

Comparison raw BF and skull shape between Brachy et Meso/Dolichocephalic dogs

```
> summary(compare.pls(plot.pls.chiens.skull.autres$res2bPLSgeomorph, plot.pls.chiens.skull.brachy$res2bPLSgeomorph))

Effect sizes

plot.pls.chiens.skull.autres$res2bPLSgeomorph plot.pls.chiens.skull.brachy$res2bPLSgeomorph
                                         1.25                                          2.85

Effect sizes for pairwise differences in PLS effect size

                                              plot.pls.chiens.skull.autres$res2bPLSgeomorph
plot.pls.chiens.skull.autres$res2bPLSgeomorph                                          0.00
plot.pls.chiens.skull.brachy$res2bPLSgeomorph                                          1.32
                                              plot.pls.chiens.skull.brachy$res2bPLSgeomorph
plot.pls.chiens.skull.autres$res2bPLSgeomorph                                          1.32
plot.pls.chiens.skull.brachy$res2bPLSgeomorph                                          0.00

P-values

                                              plot.pls.chiens.skull.autres$res2bPLSgeomorph
plot.pls.chiens.skull.autres$res2bPLSgeomorph                                        1.0000
plot.pls.chiens.skull.brachy$res2bPLSgeomorph                                        0.0926
                                              plot.pls.chiens.skull.brachy$res2bPLSgeomorph
plot.pls.chiens.skull.autres$res2bPLSgeomorph                                        0.0926
plot.pls.chiens.skull.brachy$res2bPLSgeomorph                                        1.0000
```

5. Procrustes ANOVAs

5.1. Raw bite force – skull shape

```
> summary(mod)

Analysis of Variance, using Residual Randomization
Permutation procedure: Randomization of null model residuals
Number of permutations: 1000
Estimation method: Ordinary Least Squares
Sums of Squares and Cross-products: Type I
Effect sizes (Z) based on SS distributions

          Df    SS     MS   Rsq    F    Z Pr(>SS)
bf         1 0.028 0.0281 0.056 2.68 1.76   0.057 .
Residuals 45 0.472 0.0105 0.944
Total     46 0.500
---
Signif. codes:  0 ‘***’ 0.001 ‘**’ 0.01 ‘*’ 0.05 ‘.’ 0.1 ‘ ’ 1

Call: procD.lm(f1 = skull ~ bf, iter = 999, data = gdf)
```

5.2. Residual Bite force – skull shape

```
> summary(mod)

Analysis of Variance, using Residual Randomization
Permutation procedure: Randomization of null model residuals
Number of permutations: 1000
Estimation method: Ordinary Least Squares
Sums of Squares and Cross-products: Type I
Effect sizes (Z) based on SS distributions

          Df    SS     MS   Rsq    F    Z Pr(>SS)
bf         1 0.087 0.0871 0.174 9.49 3.59   0.001 **
Residuals 45 0.413 0.0092 0.826
Total     46 0.500
---
Signif. codes:  0 ‘***’ 0.001 ‘**’ 0.01 ‘*’ 0.05 ‘.’ 0.1 ‘ ’ 1

Call: procD.lm(f1 = skull ~ bf, iter = 999, data = gdf)
```

5.3. Raw bite force – mandible shape

```
> summary(mod)

Analysis of Variance, using Residual Randomization
Permutation procedure: Randomization of null model residuals
Number of permutations: 1000
Estimation method: Ordinary Least Squares
Sums of Squares and Cross-products: Type I
Effect sizes (Z) based on SS distributions

          Df     SS     MS   Rsq    F    Z Pr(>SS)
bf         1 0.0477 0.0477 0.161 8.61 4.6   0.001 **
Residuals 45 0.2491 0.0055 0.839
Total     46 0.2968
---
Signif. codes:  0 ‘***’ 0.001 ‘**’ 0.01 ‘*’ 0.05 ‘.’ 0.1 ‘ ’ 1

Call: procD.lm(f1 = mdb ~ bf, data = gdf)
```

5.4. Residual bite force- mandible shape

```
> summary(mod)

Analysis of Variance, using Residual Randomization
Permutation procedure: Randomization of null model residuals
Number of permutations: 1000
Estimation method: Ordinary Least Squares
Sums of Squares and Cross-products: Type I
Effect sizes (Z) based on SS distributions

            Df       SS       MS     Rsq      F      Z Pr(>SS)
bf.resid.mdb  1 0.032888 0.032888 0.11082 5.6084 3.9715   0.001 **
Residuals    45 0.263883 0.005864 0.88918
Total        46 0.296771
---
Signif. codes:  0 ‘***’ 0.001 ‘**’ 0.01 ‘*’ 0.05 ‘.’ 0.1 ‘ ’ 1

Call: procD.lm(f1 = mdb ~ bf, data = gdf)
```

7. Muscles and BF

Sur BF brutes et donnees muscu brutes (size = log10(mdb size)

```
Call:
lm(formula = bf ~ mass.MS + mass.MP + mass.ZA + mass.ZP + mass.SZ +
    fl.SZ + fl.TS + fl.TP + fl.P + pcsa.MP + pcsa.ZA + pcsa.SZ +
    pcsa.TS + pcsa.TP, data = tab)

Residuals:
      Min        1Q    Median        3Q       Max
-0.049801 -0.015440 -0.002674  0.012932  0.073503

Coefficients:
             Estimate Std. Error t value Pr(>|t|)
(Intercept)  2.71574    0.17255  15.739  < 2e-16 ***
mass.MS      0.18304    0.06656   2.750 0.009716 **
mass.MP      0.09219    0.04829   1.909 0.065262 .
mass.ZA     -0.15964    0.05370  -2.973 0.005569 **
mass.ZP      0.14680    0.05836   2.515 0.017110 *
mass.SZ      0.25620    0.17235   1.486 0.146946
fl.SZ       -0.22027    0.15812  -1.393 0.173216
fl.TS       -0.17858    0.08247  -2.166 0.037909 *
fl.TP        0.10332    0.07521   1.374 0.179096
fl.P        -0.17463    0.05692  -3.068 0.004361 **
pcsa.MP      0.11114    0.04178   2.660 0.012108 *
pcsa.ZA      0.17012    0.04236   4.016 0.000335 ***
pcsa.SZ     -0.26767    0.19095  -1.402 0.170612
pcsa.TS      0.25643    0.06161   4.163 0.000221 ***
pcsa.TP      0.15009    0.06465   2.322 0.026777 *
---
Signif. codes:  0 ‘***’ 0.001 ‘**’ 0.01 ‘*’ 0.05 ‘.’ 0.1 ‘ ’ 1

Residual standard error: 0.0318 on 32 degrees of freedom
Multiple R-squared:  0.9819,   Adjusted R-squared:  0.9739
F-statistic: 123.7 on 14 and 32 DF,  p-value: < 2.2e-16
```

Sur BF residuelles et donnees muscu residuelles (size = log10(mdb size)

```
Call:
lm(formula = bf ~ mass.ZA + mass.ZP + mass.SZ + mass.TS + mass.P +
    fl.MS + fl.SZ + fl.TP + fl.P + pcsa.MP + pcsa.ZA + pcsa.SZ +
    pcsa.TS + pcsa.TP, data = tab.res)

Residuals:
      Min        1Q    Median        3Q       Max
-0.048630 -0.014122  0.001585  0.014836  0.053776

Coefficients:
             Estimate Std. Error t value Pr(>|t|)
(Intercept) -7.026e-18  4.055e-03   0.000 1.000000
mass.ZA     -1.411e-01  5.061e-02  -2.788 0.008861 **
mass.ZP      1.861e-01  5.962e-02   3.121 0.003803 **
mass.SZ      3.613e-01  1.721e-01   2.100 0.043741 *
mass.TS     -2.446e-01  9.857e-02  -2.481 0.018528 *
mass.P       2.990e-01  8.266e-02   3.618 0.001011 **
fl.MS        7.539e-02  5.638e-02   1.337 0.190587
fl.SZ       -3.522e-01  1.506e-01  -2.339 0.025722 *
fl.TP        1.663e-01  7.077e-02   2.350 0.025117 *
fl.P        -1.748e-01  5.166e-02  -3.384 0.001904 **
pcsa.MP      1.406e-01  3.110e-02   4.521 7.95e-05 ***
pcsa.ZA      1.263e-01  3.983e-02   3.171 0.003337 **
pcsa.SZ     -3.645e-01  1.853e-01  -1.966 0.057972 .
pcsa.TS      5.162e-01  9.235e-02   5.590 3.57e-06 ***
pcsa.TP      2.185e-01  5.451e-02   4.009 0.000342 ***
---
Signif. codes:  0 ‘***’ 0.001 ‘**’ 0.01 ‘*’ 0.05 ‘.’ 0.1 ‘ ’ 1

Residual standard error: 0.0278 on 32 degrees of freedom
Multiple R-squared:  0.9692,   Adjusted R-squared:  0.9558
F-statistic: 71.98 on 14 and 32 DF,  p-value: < 2.2e-16
```

```
Call:
lm(formula = bf[id] ~ size.mdb[id] + shape.mdb[id] + shape.skull[id],
    data = tab)

Residuals:
      Min        1Q    Median        3Q       Max
-0.224407 -0.067572 -0.002129  0.065820  0.178498

Coefficients:
```

```
                Estimate Std. Error t value Pr(>|t|)
(Intercept)      3.04527    0.05628  54.105  < 2e-16 ***
size.mdb[id]     0.57637    0.32279   1.786   0.0812 .
shape.mdb[id]    3.79873    0.84136   4.515 4.87e-05 ***
shape.skull[id] -1.26600    0.47690  -2.655   0.0111 *
---
Signif. codes:  0 ‘***’ 0.001 ‘**’ 0.01 ‘*’ 0.05 ‘.’ 0.1 ‘ ’ 1

Residual standard error: 0.1035 on 43 degrees of freedom
Multiple R-squared:  0.7415,   Adjusted R-squared:  0.7235
F-statistic: 41.12 on 3 and 43 DF,  p-value: 1.075e-12



lm(formula = bf ~ size.mdb + mass.m + mass.t + mass.p + fl.m +
    fl.p + pcsa.t + a.m + a.p, data = tab)

Residuals:
      Min        1Q    Median        3Q       Max
-0.069129 -0.018074 -0.003841  0.016291  0.070523

Coefficients:
             Estimate Std. Error t value Pr(>|t|)
(Intercept)  2.14357    0.12919  16.592  < 2e-16 ***
size.mdb    -0.40642    0.16881  -2.408 0.021165 *
mass.m       0.61548    0.11616   5.299 5.59e-06 ***
mass.t      -0.17767    0.09708  -1.830 0.075305 .
mass.p       0.18333    0.10482   1.749 0.088569 .
fl.m        -0.34647    0.08950  -3.871 0.000425 ***
fl.p        -0.18528    0.05471  -3.386 0.001691 **
pcsa.t       0.43771    0.09115   4.802 2.60e-05 ***
a.m         -0.09634    0.07586  -1.270 0.212024
a.p         -0.09394    0.04391  -2.139 0.039064 *
---
Signif. codes:  0 ‘***’ 0.001 ‘**’ 0.01 ‘*’ 0.05 ‘.’ 0.1 ‘ ’ 1

Residual standard error: 0.03536 on 37 degrees of freedom
Multiple R-squared:  0.9741,   Adjusted R-squared:  0.9677
F-statistic: 154.3 on 9 and 37 DF,  p-value: < 2.2e-16
```

5. Part2 – Chapter 4 – dingoes

Details of the dingoes dissected in this thesis including muscle architecture data.

head measurements			Digastric					Masseter pars superficialis				Masseter pars profunda			
length	width	height	ML	FL	PA	mass	PCSA	ML	FL	PA	mass	ML	FL	PA	mass
205	120	88	105,00	40,00	0,00	16,43	0,59	90,00	30,00	40,00	27,43	70,00	13,50	45,00	7,57
195	120	85	100,00	43,50	0,00	19,74	0,63	90,00	24,00	40,00	29,60	55,00	18,00	27,50	12,29
205	120	80	100,00	37,50	0,00	18,86	0,68	90,00	28,00	40,00	25,15	35,00	16,00	35,00	6,13
185	105	90	85,00	32,00	0,00	10,83	0,50	45,00	20,00	40,00	14,36	75,00	20,00	37,50	5,94
180	90	75	100,00	38,00	0,00	11,70	0,46	80,00	24,00	35,00	19,67	50,00	12,50	15,00	5,21
160	100	90	85,00	30,00	0,00	9,38	0,47	60,00	19,00	30,00	14,71	40,00	12,00	40,00	4,86
205	110	78	90,00	38,50	0,00	12,24	0,48	80,00	20,00	22,50	14,36	50,00	15,00	10,00	6,37
190	110	85	100,00	37,50	0,00	18,47	0,67	75,00	24,00	40,00	21,34	60,00	11,00	60,00	11,32
70	60		45,00	17,00	0,00	0,96		35,00	7,00	60,00	1,07	20,00	7,00	50,00	0,61
70	60		40,00	18,00	0,00	0,94		30,00	10,00	20,00	0,80	20,00	8,00	20,00	0,48

zygomaticomandibularis anterior				zygomaticomandibularis posterior				temporalis pars suprazygomatica				temporalis pars superficialis			
ML	FL	PA	mass	ML	FL	PA	mass	ML	FL	PA	mass	ML	FL	PA	mass
65,00	23,00	35,00	11,52	50,00	16,00	40,00	6,80	105,00	34,00	10,00	8,66	130,00	33,00	30,00	40,04
40,00	26,00	30,00	12,50	50,00	15,00	40,00	7,56	105,00	32,00	30,00	9,70	120,00	32,00	30,00	41,85
55,00	25,00	30,00	5,04	55,00	12,50	37,50	3,95	105,00	37,00	30,00	13,09	130,00	42,00	35,00	36,62
55,00	21,00	30,00	6,34	35,00	13,00	30,00	3,70	95,00	26,00	35,00	4,37	110,00	29,00	35,00	19,91
50,00	15,00	30,00	5,82	40,00	7,50	50,00	4,14	85,00	34,00	35,00	6,76	110,00	35,00	20,00	28,85
45,00	17,00	30,00	5,13	35,00	7,00	55,00	3,98	70,00	22,00	30,00	5,08	110,00	22,00	32,50	16,75
40,00	14,00	30,00	5,90	40,00	8,00	35,00	3,89	80,00	27,00	30,00	6,15	120,00	29,00	32,50	28,24
60,00	24,00	20,00	7,22	50,00	12,50	45,00	6,12	90,00	32,00	25,00	8,83	115,00	33,00	25,00	34,10
12,00	4,00		0,28	7,00	4,00		0,09	45,00	9,50		0,24	50,00	14,00	30,00	3,01
12,00	6,50	15,00	0,27	7,00			0,01	35,00	9,50	20,00	0,51	45,00	10,00	32,50	1,50

	temporalis pars profunda				pterygoideus medialis				pterygoideus lateralis			
Age	ML	FL	PA	mass	ML	FL	PA	mass	ML	FL	PA	mass
adult	125,00	32,67	30,00	61,24	90,00	13,00	40,00	15,56	35,00	6,50	50,00	1,57
adult	125,00	37,50	35,00	64,65	80,00	15,00	42,50	17,97	20,00	9,50	50,00	1,08
adult	120,00	37,00	40,00	56,79	100,00	17,00	40,00	18,00	25,00	9,50		0,89
young	110,00	28,00	41,67	33,51	90,00	18,67	65,00	10,86	15,00	9,00	60,00	0,58
adult	105,00	31,00	37,50	37,10	90,00	16,00	51,67	12,56	25,00	7,00	35,00	0,97
young	115,00	25,00	57,50	39,27	75,00	22,00	42,50	10,07	15,00	8,00		0,59
young	115,00	29,00	35,00	41,92	90,00	18,50	47,50	12,01	25,00	8,00	40,00	0,86
young	125,00	32,50	22,50	52,11	95,00	20,00	55,00	16,66	20,00	9,00	50,00	0,79
juvenile					35,00	11,00	62,50	0,85	5,00	3,00		0,04
juvenile	45,00	9,00	35,00	1,48	35,00	6,00	40,00	0,63	5,00	3,00		0,01

	Masseter complex				temporal complex				pterygoid complex			
Age	**FL**	**PA**	**mass**	**PCSA**	**FL**	**PA**	**mass**	**PCSA**	**FL**	**PA**	**mass**	**PCSA**
adult	20,63	40,00	1,73	1,24	33,22	23,33	1,69	1,44	13,00	40,00	1,23	0,98
adult	20,75	34,38	1,79	1,35	33,83	31,67	1,71	1,42	15,00	42,50	1,28	0,95
adult	20,38	35,63	1,60	1,13	38,67	35,00	1,70	1,32	17,00	40,00	1,28	0,90
young	18,50	34,38	1,48	1,09	27,67	37,22	1,39	1,18	18,67	65,00	1,06	0,39
adult	14,75	32,50	1,54	1,22	33,33	30,83	1,55	1,25	16,00	51,67	1,13	0,69
young	13,75	38,75	1,46	1,17	23,00	40,00	1,34	1,20	22,00	42,50	1,03	0,53
young	14,25	24,38	1,48	1,24	28,33	32,50	1,54	1,32	18,50	47,50	1,11	0,65
young	17,88	41,25	1,66	1,24	32,50	24,17	1,63	1,40	20,00	55,00	1,24	0,67
juvenile												
juvenile												

6. Part2 – Article 4 – supplementary material

6.1. Table S1.

Detailed information about the sample, model input and outputs and the landmarking protocol.

Sheet 2 Database

Abbreviations

ID	identification number of the specimen
I-20	Bite force at the incisors for a gape angle of 20°
C-20	Bite force at the canine for a gape angle of 20°
M-20	Bite force at the molars for a gape angle of 20°
SD	standard deviation
bite force	the bite force was estiùated using the biomechanical model
M	male
F	female
LM	length of the muscle
FL	fiber length
mandible	the mandible was used for shape analyses
skull	the skull was used for shape analyses

Sheet 3 in vivo measurements

Abbreviations

ID	identification number of the specimen
BD	Birth date
headl	head length
headw	head width
headh	headh hight
T1 to T4	trial number

Sheet 4 Contribution (%) of the different constituent bellies of the jaw muscles to the moment of the estimated bite force for different gape angles.

MS	M. masseter pars superficialis
MP	M. masseter pars profunda
ZA	M. zygomaticomandibularis anterior
ZP	M. zygomaticomandibularis posterior
SZ	M. temporalis pars suprazygomatica
TS	M. temporalis pars superficialis
TP	M. temporalis pars profunda
PM + PL	M.pterygoideus medialis and lateralis

Sheet 5 Definition of the landmarks used in this study following the Nomina Anatomica Veterinaria nomenclature (NAV, 2017).

														Digastricus			Masseter pars superficialis			Masseter pars profunda		
ID	Type	dissected	mandible	skull	bite force	I-20°	C-20°	M1-20°	I-30°	C-30°	M1-30°	AGE	SEX	fiber length	pennation angle	mass	fiber length	pennation angle	mass	fiber length	pennation angle	mass
M7	Red fox	no	yes	yes	no							c										
Ni-R1	Red fox	no	yes	no	no							c										
N-R5	Red fox	yes	yes	no	no							b	M	43,50	0,00	3,44	14,43	30,00	4,59	15,70	0,00	1,90
N-R21	Red fox	yes	yes	no	no							c	F	30,97	0,00	3,48	13,50	35,00	5,04	10,90	10,00	1,13
N-R28	Red fox	yes	yes	no	no							b	M	26,42	0,00	2,20	0,89	35,00	3,10	0,73	25,00	1,10
Ny-R1	Red fox	yes	yes	yes	no							c	M	43,13	0,00	5,63	15,07	27,50	8,89	10,88	32,50	1,57
P-R1	Red fox	no	yes	yes	no							b	M									
T-R1	Red fox	yes	yes	no	no							d	M	53,00	0,00	7,00	15,00	60,00	9,00	18,00	10,00	3,00
N-R1	Red fox	yes	yes	yes	yes	168	193	357	155	178	330	c	M	41,20	0,00	5,00	16,40	37,50	8,00	11,23	20,00	3,00
N-R10	Red fox	yes	yes	yes	yes	235	253	462	216	233	426	c	F	37,65	0,00	4,71	16,50	30,00	6,40	11,90	15,00	4,46
N-R11	Red fox	yes	yes	no	yes	89	103	208	83	96	195	a	M	30,85	0,00	2,12	9,95	28,33	3,07	9,40	0,00	0,60
N-R12	Red fox	yes	yes	yes	yes	185	213	409	171	196	376	c	F	35,47	0,00	5,42	18,13	32,50	8,70	10,50	22,50	1,92
N-R13	Red fox	yes	yes	yes	yes	254	292	524	235	271	486	c	M	40,70	0,00	6,01	23,88	25,00	11,23	12,00	5,00	3,46
N-R14	Red fox	yes	yes	yes	yes	242	276	497	226	258	466	c	M	37,40	0,00	3,43	16,15	30,00	8,52	11,73	20,00	2,43
N-R16	Red fox	yes	yes	yes	yes	203	226	434	188	210	403	c	M	33,60	0,00	5,17	18,50	28,33	8,96	13,10	0,00	3,44
N-R17	Red fox	yes	yes	no	yes	195	221	419	173	196	372	b	M	40,27	0,00	4,72	19,28	20,00	6,56	9,90	15,00	1,98
N-R18	Red fox	yes	yes	yes	yes	169	194	370	155	178	339	c	M	36,50	0,00	5,13	20,10	47,50	8,43	16,38	15,00	2,23
N-R19	Red fox	yes	yes	yes	yes	209	240	450	192	220	413	c	M	35,37	0,00	3,79	10,75	32,50	7,99	11,77	10,00	1,85
N-R2	Red fox	yes	yes	yes	yes	169	193	355	156	179	327	c	F	39,40	0,00	5,00	15,63	42,50	9,00	12,13	10,00	1,00
N-R20	Red fox	yes	yes	yes	yes	247	284	502	233	268	474	c	M	35,17	0,00	4,55	16,48	32,50	7,66	11,20	20,00	1,44
N-R22	Red fox	yes	yes	yes	yes	139	160	305	128	147	280	c	F	31,85	0,00	3,10	11,46	37,50	5,33	9,75	10,00	1,15
N-R23	Red fox	yes	yes	yes	yes	237	267	504	218	246	465	c	M	35,60	0,00	6,39	16,00	25,00	7,99	10,65	20,00	2,16
N-R24	Red fox	yes	yes	yes	yes	199	224	417	183	206	384	c	F	42,95	0,00	5,05	19,00	30,00	7,70	12,90	10,00	3,10
N-R25	Red fox	yes	yes	no	yes	97	110	218	90	101	201	a	F	36,40	0,00	1,91	11,30	20,00	3,01	10,10	20,00	1,00
N-R26	Red fox	yes	yes	yes	yes	335	376	670	326	366	652	c	F	39,97	0,00	4,39	12,20	32,50	7,26	9,80	30,00	1,63
N-R27	Red fox	yes	yes	yes	yes	173	194	363	159	178	333	d	F	38,15	0,00	4,05	12,90	27,50	6,03	10,85	20,00	2,02
N-R29	Red fox	yes	yes	yes	yes	125	146	261	118	138	247	a	F	23,25	0,00	1,70	10,91	40,00	2,50	7,32	35,00	1,10
N-R3	Red fox	yes	yes	yes	yes	210	236	440	200	224	418	c	F	34,23	0,00	5,00	14,33	27,50	6,00	19,25	0,00	1,00
N-R30	Red fox	yes	yes	yes	yes	205	233	430	187	212	391	c	M	28,89	0,00	5,20	15,52	37,50	7,60	13,45	30,00	3,80
N-R31	Red fox	yes	yes	yes	yes	229	260	496	210	239	456	c	M	25,84	0,00	6,40	28,19	42,50	14,60	9,67	30,00	1,50
N-R32	Red fox	yes	yes	yes	yes	233	256	477	215	236	440	c	M	32,28	0,00	5,00	15,27	42,50	7,60	6,55	37,50	3,00
N-R33	Red fox	yes	yes	no	yes	127	147	267	120	138	251	b	F	23,47	0,00	2,20	10,69	32,50	4,20	7,20	27,50	1,40
N-R34	Red fox	yes	yes	yes	yes	234	267	490	214	243	447	d	M	32,58	0,00	6,30	19,18	32,50	11,00	11,89	27,50	3,20
N-R35	Red fox	yes	yes	yes	yes	181	204	364	168	188	337	c	F	28,07	0,00	4,50	11,91	37,50	6,50	9,06	35,00	2,10
N-R36	Red fox	yes	yes	yes	yes	241	273	524	222	251	483	c	M	29,58	0,00	6,40	12,58	35,00	8,50	6,83	37,50	2,90
N-R37	Red fox	yes	yes	yes	yes	249	283	519	232	264	485	c	M	29,32	0,00	4,30	18,79	37,50	7,80	8,05	30,00	2,90
N-R38	Red fox	yes	yes	yes	yes	269	294	556	251	274	518	c	M	27,76	0,00	5,30	18,13	37,50	9,60	8,77	25,00	2,80
N-R39	Red fox	yes	yes	yes	yes	120	144	277	110	132	255	b	M	25,84	0,00	3,80	11,63	40,00	3,60	11,91	30,00	1,10
N-R4	Red fox	yes	yes	yes	yes	116	130	250	107	119	230	c	F	37,50	0,00	3,30	16,25	32,50	5,06	16,70	10,00	1,04
N-R40	Red fox	yes	yes	yes	yes	223	255	473	206	235	436	c	M	27,07	0,00	6,10	15,53	40,00	9,30	7,97	30,00	1,90
N-R41	Red fox	yes	yes	yes	yes	277	315	576	256	292	534	c	M	30,61	0,00	5,90	21,83	35,00	12,60	15,00	27,50	3,60
N-R42	Red fox	yes	yes	no	yes	100	119	227	91	109	207	b	F	26,82	0,00	2,30	13,56	32,50	3,50	13,13	22,50	1,40
N-R43	Red fox	yes	yes	yes	yes	217	240	445	201	223	414	c	M	31,40	0,00	6,60	22,37	37,50	11,00	17,97	30,00	3,20
N-R44	Red fox	yes	yes	yes	yes	258	288	519	238	265	478	c	M	26,12	0,00	7,10	17,06	37,50	11,00	11,38	27,50	4,10
N-R45	Red fox	yes	yes	yes	yes	245	281	592	231	265	560	c	M	24,81	0,00	4,20	11,09	40,00	6,90	12,81	20,00	2,30
N-R46	Red fox	yes	yes	yes	yes	212	237	444	195	218	407	c	M	25,98	0,00	5,40	12,82	37,50	7,80	11,16	27,50	2,60
N-R47	Red fox	yes	yes	yes	yes	248	279	544	229	258	502	c	M	25,88	0,00	5,10	14,16	37,50	8,50	9,38	30,00	3,10
N-R48	Red fox	yes	yes	yes	yes	241	271	551	223	250	509	c	M	29,09	0,00	6,50	24,88	45,00	12,60	4,72	40,00	2,00
N-R49	Red fox	yes	yes	yes	yes	184	204	392	169	187	360	c	M	29,30	0,00	4,60	17,04	30,00	8,30	8,56	35,00	2,10
N-R50	Red fox	yes	yes	no	yes	143	163	295	132	151	273	b	M	24,44	0,00	2,40	10,97	37,50	3,60	7,38	30,00	1,80
N-R6	Red fox	yes	yes	yes	yes	175	200	376	162	185	348	c	M	40,70	0,00	5,16	14,33	27,50	8,17	11,10	0,00	1,46

														Digastricus			Masseter pars superficialis			Masseter pars profunda		
ID	Type	dissected	mandible	skull	bite force	I-20°	C-20°	M1-20°	I-30°	C-30°	M1-30°	AGE	SEX	fiber length	pennation angle	mass	fiber length	pennation angle	mass	fiber length	pennation angle	mass
N-R60	Red fox	yes	yes	yes	yes	202	226	407	185	208	375	c	F	26,82	0,00	3,60	11,40	37,50	6,70	5,99	30,00	2,20
N-R61	Red fox	yes	yes	yes	yes	185	207	387	172	191	358	c	F	30,57	0,00	4,20	22,23	32,50	7,20	13,88	35,00	1,80
N-R62	Red fox	yes	yes	yes	yes	200	221	412	185	205	381	c	F	23,63	0,00	4,50	16,77	32,50	7,70	9,64	25,00	2,30
N-R63	Red fox	yes	yes	yes	yes	282	316	586	265	297	550	c	F	21,37	0,00	6,90	16,06	30,00	11,20	8,33	37,50	2,70
N-R64	Red fox	yes	yes	yes	yes	207	230	440	191	212	405	c	F	26,60	0,00	4,30	13,38	35,00	7,80	8,62	30,00	2,00
N-R7	Red fox	yes	yes	yes	yes	181	208	372	166	190	341	c	F	27,95	0,00	4,13	17,73	30,00	8,17	14,45	7,50	1,82
N-R70	Red fox	yes	yes	yes	yes	170	200	375	157	185	347	c	F	22,84	0,00	3,60	10,72	27,50	5,10	6,18	20,00	0,70
N-R8	Red fox	yes	yes	yes	yes	217	249	467	200	230	431	c	M	48,80	0,00	7,76	28,77	37,50	12,40	15,38	0,00	3,62
N-R9	Red fox	yes	yes	yes	yes	169	193	332	155	177	304	c	M	39,65	0,00	5,01	21,30	32,50	8,17	17,90	0,00	1,91
Ny-R2	Red fox	yes	yes	yes	yes	262	296	544	241	272	500	c	F	35,55	0,00	6,47	10,30		9,90	15,37	42,50	2,30
Ny-R3	Red fox	yes	yes	yes	yes	380	442	772	367	427	747	c	nc	30,63	0,00	5,97	16,63	40,00	10,93	14,05	12,50	2,66
Ny-R4	Red fox	yes	yes	yes	yes	288	339	590	264	310	540	c	M	47,80	0,00	5,48	17,45	30,00	13,59	13,93	10,00	2,96
Ny-R5	Silver fox	yes	yes	yes	yes	192	217	408	178	202	378	c		33,50	0,00	6,20	17,00	35,00	7,27	9,00	42,50	2,98
Ny-R6	Silver fox	yes	yes	yes	yes	192	218	429	178	202	398	d		32,00	0,00	4,70	10,00	55,00	6,73	10,00	30,00	2,52
Ny-R7	Silver fox	yes	yes	yes	yes	178	203	406	165	189	378	c		50,00	0,00	3,77	10,00	45,00	5,23	10,00	30,00	1,87
Ny-R8	Silver fox	yes	yes	yes	yes	247	280	514	229	260	477	c		26,00	0,00	5,23	12,00	30,00	7,16	10,00	37,50	2,00
P-R3	Red fox	yes	yes	yes	yes	170	195	358	157	180	331	b	M	40,45	0,00	4,78	15,75	22,50	6,49	9,50	15,00	1,67
MEAN						205,48	233,07	434,13	190,48	216	402,48			33,08	0,00	4,75	15,54	34,56	7,72	11,09	21,85	2,20
SD						55,39	62,45	111,41	52,95	59,84	106,64			7,25	0,00	1,39	4,65	7,14	2,67	3,44	12,04	0,87
MINIMUM						89	103	208	83	96	195			21,37	0,00	1,70	0,89	20,00	2,50	0,73	0,00	0,60
MAXIMUM						380	442	772	367	427	747			53,00	0,00	7,76	28,77	60,00	14,60	19,25	42,50	4,46

	Zygomaticomandibularis pars anterior			Zygomaticomandibularis pars posterior			Temporalis pars suprazygomatica			Temporalis pars superficialis			Temporalis pars profunda			Pterygoideus medialis	
ID	fiber length	pennation angle	mass	fiber length	pennation angle	mass	fiber length	pennation angle	mass	fiber length	pennation angle	mass	fiber length	pennation angle	mass	fiber length	pennation angle
M7																	
Ni-R1																	
N-R5	9,87		1,05	7,90	40,00	0,96	21,40	0,00	1,70	24,30	35,00	8,80	26,53	27,50	12,61	9,90	35,00
N-R21	11,10		0,84	7,35	40,00	0,77	22,55		1,65	17,35	30,00	7,81	14,93	40,00	8,97	10,18	50,00
N-R28			0,10	10,28	35,00	0,90			0,70	26,85	37,50	3,20	10,68	40,00	6,60	13,37	30,00
Ny-R1			1,80	5,70	40,00	2,05	20,47	20,00	1,93	27,45	30,00	15,35	23,20	42,50	17,58	12,43	50,00
P-R1																	
T-R1	8,00	15,00	2,00	8,00	45,00	2,00	27,00	30,00	3,00	34,00	40,00	12,00	22,00	47,00	23,00	20,00	43,00
N-R1	13,90	20,00	1,00	13,90	37,50	1,00	21,90	25,00	2,00	28,77	45,00	12,00	30,10	27,50	18,00	13,73	32,50
N-R10	11,45	10,00	1,75	10,75	25,00	1,74	18,00	0,00	2,32	24,15	35,00	11,50	20,50	22,50	18,56	9,70	60,00
N-R11	11,53		0,31	7,85	37,50	0,62	18,43	25,00	1,31	18,75	37,50	4,35	13,63	35,00	6,01	9,60	40,00
N-R12	9,60	37,50	0,84	9,75	40,00	0,94	17,76	17,50	3,62	23,32	35,00	14,81	23,04	32,50	16,80	14,20	45,00
N-R13	9,17	10,00	0,59	11,63	15,00	1,26	23,53	10,00	4,65	31,28	35,00	16,74	22,85	32,50	26,03	12,73	50,00
N-R14	9,10	42,50	1,86	14,25	30,00	1,34	25,85	22,50	3,19	26,27	35,00	11,42	20,33	32,50	18,68	10,30	50,00
N-R16	11,80	25,00	1,00	8,50	40,00	2,18	22,55	40,00	4,01	31,04	30,00	13,84	23,10	40,00	20,13	12,55	45,00
N-R17	11,90	15,00	1,00	9,05	25,00	1,89	20,45	27,50	2,23	23,00	17,50	13,32	16,07	25,00	14,07	16,08	30,00
N-R18	12,90	25,00	1,10	15,00	30,00	1,49	24,15	30,00	3,17	29,70	17,50	13,91	15,30	47,50	15,64	13,90	45,00
N-R19	10,30		0,74	9,20	30,00	2,08	17,20	17,50	2,34	20,70	30,00	13,67	20,20	40,00	13,83	9,10	50,00
N-R2	12,15	10,00	1,00	11,10	30,00	1,00	13,55	25,00	3,00	25,40	42,50	13,00	25,25	46,67	15,00	12,70	42,50
N-R20	9,25		0,99	9,67	30,00	1,14	18,47	25,00	2,84	23,50	27,50	13,41	18,53	30,00	13,83	10,67	55,00
N-R22	10,15	30,00	1,10	8,90	40,00	0,82	21,20	30,00	2,13	17,53	30,00	6,94	18,43	35,00	10,92	10,65	50,00
N-R23	13,65		1,88	10,70	40,00	2,41	22,60	35,00	2,50	20,90	27,50	13,43	14,86	45,00	18,40	12,38	50,00
N-R24	11,80	35,00	1,29	9,48	50,00	1,42	21,80	30,00	3,26	23,47	40,00	11,45	24,52	37,50	18,46	11,95	50,00
N-R25	9,95		0,54	6,65	10,00	0,55	16,20	15,00	1,85	21,50	25,00	4,24	14,37	35,00	6,45	8,33	50,00
N-R26	11,00		1,45	9,20	30,00	1,48	24,20	30,00	2,66	21,60	40,00	11,36	18,96	40,00	14,76	10,95	40,00
N-R27	12,20		0,98	7,30	30,00	1,29	24,40	30,00	3,04	21,25	50,00	9,42	19,86	35,00	15,65	13,37	50,00
N-R29	11,17	30,00	0,60	7,37	30,00	0,30	20,27	30,00	0,70	14,67	35,00	3,80	17,82	32,50	4,80	10,55	35,00
N-R3	9,93	30,00	1,00	10,00	37,50	1,00	18,60		2,00	19,35	27,50	10,00	24,83	37,50	15,00	16,50	32,50
N-R30	7,99	35,00	1,90	9,32	27,50	1,70	20,37	17,50	4,10	19,56	35,00	12,60	26,38	42,50	18,80	14,28	25,00
N-R31	18,05	35,00	2,80	6,43	30,00	2,00	25,19	25,00	4,00	23,70	25,00	13,50	31,02	30,00	24,70	6,13	35,00
N-R32	18,46	32,50	2,10	6,39	40,00	1,20	26,74	27,50	4,60	22,28	32,50	14,70	23,86	32,50	17,30	10,04	35,00
N-R33	9,28	20,00	1,00	8,42	30,00	1,00	16,67	22,50	1,30	18,79	35,00	5,90	18,70	35,00	7,20	10,14	37,50
N-R34	14,73	30,00	1,50	5,44	37,50	1,40	20,38	22,50	4,90	31,83	30,00	17,70	22,75	35,00	22,60	11,45	42,50
N-R35	13,79	27,50	1,10	10,90	27,50	0,80	29,76	25,00	2,50	27,18	17,50	11,30	26,26	32,50	13,00	10,86	27,50
N-R36	14,45	35,00	1,60	6,81	32,50	1,60	24,28	27,50	3,30	21,89	22,50	13,10	21,46	37,50	18,70	12,57	37,50
N-R37	8,36	30,00	1,80	8,63	27,50	1,90	23,16	20,00	4,10	23,50	25,00	14,10	21,54	32,50	17,00	11,16	25,00
N-R38	20,18	32,50	1,80	7,40	35,00	2,30	18,87	17,50	4,40	24,84	27,50	15,20	20,93	32,50	17,90	11,80	32,50
N-R39	9,69	35,00	1,20	9,42	27,50	0,80	20,98	32,50	3,30	22,20	27,50	7,40	16,09	37,50	7,60	11,26	30,00
N-R4	10,50	0,00	0,82	12,90	17,50	0,86	16,60	40,00	1,76	23,15	20,00	5,44	19,20	30,00	10,93	15,90	
N-R40	9,88	25,00	1,40	7,59	30,00	2,10	11,34	20,00	2,20	31,01	32,50	11,30	28,32	35,00	23,10	6,93	30,00
N-R41	11,90	20,00	2,00	7,75	35,00	1,70	28,72	17,50	5,30	24,67	35,00	20,30	28,85	42,50	27,50	10,87	35,00
N-R42	17,31	25,00	1,10	7,86	35,00	0,50	12,61	25,00	1,60	23,25	22,50	5,70	26,88	30,00	6,30	7,25	27,50
N-R43	28,53	25,00	2,60	8,06	32,50	3,10	23,68	30,00	3,40	36,32	30,00	16,00	36,33	32,50	23,70	11,79	27,50
N-R44	14,90	30,00	1,90	33,79	25,00	1,30	14,09	25,00	2,90	23,19	30,00	17,60	23,04	35,00	19,10	7,73	35,00
N-R45	15,58	37,50	1,40	5,33	30,00	1,30	20,05	30,00	2,00	27,76	27,50	11,30	23,32	35,00	12,90	6,94	37,50
N-R46	14,37	27,50	1,30	10,38	22,50	1,60	29,28	15,00	2,90	20,25	35,00	13,20	20,98	30,00	13,10	11,56	25,00
N-R47	16,61	37,50	2,70	7,55	30,00	2,00	26,90	17,50	2,20	22,07	30,00	16,90	24,48	37,50	18,80	12,05	37,50
N-R48	10,39	30,00	2,10	7,85	40,00	4,00	39,08	17,50	2,30	35,19	30,00	20,40	49,65	27,50	25,20	14,31	17,50
N-R49	16,36	30,00	1,40	10,08	30,00	1,20	21,03	25,00	2,80	20,87	20,00	13,00	21,53	30,00	13,40	15,92	30,00
N-R50	13,06	27,50	0,80	9,17	27,50	0,80	25,03	27,50	1,40	23,36	30,00	5,80	23,24	32,50	7,40	10,40	30,00
N-R6	11,65	0,00	1,04	9,65	10,00	1,45	19,10	0,00	1,81	26,67	35,00	13,41	24,77	35,00	15,50	14,00	42,50

	Zygomaticomandibularis pars anterior			Zygomaticomandibularis pars posterior			Temporalis pars suprazygomatica			Temporalis pars superficialis			Temporalis pars profunda			Pterygoideus medialis	
ID	fiber length	pennation angle	mass	fiber length	pennation angle	mass	fiber length	pennation angle	mass	fiber length	pennation angle	mass	fiber length	pennation angle	mass	fiber length	pennation angle
N-R60	22,80	20,00	1,40	8,35	25,00	2,00	16,49	30,00	2,80	24,12	25,00	8,30	23,13	35,00	12,50	7,24	27,50
N-R61	9,70	25,00	1,70	10,49	32,50	1,50	26,72	30,00	2,50	22,01	27,50	10,70	28,67	27,50	11,80	7,21	35,00
N-R62	6,32	30,00	0,20	6,34	25,00	1,30	23,91	25,00	4,40	18,40	30,00	10,90	19,19	32,50	13,60	12,76	27,50
N-R63	22,84	27,50	3,40	7,92	22,50	1,60	18,59	20,00	3,00	24,51	32,50	17,40	21,51	35,00	18,10	11,43	35,00
N-R64	14,31	25,00	1,50	10,37	20,00	1,60	16,93	27,50	3,20	21,39	20,00	13,20	24,28	32,50	15,40	8,97	37,50
N-R7	14,10	10,00	1,54	9,50	20,00	2,12	15,55	20,00	1,55	30,00	20,00	11,21	22,60	22,50	14,11	10,35	40,00
N-R70	14,81	25,00	0,90	6,56	35,00	1,10	10,81	25,00	2,20	21,99	25,00	10,20	21,49	37,50	14,20	7,53	25,00
N-R8	11,40	10,00	1,96	16,40	25,00	3,80	19,15	0,00	1,56	31,90	35,00	20,19	28,80	45,00	26,10	9,75	52,50
N-R9	10,35	0,00	0,93	8,50	35,00	1,08	19,40	10,00	3,13	25,00	22,50	10,40	24,35	32,50	18,47	10,70	37,50
Ny-R2	11,70	50,00	3,08	10,00	50,00	1,87	22,50	20,00	3,46	19,80	30,00	14,26	19,33	35,00	20,11	11,55	60,00
Ny-R3	16,10	25,00	2,13	11,35	40,00	3,23	22,50	22,50	2,74	22,07	30,00	16,40	23,60	30,00	23,76	10,25	32,50
Ny-R4	10,80	37,50	2,01	6,60	45,00	1,50	19,30	10,00	2,59	21,43	32,50	21,29	22,93	37,50	24,51	12,88	55,00
Ny-R5	13,00	35,00	1,43	7,12	45,00	1,05	32,50	30,00	3,52	30,00	45,00	15,65	27,50	42,50	21,86	16,00	45,00
Ny-R6	10,00	40,00	0,90	25,00	37,50	0,81	12,00	30,00	2,19	18,00	30,00	12,92	25,00	42,50	20,92	16,00	50,00
Ny-R7	7,00	30,00	1,23	5,00	50,00	0,65	10,00	32,50	1,30	15,00	30,00	8,74	23,00	35,00	12,10	10,00	50,00
Ny-R8	9,00	30,00	2,30	10,00	30,00	1,33	20,00	27,50	3,12	22,00	30,00	14,80	20,00	42,50	16,39	10,00	55,00
P-R3	11,00		1,06	9,80	37,50	0,74	26,13	10,00	2,04	18,00	37,50	9,41	24,47	30,00	14,65	9,60	55,00
MEAN	12,59	26,08	1,41	9,63	32,19	1,48	21,08	22,78	2,71	23,93	30,65	12,18	22,76	35,09	16,16	11,44	39,58
SD	3,99	10,77	0,67	4,27	8,61	0,73	5,27	8,95	1,01	4,72	6,82	4,16	5,63	5,67	5,52	2,71	10,10
MINIMUM	6,32	0,00	0,10	5,00	10,00	0,30	10,00	0,00	0,70	14,67	17,50	3,20	10,68	22,50	4,80	6,13	17,50
MAXIMUM	28,53	50,00	3,40	33,79	50,00	4,00	39,08	40,00	5,30	36,32	50,00	21,29	49,65	47,50	27,50	20,00	60,00

		Pterygoideus lateralis				Contribution of the muscles						
ID	mass	fiber length	pennation ang	mass	total mass	mass - digastric (%)	total mass - adductors	mass - masseter (%)	mass - temporal (%)	mass - pterygoid (%)	mass - lateral pterygoid / pterygoid (%)	
M7												
Ni-R1												
N-R5	3,00	11,90	25,00	0,44	38,49	8,94	35,05	24,25	65,93	9,81	12,79	
N-R21	2,65	7,00		0,32	32,66	10,66	29,18	26,66	63,16	10,18	10,77	
N-R28	1,90			0,10	19,90	11,06	17,70	29,38	59,32	11,30	5,00	
Ny-R1	4,83	4,75	20,00	0,29	59,92	9,40	54,29	26,36	64,21	9,43	5,66	
P-R1							0,00					
T-R1	11,00	7,00		0,40	72,40	9,67	65,40	24,46	58,10	17,43	3,51	
N-R1	4,00	9,30	32,50	1,00	55,00	9,09	50,00	26,00	64,00	10,00	20,00	
N-R10	3,85	7,95		0,25	55,54	8,48	50,83	28,23	63,70	8,07	6,10	
N-R11	1,92	6,10		0,18	20,49	10,35	18,37	25,04	63,53	11,43	8,57	
N-R12	4,41	6,75	35,00	0,25	57,71	9,39	52,29	23,71	67,37	8,91	5,36	
N-R13	5,84			0,24	76,05	7,90	70,04	23,62	67,70	8,68	3,95	
N-R14	5,03	9,00		0,00	55,90	6,14	52,47	26,97	63,45	9,59	0,00	
N-R16	4,82	7,40		0,20	63,75	8,11	58,58	26,60	64,83	8,57	3,98	
N-R17	3,45	5,45	30,00	0,15	49,37	9,56	44,65	25,60	66,34	8,06	4,17	
N-R18	3,72	6,10	30,00	0,18	55,00	9,33	49,87	26,57	65,61	7,82	4,62	
N-R19	3,81	6,55		0,22	50,32	7,53	46,53	27,21	64,13	8,66	5,46	
N-R2	3,00	12,10		1,00	52,00	9,62	47,00	25,53	65,96	8,51	25,00	
N-R20	3,53	6,00		0,24	49,63	9,17	45,08	24,91	66,73	8,36	6,37	
N-R22	2,82	6,50		0,14	34,45	9,00	31,35	26,79	63,76	9,44	4,73	
N-R23	4,61	6,27	40,00	0,31	60,08	10,64	53,69	26,90	63,94	9,16	6,30	
N-R24	4,17	7,60	40,00	0,33	56,23	8,98	51,18	26,40	64,81	8,79	7,33	
N-R25	2,06	3,90	45,00	0,15	21,76	8,78	19,85	25,69	63,17	11,13	6,79	
N-R26	4,06	5,90	50,00	0,26	49,31	8,90	44,92	26,31	64,07	9,62	6,02	
N-R27	3,65	9,25	40,00	0,25	46,38	8,73	42,33	24,38	66,41	9,21	6,41	
N-R29	1,50	4,52		0,10	17,10	9,94	15,40	29,22	60,39	10,39	6,25	
N-R3	3,00			1,00	45,00	11,11	40,00	22,50	67,50	10,00	25,00	
N-R30	3,50	4,35	30,00	0,30	59,50	8,74	54,30	27,62	65,38	7,00	7,89	
N-R31	3,50	4,33	30,00	0,10	73,10	8,76	66,70	31,33	63,27	5,40	2,78	
N-R32	3,80	7,54	40,00	0,60	59,90	8,35	54,90	25,32	66,67	8,01	13,64	
N-R33	2,30	7,04	30,00	0,50	27,00	8,15	24,80	30,65	58,06	11,29	17,86	
N-R34	4,50	4,81	30,00	0,40	73,50	8,57	67,20	25,45	67,26	7,29	8,16	
N-R35	3,50	5,96	30,00	0,50	45,80	9,83	41,30	25,42	64,89	9,69	12,50	
N-R36	3,80	3,23	25,00	0,30	60,20	10,63	53,80	27,14	65,24	7,62	7,32	
N-R37	3,60	4,49	30,00	0,30	57,80	7,44	53,50	26,92	65,79	7,29	7,69	
N-R38	3,60	10,57	30,00	0,80	63,70	8,32	58,40	28,25	64,21	7,53	18,18	
N-R39	2,70	4,34	30,00	0,30	31,80	11,95	28,00	23,93	65,36	10,71	10,00	
N-R4	2,35	10,30		0,30	31,86	10,36	28,56	27,24	63,48	9,28	11,32	
N-R40	4,00	4,26	25,00	0,10	61,50	9,92	55,40	26,53	66,06	7,40	2,44	
N-R41	5,10	6,14	35,00	0,70	84,70	6,97	78,80	25,25	67,39	7,36	12,07	
N-R42	1,90	4,37	30,00	0,30	24,60	9,35	22,30	29,15	60,99	9,87	13,64	
N-R43	4,50	3,60	20,00	0,20	74,30	8,88	67,70	29,39	63,66	6,94	4,26	
N-R44	4,20	5,07	25,00	0,60	69,80	10,17	62,70	29,19	63,16	7,66	12,50	
N-R45	3,30	5,60	25,00	0,60	46,20	9,09	42,00	28,33	62,38	9,29	15,38	
N-R46	3,60	7,52	27,50	0,50	52,00	10,38	46,60	28,54	62,66	8,80	12,20	
N-R47	3,80	5,64	27,50	0,40	63,50	8,03	58,40	27,91	64,90	7,19	9,52	
N-R48	5,50	4,97	27,50	0,20	80,80	8,04	74,30	27,86	64,47	7,67	3,51	
N-R49	3,30	6,83	20,00	0,20	50,30	9,15	45,70	28,45	63,89	7,66	5,71	
N-R50	1,80	6,35	27,50	0,30	26,10	9,20	23,70	29,54	61,60	8,86	14,29	
N-R6	4,09	7,80	30,00	0,27	52,36	9,85	47,20	25,68	65,08	9,24	6,19	

		Pterygoideus lateralis				Contribution of the muscles						
ID	mass	fiber length	pennation ang	mass		total mass	mass - digastric (%)	total mass - adductors	mass - masseter (%)	mass - temporal (%)	mass - pterygoid (%)	mass - lateral pterygoid / pterygoid (%)
N-R60	2,50	3,55		0,10		42,10	8,55	38,50	31,95	61,30	6,75	3,85
N-R61	3,50	8,88	25,00	0,70		45,60	9,21	41,40	29,47	60,39	10,14	16,67
N-R62	3,20	7,30	25,00	0,60		48,70	9,24	44,20	26,02	65,38	8,60	15,79
N-R63	4,50	4,07	22,50	0,50		69,30	9,96	62,40	30,29	61,70	8,01	10,00
N-R64	3,00	3,53	30,00	0,20		52,20	8,24	47,90	26,93	66,39	6,68	6,25
N-R7	4,28	10,10	40,00	0,28		49,21	8,39	45,08	30,28	59,61	10,12	6,14
N-R70	2,40	6,49	32,50	0,40		40,80	8,82	37,20	20,97	71,51	7,53	14,29
N-R8	4,41	2,30		0,79		82,59	9,40	74,83	29,11	63,94	6,95	15,19
N-R9	3,79	7,30		0,24		53,13	9,43	48,12	25,12	66,50	8,37	5,96
Ny-R2	5,42	8,15		0,32		67,19	9,63	60,72	28,24	62,30	9,45	5,57
Ny-R3	6,34	6,40		0,35		74,51	8,01	68,54	27,65	62,59	9,76	5,23
Ny-R4	6,25	6,50	40,00	0,32		80,50	6,81	75,02	26,74	64,50	8,76	4,87
Ny-R5	4,60	5,00	25,00	0,19		64,75	9,58	58,55	21,74	70,08	8,18	3,97
Ny-R6	3,85	7,00		0,09		55,63	8,45	50,93	21,52	70,74	7,74	2,28
Ny-R7	2,40	3,00		0,03		37,32	10,10	33,55	26,77	65,99	7,24	1,23
Ny-R8	4,25	5,50		0,19		56,77	9,21	51,54	24,82	66,57	8,61	4,28
P-R3	3,66	4,45		0,26		44,76	10,68	39,98	24,91	65,28	9,80	6,63
MEAN	3,80	6,32	30,55	0,34	Mean	52,77	9,14	47,28	26,72	64,44	8,84	8,58
SD	1,39	2,13	6,81	0,23	Sd	16,35	1,06	16,10	2,30	2,63	1,68	5,42
MINIMUM	1,50	2,30	20,00	0,00	Min	17,10	6,14	0,00	20,97	58,06	5,40	0,00
MAXIMUM	11,00	12,10	50,00	1,00	Max	84,70	11,95	78,80	31,95	71,51	17,43	25,00

ID	mass - lateral pterygoid / adductors (%)
M7	
Ni-R1	
N-R5	1,26
N-R21	1,10
N-R28	0,56
Ny-R1	0,53
P-R1	
T-R1	0,61
N-R1	2,00
N-R10	0,49
N-R11	0,98
N-R12	0,48
N-R13	0,34
N-R14	0,00
N-R16	0,34
N-R17	0,34
N-R18	0,36
N-R19	0,47
N-R2	2,13
N-R20	0,53
N-R22	0,45
N-R23	0,58
N-R24	0,64
N-R25	0,76
N-R26	0,58
N-R27	0,59
N-R29	0,65
N-R3	2,50
N-R30	0,55
N-R31	0,15
N-R32	1,09
N-R33	2,02
N-R34	0,60
N-R35	1,21
N-R36	0,56
N-R37	0,56
N-R38	1,37
N-R39	1,07
N-R4	1,05
N-R40	0,18
N-R41	0,89
N-R42	1,35
N-R43	0,30
N-R44	0,96
N-R45	1,43
N-R46	1,07
N-R47	0,68
N-R48	0,27
N-R49	0,44
N-R50	1,27
N-R6	0,57

ID	mass - lateral pterygoid / adductors (%)
N-R60	0,26
N-R61	1,69
N-R62	1,36
N-R63	0,80
N-R64	0,42
N-R7	0,62
N-R70	1,08
N-R8	1,06
N-R9	0,50
Ny-R2	0,53
Ny-R3	0,51
Ny-R4	0,43
Ny-R5	0,32
Ny-R6	0,18
Ny-R7	0,09
Ny-R8	0,37
P-R3	0,65
MEAN	0,77
SD	0,52
MINIMUM	0,00
MAXIMUM	2,50

Sheet 3

								Bite force at the incisors					Bite force at the molars				
ID	dissection	Sex	BD	body mass		headl	headw	headh	T1	T2	T3	T4	mean	T1	T2	T3	T4	mean
4246	x (ny-r5)	F	2009	6,9		160,9	91,6	89,2	183				**183**	311	256	435		**435**
4223		F	2014	6,9		151,5	93,3	67,3	231	214			**231**	386	475	484		**484**
4276		F	2014	5,25		151,3	83,8	76,1	209	250			**250**	261	291			**291**
4373		F	2017	5,7		139,1	80,9	69,1	204	215			**215**	219	255	329	329	**329**
4201		F	2014	6,8		153,3	84,6	70,9	203	149	75		**203**	206	151	216		**216**
4103		F	2017	6,25		151,7	93,6	60,1	143	183	283		**283**	373	361	370		**373**
4261		M	2014	7,3		173	82,8	77,1	81	138			**138**	284	281			**284**
4294		M	2014	7,5		166,9	91,5	88	84	98	245		**245**	281	306	349		**349**
4374		M	2017	7		179,2	89,2	75	373	184	134		**373**	226	206			**226**
4102		M	2017	5,8		157,1	75,8	72,1	134	244	294	308	**308**	254	309	253	383	**383**

Sheet 4

Contribution (%) of the different constituent bellies of the jaw muscles to the moment of the estimated bite force for different gape angles.

MS: M. masseter pars superficialis; MP: M. masseter pars profunda; ZA: M. zygomaticomandibularis anterior; ZP: M. zygomaticomandibularis posterior; SZ: M. temporalis pars suprazygomatica; TS: M. temporalis pars superficialis; TP: M. temporalis pars profunda; PM + PL: M. pterygoideus medialis and lateralis.

Gape angle	MS	MP	ZA	ZP	SZ	TS	TP	P
0°	16,22±3.27	9,78±3.42	7,15±2.55	5,43±2.55	2,58±1.03	24,23±4.41	23,51±5.25	11,11±3.85
20°	15,96±3.20	9,66±3.43	7,37±2.66	5,37±2.55	2,19±0.86	24,23±4.49	23,53±5.30	11,69±3.81
30°	15,72±3.20	9,61±3.46	7,51±2.73	5,35±2.57	2,03±0.81	24,28±4.55	23,55±5.33	11,95±3.72
40°	15,39±3.23	9,57±3.50	7,67±2.82	5,33±2.59	1,93±0.80	24,34±4.65	23,62±5.39	12,16±3.65

Sheet 5

Definition of the landmarks used in this study following the Nomina Anatomica Veterinaria nomenclature (NAV, 2017).

Landmark	Definition
Lower jaw: Mandibula	
1	Most rostromedial point of the Synchondrosis intermandibularis, at the base of the first incisor tooth
2	Most rostral point of the canine tooth, on the lateral side
3	Most caudal point of the canine tooth, on the lateral side
4	Most rostral point of the second premolar tooth, on the lateral side
5	Most rostral point of the third premolar tooth, on the lateral side
6	Most rostral point of the fourth premolar tooth, on the lateral side
7	Most caudal point of the fourth premolar tooth, on the lateral side
8	Most caudal point of the carnassial tooth, on the lateral side
9	Most caudal point of the second molar tooth, on the lateral side
10	Highest point of the tip of the Processus coronoideus
11	Most caudal point of the tip of the Processus coronoideus
12	Most caudal point of the Incisura mandibulae, at the intersection of the Processus condylaris and the Processus coronoideus
13	Most medial point of the Processus condylaris
14	Most ventral point of the Processus condylaris
15	Most lateral point of the Processus condylaris
16	Most anterior point on the curve of the Angulus mandibulae
17	Point at the tip of the Processus angularis
18	Most elevated point on the inferior border of the Ramus mandibulae
19	Lowest point on the ventral border of the Ramus mandibulae, right under the carnassial tooth
20	Most caudal and lowest point of the Synchondrosis intermandibularis on the medial side
21	Foramen mentale
22	Most rostral and ventral point of the Fossa masseterica
23	Most rostral point of the edge joining the basis of the Processus condylaris and Processus condylaris on the medial side.
24	Most rostral point of the Foramen mandibulae
25	The most lateral point on the Angulus mandibulae, at the beginning of the Processus angularis
Upper jaw	
1	Most rostral point of Os incisivum, between incisor teeth I1 in dorsal view
2	Most rostral point of Os nasale, on the midline (Sutura internasalis)
3	Most rostral point on Sutura nasoincisiva
4	Point at the junction of Os incisivum, Os nasale and Maxilla
5	Point at the junction of Os nasale, Maxilla and Os frontale
6	Most rostral point of Os temporale and most caudal point of Os nasale, on the midline (Sutura internasalis)
7	Most posterior point of the Maxilla in dorsal view
8	Most lateral point of the Processus zygomaticus of Os frontale
9	Most medial point of the curvature corresponding to the Linea temporalis, most medial point at the postorbital constriction
10	Processus frontalis of Os zygomaticum

11	Most rostral point of the curvature of the lower edge of the Fossa sacci lacrimalis
12	Bregmatic fontanel, most medial point of the Sutura coronalis, on the midline
13	Most medial point on the Sutura lambdoidea
14	Inion, posterior end of Os occipitale
15	Point at the extreme convex curvature of the Tuberculum nuchale
16	Point at the extreme convex curvature of the Crista supramastoidea
17	Fossa mandibularis, on the Sutura sphenoparietalis
18	Central point of the Sutura interincisiva in ventral view, just posterior to the two incisor teeth
19	Most rostral point of the Fissura palatina
20	Most caudal point of the Fissura palatina
21	Point on the Fissura palatina at the junction between Os incisivum and Maxilla in ventral view
22	Point between the Canina and the incisor tooth I3 at the junction between Os incisivum and Maxilla in ventral view
23	Most rostral point of Maxilla in ventral view, on the midline
24	Most rostral point of the Sutura palatomaxillaris, on the midline
25	Most caudal point of Os palatinum, on the midline
26	Point near molar tooth M2, on the Sutura palatomaxillaris
27	Ventral point on the Sutura sphenopalatina
28	Point on vomer, at the junction with Os presphenoidale (Sutura vomerosphenoidalis)
29	Most caudal point of the Synchondrosis sphenooccipitalis, on the midline
30	Most lateral point of the Synchondrosis sphenooccipitalis, rostrally to the Bulla tympanica
31	Most cranial point of the caudal curve of Os occipitale (Foramen magnum) in ventral view, on the midline
32	Most caudal point of the caudal curve of Os occipitale in ventral view
33	Point on the Foramen lacerum
34	Processus paracondylaris
35	Ventral tip of the Bulla tympanica
36	Most dorsal and caudal point of the curve of the Foramen alare caudale
37	Most ventral and posterior point at the junction of the Pars squamosa of Os temporale and Os zygomaticum, on the Arcus zygomaticus
38	Most caudal point at the junction between Maxilla and Os zygomaticum, near the molar tooth M2
39	Most cranial point of the alveolus of the canine tooth
40	Most caudal point of the alveolus of the canine tooth
41	Most cranial point of the alveolus of the upper carnassial tooth P4
42	Point between the alveolus of P4 and M1 teeth
43	Point between the alveolus of M1 and M2 teeth
44	Most caudal point of Maxilla behind tooth M2
45	Most dorsal point of the Foramen infraorbitale
46	Most ventral point of the Foramen infraorbitale
47	Point at the junction of Maxilla, Os lacrimale and Os temporale
48	Point at the junction of Maxilla, Os lacrimale and Os zygomaticum
49	Most caudal point of curvature at the junction of Maxilla and Os zygomaticum
50	Most ventral and caudal point of the Foramen alare rostrale
51	Most ventral and caudal point of the Fissura orbitalis
52	Most rostral point of Meatus acusticus externus in lateral view
53	Most caudal point of Meatus acusticus externus in lateral view
54	Opisthion, dorsal and caudal border of the Foramen magnum, on the midline

6.2. Fig. S1.

PCA on cranial shape (A), allometry-free cranial shape (B), mandibular shape (C) or allometry-free mandibular shape (D) with shapes at the maximum and minimum of the PCA axis. Illustrations represent deformations from the consensus (white) to the extreme of the axis in lateral and dorsal views, magnified by a factor three. Different ages are represented by different colours. The first two axes of the PCA on cranial shape data represent only 22.1% of the total variance and differences are rather subtle. The first axis is mostly related to variation in the breadth of the zygomatic arches, the breadth of the anterior part of the braincase, the rostro-caudal positioning of the post-orbital processes, and the height of the cranium in lateral view, in particular the height of the sagittal crest. The first axis shows significant allometry ($R^2 = 0.12$, $P < 0.01$). The second axis is driven by variation in the breadth of the cranium (zygomatic arches, orbital processes, braincase and snout), and is related to size ($R^2 = 0.12$, $P < 0.01$) and age ($R^2 = 0.10$, $P < 0.05$). The first two axes of the PCA representing the shape of the mandible account for 39.3% of the total variance. There is no significant impact of size, age, nor sex on the first axis. The second axis is related to the dorso-ventral curvature of the body, the rostro-caudal curvature of the coronoid process and is driven by variation in centroid size ($R^2 = 0.24$, $P < 0.001$) and age ($R^2 = 0.25$, $P < 0.001$).

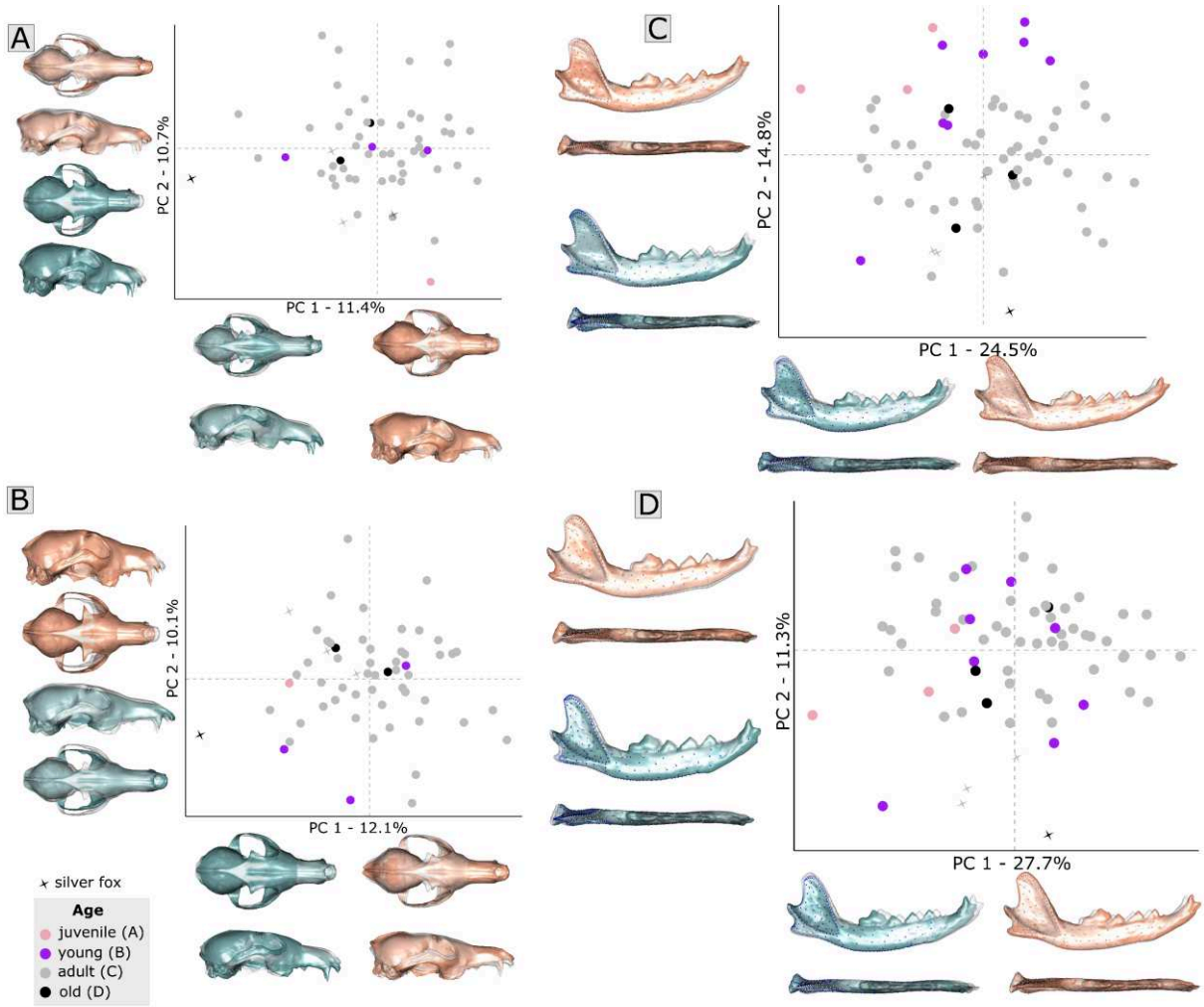

6.3. Fig. S2.

Distribution of the specimens along the allometric slope of cranial shapes (A) or mandible shapes (B) with a visualisation of the differences between large and small specimens relative to consensus shape. Ages are indicated by different colours.

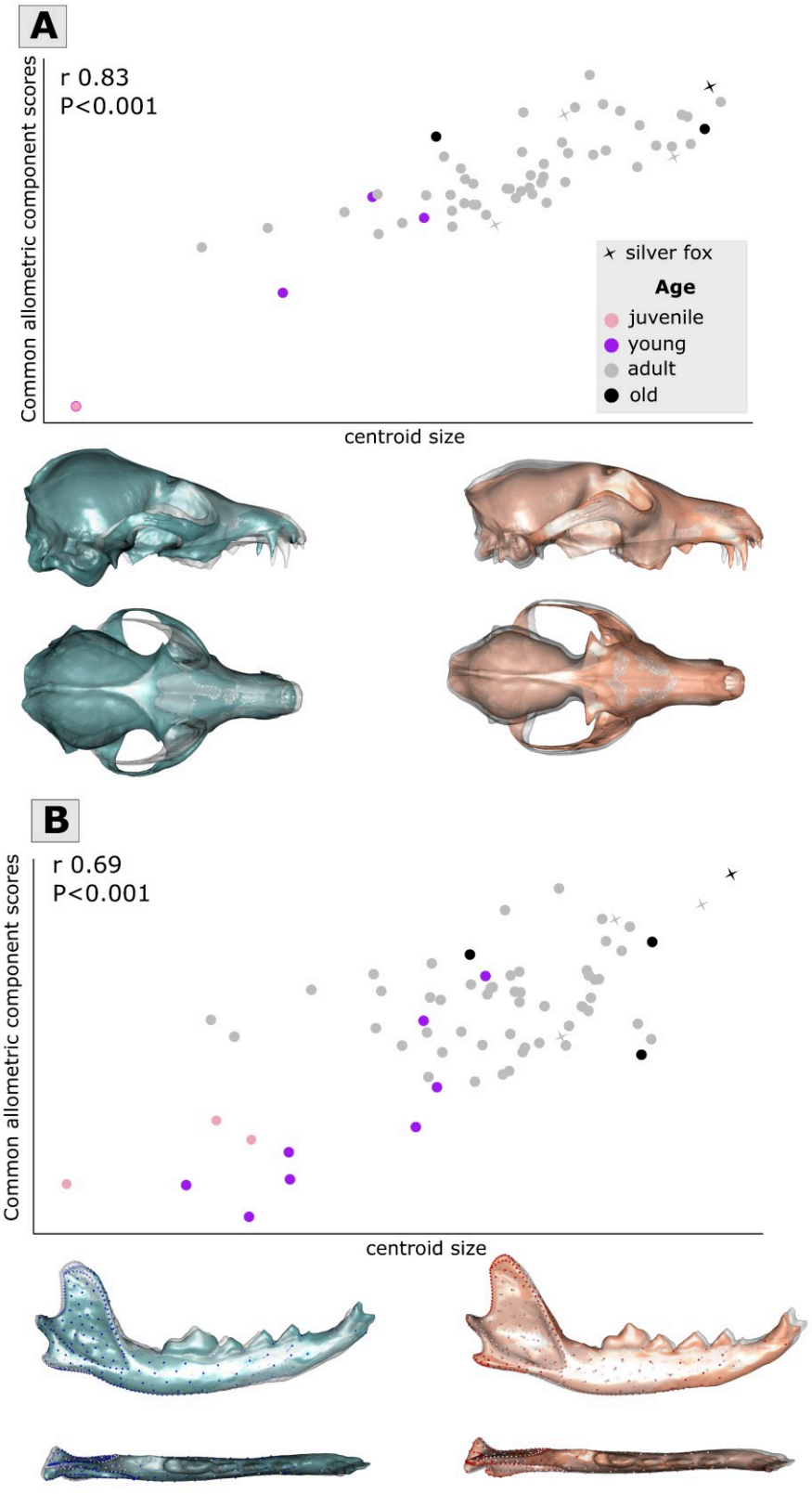

6.4. Fig. S3.

Principal Component Analyses on muscle data of foxes only with muscle loadings.
A: raw masses; B: scaled masses (regression on mandibular centroid size); C: raw PCSAs; D: scaled PCSAs (regression on mandibular centroid size). Different ages are indicated by different colours. Dig: M. digastricus; MS: M. masseter pars superficialis; MP: M. masseter pars profunda; ZA: M. zygomaticomandibularis anterior; ZP: M. zygomaticomandibularis posterior; SZ: M. temporalis pars suprazygomatica; TS: M. temporalis pars superficialis; TP: M. temporalis pars profunda; PM + PL: M. pterygoideus medialis and lateralis.

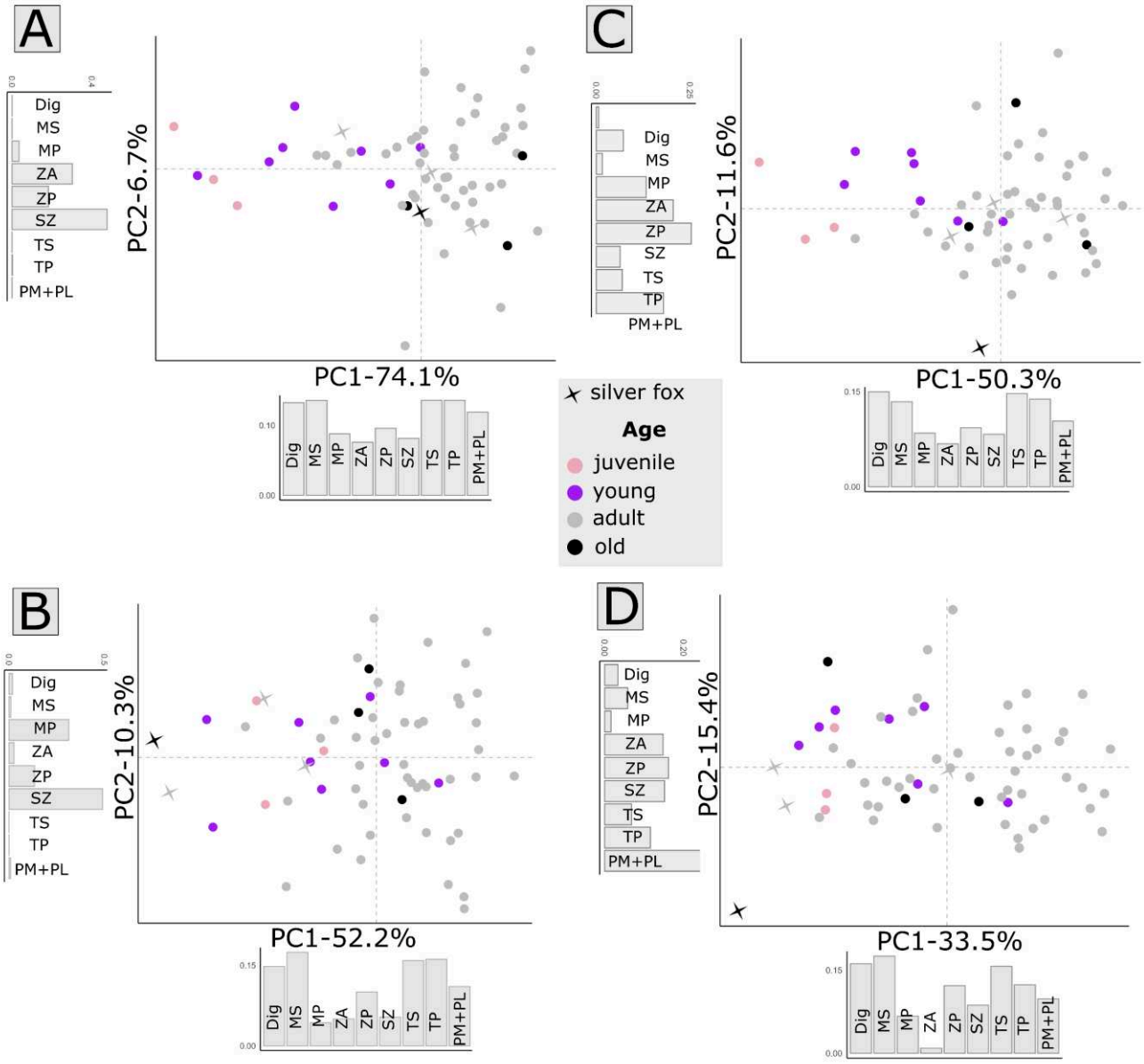

6.5. Fig. S4.

Principal Component Analyses on muscle data of dogs and foxes with muscle loadings.
A: raw PCSAs; B: scaled PCSAs (regression on mandibular centroid size). Dogs are in blue and red foxes are in orange. Beagles are in the blue polygon. A few breeds are indicated for information: Bel: Belgian Shepherd; Bult: Bull terrier; Chi: Chihuahua; Col: Collie; Dac: Dachshund; Dee: Deerhound; Kin: King Charles; Pap: Papillon. Dig: M. digastricus; MS: M. masseter pars superficialis; MP: M. masseter pars profunda; ZA: M. zygomaticomandibularis anterior; ZP: M. zygomaticomandibularis posterior; SZ: M. temporalis pars suprazygomatica; TS: M. temporalis pars superficialis; TP: M. temporalis pars profunda; PM + PL: M. pterygoideus medialis and lateralis.

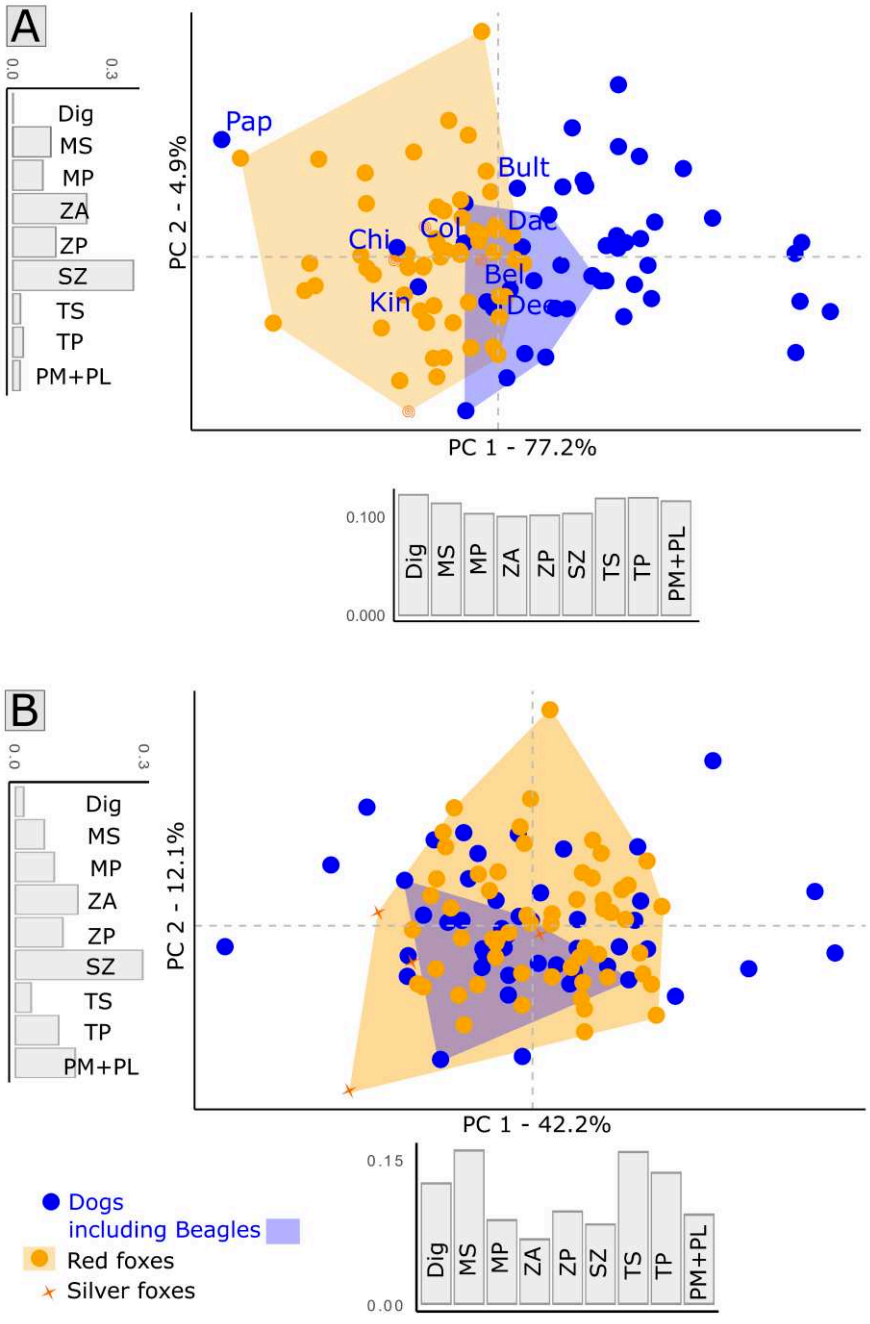

6.6. Fig. S5.

Graphs representing the model output for a given range of the food reaction force orientations at a gape angle of 20°. Foxes (orange) are compared with dogs (blue). Different bite points are represented by different dot shapes. AFRF: angle of the food reaction force (°).

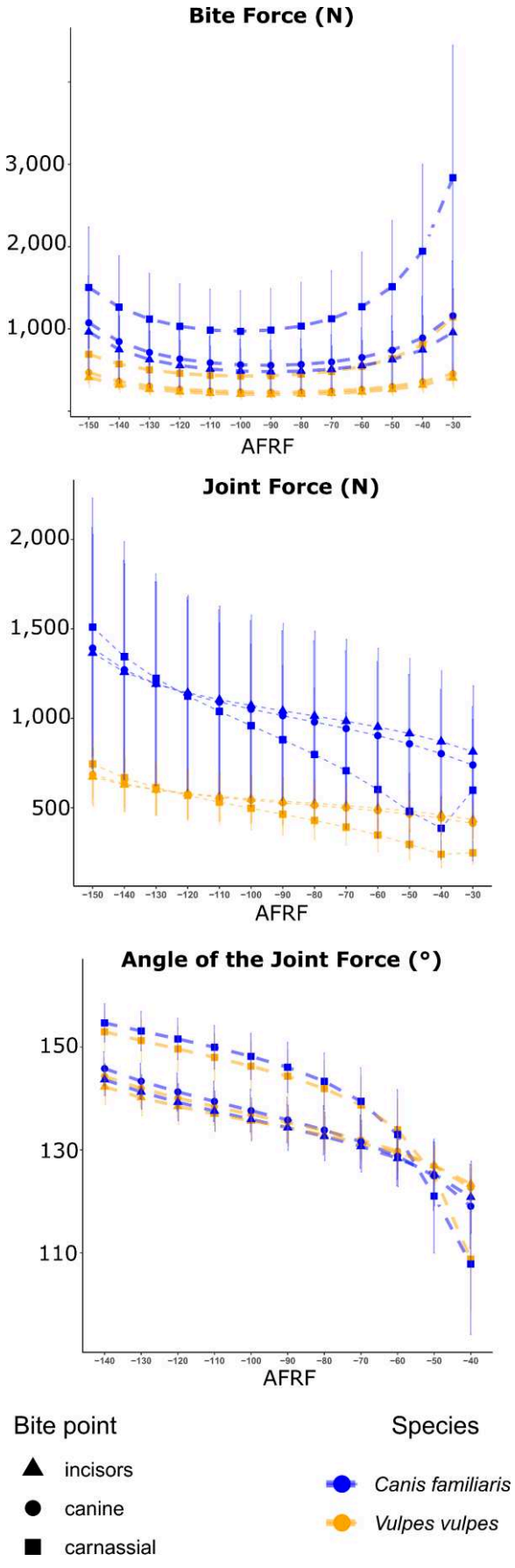

6.7. Detailed results of the statistical analyses.

Supplementary material 3 Results of the statistical analyses

Abbreviations
m=masseter
t=temporalis
p=pterygoids

1. Variability in muscle architecture data

1.1. PCA1 drivers

For the PCA on muscle PCSAs

```
>   summary(aov(pca$ind$coord[,1] ~contexte$`AGE
CRANE`+contexte$SEXE+prep_PLS$gpa.size.pcsa))
                       Df Sum Sq Mean Sq F value  Pr(>F)
contexte$`AGE CRANE`    5  155.4    31.1    23.9 3.5e-12 ***
contexte$SEXE           1   21.0    21.0    16.2   2e-04 ***
prep_PLS$gpa.size.pcsa  1   29.6    29.6    22.8 1.6e-05 ***
Residuals              50   65.1     1.3
---
Signif. codes:  0 '***' 0.001 '**' 0.01 '*' 0.05 '.' 0.1 ' ' 1
5 observations deleted due to missingness
```

1.2. PCA2 drivers

For the PCA on muscle PCSAs

```
                       Df Sum Sq Mean Sq F value Pr(>F)
contexte$`AGE CRANE`    5    3.0   0.607    0.59   0.70
contexte$SEXE           1    1.4   1.389    1.36   0.25
prep_PLS$gpa.size.pcsa  1    0.6   0.577    0.56   0.46
Residuals              50   51.1   1.023
```

1.3. Differences between foxes and dogs in muscle architecture (manova)

Raw PCSA

```
           Df  Pillai approx F num Df den Df    Pr(>F)
sp          1 0.47417   9.7191      9     97 1.838e-10 ***
Residuals 105
---
Signif. codes:  0 '***' 0.001 '**' 0.01 '*' 0.05 '.' 0.1 ' ' 1
```

Residual PCSA

```
           Df   Pillai approx F num Df den Df Pr(>F)
sp          1 0.030999  0.34479      9     97 0.9575
Residuals 105
```

1.4. Differences between foxes and dogs in muscle architecture (welch t tests)

```
> summary(na.omit(renards$`mass - masseter (%)`))
   Min. 1st Qu.  Median    Mean 3rd Qu.    Max.
   2.30   25.25   26.72   26.36   28.25   31.95
> summary(na.omit(renards$`mass - temporal (%)`))
   Min. 1st Qu.  Median    Mean 3rd Qu.    Max.
   2.63   63.16   64.44   63.56   65.99   71.51
> summary(na.omit(renards$`mass - pterygoid (%)`))
   Min. 1st Qu.  Median    Mean 3rd Qu.    Max.
```

```
  1.680   7.660   8.680   8.806   9.690  17.430
> sd(na.omit(renards$`mass - masseter (%)`))
[1] 3.810167
> sd(na.omit(renards$`mass - temporal (%)`))
[1] 7.952103
> sd(na.omit(renards$`mass - pterygoid (%)`))
[1] 2.158432
> chiens=as.data.frame(read_excel("//Desktop-p3k1mud/d/THESE/THESE/Articles/Article BF
dog/Review/Supplementary material/Table S1.xlsx",
+                                 sheet=2,skip = 2,col_names = T))
New names:
* I -> I...10
* C -> C...11
* M1 -> M1...12
* I -> I...13
* C -> C...14
* ...
> summary(na.omit(chiens$`mass - masseter (%)`))
   Min. 1st Qu.  Median    Mean 3rd Qu.    Max.
   2.30   24.89   26.31   26.16   28.62   32.06
> summary(na.omit(chiens$`mass - temporal (%)`))
   Min. 1st Qu.  Median    Mean 3rd Qu.    Max.
   2.63   61.52   63.94   62.62   66.59   71.51
> summary(na.omit(chiens$`mass - pterygoid (%)`))
   Min. 1st Qu.  Median    Mean 3rd Qu.    Max.
  1.680   8.349   9.345   9.490  10.671  17.430
> sd(na.omit(chiens$`mass - masseter (%)`))
[1] 4.373308
> sd(na.omit(chiens$`mass - temporal (%)`))
[1] 9.343351
> sd(na.omit(chiens$`mass - pterygoid (%)`))
[1] 2.307703


> t.test(renards$`mass - masseter (%)`, chiens$`mass - masseter (%)`)

        Welch Two Sample t-test

data:  renards$`mass - masseter (%)` and chiens$`mass - masseter (%)`
t = 0.25854, df = 98.942, p-value = 0.7965
alternative hypothesis: true difference in means is not equal to 0
95 percent confidence interval:
 -1.320363  1.715998
sample estimates:
mean of x mean of y
 26.36014  26.16233

> t.test(renards$`mass - temporal (%)`, chiens$`mass - temporal (%)`)

        Welch Two Sample t-test

data:  renards$`mass - temporal (%)` and chiens$`mass - temporal (%)`
t = 0.57675, df = 97.353, p-value = 0.5654
alternative hypothesis: true difference in means is not equal to 0
95 percent confidence interval:
 -2.282416  4.152437
sample estimates:
mean of x mean of y
 63.55623  62.62122

> t.test(renards$`mass - pterygoid (%)`, chiens$`mass - pterygoid (%)`)

        Welch Two Sample t-test

data:  renards$`mass - pterygoid (%)` and chiens$`mass - pterygoid (%)`
t = -1.6477, df = 103.69, p-value = 0.1025
alternative hypothesis: true difference in means is not equal to 0
95 percent confidence interval:
 -1.5055216  0.1390986
sample estimates:
mean of x mean of y
 8.806377  9.489588
```

1.5. Correlations in muscle data

(m=masseter ; t=temporalis ; p=pterygoids)

PCSA

	Pcsa.m	t	p
PCSA.m	1.0000000	0.7572205	0.5969046
PCSA.t	0.7572205	1.0000000	0.4092065
PCSA.p	0.5969046	0.4092065	1.0000000

mass

	mass.m	mass.t	mass.p
mass.m	1.0000000	0.9491922	0.8348537
mass.t	0.9491922	1.0000000	0.8613043
mass.p	0.8348537	0.8613043	1.0000000

2. Disparity tests

2.1. Mandible shape (N=59 dogs + 68 foxes)

SProcrustes.var

```
Canis familiaris    Vulpes vulpes
     0.003896853      0.002972407
```

SPV.dist

```
                Canis familiaris Vulpes vulpes
Canis familiaris      0.000000000   0.000924446
Vulpes vulpes         0.000924446   0.000000000
```

SPV.dist.Pval

```
                Canis familiaris Vulpes vulpes
Canis familiaris       1.00000000    0.06693307
Vulpes vulpes          0.06693307    1.00000000
```

2.2. Skull shape (N=58 dogs + 68 foxes)

SProcrustes.var

```
Canis familiaris    Vulpes vulpes
     0.006183231      0.002174733
```

SPV.dist

```
                Canis familiaris Vulpes vulpes
Canis familiaris      0.000000000   0.004008497
Vulpes vulpes         0.004008497   0.000000000
```

SPV.dist.Pval

```
                Canis familiaris Vulpes vulpes
Canis familiaris      1.000000000   0.000999001
Vulpes vulpes         0.000999001   1.000000000
> #dimnames(gpa$rotated)
> #cont$`ID COLLINE`
> table(cont$ESPECE)
```

2.3. Muscle masses

SProcrustes.var

```
dogs foxes
  0.644   0.359
```

SPV.dist

```
        dogs foxes
dogs   0.000   0.285
foxes  0.285   0.000
```

SPV.dist.Pval

```
        dogs foxes
dogs   1.000   0.145
foxes  0.145   1.000
```

2.4. Muscle PCSAs

SProcrustes.var

```
dogs foxes
  0.350   0.238
```

SPV.dist

```
        dogs foxes
dogs   0.000   0.112
foxes  0.112   0.000
```

SPV.dist.Pval

```
        dogs foxes
dogs   1.000   0.386
foxes  0.386   1.000
```

3. Drivers of skull shape variation

3.1. Drivers of PC1 on skull shapes (N=68) using linear regressions ('lm')

Size (N=58)

```
               Estimate Std. Error t value Pr(>|t|)
(Intercept)       0.5818     0.1952    2.98   0.0042 **
log10(gpa$size)  -0.2178     0.0731   -2.98   0.0042 **
---
Signif. codes:  0 '***' 0.001 '**' 0.01 '*' 0.05 '.' 0.1 ' ' 1
Residual standard error: 0.0122 on 56 degrees of freedom
Multiple R-squared:  0.137,   Adjusted R-squared:  0.122
F-statistic: 8.89 on 1 and 56 DF,  p-value: 0.00424
```

Age (N=58)

```
(Intercept)       0.0122     0.0125    0.97    0.335
cont$`AGE MDB`b  -0.0158     0.0145   -1.09    0.280
cont$`AGE MDB`c  -0.0112     0.0126   -0.89    0.380
cont$`AGE MDB`d  -0.0297     0.0145   -2.05    0.045 *
---
Signif. codes:  0 '***' 0.001 '**' 0.01 '*' 0.05 '.' 0.1 ' ' 1
Residual standard error: 0.0125 on 54 degrees of freedom
Multiple R-squared:  0.12,    Adjusted R-squared:  0.0712
F-statistic: 2.46 on 3 and 54 DF,  p-value: 0.0728
```

Scx (N=51)

```
            Estimate Std. Error t value Pr(>|t|)
(Intercept)  0.00444    0.00265    1.68     0.10 .
cont$SEXEM  -0.00547    0.00334   -1.64     0.11
---
Signif. codes:  0 '***' 0.001 '**' 0.01 '*' 0.05 '.' 0.1 ' ' 1
Residual standard error: 0.0115 on 49 degrees of freedom
  (7 observations deleted due to missingness)
Multiple R-squared:  0.0518,  Adjusted R-squared:  0.0324
F-statistic: 2.67 on 1 and 49 DF,  p-value: 0.108
```

3.2. Drivers of PC2 on skull shapes (N=68) using linear regressions ('lm')

Size (N=58)

```
               Estimate Std. Error t value Pr(>|t|)
(Intercept)      -0.5644     0.1892   -2.98   0.0042 **
log10(gpa$size)   0.2113     0.0708    2.98   0.0042 **
---
Signif. codes:  0 '***' 0.001 '**' 0.01 '*' 0.05 '.' 0.1 ' ' 1
Residual standard error: 0.0118 on 56 degrees of freedom
Multiple R-squared:  0.137,   Adjusted R-squared:  0.122
F-statistic:  8.9 on 1 and 56 DF,  p-value: 0.00422
```

Age (N=58)

```
               Estimate Std. Error t value Pr(>|t|)
(Intercept)      -0.0362     0.0119   -3.04   0.0037 **
cont$`AGE MDB`b   0.0354     0.0138    2.57   0.0130 *
cont$`AGE MDB`c   0.0371     0.0121    3.08   0.0033 **
cont$`AGE MDB`d   0.0347     0.0138    2.52   0.0147 *
---
Signif. codes:  0 '***' 0.001 '**' 0.01 '*' 0.05 '.' 0.1 ' ' 1

Residual standard error: 0.0119 on 54 degrees of freedom
Multiple R-squared:  0.15,    Adjusted R-squared:  0.103
F-statistic: 3.18 on 3 and 54 DF,  p-value: 0.0311
```

Sex (N=51)

```
             Estimate Std. Error t value Pr(>|t|)
(Intercept)  0.001008   0.002771    0.36     0.72
cont$SEXEM  -0.000568   0.003498   -0.16     0.87

Residual standard error: 0.0121 on 49 degrees of freedom
  (7 observations deleted due to missingness)
Multiple R-squared:  0.000538,     Adjusted R-squared:  -0.0199
F-statistic: 0.0264 on 1 and 49 DF,  p-value: 0.872
```

3.3. Results of the Procrustes ANOVAs on skull shape

Size (N=58)

```
          Df     SS      MS   Rsq    F    Z Pr(>SS)
size       1 0.0052 0.00518 0.061 3.66 4.92    0.001 **
Residuals 56 0.0794 0.00142 0.939
Total     57 0.0845
Call: procD.lm(f1 = coords ~ size, data = gdf)
```

Age (N=58)

```
          Df     SS      MS   Rsq    F    Z Pr(>SS)
age        3 0.0082 0.00272 0.097 1.93 3.11    0.002 **
Residuals 54 0.0764 0.00141 0.903
Total     57 0.0845
Call: procD.lm(f1 = coords ~ age, RRPP = T, data = gdfage)
```

Sex (N=51)

```
          Df     SS      MS  Rsq    F    Z Pr(>SS)
sex        1 0.0021 0.00211 0.03 1.52 1.86    0.041 *
Residuals 49 0.0680 0.00139 0.97
Total     50 0.0701
Call: procD.lm(f1 = coords ~ sex, data = gdf2)
```

Size + all muscle masses and PCSAs (N=54)

```
          Df       SS        MS      Rsq      F       Z Pr(>SS)
size       1 0.004458 0.0044580 0.05831 3.2183  4.6154    0.001 **
pcsa.t     1 0.001221 0.0012205 0.01597 0.8811 -0.3102    0.609
pcsa.m     1 0.001877 0.0018772 0.02456 1.3552  1.5119    0.071 .
pcsa.p     1 0.001754 0.0017536 0.02294 1.2660  1.3969    0.083 .
mass.t     1 0.001148 0.0011481 0.01502 0.8288 -0.3221    0.616
mass.m     1 0.001157 0.0011566 0.01513 0.8350 -0.1558    0.550
mass.p     1 0.001117 0.0011170 0.01461 0.8064 -0.2509    0.587
Residuals 46 0.063718 0.0013852 0.83347
Total     53 0.076449
```

PCSA of the masseter (N=54)

```
         Df       SS        MS      Rsq      F      Z Pr(>SS)
pcsa.m    1 0.002481 0.0024809 0.03245 1.7441 2.3203    0.012 *
```

```
Residuals 52 0.073968 0.0014225 0.96755
Total     53 0.076449
```

Residuals

```
         Df       SS        MS     Rsq      F      Z Pr(>SS)
pcsa.m    1 0.002093 0.0020932 0.02738 1.4639 1.6318   0.059 .
Residuals 52 0.074356 0.0014299 0.97262
Total     53 0.076449
```

PCSA of the temporal (N=54)

```
          Df       SS        MS     Rsq      F      Z Pr(>SS)
pcsa.t     1 0.002862 0.0028616 0.03743 2.0221 2.7724   0.005 **
Residuals 52 0.073588 0.0014152 0.96257
Total     53 0.076449
```

Residuals:

```
          Df       SS        MS     Rsq      F        Z Pr(>SS)
pcsa.t     1 0.001221 0.0012205 0.01597 0.8437 -0.57005   0.711
Residuals 52 0.075229 0.0014467 0.98403
Total     53 0.076449
```

PCSA of the pterygoids (N=54)

```
          Df       SS        MS     Rsq      F      Z Pr(>SS)
pcsa.p     1 0.002068 0.0020680 0.02705 1.4457 1.6993   0.044 *
Residuals 52 0.074381 0.0014304 0.97295
Total     53 0.076449
```

Residuals:

```
          Df       SS        MS     Rsq      F      Z Pr(>SS)
pcsa.p     1 0.001956 0.0019565 0.02559 1.3657 1.4097   0.084 .
Residuals 52 0.074493 0.0014326 0.97441
Total     53 0.076449
```

mass of the masseter (N=56)

```
          Df       SS        MS  Rsq     F      Z Pr(>SS)
mass.m     1 0.004034 0.0040338 0.05 2.842 4.1473   0.001 **
Residuals 54 0.076646 0.0014194 0.95
Total     55 0.080679
```

Residuals:

```
          Df       SS        MS     Rsq      F      Z Pr(>SS)
mass.m     1 0.002488 0.0024884 0.03084 1.7185 2.1094   0.023 *
Residuals 54 0.078191 0.0014480 0.96916
Total     55 0.080679
```

mass of the temporal (N=56)

```
          Df       SS        MS     Rsq      F      Z Pr(>SS)
mass.t     1 0.004738 0.0047382 0.05873 3.3692 4.7205   0.001 **
Residuals 54 0.075941 0.0014063 0.94127
```



```
Total     55 0.080679

Residuals
          Df       SS        MS     Rsq      F      Z Pr(>SS)
mass.t     1 0.002795 0.0027954 0.03465 1.9381 2.6288   0.008 **
Residuals 54 0.077884 0.0014423 0.96535
Total     55 0.080679
```

mass of the pterygoids (N=56)

```
          Df       SS        MS     Rsq      F      Z Pr(>SS)
mass.p     1 0.003904 0.0039037 0.04838 2.7456 4.0532   0.001 **
Residuals 54 0.076776 0.0014218 0.95162
Total     55 0.080679
```

Residuals

```
          Df       SS        MS     Rsq      F      Z Pr(>SS)
mass.p     1 0.002107 0.0021071 0.02612 1.4482 1.5638   0.071 .
Residuals 54 0.078572 0.0014550 0.97388
Total     55 0.080679
```

4. Drivers of mandibular shape variation

4.1. Drivers of PC1 on mandible shapes using linear regressions ('lm')

Size (N=68)

```
Residuals:
      Min        1Q    Median        3Q       Max
-0.082833 -0.021219  0.001999  0.019684  0.067298
Coefficients:
            Estimate Std. Error t value Pr(>|t|)
(Intercept)  0.01068    0.05590   0.191    0.849
size        -0.02140    0.11175  -0.192    0.849
Residual standard error: 0.03179 on 66 degrees of freedom
Multiple R-squared:  0.0005554,    Adjusted R-squared:  -0.01459
F-statistic: 0.03668 on 1 and 66 DF,  p-value: 0.8487
```

Age (N=68)

```
Residuals:
     Min       1Q   Median       3Q      Max
-0.05762 -0.02135  0.00341  0.02125  0.06385
Coefficients:
            Estimate Std. Error t value Pr(>|t|)
(Intercept) -0.04592    0.01762  -2.606  0.01138 *
ageb         0.04084    0.02066   1.977  0.05240 .
```

```
agec         0.04933    0.01811   2.724  0.00831 **
aged         0.04526    0.02331   1.942  0.05654 .
---
Signif. codes:  0 '***' 0.001 '**' 0.01 '*' 0.05 '.' 0.1 ' ' 1
Residual standard error: 0.03052 on 64 degrees of freedom
Multiple R-squared:  0.1071,  Adjusted R-squared:  0.06529
F-statistic:  2.56 on 3 and 64 DF,  p-value: 0.06269
```

Sex (N=60)

```
Residuals:
     Min       1Q   Median       3Q      Max
-0.08289 -0.01966  0.00044  0.02168  0.06575
Coefficients:
             Estimate Std. Error t value Pr(>|t|)
(Intercept) -0.002996   0.006677  -0.449    0.655
sexM         0.004510   0.008503   0.530    0.598
Residual standard error: 0.03202 on 58 degrees of freedom
  (8 observations deleted due to missingness)
Multiple R-squared:  0.004827,      Adjusted R-squared:  -0.01233
F-statistic: 0.2813 on 1 and 58 DF, p-value: 0.5979
```

4.2. Drivers of PC2 on mandible shapes (N=68) using linear regressions ('lm')

Size (N=68)

```
Residuals:
     Min       1Q   Median       3Q      Max
-0.04533 -0.01210  0.00289  0.01661  0.03826

Coefficients:
            Estimate Std. Error t value Pr(>|t|)
(Intercept)   0.1753     0.0377    4.65  1.7e-05 ***
size         -0.3512     0.0754   -4.66  1.6e-05 ***
---
Signif. codes:  0 '***' 0.001 '**' 0.01 '*' 0.05 '.' 0.1 ' ' 1

Residual standard error: 0.0214 on 66 degrees of freedom
Multiple R-squared:  0.247,   Adjusted R-squared:  0.236
F-statistic: 21.7 on 1 and 66 DF,  p-value: 1.59e-05
```

Age (N=68)

```
Residuals:
     Min       1Q   Median       3Q      Max
-0.06768 -0.01282  0.00229  0.01569  0.03879

Coefficients:
            Estimate Std. Error t value Pr(>|t|)
(Intercept)   0.0345     0.0123    2.81   0.0066 **
ageb         -0.0092     0.0144   -0.64   0.5257
agec         -0.0388     0.0126   -3.07   0.0031 **
aged         -0.0548     0.0163   -3.37   0.0013 **
---
Signif. codes:  0 '***' 0.001 '**' 0.01 '*' 0.05 '.' 0.1 ' ' 1

Residual standard error: 0.0213 on 64 degrees of freedom
```



```
Multiple R-squared:  0.281,   Adjusted R-squared:  0.247
F-statistic: 8.32 on 3 and 64 DF,  p-value: 9.38e-05
```

Sex (N=60)

```
Residuals:
     Min       1Q   Median       3Q      Max
-0.05361 -0.01600 -0.00099  0.01507  0.04827

Coefficients:
            Estimate Std. Error t value Pr(>|t|)
(Intercept)  0.00496    0.00488    1.02     0.31
sexM        -0.00545    0.00622   -0.88     0.38
Residual standard error: 0.0234 on 58 degrees of freedom
  (8 observations deleted due to missingness)
Multiple R-squared:  0.0131,  Adjusted R-squared:  -0.00396
F-statistic: 0.767 on 1 and 58 DF,  p-value: 0.385
```

4.3. Results of the Procrustes ANOVAs

Size (N=68)

```
          Df      SS        MS     Rsq     F     Z Pr(>SS)
size       1 0.01511 0.0151101 0.05543 3.873 3.628    0.002 **
Residuals 66 0.25749 0.0039014 0.94457
Total     67 0.27260
```

Age (N=68)

```
          Df       SS        MS     Rsq      F        Z Pr(>SS)
age        3 0.011229 0.0037428 0.04119 0.9165 -0.25881    0.597
Residuals 64 0.261374 0.0040840 0.95881
Total     67 0.272603
```

Sex (N=60)

```
          Df      SS        MS     Rsq      F        Z Pr(>SS)
sex        1 0.00345 0.0034497 0.01474 0.8679 -0.16031    0.536
Residuals 58 0.23054 0.0039749 0.98526
Total     59 0.23399
```

Size + all muscle masses and PCSAs (N=63)

```
          Df       SS        MS      Rsq      F       Z Pr(>SS)
size       1 0.013309 0.0133087 0.05340 3.7041 3.3488   0.003 **
pcsa.t     1 0.009217 0.0092168 0.03698 2.5652 2.4844   0.014 *
pcsa.m     1 0.004332 0.0043324 0.01738 1.2058 0.5982   0.261
pcsa.p     1 0.006003 0.0060028 0.02408 1.6707 1.5450   0.068 .
mass.t     1 0.005761 0.0057609 0.02311 1.6034 1.5021   0.082 .
mass.m     1 0.004405 0.0044055 0.01767 1.2261 0.8873   0.184
mass.p     1 0.008609 0.0086094 0.03454 2.3962 2.5842   0.009 **
Residuals 55 0.197612 0.0035929 0.79283
Total     62 0.249248
---
```

```
Signif. codes:  0 ‘***’ 0.001 ‘**’ 0.01 ‘*’ 0.05 ‘.’ 0.1 ‘ ’ 1

Call: procD.lm(f1 = coords ~ size + pcsa.t + pcsa.m + pcsa.p + mass.t +
    mass.m + mass.p + f1.m + f1.t + f1.p, RRPP = T, data = gdf)
```

PCSA of the masseter (N=63)

```
          Df       SS        MS     Rsq      F      Z Pr(>SS)
pcsa.m     1 0.013579 0.0135793 0.05448 3.5148 3.2628   0.001 **
Residuals 61 0.235669 0.0038634 0.94552
Total     62 0.249248


Residuals:
          Df       SS        MS     Rsq      F      Z Pr(>SS)
pcsa.m     1 0.008869 0.0088688 0.03558 2.2506 2.1504   0.019 *
Residuals 61 0.240379 0.0039406 0.96442
Total     62 0.249248
```

PCSA of the temporalis (N=63)

```
          Df       SS        MS     Rsq      F      Z Pr(>SS)
pcsa.t     1 0.015193 0.015193 0.06096 3.9597 3.6388   0.001 **
Residuals 61 0.234055 0.003837 0.93904
Total     62 0.249248

Residuals:
          Df       SS        MS     Rsq      F    Z Pr(>SS)
pcsa.t     1 0.009217 0.0092168 0.03698 2.3423 2.31   0.015 *
Residuals 61 0.240032 0.0039349 0.96302
Total     62 0.249248
```

PCSA of the pterygoids (N=63)

```
          Df       SS        MS     Rsq      F     Z Pr(>SS)
pcsa.p     1 0.009331 0.0093307 0.03744 2.3724 2.345   0.015 *
Residuals 61 0.239918 0.0039331 0.96256
Total     62 0.249248

Residuals:
          Df       SS        MS     Rsq      F      Z Pr(>SS)
pcsa.p     1 0.007232 0.0072317 0.02901 1.8227 1.6451   0.066 .
Residuals 61 0.242017 0.0039675 0.97099
Total     62 0.249248
```

mass of the masseter (N=65)

```
          Df       SS        MS     Rsq      F      Z Pr(>SS)
mass.m     1 0.018786 0.0187859 0.07255 4.9284 4.1946   0.001 **
Residuals 63 0.240143 0.0038118 0.92745
Total     64 0.258929

Residuals:
          Df       SS        MS     Rsq      F      Z Pr(>SS)
mass.m     1 0.012799 0.0127990 0.04943 3.2761 3.1347   0.002 **
Residuals 63 0.246130 0.0039068 0.95057
Total     64 0.258929
```

mass of the temporalis (N=65)

```
          Df       SS        MS     Rsq      F      Z Pr(>SS)
mass.t     1 0.020889 0.0208888 0.08067 5.5285 4.4706   0.001 **
```



```
Residuals 63 0.238040 0.0037784 0.91933
Total     64 0.258929

Residuals:
          Df       SS        MS     Rsq      F      Z Pr(>SS)
mass.t     1 0.013864 0.0138636 0.05354 3.564 3.4119   0.001 **
Residuals 63 0.245065 0.0038899 0.94646
Total     64 0.258929
```

mass of the pterygoids (N=65)

```
          Df       SS        MS     Rsq      F      Z Pr(>SS)
mass.p     1 0.011473 0.0114732 0.04431 2.921 2.9836   0.006 **
Residuals 63 0.247455 0.0039279 0.95569
Total     64 0.258929

Residuals:
          Df       SS        MS     Rsq      F       Z Pr(>SS)
mass.p     1 0.004807 0.0048072 0.01857 1.1918 0.70823   0.247
Residuals 63 0.254121 0.0040337 0.98143
Total     64 0.258929
```

5. Variation in bite force

```
> by(dt$bf, dt$typ,summary)
dt$typ: iv M
   Min. 1st Qu.  Median    Mean 3rd Qu.    Max.
  216.0   285.8   339.0   337.0   380.5   484.0
------------------------------------------------------------
dt$typ: est M20
   Min. 1st Qu.  Median    Mean 3rd Qu.    Max.
  208.0   368.5   432.0   434.1   506.5   772.0
------------------------------------------------------------
dt$typ: est M30
   Min. 1st Qu.  Median    Mean 3rd Qu.    Max.
  195.0   338.5   400.5   402.5   474.8   747.0
------------------------------------------------------------
dt$typ: iv I
   Min. 1st Qu.  Median    Mean 3rd Qu.    Max.
  138.0   206.0   238.0   242.9   274.8   373.0
------------------------------------------------------------
dt$typ: est I20
   Min. 1st Qu.  Median    Mean 3rd Qu.    Max.
   89.0   172.2   204.0   205.5   241.2   380.0
------------------------------------------------------------
dt$typ: est I30
   Min. 1st Qu.  Median    Mean 3rd Qu.    Max.
   83.0   158.5   187.5   190.5   223.8   367.0
> by(dt$bf, dt$typ,sd)
dt$typ: iv M
[1] 86.10072
------------------------------------------------------------
dt$typ: est M20
[1] 111.4133
------------------------------------------------------------
dt$typ: est M30
[1] 106.6417
------------------------------------------------------------
dt$typ: iv I
[1] 66.60906
------------------------------------------------------------
dt$typ: est I20
[1] 55.38968
------------------------------------------------------------
dt$typ: est I30
[1] 52.94977


> shapiro.test(dt$bf[dt$typ=="est I20"])

        Shapiro-Wilk normality test

data:  dt$bf[dt$typ == "est I20"]
W = 0.97529, p-value = 0.2624

> shapiro.test(dt$bf[dt$typ=="est M20"])

        Shapiro-Wilk normality test

data:  dt$bf[dt$typ == "est M20"]
W = 0.98301, p-value = 0.5678

> shapiro.test(dt$bf[dt$typ=="est I30"])

        Shapiro-Wilk normality test

data:  dt$bf[dt$typ == "est I30"]
W = 0.96537, p-value = 0.08636

> shapiro.test(dt$bf[dt$typ=="est M30"])

        Shapiro-Wilk normality test

data:  dt$bf[dt$typ == "est M30"]
W = 0.97571, p-value = 0.2747

> shapiro.test(dt$bf[dt$typ=="iv I"])

        Shapiro-Wilk normality test

data:  dt$bf[dt$typ == "iv I"]
W = 0.98131, p-value = 0.9718

> shapiro.test(dt$bf[dt$typ=="iv M"])

        Shapiro-Wilk normality test

data:  dt$bf[dt$typ == "iv M"]
W = 0.97155, p-value = 0.9048

> t.test(dt$bf[dt$typ=="est I20"] , dt$bf[dt$typ=="iv I"], alternative = "less")
```



```
        Welch Two Sample t-test

data:  dt$bf[dt$typ == "est I20"] and dt$bf[dt$typ == "iv I"]
t = -1.6821, df = 11.171, p-value = 0.06013
alternative hypothesis: true difference in means is less than 0
95 percent confidence interval:
     -Inf 2.475576
sample estimates:
mean of x mean of y
 205.4833  242.9000

> t.test(dt$bf[dt$typ=="est I30"] , dt$bf[dt$typ=="iv I"], alternative = "less")

        Welch Two Sample t-test

data:  dt$bf[dt$typ == "est I30"] and dt$bf[dt$typ == "iv I"]
t = -2.367, df = 10.977, p-value = 0.0187
alternative hypothesis: true difference in means is less than 0
95 percent confidence interval:
      -Inf -12.63903
sample estimates:
mean of x mean of y
 190.4833  242.9000

> t.test(dt$bf[dt$typ=="est M20"] , dt$bf[dt$typ=="iv M"], alternative = "greater")

        Welch Two Sample t-test

data:  dt$bf[dt$typ == "est M20"] and dt$bf[dt$typ == "iv M"]
t = 3.1544, df = 14.551, p-value = 0.003377
alternative hypothesis: true difference in means is greater than 0
95 percent confidence interval:
 43.04193      Inf
sample estimates:
mean of x mean of y
 434.1333  337.0000

> t.test(dt$bf[dt$typ=="est M30"] , dt$bf[dt$typ=="iv M"], alternative = "greater")

        Welch Two Sample t-test

data:  dt$bf[dt$typ == "est M30"] and dt$bf[dt$typ == "iv M"]
t = 2.1463, df = 14.05, p-value = 0.0249
alternative hypothesis: true difference in means is greater than 0
95 percent confidence interval:
 11.75897      Inf
sample estimates:
mean of x mean of y
 402.4833  337.0000
```

6. Drivers of bite force variation (N= 60 mandibles and 54 skulls)

All muscle architecture data, after stepAIC

```
Residuals:
      Min        1Q    Median        3Q       Max
-0.078330 -0.035498 -0.007342  0.026779  0.136539
Coefficients:
            Estimate Std. Error t value Pr(>|t|)
(Intercept)  2.85257    0.28283  10.086 1.21e-13 ***
mass.SZ      0.38243    0.26601   1.438 0.156759
mass.TS      0.46461    0.06942   6.692 1.82e-08 ***
fl.MS       -0.19160    0.07611  -2.517 0.015078 *
fl.SZ       -0.39299    0.27910  -1.408 0.165291
fl.TS       -0.31145    0.10273  -3.032 0.003845 **
pcsa.ZP      0.06986    0.03257   2.145 0.036843 *
pcsa.SZ     -0.49421    0.27162  -1.819 0.074830 .
pcsa.TP      0.27741    0.07432   3.732 0.000486 ***
pcsa.P       0.24649    0.05925   4.160 0.000125 ***
---
Signif. codes:  0 '***' 0.001 '**' 0.01 '*' 0.05 '.' 0.1 ' ' 1

Residual standard error: 0.04779 on 50 degrees of freedom
Multiple R-squared:  0.8628,  Adjusted R-squared:  0.8381
F-statistic: 34.95 on 9 and 50 DF,  p-value: < 2.2e-16

Residuals (size=mandible centroid size)
Coefficients:
             Estimate Std. Error t value Pr(>|t|)
(Intercept) -9.260e-18  6.169e-03   0.000 1.000000
mass.SZ      3.891e-01  2.745e-01   1.417 0.162584
mass.TS      4.703e-01  9.087e-02   5.176 4.04e-06 ***
fl.MS       -1.926e-01  7.674e-02  -2.509 0.015386 *
fl.SZ       -3.992e-01  2.862e-01  -1.395 0.169270
fl.TS       -3.096e-01  1.045e-01  -2.964 0.004648 **
pcsa.ZP      6.910e-02  3.347e-02   2.064 0.044180 *
pcsa.SZ     -5.007e-01  2.795e-01  -1.791 0.079335 .
pcsa.TP      2.783e-01  7.490e-02   3.716 0.000511 ***
pcsa.P       2.467e-01  5.928e-02   4.161 0.000124 ***
---
Signif. codes:  0 '***' 0.001 '**' 0.01 '*' 0.05 '.' 0.1 ' ' 1

Residual standard error: 0.04778 on 50 degrees of freedom
Multiple R-squared:  0.7391,   Adjusted R-squared:  0.6921
F-statistic: 15.74 on 9 and 50 DF,  p-value: 8.524e-12


n
lm(formula = bf ~ pcsa.m + pcsa.t + pcsa.p + a.m, data = tab)

Residuals:
     Min       1Q   Median       3Q      Max
-0.06546 -0.03324 -0.01300  0.01190  0.17722

Coefficients:
            Estimate Std. Error t value Pr(>|t|)
(Intercept)  1.63765    0.09159  17.880  < 2e-16 ***
pcsa.m       0.40011    0.09504   4.210 9.54e-05 ***
pcsa.t       0.39655    0.07887   5.028 5.61e-06 ***
pcsa.p       0.13591    0.05623   2.417   0.0190 *
a.m          0.11873    0.05579   2.128   0.0378 *
---
Signif. codes:  0 '***' 0.001 '**' 0.01 '*' 0.05 '.' 0.1 ' ' 1
```



```
Residual standard error: 0.05044 on 55 degrees of freedom
Multiple R-squared:  0.8319,    Adjusted R-squared:  0.8197
F-statistic: 68.04 on 4 and 55 DF,  p-value: < 2.2e-16
```

BF and mandible shape (N=60)

```
          Df       SS        MS     Rsq      F      Z Pr(>SS)
bf         1 0.016396 0.0163962 0.06873 4.2805 3.7357   0.001 **
Residuals 58 0.222166 0.0038305 0.93127
Total     59 0.238563
---
Signif. codes:  0 '***' 0.001 '**' 0.01 '*' 0.05 '.' 0.1 ' ' 1
Call: procD.lm(f1 = mdb ~ bf, data = gdf)
```

Residual BF

```
             Df       SS        MS     Rsq      F     Z Pr(>SS)
bf.resid.mdb  1 0.014829 0.0148292 0.06216 3.8443 3.353   0.001 **
Residuals    58 0.223733 0.0038575 0.93784
Total        59 0.238563
```

Skull shape (N=54)

```
          Df       SS        MS     Rsq      F      Z Pr(>SS)
bf         1 0.001826 0.0018261 0.02389 1.2725 1.0928   0.127
Residuals 52 0.074623 0.0014351 0.97611
Total     53 0.076449
Call: procD.lm(f1 = skull ~ bf, data = gdf)
```

Residual BF

```
              Df       SS        MS     Rsq      F        Z Pr(>SS)
bf.resid.skull  1 0.001316 0.0013159 0.01721 0.9107 -0.26465     0.6
Residuals      52 0.075133 0.0014449 0.98279
Total          53 0.076449
```

```
on 55 individuals : test of size+sex+age (stepAIC)
aov
 summary(s)
            Df Sum Sq Mean Sq F value   Pr(>F)
age          3 0.3719 0.12396   22.16 2.89e-09 ***
size         1 0.1002 0.10017   17.91 9.90e-05 ***
Residuals   50 0.2797 0.00559
---
Signif. codes:  0 '***' 0.001 '**' 0.01 '*' 0.05 '.' 0.1 ' ' 1
```

Student test on sex (N=55)

```
      Welch Two Sample t-test

data:  tab$bf by tab$sex
t = -2.3326, df = 38.265, p-value = 0.02503
alternative hypothesis: true difference in means is not equal to 0
```

```
95 percent confidence interval:
 -0.14154415 -0.01002874
sample estimates:
mean in group F mean in group M
       2.570918        2.646704
```

Mandible size

```
Call:
lm(formula = bf ~ size.mdb, data = tab)

Residuals:
      Min        1Q    Median        3Q       Max
-0.180392 -0.063656  0.007346  0.056322  0.206336

Coefficients:
             Estimate Std. Error t value Pr(>|t|)
(Intercept)    3.4093     0.1093  31.187  < 2e-16 ***
size.mdb       2.6013     0.3595   7.235 1.18e-09 ***
---
Signif. codes:  0 '***' 0.001 '**' 0.01 '*' 0.05 '.' 0.1 ' ' 1

Residual standard error: 0.08686 on 58 degrees of freedom
Multiple R-squared:  0.4744,  Adjusted R-squared:  0.4653
F-statistic: 52.35 on 1 and 58 DF,  p-value: 1.18e-09
```

Skull size

```
lm(formula = bf ~ size.skull, data = tab)

Residuals:
      Min        1Q    Median        3Q       Max
-0.134122 -0.047067 -0.005126  0.040383  0.193491

Coefficients:
             Estimate Std. Error t value Pr(>|t|)
(Intercept)  -4.5927     1.2894  -3.562 0.000798 ***
size.skull    2.7090     0.4826   5.613 7.81e-07 ***
---
Signif. codes:  0 '***' 0.001 '**' 0.01 '*' 0.05 '.' 0.1 ' ' 1

Residual standard error: 0.07736 on 52 degrees of freedom
  (6 observations deleted due to missingness)
Multiple R-squared:  0.3773,  Adjusted R-squared:  0.3653
F-statistic: 31.51 on 1 and 52 DF,  p-value: 7.806e-07
```


7. Covariations between skull and mandible shape (2B-PLS analyses)

	singular value	% total covar.	Corr. coefficient	p-value
1	2.52e-04	38.63277	0.699	0.003
2	1.64e-04	16.42300	0.660	0.002
3	1.35e-04	11.15313	0.826	0.001
4	1.17e-04	8.32841	0.735	0.001
5	1.02e-04	6.36732	0.684	0.001
6	8.16e-05	4.06498	0.614	0.001
7	6.91e-05	2.91568	0.633	0.009
8	5.25e-05	1.68171	0.693	0.822
9	4.67e-05	1.33190	0.695	0.884
10	4.24e-05	1.09526	0.748	0.894
11	4.03e-05	0.98978	0.690	0.681
12	3.84e-05	0.89904	0.712	0.355
13	3.61e-05	0.79673	0.672	0.218
14	3.14e-05	0.59992	0.758	0.770
15	2.92e-05	0.52020	0.678	0.754
16	2.68e-05	0.43884	0.741	0.884
17	2.48e-05	0.37375	0.751	0.950
18	2.29e-05	0.32098	0.661	0.979
19	2.22e-05	0.30129	0.671	0.903
20	2.12e-05	0.27351	0.733	0.838
21	2.04e-05	0.25504	0.722	0.599
22	1.95e-05	0.23196	0.618	0.488
23	1.86e-05	0.21112	0.812	0.381
24	1.71e-05	0.17757	0.744	0.760
25	1.63e-05	0.16262	0.802	0.646
26	1.56e-05	0.14911	0.759	0.486
27	1.45e-05	0.12752	0.789	0.818
28	1.36e-05	0.11212	0.693	0.891
29	1.27e-05	0.09831	0.639	0.950
30	1.20e-05	0.08742	0.752	0.974
31	1.14e-05	0.07947	0.799	0.979
32	1.11e-05	0.07456	0.703	0.897
33	1.06e-05	0.06862	0.728	0.854
34	9.80e-06	0.05859	0.704	0.975
35	9.62e-06	0.05643	0.708	0.844
36	9.29e-06	0.05268	0.710	0.711
37	8.68e-06	0.04599	0.722	0.891
38	8.49e-06	0.04396	0.778	0.650
39	8.04e-06	0.03947	0.752	0.765
40	7.44e-06	0.03380	0.794	0.972
41	7.38e-06	0.03326	0.805	0.661
42	7.07e-06	0.03047	0.746	0.638
43	7.00e-06	0.02984	0.733	0.193
44	6.25e-06	0.02381	0.734	0.941
45	5.80e-06	0.02051	0.812	0.999
46	5.77e-06	0.02029	0.831	0.890
47	5.53e-06	0.01867	0.794	0.865
48	5.34e-06	0.01737	0.770	0.763
49	5.20e-06	0.01649	0.774	0.477
50	4.75e-06	0.01373	0.762	0.926
51	4.68e-06	0.01339	0.793	0.637
52	4.38e-06	0.01170	0.756	0.843
53	4.18e-06	0.01065	0.841	0.843
54	4.01e-06	0.00979	0.833	0.750

55	3.91e-06	0.00933	0.797	0.419
56	3.49e-06	0.00745	0.815	0.964
57	3.33e-06	0.00678	0.773	0.930
58	3.26e-06	0.00647	0.827	0.639
59	2.96e-06	0.00534	0.731	0.911
60	2.82e-06	0.00486	0.755	0.828
61	2.66e-06	0.00433	0.732	0.736
62	2.53e-06	0.00390	0.817	0.570
63	2.19e-06	0.00292	0.801	0.947
64	1.94e-06	0.00230	0.807	0.968
65	1.72e-06	0.00180	0.854	0.964

Correlation with the log10 centroid size

```
> summary(lm(corr.m.s.renards.raw$PLScoVar$res.pls$Xscores[,1] ~
log10(corr.m.s.renards.raw$res.prepPLS$gpa.mdb$size)[corr.m.s.renards.raw$res.prepPLS$contexte$`ID COLLINE` %in%
rownames(corr.m.s.renards.raw$PLScoVar$res.pls$Xscores)]))

Call:
lm(formula = corr.m.s.renards.raw$PLScoVar$res.pls$Xscores[,
    1] ~ log10(corr.m.s.renards.raw$res.prepPLS$gpa.mdb$size)[corr.m.s.renards.raw$res.prepPLS$contexte$`ID COLLINE` %in%
    rownames(corr.m.s.renards.raw$PLScoVar$res.pls$Xscores)])

Residuals:
      Min        1Q    Median        3Q       Max
-0.05582 -0.01171  0.00203  0.01172  0.04181

Coefficients:

Estimate
(Intercept)
-0.0734
log10(corr.m.s.renards.raw$res.prepPLS$gpa.mdb$size)[corr.m.s.renards.raw$res.prepPLS$contexte$`ID COLLINE` %in%
rownames(corr.m.s.renards.raw$PLScoVar$res.pls$Xscores)]   -0.2464

Std. Error
(Intercept)
0.0286
log10(corr.m.s.renards.raw$res.prepPLS$gpa.mdb$size)[corr.m.s.renards.raw$res.prepPLS$contexte$`ID COLLINE` %in%
rownames(corr.m.s.renards.raw$PLScoVar$res.pls$Xscores)]      0.0955

t value
(Intercept)
-2.57
log10(corr.m.s.renards.raw$res.prepPLS$gpa.mdb$size)[corr.m.s.renards.raw$res.prepPLS$contexte$`ID COLLINE` %in%
rownames(corr.m.s.renards.raw$PLScoVar$res.pls$Xscores)]   -2.58

Pr(>|t|)
(Intercept)
0.013
log10(corr.m.s.renards.raw$res.prepPLS$gpa.mdb$size)[corr.m.s.renards.raw$res.prepPLS$contexte$`ID COLLINE` %in%
rownames(corr.m.s.renards.raw$PLScoVar$res.pls$Xscores)]     0.013

(Intercept)
*
log10(corr.m.s.renards.raw$res.prepPLS$gpa.mdb$size)[corr.m.s.renards.raw$res.prepPLS$contexte$`ID COLLINE` %in%
rownames(corr.m.s.renards.raw$PLScoVar$res.pls$Xscores)] *
---
Signif. codes:  0 ‘***’ 0.001 ‘**’ 0.01 ‘*’ 0.05 ‘.’ 0.1 ‘ ’ 1

Residual standard error: 0.0204 on 56 degrees of freedom
Multiple R-squared:  0.106,         Adjusted R-squared:  0.0903
F-statistic: 6.66 on 1 and 56 DF,  p-value: 0.0125

> summary(lm(corr.m.s.renards.raw$PLScoVar$res.pls$Yscores[,1] ~
log10(corr.m.s.renards.raw$res.prepPLS$gpa.mdb$size)[corr.m.s.renards.raw$res.prepPLS$contexte$`ID COLLINE` %in%
rownames(corr.m.s.renards.raw$PLScoVar$res.pls$Xscores)]))

Call:
lm(formula = corr.m.s.renards.raw$PLScoVar$res.pls$Yscores[,
    1] ~ log10(corr.m.s.renards.raw$res.prepPLS$gpa.mdb$size)[corr.m.s.renards.raw$res.prepPLS$contexte$`ID COLLINE` %in%
    rownames(corr.m.s.renards.raw$PLScoVar$res.pls$Xscores)])

Residuals:
      Min        1Q    Median        3Q       Max
-0.03526 -0.00682  0.00025  0.00744  0.02031

Coefficients:

Estimate
(Intercept)
-0.0504
log10(corr.m.s.renards.raw$res.prepPLS$gpa.mdb$size)[corr.m.s.renards.raw$res.prepPLS$contexte$`ID COLLINE` %in%
rownames(corr.m.s.renards.raw$PLScoVar$res.pls$Xscores)]   -0.1692

Std. Error
(Intercept)
0.0164
log10(corr.m.s.renards.raw$res.prepPLS$gpa.mdb$size)[corr.m.s.renards.raw$res.prepPLS$contexte$`ID COLLINE` %in%
rownames(corr.m.s.renards.raw$PLScoVar$res.pls$Xscores)]     0.0549

t value
(Intercept)
-3.07
log10(corr.m.s.renards.raw$res.prepPLS$gpa.mdb$size)[corr.m.s.renards.raw$res.prepPLS$contexte$`ID COLLINE` %in%
rownames(corr.m.s.renards.raw$PLScoVar$res.pls$Xscores)]   -3.08

Pr(>|t|)
(Intercept)
0.0033
log10(corr.m.s.renards.raw$res.prepPLS$gpa.mdb$size)[corr.m.s.renards.raw$res.prepPLS$contexte$`ID COLLINE` %in%
rownames(corr.m.s.renards.raw$PLScoVar$res.pls$Xscores)]   0.0032

(Intercept)
**
```



```
log10(corr.m.s.renards.raw$res.prepPLS$gpa.mdb$size)[corr.m.s.renards.raw$res.prepPLS$contexte$`ID COLLINE` %in%
rownames(corr.m.s.renards.raw$PLScoVar$res.pls$Xscores)] **
---
Signif. codes:  0 ‘***’ 0.001 ‘**’ 0.01 ‘*’ 0.05 ‘.’ 0.1 ‘ ’ 1

Residual standard error: 0.0117 on 56 degrees of freedom
Multiple R-squared:  0.145,         Adjusted R-squared:  0.13
F-statistic: 9.49 on 1 and 56 DF,  p-value: 0.0032
```

Without the 4 silver foxes

	singular value	% total covar.	Corr. coefficient	p-value
1	1.76e-04	24.47848	0.703	0.392
2	1.67e-04	22.08484	0.653	0.001
3	1.40e-04	15.50113	0.776	0.001
4	9.90e-05	7.72521	0.630	0.024
5	9.06e-05	6.47299	0.736	0.006
6	7.04e-05	3.90808	0.643	0.316
7	6.28e-05	3.11527	0.681	0.343
8	5.20e-05	2.13110	0.724	0.885
9	4.95e-05	1.93133	0.789	0.564
10	4.89e-05	1.88217	0.705	0.082
11	4.05e-05	1.29353	0.775	0.765
12	4.02e-05	1.27209	0.794	0.178
13	3.43e-05	0.92637	0.708	0.843
14	3.11e-05	0.76388	0.760	0.936
15	2.89e-05	0.65695	0.786	0.965
16	2.80e-05	0.61673	0.790	0.815
17	2.64e-05	0.55140	0.758	0.747
18	2.62e-05	0.54234	0.769	0.181
19	2.57e-05	0.51990	0.772	0.020
20	2.17e-05	0.37287	0.744	0.869
21	2.03e-05	0.32595	0.844	0.912
22	1.97e-05	0.30564	0.754	0.720
23	1.92e-05	0.29156	0.781	0.350
24	1.76e-05	0.24303	0.749	0.769
25	1.68e-05	0.22231	0.697	0.666
26	1.63e-05	0.20840	0.739	0.390
27	1.55e-05	0.18969	0.747	0.287
28	1.42e-05	0.15976	0.807	0.701
29	1.37e-05	0.14734	0.791	0.525
30	1.25e-05	0.12306	0.773	0.910
31	1.21e-05	0.11554	0.794	0.680
32	1.14e-05	0.10304	0.775	0.727
33	1.14e-05	0.10260	0.798	0.153
34	9.75e-06	0.07492	0.804	0.998
35	9.39e-06	0.06958	0.810	0.975
36	9.22e-06	0.06701	0.857	0.813
37	8.84e-06	0.06161	0.780	0.736
38	8.43e-06	0.05605	0.822	0.704
39	8.10e-06	0.05178	0.798	0.589
40	7.70e-06	0.04675	0.813	0.562
41	7.14e-06	0.04019	0.837	0.843
42	6.89e-06	0.03746	0.877	0.662
43	6.59e-06	0.03425	0.868	0.586
44	6.39e-06	0.03220	0.807	0.319
45	5.84e-06	0.02688	0.796	0.698
46	5.62e-06	0.02491	0.851	0.453
47	5.42e-06	0.02318	0.851	0.214
48	4.41e-06	0.01534	0.860	1.000
49	4.37e-06	0.01505	0.790	0.949
50	3.86e-06	0.01175	0.802	0.997
51	3.65e-06	0.01052	0.792	0.971
52	3.47e-06	0.00952	0.832	0.721
53	2.88e-06	0.00653	0.795	0.889

Z score to compare dogs and foxes

8. Covariations between muscle architecture and shape

8.1. Mandible – all specimens

Mass – mandible shape

Covariance explained by the singular values

	singular value	% total covar.	Corr. coefficient	p-value
1	0.008178	93.0842	0.765	0.001
2	0.001537	3.2867	0.383	0.433
3	0.000966	1.2997	0.482	0.830
4	0.000776	0.8372	0.451	0.753
5	0.000726	0.7344	0.564	0.132
6	0.000502	0.3504	0.389	0.210
7	0.000398	0.2206	0.476	0.096
8	0.000284	0.1120	0.476	0.314
9	0.000232	0.0749	0.436	0.204

PCSA – mandible shape

Covariance explained by the singular values

	singular value	% total covar.	Corr. coefficient	p-value
1	0.005956	83.881	0.687	0.001
2	0.001396	4.607	0.476	0.935
3	0.001330	4.180	0.442	0.445
4	0.001095	2.834	0.486	0.307
5	0.000815	1.572	0.477	0.623
6	0.000672	1.069	0.455	0.524
7	0.000587	0.816	0.464	0.174
8	0.000496	0.582	0.438	0.087
9	0.000441	0.459	0.448	0.004

Residual mass – mandible shape

Covariance explained by the singular values

	singular value	% total covar.	Corr. coefficient	p-value
1	0.003598	73.296	0.559	0.005
2	0.001496	12.666	0.416	0.357
3	0.000988	5.524	0.384	0.717
4	0.000763	3.293	0.521	0.712
5	0.000657	2.444	0.510	0.311
6	0.000495	1.388	0.386	0.206
7	0.000345	0.673	0.512	0.426
8	0.000283	0.453	0.459	0.281
9	0.000216	0.263	0.458	0.345

Residual PCSA – mandible shape

Covariance explained by the singular values

	singular value	% total covar.	Corr. coefficient	p-value
1	0.003718	69.981	0.543	0.006
2	0.001395	9.856	0.415	0.861
3	0.001146	6.652	0.525	0.786
4	0.000956	4.627	0.658	0.690
5	0.000816	3.369	0.424	0.489
6	0.000619	1.942	0.499	0.738
7	0.000575	1.673	0.408	0.210
8	0.000472	1.129	0.565	0.124
9	0.000390	0.771	0.448	0.078

Residual mass – allometry-free mandible shape

Covariance explained by the singular values

	singular value	% total covar.	Corr. coefficient	p-value
1	0.003314	73.483	0.513	0.009
2	0.001349	12.180	0.438	0.468
3	0.000846	4.788	0.396	0.891
4	0.000731	3.570	0.608	0.637
5	0.000646	2.795	0.472	0.179
6	0.000489	1.600	0.381	0.088
7	0.000345	0.795	0.508	0.221
8	0.000272	0.496	0.464	0.231
9	0.000209	0.293	0.497	0.290

Residual PCSA – allometry-free mandible shape

Covariance explained by the singular values

	singular value	% total covar.	Corr. coefficient	p-value
1	0.003509	68.380	0.512	0.006
2	0.001360	10.275	0.425	0.772
3	0.001143	7.253	0.544	0.552
4	0.000942	4.929	0.641	0.485
5	0.000797	3.525	0.439	0.371
6	0.000587	1.915	0.443	0.740
7	0.000562	1.756	0.425	0.116
8	0.000468	1.219	0.559	0.049
9	0.000367	0.749	0.541	0.082

8.2. Mandible – without 'A'

mass – shape

```
> pls_foxes_mdb_mass$pls_canid$res.pls
  Covariance explained by the singular values
 singular value % total covar. Corr. coefficient p-value
       0.005722         85.824             0.737   0.001
       0.001598          6.691             0.397   0.349
       0.001033          2.799             0.452   0.702
       0.000884          2.047             0.484   0.335
       0.000676          1.197             0.535   0.325
       0.000505          0.669             0.388   0.221
       0.000398          0.416             0.602   0.123
       0.000297          0.231             0.413   0.264
       0.000219          0.125             0.425   0.443
Warning message:
In as.list(X) : reached elapsed time limit
```

PCSA – shape

Covariance explained by the singular values

singular value	% total covar.	Corr. coefficient	p-value
0.003650	62.421	0.643	0.032
0.001765	14.597	0.484	0.395
0.001371	8.810	0.442	0.310
0.001048	5.142	0.479	0.464
0.000796	2.967	0.522	0.675
0.000716	2.400	0.437	0.247
0.000598	1.674	0.552	0.159
0.000497	1.156	0.442	0.081
0.000422	0.833	0.504	0.022

Residual mass – shape

Covariance explained by the singular values

singular value	% total covar.	Corr. coefficient	p-value
0.003010	63.829	0.597	0.052
0.001612	18.318	0.396	0.216

0.001075	8.147	0.416	0.465
0.000701	3.465	0.484	0.904
0.000640	2.883	0.496	0.354
0.000469	1.551	0.418	0.367
0.000359	0.908	0.525	0.376
0.000281	0.556	0.382	0.384
0.000220	0.342	0.452	0.383

Residual PCSA – shape

Covariance explained by the singular values

singular value	% total covar.	Corr. coefficient	p-value
0.003088	60.56	0.541	0.056
0.001522	14.71	0.441	0.653
0.001142	8.29	0.549	0.768
0.000912	5.28	0.635	0.814
0.000807	4.14	0.408	0.524
0.000611	2.37	0.442	0.757
0.000600	2.29	0.566	0.094
0.000465	1.37	0.511	0.178
0.000398	1.00	0.452	0.072

Residual mass – allometry-free shape

Covariance explained by the singular values

singular value	% total covar.	Corr. coefficient	p-value
0.002960	68.164	0.558	0.018
0.001362	14.426	0.427	0.455
0.000955	7.102	0.433	0.644
0.000681	3.607	0.495	0.851
0.000636	3.150	0.468	0.234
0.000468	1.701	0.416	0.197
0.000356	0.984	0.509	0.238
0.000252	0.495	0.480	0.598
0.000219	0.372	0.410	0.238

Residual PCSA – allometry-free shape

Covariance explained by the singular values

singular value	% total covar.	Corr. coefficient	p-value
0.003087	61.045	0.536	0.024
0.001522	14.842	0.441	0.461
0.001142	8.362	0.547	0.545
0.000908	5.278	0.611	0.629
0.000769	3.792	0.427	0.468
0.000606	2.350	0.460	0.613
0.000578	2.137	0.477	0.090
0.000453	1.312	0.532	0.130
0.000371	0.882	0.554	0.100

8.3. Mandible ramus – all individuals

Mass – shape

Covariance explained by the singular values

	singular value	% total covar.	Corr. coefficient	p-value
1	0.009945	91.0671	0.558	0.002
2	0.001876	3.2409	0.486	0.879
3	0.001623	2.4250	0.469	0.449
4	0.001183	1.2894	0.347	0.578
5	0.001019	0.9556	0.472	0.206
6	0.000709	0.4627	0.327	0.279

7	0.000614	0.3468	0.444	0.035
8	0.000381	0.1337	0.422	0.503
9	0.000293	0.0788	0.528	0.488

PCSA – shape

	singular value	% total covar.	Corr. coefficient	p-value
1	0.008160	82.877	0.530	0.002
2	0.002006	5.008	0.540	0.952
3	0.001713	3.652	0.390	0.815
4	0.001574	3.082	0.478	0.353
5	0.001270	2.008	0.491	0.318
6	0.001115	1.549	0.383	0.089
7	0.000823	0.843	0.449	0.242
8	0.000674	0.566	0.418	0.159
9	0.000578	0.416	0.399	0.025

Residual mass – shape

Covariance explained by the singular values

	singular value	% total covar.	Corr. coefficient	p-value
1	0.005507	79.006	0.599	0.001
2	0.001803	8.471	0.477	0.789
3	0.001273	4.220	0.384	0.870
4	0.001126	3.305	0.427	0.465
5	0.000993	2.572	0.502	0.104
6	0.000696	1.262	0.325	0.163
7	0.000516	0.695	0.459	0.176
8	0.000310	0.250	0.490	0.868
9	0.000291	0.220	0.513	0.308

Residual PCSA – shape

Covariance explained by the singular values

	singular value	% total covar.	Corr. coefficient	p-value
1	0.005894	73.38	0.551	0.003
2	0.001972	8.21	0.382	0.932
3	0.001580	5.27	0.473	0.922
4	0.001528	4.93	0.617	0.366
5	0.001255	3.33	0.420	0.283
6	0.000938	1.86	0.331	0.544
7	0.000785	1.30	0.503	0.357
8	0.000703	1.04	0.407	0.053
9	0.000563	0.67	0.439	0.032

Residual mass – allometry-free shape

Covariance explained by the singular values

	singular value	% total covar.	Corr. coefficient	p-value
1	0.005507	79.006	0.599	0.001
2	0.001803	8.471	0.477	0.789
3	0.001273	4.220	0.384	0.870
4	0.001126	3.305	0.427	0.465
5	0.000993	2.572	0.502	0.104
6	0.000696	1.262	0.325	0.163
7	0.000516	0.695	0.459	0.176
8	0.000310	0.250	0.490	0.868
9	0.000291	0.220	0.513	0.308

Residual PCSA – allometry-free shape

Covariance explained by the singular values

	singular value	% total covar.	Corr. coefficient	p-value
1	0.005643	72.992	0.577	0.001
2	0.001877	8.075	0.427	0.946
3	0.001579	5.713	0.474	0.843
4	0.001447	4.798	0.665	0.396
5	0.001253	3.600	0.406	0.166
6	0.000906	1.882	0.347	0.501
7	0.000747	1.279	0.469	0.365
8	0.000639	0.935	0.447	0.147
9	0.000563	0.727	0.437	0.022

8.4. Mandible ramus – without 'A'

mass – shape

Covariance explained by the singular values

singular value	% total covar.	Corr. coefficient	p-value
0.005789	75.146	0.562	0.126
0.002065	9.558	0.404	0.654
0.001729	6.706	0.452	0.242
0.001356	4.124	0.391	0.197
0.000923	1.909	0.515	0.511
0.000712	1.137	0.345	0.285
0.000589	0.779	0.456	0.102
0.000449	0.452	0.432	0.113
0.000290	0.189	0.495	0.585

PCSA – shape

Covariance explained by the singular values

singular value	% total covar.	Corr. coefficient	p-value
0.004857	61.039	0.449	0.115
0.002228	12.846	0.490	0.821
0.001807	8.446	0.444	0.696
0.001572	6.393	0.481	0.356
0.001259	4.103	0.544	0.336
0.001099	3.127	0.354	0.107
0.000822	1.747	0.421	0.272
0.000767	1.524	0.464	0.020
0.000547	0.773	0.444	0.125

Residual mass – shape

Covariance explained by the singular values

singular value	% total covar.	Corr. coefficient	p-value
0.004602	68.833	0.577	0.031
0.001983	12.786	0.368	0.686
0.001562	7.934	0.428	0.524
0.001191	4.613	0.430	0.532
0.000943	2.891	0.490	0.378
0.000660	1.414	0.355	0.470
0.000509	0.841	0.430	0.402
0.000357	0.413	0.412	0.727
0.000290	0.274	0.422	0.520

Residual PCSA – shape

Covariance explained by the singular values

singular value	% total covar.	Corr. coefficient	p-value
0.004867	64.283	0.529	0.036
0.002188	12.992	0.405	0.748
0.001586	6.823	0.482	0.892
0.001501	6.118	0.666	0.385
0.001107	3.324	0.387	0.717
0.000993	2.677	0.361	0.337
0.000786	1.677	0.444	0.342
0.000693	1.302	0.479	0.068
0.000544	0.803	0.448	0.081

Residual mass – allometry-free shape

Covariance explained by the singular values

singular value	% total covar.	Corr. coefficient	p-value
0.004548	69.870	0.575	0.034
0.001938	12.692	0.384	0.653
0.001443	7.033	0.375	0.605
0.001155	4.507	0.430	0.480
0.000923	2.875	0.515	0.304
0.000659	1.469	0.355	0.349
0.000509	0.874	0.432	0.280
0.000355	0.425	0.437	0.621
0.000274	0.254	0.448	0.577

Residual PCSA – allometry-free shape

Covariance explained by the singular values

singular value	% total covar.	Corr. coefficient	p-value
0.004781	64.41	0.518	0.030
0.002112	12.57	0.422	0.731
0.001585	7.08	0.483	0.829
0.001491	6.27	0.672	0.295
0.001106	3.45	0.384	0.602
0.000958	2.59	0.375	0.290
0.000773	1.68	0.475	0.265
0.000631	1.12	0.449	0.199
0.000543	0.83	0.465	0.050

8.5. Skull

Mass – shape

Covariance explained by the singular values

	singular value	% total covar.	Corr. coefficient	p-value
1	0.003623	85.220	0.844	0.001
2	0.000961	6.002	0.637	0.470
3	0.000694	3.132	0.619	0.808
4	0.000588	2.248	0.693	0.609
5	0.000481	1.503	0.631	0.548
6	0.000357	0.828	0.686	0.104
7	0.000292	0.555	0.610	0.020
8	0.000208	0.282	0.571	0.483
9	0.000188	0.230	0.713	0.125

PCSA – shape

Covariance explained by the singular values

singular value	% total covar.	Corr. coefficient	p-value
0.001630	46.04	0.695	0.244
0.000924	14.81	0.651	0.883
0.000888	13.68	0.673	0.289

	0.000751	9.77	0.666	0.248
	0.000544	5.12	0.694	0.835
	0.000500	4.33	0.713	0.391
	0.000413	2.95	0.547	0.334
	0.000321	1.79	0.624	0.594
	0.000296	1.52	0.621	0.133

Residual mass – shape

	Covariance explained by the singular values singular value	% total covar.	Corr. coefficient	p-value
1	0.001628	54.304	0.663	0.074
2	0.000942	18.179	0.633	0.216
3	0.000687	9.687	0.621	0.679
4	0.000617	7.791	0.627	0.281
5	0.000473	4.593	0.591	0.321
6	0.000346	2.456	0.698	0.141
7	0.000290	1.722	0.634	0.028
8	0.000194	0.769	0.662	0.700
9	0.000156	0.499	0.714	0.588

Residual PCSA – shape

	Covariance explained by the singular values singular value	% total covar.	Corr. coefficient	p-value
1	0.002303	61.233	0.757	0.006
2	0.001049	12.708	0.633	0.542
3	0.000887	9.095	0.730	0.427
4	0.000762	6.713	0.634	0.351
5	0.000547	3.461	0.700	0.851
6	0.000491	2.780	0.711	0.492
7	0.000403	1.880	0.545	0.482
8	0.000313	1.134	0.616	0.721
9	0.000294	0.997	0.607	0.151

Residual mass – allometry-free shape

	Covariance explained by the singular values singular value	% total covar.	Corr. coefficient	p-value
1	0.001617	54.665	0.650	0.047
2	0.000941	18.502	0.634	0.103
3	0.000684	9.800	0.620	0.499
4	0.000588	7.236	0.704	0.323
5	0.000451	4.262	0.634	0.355
6	0.000346	2.504	0.697	0.061
7	0.000290	1.757	0.634	0.006
8	0.000192	0.770	0.703	0.573
9	0.000155	0.504	0.716	0.462

Residual PCSA – allometry-free shape

	Covariance explained by the singular values singular value	% total covar.	Corr. coefficient	p-value
1	0.001674	51.49	0.687	0.032
2	0.000888	14.51	0.729	0.798
3	0.000785	11.33	0.689	0.605
4	0.000678	8.46	0.670	0.559
5	0.000503	4.65	0.729	0.920
6	0.000467	4.00	0.584	0.528
7	0.000382	2.68	0.640	0.479
8	0.000294	1.59	0.577	0.724
9	0.000265	1.29	0.529	0.250

8.6. Z-scores

```
> compare.pls(  Z_scores_foxes_tous$PLS_foxes_mass,
+               Z_scores_foxes_tous$PLS_foxes_PCSA,
+               Z_scores_foxes_tous$PLS_foxes_arr_mass,
-               Z_scores_foxes_tous$PLS_foxes_arr_PCSA,
+
-             Z_scores1$PLS_dogs_mass,
+             Z_scores1$PLS_dogs_PCSA,
+             Z_scores1$PLS_dogs_arr_mass,
+             Z_scores1$PLS_dogs_arr_PCSA,
+
-             Z_scores_foxes_skull$PLS_foxes_skull_mass,
+             Z_scores_foxes_skull$PLS_foxes_skull_PCSA,
-
-             Z_scores_dog_skull$PLS_dogs_skull_mass,
+             Z_scores_dog_skull$PLS_dogs_skull_PCSA
-
-             )
```

Effect sizes

```
          Z_scores_foxes_tous$PLS_foxes_mass        Z_scores_foxes_tous$PLS_foxes_PCSA
                                        3.50                                      4.19
      Z_scores_foxes_tous$PLS_foxes_arr_mass    Z_scores_foxes_tous$PLS_foxes_arr_PCSA
                                        2.55                                      2.41
                     Z_scores1$PLS_dogs_mass                   Z_scores1$PLS_dogs_PCSA
                                        4.22                                      4.11
                 Z_scores1$PLS_dogs_arr_mass               Z_scores1$PLS_dogs_arr_PCSA
                                        2.74                                      2.15
  Z_scores_foxes_skull$PLS_foxes_skull_mass Z_scores_foxes_skull$PLS_foxes_skull_PCSA
                                        4.30                                      2.46
       Z_scores_dog_skull$PLS_dogs_skull_mass      Z_scores_dog_skull$PLS_dogs_skull_PCSA
                                        6.84                                      6.39
```

Effect sizes for pairwise differences in PLS effect size

```
                                                Z_scores_foxes_tous$PLS_foxes_mass
Z_scores_foxes_tous$PLS_foxes_mass                                           0.000
Z_scores_foxes_tous$PLS_foxes_PCSA                                           1.128
Z_scores_foxes_tous$PLS_foxes_arr_mass                                       2.073
Z_scores_foxes_tous$PLS_foxes_arr_PCSA                                       2.243
Z_scores1$PLS_dogs_mass                                                      0.109
Z_scores1$PLS_dogs_PCSA                                                      0.155
Z_scores1$PLS_dogs_arr_mass                                                  1.728
Z_scores1$PLS_dogs_arr_PCSA                                                  2.139
Z_scores_foxes_skull$PLS_foxes_skull_mass                                    1.313
Z_scores_foxes_skull$PLS_foxes_skull_PCSA                                    2.577
Z_scores_dog_skull$PLS_dogs_skull_mass                                       2.583
Z_scores_dog_skull$PLS_dogs_skull_PCSA                                       2.085
                                                Z_scores_foxes_tous$PLS_foxes_PCSA
Z_scores_foxes_tous$PLS_foxes_mass                                           1.128
Z_scores_foxes_tous$PLS_foxes_PCSA                                           0.000
Z_scores_foxes_tous$PLS_foxes_arr_mass                                       1.006
Z_scores_foxes_tous$PLS_foxes_arr_PCSA                                       1.168
Z_scores1$PLS_dogs_mass                                                      0.871
Z_scores1$PLS_dogs_PCSA                                                      0.817
Z_scores1$PLS_dogs_arr_mass                                                  0.692
Z_scores1$PLS_dogs_arr_PCSA                                                  1.119
Z_scores_foxes_skull$PLS_foxes_skull_mass                                    0.149
Z_scores_foxes_skull$PLS_foxes_skull_PCSA                                    1.443
Z_scores_dog_skull$PLS_dogs_skull_mass                                       3.523
Z_scores_dog_skull$PLS_dogs_skull_PCSA                                       3.035
                                                Z_scores_foxes_tous$PLS_foxes_arr_mass
Z_scores_foxes_tous$PLS_foxes_mass                                           2.073
Z_scores_foxes_tous$PLS_foxes_PCSA                                           1.006
Z_scores_foxes_tous$PLS_foxes_arr_mass                                       0.000
Z_scores_foxes_tous$PLS_foxes_arr_PCSA                                       0.144
Z_scores1$PLS_dogs_mass                                                      1.711
Z_scores1$PLS_dogs_PCSA                                                      1.652
```

```
Z_scores1$PLS_dogs_arr_mass                                0.268
Z_scores1$PLS_dogs_arr_PCSA                              0.151
Z_scores_foxes_skull$PLS_foxes_skull_mass                 0.898
Z_scores_foxes_skull$PLS_foxes_skull_PCSA               0.342
Z_scores_dog_skull$PLS_dogs_skull_mass                     4.238
Z_scores_dog_skull$PLS_dogs_skull_PCSA                   3.773

Z_scores_foxes_tous$PLS_foxes_mass                         2.2428
Z_scores_foxes_tous$PLS_foxes_PCSA                       1.1678
Z_scores_foxes_tous$PLS_foxes_arr_mass                     0.1436
Z_scores_foxes_tous$PLS_foxes_arr_PCSA                   0.0000
Z_scores1$PLS_dogs_mass                                    1.8539
Z_scores1$PLS_dogs_PCSA                                  1.7930
Z_scores1$PLS_dogs_arr_mass                                0.4096
Z_scores1$PLS_dogs_arr_PCSA                              0.0149
Z_scores_foxes_skull$PLS_foxes_skull_mass                  1.0638
Z_scores_foxes_skull$PLS_foxes_skull_PCSA                0.1918
Z_scores_dog_skull$PLS_dogs_skull_mass                     4.3882
Z_scores_dog_skull$PLS_dogs_skull_PCSA                   3.9225

Z_scores_foxes_tous$PLS_foxes_mass                         0.1086
Z_scores_foxes_tous$PLS_foxes_PCSA                       0.8710
Z_scores_foxes_tous$PLS_foxes_arr_mass                     1.7109
Z_scores_foxes_tous$PLS_foxes_arr_PCSA                   1.8539
Z_scores1$PLS_dogs_mass                                    0.0000
Z_scores1$PLS_dogs_PCSA                                  0.0422
Z_scores1$PLS_dogs_arr_mass                                1.4235
Z_scores1$PLS_dogs_arr_PCSA                              1.7906
Z_scores_foxes_skull$PLS_foxes_skull_mass                  1.0192
Z_scores_foxes_skull$PLS_foxes_skull_PCSA                2.1074
Z_scores_dog_skull$PLS_dogs_skull_mass                     2.4509
Z_scores_dog_skull$PLS_dogs_skull_PCSA                   1.9913

Z_scores_foxes_tous$PLS_foxes_mass                         1.728
Z_scores_foxes_tous$PLS_foxes_PCSA                       0.692
Z_scores_foxes_tous$PLS_foxes_arr_mass                     0.268
Z_scores_foxes_tous$PLS_foxes_arr_PCSA                   0.410
Z_scores1$PLS_dogs_mass                                    1.424
Z_scores1$PLS_dogs_PCSA                                  1.388
Z_scores1$PLS_dogs_arr_mass                                0.000
Z_scores1$PLS_dogs_arr_PCSA                              0.404
Z_scores_foxes_skull$PLS_foxes_skull_mass                  0.576
Z_scores_foxes_skull$PLS_foxes_skull_PCSA                0.615
Z_scores_dog_skull$PLS_dogs_skull_mass                     3.916
Z_scores_dog_skull$PLS_dogs_skull_PCSA                   3.455

Z_scores_foxes_tous$PLS_foxes_mass                         2.1391
Z_scores_foxes_tous$PLS_foxes_PCSA                       1.1186
Z_scores_foxes_tous$PLS_foxes_arr_mass                     0.1509
Z_scores_foxes_tous$PLS_foxes_arr_PCSA                   0.0149
Z_scores1$PLS_dogs_mass                                    1.7906
Z_scores1$PLS_dogs_PCSA                                  1.7332
Z_scores1$PLS_dogs_arr_mass                                0.4041
Z_scores1$PLS_dogs_arr_PCSA                              0.0000
Z_scores_foxes_skull$PLS_foxes_skull_mass                  1.0170
Z_scores_foxes_skull$PLS_foxes_skull_PCSA                0.1846
Z_scores_dog_skull$PLS_dogs_skull_mass                     4.2458
Z_scores_dog_skull$PLS_dogs_skull_PCSA                   3.7919

Z_scores_foxes_tous$PLS_foxes_mass                         1.313
Z_scores_foxes_tous$PLS_foxes_PCSA                       0.149
Z_scores_foxes_tous$PLS_foxes_arr_mass                     0.898
Z_scores_foxes_tous$PLS_foxes_arr_PCSA                   1.064
Z_scores1$PLS_dogs_mass                                    1.019
Z_scores1$PLS_dogs_PCSA                                  0.962
Z_scores1$PLS_dogs_arr_mass                                0.576
Z_scores1$PLS_dogs_arr_PCSA                              1.017
Z_scores_foxes_skull$PLS_foxes_skull_mass                  0.000
Z_scores_foxes_skull$PLS_foxes_skull_PCSA                1.346
Z_scores_dog_skull$PLS_dogs_skull_mass                     3.715
Z_scores_dog_skull$PLS_dogs_skull_PCSA                   3.221
```



```
Z_scores_foxes_tous$PLS_foxes_mass                         2.577
Z_scores_foxes_tous$PLS_foxes_PCSA                       1.443
Z_scores_foxes_tous$PLS_foxes_arr_mass                     0.342
Z_scores_foxes_tous$PLS_foxes_arr_PCSA                   0.192
Z_scores1$PLS_dogs_mass                                    2.107
Z_scores1$PLS_dogs_PCSA                                  2.041
Z_scores1$PLS_dogs_arr_mass                                0.615
Z_scores1$PLS_dogs_arr_PCSA                              0.765
Z_scores_foxes_skull$PLS_foxes_skull_mass                  1.346
Z_scores_foxes_skull$PLS_foxes_skull_PCSA                0.000
Z_scores_dog_skull$PLS_dogs_skull_mass                     4.714
Z_scores_dog_skull$PLS_dogs_skull_PCSA                   4.239

Z_scores_foxes_tous$PLS_foxes_mass                         2.583
Z_scores_foxes_tous$PLS_foxes_PCSA                       3.523
Z_scores_foxes_tous$PLS_foxes_arr_mass                     4.238
Z_scores_foxes_tous$PLS_foxes_arr_PCSA                   4.388
Z_scores1$PLS_dogs_mass                                    2.451
Z_scores1$PLS_dogs_PCSA                                  2.477
Z_scores1$PLS_dogs_arr_mass                                3.916
Z_scores1$PLS_dogs_arr_PCSA                              4.246
Z_scores_foxes_skull$PLS_foxes_skull_mass                  3.715
Z_scores_foxes_skull$PLS_foxes_skull_PCSA                4.714
Z_scores_dog_skull$PLS_dogs_skull_mass                     0.000
Z_scores_dog_skull$PLS_dogs_skull_PCSA                   0.466

Z_scores_foxes_tous$PLS_foxes_mass                         2.085
Z_scores_foxes_tous$PLS_foxes_PCSA                       3.035
Z_scores_foxes_tous$PLS_foxes_arr_mass                     3.773
Z_scores_foxes_tous$PLS_foxes_arr_PCSA                   3.922
Z_scores1$PLS_dogs_mass                                    1.991
Z_scores1$PLS_dogs_PCSA                                  2.020
Z_scores1$PLS_dogs_arr_mass                                3.455
Z_scores1$PLS_dogs_arr_PCSA                              3.792
Z_scores_foxes_skull$PLS_foxes_skull_mass                  3.221
Z_scores_foxes_skull$PLS_foxes_skull_PCSA                4.239
Z_scores_dog_skull$PLS_dogs_skull_mass                     0.466
Z_scores_dog_skull$PLS_dogs_skull_PCSA                   0.000
```

P-values

```
Z_scores_foxes_tous$PLS_foxes_mass                         1.00000
Z_scores_foxes_tous$PLS_foxes_PCSA                       0.12963
Z_scores_foxes_tous$PLS_foxes_arr_mass                     0.01811
Z_scores_foxes_tous$PLS_foxes_arr_PCSA                   0.01245
Z_scores1$PLS_dogs_mass                                    0.45675
Z_scores1$PLS_dogs_PCSA                                  0.43855
Z_scores1$PLS_dogs_arr_mass                                0.04204
Z_scores1$PLS_dogs_arr_PCSA                              0.01621
Z_scores_foxes_skull$PLS_foxes_skull_mass                  0.09459
Z_scores_foxes_skull$PLS_foxes_skull_PCSA                0.00498
Z_scores_dog_skull$PLS_dogs_skull_mass                     0.00490
Z_scores_dog_skull$PLS_dogs_skull_PCSA                   0.01854

Z_scores_foxes_tous$PLS_foxes_mass                         0.129631
Z_scores_foxes_tous$PLS_foxes_PCSA                       1.000000
Z_scores_foxes_tous$PLS_foxes_arr_mass                     0.157114
Z_scores_foxes_tous$PLS_foxes_arr_PCSA                   0.121444
Z_scores1$PLS_dogs_mass                                    0.191869
Z_scores1$PLS_dogs_PCSA                                  0.207096
Z_scores1$PLS_dogs_arr_mass                                0.244488
Z_scores1$PLS_dogs_arr_PCSA                              0.131662
Z_scores_foxes_skull$PLS_foxes_skull_mass                  0.440775
Z_scores_foxes_skull$PLS_foxes_skull_PCSA                0.074527
Z_scores_dog_skull$PLS_dogs_skull_mass                     0.000214
Z_scores_dog_skull$PLS_dogs_skull_PCSA                   0.001204

Z_scores_foxes_tous$PLS_foxes_mass                         1.91e-02
Z_scores_foxes_tous$PLS_foxes_PCSA                       1.57e-01
```

```
Z_scores_foxes_tous$PLS_foxes_arr_mass                    1.00e+00
Z_scores_foxes_tous$PLS_foxes_arr_PCSA                    4.43e-01
Z_scores1$PLS_dogs_mass                                   4.35e-02
Z_scores1$PLS_dogs_PCSA                                   4.93e-02
Z_scores1$PLS_dogs_arr_mass                               3.94e-01
Z_scores1$PLS_dogs_arr_PCSA                               4.40e-01
Z_scores_foxes_skull$PLS_foxes_skull_mass                 1.85e-01
Z_scores_foxes_skull$PLS_foxes_skull_PCSA                 3.66e-01
Z_scores_dog_skull$PLS_dogs_skull_mass                    1.13e-05
Z_scores_dog_skull$PLS_dogs_skull_PCSA                    8.07e-05

Z_scores_foxes_tous$PLS_foxes_mass                        1.25e-02
Z_scores_foxes_tous$PLS_foxes_PCSA                        1.21e-01
Z_scores_foxes_tous$PLS_foxes_arr_mass                    4.43e-01
Z_scores_foxes_tous$PLS_foxes_arr_PCSA                    1.00e+00
Z_scores1$PLS_dogs_mass                                   3.19e-02
Z_scores1$PLS_dogs_PCSA                                   3.65e-02
Z_scores1$PLS_dogs_arr_mass                               3.41e-01
Z_scores1$PLS_dogs_arr_PCSA                               4.94e-01
Z_scores_foxes_skull$PLS_foxes_skull_mass                 1.44e-01
Z_scores_foxes_skull$PLS_foxes_skull_PCSA                 4.24e-01
Z_scores_dog_skull$PLS_dogs_skull_mass                    5.71e-06
Z_scores_dog_skull$PLS_dogs_skull_PCSA                    4.38e-05

Z_scores_foxes_tous$PLS_foxes_mass                        0.45675
Z_scores_foxes_tous$PLS_foxes_PCSA                        0.19187
Z_scores_foxes_tous$PLS_foxes_arr_mass                    0.04355
Z_scores_foxes_tous$PLS_foxes_arr_PCSA                    0.03188
Z_scores1$PLS_dogs_mass                                   1.00000
Z_scores1$PLS_dogs_PCSA                                   0.48316
Z_scores1$PLS_dogs_arr_mass                               0.07729
Z_scores1$PLS_dogs_arr_PCSA                               0.03668
Z_scores_foxes_skull$PLS_foxes_skull_mass                 0.15406
Z_scores_foxes_skull$PLS_foxes_skull_PCSA                 0.01754
Z_scores_dog_skull$PLS_dogs_skull_mass                    0.00713
Z_scores_dog_skull$PLS_dogs_skull_PCSA                    0.02322

Z_scores_foxes_tous$PLS_foxes_mass                        4.20e-02
Z_scores_foxes_tous$PLS_foxes_PCSA                        2.44e-01
Z_scores_foxes_tous$PLS_foxes_arr_mass                    3.94e-01
Z_scores_foxes_tous$PLS_foxes_arr_PCSA                    3.41e-01
Z_scores1$PLS_dogs_mass                                   7.73e-02
Z_scores1$PLS_dogs_PCSA                                   8.56e-02
Z_scores1$PLS_dogs_arr_mass                               1.00e+00
Z_scores1$PLS_dogs_arr_PCSA                               3.43e-01
Z_scores_foxes_skull$PLS_foxes_skull_mass                 2.82e-01
Z_scores_foxes_skull$PLS_foxes_skull_PCSA                 2.69e-01
Z_scores_dog_skull$PLS_dogs_skull_mass                    4.51e-05
Z_scores_dog_skull$PLS_dogs_skull_PCSA                    2.76e-04

Z_scores_foxes_tous$PLS_foxes_mass                        1.62e-02
Z_scores_foxes_tous$PLS_foxes_PCSA                        1.32e-01
Z_scores_foxes_tous$PLS_foxes_arr_mass                    4.40e-01
Z_scores_foxes_tous$PLS_foxes_arr_PCSA                    4.94e-01
Z_scores1$PLS_dogs_mass                                   3.67e-02
Z_scores1$PLS_dogs_PCSA                                   4.15e-02
Z_scores1$PLS_dogs_arr_mass                               3.43e-01
Z_scores1$PLS_dogs_arr_PCSA                               1.00e+00
Z_scores_foxes_skull$PLS_foxes_skull_mass                 1.55e-01
Z_scores_foxes_skull$PLS_foxes_skull_PCSA                 4.35e-01
Z_scores_dog_skull$PLS_dogs_skull_mass                    1.09e-05
Z_scores_dog_skull$PLS_dogs_skull_PCSA                    7.47e-05

Z_scores_foxes_tous$PLS_foxes_mass                        0.094586
Z_scores_foxes_tous$PLS_foxes_PCSA                        0.440775
Z_scores_foxes_tous$PLS_foxes_arr_mass                    0.184664
Z_scores_foxes_tous$PLS_foxes_arr_PCSA                    0.143706
Z_scores1$PLS_dogs_mass                                   0.154061
Z_scores1$PLS_dogs_PCSA                                   0.168059
Z_scores1$PLS_dogs_arr_mass                               0.282188
Z_scores1$PLS_dogs_arr_PCSA                               0.154586
```



```
Z_scores_foxes_skull$PLS_foxes_skull_mass                 1.000000
Z_scores_foxes_skull$PLS_foxes_skull_PCSA                 0.089223
Z_scores_dog_skull$PLS_dogs_skull_mass                    0.000102
Z_scores_dog_skull$PLS_dogs_skull_PCSA                    0.000639

Z_scores_foxes_tous$PLS_foxes_mass                        4.98e-03
Z_scores_foxes_tous$PLS_foxes_PCSA                        7.45e-02
Z_scores_foxes_tous$PLS_foxes_arr_mass                    3.66e-01
Z_scores_foxes_tous$PLS_foxes_arr_PCSA                    4.24e-01
Z_scores1$PLS_dogs_mass                                   1.75e-02
Z_scores1$PLS_dogs_PCSA                                   2.06e-02
Z_scores1$PLS_dogs_arr_mass                               2.69e-01
Z_scores1$PLS_dogs_arr_PCSA                               4.35e-01
Z_scores_foxes_skull$PLS_foxes_skull_mass                 8.92e-02
Z_scores_foxes_skull$PLS_foxes_skull_PCSA                 1.00e+00
Z_scores_dog_skull$PLS_dogs_skull_mass                    1.21e-06
Z_scores_dog_skull$PLS_dogs_skull_PCSA                    1.12e-05

Z_scores_foxes_tous$PLS_foxes_mass                        4.90e-03
Z_scores_foxes_tous$PLS_foxes_PCSA                        2.14e-04
Z_scores_foxes_tous$PLS_foxes_arr_mass                    1.13e-05
Z_scores_foxes_tous$PLS_foxes_arr_PCSA                    5.71e-06
Z_scores1$PLS_dogs_mass                                   7.13e-03
Z_scores1$PLS_dogs_PCSA                                   6.62e-03
Z_scores1$PLS_dogs_arr_mass                               4.51e-05
Z_scores1$PLS_dogs_arr_PCSA                               1.09e-05
Z_scores_foxes_skull$PLS_foxes_skull_mass                 1.02e-04
Z_scores_foxes_skull$PLS_foxes_skull_PCSA                 1.21e-06
Z_scores_dog_skull$PLS_dogs_skull_mass                    1.00e+00
Z_scores_dog_skull$PLS_dogs_skull_PCSA                    3.20e-01

Z_scores_foxes_tous$PLS_foxes_mass                        1.85e-02
Z_scores_foxes_tous$PLS_foxes_PCSA                        1.20e-03
Z_scores_foxes_tous$PLS_foxes_arr_mass                    8.07e-05
Z_scores_foxes_tous$PLS_foxes_arr_PCSA                    4.38e-05
Z_scores1$PLS_dogs_mass                                   2.32e-02
Z_scores1$PLS_dogs_PCSA                                   2.17e-02
Z_scores1$PLS_dogs_arr_mass                               2.76e-04
Z_scores1$PLS_dogs_arr_PCSA                               7.47e-05
Z_scores_foxes_skull$PLS_foxes_skull_mass                 6.39e-04
Z_scores_foxes_skull$PLS_foxes_skull_PCSA                 1.12e-05
Z_scores_dog_skull$PLS_dogs_skull_mass                    3.20e-01
Z_scores_dog_skull$PLS_dogs_skull_PCSA                    1.00e+00
```

9. Covariations between bite force and shape

9.1. 2B-PLS between bite force and mandibular shape – all specimens

Bite Force – mandible shape

```
  Covariance explained by the singular values
 singular value % total covar. Corr. coefficient p-value
       0.003549        99.8663             0.629   0.001
       0.000125         0.1240             0.579   0.129
       0.000035         0.0097             0.538   0.817
```

Linear model: PLS1 of mandible shape by size + age

```
                  Df  Sum Sq Mean Sq F value  Pr(>F)
log(gpa$size)      1 0.00714 0.00714    16.9 0.00013 ***
contexte$`AGE MDB` 3 0.01143 0.00381     9.0   6e-05 ***
Residuals         55 0.02328 0.00042
---
Signif. codes:  0 '***' 0.001 '**' 0.01 '*' 0.05 '.' 0.1 ' ' 1
```

Residual Bite Force – mandible shape

```
  Covariance explained by the singular values
 singular value % total covar. Corr. coefficient p-value
       0.002486        99.7484             0.549   0.001
       0.000119         0.2295             0.555   0.161
       0.000037         0.0221             0.510   0.692
```

Residual Bite Force – allometry-free mandible shape

```
  Covariance explained by the singular values
 singular value % total covar. Corr. coefficient p-value
       2.46e-03         99.751             0.545   0.001
       1.18e-04          0.229             0.576   0.091
       3.49e-05          0.020             0.535   0.684
```

9.2. 2B-PLS between bite force and mandibular shape – without 'A'

Bite Force – mandible shape without 'A'

```
  Covariance explained by the singular values
 singular value % total covar. Corr. coefficient p-value
       2.06e-03         99.612             0.528   0.053
       1.23e-04          0.355             0.589   0.116
       3.74e-05          0.033             0.535   0.711
```

Residual Bite Force – mandible shape without 'A'

```
  Covariance explained by the singular values
 singular value % total covar. Corr. coefficient p-value
       1.98e-03        99.5847             0.498   0.009
       1.22e-04         0.3771             0.567   0.106
       3.88e-05         0.0382             0.545   0.612
```


Residual Bite Force – allometry-free mandible shape without 'A'

```
  Covariance explained by the singular values
 singular value % total covar. Corr. coefficient p-value
       1.88e-03        99.5492             0.511   0.003
       1.21e-04         0.4115             0.583   0.074
       3.74e-05         0.0393             0.546   0.575
```

9.3. 2B-PLS between bite force and mandibular ramus shape – all specimens

Bite Force – mandibular ramus shape

```
  Covariance explained by the singular values
 singular value % total covar. Corr. coefficient p-value
       0.005505        99.8546             0.571   0.001
       0.000202         0.1347             0.506   0.065
       0.000057         0.0107             0.550   0.534
```

Residual Bite Force – mandibular ramus shape

```
  Covariance explained by the singular values
 singular value % total covar. Corr. coefficient p-value
       4.15e-03        99.7660             0.578   0.001
       1.92e-04         0.2149             0.456   0.100
       5.74e-05         0.0191             0.570   0.543
```

Residual Bite Force – allometry-free mandibular ramus shape

```
  Covariance explained by the singular values
 singular value % total covar. Corr. coefficient p-value
       3.84e-03        99.7502             0.609   0.001
       1.84e-04         0.2303             0.480   0.060
       5.37e-05         0.0195             0.580   0.557
```

9.4. 2B-PLS between bite force and mandibular ramus shape – without 'A'

Bite Force – mandibular ramus shape without 'A'

```
  Covariance explained by the singular values
 singular value % total covar. Corr. coefficient p-value
       3.25e-03        99.5937             0.446   0.029
       1.99e-04         0.3732             0.493   0.055
       5.93e-05         0.0331             0.626   0.530
```

Residual Bite Force – mandibular ramus shape without 'A'

```
  Covariance explained by the singular values
 singular value % total covar. Corr. coefficient p-value
       3.22e-03        99.5937             0.531   0.004
       1.97e-04         0.3725             0.462   0.066
       5.94e-05         0.0338             0.639   0.500
```

Residual Bite Force – allometry-free mandibular ramus shape without 'A'

```
  Covariance explained by the singular values
 singular value % total covar. Corr. coefficient p-value
       0.003156        99.6084             0.512   0.005
```

0.000189	0.3579	0.486	0.064
0.000058	0.0337	0.631	0.469

9.5. 2B-PLS between bite force and skull shape – all specimens

Bite Force – skull shape

Covariance explained by the singular values

singular value	% total covar.	Corr. coefficient	p-value
1.01e-03	99.018	0.655	0.128
9.41e-05	0.854	0.706	0.001
3.65e-05	0.128	0.663	0.021

Residual Bite Force – skull shape

Covariance explained by the singular values

singular value	% total covar.	Corr. coefficient	p-value
7.09e-04	98.18	0.553	0.438
8.89e-05	1.55	0.679	0.013
3.72e-05	0.27	0.667	0.018

Residual Bite Force – allometry-free skull shape

Covariance explained by the singular values

singular value	% total covar.	Corr. coefficient	p-value
6.90e-04	99.112	0.659	0.413
6.09e-05	0.773	0.639	0.524
2.35e-05	0.115	0.648	0.879

9.6. 2B-PLS between bite force and skull shape – without 'A'

Bite Force – skull shape without 'A'

Covariance explained by the singular values

singular value	% total covar.	Corr. coefficient	p-value
7.71e-04	98.377	0.711	0.747
9.23e-05	1.410	0.668	0.004
3.58e-05	0.213	0.683	0.022

Residual Bite Force – skull shape without 'A'

Covariance explained by the singular values

singular value	% total covar.	Corr. coefficient	p-value
7.20e-04	98.206	0.553	0.377
9.04e-05	1.549	0.672	0.008
3.59e-05	0.245	0.685	0.020

Residual Bite Force – allometry-free skull shape without 'A'

Covariance explained by the singular values

singular value	% total covar.	Corr. coefficient	p-value
6.72e-04	99.178	0.657	0.505
5.46e-05	0.654	0.713	0.874
2.76e-05	0.167	0.635	0.407

9.7. Z-scores

Effect sizes

plot.pls.dogs$res2bPLSgeomorph	4.038
plot.pls.dogs.rbf$res2bPLSgeomorph	2.839
plot.pls.dogs.rbf.rsh$res2bPLSgeomorph	3.396
plot.pls.foxes$res2bPLSgeomorph	0.377
plot.pls.foxes.rbf$res2bPLSgeomorph	0.649
plot.pls.foxes.rbf.rsh$res2bPLSgeomorph	0.493

Effect sizes for pairwise differences in PLS effect size

	plot.pls.dogs$res2bPLSgeomorph
plot.pls.dogs$res2bPLSgeomorph	0.000
plot.pls.dogs.rbf$res2bPLSgeomorph	0.812
plot.pls.dogs.rbf.rsh$res2bPLSgeomorph	0.895
plot.pls.foxes$res2bPLSgeomorph	2.942
plot.pls.foxes.rbf$res2bPLSgeomorph	2.723
plot.pls.foxes.rbf.rsh$res2bPLSgeomorph	2.742

	plot.pls.dogs.rbf$res2bPLSgeomorph
plot.pls.dogs$res2bPLSgeomorph	0.81156
plot.pls.dogs.rbf$res2bPLSgeomorph	0.00000
plot.pls.dogs.rbf.rsh$res2bPLSgeomorph	0.00988
plot.pls.foxes$res2bPLSgeomorph	2.01075
plot.pls.foxes.rbf$res2bPLSgeomorph	1.80644
plot.pls.foxes.rbf.rsh$res2bPLSgeomorph	1.84590

	plot.pls.dogs.rbf.rsh$res2bPLSgeomorph
plot.pls.dogs$res2bPLSgeomorph	0.89453
plot.pls.dogs.rbf$res2bPLSgeomorph	0.00988
plot.pls.dogs.rbf.rsh$res2bPLSgeomorph	0.00000
plot.pls.foxes$res2bPLSgeomorph	2.22485
plot.pls.foxes.rbf$res2bPLSgeomorph	1.99189
plot.pls.foxes.rbf.rsh$res2bPLSgeomorph	2.02579

	plot.pls.foxes$res2bPLSgeomorph
plot.pls.dogs$res2bPLSgeomorph	2.942
plot.pls.dogs.rbf$res2bPLSgeomorph	2.011
plot.pls.dogs.rbf.rsh$res2bPLSgeomorph	2.225
plot.pls.foxes$res2bPLSgeomorph	0.000
plot.pls.foxes.rbf$res2bPLSgeomorph	0.204
plot.pls.foxes.rbf.rsh$res2bPLSgeomorph	0.108

	plot.pls.foxes.rbf$res2bPLSgeomorph
plot.pls.dogs$res2bPLSgeomorph	2.7229
plot.pls.dogs.rbf$res2bPLSgeomorph	1.8064
plot.pls.dogs.rbf.rsh$res2bPLSgeomorph	1.9919
plot.pls.foxes$res2bPLSgeomorph	0.2040
plot.pls.foxes.rbf$res2bPLSgeomorph	0.0000
plot.pls.foxes.rbf.rsh$res2bPLSgeomorph	0.0884

	plot.pls.foxes.rbf.rsh$res2bPLSgeomorph
plot.pls.dogs$res2bPLSgeomorph	2.7416

```
plot.pls.dogs.rbf$res2bPLSgeomorph                    1.8459
plot.pls.dogs.rbf.rsh$res2bPLSgeomorph                2.0258
plot.pls.foxes$res2bPLSgeomorph                       0.1084
plot.pls.foxes.rbf$res2bPLSgeomorph                   0.0884
plot.pls.foxes.rbf.rsh$res2bPLSgeomorph               0.0000

P-values

                                      plot.pls.dogs$res2bPLSgeomorph
plot.pls.dogs$res2bPLSgeomorph                               1.00000
plot.pls.dogs.rbf$res2bPLSgeomorph                           0.20852
plot.pls.dogs.rbf.rsh$res2bPLSgeomorph                       0.18552
plot.pls.foxes$res2bPLSgeomorph                              0.00163
plot.pls.foxes.rbf$res2bPLSgeomorph                          0.00324
plot.pls.foxes.rbf.rsh$res2bPLSgeomorph                      0.00306
                                      plot.pls.dogs.rbf$res2bPLSgeomorph
plot.pls.dogs$res2bPLSgeomorph                                   0.2085
plot.pls.dogs.rbf$res2bPLSgeomorph                               1.0000
plot.pls.dogs.rbf.rsh$res2bPLSgeomorph                           0.4961
plot.pls.foxes$res2bPLSgeomorph                                  0.0222
plot.pls.foxes.rbf$res2bPLSgeomorph                              0.0354
plot.pls.foxes.rbf.rsh$res2bPLSgeomorph                          0.0325
                                      plot.pls.dogs.rbf.rsh$res2bPLSgeomorph
plot.pls.dogs$res2bPLSgeomorph                                       0.1855
plot.pls.dogs.rbf$res2bPLSgeomorph                                   0.4961
plot.pls.dogs.rbf.rsh$res2bPLSgeomorph                               1.0000
plot.pls.foxes$res2bPLSgeomorph                                      0.0130
plot.pls.foxes.rbf$res2bPLSgeomorph                                  0.0232
plot.pls.foxes.rbf.rsh$res2bPLSgeomorph                              0.0214
                                      plot.pls.foxes$res2bPLSgeomorph
plot.pls.dogs$res2bPLSgeomorph                               0.00163
plot.pls.dogs.rbf$res2bPLSgeomorph                           0.02218
plot.pls.dogs.rbf.rsh$res2bPLSgeomorph                       0.01305
plot.pls.foxes$res2bPLSgeomorph                              1.00000
plot.pls.foxes.rbf$res2bPLSgeomorph                          0.41919
plot.pls.foxes.rbf.rsh$res2bPLSgeomorph                      0.45682
                                      plot.pls.foxes.rbf$res2bPLSgeomorph
plot.pls.dogs$res2bPLSgeomorph                                   0.00324
plot.pls.dogs.rbf$res2bPLSgeomorph                               0.03542
plot.pls.dogs.rbf.rsh$res2bPLSgeomorph                           0.02319
plot.pls.foxes$res2bPLSgeomorph                                  0.41919
plot.pls.foxes.rbf$res2bPLSgeomorph                              1.00000
plot.pls.foxes.rbf.rsh$res2bPLSgeomorph                          0.46478
                                      plot.pls.foxes.rbf.rsh$res2bPLSgeomorph
plot.pls.dogs$res2bPLSgeomorph                                       0.00306
plot.pls.dogs.rbf$res2bPLSgeomorph                                   0.03245
plot.pls.dogs.rbf.rsh$res2bPLSgeomorph                               0.02139
plot.pls.foxes$res2bPLSgeomorph                                      0.45682
plot.pls.foxes.rbf$res2bPLSgeomorph                                  0.46478
plot.pls.foxes.rbf.rsh$res2bPLSgeomorph                              1.00000
```

7. Part2 – Article 5 & 6 – supplementary material

7.1. Table S1 articles 5 and 6.

					Environmental data																		Muscle ar			
					GPA coordinates					Climatic data			Diet (Forbes-Harper et al., 2017)										PCSA			
ID	cat	sex	age	body mass	location	x	y	urban	demographics	bio5	bio6	bio12	sheep	rodent	rabbit	marsupials	bird	reptile/frog	invertebrates	mammal	plant	other	digastric	masseter	temporal	pterygoid
FO-23	AUSTRALIAN RED FOX	NA	NA	NA	Australia	NA	NA	NA	NA	NA	NA	NA	NA	NA	NA	NA	NA	NA	NA	NA	NA	NA	1,81	10,81	10,96	2,67
FO-24	AUSTRALIAN RED FOX	NA	NA	NA	Australia	NA	NA	NA	NA	NA	NA	NA	NA	NA	NA	NA	NA	NA	NA	NA	NA	NA	1,72	8,81	8,58	2,95
FO-25	AUSTRALIAN RED FOX	NA	NA	NA	Australia	NA	NA	NA	NA	NA	NA	NA	NA	NA	NA	NA	NA	NA	NA	NA	NA	NA	1,29	8,56	9,47	2,50
FO-27	AUSTRALIAN RED FOX	NA	NA	NA	Australia	NA	NA	NA	NA	NA	NA	NA	NA	NA	NA	NA	NA	NA	NA	NA	NA	NA	1,79	8,95	9,74	2,69
FO-50	AUSTRALIAN RED FOX	NA	NA	NA	Australia	NA	NA	NA	NA	NA	NA	NA	NA	NA	NA	NA	NA	NA	NA	NA	NA	NA	1,86	6,94	11,18	4,00
FO-51	AUSTRALIAN RED FOX	NA	NA	NA	Australia	NA	NA	NA	NA	NA	NA	NA	NA	NA	NA	NA	NA	NA	NA	NA	NA	NA	2,17	10,51	14,38	2,81
FO-52	AUSTRALIAN RED FOX	NA	NA	NA	Australia	NA	NA	NA	NA	NA	NA	NA	NA	NA	NA	NA	NA	NA	NA	NA	NA	NA	1,23	9,67	10,78	3,46
FO-53	AUSTRALIAN RED FOX	NA	NA	NA	Australia	NA	NA	NA	NA	NA	NA	NA	NA	NA	NA	NA	NA	NA	NA	NA	NA	NA	0,95	8,21	11,04	3,78
FO-54	AUSTRALIAN RED FOX	NA	NA	NA	Australia	NA	NA	NA	NA	NA	NA	NA	NA	NA	NA	NA	NA	NA	NA	NA	NA	NA	1,58	8,35	9,95	2,03
FO-55	AUSTRALIAN RED FOX	NA	NA	NA	Australia	NA	NA	NA	NA	NA	NA	NA	NA	NA	NA	NA	NA	NA	NA	NA	NA	NA	1,54	6,46	7,87	3,49
FO-56	AUSTRALIAN RED FOX	NA	NA	NA	Australia	NA	NA	NA	NA	NA	NA	NA	NA	NA	NA	NA	NA	NA	NA	NA	NA	NA	1,82	9,25	13,53	4,22
FO-57	AUSTRALIAN RED FOX	NA	NA	NA	Australia	NA	NA	NA	NA	NA	NA	NA	NA	NA	NA	NA	NA	NA	NA	NA	NA	NA	1,43	8,46	13,81	2,56
FO-59	AUSTRALIAN RED FOX	NA	NA	NA	Australia	NA	NA	NA	NA	NA	NA	NA	NA	NA	NA	NA	NA	NA	NA	NA	NA	NA	2,44	9,22	11,02	2,00
FO-60	AUSTRALIAN RED FOX	NA	NA	NA	Australia	NA	NA	NA	NA	NA	NA	NA	NA	NA	NA	NA	NA	NA	NA	NA	NA	NA	1,29	10,65	12,09	3,22
M7	RED FOX	NA	NA	NA	France	NA	NA	NA	NA	NA	NA	NA	NA	NA	NA	NA	NA	NA	NA	NA	NA	NA	NA	NA	NA	NA
Ni-R1	RED FOX	NA	NA	NA	France	NA	NA	NA	NA	NA	NA	NA	NA	NA	NA	NA	NA	NA	NA	NA	NA	NA	NA	NA	NA	NA
N-R1	RED FOX	M	NA	NA	France	NA	NA	NA	NA	NA	NA	NA	NA	NA	NA	NA	NA	NA	NA	NA	NA	NA	1,14	7,19	8,57	2,90
N-R10	RED FOX	F	NA	NA	France	NA	NA	NA	NA	NA	NA	NA	NA	NA	NA	NA	NA	NA	NA	NA	NA	NA	1,18	9,39	12,79	1,99
N-R11	RED FOX	M	NA	NA	France	NA	NA	NA	NA	NA	NA	NA	NA	NA	NA	NA	NA	NA	NA	NA	NA	NA	0,65	3,98	5,75	1,58
N-R12	RED FOX	F	NA	NA	France	NA	NA	NA	NA	NA	NA	NA	NA	NA	NA	NA	NA	NA	NA	NA	NA	NA	1,44	6,76	12,54	2,19
N-R13	RED FOX	M	NA	NA	France	NA	NA	NA	NA	NA	NA	NA	NA	NA	NA	NA	NA	NA	NA	NA	NA	NA	1,39	8,32	15,04	2,90
N-R14	RED FOX	M	NA	NA	France	NA	NA	NA	NA	NA	NA	NA	NA	NA	NA	NA	NA	NA	NA	NA	NA	NA	0,87	8,34	11,75	2,96
N-R15	RED FOX	M	NA	NA	France	NA	NA	NA	NA	NA	NA	NA	NA	NA	NA	NA	NA	NA	NA	NA	NA	NA	NA	NA	NA	NA
N-R16	RED FOX	M	NA	NA	France	NA	NA	NA	NA	NA	NA	NA	NA	NA	NA	NA	NA	NA	NA	NA	NA	NA	1,45	9,08	11,23	2,67
N-R17	RED FOX	M	NA	NA	France	NA	NA	NA	NA	NA	NA	NA	NA	NA	NA	NA	NA	NA	NA	NA	NA	NA	1,11	7,39	13,61	1,83
N-R18	RED FOX	M	NA	NA	France	NA	NA	NA	NA	NA	NA	NA	NA	NA	NA	NA	NA	NA	NA	NA	NA	NA	1,33	5,45	11,80	1,87
N-R19	RED FOX	M	NA	NA	France	NA	NA	NA	NA	NA	NA	NA	NA	NA	NA	NA	NA	NA	NA	NA	NA	NA	1,01	9,83	11,57	2,69
N-R2	RED FOX	F	NA	NA	France	NA	NA	NA	NA	NA	NA	NA	NA	NA	NA	NA	NA	NA	NA	NA	NA	NA	1,20	6,27	9,30	2,19
N-R20	RED FOX	M	NA	NA	France	NA	NA	NA	NA	NA	NA	NA	NA	NA	NA	NA	NA	NA	NA	NA	NA	NA	1,22	6,71	12,19	1,91
N-R21	RED FOX	F	NA	NA	France	NA	NA	NA	NA	NA	NA	NA	NA	NA	NA	NA	NA	NA	NA	NA	NA	NA	1,06	5,24	8,65	1,77
N-R22	RED FOX	F	NA	NA	France	NA	NA	NA	NA	NA	NA	NA	NA	NA	NA	NA	NA	NA	NA	NA	NA	NA	0,92	6,13	8,63	1,69
N-R23	RED FOX	M	NA	NA	France	NA	NA	NA	NA	NA	NA	NA	NA	NA	NA	NA	NA	NA	NA	NA	NA	NA	1,69	8,86	14,49	2,41
N-R24	RED FOX	F	NA	NA	France	NA	NA	NA	NA	NA	NA	NA	NA	NA	NA	NA	NA	NA	NA	NA	NA	NA	1,11	7,30	10,38	2,28
N-R25	RED FOX	F	NA	NA	France	NA	NA	NA	NA	NA	NA	NA	NA	NA	NA	NA	NA	NA	NA	NA	NA	NA	0,50	4,47	6,20	1,61
N-R26	RED FOX	F	NA	NA	France	NA	NA	NA	NA	NA	NA	NA	NA	NA	NA	NA	NA	NA	NA	NA	NA	NA	1,04	8,52	10,32	2,85
N-R27	RED FOX	F	NA	NA	France	NA	NA	NA	NA	NA	NA	NA	NA	NA	NA	NA	NA	NA	NA	NA	NA	NA	1,00	7,68	9,80	1,77
N-R28	RED FOX	M	NA	NA	France	NA	NA	NA	NA	NA	NA	NA	NA	NA	NA	NA	NA	NA	NA	NA	NA	NA	0,79	NA	NA	1,22
N-R29	RED FOX	F	NA	NA	France	NA	NA	NA	NA	NA	NA	NA	NA	NA	NA	NA	NA	NA	NA	NA	NA	NA	0,69	3,59	4,43	1,17
N-R3	RED FOX	F	NA	NA	France	NA	NA	NA	NA	NA	NA	NA	NA	NA	NA	NA	NA	NA	NA	NA	NA	NA	1,38	5,56	9,77	1,93
N-R30	RED FOX	M	NA	NA	France	NA	NA	NA	NA	NA	NA	NA	NA	NA	NA	NA	NA	NA	NA	NA	NA	NA	1,70	9,34	11,75	2,28
N-R31	RED FOX	M	NA	NA	France	NA	NA	NA	NA	NA	NA	NA	NA	NA	NA	NA	NA	NA	NA	NA	NA	NA	2,34	8,61	12,73	4,54
N-R32	RED FOX	M	NA	NA	France	NA	NA	NA	NA	NA	NA	NA	NA	NA	NA	NA	NA	NA	NA	NA	NA	NA	1,46	9,15	12,46	3,39
N-R33	RED FOX	F	NA	NA	France	NA	NA	NA	NA	NA	NA	NA	NA	NA	NA	NA	NA	NA	NA	NA	NA	NA	0,88	6,68	6,08	2,07
N-R34	RED FOX	M	NA	NA	France	NA	NA	NA	NA	NA	NA	NA	NA	NA	NA	NA	NA	NA	NA	NA	NA	NA	1,82	9,57	14,32	2,98
N-R35	RED FOX	F	NA	NA	France	NA	NA	NA	NA	NA	NA	NA	NA	NA	NA	NA	NA	NA	NA	NA	NA	NA	1,51	7,16	8,40	3,08
N-R36	RED FOX	M	NA	NA	France	NA	NA	NA	NA	NA	NA	NA	NA	NA	NA	NA	NA	NA	NA	NA	NA	NA	2,04	11,13	12,88	2,44
N-R37	RED FOX	M	NA	NA	France	NA	NA	NA	NA	NA	NA	NA	NA	NA	NA	NA	NA	NA	NA	NA	NA	NA	1,38	9,66	12,98	2,99
N-R38	RED FOX	M	NA	NA	France	NA	NA	NA	NA	NA	NA	NA	NA	NA	NA	NA	NA	NA	NA	NA	NA	NA	1,80	9,80	14,02	2,97
N-R39	RED FOX	M	NA	NA	France	NA	NA	NA	NA	NA	NA	NA	NA	NA	NA	NA	NA	NA	NA	NA	NA	NA	1,39	4,66	7,58	2,18
N-R4	RED FOX	F	NA	NA	France	NA	NA	NA	NA	NA	NA	NA	NA	NA	NA	NA	NA	NA	NA	NA	NA	NA	0,83	4,39	7,50	1,20
N-R40	RED FOX	M	NA	NA	France	NA	NA	NA	NA	NA	NA	NA	NA	NA	NA	NA	NA	NA	NA	NA	NA	NA	2,13	9,75	10,92	4,84
N-R41	RED FOX	M	NA	NA	France	NA	NA	NA	NA	NA	NA	NA	NA	NA	NA	NA	NA	NA	NA	NA	NA	NA	1,82	9,66	14,65	4,12
N-R42	RED FOX	F	NA	NA	France	NA	NA	NA	NA	NA	NA	NA	NA	NA	NA	NA	NA	NA	NA	NA	NA	NA	0,81	4,02	5,14	2,54
N-R43	RED FOX	M	NA	NA	France	NA	NA	NA	NA	NA	NA	NA	NA	NA	NA	NA	NA	NA	NA	NA	NA	NA	1,98	8,97	9,96	3,34
N-R44	RED FOX	M	NA	NA	France	NA	NA	NA	NA	NA	NA	NA	NA	NA	NA	NA	NA	NA	NA	NA	NA	NA	2,56	9,21	14,37	4,80
N-R45	RED FOX	M	NA	NA	France	NA	NA	NA	NA	NA	NA	NA	NA	NA	NA	NA	NA	NA	NA	NA	NA	NA	1,60	8,75	8,50	4,21
N-R46	RED FOX	M	NA	NA	France	NA	NA	NA	NA	NA	NA	NA	NA	NA	NA	NA	NA	NA	NA	NA	NA	NA	1,96	8,60	11,04	3,03
N-R47	RED FOX	M	NA	NA	France	NA	NA	NA	NA	NA	NA	NA	NA	NA	NA	NA	NA	NA	NA	NA	NA	NA	1,86	10,58	12,74	2,61
N-R48	RED FOX	M	NA	NA	France	NA	NA	NA	NA	NA	NA	NA	NA	NA	NA	NA	NA	NA	NA	NA	NA	NA	2,11	11,78	9,51	3,58
N-R49	RED FOX	M	NA	NA	France	NA	NA	NA	NA	NA	NA	NA	NA	NA	NA	NA	NA	NA	NA	NA	NA	NA	1,48	7,55	11,75	1,80
N-R5	RED FOX	M	NA	NA	France	NA	NA	NA	NA	NA	NA	NA	NA	NA	NA	NA	NA	NA	NA	NA	NA	NA	0,75	5,52	7,52	2,69
N-R50	RED FOX	M	NA	NA	France	NA	NA	NA	NA	NA	NA	NA	NA	NA	NA	NA	NA	NA	NA	NA	NA	NA	0,93	5,69	5,03	1,65
N-R6	RED FOX	M	NA	NA	France	NA	NA	NA	NA	NA	NA	NA	NA	NA	NA	NA	NA	NA	NA	NA	NA	NA	1,20	8,25	9,62	2,17
N-R60	RED FOX	F	NA	NA	France	NA	NA	NA	NA	NA	NA	NA	NA	NA	NA	NA	NA	NA	NA	NA	NA	NA	1,27	9,99	8,51	3,01
N-R61	RED FOX	F	NA	NA	France	NA	NA	NA	NA	NA	NA	NA	NA	NA	NA	NA	NA	NA	NA	NA	NA	NA	1,30	6,22	8,28	4,50
N-R62	RED FOX	F	NA	NA	France	NA	NA	NA	NA	NA	NA	NA	NA	NA	NA	NA	NA	NA	NA	NA	NA	NA	1,80	7,70	12,05	2,49
N-R63	RED FOX	F	NA	NA	France	NA	NA	NA	NA	NA	NA	NA	NA	NA	NA	NA	NA	NA	NA	NA	NA	NA	3,05	11,13	13,58	3,38
N-R64	RED FOX	F	NA	NA	France	NA	NA	NA	NA	NA	NA	NA	NA	NA	NA	NA	NA	NA	NA	NA	NA	NA	1,53	8,67	12,10	2,67
N-R7	RED FOX	F	NA	NA	France	NA	NA	NA	NA	NA	NA	NA	NA	NA	NA	NA	NA	NA	NA	NA	NA	NA	1,39	7,94	9,64	3,18
N-R70	RED FOX	F	NA	NA	France	NA	NA	NA	NA	NA	NA	NA	NA	NA	NA	NA	NA	NA	NA	NA	NA	NA	1,49	6,80	10,65	3,18
N-R8	RED FOX	M	NA	NA	France	NA	NA	NA	NA	NA	NA	NA	NA	NA	NA	NA	NA	NA	NA	NA	NA	NA	1,50	9,03	11,71	3,06
N-R9	RED FOX	M	NA	NA	France	NA	NA	NA	NA	NA	NA	NA	NA	NA	NA	NA	NA	NA	NA	NA	NA	NA	1,19	5,89	11,16	2,82

						Environmental data																					Muscle ar			
						GPA coordinates				Climatic data			Diet (Forbes-Harper et al., 2017)													PCSA			
ID	cat	sex	age	body mass	location	x	y	urban	demographics	bio5	bio6	bio12	sheep	rodent	rabbit	marsupials	bird	reptile/frog	invertebrates	mammal	plant	other	digastric	masseter	temporal	pterygoid
Ny-R1	RED FOX	M	NA	NA	France	NA	NA	NA	NA	NA	NA	NA	NA	NA	NA	NA	NA	NA	NA	NA	NA	NA	1,23	NA	10,68	2,50
Ny-R2	RED FOX	F	NA	NA	France	NA	NA	NA	NA	NA	NA	NA	NA	NA	NA	NA	NA	NA	NA	NA	NA	NA	1,72	11,21	15,29	2,34
Ny-R3	RED FOX	NA	NA	NA	France	NA	NA	NA	NA	NA	NA	NA	NA	NA	NA	NA	NA	NA	NA	NA	NA	NA	1,84	9,68	15,36	5,19
Ny-R4	RED FOX	M	NA	NA	France	NA	NA	NA	NA	NA	NA	NA	NA	NA	NA	NA	NA	NA	NA	NA	NA	NA	1,08	11,25	17,15	2,76
Ny-R5	SILVER FOX	NA	NA	NA	France	NA	NA	NA	NA	NA	NA	NA	NA	NA	NA	NA	NA	NA	NA	NA	NA	NA	1,75	7,44	9,89	2,00
Ny-R6	SILVER FOX	NA	NA	NA	France	NA	NA	NA	NA	NA	NA	NA	NA	NA	NA	NA	NA	NA	NA	NA	NA	NA	1,39	6,59	13,18	1,49
Ny-R7	SILVER FOX	NA	NA	NA	France	NA	NA	NA	NA	NA	NA	NA	NA	NA	NA	NA	NA	NA	NA	NA	NA	NA	0,71	7,24	9,86	1,47
Ny-R8	SILVER FOX	NA	NA	NA	France	NA	NA	NA	NA	NA	NA	NA	NA	NA	NA	NA	NA	NA	NA	NA	NA	NA	1,90	9,55	12,50	2,40
P-R1	RED FOX	NA	NA	NA	France	NA	NA	NA	NA	NA	NA	NA	NA	NA	NA	NA	NA	NA	NA	NA	NA	NA	NA	NA	NA	NA
P-R3	RED FOX	M	NA	NA	France	NA	NA	NA	NA	NA	NA	NA	NA	NA	NA	NA	NA	NA	NA	NA	NA	NA	1,11	6,57	9,53	2,21
T-R1	RED FOX	M	NA	NA	France	NA	NA	NA	NA	NA	NA	NA	NA	NA	NA	NA	NA	NA	NA	NA	NA	NA	1,25	8,32	10,18	3,93
1,00	AUSTRALIAN RED FOX WITH DIET	F	2,00	4.96	Dumbleyung	-33.526934	117.572106	rural	21	300,00	51,00	437,00	0,00	0,46	0,00	0,99	0,00	0,00	0,00	0,00	0,32	0,00	NA	NA	NA	NA
4,00	AUSTRALIAN RED FOX WITH DIET	F	3,00	4.395	Dumbleyung	-33.526934	117.572106	rural	21	300,00	51,00	437,00	1,25	0,00	0,00	0,00	0,32	0,00	0,00	0,00	0,00	0,00	NA	NA	NA	NA
6,00	AUSTRALIAN RED FOX WITH DIET	F	2,00	6.48	Dumbleyung	-33.526934	117.572106	rural	21	300,00	51,00	437,00	0,00	1,25	0,00	0,00	0,00	0,00	0,00	0,00	0,00	0,32	NA	NA	NA	NA
7,00	AUSTRALIAN RED FOX WITH DIET	M	4+	7.195	Dumbleyung	-33.526934	117.572106	rural	21	300,00	51,00	437,00	1,57	0,00	0,00	0,00	0,00	0,00	0,00	0,00	0,00	0,00	NA	NA	NA	NA
9,00	AUSTRALIAN RED FOX WITH DIET	M	2,00	6.6	Dumbleyung	-33.526934	117.572106	rural	21	300,00	51,00	437,00	0,00	0,68	0,00	0,00	0,00	0,00	0,00	0,00	0,89	0,00	NA	NA	NA	NA
10,00	AUSTRALIAN RED FOX WITH DIET	F	2,00	5.46	Dumbleyung	-33.526934	117.572106	rural	21	300,00	51,00	437,00	1,57	0,00	0,00	0,00	0,00	0,00	0,00	0,00	0,00	0,00	NA	NA	NA	NA
11,00	AUSTRALIAN RED FOX WITH DIET	F	2,00	6.67	Dumbleyung	-33.526934	117.572106	rural	21	300,00	51,00	437,00	1,11	0,40	0,00	0,00	0,00	0,00	0,00	0,00	0,23	0,00	NA	NA	NA	NA
12,00	AUSTRALIAN RED FOX WITH DIET	M	1,00	4.245	Dumbleyung	-33.526934	117.572106	rural	21	300,00	51,00	437,00	0,63	0,84	0,14	0,00	0,00	0,00	0,00	0,00	0,29	0,00	NA	NA	NA	NA
13,00	AUSTRALIAN RED FOX WITH DIET	M	1,00	5.715	Dumbleyung	-33.526934	117.572106	rural	21	300,00	51,00	437,00	1,57	0,00	0,00	0,00	0,00	0,00	0,00	0,00	0,00	0,00	NA	NA	NA	NA
15,00	AUSTRALIAN RED FOX WITH DIET	F	2,00	5.48	Dumbleyung	-33.526934	117.572106	rural	21	300,00	51,00	437,00	0,00	0,58	0,00	0,00	0,00	0,00	0,58	0,00	0,68	0,00	NA	NA	NA	NA
16,00	AUSTRALIAN RED FOX WITH DIET	M	1,00	5.025	Dumbleyung	-33.526934	117.572106	rural	21	300,00	51,00	437,00	0,00	0,31	0,31	0,00	0,00	0,00	0,38	0,00	0,97	0,00	NA	NA	NA	NA
20,00	AUSTRALIAN RED FOX WITH DIET	M	3,00	6.395	Katanning	-33.690697	117.555314	urban	3768	298,00	53,00	467,00	1,57	0,00	0,00	0,00	0,00	0,00	0,00	0,00	0,00	0,00	NA	NA	NA	NA
21,00	AUSTRALIAN RED FOX WITH DIET	M	3,00	6.62	Katanning	-33.690697	117.555314	urban	3768	298,00	53,00	467,00	0,66	0,00	0,00	0,63	0,52	0,00	0,10	0,00	0,00	0,10	NA	NA	NA	NA
22,00	AUSTRALIAN RED FOX WITH DIET	M	2,00	7.215	Katanning	-33.690697	117.555314	urban	3768	298,00	53,00	467,00	0,49	0,00	0,00	0,00	1,08	0,00	0,00	0,00	0,00	0,00	NA	NA	NA	NA
23,00	AUSTRALIAN RED FOX WITH DIET	M	1,00	4.54	Katanning	-33.690697	117.555314	urban	3768	298,00	53,00	467,00	0,68	0,58	0,00	0,00	0,00	0,00	0,00	0,00	0,58	0,00	NA	NA	NA	NA
25,00	AUSTRALIAN RED FOX WITH DIET	F	1,00	4.165	Katanning	-33.690697	117.555314	urban	3768	298,00	53,00	467,00	0,79	0,00	0,00	0,00	0,00	0,00	0,46	0,00	0,58	0,00	NA	NA	NA	NA
26,00	AUSTRALIAN RED FOX WITH DIET	F	1,00	4.95	Katanning	-33.690697	117.555314	urban	3768	298,00	53,00	467,00	1,09	0,00	0,00	0,00	0,00	0,00	0,00	0,00	0,00	0,48	NA	NA	NA	NA
27,00	AUSTRALIAN RED FOX WITH DIET	M	3,00	7.04	Katanning	-33.690697	117.555314	urban	3768	298,00	53,00	467,00	0,00	0,32	0,00	0,00	0,00	0,00	0,10	0,00	1,23	0,00	NA	NA	NA	NA
28,00	AUSTRALIAN RED FOX WITH DIET	M	2,00	6.45	Katanning	-33.690697	117.555314	urban	3768	298,00	53,00	467,00	0,89	0,30	0,00	0,00	0,59	0,00	0,00	0,00	0,00	0,00	NA	NA	NA	NA
29,00	AUSTRALIAN RED FOX WITH DIET	M	2,00	6.56	Katanning	-33.690697	117.555314	urban	3768	298,00	53,00	467,00	1,32	0,00	0,00	0,00	0,10	0,00	0,00	0,00	0,23	0,00	NA	NA	NA	NA
30,00	AUSTRALIAN RED FOX WITH DIET	F	4+	5.335	Katanning	-33.690697	117.555314	urban	3768	298,00	53,00	467,00	0,89	0,58	0,00	0,00	0,00	0,00	0,14	0,10	0,00	0,27	NA	NA	NA	NA
31,00	AUSTRALIAN RED FOX WITH DIET	F	1,00	3.75	Katanning	-33.690697	117.555314	urban	3768	298,00	53,00	467,00	1,57	0,00	0,00	0,00	0,00	0,00	0,00	0,00	0,00	0,00	NA	NA	NA	NA
32,00	AUSTRALIAN RED FOX WITH DIET	F	1,00	4.3	Katanning	-33.690697	117.555314	urban	3768	298,00	53,00	467,00	1,57	0,00	0,00	0,00	0,00	0,00	0,00	0,00	0,00	0,00	NA	NA	NA	NA
34,00	AUSTRALIAN RED FOX WITH DIET	M	1,00	5.39	Nyabing	-33.594708	118.032603	rural	11	299,00	53,00	368,00	1,25	0,00	0,00	0,00	0,00	0,00	0,00	0,00	0,32	0,00	NA	NA	NA	NA
35,00	AUSTRALIAN RED FOX WITH DIET	M	3,00	7.745	Katanning	-33.690697	117.555314	urban	3768	298,00	53,00	467,00	0,98	0,00	0,00	0,58	0,00	0,00	0,00	0,00	0,10	0,00	NA	NA	NA	NA
36,00	AUSTRALIAN RED FOX WITH DIET	M	1,00	4.535	Nyabing	-33.594708	118.032603	rural	11	299,00	53,00	368,00	1,23	0,00	0,00	0,00	0,10	0,00	0,00	0,00	0,32	0,00	NA	NA	NA	NA
37,00	AUSTRALIAN RED FOX WITH DIET	F	1,00	3.865	Nyabing	-33.594708	118.032603	rural	11	299,00	53,00	368,00	1,43	0,00	0,00	0,00	0,00	0,00	0,00	0,00	0,00	0,14	NA	NA	NA	NA
38,00	AUSTRALIAN RED FOX WITH DIET	F	1,00	4.375	Nyabing	-33.594708	118.032603	rural	11	299,00	53,00	368,00	0,92	0,00	0,58	0,00	0,27	0,00	0,00	0,00	0,00	0,00	NA	NA	NA	NA
39,00	AUSTRALIAN RED FOX WITH DIET	M	1,00	5.01	Nyabing	-33.594708	118.032603	rural	11	299,00	53,00	368,00	1,23	0,17	0,00	0,00	0,00	0,00	0,14	0,00	0,23	0,10	NA	NA	NA	NA
41,00	AUSTRALIAN RED FOX WITH DIET	M	1,00	5.45	Katanning	-33.690697	117.555314	urban	3768	298,00	53,00	467,00	0,00	0,74	0,00	0,00	0,00	0,23	0,00	0,00	0,79	0,00	NA	NA	NA	NA
43,00	AUSTRALIAN RED FOX WITH DIET	F	2,00	5.58	Katanning	-33.690697	117.555314	urban	3768	298,00	53,00	467,00	0,68	0,00	0,00	0,00	0,00	0,00	0,00	0,00	0,89	0,00	NA	NA	NA	NA
46,00	AUSTRALIAN RED FOX WITH DIET	F	2,00	5.41	Katanning	-33.690697	117.555314	urban	3768	298,00	53,00	467,00	0,00	0,46	0,00	0,00	0,00	0,00	0,00	0,00	1,11	0,00	NA	NA	NA	NA
48,00	AUSTRALIAN RED FOX WITH DIET	F	2,00	5.315	Nyabing	-33.594708	118.032603	rural	11	299,00	53,00	368,00	1,25	0,00	0,00	0,00	0,00	0,00	0,32	0,00	0,00	0,00	NA	NA	NA	NA
49,00	AUSTRALIAN RED FOX WITH DIET	F	4+	5.865	Nyabing	-33.594708	118.032603	rural	11	299,00	53,00	368,00	1,35	0,00	0,00	0,00	0,00	0,00	0,00	0,00	0,00	0,23	NA	NA	NA	NA
51,00	AUSTRALIAN RED FOX WITH DIET	M	2,00	5.935	Katanning	-33.690697	117.555314	urban	3768	298,00	53,00	467,00	0,00	0,00	0,00	0,00	0,00	0,00	0,00	0,00	1,57	0,00	NA	NA	NA	NA
52,00	AUSTRALIAN RED FOX WITH DIET	F	1,00	3.415	Katanning	-33.690697	117.555314	urban	3768	298,00	53,00	467,00	1,35	0,00	0,00	0,00	0,00	0,00	0,00	0,00	0,17	0,14	NA	NA	NA	NA
53,00	AUSTRALIAN RED FOX WITH DIET	F	1,00	4.038	Katanning	-33.690697	117.555314	urban	3768	298,00	53,00	467,00	NA	NA	NA	NA	NA	NA	NA	NA	NA	NA	NA	NA	NA	NA
58,00	AUSTRALIAN RED FOX WITH DIET	F	1,00	4.31	Nyabing	-33.594708	118.032603	rural	11	299,00	53,00	368,00	1,57	0,00	0,00	0,00	0,00	0,00	0,00	0,00	0,00	0,00	NA	NA	NA	NA
59,00	AUSTRALIAN RED FOX WITH DIET	F	2,00	5.455	Nyabing	-33.594708	118.032603	rural	11	299,00	53,00	368,00	0,00	0,00	0,00	0,00	0,00	0,00	1,35	0,23	0,00	0,00	NA	NA	NA	NA
60,00	AUSTRALIAN RED FOX WITH DIET	NA	1,00	4.4	Katanning	-33.690697	117.555314	urban	3768	298,00	53,00	467,00	NA	NA	NA	NA	NA	NA	NA	NA	NA	NA	NA	NA	NA	NA
63,00	AUSTRALIAN RED FOX WITH DIET	M	2,00	5.315	Nyabing	-33.594708	118.032603	rural	11	299,00	53,00	368,00	NA	NA	NA	NA	NA	NA	NA	NA	NA	NA	NA	NA	NA	NA
64,00	AUSTRALIAN RED FOX WITH DIET	F	2,00	6.42	Nyabing	-33.594708	118.032603	rural	11	299,00	53,00	368,00	1,57	0,00	0,00	0,00	0,00	0,00	0,00	0,00	0,00	0,00	NA	NA	NA	NA
65,00	AUSTRALIAN RED FOX WITH DIET	F	1,00	3.9	Nyabing	-33.594708	118.032603	rural	11	299,00	53,00	368,00	1,25	0,00	0,00	0,00	0,00	0,00	0,00	0,00	0,32	0,00	NA	NA	NA	NA
66,00	AUSTRALIAN RED FOX WITH DIET	M	3,00	7.185	Katanning	-33.690697	117.555314	urban	3768	298,00	53,00	467,00	0,88	0,68	0,00	0,00	0,10	0,00	0,00	0,00	0,00	0,00	NA	NA	NA	NA
67,00	AUSTRALIAN RED FOX WITH DIET	M	2,00	5.75	Katanning	-33.690697	117.555314	urban	3768	298,00	53,00	467,00	1,57	0,00	0,00	0,00	0,00	0,00	0,00	0,00	0,00	0,00	NA	NA	NA	NA
68,00	AUSTRALIAN RED FOX WITH DIET	F	1,00	5.195	Nyabing	-33.594708	118.032603	rural	11	299,00	53,00	368,00	1,57	0,00	0,00	0,00	0,00	0,00	0,00	0,00	0,00	0,00	NA	NA	NA	NA
69,00	AUSTRALIAN RED FOX WITH DIET	F	1,00	6.425	Katanning	-33.690697	117.555314	urban	3768	298,00	53,00	467,00	1,11	0,00	0,00	0,00	0,00	0,00	0,00	0,00	0,46	0,00	NA	NA	NA	NA
70,00	AUSTRALIAN RED FOX WITH DIET	F	1,00	4.35	Nyabing	-33.594708	118.032603	rural	11	299,00	53,00	368,00	1,57	0,00	0,00	0,00	0,00	0,00	0,00	0,00	0,00	0,00	NA	NA	NA	NA
71,00	AUSTRALIAN RED FOX WITH DIET	F	1,00	4.885	Nyabing	-33.594708	118.032603	rural	11	299,00	53,00	368,00	1,15	0,00	0,00	0,00	0,00	0,00	0,00	0,10	0,40	0,10	NA	NA	NA	NA
72,00	AUSTRALIAN RED FOX WITH DIET	F	1,00	4.765	Katanning	-33.690697	117.555314	urban	3768	298,00	53,00	467,00	0,99	0,00	0,00	0,00	0,00	0,00	0,00	0,00	0,58	0,00	NA	NA	NA	NA
73,00	AUSTRALIAN RED FOX WITH DIET	M	4+	6.345	Nyabing	-33.594708	118.032603	rural	11	299,00	53,00	368,00	1,57	0,00	0,00	0,00	0,00	0,00	0,00	0,00	0,00	0,00	NA	NA	NA	NA
74,00	AUSTRALIAN RED FOX WITH DIET	M	1,00	6.315	Katanning	-33.690697	117.555314	urban	3768	298,00	53,00	467,00	1,35	0,00	0,00	0,00	0,00	0,00	0,00	0,00	0,23	0,00	NA	NA	NA	NA
75,00	AUSTRALIAN RED FOX WITH DIET	M	1,00	3.78	Nyabing	-33.594708	118.032603	rural	11	299,00	53,00	368,00	1,23	0,00	0,00	0,00	0,00	0,00	0,00	0,00	0,32	0,10	NA	NA	NA	NA
76,00	AUSTRALIAN RED FOX WITH DIET	F	2,00	5.169	Katanning	-33.690697	117.555314	urban	3768	298,00	53,00	467,00	NA	NA	NA	NA	NA	NA	NA	NA	NA	NA	NA	NA	NA	NA
77,00	AUSTRALIAN RED FOX WITH DIET	F	1,00	4.685	Katanning	-33.690697	117.555314	urban	3768	298,00	53,00	467,00	1,35	0,00	0,00	0,00	0,00	0,00	0,00	0,00	0,23	0,00	NA	NA	NA	NA
80,00	AUSTRALIAN RED FOX WITH DIET	M	1,00	4.45	Katanning	-33.690697	117.555314	urban	3768	298,00	53,00	467,00	1,25	0,00	0,00	0,00	0,00	0,00	0,00	0,00	0,00	0,32	NA	NA	NA	NA
81,00	AUSTRALIAN RED FOX WITH DIET	F	1,00	5.095	Katanning	-33.690697	117.555314	urban	3768	298,00	53,00	467,00	0,00	0,52	0,00	0,94	0,00	0,00	0,00	0,00	0,00	0,32	NA	NA	NA	NA
82,00	AUSTRALIAN RED FOX WITH DIET	F	2,00	4.185	Katanning	-33.690697	117.555314	urban	3768	298,00	53,00	467,00	1,15	0,27	0,00	0,00	0,23	0,10	0,00	0,00	0,17	0,10	NA	NA	NA	NA
83,00	AUSTRALIAN RED FOX WITH DIET	M	1,00	5.24	Katanning	-33.690697	117.555314	urban	3768	298,00	53,00	467,00	1,57	0,00	0,00	0,00	0,00	0,00	0,00	0,00	0,00	0,00	NA	NA	NA	NA
85,00	AUSTRALIAN RED FOX WITH DIET	M	4+	7.5	Katanning	-33.690697	117.555314	urban	3768	298,00	53,00	467,00	0,42	0,40	0,00	0,00	0,00	0,00	0,00	0,00	0,29	0,89	NA	NA	NA	NA
87,00	AUSTRALIAN RED FOX WITH DIET	F	1,00	3.725	Katanning	-33.690697	117.555314	urban	3768	298,00	53,00	467,00	0,00	0,00	0,00	0,00	0,00	0,00	0,23	0,00	1,35	0,00	NA	NA	NA	NA

						GPA coordinates			Environmental data				Diet (Forbes-Harper et al., 2017)										PCSA			Muscle ar
										Climatic data																
ID	cat	sex	age	body mass	location	x	y	urban	demographics	bio5	bio6	bio12	sheep	rodent	rabbit	marsupials	bird	reptile/frog	invertebrates	mammal	plant	other	digastric	masseter	temporal	pterygoid
90,00	AUSTRALIAN RED FOX WITH DIET	M	2,00	7.228	Katanning	-33.690697	117.555314	urban	3768	298,00	53,00	467,00	NA	NA	NA	NA	NA	NA	NA	NA	NA	NA	NA	NA	NA	NA
92,00	AUSTRALIAN RED FOX WITH DIET	M	1,00	4.89	Katanning	-33.690697	117.555314	urban	3768	298,00	53,00	467,00	1,25	0,00	0,00	0,00	0,00	0,00	0,32	0,00	0,00	0,00	NA	NA	NA	NA
93,00	AUSTRALIAN RED FOX WITH DIET	F	1,00	3.42	Katanning	-33.690697	117.555314	urban	3768	298,00	53,00	467,00	1,57	0,00	0,00	0,00	0,00	0,00	0,00	0,00	0,00	0,00	NA	NA	NA	NA
95,00	AUSTRALIAN RED FOX WITH DIET	M	3,00	6.37	Katanning	-33.690697	117.555314	urban	3768	298,00	53,00	467,00	1,40	0,00	0,00	0,00	0,00	0,00	0,14	0,00	0,10	0,00	NA	NA	NA	NA
96,00	AUSTRALIAN RED FOX WITH DIET	F	1,00	4.72	Katanning	-33.690697	117.555314	urban	3768	298,00	53,00	467,00	1,07	0,00	0,00	0,00	0,00	0,00	0,37	0,00	0,32	0,00	NA	NA	NA	NA
100,00	AUSTRALIAN RED FOX WITH DIET	F	4+	6.165	Katanning	-33.690697	117.555314	urban	3768	298,00	53,00	467,00	0,58	0,89	0,00	0,00	0,00	0,00	0,00	0,00	0,32	0,00	NA	NA	NA	NA
101,00	AUSTRALIAN RED FOX WITH DIET	F	4+	4.152	Nyabing	-33.594708	118.032603	rural	11	299,00	53,00	368,00	1,57	0,00	0,00	0,00	0,00	0,00	0,00	0,00	0,00	0,00	NA	NA	NA	NA
104,00	AUSTRALIAN RED FOX WITH DIET	M	3,00	6.7	Katanning	-33.690697	117.555314	urban	3768	298,00	53,00	467,00	0,00	0,00	0,00	0,00	0,10	0,00	0,00	0,10	1,40	0,10	NA	NA	NA	NA
105,00	AUSTRALIAN RED FOX WITH DIET	M	2,00	5.4	Katanning	-33.690697	117.555314	urban	3768	298,00	53,00	467,00	1,13	0,40	0,00	0,00	0,00	0,00	0,00	0,00	0,17	0,00	NA	NA	NA	NA
106,00	AUSTRALIAN RED FOX WITH DIET	M	3,00	6.21	Nyabing	-33.594708	118.032603	rural	11	299,00	53,00	368,00	0,58	0,89	0,00	0,00	0,00	0,00	0,00	0,00	0,32	0,00	NA	NA	NA	NA
107,00	AUSTRALIAN RED FOX WITH DIET	M	3,00	6.37	Nyabing	-33.594708	118.032603	rural	11	299,00	53,00	368,00	1,25	0,00	0,00	0,00	0,00	0,00	0,00	0,00	0,00	0,32	NA	NA	NA	NA
109,00	AUSTRALIAN RED FOX WITH DIET	M	1,00	6.71	Katanning	-33.690697	117.555314	urban	3768	298,00	53,00	467,00	1,23	0,00	0,00	0,00	0,00	0,00	0,32	0,00	0,00	0,10	NA	NA	NA	NA
110,00	AUSTRALIAN RED FOX WITH DIET	M	1,00	4.79	Katanning	-33.690697	117.555314	urban	3768	298,00	53,00	467,00	0,68	0,52	0,00	0,00	0,00	0,00	0,46	0,00	0,40	0,00	NA	NA	NA	NA
111,00	AUSTRALIAN RED FOX WITH DIET	F	2,00	5,00	Katanning	-33.690697	117.555314	urban	3768	298,00	53,00	467,00	1,28	0,00	0,00	0,00	0,00	0,00	0,00	0,00	0,29	0,00	NA	NA	NA	NA
112,00	AUSTRALIAN RED FOX WITH DIET	F	2,00	5.185	Katanning	-33.690697	117.555314	urban	3768	298,00	53,00	467,00	0,90	0,23	0,00	0,00	0,62	0,00	0,00	0,00	0,00	0,00	NA	NA	NA	NA
113,00	AUSTRALIAN RED FOX WITH DIET	F	2,00	5.99	Katanning	-33.690697	117.555314	urban	3768	298,00	53,00	467,00	0,00	0,00	0,00	0,00	0,00	0,68	0,32	0,00	0,00	0,79	NA	NA	NA	NA
114,00	AUSTRALIAN RED FOX WITH DIET	F	1,00	3.875	Katanning	-33.690697	117.555314	urban	3768	298,00	53,00	467,00	0,63	0,79	0,00	0,00	0,00	0,00	0,23	0,00	0,32	0,00	NA	NA	NA	NA
116,00	AUSTRALIAN RED FOX WITH DIET	M	1,00	5.665	Katanning	-33.690697	117.555314	urban	3768	298,00	53,00	467,00	0,58	0,00	0,00	0,00	0,00	0,58	0,40	0,46	0,00	0,23	NA	NA	NA	NA
117,00	AUSTRALIAN RED FOX WITH DIET	F	1,00	4.225	Katanning	-33.690697	117.555314	urban	3768	298,00	53,00	467,00	1,11	0,00	0,00	0,00	0,00	0,00	0,40	0,00	0,23	0,00	NA	NA	NA	NA
118,00	AUSTRALIAN RED FOX WITH DIET	F	1,00	3.49	Woodanilling	-33.563404	117.431114	rural	29	301,00	54,00	449,00	1,57	0,00	0,00	0,00	0,00	0,00	0,00	0,00	0,00	0,00	NA	NA	NA	NA
119,00	AUSTRALIAN RED FOX WITH DIET	M	1,00	4.17	Woodanilling	-33.563404	117.431114	rural	29	301,00	54,00	449,00	1,57	0,00	0,00	0,00	0,00	0,00	0,00	0,00	0,00	0,00	NA	NA	NA	NA
120,00	AUSTRALIAN RED FOX WITH DIET	F	1,00	4.675	Woodanilling	-33.563404	117.431114	rural	29	301,00	54,00	449,00	1,35	0,00	0,00	0,00	0,00	0,00	0,00	0,00	0,00	0,23	NA	NA	NA	NA
121,00	AUSTRALIAN RED FOX WITH DIET	M	2,00	5.995	Woodanilling	-33.563404	117.431114	rural	29	301,00	54,00	449,00	1,35	0,00	0,00	0,00	0,00	0,00	0,00	0,00	0,23	0,00	NA	NA	NA	NA
122,00	AUSTRALIAN RED FOX WITH DIET	M	3,00	6.32	Woodanilling	-33.563404	117.431114	rural	29	301,00	54,00	449,00	1,57	0,00	0,00	0,00	0,00	0,00	0,00	0,00	0,00	0,00	NA	NA	NA	NA
123,00	AUSTRALIAN RED FOX WITH DIET	M	1,00	5.04	Woodanilling	-33.563404	117.431114	rural	29	301,00	54,00	449,00	0,79	0,00	0,00	0,00	0,00	0,00	0,32	0,00	0,68	0,00	NA	NA	NA	NA
124,00	AUSTRALIAN RED FOX WITH DIET	M	4+	5.775	Woodanilling	-33.563404	117.431114	rural	29	301,00	54,00	449,00	1,47	0,00	0,00	0,00	0,00	0,00	0,00	0,00	0,00	0,10	NA	NA	NA	NA
125,00	AUSTRALIAN RED FOX WITH DIET	M	4+	5.665	Woodanilling	-33.563404	117.431114	rural	29	301,00	54,00	449,00	0,89	0,52	0,00	0,00	0,00	0,00	0,27	0,00	0,29	0,00	NA	NA	NA	NA
126,00	AUSTRALIAN RED FOX WITH DIET	F	2,00	5.52	Woodanilling	-33.563404	117.431114	rural	29	301,00	54,00	449,00	0,79	0,32	0,00	0,00	0,00	0,32	0,38	0,00	0,40	0,10	NA	NA	NA	NA
127,00	AUSTRALIAN RED FOX WITH DIET	F	2,00	5.215	Woodanilling	-33.563404	117.431114	rural	29	301,00	54,00	449,00	1,34	0,00	0,00	0,00	0,00	0,00	0,00	0,00	0,00	0,23	NA	NA	NA	NA
128,00	AUSTRALIAN RED FOX WITH DIET	M	2,00	6.35	Woodanilling	-33.563404	117.431114	rural	29	301,00	54,00	449,00	0,00	0,46	0,00	0,00	0,00	0,00	0,68	0,00	0,00	0,68	NA	NA	NA	NA
129,00	AUSTRALIAN RED FOX WITH DIET	F	2,00	4.735	Woodanilling	-33.563404	117.431114	rural	29	301,00	54,00	449,00	1,05	0,32	0,00	0,00	0,00	0,00	0,00	0,00	0,40	0,00	NA	NA	NA	NA
130,00	AUSTRALIAN RED FOX WITH DIET	F	3,00	5.935	Woodanilling	-33.563404	117.431114	rural	29	301,00	54,00	449,00	1,47	0,00	0,00	0,00	0,10	0,00	0,00	0,00	0,00	0,00	NA	NA	NA	NA
131,00	AUSTRALIAN RED FOX WITH DIET	F	1,00	5.56	Woodanilling	-33.563404	117.431114	rural	29	301,00	54,00	449,00	0,52	0,00	1,02	0,00	0,14	0,00	0,00	0,00	0,00	0,00	NA	NA	NA	NA
132,00	AUSTRALIAN RED FOX WITH DIET	M	2,00	6.258	Woodanilling	-33.563404	117.431114	rural	29	301,00	54,00	449,00	NA	NA	NA	NA	NA	NA	NA	NA	NA	NA	NA	NA	NA	NA
133,00	AUSTRALIAN RED FOX WITH DIET	M	4+	6.03	Woodanilling	-33.563404	117.431114	rural	29	301,00	54,00	449,00	0,74	0,00	0,00	0,00	0,00	0,00	0,00	0,00	0,84	0,00	NA	NA	NA	NA
135,00	AUSTRALIAN RED FOX WITH DIET	F	1,00	5.065	Woodanilling	-33.563404	117.431114	rural	29	301,00	54,00	449,00	0,00	0,00	0,00	0,00	0,00	0,00	1,57	0,00	0,00	0,00	NA	NA	NA	NA
136,00	AUSTRALIAN RED FOX WITH DIET	M	1,00	5.96	Woodanilling	-33.563404	117.431114	rural	29	301,00	54,00	449,00	1,57	0,00	0,00	0,00	0,00	0,00	0,00	0,00	0,00	0,00	NA	NA	NA	NA
137,00	AUSTRALIAN RED FOX WITH DIET	M	2,00	5.96	Woodanilling	-33.563404	117.431114	rural	29	301,00	54,00	449,00	1,05	0,00	0,00	0,00	0,23	0,00	0,00	0,00	0,46	0,00	NA	NA	NA	NA
138,00	AUSTRALIAN RED FOX WITH DIET	F	1,00	3.85	Woodanilling	-33.563404	117.431114	rural	29	301,00	54,00	449,00	1,40	0,00	0,00	0,00	0,00	0,00	0,00	0,00	0,00	0,17	NA	NA	NA	NA
139,00	AUSTRALIAN RED FOX WITH DIET	F	2,00	4.305	Woodanilling	-33.563404	117.431114	rural	29	301,00	54,00	449,00	1,47	0,00	0,00	0,00	0,00	0,00	0,00	0,00	0,00	0,10	NA	NA	NA	NA
140,00	AUSTRALIAN RED FOX WITH DIET	M	1,00	6.09	Woodanilling	-33.563404	117.431114	rural	29	301,00	54,00	449,00	0,93	0,63	0,00	0,00	0,00	0,00	0,10	0,00	0,00	0,00	NA	NA	NA	NA
141,00	AUSTRALIAN RED FOX WITH DIET	M	1,00	4.78	Woodanilling	-33.563404	117.431114	rural	29	301,00	54,00	449,00	1,57	0,00	0,00	0,00	0,00	0,00	0,00	0,00	0,00	0,00	NA	NA	NA	NA
142,00	AUSTRALIAN RED FOX WITH DIET	F	1,00	4.66	Woodanilling	-33.563404	117.431114	rural	29	301,00	54,00	449,00	1,57	0,00	0,00	0,00	0,00	0,00	0,00	0,00	0,00	0,00	NA	NA	NA	NA
143,00	AUSTRALIAN RED FOX WITH DIET	M	3,00	6.67	Woodanilling	-33.563404	117.431114	rural	29	301,00	54,00	449,00	1,57	0,00	0,00	0,00	0,00	0,00	0,00	0,00	0,00	0,00	NA	NA	NA	NA
144,00	AUSTRALIAN RED FOX WITH DIET	M	1,00	5.295	Woodanilling	-33.563404	117.431114	rural	29	301,00	54,00	449,00	0,99	0,00	0,00	0,00	0,00	0,00	0,00	0,00	0,00	0,58	NA	NA	NA	NA
145,00	AUSTRALIAN RED FOX WITH DIET	F	1,00	5.53	Woodanilling	-33.563404	117.431114	rural	29	301,00	54,00	449,00	NA	NA	NA	NA	NA	NA	NA	NA	NA	NA	NA	NA	NA	NA
146,00	AUSTRALIAN RED FOX WITH DIET	F	1,00	5.075	Woodanilling	-33.563404	117.431114	rural	29	301,00	54,00	449,00	1,57	0,00	0,00	0,00	0,00	0,00	0,00	0,00	0,00	0,00	NA	NA	NA	NA
147,00	AUSTRALIAN RED FOX WITH DIET	M	2,00	6.25	Woodanilling	-33.563404	117.431114	rural	29	301,00	54,00	449,00	1,57	0,00	0,00	0,00	0,00	0,00	0,00	0,00	0,00	0,00	NA	NA	NA	NA
149,00	AUSTRALIAN RED FOX WITH DIET	M	2,00	6.805	Woodanilling	-33.563404	117.431114	rural	29	301,00	54,00	449,00	1,57	0,00	0,00	0,00	0,00	0,00	0,00	0,00	0,00	0,00	NA	NA	NA	NA
150,00	AUSTRALIAN RED FOX WITH DIET	M	1,00	4.69	Woodanilling	-33.563404	117.431114	rural	29	301,00	54,00	449,00	0,89	0,00	0,00	0,00	0,00	0,00	0,00	0,00	0,68	0,00	NA	NA	NA	NA
151,00	AUSTRALIAN RED FOX WITH DIET	M	1,00	4.815	Woodanilling	-33.563404	117.431114	rural	29	301,00	54,00	449,00	1,20	0,10	0,00	0,00	0,00	0,14	0,00	0,00	0,32	0,00	NA	NA	NA	NA
152,00	AUSTRALIAN RED FOX WITH DIET	F	3,00	4.89	Woodanilling	-33.563404	117.431114	rural	29	301,00	54,00	449,00	NA	NA	NA	NA	NA	NA	NA	NA	NA	NA	NA	NA	NA	NA
154,00	AUSTRALIAN RED FOX WITH DIET	M	1,00	4.579	Mt. Baker	-34.630755	117.665356	rural	85	266,00	61,00	726,00	NA	NA	NA	NA	NA	NA	NA	NA	NA	NA	NA	NA	NA	NA
155,00	AUSTRALIAN RED FOX WITH DIET	M	2,00	5.48	Mt. Baker	-34.630755	117.665356	rural	85	266,00	61,00	726,00	0,00	0,00	0,00	0,00	0,00	0,00	0,79	0,00	0,79	0,00	NA	NA	NA	NA
156,00	AUSTRALIAN RED FOX WITH DIET	M	4+	5.23	Mt. Baker	-34.630755	117.665356	rural	85	266,00	61,00	726,00	1,35	0,00	0,00	0,00	0,00	0,00	0,14	0,00	0,17	0,00	NA	NA	NA	NA
157,00	AUSTRALIAN RED FOX WITH DIET	M	1,00	5.067	Mt. Baker	-34.630755	117.665356	rural	85	266,00	61,00	726,00	0,00	0,00	0,00	0,00	0,00	0,00	0,00	0,00	1,57	0,00	NA	NA	NA	NA
159,00	AUSTRALIAN RED FOX WITH DIET	F	2,00	4.96	Mt. Baker	-34.630755	117.665356	rural	85	266,00	61,00	726,00	0,74	0,00	0,00	0,00	0,00	0,32	0,23	0,00	0,68	0,00	NA	NA	NA	NA
160,00	AUSTRALIAN RED FOX WITH DIET	M	2,00	7.12	Mt. Baker	-34.630755	117.665356	rural	85	266,00	61,00	726,00	0,68	0,00	0,00	0,00	0,00	0,00	0,00	0,00	0,89	0,00	NA	NA	NA	NA
162,00	AUSTRALIAN RED FOX WITH DIET	F	1,00	2.845	Mt. Baker	-34.630755	117.665356	rural	85	266,00	61,00	726,00	1,57	0,00	0,00	0,00	0,00	0,00	0,00	0,00	0,00	0,00	NA	NA	NA	NA
164,00	AUSTRALIAN RED FOX WITH DIET	F	1,00	4.475	Mt. Baker	-34.630755	117.665356	rural	85	266,00	61,00	726,00	0,32	0,96	0,00	0,00	0,00	0,00	0,17	0,00	0,46	0,00	NA	NA	NA	NA
167,00	AUSTRALIAN RED FOX WITH DIET	F	2,00	5.485	Mt. Baker	-34.630755	117.665356	rural	85	266,00	61,00	726,00	0,99	0,00	0,00	0,00	0,00	0,00	0,58	0,00	0,00	0,00	NA	NA	NA	NA
168,00	AUSTRALIAN RED FOX WITH DIET	M	1,00	5.8	Mt. Baker	-34.630755	117.665356	rural	85	266,00	61,00	726,00	1,57	0,00	0,00	0,00	0,00	0,00	0,00	0,00	0,00	0,00	NA	NA	NA	NA
170,00	AUSTRALIAN RED FOX WITH DIET	M	4+	6.585	Mt. Baker	-34.630755	117.665356	rural	85	266,00	61,00	726,00	0,38	0,00	0,00	0,00	0,00	0,00	0,00	0,10	1,17	0,00	NA	NA	NA	NA
172,00	AUSTRALIAN RED FOX WITH DIET	M	4+	6,00	Mt. Baker	-34.630755	117.665356	rural	85	266,00	61,00	726,00	0,99	0,00	0,00	0,00	0,00	0,00	0,00	0,00	0,58	0,00	NA	NA	NA	NA
173,00	AUSTRALIAN RED FOX WITH DIET	M	1,00	5.505	Mt. Baker	-34.630755	117.665356	rural	85	266,00	61,00	726,00	0,58	0,00	0,00	0,00	0,00	0,99	0,00	0,00	0,00	0,00	NA	NA	NA	NA
174,00	AUSTRALIAN RED FOX WITH DIET	M	1,00	5.94	Mt. Baker	-34.630755	117.665356	rural	85	266,00	61,00	726,00	0,00	0,00	0,00	0,00	1,47	0,00	0,00	0,10	0,00	0,00	NA	NA	NA	NA
175,00	AUSTRALIAN RED FOX WITH DIET	M	2,00	6.535	Mt. Baker	-34.630755	117.665356	rural	85	266,00	61,00	726,00	0,00	0,00	0,00	0,75	0,00	0,20	0,46	0,00	0,46	0,32	NA	NA	NA	NA
176,00	AUSTRALIAN RED FOX WITH DIET	M	3,00	8.23	Mt. Baker	-34.630755	117.665356	rural	85	266,00	61,00	726,00	1,35	0,00	0,00	0,00	0,00	0,00	0,17	0,00	0,14	0,00	NA	NA	NA	NA
178,00	AUSTRALIAN RED FOX WITH DIET	F	1,00	4.845	Mt. Baker	-34.630755	117.665356	rural	85	266,00	61,00	726,00	1,35	0,00	0,00	0,00	0,00	0,00	0,00	0,00	0,00	0,23	NA	NA	NA	NA
179,00	AUSTRALIAN RED FOX WITH DIET	M	1,00	4.66	Mt. Baker	-34.630755	117.665356	rural	85	266,00	61,00	726,00	1,20	0,00	0,00	0,00	0,00	0,00	0,29	0,00	0,17	0,14	NA	NA	NA	NA
180,00	AUSTRALIAN RED FOX WITH DIET	F	4+	5.19	Mt. Baker	-34.630755	117.665356	rural	85	266,00	61,00	726,00	0,99	0,58	0,00	0,00	0,00	0,00	0,00	0,00	0,00	0,00	NA	NA	NA	NA
181,00	AUSTRALIAN RED FOX WITH DIET	F	1,00	4.04	Mt. Baker	-34.630755	117.665356	rural	85	266,00	61,00	726,00	0,99	0,00	0,00	0,00	0,00	0,00	0,00	0,00	0,58	0,00	NA	NA	NA	NA

										Environmental data														Muscle ar			
					GPA coordinates					Climatic data			Diet (Forbes-Harper et al., 2017)										PCSA			
ID	cat	sex	age	body mass	location	x	y	urban	demographics	bio5	bio6	bio12	sheep	rodent	rabbit	marsupials	bird	reptile/frog	invertebrates	mammal	plant	other	digastric	masseter	temporal	pterygoid
182,00	AUSTRALIAN RED FOX WITH DIET	F	1,00	5.31	Mt. Baker	-34.580594	117.499284	rural	85	270,00	62,00	673,00	1,35	0,00	0,00	0,00	0,00	0,00	0,00	0,00	0,23	0,00	NA	NA	NA	NA
183,00	AUSTRALIAN RED FOX WITH DIET	M	1,00	5.445	Mt. Baker	-34.580594	117.499284	rural	85	270,00	62,00	673,00	0,00	0,00	0,00	0,00	0,00	0,00	0,99	0,00	0,00	0,58	NA	NA	NA	NA
184,00	AUSTRALIAN RED FOX WITH DIET	F	1,00	3.755	Mt. Baker	-34.580594	117.499284	rural	85	270,00	62,00	673,00	1,25	0,00	0,00	0,00	0,00	0,00	0,23	0,00	0,23	0,00	NA	NA	NA	NA
185,00	AUSTRALIAN RED FOX WITH DIET	F	4+	5.955	Mt. Baker	-34.580594	117.499284	rural	85	270,00	62,00	673,00	1,57	0,00	0,00	0,00	0,00	0,00	0,00	0,00	0,00	0,00	NA	NA	NA	NA
186,00	AUSTRALIAN RED FOX WITH DIET	M	2,00	6.135	Mt. Baker	-34.580594	117.499284	rural	85	270,00	62,00	673,00	1,17	0,00	0,00	0,00	0,00	0,00	0,32	0,00	0,23	0,00	NA	NA	NA	NA
187,00	AUSTRALIAN RED FOX WITH DIET	M	1,00	5.575	Mt. Baker	-34.580594	117.499284	rural	85	270,00	62,00	673,00	1,57	0,00	0,00	0,00	0,00	0,00	0,00	0,00	0,00	0,00	NA	NA	NA	NA
188,00	AUSTRALIAN RED FOX WITH DIET	M	3,00	6.03	Mt. Baker	-34.580594	117.499284	rural	85	270,00	62,00	673,00	1,57	0,00	0,00	0,00	0,00	0,00	0,00	0,00	0,00	0,00	NA	NA	NA	NA
192,00	AUSTRALIAN RED FOX WITH DIET	M	3,00	8.918	Mt. Baker	-34.630755	117.665356	rural	85	266,00	61,00	726,00	NA	NA	NA	NA	NA	NA	NA	NA	NA	NA	NA	NA	NA	NA
193,00	AUSTRALIAN RED FOX WITH DIET	F	3,00	5.88	Mt. Baker	-34.630755	117.665356	rural	85	266,00	61,00	726,00	0,58	0,52	0,00	0,00	0,00	0,00	0,00	0,00	0,74	0,00	NA	NA	NA	NA
194,00	AUSTRALIAN RED FOX WITH DIET	M	3,00	6.175	Mt. Baker	-34.630755	117.665356	rural	85	266,00	61,00	726,00	0,00	0,68	0,00	0,00	0,00	0,00	0,00	0,00	0,89	0,00	NA	NA	NA	NA
195,00	AUSTRALIAN RED FOX WITH DIET	M	1,00	4.6	Mt. Baker	-34.630755	117.665356	rural	85	266,00	61,00	726,00	1,57	0,00	0,00	0,00	0,00	0,00	0,00	0,00	0,00	0,00	NA	NA	NA	NA
196,00	AUSTRALIAN RED FOX WITH DIET	M	1,00	5.12	Mt. Baker	-34.630755	117.665356	rural	85	266,00	61,00	726,00	1,57	0,00	0,00	0,00	0,00	0,00	0,00	0,00	0,00	0,00	NA	NA	NA	NA
197,00	AUSTRALIAN RED FOX WITH DIET	F	1,00	4.835	Mt. Baker	-34.630755	117.665356	rural	85	266,00	61,00	726,00	1,09	0,00	0,00	0,00	0,00	0,00	0,40	0,00	0,23	0,10	NA	NA	NA	NA
198,00	AUSTRALIAN RED FOX WITH DIET	F	2,00	6.59	Mt. Baker	-34.630755	117.665356	rural	85	266,00	61,00	726,00	0,00	0,00	0,00	0,00	0,00	0,00	1,57	0,00	0,00	0,00	NA	NA	NA	NA
199,00	AUSTRALIAN RED FOX WITH DIET	M	1,00	4.265	Mt. Baker	-34.630755	117.665356	rural	85	266,00	61,00	726,00	0,00	0,00	0,00	0,00	0,14	0,00	0,46	0,10	1,00	0,25	NA	NA	NA	NA
200,00	AUSTRALIAN RED FOX WITH DIET	M	2,00	7.015	Mt. Baker	-34.580594	117.499284	rural	85	270,00	62,00	673,00	1,43	0,00	0,00	0,00	0,00	0,00	0,00	0,00	0,00	0,14	NA	NA	NA	NA
201,00	AUSTRALIAN RED FOX WITH DIET	M	1,00	6.14	Mt. Baker	-34.580594	117.499284	rural	85	270,00	62,00	673,00	1,25	0,00	0,00	0,00	0,00	0,00	0,32	0,00	0,00	0,00	NA	NA	NA	NA
202,00	AUSTRALIAN RED FOX WITH DIET	M	1,00	4.09	Mt. Baker	-34.580594	117.499284	rural	85	270,00	62,00	673,00	1,05	0,00	0,46	0,00	0,00	0,00	0,00	0,00	0,00	0,23	NA	NA	NA	NA
203,00	AUSTRALIAN RED FOX WITH DIET	M	3,00	6.35	Mt. Baker	-34.580594	117.499284	rural	85	270,00	62,00	673,00	0,73	0,58	0,00	0,00	0,10	0,00	0,00	0,00	0,00	0,52	NA	NA	NA	NA
204,00	AUSTRALIAN RED FOX WITH DIET	F	1,00	5.12	Mt. Baker	-34.580594	117.499284	rural	85	270,00	62,00	673,00	1,25	0,00	0,00	0,00	0,00	0,00	0,23	0,00	0,00	0,23	NA	NA	NA	NA
205,00	AUSTRALIAN RED FOX WITH DIET	M	1,00	7.855	Mt. Baker	-34.580594	117.499284	rural	85	270,00	62,00	673,00	0,58	0,79	0,00	0,00	0,00	0,00	0,00	0,00	0,46	0,00	NA	NA	NA	NA
206,00	AUSTRALIAN RED FOX WITH DIET	F	2,00	5.73	Mt. Baker	-34.580594	117.499284	rural	85	270,00	62,00	673,00	1,17	0,32	0,00	0,00	0,00	0,00	0,23	0,00	0,00	0,00	NA	NA	NA	NA
209,00	AUSTRALIAN RED FOX WITH DIET	M	1,00	4.45	Mt. Baker	-34.580594	117.499284	rural	85	270,00	62,00	673,00	0,00	1,17	0,00	0,00	0,00	0,00	0,23	0,00	0,00	0,32	NA	NA	NA	NA
210,00	AUSTRALIAN RED FOX WITH DIET	M	1,00	5.55	Mt. Baker	-34.630755	117.665356	rural	85	266,00	61,00	726,00	0,94	0,00	0,00	0,00	0,63	0,00	0,00	0,00	0,00	0,00	NA	NA	NA	NA
211,00	AUSTRALIAN RED FOX WITH DIET	M	3,00	6.595	Mt. Baker	-34.580594	117.499284	rural	85	270,00	62,00	673,00	0,00	0,00	0,00	0,00	0,00	0,00	0,23	0,00	0,00	1,35	NA	NA	NA	NA
212,00	AUSTRALIAN RED FOX WITH DIET	F	4+	5.73	Mt. Baker	-34.580594	117.499284	rural	85	270,00	62,00	673,00	1,57	0,00	0,00	0,00	0,00	0,00	0,00	0,00	0,00	0,00	NA	NA	NA	NA
213,00	AUSTRALIAN RED FOX WITH DIET	M	4+	6.11	Mt. Baker	-34.580594	117.499284	rural	85	270,00	62,00	673,00	0,46	0,68	0,00	0,00	0,00	0,00	0,00	0,00	0,68	0,00	NA	NA	NA	NA
214,00	AUSTRALIAN RED FOX WITH DIET	M	1,00	4.1	Mt. Baker	-34.580594	117.499284	rural	85	270,00	62,00	673,00	0,46	0,00	0,00	0,00	0,10	0,00	0,61	0,10	0,74	0,00	NA	NA	NA	NA
215,00	AUSTRALIAN RED FOX WITH DIET	M	1,00	6.63	Mt. Baker	-34.630755	117.665356	rural	85	266,00	61,00	726,00	NA	NA	NA	NA	NA	NA	NA	NA	NA	NA	NA	NA	NA	NA
216,00	AUSTRALIAN RED FOX WITH DIET	F	3,00	5.425	Mt. Baker	-34.630755	117.665356	rural	85	266,00	61,00	726,00	0,00	0,99	0,00	0,00	0,00	0,00	0,46	0,00	0,00	0,32	NA	NA	NA	NA
220,00	AUSTRALIAN RED FOX WITH DIET	F	1,00	2.85	Armadale	-32.147053	116.002545	urban	45952	312,00	78,00	962,00	0,00	0,00	0,00	0,00	0,58	0,10	0,38	0,00	0,84	0,00	NA	NA	NA	NA
221,00	AUSTRALIAN RED FOX WITH DIET	F	2,00	5.105	Quairading	-32.013423	117.395801	semirural2	663	332,00	50,00	362,00	0,00	0,00	0,00	0,00	0,00	0,00	1,17	0,00	0,40	0,00	NA	NA	NA	NA
224,00	AUSTRALIAN RED FOX WITH DIET	F	1,00	3.25	Quairading	-32.013423	117.395801	semirural2	663	332,00	50,00	362,00	0,63	0,23	0,00	0,00	0,00	0,00	0,79	0,00	0,32	0,00	NA	NA	NA	NA
226,00	AUSTRALIAN RED FOX WITH DIET	F	1,00	4.28	Quairading	-32.013423	117.395801	semirural2	663	332,00	50,00	362,00	1,05	0,40	0,00	0,00	0,00	0,00	0,32	0,00	0,00	0,00	NA	NA	NA	NA
227,00	AUSTRALIAN RED FOX WITH DIET	M	4+	6.548	Quairading	-32.013423	117.395801	semirural2	663	332,00	50,00	362,00	NA	NA	NA	NA	NA	NA	NA	NA	NA	NA	NA	NA	NA	NA
228,00	AUSTRALIAN RED FOX WITH DIET	F	1,00	4.365	Quairading	-32.013423	117.395801	semirural2	663	332,00	50,00	362,00	0,00	0,32	0,00	0,00	0,00	0,00	1,11	0,00	0,32	0,00	NA	NA	NA	NA
229,00	AUSTRALIAN RED FOX WITH DIET	M	1,00	4.91	Quairading	-32.013423	117.395801	semirural2	663	332,00	50,00	362,00	0,00	1,57	0,00	0,00	0,00	0,00	0,00	0,00	0,00	0,00	NA	NA	NA	NA
230,00	AUSTRALIAN RED FOX WITH DIET	F	4+	6.325	Quairading	-32.013423	117.395801	semirural2	663	332,00	50,00	362,00	0,79	0,67	0,00	0,00	0,00	0,00	0,17	0,10	0,17	0,20	NA	NA	NA	NA
231,00	AUSTRALIAN RED FOX WITH DIET	M	1,00	4.105	Quairading	-32.013423	117.395801	semirural2	663	332,00	50,00	362,00	1,57	0,00	0,00	0,00	0,00	0,00	0,00	0,00	0,00	0,00	NA	NA	NA	NA
232,00	AUSTRALIAN RED FOX WITH DIET	F	1,00	3.59	Quairading	-32.013423	117.395801	semirural2	663	332,00	50,00	362,00	NA	NA	NA	NA	NA	NA	NA	NA	NA	NA	NA	NA	NA	NA
233,00	AUSTRALIAN RED FOX WITH DIET	F	2,00	4.34	Quairading	-32.013423	117.395801	semirural2	663	332,00	50,00	362,00	NA	NA	NA	NA	NA	NA	NA	NA	NA	NA	NA	NA	NA	NA
234,00	AUSTRALIAN RED FOX WITH DIET	F	1,00	4.35	Quairading	-32.013423	117.395801	semirural2	663	332,00	50,00	362,00	1,05	0,00	0,00	0,00	0,00	0,32	0,40	0,00	0,00	0,00	NA	NA	NA	NA
235,00	AUSTRALIAN RED FOX WITH DIET	M	1,00	5.295	Quairading	-32.013423	117.395801	semirural2	663	332,00	50,00	362,00	1,25	0,00	0,00	0,00	0,00	0,00	0,00	0,00	0,32	0,00	NA	NA	NA	NA
238,00	AUSTRALIAN RED FOX WITH DIET	F	2,00	5.28	Quairading	-32.013423	117.395801	semirural2	663	332,00	50,00	362,00	0,46	0,23	0,00	0,00	0,14	0,82	0,00	0,00	0,46	0,00	NA	NA	NA	NA
240,00	AUSTRALIAN RED FOX WITH DIET	F	2,00	5.535	Quairading	-32.013423	117.395801	semirural2	663	332,00	50,00	362,00	0,79	0,00	0,00	0,00	0,32	0,00	0,58	0,00	0,00	0,32	NA	NA	NA	NA
241,00	AUSTRALIAN RED FOX WITH DIET	F	4+	5.435	Quairading	-32.013423	117.395801	semirural2	663	332,00	50,00	362,00	NA	NA	NA	NA	NA	NA	NA	NA	NA	NA	NA	NA	NA	NA
243,00	AUSTRALIAN RED FOX WITH DIET	M	2,00	5.34	Quairading	-32.013423	117.395801	semirural2	663	332,00	50,00	362,00	0,93	0,10	0,00	0,00	0,17	0,00	0,14	0,00	0,58	0,00	NA	NA	NA	NA
244,00	AUSTRALIAN RED FOX WITH DIET	M	1,00	4.849	Quairading	-32.013423	117.395801	semirural2	663	332,00	50,00	362,00	NA	NA	NA	NA	NA	NA	NA	NA	NA	NA	NA	NA	NA	NA
245,00	AUSTRALIAN RED FOX WITH DIET	M	2,00	6.87	Quairading	-32.013423	117.395801	semirural2	663	332,00	50,00	362,00	0,23	0,00	0,00	0,00	0,00	0,00	0,23	0,00	1,25	0,00	NA	NA	NA	NA
246,00	AUSTRALIAN RED FOX WITH DIET	F	2,00	5.8	Quairading	-32.013423	117.395801	semirural2	663	332,00	50,00	362,00	1,17	0,00	0,00	0,00	0,00	0,00	0,14	0,00	0,32	0,17	NA	NA	NA	NA
247,00	AUSTRALIAN RED FOX WITH DIET	M	1,00	4.055	Quairading	-32.013423	117.395801	semirural2	663	332,00	50,00	362,00	1,47	0,00	0,00	0,00	0,00	0,00	0,10	0,00	0,00	0,00	NA	NA	NA	NA
248,00	AUSTRALIAN RED FOX WITH DIET	F	4+	5.065	Quairading	-32.013423	117.395801	semirural2	663	332,00	50,00	362,00	0,00	0,68	0,00	0,00	0,10	0,00	0,32	0,00	0,78	0,00	NA	NA	NA	NA
249,00	AUSTRALIAN RED FOX WITH DIET	F	1,00	5.405	Quairading	-32.013423	117.395801	semirural2	663	332,00	50,00	362,00	0,40	0,58	0,00	0,00	0,00	0,00	0,23	0,00	0,79	0,00	NA	NA	NA	NA
250,00	AUSTRALIAN RED FOX WITH DIET	M	3,00	8.24	Quairading	-32.013423	117.395801	semirural2	663	332,00	50,00	362,00	0,00	1,57	0,00	0,00	0,00	0,00	0,00	0,00	0,00	0,00	NA	NA	NA	NA
253,00	AUSTRALIAN RED FOX WITH DIET	F	1,00	4.1	Quairading	-32.013423	117.395801	semirural2	663	332,00	50,00	362,00	0,14	0,84	0,00	0,00	0,00	0,00	0,23	0,00	0,00	0,66	NA	NA	NA	NA
255,00	AUSTRALIAN RED FOX WITH DIET	M	1,00	4.775	Quairading	-32.013423	117.395801	semirural2	663	332,00	50,00	362,00	1,47	0,00	0,00	0,00	0,00	0,00	0,00	0,00	0,00	0,10	NA	NA	NA	NA
256,00	AUSTRALIAN RED FOX WITH DIET	F	1,00	4.6	Quairading	-32.013423	117.395801	semirural2	663	332,00	50,00	362,00	1,09	0,00	0,00	0,00	0,10	0,00	0,00	0,00	0,00	0,46	NA	NA	NA	NA
262,00	AUSTRALIAN RED FOX WITH DIET	M	2,00	5.85	Boyup Brook	-33.835060	116.388186	semirural1	346	293,00	50,00	719,00	NA	NA	NA	NA	NA	NA	NA	NA	NA	NA	NA	NA	NA	NA
263,00	AUSTRALIAN RED FOX WITH DIET	M	1,00	5.475	Boyup Brook	-33.835060	116.388186	semirural1	346	293,00	50,00	719,00	1,20	0,00	0,00	0,00	0,00	0,00	0,17	0,00	0,23	0,23	NA	NA	NA	NA
264,00	AUSTRALIAN RED FOX WITH DIET	M	1,00	5.395	Boyup Brook	-33.835060	116.388186	semirural1	346	293,00	50,00	719,00	1,57	0,00	0,00	0,00	0,00	0,00	0,00	0,00	0,00	0,00	NA	NA	NA	NA
265,00	AUSTRALIAN RED FOX WITH DIET	M	1,00	7.035	Boyup Brook	-33.835060	116.388186	semirural1	346	293,00	50,00	719,00	0,84	0,00	0,00	0,00	0,00	0,00	0,46	0,00	0,52	0,00	NA	NA	NA	NA
268,00	AUSTRALIAN RED FOX WITH DIET	F	1,00	3.45	Boyup Brook	-33.835060	116.388186	semirural1	346	293,00	50,00	719,00	NA	NA	NA	NA	NA	NA	NA	NA	NA	NA	NA	NA	NA	NA
269,00	AUSTRALIAN RED FOX WITH DIET	F	1,00	4.8	Boyup Brook	-33.835060	116.388186	semirural1	346	293,00	50,00	719,00	0,68	0,00	0,00	0,00	0,00	0,00	0,52	0,00	0,00	0,63	NA	NA	NA	NA
270,00	AUSTRALIAN RED FOX WITH DIET	M	1,00	5.955	Boyup Brook	-33.835060	116.388186	semirural1	346	293,00	50,00	719,00	1,07	0,00	0,00	0,00	0,00	0,00	0,27	0,00	0,00	0,41	NA	NA	NA	NA
271,00	AUSTRALIAN RED FOX WITH DIET	F	1,00	4.725	Boyup Brook	-33.835060	116.388186	semirural1	346	293,00	50,00	719,00	0,89	0,00	0,00	0,00	0,00	0,00	0,46	0,00	0,00	0,46	NA	NA	NA	NA
272,00	AUSTRALIAN RED FOX WITH DIET	M	1,00	6.14	Boyup Brook	-33.835060	116.388186	semirural1	346	293,00	50,00	719,00	0,99	0,00	0,00	0,00	0,00	0,00	0,00	0,00	0,00	0,58	NA	NA	NA	NA
273,00	AUSTRALIAN RED FOX WITH DIET	F	1,00	4.92	Boyup Brook	-33.835060	116.388186	semirural1	346	293,00	50,00	719,00	1,04	0,00	0,00	0,00	0,00	0,00	0,32	0,10	0,32	0,23	NA	NA	NA	NA
275,00	AUSTRALIAN RED FOX WITH DIET	M	1,00	5.79	Boyup Brook	-33.835060	116.388186	semirural1	346	293,00	50,00	719,00	1,57	0,00	0,00	0,00	0,00	0,00	0,00	0,00	0,00	0,00	NA	NA	NA	NA
276,00	AUSTRALIAN RED FOX WITH DIET	F	1,00	3.93	Boyup Brook	-33.835060	116.388186	semirural1	346	293,00	50,00	719,00	NA	NA	NA	NA	NA	NA	NA	NA	NA	NA	NA	NA	NA	NA
277,00	AUSTRALIAN RED FOX WITH DIET	F	1,00	5.31	Boyup Brook	-33.835060	116.388186	semirural1	346	293,00	50,00	719,00	0,89	0,00	0,00	0,00	0,00	0,00	0,10	0,00	0,00	0,67	NA	NA	NA	NA
278,00	AUSTRALIAN RED FOX WITH DIET	F	1,00	5.6	Boyup Brook	-33.835060	116.388186	semirural1	346	293,00	50,00	719,00	0,68	0,00	0,00	0,00	0,00	0,00	0,52	0,00	0,00	0,63	NA	NA	NA	NA
279,00	AUSTRALIAN RED FOX WITH DIET	F	1,00	5.285	Boyup Brook	-33.835060	116.388186	semirural1	346	293,00	50,00	719,00	1,30	0,00	0,00	0,00	0,00	0,00	0,25	0,10	0,00	0,00	NA	NA	NA	NA

						GPA coordinates				Environmental data																Muscle ar			
											Climatic data			Diet (Forbes-Harper et al., 2017)											PCSA			
ID		cat	sex	age	body mass	location	x	y	urban	demographics	bio5	bio6	bio12	sheep	rodent	rabbit	marsupials	bird	reptile/frog	invertebrates	mammal	plant	other	digastric	masseter	temporal	pterygoid
	280,00	AUSTRALIAN RED FOX WITH DIET	F	1,00	4.625	Boyup Brook	-33.835060	116.388186	semirural1	346	293,00	50,00	719,00	0,00	0,00	0,00	0,00	1,11	0,00	0,00	0,00	0,46	0,00	NA	NA	NA	NA
	281,00	AUSTRALIAN RED FOX WITH DIET	F	1,00	4.055	Boyup Brook	-33.835060	116.388186	semirural1	346	293,00	50,00	719,00	1,25	0,25	0,00	0,00	0,00	0,00	0,20	0,00	0,00	0,00	NA	NA	NA	NA
	282,00	AUSTRALIAN RED FOX WITH DIET	M	2,00	6.01	Boyup Brook	-33.835060	116.388186	semirural1	346	293,00	50,00	719,00	1,11	0,00	0,00	0,00	0,23	0,00	0,23	0,00	0,32	0,00	NA	NA	NA	NA
	283,00	AUSTRALIAN RED FOX WITH DIET	M	1,00	5.43	Boyup Brook	-33.835060	116.388186	semirural1	346	293,00	50,00	719,00	0,00	0,00	0,00	1,57	0,00	0,00	0,00	0,00	0,00	0,00	NA	NA	NA	NA
	286,00	AUSTRALIAN RED FOX WITH DIET	M	2,00	6.175	Boyup Brook	-33.835060	116.388186	semirural1	346	293,00	50,00	719,00	0,96	0,00	0,00	0,00	0,17	0,00	0,23	0,00	0,52	0,00	NA	NA	NA	NA
	287,00	AUSTRALIAN RED FOX WITH DIET	M	1,00	5.27	Boyup Brook	-33.835060	116.388186	semirural1	346	293,00	50,00	719,00	0,46	0,00	0,00	0,00	0,00	0,00	0,67	0,10	0,00	0,68	NA	NA	NA	NA
	288,00	AUSTRALIAN RED FOX WITH DIET	F	1,00	5.18	Boyup Brook	-33.835060	116.388186	semirural1	346	293,00	50,00	719,00	0,00	0,00	0,00	0,00	0,23	0,00	0,00	0,00	1,25	0,23	NA	NA	NA	NA
	289,00	AUSTRALIAN RED FOX WITH DIET	M	1,00	4.78	Boyup Brook	-33.835060	116.388186	semirural1	346	293,00	50,00	719,00	0,68	0,00	0,00	0,00	0,00	0,00	0,79	0,00	0,00	0,32	NA	NA	NA	NA
	290,00	AUSTRALIAN RED FOX WITH DIET	M	4+	6.74	Boyup Brook	-33.835060	116.388186	semirural1	346	293,00	50,00	719,00	0,00	0,00	0,00	0,00	0,00	0,00	0,00	0,00	1,57	0,00	NA	NA	NA	NA
	291,00	AUSTRALIAN RED FOX WITH DIET	F	2,00	5.55	Boyup Brook	-33.835060	116.388186	semirural1	346	293,00	50,00	719,00	1,17	0,00	0,00	0,00	0,00	0,00	0,00	0,00	0,00	0,40	NA	NA	NA	NA
	292,00	AUSTRALIAN RED FOX WITH DIET	F	3,00	4.9	Boyup Brook	-33.835060	116.388186	semirural1	346	293,00	50,00	719,00	1,17	0,00	0,00	0,00	0,00	0,00	0,14	0,00	0,32	0,17	NA	NA	NA	NA
	293,00	AUSTRALIAN RED FOX WITH DIET	M	1,00	6.34	Boyup Brook	-33.835060	116.388186	semirural1	346	293,00	50,00	719,00	1,17	0,00	0,00	0,00	0,23	0,23	0,10	0,00	0,20	0,00	NA	NA	NA	NA
	294,00	AUSTRALIAN RED FOX WITH DIET	M	1,00	7.195	Boyup Brook	-33.835060	116.388186	semirural1	346	293,00	50,00	719,00	1,37	0,00	0,00	0,00	0,00	0,00	0,00	0,10	0,17	0,00	NA	NA	NA	NA
	296,00	AUSTRALIAN RED FOX WITH DIET	M	1,00	6.265	Boyup Brook	-33.835060	116.388186	semirural1	346	293,00	50,00	719,00	0,32	0,00	0,00	0,00	1,17	0,00	0,00	0,00	0,23	0,00	NA	NA	NA	NA
	297,00	AUSTRALIAN RED FOX WITH DIET	M	1,00	6.59	Boyup Brook	-33.835060	116.388186	semirural1	346	293,00	50,00	719,00	0,23	0,00	0,00	0,00	1,32	0,00	0,00	0,00	0,00	0,10	NA	NA	NA	NA
	298,00	AUSTRALIAN RED FOX WITH DIET	M	2,00	7.15	Boyup Brook	-33.835060	116.388186	semirural1	346	293,00	50,00	719,00	1,35	0,00	0,00	0,00	0,00	0,00	0,14	0,00	0,17	0,00	NA	NA	NA	NA
	299,00	AUSTRALIAN RED FOX WITH DIET	F	1,00	4.025	Boyup Brook	-33.835060	116.388186	semirural1	346	293,00	50,00	719,00	1,35	0,00	0,00	0,00	0,00	0,00	0,10	0,10	0,17	0,00	NA	NA	NA	NA
	300,00	AUSTRALIAN RED FOX WITH DIET	M	1,00	4.725	Boyup Brook	-33.835060	116.388186	semirural1	346	293,00	50,00	719,00	1,11	0,00	0,00	0,00	0,00	0,00	0,44	0,00	0,14	0,00	NA	NA	NA	NA
	302,00	AUSTRALIAN RED FOX WITH DIET	M	1,00	5.91	Boyup Brook	-33.835060	116.388186	semirural1	346	293,00	50,00	719,00	0,58	0,59	0,00	0,00	0,00	0,00	0,67	0,00	0,00	0,00	NA	NA	NA	NA
	304,00	AUSTRALIAN RED FOX WITH DIET	F	1,00	4.45	Boyup Brook	-33.835060	116.388186	semirural1	346	293,00	50,00	719,00	NA	NA	NA	NA	NA	NA	NA	NA	NA	NA	NA	NA	NA	NA
	305,00	AUSTRALIAN RED FOX WITH DIET	F	1,00	4.59	Boyup Brook	-33.835060	116.388186	semirural1	346	293,00	50,00	719,00	1,40	0,00	0,00	0,00	0,00	0,00	0,14	0,00	0,00	0,10	NA	NA	NA	NA
	306,00	AUSTRALIAN RED FOX WITH DIET	M	2,00	7.04	Boyup Brook	-33.835060	116.388186	semirural1	346	293,00	50,00	719,00	1,57	0,00	0,00	0,00	0,00	0,00	0,00	0,00	0,00	0,00	NA	NA	NA	NA
	307,00	AUSTRALIAN RED FOX WITH DIET	M	1,00	6.39	Boyup Brook	-33.835060	116.388186	semirural1	346	293,00	50,00	719,00	1,57	0,00	0,00	0,00	0,00	0,00	0,00	0,00	0,00	0,00	NA	NA	NA	NA
	308,00	AUSTRALIAN RED FOX WITH DIET	M	4+	7.55	Boyup Brook	-33.835060	116.388186	semirural1	346	293,00	50,00	719,00	1,35	0,00	0,00	0,00	0,00	0,00	0,00	0,00	0,23	0,00	NA	NA	NA	NA
	309,00	AUSTRALIAN RED FOX WITH DIET	F	2,00	5.275	Boyup Brook	-33.835060	116.388186	semirural1	346	293,00	50,00	719,00	1,17	0,23	0,00	0,00	0,00	0,00	0,00	0,00	0,32	0,00	NA	NA	NA	NA
	310,00	AUSTRALIAN RED FOX WITH DIET	M	1,00	4.58	Boyup Brook	-33.835060	116.388186	semirural1	346	293,00	50,00	719,00	0,68	0,00	0,85	0,00	0,00	0,00	0,10	0,00	0,00	0,17	NA	NA	NA	NA
	311,00	AUSTRALIAN RED FOX WITH DIET	F	1,00	4.985	Boyup Brook	-33.835060	116.388186	semirural1	346	293,00	50,00	719,00	0,79	0,00	0,00	0,00	0,00	0,00	0,79	0,00	0,00	0,00	NA	NA	NA	NA
	312,00	AUSTRALIAN RED FOX WITH DIET	F	1,00	3.42	Boyup Brook	-33.835060	116.388186	semirural1	346	293,00	50,00	719,00	NA	NA	NA	NA	NA	NA	NA	NA	NA	NA	NA	NA	NA	NA
	313,00	AUSTRALIAN RED FOX WITH DIET	M	4+	5.915	Boyup Brook	-33.835060	116.388186	semirural1	346	293,00	50,00	719,00	0,79	0,17	0,00	0,00	0,40	0,00	0,27	0,00	0,52	0,00	NA	NA	NA	NA
	315,00	AUSTRALIAN RED FOX WITH DIET	M	2,00	6.57	Boyup Brook	-33.835060	116.388186	semirural1	346	293,00	50,00	719,00	0,73	0,62	0,00	0,00	0,41	0,00	0,11	0,00	0,24	0,00	NA	NA	NA	NA
	316,00	AUSTRALIAN RED FOX WITH DIET	M	1,00	5.215	Boyup Brook	-33.835060	116.388186	semirural1	346	293,00	50,00	719,00	0,63	0,00	0,00	0,00	0,00	0,00	0,52	0,00	0,00	0,68	NA	NA	NA	NA
	317,00	AUSTRALIAN RED FOX WITH DIET	F	1,00	3.93	Boyup Brook	-33.835060	116.388186	semirural1	346	293,00	50,00	719,00	0,46	0,00	0,00	0,00	1,11	0,00	0,00	0,00	0,00	0,00	NA	NA	NA	NA
	318,00	AUSTRALIAN RED FOX WITH DIET	F	2,00	5.205	Boyup Brook	-33.835060	116.388186	semirural1	346	293,00	50,00	719,00	1,47	0,00	0,00	0,00	0,00	0,00	0,10	0,00	0,00	0,00	NA	NA	NA	NA
	319,00	AUSTRALIAN RED FOX WITH DIET	F	1,00	5.66	Boyup Brook	-33.835060	116.388186	semirural1	346	293,00	50,00	719,00	1,47	0,00	0,00	0,00	0,00	0,00	0,00	0,10	0,00	0,00	NA	NA	NA	NA
	321,00	AUSTRALIAN RED FOX WITH DIET	M	2,00	8.1	Boyup Brook	-33.835060	116.388186	semirural1	346	293,00	50,00	719,00	0,74	0,63	0,00	0,00	0,14	0,00	0,23	0,00	0,32	0,17	NA	NA	NA	NA
	341,00	AUSTRALIAN RED FOX WITH DIET	F	2,00	4.215	Boyup Brook	-33.835060	116.388186	semirural1	346	293,00	50,00	719,00	0,32	0,52	0,00	0,00	0,00	0,00	0,00	0,00	0,94	0,00	NA	NA	NA	NA
	342,00	AUSTRALIAN RED FOX WITH DIET	F	1,00	4.098	Armadale	-32.147053	116.002545	urban	45952	312,00	78,00	962,00	0,99	0,00	0,00	0,00	0,00	0,00	0,58	0,00	0,00	0,00	NA	NA	NA	NA
	343,00	AUSTRALIAN RED FOX WITH DIET	M	1,00	6.365	Armadale	-32.147053	116.002545	urban	45952	312,00	78,00	962,00	NA	NA	NA	NA	NA	NA	NA	NA	NA	NA	NA	NA	NA	NA
	348,00	AUSTRALIAN RED FOX WITH DIET	M	1,00	4.85	Williams-Darkan	-33.263573	116.770016	rural	18	307,00	48,00	540,00	0,84	0,14	0,00	0,00	0,00	0,00	0,46	0,00	0,44	0,23	NA	NA	NA	NA
	352,00	AUSTRALIAN RED FOX WITH DIET	F	2,00	5.26	Gingin	-31.349781	115.906833	semirural2	788	322,00	80,00	700,00	0,00	0,00	0,00	0,00	0,00	0,00	1,57	0,00	0,00	0,00	NA	NA	NA	NA
	354,00	AUSTRALIAN RED FOX WITH DIET	F	2,00	5.355	Gingin	-31.349781	115.906833	semirural2	788	322,00	80,00	700,00	0,00	0,10	0,00	0,00	0,00	0,00	1,47	0,00	0,00	0,00	NA	NA	NA	NA
	357,00	AUSTRALIAN RED FOX WITH DIET	M	2,00	6.345	Gingin	-31.349781	115.906833	semirural2	788	322,00	80,00	700,00	1,11	0,00	0,00	0,00	0,00	0,00	0,29	0,00	0,00	0,35	NA	NA	NA	NA
	358,00	AUSTRALIAN RED FOX WITH DIET	M	4+	6.445	Gingin	-31.349781	115.906833	semirural2	788	322,00	80,00	700,00	1,11	0,00	0,00	0,00	0,32	0,00	0,32	0,00	0,00	0,00	NA	NA	NA	NA
	360,00	AUSTRALIAN RED FOX WITH DIET	M	2,00	7.245	Gingin	-31.349781	115.906833	semirural2	788	322,00	80,00	700,00	0,58	0,00	0,00	0,00	0,00	0,00	0,99	0,00	0,00	0,00	NA	NA	NA	NA
	363,00	AUSTRALIAN RED FOX WITH DIET	F	4+	7.03	Gingin	-31.349781	115.906833	semirural2	788	322,00	80,00	700,00	0,23	0,00	0,00	0,00	0,00	0,00	1,35	0,00	0,00	0,00	NA	NA	NA	NA
	364,00	AUSTRALIAN RED FOX WITH DIET	M	4+	6.405	Gingin	-31.349781	115.906833	semirural2	788	322,00	80,00	700,00	1,57	0,00	0,00	0,00	0,00	0,00	0,00	0,00	0,00	0,00	NA	NA	NA	NA
	368,00	AUSTRALIAN RED FOX WITH DIET	F	1,00	3.945	Gingin	-31.349781	115.906833	semirural2	788	322,00	80,00	700,00	1,57	0,00	0,00	0,00	0,00	0,00	0,00	0,00	0,00	0,00	NA	NA	NA	NA
	371,00	AUSTRALIAN RED FOX WITH DIET	M	2,00	6.22	Gingin	-31.349781	115.906833	semirural2	788	322,00	80,00	700,00	1,05	0,00	0,00	0,00	0,00	0,00	0,00	0,00	0,00	0,52	NA	NA	NA	NA
	372,00	AUSTRALIAN RED FOX WITH DIET	M	1,00	5.685	Gingin	-31.349781	115.906833	semirural2	788	322,00	80,00	700,00	1,57	0,00	0,00	0,00	0,00	0,00	0,00	0,00	0,00	0,00	NA	NA	NA	NA
	373,00	AUSTRALIAN RED FOX WITH DIET	F	2,00	6.185	Gingin	-31.349781	115.906833	semirural2	788	322,00	80,00	700,00	1,11	0,00	0,00	0,00	0,00	0,00	0,32	0,00	0,00	0,32	NA	NA	NA	NA
	375,00	AUSTRALIAN RED FOX WITH DIET	F	2,00	5.415	Gingin	-31.349781	115.906833	semirural2	788	322,00	80,00	700,00	0,68	0,00	0,00	0,00	0,00	0,00	0,89	0,00	0,00	0,00	NA	NA	NA	NA
	379,00	AUSTRALIAN RED FOX WITH DIET	M	1,00	5.755	Gingin	-31.349781	115.906833	semirural2	788	322,00	80,00	700,00	1,37	0,00	0,00	0,00	0,00	0,00	0,14	0,00	0,10	0,10	NA	NA	NA	NA
	380,00	AUSTRALIAN RED FOX WITH DIET	M	1,00	4.82	Gingin	-31.349781	115.906833	semirural2	788	322,00	80,00	700,00	1,25	0,00	0,00	0,00	0,00	0,00	0,32	0,00	0,00	0,00	NA	NA	NA	NA
	386,00	AUSTRALIAN RED FOX WITH DIET	F	NA	4.78	Williams-Darkan	-33.263573	116.770016	rural	18	307,00	48,00	540,00	0,79	0,00	0,00	0,00	0,00	0,00	0,79	0,00	0,00	0,00	NA	NA	NA	NA
	389,00	AUSTRALIAN RED FOX WITH DIET	M	NA	6.54	Kemerton	-33.238566	115.746079	urban	10182	305,00	68,00	855,00	0,32	0,00	0,00	0,00	1,17	0,00	0,00	0,00	0,00	0,23	NA	NA	NA	NA
	391,00	AUSTRALIAN RED FOX WITH DIET	F	NA	3.945	Quindanning-Darkan	-33.261074	116.650991	rural	18	304,00	43,00	604,00	0,00	0,00	0,00	0,00	0,00	0,00	0,00	0,00	0,00	1,57	NA	NA	NA	NA
	394,00	AUSTRALIAN RED FOX WITH DIET	M	NA	5.9	Quindanning-Darkan	-33.261074	116.650991	rural	18	304,00	43,00	604,00	NA	NA	NA	NA	NA	NA	NA	NA	NA	NA	NA	NA	NA	NA
	395,00	AUSTRALIAN RED FOX WITH DIET	F	NA	5.83	Darkan	-33.33516	116.732931	semirural1	235	303,00	46,00	558,00	0,40	0,00	0,00	0,00	0,00	0,17	0,68	0,00	0,00	0,71	NA	NA	NA	NA
	396,00	AUSTRALIAN RED FOX WITH DIET	M	NA	2.05	Quindanning-Darkan	-33.261074	116.650991	rural	18	304,00	43,00	604,00	NA	NA	NA	NA	NA	NA	NA	NA	NA	NA	NA	NA	NA	NA
	397,00	AUSTRALIAN RED FOX WITH DIET	M	NA	2.495	Quindanning-Darkan	-33.261074	116.650991	rural	18	304,00	43,00	604,00	1,57	0,00	0,00	0,00	0,00	0,00	0,00	0,00	0,00	0,00	NA	NA	NA	NA
	399,00	AUSTRALIAN RED FOX WITH DIET	M	NA	6.478	Williams-Darkan	-33.263573	116.770016	rural	18	307,00	48,00	540,00	NA	NA	NA	NA	NA	NA	NA	NA	NA	NA	NA	NA	NA	NA
	400,00	AUSTRALIAN RED FOX WITH DIET	F	NA	5.385	Williams-Darkan	-33.263573	116.770016	rural	18	307,00	48,00	540,00	0,77	0,00	0,10	0,00	0,00	0,00	0,32	0,00	0,00	0,69	NA	NA	NA	NA
Co01		AUSTRALIAN RED FOX WITH DIET	F	4+	4.635	Corrigin	-32.305662	117.783758	semirural2	668	319,00	44,00	352,00	0,00	1,57	0,00	0,00	0,00	0,00	0,00	0,00	0,00	0,00	NA	NA	NA	NA
Co03		AUSTRALIAN RED FOX WITH DIET	F	4+	4.85	Corrigin	-32.305662	117.783758	semirural2	668	319,00	44,00	352,00	1,25	0,00	0,00	0,00	0,00	0,00	0,32	0,00	0,00	0,00	NA	NA	NA	NA
Co04		AUSTRALIAN RED FOX WITH DIET	F	3,00	5.29	Corrigin	-32.305662	117.783758	semirural2	668	319,00	44,00	352,00	0,00	0,68	0,00	0,00	0,89	0,00	0,00	0,00	0,00	0,00	NA	NA	NA	NA
Co05		AUSTRALIAN RED FOX WITH DIET	M	3,00	6.91	Corrigin	-32.305662	117.783758	semirural2	668	319,00	44,00	352,00	0,99	0,58	0,00	0,00	0,00	0,00	0,00	0,00	0,00	0,00	NA	NA	NA	NA
Co06		AUSTRALIAN RED FOX WITH DIET	F	2,00	5.26	Corrigin	-32.305662	117.783758	semirural2	668	319,00	44,00	352,00	0,10	0,10	0,00	0,00	0,00	0,00	1,40	0,00	0,10	0,00	NA	NA	NA	NA
Co07		AUSTRALIAN RED FOX WITH DIET	M	1,00	4.61	Corrigin	-32.305662	117.783758	semirural2	668	319,00	44,00	352,00	0,10	0,00	0,00	0,00	0,00	0,00	1,47	0,00	0,00	0,00	NA	NA	NA	NA
Co08		AUSTRALIAN RED FOX WITH DIET	M	2,00	5.125	Corrigin	-32.305662	117.783758	semirural2	668	319,00	44,00	352,00	0,91	0,46	0,00	0,00	0,00	0,00	0,44	0,00	0,00	0,00	NA	NA	NA	NA
Co09		AUSTRALIAN RED FOX WITH DIET	F	1,00	3.865	Corrigin	-32.305662	117.783758	semirural2	668	319,00	44,00	352,00	0,00	0,46	0,00	0,00	0,00	0,00	0,00	0,00	1,11	0,00	NA	NA	NA	NA
Co10		AUSTRALIAN RED FOX WITH DIET	M	2,00	5.18	Corrigin	-32.305662	117.783758	semirural2	668	319,00	44,00	352,00	1,43	0,10	0,00	0,00	0,00	0,00	0,10	0,00	0,00	0,00	NA	NA	NA	NA
Co11		AUSTRALIAN RED FOX WITH DIET	F	4+	4.95	Corrigin	-32.305662	117.783758	semirural2	668	319,00	44,00	352,00	0,00	0,32	0,00	0,00	0,00	0,00	1,25	0,00	0,00	0,00	NA	NA	NA	NA

										Environmental data																Muscle ar			
					GPA coordinates					Climatic data			Diet (Forbes-Harper et al., 2017)												PCSA			
ID	cat	sex	age	body mass	location	x	y	urban	demographics	bio5	bio6	bio12	sheep	rodent	rabbit	marsupials	bird	reptile/frog	invertebrates	mammal	plant	other	digastric	masseter	temporal	pterygoid
Co12	AUSTRALIAN RED FOX WITH DIET	M	4+	6.595	Corrigin	-32.305662	117.783758	semirural2	668	319,00	44,00	352,00	0,32	0,46	0,00	0,00	0,10	0,00	0,00	0,00	0,98	0,00	NA	NA	NA	NA
Co15	AUSTRALIAN RED FOX WITH DIET	F	1,00	2.8	Corrigin	-32.305662	117.783758	semirural2	668	319,00	44,00	352,00	0,68	0,79	0,00	0,00	0,00	0,14	0,29	0,00	0,00	0,00	NA	NA	NA	NA
Co16	AUSTRALIAN RED FOX WITH DIET	F	2,00	4.269	Corrigin	-32.305662	117.783758	semirural2	668	319,00	44,00	352,00	0,00	1,25	0,00	0,00	0,00	0,00	0,32	0,00	0,00	0,00	NA	NA	NA	NA
Co17	AUSTRALIAN RED FOX WITH DIET	M	1,00	3.25	Corrigin	-32.305662	117.783758	semirural2	668	319,00	44,00	352,00	0,00	0,27	0,00	0,00	0,00	0,00	0,17	0,00	1,25	0,00	NA	NA	NA	NA
Co18	AUSTRALIAN RED FOX WITH DIET	M	4+	4.41	Corrigin	-32.305662	117.783758	semirural2	668	319,00	44,00	352,00	0,00	0,00	0,00	0,00	0,00	0,00	0,00	0,00	0,00	1,57	NA	NA	NA	NA
Da01	AUSTRALIAN RED FOX WITH DIET	M	1,00	5.06	Darkan	-33.33516	116.732931	semirural1	235	303,00	46,00	558,00	1,57	0,00	0,00	0,00	0,00	0,00	0,00	0,00	0,00	0,00	NA	NA	NA	NA
Da02	AUSTRALIAN RED FOX WITH DIET	M	3,00	7.41	Darkan	-33.33516	116.732931	semirural1	235	303,00	46,00	558,00	NA	NA	NA	NA	NA	NA	NA	NA	NA	NA	NA	NA	NA	NA
Da03	AUSTRALIAN RED FOX WITH DIET	M	1,00	NA	Darkan	-33.33516	116.732931	semirural1	235	303,00	46,00	558,00	1,28	0,00	0,00	0,14	0,00	0,10	0,23	0,00	0,00	0,00	NA	NA	NA	NA
Da04	AUSTRALIAN RED FOX WITH DIET	F	1,00	3.935	Darkan	-33.33516	116.732931	semirural1	235	303,00	46,00	558,00	0,00	1,23	0,00	0,00	0,00	0,29	0,10	0,10	0,00	0,10	NA	NA	NA	NA
Da05	AUSTRALIAN RED FOX WITH DIET	M	1,00	5.245	Darkan	-33.33516	116.732931	semirural1	235	303,00	46,00	558,00	1,43	0,00	0,00	0,00	0,00	0,00	0,10	0,00	0,10	0,00	NA	NA	NA	NA
Da06	AUSTRALIAN RED FOX WITH DIET	F	1,00	4.975	Darkan	-33.33516	116.732931	semirural1	235	303,00	46,00	558,00	NA	NA	NA	NA	NA	NA	NA	NA	NA	NA	NA	NA	NA	NA
Da07	AUSTRALIAN RED FOX WITH DIET	M	1,00	4.67	Darkan	-33.33516	116.732931	semirural1	235	303,00	46,00	558,00	1,40	0,00	0,00	0,00	0,00	0,00	0,17	0,00	0,00	0,00	NA	NA	NA	NA
Da08	AUSTRALIAN RED FOX WITH DIET	M	1,00	6.4	Darkan	-33.33516	116.732931	semirural1	235	303,00	46,00	558,00	1,25	0,00	0,00	0,00	0,00	0,00	0,23	0,00	0,00	0,23	NA	NA	NA	NA
Da09	AUSTRALIAN RED FOX WITH DIET	M	1,00	4.62	Darkan	-33.33516	116.732931	semirural1	235	303,00	46,00	558,00	1,47	0,00	0,00	0,00	0,00	0,00	0,00	0,00	0,00	0,10	NA	NA	NA	NA
Da10	AUSTRALIAN RED FOX WITH DIET	M	1,00	6.775	Darkan	-33.33516	116.732931	semirural1	235	303,00	46,00	558,00	1,43	0,00	0,00	0,00	0,00	0,00	0,10	0,00	0,00	0,10	NA	NA	NA	NA
Da100	AUSTRALIAN RED FOX WITH DIET	M	2,00	5.695	Darkan	-33.33516	116.732931	semirural1	235	303,00	46,00	558,00	0,58	0,79	0,00	0,00	0,00	0,00	0,32	0,00	0,32	0,00	NA	NA	NA	NA
Da101	AUSTRALIAN RED FOX WITH DIET	M	1,00	4.075	Darkan	-33.33516	116.732931	semirural1	235	303,00	46,00	558,00	0,00	0,00	0,00	0,00	0,00	0,00	1,11	0,00	0,46	0,00	NA	NA	NA	NA
Da104	AUSTRALIAN RED FOX WITH DIET	F	1,00	4.19	Darkan	-33.33516	116.732931	semirural1	235	303,00	46,00	558,00	0,79	0,00	0,00	0,00	0,00	0,00	0,74	0,00	0,23	0,00	NA	NA	NA	NA
Da105	AUSTRALIAN RED FOX WITH DIET	F	2,00	5.46	Darkan	-33.33516	116.732931	semirural1	235	303,00	46,00	558,00	0,79	0,00	0,00	0,00	0,10	0,00	0,00	0,00	0,78	0,00	NA	NA	NA	NA
Da106	AUSTRALIAN RED FOX WITH DIET	M	1,00	4.13	Darkan	-33.33516	116.732931	semirural1	235	303,00	46,00	558,00	1,57	0,00	0,00	0,00	0,00	0,00	0,00	0,00	0,00	0,00	NA	NA	NA	NA
Da107	AUSTRALIAN RED FOX WITH DIET	F	1,00	3.04	Darkan	-33.33516	116.732931	semirural1	235	303,00	46,00	558,00	1,57	0,00	0,00	0,00	0,00	0,00	0,00	0,00	0,00	0,00	NA	NA	NA	NA
Da108	AUSTRALIAN RED FOX WITH DIET	F	1,00	3.24	Darkan	-33.33516	116.732931	semirural1	235	303,00	46,00	558,00	0,79	0,00	0,00	0,00	0,79	0,00	0,00	0,00	0,00	0,00	NA	NA	NA	NA
Da109	AUSTRALIAN RED FOX WITH DIET	F	1,00	3.735	Darkan	-33.33516	116.732931	semirural1	235	303,00	46,00	558,00	1,35	0,00	0,00	0,00	0,00	0,00	0,10	0,00	0,14	0,14	NA	NA	NA	NA
Da11	AUSTRALIAN RED FOX WITH DIET	F	2,00	5.555	Darkan	-33.33516	116.732931	semirural1	235	303,00	46,00	558,00	1,40	0,00	0,00	0,00	0,00	0,00	0,14	0,00	0,00	0,10	NA	NA	NA	NA
Da111	AUSTRALIAN RED FOX WITH DIET	F	1,00	5.06	Darkan	-33.33516	116.732931	semirural1	235	303,00	46,00	558,00	1,11	0,40	0,00	0,00	0,00	0,00	0,00	0,00	0,00	0,23	NA	NA	NA	NA
Da112	AUSTRALIAN RED FOX WITH DIET	M	1,00	3.94	Darkan	-33.33516	116.732931	semirural1	235	303,00	46,00	558,00	0,89	0,00	0,00	0,00	0,00	0,00	0,58	0,00	0,32	0,00	NA	NA	NA	NA
Da113	AUSTRALIAN RED FOX WITH DIET	M	2,00	4.81	Darkan	-33.33516	116.732931	semirural1	235	303,00	46,00	558,00	1,43	0,00	0,00	0,00	0,00	0,00	0,10	0,00	0,10	0,00	NA	NA	NA	NA
Da114	AUSTRALIAN RED FOX WITH DIET	F	1,00	4.38	Darkan	-33.33516	116.732931	semirural1	235	303,00	46,00	558,00	0,00	1,57	0,00	0,00	0,00	0,00	0,00	0,00	0,00	0,00	NA	NA	NA	NA
Da115	AUSTRALIAN RED FOX WITH DIET	F	NA	5.09	Darkan	-33.33516	116.732931	semirural1	235	303,00	46,00	558,00	0,98	0,58	0,00	0,00	0,10	0,00	0,00	0,00	0,00	0,00	NA	NA	NA	NA
Da116	AUSTRALIAN RED FOX WITH DIET	M	1,00	5.06	Darkan	-33.33516	116.732931	semirural1	235	303,00	46,00	558,00	1,35	0,00	0,00	0,00	0,00	0,00	0,14	0,00	0,17	0,00	NA	NA	NA	NA
Da117	AUSTRALIAN RED FOX WITH DIET	M	1,00	4.71	Darkan	-33.33516	116.732931	semirural1	235	303,00	46,00	558,00	1,57	0,00	0,00	0,00	0,00	0,00	0,00	0,00	0,00	0,00	NA	NA	NA	NA
Da118	AUSTRALIAN RED FOX WITH DIET	F	1,00	4.57	Darkan	-33.33516	116.732931	semirural1	235	303,00	46,00	558,00	0,00	0,00	0,00	0,00	0,00	0,00	1,11	0,00	0,46	0,00	NA	NA	NA	NA
Da119	AUSTRALIAN RED FOX WITH DIET	F	1,00	4.035	Darkan	-33.33516	116.732931	semirural1	235	303,00	46,00	558,00	1,47	0,00	0,00	0,00	0,00	0,00	0,00	0,00	0,10	0,00	NA	NA	NA	NA
Da12	AUSTRALIAN RED FOX WITH DIET	F	2,00	6.095	Darkan	-33.33516	116.732931	semirural1	235	303,00	46,00	558,00	1,43	0,00	0,00	0,00	0,00	0,14	0,00	0,00	0,00	0,00	NA	NA	NA	NA
Da121	AUSTRALIAN RED FOX WITH DIET	F	1,00	4.63	Darkan	-33.33516	116.732931	semirural1	235	303,00	46,00	558,00	1,25	0,00	0,00	0,00	0,00	0,00	0,00	0,00	0,32	0,00	NA	NA	NA	NA
Da124	AUSTRALIAN RED FOX WITH DIET	F	1,00	4.605	Darkan	-33.33516	116.732931	semirural1	235	303,00	46,00	558,00	1,35	0,00	0,00	0,00	0,00	0,00	0,00	0,00	0,23	0,00	NA	NA	NA	NA
Da125	AUSTRALIAN RED FOX WITH DIET	M	2,00	5.42	Darkan	-33.33516	116.732931	semirural1	235	303,00	46,00	558,00	0,84	0,00	0,00	0,00	0,00	0,58	0,23	0,00	0,32	0,00	NA	NA	NA	NA
Da126	AUSTRALIAN RED FOX WITH DIET	F	1,00	4.31	Darkan	-33.33516	116.732931	semirural1	235	303,00	46,00	558,00	1,47	0,00	0,00	0,00	0,00	0,00	0,00	0,00	0,10	0,00	NA	NA	NA	NA
Da129	AUSTRALIAN RED FOX WITH DIET	M	2,00	7.06	Darkan	-33.33516	116.732931	semirural1	235	303,00	46,00	558,00	1,57	0,00	0,00	0,00	0,00	0,00	0,00	0,00	0,00	0,00	NA	NA	NA	NA
Da131	AUSTRALIAN RED FOX WITH DIET	F	1,00	3.135	Darkan	-33.33516	116.732931	semirural1	235	303,00	46,00	558,00	0,89	0,00	0,68	0,00	0,00	0,00	0,00	0,00	0,00	0,00	NA	NA	NA	NA
Da132	AUSTRALIAN RED FOX WITH DIET	F	1,00	4.51	Darkan	-33.33516	116.732931	semirural1	235	303,00	46,00	558,00	0,93	0,00	0,00	0,00	0,40	0,00	0,48	0,00	0,00	0,00	NA	NA	NA	NA
Da135	AUSTRALIAN RED FOX WITH DIET	M	1,00	4.37	Darkan	-33.33516	116.732931	semirural1	235	303,00	46,00	558,00	1,30	0,00	0,00	0,00	0,00	0,00	0,17	0,00	0,17	0,10	NA	NA	NA	NA
Da136	AUSTRALIAN RED FOX WITH DIET	M	1,00	3.43	Darkan	-33.33516	116.732931	semirural1	235	303,00	46,00	558,00	0,99	0,46	0,00	0,00	0,00	0,00	0,23	0,23	0,00	0,00	NA	NA	NA	NA
Da137	AUSTRALIAN RED FOX WITH DIET	M	1,00	5.83	Darkan	-33.33516	116.732931	semirural1	235	303,00	46,00	558,00	0,94	0,58	0,00	0,00	0,00	0,00	0,23	0,00	0,00	0,00	NA	NA	NA	NA
Da139	AUSTRALIAN RED FOX WITH DIET	M	1,00	4.87	Darkan	-33.33516	116.732931	semirural1	235	303,00	46,00	558,00	1,57	0,00	0,00	0,00	0,00	0,00	0,00	0,00	0,00	0,00	NA	NA	NA	NA
Da140	AUSTRALIAN RED FOX WITH DIET	M	1,00	5.575	Darkan	-33.33516	116.732931	semirural1	235	303,00	46,00	558,00	0,99	0,58	0,00	0,00	0,00	0,00	0,00	0,00	0,00	0,00	NA	NA	NA	NA
Da141	AUSTRALIAN RED FOX WITH DIET	M	1,00	4.76	Darkan	-33.33516	116.732931	semirural1	235	303,00	46,00	558,00	1,47	0,00	0,00	0,00	0,00	0,00	0,10	0,00	0,00	0,00	NA	NA	NA	NA
Da143	AUSTRALIAN RED FOX WITH DIET	M	2,00	5.8	Darkan	-33.33516	116.732931	semirural1	235	303,00	46,00	558,00	0,00	0,00	0,00	0,00	0,00	0,00	0,32	0,00	1,25	0,00	NA	NA	NA	NA
Da145	AUSTRALIAN RED FOX WITH DIET	F	1,00	4.27	Darkan	-33.33516	116.732931	semirural1	235	303,00	46,00	558,00	1,23	0,00	0,00	0,00	0,00	0,00	0,10	0,00	0,32	0,00	NA	NA	NA	NA
Da146	AUSTRALIAN RED FOX WITH DIET	F	1,00	4.32	Darkan	-33.33516	116.732931	semirural1	235	303,00	46,00	558,00	1,09	0,00	0,00	0,00	0,10	0,00	0,32	0,00	0,32	0,00	NA	NA	NA	NA
Da148	AUSTRALIAN RED FOX WITH DIET	M	1,00	4.68	Darkan	-33.33516	116.732931	semirural1	235	303,00	46,00	558,00	0,79	0,00	0,00	0,00	0,74	0,00	0,00	0,00	0,23	0,00	NA	NA	NA	NA
Da15	AUSTRALIAN RED FOX WITH DIET	M	1,00	5.54	Darkan	-33.33516	116.732931	semirural1	235	303,00	46,00	558,00	1,40	0,10	0,00	0,00	0,00	0,00	0,10	0,00	0,00	0,10	NA	NA	NA	NA
Da150	AUSTRALIAN RED FOX WITH DIET	M	1,00	4.185	Darkan	-33.33516	116.732931	semirural1	235	303,00	46,00	558,00	0,00	0,00	1,57	0,00	0,00	0,00	0,00	0,00	0,00	0,00	NA	NA	NA	NA
Da151	AUSTRALIAN RED FOX WITH DIET	M	2,00	6.45	Darkan	-33.33516	116.732931	semirural1	235	303,00	46,00	558,00	1,37	0,00	0,00	0,00	0,00	0,00	0,10	0,00	0,00	0,17	NA	NA	NA	NA
Da152	AUSTRALIAN RED FOX WITH DIET	F	4+	6.1	Darkan	-33.33516	116.732931	semirural1	235	303,00	46,00	558,00	1,43	0,00	0,00	0,00	0,00	0,00	0,00	0,00	0,10	0,10	NA	NA	NA	NA
Da154	AUSTRALIAN RED FOX WITH DIET	F	3,00	5.27	Darkan	-33.33516	116.732931	semirural1	235	303,00	46,00	558,00	1,57	0,00	0,00	0,00	0,00	0,00	0,00	0,00	0,00	0,00	NA	NA	NA	NA
Da155	AUSTRALIAN RED FOX WITH DIET	F	1,00	3.98	Darkan	-33.33516	116.732931	semirural1	235	303,00	46,00	558,00	NA	NA	NA	NA	NA	NA	NA	NA	NA	NA	NA	NA	NA	NA
Da156	AUSTRALIAN RED FOX WITH DIET	F	1,00	3.63	Darkan	-33.33516	116.732931	semirural1	235	303,00	46,00	558,00	0,00	0,00	1,37	0,00	0,00	0,10	0,00	0,00	0,10	0,14	NA	NA	NA	NA
Da158	AUSTRALIAN RED FOX WITH DIET	F	1,00	3.96	Darkan	-33.33516	116.732931	semirural1	235	303,00	46,00	558,00	1,25	0,32	0,00	0,00	0,00	0,00	0,00	0,00	0,00	0,00	NA	NA	NA	NA
Da159	AUSTRALIAN RED FOX WITH DIET	M	1,00	3.53	Darkan	-33.33516	116.732931	semirural1	235	303,00	46,00	558,00	1,57	0,00	0,00	0,00	0,00	0,00	0,00	0,00	0,00	0,00	NA	NA	NA	NA
Da16	AUSTRALIAN RED FOX WITH DIET	F	1,00	5.14	Darkan	-33.33516	116.732931	semirural1	235	303,00	46,00	558,00	1,43	0,00	0,00	0,00	0,00	0,00	0,14	0,00	0,00	0,00	NA	NA	NA	NA
Da160	AUSTRALIAN RED FOX WITH DIET	M	2,00	7.105	Darkan	-33.33516	116.732931	semirural1	235	303,00	46,00	558,00	1,57	0,00	0,00	0,00	0,00	0,00	0,00	0,00	0,00	0,00	NA	NA	NA	NA
Da161	AUSTRALIAN RED FOX WITH DIET	M	1,00	3.89	Darkan	-33.33516	116.732931	semirural1	235	303,00	46,00	558,00	1,43	0,00	0,00	0,00	0,00	0,00	0,00	0,00	0,14	0,00	NA	NA	NA	NA
Da162	AUSTRALIAN RED FOX WITH DIET	M	1,00	5.57	Darkan	-33.33516	116.732931	semirural1	235	303,00	46,00	558,00	0,46	0,00	1,11	0,00	0,00	0,00	0,00	0,00	0,00	0,00	NA	NA	NA	NA
Da163	AUSTRALIAN RED FOX WITH DIET	M	1,00	5.43	Darkan	-33.33516	116.732931	semirural1	235	303,00	46,00	558,00	1,47	0,00	0,00	0,00	0,00	0,00	0,00	0,00	0,10	0,00	NA	NA	NA	NA
Da164	AUSTRALIAN RED FOX WITH DIET	F	NA	4.465	Darkan	-33.33516	116.732931	semirural1	235	303,00	46,00	558,00	0,32	0,00	0,00	0,00	0,00	0,00	1,11	0,00	0,32	0,00	NA	NA	NA	NA
Da165	AUSTRALIAN RED FOX WITH DIET	F	1,00	4.12	Darkan	-33.33516	116.732931	semirural1	235	303,00	46,00	558,00	1,35	0,00	0,00	0,00	0,00	0,23	0,00	0,00	0,00	0,00	NA	NA	NA	NA
Da167	AUSTRALIAN RED FOX WITH DIET	M	1,00	4.86	Darkan	-33.33516	116.732931	semirural1	235	303,00	46,00	558,00	1,35	0,00	0,00	0,00	0,00	0,00	0,14	0,00	0,00	0,17	NA	NA	NA	NA
Da17	AUSTRALIAN RED FOX WITH DIET	F	1,00	5.02	Darkan	-33.33516	116.732931	semirural1	235	303,00	46,00	558,00	0,00	0,00	1,47	0,00	0,00	0,00	0,10	0,00	0,00	0,00	NA	NA	NA	NA
Da170	AUSTRALIAN RED FOX WITH DIET	M	1,00	4.02	Darkan	-33.33516	116.732931	semirural1	235	303,00	46,00	558,00	1,40	0,00	0,00	0,00	0,00	0,00	0,10	0,00	0,14	0,00	NA	NA	NA	NA
Da171	AUSTRALIAN RED FOX WITH DIET	M	1,00	5.45	Darkan	-33.33516	116.732931	semirural1	235	303,00	46,00	558,00	1,47	0,00	0,00	0,00	0,00	0,00	0,00	0,00	0,00	0,10	NA	NA	NA	NA
Da172	AUSTRALIAN RED FOX WITH DIET	M	2,00	6.425	Darkan	-33.33516	116.732931	semirural1	235	303,00	46,00	558,00	0,68	0,00	0,00	0,00	0,00	0,00	0,89	0,00	0,00	0,00	NA	NA	NA	NA

										Environmental data																		Muscle ar
					GPA coordinates					Climatic data			Diet (Forbes-Harper et al., 2017)												PCSA			
ID	cat	sex	age	body mass	location	x	y	urban	demographics	bio5	bio6	bio12	sheep	rodent	rabbit	marsupials	bird	reptile/frog	invertebrates	mammal	plant	other	digastric	masseter	temporal	pterygoid
Da173	AUSTRALIAN RED FOX WITH DIET	M	1,00	6.375	Darkan	-33.33516	116.732931	semirural1	235	303,00	46,00	558,00	0,40	0,00	0,00	0,00	0,00	0,00	0,23	0,00	1,09	0,10	NA	NA	NA	NA
Da175	AUSTRALIAN RED FOX WITH DIET	M	1,00	5.77	Darkan	-33.33516	116.732931	semirural1	235	303,00	46,00	558,00	NA	NA	NA	NA	NA	NA	NA	NA	NA	NA	NA	NA	NA	NA	NA
Da177	AUSTRALIAN RED FOX WITH DIET	M	2,00	6.829	Darkan	-33.33516	116.732931	semirural1	235	303,00	46,00	558,00	NA	NA	NA	NA	NA	NA	NA	NA	NA	NA	NA	NA	NA	NA	NA
Da179	AUSTRALIAN RED FOX WITH DIET	F	1,00	4.18	Darkan	-33.33516	116.732931	semirural1	235	303,00	46,00	558,00	0,32	1,25	0,00	0,00	0,00	0,00	0,00	0,00	0,00	0,00	NA	NA	NA	NA
Da18	AUSTRALIAN RED FOX WITH DIET	F	1,00	4.46	Darkan	-33.33516	116.732931	semirural1	235	303,00	46,00	558,00	0,79	0,00	0,00	0,00	0,00	0,00	0,00	0,00	0,00	0,79	NA	NA	NA	NA
Da19	AUSTRALIAN RED FOX WITH DIET	M	1,00	4.77	Darkan	-33.33516	116.732931	semirural1	235	303,00	46,00	558,00	0,00	0,00	0,00	0,00	0,89	0,00	0,68	0,00	0,00	0,00	NA	NA	NA	NA
Da21	AUSTRALIAN RED FOX WITH DIET	F	1,00	4.435	Darkan	-33.33516	116.732931	semirural1	235	303,00	46,00	558,00	0,32	0,00	0,00	0,00	0,00	1,17	0,14	0,00	0,00	0,17	NA	NA	NA	NA
Da22	AUSTRALIAN RED FOX WITH DIET	M	1,00	5.43	Darkan	-33.33516	116.732931	semirural1	235	303,00	46,00	558,00	1,40	0,00	0,00	0,00	0,00	0,00	0,10	0,00	0,10	0,10	NA	NA	NA	NA
Da24	AUSTRALIAN RED FOX WITH DIET	F	2,00	6.22	Darkan	-33.33516	116.732931	semirural1	235	303,00	46,00	558,00	0,00	0,00	1,35	0,00	0,00	0,00	0,00	0,00	0,23	0,00	NA	NA	NA	NA
Da25	AUSTRALIAN RED FOX WITH DIET	F	1,00	3.89	Darkan	-33.33516	116.732931	semirural1	235	303,00	46,00	558,00	1,57	0,00	0,00	0,00	0,00	0,00	0,00	0,00	0,00	0,00	NA	NA	NA	NA
Da26	AUSTRALIAN RED FOX WITH DIET	M	2,00	6.48	Darkan	-33.33516	116.732931	semirural1	235	303,00	46,00	558,00	1,11	0,00	0,00	0,00	0,32	0,00	0,00	0,00	0,00	0,32	NA	NA	NA	NA
Da28	AUSTRALIAN RED FOX WITH DIET	M	1,00	5.245	Darkan	-33.33516	116.732931	semirural1	235	303,00	46,00	558,00	0,00	0,58	0,00	0,00	0,00	0,00	0,00	0,00	0,99	0,00	NA	NA	NA	NA
Da29	AUSTRALIAN RED FOX WITH DIET	M	1,00	5.775	Darkan	-33.33516	116.732931	semirural1	235	303,00	46,00	558,00	1,25	0,00	0,00	0,00	0,00	0,00	0,00	0,00	0,32	0,00	NA	NA	NA	NA
Da32	AUSTRALIAN RED FOX WITH DIET	M	1,00	5.279	Darkan	-33.33516	116.732931	semirural1	235	303,00	46,00	558,00	0,32	0,00	0,00	0,00	1,11	0,00	0,32	0,00	0,00	0,00	NA	NA	NA	NA
Da33	AUSTRALIAN RED FOX WITH DIET	F	1,00	3.855	Darkan	-33.33516	116.732931	semirural1	235	303,00	46,00	558,00	0,00	0,00	0,00	0,00	0,00	0,58	0,68	0,00	0,00	0,58	NA	NA	NA	NA
Da34	AUSTRALIAN RED FOX WITH DIET	M	2,00	6.39	Darkan	-33.33516	116.732931	semirural1	235	303,00	46,00	558,00	1,43	0,00	0,00	0,00	0,00	0,00	0,00	0,00	0,14	0,00	NA	NA	NA	NA
Da35	AUSTRALIAN RED FOX WITH DIET	F	1,00	4,00	Darkan	-33.33516	116.732931	semirural1	235	303,00	46,00	558,00	0,00	0,00	0,00	0,00	0,23	0,00	0,84	0,00	0,68	0,00	NA	NA	NA	NA
Da38	AUSTRALIAN RED FOX WITH DIET	M	1,00	4.825	Darkan	-33.33516	116.732931	semirural1	235	303,00	46,00	558,00	0,00	0,46	0,00	0,00	0,00	0,00	0,00	0,00	1,11	0,00	NA	NA	NA	NA
Da39	AUSTRALIAN RED FOX WITH DIET	M	1,00	4.83	Darkan	-33.33516	116.732931	semirural1	235	303,00	46,00	558,00	NA	NA	NA	NA	NA	NA	NA	NA	NA	NA	NA	NA	NA	NA	NA
Da40	AUSTRALIAN RED FOX WITH DIET	M	1,00	5.995	Darkan	-33.33516	116.732931	semirural1	235	303,00	46,00	558,00	0,32	0,00	0,00	0,00	1,25	0,00	0,00	0,00	0,00	0,00	NA	NA	NA	NA
Da41	AUSTRALIAN RED FOX WITH DIET	M	2,00	5.33	Darkan	-33.33516	116.732931	semirural1	235	303,00	46,00	558,00	1,57	0,00	0,00	0,00	0,00	0,00	0,00	0,00	0,00	0,00	NA	NA	NA	NA
Da42	AUSTRALIAN RED FOX WITH DIET	F	1,00	5.62	Darkan	-33.33516	116.732931	semirural1	235	303,00	46,00	558,00	1,35	0,00	0,00	0,00	0,00	0,00	0,17	0,00	0,00	0,14	NA	NA	NA	NA
Da43	AUSTRALIAN RED FOX WITH DIET	F	1,00	3.955	Darkan	-33.33516	116.732931	semirural1	235	303,00	46,00	558,00	1,57	0,00	0,00	0,00	0,00	0,00	0,00	0,00	0,00	0,00	NA	NA	NA	NA
Da46	AUSTRALIAN RED FOX WITH DIET	F	1,00	4.23	Darkan	-33.33516	116.732931	semirural1	235	303,00	46,00	558,00	1,23	0,00	0,00	0,00	0,00	0,00	0,23	0,10	0,23	0,00	NA	NA	NA	NA
Da47	AUSTRALIAN RED FOX WITH DIET	M	2,00	4.92	Darkan	-33.33516	116.732931	semirural1	235	303,00	46,00	558,00	1,11	0,46	0,00	0,00	0,00	0,00	0,00	0,00	0,00	0,00	NA	NA	NA	NA
Da48	AUSTRALIAN RED FOX WITH DIET	M	1,00	4.04	Darkan	-33.33516	116.732931	semirural1	235	303,00	46,00	558,00	1,57	0,00	0,00	0,00	0,00	0,00	0,00	0,00	0,00	0,00	NA	NA	NA	NA
Da49	AUSTRALIAN RED FOX WITH DIET	M	1,00	2.81	Darkan	-33.33516	116.732931	semirural1	235	303,00	46,00	558,00	0,00	0,00	0,14	0,00	0,00	0,00	1,43	0,00	0,00	0,00	NA	NA	NA	NA
Da50	AUSTRALIAN RED FOX WITH DIET	M	2,00	6.355	Darkan	-33.33516	116.732931	semirural1	235	303,00	46,00	558,00	0,32	0,00	0,00	0,00	0,63	0,00	0,00	0,00	0,84	0,00	NA	NA	NA	NA
Da51	AUSTRALIAN RED FOX WITH DIET	M	1,00	4.52	Darkan	-33.33516	116.732931	semirural1	235	303,00	46,00	558,00	1,57	0,00	0,00	0,00	0,00	0,00	0,00	0,00	0,00	0,00	NA	NA	NA	NA
Da52	AUSTRALIAN RED FOX WITH DIET	M	1,00	4.685	Darkan	-33.33516	116.732931	semirural1	235	303,00	46,00	558,00	0,40	0,00	1,17	0,00	0,00	0,00	0,00	0,00	0,00	0,00	NA	NA	NA	NA
Da54	AUSTRALIAN RED FOX WITH DIET	F	1,00	3.345	Darkan	-33.33516	116.732931	semirural1	235	303,00	46,00	558,00	0,52	0,00	0,00	0,00	0,00	0,89	0,32	0,00	0,23	0,00	NA	NA	NA	NA
Da56	AUSTRALIAN RED FOX WITH DIET	M	2,00	5.255	Darkan	-33.33516	116.732931	semirural1	235	303,00	46,00	558,00	0,94	0,00	0,00	0,00	0,14	0,58	0,10	0,10	0,00	0,10	NA	NA	NA	NA
Da57	AUSTRALIAN RED FOX WITH DIET	F	1,00	3.425	Darkan	-33.33516	116.732931	semirural1	235	303,00	46,00	558,00	0,89	0,52	0,00	0,00	0,00	0,32	0,23	0,00	0,00	0,00	NA	NA	NA	NA
Da58	AUSTRALIAN RED FOX WITH DIET	F	4+	5.285	Darkan	-33.33516	116.732931	semirural1	235	303,00	46,00	558,00	1,25	0,00	0,00	0,00	0,00	0,00	0,00	0,00	0,32	0,00	NA	NA	NA	NA
Da59	AUSTRALIAN RED FOX WITH DIET	M	3,00	6.38	Darkan	-33.33516	116.732931	semirural1	235	303,00	46,00	558,00	1,25	0,00	0,00	0,00	0,00	0,00	0,23	0,00	0,23	0,00	NA	NA	NA	NA
Da60	AUSTRALIAN RED FOX WITH DIET	F	3,00	4.5	Darkan	-33.33516	116.732931	semirural1	235	303,00	46,00	558,00	0,57	0,00	0,00	0,10	0,10	0,00	0,98	0,00	0,00	0,00	NA	NA	NA	NA
Da61	AUSTRALIAN RED FOX WITH DIET	M	3,00	6.01	Darkan	-33.33516	116.732931	semirural1	235	303,00	46,00	558,00	1,11	0,46	0,00	0,00	0,00	0,00	0,00	0,00	0,00	0,00	NA	NA	NA	NA
Da62	AUSTRALIAN RED FOX WITH DIET	M	1,00	5.31	Darkan	-33.33516	116.732931	semirural1	235	303,00	46,00	558,00	1,43	0,00	0,00	0,00	0,00	0,00	0,10	0,00	0,00	0,10	NA	NA	NA	NA
Da63	AUSTRALIAN RED FOX WITH DIET	M	1,00	5.04	Darkan	-33.33516	116.732931	semirural1	235	303,00	46,00	558,00	0,00	0,00	1,17	0,00	0,00	0,00	0,32	0,00	0,23	0,00	NA	NA	NA	NA
Da64	AUSTRALIAN RED FOX WITH DIET	F	1,00	4.03	Darkan	-33.33516	116.732931	semirural1	235	303,00	46,00	558,00	0,79	0,00	0,00	0,00	0,63	0,00	0,32	0,00	0,23	0,00	NA	NA	NA	NA
Da65	AUSTRALIAN RED FOX WITH DIET	M	1,00	3.815	Darkan	-33.33516	116.732931	semirural1	235	303,00	46,00	558,00	0,67	0,00	0,00	0,00	0,00	0,00	0,58	0,10	0,58	0,00	NA	NA	NA	NA
Da67	AUSTRALIAN RED FOX WITH DIET	F	3,00	3.99	Darkan	-33.33516	116.732931	semirural1	235	303,00	46,00	558,00	0,00	0,58	0,00	0,00	0,00	0,00	0,79	0,00	0,46	0,00	NA	NA	NA	NA
Da70	AUSTRALIAN RED FOX WITH DIET	M	1,00	6.18	Darkan	-33.33516	116.732931	semirural1	235	303,00	46,00	558,00	0,58	0,00	0,00	0,00	0,00	0,00	0,00	0,00	0,99	0,00	NA	NA	NA	NA
Da71	AUSTRALIAN RED FOX WITH DIET	F	1,00	4.6	Darkan	-33.33516	116.732931	semirural1	235	303,00	46,00	558,00	1,25	0,00	0,00	0,00	0,00	0,00	0,00	0,00	0,23	0,23	NA	NA	NA	NA
Da72	AUSTRALIAN RED FOX WITH DIET	F	NA	3.43	Darkan	-33.33516	116.732931	semirural1	235	303,00	46,00	558,00	1,43	0,00	0,00	0,00	0,10	0,00	0,10	0,00	0,00	0,00	NA	NA	NA	NA
Da73	AUSTRALIAN RED FOX WITH DIET	F	1,00	4.7	Darkan	-33.33516	116.732931	semirural1	235	303,00	46,00	558,00	1,43	0,00	0,00	0,00	0,00	0,00	0,10	0,00	0,10	0,00	NA	NA	NA	NA
Da74	AUSTRALIAN RED FOX WITH DIET	M	1,00	4.86	Darkan	-33.33516	116.732931	semirural1	235	303,00	46,00	558,00	1,11	0,00	0,00	0,00	0,00	0,00	0,00	0,00	0,00	0,46	NA	NA	NA	NA
Da75	AUSTRALIAN RED FOX WITH DIET	M	1,00	3.65	Darkan	-33.33516	116.732931	semirural1	235	303,00	46,00	558,00	0,23	0,00	0,00	0,00	0,00	0,00	1,35	0,00	0,00	0,00	NA	NA	NA	NA
Da76	AUSTRALIAN RED FOX WITH DIET	F	1,00	3.715	Darkan	-33.33516	116.732931	semirural1	235	303,00	46,00	558,00	0,00	0,00	0,00	0,00	0,00	0,00	0,32	0,00	1,25	0,00	NA	NA	NA	NA
Da77	AUSTRALIAN RED FOX WITH DIET	F	1,00	3.13	Darkan	-33.33516	116.732931	semirural1	235	303,00	46,00	558,00	0,00	0,00	0,00	0,00	1,57	0,00	0,00	0,00	0,00	0,00	NA	NA	NA	NA
Da78	AUSTRALIAN RED FOX WITH DIET	M	1,00	5.76	Darkan	-33.33516	116.732931	semirural1	235	303,00	46,00	558,00	1,47	0,00	0,00	0,00	0,00	0,00	0,10	0,00	0,00	0,00	NA	NA	NA	NA
Da79	AUSTRALIAN RED FOX WITH DIET	M	1,00	3.605	Darkan	-33.33516	116.732931	semirural1	235	303,00	46,00	558,00	1,43	0,00	0,00	0,00	0,10	0,00	0,00	0,00	0,10	0,00	NA	NA	NA	NA
Da80	AUSTRALIAN RED FOX WITH DIET	F	3,00	5.45	Darkan	-33.33516	116.732931	semirural1	235	303,00	46,00	558,00	0,00	0,00	0,00	0,00	0,00	0,00	0,89	0,00	0,68	0,00	NA	NA	NA	NA
Da82	AUSTRALIAN RED FOX WITH DIET	F	1,00	4,00	Darkan	-33.33516	116.732931	semirural1	235	303,00	46,00	558,00	1,47	0,00	0,00	0,00	0,10	0,00	0,00	0,00	0,00	0,00	NA	NA	NA	NA
Da83	AUSTRALIAN RED FOX WITH DIET	F	1,00	3.145	Darkan	-33.33516	116.732931	semirural1	235	303,00	46,00	558,00	0,00	0,00	0,00	0,00	0,00	0,00	0,00	0,00	1,57	0,00	NA	NA	NA	NA
Da84	AUSTRALIAN RED FOX WITH DIET	M	1,00	4.145	Darkan	-33.33516	116.732931	semirural1	235	303,00	46,00	558,00	0,79	0,00	0,00	0,00	0,00	0,00	0,00	0,00	0,79	0,00	NA	NA	NA	NA
Da85	AUSTRALIAN RED FOX WITH DIET	F	NA	4.19	Darkan	-33.33516	116.732931	semirural1	235	303,00	46,00	558,00	0,00	0,23	0,00	0,00	0,00	0,00	0,74	0,00	0,79	0,00	NA	NA	NA	NA
Da86	AUSTRALIAN RED FOX WITH DIET	M	1,00	4.01	Darkan	-33.33516	116.732931	semirural1	235	303,00	46,00	558,00	1,35	0,00	0,00	0,00	0,00	0,00	0,14	0,00	0,17	0,00	NA	NA	NA	NA
Da87	AUSTRALIAN RED FOX WITH DIET	M	1,00	5.03	Darkan	-33.33516	116.732931	semirural1	235	303,00	46,00	558,00	0,52	0,00	0,00	0,00	0,00	0,00	1,05	0,00	0,00	0,00	NA	NA	NA	NA
Da88	AUSTRALIAN RED FOX WITH DIET	F	NA	4.5	Darkan	-33.33516	116.732931	semirural1	235	303,00	46,00	558,00	1,11	0,00	0,00	0,00	0,00	0,00	0,00	0,00	0,46	0,00	NA	NA	NA	NA
Da89	AUSTRALIAN RED FOX WITH DIET	F	1,00	4.15	Darkan	-33.33516	116.732931	semirural1	235	303,00	46,00	558,00	NA	NA	NA	NA	NA	NA	NA	NA	NA	NA	NA	NA	NA	NA	NA
Da90	AUSTRALIAN RED FOX WITH DIET	M	2,00	6.4	Darkan	-33.33516	116.732931	semirural1	235	303,00	46,00	558,00	1,57	0,00	0,00	0,00	0,00	0,00	0,00	0,00	0,00	0,00	NA	NA	NA	NA
Da91	AUSTRALIAN RED FOX WITH DIET	F	1,00	5.21	Darkan	-33.33516	116.732931	semirural1	235	303,00	46,00	558,00	1,47	0,00	0,00	0,00	0,00	0,00	0,10	0,00	0,00	0,00	NA	NA	NA	NA
Da92	AUSTRALIAN RED FOX WITH DIET	M	1,00	5.8	Darkan	-33.33516	116.732931	semirural1	235	303,00	46,00	558,00	1,57	0,00	0,00	0,00	0,00	0,00	0,00	0,00	0,00	0,00	NA	NA	NA	NA
Da93	AUSTRALIAN RED FOX WITH DIET	F	1,00	3.845	Darkan	-33.33516	116.732931	semirural1	235	303,00	46,00	558,00	0,00	0,00	0,00	0,00	0,00	0,00	1,57	0,00	0,00	0,00	NA	NA	NA	NA
Da94	AUSTRALIAN RED FOX WITH DIET	F	1,00	4.61	Darkan	-33.33516	116.732931	semirural1	235	303,00	46,00	558,00	1,25	0,00	0,00	0,00	0,00	0,00	0,00	0,00	0,32	0,00	NA	NA	NA	NA
Da95	AUSTRALIAN RED FOX WITH DIET	M	NA	6.21	Darkan	-33.33516	116.732931	semirural1	235	303,00	46,00	558,00	1,47	0,00	0,00	0,00	0,00	0,00	0,10	0,00	0,00	0,00	NA	NA	NA	NA
Da96	AUSTRALIAN RED FOX WITH DIET	F	2,00	5.115	Darkan	-33.33516	116.732931	semirural1	235	303,00	46,00	558,00	0,00	0,00	0,00	0,00	0,00	0,00	0,79	0,00	0,79	0,00	NA	NA	NA	NA
Da97	AUSTRALIAN RED FOX WITH DIET	F	1,00	3.85	Darkan	-33.33516	116.732931	semirural1	235	303,00	46,00	558,00	0,00	0,00	0,00	0,00	0,40	0,00	1,11	0,00	0,23	0,00	NA	NA	NA	NA
Da98	AUSTRALIAN RED FOX WITH DIET	M	2,00	6.875	Darkan	-33.33516	116.732931	semirural1	235	303,00	46,00	558,00	1,35	0,00	0,00	0,00	0,00	0,00	0,00	0,00	0,20	0,10	NA	NA	NA	NA

	chitecture							Bite Force		
	Mass				dissection			Dry skull	this study - models	
ID	digastric	masseter	temporal	pterygoid	I	C	M	(Forbes-Harper et al., 2017)	model 1	model 2
FO-23	4,79	17,87	14,50	5,06	NA	NA	NA	NA	237,51	233,35
FO-24	5,20	13,82	14,84	4,42	NA	NA	NA	NA	206,97	236,88
FO-25	4,18	12,96	11,60	4,15	NA	NA	NA	NA	200,39	226,20
FO-27	5,02	16,12	16,87	4,83	NA	NA	NA	NA	219,72	239,93
FO-50	5,04	13,29	13,60	5,18	NA	NA	NA	NA	194,20	243,17
FO-51	5,17	14,85	15,72	5,09	NA	NA	NA	NA	266,46	225,50
FO-52	5,16	14,19	14,05	4,79	NA	NA	NA	NA	211,64	265,74
FO-53	3,28	12,29	12,50	3,91	NA	NA	NA	NA	207,88	198,23
FO-54	4,61	15,22	12,91	4,46	NA	NA	NA	NA	192,56	222,86
FO-55	3,67	9,32	8,95	3,86	NA	NA	NA	NA	188,71	196,50
FO-56	5,39	17,07	15,26	6,77	NA	NA	NA	NA	217,48	236,50
FO-57	3,80	11,12	11,59	3,80	NA	NA	NA	NA	194,97	186,35
FO-59	4,40	14,34	15,41	4,46	NA	NA	NA	NA	256,56	245,66
FO-60	4,10	15,21	15,62	4,80	NA	NA	NA	NA	240,03	208,28
M7	NA	NA	NA	NA	NA	NA	NA	NA	210,42	274,45
NI-R1	NA	NA	NA	NA	NA	NA	NA	NA	270,07	234,96
N-R1	5,00	13,00	14,00	5,00	168,29	192,88	357,08	NA	204,17	223,87
N-R10	4,71	14,35	13,82	4,10	234,65	252,93	461,94	NA	271,45	231,14
N-R11	2,12	4,60	5,66	2,10	88,53	102,95	208,14	NA	102,70	131,90
N-R12	5,42	12,40	18,43	4,66	185,46	213,37	408,58	NA	244,76	217,02
N-R13	6,01	16,54	21,39	6,08	253,82	292,31	524,11	NA	243,49	280,59
N-R14	3,43	14,15	14,61	5,03	241,52	275,89	497,09	NA	264,20	253,04
N-R15	NA	NA	NA	NA	NA	NA	NA	NA	137,35	127,79
N-R16	5,17	15,58	17,85	5,02	202,76	226,12	434,48	NA	269,51	239,54
N-R17	4,72	11,43	15,55	3,60	195,47	220,88	419,37	NA	196,78	192,98
N-R18	5,13	13,25	17,08	3,90	169,11	194,32	369,77	NA	203,75	267,51
N-R19	3,79	12,66	16,01	4,03	208,88	239,55	449,88	NA	252,77	195,64
N-R2	5,00	12,00	16,00	4,00	168,56	193,37	354,58	NA	255,65	234,99
N-R20	4,55	11,23	16,25	3,77	247,09	283,64	501,92	NA	281,21	273,73
N-R21	3,48	7,78	9,46	2,97	NA	NA	NA	NA	253,62	226,78
N-R22	3,10	8,40	9,07	2,96	139,10	160,22	305,38	NA	195,95	164,24
N-R23	6,39	14,44	15,93	4,92	236,74	267,21	503,86	NA	236,94	266,50
N-R24	5,05	13,51	14,71	4,50	198,57	223,63	416,62	NA	257,73	246,27
N-R25	1,91	5,10	6,09	2,21	97,14	109,94	217,74	NA	116,71	151,85
N-R26	4,39	11,82	14,02	4,32	335,06	375,99	669,85	NA	241,12	254,98
N-R27	4,05	10,32	12,46	3,90	173,33	193,77	362,80	NA	218,08	211,31
N-R28	2,20	5,20	3,90	2,00	NA	NA	NA	NA	128,48	143,11
N-R29	1,70	4,50	4,50	1,60	124,98	145,76	260,98	NA	132,41	133,76
N-R3	5,00	9,00	12,00	4,00	210,43	236,15	440,27	NA	249,40	230,36
N-R30	5,20	15,00	16,70	3,80	205,00	232,58	429,64	NA	231,91	265,95
N-R31	6,40	20,90	17,50	3,60	228,79	259,99	496,36	NA	266,94	239,27
N-R32	5,00	13,90	19,30	4,40	232,77	256,24	477,41	NA	273,62	229,50
N-R33	2,20	7,60	7,20	2,80	127,26	147,04	267,24	NA	166,62	155,35
N-R34	6,30	17,10	22,60	4,90	234,48	266,79	490,28	NA	284,57	329,65
N-R35	4,50	10,50	13,80	4,00	181,13	203,51	364,30	NA	236,44	273,84
N-R36	6,40	14,60	16,40	4,10	241,04	272,84	523,86	NA	251,94	223,38
N-R37	4,30	14,40	18,20	3,90	248,88	283,00	518,94	NA	246,31	262,34
N-R38	5,30	16,50	19,60	4,40	269,26	293,53	555,73	NA	231,20	230,96
N-R39	3,80	6,70	10,70	3,00	120,03	144,11	277,01	NA	131,51	153,44
N-R4	3,30	7,78	7,20	2,65	116,21	129,60	249,76	NA	186,25	177,54
N-R40	6,10	14,70	13,50	4,10	223,33	254,97	473,43	NA	258,19	242,03
N-R41	5,90	19,90	25,60	5,80	277,02	315,14	576,40	NA	304,73	295,59
N-R42	2,30	6,50	7,30	2,20	100,22	119,39	227,13	NA	137,67	147,76
N-R43	6,60	19,90	19,40	4,70	216,68	240,23	445,39	NA	294,17	301,94
N-R44	7,10	18,30	20,50	4,80	258,38	287,80	518,72	NA	274,38	288,55
N-R45	4,20	11,90	13,30	3,90	244,88	280,80	592,23	NA	220,33	205,87
N-R46	5,40	13,30	16,10	4,10	212,17	237,21	443,95	NA	248,83	265,90
N-R47	5,10	16,30	19,10	4,20	248,14	279,34	544,08	NA	233,02	233,52
N-R48	6,50	20,70	22,70	5,70	241,18	270,88	551,08	NA	257,95	265,91
N-R49	4,60	13,00	15,80	3,50	183,85	204,20	391,63	NA	244,28	217,38
N-R5	3,44	8,50	10,50	3,44	NA	NA	NA	NA	158,89	182,06
N-R50	2,40	7,00	7,20	2,10	142,71	163,42	295,15	NA	152,62	142,41
N-R6	5,16	12,12	15,22	4,36	174,60	200,36	375,99	NA	199,03	223,71
N-R60	3,60	12,30	11,10	2,60	201,51	226,27	407,22	NA	207,23	199,13
N-R61	4,20	12,20	13,20	4,20	185,37	206,96	386,99	NA	261,47	225,49
N-R62	4,50	11,50	15,30	3,80	200,05	221,32	412,17	NA	227,04	220,23
N-R63	6,90	18,90	20,40	5,00	282,29	316,42	586,41	NA	256,88	246,71
N-R64	4,30	12,90	16,40	3,20	207,20	230,28	440,04	NA	260,13	286,76
N-R7	4,13	13,65	12,76	4,56	180,65	207,88	372,00	NA	227,30	235,23
N-R70	3,60	7,80	12,40	2,80	169,54	199,59	374,49	NA	197,48	176,91
N-R8	7,76	21,78	21,75	5,20	216,85	248,82	467,10	NA	245,85	231,11
N-R9	5,01	12,09	13,53	4,03	169,10	192,99	332,18	NA	260,24	240,87

chitecture		Mass			dissection			Bite Force	this study - models	
ID	digastric	masseter	temporal	pterygoid	I	C	M	Dry skull (Forbes-Harper et al., 2017)	model 1	model 2
Ny-R1	5,63	14,31	17,28	5,12	NA	NA	NA	NA	249,05	233,13
Ny-R2	6,47	17,15	17,72	5,74	262,12	295,93	544,07	NA	248,48	191,37
Ny-R3	5,97	18,95	19,14	6,69	379,86	441,92	772,45	NA	292,62	257,90
Ny-R4	5,48	20,06	23,88	6,57	287,92	338,62	589,77	NA	297,19	266,35
Ny-R5	6,20	12,73	19,17	4,79	192,22	217,35	407,97	NA	191,41	260,62
Ny-R6	4,70	10,96	15,11	3,94	192,21	217,88	428,91	NA	234,91	276,46
Ny-R7	3,77	8,98	10,04	2,43	177,71	203,37	406,22	NA	172,89	211,79
Ny-R8	5,23	12,79	17,92	4,44	247,07	279,91	513,64	NA	218,70	238,22
P-R1	NA	NA	NA	NA	NA	NA	NA	NA	293,66	221,94
P-R3	4,78	9,96	11,45	3,92	169,55	194,96	357,96	NA	225,78	211,45
T-R1	7,00	16,00	15,00	11,40	NA	NA	NA	NA	195,39	271,71
1,00	NA	NA	NA	NA	NA	NA	NA	2,40	223,59	209,42
4,00	NA	NA	NA	NA	NA	NA	NA	NA	221,17	220,40
6,00	NA	NA	NA	NA	NA	NA	NA	2,44	247,14	275,17
7,00	NA	NA	NA	NA	NA	NA	NA	2,47	254,36	253,96
9,00	NA	NA	NA	NA	NA	NA	NA	NA	290,16	291,48
10,00	NA	NA	NA	NA	NA	NA	NA	2,39	255,34	227,36
11,00	NA	NA	NA	NA	NA	NA	NA	2,38	235,32	191,65
12,00	NA	NA	NA	NA	NA	NA	NA	2,31	157,03	187,88
13,00	NA	NA	NA	NA	NA	NA	NA	2,36	193,52	203,36
15,00	NA	NA	NA	NA	NA	NA	NA	NA	210,32	215,19
16,00	NA	NA	NA	NA	NA	NA	NA	2,37	205,44	222,11
20,00	NA	NA	NA	NA	NA	NA	NA	2,44	230,84	226,82
21,00	NA	NA	NA	NA	NA	NA	NA	2,48	233,29	298,83
22,00	NA	NA	NA	NA	NA	NA	NA	2,45	297,79	331,65
23,00	NA	NA	NA	NA	NA	NA	NA	NA	187,72	200,88
25,00	NA	NA	NA	NA	NA	NA	NA	NA	160,57	157,11
26,00	NA	NA	NA	NA	NA	NA	NA	NA	188,42	153,49
27,00	NA	NA	NA	NA	NA	NA	NA	NA	230,45	254,45
28,00	NA	NA	NA	NA	NA	NA	NA	2,43	291,53	293,31
29,00	NA	NA	NA	NA	NA	NA	NA	2,45	289,25	284,07
30,00	NA	NA	NA	NA	NA	NA	NA	NA	213,79	235,30
31,00	NA	NA	NA	NA	NA	NA	NA	2,26	167,81	157,69
32,00	NA	NA	NA	NA	NA	NA	NA	2,31	181,68	171,31
34,00	NA	NA	NA	NA	NA	NA	NA	2,36	201,81	192,14
35,00	NA	NA	NA	NA	NA	NA	NA	2,47	260,12	264,58
36,00	NA	NA	NA	NA	NA	NA	NA	2,38	201,54	198,33
37,00	NA	NA	NA	NA	NA	NA	NA	2,28	170,15	172,20
38,00	NA	NA	NA	NA	NA	NA	NA	2,34	166,18	178,39
39,00	NA	NA	NA	NA	NA	NA	NA	2,29	152,42	176,50
41,00	NA	NA	NA	NA	NA	NA	NA	2,40	257,44	266,10
43,00	NA	NA	NA	NA	NA	NA	NA	2,31	188,17	210,02
46,00	NA	NA	NA	NA	NA	NA	NA	NA	234,62	241,07
48,00	NA	NA	NA	NA	NA	NA	NA	2,40	202,03	218,36
49,00	NA	NA	NA	NA	NA	NA	NA	NA	276,82	241,29
51,00	NA	NA	NA	NA	NA	NA	NA	2,44	217,57	235,39
52,00	NA	NA	NA	NA	NA	NA	NA	2,30	159,88	175,08
53,00	NA	NA	NA	NA	NA	NA	NA	2,30	179,73	169,63
58,00	NA	NA	NA	NA	NA	NA	NA	2,25	154,97	152,02
59,00	NA	NA	NA	NA	NA	NA	NA	2,40	229,79	244,97
60,00	NA	NA	NA	NA	NA	NA	NA	2,34	160,99	183,17
63,00	NA	NA	NA	NA	NA	NA	NA	2,42	252,16	223,18
64,00	NA	NA	NA	NA	NA	NA	NA	2,39	178,85	220,80
65,00	NA	NA	NA	NA	NA	NA	NA	2,27	157,61	177,52
66,00	NA	NA	NA	NA	NA	NA	NA	2,45	237,26	294,26
67,00	NA	NA	NA	NA	NA	NA	NA	2,35	193,11	226,64
68,00	NA	NA	NA	NA	NA	NA	NA	2,33	207,46	202,46
69,00	NA	NA	NA	NA	NA	NA	NA	2,37	177,29	198,62
70,00	NA	NA	NA	NA	NA	NA	NA	2,35	159,41	176,20
71,00	NA	NA	NA	NA	NA	NA	NA	NA	165,11	191,80
72,00	NA	NA	NA	NA	NA	NA	NA	2,30	162,47	212,50
73,00	NA	NA	NA	NA	NA	NA	NA	2,43	209,11	226,38
74,00	NA	NA	NA	NA	NA	NA	NA	2,38	203,21	200,93
75,00	NA	NA	NA	NA	NA	NA	NA	2,33	179,64	176,58
76,00	NA	NA	NA	NA	NA	NA	NA	2,44	283,07	225,76
77,00	NA	NA	NA	NA	NA	NA	NA	2,27	175,61	159,38
80,00	NA	NA	NA	NA	NA	NA	NA	2,28	149,84	159,43
81,00	NA	NA	NA	NA	NA	NA	NA	2,29	156,21	173,10
82,00	NA	NA	NA	NA	NA	NA	NA	2,36	193,74	210,46
83,00	NA	NA	NA	NA	NA	NA	NA	2,31	183,52	163,47
85,00	NA	NA	NA	NA	NA	NA	NA	2,46	213,52	257,84
87,00	NA	NA	NA	NA	NA	NA	NA	2,28	154,18	178,62

	chitecture	Mass			dissection			Bite Force Dry skull	this study - models	
ID	digastric	masseter	temporal	pterygoid	I	C	M	(Forbes-Harper et al., 2017)	model 1	model 2
90,00	NA	NA	NA	NA	NA	NA	NA	2,44	273,04	325,09
92,00	NA	NA	NA	NA	NA	NA	NA	2,36	178,08	184,57
93,00	NA	NA	NA	NA	NA	NA	NA	NA	139,64	165,20
95,00	NA	NA	NA	NA	NA	NA	NA	2,44	283,09	300,32
96,00	NA	NA	NA	NA	NA	NA	NA	2,32	176,86	204,84
100,00	NA	NA	NA	NA	NA	NA	NA	2,37	199,01	226,43
101,00	NA	NA	NA	NA	NA	NA	NA	2,39	220,59	219,82
104,00	NA	NA	NA	NA	NA	NA	NA	2,40	281,95	240,20
105,00	NA	NA	NA	NA	NA	NA	NA	2,44	256,78	250,13
106,00	NA	NA	NA	NA	NA	NA	NA	NA	223,74	233,43
107,00	NA	NA	NA	NA	NA	NA	NA	2,40	252,60	242,19
109,00	NA	NA	NA	NA	NA	NA	NA	2,41	188,13	225,94
110,00	NA	NA	NA	NA	NA	NA	NA	2,36	178,39	173,72
111,00	NA	NA	NA	NA	NA	NA	NA	2,40	198,54	182,66
112,00	NA	NA	NA	NA	NA	NA	NA	2,38	235,13	213,42
113,00	NA	NA	NA	NA	NA	NA	NA	2,40	226,76	272,05
114,00	NA	NA	NA	NA	NA	NA	NA	NA	179,92	196,57
116,00	NA	NA	NA	NA	NA	NA	NA	2,41	169,38	180,32
117,00	NA	NA	NA	NA	NA	NA	NA	2,30	220,41	235,78
118,00	NA	NA	NA	NA	NA	NA	NA	2,27	169,35	163,71
119,00	NA	NA	NA	NA	NA	NA	NA	2,28	181,63	201,95
120,00	NA	NA	NA	NA	NA	NA	NA	2,36	193,38	186,83
121,00	NA	NA	NA	NA	NA	NA	NA	2,40	203,67	260,63
122,00	NA	NA	NA	NA	NA	NA	NA	2,43	213,35	193,24
123,00	NA	NA	NA	NA	NA	NA	NA	NA	169,76	170,94
124,00	NA	NA	NA	NA	NA	NA	NA	2,37	205,50	197,04
125,00	NA	NA	NA	NA	NA	NA	NA	2,46	307,42	243,10
126,00	NA	NA	NA	NA	NA	NA	NA	2,36	231,93	236,78
127,00	NA	NA	NA	NA	NA	NA	NA	2,39	177,36	173,17
128,00	NA	NA	NA	NA	NA	NA	NA	2,38	225,54	243,83
129,00	NA	NA	NA	NA	NA	NA	NA	2,35	227,73	218,18
130,00	NA	NA	NA	NA	NA	NA	NA	2,47	224,05	217,97
131,00	NA	NA	NA	NA	NA	NA	NA	2,37	200,10	210,91
132,00	NA	NA	NA	NA	NA	NA	NA	2,38	260,52	245,06
133,00	NA	NA	NA	NA	NA	NA	NA	2,44	292,43	239,00
135,00	NA	NA	NA	NA	NA	NA	NA	2,36	183,43	187,45
136,00	NA	NA	NA	NA	NA	NA	NA	2,35	205,55	206,79
137,00	NA	NA	NA	NA	NA	NA	NA	2,41	211,35	262,25
138,00	NA	NA	NA	NA	NA	NA	NA	2,28	188,67	157,77
139,00	NA	NA	NA	NA	NA	NA	NA	2,35	202,83	179,33
140,00	NA	NA	NA	NA	NA	NA	NA	2,44	247,61	235,40
141,00	NA	NA	NA	NA	NA	NA	NA	NA	167,77	181,92
142,00	NA	NA	NA	NA	NA	NA	NA	2,30	193,34	149,98
143,00	NA	NA	NA	NA	NA	NA	NA	2,41	237,68	211,90
144,00	NA	NA	NA	NA	NA	NA	NA	2,40	178,70	198,96
145,00	NA	NA	NA	NA	NA	NA	NA	2,36	184,00	208,62
146,00	NA	NA	NA	NA	NA	NA	NA	2,34	211,91	196,42
147,00	NA	NA	NA	NA	NA	NA	NA	2,38	263,10	269,92
149,00	NA	NA	NA	NA	NA	NA	NA	NA	242,79	237,30
150,00	NA	NA	NA	NA	NA	NA	NA	2,33	176,29	202,22
151,00	NA	NA	NA	NA	NA	NA	NA	2,33	175,90	196,67
152,00	NA	NA	NA	NA	NA	NA	NA	2,40	278,60	227,34
154,00	NA	NA	NA	NA	NA	NA	NA	2,34	167,82	186,28
155,00	NA	NA	NA	NA	NA	NA	NA	2,39	193,67	216,28
156,00	NA	NA	NA	NA	NA	NA	NA	NA	212,55	242,92
157,00	NA	NA	NA	NA	NA	NA	NA	2,38	200,60	216,00
159,00	NA	NA	NA	NA	NA	NA	NA	2,36	160,47	180,27
160,00	NA	NA	NA	NA	NA	NA	NA	2,45	231,75	232,29
162,00	NA	NA	NA	NA	NA	NA	NA	2,27	129,25	153,13
164,00	NA	NA	NA	NA	NA	NA	NA	2,38	170,36	178,53
167,00	NA	NA	NA	NA	NA	NA	NA	2,33	197,70	215,67
168,00	NA	NA	NA	NA	NA	NA	NA	2,36	192,52	180,53
170,00	NA	NA	NA	NA	NA	NA	NA	NA	236,77	220,69
172,00	NA	NA	NA	NA	NA	NA	NA	2,46	264,06	290,36
173,00	NA	NA	NA	NA	NA	NA	NA	2,33	130,61	191,36
174,00	NA	NA	NA	NA	NA	NA	NA	2,41	214,77	213,26
175,00	NA	NA	NA	NA	NA	NA	NA	2,41	235,35	226,22
176,00	NA	NA	NA	NA	NA	NA	NA	2,48	318,61	256,90
178,00	NA	NA	NA	NA	NA	NA	NA	2,33	236,38	184,18
179,00	NA	NA	NA	NA	NA	NA	NA	2,32	157,14	169,85
180,00	NA	NA	NA	NA	NA	NA	NA	2,39	247,32	209,89
181,00	NA	NA	NA	NA	NA	NA	NA	2,29	167,70	179,83

	chitecture	Mass			dissection			Bite Force	this study - models	
ID	digastric	masseter	temporal	pterygoid	I	C	M	Dry skull (Forbes-Harper et al., 2017)	model 1	model 2
182,00	NA	NA	NA	NA	NA	NA	NA	2,39	197,84	217,56
183,00	NA	NA	NA	NA	NA	NA	NA	2,42	182,80	228,93
184,00	NA	NA	NA	NA	NA	NA	NA	2,28	168,21	143,53
185,00	NA	NA	NA	NA	NA	NA	NA	2,40	267,92	230,93
186,00	NA	NA	NA	NA	NA	NA	NA	2,45	244,87	241,93
187,00	NA	NA	NA	NA	NA	NA	NA	2,34	153,26	170,50
188,00	NA	NA	NA	NA	NA	NA	NA	2,48	240,18	255,10
192,00	NA	NA	NA	NA	NA	NA	NA	NA	253,30	306,52
193,00	NA	NA	NA	NA	NA	NA	NA	NA	265,74	227,13
194,00	NA	NA	NA	NA	NA	NA	NA	2,47	294,45	277,08
195,00	NA	NA	NA	NA	NA	NA	NA	2,41	157,97	187,13
196,00	NA	NA	NA	NA	NA	NA	NA	2,34	188,31	216,09
197,00	NA	NA	NA	NA	NA	NA	NA	2,35	187,43	209,51
198,00	NA	NA	NA	NA	NA	NA	NA	2,44	227,39	258,79
199,00	NA	NA	NA	NA	NA	NA	NA	2,33	207,44	176,53
200,00	NA	NA	NA	NA	NA	NA	NA	NA	235,81	276,98
201,00	NA	NA	NA	NA	NA	NA	NA	2,39	215,26	268,40
202,00	NA	NA	NA	NA	NA	NA	NA	2,34	137,42	167,22
203,00	NA	NA	NA	NA	NA	NA	NA	2,49	289,92	285,51
204,00	NA	NA	NA	NA	NA	NA	NA	2,36	179,14	191,29
205,00	NA	NA	NA	NA	NA	NA	NA	2,40	194,36	221,67
206,00	NA	NA	NA	NA	NA	NA	NA	2,35	180,16	218,32
209,00	NA	NA	NA	NA	NA	NA	NA	2,33	169,51	152,20
210,00	NA	NA	NA	NA	NA	NA	NA	NA	191,39	223,82
211,00	NA	NA	NA	NA	NA	NA	NA	2,42	268,90	245,03
212,00	NA	NA	NA	NA	NA	NA	NA	2,42	243,23	223,19
213,00	NA	NA	NA	NA	NA	NA	NA	2,43	235,83	238,03
214,00	NA	NA	NA	NA	NA	NA	NA	2,33	185,33	193,16
215,00	NA	NA	NA	NA	NA	NA	NA	2,44	163,66	179,64
216,00	NA	NA	NA	NA	NA	NA	NA	2,34	234,80	201,35
220,00	NA	NA	NA	NA	NA	NA	NA	NA	180,22	154,50
221,00	NA	NA	NA	NA	NA	NA	NA	2,33	193,36	192,97
224,00	NA	NA	NA	NA	NA	NA	NA	2,28	169,76	169,76
226,00	NA	NA	NA	NA	NA	NA	NA	2,34	167,66	206,90
227,00	NA	NA	NA	NA	NA	NA	NA	2,47	239,93	280,96
228,00	NA	NA	NA	NA	NA	NA	NA	2,32	191,18	169,21
229,00	NA	NA	NA	NA	NA	NA	NA	2,33	170,13	202,75
230,00	NA	NA	NA	NA	NA	NA	NA	2,37	209,83	237,33
231,00	NA	NA	NA	NA	NA	NA	NA	2,29	187,06	193,50
232,00	NA	NA	NA	NA	NA	NA	NA	2,29	163,71	148,91
233,00	NA	NA	NA	NA	NA	NA	NA	2,37	170,46	159,46
234,00	NA	NA	NA	NA	NA	NA	NA	2,32	165,47	162,19
235,00	NA	NA	NA	NA	NA	NA	NA	2,38	207,75	232,89
238,00	NA	NA	NA	NA	NA	NA	NA	2,42	218,48	254,51
240,00	NA	NA	NA	NA	NA	NA	NA	2,34	192,49	194,40
241,00	NA	NA	NA	NA	NA	NA	NA	2,37	209,12	188,47
243,00	NA	NA	NA	NA	NA	NA	NA	2,41	215,73	213,43
244,00	NA	NA	NA	NA	NA	NA	NA	NA	191,60	229,72
245,00	NA	NA	NA	NA	NA	NA	NA	2,42	188,96	219,48
246,00	NA	NA	NA	NA	NA	NA	NA	NA	215,58	234,71
247,00	NA	NA	NA	NA	NA	NA	NA	2,32	173,68	188,65
248,00	NA	NA	NA	NA	NA	NA	NA	2,37	232,10	209,66
249,00	NA	NA	NA	NA	NA	NA	NA	2,41	129,80	188,46
250,00	NA	NA	NA	NA	NA	NA	NA	2,46	229,31	234,89
253,00	NA	NA	NA	NA	NA	NA	NA	2,26	190,13	172,14
255,00	NA	NA	NA	NA	NA	NA	NA	2,36	179,61	217,74
256,00	NA	NA	NA	NA	NA	NA	NA	2,33	195,65	175,51
262,00	NA	NA	NA	NA	NA	NA	NA	2,45	230,04	250,94
263,00	NA	NA	NA	NA	NA	NA	NA	2,41	196,44	201,93
264,00	NA	NA	NA	NA	NA	NA	NA	2,37	178,94	199,88
265,00	NA	NA	NA	NA	NA	NA	NA	2,43	232,30	216,64
268,00	NA	NA	NA	NA	NA	NA	NA	2,29	172,34	148,99
269,00	NA	NA	NA	NA	NA	NA	NA	2,34	141,89	164,22
270,00	NA	NA	NA	NA	NA	NA	NA	2,44	176,20	224,27
271,00	NA	NA	NA	NA	NA	NA	NA	2,37	199,56	198,22
272,00	NA	NA	NA	NA	NA	NA	NA	2,42	205,60	222,19
273,00	NA	NA	NA	NA	NA	NA	NA	2,32	181,37	184,58
275,00	NA	NA	NA	NA	NA	NA	NA	2,38	168,67	175,14
276,00	NA	NA	NA	NA	NA	NA	NA	2,30	156,08	167,42
277,00	NA	NA	NA	NA	NA	NA	NA	2,43	163,99	187,46
278,00	NA	NA	NA	NA	NA	NA	NA	2,33	215,38	199,77
279,00	NA	NA	NA	NA	NA	NA	NA	2,37	212,88	216,56

	chitecture	Mass			dissection			Bite Force	this study - models	
ID	digastric	masseter	temporal	pterygoid	I	C	M	Dry skull (Forbes-Harper et al., 2017)	model 1	model 2
280,00	NA	NA	NA	NA	NA	NA	NA	2,31	205,76	195,60
281,00	NA	NA	NA	NA	NA	NA	NA	NA	171,56	180,59
282,00	NA	NA	NA	NA	NA	NA	NA	2,43	283,54	213,80
283,00	NA	NA	NA	NA	NA	NA	NA	2,40	221,29	210,52
286,00	NA	NA	NA	NA	NA	NA	NA	2,46	277,87	246,79
287,00	NA	NA	NA	NA	NA	NA	NA	2,39	222,44	230,80
288,00	NA	NA	NA	NA	NA	NA	NA	2,33	189,55	195,84
289,00	NA	NA	NA	NA	NA	NA	NA	2,38	166,03	197,27
290,00	NA	NA	NA	NA	NA	NA	NA	2,47	229,00	264,44
291,00	NA	NA	NA	NA	NA	NA	NA	NA	228,12	250,00
292,00	NA	NA	NA	NA	NA	NA	NA	2,32	177,40	209,05
293,00	NA	NA	NA	NA	NA	NA	NA	2,42	212,61	262,32
294,00	NA	NA	NA	NA	NA	NA	NA	2,41	184,34	239,51
296,00	NA	NA	NA	NA	NA	NA	NA	NA	202,83	255,87
297,00	NA	NA	NA	NA	NA	NA	NA	2,39	199,22	212,49
298,00	NA	NA	NA	NA	NA	NA	NA	2,47	232,08	273,67
299,00	NA	NA	NA	NA	NA	NA	NA	2,30	180,79	162,80
300,00	NA	NA	NA	NA	NA	NA	NA	NA	174,84	183,36
302,00	NA	NA	NA	NA	NA	NA	NA	2,41	210,70	205,74
304,00	NA	NA	NA	NA	NA	NA	NA	2,38	218,44	203,66
305,00	NA	NA	NA	NA	NA	NA	NA	2,33	210,73	181,88
306,00	NA	NA	NA	NA	NA	NA	NA	2,50	282,39	319,04
307,00	NA	NA	NA	NA	NA	NA	NA	2,35	209,79	274,60
308,00	NA	NA	NA	NA	NA	NA	NA	2,52	306,27	330,06
309,00	NA	NA	NA	NA	NA	NA	NA	2,37	192,82	225,98
310,00	NA	NA	NA	NA	NA	NA	NA	2,35	151,62	181,34
311,00	NA	NA	NA	NA	NA	NA	NA	2,41	256,86	224,03
312,00	NA	NA	NA	NA	NA	NA	NA	2,24	144,40	148,14
313,00	NA	NA	NA	NA	NA	NA	NA	NA	231,60	269,24
315,00	NA	NA	NA	NA	NA	NA	NA	2,41	284,64	257,22
316,00	NA	NA	NA	NA	NA	NA	NA	2,38	155,64	174,76
317,00	NA	NA	NA	NA	NA	NA	NA	2,23	155,79	170,52
318,00	NA	NA	NA	NA	NA	NA	NA	2,37	235,02	210,87
319,00	NA	NA	NA	NA	NA	NA	NA	2,35	221,94	201,17
321,00	NA	NA	NA	NA	NA	NA	NA	2,46	200,50	258,30
341,00	NA	NA	NA	NA	NA	NA	NA	NA	179,72	200,55
342,00	NA	NA	NA	NA	NA	NA	NA	NA	197,92	211,03
343,00	NA	NA	NA	NA	NA	NA	NA	NA	229,28	279,90
348,00	NA	NA	NA	NA	NA	NA	NA	2,41	179,40	178,35
352,00	NA	NA	NA	NA	NA	NA	NA	2,40	210,72	247,68
354,00	NA	NA	NA	NA	NA	NA	NA	2,40	198,17	220,92
357,00	NA	NA	NA	NA	NA	NA	NA	2,49	235,96	240,09
358,00	NA	NA	NA	NA	NA	NA	NA	NA	245,23	207,23
360,00	NA	NA	NA	NA	NA	NA	NA	2,41	219,24	205,47
363,00	NA	NA	NA	NA	NA	NA	NA	NA	216,90	207,96
364,00	NA	NA	NA	NA	NA	NA	NA	2,45	249,69	249,90
368,00	NA	NA	NA	NA	NA	NA	NA	2,37	171,42	175,93
371,00	NA	NA	NA	NA	NA	NA	NA	2,40	218,94	254,24
372,00	NA	NA	NA	NA	NA	NA	NA	2,40	219,93	213,04
373,00	NA	NA	NA	NA	NA	NA	NA	2,36	217,80	256,92
375,00	NA	NA	NA	NA	NA	NA	NA	2,38	164,82	185,20
379,00	NA	NA	NA	NA	NA	NA	NA	2,42	207,89	218,82
380,00	NA	NA	NA	NA	NA	NA	NA	2,39	177,91	209,16
386,00	NA	NA	NA	NA	NA	NA	NA	2,45	177,71	187,07
389,00	NA	NA	NA	NA	NA	NA	NA	2,43	184,17	233,84
391,00	NA	NA	NA	NA	NA	NA	NA	2,36	268,17	223,49
394,00	NA	NA	NA	NA	NA	NA	NA	2,45	211,65	237,85
395,00	NA	NA	NA	NA	NA	NA	NA	2,45	225,40	256,92
396,00	NA	NA	NA	NA	NA	NA	NA	NA	111,30	95,72
397,00	NA	NA	NA	NA	NA	NA	NA	NA	151,36	101,67
399,00	NA	NA	NA	NA	NA	NA	NA	2,47	267,59	289,17
400,00	NA	NA	NA	NA	NA	NA	NA	2,37	245,07	237,42
Co01	NA	NA	NA	NA	NA	NA	NA	NA	197,84	197,87
Co03	NA	NA	NA	NA	NA	NA	NA	NA	242,59	213,31
Co04	NA	NA	NA	NA	NA	NA	NA	2,38	188,71	241,64
Co05	NA	NA	NA	NA	NA	NA	NA	2,46	232,54	291,13
Co06	NA	NA	NA	NA	NA	NA	NA	2,36	179,77	216,13
Co07	NA	NA	NA	NA	NA	NA	NA	2,35	175,98	174,19
Co08	NA	NA	NA	NA	NA	NA	NA	NA	204,30	256,19
Co09	NA	NA	NA	NA	NA	NA	NA	2,27	138,65	163,24
Co10	NA	NA	NA	NA	NA	NA	NA	2,40	219,83	215,49
Co11	NA	NA	NA	NA	NA	NA	NA	2,41	247,63	242,36

	chitecture	Mass			dissection			Bite Force Dry skull (Forbes-Harper et al., 2017)	this study - models	
ID	digastric	masseter	temporal	pterygoid	I	C	M		model 1	model 2
Co12	NA	NA	NA	NA	NA	NA	NA	2,45	257,08	272,14
Co15	NA	NA	NA	NA	NA	NA	NA	NA	118,73	156,90
Co16	NA	NA	NA	NA	NA	NA	NA	NA	205,34	203,32
Co17	NA	NA	NA	NA	NA	NA	NA	NA	125,06	138,81
Co18	NA	NA	NA	NA	NA	NA	NA	2,40	279,41	198,31
Da01	NA	NA	NA	NA	NA	NA	NA	NA	141,63	177,85
Da02	NA	NA	NA	NA	NA	NA	NA	2,48	275,84	280,75
Da03	NA	NA	NA	NA	NA	NA	NA	NA	165,92	195,94
Da04	NA	NA	NA	NA	NA	NA	NA	2,26	129,44	165,18
Da05	NA	NA	NA	NA	NA	NA	NA	2,33	225,25	218,65
Da06	NA	NA	NA	NA	NA	NA	NA	NA	136,33	185,82
Da07	NA	NA	NA	NA	NA	NA	NA	2,34	185,00	202,11
Da08	NA	NA	NA	NA	NA	NA	NA	2,41	185,18	244,20
Da09	NA	NA	NA	NA	NA	NA	NA	2,33	160,33	175,07
Da10	NA	NA	NA	NA	NA	NA	NA	2,39	185,63	238,81
Da100	NA	NA	NA	NA	NA	NA	NA	2,35	234,07	229,88
Da101	NA	NA	NA	NA	NA	NA	NA	NA	153,06	173,77
Da104	NA	NA	NA	NA	NA	NA	NA	2,33	166,91	187,17
Da105	NA	NA	NA	NA	NA	NA	NA	2,37	190,80	222,75
Da106	NA	NA	NA	NA	NA	NA	NA	2,32	155,65	170,56
Da107	NA	NA	NA	NA	NA	NA	NA	2,23	119,15	144,82
Da108	NA	NA	NA	NA	NA	NA	NA	NA	142,25	146,07
Da109	NA	NA	NA	NA	NA	NA	NA	NA	133,66	166,38
Da11	NA	NA	NA	NA	NA	NA	NA	2,37	255,36	212,17
Da111	NA	NA	NA	NA	NA	NA	NA	2,30	134,45	168,07
Da112	NA	NA	NA	NA	NA	NA	NA	NA	158,61	183,19
Da113	NA	NA	NA	NA	NA	NA	NA	2,41	257,62	246,18
Da114	NA	NA	NA	NA	NA	NA	NA	NA	149,07	148,92
Da115	NA	NA	NA	NA	NA	NA	NA	2,35	169,67	195,78
Da116	NA	NA	NA	NA	NA	NA	NA	NA	123,74	174,21
Da117	NA	NA	NA	NA	NA	NA	NA	2,30	177,92	178,33
Da118	NA	NA	NA	NA	NA	NA	NA	NA	140,53	161,19
Da119	NA	NA	NA	NA	NA	NA	NA	NA	180,82	173,25
Da12	NA	NA	NA	NA	NA	NA	NA	2,38	214,17	224,17
Da121	NA	NA	NA	NA	NA	NA	NA	2,30	171,49	179,30
Da124	NA	NA	NA	NA	NA	NA	NA	2,30	186,36	171,32
Da125	NA	NA	NA	NA	NA	NA	NA	2,43	224,18	197,34
Da126	NA	NA	NA	NA	NA	NA	NA	NA	118,18	136,28
Da129	NA	NA	NA	NA	NA	NA	NA	NA	256,16	267,48
Da131	NA	NA	NA	NA	NA	NA	NA	2,26	143,35	153,05
Da132	NA	NA	NA	NA	NA	NA	NA	NA	139,45	164,00
Da135	NA	NA	NA	NA	NA	NA	NA	NA	141,02	160,67
Da136	NA	NA	NA	NA	NA	NA	NA	NA	136,76	163,23
Da137	NA	NA	NA	NA	NA	NA	NA	2,45	170,36	185,14
Da139	NA	NA	NA	NA	NA	NA	NA	2,32	164,88	186,24
Da140	NA	NA	NA	NA	NA	NA	NA	2,39	183,40	208,58
Da141	NA	NA	NA	NA	NA	NA	NA	2,31	150,85	200,18
Da143	NA	NA	NA	NA	NA	NA	NA	2,45	258,74	265,80
Da145	NA	NA	NA	NA	NA	NA	NA	NA	167,99	183,43
Da146	NA	NA	NA	NA	NA	NA	NA	2,31	170,57	182,93
Da148	NA	NA	NA	NA	NA	NA	NA	2,34	162,72	161,67
Da15	NA	NA	NA	NA	NA	NA	NA	2,37	177,66	206,98
Da150	NA	NA	NA	NA	NA	NA	NA	2,32	143,06	179,01
Da151	NA	NA	NA	NA	NA	NA	NA	2,45	253,90	331,04
Da152	NA	NA	NA	NA	NA	NA	NA	NA	147,70	163,32
Da154	NA	NA	NA	NA	NA	NA	NA	2,42	230,97	244,61
Da155	NA	NA	NA	NA	NA	NA	NA	NA	173,63	205,23
Da156	NA	NA	NA	NA	NA	NA	NA	2,28	144,79	158,29
Da158	NA	NA	NA	NA	NA	NA	NA	2,28	163,53	157,78
Da159	NA	NA	NA	NA	NA	NA	NA	2,29	170,87	158,21
Da16	NA	NA	NA	NA	NA	NA	NA	NA	184,33	208,36
Da160	NA	NA	NA	NA	NA	NA	NA	2,45	218,95	300,55
Da161	NA	NA	NA	NA	NA	NA	NA	2,30	180,41	192,55
Da162	NA	NA	NA	NA	NA	NA	NA	2,40	188,35	197,59
Da163	NA	NA	NA	NA	NA	NA	NA	2,40	165,62	196,67
Da164	NA	NA	NA	NA	NA	NA	NA	NA	140,54	163,10
Da165	NA	NA	NA	NA	NA	NA	NA	2,29	168,62	180,08
Da167	NA	NA	NA	NA	NA	NA	NA	NA	169,47	227,51
Da17	NA	NA	NA	NA	NA	NA	NA	2,30	181,04	198,37
Da170	NA	NA	NA	NA	NA	NA	NA	2,29	179,20	199,14
Da171	NA	NA	NA	NA	NA	NA	NA	NA	156,53	204,30
Da172	NA	NA	NA	NA	NA	NA	NA	2,42	191,40	252,86

	chitecture		Mass		dissection			Bite Force	this study - models	
ID	digastric	masseter	temporal	pterygoid	I	C	M	Dry skull (Forbes-Harper et al., 2017)	model 1	model 2
Da173	NA	NA	NA	NA	NA	NA	NA	NA	200,60	267,81
Da175	NA	NA	NA	NA	NA	NA	NA	2,36	143,64	194,95
Da177	NA	NA	NA	NA	NA	NA	NA	2,53	230,68	306,30
Da179	NA	NA	NA	NA	NA	NA	NA	2,32	175,99	178,99
Da18	NA	NA	NA	NA	NA	NA	NA	2,34	196,06	201,75
Da19	NA	NA	NA	NA	NA	NA	NA	2,30	166,86	200,12
Da21	NA	NA	NA	NA	NA	NA	NA	2,36	154,38	189,52
Da22	NA	NA	NA	NA	NA	NA	NA	2,35	147,60	170,38
Da24	NA	NA	NA	NA	NA	NA	NA	2,35	233,53	240,03
Da25	NA	NA	NA	NA	NA	NA	NA	2,31	162,91	164,69
Da26	NA	NA	NA	NA	NA	NA	NA	2,44	233,51	203,89
Da28	NA	NA	NA	NA	NA	NA	NA	2,35	128,25	177,82
Da29	NA	NA	NA	NA	NA	NA	NA	2,35	171,67	193,74
Da32	NA	NA	NA	NA	NA	NA	NA	NA	218,34	211,09
Da33	NA	NA	NA	NA	NA	NA	NA	NA	178,33	154,84
Da34	NA	NA	NA	NA	NA	NA	NA	2,42	312,02	301,62
Da35	NA	NA	NA	NA	NA	NA	NA	NA	150,06	155,29
Da38	NA	NA	NA	NA	NA	NA	NA	2,32	158,75	182,23
Da39	NA	NA	NA	NA	NA	NA	NA	NA	199,55	166,56
Da40	NA	NA	NA	NA	NA	NA	NA	2,31	140,03	182,19
Da41	NA	NA	NA	NA	NA	NA	NA	2,42	233,90	241,02
Da42	NA	NA	NA	NA	NA	NA	NA	NA	217,19	186,94
Da43	NA	NA	NA	NA	NA	NA	NA	2,23	142,04	147,98
Da46	NA	NA	NA	NA	NA	NA	NA	2,29	170,52	183,43
Da47	NA	NA	NA	NA	NA	NA	NA	2,37	221,49	210,30
Da48	NA	NA	NA	NA	NA	NA	NA	NA	149,79	140,20
Da49	NA	NA	NA	NA	NA	NA	NA	2,28	162,76	160,92
Da50	NA	NA	NA	NA	NA	NA	NA	2,46	222,21	250,82
Da51	NA	NA	NA	NA	NA	NA	NA	2,28	167,08	181,85
Da52	NA	NA	NA	NA	NA	NA	NA	2,34	177,13	191,35
Da54	NA	NA	NA	NA	NA	NA	NA	NA	171,92	184,33
Da56	NA	NA	NA	NA	NA	NA	NA	2,38	265,62	266,18
Da57	NA	NA	NA	NA	NA	NA	NA	NA	157,13	171,90
Da58	NA	NA	NA	NA	NA	NA	NA	2,36	197,61	203,51
Da59	NA	NA	NA	NA	NA	NA	NA	2,46	216,57	267,97
Da60	NA	NA	NA	NA	NA	NA	NA	NA	191,66	217,32
Da61	NA	NA	NA	NA	NA	NA	NA	2,45	214,24	219,47
Da62	NA	NA	NA	NA	NA	NA	NA	NA	157,05	230,63
Da63	NA	NA	NA	NA	NA	NA	NA	2,37	164,97	216,51
Da64	NA	NA	NA	NA	NA	NA	NA	NA	189,84	184,63
Da65	NA	NA	NA	NA	NA	NA	NA	2,34	134,51	140,02
Da67	NA	NA	NA	NA	NA	NA	NA	2,40	239,02	212,60
Da70	NA	NA	NA	NA	NA	NA	NA	NA	189,58	193,89
Da71	NA	NA	NA	NA	NA	NA	NA	NA	192,78	192,71
Da72	NA	NA	NA	NA	NA	NA	NA	NA	139,61	132,29
Da73	NA	NA	NA	NA	NA	NA	NA	2,32	139,13	165,61
Da74	NA	NA	NA	NA	NA	NA	NA	2,30	179,20	200,34
Da75	NA	NA	NA	NA	NA	NA	NA	NA	145,65	162,50
Da76	NA	NA	NA	NA	NA	NA	NA	2,31	153,71	150,44
Da77	NA	NA	NA	NA	NA	NA	NA	2,27	129,28	124,27
Da78	NA	NA	NA	NA	NA	NA	NA	2,37	186,63	221,99
Da79	NA	NA	NA	NA	NA	NA	NA	2,33	122,67	149,85
Da80	NA	NA	NA	NA	NA	NA	NA	2,36	190,34	217,43
Da82	NA	NA	NA	NA	NA	NA	NA	2,31	163,12	169,93
Da83	NA	NA	NA	NA	NA	NA	NA	NA	133,60	134,58
Da84	NA	NA	NA	NA	NA	NA	NA	NA	192,57	170,41
Da85	NA	NA	NA	NA	NA	NA	NA	NA	203,11	208,29
Da86	NA	NA	NA	NA	NA	NA	NA	NA	126,90	167,19
Da87	NA	NA	NA	NA	NA	NA	NA	NA	167,62	182,14
Da88	NA	NA	NA	NA	NA	NA	NA	NA	144,26	162,11
Da89	NA	NA	NA	NA	NA	NA	NA	2,23	151,72	164,69
Da90	NA	NA	NA	NA	NA	NA	NA	NA	242,41	253,70
Da91	NA	NA	NA	NA	NA	NA	NA	2,30	182,02	170,14
Da92	NA	NA	NA	NA	NA	NA	NA	NA	194,34	231,47
Da93	NA	NA	NA	NA	NA	NA	NA	NA	172,10	178,14
Da94	NA	NA	NA	NA	NA	NA	NA	NA	141,91	173,85
Da95	NA	NA	NA	NA	NA	NA	NA	NA	185,54	226,79
Da96	NA	NA	NA	NA	NA	NA	NA	2,40	277,83	237,01
Da97	NA	NA	NA	NA	NA	NA	NA	2,29	143,68	157,10
Da98	NA	NA	NA	NA	NA	NA	NA	2,48	269,81	270,78

7.2. Article 5 – Fig. S1

First axis of the 2B-PLS analyses on mandible shape and muscle masses with loadings. The deformations from the consensus to the minimum (in blue) and maximum (in red) are represented on lateral, dorsal and cauda views.

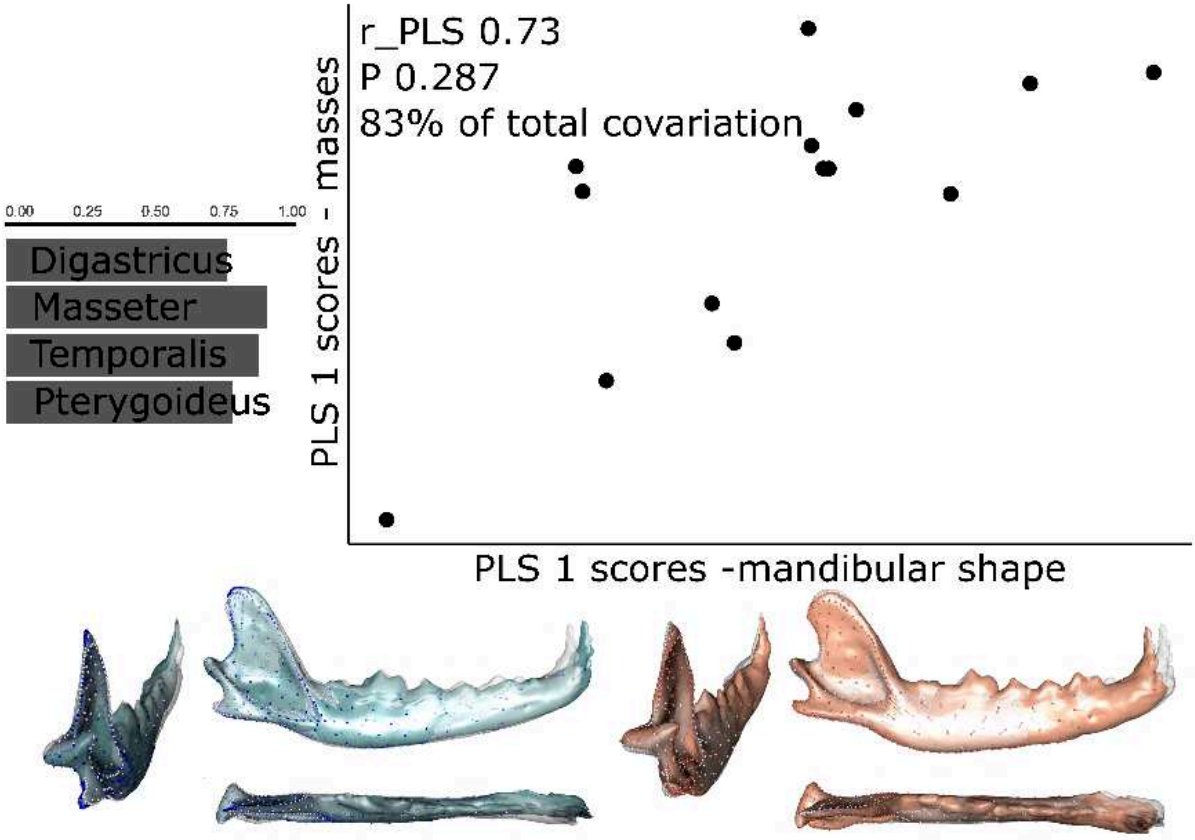

7.3. Article 5 – Fig. S2

First axes of the PCA on muscle data and boxplot representing values in French and Australian red foxes. A: mass; B: PCSA; C; residual mass; D: residual PCSA. P-KW: p-value of a Kruskall-Wallis test (reported only for significant results). French red foxes are in black and Australian red foxes are in orange.

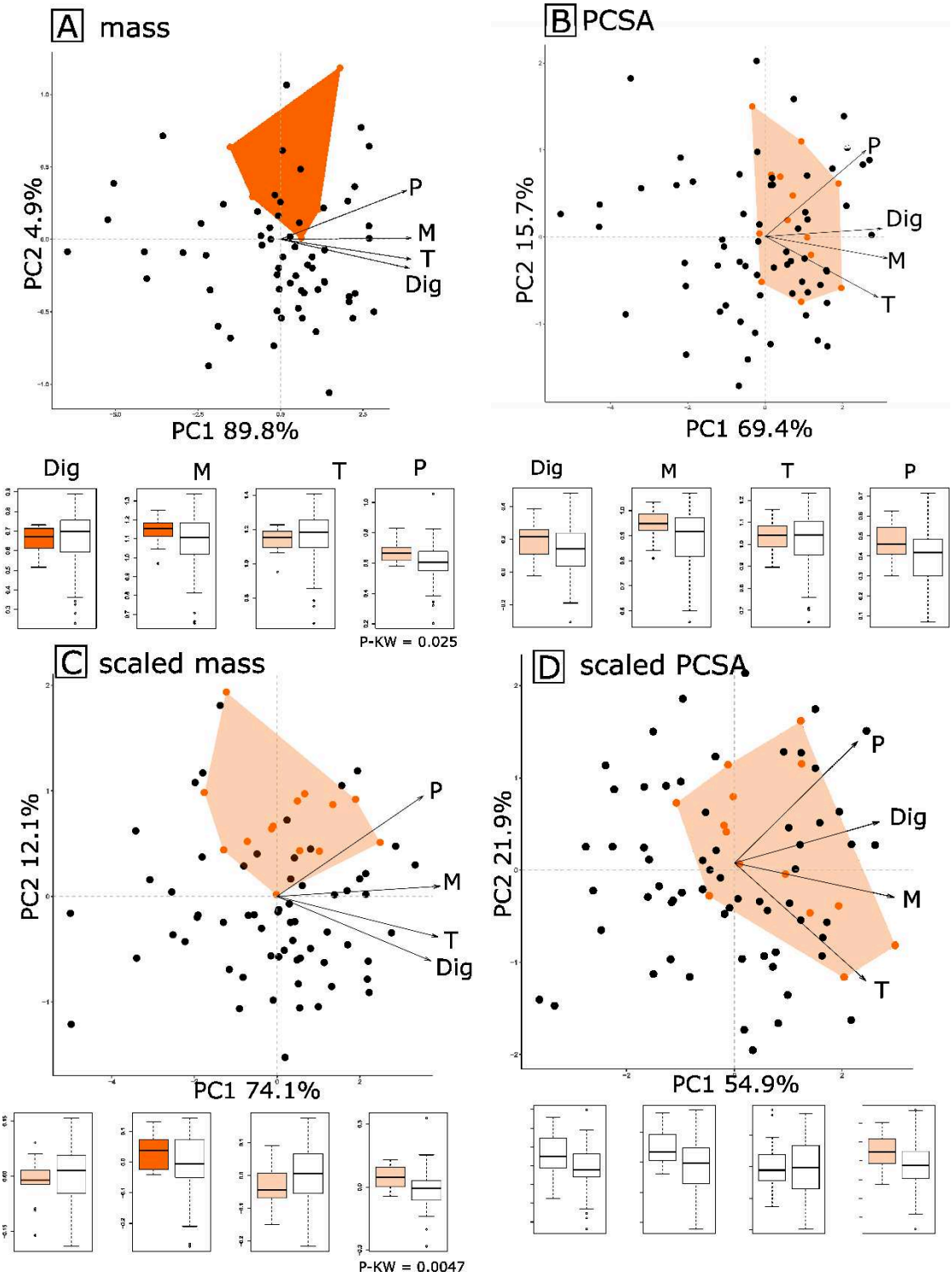

7.4. Article 6 – Table S2

Table S2. Definition of the landmarks used in this study.

Landmark	Definition
Mandible	
1	Most rostromedial point of the mandiblular symphysis, at the base of the first incisor
2	Most rostral point of the canid, on the lateral side
3	Most caudal point of the canid, on the lateral side
4	Most rostral point of the second premolar, on the lateral side
5	Most rostral point of the third premolar, on the lateral side
6	Most rostral point of the fourth premolar, on the lateral side
7	Most caudal point of the fourth premolar, on the lateral side
8	Most caudal point of the carnassial, on the lateral side
9	Most caudal point of the second molar, on the lateral side
10	Highest point of the tip of the coronoid process
11	Most caudal point of the tip of the coronoid process
12	Most caudal point of the mandibular notch, at the intersection of the condyle and the coronoid process. This point is considered as the centre of rotation of the mandible with respect to the skull for predictions in model 2.
13	Most medial point of the condyle (tip of the head of the mandible)
14	Most ventral point of the condyle
15	Most lateral point of the condyle
16	Most anterior point on the curve of the angle of mandible
17	Point at the tip of the angular process
18	Most elevated point on the inferior border of the ramus
19	Lowest point on the ventral border of the ramus, right under the carnassial
20	Most caudal and lowest point of the intermandibular suture on the medial side
21	Main mental foramen
22	Rostral point of intersection between the coronoid crest and the condyloid crest
23	Most rostral point of the edge joining the basis of the coronoid process and the condyle on the medial side.
24	Most rostral point of the mandibular foramen
25	The most lateral point on the angle of mandible, at the beginning of the angular process

8. Part 3 – Chapter 6. Verification of species identification for fragmented archaeological mandibles

Before conducting any further analyses, we wanted to make sure we did not misclassify any of our bones. Indeed, species were identified base on the aspect of the teeth and the overall shape and size of the mandible and the probability to find this species given the chrono-cultural context of the site, but small fragments can be misleading. Since we had a lot of small pieces of mandibles in our archaeological sample, we wanted to make sure that we did not make any identification errors. In particular, we wanted to make sure that some small fragments identified as dog or fox could not be of the opposite species, or even of another small carnivore also present on certain sites such as badgers or other small mustelids that can be relatively abundant at some sites (Chalain, Herxheim). The cat is rare (we found 2 cats but we did not include them in the analyses because the dental formula is very different and it is not possible to place the landmarks of the 10 landmarks in a homologous way (M2 is absent for example).

For this purpose, we performed non-supervised analyses to classify the mandibles of our archaeological sample based on morphological similarities (this method does not require any comparison with modern canids). for each template, we compared our identifications with the classifications or predictions.

We performed a **GPA** on all the archaeological mandibles of our ample, including mandibles that we identified as other carnivorous species (47 mustelids). Even the youngest individuals (including some 'juveniles') were included in these analyses.

For each template, we performed a **Principal Component Analyses** on the Procrustes coordinates from the GPA to visualize the morphological spaces occupied by each species in the two first principal component axes. However, this visualisation method may not be sufficient to separate clearly all the species, because only two axes of variation are represented together within a single plot.

Accordingly, we also performed classification analyses directly on the Procrustes coordinates (gaussian mixture models), or on the distance matrix (UPGMA clustering).

- **Gaussian mixture models**

We used the function Mclust() from package « mclust » to identify groups. This method of clustering is based on finite Gaussian mixture models. Models are estimated by EM algorithm initialized by hierarchical model-based agglomerative clustering. The optimal model is then selected according to BIC.

- **UPGMA clustering**

We calculated a Procrustes distance matrix using the function dist().We calculated the Euclidean distance between all pairs of observations, represented by a two-dimensional matrix of the Procrustes coordinates from the GPA. We then used the function upgma() from the

package “phangorn” to perform UPGMA clustering, using method “ward.D2”. We obtained a tree with ggtree (Yu *et al.*, 2017).

Template A

For template A, the mustelids are clearly separated from the canids. The tree clearly separates all species with the exception of a mustelid (Cha71) which is grouped with dogs. The characteristic aspect of the teeth of the two mandibles, however, confirms our previous identification. The wolves are grouped together close to other dogs in the tree, but they significantly differ is size. The biggest mustelids and close in centroid size with foxes.

The GM method leads to a better classification.

Here are the results of the comparison between the GM classification and our own identifications, when only the shape is used for the construction of the distance matrix:

Mclust VEI (diagonal, equal shape) model with 9 components:

```
 log-likelihood   n    df     BIC     ICL
      959732.1 160 11656 1860308 1860308

Clustering table:
 1  2  3  4  5  6  7  8  9
27 21 32 21 26  4  8  6 15
> table(mc$classification, res.pca$contexte$species)

   dog fox mustelid wolf
 1  27   0       0    0
 2  21   0       0    0
 3  32   0       0    0
 4  21   0       0    0
 5  26   0       0    0
 6   0   0       0    4
 7   0   8       0    0
 8   0   0       6    0
 9   0   0      15    0
```

The best GM model was a clustering in 8 groups. There are 4 groups with dogs, 1 with wolves, 1 with foxes and 2 with mustelids. Our identifications overall correspond to the classification proposed by mclust: all species are clearly separated with the exception of Cla8 that was grouped with dogs. Wolves are clearly identified by the GM method.

Template B

For template B, results are similar. In the tree, mustelids are clearly separated. Most are on the same branch, but 3 mustelids are classified in another group, closer to dogs but on a distinct branch and they have a much smaller centroid size. Cha52 is isolated on a branch closer to dogs than other canids but it is smaller than the smallest dog and it well classified with template A.

One subadult fox (Vit23) is grouped with dogs (it P2 and P4 teeth are still erupting). Wolves are separated on two different branches but the centroid size is still discriminatory.

Mclust VEI (diagonal, equal shape) model with 9 components:

```
 log-likelihood   n   df     BIC     ICL
      689832.4 268 5296 1350055 1350055

Clustering table:
 1  2  3  4  5  6  7  8  9
37 31 40 43 44 38 12 16  7
> table(mc$classification, res.pca$contexte$species)

    dog fox mustelid wolf
 1  36   1       0    0
 2  30   0       0    1
 3  40   0       0    0
 4  40   0       0    3
 5  44   0       0    0
 6  38   0       0    0
 7   0  12       0    0
 8   0   0      16    0
 9   0   0       7    0
```

Template C

With template C, Cha71 and Cha52 are still misclassified, but they still have smaller sample sizes than the smallest dogs.

Additionally, 2 foxes are misclassified. Har80 is classified with dogs and has a centroid size that is compatible with dogs (0.36). It was classified with other dogs in analyses with template A. Har78 is classified with two small mustelids but its centroid size (0.35) is bigger than the biggest centroid size of large mustelids. Moreover, the teeth confirm the attribution as a fox.

Rob4 is classified with this fox and the two small mustelids. However, it is clearly a dog according to its centroid size.

Wolves are separated on two different branches but the centroid size is still discriminant, as in analyses with template B.

With the GM models, all classifications match our identifications:

Mclust VEI (diagonal, equal shape) model with 9 components:

```
 log-likelihood   n   df     BIC     ICL
      743960.3 258 5806 1455680 1455679

Clustering table:
 1  2  3  4  5  6  7  8  9
```

```
34 43 37 39 45 16 11 26  7
> table(mc$classification, res.pca$contexte$species)

   dog fox mustelid wolf
1  33   1       0    0
2  41   2       0    0
3  33   0       0    4
4  39   0       0    0
5  45   0       0    0
6   0   0      16    0
7   0   0      11    0
8  26   0       0    0
9   0   7       0    0
```

Mustelids are in two groups, foxes in a third group, and dogs are in 5 different groups. The 4 wolves are classified with dogs in group 3.

Template D

Misclassifications are more frequent. The two mustelids Cha71 and Cha52 are still with dogs but the centroid size of Cha71 is only compatible with mustelids (0.19) and Cha52 is isolated with Cha40, another mustelid. Four dogs are classified with foxes but their centroid sizes are bigger than the those of the biggest foxes (Twa152: 0.28; Har30: 0.26; Har31: 0.25; Cas4: 0.259), Har30 and Har31 have teeth that confirm the attribution as dogs and Cas4 was classified as a dog in analyses with template B.

Three foxes are with dogs. Their centroid size is compatible with large foxes or small dogs (Tar1: 0.23; Tev3: 0.22; Vit23: 0.205). Vit23 was classified as a fox in analyses with template B. Tar1 and Tev3 have teeth that confirm the attribution a a fox.

One dog is with mustelids (Mas7). However, the teeth and the centroid size (0.25) clearly confirm that it is not a mustelid.

Template E

There is more misclassification than in the trees with template C and D. template E is not effective at distinguishing dogs/foxes/mustelids using shape only. We checked each mandible that did not seem well classified considering the results of previous analyses with templates ABCD but we did not notify any mistakes.

The dog Mas7 is still classified with mustelids but its centroid size (0.14) is too big for mustelids, as in analyses with template D. The mustelid Cha73 is still misclassified with dogs (see template A). Cha33 and Cha64 are classified with dogs but they were classified as mustelids in analyses with template D. The fox Har78 is close to these mustelids. This fox was really close to mustelids in analyses with template C. The mustelids Cha52 and Cha49 are still grouped with dogs (as in analyses with template D). Cha40 is classified with dogs, as in analyses with template C and D.

Some foxes are closer to dogs than to other foxes (Har80, Cla5, Cla6 ➔ attribution to the fox species confirmed by previous templates and the aspect of the teeth; Twa184 ➔ teeth confirm the attribution to the fox species). Vit23 is still grouped with dogs, as in previous analyses with other templates.

Some dogs are classified with foxes but they are too big to be foxes (Tev13: 0.137 and teeth of a dog; Twa28: 0.146) and Twa28 was classified as a dog in analyses with template A).

Mustelids and dogs are mixed at the bottom of the tree.

GM models identify no clear structure in the data (only 1 group is identified).

The wolves and dogs overlap in centroid sizes. Bur2 is still large in centroid size for dogs and in the range of variation of ancient wolves. The same holds for Her4, however, it was clearly a dog in analyses with template A (the ramus is confusing).

GM models identify no clear structure in the data (only 1 group is identified).

Template F

Template F seems as effective as template A. Only the young fox Her15 is grouped with dogs but its centroid size is compatible with foxes, not dogs (0.226). Besides, it is close to Bor27, a young dog (centroid size: 0.228).

The GM models identify 9 groups. Group 5 and 9 contain mustelids only. Dogs are in six groups (one dog is isolated in one group) and one of them contains the 4 wolves. All foxes are isolated in another group.

Mclust EEI (diagonal, equal volume and shape) model with 9 components:

```
 log-likelihood   n   df     BIC     ICL
      666819.8 199 7178 1295644 1295644

Clustering table:
 1  2  3  4  5  6  7  8  9
33 32 28 14 19 41  1 25  6
> table(mc$classification, res.pca$contexte$species)

   dog fox mustelid wolf
 1  33   0       0    0
 2  31   0       0    1
 3  28   0       0    0
 4   0  14       0    0
 5   0   0      19    0
 6  37   0       0    4
 7   1   0       0    0
 8  25   0       0    0
 9   0   0       6    0
```

Template G

We have quite excellent results even though the template is very small.

Some mustelids are grouped with dogs. Her29 is, however, very small (0.038). Cha51 (0.07) and Her24 (0.044) were classified as mustelids in analyses with template D.

Some foxes are closer to dogs in both size and shape: the young fox Her15 (as in template F but correctly classified with template A), Har80as previously seen with template A, Her14 was correctly classified with previous templates (C and D). Cla2, Cla9, Cha42 and Har79 were also correctly classified as dogs in analyses with more complete templates (A/B). Twa15 is clearly a fox considering its centroid size (0.48; as it is pathological it was not included in analyses with more complete templates). Cha28 is close to dogs but also to the fox Har80. Its centroid size (0.064) is compatible with fox or small dogs. It could not be analyzed with more complete templates but we chose to keep our identification as a fox.

GM models identify no clear structure in the data (only 1 group is identified).

Template H

Template H is surprisingly not too bad in distinguishing species. A few dogs are with foxes (Twa128, Cla7 and Bor91 are dogs according to analyses with template A). the centroid size is a good complementary indicator.

Wolves are not clearly isolated in shape but they have much bigger centroid sizes than dogs.

A few foxes are with dogs. Cha18, Cha31 and her15 have been correctly classified as fox with previous templates.

The young fox Cla8 is classified with mustelids. In analyses with template A it was classified with dogs.

GM models identify no clear structure in the data (only 1 group is identified).

Template I

Some dogs are grouped with mustelids but the centroid size is indicative of the attribution to the dog group (Vit10, Tev15, Twa90, Pir6, Vit25, Aur7).

Some foxes are grouped with dogs but previous analyses confirm our attributions (Tev1, Tev7, Tev10, Twa183, Vit23).

The differences in centroid size between wolves and dogs is less clear than for other templates.

Ico9 is bigger than the other dogs and is in the range of variation of ancient wolves. It was not included in analyses with other templates.

GM models identify no clear structure in the data (only 1 group is identified).

Template J

We observe almost the same things as with template A. The mustelid Cha71 is correctly classified, contrary to analyses with template A. The foxes Her15 and Cla10 are with dogs but their attribution was confirmed by more complete templates.

The centroid size is useful to distinguish dogs and wolves.

GM models identify no clear structure in the data (only 1 group is identified).

Conclusion

This long step was necessary to validate our species identifications. We only presented the final results but preliminary steps allowed us to correct some errors that occurred during the registration process. For example, Cha33 (based on template D, E, G) and Twa137 (based on template G) were re-identified as mustelids whereas they had been recorded as foxes. Indeed, the NJ trees for template D, E (Cha33) and G (Cha33, Twa187) indicate that these specimens are close to other mustelids.

Cha33 Twa187

The results of the gaussian models and those of the UPGMA clustering are also relevant to determine which templates are useful to describe the overall morphological variability in mandibular shape and size. Only MG models on templates A, B, C and F were successful at identifying groups. No structure in the data was found for the other templates. Trees and boxplots obtained for templates A, B, F and J were the best at distinguishing species. The tree with template C lead to a more important number of misclassifications.

We thus used only the templates A, B, C F and J to explore the variation in morphotypes, which represents 405 different archaeological dogs.

However, even for these most complete patterns we obtain (few) erroneous classifications, revealing the risk of confusion between dogs and foxes or foxes and mustelids, which is partly related to the younger age of the individuals that are less well classified. It will thus be fundamental to remove the juveniles from our analyses (when the carnassial is not erupted) and to indicate the age of the individuals (subadults, young, adult, old)

For the smallest fragments, different species are not always on different branches. Mustelids can be closer to dogs than to other mustelids, and the same goes for foxes. The NJ reflect convergence in shape in specific areas, that could match convergence in functional demands.

The smallest patterns may thus be more appropriate to explore functional diversity than the overall morphological diversity.

Wolves have significantly larger centroid sizes. Bur2 is slightly smaller than the smallest wolves, but its attribution to the wolf species is to be considered. The tree does not allow to clearly distinguish wolves and dogs with the shape of the mandible only, and Bur2 was not included in the previous analyses with templates A to C. However, we confirm our attribution to the dog species, given the archaeological context. Bur2 comes from Bury, an archaeological site dated back to the transition between the Late Neolithic and the Bronze age. It is known that bigger dogs can be found at this time. Moreover, the mandible was from a complete skeleton, and the attribution as a dog (rather than wolf) is based on the observation of the complete skeleton.
GM models identify no clear structure in the data (only 1 group is identified).

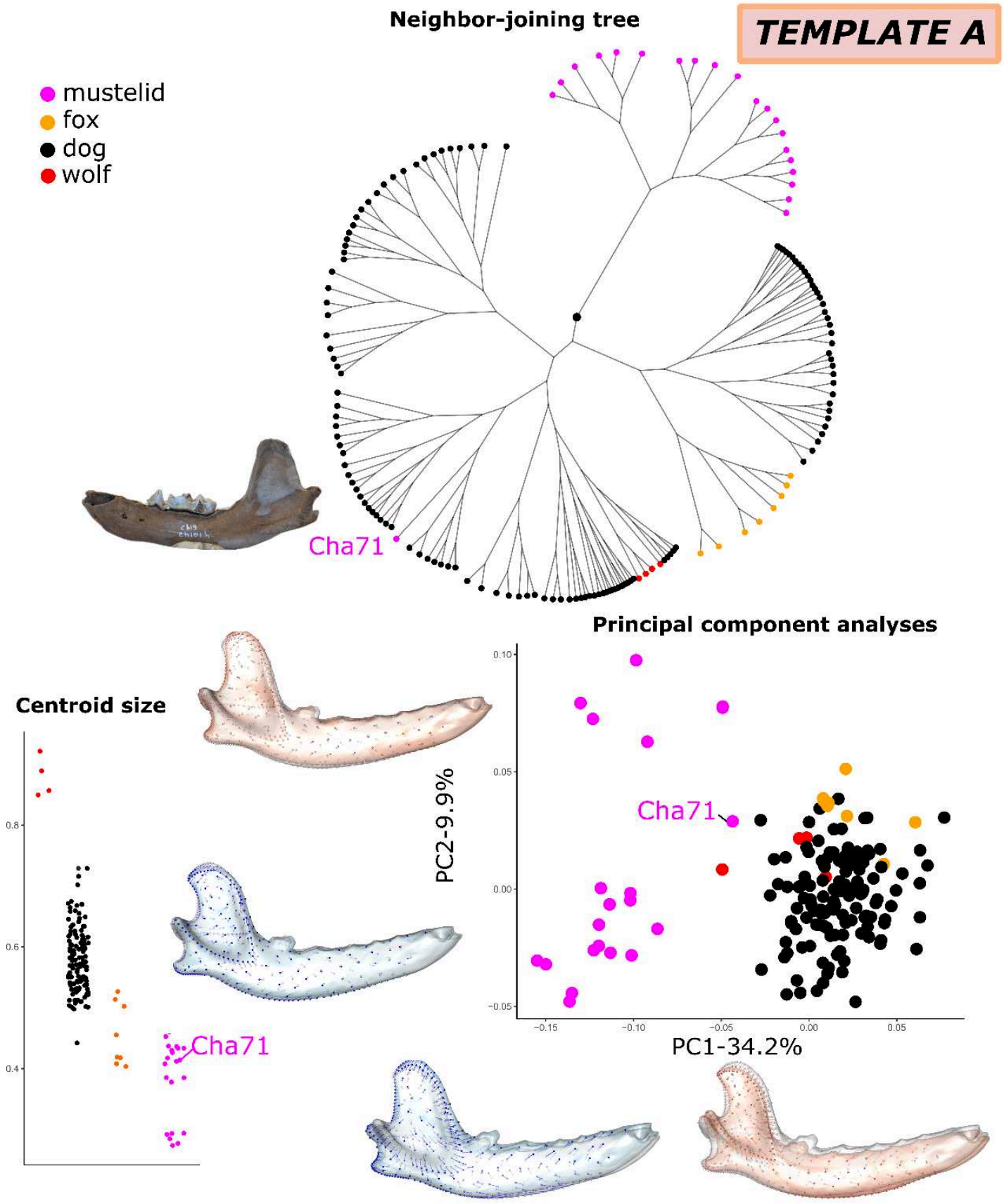

Figure 165. Verification of species identification, using comparison of shapes (classification tree and Principal Component Analyses) based on template A.

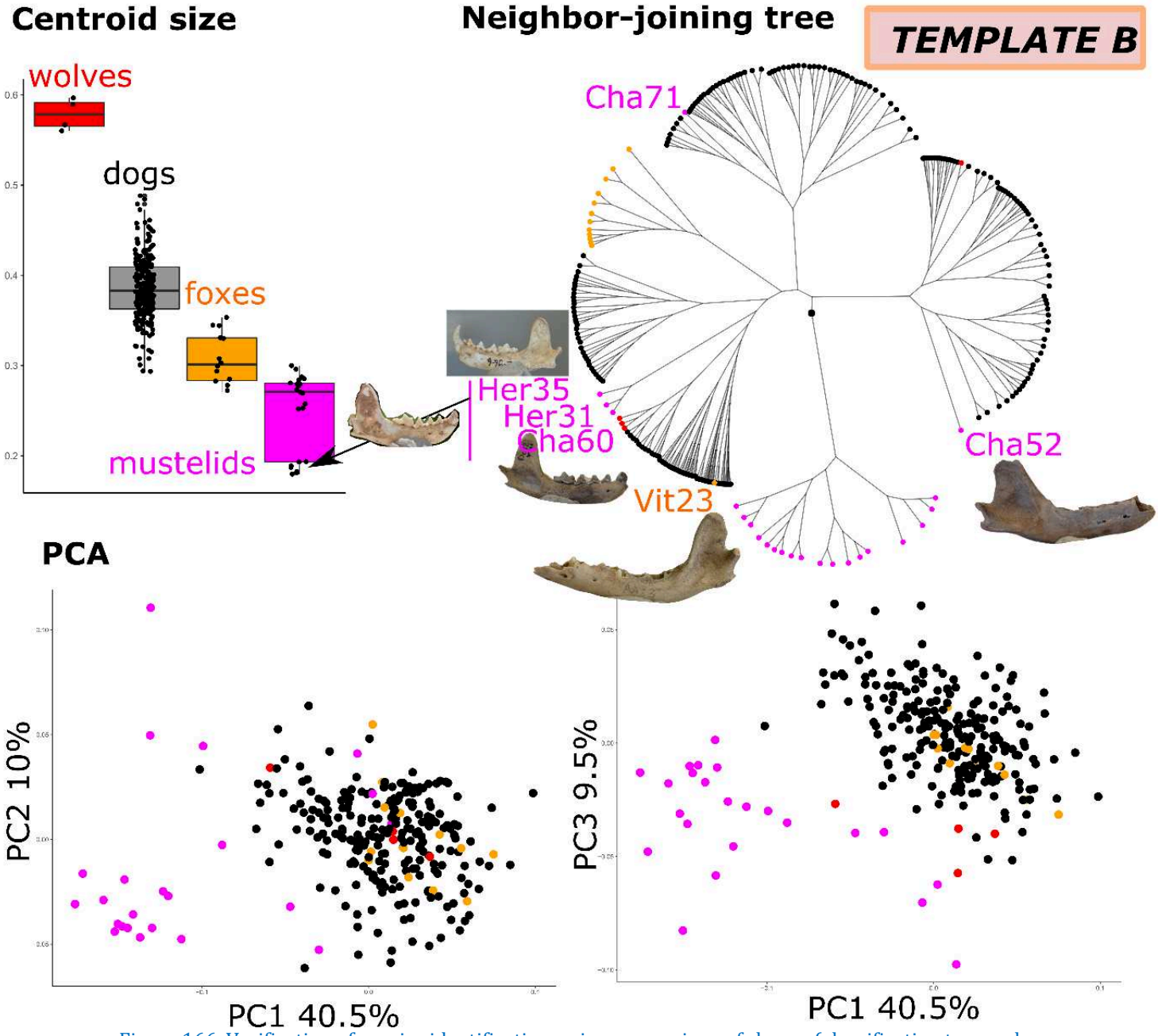

Figure 166. Verification of species identification, using comparison of shapes (classification tree and Principal Component Analyses) based on template B.

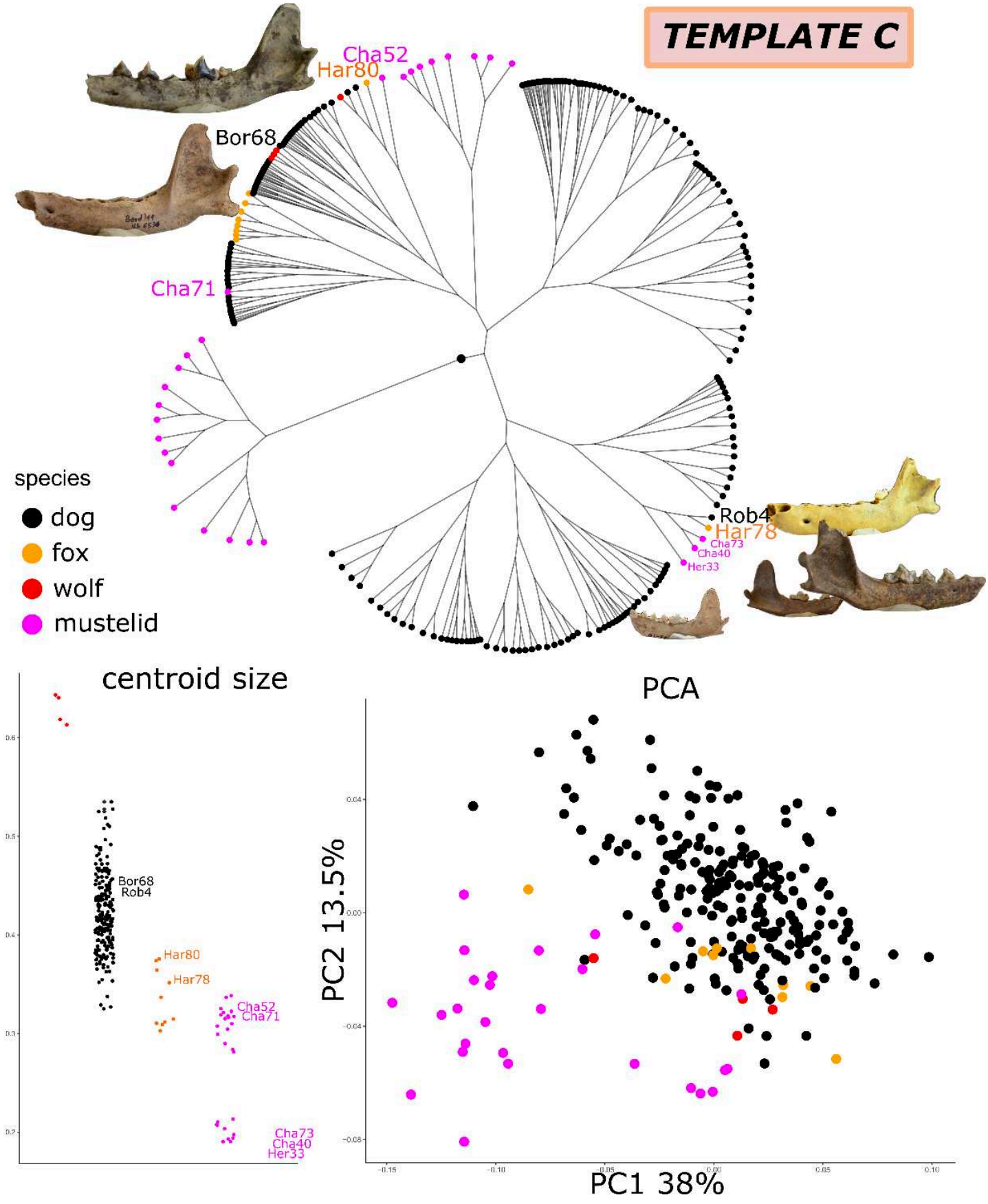

Figure 167. Verification of species identification, using comparison of shapes (classification tree and Principal Component Analyses) based on template C.

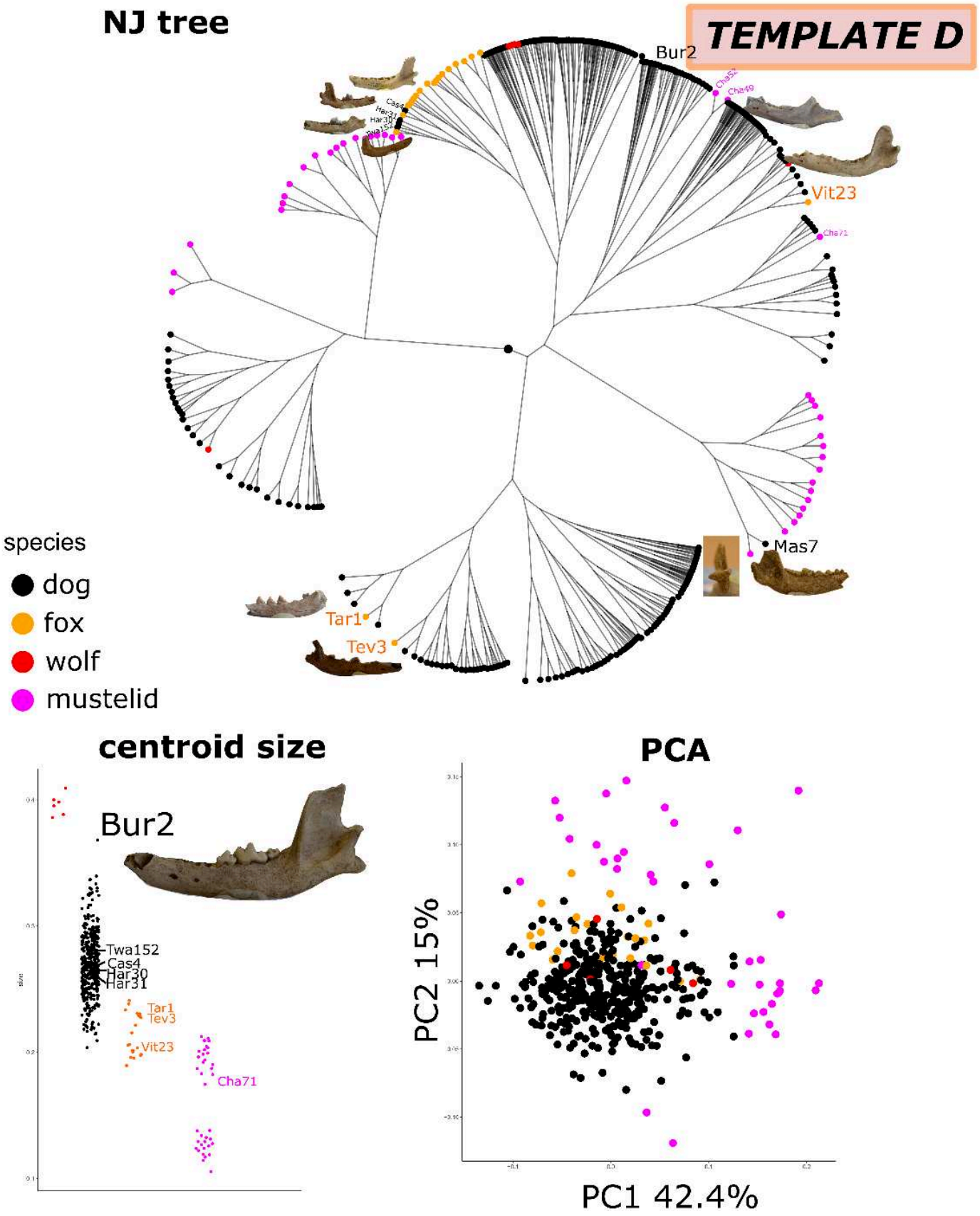

Figure 168. Verification of species identification, using comparison of shapes (classification tree and Principal Component Analyses) based on template D.

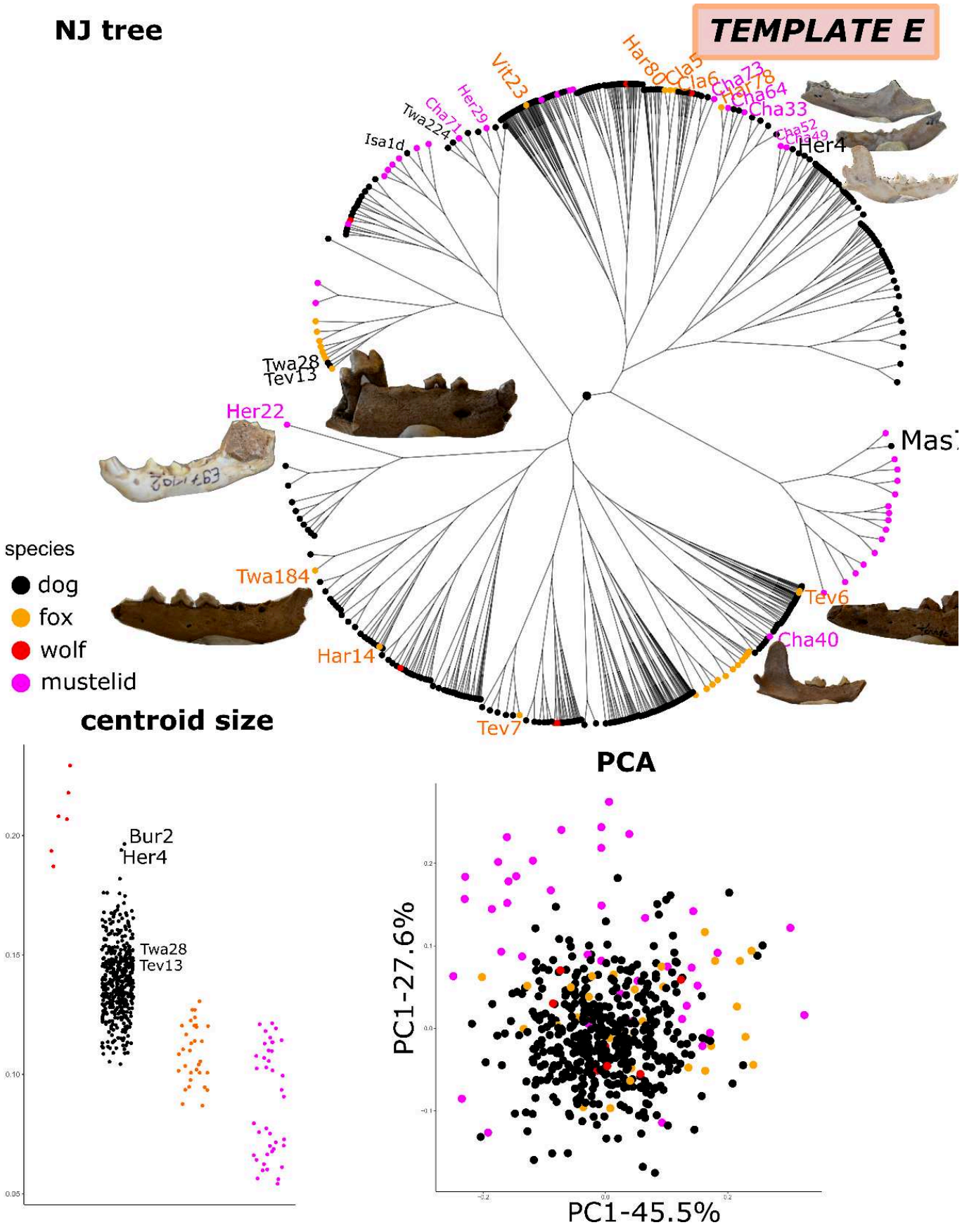

Figure 169. Verification of species identification, using comparison of shapes (classification tree and Principal Component Analyses) based on template E.

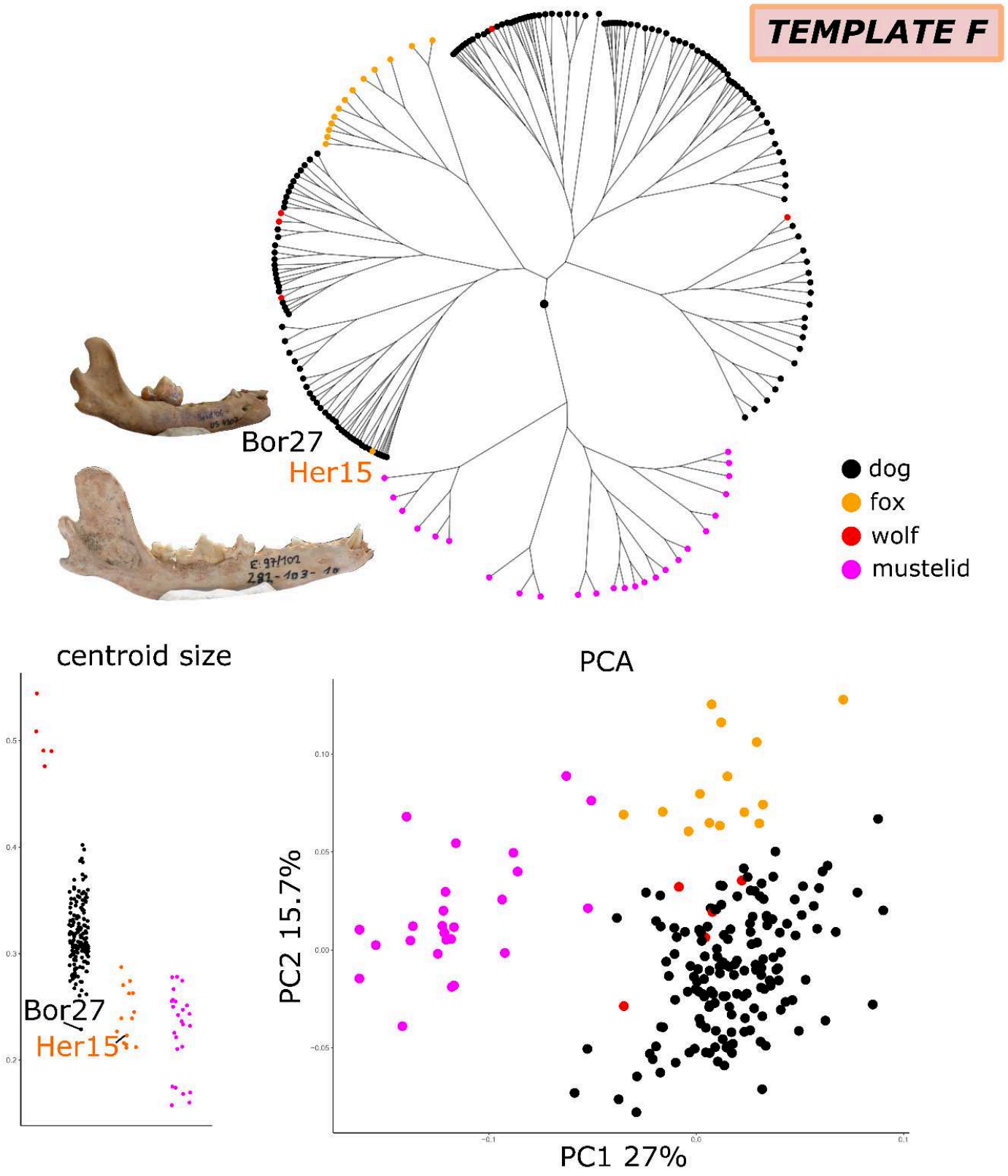

Figure 170. Verification of species identification, using comparison of shapes (classification tree and Principal Component Analyses) based on template F.

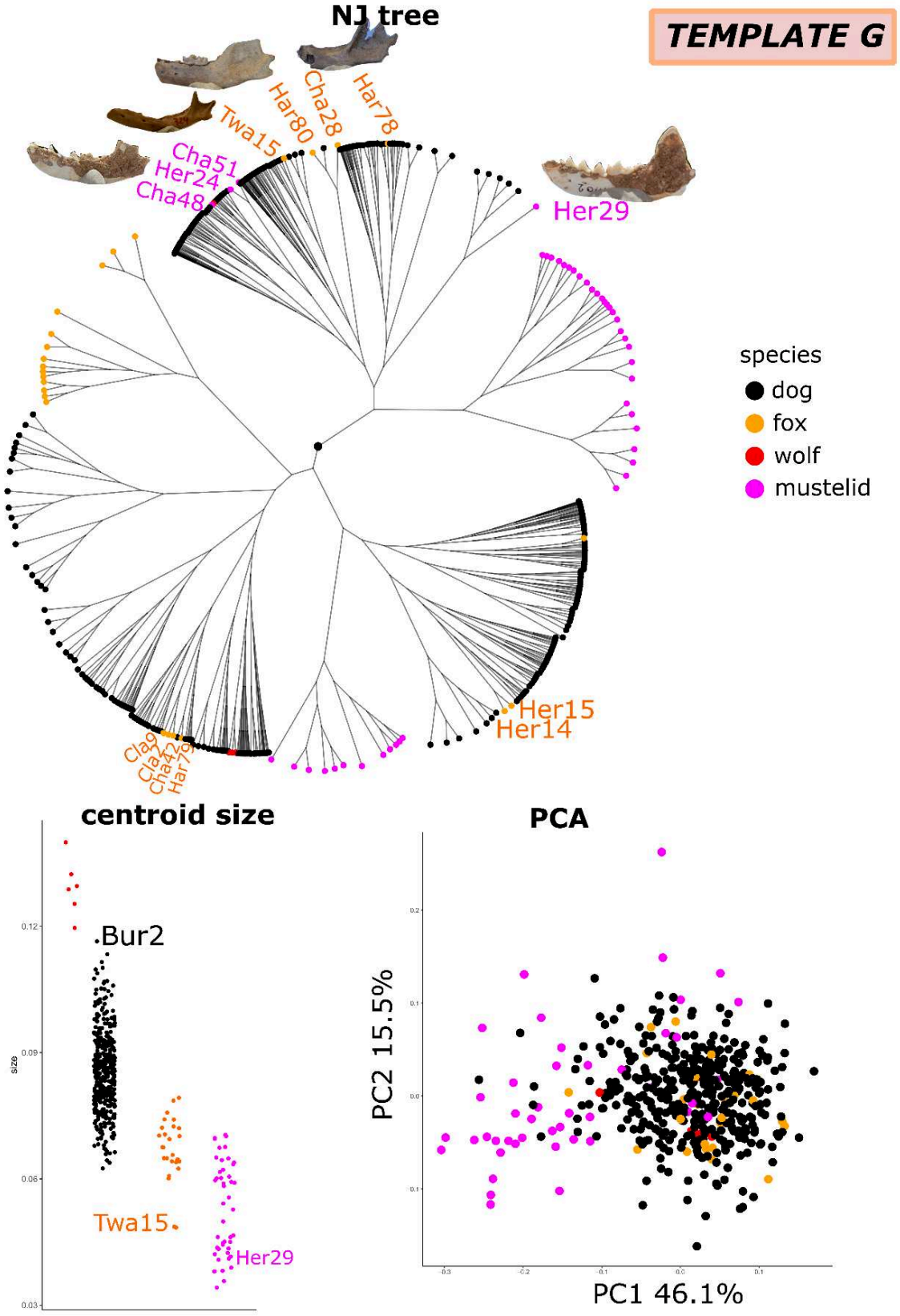

Figure 171. Verification of species identification, using comparison of shapes (classification tree and Principal Component Analyses) based on template G.

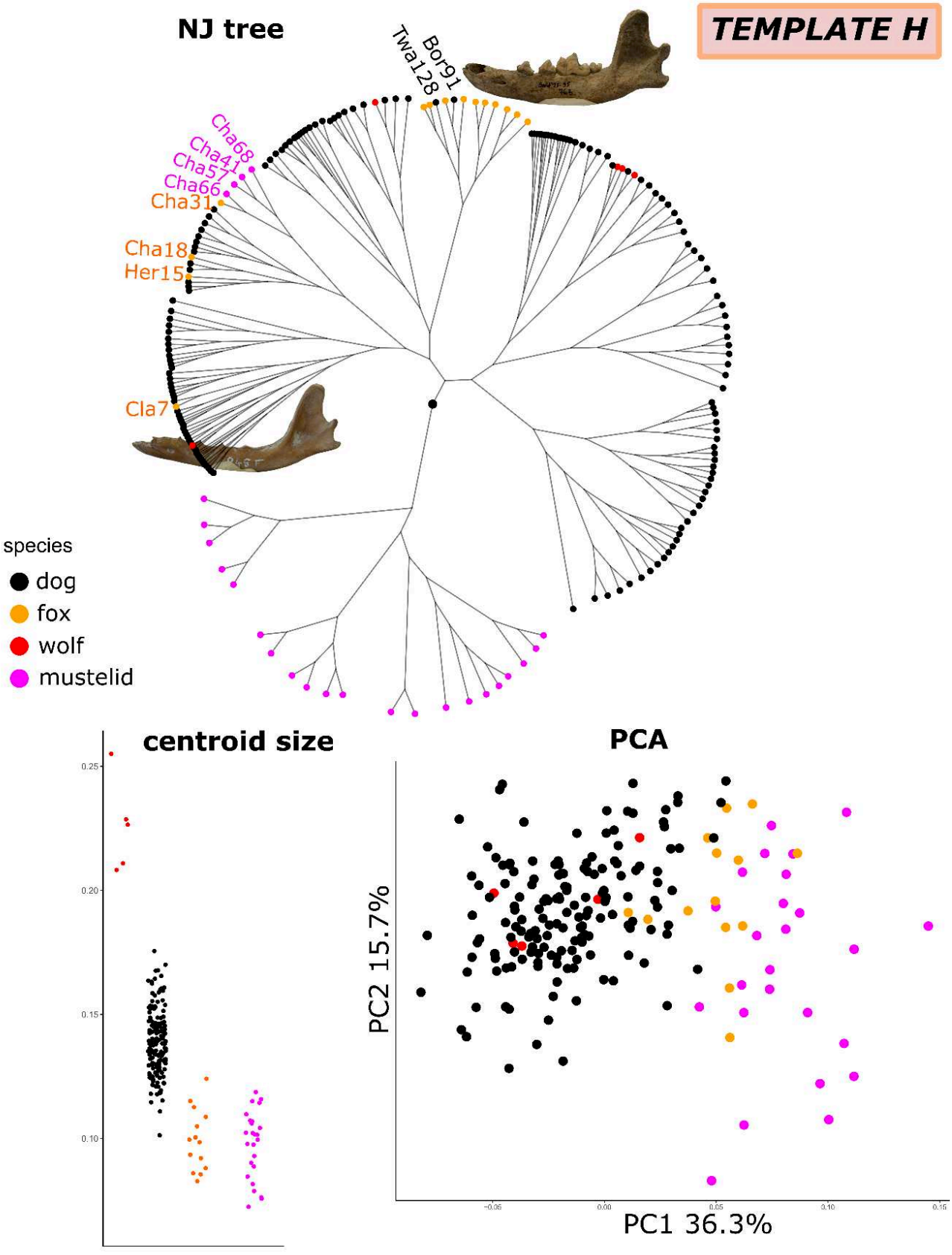

* Figure 172. Verification of species identification, using comparison of shapes (classification tree and Principal Component Analyses) based on template H.

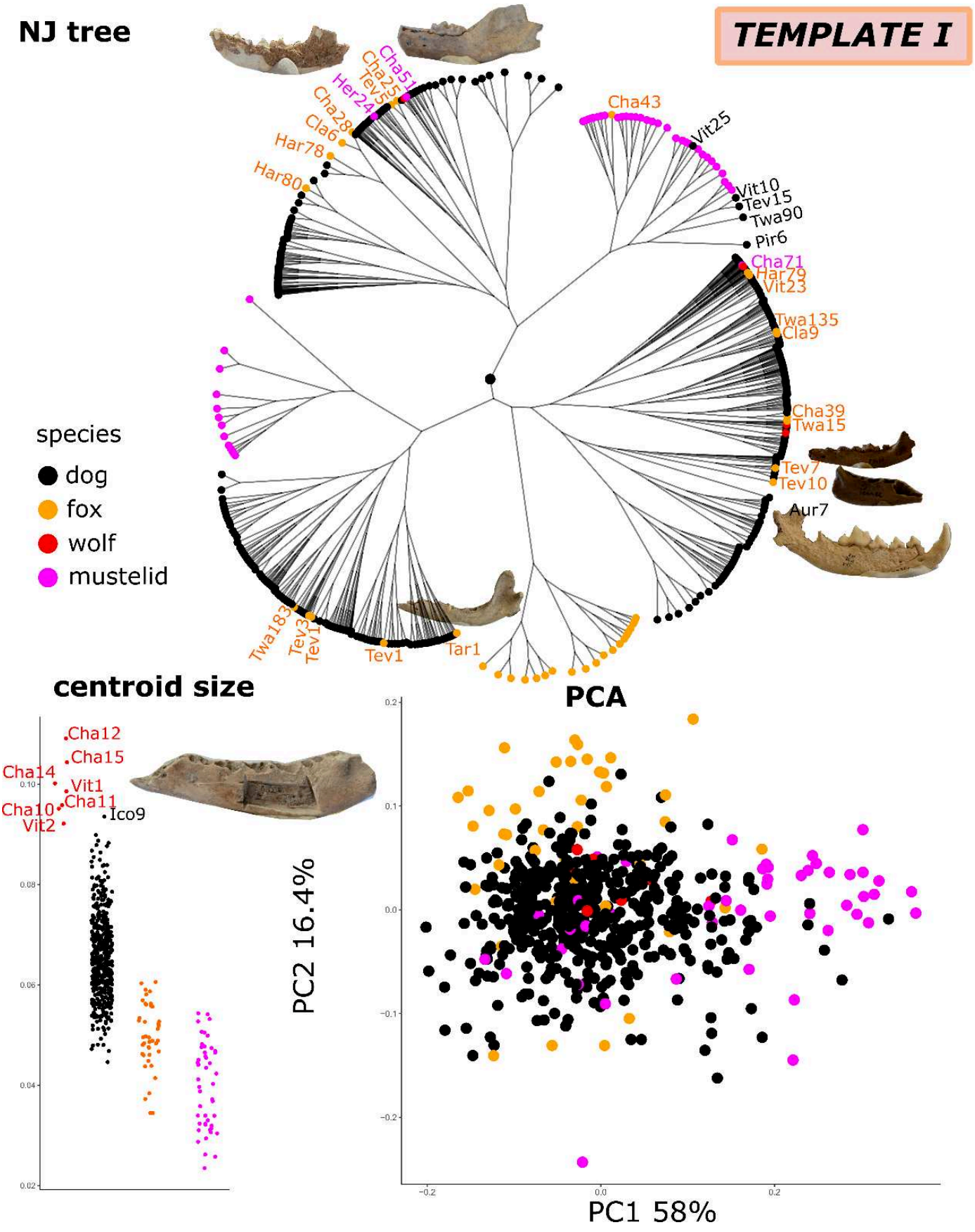

Figure 173. Verification of species identification, using comparison of shapes (classification tree and Principal Component Analyses) based on template I.

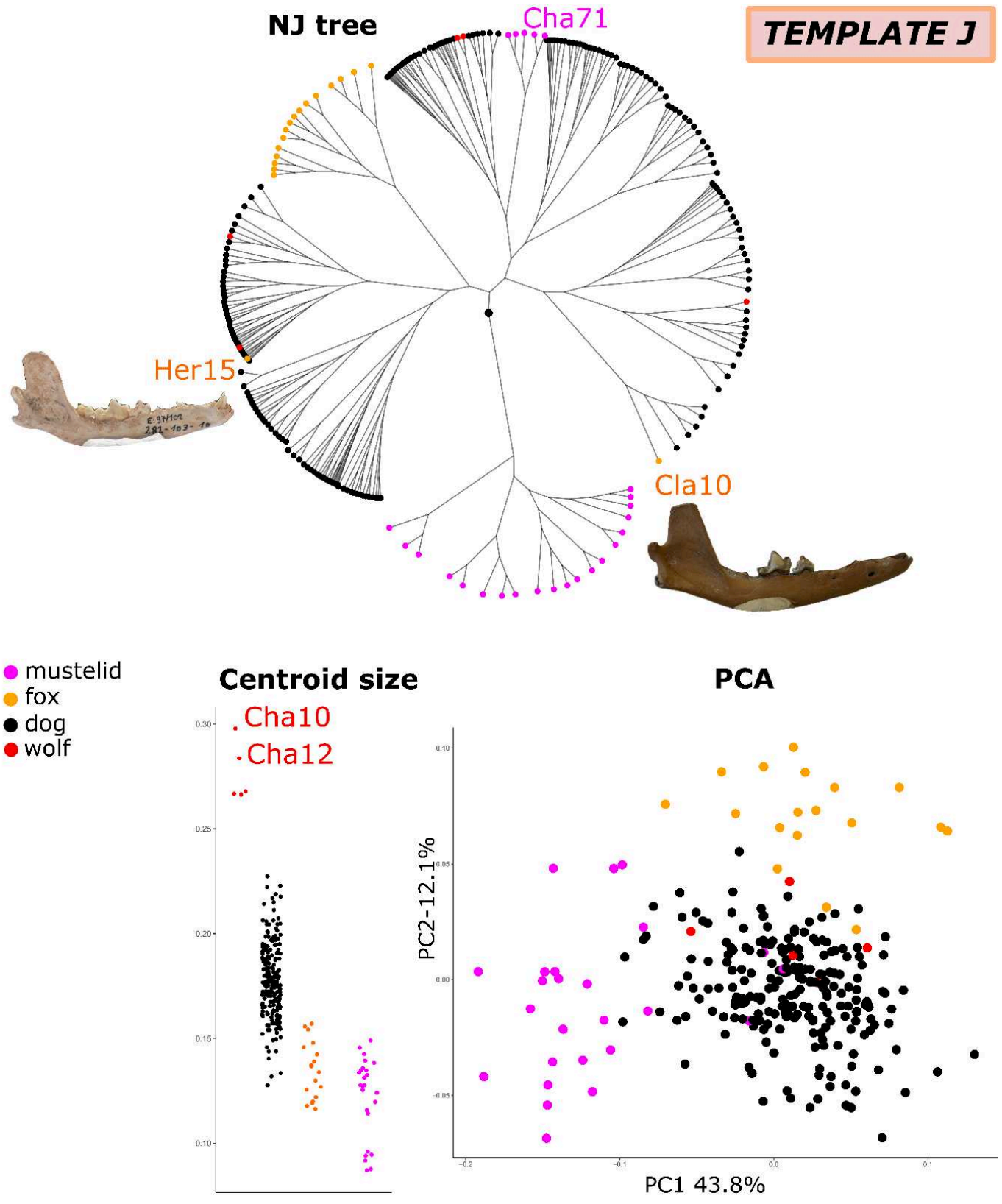

Figure 174. Verification of species identification, using comparison of shapes (classification tree and Principal Component Analyses) based on template J.

9. Part 3. Analyses performed on the predicted mandible shapes.

9.1. Chapter 7

We have tried to conduct the analyses not on the coordinates of template I, but on the complete shape of the mandible for the 491 individuals described by template I. To do this, we predicted the coordinates of the complete shape of the mandible following the method proposed (see section 1.2.5).

We predicted the shape only for the 127 dogs with complete mandibles in order to verify the accuracy of the predictions. A tree similar to that of the Figure 99 should be obtained.

If the 15 first PLS axes (all the axes that show significant *P*-values) are used for the predictions, some outlandish forms are predicted based on the mandibles of pre-Bronze Age dogs (Figure 179). Accordingly, we prefer to keep only the three axes that represent more than 1% of the total covariation for the analyses (Figure 175).

We observe that the separation between modern and ancient dogs is clearer (Figure 175) than in analyses with template A (Figure 99, see page 370), but this is probably a methodological bias. Indeed, the decision rules are established on all modern dogs and then applied to archaeological dogs, which artificially increases the differences.

Then we conducted the analyses with the predicted shapes for all the specimens represented by template I (Figure 176).

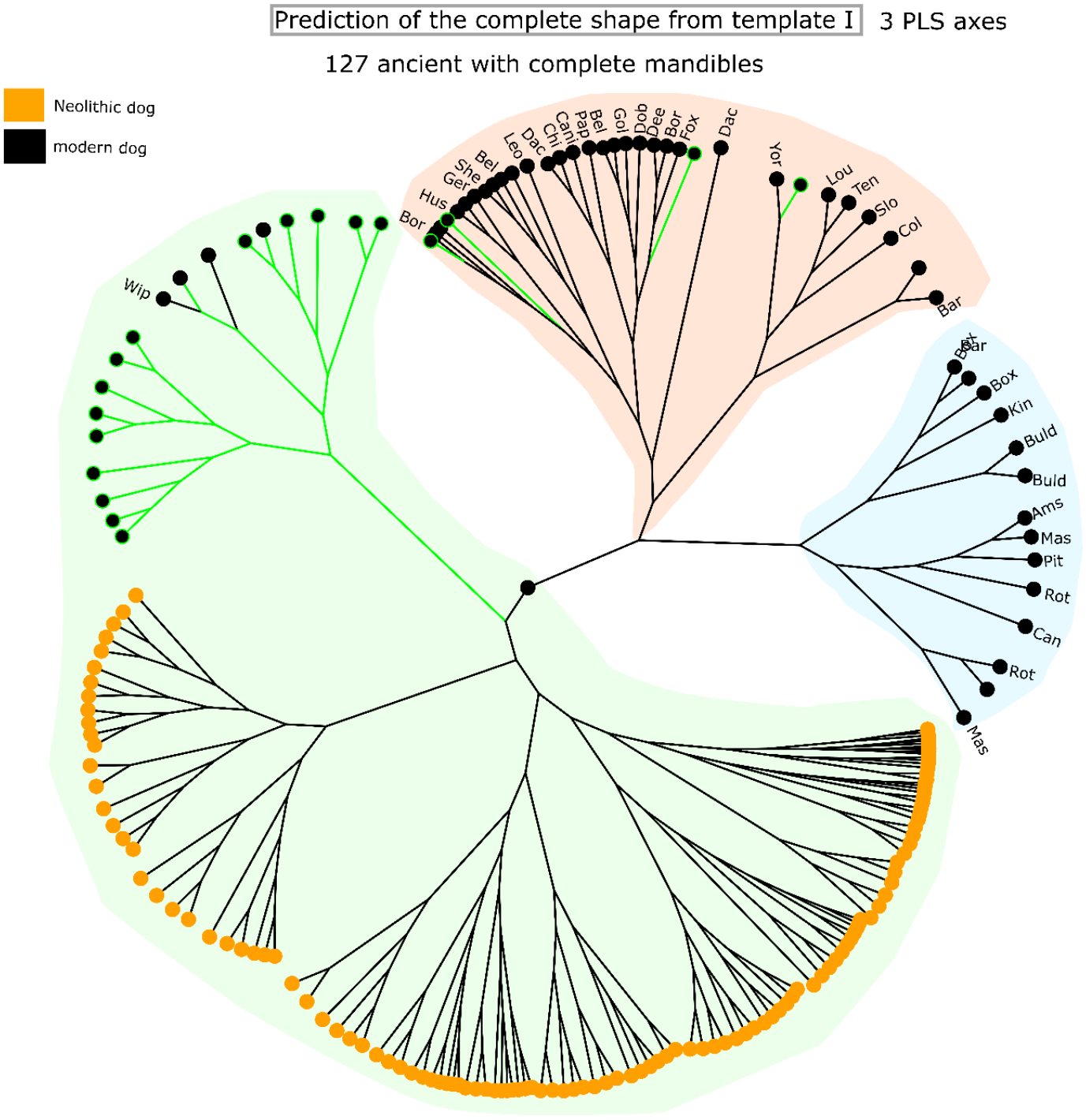

Figure 175. Verification of species identification, using comparison of shapes (classification tree and Principal Component Analyses) based on shape predictions using template I for the complete mandibles. Only the 3 first PLS axes were used for the predictions.

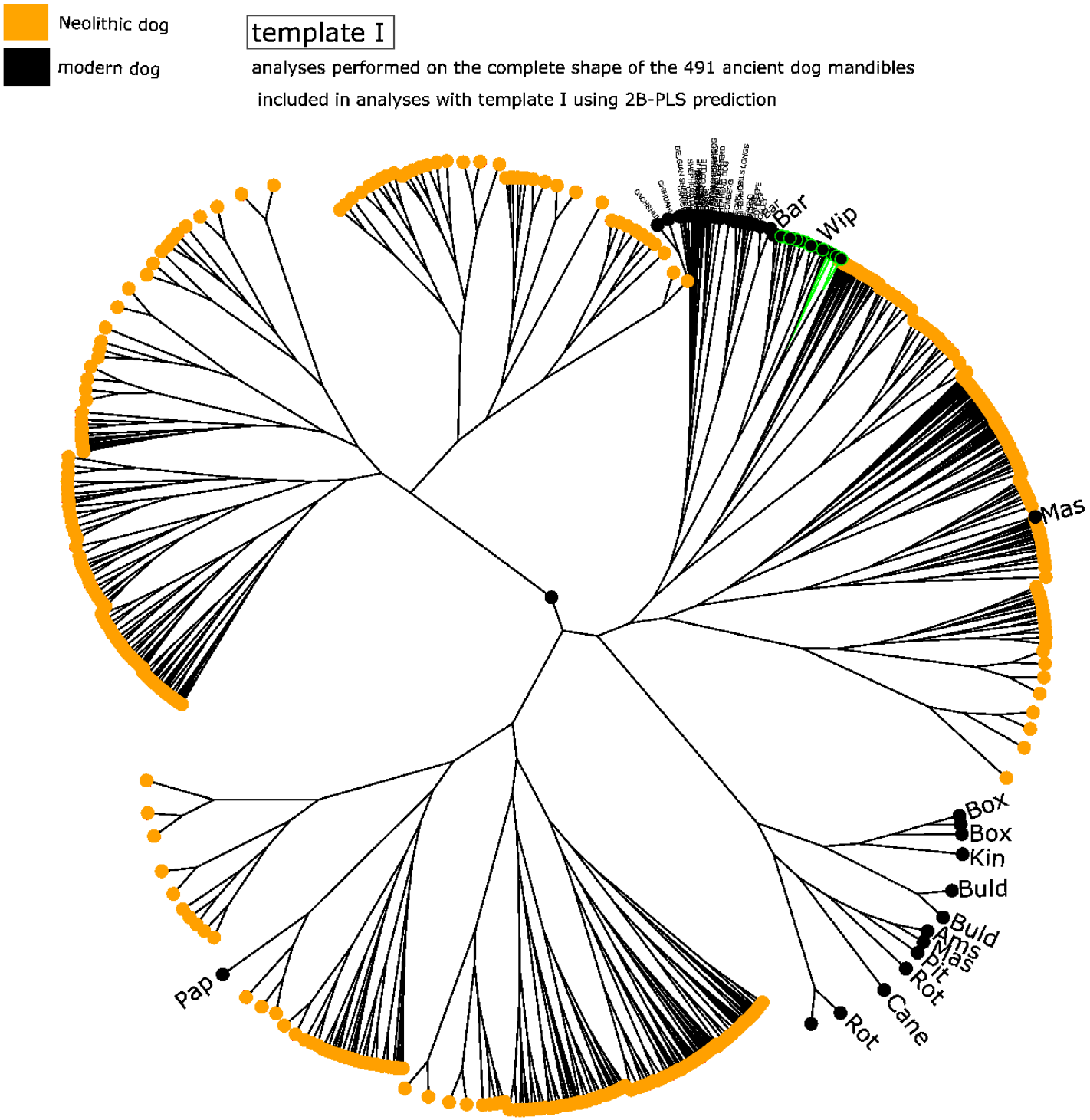

Figure 176. Verification of species identification, using comparison of shapes (classification tree and Principal Component Analyses) based on shape predictions using template I for all the mandibles. Only the 3 first PLS axes were used for the predictions.

9.2. Chapter 9 – comparison of ancient dogs from Eastern and Western Europe

In Part 3 Chapter 9 section 1 (page 414), we performed parallel analyses on the predicted shapes of the complete mandible based on the Procrustes coordinates of template I, using PLS regression as explained in Chapter 7 section 1.2.6.2 (page 382).

We performed analyses on 2 sets of predictions: the first one uses only the 3 first PLS axes (that represent 96% of the total covariations), and the second set uses the 15 first axes that show significant levels of covariation. The results are indicated in Table 38.

To ensure the relevance of using predicted shapes for analyses, we compared the results we obtained using template A (Table 38) to those we obtained using PLS predictions from template I for the 127 mandibles included in analyses with template A (Figure 181). Unfortunately, it seems that the results with shape predictions are too distorted to be fully exploited. Indeed, the success rate of the CVA is lower in analyses with predicted shapes and the CVA is particularly bad at classifying dogs from Eastern Europe. The CVA more easily classifies dogs from Western Europe. As a consequence, we do not feel it appropriate to interpret the results of the analyses we performed on the predicted complete shapes of the 492 mandibles corresponding to template I (the results are reported for discussion only).

If we consider the second set of predictions (using the 15 first PLS axes, Figure 179) the results are slightly closer to those obtained with template A (which is consistent with the fact that the more PLS axes are taken into account in the analyses, the more accurate the predictions, at least for the mandibles that contribute to build the decision rules). However, the classification tree leads to different classifications and some predicted shapes are absurd, which demonstrates that the method is not appropriate for our sample of 491 mandibles. We do not encounter this problem when using only 3 PLS axes for prediction. This is likely because the decision rules were established on a less variable sample (only 127 dogs). Moreover, some small fragments could be slightly damaged, creating some noise in the data. If more PLS axes are used for the prediction, more importance can be given to some points that are likely to be misplaced because of the fragmentation in template I.

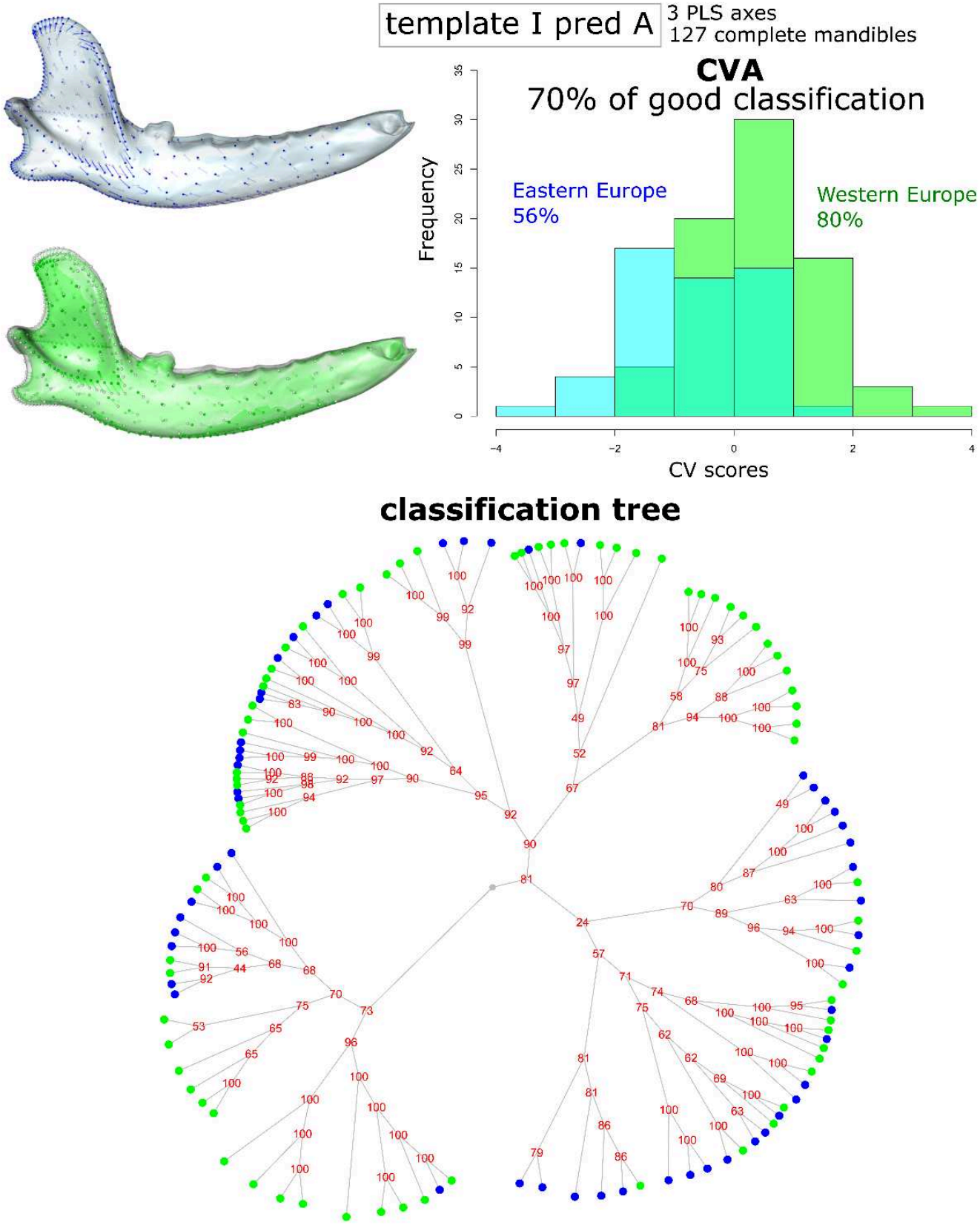

Figure 177. Visualisation of differences in mandible form between ancient dogs from Eastern and Western Europe. Analyses based on the predicted shapes of the complete mandibles using template I for the 127 ancient dogs with complete mandibles. 3PLS axes were used for the prediction using PLS regression.

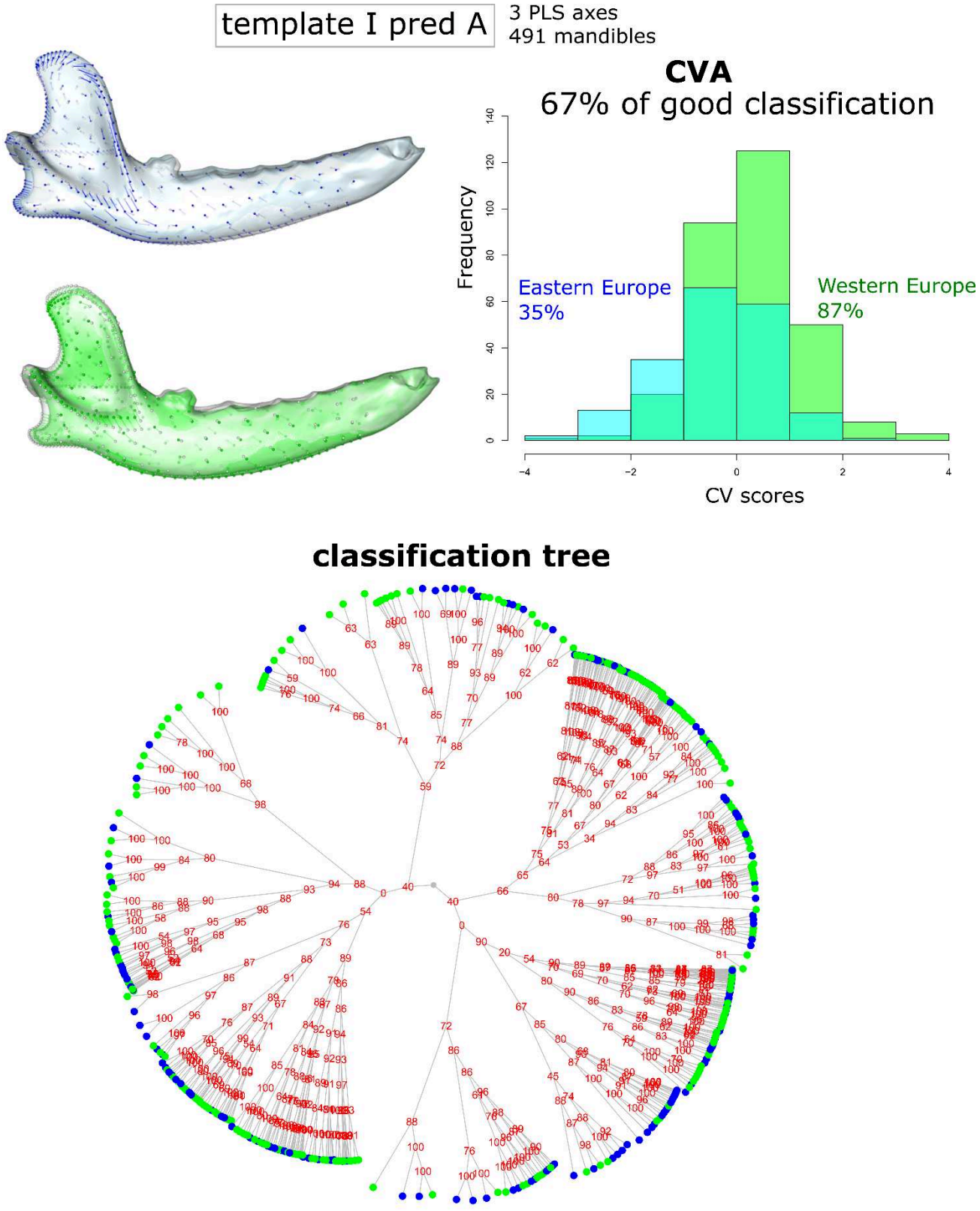

Figure 178. Visualisation of differences in mandible form between ancient dogs from Eastern and Western Europe. Analyses based on the predicted shapes of the complete mandibles using template I for the 491 ancient dogs represented by template I. 3PLS axes were used for the prediction using PLS regression.

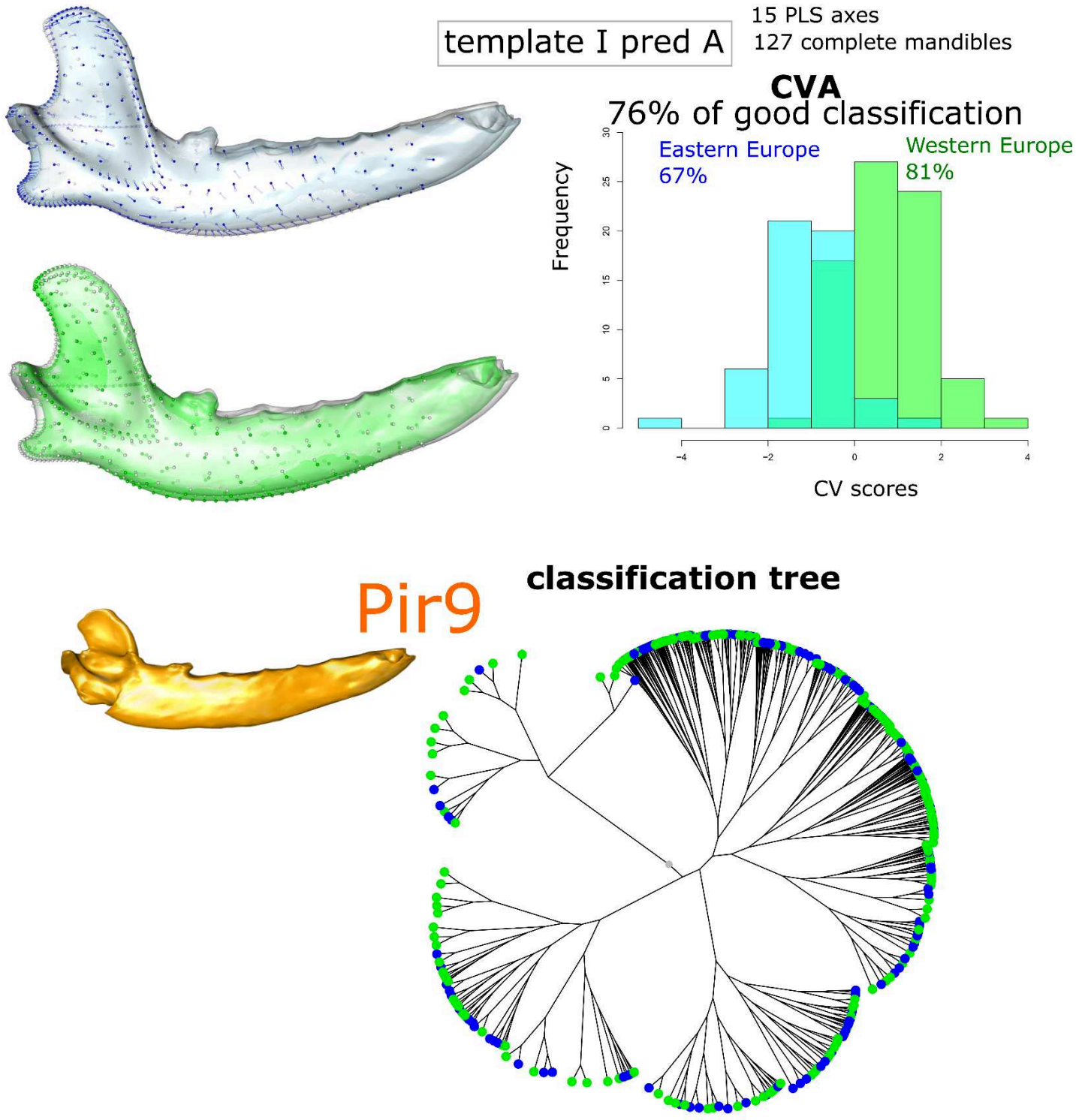

Figure 179. Visualisation of differences in mandible form between ancient dogs from Eastern and Western Europe. Analyses based on the predicted shapes of the complete mandibles using template I for the 127 ancient dogs with complete mandibles. 15 PLS axes were used for the prediction using PLS regression.

10. Efficiency of each template to predict cranial shape

In Part 2 (see Article 2, Chapter 3, page 163), we demonstrated that cranial and mandibular shape strongly covary in modern dogs and red foxes. This strong covariation may allow to predict the shape of the cranium using the shape of the complete mandible or even that of a part of the mandible. In order to test whether integration is strong enough with small fragments to enable accurate predictions, we performed a two-block partial-least-square analysis between the Procrustes coordinates of cranial shape and the Procrustes coordinates of each template used to study mandibular shape in archaeological canids. Then we use the results of the 2B-PLS to buid predictive models and compare the results of our predictions with real cranial shapes.

This section is exploratory and is provided for information purposes only. We had indeed only a small number of archaeological crania associated with mandibles, allowing us to verify the accuracy of our predictions.

The results are nevertheless discussed here because they allow us to confirm that even small portions of the mandible can provide information on the overall shape of the head and thus the morphotype. However, the loss of information is more or less important depending on the fragments. The loss of information is very important for templates E and H. Interestingly, template I is informative enough to reflect strong differences between the different populations in a sample (between brachycephals and modern dolichocephals in particular).

However, since the modularity was likely not the same in the past (see Part 3, Chapter 7, section 1.2.6), it is not possible to be sure that these results are fully transposable to archaeological canids.

10.1. Prediction of cranial shape in modern dogs

10.1.1. Establishment of the decision rules on all the modern dogs of our sample

Procrustes coordinates for the block 1 (mandibular shape) were obtained from a general Procrustes Analyses (GPA) performed on the raw coordinates of the mandibular shape for the modern dogs and dingoes for which both the upper and lower jaw have been landmarked, plus all the archaeological dogs for which skull shape is to be predicted. The Procrustes coordinates for the block 2 (cranial shape) were obtained from a GPA performed on the raw coordinates of cranial shape for all the modern dogs and dingoes for which both the upper and lower jaw have been landmarked.

We also used the dingoes for the construction of the model since we demonstrated that dingoes are close is shape to ancient dogs (see classification trees). The juveniles were excluded from the construction of the model.

We used the function “pls2B” from the package “Morpho” to build a predictive model on the modern canids and we used 1000 permutations to compute the p-value. We then used the function predictPLSfromData to predict the shape of the cranium of the archaeological dogs.

Only one Beagle (M2) was 3D modelled using photogrammetry. We compared the predicted shape using the model established for each template and the real shape of the cranium using the function meshDist. This function calculates and visualizes distances between the two surface meshes.

The results of the covariation analyses are provided in Table 50. Visualisation of the deformations along the first PLS axes for analyses performed on coordinates from template A and I are provided in Figure 180 and Figure 181, respectively. The differences between the real shape and the predicted shape for beagle M1 are reported in Figure 182.

We observe that all models show strong covariations between cranial and mandibular shape, with the exception of templates E and H ($0.01 < P < 0.05$ and coefficients of covariation below 0.7) and template G ($0.001 < P < 0.01$ and r-pls below 0.7). However, for template G, the comparison between mesh surfaces for beagle M1 is quite good. The most obvious differences are located on the zygomatic arch. For template A, the differences are mostly located on the curvature of the snout and these differences get more important when we consider templates B, C, F. Interestingly, the lowest differences between the real mesh and the predicted mesh are obtained for template I (Table 51, Figure 182, Figure 183). Most of the templates are thus interesting to predict cranial shape, even the template I, although it corresponds to the smallest fragment. The robustness and curvature are particularly distinctive of brachycephalic and dolichocephalic dogs (Figure 180 and Figure 181).

Table 50. Results of the 2B-PLS analyses between cranial and mandibular shape in the 56 modern dogs and 7 dingoes with cranium and mandible, for all the templates used in analyses of ancient dogs.

template	% of total covariation of PLS1	r-PLS	P
A	86%	0.82	0.001
B	85%	0.77	0.001
C	82%	0.74	0.001
D	79%	0.79	0.001
E	69%	0.60	0.040
F	73%	0.79	0.001
G	71%	0.69	0.005
H	62%	0.56	0.009
I	67%	0.73	0.038
J	77%	0.73	0.001

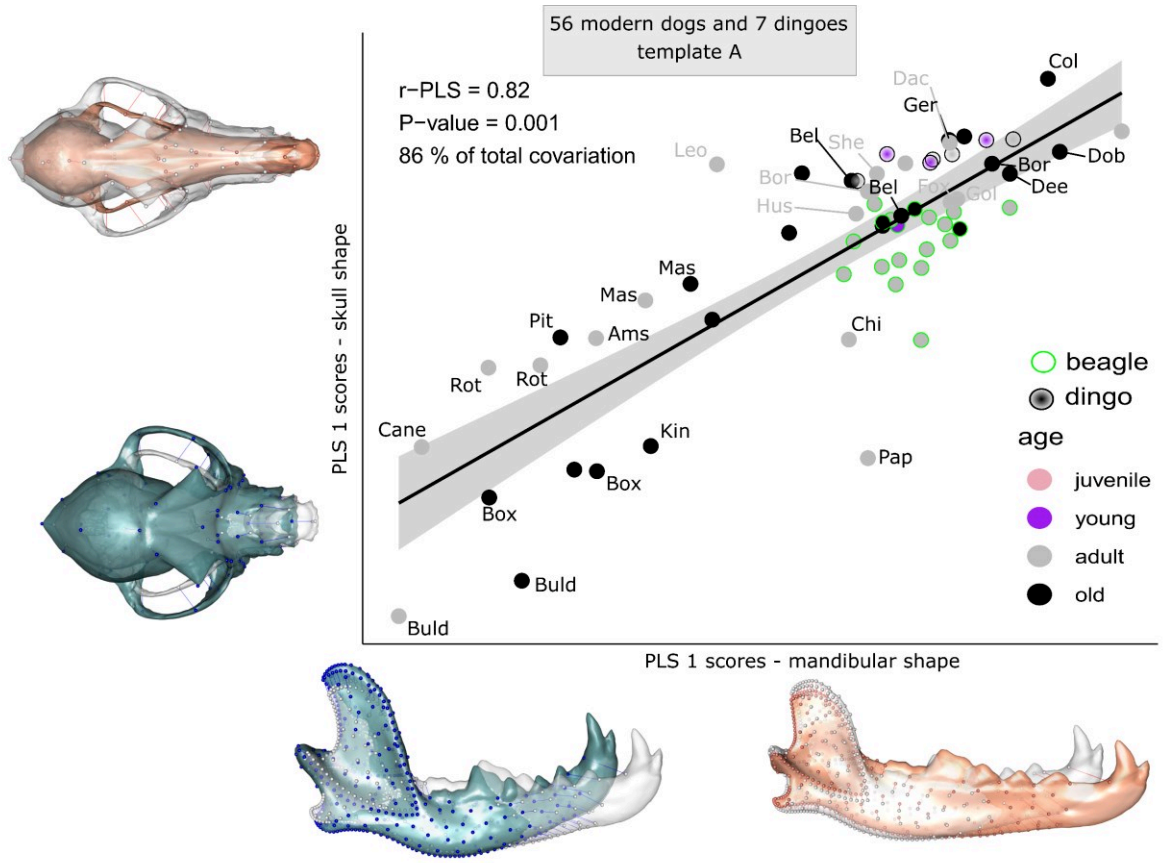

Figure 180. 2B-PLS between the cranial and mandibular shape in modern dogs (56) and dingoes (7) – analyses performed with template A.

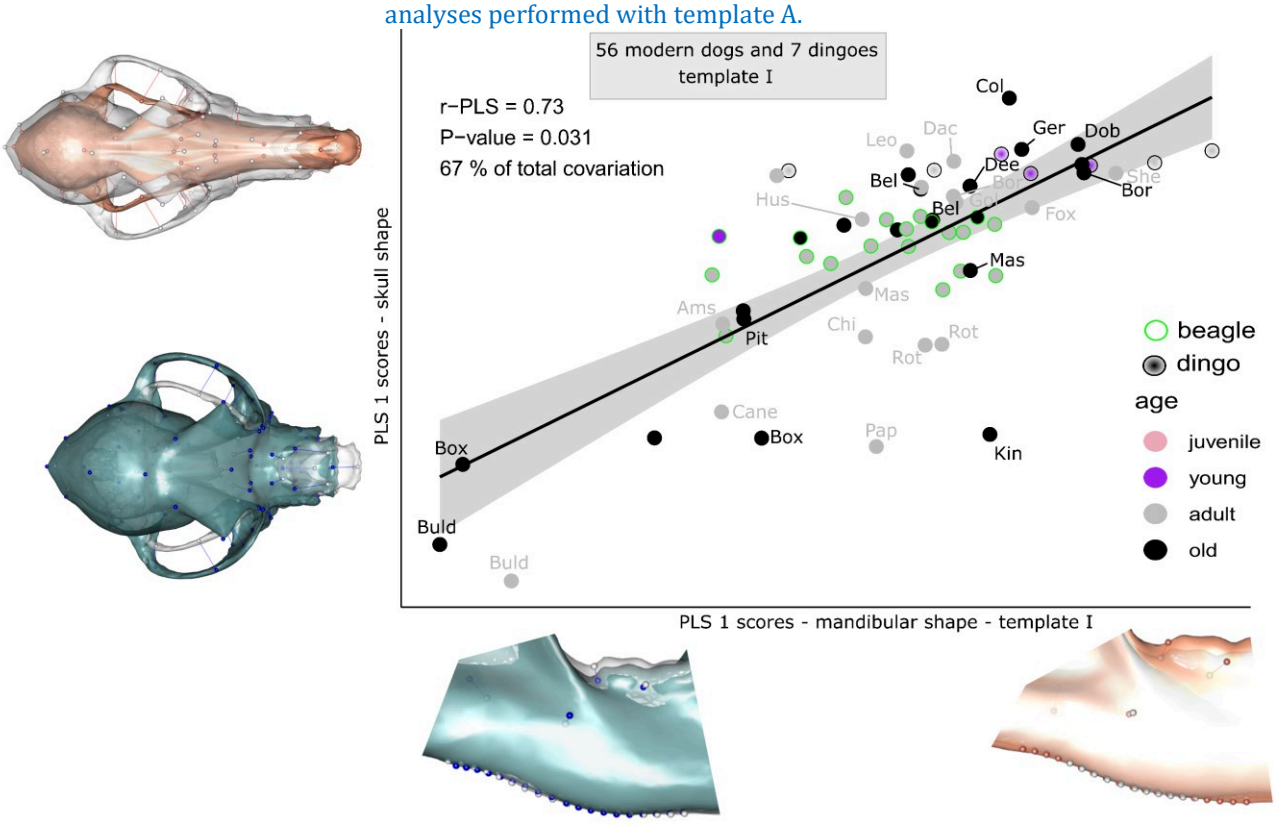

Figure 181. 2B-PLS between the cranial and mandibular shape in modern dogs (56) and dingoes (7) – analyses performed with template I.

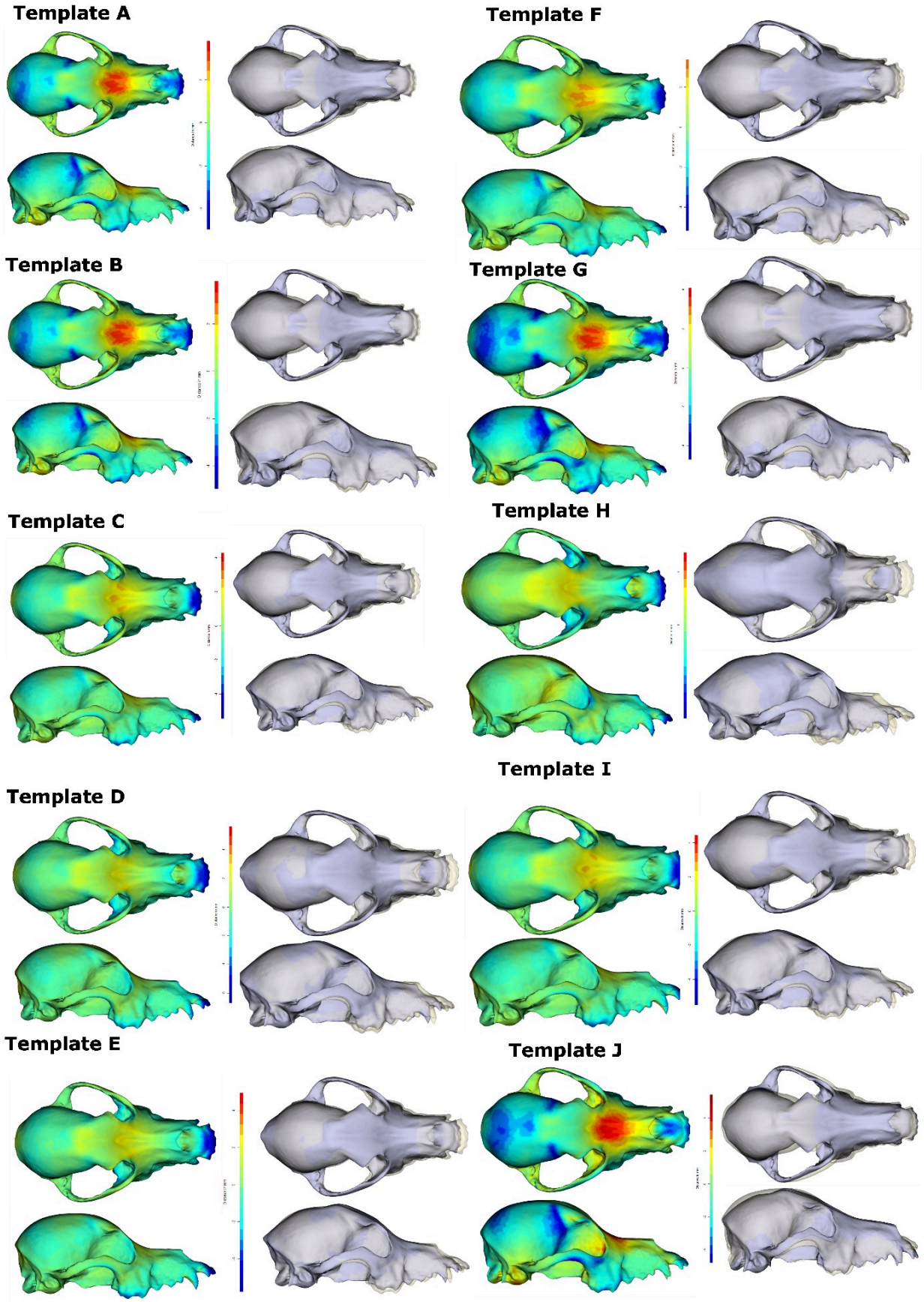

Figure 182. Comparison between the surfaces of the real cranial shape (white) of Beagle M1 and that of the predicted shape using the shape of the mandible for the 10 templates. The PLS model is based on the 7 modern dingoes and 56 modern dogs. The distances between the surfaces are represented using colors on the real surface of Beagle M1. They are listed in Table 51.

Table 51. Summary of the distances between the real mesh of Beagle M1 (obtained using photogrammetry) and the mesh obtained after prediction using the 10 fragmentation patterns of mandible shape. The PLS model is based on the 7 modern dingoes and 56 modern dogs.

Template	Min.	Median	Mean	Max
A	-4.9553	-0.1532	-0.2342	3.8003
B	-5.2394	-0.1276	-0.2329	3.5710
C	-5.4239	-0.1846	-0.2690	4.2764
D	-6.6860	-0.1606	-0.3245	5.6254
E	-0.8281	-0.1617	-0.2818	4.9609
F	-5.1745	-0.1255	-0.2381	3.3765
G	-4.6653	-0.1921	-0.2370	4.0855
H	-8.8051	0.1970	-0.4475	6.7980
I	-5.4830	-0.1780	-0.2692	4.4551
J	1.4687	-0.2860	-0.2678	5.4039

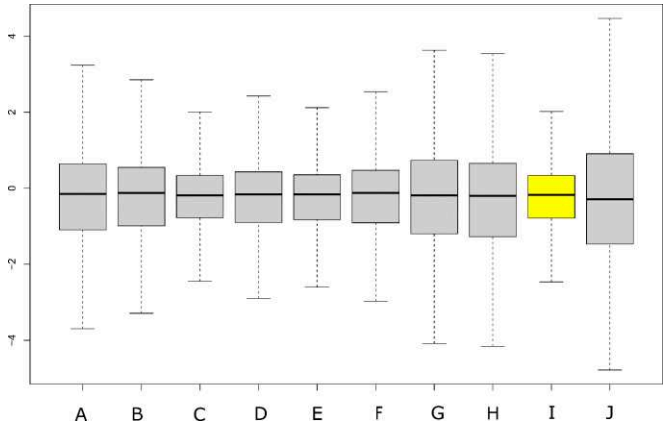

Figure 183. Distances between the real mesh of Beagle M1 (obtained using photogrammetry) and the mesh obtained after prediction using the 10 fragmentation patterns of mandible shape.

10.1.2. Establishment of the decision rules on the modern dogs that are the closest in size and shape to the ancient dogs

We also performed similar analyses with only the 52 modern dogs and dingoes that are closer in size and shape (we removed from the analyses the dogs in group B and B' in the classification tree with modern and ancient dogs, the shepherd sheepdog and the 2 barzoïs that are much larger, and the chihuahua and papillon that are smaller).

The covariations are lower than in the previous section and they are no longer significant for template E (Table 52). The covariations are less good for template I. Beagles are clearly isolated on the left part of the graph (Table 52, Figure 184).

Table 52. Results of the 2B-PLS analyses between cranial and mandibular shape in the 52 modern dogs and dingoes for all the templates used in analyses of ancient dogs.

template	% of total covariation of PLS1	r-PLS	P
A	70 %	0.86	0.001
B	68	0.85	0.001
C	70	0.82	0.001
D	58	0.82	0.011
E	66	0.56	0.062
F	74	86	0.001
G	58	0.64	0.005
H	76	0.80	0.001
I	66	0.55	0.008
J	75	0.75	0.001

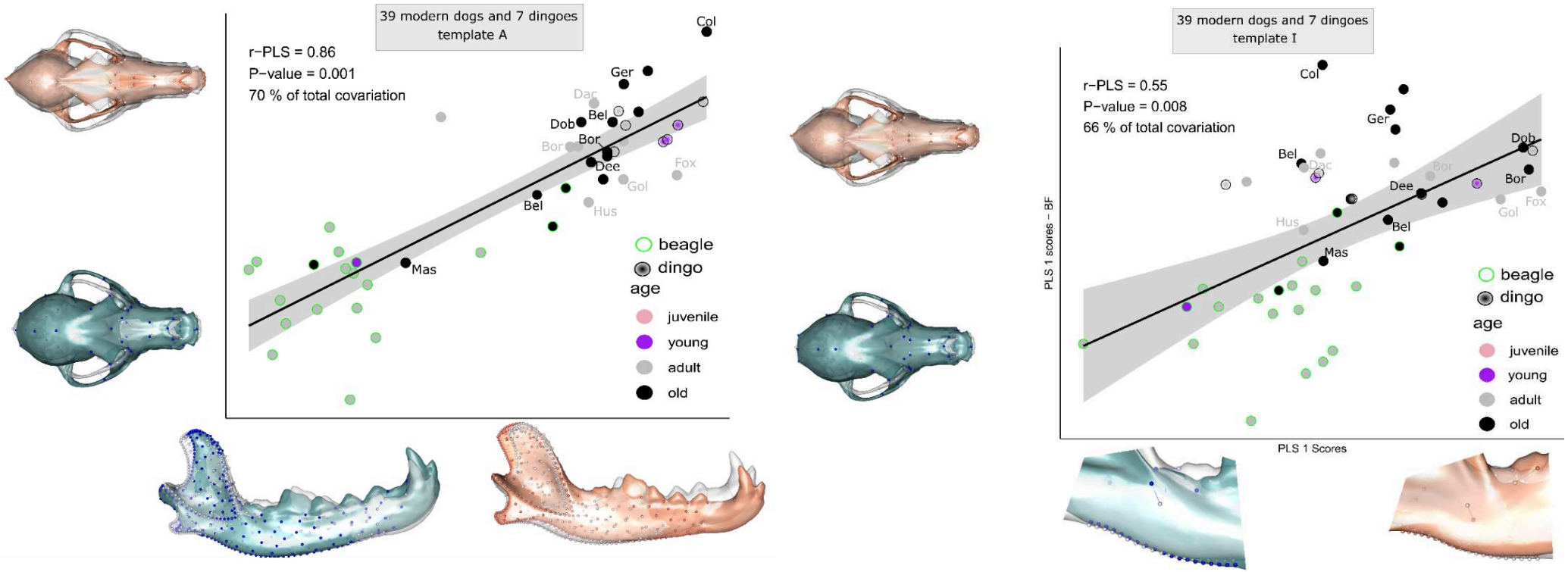

Figure 184. 2B-PLS between the cranial and mandibular shape in a subsample of the modern dogs (39) and dingoes (7) – analyses performed with template A (left) or template I (right)

10.1.3. Application to ancient dogs

Five crania of ancient dogs were reconstructed using photogrammetry (Pir12, Aur3, Cha19, Cla1, Cad3), but only one of these crania (Cad3) correspond to a complete mandible of our corpus (Cad2). Cad2 is a complete mandible that is included in all templates. We used the Procrustes coordinates from templates A (Figure 185) and I (Figure 186) of mandible Cad2 to predict the cranial shape and we compared it with the real shape of the cranium (Cad3). For template A, better results are obtained when only 52 dogs are used to establish the decision rules. For template I, better results are obtained when all modern dogs are used to establish the decision rules.

We have also photographed the skull (cranium and mandible still in connection) Pir2 for which the corresponding mandible (Pir3) is included in analyses with templates B, D, E, G, I, and J. We used the Procrustes coordinates from template I (Figure 187) of the mandible to predict the cranial shape and we compared it with the real shape of the cranium. Better results are obtained with template A and when all modern dogs are used to establish the decision rules. Better results are obtained when only 52 dogs are used to establish the decision rules.

The other crania are unfortunately too damaged to be used to test the correspondence between the predicted and the real cranial shape.

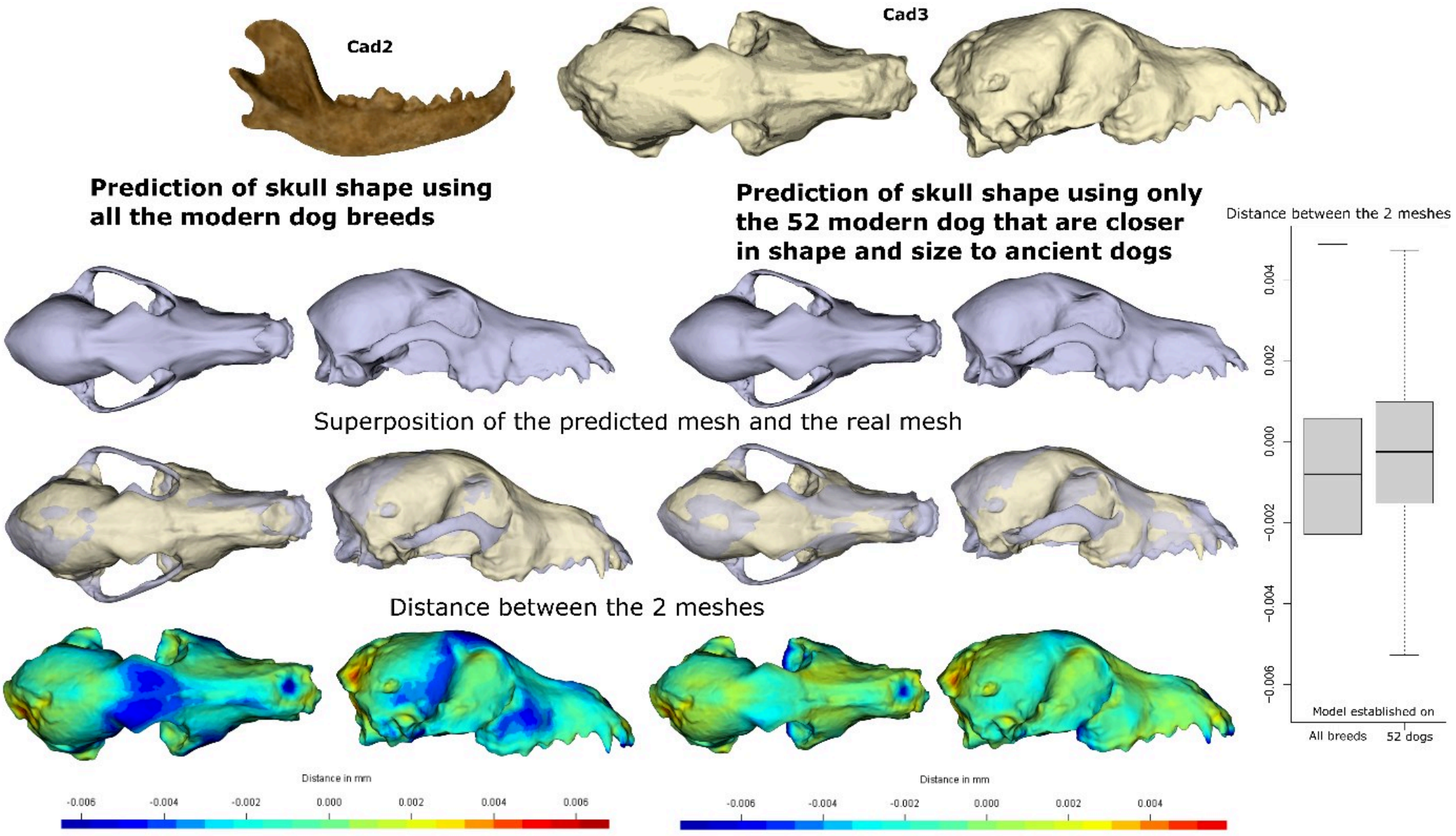

Figure 185. Comparison between the surfaces of the real cranial shape (white) that correspond to mandible Cad2 (id Cad3) and that of the predicted shape using the shape of the mandible for the template A.

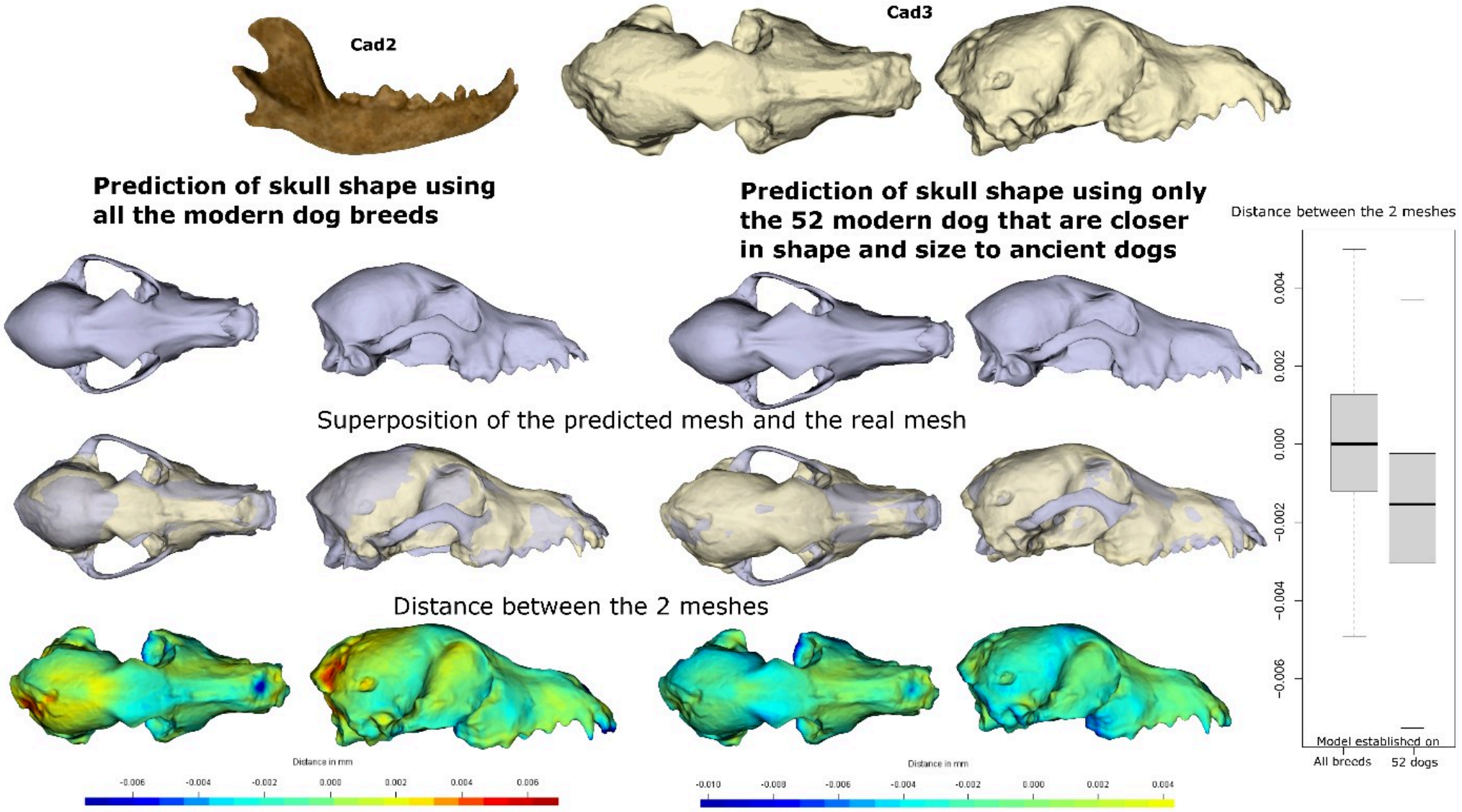

Figure 186. Comparison between the surfaces of the real cranial shape (white) that correspond to mandible Cad2 (id Cad3) and that of the predicted shape using the shape of the mandible for the template I.

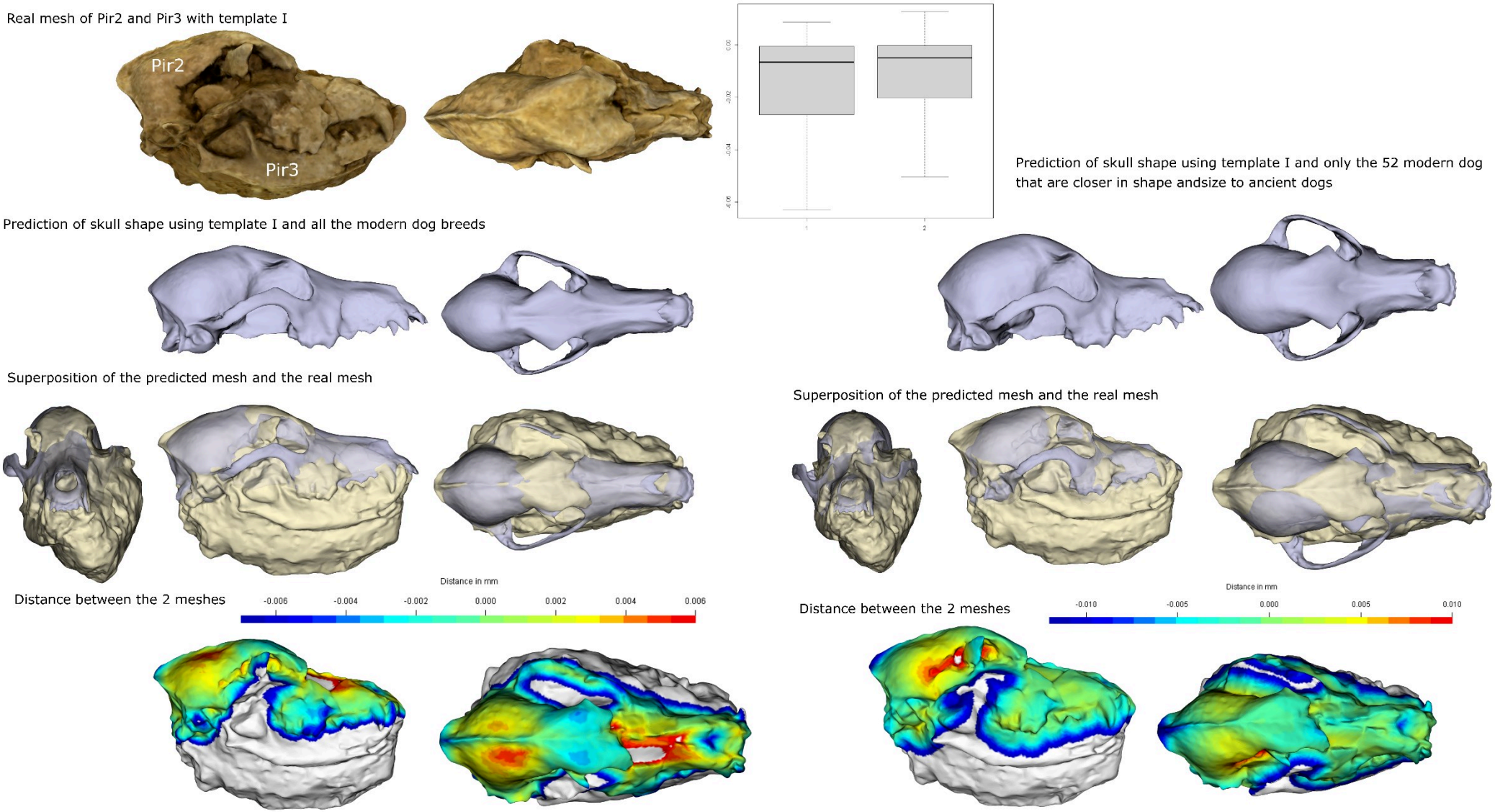

Figure 187. Comparison between the surfaces of the real cranial shape (white) that correspond to mandible Pir2 (id Pir3) and that of the predicted shape using the shape of the mandible for the template I.

11. Part 3 – Chapter 7. A consequence of differences between modern and ancient canids: the inadequacy of supervised learning for species prediction

We performed supervised analyses to predict the species of archaeological remains based on decision rules established on modern canids.

In the following section, we used Canonical Variate Analysis to separate modern canids species (dog/dingo/wolf/fox) and then applied the decision rules to archaeological remains. For each template, we first performed a GPA on the landmark coordinates of both the modern and archaeological mandibles. We then performed a Canonical Variate Analysis on the rotated configurations projected into tangent space of the modern canids (70 dogs, 10 dingoes, 8 wolves, 72 foxes, young and adults are included) of the sample using the function CVA() from package Morpho. We measured the success rates after a leave-one-out procedure. After this, we predicted the scores of the archaeological canids in this CVA using the function predict(). We applied the function typprobClass() on these scores to predict the species of the archaeological canids based on the decision rules established on the modern canids. This function calculates the probability for an observation belonging to a given multivariate normal distribution. The specimens for which the probability to belong to any group is under 0.1% were not assigned to any group. Since we did not have modern mustelids, the predictive model was not built to detect the presence of another species. Although one could expect the model not to be able to classify them in any of the modern canid groups (they should appear as not classified if the model is specific enough).

The success rates on modern canids are generally excellent (Table 53). Templates G and I have the lowest success rates on modern canids (87% and 81%, respectively).

However, the correspondence between our identifications and CVA predictions for the archaeological remains is not good. Actually, for all templates there are many unclassifiable individuals, including for the most complete templates (A and B), which likely reflects differences in morphology and morphological variability between modern and archaeological canids, suggesting that **modern canids are not good models to compare with archaeological canids, at least for identification purposes**. We have better results for the smallest templates (G, H, I and J). However, with these templates, most of the mustelids were classified in one of the canid species (while for most templates, the archaeological mustelids were not classified, which is good). This is likely because these templates are less impacted by slight variations in shape and thus the differences between archaeological and modern mandibles are lower. The CVA is consequently more successful at finding a group for attribution. This does not mean, however, that these fragments are more akin to reflect fundamental differences between species.

The visualisation of the results for template A and B reinforces this hypothesis: many dogs are plotted outside of the range of modern dogs. The same is observed for foxes, at a lower scale. Mustelids are plotted between them and tend to be clearly isolated however.

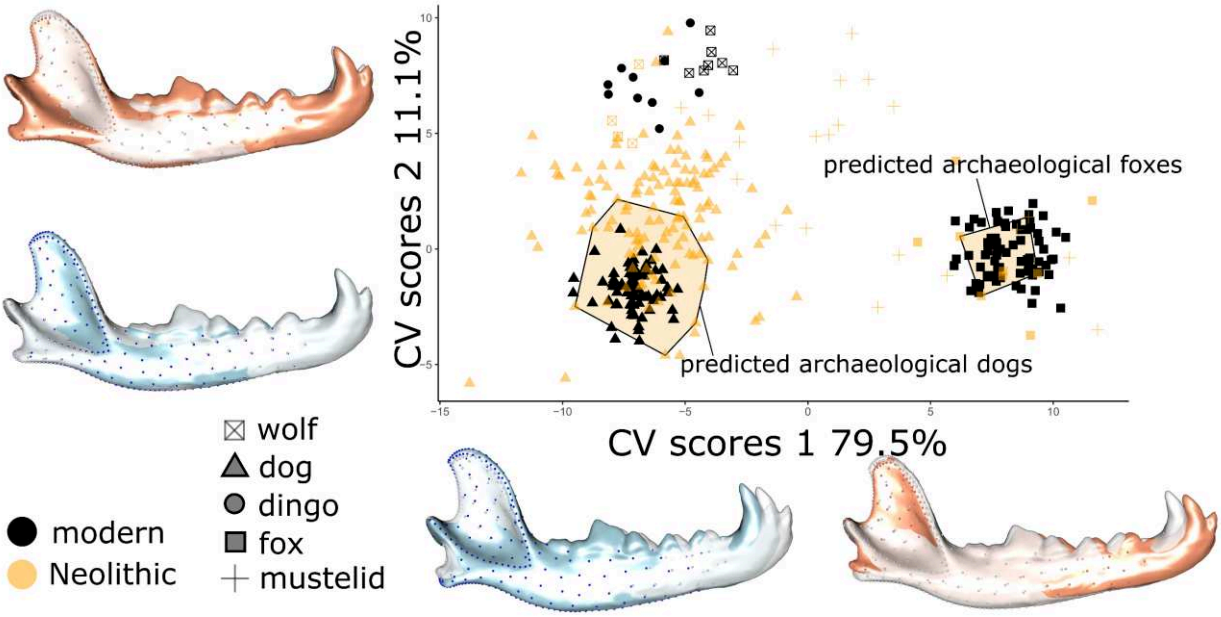

Figure 188. CVA scores of the modern and archaeological canids and mustelids with template A, with visualisation of the deformations along CVA axes. The area of prediction of archaeological dogs or foxes around modern dogs or foxes are reported.

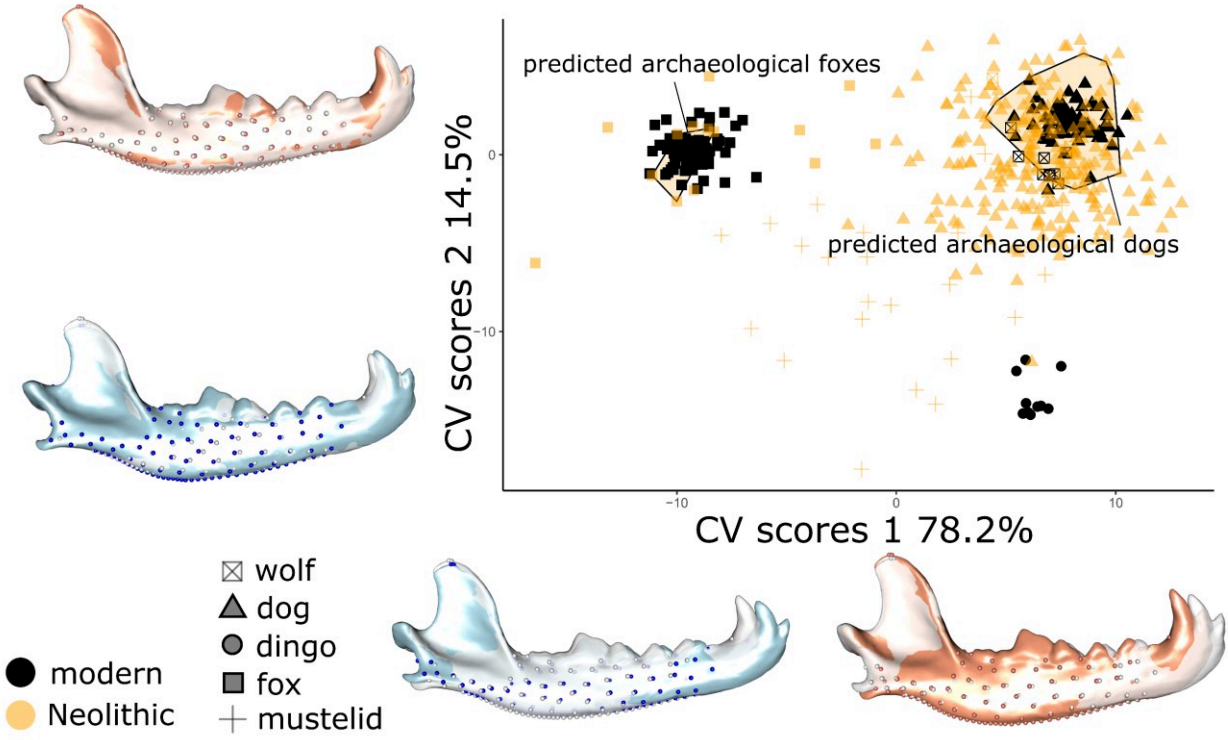

Figure 189. CVA scores of the modern and archaeological canids and mustelids with template B, with visualisation of the deformations along CVA axes. The area of prediction of archaeological dogs or foxes around modern dogs or foxes are reported.

As a result, the use of non-supervised analyses may be more relevant to identify clusters of individuals which are likely attributable to the species in the first place.

Table 53. Success rates with the CVA.

	Success by cross-validation on:		Unclassified	
	modern canids	archaeological canids	archaeological canids	archaeological mustelids
A	98%	29% (36/127 dogs +4/8 foxes+0/4 wolves)	72% (4/4 wolves + 4/8 foxes + 91/127 dogs)	90% 19/21
B	98%	38% (84/228 dogs + 9/13 foxes + 1/4 wolves)	60% (3/4 wolves + 4/13 foxes + 140/228 dogs)	83% 19/23
C	95%	24% (46/217 dogs + 7/10 foxes +2/4 wolves)	73% (2/4 wolves + 3/10 foxes +163 /217 dogs)	89% 24/27
D	93%	56% (221/395 dogs + 17/22 foxes + 1/7 wolves)	38% (3/7 wolves + 5/22 foxes + 154/395 dogs)	58% 22/38
E	88%	43% (208/440 dogs + 20/32 foxes + 1/8 wolves)	44% (0/8 wolves + 10/32 foxes +199/440 dogs)	78% 31/40
F	96%	25% (37/155 dogs + 5/14 foxes + 2/5 wolves)	74% (3/5 wolves + 9/14 foxes + 117/155 dogs)	88% 22/25
G	87%	71% (276/389 dogs + 20/25 foxes + 4/7 wolves)	4% (0/7 wolves + 2/25 foxes + 13/389 dogs)	20% 9/45
H	91%	70% (113/160 dogs + 10/14 foxes + 2/5 wolves)	4% (0/5 wolves + 3/14 foxes + 4/160 dogs)	20% 5/25
I	81%	82% (409/491 dogs + 31/40 foxes + 3/9 wolves)	3% (0/9 wolves + 1/40 fox + 15/491 dogs)	4% 2/47
J	93%	73% (158/215 dogs + 14/18 foxes + 1/5 wolves)	12% (0/5 wolves + 4/19 fox + 25/215 dogs)	36% 9/25

Variabilité morphologique des chiens et renards roux dans les premières sociétés agricoles d'Europe : approche morpho-fonctionnelle basée sur la mandibule

Les changements culturels et techno-économiques majeurs survenus en Europe entre 7000 et 4000 ans avant J.-C., notamment le développement de l'agriculture, ont eu d'importantes répercussions sur les animaux qui vivaient près des hommes. Le chien, seul animal domestiqué depuis déjà plusieurs millénaires, est probablement un bon marqueur de l'évolution des sociétés humaines à cette époque. Bien que de nombreuses données nous informent sur son statut et sa diversité génétique, très peu d'études ont documenté sa variabilité morphologique et les éventuelles adaptations fonctionnelles en découlant, en lien avec les contraintes anthropiques. En outre, à ce jour, aucune étude n'a exploré la variabilité des renards roux anciens, bien qu'ils soient susceptibles de développer les mêmes adaptations que les chiens (mais dans une moindre mesure en raison de leur nature commensale). Dans cette thèse, une approche morpho-fonctionnelle innovante est utilisée pour décrire l'évolution de la mandibule (l'os le mieux préservé dans les séries archéologiques et un élément fonctionnel important de l'appareil masticateur) du Mésolithique au tout début de l'âge du Bronze en Europe occidentale et au sud de la Roumanie. La photogrammétrie et la morphométrie géométrique sont utilisées pour quantifier la forme des os en 3D. Dans un premier temps, les facteurs de forme et les relations forme-fonction au sein de l'appareil masticateur sont explorés dans un échantillon de chiens et de renards modernes. Les muscles masticateurs d'environ 120 chiens de différentes races et de renards ont été disséqués. Un modèle biomécanique d'estimation de la force de morsure à partir des données musculaires est établi et validé par des mesures in vivo. De fortes interrelations entre le crâne, la mandibule, les muscles masticateurs et la force de morsure sont démontrées pour les deux espèces, soulignant la forte intégration malgré les sélections artificielles extrêmes chez les chiens modernes. Un modèle prédictif de la force de morsure utilisant la forme des fragments mandibulaires est donc développé pour interpréter les variations de forme dans l'échantillon archéologique. Les impacts des facteurs de développement et environnementaux (climat, urbanisme, alimentation) sur la forme ou la fonction sont quantifiés par l'étude de 433 renards australiens. Ensuite, la variabilité des chiens et des renards anciens (528 chiens et 50 renards) est comparée à celle des canidés modernes (70 chiens, 8 dingos, 8 loups, 68 renards). De fortes différences morphologiques sont démontrées pour les deux espèces, ce qui suggère des différences fonctionnelles. Les chiens anciens semblent très variables en termes de taille et de forme, bien que moins variables que les chiens modernes. Les hypertypes récents n'ont pas d'équivalent dans notre échantillon archéologique. Plus surprenant, certaines formes anciennes ne sont pas trouvées dans l'échantillon moderne. Enfin, la variabilité existant chez les chiens avant l'âge du Bronze est explorée et mise en relation avec les informations déjà disponibles. De fortes différences entre l'Europe de l'Est et de l'Ouest sont mises en évidence, reflétant les histoires très différentes des populations canines dans ces deux régions. Dans chaque zone géographique, des différences temporelles mais aussi culturelles dans la taille et la forme des chiens sont démontrées. L'étude des renards, bien que limitée en raison de la rareté des restes, révèle l'existence d'une diversité relativement importante. Les variations de taille et de forme sont alors probablement plus liées à des variations géographiques et climatiques qu'à des contraintes anthropiques. Des différences dans la force de morsure au fil du temps sont suggérées pour les deux espèces, ce qui laisse supposer des changements dans la fonction du chien, et peut-être des adaptations fonctionnelles à un régime alimentaire de plus en plus influencé par les pratiques humaines.

Mots clefs : canidé, *Canis familiaris*, *Vulpes vulpes*, Neolithique-Chalcolithique, morphométrie géométrique, appareil masticateur

Morphological variability in dogs and red foxes from the first European agricultural societies: a morpho-functional approach based on the mandible

The major cultural and techno-economic changes that occurred in Europe between 7,000 and 4,000 BC, including the development of agriculture, had major repercussions on the animals that lived close to humans. The dog, the only animal that has been domesticated for thousands of years is probably a good marker of the evolution of human societies at that time. Although many data inform us about its status and genetic diversity, very few studies have documented its morphological variability and the resulting possible functional adaptations in relation to anthropogenic constraints. Furthermore, to date no studies have explored the variability in ancient red foxes although they are likely to develop the same adaptations as dogs (but to a lesser extent due to their commensal nature). In this thesis, an innovative morpho-functional approach is used to describe the evolution of mandible (the best preserved bone in archaeological series and an important functional element of the masticatory apparatus) from the Mesolithic to the very early Bronze Age in Western Europe and Southern Romania. Photogrammetry and geometric morphometrics are used to quantify the shape of the bones in 3D. In a first step, shape drivers and form-function relationships within the masticatory apparatus are explored in a sample of modern dogs and foxes. The masticatory muscles of approximately 120 dogs of various breeds and foxes were dissected. A biomechanical model for estimating bite force using muscle data is established and validated by in vivo measurements. Strong interrelationships between the cranium, mandible, masticatory muscles and bite force are demonstrated for both species, highlighting the strong integration despite the extreme artificial selections in modern dogs. A predictive model of bite force using the shape of mandibular fragments is therefore developed to interpret the variations in shape in the archaeological sample. The impacts of developmental and environmental factors (climate, urbanism, diet) on the form or function are quantified by studying 433 Australian foxes. Secondly, the variability of ancient dogs and foxes (528 dogs and 50 foxes) is compared with that of modern canids (70 dogs, 8 dingoes, 8 wolves, 68 foxes). Strong morphological differences are demonstrated for both species, suggesting functional differences. Ancient dogs appear highly variable in terms of size and shape, although less variable than modern dogs. Modern hypertypes have no equivalent in our archaeological sample. More surprisingly, some ancient shapes are not found in the extant sample. Finally, the variability existing in dogs prior to the Bronze Age is explored and linked to the information already available. Strong differences between eastern and western Europe are highlighted, reflecting the very different histories of dog populations in these two areas. In each geographical area, temporal but also cultural differences in the size and shape of the dogs are demonstrated. The study of foxes, although limited due to the scarcity of remains, reveals the existence of a relatively large diversity. Variation in size and shape are then probably more related to geographical and climatic variation than to anthropogenic constraints. Differences in bite force over time are suggested for both dogs and foxes, suggesting changes in dog function, and possibly functional adaptations to a diet that has become increasingly influenced by human practices.

Key words: canid, *Canis familiaris*, *Vulpes vulpes*, Neolithic-Chalcolithic, geometric morphometrics, masticatory apparatus